

UNCLASSIFIED

AD 273 887

*Reproduced
by the*

**ARMED SERVICES TECHNICAL INFORMATION AGENCY
ARLINGTON HALL STATION
ARLINGTON 12, VIRGINIA**



UNCLASSIFIED

NOTICE: When government or other drawings, specifications or other data are used for any purpose other than in connection with a definitely related government procurement operation, the U. S. Government thereby incurs no responsibility, nor any obligation whatsoever; and the fact that the Government may have formulated, furnished, or in any way supplied the said drawings, specifications, or other data is not to be regarded by implication or otherwise as in any manner licensing the holder or any other person or corporation, or conveying any rights or permission to manufacture, use or sell any patented invention that may in any way be related thereto.

UNEDITED ROUGH DRAFT TRANSLATION

273 887

THEORETICAL BASES FOR THE DESIGN OF LIQUID-FUELED
ROCKET ENGINES

BY: M. I. Shevel'yuk

English Pages: 952

THIS TRANSLATION IS A RENDITION OF THE ORIGINAL FOREIGN TEXT WITHOUT ANY ANALYTICAL OR EDITORIAL COMMENT. STATEMENTS OR THEORIES ADVOCATED OR IMPLIED ARE THOSE OF THE SOURCE AND DO NOT NECESSARILY REFLECT THE POSITION OR OPINION OF THE FOREIGN TECHNOLOGY DIVISION.

PREPARED BY:

TRANSLATION SERVICES BRANCH
FOREIGN TECHNOLOGY DIVISION
WP-AFB, OHIO.

M. I. Shevelyuk

TEORETICHESKIYE OSNOVY PROYEKTIROVANIYA ZHIDKOSTNYKH
RAKETNYKH DVIGATELEY

Gosudarstvennoye Nauchno-Tekhnicheskoye Izdatel'stvo
Oborongiz, Moskva - 1960

Pages: 1-684

MCL-1358/1+2

This volume sets forth the theoretical foundations of the design of liquid-fueled rocket engines; using data published in the foreign literature as a basis, it discusses the operating modes, working processes, and characteristics of the ZhRD* and its chamber, the planning and design of atomizing devices and systems for delivering fuel into the chamber of the ZhRD, as well as the specifications of the fuels used. The book also illuminates the problems of chamber cooling and operation and testing of ZhRD.

The volume is designed as a study aid for the higher technical schools in the corresponding specialties; it can also be used as a textbook for engineers and technicians working in this field.

Reviewer: Doctor of Technical Sciences Professor A.V. Kvasnikov

Editor: Engineer I.L. Yanovskiy

. Editor-in-Chief: Engineer S.D. Krasil'nikov

*[ЖРД = ZhRD = Zhidkostnyy Raketnyy Dvigatel' = Liquid-Fueled Rocket Engine(s).]

TABLE OF CONTENTS

Foreword	1
Chapter I. Introduction	3
1. Brief History of the Development of Liquid-Fueled Rocket Engines	4
2. Directions in the Development of <u>ZhRD</u>	15
Chapter II. General <u>ZhRD</u> Characteristics	26
1. Basic <u>ZhRD</u> Design Elements	26
2. Classifications of Existing <u>ZhRD</u>	30
3. Basic <u>ZhRD</u> Parameters	39
4. Advantages and Disadvantages of <u>ZhRD</u>	43
5. Fields of Application of <u>ZhRD</u>	47
6. Requirements Demanded of Weapon Engines	49
7. Factors Affecting Velocity and Range of Missiles With <u>ZhRD</u>	51
8. Basic Problems to be Solved in Planning and Designing <u>ZhRD</u>	58
Chapter III. Engine Operating Cycles and Efficiency	61
1. Operating Cycle of an Ideal Engine	61
2. Operating Cycle of a Real Engine	65
3. Classification of Velocities of Gas Outflow From the Chamber Nozzle of a <u>ZhRD</u>	67
4. Engine Efficiencies	72
5. Change of Working Fluid's Basic Parameters Along the Chamber Length of a <u>ZhRD</u>	82
6. Equations Characterizing the Quantitative Relationships in the Change of Gas-Flow Parameters Along the Length of the <u>ZhRD</u> Nozzle	85
Chapter IV. <u>ZhRD</u> Operating Regimes	99
1. Rated and Nonrated Engine Operating Regimes	100
2. Operational Engine Operating Regimes	102
3. Factors Affecting the Intensity of <u>ZhRD</u> Thrust.	104
4. The Absolute Thrust of an Engine	106
5. Engine Chamber Nozzle Operation at Nonoptimum Regimes	118
6. The Thrust Coefficient of an Engine	122
7. Specific Thrust of an Engine	126
8. Fuel Flow Rates in an Engine	133
9. Methods and Limits of Regulating Engine Thrust.	138
10. Flow-Rate Characteristics of an Engine	146
11. Real <u>ZhRD</u> Flow-Rate Characteristics	155
12. Engine Altitude Characteristics	157
13. Real <u>ZhRD</u> Altitude Characteristics	163
14. Selection of Optimum Engine-Chamber Nozzle Design Altitude	167
15. Regulating an Engine-Chamber Nozzle's Design Altitude	172
16. Basic Characteristics of the A-4 Oxygen <u>ZhRD</u>	174

Chapter V. Characteristics of <u>ZhRD</u> Fuels	175
1. Basic Types of <u>ZhRD</u> Fuels	176
2. Parameters Characterizing Quality of Fuel	182
3. Methods of Converting Elementary Weight Compo- sitions of Fuel Components Into Conventional Chemical Formulas and Vice Versa	188
4. Determination of Theoretical and Actual Quantity of Oxidizer Required for Complete Combustion of a Unit of Combustible	193
5. Determination of Excess Oxidizer Ratio for Fuel	199
6. Determination of Proportions by Weight and Vol- ume, Specific Gravity, and Specific Volume of Fuel	205
7. Determination of Heat Value of Fuel	206
8. Determining Energy Content of Fuel	215
9. Specifications Set Forth for a <u>ZhRD</u> Fuel	227
10. Basic Characteristics of <u>ZhRD</u> Combustibles	234
11. Basic Characteristics of Oxidizers for <u>ZhRD</u> Combustibles	248
12. Basic Characteristics of <u>ZhRD</u> Fuels	263
13. Methods of Improving the Quality of <u>ZhRD</u> Fuels	270
14. Selection of Fuel Components for Engine in De- sign Stage	272
15. Use of Atomic Energy in Rocket Engines	279
Chapter VI. Cycles in <u>ZhRD</u> Chambers	297
1. Cycles of Fuel Preparation and Combustion in the Engine Chamber	298
2. Heat Balance for an Engine Combustion Chamber.	309
3. The Fuel Heat-Liberation Coefficient in an En- gine Combustion Chamber	313
4. Ideal, Theoretical, and Actual Thermodynamic Temperatures of Fuel Combustion	317
5. Determining the Composition and Ideal Tempera- ture for Products of Fuel Combustion	320
6. Determining the Energy Content of Products of Fuel Combustion	324
7. The Essence of <u>ZhRD</u> Chamber Thermodynamic De- sign	326
8. Equations of the Constants of Equilibrium of Gas-Dissociation Reactions and Equations of Material Balance	330
9. Determining the Theoretical Temperature and Composition of Products of Fuel Combustion in a <u>ZhRD</u> Combustion Chamber	337
10. Methods for Solving Systems of Equations for Determining Theoretical Temperature and Compo- sition of Products of Fuel Combustion	346
11. Determining the Theoretical Temperature and Composition for Products of Fuel Combustion in an Engine-Chamber Nozzle Outlet Section	365
12. Determining the True Parameters and Characteris- tics of a <u>ZhRD</u>	374

Chapter VII. Planning and Designing <u>ZhRD</u> Chambers . . .	387
1. <u>ZhRD</u> Chamber Requirements	388
2. <u>Lateral</u> and Volumetric Intensities of Flow Rate and Heat Liberation in Engine Combustion Chambers	390
3. Determination of Combustion-Chamber Volume in Engines	395
4. Advantages and Shortcomings of Combustion Chambers, of Various Structural Shapes, and Their Heads	402
5. Selection of Shape for <u>ZhRD</u> Combustion Chamber .	408
6. Selection of Relative Area in Engine Combustion Chambers	413
7. Determination of Basic Geometric Characteristics of Engine Chamber	419
8. Selection of Shape and Angle for Engine-Chamber Nozzle	428
9. Graphical Methods to Shape the Nozzle of an Engine Chamber	437
10. Engine-Chamber Liner Loads	440
11. Requirements for Materials used in Engine Chambers	449
12. Determination of Optimum Pressure in <u>ZhRD</u> Combustion Chamber	453
13. Determination of Engine Weight	460
14. Determination of Engine Dimensions	471
15. Methods of Igniting Fuel on Engine Start	472
16. General Problems in Planning and Designing <u>ZhRD</u> Chambers	480
Chapter VIII. Theory and Design of Atomizing Devices for <u>ZhRD</u>	486
1. Specifications Set Forth for Atomizing Device of <u>ZhRD</u>	487
2. Methods of Atomizing Fuel Components in <u>ZhRD</u> . .	494
3. Types of Fuel Spray Nozzles	497
4. Factors Exerting Qualitative Influence on Atomization of Fuel Components	507
5. Design of Jet-Type Atomizing System	516
6. Design of Single-Component Centrifugal Spray Nozzles	523
7. Design of Two-Component Centrifugal Emulsion-Type Nozzles	540
8. Placement of Fuel Nozzles and Other Devices on Engine-Chamber Head	543
Chapter IX. Planning and Designing <u>ZhRD</u> Cooling Systems.	552
1. Methods of Protecting <u>ZhRD</u> Chambers against Overheating; Their Advantages and Shortcomings .	554
2. Heat-Transfer Processes in a <u>ZhRD</u> Chamber . . .	564
3. Requirements Imposed on a <u>ZhRD</u> Regenerative Cooling System	576
4. Factors Affecting Heat Transfer in a <u>ZhRD</u> Chamber	582

5. Similarity Criteria in the <u>ZhRD</u> Heat Exchange Processes	594
6. Determining Specific Convective Heat Flows From the Gas to the Engine-Chamber Liner	598
7. Determining Specific Radiation Heat Flows From a Gas to an Engine-Chamber Liner	606
8. Selecting Shapes and Dimensions for an Engine-Chamber Coolant Passage	617
9. Determining Degree of Coolant Preheating Throughout Engine-Chamber Coolant-Passage Length	624
10. Determining Liquid-Side and Gas-Side Engine-Chamber Liner Temperatures	629
11. Protective Curtains for an Engine-Chamber Inner Liner	637
12. The Sequence of Designing a <u>ZhRD</u> -Chamber Cooling System	647
13. Determining Temperature Stresses in a <u>ZhRD</u> -Chamber Liner	653
14. Selecting Material for Engine-Chamber Inner Liner and Determining Liner Thickness	661
Chapter X. Planning and Design of <u>ZhRD</u> Fuel-Feed Systems.	667
1. Basic Types of <u>ZhRD</u> Fuel-Feed Systems, Their Advantages, Disadvantages, and Ranges of Application	668
2. Fundamentals of Planning and Design of <u>ZhRD</u> Fuel Tanks	678
3. Design of Gas Pressure Accumulator for Engine Fuel-Feed System	694
4. Design of Powder Pressure Accumulator for Engine Fuel-Feed System	711
5. Calculations for Liquid-Propellant Pressure Accumulator for Fuel-Feed System	725
6. Methods of Powering <u>TNA</u> Turbines and Their Advantages and Disadvantages	735
7. Design of Hydrogen-Peroxide Vapor-Gas Generators for <u>ZhRD</u>	743
8. Two-Component <u>ZhRD</u> Gas Generators	759
9. Determining Power of <u>TNA</u> Turbine and Per-Second Flow of Gas Required to Feed it	771
10. Characteristics of <u>ZhRD</u> Fuel-Feed System Turbines and Special Points for Their Design	776
11. Characteristics of Pumps for <u>ZhRD</u> Fuel-Feed System and Special Points in Their Design.	787
12. Fittings, Pipelines, and Other Elements of <u>ZhRD</u> Fuel-Feed System	800
13. Hydraulic Calculations for <u>ZhRD</u> Fuel-Feed System.	810
14. Tuning of <u>ZhRD</u> to Operate at Design Parameters.	815
15. Comparison of Different <u>ZhRD</u> Fuel-Feed-System Layouts	820

Chapter XI. Stable and Unstable <u>ZhRD</u> Regimes and Auto- matic Operating Control	826
1. Stable and Nonstable <u>ZhRD</u> Operating Regimes	827
2. Automatic Regulation of <u>ZhRD</u> Operating Regime.	843
Chapter XII. Certain Problems Encountered in <u>ZhRD</u> Opera- tion	861
1. Engine Operating Reliability	862
2. Start and Stopping the <u>ZhRD</u>	866
3. "Charge" <u>ZhRD</u> Starting, with Hypergolic Fuel Com- ponents	873
4. Engine Service Life	881
Chapter XIII. Stages in the Planning and Final Tests of <u>ZhRD</u>	884
1. Stages in the Planning of a <u>ZhRD</u>	884
2. Static Tests of <u>ZhRD</u>	896
3. Processing Data From Hot-Firing Static Tests of an Engine	916
Appendices	926
Bibliography	948

FOREWORD

During recent years, a number of papers and independent volumes devoted to the theory and design of liquid-fueled rocket engines (ZhRD) have been published at home and abroad.

Among these studies, the textbooks written by the Soviet scientists A.V. Bolgarskiy and V.K. Shchukin, G.B. Sinyarev and M.V. Dobrovol'skiy, V.I. Feodos'yev and G.B. Sinyarev, and others merit special attention.

The present volume represents an attempt to generalize the material available on the theory and design of liquid-fueled rocket engines for aerospace equipment designed for various purposes.

Certain problems of reaction-thrust technique have not been highly developed up to the present time. In many cases, this obliged the author to restrict himself to qualitative analysis of such problems as they might apply to specific tasks of engineering engine-design practice.

The author has systematized, refined, and, in some cases, developed further certain questions relating to the theory and design of ZhRD.

Diagrams, tables, and sample calculations are included in the volume to assist in practical utilization of the information embodied in it.

The exposition may be used as a basis for selection of the appropriate type of engine for a specified application and the type of fuel

required, establishment of the optimum operational and design parameters for it, selection of materials, computation of the geometrical, operational, hydraulic, and other specifications, establishment of physical designs for its individual elements, and, on the whole, the first-approximation planning of an economical and operationally dependable engine that ensures the maximum flight range for the equipment in question.

The author has made an attempt to follow a terminology and set of letter symbols that corresponds most fully to the physical essence of the concepts and will be convenient to use.

The information presented in the volume does not pretend to be a full exposition of the problems encountered in the field and, naturally, requires further work.

The author requests that all errors and deficiencies noted be reported to the address: Moscow, I-51, Petrovka, 24, Oborongiz.

The Author

Chapter I

INTRODUCTION

In the various types of rocket missiles, the basic element is the engine.

The type of engine is determined basically by the design, overall dimensions, and flight characteristics of these missiles. The missile's range depends on the type of engine selected, the type of fuel components used in it, and on its design, operational, and other characteristics.

It is the object of the present volume to provide students in the higher technical educational institutions and engineering-technical workers with a brief outline of the theory and basic design principles of liquid-fueled rocket engines. This information may be used as a basis in each specific case for making a rational selection of a basic ZhRD design for development, the fuel components for it, and its starting and design parameters, and for making the necessary calculations of its operational, geometrical, and other characteristics, as well as solving other problems related to the creation of a dependable and operationally economical engine design.

In addition to general engineering preparation, it will be necessary for successful completion of this course to have a clear conception of existing ZhRD and ZhRS* (liquid-fueled rocket missile) designs, *[XPC = ZhRS = Zhidkostnyy Raketnyy Snaryad = Liquid-Fueled Rocket Missile(s).]

as well as to know the chemistry and combustion theory of liquid fuels, the fundamentals of heat exchange and heat transfer, the theory of strength and rigidity of structures, high-speed aerodynamics, ballistics, and automatic-control theory.

SECTION 1. BRIEF HISTORY OF THE DEVELOPMENT OF LIQUID-FUELED ROCKET ENGINES

Our country can take the basic credit for developing the foundations of the theory of liquid-fueled rocket engines and the missiles for them, as well as for building the first models.

The founder of reaction-engine theory was the great Russian scientist N.Ye. Zhukovskiy, who, in his 1882 paper entitled "O reaktsii vytekayushchey i vtekayushchey zhidkosti" ("Concerning the reaction of outflowing and inflowing liquids"), was the first to derive the equation for the reaction force of an outflowing fluid, and who presented the equation for the efficiency of the fluid stream in his later papers.

The Russian scientist I.V. Meshcherskiy, whose outstanding works on the mechanics of bodies of variable mass, which were published in 1897, formed the basis for the contemporary theory of motion of reaction-thrust missiles, must be ascribed an important part in the creation of reaction-engine theory.

K.E. Tsiolkovskiy, who originated the idea of the liquid-fueled rocket engine, created the theory of flight of reaction-powered machines, and authored a number of systems for such machines and other suggestions, must be included among the Russian scientists who have made the inventive genius of their Motherland famous.

K.E. Tsiolkovskiy published his first paper in the journal "Nauchnoye obozreniye" ("Scientific Review"), No. 5, under the title "Issledovaniye mirovykh prostranstv reaktivnymi priborami" ("Investigation of

interstellar space by means of reaction-engined devices"). In this 1903 paper, and in the supplementary papers that followed it between 1911 and 1914, and then in 1924-1925 and thereafter, K.E. Tsiolkovskiy showed the insight of a genius in formulating and solving the basic problems of the theory and working principles of the liquid-fueled rocket missile.

He was first to propose the following:

- 1) a design for a liquid-fueled rocket engine (1903);
- 2) the use of liquid oxygen as an oxidizer for the fuel (1903);
- 3) pump delivery of the fuel into the engine's chamber (1903);
- 4) graphite and high-melting metals for fabrication of engine chambers (1903);
- 5) cooling of the engine chamber by one of the fuel components (1903);
- 6) closed-cycle cooling of the engine chamber (1903);
- 7) the use of nuclear and electric energy to power reaction engines (1911);
- 8) the use of ozone as an oxidizer and liquid methane and turpentine as fuels (1914);
- 9) the use of oxides of nitrogen as oxidizers (1926);
- 10) the use of nitrogen pentoxide as an oxidizer and monatomic hydrogen as a fuel (1927);
- 11) placing control surfaces in the stream of gases behind the nozzle of the engine chamber to control the missile in its flight in the rarefied layers of the atmosphere and in space (1929), etc.

K.E. Tsiolkovskiy also considered other problems of reaction-thrust motion in his papers, and specifically:

- 1) he demonstrated that a reaction-thrust engine can develop thrust even in airless space;

2) he made reference to the high promise of practical utilization of reaction-thrust missiles for study of cosmic space;

3) he demonstrated that an inclined ascent is more efficient for a reaction-thrust missile than vertical ascent;

4) he proved that liquid fuels are superior to solid fuels (powder) for medium- and long-range reaction-thrust machines;

5) he showed that medium- and long-range reaction-thrust missiles must have control and automatic-control devices in operation during flight;

6) he studied the motion of the reaction-thrust missile in vacuo, with and without consideration of gravity;

7) he derived a celebrated formula for determining the maximum flight speed of a reaction-thrust missile in airless space at the end of its powered trajectory;

8) he made note of the expediency of raising the gas pressure in the engine's combustion chamber with the object of increasing its specific thrust;

9) he determined the efficiency of the reaction-thrust engine during flight and indicated a number of paths for development of this type of technique and the promise that it offered.

K.E. Tsiolkovskiy established a solid scientific footing for the study of the rocket's motion as a body of variable mass.

K.E. Tsiolkovskiy advanced the following ingenious ideas:

1) that of building multiple-stage reaction-thrust missiles to attain long flight ranges;

2) the expediency of using winged reaction-thrust missiles to attain long ranges;

3) the design of reaction-engined aircraft;

4) the idea of cosmic stations, i.e., artificial Earth satellites

in the form of specialized reaction-thrust missiles, etc.

Contemporary reaction-thrust technology is based for the most part on the work of K.E. Tsiolkovskiy. His ideas were popularized to some extent in the book "Mezhplanetnyye puteshestviya" ("Interplanetary Travel") by Ya.I. Perel'man, which appeared in 1915.

K.E. Tsiolkovskiy began to show interest in problems of reaction-thrust motion in 1883. Between February and May of that year, he wrote a paper entitled "Svobodnoye prostranstvo" ("Free space"), in which he analyzed certain problems related to the use of reaction-thrust motion. In 1896, he wrote a novel entitled "Vne zemli" ("Outside the earth"), in which he also made reference to the reaction-thrust missile as an apparatus for interplanetary travel.

The Great October Socialist Revolution gave K.E. Tsiolkovskiy a full opportunity to develop his creative activity. The daily attention paid to his scientific research work by the Communist Party and the Soviet Government contributed to its widespread dissemination and recognition.

Before the Great October Socialist Revolution, he had written 80 papers, of which 50 had been published, while after the revolution, he wrote and published 150 articles.

The numerous works of K.E. Tsiolkovskiy in the field of reaction-engine technology made him world-famous. Professor H. Oberth wrote K.E. Tsiolkovskiy from Germany in September of 1929 as follows: "My compliments... May you live to see the attainment of your glorious goals... You have lighted the lamp, and we shall work until the most grandiose dream of humanity comes true."

In 1917, the Russian scientist Yu.M. Kondratyuk began his research work in the field of reaction-thrust motion, and in 1929 he published a paper entitled "Zavoyevaniye mezhplanetnykh prostranstv"

("Conquest of interplanetary space") (republished by Oborongiz in 1947). In this paper, he derived a series of important conclusions and gave expression to many original ideas in the field of reaction-thrust technique;

- 1) he demonstrated that a missile that does not jettison its fuel tanks during flight as they are exhausted cannot escape the range of terrestrial gravity;

- 2) he investigated the takeoff dynamics of the winged reaction-thrust missile;

- 3) he introduced new proposals on the realization of space stations and interplanetary flights using reaction-thrust machines;

- 4) he proposed the use of solids (lithium, boron, etc.) as fuels for ZhRD.

He also investigated the problem of heating of reaction-thrust missiles during flight in the atmosphere.

Our compatriot F.A. Tsander began his studies of reaction propulsion in 1908, and in his 1932 book entitled "Problemy poleta pri pomoshchi reaktivnykh apparatov" ("Problems of flight using reaction-thrust machines") set forth the results of his investigations of a number of highly important problems of reaction-thrust engineering and mapped out paths for its development, as follows:

- 1) he made note of the expediency of using metallic elements of the reaction-thrust missile as fuel after they had performed their immediate functions, with the object of attaining maximum range;

- 2) he developed a theory of spray injectors and a theory of the ZhRD, analyzing the basic principles of heat-exchange calculation and cooling for the engine chamber;

- 3) he proposed a number of operating cycles for the ZhRD and derived their efficiencies;

4) he developed a theory of missile flight along elliptical trajectories;

5) he investigated the climbing properties of a reaction-engined aircraft;

6) he investigated various types of liquid fuels with the object of selecting the most efficient fuels for use in reaction-thrust engines, and considered a number of other problems related to reaction-thrust engineering.

In 1930-1932, F.A. Tsander built and tested his OR-1 reaction engine, which worked on a mixture of air and gasoline and developed up to 5 kg of thrust. A second experimental engine, the OR-2, which had been built after his drawings in 1932 for operation on liquid oxygen and gasoline, underwent firing tests in 1933 without participation of F.A. Tsander, who had died ten days after the first test of the engine. The combustion chamber of this engine was oxygen-cooled, and the nozzle was water-cooled. The fuel components were fed into this engine's combustion chamber by compressed air.

Abroad, the first investigations of cosmic-flight problems appeared beginning with the second decade of the 20th century, and these were followed by studies of liquid-fueled rocket missiles. Among the scientists who devoted their efforts to these problems, we should take note of R. Eno-Peltri (France), whose first paper was published in 1903, and R. Goddard (USA), who began his work in 1915 and subsequently built several types of meteorological missiles with liquid-fueled engines. The work of H. Oberth (Germany), which was published in 1927, and that of E. Zenger (Austria), which appeared in 1933, made large contributions to the theory of reaction-engined flight.

The first dependable ZhRD were built in the USSR. The engines of the reaction-thrust institute at Peenemunde (the A-4 and "Wasserfall")

and the firms BMW [Bayerische Motoren Werke] and Walther appeared in Germany, and those of the California Institute of Technology and the firms Aerojet Engineering, Reaction Motors, etc. in the USA all appeared somewhat later than the first ones built in the USSR.

The appearance of the first dependable engines made definite the possibility of applying them in practice in long-range and anti-aircraft missiles of various types, aerial torpedos, etc.

A tremendous achievement in the field of developing reaction-thrust science and technology was the building and successful testing of the world's first intercontinental ballistic missile in the Soviet Union.

Test results for this rocket indicated that perfection of the intercontinental ballistic missiles will make it possible to reach any region of the globe, no matter how remote, without resorting to strategic aviation.

The greatest achievement of Soviet science and technology in the field of rocketry was the launching, on 4 October 1957, of the world's first artificial satellite.

In its launching, this satellite, which had the shape of a sphere 58 cm in diameter and weighing 83.6 kg, received its 8000-m/sec orbital velocity and its 900-km maximum distance from the earth's surface from a rocket carrier; it completed one revolution about the earth in 1 hour 35 minutes.

This satellite completed 1400 revolutions about the earth and traveled about 60 million kilometers.

This successful launching of a man-made Earth satellite was the greatest contribution ever made to the treasury of the world's science and culture.

The second artificial Earth satellite was launched in the Soviet

Union on 3 November 1957 (as part of the program of the International Geophysical Year).

This Earth satellite was the last stage of a rocket vehicle and carried a container for scientific apparatus and an experimental animal (a dog) and weighed a total of 508.3 kg.

The initial orbital characteristics of the satellite were as follows: shape, elliptical; altitude at apogee, 1671 km; inclination of orbit to equator, $65^{\circ}17'$; period of revolution, 103.74 min. The orbital velocity of the satellite at launch was 8000 m/sec.

This satellite completed about 2370 revolutions around the earth, and traveled a distance of 100 million kilometers.

With the successful launching of an artificial Earth satellite carrying various scientific apparatus and an experimental animal, Soviet scientists expanded their investigation of cosmic space and the upper layers of the atmosphere.

On 15 May 1958, a third Earth satellite — the largest in the world — was launched in the Soviet Union. It weighed 1327 kg. It was 3.57 m long and had a largest diameter of 1.73 m.

The initial orbital characteristics of this satellite were as follows: shape, elliptical; altitude at apogee, 1880 km; inclination of orbit to equator, 65° ; period of revolution, 105.95 min.

This satellite continues in its motion about the earth. On 15 February 1960, it had completed 9221 revolutions.

The next magnificent attainment of Soviet rocket science and engineering was the creation of a multi-stage rocket the last stage of which was capable of reaching the second cosmic [parabolic] velocity (11.2 km/sec), thus making interplanetary flight possible. Such a cosmic rocket was successfully launched toward the moon in the USSR on 2 January 1959.

The last stage of the rocket, which weighed 1472 kg without fuel, was equipped with a special container for measuring apparatus and radio transmitters to carry out scientific investigations. The total weight of the scientific and measurement apparatus with their power sources and container came to 361.3 kg.

Thirty-four hours after blastoff, this cosmic rocket flew past the moon (at a distance of about 6-7 thousand kilometers) and was 597,000 kilometers from the earth in the 62nd hour of its flight, at 10 hours on 5 January. Having overcome the attraction of the earth and the moon, it emerged into its orbit about the sun.

Dependable radio contact between the rocket and the earth was maintained for 62 hours, in accordance with the program.

Evaluation of the measurement data obtained made it possible to establish that the cosmic rocket finally entered the periodic orbit of an artificial planet of the solar system on 7-8 January 1959. The largest diameter of the rocket's orbit, which lay between those of the earth and Mars, was found to be 343.6 million kilometers. The rocket's period of revolution about the sun is 15 months (450 earth days).

The launching of the cosmic rocket, which had become for all eternity the first artificial planet of our solar system, opened the era of interplanetary flight and demonstrated to the entire world the outstanding achievements of Soviet science and engineering.

Another historical first was scored in the period from 12 through 14 September 1959 with the successful launching of a second multiple-stage Soviet cosmic rocket to the moon; this device delivered to its surface a pennant with the coat of arms of the Soviet Union.

Valuable scientific data which opened up a new stage in the exploration and conquest of the cosmos by man were transmitted from the rocket and received on the earth during this flight.

The landing of a Soviet rocket on the moon represents an outstanding success for Soviet science and engineering and marks the beginning of flight from the earth to other planets.

On 4 October 1959, a third multiple-stage cosmic rocket was launched in the USSR to continue the investigation of cosmic space and photograph that side of the moon which is invisible from the earth.

For this purpose, an interplanetary space station that could be controlled automatically from the earth was designed, built, and placed by a rocket in a previously calculated orbit around the moon. As planned, this station passed at a distance of several thousand kilometers from the moon, photographed its other side on 18 October, and transmitted these images to the earth on command by means of a special radio communications system.

This rocket launching to the moon, which resulted in the acquisition of extremely valuable and hitherto unavailable scientific data concerning cosmic space, including the photographs of that side of the moon which is invisible from the earth, required solution of a number of highly diverse and complex problems by Soviet experts. These attainments of Soviet science and engineering have shaken the entire world and have been an occasion for enormous delight for all progressive humanity.

On the basis of the progress made in the Soviet Union in investigating cosmic space by means of ballistic rockets, Soviet scientists and designers are working in accordance with a scientific-research program on the creation of a more powerful rocket to be used in launching heavy Earth satellites and making space flights to other planets of the solar system.

On 8 January 1960, TASS reported that this rocket would be launched into the central part of the Pacific Ocean without its last

stage during the first few months of 1960, as part of the development of a high-accuracy rocket of this type. The area in which the stage [sic] of the rocket was expected to fall was indicated in this report.

The first launching of this rocket took place in the evening of 20 January 1960.

At 20 hours 15 minutes Moscow time on the same day, the next-to-last stage of this rocket, having moved exactly along the specified trajectory with a dummy of the last stage and having developed a speed better than 26 thousand kilometers/hour, reached the specified area in the equatorial Pacific Ocean, which was 12.5 thousand kilometers across the earth's surface from the point of launching.

The last-stage dummy, which was adapted to pass through the dense layers of the atmosphere, reached the surface of the sea near the calculated impact point.

Special ships of the Soviet fleet waiting in the rocket's expected area of impact made valuable telemetric measurements on the descending branch of the flight trajectory.

The dummy of the rocket's last stage was observed during its flight through the atmosphere and was pinpointed where it dropped into the water by radar, optical, and sonar stations on the ships.

It was established by the measurements carried out that the rocket's impact point was less than 2 km from the predicted position, so that the high accuracy of the rocket's control system was confirmed.

The rocket was launched exactly at the specified time. The rocket's flight and the operation of all of its stages took place in conformity with the predetermined program. The measurement systems and facilities on board the rocket transmitted the necessary data to ground and shipborne stations over the entire flight path.

A second such rocket was launched for the same purpose in the evening of 31 January 1960.

The last stage of the rocket with its dummy reached the specified area in the equatorial Pacific Ocean at 19 hours 58 minutes Moscow time.

The last-stage dummy was again observed during flight through the atmosphere and was pinpointed on impact with the water by ship-borne radar, optical, and sonar stations.

The measurement data again confirmed the high precision with which the rocket's flight was controlled.

The successful launchings of this powerful Soviet multiple-stage ballistic rocket have further advanced Soviet science along the path to the conquest of cosmic space and study of the solar system.

SECTION 2. DIRECTIONS IN THE DEVELOPMENT OF ZhRD

Analysis of the designs of existing ZhRD enable us to establish the basic directions being taken in the development of this branch of engineering.

Oxygen-, nitric-acid-, and hydrogen-peroxide engines were developed during the Second World War and used in missiles, aerial torpedos, and aircraft.

The oxygen-carrying rocket engines used at that time for long-range missiles developed absolute thrusts no greater than 26 tons, worked on fuels with relatively low calorific values (75% ethyl alcohol and liquid oxygen) with low combustion-chamber gas pressures (16 atmospheres absolute) and low thrusts per liter (about 60-80 kg per liter of volume) and, as a result, developed low specific thrusts [of the order of 200 kg of thrust/(kg of fuel/sec)].

The ZhRD of the A-4 long-range missile (Figs. 1.1 and 1.2) can be



Fig. 1.1. External appearance and cutaway of A-4 long-range missile with 25-26 tons of thrust at the surface. 1) Engine chamber; 2) turbopump set; 3) oxygen tank; 4) ethyl-alcohol tank; 5) instrument compartment; 6) warhead; 7) framework of missile.

cited as an example of an oxygen engine of this type.

A tank for 75%-by-weight ethyl alcohol (the fuel) and a tank for liquid oxygen (the oxidizer) are located in the middle of the rocket. The 4600-liter fuel tank weighs 76 kg; it holds 3900 kg of fuel. The oxidizer tank has a capacity of 4470 liters and weighs 120 kg; 4900 kg of oxidizer are pumped into it.

The engine, which weighs 930 kg, is mounted inside the tail section of the missile.

The engine (see Fig. 1.2) develops a surface thrust of 25-26 tons for 60-70 sec and consumes about 125 kg of fuel per second during this process. The basic elements of the engine are the welded pear-shaped combustion chamber (see Fig. 1.3), and the turbopump set and gas generator of the fuel-supply system. The gas mixture developed in the gas generator from 80%-by-weight hydrogen peroxide with the aid of a liquid catalyst (sodium permanganate) is used to drive the turbine of the pump set. The greatest outside diameter of the engine's chamber is 1190 mm, and it is 2020 mm long. The chamber weighs 422 kg.

Figure 1.4 shows an A-4 missile at takeoff.

During the Second World War, nitric-acid reaction engines were



Fig. 1.2. External appearance of A-4 rocket engine without fuel tanks.

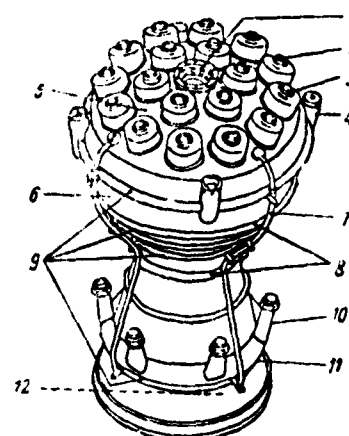


Fig. 1.3. External appearance of chamber of A-4 engine. 1) Flange for attachment of main alcohol valve; 2) oxygen nozzle; 3) pre-combustion chamber; 4) mounts; 5) chamber head; 6) combustion chamber; 7) cooling-system pipeline; 8) corrugations to offset thermal expansion of chamber outer shell; 9) rings for alcohol supply to chamber; 10) connecting pieces for delivery of ethyl alcohol into space between tanks; 11) fuel-collector ring; 12) boundary of cooled section of nozzle.

about 190-200 kg of thrust/(kg of fuel/sec).

The S-2 liquid-fueled engine of the "Wasserfall" radio-controlled antiaircraft missile, which developed a surface thrust of 8 tons (Fig. 1.5) can serve as an example of a nitric-acid engine.

This missile was also developed in Germany and reached the flight-testing stage during the Second World War. In external appearance, it resembles the A-4 missile, but it is considerably simpler and has smaller over-all dimensions. Its most significant departure from the A-4 consists in the fact that it is equipped with four small, broad wings. It was the largest of all the guided antiaircraft missiles de-



Fig. 1.4. Launching of A-4 missile.

veloped during this period of time for defense against enemy aircraft flying as high as 20 kilometers. Its body had a maximum diameter of 880 mm and a length of 7835 mm, its wing span was 1875 mm, and its tailfin span was 2510 mm.

The missile's warhead weighed 145 kg, of which 125 kg was explosive. The total blastoff weight of the rocket was 3245 kg.

This rocket's engine consists basically of an elliptical combustion chamber and the gas-bottle fuel-supply system. The combustion chamber (welded from sheet steel and integral with the nozzle) has a flat removable head with sprayers for the fuel components. The chamber is cooled by the oxidizer.

The engine is powered by components that ignite spontaneously on mixing: Tonka-841 compound (fuel) and M-10 compound (oxidizer). Compound 841 consists of 12% Optol, 20% benzene, 15% xylene, 30% of vinyl-ethyl ether, and 23% of aniline, while the M-10 compound consists of 90% of 98%-by-weight nitric acid and 10% of 96% sulfuric acid. One tank holds 335 kg of fuel and the other 1480 kg of oxidizer.

The components are fed into the combustion chamber of the engine under a pressure of 25 atmospheres, with the combustion chamber at 22.5 atmospheres. The compressed-nitrogen pressure in the tanks of the fuel-supply system is 300 atmospheres. The engine operates for 43 sec. The chamber weighs 43 kg, and the dry weight of the entire engine is 150 kg.

Work on the design of this engine was begun in the middle of 1941, and its first phase was completed in 1943. About 20 trial launchings

of the missile had been carried out during this same span of time. The results of flight tests with the missile indicated the necessity of further work on it.

Series-production and experimental models of liquid-fueled rocket engines were designed and built during the Second World War for use in aerial torpedos and aircraft; these included "cold-type" hydrogen-peroxide engines.

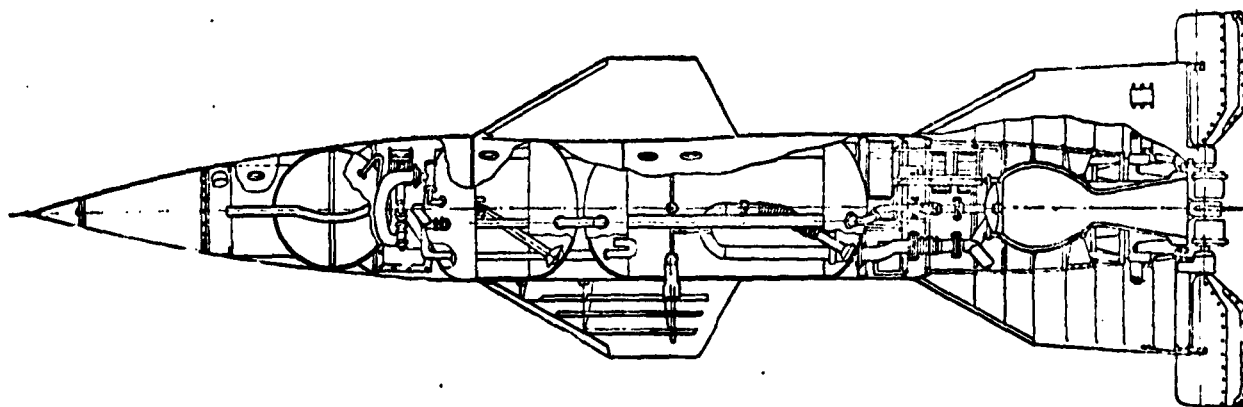


Fig. 1.5. "Wasserfall" liquid-fueled missile.



Fig. 1.6. Walther hydrogen-peroxide aerial-torpedo ZhRD with thrust of 550-590 kg. 1) Hydrogen-peroxide tank; 2) engine mount; 3) air bottles; 4) sodium-permanganate tank; 5) mixing chamber.

The hydrogen-peroxide engines of this type which were constructed in this period of time and somewhat later developed small specific thrusts [about 100-110 kg of thrust/(kg of fuel/sec)], and were therefore not developed and used further.

The Type 109-507 aerial-torpedo ZhRD (Walther), which develops a thrust of 550-590 kg for 10-13 sec (Fig. 1.6) may serve as an example of the hydrogen-peroxide engine.

The 80% hydrogen peroxide used as a fuel in this engine is decomposed by a liquid catalyst (23%-by-weight sodium permanganate). The working components are fed into the reaction chamber by compressed air. The initial air pressure in the bottle is 150 atmospheres, and the working components are delivered at a pressure of 30-35 atmospheres. The reaction-chamber pressure is 22 atmospheres, and the temperature of the vapor gas formed in it reaches 420-440°C.

The engine can work until the hydrogen-peroxide supply in its tank is fully exhausted.

The cowling length of the engine is 2210 mm, and its largest diameter is 330 mm. Its dry weight is 17.5 kg, and when supplied with the working substances (hydrogen peroxide, aqueous solution of sodium permanganate, and compressed air), the engine weighs 143 kg.

All of the hydrogen-peroxide engine types developed in Germany by the firm Walther were used by the Germans during the Second World War as main and auxiliary engines for aircraft, aerial torpedos, and submarine torpedos.

However, despite the fact that hydrogen peroxide has no advantages over nitric acid, hydrogen-peroxide engines were used on a broader scale during the Second World War than nitric-acid engines. This is accounted for by the fact that they were brought to the operational state earlier.

The mastery of hydrogen-peroxide engines developing large absolute thrusts was paralleled by research in a number of countries toward the creation of oxygen-, nitric-acid-, and other engine types for high-powered long-range rocket missiles and antiaircraft-defense

missiles.

The postwar development of reaction-engine technique required the creation of ZhRD developing large thrusts with minimal specific weights and specific fuel consumptions.

Solution of this problem required taking the course of increasing combustion-chamber dimensions, forcing the fuel-combustion process in it to increased pressures and temperatures, increasing the engine's fuel-consumption rate and per-liter thrust, and using more efficient fuels.

At the present time, the development of ZhRD is moving toward perfection of the designs of individual modifications and development of new high-thrust engine designs to use high-efficiency fuels and develop high specific thrusts. The combustion temperatures of some of these fuels may reach 4000°C , and the gas-discharge velocity through the nozzle may run as high as 3000-4000 m/sec.*

The fuels in use at the present time include Tonka-250,** kerosene, ethyl alcohol diluted with water, etc.; aniline, Diesel fuel, furfuryl alcohol, etc. are in use abroad.

The following fuels are receiving a great deal of attention at the present time: hydrazine and fuels based on it (methyl hydrazine, dimethyl hydrazine), diethylamine, fuel mixtures based on kerosene and pyrolysis oil, etc. Liquid fluorine, oxygen fluoride, ozone-enriched oxygen, etc. are of great interest as oxidizers.

At the present stage in their development, long-range missiles require:

1) a sharp increase in the absolute thrust of the engines up to several hundred tons for a single unit;

*Ekspress-informatsiya AN SSSR, No. 8, RT-22, 1958.
**G. Mebus [sic], Raschet raketnykh dvigateley (Design of Rocket Engines), IL (Foreign Literature Press), 1959.

- 2) an increase in the specific thrust of the engines up to many tens of tons per unit;
- 3) a further reduction of engine weight per unit of thrust developed;
- 4) the creation of multiple-chamber engines with automatic operation of all units.

As science develops the field of liquid-fueled rocket engines, increasing amounts of attention are being concentrated on such problems as the reliability of the designs, simplicity of control, etc.

Great difficulties are encountered in the development of high-power engines. The inordinate intensity of the combustion process in the engine chamber, the high gas velocities, pressures, and temperatures, which are considerably higher than any values hitherto attained in chemically fueled machines, the enormous per-second fuel flow rate, which requires servicing by feeder units developing several tens of thousands of horsepower, the power of the engine itself, which may run to tens of millions of horsepower — all this renders particularly acute the problems of chamber cooling, making the chambers explosion-proof, starting the engine and controlling its operation, perfection of the TNA* and methods of supplying its turbine, the development of new high-efficiency fuels, high-strength welding steels, and many other extremely complex problems.

The most complex problem encountered in designing high-thrust engines is that of ensuring stable operating modes. This is due to the fact that difficulties are encountered with large engines of the A-4 type in connection with the necessity of making the inner chamber shell quite thick (over 5 mm). During operation, large temperature

*[THA = TNA = Turbo-Nasosnyy Agregat = Turbopump set.]

gradients arise in this shell, with the resulting complex distribution of thermal stresses across its thickness, the latter reducing its strength margin considerably because of the difficulty of arranging suitable cooling for such a thick shell, which has a large coefficient of thermal conductivity (materials possessing high thermal-conductivity coefficients frequently have relatively low strengths).

In a number of cases, this effect is further complicated by elastic instability of the shell as a result of the high pressure exerted on it by the cooling fluid and the thrust from the nozzle end. Moreover, high-thrust engines have large nozzles, which make up the basic part of the engine chamber's weight. And the use of monobloc engine designs involves great difficulty in synchronizing and controlling the operation of the block.

The development of high-thrust oxygen engines for SDD* is being paralleled in many countries by work on the creation of nitric-acid engines for these purposes (ZhRD "Erlikon" [sic] 54).

The development of high-powered liquid-fueled rocket engines has been accompanied by problems of controlling them, foremost among which are:

- 1) maintaining thrust and chamber pressure constant or varying them in accordance with a specified program;
- 2) maintaining the specified proportions between the fuel components, i.e., the weight ratio of oxidizer to fuel;
- 3) maintenance of dynamic stability in the fuel-supply system and the fuel-combustion process in the engine chamber;
- 4) programming the pressure variation in the combustion chamber and the proportions between the fuel components during static testing

*[СДЛ = SDD = Snaryad Dal'nego Deystviya = Long-Range Missile.]

of the engine;

5) compensation of periodic or constant errors stemming from tolerances in production of the engine.

Regulation of the fuel-component proportions during the engine's operation is necessary for maintenance of optimum specific thrust, which prolongs the engine's operation time and reduces the final mass of the missile, thereby increasing its range.

For ballistic missiles, the thrust must either be varied in accordance with a specified program dictated by the acceleration permissible or held constant. The latter case occurs only in the absence of aerodynamic drag and may therefore be used in the last stages of multiple-stage missiles. In other cases, optimum programming of the thrust value is required for attainment of maximum terminal velocity. This also applies to winged missiles.

One important problem encountered even when automatic-control systems are used, is that of ensuring dynamic stability of the fuel-combustion process in the chamber — a process strongly influenced by the time delay and nonlinearity of the combustion process, the rigidity of the design, including the fuel tanks and lines, the compressibility of the fuel components, and aerodynamic forces in addition to the shape of the chamber and its head and the chemical and physical properties of the fuel components used. Despite the availability of a number of studies devoted to theoretical investigation of this problem, the struggle with high- and low-frequency gas-pressure fluctuations in the combustion chamber is still being carried on by empirical methods.

Liquid-fueled rocket engines developing thrusts measured in hundreds of tons* were required in connection with the development of cosmic and super-long-range missiles in recent years, as well as mis-

*Interavia, No. 4038, 1958.

siles used in launching large Earth satellites. Nuclear energy will obviously come into use in the future for high-thrust engines.

Chapter II

GENERAL ZhRD CHARACTERISTICS

The basic element of liquid-fueled long-range, antiaircraft, and other rocket missiles is their engine — the ZhRD. The range of the missiles, other things being equal, depends to a large measure on the perfection of the engine's design, the type of fuel components used in it, and also its design and operational characteristics.

To evaluate the operational properties of existing types of ZhRD and to choose an engine as required by the tactical and technical conditions, at first one must become acquainted with some concepts, definitions, basic data and characteristics of the ZhRD.

In this chapter, the classification of existing ZhRD is stated, and their general characteristics are shown, permitting the ascertainment of their virtues and shortcomings, comparison of their qualities, and establishment of expedient fields of application for this or some other type of engine. Tables of the numerical values of basic parameters and brief data concerning the design particulars of existing ZhRD are included. Analyses of the basic factors affecting range and of the requirements for weapon engines are also shown. At the same time, other problems concerning the theory and bases of designing ZhRD are also considered.

SECTION 1. BASIC ZhRD DESIGN ELEMENTS

A heat engine is referred to as a reaction engine if it develops

thrust because of the resultant of gasdynamic forces on the engine combustion chamber (as fuel is spent) and because of the discharge of the products of combustion through the nozzle into the atmosphere.

A reaction engine using liquid fuel for its operation is called a liquid-fueled rocket engine.

The basic design elements of a ZhRD are generally as follows.

1. The engine chamber, in which fuel combustion is accomplished and the heat energy of the gases is changed to kinetic energy in the outflowing stream, as a result of which thrust is developed.

The engine chamber consists of a head, combustion chamber, and nozzle. The head of the engine chamber serves for atomization of the fuel components, which are fed into the combustion chamber in a fixed weight relationship.

Spontaneous blending, heating, evaporation and combustion of the fuel occurs in the combustion chamber of the engine.

In the engine chamber nozzle, as the products of fuel combustion flow out into the surrounding medium, their heat energy is changed into kinetic energy. These processes have an enormous influence on the economy of operation and thrust characteristics of the engine.

The processes in the combustion chamber and in the engine nozzle are closely related to each other. The amount of chemical energy which may be liberated in the nozzle as the result of fuel combustion and recombination of gas molecules depends on the stage of completeness of the process of combustion in the combustion chamber.

2. The engine propellant-feed system, ordinarily consisting of one, two, or several fuel tanks, a mechanism for forced delivery of the fuel components to the engine chamber, a source of energy for starting this mechanism, communication systems and fittings (pipelines, valves, vents, flow-meter washers, and the like), which, in totality, provide

for normal launching, operating regime, and stopping of the engine.

In some cases, the fuel tanks are not included among the engine elements, but are part of the vehicle.

The engine may have such fuel-feed systems and controls as to permit it to be started and stopped if necessary.

3. The engine ignition system, which is a device for igniting the fuel when the ZhRD is launched.

In some types of ZhRD, the ignition system is not structurally connected with the engine chamber, and sometimes is even entirely lacking, if self-igniting fuel components are used.

4. The engine thrust frame, or other means of fastening engine assemblies to one another, and transmitting thrust to the weapon.

There are autonomous or on-board methods of feeding the engine units with compressed gases. For autonomous feeding, sometimes an air flask with a self-contained unit of reducers, pipelines, fittings, and valves which are necessary to create a pressure head in the fuel tanks and for other purposes, is used.

The rigid requirements demanded of an engine because of the great concentration of energy in the fuels used, the complexity of the physicochemical processes proceeding in it, and safety requirements during operation have led to the fact that contemporary ZhRD, in many cases, are, in their design relationships, extremely complex thrust frames with a highly developed automatic control system.

The aspiration for maximum automation of the engine's operation can be explained by the fundamental features of the ZhRD. In these engines, within a short period of time, it is necessary to carry out all operations which are required for dependable fuel ignition, increasing its delivery to the combustion chamber up to nominal value, maintaining this rate of flow constant or changing it in accordance with the

programmed operation of the engine, and, finally, stopping the engine at the proper instant.

One must not forget that the fuel which is fed into the combustion chamber is an explosive fuel mixture. Considering the great expenditure of fuel per second in the engine, it is clear that the smallest disruption of the regularity of operation of the feed system or delay at the instant of ignition of the fuel may lead to its concentration in the combustion chamber and, consequently, to a sudden ignition with a sharp rise of pressure in the combustion chamber to a great quantity, and even, as a consequence of this, to explosion of the engine. The same thing may occur when fuel combustion is accidentally interrupted or a fuel is again fed into the hot combustion chamber after the engine is stopped. In this case, the ignition of the fuel by the hot surface of the chamber also may lead to explosion of the engine.

From what has been said it is clear that the fuel-feed system has to function without fail. In practice, this is attained by automation and the blocking of the engine fuel-feed system. By an automatic blocking system one understands the creation of such conditions as to prevent the following operation to be performed in an engine feed system from being carried out until such time as the previous operation has been accomplished.

The automation of the fuel-feed system in contemporary ZhRD is being carried to such a degree of perfection that all operations in launching, placing the engine on the chosen operating mode, and stopping it are carried out by delivering only one command to the engine.

Such a high level of ZhRD automation is also necessary because of the fact that they are usually installed in pilotless aircraft.

The missile's purpose determines its type of engine, thrust, and

operation time, which in turn influences chamber dimensions, fuel-tank volume, and choice of fuel components.

SECTION 2. CLASSIFICATIONS OF EXISTING ZhRD

Existing liquid-fueled rocket engines are extremely diversified in their designs, operating characteristics, and other features. This is explained:

- 1) by the great diversity of fuels used in them;
- 2) by the purpose of this or that type of engine, which determines the magnitude of its thrust, program, and operation time;
- 3) by the features of the process involved in converting the chemical energy of the fuel, in the engine, into the kinetic energy of the gas stream, from the nozzle outlet to the surrounding medium;
- 4) by economic, production, and similar considerations, as well as by the features encountered in engine development trends at various design bureaus.

The field of application and the type of fuel used have the greatest influence on the design of a ZhRD.

To elucidate the virtues and shortcomings of these or those types and designs of engines, to establish expedient fields of application for them, and to study their design and operational details, it is expedient to divide existing ZhRD according to the following most characteristic features.

1. According to engine designation:
 - a) sustainer or basic, when each engine is basic in the given vehicle and operates during the entire flight or its greater part;
 - b) booster, used to facilitate launching of a weapon which has a sustaining engine;

c) verniers, used in a weapon during flight in addition to the basic engine for the purpose of providing a short increase in thrust and speed to the weapon.

Liquid-fueled rocket verniers are often used in aviation; they often have pump-fed fuel systems with mechanical drive from the main engine of the aircraft. The verniers may be started many times during the aircraft's flight.

Besides this, ZhRD may be intended for one-time (one-shot) operation, that is, for use during only one flight after installation in the vehicle, or multi-time (multi-shot) operation, that is, for use in several flights.

2. According to the type of fuel used, ZhRD are divided into engines operating with hypergolic and nonhypergolic fuel components. The various properties of fuels impose specific features on the design of the engine.

The selection of liquid-fuel components for a given engine is generally based on the methods of application, availability of components, characteristics, properties, and similar factors.

ZhRD fuels may be monopropellant, when only one liquid fuel component (isopropyl nitrate, nitromethane, hydrazine, and others) is used, and bipropellant, when two liquid fuel components — the fuel and oxidizer — are used. Tripropellant fuels also exist.

At the present time, bipropellant engines are most widely used.

3. According to the type of oxidizer used for the fuel, engines are divided into:

a) oxygen, using liquid oxygen or its allotropic modifications and compounds with the fuel elements as an oxidizer;

b) nitric acid, using, as the oxidizer, nitric acid and oxidizers which are derivatives of the nitric acid or which contain nitric acid;

c) hydrogen peroxide, using hydrogen peroxide with a liquid or solid catalyst;

d) fluoride, using fluorine, fluorides of oxygen, and other fluorine-containing compounds as oxidizers;

e) chlorine, using chlorine, oxides of chlorine, or other oxidizers containing oxides of chlorine or their derivatives.

Complex oxidizers, containing, in various combinations, molecules of oxygen, nitrogen, chlorine, and fluorine, as well as solutions of several oxides, acids, and other components in each other are also known.*

Engines which operate on suspensions of metals and metalloids, with liquid fuels, are also possible.**

The classification of engines according to the type of oxidizer used is most essential, since differences in oxidizer properties determine the design shape of the engines. There is no engine which can operate with several different oxidizers.

Every engine is developed for a previously determined oxidizer, and, as a rule, the design of one engine differs from the design of another because of the differences in the properties of the oxidizers used. The development of a ZhRD always begins with the choice of oxidizer and fuel for the engine.

4. According to the method of propellant feed to the combustion chamber, ZhRD are divided into the following classes:

a) with a pressure-fed system of fuel feed by means of:

— gas pressure generators (GAD),*** that is, the pressure of a

*Ekspress-informatsiya AN SSSR, No. 21, RT-60, 1959.

**Voprosy raketnoy tekhniki (Problems of rocket engineering), No. 12, IL, 1959.

***[ГАП = GAD = Gazovoy Akkumulyator Davleniya = Gas Pressure Generator.]

cold gas, ordinarily air (VAD),* fed to the fuel tanks from a special flask;

- solid propellant hot gas generator (PAD),** that is, the pressure of the hot powder gases, which form during the operation of the engine in a special chamber by the ignition of a powder charge;

- liquid gas pressure generator (ZhAD),*** that is, the pressure of the hot combustion products of self-igniting fuel components, formed during the operation of the engine in one general or in two special separate chambers (gas generators), installed on the upper end plates of the fuel tanks;

b) with a pump-fed system of fuel feed by means of:

- turbopump unit, that is, with delivery of fuel components from the tanks to the engine's combustion chamber by centrifugal pumps, which are started by a gas-vapor turbine, fed with gas vapor produced in a special gas generator from hydrogen peroxide, isopropyl nitrate, or hydrazine, from ignition of the basic fuel components, or from gas obtained from the engine combustion chamber;

- injectors, whose operation is based on the principle of using the kinetic energy developed by a gas when it expands in a special nozzle (the gas required for injector operation is obtained from the combustion chamber or produced in a special gas-vapor generator).

A pump-fed propellant-feed system with a gas-pressure generator (GAD) is often called a pressurized fuel-feed system.

5. According to the heat load, ZhRD are:

*[BAI = VAD = Vozdushnyy Akkumulyator Davleniya = Compressed Air Flask.]

**[PAI = PAD = Porokhovoy Akkumulyator Davleniya = Powder (Solid-Propellant) Pressure Generator.]

***[ZAI = ZhAD = Zhidkostnyy Akkumulyator Davleniya = Liquid-Fueled Pressure Generator.]

a) of the "hot" type, in which the fuel burns at a high temperature (about 2700-3600°C), and

b) of the "cold" type, in which decomposition of hydrogen peroxide occurs at a comparatively low temperature (about 320-480°C).

6. According to the method of cooling the chamber, ZhRD are divided into engines having:

a) regenerative cooling, which involves the fact, that one of the fuel components (or sometimes both components), before arriving in the combustion chamber, pass through the interliner space of the chamber, and thus cools the inner liner of the nozzle and the combustion chamber;

b) sweat cooling, in which the coolant flows from the interliner space into the chamber through small pores in the inner liner which is made of a special porous material; thus the chamber wall is cooled and, simultaneously, a vaporized gas film is formed on the inner surface, protecting the liner from excessive heating by hot gases; gases;

c) flowing water cooling, ordinarily used in test stands.

It is also possible to cool engine chambers by circulating water, which is at the same time the working fluid for the turbine of the pump unit of the engine propellant feed system (closed-cycle regenerative engine cooling).

The heat release rate of the combustion chamber and nozzle have a basic influence on the choice of the appropriate method of engine cooling.

At the present time, the regenerative method of cooling is the most widespread, since it is most dependable and economical. In this case, the heat which is transferred from the inner liner to the coolant is returned to the combustion chamber.

For regenerative engine cooling, the fuel component which has the least corrosive properties, the highest values of heat capacity, thermal conductivity, and other characteristics useful for this purpose is ordinarily used. The oxidizer is ordinarily used for cooling the chambers of small-thrust engines, since the fuel in these is insufficient for dependable cooling.

7. According to the method of protecting the inner liner of the chamber from overheating (with regenerative cooling), ZhRD may be divided into engines:

a) with a gas fuel curtain, created on the head side of the chamber through peripheral low-capacity spray nozzles;

b) with film fuel curtains, created in the most intensely heated parts of the engine chamber; the fuel is fed to the inner liner surface through special apertures or slits in it, by which means the liquid flows along this surface in the direction of the gas stream; it is gradually heated and vaporized, and thus protects the liner against excessive heating;

c) with insulation of the liner gas surface against heat of the gas flow (ceramics, graphite, metallic oxides, and other substances may serve as insulators).

Protection of the chamber liner against overheating by a gas or film fuel curtain, like the sweating method of cooling, is ordinarily applied in those cases when, as a consequence of the high heat release rate in the engine chamber, it cannot be cooled by the most simple and economical manner, or when the use of the latter is accompanied with great difficulties under the particular conditions.

The coolant duct of a ZhRD chamber may be slotted, spiral, spiral slotted, and of other shapes.

The ring-shaped coolant duct is the simplest and cheapest from a

design viewpoint.

There are single-liner and double-liner chambers. Engines of the "cold" type and uncooled engines of the "hot" type which are intended for operation for not longer than 5-15 seconds have single-liner chambers. Cooled engines of the "hot" type with a relatively long operating period have double-liner chambers.

The engine chamber cooling system must permit the coolant to remove local heat flows, which have maximum value near the critical nozzle section, from the inner chamber liner with permissible heating of this fluid in the duct.

8. According to the number of combustion chambers, engines are divided into:

a) monochambered, that is, having only one combustion chamber in their design, and

b) multichambered, that is, having in their design several combustion chambers, capable of operating, as desired, either simultaneously or separately for the purpose of changing the magnitude of the engine's thrust.

ZhRD chambers are fabricated of steel, copper and steel, aluminum, ceramics and steel, and from other materials.

There are cylindrical, conically tapering, elliptical, pear-shaped, spherical, and other shapes of ZhRD combustion chambers.

The type of fuel used, method of atomization, pressure in the combustion chamber, magnitude of thrust and operation time of the engine, technology of its manufacture, cost, and other factors influence the selection of an expedient shape for an engine combustion chamber.

The outlet portion of a ZhRD chamber nozzle is constructed either:

a) conical (the flare angle of the outlet section of

the nozzle usually varies from 25 to 35°) or

b) shaped (to obtain a flow of gases which is axial, or close to it, in the outlet section of the nozzle).

Nozzle-section height may be controlled or noncontrolled.

9. According to the method of atomizing fuel components, there are ZhRD chambers:

a) with jet atomization (resembling the "Wasserfall" guided anti-aircraft missile's engine);

b) with flat-spray atomization (resembling the "Rheintochter" anti-aircraft missile's engine);

c) with centrifugal atomization;

d) with prechamber atomization (resembling the A-4 engine).

Both monocomponent and bicomponent centrifugal nozzles are made.

In construction, welded and detachable chamber heads have flat, tent-shaped, spherical, and other shapes. In a combustion chamber of spherical shape, that part in which the fuel-atomizing devices are located is called the head.

10. According to the method of igniting the basic fuel components in launching, ZhRD are divided into engines:

a) with chemical ignition, that is, by means of fuel components, basic or launching, which are self-igniting upon contact;

b) with electrical ignition, that is, by means of electrical devices (electric spark plugs or arcs);

c) with pyrotechnical ignition, that is, by means of a pyroelectric cartridge (a flame formed by the burning of a propellant grain).

11. According to the magnitude of nominal thrust, one may conventionally divide ZhRD into engines:

a) of small thrust (of the order of 0.5-5 tons), intended for aerial torpedos of various purposes, small antiaircraft missiles,

launching engines, and for main engines for aircraft;

b) of medium thrust (of the order of 5-25 tons), intended for large antiaircraft missiles and aircraft, small long-range missiles, high-performance and super-hypersonic fighter, interceptor, and reconnaissance aircraft, and

c) of high thrust (over 25 tons), intended for large and extra long-range missiles.

ZhRD are produced to provide both for controlled and noncontrolled thrust during engine operation.

Control of the magnitude of thrust of a ZhRD is accomplished:

a) by changing the fuel rate of flow per second in the combustion chamber by means of changing feed pressure and

b) switching on or switching off part of the fuel nozzles, or separate chambers (if the engine is multichambered).

If the fuel tanks are among the engine elements, ZhRD differ as follows:

a) with sequential tank arrangement (one tank arranged behind the other, along one axis);

b) with concentric tank arrangement (one tank placed inside the other).

Fuel tanks may also be subdivided as follows:

a) airframe, which are both missile body and load carrier, and nonairframe, which are placed in the missile body and carry only the static load of the working components which are located in them;

b) relieved of working gas pressure (with turbopump fuel delivery) and loaded with working gas pressure (with a pressure-fed fuel feed system with a VAD, PAD, or ZhAD);

c) "cold," intended for liquid oxygen; hot, from which a fuel component is injected by a hot gas, and normal, from which a fuel component

is injected into the combustion chamber by a cold gas.

12. According to the engine's connection with the weapon, ZhRD may be distinguished as follows:

- a) constructions which are independent of the weapon (the engine is suspended from the weapon or installed in it);
- b) constructions, which are part of the weapon (the engines of antiaircraft, short-range, and long-range missiles).

SECTION 3. BASIC ZhRD PARAMETERS

The basic parameters characterizing the flight and operational properties of a ZhRD of any type and design are as follows.

1. Absolute or total thrust, developed by the engine in operation at a rated operating regime, P_{Σ} (kg, ton).

The absolute thrust of the engine chamber, relative to the volume of the combustion chamber V_k ,* is called volumetric thrust:

$$P_{\underline{1}} = P/V_k \text{ kg thrust/liter.**} \quad (2.1)$$

2. Specific engine thrust, that is, the thrust relative to the sum of the fuel rate of flow per second in the engine:

$$P_{ud\Sigma} = P_{\Sigma}/G_{\Sigma} \frac{\text{kg thrust}}{\text{kg fuel/sec}} \quad (2.2)$$

or

$$P'_{ud} = \gamma_t P_{ud} \frac{\text{kg thrust}}{\text{liter fuel/sec}},$$

where P_{Σ} is the sum of the engine thrust in kg; G_{Σ} is the total rate of fuel flow in the engine, consisting, in the aggregate, of rate of fuel flow G_s in the combustion chamber, and G'_s in the gas generator of the fuel supply system, and the rate of fuel flow G_{zav} *** in forming the protective curtain around the surface of the burner liner,

*[$V_k = V_k = V_{kamera} = V_{chamber}$.]

**[$P_{\underline{1}} = P_{\underline{1}} = P_{litrovaya} = P_{volumetric}$.]

***[$G_{zav} = G_{zav} = G_{zaves} = G_{curtain}$.]

in kg/sec; γ_t^* is specific gravity of the fuel in kg/liter; P_{ud}^{**} is specific chamber thrust.

In existing ZhRD, it is possible to determine specific thrust from the thrust value and the rates of fuel flow into the combustion chamber, obtained by test-stand measurements.

Absolute thrust is not characteristic of the degree of perfection in ZhRD operation. An operational characteristic of an engine's operation is its specific thrust, sometimes called the specific impulse.

The greater the engine's specific thrust, the less the consumption of fuel per second will be at a given quantity of absolute thrust, and, consequently, the smaller the required supply of fuel in the tanks will be for any given period of operation, dimensions, and weight of the engine.

The greater the specific thrust of a ZhRD in operation on a given fuel, other things being equal, the better established the operating cycle in the engine and the more perfect the engine from a design viewpoint.

Absolute and specific engine-chamber thrust are constant quantities, with a given regime, for operations in space.

The required thrust of a ZhRD is determined in the design of the given weapon (depending on range, quantity of payload, and other factors).

3. The specific fuel consumption in the engine, that is, fuel consumption referred to a unit of engine thrust per second or per hour:

$$C_{ud} = \frac{1}{P_{ud}} \frac{\text{kg fuel/sec}}{\text{kg thrust}} = \frac{1}{P_{ud}} 3600 \frac{\text{kg fuel/hour}}{\text{kg thrust}}. *** \quad (2.3)$$

$$*[\gamma_T = \gamma_t = \gamma_{\text{toplivo}} = \gamma_{\text{fuel}}.]$$

$$**[P_{yd} = P_{ud} = P_{\text{udel'nyy}} = P_{\text{specific}}.]$$

$$***[C_{yd} = C_{ud} = C_{\text{udel'nyy}} = C_{\text{specific}}.]$$

The specific fuel consumption, equally with the specific thrust, is an important operating characteristic of the engine, since the greater its value, other conditions being equal, the greater the range and operating period of a weapon will be with the given engine.

The quantity C_{ud} depends on the pressure in the combustion chamber, the type of fuel used, and the establishment of the operating cycle in the engine chamber.

4. The specific weight of the engine, that is, the weight, referred to unit of engine thrust:

$$\gamma_{dv} = G_{dv}/P_{\Sigma} \text{ kg/kg thrust,*} \quad (2.4)$$

where G_{dv} is the dry weight of the engine in kg, and γ_{dv} is the specific weight of the engine.

By the dry weight of the engine is meant the weight of its entire structure when the tanks are not filled with operating components (fuel, gas, and the like).

At a given magnitude of absolute thrust, specific weight determines the total dry weight of the engine, which affects the weapon's characteristics to a considerable measure.

5. The engine's frontal thrust, that is, the thrust relative to 1 cm² of the greatest cross-section of the engine:

$$P_{lob} = P_{\Sigma}/F_{dv} \text{ kg thrust/cm}^2,** \quad (2.5)$$

where F_{dv} is the greatest area of cross-section of the engine in cm².

The specific frontal thrust is very important when evaluating the aerodynamic qualities of the engine, since the greater its value at a given thrust, the less the greatest cross-section of the weapon may be

*[$\gamma_{dv} = \gamma_{dv} = \gamma_{dvigatel'} = \gamma_{engine}$;
 $G_{dv} = G_{dv} = G_{dvigatel'} = G_{engine}$.]
 **[$P_{lob} = P_{lob} = P_{lobovaya} = P_{frontal}$;
 $F_{dv} = F_{dv} = F_{dvigatel'} = F_{engine}$.]

with this engine. Existing engines have a $P_{lob} = 1-4 \text{ kg thrust/cm}^2$.

To parameters characterizing the engine we should add the effective efficiency, i.e., a relationship between fuel components χ , combustion-chamber volume V_k , and chamber pressure p_k .*

Ordinarily, the initial parameters of a ZhRD are given as its relative parameters in operation in a rated operating regime, reduced to standard atmospheric conditions.

Under the conditions mentioned, existing missile ZhRD (the "Vanguard" missile and others) have $P_{ud} \approx 200-240 \frac{\text{kg thrust}}{\text{kg fuel/sec}}$; $C_{ud} \approx 15-18 \frac{\text{kg fuel/hour}}{\text{kg thrust}} = 4.0-5.0 \frac{\text{kg fuel/sec}}{\text{tons, thrust}}$; $\gamma_{dv} = 10-40 \text{ kg/ton thrust}$.

The operation qualities of an engine are its adaptability and dependability of operation, lifetime, simplicity of maintenance, and others.

The engine parameters enumerated above facilitate evaluation of a given type of engine with respect to thrust force, economy of operation, external dimensions, and operational qualities, and determine, in the first approximation, the basic virtues and shortcomings of this or that engine; and establish rational fields for its application.

The basic parameters of an engine, which determine its qualities, depend on design particulars, operation modes of the engine itself, external conditions, and a number of other factors. The effective caloric value of the fuel and the pressure in the combustion chamber and in the nozzle outlet section have a substantial influence on specific thrust, specific fuel consumption, and efficiency of the engine. Therefore, to determine the basic qualities of a projected engine and properly choose its parameters, it is necessary to know the dependence of absolute and specific thrust, and of specific and per-second fuel con-

*[$p_k = p_k = p_{kamera} = p_{chamber}$.]

sumption on flight altitude, pressure in the combustion chamber, and other factors.

SECTION 4. ADVANTAGES AND DISADVANTAGES OF ZhRD

At the present stage of development of reaction engineering, only reaction engines which operate by the chemical energy of decomposition and oxidation of fuel have been realized and are in practical use.

Such engines include reaction engines operating on solid fuel (solid-propellant or PRD*), on liquid fuel in an air atmosphere (VRD**), and the ZhRD, operating on liquid fuel; these engines are, at the present time, experiencing their greatest development and application.

Liquid-fueled rocket engines have the following advantages in comparison to air-breathing reaction motors:

1) they can develop thrust even in an airless space, since their operation does not depend on the surrounding medium (flying altitude is limited only by the supply of fuel in the tanks and the engine's specific thrust);

2) absolute thrust, in contrast to the air-breathing reaction motors, increases with ascent in altitude, and is little dependent on flying speed in the dense layers of the atmosphere;

3) the possibility of concentrating extremely high thrust (up to 1000 tons) in one engine at comparatively small dimensions and specific engine weight (from 0.01 to 0.040 kg/kg of thrust)***;

4) the total weight of the engine is less than the weight of any air-breathing engine of the same power;

5) the convenience of using the engine with a weapon as a result

*[ПРД = PRD = Porokhovoy Raketnyy Dvigatel' = Solid-Propellant Rocket Motor.]

**[БРД = VRD = Vozdushno-Reaktivnyy Dvigatel' = Ram-Jet Engine.]

***Ekspress-informatsiya, AN SSSR, No. 20, ADS-78, 1958.

of the relatively small external dimensions;

6) the possibility of obtaining relatively great speeds and flying altitudes, which are not attainable for a VRD (the A-4 long-range missile has a flying speed of about 1520 m/sec for 5500 km/hr at an altitude of 35-37 km);

7) a special engine is not required for launching.

Like other types of engines, the ZhRD permits the accomplishment of multiple start-ups and regulation of thrust force by changing per-second fuel rate of flow in the combustion chamber.

The basic disadvantages of the ZhRD are:

1) the low economy of operation at low flying speeds (a great specific fuel consumption);

2) the short operating time of the engine, which is governed by the extremely high specific fuel consumption [up to 15-20 (kg of fuel per hour/kg of thrust)];

3) the insignificant operational line of the engine (from 2.5 sec up to 2 hours instead of 50-300 hours for a VRD and 100-350 hours for piston engines);

4) the payload of the weapon is decreased with increase of range by the increase of the supply of fuel in the tanks;

5) the necessity of having a liquid fuel oxidizer in the rocket aircraft, the handling of which is often attended with great difficulties.

The advantages and disadvantages of the ZhRD mentioned above have determined their fields of application.

However, in comparison with engines of other types, these virtues and shortcomings of a given ZhRD may be more fully elucidated only by inspection of the concrete conditions of its operation, such as thrust program, altitude and flying speed, and so forth.

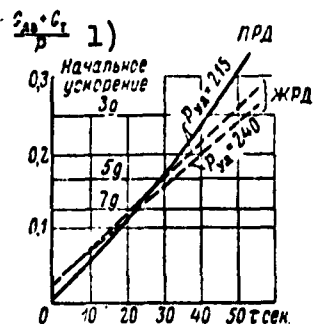


Fig. 2.1. Approximate comparison of weight characteristics (including fuel) of a PRD and ZhRD at various operation times. 1) Initial acceleration.

In some cases (with short operation times, small amount of thrust, or in special fields of application) the solid-propellant rocket engine (PRD) can successfully rival the ZhRD.

Among the virtues of the PRD there are, first of all, simplicity of its construction and method of loading the fuel, constant readiness for operation, reliability in operation, cheapness, less specific weight, less

TABLE 2.1

1) Тип двигателя	Максимально достижимая скорость полета км/час 2)
3) Поршневые	600
4) Турбовинтовые	900
5) Турбореактивные	2000
6) Прямоточные ВРД	6000
7) Пороховые РД	28 000
8) Жидкостные РД	50 000
9) Термоядерные РД	100 000
10) Электрохимические РД	500 000
11) Фотонные РД	300 · 10 ⁶

1) Type of engine; 2) maximum flying speed attained, km/hr; 3) piston; 4) turboprop; 5) turbojet; 6) ram-jet; 7) solid-propellant rocket engine; 8) liquid-propellant rocket engine; 9) nuclear-heated rocket engine; 10) electric-(system) rocket engines; 11) photon rocket engine.

dependence of the construction on the type of weapon, and widespread application in most diverse fields of contemporary engineering. Moreover, the operation of a solid-propellant engine does not depend on the maneuvering of the missile and its acceleration in flight.

Solid fuels (powders) have a somewhat smaller specific impulse

than liquid fuels and are more expensive, but their comparative advantage lies in their greater specific weight. Powders, in comparison with liquid fuels, are more reliable and safe in operation. They can be better stored over extensive periods at any atmospheric temperature, they are not toxic, not aggressive in relation to metals, are ready for use at any moment, do not require any sort of prolonged and complex preparations before use, and so forth.

However, the weight characteristics of solid-propellant engines can be better, in comparison with the ZhRD, only when they are operated for short periods. When the engine operates for more than 20 seconds, the ZhRD has a smaller relationship of engine weight (including fuel as well) to the developed thrust than a PRD. Even with equal specific thrust [$P_{ud} = 215$ (kg of thrust/kg of fuel per second)], the weight characteristics of a PRD may be compared to those of a ZhRD only when time of operation is of the order of 26 sec (Fig. 2.1). When the time of operation is less, the PRD has better weight and thrust characteristics than the ZhRD, since they provide an increased thrust without proportional increase of the weight of the dry construction for a given weight of charge. Moreover, as a consequence of the lower relationship of weight to thrust, the PRD permits the attainment of greater missile accelerations.

Another basic reason for the limited application of solid-propellant rocket missiles in a number of cases is the high cost of powder, the large dimensions of the powder chamber for a considerable time of operation, and the appearance of an unstable, resonant combustion of powder in long chambers of small diameter, when the hot powder gases flow in the chamber with great speeds.

The tentative values of flying speeds attained in practice for

aircraft with different types of engines are shown in Table 2.1.*

SECTION 5. FIELDS OF APPLICATION OF ZhRD

Liquid-fueled rocket engines have extremely extensive fields of application.

At the present time ZhRD are basically used for:

1) guided and nonguided missiles (antiaircraft, short and long range, cosmic, and others);

2) fighter aircraft, as the basic power plant, and bombing aircraft, as a booster engine, intended for short aircraft maneuvers, increasing horizontal and vertical flying speeds, and altitudes.

The ZhRD has a comparatively limited application in meteorological missiles, racing automobiles and motorcycles, and cargo trucks intended for operation on bad country and mountain roads (to facilitate motor-vehicle movement).

Unguided liquid-fueled rocket missiles (NRS**) are chiefly used as a tactical weapon for bombardment at short distances.

Guided liquid-fueled rocket missiles (UZhRS***) basically resemble unguided missiles in their external appearance and are guided during flight by means of special devices. These missiles may be used for strategic targets, as a means of PVO**** and for carrying out scientific studies of outer space. Such missiles have extremely diverse purposes ("ground-ground," "ground-air," "ground-water," "air-air," and others).

Since the direction of flight is corrected by devices in these

*Ekspress-informatsiya, AN SSSR, No. 8, RT-23, 1958.

**[HPC = NRS = Nepravlyaemyy Raketnyy Snaryad = Unguided Rocket Missile.]

***[YKPC = UZhRS = Upravlyaemyy zhidkostnyy raketnyy snaryad = Guided Liquid-Fueled Rocket Missile.]

****[ПВО = PVO = Protivovozdushnaya Oborona = Air Defense.]

missiles, the accuracy of fire in this case considerably exceeds the accuracy of fire of unguided liquid-fueled and solid-propellant rocket missiles.

Flight range and altitude of single-stage UZhRS without booster motors is limited by the difficulties of constructing such missiles with great relationship of weight of dry construction and payload to gross take-off weight of the missile, and the comparatively low effectiveness of the fuels used.

Aircraft with a ZhRD as their main engines, in comparison with aircraft having engines of other types (VMG, TVRD, TRD,* and PRD), have advantages in regard to ceiling, flying speed, and rate of climb.

At the present time, an aircraft with this engine is the only vehicle which can accomplish a flight at exceptionally high altitudes and with very great speeds. However, the great rate of fuel flow per second in a ZhRD limits the range and duration of flight and other important characteristics of the aircraft. Moreover, methods of increasing the range of an aircraft with this engine are not promising. Therefore, it is expedient to use the ZhRD only for aircraft intended for short flights and high altitudes.

Rocket engines have created the possibility of conquering interplanetary space. However, the solution of this problem still requires enormous work along the lines of increasing the efficiency of the engine, using the more effective liquid fuels which are exploited with difficulty, constructing missiles with maximum relative fuel conservation, and with the use of multistage missile plans, etc.

*[BMT = VMG = Vintomotornaya Gruppa = Engine-Propellor Unit;

TBPd = TVRD = Turbovintovyy Reaktivnyy Dvigatel' = Turboprop Engine;

TPd = TRD = Turboreaktivnyy Dvigatel' = Turbojet Engine.]

Atomic reaction engines will be applied without limitations both for flights from the earth and beyond the earth, given the condition that the basic problems connected with their development are satisfactorily solved.

SECTION 6. REQUIREMENTS DEMANDED OF WEAPON ENGINES

Weapon engines demand the following basic requirements:

- 1) compactness and simplicity of construction, and cheapness of mass production and operation;
- 2) automation of operation and reliability of hermetic sealing of fuel-feed equipment;
- 3) small specific weight and dimensions for an engine of given thrust;
- 4) continuous combat readiness for launching within the temperature range of -40 to $+50^{\circ}\text{C}$;
- 5) reliability of launching, operation, and stopping;
- 6) good response — stable thrust increase (for missile engines, the time required to reach an operating regime of 90% nominal thrust must not exceed 1-3 sec, counting from the instant at which the launching pulse is delivered);
- 7) high economy of operation (the greatest possible value of specific thrust);
- 8) the fuel combustion process in the engine chamber must be dynamically stable in a given thrust range, during the weapon's maneuvers and perturbations during flight;
- 9) constancy of developed thrust for the established operating regime;
- 10) possibility of stopping the engine before complete expenditure of the fuel supply in the tanks (if necessary);

11) possibility of prolonged storage of the engine, filled up with fuel, and transporting it by motor or railway transportation (this is especially important for the engines of antiaircraft missiles and aerial torpedos);

12) materials of the engine and its anticorrosive covering must permit its prolonged storage;

13) convenience of assembling the engine and the weapon, and others.

This list of requirements is equally applicable to expendable engines (antiaircraft and long-range guided missiles and others) and multi-shot engines (the aviation type).

Aircraft engines for multi-shot operation, boosters, and launching engines demand the following additional requirements.

a) For multi-shot engines:

1) possibility of starting it at any flight altitude in not more than 3 sec;

2) possibility of not less than 6-7 starts during flight;

3) regulation of thrust within the limits from maximum value to 0.1;

4) control of operation from one control unit;

5) operating life must be not less than 2 hours.

b) For boosters for main engines:

1) possibility of starting at any altitude in not more than 3 sec;

2) possibility of not less than 3-4 starts during flight;

3) regulation of thrust (if necessary) from maximum value to 0.3;

4) operating life of the combustion chamber must be not less than 1 hour.

c) For launching engines:

1) possibility of synchronized starting of several engines operating in parallel;

2) possibility of jettisoning to the earth by parachute after completion of operation.

Blastoff of unguided aircraft and ballistic missiles and transmitting the initial acceleration of flight to them are possible by means of the application of a powder charge in the combustion chamber of the sustaining ZhRD.

The above list of requirements, in general, is entirely complete, and, moreover, it characterizes the operational potentials of engines of various designations rather fully.

In each separate case, an engine may also demand other additional requirements.

In designing nitric-acid engines, it is necessary to consider additionally the extremely high toxicity and corrosive properties of nitric acid, and its continuous vaporization (fuming). The insulation of a nitric-acid engine and tanks in a weapon require a special method, which provides complete insulation of the engine from the other parts of the vehicle. Materials used for engines of this type must be corrosion-resistant to nitric acid.

SECTION 7. FACTORS AFFECTING VELOCITY AND RANGE OF MISSILES WITH ZhRD

Many various factors, of which the following are the most basic, affect a missile's velocity V_{kon}^* at the end of the powered phase and range L :

1) the fuel-weight ratio in the missile:

$$a = G_t / G_0; ** \quad (2.6)$$

*[$V_{kon} = V_{konets} = V_{end}$.]

**[$G_t = G_{topliva} = G_{fuel}$.]

2) the missile's thrust-weight ratio:

$$b = P_0/G_0; \quad (2.7)$$

3) the engine's specific thrust:

$$P_{ud_0} = P_0/G_\Sigma, \quad (2.8)$$

where G_t is the supply of fuel in the missile's tanks before blastoff; G_0 is the total starting (initial) weight of the missile; P_0 is the engine's absolute thrust at missile blastoff; G_Σ is fuel rate of flow per second in the engine;

4) the angle of the missile's flight trajectory at the end of the powered phase relative to the vertical;

5) the aerodynamic shape of the missile, principle of its multiple stage design, and others.

The fuel-weight ratio a for the missile has the greatest effect on V_{kon} and L , but in practice it is limited by the structural features of the missile and the materials used.

In existing antiaircraft missiles $a \sim 0.60-0.65$, and in long-range missiles $a \approx 0.72-80$.

The lower value of the coefficient a in antiaircraft missiles, compared with long-range ballistic missiles, can be explained by the fact that the antiaircraft missiles are more rugged and heavier since they are likely to encounter greater lateral acceleration during flight, and consequently greater loads.

Long-range missiles that are more highly perfected with respect to weight are possible, but at the present time it is possible to attain this only at great cost (by the application of multistage missiles, use of more efficient fuel, etc.).

At given values of P_{ud} and b , the quantities V_{kon} and L are directly proportional to a .

The missile's thrust-weight ratio b has the least influence on

V_{kon} and L relative to \underline{a} and P_{ud} , and, moreover, has limited practical potential. When \underline{b} is increased, flight range, at first, increases swiftly, but when \underline{b} is greater than 10 it remains almost constant. With given values of \underline{a} and P_{ud} , an increase of \underline{b} increases the values of V_{kon} and L in direct proportion to \underline{a} . In practice, even when \underline{a} is equal to 0.80 (a long-range missile), it is expedient to assume a value of \underline{b} greater than 3, since to increase \underline{b} , it is necessary to increase the absolute engine thrust, and, consequently, the dimensions and weight of the engine and missile, which under certain conditions causes the gain due to increased \underline{b} to vanish.

In existing antiaircraft missiles, $b \approx 2.5-6$ and higher, and in long-range missiles, $b \approx 1.8-2.5$.

At a lower thrust-weight ratio, the missile has bad blastoff properties, and at higher thrust-weight ratios, bad weight characteristics, which decreases the effective use of the missile.

The theoretical optimum of the missile's thrust-weight ratio depends basically upon its designation, type, degree of design perfection, and launching method used.

The greater the thrust-weight ratio of the missile, the greater its rate of climb and axial overload. One of the factors determining the upper limit of the missile's thrust-weight ratio is the axial overload permitted by operating conditions and durability of the missile's on-board guidance system devices.

The engine's specific thrust P_{ud} is the second most important factor after the coefficient \underline{a} , in increasing V_{kon} and L (the velocity V_{kon} is proportional in the first stage, and L in the second stage, to the quantity P_{ud}).

With a given value of \underline{b} , the influence of P_{ud} on V_{kon} and L is directly proportional to the factor \underline{a} . However, an increase of P_{ud} re-

TABLE 2.2

1) Увеличение \underline{a} при $P_{ud_0} = 200 \text{ кгсек/кг}$ %	2) Повышение L относительно дальности снаряда А-4 за счет увеличения \underline{a} при $P_{ud_0} = 200 \text{ кгсек/кг}$ $L=350 \text{ км}$ принята за единицу	3) Увеличение P_{ud} для такого же повышения L , как и за счет роста \underline{a} для $\underline{a}=70\%$
70	1	4) $P_{ud_0} = 200 \text{ кгсек/кг}$
85	2,3	350
90	4	350
95	6	400

- 1) Increase in \underline{a} , at $P_{ud_0} = 200 \text{ kg sec/kg}$, %;
- 2) increase in L , relative to range of A-4 missile, due to increase in \underline{a} , at $P_{ud_0} = 200 \text{ kg sec/kg}$, $L = 350 \text{ km}$ is the unit; 3) increase in P_{ud} for the same increase in L , as well as for the increase in \underline{a} , at $\underline{a} = 70\%$; 4) $P_{ud_0} = 200 \text{ kg sec/kg}$.

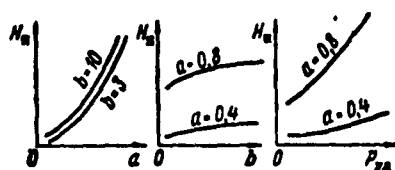


Fig. 2.2. Flight altitude H of missile, as function of values of \underline{a} , \underline{b} , and P_{ud} .

quires raising the pressure in the engine combustion chamber, the use of fuels with higher heating values at high combustion temperatures and, thus a structurally more complex cooling system for both combustion chamber and nozzle; also, other measures are needed, and

these complicate engine design, raising specific weight and cost. It is obvious that in practice the increase of V_{kon} and L will be attained by simultaneous increase of \underline{a} and P_{ud} , as well as in other ways. It is always necessary to try to develop an engine with the greatest P_{ud} and the least specific weight.

In Fig. 2.2, the curves showing flight altitude H_p^* of a long-range missile as functions of the values of \underline{a} , \underline{b} , and P_{ud} are shown, no allowance being made for the resistance of the surrounding medium

$$*[H_{\Pi} = H_p = H_{polet} = H_{flight}.]$$

and the influence of the acceleration of gravity.

In Table 2.2, there are shown data concerning the tentative dependence of L on a and P_{ud} for the A-4 long-range missile, without allowing for the resistance of the surrounding medium and the acceleration of gravity.

The approximate data given in this table indicate that an increase in a rapidly attains its practical limit, since it would almost be impossible to design a single-stage missile in which 90% of the weight would be due to the fuel, i.e., at $a = 90\%$.

The increase in P_{ud} effectively increases L , in practice, within great limits. In addition, it is, in practice, possible to increase P_{ud} to its upper limits, if not restricted by a fixed energy source.

The range of a liquid-fueled rocket missile of any type is determined to a considerable degree by the velocity V_{kon} .

The development of rocket aerospace equipment is determined by the following magnitudes of flight speed at the end of the powered trajectory*:

- a) missiles for hitting bombers and fighters, 1-2 km/sec;
- b) missiles for shooting down intercontinental rockets, about 3-7 km/sec;
- c) long-range missiles ($L = 1000-10,000$ km), about 2-8 km/sec;
- d) pilotless aircraft ($L = 1000-20,000$ km), about 1-6 km/sec;
- e) rocket vehicles for artificial satellites, about 8 kg/sec [sic];
- f) rockets for space flights, about 11.2 kg/sec [sic].

The optimum solution of these requirements depends primarily upon the magnitude of specific thrust attained.

Each of the above-mentioned types of rocket missiles requires different design solutions in the process of development. However, all

*Voprosy raketnoy tekhniki, 1958, No. 5, IL.

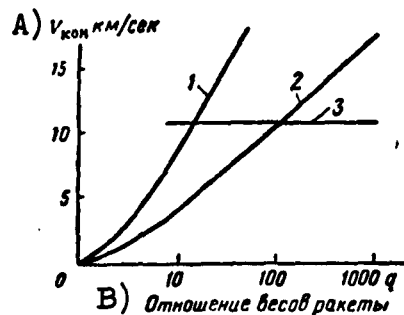


Fig. 2.3. Flight speed of single-stage rocket at end of fuel cutoff, as function of q . 1) $P_{ud} = 300 \text{ kg sec/kg}$; 2) $P_{ud} = 600 \text{ kg sec/kg}$; 3) escape velocity. A) V_{kon} , km/sec; B) rocket-weight ratio.

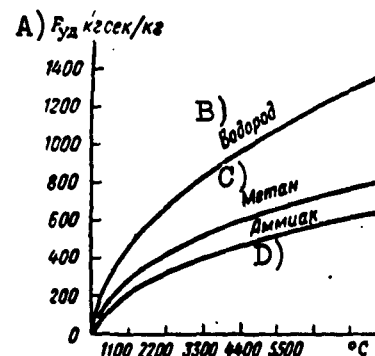


Fig. 2.4. Theoretical specific thrust, dependent on temperature of mass carrier in the reactor of an atomic engine. A) P_{ud} , kgsec/kg; B) hydrogen; C) methane; D) ammonia.

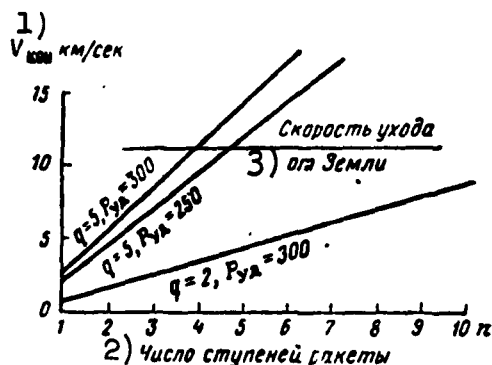


Fig. 2.5. Flight speed at end of fuel cutoff attained by multi-stage rockets having various q and specific thrusts. 1) V_{kon} , km/sec; 2) number of rocket stages; 3) escape velocity.

the problems connected with them may be solved in principle by the use of molecular chemical fuels.

In Fig. 2.3 there are shown the roughly calculated values of attainable flight speeds of a single-stage rocket at the end of fuel cutoff, allowing for atmospheric resistance and the effect of gravity,

as a function of the weight ratio $q = G_0/G_k$,* where G_0 is the takeoff weight of the missile and the fuel, and G_k is the weight of the missile at the end of fuel cutoff.**

The curves shown in this figure indicate that at $P_{ud} = 300$ kg sec/kg, in order to attain the cosmic (11 km/sec) [escape] velocity altitude a single-stage rocket with a clearly unrealistic weight ratio of $q \geq 150$ is required. At $P_{ud} = 600$ kg sec/kg the development of a rocket with a weight ratio of $q = 9$ is conceivable from a practical standpoint (for example, for a flight to the moon).

The theoretical values of P_{ud} depending on reactor temperature of an atomic engine and the properties of its mass carrier (the energy heat carrier) are shown in Fig. 2.4.

Figure 2.5 gives the calculated approximate values of the attainable flight speeds for multistage rockets at the end of fuel burnout.

The curves in this figure indicate that with a weight ratio of $q = 2$ and with $P_{ud} = 300$ kg sec/kg, the "cosmic" flight velocity can be attained only with 12-13-stage rockets. At $q = 5$ and $P_{ud} = 300$ kg sec/kg, three- or four-stage rockets (with ZhRD) are required for space flights.

The principal task in designing and constructing ZhRD is to achieve the highest possible values of pressure and gas temperature in the combustion chamber, compatible with the required chamber strength. The level of perfection of the chamber nozzle, its cooling method, and other factors substantially affect the magnitude of P_{ud} .

Development of an improved missile design requires new design solutions and more improved methods of production of the missile itself as well as the engine.

*[$G_k = G_k = G_{konets} = G_{end}$.]

**Aviation Age, Vol. 28, No. 1, January 1957.

SECTION 8. BASIC PROBLEMS TO BE SOLVED IN PLANNING AND DESIGNING ZhRD

The basic problems which must be solved in planning and designing a liquid-fueled rocket engine for a craft of any designation can generally be broken down as follows.

For a rational choice:

- a) type of fuel, system of its supply and atomization;
- b) basic parameters of the engine, providing for a solution of the problem posed (pressure in the combustion chamber and in the nozzle outlet section and others);
- c) combustion-chamber and engine-nozzle shapes;
- d) method (system) of engine cooling;
- e) systems for starting and controlling the engine's operation, switching on various valves (electrical, hydraulic, pneumatic) and other elements;
- f) designs of the separate elements of the engine;
- g) materials used for manufacturing the engine.

For calculations to determine:

- a) characteristics of the engine (altitude, throttling, hydraulic, and others);
- b) geometrical dimensions of the combustion chamber and nozzle of the engine;
- c) parameters and geometric dimensions of the fuel-feed and atomization systems as well as of the engine cooling duct.

The solution of these problems is usually based:

- 1) on proved theoretical and operational data, and
- 2) on the results of subsequent tests carried out on the projected and built prototype for purposes of checking and adjusting to achieve economy and reliability of operation.

In determining the basic parameters and dimensions of the engine being designed, we generally make use of the relative data (coefficients) applicable to contemporary engines.

In designing a ZhRD, it is necessary to follow departmental and all-union standards and norms, as well as the technical conditions for manufacture, assembly, and testing.

It is impossible to give general rules for designing a ZhRD, because the development of each separate construction of an engine depends on its use, type of fuel, available data, and other factors. However, the usual methods of choosing the shape of the combustion chamber and nozzle of the engine, the values of its basic parameters, as well as calculations of heat transfer, operational, geometrical, and hydraulic characteristics, systems for fuel feed and injection, are, with some exceptions, suitable for all types of ZhRD.

In designing an engine, we devote great attention to the problems of simplicity and cheapness of construction, convenience of guidance and operation, reliability and economy of operation, and so forth.

The solution of the problem of developing a reliable construction for a ZhRD of great thrust is impeded by the fact that it is attended with constant intensification of the heat processes in the combustion chamber, increase of fuel consumption, and the use of more efficient fuels. An expedient choice of fuel components for a specific engine intended to fulfill a certain function is the first and most obligatory condition for success in developing an engine. However, the greatest difficulties arise in working out the design of the engine.

After completion of the engine design to meet the requirements of the selected fuel type, structural and similar measures are worked out to provide for stable combustion within the combustion chamber of the

engine, without fluctuations in pressure and detonation phenomena capable of destroying the engine (because of powerful vibrations and explosions within the engine) during the first seconds of engine operation as it enters the nominal regime, or at any subsequent instant of time.

The following basic stage of engine development is the solution of the problem of cooling the combustion chamber and nozzle. Reliable cooling of a ZhRD always presents great difficulties in developing any engines of prolonged operation, which develop a considerable specific thrust.

The following stage is the development of the engine fuel-feed system and, finally, the last stage involves the development of systems for starting and controlling the engine.

Successful solution of these problems is possible only upon condition of considering the latest scientific achievements in the development of ZhRD and in other associated fields of engineering.

Chapter III

ENGINE OPERATING CYCLES AND EFFICIENCY

The work of a ZhRD consists of changing the chemical energy of liquid fuel into heat energy and then into the kinetic energy of combustion products flowing from the nozzle into the atmosphere, as a result of which a reactive force — the engine's thrust — is developed.

This change of the chemical energy of the fuel in a ZhRD into the other corresponding forms of energy, as in any other engine, is, in practice, accompanied by an unproductive expenditure of part of the energy of the fuel burned. The smaller the magnitude of this loss, the more perfect the engine.

In the present chapter, the thermodynamic processes which form the basis of the change of the chemical energy of the fuel in a ZhRD into the kinetic energy of the gas flow are considered.

SECTION 1. OPERATING CYCLE OF AN IDEAL ENGINE

By the operating cycle of a ZhRD is meant the totality of the thermodynamic processes in the mass carrier in the engine chamber, as a result of which the chemical energy of the fuel is turned into the kinetic energy of the gases issuing from the nozzle into the surrounding medium.

To ascertain and analyze the most important parameters which influence the operating economy of the engine and serve for comparative evaluation of real engines, the concept of the operating cycle of an

ideal engine has been introduced into the theory of the ZhRD.

By the operating cycle of an ideal engine, we mean, conventionally, a certain closed and reversible thermodynamic cycle consisting of the simplest thermodynamic processes and constituting a simplified scheme of the combination of the actual processes occurring in real ZhRD.

In accordance with this, the following assumptions are accepted for the operating cycle of an ideal engine:

1) the fuel components are compressed and fed to the combustion chamber without hydraulic resistances in the line and with a negligible loss of energy on these processes, relative to the mechanical work performed by the products of fuel combustion;

2) by means of atomization and mixing of the fuel components fed to the combustion chamber, an absolutely uniform (homogeneous) fuel mixture is formed.

3) the fuel components flow into the combustion chamber at a constant rate;

4) the fuel in the engine's chamber burns at constant pressure and with complete heat liberation (when $\varphi_k = 1^*$);

5) the combustion products of the fuel form an ideal gas;

6) the products of combustion expand adiabatically in the nozzle, i.e., without transfer of heat to the surrounding medium, and without complete fuel combustion, recombination, relaxation, and without viscosity friction between the molecules of the gases;

7) the same fields of pressure, temperature, and velocity are to be found in any cross section of the combustion chamber and nozzle throughout their lengths;

*[$\varphi_k = \varphi_k = \varphi_{k\text{amera}} = \varphi_{\text{chamber}}$.]

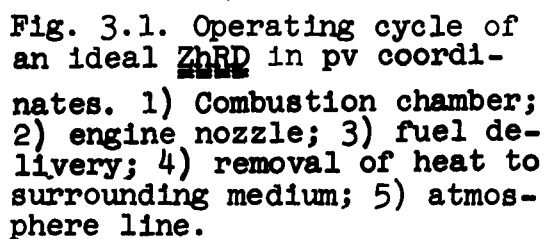


Fig. 3.1. Operating cycle of an ideal ZHRD in pv coordinates. 1) Combustion chamber; 2) engine nozzle; 3) fuel delivery; 4) removal of heat to surrounding medium; 5) atmosphere line.

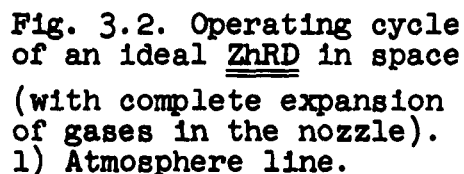


Fig. 3.2. Operating cycle of an ideal ZhRD in space (with complete expansion of gases in the nozzle).
1) Atmosphere line.

8) the movement of the gases in the nozzle outlet is one-dimensional and the gas flow lines are parallel to each other;

9) all the heat is used in the engine with the exception of the heat escaping with the outgoing gas.

1) Atmosphere line. With these assumptions, the operating cycle of an ideal engine consists of one isochor, two isobars, and one adiabatic line (Fig. 3.1):

1) the isochor of fuel pressurization and feed into the combustion chamber, characterizing the processes in the fuel-supply system of the engine (line an [aH]);

2) the isobar of fuel combustion in the engine's chamber (line $n_k [H_k]$);

3) the adiabatic line of the gases' expansion in the engine's nozzle (line kv [ka]);

4) the isobar of the heat transfer from the mass carrier to the surrounding medium, representing the conditional closure of the operating cycle (line va [sa]).

All the basic parameters characterizing the work of one kilogram of gas in the cycle of an ideal engine have values of maximum quantity, and the degree to which the parameters of a real engine approach these determines the perfection of the latter.

The full useful work of one kilogram of gas in the cycle of an ideal engine is expressed in Fig. 3.1 by the area of the shaded diagram, and is expressed analytically thus:

$$\begin{aligned} L_t &= \text{area } OHKE + \text{area } EKBM - \text{area } OABM = p_k v_k + \\ &+ \frac{1}{k-1} (p_k v_k - p_a v_a) - p_a v_a = \frac{k}{k-1} (p_k v_k - p_a v_a) = \\ &= \frac{k}{k-1} (R_k T_k - R_a T_a) = \frac{k}{k-1} R_k (T_k - T_a) = \frac{k}{k-1} R_k T_k \left(1 - \frac{T_a}{T_k}\right) = \\ &= \frac{k}{k-1} R_k T_k \left[1 - \left(\frac{p_a}{p_k}\right)^{\frac{k-1}{k}}\right] = \frac{w_{\max}^2}{2g} \text{ kg-m/kg.} \end{aligned}$$

The full work of one kilogram of gas in the cycle of an ideal engine when operating in space with complete expansion of gas in the nozzle ($p_v = p_a = 0$)* would be

$$L_{t\max} = \frac{k}{k-1} R_k T_k = \frac{k}{k-1} p_k v_k = \frac{w_{\max}^2}{2g} \text{ kg-m/kg, ***} \quad (3.1)$$

where $w_{v.1}$ ** is the ideal velocity of gas outflow from the engine's chamber nozzle; w_{\max} is the maximum ideal velocity of gas outflow from the nozzle with complete expansion (up to $p_v = 0$).

The accepted evaluation of the economy of a real engine in relationship to quantity L_t is its operating cycle as accomplished with the same gas pressures in the combustion chamber and in the outlet

*[$p_B = p_v = p_{\text{vykhod}} = p_{\text{outlet}}$.]***[$L_{\text{TP}} = L_{\text{tp}} = L_{\text{tpustota}} = L_{\text{tspace}}$.]
 **[$w_{B.H} = w_{v.1} = w_{\text{vykhod.ideal'noy}} = w_{\text{outlet.ideal}}$.]

nozzle, but with fuel energy losses and other deviations from the conditions of the operation of an ideal engine.

The operating cycle of an ideal engine in space (with complete expansion of the gases in the nozzle) is shown in Fig. 3.2.

The degree of perfection for an ideal ZhRD is conventionally evaluated in terms of the thermal efficiency η_t which takes into consideration only the heat losses in the fuel due to the escape of the gases to the surrounding medium, according to the second law of thermodynamics.

SECTION 2. OPERATING CYCLE OF A REAL ENGINE

The operating conditions of a real engine differ considerably from the operating conditions of an ideal engine. In the operation of a real engine one must consider:

- 1) hydraulic losses in the line during delivery of liquid fuel components to the combustion chamber;
- 2) the heterogeneity of the velocity and concentration fields of the fuel components in the cross sections throughout the length of the combustion chamber as a result of their imperfect atomization and mixing;
- 3) the fuel's heat losses in the form of dissociation, incomplete combustion, and heat transfer to the surrounding medium;
- 4) the mass carrier's pressure difference along the length of the combustion chamber as a consequence of hydraulic losses and flow acceleration during heating up;
- 5) the complete combustion of the fuel components in the nozzle which were not fully consumed in the chamber because of their imperfect atomization and mixing, and due to their limited chamber stay time.
- 6) the establishment of a chemical and energy state of equilibrium of the fuel combustion products as they flow and expand in the nozzle;

7) losses as a consequence of the viscosity friction of the gases, i.e., the molecules' friction against each other and the wall of the chamber;

8) the irregularity of the outflow of gases in the supercritical part of the nozzle and the nonparallelism of the flow of gases into the surrounding medium;

9) The underexpansion or overexpansion of the gas in the nozzle as a consequence of various operating regimes and external conditions of the operation of the engine, and other factors.

Because of this the operating cycle of the real engine differs from the cycle of an ideal engine (see Fig. 3.1), and the total work L_1 of one kilogram of gas in it is less than the theoretically conceivable total work L_t of an ideal cycle by the magnitude of the auxiliary losses L_{pot}^* in fuel energy, i.e.,

$$L_1 = L_t - L_{pot}. \quad (3.2)$$

The work L_1 of the cycle determines the specific thrust of the engine. The greater L_1 is, the greater the engine's P_{ud}^{**}

The magnitude of auxiliary heat losses of the fuel in a real engine L_{pot} is most affected by:

1) the design of the chamber's burner cup (the method of atomization and mixing of the fuel components, and the type and distribution of the sprayers in the chamber head);

2) the chemical composition of the fuel components and their relationship to each other;

3) the volume of the combustion chamber and its shape;

4) the geometrical characteristics of the nozzle and its profile;

*[$L_{not} = L_{pot} = L_{poterya} = L_{loss}$.]

**[$P_{уд} = P_{specific}$.]

5) the external operating conditions of the engine (operation at land or sea level or at some altitude above the earth), and other factors.

Because of a number of enumerated factors accompanying and complicating the operating cycles in the combustion chamber and nozzle of a real engine, it is practically impossible to precisely define the parameters of the mass carrier even in the characteristic sections of the engine's chamber; therefore, in planning an engine's design, the derivation of a number of assumptions and coefficients simplifying the solution of the problem is often required.

SECTION 3. CLASSIFICATION OF VELOCITIES OF GAS OUTFLOW FROM THE CHAMBER NOZZLE OF A ZhRD

The process of gas outflow from a chamber nozzle of an engine is characterized by the magnitude of the flow's absolute velocity at the nozzle.

To evolve formulas for the efficiency of an engine, it is necessary to understand the physical essence of the conditional concepts of the velocities of gas outflow from an engine chamber nozzle.

In ZhRD theory, the following distinct gas outflow velocities are accepted:

1) maximum ideal w_{\max} ; 2) ideal $w_{v.1}$; 3) theoretical $w_{v.t}^*$; 4) true w_v^* ; 5) effective w_{ef}^* ; 6) critical w_{kr}^* .

Maximum ideal velocity is that exhaust velocity which a gas would have in an ideal engine's chamber nozzle outlet section with complete change of the available chemical energy of one kilogram of fuel into

$$\begin{aligned} & * [w_{B.T} = w_{v.t} = w_{vykhod.teoreticheskaya} = w_{outlet.theoretical}; \\ & w_B = w_v = w_{vykhod} = w_{outlet}; \\ & w_{\text{эф}} = w_{ef} = w_{effektivnaya} = w_{effective}; \\ & w_{kp} = w_{kr} = w_{kriticheskaya} = w_{critical}.] \end{aligned}$$

the kinetic energy of the gas at an infinitely high level of expansion, i.e.,

$$w_{\max} = \sqrt{2gH_u} = 91,53 \sqrt{H_u} = \sqrt{2g \frac{k}{k-1} R_k T_k} \text{ m/sec}, \quad (3.3)$$

where H_u kcal/kg is the lowest calorific value of the fuel.

The magnitude of the ideal exhaust velocity is characteristic of the fuel's properties.

Ideal velocity is the exhaust velocity which a gas would have in an ideal engine's chamber nozzle outlet section, assuming adiabatic change of condition and allowing for the counter-pressure of the atmospheric air; i.e.,

$$\begin{aligned} w_{s,u} &= \sqrt{2gH_u \eta_t} = 91,53 \sqrt{H_u \eta_t} = \sqrt{2g \frac{k}{k-1} R_k T_k \left[1 - \left(\frac{p_a}{p_k} \right)^{\frac{k-1}{k}} \right]} = \\ &= \sqrt{2g \frac{k}{k-1} R_k T_k \eta_t} = w_{\max} \sqrt{\eta_t} \text{ m/sec}, \end{aligned} \quad (3.4)$$

where η_t is the thermal efficiency of the engine.

Theoretical velocity is the exhaust velocity of the chemically active gases in the chamber nozzle outlet of a real engine, theoretically calculated with regard to only one fuel heat loss in the combustion chamber in the form of dissociation of gases, and with the assumption of complete chemical- and energy-equilibrium isentropic change in the state of the products of combustion in the chamber nozzle, i.e.,

$$w_{s,r} = \sqrt{2g \frac{k}{k-1} R_{k,r} T_{k,r} \left[1 - \left(\frac{p_a}{p_k} \right)^{\frac{k-1}{k}} \right]} = 91,53 \sqrt{I_k - I_a} \text{ m/sec},$$

where k is the mean value of the exponent of the level of the isentropes equation; I_k and I_v^* are the energy content of the gases in the combustion chamber and the chamber nozzle outlet section, respectively, of a real engine in kcal/kg.

*[$I_k = I_{\text{chamber}}$; $I_a = I_{\text{outlet}}$.]

True velocity is the mean velocity of gas outflow in the chamber nozzle outlet of a real engine, usually defined with the assumption of polytropic expansion of the gases in the nozzle:

$$w_v = \sqrt{2gH_u 427 \eta_i} = 91.53 \sqrt{H_u \eta_i} = \\ = \sqrt{2g \frac{n}{n-1} R_u T_u \left[1 - \left(\frac{p_u}{p_u} \right)^{\frac{n-1}{n}} \right]} \text{ m/sec,} \quad (3.5)$$

where η_i is the internal efficiency of the engine.

In deriving equations for determining the velocity of gas outflow from an engine chamber nozzle, the following are disregarded:

1) the velocity at which fuel components are injected into the combustion chamber, as a consequence of their negligibly small magnitudes relative to gas exhaust velocity from the nozzle;

2) the heat resistance of the engine's combustion chamber (the drop in pressure along the length of the chamber because of the combustion products' heating up and attaining a movement up to the velocity w_k^*), which, if necessary, is calculated by a special coefficient (see Section 13, Chapter VI [sic]);

3) energy loss of the gas flow as a consequence of radially composed velocity at the exit from the expanding part of the chamber nozzle, which is usually also computed by a special coefficient.

The velocity w_v is the summary of the characteristics of an engine's operating efficiency.

In existing ZhRD $w_v \approx 2000-2500$ m/sec. For the most efficient chemical fuels' products of combustion, the possible exhaust velocity amounts to about 4.5 km/sec.

Obtaining the maximum velocity of exit gases from the chamber nozzle is one of the basic tasks of the designer of an engine.

*[$w_k = w_{\text{chamber}}$.]

The greater the velocity w_v , the greater the specific thrust of the engine proportional to it, since $P_{ud} = w_v/g \approx 0.1w_v$ (when $p_v = p_a$).*

Effective velocity is the conditional velocity of the gases behind the chamber nozzle of a real engine, computed in accordance with the general equation for the thrust of an engine working on the corresponding operating regime and flight altitude:

$$P_s = \frac{G_s}{g} w_s + F_s (p_s - p_a) = \frac{G_s}{g} w_{s\phi}, \quad ** \quad (3.6)$$

i.e.,

$$w_{s\phi} = \frac{gP_s}{G_s} = w_s + \frac{gF_s}{G_s} (p_s - p_a) = gP_{y.s.} \text{ m/sec.} *** \quad (3.7)$$

When $p_v = p_a$ we have $w_{ef.n} = w_{ef} = w_v$.****

One may distinguish the following effective exhaust velocities:

- 1) at ground or sea level w_{ef_0} ;
- 2) in flight at a specified altitude $w_{ef.H}$;
- 3) during flight in space $w_{ef.p}$.*****

Critical velocity is the velocity of gas outflow in the outlet of the engine chamber nozzle:

$$w_{cp} = \sqrt{2g \frac{n}{n+1} R_k T_k} = \sqrt{ngRT_{cp}} \text{ m/sec.} \quad (3.8)$$

Increase of velocity w_v is, in principle, possible by increasing parameters H_u , R_k , \underline{n} , p_k/p_v , T_k , and η_1 . Some of these parameters are, in practice, extremely limited.

Within the widest limits, one may increase w_v by using fuel of high calorific values in the ZhRD, as well as fuels whose combustion

*[$p_a = p_a = p_{atmosfera} = p_{atmosphere}$.]
 **[$p_n = p_n = p_{neogranichennaya} = p_{absolute}$.]
 ***[$gP_{y.d.n} = gP_{ud.n} = gP_{udel'naya.neogranichennaya} = gP_{specific.absolute}$.]
 ****[$w_{\phi.n} = w_{ef.n}$.]
 *****[$w_{\phi.p} = w_{ef.p} = w_{effektivnaya.pustota} = w_{effective.space}$.]

products, other things being equal, have the greatest value of R_k .

The use of fuels of high calorific value to increase exhaust velocity, other things being equal, usually raises combustion temperature and therefore requires more intensive cooling of the engine chamber, more intensive removal of heat from the heated inner liner of the chamber, and the use of more expensive heat-resistant metals for manufacturing the chamber.

When the chamber liner has a high heat liberation rate, an engine cooling system which is more complicated in construction, relatively expensive, and less economical may be required.

Increase of gas exhaust velocity by raising pressure in the combustion chamber above a determined limit, different for every type of engine, is limited in practice because of the increase of engine weight and the difficulties of cooling the chamber.

Increasing w_v by decreasing gas pressure p_v at the outlet from the engine nozzle is also, in practice, limited by the tactical purpose of the weapon, engine operating conditions relative to the surrounding medium, and other factors.

In existing engines, pressure difference in the nozzle amounts to $p_k/p_v \approx 16-60$ and more. Further increase of the initial gas pressure in the combustion chamber leads to a comparatively small increase of exhaust velocity but, in return, to a more considerable increase of the specific weight of the engine. Therefore, one may scarcely expect that from the economic point of view a pressure above 60-100 atmospheres absolute would be used in the combustion chamber. By decrease of the gas pressure in the engine nozzle outlet, the blastoff thrust of the engine is lowered and nozzle weight is increased, so that decreasing pressure is, in each separate case, held within fixed limits.

SECTION 4. ENGINE EFFICIENCIES

The accepted definition of efficiency is the degree of perfection, in a ZhRD, of the change of the chemical energy of the fuel into the kinetic energy of the combustion products at the outlet from the chamber nozzle: thermal efficiency η_t ; internal efficiency η_i ; relative efficiency η_o^* ; mechanical efficiency η_m , and effective efficiency η_e . Besides this, there are additional efficiencies which have been accepted to define the engine's work during the missile's flight: thrust efficiency η_p and total efficiency η_{ob}^* .

Thermal efficiency η_t of the engine shows what part of the available chemical energy of the fuel fed to the combustion chamber would be changed to the kinetic energy of the gases at the outlet from the chamber nozzle in case of an ideal ZhRD, i.e.,

$$\eta_t = \frac{L_t}{H_{\text{fuel}}} = \frac{w_{\text{ex}}^2/2g}{w_{\text{max}}^2/2g} = \left(\frac{w_{\text{ex}}}{w_{\text{max}}} \right)^2 =$$

$$= \left(\frac{\sqrt{2g \frac{k}{k-1} R_g T_g \left[1 - \left(\frac{p_e}{p_g} \right)^{\frac{k-1}{k}} \right]}}{\sqrt{2g \frac{k}{k-1} R_g T_g}} \right)^2 = 1 - \left(\frac{p_e}{p_g} \right)^{\frac{k-1}{k}},$$

i.e.,

$$\eta_t = \left(\frac{w_{\text{ex}}}{w_{\text{max}}} \right)^2 = 1 - \left(\frac{p_e}{p_g} \right)^{\frac{k-1}{k}}. \quad (3.9)$$

Consequently, when determining an engine's thermal efficiency, only the heat loss of the working fluid as stated in the second law of thermodynamics is considered.

The value of η_t depends on the expansion level p_k/p_v of the gases in the nozzle and the adiabatic exponent k (depending on the type of fuel).

$$*[\eta_o = \eta_o = \eta_{\text{otnositel'nyy}} = \eta_{\text{relative}};$$

$$\eta_{ob} = \eta_{ob} = \eta_{\text{obshchiy}} = \eta_{\text{total}}.]$$

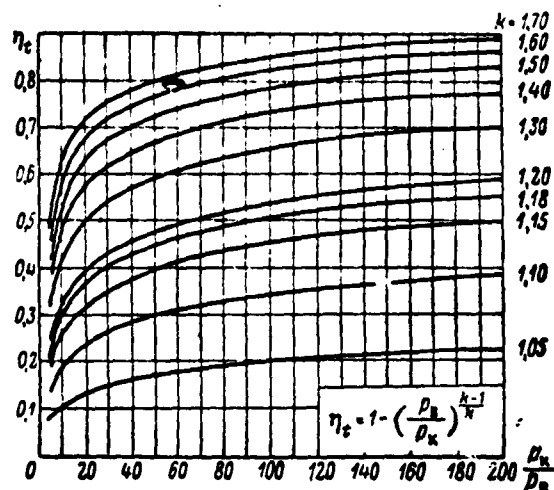


Fig. 3.3. Thermal efficiency η_t of an engine, as a function of p_k and k .

In practice, different fuels at the same conditions have different speeds of combustion and recombination, which are differentiated by the composition of the gases, their specific heat, and, consequently, by the magnitude of k .

In Table 3.1 and in Fig. 3.3 the values of η_t when $p_v = 1$ atm-abs and at various magnitudes of p_k and k are shown. The data in the table and the curves of Fig. 3.3 show that when p_k is increased, the value of η_t , at first, grows rapidly (in direct proportion to k), and then slower, and at about 200 atm-abs becomes almost constant.

Consequently, to obtain the greatest value of η_t it is necessary for the engine to operate at the highest possible p_k , and also using a fuel whose combustion products have the greatest possible specific heat ratio ($k = c_p/c_v$).*

With a rise in p_k the pressure difference p_k/p_v in the nozzle is increased and the operating cycle in the engine is intensified, basically by decreasing the dissociation of the gases in the combustion chamber. In some cases an increase of p_k to 100 atm-abs may be justified for decreasing the dimensions and weight of the engine chamber.

*[The specific heat ratio k , not to be confused with the adiabatic exponent k just mentioned. The specific heat ratio k is a Russian lower-case italic letter.]

TABLE 3.1

Values of η_t Depending on p_k and k when $p_v =$
 $= 1$ Atmosphere Absolute

$k \backslash p_k/p_k$	1/5	1/10	1/20	1/50	1/100	1/200
1,0	0	0	0	0	0	0
1,05	0,074	0,104	0,133	0,150	0,197	0,223
1,10	0,136	0,189	0,238	0,299	0,342	0,382
1,15	0,189	0,259	0,323	0,400	0,451	0,499
1,18	0,218	0,196	0,367	0,449	0,505	0,554
1,20	0,232	0,319	0,393	0,479	0,536	0,586
1,30	0,310	0,412	0,449	0,595	0,654	0,706
1,40	0,369	0,482	0,575	0,673	0,732	0,780
1,50	0,415	0,536	0,632	0,729	0,785	0,829
1,60	0,453	0,578	0,675	0,769	0,822	0,863
1,70	0,482	0,613	0,709	0,800	0,850	0,887

If the engine operates with underexpansion of the gases in the nozzle ($p_v > p_a$), in this case the thermal efficiency is expressed by the formula

$$\eta_{ned} = \varphi_{ned} \eta_t \quad * \quad (3.10)$$

where φ_{ned} is the factor of completeness of gas expansion in the nozzle relative to atmospheric pressure:

$$\varphi_{ned} = \frac{1 - (p_v/p_a)^{\frac{k-1}{k}}}{1 - (p_a/p_a)^{\frac{k-1}{k}}};$$

here p_v is the pressure in the outlet of the engine nozzle with underexpansion of the gases ($p_v > p_a$); and p_a is the pressure of the atmospheric air.

Existing engines have a $\eta_t \approx 0.40-0.70$.

The internal efficiency of an engine shows what part of the available chemical energy of the fuel fed to the combustion chamber of a

*[$\varphi_{ned} = \varphi_{ned} = \varphi_{nedorasshireniye} = \varphi_{underexpansion}$;
 $\eta_{ned} = \eta_{underexpansion}$]

real engine is turned into kinetic energy of the gases in the outlet from the nozzle, i.e.,

$$\eta_l = \frac{L_l}{H_u 427} = \frac{w_v^2 / 2g}{w_{max}^2 / 2g} = \left(\frac{w_v}{w_{max}} \right)^2. \quad (3.11)$$

When $p_v \neq p_a$, the value of w_v must be replaced by the value of w_{ef} . Since when $p_v = p_a$ the absolute thrust of the engine chamber is

$$P = G_s / g (w_v), \text{ from which } w_v = gP / G_s \text{ m/sec,}$$

then

$$\eta_l = \frac{w_v^2 / 2g}{H_u 427} = \frac{\left(\frac{gP}{G_s} \right)^2 / 2g}{H_u 427} = \frac{P^2}{87.05 H_u G_s^2}.$$

Since $P_{ud} = P / G_s$, then

$$\eta_l = \frac{P_{ud}^2}{87.05 H_u} = 0.0115 \frac{P_{ud}}{H_u}. \quad (3.12)$$

If P and G_s have been measured during the engine's trials on a test stand, it is possible to compute η_l and w_v extremely precisely by the latter equation.

Existing engines have an $\eta_l \approx 0.30-0.50$.

Relative efficiency of an engine shows the degree of deviation of the operating cycle in the chamber of a real engine from the operating cycle in the chamber of an ideal engine, i.e.,

$$\eta_o = \frac{L_l}{L_e} = \frac{w_v^2 / 2g}{H_u 427 \eta_l} = \frac{\eta_l}{\eta_l}. \quad (3.13)$$

This efficiency considers the losses of fuel energy in a real engine which are conditional upon the physical incompleteness of fuel combustion as a result of imperfect mixing of its components and inadequate speed of combustion and recombination of gases during expansion in the nozzle, as well as losses caused by the energetic instability of outflow of gases from the nozzle and the nonadiabatic character of the process (heat transfer to the surrounding medium and heat transfer

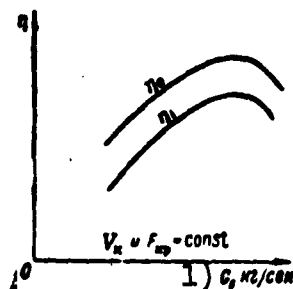


Fig. 3.4. Factors η_1 and η_0 dependent on G_s of an engine, with unchanging values of V_k and F_{kr} .
1) G_s , kg/sec.

to the liner as a result of friction and radiation).

Existing engines (the "Vanguard" missile and others) have a $\eta_0 \approx 0.65-0.90$.

By raising p_k , the values of η_1 and η_0 are increased by increasing the fuel's heat liberation coefficient ϕ_k . Increase of p_k by increasing G_s without changing the dimensions of the combustion chamber and nozzle of the engine leads at first to an increase of η_1 and

η_0 because the operating regime is close to the optimum regime in regard to flow rate of the fuel in a given combustion chamber's volume, and then to their decrease as a consequence of the discrepancy of the volume of the combustion chamber V_k to the ever-increasing fuel flow rate G_s per second and the decrease of ϕ_k by this means (Fig. 3.4).

Mechanical efficiency of an engine considers the decrease of the internal efficiency of the engine caused by possible additional flow rates in serving the fuel-feeder system and in forming the protective curtain around the surface of the burner liner.

When $p_s = p_a$,* the specific thrust may be expressed as follows:

1) combustion chamber:

$$P_{y,z} = \frac{P_z}{G_s} = \frac{v_z}{g} = \frac{91.53 \sqrt{H_s \eta_1}}{g} = 9.33 \sqrt{H_s \eta_1} \frac{\text{kg thrust}}{\text{kg fuel/sec}};$$

2) engine as a whole:

$$P_{y,z} = \frac{P_z}{G_s} = 9.33 \sqrt{H_s \eta_1 \eta_m} \frac{\text{kg thrust}}{\text{kg fuel/sec}},$$

where G_s is the total flow rate in the engine in kg/sec.

The absolute thrust of an engine with a TNA may be greater than

*[$p_c = p_s = p_{\text{система}} = p_{\text{system}}$.]

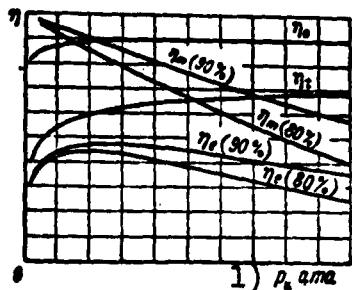


Fig. 3.5. Engine efficiency η_t , η_1 , η_0 , η_e , and η_m depending on p_k . 1) Atmosphere absolute.

the thrust of an engine without a TNA, if the gases which have worked in the turbine, flowing out into the surrounding medium, create an additional thrust $\Delta P_{\underline{TNA}}$ or are burned in the basic chamber or an auxiliary engine chamber.

Having divided the expression mentioned above for $P_{ud.k}$ into the expression for $P_{ud\Sigma}$, we will obtain a formula for computation of the mechanical efficiency of an engine, i.e.,

$$\eta_m = \left(\frac{P_{y\Delta\Sigma}}{P_{y\Delta.k}} \right)^2 = \left(\frac{P_2}{P_k} \right)^2 \left(\frac{G_s}{G_s + G'_s} \right)^2 = \left(\frac{P_2}{P_k} \right)^2 \left(\frac{1}{1 + G_s/G'_s} \right)^2 = \left(\frac{P_2}{P_k} \right)^2 \left(\frac{1}{1 + \zeta_{rr}} \right)^2, \quad (3.14)$$

whence

$$P_{y\Delta\Sigma} = P_{y\Delta.k} \sqrt{\eta_m} = P_{y\Delta.k} \frac{P_2}{P_k} \frac{1}{1 + \zeta_{rr}} \frac{\text{kg thrust}}{\text{kg fuel/sec}},$$

or when $P_\Sigma = P_k$, we will obtain

$$P_{y\Delta\Sigma} = P_{y\Delta.k} \frac{1}{1 + \zeta_{rr}} \frac{\text{kg thrust}}{\text{kg fuel/sec}},$$

where $\zeta_{gg} = G'_s/G_s \approx f(P_k, p_p)^*$ is the relative fuel consumption in serving the fuel-feed system (gas generator) of the engine.

In existing engines with turbopump units we have:

1) in missile engines $\zeta_{gg} \approx 0.015-0.030$;

2) in aircraft engines $\zeta_{gg} \approx 0.050-0.060$.

For existing missile engines feeding the turbine of the turbopump unit with gas vapor from 80% hydrogen peroxide or fuel combustion products removed from the engine combustion chamber (the "Atlas" mis-

*[$\zeta_{rr} = \zeta_{gg} = \zeta_{\text{gazogenerator}} = \zeta_{\text{gas generator}}$;
 $p_\Pi = p_p = p_{\text{podacha}} = p_{\text{feed}}$.]

side and others) $\eta_m \approx 0.97-0.98$.

By raising p_k , the value of η_m is decreased almost in accordance with the linear law (Fig. 3.5). The more effective an engine's fuel-feed system is, the greater its η_m .

In engines with a closed system for cooling and feeding the turbine $\eta_m \approx 1$, since the expenditure of energy in starting the circulation pump of this system is negligibly small. For engines supplied by means of a VAD, whose $G_s = 0$, nominally $\eta_m = 1$. However, in comparing the effectiveness of operation of these engines with a ZhRD having a turbopump unit, one should not lose sight of the preliminary expenditure of energy in obtaining the compressed gas for the fuel-feed system.

The effective efficiency of an engine shows what part of the available chemical energy of the total flow rate in a real engine is turned into the kinetic energy of gases as a result of which thrust force is developed; i.e.,

$$\eta_e = \eta_i \eta_m = \eta_i \eta_o \eta_m. \quad (3.15)$$

This efficiency may be expressed as follows:

$$\eta_e = \frac{L_i}{\left(H_u + H'_u \frac{G'_s}{G_s}\right) 427} = \frac{w_s^2/2g}{(H_u + H'_u \zeta_{rr}) 427}. \quad (3.15')$$

If the same fuel which is expended in the combustion chamber of the engine is used to start the turbopump unit, $H_u = H'_u$ and

$$\eta_e = \frac{w_s^2/2g}{(1 + \zeta_{rr}) H_u 427} = \frac{\eta_i}{1 + \zeta_{rr}},$$

from whence

$$w_s = \sqrt{2g H_u 427 (1 + \zeta_{rr}) \eta_e} \text{ m/sec.}$$

Some engines have a G'_s equal to zero, and, consequently $\eta_e = \eta_i$.

Existing engines have a $\eta_e \approx 0.25-0.45$ and over.

In a number of ZhRD now manufactured, 80% hydrogen peroxide is

sometimes used to start the TNA.

For an engine in flight, the effective efficiency must be determined by consideration of the kinetic energy of the basic and auxiliary fuels which are moving with the weapon at a velocity V in m/sec, using the formula

$$\eta_{eV} = \frac{w_{\phi}^2/2g + V^2/2g}{(H_u + H'_u \zeta_{rr}) 427 + \frac{V^2}{2g} (1 + \zeta_{rr})} = \frac{w_{\phi}^2 + V^2}{2g (H_u + H'_u \zeta_{rr}) 427 + V^2 (1 + \zeta_{rr})} \quad (3.16)$$

If the TNA operates on the basic fuel, $H_u = H'_u$, and therefore

$$\eta_{eV} = \frac{w_{\phi}^2 + V^2}{2g (H_u 427 + \frac{V^2}{2g}) (1 + \zeta_{rr})} \quad (3.16')$$

With a heat value of the fuel of the order of $H_u = 2000$ kcal/kg and a flight velocity $V_{kon} = 3000$ m/sec* ($M \approx 10$) the kinetic energy of the fuel amounts to about 50% of its heating value. One may not disregard such a quantity of energy.

The thrust efficiency of an engine shows what part of the available kinetic energy of the gases in the chamber nozzle of a real engine is used during the flight of a weapon, i.e.,

$$\eta_p = \frac{L_{кин.исп}}{L_{кин.расп}} = \frac{L_{кин.исп}}{L_{кин.исп} + L_{кин.неисп}} = \frac{P_{ya} V}{P_{ya} V + \frac{(w_{\phi} - V)^2}{2g}} = \frac{\frac{(w_{\phi}/g) V}{\frac{w_{\phi}}{g} V + \frac{(w_{\phi} - V)^2}{2g}}}{\frac{2w_{\phi} V}{w_{\phi}^2 + V^2}} = \frac{2(V/w_{\phi})}{1 + (V/w_{\phi})^2} \quad ** \quad (3.17)$$

*[$V_{kon} = V_{kon} = V_{konets} = V_{end}$.]

**[$L_{кин.исп} = L_{кин.исп} = L_{kineticheskaya.ispolzovat'sya} = L_{kinetic.used}$;

$L_{кин.расп} = L_{кин.расп} = L_{kineticheskaya.raspolagaemaya} = L_{kinetic.available}$;

$L_{кин.неисп} = L_{кин.неисп} = L_{kineticheskaya.neispolzovat'sya} = L_{kinetic.not used}$.]

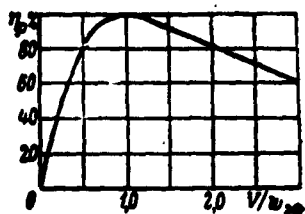


Fig. 3.6. Thrust efficiency of an engine η_p depending on the relationship of velocities V/w_{ef} .

When $V/w_{ef} = 0$, $\eta_p = 0$; when $w_{ef} = V$, $\eta_p = 1$, i.e., it attains the maximum when $w_{ef} = 0$ relative to the earth, and when $V/w_{ef} > 1$, it is decreased (Fig. 3.6).

The A-4 long-range missile, with a flight velocity at the end of the boost phase $V_{kon} = 1525$ m/sec, and a velocity $w_{ef} = 2135$ m/sec had an $\eta_p = 0.94$.

The total efficiency of an engine shows what part of the available energy of the total flow rate in a real liquid-propellant rocket engine is usefully utilized during the weapon's flight, i.e.,

$$\eta_{\text{total}} = \eta_{\text{lv}} \eta_p. * \quad (3.18)$$

The magnitude of the specific thrust of the engine is used for evaluation and comparison between the work of different liquid-fueled rocket engines.

In the theoretical calculation of efficiency and specific thrust of an engine, it is necessary to know the precise values of the heats of reaction and phase transitions, specific heat, and the constant of equilibrium of the combustion products of the given fuel.

The values of all the above-mentioned efficiencies of an engine depend, to a considerable degree, on the type of fuel used. It follows that one must keep in mind that for a ZhRD not the effective efficiency η_e , but the specific thrust, determined by the effective out-flow velocity, is distinctive, since cases are possible when by dilution of the fuel mixture with water and lowering its heating value, it is possible to raise even η_t or η_o , and, consequently, even η_e , at the same time lowering P_{ud} . Therefore the best engine is not the one which

$$*[\eta_{\text{total}} = \eta_{\text{obshch}} = \eta_{\text{obshchiy}} = \eta_{\text{total}}.]$$

is more economical in using the available heat, but the one which develops the greatest specific thrust.

For this reason, efficiency values may be used only for comparative evaluation of a ZhRD, operating on the same fuel and at identical combustion conditions or in the operation of a given engine with various flight speeds.

Example 1. An engine develops a thrust $P = 908$ kg at a flow rate $G_s = 4.86$ kg/sec and $H_u = 1665$ kcal/kg. *

Flight speed of missile $V = 1285$ m/sec.

Determine w_{ef} , L_{kin} , η_i , η_p , η_{obshch} , and P_{ud} .

Solution.

1. Effective velocity of gas outflow

$$w_{ef} = \frac{gP}{G_s} = \frac{9.81 \cdot 908}{4.86} = 1840 \text{ m/sec.}$$

2. Kinetic energy of 1 kg of gases behind the engine nozzle

$$L_{kin} = \frac{w_{ef}^2}{2g} = \frac{1840^2}{2 \cdot 9.81} = 17.2 \cdot 10^5 \text{ kgm/kg.}$$

3. Engine efficiency:

a) internal

$$\eta_i = \frac{w_{ef}^2/2g}{H_u \cdot 427} = \frac{1840^2/2 \cdot 9.81}{1665 \cdot 427} = \frac{7.2 \cdot 10^5}{1665 \cdot 427} = 0.242 = 24.2\%;$$

b) thrust

$$\eta_p = \frac{2 \frac{V}{w_{ef}}}{1 + \left(\frac{V}{w_{ef}}\right)^2} = \frac{2 \frac{1285}{1840}}{1 + \left(\frac{1285}{1840}\right)^2} = 0.375 = 37.5\%;$$

c) total

$$\begin{aligned} \eta_{obshch} &= \frac{PV}{G_s H_u 427 + \frac{V^2}{2g} G_s} = \frac{w_{ef} V}{g H_u 427 + V^2/2} = \frac{2(V/w_{ef})}{\frac{1}{\eta_i} + (V/w_{ef})^2} = \\ &= \frac{2(1285/1840)}{\frac{1}{0.242} + \left(\frac{1285}{1840}\right)^2} = 0.0936 = 9.36\%. \end{aligned}$$

*D. Satton [probably George Sutton], Rocket Engines, IL, 1950.

4. Specific thrust

$$P_{ya} = \frac{w_{00}}{g} = \frac{1840}{9.81} = 187 \frac{\text{kg thrust}}{\text{kg fuel/sec}}$$

5. Specific fuel consumption

$$\begin{aligned} C_{ud} &= G_s/P = 4.86/908 = 0.00535 \frac{\text{kg fuel/sec}}{\text{kg thrust}} = \\ &= 5.35 \frac{\text{kg fuel/sec}}{\text{tons of thrust}} \end{aligned}$$

SECTION 5. CHANGE OF WORKING FLUID'S BASIC PARAMETERS ALONG THE CHAMBER LENGTH OF A ZhRD

In the operating cycle in a ZhRD, the state of the mass carrier (fuel and combustion products) is changed during its movement along the combustion chamber and nozzle. By this means, the change of the mass carrier's parameters (pressure, temperature, velocity, and others) along the length of the engine chamber is conditional upon the character of the operating cycle occurring in the chamber.

In the majority of existing ZhRD fuel components are fed from the tanks to the combustion chamber under a pressure $p_p \approx 20-60$ atm abs or above (Fig. 3.7).

The pressure of the fuel components in the cooling jacket and in the injectors in the engine chamber head is decreased to approximately 10-18 atm abs as a consequence of the increase of the velocity of their outflow and the hydraulic resistances in the lines and in the burner cup.

Directly along the length of the combustion chamber, gas-flow pressure is slowly decreased as the result of losses by friction against the surface of the liner and the increase of the velocity of movement under the influence of the inflow of the compressed fuel's heat (and sometimes also by the change in the cross section of the combustion chamber along its length). Decrease of gas pressure

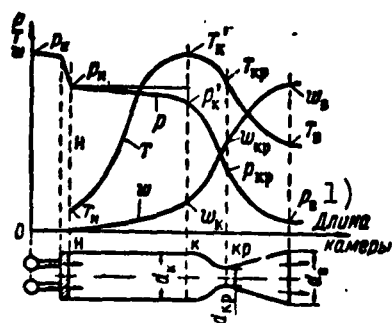


Fig. 3.7. Picture of change of basic parameters of mass carrier (working fluid) along the length of a real engine's chamber. 1) Length of chamber.

along the length of an ordinary cylindrical combustion chamber is insignificant.

Decrease of gas pressure at the end of a cylindrical combustion chamber usually does not exceed 0.5-1% of the pressure at the chamber head. Therefore, in calculating the pressure difference of the gases in the combustion chamber one may accept it as constant, and consider

the combustion chamber as an isobaric chamber, if $f_k = F_k/F_{kr} \geq 5-6$.

In the engine nozzle, gas-flow pressure is considerably decreased, since here the geometrical influence on the flow takes place, and at the outlet from the chamber to the atmosphere it ordinarily amounts to 0.6-1.2 atm abs.

Pressure at a cross section of the chamber nozzle is established by considering the external conditions of the engine's use, and therefore must be different for engines of different designations.

The temperature of the fuel components fed from the tanks to the engine combustion chamber (liquid under normal physical conditions) is practically equal to the temperature of the surrounding medium.

If a fuel component is used for cooling the combustion chamber and nozzle of the engine, by this means it is ordinarily heated up by 50-100°C or more, but not higher than its boiling temperature at the given local pressure in the cooling duct.

The fuel components injected into the combustion chamber are, at first, heated up by means of the combustion heat of the previous portions of the fuel, are vaporized, and then by means of mixing with each other are ignited and burn.

The temperature of the gases in the zone where the fuel is prepared for combustion remains almost constant, increases sharply in the combustion zone, and decreases during the gases' expansion in the nozzle. Temperature at the combustion chamber head ordinarily amounts to 600-900°C. In the presence of prechamber vaporization of the fuel components, this temperature is higher.

Temperature of the gases at the end of the combustion chamber (before the nozzle) amounts to 2800-3300°C, and in the outlet section of the nozzle, 1000-2000°C. These temperatures considerably exceed the melting temperature of the materials of the chamber's inner liner, which creates the necessity of cooling it reliably.

Injection velocity w_{vpr}^* of the fuel components into the combustion chamber depends chiefly on the feed pressure, design of the vaporizing unit, pressure in the combustion chamber, and other factors, and usually varies from 20 to 40 m/sec.

The velocity of the gases grows slowly along the length of the combustion chamber and is sharply increased in the engine nozzle.

In ZhRD combustion chambers, $w_k \approx 50-200$ m/sec, and $w_v \approx 2000$ to 2500 m/sec.

As a consequence of the considerable turbulence of the gas flow and the extremely uneven distribution of the gas-flow velocities in all sections of the combustion chamber and nozzle, one may speak only of the average parameters of the working fluid, somewhat different from their true values.

One must also keep in mind that the computed values of the parameters of the mass carrier in the characteristic sections of the combustion chamber and nozzle of the engine as mentioned above are approx-

$$*[w_{\text{вп}} = w_{\text{vpr}} = w_{\text{vпрыск}} = w_{\text{injection}}.]$$

imate; in each individual case, it is necessary to determine them either by calculations or experimentally (the latter method is suitable for existing engines).

SECTION 6. EQUATIONS CHARACTERIZING THE QUANTITATIVE RELATIONSHIPS IN THE CHANGE OF GAS-FLOW PARAMETERS ALONG THE LENGTH OF THE ZhRD NOZZLE

In planning and designing a ZhRD, one must know the quantitative relationships in the change of gas-flow parameters (pressure, temperature, velocity, etc.) along the length of the combustion chamber and nozzle.

The connections between the temperatures of the gas flow in various sections of the engine chamber, on the one hand, and velocities, pressures, and densities of this flow, on the other hand, may be expressed by the corresponding equations of gas dynamics. In using these equations, we usually make the assumption that temperatures, velocities, and pressures of the gases in the sections of the flow channel being studied are the same. These assumptions are actually valid only for the nozzle portion of the engine chamber, and are completely inapplicable to the operating conditions of the combustion chamber, where the characteristics of the working fluid are extremely changeable, and do not lend themselves to precise quantitative analysis.

The parameters of the gas flow in the chamber of a ZhRD are changed as a consequence of:

- 1) geometrical influence on the flow, i.e., changes in the cross section of the channel for the gas flow;
- 2) heat influence on the flow, i.e., transfer of heat from the gas flow to vaporization of fuel components, to the surrounding medium, and as a result of the dissociation of fuel combustion products, as well as the feeding of heat to the gas flow as the result of fuel com-

bustion and recombination of the products of gas dissociation;

3) flow-rate influence on the stream, i.e., increase of the quantity of gas per second as the result of vaporization and combustion of fuel components (the presence of the smallest liquid particles of the fuel in the gas flow may be disregarded because of their relatively trifling amount), and

4) chemical influence on the flow, i.e., change of the number of moles per unit mass in the gas stream resulting from the chemical reactions occurring (fuel combustion, dissociation, and recombination of the gas molecules).

The intensity of the above-enumerated influences on the gas flow in a ZhRD is diverse and its quantitative calculation is extremely difficult.

The velocity of the gas flow in the engine is increased basically because of geometrical influence. In the combustion chamber the gas velocity is increased chiefly by means of heat and chemical influences. However, the latter lead to a considerable increase of the velocity of the gas flow only in a high-speed engine combustion chamber, where the relative area $f_k < 3$. The requirement for such a high-speed combustion chamber practically never arises.

Flow-rate influence on the gas stream in a ZhRD nozzle is even less significant.

Since, in the combustion chambers of conventional engines, $f_k > 4$, and, therefore, the velocity of the gas flow at the outlet to the nozzle is comparatively small, in calculations of a ZhRD its value may be accepted as equal to zero. This assumption permits the determination of the parameters of the gas flow at the outlet from the combustion chamber to the nozzle only on the basis of the data of the thermodynamic calculations of the engine. In those cases when this gas velocity

cannot be disregarded, its value may be determined after the thermodynamic calculation of the fuel combustion process.

When designing a ZhRD, one ordinarily computes the quantitative relationships of the geometrical influence on the gas flow in the nozzle, the effect of the other influences on the gas being thus calculated by using the polytropic exponent n or by other parameters on the basis of the principles of technical thermodynamics and gasdynamics.

The quantitative relationships of geometrical influence on the gas flow may be most easily obtained in the form of the dependences of the separate gas parameters on the velocity regime, i.e., on the Mach number ($M = w/a$, where w is the velocity of the stream and a the local speed of sound).

The velocity regime of an adiabatic gas-stream current in the geometrical nozzle of an engine may be expressed as follows:

a) at the entrance to the chamber nozzle

$$M_x = \frac{w_x}{a_x} = \frac{w_x}{\sqrt{k g R_x T_x}} = \frac{w_x}{\sqrt{k \frac{p_x}{\rho_x}}}; \quad (3.19)$$

b) in any nozzle cross section

$$M = \frac{w}{a} = \frac{w}{\sqrt{k g R T}} = \frac{w}{\sqrt{k \frac{p}{\rho}}}, \quad (3.19')$$

with $RT = pv = p/\gamma = p/g\rho$.

For a subsonic flow $M < 1$, for a supersonic flow $M > 1$, and when $w = a$, $M = 1$.

In the presence of an adiabatic current, the temperature of a completely decelerated gas flow in any cross section at all in a combustion chamber and nozzle of the engine remains the same, i.e.,

$$T^* = T + \Delta T_{\text{дин}} = T + A \frac{w^2}{2gc_p} = \text{const}, * \quad (3.20)$$

where T and w are, respectively, the true temperature and velocity

$$*[\Delta T_{\text{дин}} = \Delta T_{\text{din}} = \Delta T_{\text{dinamicheskij}} = \Delta T_{\text{dynamic}}.]$$

of the gas flow before deceleration; and ΔT_{din} is the dynamic increase of the temperature as a consequence of the deceleration of the gas flow, attaining a considerable magnitude at velocities close to the speed of sound (for example, with a velocity $w = 10$ m/sec, $\Delta T_{\text{din}} = 0.05^\circ\text{C}$; when $w = 100$ m/sec, $\Delta T_{\text{din}} = 5.0^\circ\text{C}$, and when $w = 350$ m/sec, $\Delta T_{\text{din}} = 60^\circ\text{C}$).

Since from the equation of state for 1 kg of gas

$$c_p = \frac{k}{k-1} AR = \frac{k}{k-1} A \frac{p}{\rho T},$$

Expression (3.20) may be given the form

$$T^* = T + T \frac{k-1}{2} \frac{w^2}{k \frac{p}{\rho}} = T \left(1 + \frac{k-1}{2} M^2 \right). \quad (3.20')$$

We obtain an analogous expression for the temperature of the adiabatic deceleration of the gas flow in the inlet section of the engine nozzle:

$$T^* = T'_k \left(1 + \frac{k-1}{2} M_k^2 \right), \quad (3.20'')$$

where T'_k is the true temperature of the gas flow at the entrance to the nozzle with a velocity w_k .

Since, in existing engines, gas velocity w_k at the entrance to the nozzle is about 60-200 m/sec, one may assume that the values of the true temperature T'_k and the temperature T_k determined by the thermodynamic calculation of the engine, and the temperature T^*_k of the adiabatic deceleration of the gas flow (corresponding to $w_k = 0$) differ very little in practice.

By comparing the right-hand parts of Eqs. (3.20'') and (3.20'), we learn the relationship of the true temperatures of the gas flow for any two sections of the engine nozzle being studied:

$$\frac{T}{T'_k} = \frac{1 + \frac{k-1}{2} M_k^2}{1 + \frac{k-1}{2} M^2}. \quad (3.21)$$

Since, for these nozzle sections in the presence of an adiabatic gas flow, the temperatures are associated with the pressures and densities by the well-known equations

$$\frac{T}{T_k} = \left(\frac{p}{p_k}\right)^{\frac{k-1}{k}} = \left(\frac{\rho}{\rho_k}\right)^{\frac{k-1}{k}},$$

from which

$$\frac{p}{p_k} = \left(\frac{T}{T_k}\right)^{\frac{k}{k-1}} \quad \text{and} \quad \frac{\rho}{\rho_k} = \left(\frac{T}{T_k}\right)^{\frac{1}{k-1}},$$

then Eq. (3.21) may be given the form

$$\frac{p}{p_k} = \left(\frac{1 + \frac{k-1}{2} M_k^2}{1 + \frac{k-1}{2} M^2} \right)^{\frac{k}{k-1}}$$

and

$$\frac{\rho}{\rho_k} = \left(\frac{1 + \frac{k-1}{2} M_k^2}{1 + \frac{k-1}{2} M^2} \right)^{\frac{1}{k-1}}. \quad (3.21')$$

Analogously, one may obtain the relationships of the gas-flow parameters for the critical, outlet, or any of the cross sections of the engine nozzle.

If the velocity w_k of the gas flow at the outlet to the nozzle is practically negligible, and therefore one may accept $M_k = 0$, Eqs. (3.21) and (3.21') take the form

$$T/T'_k = T/T_k = (p/p_k)^{k-1/k} = 1/[1 + (k-1)/2M^2],$$

from which

$$M = \sqrt{\frac{2}{k-1} \left(\frac{T_k}{T} - 1 \right)} = \sqrt{\frac{2}{k-1} \left[\left(\frac{p_k}{p} \right)^{\frac{k-1}{k}} - 1 \right]};$$

$$\frac{p}{p_k} = \frac{p}{p_k} = \left(\frac{T}{T_k} \right)^{\frac{k}{k-1}} = \left(\frac{1}{1 + \frac{k-1}{2} M^2} \right)^{\frac{k}{k-1}}$$

and

$$\frac{\rho}{\rho_k} = \frac{\rho}{\rho_k} = \left(\frac{T}{T_k} \right)^{\frac{1}{k-1}} = \left(\frac{1}{1 + \frac{k-1}{2} M^2} \right)^{\frac{1}{k-1}}. \quad (3.21'')$$

Applying these expressions to the critical section of the nozzle, i.e., using $M = M_{kr} = 1$ in them, we will obtain, accordingly,

$$\frac{T_{kp}}{T_k} = \frac{2}{k+1}; \quad \frac{p_{kp}}{p_k} = \left(\frac{2}{k+1} \right)^{\frac{k}{k-1}} \text{ and } \frac{\rho_{kp}}{\rho_k} = \left(\frac{2}{k+1} \right)^{\frac{1}{k-1}}$$

For the combustion products of a ZhRD having a power of $k = 1.2$, we find $p_{kr} = 0.56 p_k$; $T_{kr} = 0.909 T_k$, and $\rho_{kr} = 0.621 \rho_k$.

The pressure of the adiabatically decelerated gas flow in any of the cross sections in the engine nozzle is determined by the adiabatic dependence of the gas's parameters, as well known from the techniques of thermodynamics:

$$p^* = p \left(\frac{T^*}{T} \right)^{\frac{k}{k-1}} \text{ atm abs,}$$

where p and T are the static absolute pressure and the corresponding temperature in any nozzle cross section.

The introduction into ZhRD theory of the concepts of the parameters of adiabatic gas deceleration considerably simplifies calculations in a number of cases, since by this means the necessity of considering the change of the kinetic energy of the gas flow along the length of the combustion chamber and nozzle of the engine is excluded.

The relationship of the velocities of the gas flow for the two sections of the engine nozzle being studied are determined from the expression

$$\frac{M}{M_k} = \frac{\frac{w}{\sqrt{k g R T}}}{\frac{w_k}{\sqrt{k g R T_k}}} = \frac{w}{w_k} \sqrt{\frac{T_k}{T}},$$

i.e.,

$$\frac{w}{w_k} = \frac{M}{M_k} \sqrt{\frac{T}{T_k}}, \quad (3.22)$$

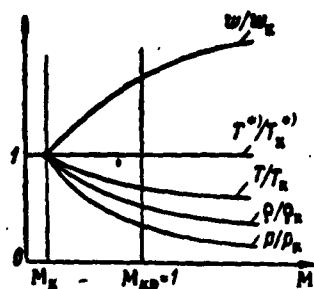


Fig. 3.8. Change of basic parameters of gas in the presence of an adiabatic current in an engine's geometrical chamber, dependent upon the Mach number.

since in the presence of an adiabatic gas flow $R_k = R'_k = \text{const.}$

After replacing T/T'_k in this formula with the expression from Eq. (3.21), we finally obtain

$$\frac{w}{w_k} = \frac{M}{M_k} \sqrt{\frac{1 + \frac{k-1}{2} M_k^2}{1 + \frac{k-1}{2} M^2}}. \quad (3.23) \quad (3.23)$$

Figure 3.8 shows the dependence of the parameters of the gas flow along the length of the geometrical nozzle on the Mach number.

In some cases design formulas are simplified if the parameters of the gas condition are determined in the form of dependences not on the Mach number, but on velocity factor $\lambda = w/w_{kr} = w/a_{kr}$.

The dependences of the change of temperature, pressure, and other parameters of the gas on the velocity factor λ are expressed by the following well-known formulas:

$$\frac{T}{T_k} = 1 - \frac{k-1}{k+1} \lambda^2;$$

$$\frac{p}{p_k} = \left(1 - \frac{k-1}{k+1} \lambda^2\right)^{\frac{k}{k-1}};$$

$$\frac{\rho}{\rho_k} = \left(1 - \frac{k-1}{k+1} \lambda^2\right)^{\frac{1}{k-1}};$$

$$\sqrt{\frac{k+1}{k-1} \left[1 - \left(\frac{p}{p_k}\right)^{\frac{k-1}{k}}\right]} = \sqrt{\frac{k+1}{k-1 + \frac{2}{M^2}}};$$

$$M = \lambda \sqrt{\frac{2}{k+1 - (k-1)\lambda^2}}.$$

Since in the calculations of a ZhRD a one-dimensional gas flow is being investigated, then, regardless of the nozzle profile, the only variable magnitude applicable to the nozzle is the area F of its flow-through section.

Because pressure p is the basic parameter characterizing the change in the state of the gas stream along the length of the nozzle, we ordinarily determine the dependence of the change of p on F , and then compute the other parameters of the gas corresponding to this pressure.

The relationship of the arbitrary and critical cross sections of the engine nozzle, depending on the pressure of the gas flow, is determined from the equation of continuity of flow, written in conformity to these nozzle sections:

$$G = F w p = F_{kp} w_{kp} p_{kp} = \text{const}, \quad (3.24)$$

i.e.,

$$\frac{F}{F_{kp}} = \frac{w_{kp}}{w} \frac{p_{kp}}{p}.$$

After substitution in this equation of the well-known expressions for w_{kp} , w , p_{kp} , and p and the corresponding changes, we finally obtain

$$\begin{aligned} f = \frac{F}{F_{kp}} &= \left[\frac{2}{k+1} \right]^{\frac{1}{k-1}} \left(\frac{p_k}{p} \right)^{\frac{1}{k}} \sqrt{\frac{k-1}{k+1} \left[1 - \left(\frac{p_k}{p} \right)^{\frac{k-1}{k}} \right]} = \\ &= \frac{1}{M} \left(\frac{1 + \frac{k-1}{2} M^2}{\frac{k+1}{2}} \right)^{\frac{k+1}{2(k-1)}} = \frac{1}{\lambda} \left(\frac{\frac{2}{k+1}}{1 - \frac{k-1}{k+1} \lambda^2} \right)^{\frac{1}{k-1}}. \end{aligned} \quad (3.25)$$

This equation gives the necessary connection between the magnitude F of the nozzle's (flow-through) cross section and the pressure of the gas flow in the given section (with given values of F_{kp} and p_k) and also may be used to determine the outlet section F_v of the nozzle at a gas pressure p_v .

The connection between F and p is not direct, but, having established the necessary relationship p_k/p , we may determine the unknown relationship of areas $f = F/F_{kp}$ (Fig. 3.9) in accordance with the equation given.

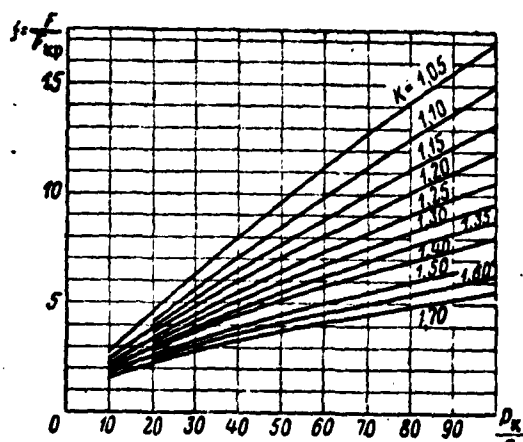


Fig. 3.9. Values of F/F_{kr} , dependent on relationship p_k/p_v and adiabatic exponent k or polytropic exponent n .

Assuming a series of values for gas-stream pressures along the length of the engine chamber nozzle, one may compute the other gas parameters corresponding to them:

$$T = T_k \left(\frac{p}{p_k} \right)^{\frac{k-1}{k}}; \quad \rho = \rho_k \left(\frac{p}{p_k} \right)^{\frac{1}{k}};$$

$$\gamma = \gamma_k \left(\frac{p}{p_k} \right)^{\frac{1}{k}}; \quad v = v_k \left(\frac{p_k}{p} \right)^{\frac{1}{k}};$$

$$w = \lambda w_{kp} = \sqrt{\frac{k+1}{k-1} \left[1 - \left(\frac{p}{p_k} \right)^{\frac{k-1}{k}} \right]} =$$

$$= \sqrt{2g \frac{k}{k-1} R_k T_k \left[1 - \left(\frac{p}{p_k} \right)^{\frac{k-1}{k}} \right]},$$

where

$$w_{kp} = \sqrt{2g \frac{k}{k+1} R_k T_k} = \sqrt{g k R_k T_{kp}}.$$

Having the basic geometrical dimensions of the nozzle and having drawn it in the corresponding scale, according to the expression $d = \sqrt{4F/\pi}$ one may determine the sections which will correspond to the computed values of the parameters of the gas flow and plot the curves of their change along the length of the chamber nozzle (Fig. 3.10).

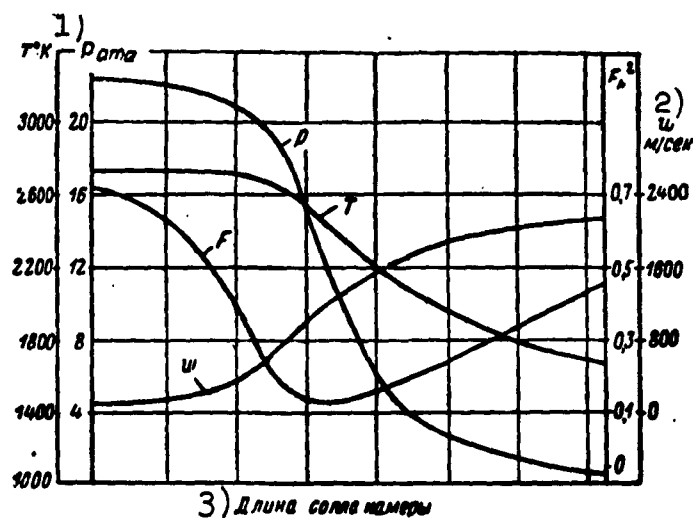


Fig. 3.10. Change of gas-flow parameters along the length of an engine chamber nozzle. 1) p , atm abs; 2) w , m/sec; 3) length of chamber nozzle.

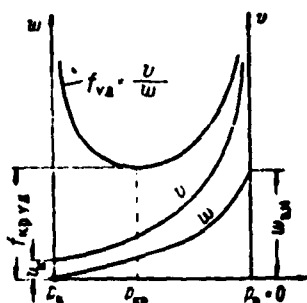


Fig. 3.11. Dimensionless area of an engine's geometrical nozzle, dependent on Mach number in the presence of an adiabatic gas current.

The equations derived here for an adiabatic gas current are also applied for isentropic and polytropic processes of gas expansion in the engine nozzle upon condition that the adiabatic exponent k in these equations is replaced by the isentropic or polytropic exponent n .

Ordinarily the polytropic exponent $n \approx 1.10-1.20$ and $F_v/F_{kr} \approx 3-4$.

Upon increase of k , the relationship F_v/F_{kr} is decreased, which shows the advantage of using fuels whose combustion products have a greater value of k .

The greater the pressure difference p_k/p_v of the gases in the nozzle, the greater the length of the nozzle at a given flare angle, the nozzle surface, and its weight.

In the presence of a subsonic current, gas velocity w is increased more intensively than specific volume v , and just the opposite in the presence of a supersonic current. Therefore the area of the

nozzle channel in the subsonic region must be decreased, and increased in the supersonic region, which is obvious from the equation of continuity of the gas stream $F = Gv/w$ (Fig. 3.11).

Consequently, the critical section of the engine nozzle is the boundary where the character of the geometrical influence on the gas flow changes to the opposite sign.

In an actual process, heat $dQ > 0$, and the gas friction work $dL > 0$; therefore the equality of velocities $w = a$ is established where $dF > 0$, i.e., in the expanding portion of the nozzle. This means that the gases' velocity in the narrowest section of the nozzle is less than the speed of sound.

Example 2. Construct the curves of the adiabatic change of gas flow parameters v , T , w , F , and M , depending on the length of the nozzle, if $p_k = 21$ atm abs; $p_v = 1.03$ atm abs; $T_k = 2200^\circ\text{K}$; $G_g = G_s = 1$ kg/sec; $v_k = 0.373$ m³/kg; $R_k = 35.3$ kg-m/kg-^oC, and $k = 1.3$.

Solution.

We assume throughout the nozzle length, a series of values for gas pressure: $p = 17.5, 14.0, 11.5, 7.0$ and 4.2 atmospheres absolute and for each of them we determine the area of the cross section of the nozzle.

With a pressure $p = 17.5$ atm abs we have:

1) specific volume of gases

$$v = v_k \left(\frac{p_k}{p} \right)^{\frac{1}{k}} = 0.373 \left(\frac{21}{17.5} \right)^{1/1.3} = 0.43 \text{ m}^3/\text{kg};$$

2) gas temperature

$$T = T_k \left(\frac{p}{p_k} \right)^{\frac{k-1}{k}} = 2200 \left(\frac{17.5}{21} \right)^{\frac{1.3-1}{1.3}} = 2100^\circ\text{K};$$

3) exit velocity

$$w = \sqrt{2g \frac{k}{k-1} R_k T_k \left[1 - \left(\frac{p}{p_k} \right)^{\frac{k-1}{k}} \right]} -$$

$$= \sqrt{2 \cdot 9,81 \cdot 35,3 \cdot 2220 \left[1 - \left(\frac{17,5}{21} \right)^{\frac{1,3-1}{1,3}} \right]} = 530 \text{ m/sec};$$

4) area of the nozzle cross section

$$F = \frac{G_s v}{w} = \frac{10 \cdot 0,43}{530} = 0,000812 \text{ m}^2 = 8,12 \text{ cm}^2;$$

5) relationship of local velocity to the speed of sound

$$M = \frac{w}{\sqrt{k g R T}} = \frac{530}{\sqrt{9,81 \cdot 1,3 \cdot 35,3 \cdot 2100}} = 0,53.$$

Analogously, we determine the parameters of the gas flow at the other chosen values of pressure and reduce the results of the calculations in Table 3.2.

TABLE 3.2

1) p kg/cm ²	2) v m ³ /kg	T °K	3) w m/sec	w/v	F cm ²	M
$p_k=21$	0,37	2200	0	0	—	0
17,5	0,43	2100	530	1230	3,12	0,53
14,0	0,51	2020	775	1520	6,50	0,81
$p_{kp}=11,5$	0,60	1930	980	1550	6,32	1,00
7,0	0,88	1720	1220	1390	7,10	1,42
4,2	1,30	1530	1440	1110	8,82	1,79
$p_n=1,03$	3,80	1105	1830	482	20,20	2,89

1) p , kg/cm²; 2) v , m³/kg; 3) w , m/sec.

Example 3. Determine the basic geometrical dimensions of an engine chamber nozzle if $G_s = 13.54$ kg/sec; $p_k = 20$ atm abs; $T_k = 2787^\circ\text{K}$; $\gamma_k = 2.023$ kg/m³; $w_v = 2174$ m/sec; $\gamma_v = 0.153$ kg/m³; $R = 35.25$ kg-m/kg-°C, and $n = 1.16$.

Solution.

1. Parameters of the gas mixture in the critical section of the nozzle

$$T_{kp} = \frac{2T_k}{n+1} = \frac{2 \cdot 2787}{1,16+1} = 2580^\circ\text{K};$$

$$p_{kp} = p_k \left(\frac{2}{n+1} \right)^{\frac{n}{n-1}} = 20 \left(\frac{2}{1.16+1} \right)^{\frac{1.16}{1.16-1}} = 11.43 \text{ kg/cm}^3;$$

$$\gamma_{kp} = \frac{p_{kp}}{R T_{kp}} = \frac{11.43 \cdot 10^4}{35.27 \cdot 2580} = 1.257 \text{ kg/cm}^3;$$

$$w_{kp} = \sqrt{g n R T_{kp}} = \sqrt{9.81 \cdot 1.16 \cdot 35.27 \cdot 2580} = 1017 \text{ m/sec.}$$

2. Basic geometrical dimensions of the nozzle:

$$F_{kp} = \frac{G_g}{w_{kp} \gamma_{kp}} = \frac{13.54 \cdot 10^4}{1017 \cdot 1.257} = 105.9 \text{ cm}^2;$$

$$d_{kp} = 1.128 \sqrt{F_{kp}} = 1.128 \sqrt{105.9} = 13.17 \text{ cm} = 131.7 \text{ mm};$$

$$F_g = \frac{G_g}{w_g \gamma_g} = \frac{13.54 \cdot 10^4}{2174 \cdot 0.153} = 407.1 \text{ cm}^2;$$

$$d_g = 1.128 \sqrt{F_g} = 1.128 \sqrt{407.1} = 25.6 \text{ cm} = 256 \text{ mm}.$$

Example 4. Determine the theoretical specific thrust at ground level and the specific areas of the critical and outlet sections of the nozzle of an engine chamber, operating on kerosene and nitric acid of 96% weight concentration, when $\alpha = 0.78$; $p_k = 40 \text{ atm abs}$, and $p_v = 0.8 \text{ atm abs}$, if the thermodynamic calculations produce the following theoretical parameters of the gases in the combustion chamber: $T_k = 2900^\circ\text{K}$, $R_k = 34 \text{ kg-m/kg-}^\circ\text{C}$, and $k = 1.16$.

Solution.

1. Density of the gas in the combustion chamber

$$\gamma_k = \frac{p_k}{R_k T_k} = \frac{40 \cdot 10^4}{34 \cdot 2900} = 4.06 \text{ kg/m}^3.$$

2. Parameters of the gas in the outlet section of the chamber nozzle:

a) temperature

$$T_g = T_k \left(\frac{p_g}{p_k} \right)^{\frac{k-1}{k}} = 2900 \left(\frac{0.8}{40} \right)^{\frac{1.16-1}{1.16}} = 2900 \cdot 0.5839 = 1690^\circ\text{K};$$

b) density

$$\gamma_g = \gamma_k \left(\frac{T_g}{T_k} \right)^{\frac{1}{k-1}} = 4.06 \left(\frac{1690}{2900} \right)^{\frac{1}{1.16-1}} = 4.06 \cdot 0.052 = 0.21 \text{ kg/m}^3;$$

c) velocity factor

$$\lambda_g = \sqrt{\frac{k+1}{k-1} \left[1 - \left(\frac{p_g}{p_k} \right)^{\frac{k-1}{k}} \right]} = \sqrt{\frac{1.16+1}{1.16-1} \left[1 - \left(\frac{0.8}{40} \right)^{\frac{1.16-1}{1.16}} \right]} = 2.37;$$

d) exit velocity

$$w_0 = \lambda_{\text{кр}} a_{\text{кр}} = \lambda_{\text{с}} \sqrt{2g \frac{k}{k+1} R_k T_k} =$$

$$= 2,37 \sqrt{2 \cdot 9,81 \frac{1,16}{1,16+1} 34 \cdot 2900} = 2418 \text{ m/sec};$$

e) relative area of the outlet section of the chamber nozzle

$$f_{\text{с}} = \frac{F_{\text{с}}}{F_{\text{кр}}} = \frac{1}{\lambda_{\text{с}}} \left(\frac{\frac{2}{k+1}}{1 - \frac{k-1}{2} \lambda_{\text{с}}^2} \right)^{\frac{1}{k-1}} =$$

$$= \frac{1}{2,37} \left(\frac{\frac{2}{1,16+1}}{1 - \frac{1,16-1}{2} \cdot 2,37^2} \right)^{\frac{1}{1,16-1}} = 5,024;$$

f) specific area of the outlet section of the chamber nozzle

$$f_{y_{\text{с.с}}} = \frac{1}{w_0 \gamma_0} = \frac{1}{2418 \cdot 0,21} = 0,001974 \text{ m}^2/\text{kg} = 19,74 \text{ cm}^2/\text{kg};$$

g) specific area of the critical section of the chamber nozzle

$$f_{y_{\text{к.кр}}} = f_{\text{с}} f_{y_{\text{с.с}}} = 5,024 \cdot 19,74 = 99,3 \text{ cm}^2/\text{kg}.$$

3. Specific thrust of the engine chamber

$$P_{y_{\text{с.с}}} = \frac{P_{\text{с}}}{G_{\text{с}}} = \frac{\frac{Q_{\text{с}}}{g} w_0 + F_{\text{с}} (p_{\text{с}} - p_{\text{а}})}{G_{\text{с}}} = \frac{w_0}{g} + \frac{F_{\text{с}}}{G_{\text{с}}} (p_{\text{с}} - p_{\text{а}}) =$$

$$= \frac{w_0}{g} + f_{y_{\text{с.с}}} (p_{\text{с}} - p_{\text{а}}) = \frac{2418}{9,81} + 19,34 (0,8 - 1) = 243,052 \text{ kg-sec/kg}.$$

Chapter IV

ZhRD OPERATING REGIMES

In use, a ZhRD operates under various internal regimes and external conditions.

Control of the magnitude of engine thrust is usually accomplished by a change in the per-second rate of fuel flow into the combustion chamber and by a pressure change in the latter. By this means, not only is the thrust changed, but the engine operating economy as well.

With a change in the conditions of the surrounding medium, the basic parameters of the ZhRD are also changed, since, in this case, the back pressure behind the nozzle is reduced, which, other things being equal, is also reflected in the magnitudes of the engine's absolute and specific thrusts. In designing ZhRD weapons, one must know the basic parameters of the engine (absolute and specific thrusts) under rated and various nonrated static operating regimes at ground or sea level or in flight conditions. The basic factors determining the operating regime of the engine and upon which absolute and specific thrust depend, i.e., pressure in the combustion chamber, flight altitude, etc., are called engine characteristics.

In this chapter there is a discussion of ZhRD characteristics under possible internal regimes and conditions of operation, and methods are laid down for thus determining absolute and specific thrust as well as specific fuel consumption and other parameters for engine design.

Furthermore, a brief analysis of the factors affecting the magnitude of specific thrust is given, and suggestions are made for increasing engine operating economy.

This material facilitates determination of the optimum parameters and selection of an expedient operating regime for the engine being designed.

SECTION 1. RATED AND NONRATED ENGINE OPERATING REGIMES

The operational condition of a ZhRD is characterized by a set of parameters determining its efficiency, absolute and specific thrusts, and the heat, static, and dynamic loads on individual engine elements; the accepted designation of this state is the operating regime of the engine and the parameters of the operating process in the engine which correspond to it, such as fuel flow rate per second and composition factor, pressure in the combustion chamber and in the nozzle outlet section, and others, as engine operating-regime parameters.

By the use of a ZhRD thermodynamic rating, one may evaluate the basic engine characteristics only under certain rated operational conditions alone.

In operational conditions, absolute and specific engine thrusts may change subject to the internal operating regime of the engine (from a change of gas pressure in the combustion chamber as a result of a change of the per-second fuel flow rate in it or the weight relationship of its components) and external conditions (flight altitude and velocity or pressure of the surrounding medium).

If a ZhRD operates at a rated per-second rate of fuel flow into the combustion chamber (i.e., rated pressure in the chamber), the regime is referred to as rated, and if the per-second fuel flow rate to the combustion chamber is greater or smaller than rated, the regime is

referred to as nonrated.

The ratio of gas pressure p_k in the combustion chamber at a given engine operating regime to the gas pressure p_v in the outlet section of the nozzle of this chamber is called the gas expansion ratio in the nozzle.

If, in the chamber nozzle, the gases expand up to the ambient air pressure ($p_v = p_a$), the gas expansion ratio in the nozzle and the nozzle operating regime are referred to as optimum; if the gases in the nozzle exceed or fail to attain the ambient air pressure ($p_v \gtrless p_a$), the gas expansion ratio in the nozzle and the nozzle operating regime is called nonoptimum.

A change in the operating regime of an engine nozzle may be caused by a change in the per-second fuel flow rate to the combustion chamber relative to the rated value, or by a change in flight altitude (atmospheric pressure). An engine nozzle may operate on an optimum regime only if the values of altitude and flight speed of the missile and the per-second rate of fuel flow to the combustion chamber are constant. Under operating conditions the chamber nozzles of missile engines usually operate at nonoptimum regimes of overexpansion and underexpansion of the gases.

The most advantageous engine operating regime is the regime rated at optimum gas expansion in the nozzle. This operating regime is called optimum, since it corresponds to the greatest values of actual efficiency and specific thrust relative to their values when the chamber nozzles operate under nonoptimum regimes (underexpansion and overexpansion of the gases in the nozzle). Numerical values of operating parameters are usually given for the engine's work at this regime.

Existing ZhRD may be divided into two groups depending on the operating regime of the engine nozzle at ground or sea level:

1) low-altitude engines, in which, during normal operation at ground or sea level, gas pressure in the outlet section of the nozzle is equal to or greater than atmospheric pressure, i.e., when $p_v = p_a$;

2) high-altitude engines, in which, during normal operation at ground or sea level, gas pressure in the outlet section of the nozzle is less than the pressure of the atmospheric air, i.e., when $p_v < p_a$.

A high-altitude engine may operate on a regime of optimal gas expansion in the nozzle only at a rated altitude H_{rasch} ,* where an equality between p_v and p_a is attained.

The basic characteristic of a high-altitude engine is the magnitude of the gas pressure p_v in the nozzle outlet section. Consequently, by a rated altitude of an engine nozzle, we understand that rated flight altitude where $p_v = p_a$.

Depending on the rated altitude of the nozzle, the accepted subdivision of liquid-fuel rocket engines is into engines of moderate altitude (when $p_v > 0.6$ atm abs) and of high altitude (when $p_v < 0.6$ atm abs). The engines of the last stages of multistage missiles are of the high-altitude type.

SECTION 2. OPERATIONAL ENGINE OPERATING REGIMES

With regard to the per-second fuel flow rate into the combustion chamber, we may distinguish the following characteristic operating regimes (thrusters) of an engine.

1. Starting, constituting the operation of an engine in the period from the instant fuel is ignited in the combustion chamber until the engine reaches its operating regime.

2. Nominal thrust regime, corresponding to continuous normal load of the engine at a nominal (specific) rate of propellant consumption

*[$H_{\text{pacu}} = H_{\text{rasch}} = H_{\text{raschetnaya}} = H_{\text{rated}}$.]

by the engine chamber.

3. Maximum thrust regime, corresponding to a brief maximum engine load at the maximum permissible flow rate intensity of its combustion chamber and an increase in the specific propellant (fuel) consumption in comparison to the nominal regime.

Other conditions being equal, such forced engine operation is combined with a deterioration in engine operating economy because of the inadequate volume of the combustion chamber or the nonrated per-second fuel flow rate into the combustion chamber, and other reasons.

A temporary increase in engine thrust relative to the rated nominal thrust may necessitate an increase in the weapon's rate of climb, decrease of the length of the aerodynamic vehicle's run at blastoff, or a temporary increase of maximum flight speed.

In operation, a ZhRD seldom operates at a maximum thrust regime. Usually, an engine operates with a thrust less than maximum the greater part of the time.

4. Minimum thrust regime, corresponding to the minimum permissible load of the engine, below which its operation becomes unstable.

The value of minimum thrust depends on the engine design and designation and sometimes amounts to about 10-30% of nominal thrust.

5. Operational regime, corresponding to engine loads in the range from minimum to established maximum thrust magnitude, within which stable engine operation is ensured.

The duration of ZhRD operation at pertinent regimes is established by the engine designer.

The above classification of operating (thrust) regimes of an engine may have particular significance for main engines and aircraft vernier engines. Boosters have only one operating regime.

6. Stable operating regime of the engine, corresponding to the

load at which the fuel combustion process in the chamber occurs without anomalous pulsations in gas pressure.

SECTION 3. FACTORS AFFECTING THE INTENSITY OF ZhRD THRUST

The result of all hydrodynamic pressure forces operating on an engine chamber in the presence of outflow of gases from it to the surrounding medium is called the thrust of a ZhRD.

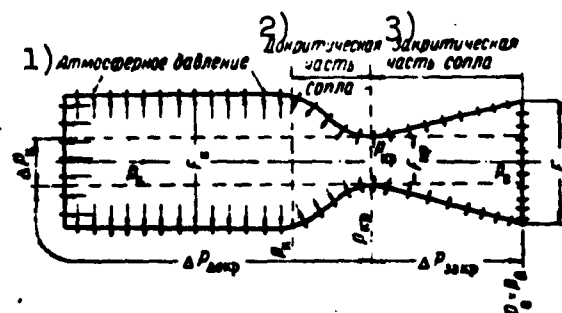


Fig. 4.1. Definition of the thrust of a ZhRD as the force resulting from the influence of gas pressure on the internal surface and air pressure on the external surface of the engine chamber. 1) Atmospheric pressure; 2) subcritical part of the nozzle; 3) hypercritical part of the nozzle.

The thrust of an engine, neglecting atmospheric air pressure (when the engine is operating in space), is dependent upon the following three forces of gas pressure working on the combustion chamber and nozzle in the direction of the nozzle-combustion chamber axis (Fig. 4.1):

1) the unbalanced force of gas pressure on the surface of the combustion chamber head, equal to the pressure p_k produced in the chamber on the area of the head, in a magnitude equal to the area F_{kr} , of the critical section of the nozzle, i.e.,

$$\Delta P_k = p_k F_{kr}; \quad (4.1)$$

2) a force equal to the difference of the gas pressure forces act-

ing on the remaining part of the combustion chamber head (area $F_k - F_{kr}$), and the subcritical part of the nozzle which has the same area in the direction of the engine's axis:

$$\Delta P_{dokr} = (p_k - p_{rez.dokr})(F_k - F_{kr}); * \quad (4.2)$$

3) the unbalanced force of the gas pressure on the hypercritical part of the nozzle which has the area $F_v - F_{kr}$ in the direction of the engine's axis

$$\Delta P_{zagr} = p_{rez.zagr}(F_v - F_{kr}), ** \quad (4.3)$$

that is,

$$P_p = \Delta P_k + \Delta P_{dokr} + \Delta P_{zagr}, \quad (4.4)$$

where p_k is the absolute gas pressure in the combustion chamber (pressure on the chamber head) in atm abs; F_k and F_v are the area of the greatest cross sections in the combustion chamber and the outlet section of the nozzle, respectively; $p_{rez.dokr}$ and $p_{rez.zagr}$ are the resultant absolute gas pressures on the subcritical and hypercritical nozzle sections, respectively, in atm abs.

Gas-pressure forces on the engine chamber in a direction perpendicular to its axis balance each other in a manner analogous to the forces of air pressure on an engine during its operation in the atmosphere (see Fig. 4.1).

The resultant of all axial forces caused by the pressure of the liquid in the cooling duct of the engine chamber is usually negligible.

The absolute thrust of an engine chamber when operating in the atmosphere is expressed by the equation

$$* [p_{pez.dokr} = p_{rez.dokr} = p_{rezul'tiruyushchaya.dokriticheskaya} = p_{resultant.subcritical}]$$

$$** [p_{pez.zagr} = p_{rez.zagr} = p_{rezul'tiruyushchaya.zakriticheskaya} = p_{resultant.hypercritical}]$$

$$P_H = P_p - F_v p_a, \quad (4.5)$$

where $F_v p_a$ is the force of the counter pressure of the atmospheric air on the gas flow in the outlet section of the engine chamber nozzle.

Thrust magnitude P_p depends only on the internal conditions of the operation of a given engine, characterized by the pressure p_k in the combustion chamber, and the term $F_v p_a$ depends only on the external conditions of the engine's operation, i.e., on the pressure p_a of the surrounding medium. When the engine is operating in space, where $p_a = 0$, the term $F_v p_a = 0$.

The thrust of an existing engine may be determined on a test stand under fixed atmospheric conditions.

SECTION 4. THE ABSOLUTE THRUST OF AN ENGINE

The absolute thrust of a liquid-fueled rocket engine chamber usually consists of:

1) the dynamic thrust component, equal to the change of momentum of the combustion products of the per-second fuel flow rate to the combustion chamber of the engine:

$$P_{dyn} = \frac{G_s}{g} \cdot w \text{ kg}; \quad (4.6)$$

2) the static thrust component, equal to the force of the pressure on the engine of the fuel combustion products which are expanding behind the nozzle:

$$P_{st} = F_s (p_s - p_a) \text{ kg}, * \quad (4.7)$$

that is,

$$\begin{aligned} P_s &= P_{dyn} + P_{st} = \frac{G_s}{g} w_s + F_s (p_s - p_a) = \\ &= \frac{G_s}{g} w_s + F_s p_s \left(1 - \frac{p_a}{p_s}\right) = \frac{G_s}{g} w_{s, \phi, n}. \end{aligned} \quad (4.8)$$

*[$P_{st} = P_{st} = P_{sticheskiy} = P_{static}$.]

This expression is called the general thrust equation of an engine. This equation may be given other expressions, often encountered in the literature, if you consider that

$$\left. \begin{aligned} w_s &= 91,53 \sqrt{H_s \gamma_s}; F_s = G_s / w_s \gamma_s = G_s v_s / w_s \text{ и } p_s v_s = R_s T_s, \\ \text{i.e.,} \\ p_s &= \frac{G_s}{g} 91,53 \sqrt{H_s \gamma_s} + F_s (p_s - p_a) = \\ &= 9,33 G_s \sqrt{H_s \gamma_s} + F_s (p_s - p_a) = \frac{G_s}{g} w_{s\phi s}; \\ p_s &= \frac{G_s}{g} w_s + \frac{G_s}{w_s \gamma_s} (p_s - p_a) = \frac{G_s}{g} \left(w_s + g \frac{p_s - p_a}{w_s \gamma_s} \right); \\ p_s &= \frac{G_s}{g} w_s + \frac{G_s v_s}{w_s} p_s \left(1 - \frac{p_s}{p_a} \right) = \frac{G_s}{g} \left[w_s + \frac{g R_s T_s}{w_s} \left(1 - \frac{p_s}{p_a} \right) \right]. \end{aligned} \right\} \quad (4.8')$$

The latter two equations permit the determination of an engine's thrust independently of its geometrical dimensions.

The thrust equation may also be given this form:

$$\begin{aligned} P_s &= \frac{G_s}{g} w_s + F_s p_s - F_a p_a = F_s p_s \left(1 + \frac{G_s w_s}{g F_s p_s} \right) - F_a p_a = \\ &= F_s p_s \left(1 + \frac{F_s w_s \gamma_s w_s}{g F_s p_s} \right) - F_a p_a = F_s p_s \left(1 + \frac{n}{n} \frac{w_s^2}{g} \frac{\gamma_s}{p_s} \right) - F_a p_a = \\ &= F_s p_s \left(1 + n \frac{w_s^2}{n g R_s T_s} \right) - F_a p_a \end{aligned}$$

or, finally,

$$P_s = F_s p_s (1 + n M_s^2) - F_a p_a = \frac{G_s}{g} w_{s\phi s}, \quad (4.8'')$$

where n is the exponent of polytropic gas expansion in the nozzle, $M_v = w_v / a_v$ is the ratio of the gas exhaust velocity w_v in the outlet section of the nozzle to the local speed of sound a_v (Mach number).

The general thrust equation may be used for calculation of engine characteristics.

In the chamber of an engine operating on a given fuel when $p_v / p_a \geq 0.3-0.4$, the value of p_k / p_v is not dependent on G_s or p_k ; the pressure p_v does not depend on p_a , but upon p_k ; velocity w_v does not depend on p_k and p_a , but upon p_k / p_v (on the dimensions of the chamber

nozzle), i.e., for a given chamber at standard operating conditions, the magnitude of w_v is constant.

For calculating flow rate characteristics, the general thrust equation must be reduced to another form.

If, in the general thrust equation of an engine

$$P_n = \frac{G_s}{g} w_s + F_s (p_s - p_a)$$

we substitute

$$G_s = \frac{F_{kp} w_{kp}}{v_{kp}}, \text{ then } w_s = \sqrt{2g \frac{n}{n-1} p_k v_k \left[1 - \left(\frac{p_s}{p_k} \right)^{\frac{n-1}{n}} \right]},$$

$$w_{kp} = \sqrt{2g \frac{n}{n+1} p_k v_k} \text{ and } v_{kp} = v_k \left(\frac{n+1}{2} \right)^{\frac{1}{n-1}},$$

we will obtain

$$P_n = \frac{F_{kp} w_{kp}}{v_{kp}} \frac{w_s}{g} + F_s (p_s - p_a) =$$

$$= p_k F_{kp} \sqrt{\frac{2n^2}{n-1} \left(\frac{2}{n+1} \right)^{\frac{n+1}{n-1}} \left[1 - \left(\frac{p_s}{p_k} \right)^{\frac{n-1}{n}} \right]} + F_s (p_s - p_a). \quad (4.8''')$$

This equation shows that the absolute thrust of an engine is proportional to the pressure p_k in the combustion chamber and the area F_{kr} of the critical section of the nozzle.

When an engine is operating in space, where $p_a = 0$ and therefore $F_v p_a = 0$, Eqs. (4.8) through (4.8''') are expressed as follows:

$$\left. \begin{aligned} P_n &= 9.33 G_s \sqrt{H_n T_n} + F_s p_s = \frac{G_s}{g} w_{s,n}; \\ P_n &= \frac{G_s}{g} w_s + F_s p_s; \\ P_n &= \frac{G_s}{g} \left(w_s + \frac{g R_s T_s}{w_s} \right); \\ P_n &= F_s p_s (1 + n M_n^2); \\ P_n &= p_k F_{kp} \sqrt{\frac{2n^2}{n-1} \left(\frac{2}{n+1} \right)^{\frac{n+1}{n-1}} \left[1 - \left(\frac{p_s}{p_k} \right)^{\frac{n-1}{n}} \right]} + F_s p_s. \end{aligned} \right\} \quad (4.9)$$

When changes occur in combustion chamber pressure p_k , altitude H , and flight speed V , the absolute thrust of a given engine changes,

since

$$p_v = f(p_k) \text{ and } p_a = f'(H, V).$$

With a constant G_s and the same nozzle dimensions, P_{din} is not changed, and P_{st} may be changed only by a change of p_a . When $p_v = p_a$ the value of $P_{st} = 0$, when $p_v > p_a$ it is positive, and when $p_v < p_a$, it is negative (Fig. 4.2).

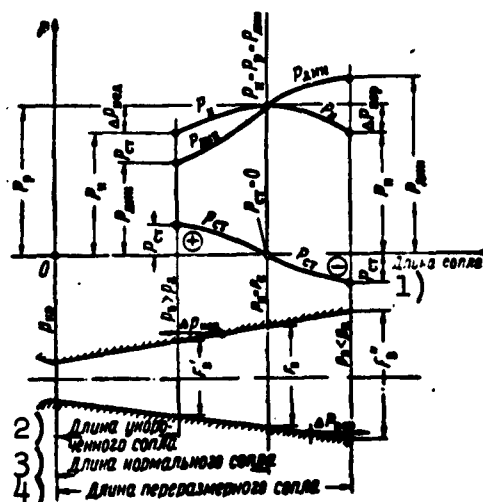


Fig. 4.2. Absolute thrust of an engine as a function of nozzle length at rate of fuel flow to combustion chamber. 1) Nozzle length; 2) length of a shortened nozzle; 3) normal nozzle length; 4) extended nozzle length.

Expansion of the gases in an engine chamber nozzle up to the pressure of the surrounding medium is possible only when the nozzle is of normal length.

The absolute thrust of an engine when the nozzle is operating on an optimum (rated) regime is expressed as follows

$$P_{opt} = P_p = P_r = P_{raschetnyy} = \frac{G_s}{g} w_s^* \quad (4.10)$$

$$*[P_{ont} = P_{opt} = P_{optimal'nyy} = P_{optimum}; P_p = P_r = P_{raschetnyy} = P_{rated}']$$

The optimum operating regime of a ZhRD nozzle is the most advantageous since, other conditions being equal, the engine develops maximum thrust under this regime.

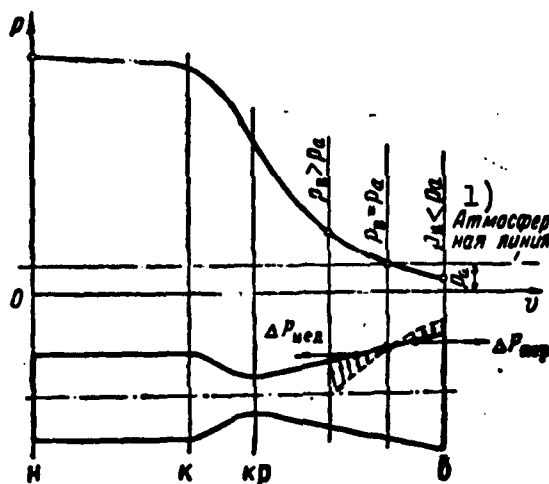


Fig. 4.3. Change of gas pressure on the surface of a shortened, normal, and lengthened nozzle. 1) Atmosphere line.

An engine's thrust P_n when the nozzle operates at a regime of underexpansion or overexpansion of gases is always less than the engine's thrust P_{opt} obtained at rated optimum operating regime of the combustion chamber and nozzle, according to the magnitudes (Fig. 4.2 and 4.3):

$$\Delta P_{ned} = (F_n - F_s) p_{rez.ned}^*$$

and

$$\Delta P_{nep} = (F_n - F_s) p_{rez.nep}^{**} \quad (4.11)$$

where $p_{rez.ned}$ and $p_{rez.per}$ are the resultant true gas pressures on the surface of the shortened and lengthened parts, respectively, of the engine chamber nozzle.

$$\begin{aligned} &^*[\Delta P_{ned} = \Delta P_{ned} = \Delta P_{nedorasshirenie} = \Delta P_{underexpansion}; \\ &\quad p_{rez.ned} = p_{resultant.underexpansion}.] \\ &^{**}[\Delta P_{nep} = \Delta P_{nep} = \Delta P_{pererasshirenie} = \Delta P_{overexpansion}; \\ &\quad p_{rez.nep} = p_{resultant.overexpansion}.] \end{aligned}$$

Therefore, the absolute thrust of an engine chamber, when the nozzle is operating on a nonoptimum regime, will be:

1) in case of underexpansion of the gases in the nozzle

$$P_n = P_{out} - \Delta P_{ned}$$

from whence $P_{opt} = P_n + \Delta P_{ned}$;

2) in case of overexpansion of the gases in the nozzle

$$P_n = P_{out} - \Delta P_{sep}$$

from whence $P_{opt} = P_n + \Delta P_{per}$.

Consequently, at given values of G_s and p_k , shortening or lengthening of a given engine nozzle will lead to a change in the magnitudes of p_v and w_v , and P_{din} and P_{st} . For example, when a nozzle of normal length is shortened, p_v increases and P_{din} decreases as the consequence of some underexpansion of the gases in the nozzle, and P_{st} increases because of the increase in the pressure difference of the gases behind the nozzle, as a result of which the engine's thrust is, accordingly, decreased relative to the rated optimum magnitude P_{opt} .

Change of an engine's absolute thrust, depending on the change of nozzle length, corresponds to a definite change of altitude H or flying speed V .

The thrust of a low-altitude engine, when operating at a certain altitude H , is expressed by the equation

$$P_H = P_{out} + F_s (\rho_s - \rho_a). \quad (4.12)$$

A low-altitude engine in space develops approximately 10 to 20% greater thrust than at ground level.

Since the engine of a long-range missile usually operates in the rarefied layers of the atmosphere during the greater part of the time, it is expedient to make it a high-altitude engine, i.e., with a relatively lengthened nozzle at ground or sea level (when $p_v < p_a$).

Such a high-altitude engine, when operating at ground level or at

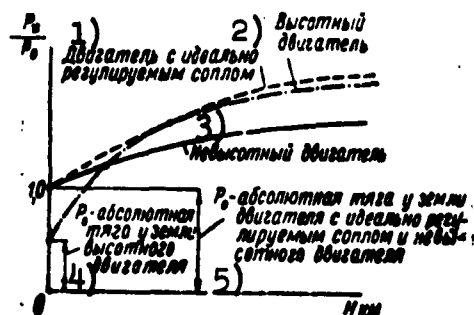


Fig. 4.4. Change of absolute thrust of low-altitude and high-altitude engines, depending on flight altitude H . 1) Engine with ideal regulating nozzle; 2) high-altitude engine; 3) low-altitude engine; 4) P_0 - absolute thrust of a high-altitude engine at ground level; 5) P_0 - absolute thrust at ground level of an engine with ideal regulating nozzle and low-altitude engine.

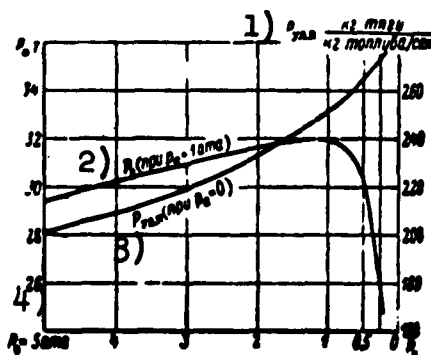


Fig. 4.5. Absolute thrust of an engine chamber operating at ground level and its specific thrust in space, depending on p_v when p_k is constant. 1) $P_{ud.p}$, kg thrust/kg fuel per sec; 2) P_0 (when $p_a = 1$ atm abs); 3) $P_{ud.p}$ (when $p_a = 0$); 4) $P_v = 5$ atm abs.

low altitudes, will develop less thrust than a low-altitude engine (with a normal nozzle length). However, to make up for that, as it rises in altitude the thrust of such an engine becomes, other things being equal, greater than the thrust of a low-altitude engine within a short time (Fig. 4.4).

A missile with such a high-altitude engine, other things being equal, will have a relatively great range. For this reason, at the present time high-altitude engines are made for long-range missiles and for some antiaircraft missiles. The design altitude for an engine being designed is usually chosen with due regard to the missile's type and tactical designation. The absolute thrust of a high-altitude engine is determined according to the general thrust equation given above.

Figure 4.5 shows the results of rough calculations for determining the absolute and specific thrusts of the A-4 engine at sea level and in space, operating on 80% weight concentration ethyl alcohol and liquid oxygen, with $p_k = 20$ atm abs, $n = 1.16$, and different values of p_v (depending on the different

lengths of the chamber nozzle).

The curves of this graph show that:

1) shortening the nozzle relative to its normal terrestrial length leads to a decrease in the engine's absolute and specific thrusts in operation at ground level, in the rarefied layers of the atmosphere, and in space;

2) lengthening the nozzle relative to its normal terrestrial length leads to a decrease in the engine's absolute and specific thrusts at blastoff and to increasing them considerably as the engine operates in the rarefied layers of the atmosphere;

3) increasing the area of the nozzle outlet section by 30% and its length by 6% relative to the normal-length nozzle at ground level increases the absolute and specific thrusts of the engine in space by approximately 5%, and its internal efficiency by almost 10%.

The engine thrust vector must concur strictly with the axis of the missile's flight. In practice it is extremely difficult to accomplish this condition, since, in fact, an engine's thrust in relationship to the missile is always somewhat noncoaxial.

Calculations show that disruption of the centrality of the thrust vector of a ~~ZhRD~~ by 0.5% can cause a lateral force of about 0.1% of the thrust of the engine. For a missile with a mass ratio of 7:1 at the end of the power phase, the lateral acceleration may reach 0.1 g, and the lateral velocity about 60 m/sec.

This circumstance compels the application of some means for steering the missile during blastoff and in flight, as well as for changing the direction of its flight if necessary. One may use gas rudders, which are started by a hydraulic system (steering engines) for this purpose in missiles of large and medium thrust. Gas rudders may cause a lateral force of up to 20% of the axial value of the engine's thrust.

If gas rudders are placed in the gas flow at the rear of the engine nozzle, the engine thrust decreases by the magnitude ΔP_{rul}^* kg. The magnitude of the resistance of the gas rudders of a missile depends on their design, dimensions, turning angle in the gas flow, and their burnout level during the engine's operation. In ballistic missiles a turn by gas rudders is possible within the limits of $\pm 25^\circ$, and their working turns are usually accomplished in the interval of $\pm 12^\circ$. This shows that the forces operating on gas rudders in the missile's guided-flight phase change within wide limits.

The frontal drag for the A-4 long-range missile's gas rudders, in a nondivergent position, is equal to about 640 kg, and in a divergent position attains 1560 kg.

In calculations, thrust losses of liquid-fuel rocket engines due to gas rudders are usually accepted, in accordance with the statistical data, as equal to about 1-3% for finned missiles and to about 2-4% for finless missiles, computed from ground-level engine thrust. This is convenient from the practical point of view, since one may determine the resistance of the gas rudders experimentally at ground level.

The quantity ΔP_{rul} is practically independent of flight altitude, since density and velocity of the stream of gases flowing out of the engine nozzle do not depend on the pressure of the surrounding medium, i.e., are not functions of flight altitude.

Instead of gas rudders, in some cases special steering combustion chambers, which may also be used as the final stage of an engine, are applied for steering a missile in flight. By changing the corresponding mode of fuel flow rate to the separate chambers, one may turn the missile in the required direction.

$$*[\Delta P_{pyл} = \Delta P_{rul} = \Delta P_{rul'} = \Delta P_{rudder}]$$

If the fuel system contains a turbopump unit whose exhaust gas flows into the atmosphere through the expanding nozzle of an exhaust pipe which is parallel to the engine axis, a supplementary engine thrust is developed:

$$\Delta P_{TNA} = \varepsilon_1 G'_s P_{ya.TNA}$$

where ε_1 is the factor accounting for the shortage of specific thrust due to part of the fuel being expended in the gas generator (as a consequence of partial use of the gases' heat differential in the turbine and their partial ejection through the constant-pressure valve if such a valve exists); G'_s is the fuel flow rate to the gas generator of the turbopump unit in kg/sec; $P_{ud.TNA}$ is the specific thrust developed by the gases when they flow out of the exhaust pipe of the turbopump unit's nozzle in kg thrust/kg fuel/sec.

Experience shows that the value of ΔP_{TNA} may amount to about 0.2 to 0.5% of the thrust of the engine chamber.

Allowing for this, the summary absolute thrust of an engine is expressed by the equation

$$P_s = P_s + \Delta P_{TNA} - \Delta P_{py} = \varepsilon_2 P_s + \Delta P_{TNA} = \varepsilon_2 G'_s P_{ya} + \varepsilon_1 G'_s P_{ya.TNA}$$

where ε_2 is the factor allowing for the engine's thrust loss as a consequence of gas rudders at the rear of the nozzle.

The absolute thrust of a ~~ZhrD~~ at ground or sea level is an extremely important characteristic of the engine, since it determines the stability of the weapon at the instant of launching.

The magnitude of engine thrust at ground level is usually dependent upon the weapon's tactical designation. Thus, for example, for existing long-range missiles of the A-4 type, the magnitude of the thrust at ground level must be almost twice as great as the missile's launching weight.

Requirements for increasing range and weight of payload of a

weapon leads to a great increase in the engine's absolute thrust.

Toward the end of the Second World War, engine thrusts reached 26 tons.

Experience has shown that the development of a single-chamber engine is not practicable for extremely great thrusts because of the excessive increase in the dimensions and weight of the engine and the difficulties in its experimental development. The published literature reports that single-chamber engines with a thrust of several hundred tons may be developed.

Probably missiles with greater thrusts will be multichambered with synchronized thrust of the separate combustion chambers. Such an engine permits steering the missile's flight by differential throttling of the separate combustion chambers or turning them relative to the missile axis.

In practice, the thrust of a multichambered engine may attain extremely great magnitudes.

Calculations show that an engine in the form of clusters of several chambers of smaller size has a smaller total weight than a single-chambered engine of the same thrust operating under the same conditions. The advantage of a multichamber engine also lies in the convenience of regulating thrust; however, its external dimensions are greater than the dimensions of a single-chamber engine.

One must bear in mind that a liquid-fuel rocket engine, at launching, usually works up to full thrust only after a short interval of time after the trigger pulse is delivered. Again, in cutting off (stopping) the engine, its thrust does not cease simultaneously, but, as they say, the phenomenon of aftereffects is observed, leading to range dispersion, especially in ballistic missiles.

The magnitude of the aftereffect momentum and some amount of dispersion of its values, in a ZhRD, depends upon the length of time that

fuel which was not cut off, because of the design particulars of the engine, continues to arrive in the combustion chamber and burn there.

At the moment the cut-off signal is given for the fuel components, some quantity of fuel is arriving in the chamber, where it burns after a certain time interval equal to its delay in ebullition. The cut-off valves are late in operating after the signal is given for their closure; the process of closing also does not take place simultaneously, since at this moment a certain amount of fuel continues to arrive in the chamber and burn there. After the cut-off valves close, the fuel which was not cut off rushes into the combustion chamber partly as a consequence of inertial effect, and also by partial vapor formation because of the decrease in the pressure in the lines, especially in the cooling duct of the engine chamber. Besides this, at the moment the supply of the components is cut off, there is some amount of gases of a certain pressure in the chamber. Because of all these things, the engine has an aftereffect momentum, which leads to a considerable range dispersion in ballistic missiles.

In order to decrease the range dispersion of these missiles, sometimes, before complete cutoff of fuel delivery to the combustion chamber, the engine at first shifts to operation with a smaller per-second flow rate, i.e., at the final thrust stage. For this same purpose, the extremely perfected instruments in systems for guiding the missile in the power phase of its trajectory are applied. Decreasing the scattering (dispersion) of the range of long-range missiles is possible by means of decreasing the liquid-fueled rocket engine's aftereffect momentum, as well as by careful calculation of its magnitude in working out the mechanism for separating the warhead from the body of the missile.

SECTION 5. ENGINE CHAMBER NOZZLE OPERATION AT NONOPTIMUM REGIMES

At the rear of the chamber nozzle, when operating on nonoptimum regimes, transformation of the supersonic gas flow into a subsonic gas flow occurs, with the restoration of the pressure from p_v to p_a , because of the system of compression waves (Fig. 4.6).

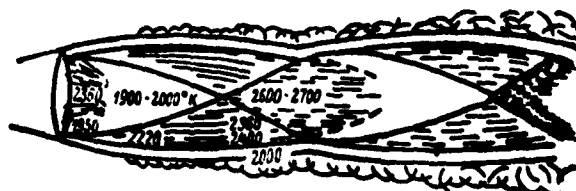


Fig. 4.6. Transformation of gas flow in the rear of an engine nozzle by compression waves as the consequence of underexpansion, relative to the pressure of the atmospheric air (when $p_v > p_a$), of the exhaust from the nozzle.

In the ranges of the operating regimes for underexpansion and overexpansion of the gases in the engine nozzle exhaust section, ordinarily the rated exhaust velocity w_v is established, whose magnitude is independent of the conditions of the surrounding medium and is determined only by the parameters of the gases in the combustion chamber and the geometrical form of the nozzle.

In cases where the nozzle operates with $p_v > p_a$ the stream of gas at the end of the nozzle at first expands with an increase in velocity, and then, as a consequence of its inertial velocity of overexpansion, is subjected to compression by the influence of the relatively great pressure of the surrounding layers of air on it, and so forth. These processes of overexpansion and overcompression of the gas stream and the layers of the atmospheric air adjoining it, relative to its pressure in an unperturbed condition, are usually accompanied by oblique

compression wave.

The further a nonoptimum operating regime of the chamber nozzle varies from optimum, the stronger the perturbation in the stream of gases at the end of the engine chamber.

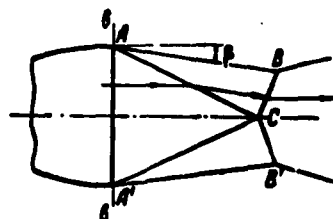


Fig. 4.7. Transformation of gas flow at rear of engine nozzle through compression waves as a consequence of its overexpansion relative to the atmospheric air pressure (when $p_v < p_a$).

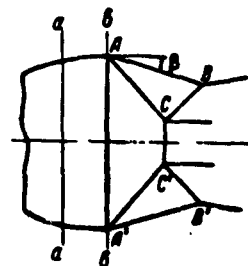


Fig. 4.8. Transformation of flow of exhaust gases from an engine nozzle with appearance of a normal compression wave due to the considerable overexpansion of gases relative to the atmospheric air pressure.

When a nozzle operates with $p_v < p_a$, transformation of the supersonic gas flow to subsonic is considerably more complex (Figs. 4.7 and 4.8). Here the pressure of the gas is restored to the pressure of the surrounding medium by means of a system of oblique and even, possibly, normal compression waves.

A decrease in the pressure ratio p_v/p_a causes an increase in the angle β (see Fig. 4.7), and when it exceeds a certain limiting value β' , depending on Mach number (M_v), the gas-flow transformation scheme in the rear of the nozzle is even more complicated (see Fig. 4.8). In this case, a normal (or, more exactly, curvilinear) compression wave appears around the gas-flow axis, and this, when p_v/p_a is decreased to a fixed value, will be shifted to the nozzle's outlet section.

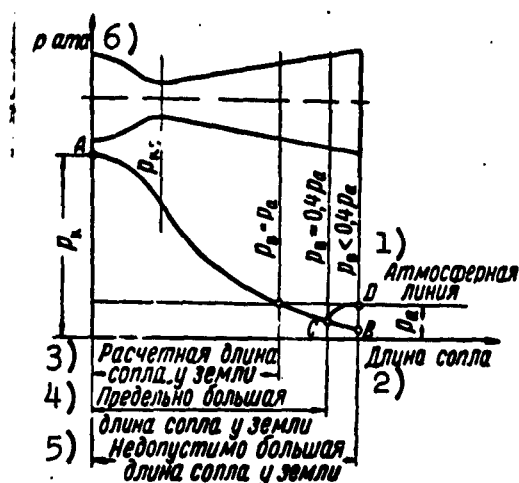


Fig. 4.9. Compression waves in flow in an engine nozzle as a consequence of excessive over-expansion relative to atmospheric air pressure. 1) Atmosphere line; 2) nozzle length; 3) rated nozzle length at ground level; 4) maximum nozzle length at ground level; 5) inadmissible nozzle length at ground level; 6) p , atm abs.

Until this normal compression wave approaches the chamber-nozzle outlet section, exhaust velocity will be supersonic, since in this case its magnitude is determined only by the parameters of the gases at the end of the combustion chamber and the design of the nozzle. By this means, the pressure in the gas flow at the rear of the nozzle will be restored up to the pressure of the atmospheric air by means of oblique compression waves.

After the normal compression wave moves to the chamber-nozzle exhaust section, gas outflow velocity will be sonic.

With a further decrease in p_v/p_a , the gases' normal compression wave enters the nozzle. Then, in the nozzle behind the plane of this compression wave, the gas stream becomes subsonic and strongly perturbed, as a result of which it may become detached from the surface of the nozzle wall (Fig. 4.9), and to considerable

decrease of the engine's specific thrust.

In practice, we find that the gases' detachment from the wall of the chamber nozzle in a liquid-fueled rocket engine may occur when $p_v/p_a = 0.3-0.4$.

Regimes when normal compression waves occur within the nozzle are inefficient, and are therefore not desirable during normal operation of the engine. Such regimes may take place only when starting and stopping the engine, and also during test-stand trials of high-altitude engines.

For a variation in a ZhRD chamber operating regime until normal compression waves occur in the gases inside the nozzle, engine thrust may be determined by the above-mentioned general equations (4.8) and (4.9); in other cases these equations will give incorrect results to the computations.

Studies have established that the gas streams behind the nozzle of an engine affect the aerodynamic characteristics of the missile by decreasing frontal drag at supersonic flight speeds and increasing it at subsonic flight speeds.

With a subsonic flight speed the gas streams flowing out of the engine nozzle with a supersonic velocity operate like an ejector and create an inflow of the surrounding air behind the flying missile. This phenomenon considerably affects such devices as missiles, aerial torpedoes, and some types of jet aircraft, in which the engine is installed in the conical tail section.

The ejecting action of the gases flowing out of the engine nozzle creates an acceleration of the surrounding air and, consequently, a local increase in surface friction, as well as a decrease in the pressure on the surface of the missile close to the nozzle. This leads to an increase of the frontal drag through the moving air and a de-

crease in the atmospheric pressure at the exhaust from the nozzle (this decrease in pressure causes an increase in thrust, which is developed by the difference of pressures between the gases at the exhaust from the nozzle and the atmospheric air).

During the flight of a missile with supersonic speed, a turbulent wake with decreased local pressure is excited at its tail section. Under the influence of the reactive stream, the area of lowered pressure is filled by the gases flowing out of the engine, which leads to an increase in the pressure on the missile's tail section. By this means frontal drag is decreased, i.e., thrust is increased.

SECTION 6. THE THRUST COEFFICIENT OF AN ENGINE

To simplify calculations, the concept of an engine's thrust coefficient, which is the ratio of the chamber's absolute thrust P to the product of the gas pressures p_k in the combustion chamber and the area F_{kr} of the nozzle's critical section, i.e.,

$$K = \frac{P}{p_k F_{kr}}, \quad (4.13)$$

has been introduced into liquid-fueled rocket engine theory.

This coefficient shows how many times the thrust of the engine chamber is increased relative to the basic term of thrust ($p_k F_{kr}$) by means of the convergent and divergent parts of the nozzle.

Using the concept of an engine chamber's thrust coefficient, the general thrust equation

$$P_a = \frac{G_e}{g} w_e + F_e p_e - F_e p_a = P_e - F_e p_a$$

may be given the following dimensionless form:

$$\frac{P_a}{p_k F_{kr}} = \frac{P_e}{p_k F_{kr}} - \frac{F_e p_a}{p_k F_{kr}} *$$

$$\begin{aligned} & * [P_H = P_{\text{absolute}}; P_{\Pi} = P_{\text{space}}; \\ & F_p = F_r = F_{\text{raschetny}} = F_{\text{rated (calculated)}}.] \end{aligned}$$

or

$$K_n = K_n - f_v \frac{p_a}{p_n}, \quad (4.14)$$

where $K_n = p_n / p_k F_{kr}$ is the thrust coefficient of an engine when the gases flow out of the nozzle into the atmosphere; $K_p = P_p / p_k F_{kr}$ is the thrust coefficient of an engine when the gases flow out of the nozzle into space; and $f_v = F_v / F_{kr}$ is the relative area of the nozzle's exhaust section.

By this means, we will obtain the following additional expressions for determining the thrust of an engine chamber:

$$P = p_n F_{vp} K; \quad P_n = p_n F_{vp} K_n; \quad P_a = p_a F_{vp} K_n.$$

Bearing in mind that the absolute thrust of a chamber is also expressed by the equation

$$P_n = p_n F_{vp} \sqrt{\frac{2n^2}{n-1} \left(\frac{2}{n+1}\right)^{\frac{n+1}{n-1}} \left[1 - \left(\frac{p_a}{p_n}\right)^{\frac{n-1}{n}}\right]} + F_{vp} (p_n - p_a) = p_n F_{vp} K_n,$$

we will obtain

$$K_n = \sqrt{\frac{2n^2}{n-1} \left(\frac{2}{n+1}\right)^{\frac{n+1}{n-1}} \left[1 - \left(\frac{p_a}{p_n}\right)^{\frac{n-1}{n}}\right]} + \frac{F_{vp} (p_n - p_a)}{p_n F_{vp}}. \quad (4.15)$$

This formula shows that K_n is also dependent upon atmospheric air pressure p_a , the value of which, with an increase in altitude, is lowered, and in space is equal to zero. Therefore, at a given operating regime in the chamber, the thrust coefficient K_n is increased with a rise in altitude, and in space attains maximum value, K_p .

Since the thrust of the chamber in space is expressed by the equation $P_p = F_{vp} p_v (1 + n M_v^2)$, the thrust coefficient of a liquid-fueled rocket engine, when operating in space, may be expressed as follows:

$$K_n = \frac{P_n}{p_n F_{vp}} = \frac{F_{vp} p_n (1 + n M_v^2)}{p_n F_{vp}} = f_v \frac{p_n}{p_n} (1 + n M_v^2). \quad (4.16)$$

If, in this formula, we replace f_v and p_v / p_k with the already

well-known expressions of them which are functions of Mach number (M_v), and then replace this figure with its value dependent on the velocity coefficient λ_v , or express the latter by the ratio p_v/p_k , after the appropriate transformations, we will obtain the following expressions for the coefficient of the thrust of an engine when operating in space:

$$K_s = \left(\frac{2}{n+1}\right)^{\frac{n+1}{2(n-1)}} \frac{1+nM_s^2}{M_s \sqrt{1+\frac{k-1}{2}M_s^2}} = \left(\frac{2}{n+1}\right)^{\frac{1}{n-1}} \frac{\lambda_s^2+1}{\lambda_s} =$$

$$= 2 \left(\frac{2}{n+1}\right)^{\frac{1}{n-1}} \frac{n}{\sqrt{n^2-1}} \sqrt{1-\left(\frac{p_s}{p_k}\right)^{\frac{n-1}{n}}} \left[1 + \frac{n-1}{2n} \frac{(p_s/p_k)^{\frac{n-1}{n}}}{1-(p_s/p_k)^{\frac{n-1}{n}}} \right]. \quad (4.16')$$

In accordance with these same formulas, one may also determine the theoretical engine thrust coefficient $K_{p.t}^*$ when operating in space if we replace the corresponding actual parameters with their theoretical values which were obtained during thermodynamic computation of the engine chamber.

The following relationship exists between the actual thrust coefficient K_p of the engine when operating in space and its theoretical value $K_{p.t}$:

$$K_s = \varphi_s K_{s.t} \quad (4.17)$$

where φ_s^{**} is the correction factor for the nozzle efficiency of this specific engine chamber nozzle.

It is simplest to determine the theoretical coefficient of thrust in space by means of Eq. (4.16'), having replaced the polytropic exponent n in it with the specific heat ratio k .

In existing engines $K_p \approx 1.5-1.8$. By increasing p_k and decreasing n or k , the value of K_p is increased.

By considering these factors, one may also express an engine cham-

*[$K_{p.t} = K_{p.t} = K_{pustota.theoreticheskiy} = K_{space.theoretical}$.]
 **[$\varphi_c = \varphi_s = \varphi_{soplo} = \varphi_{nozzle}$.]

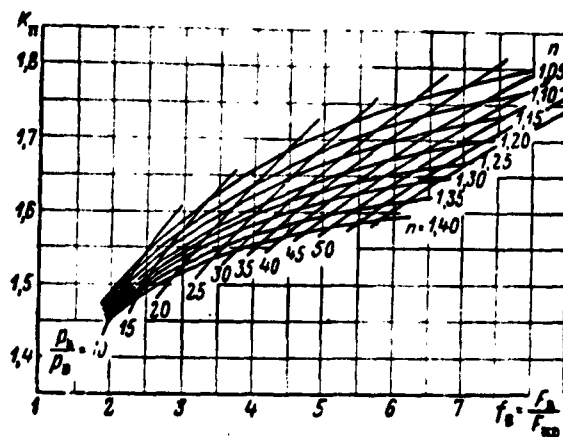


Fig. 4.10. Nomogram for determining geometrical dimensions of an engine nozzle.

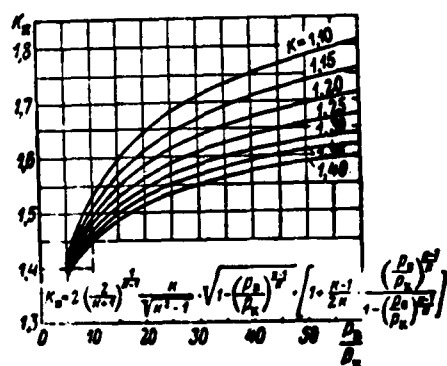


Fig. 4.11. Thrust coefficient of an engine in space, dependent on gas-expansion ratio in the nozzle and specific heat ratio k .

ber's thrust thus:

$$P_n = p_n F_{sp} \varphi_c K_{n,r} - F_n p_n; \quad P_n = p_n F_{sp} \varphi_c K_{n,r}$$

The formulas given here permit the

determination of the basic geometrical dimensions of the chamber nozzle and some of its operating parameters. By this means, one may use the curves in Figs. 3.9, 4.10, and 4.11 for approximate calculations.

Example 1. Determine the absolute

thrust of an engine when operating in space and the geometrical dimensions of the chamber nozzle, if $p_k = 40$ atm abs, $p_v = 1$ atm abs, $n = 1.15$, and $F_{kr} = 39$ cm².

Solution.

1. According to the graph in Fig. 4.10, when $p_k/p_v = 40/1 = 40$ and $n = 1.15$, we find $K_p = 1.725$ and $f_v = 6.5$.

2. Thrust of the engine chamber in space

$$P_n = p_n F_{sp} K_n = 40 \cdot 39 \cdot 1.725 = 2667 \text{ kg.}$$

3. Area of the nozzle cross section at outlet

$$F_s = f_s F_{kp} = 6,5 \cdot 39 = 253,5 \text{ cM}^2.$$

4. Diameters of the critical and exhaust sections of the nozzle:

$$d_{kp} = \sqrt{\frac{4F_{kp}}{\pi}} = \sqrt{\frac{4 \cdot 39}{3,14}} = 7,042 \text{ cM}; \quad d_s = \sqrt{\frac{4 \cdot 253,5}{3,14}} = 17,92 \text{ cM}.$$

We will also determine the thrust of the engine chamber in space and the pressure of the gases in the nozzle exhaust section when $p_k = 40 \text{ atm abs}$, $n = 1.15$, $d_{kr} = 7 \text{ cm}$, and $d_v = 21 \text{ cm}$.

We solve this problem in the following manner.

1. The relative area of the exhaust section of the chamber nozzle will be

$$f_s = F_s / F_{kp} = d_s^2 / d_{kp}^2 = 21^2 / 7^2 = 8,9.$$

2. According to the graph in Fig. 4.10, when $f_v = 8.9$ and $n = 1.15$, we find the level of gas expansion in the nozzle:

$$p_k / p_v = 60,$$

from whence $p_v = p_k / 60 = 40 / 60 \approx 0.67 \text{ atm abs}$.

3. According to the graph in Fig. 4.11, when $p_k / p_v = 60$ and $n = 1.15$, we find the chamber's thrust coefficient K_p in space is equal to 1.76.

4. We will determine the area of the critical section of the nozzle according to the formula

$$F_{kp} = \frac{\pi d_{kp}^2}{4} = \frac{3,14 \cdot 7^2}{4} = 38,48 \text{ cM}^2.$$

5. The thrust of the engine chamber when operating in space:

$$P_s = K_p p_k F_{kp} = 1,76 \cdot 40 \cdot 38,4 = 2703,36 \text{ kg}.$$

SECTION 7. SPECIFIC THRUST OF AN ENGINE

The usual accepted evaluation of the operating economy of a ZhRD on a given fuel and on the corresponding regime is by the magnitude of specific thrust.

In calculating the characteristics of a liquid-fueled rocket en-

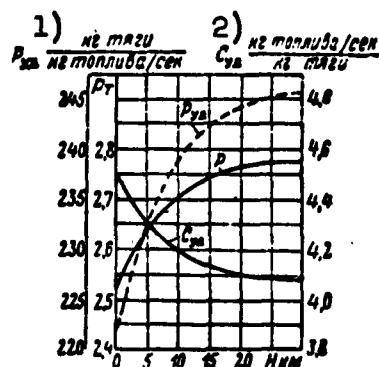


Fig. 4.12. Rated dependence of absolute thrust, specific thrust, and specific consumption on flight altitude. 1) P_{ud} , kg thrust/(kg fuel/sec); 2) C_{ud} , kg fuel/sec per kg thrust.

engine for evaluation of the fuel used in it and the quality of the operating cycle, the magnitude of the specific thrust, depending on the regime and operating conditions of the engine, should be determined by taking into consideration the per-second fuel-component flow rate to the combustion chamber and the flow rates for servicing the fuel-feed system and forming the protective curtain around the surface of the engine-chamber burner liner.

Calculations show that the specific thrust of an engine is quite dependent on flight altitude H of the weapon (see Fig. 4.12); the less pressure p_k in the combustion chamber, the greater the dependence of P_{ud} on H .

Considering the above, one should distinguish the specific thrust of the chamber only and of the engine as a whole, i.e.,

1. The engine chamber:

a) in general

$$P_{y_{1.2}} = P_u / G_u; \quad (4.18)$$

b) when the nozzle is operating in the optimum regime ($p_v = p_a$),

$$P_{y_{1.2opt}} = P_{out} / G_u = w_u / g;$$

c) when the nozzle operates in a nonoptimum regime ($p_v \neq p_a$),

$$P_{y_{1.2}} = P_u / G_u = w_{u0} / g; *$$

d) when operating at ground or sea level ($H = 0$)

$$P_{y_{1.2}} = P_u / G_u; **$$

*[$P_{y_{1.2}} = P_{ud.n} = P_{udel'nyy.neoptimal'nyy} = P_{specific.nonoptimum}$]
 **[$P_{y_{1.2}} = P_{ud.0} = P_{udel'nyy.0} = P_{specific.(H-) zero}$]

e) when operating in space ($p_a = 0$), $P_{ud.p} = P_p/G_s$.

2. The engine as a whole:

a) in general

$$P_{y_{\Sigma}} = P_{\Sigma}/G_{\Sigma}; \quad (4.19)$$

b) when the nozzle is operating in a nonoptimum regime ($p_v \geq p_a$),

$$P_{y_{\Sigma}} = P_{\Sigma}/G_{\Sigma};$$

c) when operating at ground or sea level ($H = 0$)

$$P_{y_{\Sigma}} = P_{\Sigma}/G_{\Sigma};$$

d) when operating in space ($p_a = 0$), $P_{ud\Sigma p} = P_{\Sigma p}/G_{\Sigma}$.

The specific thrust of an engine chamber when operating in space may also be expressed by the formula

$$P_{y_{\Sigma}} = P_{\Sigma}/G_{\Sigma} = p_{kr} F_{kr} K_{\Sigma}/G_{\Sigma} = \beta K_{\Sigma}$$

where $\beta = p_{kr} F_{kr}/G_{\Sigma}$ is the actual gas-pressure impulse in the combustion chamber in kg-sec/kg.

Thus, the specific thrust of an engine chamber, when the nozzle is operating in a nonoptimum regime ($p_v \neq p_a$), will be

$$\begin{aligned} P_{y_{\Sigma}} &= \frac{P_{\Sigma}}{G_{\Sigma}} = \frac{P_{\Sigma} - F_{\Sigma} p_a}{G_{\Sigma}} = \beta K_{\Sigma} - f_{y_{\Sigma}} p_a = \\ &= \beta K_{\Sigma} - \beta f_{\Sigma} \frac{p_a}{p_{kr}} = \beta \left(K_{\Sigma} - f_{\Sigma} \frac{p_a}{p_{kr}} \right), \end{aligned}$$

where $f_{ud.v} = F_v/G_{\Sigma}^*$ is the true specific area of the exhaust section of the chamber nozzle in kg/cm²; and $f_v = F_v/F_{kr}$ is the relative area of the exhaust section of the chamber nozzle.

In liquid-fueled rocket engine theory, there is also an accepted distinction of the theoretical specific thrust of an engine chamber:

$$P_{y_{\Sigma}} = w_{\Sigma}/g^{**}$$

Since the actual operating characteristics of a chamber may be

*[$f_{y_{\Sigma}} = f_{ud.v} = f_{udel'nyy.vykhod} = f_{specific.outlet}$]
 **[$P_{y_{\Sigma}} = P_{specific.theoretical}$]

expressed in the following manner by means of the corresponding theoretical characteristics computed during the thermodynamic computation of the engine:

$$K_n = \varphi_c K_{n,t}; \quad \beta = \varphi_{p_k} \beta_t; \quad P_{ya} = \varphi_{ya} P_{ya,t}; \quad f_{ya,n} = \varphi_{p_k} f_{ya,n,t} *$$

the specific thrust of the engine chamber may be determined thus:

$$P_{ya,n} = \varphi_{p_k} \beta_t \varphi_c K_{n,t};$$

$$P_{ya,n} = (\beta_t \varphi_c K_{n,t} - f_{ya,n,t} P_a) = \varphi_{p_k} \beta_t (\varphi_c K_{n,t} - f_{ya,n,t} \frac{P_a}{\beta_t});$$

$$P_{ya,n} = \varphi_{ya} P_{ya,t} + \varphi_{p_k} f_{ya,n,t} (P_a - P_a),$$

where $\varphi_{p_k} = \beta/\beta_t$ is the gas-pressure coefficient (correction factor) for the engine combustion chamber; and $P_{ud} = w_v/g$ and $P_{ud,t} = w_{v,t}/g$ are the true and theoretical dynamic specific thrusts, respectively, of the engine chamber.

The chamber's specific thrust $P_{ud,n}$, during nonoptimum nozzle operation, may be converted into the specific thrust $P_{ud,opt}$ during optimum nozzle operation according to the formula

$$P_{ya,opt} \approx P_{ya,n} \frac{\sqrt{1 - (P_a/P_n)^{\frac{n-1}{n}}}}{\sqrt{1 - (P_a/P_n)^{\frac{n-1}{n}}}} \frac{\text{kg thrust}}{\text{kg-fuel/sec}}. \quad (4.19')$$

In accordance with an analogous formula, one may evaluate the specific thrusts of engines operating at various values of p_k and the same values of p_v . The magnitude of specific thrust is affected by the regime and operating conditions of the engine, its design particulars, and other factors, such as:

- 1) type of fuel, its composition, and method of atomization;
- 2) pressure in the combustion chamber;
- 3) level of gas expansion in the nozzle;
- 4) shape and dimensions of the combustion chamber;
- 5) engine-nozzle divergence angle and configuration;

* [$\varphi_{p_k} = \varphi_{p_{\text{chamber}}}$.]

- 6) relative area ($f_k = F_k/F_{kr}$) of the combustion chamber;
- 7) engine cooling system;
- 8) nature of the methods used to protect the chamber liner and nozzle liner from overheating;
- 9) propellant-feed system, its design and performance, and operating economy;
- 10) pressure at which fuel is fed to the combustion chamber;
- 11) flight altitude (see Fig. 4.12), etc.

By the improvement of vaporization and mixing of fuel components, and by eliminating enrichment of the peripheral spray with combustible, which is often used to protect the chamber liner from overheating, as well as using a number of other methods, one may considerably increase an engine's specific thrust.

When raising the pressure in the combustion chamber to $p_k \approx 60$ atm abs, at first the specific thrust increases sharply, from 60 to 100 atm abs its growth gradually slows down, and at about 200 atm abs it remains almost constant (Figs. 4.13 and 4.14).

Increasing P_{ud} by raising p_k above a certain value is limited in practice. Raising p_k , other things being equal, causes:

- 1) decrease in the external dimensions of the combustion chamber because of the smaller specific volume of the fuel combustion products formed;

- 2) increase in the thermal efficiency η_t of the engine because of the increase in the gas-pressure difference in the nozzle;

- 3) increasing the heat liberation coefficient φ_k of the fuel in the combustion chamber as a consequence of the intensification in the working cycle by decreasing the dissociation of the gases and increasing the physical coefficient $\varphi_{p.k}^*$ of completeness of fuel combustion,
 $*[\varphi_{п.к} = \varphi_{p.k} = \varphi_{полнота.камера} = \varphi_{completeness (of combustion).chamber}]$

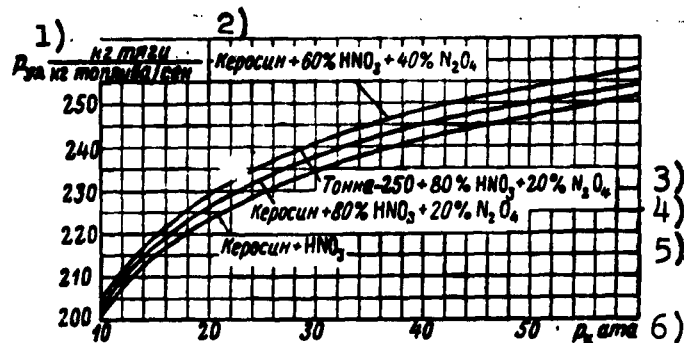


Fig. 4.13. Dependence of an engine's theoretical specific thrust on combustion chamber pressure for several fuels when $p_v = 1$ atm abs and $\alpha = 0.8$.

- 1) P_{ud} , kg thrust/(kg fuel/sec); 2) kerosene + 60% HNO_3 + 40% N_2O_4 ; 3) Tonka-250 + 80% HNO_3 + 20% N_2O_4 ; 4) kerosene + 80% HNO_3 + 20% N_2O_4 ; 5) kerosene + HNO_3 ; 6) p_k , atm abs.

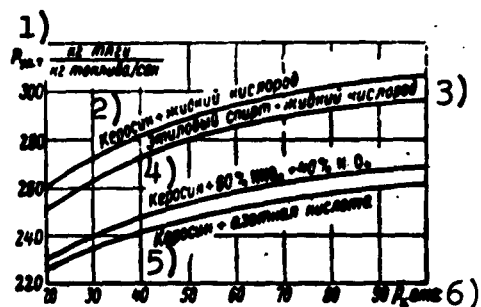


Fig. 4.14. Theoretical specific engine thrust as dependent on combustion chamber pressure for several fuels when $p_v = 1$ atm abs and $\alpha = 0.8$.

- 1) P_{ud} , kg thrust per kg fuel/sec; 2) kerosene and liquid oxygen; 3) ethyl alcohol and liquid oxygen; 4) kerosene + 60% HNO_3 + 40% N_2O_4 ; 5) kerosene + nitric acid; 6) p_k , atm abs.

which, in conjunction with the first factor, increases the velocity of the gases in the nozzle exhaust and, proportionally, the specific thrust of the engine;

4) decreasing the time τ_{pr}^* the fuel remains in the combustion chamber, which also decreases its required volume, dimensions, and weight.

However, beginning at some magnitude of p_k , increasing it further does not give noticeable advantages.

On the other hand, raising p_k basically leads to the following phenomena:

$$*[\tau_{np} = \tau_{pr} = \tau_{prebyvaniye} = \tau_{stay}.]$$

1) raising the temperature in the engine combustion chamber and complication of its cooling system;

2) changing the engine-chamber nozzle length due to the necessity for setting up a great gas-pressure difference across the nozzle;

3) increasing the weight of the engine as the consequence of the requirement for greater strength of the combustion chamber, nozzle, and other elements of the engine;

4) increasing the energy losses in supplying fuel to the combustion chamber under a great pressure head, and

5) increasing the cost of the engine.

In practice, gas pressure in the engine combustion chamber is chosen in each separate case on the basis of comparative calculations showing its effect on specific thrust, dimensions and weight of the chamber and propellant-feed system of the engine, on the possibility of effective cooling of the engine, etc.

In future engines, one may expect an increase in the ratio p_k/p_v by means of increasing p_k and decreasing p_v , which is especially suitable for long-range missiles and some types of aircraft.*

The design of reaction engines with a combustion chamber pressure of up to 100-200 atm abs and above is entirely possible, when atomic reactors, intended for using the heat of nuclear reactions, are constructed.

The most radical method of increasing P_{ud} is the use of exotic fuels. However, this means of increasing P_{ud} leads to an increase in T_k , which considerably complicates the problem of cooling the engine.

Calculations show that, in practice, the possible limit of in-

*Problems of Rocket Engineering, Nos. 1 and 2, 1954, IL.

creasing P_{ud} by means of the chemical energy of the fuel is about 350 to 450 kg-thrust/(kg-fuel/sec).

Magnitude of specific thrust, characterizing the engine's operating economy, does not reveal the specific nature of the heat process occurring in the combustion chamber and in the engine nozzle, or the cycle's reserves for increasing operating economy. In this relationship, the engine efficiencies are the best indices.

Ground-level data for specific thrust have considerable value only for low-altitude engines.

The specific thrust in space should be considered the basic characteristic of the operating economy of high-altitude ZhRD.

The most complete characteristic of the operating economy for a high-altitude engine is its mean specific thrust with regard to the trajectory of the flight, expressed by the formula

$$P_{sp, cp} = \frac{Q_L \cdot w_s + F_s (P_s - P_{a, cp})}{G_s} \frac{\text{kg thrust}}{\text{kg fuel/sec}}, * \quad (4.19")$$

where $p_{a, sr}$ is the mean atmospheric pressure in atm abs along the trajectory of the flight.

SECTION 8. FUEL FLOW RATES IN AN ENGINE

To determine the dimensions of a combustion chamber, chamber burner cup, fuel tanks, and propellant-feed system, also including start-control devices, one must know the per-second flow rate of the fuel components in the engine into the chamber and for supplying the feed system.

In a liquid-propellant rocket engine, in general, we accept the distinction of the following per-second fuel flow rates:

$$\begin{aligned} * [P_{yd, cp} &= P_{ud, sr} = P_{udel'nyy, srednyaya} = P_{specific, mean}; \\ P_{a, cp} &= P_{a, sr} = P_{atmosfera, srednyaya} = P_{atmosphere, mean}.] \end{aligned}$$

1) basic - in the engine combustion chamber when it is operating in a given regime G_s in kg/sec;

2) starting - in the combustion chamber, corresponding to the operating regime of the engine at the first starting stage, $G_{s p}^*$ in kg/sec;

3) auxiliary - in servicing the propellant-feed system (TNA, ZhAD) G'_s in kg/sec.

The per-second propellant flow rate to the combustion chamber, when the engine is operating on the corresponding operating regime, is determined in accordance with the formula

$$G_s = \frac{P_{\text{с}}}{P_{\text{г.с}}} = \frac{P_{\text{с}}}{w_{\text{с}}/g} = \frac{gP_{\text{с}}}{w_{\text{с}}} \text{ kg/sec.} \quad (4.20)$$

In planning and designing an engine, it is necessary to know the relationships between the per-second propellant-flow rate G_s into the chamber, the magnitude of the area F_{kr} of the cross section of the nozzle throat and the parameters of the gases at the entrance to the nozzle from the combustion chamber.

Gasdynamics give the following interdependence between G_s , F_{kr} , and the parameters of the gas at the entrance into the nozzle of a ZhRD:

$$G_s = p_{\text{с}} F_{\text{ср}} \sqrt{\frac{n g}{R_{\text{с}} T_{\text{с}}}} \left(\frac{2}{n+1} \right)^{\frac{n+1}{2(n-1)}} = p_{\text{с}} B = F_{\text{ср}} C \text{ kg/sec} \quad (4.21)$$

or

$$G_s = \frac{p_{\text{с}} F_{\text{ср}} A}{\sqrt{R_{\text{с}} T_{\text{с}}}} = p_{\text{с}} F_{\text{ср}} \frac{A}{\sqrt{R_{\text{с}} T_{\text{с}}}} = \frac{p_{\text{с}} F_{\text{ср}}}{\beta},$$

where $A = \sqrt{2g \frac{n}{n+1} \left(\frac{2}{n+1} \right)^{\frac{2}{n-1}}} = \sqrt{ng} \left(\frac{2}{n+1} \right)^{\frac{n+1}{2(n-1)}}$ - a coefficient which is only slightly dependent on polytropic exponent n (when n is increased from 1.1 to 1.2, the magnitude of A is increased from 1.98 to 2.03); and $\beta = \sqrt{R_k T_k} / A = p_k F_{kr} / G_s$, the specific impulse of the pressure of the

*[$G_{s n} = G_{s p} = G_{s \text{ пусковой}} = G_{s \text{ starting}}$.]

gases in the combustion chamber, which characterizes the properties of the propellant and the completeness of its combustion.

In the case of decrease in gas pressure along the length of the combustion chamber we have

$$G_s = p_k F_{kr} \sqrt{\frac{ng}{R_k T_k} \left(\frac{1 + \frac{n-1}{2} M_k^2}{\frac{n+1}{2}} \right)^{\frac{n+1}{2(n-1)}}} \text{ kg/sec.} \quad (4.22)$$

These formulas show that under conditions of constant temperature and composition of the products of propellant combustion, the values of p_k and F_{kr} change in direct proportion to the change in G_s .

Using these formulas with the assumption mentioned, one may compute the dependence of G_s on p_k or F_{kr} , and of thrust P on G_s or p_k , and construct the graphs accordingly.

For engines of great thrust, great per-second propellant-flow rates are required, which is one of the basic difficulties in the field of development of such engines.

The per-second flow rates of the oxidizer and combustible are determined from the equation of the summary propellant-flow rate to the combustion chamber:

$$G_s = G_{s g} + G_{s o} \text{ kg/sec; *} \\ \text{bearing in mind that } G_{s o} = \chi G_{s g}, \text{ we obtain} \\ G_s = G_{s g} + \chi G_{s g} = G_{s g} (1 + \chi). \quad (4.23)$$

whence

$$\left. \begin{aligned} G_{s g} &= \frac{G_s}{1 + \chi} \text{ kg/sec;} \\ G_{s o} &= \frac{\chi G_s}{1 + \chi} \text{ kg/sec,} \end{aligned} \right\} \quad (4.24)$$

where $\chi = G_{s o} / G_{s g}$, the true weight coefficient of the propellant

$$\begin{aligned} * [G_{s r} &= G_{s g} = G_{s \text{ goryuchyeye}} = G_{s \text{ combustible}}; \\ G_{s o} &= G_{s o} = G_{s \text{ okislitel'}} = G_{s \text{ oxidizer}}.] \end{aligned}$$

compound.

The per-second flow rates of the oxidizer and combustible to the combustion chamber of the engine may also be determined in accordance with the formulas:

$$\begin{aligned} G_{o,0} &= g_o G, \text{ kg/sec;} \\ G_{o,r} &= g_r G, \text{ kg/sec,} \end{aligned} \quad (4.25)$$

where g_o and g_g are the weight proportions of the propellant components in kg/kg.

Some engines of great thrusts intended for long-range missiles are made with two stages of thrust, the starting and operating stages. For example, the A-4 engine has a starting and final thrust of 8 tons and an operating thrust of 26 tons. Shifting the engine from the first stage to the second is carried out after it has worked up normally to the previous starting stage.

A starting stage of thrust is introduced for the purpose of starting the engine with a per-second propellant-flow rate to the combustion chamber which is less than the flow rate in the operating regime (resembling the A-4 engine), and, by the same means, avoiding possible engine explosion during ignition of the propellant mixture which has accumulated in the combustion chamber in case of a malfunction in igniting the propellant during starting.

In some existing engines for long-range missiles starting flow rate $G_{s\ p} \approx 20-30\%*$ of G_s .

The per-second propellant-flow rate G'_s in servicing the fuel-feed system, when operating in a rated regime, amounts to about 1.5-3% of the per-second propellant-flow rate G_s to the engine combustion chamber.

When engine thrust is decreased by means of throttling the per-

*[$G_{s\ n} = G_{s\ p} = G_{s\ \text{puskovoy}} = G_{s\ \text{starting}}$.]

second propellant-flow rate to the combustion chamber, the percentage of the propellant-flow rate used to start the turbine of the pump assembly grows as a consequence of the disruption, by this means, of the optimum operating conditions of the gas generator and turbine of the propellant-feed system. For example, with an engine thrust equal to 20% of the rated value, the propellant-flow rate for starting the TNA may amount to 10% of G_s .

The operating economy of the engine is sometimes evaluated by the magnitude of the specific fuel consumption:

- 1) per kg of thrust, per hour

$$C_{ya} = \frac{G_s}{P_n} 3600 = \frac{1}{P_{ya}} 3600 = \frac{1}{\eta_{sp}} \text{ kg-fuel/kg-thrust}, \quad (4.26)$$

- 2) per thrust-hour

$$C_p = \frac{G_s}{N_p} 3600 = \frac{G_s}{P_n V} 3600 = C_{ya} \frac{75}{V} \text{ kg/hp-hr}, \quad (4.27)$$

where V is the missile's flight speed in m/sec.

The specific fuel consumption in a ZhRD depends to a considerable degree on the quality of the propellant itself.

The theoretical specific consumptions for some fuels in a ZhRD at an optimum ratio of components, $p_k = 40$ atm abs and $p_v = 1$ atm abs, have the following approximate values:

	kg/m-sec
1) kerosene + 98% nitric acid.....	4.35
2) Tonka-250 and 98% nitric acid.....	4.09
3) kerosene + 60% of 98% concentration HNO_3 + 40% N_2O_4	3.98
4) Tonka-250 + 60% of 98% HNO_3 + 40% N_2O_4	3.95
5) dimazine (DMG)* + 60% of 98% HNO_3 and 40% N_2O_4	3.82
6) 93.5% ethyl alcohol + liquid oxygen.....	3.68
7) kerosene + liquid oxygen.....	3.56
8) hydrazine + chlorine trifluoride.....	3.51
9) dimazine (DMG) + liquid oxygen.....	3.41
10) hydrazine + liquid oxygen.....	3.36

*[DMG = DMG = dimetil gidrazin = unsymmetrical dimethyl hydrazine - UDMH (dimazine).]

11)	hydrazine + nitrogen trifluoride.....	3.24
12)	kerosene + fluorine monoxide.....	3.00
13)	ammonia + liquid fluorine.....	2.92
14)	hydrazine + liquid fluorine.....	2.90

The figures indicated show that fluorine engines have a relatively small specific fuel consumption which is explained by the higher H_u of the propellant based on fluorine.

By increasing flight altitude, specific fuel consumption is decreased in inverse proportion to $P_{ud.n}$, if the inertia load is ignored.

Specific fuel consumption when the engine is operating on a given regime in space is independent of flight altitude and is of a constant magnitude.

One may consider that a 1% savings in fuel consumption, other conditions being equal, would increase the payload of a missile by approximately 10%.

Example 2. An engine develops a thrust of 1000 kg at a per-second fuel-flow rate to the combustion chamber of 4.86 kg. Determine the specific fuel consumption in the engine.

Solution.

1) specific thrust of the engine

$$P_{ud} = P/G_s = 1000/4.86 = 206 \text{ kg-thrust/(kg-fuel/sec)};$$

2) specific fuel consumption

$$C_{ud} = 1/P_{ud} = 1/206 = 0.00485 \text{ (kg-fuel/sec)/kg-thrust} = \\ = 4.85 \text{ (kg-fuel/sec)/m-thrust.}$$

SECTION 9. METHODS AND LIMITS OF REGULATING ENGINE THRUST

In some cases in a ZhRD the requirement arises for the possibility of regulating the magnitude of thrust within greater or smaller limits. This may be required, for example, to accomplish a given rule for changing the thrust and acceleration of the rocket from time to time,

obtaining a given flight speed at the instant the engine is cut off, or compensating the changes in the characteristics of the engine units and the change in the atmospheric pressure with altitude, to ensure an optimum operating regime, and by this means to obtain the best thrust characteristics.

A liquid-propellant rocket engine with an invariable per-second fuel-flow rate to the combustion chamber gives the missile a flight of changing acceleration, because of the decrease in the back pressure of the atmosphere with rise in altitude (increase of the static thrust component) and the decrease of the missile's weight as fuel components are consumed in the missile. In practice, for the flight of ballistic rockets in an atmosphere of fixed density, a flight with constant acceleration may be more practicable, which may be accomplished by regulating the engine thrust. During these rockets' flight in space, it is advantageous to have an engine with constant thrust. Calculations show that to obtain the best flight characteristics for rockets of various designations, it is necessary to regulate the engine thrust from time to time in accordance with a set of optimum rules. This permits a considerable increase of the payload of the rocket in comparison with its value during a flight with constant thrust.

In cases of application of ZhRD for piloted aircraft, the regulation of their thrust from time to time must be carried out in accordance with the most advantageous climb conditions, for providing maximum speed, range, and duration of flight. For example, to obtain the maximum flight speed of an aircraft, the greatest possible engine thrust is required, while for maximum range and duration of flight it is necessary for the engine to operate with a relatively small thrust. For an aircraft's flight in cruising regimes and at high altitudes, one may regulate the thrust in order to provide the optimum expansion

of gases in the chamber nozzle.

In practice, regulating the thrust of a ZhRD may be accomplished by means of:

1) changing the per-second fuel-flow rate to the combustion chamber (throttle control of the engine), i.e., changing the pressure in it;

2) switching separate combustion chambers in or out of operation, if the engine is multichambered.

It is possible to change the per-second fuel-flow rate to the combustion chamber of an engine by means of:

a) changing the fuel-flow pressure to the combustion chamber through a constant number of injectors; for example, regulating the fuel feed to the gas generator, as a result of which the number of revolutions of the turbine and the capacity of the pumps of the fuel-feed system of the engine are changed;

b) adaptation of rotary valves (resembling the BMW-R3386 engine), by means of which part of the injector orifices in the combustion-chamber head are opened or closed as necessary for feeding fuel;

c) adaptation of a group-injector system for the same purpose (resembling the "Walther" 109-509A engine), permitting switching of separate groups of fuel injectors in or out of operation as convenient.

In the BMW-R3386 engine, turning the regulating valves is accomplished, depending on change of altitude and flight speed, by a special automatic device for keeping a constant Mach number. In the "Walther" 109-509A engine, the chamber has 12 injectors of the flat-spray type. All of these injectors are connected in two groups of three injectors each and one of six injectors. The pilot controls the operations of these groups of injectors as convenient.

The throttle control method of regulating the thrust of a ZhRD is

the simplest, but it is extremely uneconomical, since by increase or decrease of the per-second fuel-flow rate to the combustion chamber in relationship to its optimum value, the following factors deteriorate:

1) the processes of vaporization and mixing of the fuel components, because of the change in the normal pressure difference of the components in the injectors;

2) the quality of the cycle in the engine chamber, as a consequence of a decrease in the pressure of the gases in it, deterioration in the quality of vaporization, and the fact that the volume of the combustion chamber and the dimensions of the nozzle do not correspond to the changed per-second fuel-flow rate;

3) the state of engine chamber cooling by the regenerative method, especially when one of the propellant components serves as the coolant; this may lead to overheating and even burning out the inner liner of the chamber as a consequence of the decreased amount of fuel because of the decreased thrust and, hence, deterioration in the conditions of heat transfer to the liner, which do not correspond to the changed thermal operating regime of the engine.

Besides this, the pressure in the combustion chamber is lowered by a decrease in the fuel-flow rate, and therefore the level of dissociation of the products of combustion is increased, which, in general, decreases the specific thrust of the engine and disrupts the stability of its operation.

This shows that regulating the thrust of an engine by throttle control may be practicable only within comparatively narrow limits.

Loss ΔP_{ud} of specific thrust by throttle control of the fuel-flow rate to the chamber of the engine depends on flight altitude and intensity of throttling. With an increase in altitude, the loss ΔP_{ud} decreases, and in space is theoretically equal to zero. One may consider

that a five-fold decrease in the engine chamber's thrust by throttle control at sea level is accompanied by a decrease in the specific thrust of almost 20%, and losses in thrust of approximately 8% of nominal value.

Decreasing the loss in specific thrust, which is conditional upon the decrease of the pressure difference in the injectors because of throttle control of the fuel-flow rate, is possible by regulating the thrust by means of application of the above-mentioned rotary valves or by a group system of injectors. In these methods of regulation, those injectors which are not switched off operate at rated (optimum) pressure differences. However, such thrust regulation is also accompanied by an unavoidable deterioration in the method used in cooling the engine chamber, because of the reasons mentioned above. Besides this, switching off part of the injectors does not provide equal distribution of the fuel components across a cross section of the combustion chamber, the propellant combustion in the relatively large volume of the chamber deteriorates, and a fusion of the nonoperating part of the injectors is caused as the consequence of the inflow of gases of high temperature through them, as well as causing some asymmetry in the engine-chamber thrust.

Satisfactory propellant-component vaporization during regulation of engine thrust by throttle control of the fuel-flow rate is made possible by using injectors with regulated nozzles. However, such injectors are complicated in construction.

Multichambered engines permit stage regulation of thrust by cutting the separate chambers in or out of operation in the optimum regime without decreasing the operating economy of the engine. However, multichamber (bloc) engines have comparatively complicated fuel-feed systems because of the necessity of synchronizing the thrust of the

separate chambers, and greater dimensions. In changing the per-second fuel-flow rate to the combustion chamber of engines operating with variable thrust, the pressure of the gases in the chamber must be constant; considerable decrease in its magnitude leads to deterioration of the cycle in the combustion chamber, to the origin of an unstable propellant-combustion regime, and other unfavorable consequences.

Consequently, regulating the thrust of a ZhRD by means of throttle control of the per-second fuel-flow rate is accompanied by a decrease in the operating economy of the engine, disruption of the normal conditions of chamber cooling, and the origination of unstable operation.

The lower limit for reducing the thrust of an engine by throttle control of the fuel-flow rate may, in practice, be established either by the given coolant's maximum permissible heat in the chamber passage, or by compression waves originating in the gases in the nozzle, which may take place when the ratio of the pressures of the gases in the outlet from the nozzle and in the atmospheric air is about $p_v/p_a \leq 0.4$.

The ratio of pressures mentioned above shows that, in practice, the possible intensity of throttling an engine for changing the thrust, according to this parameter, is less at ground level and at low altitudes than at high altitudes. One may consider that by lowering the thrust and the pressure of the gases in the combustion chamber of the engine by 80%, the temperature of the coolant may be raised by almost 50%.

If the coolant permits only an insignificant rise of temperature, or if an extremely intense throttling of the engine chamber is required for decreasing the thrust, then it may become necessary to change the composition of the propellant for decreasing the tempera-

ture of the products of propellant combustion at extremely small thrusts, to use a film protection against overheating of the chamber liner, and so forth.

Regulating the thrust of an engine below 10% of its nominal value is, in practice, impossible to accomplish because of the instability of the combustion of the propellant in the combustion chamber, excessive increase in the temperature of the coolant, and the sharp decrease in specific thrust. In some existing types of aircraft ~~ZhRD~~ which operate on nitric acid and kerosene, the thrust is regulated within the limits of 30-100%. Somewhat wider limits of thrust regulation (12-100%) are possible for engines operating on hypergolic propellant components (Table 4.1).

A good start-up and smooth thrust control of an engine within wide limits may be provided only by preserving the necessary propellant-component ratio. This applies also to the composition of the fuel used to operate the gas generator. If these conditions are not fulfilled, an excessively high temperature in the chamber of the gas generator or uneven combustion may take place, and the reaction may even stop.

In designing any system for regulating an engine, it is necessary to consider the requirements demanded of the system during regimes in launching, normal operation, and operation at the instant of propellant cutoff. In general, very precise regulation of all three operating regimes of the engine is desirable; however, the designer's potentialities in this relationship are limited for reasons of a practical nature.

This circumstance leads to the emergence of new problems, particularly in providing pumps of identical characteristics, and to the complication of the system of regulation (the presence of several feed-

TABLE 4.1

Limits of Thrust Regulation of Some Existing
ZhRD

1) Марка двигателя	2) Назначение двигателя	3) Способ регулирования тяги	4) Тяга двигателя кг		7) Пределы регулиру- рования тяги %
			5) максим.	6) миним.	
8) "Вальтер" 109-509A	9) Авиационный	10) Групповые форсунки	1700	200	11,7
11) BMW-P3386	12) Зенитный снаряд	13) Поворотные золотники	380	60	15,7
14) "Скреймер"	15) Авиационный	16) Дросселирование расхода	3000	450	12,5

1) Brand of engine; 2) purpose of engine; 3) method of thrust regulation; 4) engine thrust, kg; 5) maximum; 6) minimum; 7) limits of thrust regulation, %; 8) "Walther" 109-509A; 9) aircraft; 10) group injectors; 11) BMW-R3386; 12) antiaircraft missile; 13) rotary valves; 14) "Screamer"; 15) aircraft; 16) flow-rate throttling.

back circuits). The use of a bloc of single-chambered engines leads to further complication of the system as the result of the emergence of several regulation circuits.

Since ZhRD with thrust regulated in accordance with a fixed rule are very complicated in structure, their application has turned out to be impractical in a number of cases. For this reason the thrust of the majority of the contemporary missiles which are being manufactured is not regulated. The engines of long-range missiles may accomplish thrust regulation in the form of one stage during launching and several seconds before engine cutoff, which creates the necessity of providing reliable starting and stopping of the engine according to a given program.

SECTION 10. FLOW-RATE CHARACTERISTICS OF AN ENGINE

The dependence of absolute and specific thrusts (P and P_{ud}) of an engine, in the presence of fixed values of altitude and flight speed, on the pressure p_k in the combustion chamber, i.e.,

$$P \text{ and } P_{ud} = f(p_k),$$

is called the flow-rate or throttle characteristics of a ZhRD; these characteristics may also be dependent upon the factors determining the magnitude of its pressure p_k , i.e., per-second fuel-flow rate G_s [sic] to the combustion chamber; feed pressure p_p of the propellant components to the combustion chamber; and number of revolutions n of the turbo-pump unit, if one is included in the engine fuel-feed system, and other factors.

By means of the flow-rate characteristics, the most advantageous operating regime of the engine under operating conditions is ordinarily established, and the practicability and limits of thrust regulation by changing the per-second propellant-flow rate to the combustion chamber are ascertained.

Flow-rate characteristics of a ZhRD, in accordance with the pressure of the gases in the combustion chamber, may be constructed in accordance with the data from ground-level tests of the engine on a stand, and analytical calculations for ground-level or arbitrary values of altitude and flight speed.

Flow-rate characteristics for an engine operating on a test stand are usually derived from an invariable weight ratio of the propellant components. Fulfilling this condition, with the changing operating regimes of an engine is, in practice, extremely difficult. Flow-rate characteristics may also be derived for determining the specific thrust of an engine at different weight ratios of the propellant components.

In practice, one may calculate flow-rate characteristics of an engine only approximately, since one cannot precisely evaluate the decrease in the heat-liberation coefficient φ_k of the fuel and the change in the polytropic exponent n of the expansion of the gases in the nozzle, because of the change in the per-second flow rate G_s of the propellant to the combustion chamber in relationship to its rated nominal value $G_{s.r}$. In calculating flow-rate characteristics, the values of φ_k and n are assumed as being constant, and equal to their values when the engine is operating in the optimum regime.

Ignoring changes of φ_k and n , these ratios are found in accordance with the flow-rate characteristics of an engine:

$$\frac{G_s}{G_{s.p}} = \frac{p_k}{p_{k.p}},$$

whence $C_s = G_{s.r} (p_k/p_{k.r})$ kg/sec;

$$\frac{p_o}{p_{o.p}} = \frac{p_k}{p_{k.p}},$$

whence $p_v = p_k p_{v.r}/p_{k.r}$ atm abs;

$$\frac{\Delta p_{c.p}}{\Delta p_{c.p.p}} = \left(\frac{G_s}{G_{s.p}} \right)^2,$$

whence $\Delta p_{s.p} = \Delta p_{s.p.r} (G_s/G_{s.r})^2 = \Delta p_{s.p.r} (p_k/p_{k.r})^2$, where $\Delta p_{s.p.r}$ and $\Delta p_{s.p}^*$ are the summary pressure differences of the fuel in the pressurized feed system of the engine when the chamber is operating in rated and nonrated operating regimes, respectively, in kg/cm².

Considering these ratios, the general thrust equation of an engine chamber may be given the form

$$P_s = \frac{w_s}{g} G_s + F_s p_s - F_s p_o = \frac{w_s}{g} G_{s.p} \frac{p_k}{p_{k.p}} + F_s p_k \frac{p_{o.p}}{p_{k.p}} - F_s p_o =$$

$$= \left(\frac{w_s}{g} \frac{G_{s.p}}{p_{k.p}} + F_s \frac{p_{o.p}}{p_{k.p}} \right) p_k - F_s p_o = \left(\frac{P_{sm}}{p_{k.p}} + F_s \frac{p_{o.p}}{p_{k.p}} \right) p_k - F_s p_o.$$

$$*[\Delta p_{c.p.p} = \Delta p_{s.p.r} = \Delta p_{\text{summary.perepad.raschetny}} =$$

$$= \Delta p_{\text{summary.difference.rated}};$$

$$\Delta p_{c.p} = \Delta p_{\text{summary.difference}}.]$$

Replacing the constant value for a given engine $P_{din}/p_{k.r} + F_v p_{v.r}/p_{k.r} = A$ in this expression, we will finally obtain an equation for computing the thrust of an engine under chosen values of pressure in the combustion chamber:

$$P_s = Ap_k - F_s p_s.$$

Since, according to the ratio $p_k = (p_{k.r}/G_{s.r})G_s$ given above, the latter equation may be given the form

$$P_s = Ap_k - F_s p_s = A \frac{p_{k.r}}{G_{s.r}} G_s - F_s p_s = A' G_s - F_s p_s,$$

where $A' = (P_{din} + F_v p_{v.r})/G_{s.r}$ is a constant magnitude for the given engine.

The per-second propellant-flow rate $G_{s.r}$ to the combustion chamber when the engine is operating in a rated regime is determined according to the formulas in Section 8 of this chapter.

The thrust of the engine chamber when operating in space, i.e., when $F_v p_a = 0$, is determined in accordance with the formulas:

$$P_p = Ap_k \text{ or } P_p = A' G_s.$$

These formulas show that when the engine is operating in space the dependence of P_p on p_k or G_s is a straight line passing through the beginning of the coordinates, and when operating in an atmosphere it is a straight line arranged below the previous line due to the effect of $F_v p_a$ (Figs. 4.15 and 4.16). One must bear in mind that the flow-rate characteristics of an engine, in real conditions, are an almost straight line only until a propellant-flow rate to the chamber equal to about 30-40% of nominal is achieved. At lower propellant-flow rates, the flow-rate characteristic runs along a sharply increasing curve with its left branch directed downward.

The specific thrust of an engine chamber, with a corresponding value of p_k , is determined in accordance with the formula

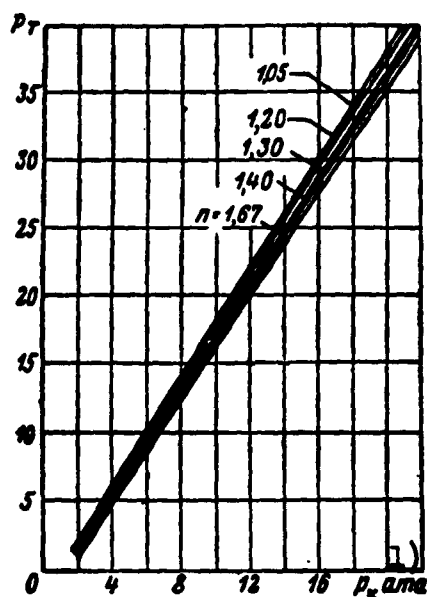


Fig. 4.16. Flow-rate characteristics of the A-4 engine when operating at sea level, computed for various polytropic exponents n . 1) p_k , atm abs.

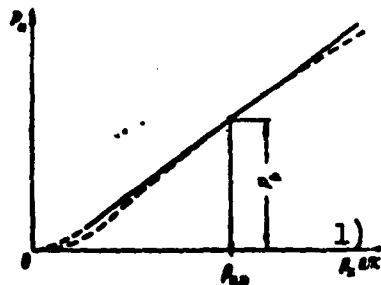


Fig. 4.17. Approximate curves of rated (solid line) and experimental (dotted line) flow-rate characteristics of an engine when operating at ground level. 1) p_k , atm abs.

ence of thrust on pressure in the combustion chamber is a slightly curved line, almost straight (Fig. 4.17). Since the curvature of this line is extremely small, when there is a lack of test-stand data for an engine, one may fully rely upon the calculated flow-rate characteristics.

Calculation of a change in an engine's thrust, depending on p_k , may be carried out by means of the nomogram in Fig. 4.10 by the following method:

1) for a given value of $f_v = F_v/F_{kr}$ and a chosen magnitude of n , determine, in accordance with the nomogram, the relationship of p_k/p_v and the thrust coefficient K_p in space;

2) for every chosen value of p_k , determine $K_n = K_p - f_v p_a/p_k$, and compute the thrust of the engine in accordance with the formula $P_n = K_n p_k F_{kr}$.

On the basis of calculating the dependence of P_n and $P_{ud.n}$ on p_k , the already well-known general formula of the thrust of an engine may be laid down:

$$P_n = p_k F_{kr} \sqrt{\frac{2n^2}{n-1} \left(\frac{2}{n+1}\right)^{\frac{n+1}{n-1}} \left[1 - \left(\frac{p_a}{p_k}\right)^{\frac{n-1}{n}}\right]} + F_a (p_a - p_k).$$

For computing the thrust of an engine in accordance with this formula at chosen values of p_k (for example, with $p_k = 5, 10, 15, 20$

atm abs, etc.), one must set down the assumed mean values for the polytropic exponent \underline{n} and, by means of the graphs in Fig. 3.9, determine, according to the $f_v = F_v/F_{kr}$ of the given engine, and the chosen value of \underline{n} , the relationship of p_k/p_v and then of p_v .

The results of such calculations of the throttle characteristics of an A-4 engine, when operating at sea level with various values of \underline{n} , are shown in Fig. 4.16. For this engine, $f_v = 3.42$.

The curves of this figure show that \underline{n} has an insignificant influence on the throttle characteristics of an engine. For example, when \underline{n} is changed from 1 to 1.67, the thrust of an A-4 engine, at a given p_k , is changed by approximately 10%. Changing \underline{n} at an invariable value of p_k causes a decrease in the engine's thrust.

Since, with corresponding values of p_k , it is impossible to evaluate the magnitude of the polytropic exponent \underline{n} of the expansion of the gases in the nozzle precisely, in this case the results of the flow-rate characteristics of the engine are obtained in approximation.

For existing engines, the mean value of \underline{n} may be determined with sufficient accuracy by the magnitudes of p_k and p_v measured during experiments.

For construction of the flow-rate characteristics of an engine chamber, one may use the formulas:

$$P_s = p_s F_{sp} K_{s,r} - F_s p_s; G_s = \frac{G_{s,p}}{p_{s,p}} p_s \text{ and } P_{y,s} = \frac{P_s}{G_s}.$$

For calculating the flow-rate characteristics of an engine in accordance with the feed pressure p_p of the propellant components to the combustion chamber, one may use the formula

$$P_s = p_s + \Delta p_{c,s} = p_s + \Delta p_{c,s,p} \left(\frac{p_s}{p_{s,p}} \right)^2 = p_s + \Delta p_{c,s,p} \left(\frac{G_s}{G_{s,p}} \right)^2.$$

Engines of the final stages of multistage missiles must begin and end their operation in space. This circumstance requires knowledge of

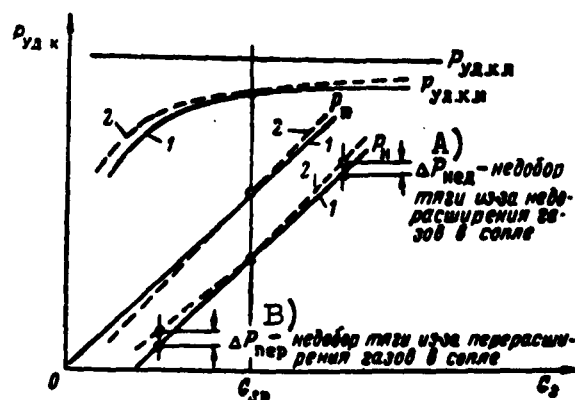


Fig. 4.18. Flow-rate characteristics of an engine with nonregulated and with ideally regulated nozzle in accordance with altitude. 1) Engine with nozzle which is not regulated in accordance with flight altitude; 2) engine with ideally regulated nozzle. A) ΔP_{ned} - shortage of thrust because of underexpansion of the gases in the nozzle; B) ΔP_{per} - shortage of thrust because of overexpansion of the gases in the nozzle.

the flow-rate characteristics of high-altitude and super-high-altitude engines and the capability of constructing them on the basis of data from ground-level static tests.

Figure 4.18 shows the flow-rate characteristics of a ZhRD with a nonregulated high-altitude nozzle in accordance with flow-rate G_s (solid lines) and with an ideally regulated nozzle in accordance with the rated conditions of operation (when $p_v = p_a$).

In a given case, when G_s deviates from the rated magnitude $G_{s, r}$, nozzle regulation is accomplished by shortening or elongating the nozzle. Thus, an unregulated engine nozzle operates under nonoptimum conditions, i. e., the gases overexpand or underexpand in relationship to the surrounding medium's pressure p_a .

Figure 4.19 shows the flow-rate characteristics of a low-altitude

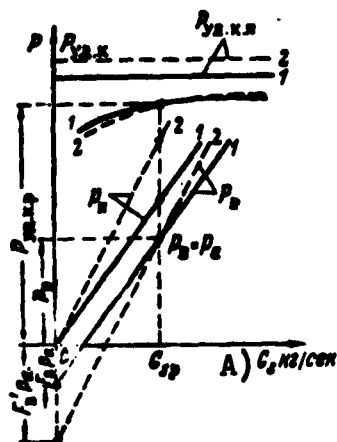


Fig. 4.19. Flow-rate characteristics of a low-altitude and of a high-altitude engine. 1) Low-altitude engine; 2) high-altitude engine. A) G_s , kg/sec.

and of a high-altitude ZhRD when operating in the atmosphere and in space (the dashed lines refer to the high-altitude engine).

Comparing the rated and experimental flow-rate characteristics of ZhRD is possible only if they are reduced to the same conditions (preferably to normal conditions).

The following approximate characteristics are also of interest in selecting the most advantageous engine operating regime (Fig. 4.20):

1) the dependence of specific fuel consumption C_{ud} and the engine's internal effi-

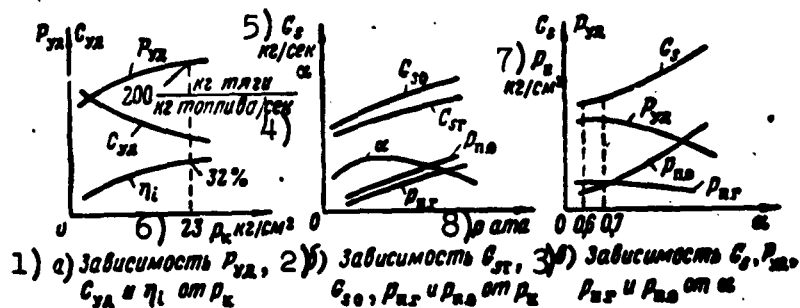


Fig. 4.20. Some engine cycle parameters as functions of combustion chamber pressure and the fuel's excess oxidation coefficient. 1) a) P_{ud} , C_{ud} , and η_i as functions of p_k ; 2) b) $G_{s g}$, $G_{s o}$, $p_{p.g}$, and $p_{p.o}$ as functions of p_k ; 3) c) G_s , P_{ud} , $p_{p.g}$, and $p_{p.o}$ as functions of α ; 4) kg-thrust/(kg-fuel/sec); 5) G_s , kg/sec; 6) p_k , kg/cm²; 7) p_p , kg/cm²; 8) p , atm abs.

ciency η_i on combustion chamber pressure p_k ;

2) the dependence of the per-second flow rates of the combustible ($G_{s g}$) and oxidizer ($G_{s o}$) to the combustion chamber, their feed pressures ($p_{p.g}$ and $p_{p.o}$), and the fuel's excess oxidation coefficient α on com-

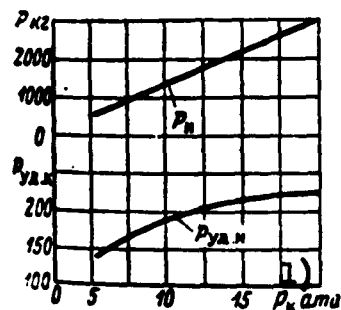


Fig. 4.21. Rated flow-rate engine characteristics (example No. 3). 1) p_k , atm abs.

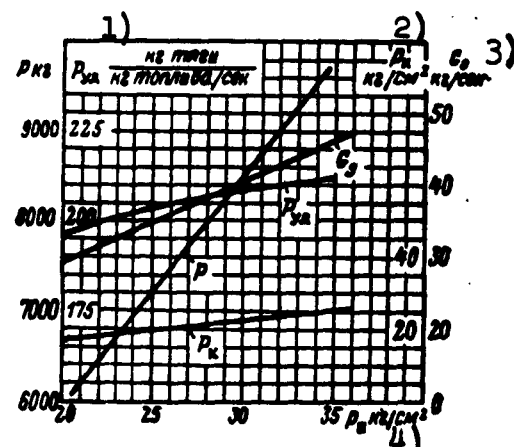


Fig. 4.22. Rated flow-rate engine characteristics. 1) P_{ud} , kg-thrust/(kg-fuel/sec); 2) p_k , kg/cm²; 3) G_s , kg/sec; 4) p_p , kg/cm².

TABLE 4.2

1) p_k , kg/cm ²	20	15	10	5
2) P_n , kg	3000	2150	1296	445
3) $P_{u, n}$ $\frac{\text{kg thrust}}{\text{kg fuel/sec}}$	221	210	191	131

1) p_k , kg/cm²; 2) P_n , kg; 3) $P_{ud, n}$, kg-thrust/(kg-fuel/sec).

bustion chamber pressure;

3) the dependence of the per-second fuel-flow rate G_s to the combustion chamber, fuel-component supply pressures $p_{p, g}$ and $p_{p, o}$, and absolute P and specific p_{ud} [sic] engine thrusts on the excess oxidation coefficient α .

The aggregate of the different flow-rate and altitude characteristics permits sufficiently accurate evaluation of Z_{HRD} of any type and design from the viewpoint of per-second fuel-flow rate, thrust, operating efficiency, and those requirements which are demanded for the chamber, fuel-feed system units, and engine operation regulation.

Example 3. Calculate the flow-rate characteristics of an engine when $p_k = 20, 15, 10,$ and 5 kg/cm^2 for a $V = 0$ and $H = 0$, if $P_r = 3000 \text{ kg}$, $F_v = 407.1 \text{ cm}^2$, $p_{k.r} = 20 \text{ kg/cm}^2$, $G_{s.r} = 13.54 \text{ kg/sec}$, and $p_{v.r} = 1.00 \text{ kg/cm}^2$.

Solution.

1. At the given initial data for the engine, the flow-rate characteristic computation formulas take the form

$$P_n = 170.3p_k - 407.1 \text{ kg};$$

$$P_{ud.n} = 251.1 - 602/p_k \text{ kg-thrust/(kg-fuel/sec)}.$$

2. The results of the computations for absolute and specific thrust for the given gas pressures in the combustion chamber are reduced in Table 4.2 and presented graphically in Fig. 4.21.

Figure 4.22 shows the flow-rate characteristics of an engine as a function of fuel-feed pressure, with a rated thrust of 8500 kg at ground level and a specific thrust of 213 kg-thrust/(kg-fuel/sec), combustion chamber pressure of 22 atm abs, nozzle outlet-section pressure 1 atm abs, per-second fuel-flow rate to the combustion chamber 39.9 kg/sec, and pressure difference of 7.7 atm abs in the fuel line. The chamber-nozzle outlet-section area is 1052 cm^2 .

SECTION 11. REAL ZhRD FLOW-RATE CHARACTERISTICS

Real flow-rate characteristics may be constructed in accordance with the data from ZhRD static firing tests, i.e., considering the factual values of the different additional engine parameters which affect its operation at any instant of time.

During an engine's operation under real conditions, the following parameters, which affect the magnitudes of absolute and specific thrust, are changed:

- 1) the engine operating components' (fuel and vapor-gas genera-

tion devices) specific weights, caused by their temperature change;

2) the fuel components' pressure head to the pumps in accordance with the degree of their consumption;

3) the ratio of the fuel components (their weight concentration);

4) the gas-vapor pressure to the TNA or the tank pressure in other propellant-feed systems, and similar.

When these parameters are changed, the TNA rpm change accordingly, as well as the working components' per-second flow rate in the engine, combustion chamber pressure, and, consequently, engine thrust.

Zhrd flow-rate and altitude characteristics are usually computed at these parameters' fixed nominal values. They are always differentiated from experimental characteristics. To construct precise engine characteristics by calculations, one must consider an engine's change due to the factors mentioned above; thus, the following system of equations is obtained:

$$\left. \begin{aligned} \Delta G_{s,o} &= a\Delta p_o + b\Delta p_r + c\Delta \gamma_o + e\Delta \gamma_r + f\Delta G_{nr} + i\Delta c_1; \\ \Delta G_{s,r} &= a'\Delta p_o + b'\Delta p_r + c'\Delta \gamma_o + e'\Delta \gamma_r + f'\Delta G_{nr} + i'\Delta c_1; \\ \Delta n &= l\Delta G_{s,o} + m\Delta G_{s,r} + o\Delta \gamma_o + q\Delta \gamma_r + r\Delta G_{nr} + s\Delta c_1, \end{aligned} \right\} \quad (4.28)$$

where $\Delta G_{s,o}$ and $\Delta G_{s,g}$ are the changes in the per-second flow rate of the oxidizer and the combustible, respectively, in kg/sec; Δp_o and Δp_g are the changes of fuel components' pressure heads to the pumps; $\Delta \gamma_o$ and $\Delta \gamma_g$ are the changes in specific weight of the fuel components; ΔG_{pg}^* is the change in gas-vapor flow rate in kg/sec; Δc_1 is the change in nozzle velocity at the outlet from the TNA turbine nozzles, determined by the change in temperature and composition of the working fluid during gas-vapor generation; Δn is the change in TNA rpm; and $a, b, c, \dots, a', b', c', \dots$ are constant coefficients.

Thus, a change in the per-second fuel-flow rate to the engine

$$*[\Delta G_{nr} = \Delta G_{pg} = \Delta G_{parogaz} = \Delta G_{gas \text{ vapor}}.]$$

combustion chamber is expressed by the formula

$$\Delta G_s = \Delta G_{s,0} + \Delta G_{s,r} = (a + a') \Delta p_0 + (b + b') \Delta p_r + (c + c') \Delta \gamma_0 + (e + e') \Delta \gamma_r + (f + f') \Delta G_{nr} + (i + i') \Delta c_1. \quad (4.29)$$

The change in the weight coefficient of the fuel composition will be

$$\Delta \chi = \frac{G_{s,0} + \Delta G_{s,0}}{G_{s,r} + \Delta G_{s,r}} - \chi, \quad (4.30)$$

where χ is the fuel-composition coefficient when the engine is operating in a nominal regime (when all changes in the additional parameters are equal to zero).

Thus, a change in engine thrust is found by means of the flow-rate characteristics, using the values of ΔG_s and $\Delta \chi$ which have been found.

During an engine's flight at various altitudes, with great velocities or accelerations, the number of additional factors affecting the engine's operation increases.

A weapon's acceleration during flight depends basically on the device's weight decrease as a consequence of the consumption of the fuel in the tanks and the decrease in atmospheric air resistance with increased altitude.

SECTION 12. ENGINE ALTITUDE CHARACTERISTICS

For practicable use of an engine, it is important to know how its characteristics are changed by changes in the external operating conditions, i.e., altitude H and flight speed V .

The dependence of absolute P and specific P_{ud} engine thrusts on flight altitude H , at a fixed combustion-chamber pressure p_k and constant flight speed V , is called the altitude characteristics of a ZhRD.

Since an engine may operate in maximum, nominal, and minimal thrust regimes, an engine's altitude characteristics must be con-

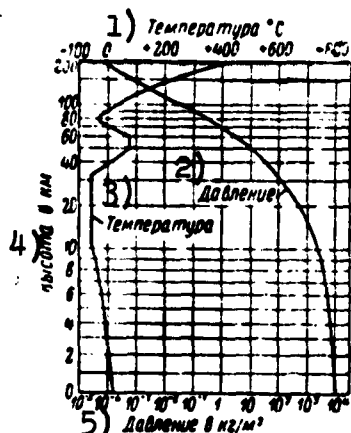


Fig. 4.23. Temperature and pressure in the atmosphere at altitudes of zero to 200 km. 1) Temperature, °C; 2) pressure; 3) temperature; 4) altitude, km; 5) pressure, kg/m^2 .

constructed for several combustion-chamber pressures which control these operating regimes.

Constructing the altitude and velocity characteristics of a ZhRD by the experimental method is attended with extremely great difficulties, since the use of very complicated equipment is required for this — special wind tunnels and pressure chambers, and providing actual operational tests for the engine installed in a missile provided with apparatus capable of measuring the required parameters with sufficient accuracy. Therefore these ZhRD characteristics are usually

constructed by the calculation method. Thus, precise calculation of these characteristics is made extremely complicated by the impossibility of precisely evaluating the change in atmospheric air pressure around the engine and behind its nozzle during changes in altitude and flight speed.

The pressure p_a of the surrounding medium, into which gases flow from the engine nozzle, is the basic external factor affecting the magnitudes of the engine's absolute and specific thrusts. This pressure is changed as a function of the change in altitude and flight speed.

For constructing the altitude characteristics of a ZhRD, ignoring the change in air pressure behind the engine nozzle as a consequence of the change in flight speed (the engine's ideal altitude characteristics), we may take the values of p_a , as a function of flight altitude, from Table 4.3, the Standard International Atmosphere, which has been computed up to an altitude of 75 km.

TABLE 4.3
Standard International Atmosphere

Высота км 1)	Давление кг/см ² 2)	Темпера- тура T °K 3)	Высота км 1)	Давление кг/см ² 2)	Темпера- тура T °K 3)
0	1,033	288	16	0,113	216,5
1	0,917	281,5	17	0,089	216,5
2	0,811	275	18	0,076	216,5
3	0,715	268,5	19	0,065	216,5
4	0,620	262	20	0,056	216,5
5	0,550	255,5	21	0,048	216,5
6	0,481	249	22	0,041	216,5
7	0,418	242,5	23	0,035	216,5
8	0,363	236	24	0,030	216,5
9	0,314	229,5	25	0,025	216,5
10	0,269	223	26	0,020	216,5
11	0,231	216,5	30	0,0124	
12	0,197	216,5	40	0,003	
13	0,168	216,5	50	0,00093	
14	0,143	216,5	60	0,00031	
15	0,122	216,5	75	0,000031	

1) Altitude, km; 2) pressure, kg/cm²; 3) temperature T, °K.

At altitudes above 25 km, the value of p_a may be evaluated according to the curves in Fig. 4.23. These curves show that at great altitudes p_a is so small that it may be neglected; if we consider that $p_a = 0$ at an altitude of 20 km, the error in computing thrust would not exceed 1%. Therefore, engine altitude characteristics may be computed with sufficient precision from the data in Table 4.3 alone.

Relative $\frac{Z_{HRD}}{Z_{HDD}}$ thrust increase as altitude increases depends on the designed altitude of the nozzle, and in contemporary engines, within the limits of atmospheric pressure change from one atmosphere to space, it may attain 10-20%.

The determination of p_a as a function of flight speed presents great difficulties and is possible only on the basis of the weapon's aerodynamic design, allowing for the weapon's shape.

Figure 4.24 shows the altitude characteristics for an A-4 engine,

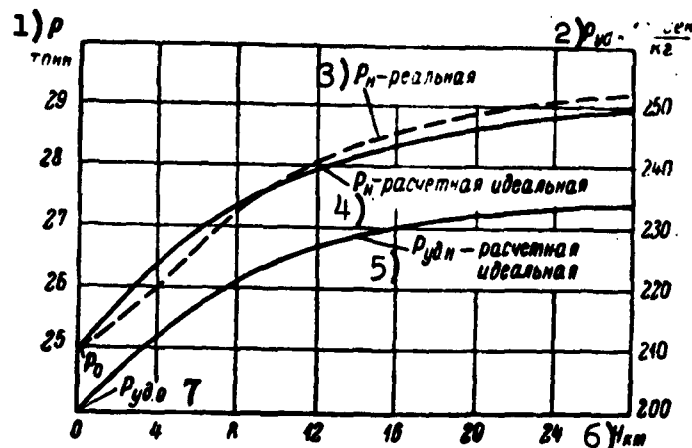


Fig. 4.24. A-4 engine altitude characteristics (dashed line shows real characteristics). 1) P , tons; 2) $P_{ud.n}$, kg-sec/kg; 3) P_n - real; 4) P_n - rated ideal; 5) $P_{ud.n}$ - rated ideal; 6) H , km; 7) $P_{ud.0}$.

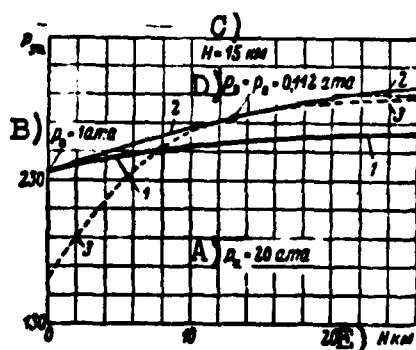


Fig. 4.25. Altitude characteristics of low-altitude and high-altitude engines, and of an engine with ideal nozzle, regulated in accordance with altitude. 1) Low-altitude engine; 2) engine with ideal nozzle, regulated in accordance with altitude; 3) high-altitude engine. A) $p_k = 20$ atm abs; B) $p_v = 1$ atm abs; C) $H = 15$ km; D) $p_v = p_a = 0.112$ atm abs; E) H , km.

where $F_v = 4295 \text{ cm}^2$, $p_v = 0.85 \text{ atm abs}$, $P_0 = 25$ tons, and $P_{ud.0} = 200$ kg-thrust per kg-fuel/sec.

The curves in this graph show that at an altitude of 28 km the engine develops approximately 15.5% greater thrust than at ground level, and, when operating in space, 17% greater thrust. At a fixed flow rate to the combustion chamber, not only these percentages grow, but the engine's specific thrust as well.

Figure 4.25 shows the approximate rated altitude characteristics for low-altitude and high-altitude engines, also that of an engine with an ideal nozzle, regulated in accordance with flight altitude, as constructed in accordance

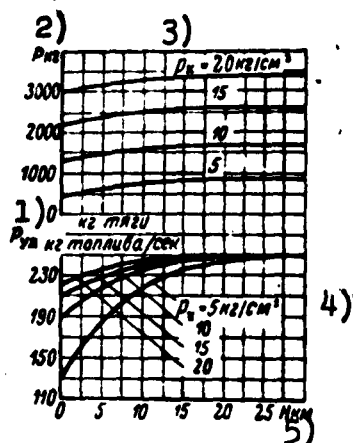


Fig. 4.26. Rated engine altitude characteristics (see example No. 4). 1) P_{ud} , kg-thrust/kg-fuel per sec; 2) P , kg; 3) $p_k = 20$ kg/cm²; 4) $p_k = 5$ kg/cm²; 5) H , km.

with the values of p_a taken from Table 4.7 [sic]. All these engines are identical, i.e., they all operate on the same fuel and at the same combustion-chamber pressure.

The curves of this graph show that:

- 1) a high-altitude engine has a relatively small thrust at ground level, which gives the weapon poor launching properties;
- 2) as flight altitude increases, the absolute thrust of a high-altitude engine increases more intensively than that of a low-altitude engine, in direct proportion to the engine's design altitude;
- 3) an engine with an ideal nozzle, regulated in accordance with flight altitude, has, relatively speaking, more favorable characteristics, which shows the necessity of making such an engine with a regulated design altitude, even if it has only one or two fixed positions.

Besides high operating economy, an engine must provide the weapon with a good takeoff, i.e., its thrust at ground level must exceed the missile's blastoff weight by a given number. An engine's relative thrust coefficient $b = P_0/G_0$ is a function of the tactical designation of the missile. Calculations show that as combustion-chamber pressure rises, the increase in an engine's absolute and specific thrusts becomes less and less significant as flight altitude increases. One should therefore bear in mind that specific thrust will be changed as a function of the engine's absolute thrust, since G_s is independent of p_a and remains constant in calculating the external characteristics.

Example 4. Calculate the altitude characteristics for an engine

TABLE 4.4

1) $H, \text{ км}$	0	5	10	20	30
2) $p_a, \text{ кг/см}^2$	1,033	0,550	0,269	0,055	0,011

1) $H, \text{ км}$; 2) $p_a, \text{ кг/см}^2$.

TABLE 4.5

Values of $P_n/P_{ud,n}$ in Accordance with Flight Altitude

Давление в камере сгорания P_k кг/см^2 1)	2) Высота полета H в км				
	0	5	10	20	30
20	$\frac{2986}{220}$	$\frac{3198}{235}$	$\frac{3298}{243}$	$\frac{3385}{250}$	$\frac{3404}{251}$
15	$\frac{2137}{210}$	$\frac{2333}{229}$	$\frac{2448}{240}$	$\frac{2535}{249}$	$\frac{2553}{251}$
10	$\frac{1283}{189}$	$\frac{1479}{218}$	$\frac{1594}{235}$	$\frac{1681}{248}$	$\frac{1699}{251}$
5	$\frac{432}{127}$	$\frac{628}{185}$	$\frac{743}{210}$	$\frac{830}{245}$	$\frac{848}{250}$

1) Pressure p_k in combustion chamber, кг/см^2 ; 2) flight altitude H , км.

when $p_k = 20, 15, 10$, and 5 кг/см^2 for flight altitudes $H = 0, 5, 10, 20$, and 30 км , if $P_r = 3000 \text{ кг}$, $F_v = 407.1 \text{ см}^2$, $p_k = 20 \text{ кг/см}^2$, $G_{s,r} = 13.54 \text{ кг/сек}$, and $p_{v,r} = 1.00 \text{ кг/см}^2$.

Solution.

1. We determine the absolute and specific thrusts of the engine in accordance with the formulas:

$$P_n = AP_k - F_v p_a \text{ and } P = \frac{P_n}{G_s} = B - C \frac{P_k}{p_a},$$

which, at the given parameters, is reduced to the form:

$$a) \text{ when } p_k = 20 \text{ кг/см}^2 \quad P_n = 3407 - 407.1 p_a;$$

$$P_{ud.n} = 251.1-30.1 p_a;$$

b) when $p_k = 15 \text{ kg/cm}^2$ $P_n = 2557-407.1 p_a;$

$$P_{ud.n} = 251.1-20.1 p_a;$$

c) when $p_k = 10 \text{ kg/cm}^2$ $P_n = 1703-407.1 p_a;$

$$P_{ud.n} = 251.1-60.2 p_a;$$

d) when $p_k = 5 \text{ kg/cm}^2$ $P_n = 852-407.1 p_a;$

$$P_{ud.n} = 251.1-120.4 p_a,$$

where p_a is in kg/cm^2 and $P_{ud.n}$ is in $\text{kg-thrust}/(\text{kg-fuel/sec})$.

2. The atmospheric pressure for the given altitudes, taken from Table 4.7 [sic], is reduced in Table 4.4.

3. The results of the computations of absolute and specific thrusts, at the given flight altitudes, are shown in Table 4.5 and presented graphically in Fig. 4.26.

SECTION 13. REAL Zhrd ALTITUDE CHARACTERISTICS

In the previous section, we considered the change in an engine's absolute and specific thrusts as a function of the natural pressure change in the unperturbed atmospheric air as a function of flight altitude. Under real engine operating conditions, the pressure of the surrounding medium behind the chamber nozzle is always less than the pressure of the unperturbed air. This phenomenon is caused by the rarefaction developed behind the engine nozzle as the missile flies with great velocities and accelerations, and affects the magnitude of the engine's thrust. Therefore, in precise calculation of an engine's altitude characteristics, one must consider its specific external operating conditions.

In real operating conditions, an engine's absolute thrust depends on the following factors:

- 1) the weapon's flight altitude, speed, and acceleration;

- 2) the fuel tanks' pressurization system;
- 3) the engine's propellant-feed system;
- 4) the specific weight and level of the fuel components in the tank, etc.

Some of these factors tend to increase, and some to decrease, the engine's absolute thrust. For example, as the flight altitude and speed of a weapon of the A-4 type are increased, the pressure of the air around the engine decreases in relationship to the atmospheric pressure, and in the presence of a great flight speed (above Mach number 2.6) the rarefaction formed behind the engine nozzle may even attain absolute vacuum, as a result of which the following things take place.

1. The expansion ratio of the gases behind the engine nozzle increases as a consequence of the decreased back pressure p_a , because of which the engine thrust increases by means of the increase in the statistic member $P_{st} = F_v (p_v - p_a)$ (subscript st = statistic).

2. The expansion ratio of the turbopump unit exhaust gases increases as they flow out into the surrounding medium, and volume of turbopump unit exhaust gases increases as a consequence of the decreased back pressure p_a (if a TNA is part of the engine propellant-feed system and the turbine exhaust gases continue to expand as they flow out into the surrounding medium and develop a thrust).

3. The on-board gas pressure on the engine fuel-system pressure reducer is reduced at the outlet as a consequence of the decreased pressure p_a of the surrounding medium on the reducer diaphragm, because of which the gas-vapor feed to the turbine is reduced, turbine rpm drops, and the pumps' capacity is lowered, which leads to a decrease in engine thrust. An analogous effect on engine thrust is possible when other instruments which are sensitive to pressure changes

in the surrounding medium are installed.

4. The pressure for the engine fuel-pump suction is changed as a consequence of a change in fuel-tank pressurization (if pressurization by velocity head or from an on-board source of compressed gas is used), because of which changes occur in the per-second fuel-flow rate to the combustion chamber and, consequently, in the engine thrust.

5. The fuel components' pressure head to the pumps is increased by means of the inertial forces developed as the weapon is accelerated, in direct proportion to the specific weight and the level of the fuel components in the tanks before they reach the pumps, which, similar to item No. 4, changes the engine thrust.

6. The fuel components' weight ratio as they are fed to the engine combustion chamber is decreased under the influence of the factors mentioned in items 3-5, because of which the fuel's thermal efficiency is changed and, consequently, the engine thrust as well.

To calculate the effect of all the factors enumerated above on thrust magnitude and to construct the real altitude characteristics, it is necessary to have the following basic characteristics:

a) engine combustion chamber and nozzle — the pressure of the gases in the chamber and at the outlet from the nozzle, the area of the nozzle outlet section;

b) propellant-feed system — turbines, pumps, pressure regulators, and the like, and

c) weapon — flight altitude, speed and acceleration, and angle of shift in accordance with time, as the same engine may show different real characteristics when installed in different missiles.

In practice, this problem is brought to compilation by simultaneous approximate solution of several equations, considering the effect of the factors enumerated above on the engine's operation.

The most important of these factors is the pressure of the atmospheric air behind the engine nozzle; therefore, its magnitude must be evaluated by computing with the specific engine operating conditions when designing a ZhRD.

An engine's real altitude characteristics, i.e., allowing for the effect of all the factors enumerated above on engine operation, is expressed by the equation

$$P_{zH} = P_p \left(1 + \frac{\Delta G_z}{G_z} \right) + F_z (P_z - P_a) + \Delta P_{TNA} - \Delta P_{pyz}, \quad (4.31)$$

where P_p is the engine thrust at ground level at the rated nominal regimes; ΔP_{TNA} is the thrust developed by TNA exhaust gases; ΔP_{rul} is the engine thrust loss due to gas rudders; $\Delta G_z = \Delta G_{zg} + \Delta G_{zo}$ is the change in per-second fuel flow to the combustion chamber in kg/sec as the consequence of:

a) the effect of the pressure change in the surrounding air on the pressure reducer's operation, determined, in turn, by the operating regimes of the PGG and TNA (if such devices are included in the engine propellant-feed system);

b) the effect of variation in velocity-head fuel-tank pressurization on the pumps' operation; as flight altitude increases, velocity-head pressurization decreases, and as flight speed increases, velocity-head pressurization increases;

c) the effect of the change in fuel component level in the tanks as a consequence of their consumption;

d) the effect of the changing fuel-component pressure head in the tanks because of the inertial forces developed during the weapon's acceleration, and other reasons.

Figure 4.24 shows the results of the calculation of an A-4 engine's real altitude characteristics when it is installed in a long-range missile.

It is obvious that the same engine may have different real altitude characteristics, depending on the particulars of the aircraft in which it is installed. A change in construction, fuel-tank volume, takeoff velocity or acceleration, head of fuel-tank pressurization, or the like leads unavoidably to a change in the fuel components' feed pressure to the combustion chamber, and, consequently, change in engine thrust.

The construction of real ZhRD altitude characteristics for aircraft is closely connected with the calculation of the trajectory elements for these craft. Therefore, the engine altitude characteristics and the aircraft flight trajectory must be determined by simultaneous calculations.

The curves in Fig. 4.24 show that the real altitude characteristics of an engine differ very little (by 1-3%) from the ideal characteristics (dashed line) when computed under the same initial conditions in conformance to the simplified formula which considers only the normal pressure of the unperturbed air behind the engine nozzle in accordance with flight altitude. Bearing this circumstance in mind, one may use the simplified thrust formula for calculating altitude characteristics.

SECTION 14. SELECTION OF OPTIMUM ENGINE-CHAMBER NOZZLE DESIGN ALTITUDE

One of the basic parameters which directly affects the magnitude of an engine's absolute thrust is the pressure of the surrounding medium, which may change during an aircraft's flight as a function of flight altitude and speed.

The majority of aircraft engines operate without a change of the gas pressure in the combustion chamber as altitude increases, but since atmospheric pressure p_a is thus decreased, the necessity arises

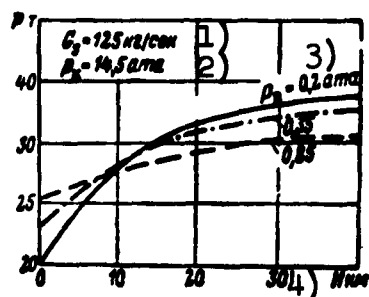


Fig. 4.27. Rated altitude characteristics of an A-4 engine with different conventional nozzle lengths. 1) $G_s = 125 \text{ kg/sec}$; 2) $p_k = 14.5 \text{ atm abs}$; 3) $p_v = 0.2 \text{ atm abs}$; 4) $H, \text{ km}$.

for craft of this type to use high-altitude engines, in which, when operating at ground level, the gas pressure p_v in the nozzle outlet section is somewhat less than the pressure p_a of the atmospheric air.

If the magnitude of p_v is properly selected, the engine may develop the greatest mean specific thrust $P_{ud.sr}$ in accordance with its flight trajectory and give the aircraft, other things being equal, the maximum flight range.

The results of the computations and construction of the altitude characteristics for an A-4 engine with nozzles of different design altitudes, under otherwise equal conditions (see Fig. 4.27), show that:

1) an engine of low design altitude ($p_v = 0.85 \text{ atm abs}$), when operating at ground level, develops a relatively greater thrust than a high-altitude engine (see the curve for $p_v = 0.85 \text{ atm abs}$), but then as it rises in altitude its thrust increases less rapidly, and, as a result, at a high altitude becomes relatively low; because of this $P_{ud.sr}$ will also be low;

2) an engine of excessively high design altitude develops a relatively great thrust at considerable altitudes, but it has an extremely small thrust at ground level and at low flight altitudes (see the curve for $p_v = 0.2 \text{ atm abs}$), as a result of which the $P_{ud.sr}$ obtained is also small;

3) an engine of moderate design altitude, obviously, will have a relatively great $P_{ud.sr}$ (see the curve for a $p_v = 0.35 \text{ atm abs}$);

4) the A-4 missile's increase in flight range when $p_v = 0.35$

atm abs amounts to about 8% of the range obtained when $p_v = 0.85$ atm abs.

Since the operation time of a ZhRD in different regimes according to thrust and flight altitude depends basically on the aircraft's flight trajectory, it is necessary to choose a nozzle design altitude for an engine being designed only for the specific reaction device in which the engine will be installed.

In designing an engine it is necessary to select a p_v that, other things being equal, will give the greatest $P_{ud.sr}$ and, consequently, the greatest missile range.

The optimum engine-nozzle design altitude depends on the aircraft's flight trajectory, which shows that there is some difficulty in computing $p_{v.opt}$,* which is required in advance in order to know the flight trajectory of the installation being designed. The greater the aircraft's perfection from the design viewpoint, i.e., the smaller its relative final weight μ_{kon} ** (for the A-4 missile we have a $\mu_{kon} = G_k/G_0 = 0.32$) and the greater the engine's specific thrust, the less the value of $p_{v.opt}$ will be and the greater the effect that may be expected from using a nozzle of optimum design altitude.

The use of high-altitude nozzles provides a considerable increase in aircraft range in comparison to a low-altitude nozzle, in direct proportion to the aircraft's degree of perfection.

In selecting a nozzle design altitude for an engine being designed, one should bear in mind that:

1) increasing the design altitude of the nozzle increases its dimensions and weight, because of which difficulties arise in cooling its greater surface, and also the expenditures of energy in climbing

*[$p_{v.opt} = P_{outlet.optimum}$]

**[$\mu_{kon} = \mu_{kon} = \mu_{konechnyy} = \mu_{final}$]

and acceleration increase sharply because of the engine's increase in weight and the decrease in p_v ;

2) the engine thrust at ground level is decreased considerably, which greatly impairs the missile's launching properties;

3) when the gases in the nozzle overexpand up to a pressure of less than $p_v \approx 0.3p_a$ the gas flow becomes detached from the nozzle walls, because of which compression waves appear, which decrease the engine's specific thrust considerably.

In view of these reasons, and also because the launching thrust of fast-climbing, heavy missiles of the A-4 type must, in practice, be not less than double the weight of the missile at blastoff, some pressure increase in the nozzle outlet section relative to its optimum value is advisable. Thus, the engine nozzle is shortened, its weight is decreased, and launching thrust increases. The latter circumstance indicates the necessity for comparative evaluation of the effect of the engine's weight and specific thrust on the missile's range (to attain the greatest range, one must determine the weight equivalent of the thrust).

In designing an engine, we often base the magnitude of the pressure in the nozzle outlet section on statistical data (considering the missile's designation).

At the present time, for single-stage missile engines, it is assumed that in the nozzle outlet section the gas pressure $p_v = 0.6-0.85$ atm abs.

Sometimes the magnitude of p_v is assumed as equal to the atmospheric air pressure p_a at the altitude which the missile reaches after expending half of the supply of fuel in the tanks. One cannot consider such a solution to this problem as valid.

For engine nozzles intended for the second and following stages

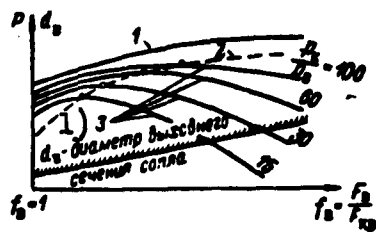


Fig. 4.28. Absolute engine thrust as a function of the dimensionless area f_v of a nozzle cross section. 1) d_v - diameter of nozzle outlet section.

of a multistage missile, in order not to increase the nozzle outlet section by a considerable degree, one may assume $p_v = 0.1-0.3$ atm abs.

As we select the magnitude of p_v it is necessary to consider the real engine design altitude, the missile's designation, the character of its flight trajectory, nozzle cooling system, the effect of increasing the engine's weight on the missile's range be-

cause of the change in p_v , and a number of other factors.

Figure 4.28 shows the curves for the absolute thrust P of an engine chamber as a function of the nozzle's dimensionless area $f_v = \frac{F_v}{F_{kr}}$ at various operating conditions. Curve 1 shows the change in P as a function of the change in f_v when the engine is operating in space; as f_v increases, the magnitude of P increases.

The dashed curve 2 shows the change in P as a function of f_v when the engine is operating continuously at the rated regime; this regime is maintained by changing the per-second fuel-flow rate to the combustion chamber.

The other curves 3 show the change in P as a function of the different ratios of gas expansion within the nozzle; for example $\epsilon_s = p_k/p_v = 15, 30, 60$, and 100. Each of these curves has its maximum when $p_v = p_a$, i.e., when the corresponding curve intersects with curve 2.

The curves of this graph show that an engine with a small pressure p_k in the combustion chamber is more sensitive to a change in the nozzle length than when p_k is great. They also indicate that engines with large values of p_k should be made as low-altitude engines, since

by this means they will have a relatively small loss of thrust.

SECTION 15. REGULATING AN ENGINE-CHAMBER NOZZLE'S DESIGN ALTITUDE

An engine with a chamber nozzle which was ideally regulated to conform with flight altitude [i.e., a nozzle which was elongated in accordance with flight altitude to maintain the engine's optimum rated operating conditions ($p_v = p_a$)] would have the best altitude characteristics.

This shows the requirement for developing engine chambers with nozzles which are regulated in accordance with flight altitude, even if they have only one or two fixed positions, which, other things being equal, considerably increases a missile's range without decreasing its launching thrust as compared to a missile with a low-altitude engine.

Figure 4.29 shows the altitude characteristics of an engine:

- 1) with normal ground-level nozzle (curve 1-4-2);
- 2) with an oversized ground-level nozzle (curves 3-4-5-6-7 and 8-6-9-10);
- 3) with an ideal nozzle, regulated in accordance with altitude (curve 1-5-9-11);
- 4) with a two-stage regulated nozzle (curve 1-4-5-6-9-10), with the first stage of regulation switched into operation at point 4 and the second at point 6.

The curves of these altitude characteristics show that the use of nozzle design-altitude regulation permits:

- 1) increasing the engine's launching thrust;
- 2) increasing the engine's operating economy, determined by the magnitude of $P_{ud.sr}$, and
- 3) increasing the aircraft's range (by means of the first two factors).

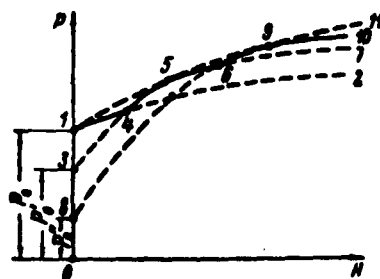


Fig. 4.29. Character of two-stage regulation of engine-nozzle design altitude.

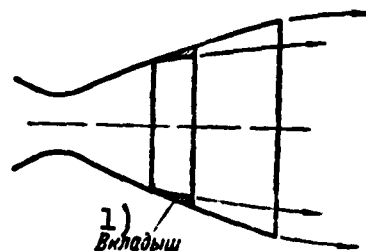


Fig. 4.30. Simplified diagram of single-stage regulation of engine-nozzle design altitude.
1) Liner.

Regulating the nozzle's design altitude as altitude increases is most effective for long-range and super-long-range missiles, whose powered trajectory is close to vertical.

Practical accomplishment of chamber-nozzle design-altitude regulation, even in the simplest form (with one or two fixed values of $f_v = F_v/F_{kr}$), is extremely complicated. The engine nozzle usually operates under high temperature conditions; therefore it is very difficult to regulate it and cool it at the same time.

One-stage nozzle design-altitude regulation may be accomplished without great design difficulties by the use of a special nozzle liner (Fig. 4.30). During the missile's launching and as it climbs to a predetermined flight altitude, this liner will detach the stream of gases from the engine chamber nozzle walls, and therefore it will operate as a normal ground-level nozzle. After a certain altitude is reached, the nozzle liner burns up or is mechanically ejected and the nozzle begins to operate as a high-altitude nozzle.

In practice, other methods of one-stage engine-nozzle design-altitude regulation are possible.

SECTION 16. BASIC CHARACTERISTICS OF THE A-4 OXYGEN ZhRD

The basic data of the German A-4 engine, intended for long-range missiles, are shown below.

Combustion chamber pressure in kg/cm ²	14.5
Per-second fuel-flow rate in kg/sec:	
liquid oxygen.....	69
ethyl alcohol of 75% weight concentration.....	56
total.....	125
Temperature in combustion chamber (measured) in °C.....	2367
Absolute thrust at sea level in kg.....	25,000
Velocity of gas outflow from the nozzle at sea level in m/sec:	
actual.....	1995
theoretical.....	2200
Nozzle efficiency.....	0.90
Pressure difference in the cooling system in kg/cm ²	4.3
Pressure difference of the alcohol in the injectors (mean) in kg/cm ²	2.4
Diameter of the combustion chamber (maximum) in mm.....	920
Diameter of the nozzle critical section in mm.....	400
Diameter of the outlet section of the nozzle in mm.....	740
Characteristic equivalent length of the combustion chamber in m.....	2.87
Consumption of ethyl alcohol for developing the chamber film curtain (out of the total flow rate of the alcohol into the chamber) in %.....	13
Mean value of the specific heat flow in kcal/m ² -sec.....	510
or in kcal/m ² -hr.....	1.83 · 10 ⁶
Alcohol temperature increase in the chamber cooling jacket in °C.....	35
Number of antechambers of the pear-shaped combustion chamber.....	18
Dry weight in kg:	
engine chamber.....	422
turbopump unit.....	160
vapor-gas generator.....	73
compressed-air flasks.....	75
engine thrust frame.....	56
total weight of the engine (without tanks).....	930
oxygen tank.....	120
alcohol tank.....	76
Weight of the working components in the engine tanks in kg:	
ethyl alcohol.....	3814
liquid oxygen.....	4900
hydrogen peroxide of 80% weight concentration.....	177
potassium permanganate of 28% weight concentration...	14

Chapter V

CHARACTERISTICS OF ZhRD FUELS

The liquid substance or combination of liquid substances used in a ZhRD as a source of energy and a mass carrier in setting up the reaction thrust is commonly known as the engine fuel. Each of these liquid substances, which are stored separately and delivered separately to the combustion chamber and, taken together, compose the fuel used by the engine, is known as a fuel component.

The fuel component subjected to oxidation during the combustion process in the engine chamber is customarily referred to as the combustible, while the fuel component that oxidizes the combustible in the engine's combustion chamber is known as the oxidizer. Here the term "oxidation" is used in its broad sense, i.e., to cover oxidation proper (the reaction of the fuel elements with oxygen), fluorination (the reaction of a fuel with fluorine), chlorination (reaction of fuel with chlorine), etc.

In the early stages of development of ZhRD, hydrocarbons with low calorific values, such as alcohols, amines, and hydrazine hydrate were used as fuels; kerosene was used only in rare cases; an 80% aqueous solution of hydrogen peroxide or nitric acid was employed as an oxidizer, with liquid oxygen the exception.

At the present time, the principal attention is being devoted to more efficient fuels with high calorific values. The use of these fuels in ZhRD makes it possible to obtain higher specific thrusts

from the engine, reduce the quantity of fuel for a given absolute thrust and burning rate, and, consequently, to reduce the capacity of the fuel tanks, the size of the missile, and, all other things equal, to achieve longer ranges.

The first step in designing an engine is to select the fuel components on the basis of operational considerations, with the object of achieving the optimum flight characteristics in the missile.

The present chapter presents brief discussions of existing fuel types for ZhRD, gives the parameters that characterize the quality of fuel components, and sets forth the basic specifications for ZhRD fuels.

The physical, thermal, and other properties of the fuels and oxidizers considered in this chapter are borrowed in part from the Technical Encyclopedia, the Handbook of Chemistry, and other sources.

SECTION 1. BASIC TYPES OF ZhRD FUELS

A fuel is generally known as basic, starting, or auxiliary, depending on the manner in which it is used in a ZhRD.

Liquid fuel components used directly for operation of the engine chamber are known as the basic fuel, while the starting fuel is composed of liquid hypergolic propellants that are used only when the engine is being started, and then only to trigger combustion of the nonhypergolic components of the basic working fuel in the combustion chamber.

Substances used in an engine as a source of thermal energy and working mass to power the gas generator of the pump-unit turbine and the fluid-pressure accumulator of the system that delivers the basic fuel components from the tanks to the combustion chamber are sometimes known as an auxiliary fuel. Small portions of the basic fuel

components or gases withdrawn from the engine chamber can also be used for this purpose.

The following may be used in ZbRD:

1) monopropellant liquid fuels, in which the combustible and oxidizer are combined in a single liquid substance as a chemical compound or into a stable mechanical mixture (monofuels);

2) bipropellant and multipropellant liquid fuels, which consist of two or more separately stored combustible and oxidizer components that are delivered separately to the engine combustion chamber.

The monopropellant fuels include nitromethane (CH_3NO_2), which is a high-energy but comparatively cheap and explosionproof monofuel, nitroglycerine ($\text{C}_3\text{H}_5\text{N}_3\text{O}_9$), and nitric-acid solutions of nitrogen tetroxide, tetranitromethane, and other oxidizers with combustible.*

Monopropellant liquid fuels are characterized by the following special properties:

- a) uniformity of the combustible mixture;
- b) constancy of all of its basic characteristics (the values of the excess oxidizer ratio, heating value, combustion rate, etc.);
- c) smooth combustion in the primary phase (irrespective of hydrodynamic factors);
- d) a strong tendency of certain fuels to decompose, detonate, and explode.

When a monofuel is used, the entire fuel-supply system can be simplified considerably and the engine made considerably lighter than an engine operating on a bipropellant fuel. However, existing monofuels are considerably inferior to bipropellant fuels for the following reasons:

- 1) they present considerable explosion hazard (with a powerful

*Ekspress-informatsiya AN SSSR, No. 10, ADS-39, 1959.

shattering effect) when they have satisfactory heating values, or

2) they have relatively low heating values when the necessary explosion safety is assured.

Attempts to reconcile these contradictions have not yet given the desired results. In spite of many attempts on the part of the designers, not a single engine has as yet been built to operate dependably on a liquid monofuel.

A particularly dangerous and toxic explosive is nitromethane, which is a slightly oily liquid at normal temperature and is used in industry as a solvent and as a component in lacquers and paints. Its boiling point is $+110^{\circ}\text{C}$, its melting point is -29°C , and the temperature of the combustion products at 35 atm abs is about $2,170^{\circ}\text{C}$, indicating that its use will be attractive from a thermodynamic standpoint. Nitromethane burns with a pale, almost invisible flame.

Since the detonation speed of nitromethane is many times greater than the speed of normal combustion, and the pressure at which it is injected into the combustion chamber must be adjusted in such a way as to exceed by a slight margin the chamber pressure itself, the detonation wave may propagate through the fuel lines, trigger explosions in them, and cause the engine to misfire.

A special ignition system is required to start engines operating on nitromethane, and a small quantity of gaseous oxygen is used in the initial firing.

The most widely used bipropellant fuels include:

- a) aqueous solutions of ethyl alcohol with liquid oxygen;
- b) kerosenes with nitric acid (96 or 98% concentration by weight) or with solutions of this acid, etc.

Bipropellant liquid fuels are characterized by the following

special properties:

- a) separate storage and delivery to the engine combustion chamber;
- b) comparative explosionproofness during storage and use in the engine;
- c) a (basically) diffusive combustion process in a turbulent stream, with simultaneous displacement of the combustible and oxidizer particles (the combustion rate is determined by the rate at which the mixture forms);
- d) opportunities for selecting stable, maximum-efficiency fuel components and adjusting their combustion rate by varying the mixing rate, since the rate of the chemical reaction is immeasurably greater than that of mixing at the high temperatures developed in the focus of combustion, etc.

In diffusive combustion of the fuel, the admissible forcing range in which the stability of combustion is not disturbed is much wider than in kinetic combustion, a fact accounted for basically by the extreme nonuniformity of the gas stream as regards the propellant concentrations, i.e., the oxidizer excess.

Bipropellant and multipropellant fuels are classed as:

- 1) nonhypergolic fuels, the liquid components of which do not ignite on contact with one another and require an outside heat source for ignition, and
- 2) hypergolic fuels, the liquid components of which begin to burn without an outside heat source when they come into contact with one another.

Alcohol and oxygen, kerosene and nitric acid, etc., are examples of nonhypergolic fuels.

An oxidizer with which the combustible under consideration

will be autoigniting at normal temperature can be selected for each combustible. For this reason, there is no point in classifying combustibles as autoigniting and nonautoigniting unless we note the specific oxidizer to be used in combination with the fuel.

Most combustibles are autoigniting with fluorine and ozone. The number of combustibles that ignite spontaneously with oxygen is quite large (phosphorous, boron hydrides, certain organometallic compounds, and many others). A number of combustibles ignite spontaneously with fluorine monoxide. As a rule, combustibles that are autoigniting with nitric acid are also autoigniting with liquid nitrogen oxides, solutions of these oxides in tetranitromethane, oxides of chlorine and perchloric acid or solutions of them, and with fluorine monoxide.

Autoignition depends to a considerable degree on the conditions under which the reacting components are mixed.

At the present time, combustibles that are autoigniting on contact with nitric acid and hydrogen peroxide are used in ZhRD. The group of combustibles that form hypergolic combinations with these oxidizers includes:

- a) a mixture of xylidene and triethylamine with nitric acid;
- b) a mixture of aniline (65% by weight) and furfuryl alcohol (35%) with nitric acid;
- c) a mixture of optol, aniline, xylol, benzene, and vinyl-ethyl alcohol with nitric acid;
- d) hydrazine hydrate with hydrogen peroxide;
- e) xylidene with AM-50 mixture (this consists of 50% by weight of 98% nitric acid and 50% of nitration oleum, GOST 701-41) and certain other fuels, which are used in different combinations and with

^WA.V. Bolgarskiy and V.K. Shchukin, *Rabochiy protsess v zhidkostnykh raketnykh dvigatelyakh* (Working process in liquid-fuel rocket engines), Oborongiz, 1953.

ignition catalyzers as both basic and starting combustible components of the fuel.

Xylidene with AM-40 or AM-50 mixture and other combustible-oxidizer combinations are being used successfully as starting hypergolic fuel components.

The basic advantage gained by using hypergolic components in ZhRD as basic and starting fuels consists in the following:

a) the system for starting the engine is considerably simplified because it is no longer necessary to have a special device to ignite the fuel;

b) the danger that the fuel mixture will explode in the combustion chamber on starting and stopping of the engine is reduced, since it is almost impossible for unburned fuel to accumulate in the chamber;

c) the volume and weight of the combustion chamber are reduced, since autoreacting components do not require any significant time for priming for the combustion process, and this raises the per-liter thrust of the engine.

The basic shortcomings of autoigniting fuels are as follows:

a) the production of these fuels is considerably more complex, with the result that they are more expensive than nonhypergolic fuels, and

b) the great fire hazard in the event of leakage in the engine's plumbing system.

The conditions of ignition and combustion of the fuel in the combustion chamber require that nonautoigniting fuel components have the lowest possible flash points, and that autoigniting fuel components have the shortest possible delay before autoignition begins (induction period). The latter requirement is particularly important.

() By the term "autoignition delay," we mean the time that passes from the instant at which the hypergolic liquid components come into contact to the instant at which they ignite.

For safety in starting the engine, the autoignition delay time of the fuel components should not exceed 0.03 sec. For reliability in starting the engine under various meteorological conditions and at various altitudes, it is necessary that the autoignition delay time not increase excessively as the fuel temperature declines and as the atmospheric pressure drops off.

() The lower the flash point of autoigniting fuel components, the smaller will be the energy necessary to activate them for ignition, i.e., the smaller will be the amount of external thermal energy required to fire these components. If combustion begins in any given group of fuel-mixture particles, the activation energy for the other particles will be transmitted from fuel-component particles that have already undergone chemical reaction.

The activation-energy values for different fuel mixtures are different. The higher the required activation energy, the more difficult will it be to ignite the fuel mixture.

Below we present the basic characteristics of those combustibles, oxidizers, and resultant fuels that are of greatest interest for use in ZhRD.

SECTION 2. PARAMETERS CHARACTERIZING QUALITY OF FUEL

To select a fuel type and compute its combustion processes, as well as for the general design of the engine, it is necessary to have complete and accurate information concerning the (physicochemical and other) parameters of the combustible, the oxidizer, and the fuel as a whole.

These parameters characterizing the quality of the fuel include:

- 1) the specific gravity of the fuel and its components as a function of temperature;
- 2) the solidification (melting) and boiling points of these fuel components at the pressure in question;
- 3) their specific heat capacity, viscosity, and surface tension;
- 4) the elementary compositions of the fuel components;
- 5) the mixture ratio of the fuel (ratio of oxidizer to combustible) or the fuel's oxidizer-excess factor;
- 6) the heating values or energy contents of the fuel and its components;
- 7) the flash- and autoignition temperatures, the induction period, and the ignition range of the fuel in question;
- 8) the combustion temperature of the fuel under the specific conditions involved;
- 10) [sic] the specific gas yield of the fuel, i.e., the volume of the gases that form on combustion of a unit weight or volume of the fuel, reduced to standard conditions;
- 11) the specific thrust developed by the engine in operation on the fuel in question under specified conditions;
- 12) the chemical stability of the fuel components and the products of its combustion;
- 13) the corrosion of the physical parts of the engine by the fuel components and the combustion products of the fuel;
- 14) the mutual solubility of the fuel components and their chemical action on one another;
- 15) the foreign-impurity content in the fuel components and

their influence on the engine's operation;

16) the chemical activity of the fuel components, i.e., the ability of the combustible and oxidizer to enter reaction with one another, which is characterized by the rate of chemical conversion of the reacting substances under the specific conditions involved;

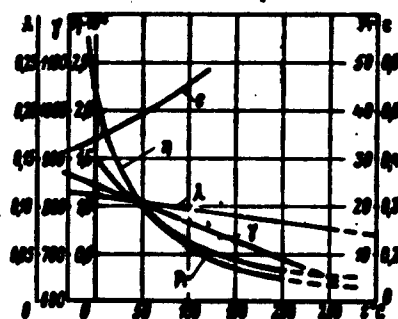


Fig. 5.1. Physical constants of tractor kerosene as a function of temperature (at standard pressure).

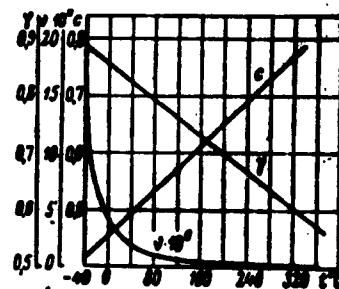


Fig. 5.2. Physical constants of kerosene as a function of temperature (at standard pressure).

17) the heat of formation of the component, the heat required to bring it to the boiling point, and the heat of evaporation of the fuel components;

18) the hygroscopicity, volatility, and toxicity of the fuel components;

19) the technical availability, cost, and other characteristics of the fuel components.

The above properties and characteristics of the fuel determine the efficiency and specific thrust of the engine, the possibility of cooling it with one of the fuel components, the fuel-supply system, operational reliability, simplicity, and safety, and the possibility and expediency of using the fuel in the engine.

The basic indicators that determine the quality of a given fuel are the specific thrusts that it develops per unit weight and volume.

The specific gravities and freezing and melting points for specified conditions are listed in tables borrowed from the handbooks and other literature sources, together with other characteristics of certain fuel components.

Figures 5.1-5.7 show the physical constants (specific gravity, specific heat capacity, thermal conductivity, viscosity, etc.) of the most widely used combustibles and oxidizers as functions of temperature.

Certain physical constants of a fuel or its individual components can be determined by the following formulas:

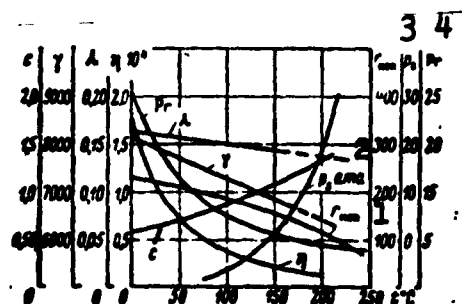


Fig. 5.3. Physical constants of ethyl alcohol of 100% concentration by weight as a function of temperature (at standard pressure). 1) r_{isp}^* ; 2) p_s , atmospheres absolute; 3) p_s , $p_s = p_z$ [not identified]; 4) p_r [not identified].

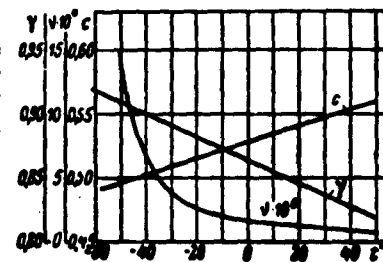


Fig. 5.4. Physical constants of Tonka-250 combustible as a function of temperature (at standard pressure).

1) the specific gravity of the fuel,

$$\gamma_r = \frac{\gamma_r + \chi' \gamma_o}{1 + \chi'} = \frac{\gamma_o \gamma_r (1 + \chi)}{\gamma_o + \chi \gamma_r}, \quad ** \quad (5.1)$$

where γ_g and γ_o are the specific gravities of the combustible and oxidizer, respectively, under the specified temperature and pressure conditions, and χ' and χ are the volume and weight proportions of the fuel components;

*[$r_{исп} = r_{исп} = r_{испарение} = r_{evaporation}$.]

**[$\gamma_r = \gamma_t = \gamma_{топливо} = \gamma_{fuel, propellant}$; $\gamma_r = \gamma_g = \gamma_{горючее} = \gamma_{combustible}$; $\gamma_o = \gamma_o = \gamma_{окислитель} = \gamma_{oxidizer}$.]

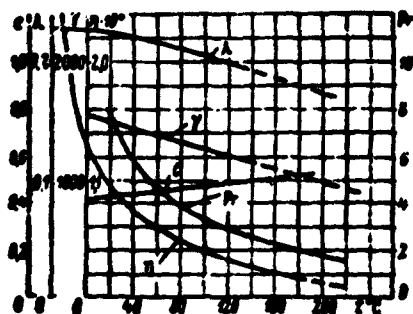


Fig. 5.5. Physical constants of nitric acid of 100% concentration by weight as a function of temperature (at standard pressure).

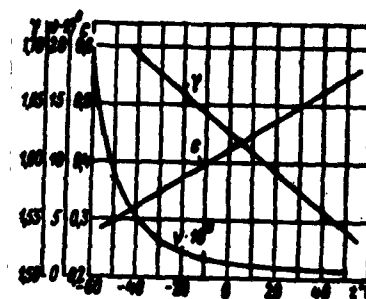


Fig. 5.6. Physical constants as a function of temperature for an oxidizer consisting of 80% of 98% HNO₃ and 20% of N₂O₄ (at standard pressure).

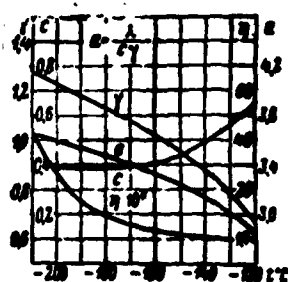


Fig. 5.7. Physical constants of liquid oxygen as a function of temperature.

2) the specific gravity of a mixture of several components:

$$\gamma = g_1 \gamma_1 + g_2 \gamma_2 + \dots + \text{etc.}, \quad (5.2)$$

where g_1, g_2 , etc., are the weight fractions of the corresponding components in one kg of mixture; γ_1, γ_2 , etc., are the specific gravities of these components under the specified temperature and pressure conditions;

3) the heat capacity of a mixture of components:

$$c = g_1 c_1 + g_2 c_2 + \dots + \text{etc.}, \quad (5.3)$$

where c_1, c_2 , etc., are the heat capacities of the corresponding components in the mixture for the specified temperature and pressure values;

4) the thermal conductivity of a given unassociated liquid component;

$$\lambda = \lambda_0 \left(\frac{T}{T_0} \right)^{0.4} \text{ kcal/m-hour-}^\circ\text{C}, \quad (5.4)$$

where $\lambda_0 = \frac{1.52 \cdot 10^{-4}}{\mu^{1.8}} c_p \gamma^{0.5}$ is the thermal conductivity in kcal/m-hour- $^\circ\text{C}$,

c_0 is the heat capacity, γ_0 is the specific weight of the component at the temperature and pressure specified, and μ is the molecular weight of this component;

5) the thermal conductivity of a component mixture (approximate determination):

$$\lambda = g_1\lambda_1 + g_2\lambda_2 + \dots + \text{etc.}, \quad (5.5)$$

where λ_1 , λ_2 , etc., are the thermal conductivity coefficients of the corresponding fuel components at the temperature and pressure specified;

6) the kinematic viscosity coefficient of a mixture of components,

$$\nu = \frac{1}{(g_1/\nu_1) + (g_2/\nu_2) + \dots + \text{etc.}} \quad \text{m}^2/\text{sec} \quad (5.6)$$

where ν_1 , ν_2 , etc., are the kinematic viscosity coefficients of the corresponding components at the temperature and pressure specified ($\nu = \eta/\rho$, where ρ is the density of the component).

The basic parameters characterizing the quality of a fuel also include its efficiency, i.e., the missile velocity attainable at the end of the powered trajectory with the engine operating on this fuel, since this velocity is the basic factor determining the range of a reaction-thrust missile.

The relative efficiency of a given fuel or its components under a given set of operating conditions (given values of the ZhRD's thrust, combustion-chamber pressure, constant per-second fuel flow rates, etc.) can be estimated from the corresponding formulas.

Table 5.1 lists the saturation vapor pressures of certain fuel components, and Appendix VIII shows the vapor pressures of certain liquids as functions of temperature.

Table 5.1.

Saturation Vapor Pressures of Certain Fuel Components Used in Foreign Rocket Types

1 Вещество	2 Химическая формула	3 Давление в атм								4 Критические параметры	
		2	5	10	20	30	40	50	60	5 $t_{кр}$ °C	6 $p_{кр}$ атм
7 Температура, °C											
8 Этиловый спирт 100%-ный	C_2H_5OH	97,5	126,0	151,8	183,0	203,0	218,0	230,0	242,0	243	63,1
9 То же 92%-ный	—	100	128	155	183	210	232	250	266	—	—
10 Метиловый спирт 100%-ный	CH_3OH	84,0	112,5	138,0	167,8	186,5	203,5	214,0	224,0	240	78,7
11 Изопропиловый спирт 100%-ный	C_3H_7OH	101,3	130,2	155,7	186,0	206,0	220,2	232,0	—	235	53,0
12 Анилин	C_6H_5N	212,8	254,8	292,7	342,0	375,5	400,0	424,4	—	426	52,4
13 Аммиак	NH_3	-18,7	+4,7	25,7	50,1	66,1	78,9	89,3	98,3	132,4	111,5
14 Керосин	—	185	225	287	340	330	—	—	—	404,0	30,6
15 Тонка-250	—	100	170	214	270	304	—	—	—	358	34
16 Гидразин	N_2H_4	135	175	205	235	262	275	290	300	380	145
17 Диметилгидразин несимметричный (димазин)	$C_2H_5N_2$	84	110	142	173	190	208	224	235	249	62
18 Метилгидразин	CH_3N_2	—	—	—	—	—	—	—	—	257	75
19 Кислород жидкий	O_2	-176,0	-164,5	-153,1	-140,0	-130,7	-124,1	—	—	-118,9	49,7
20 Азотная кислота 100%-ная	HNO_3	120	150	190	230	264	290	312	—	—	—
21 То же 98%-ная	—	100	138	160	205	226	240	—	—	—	—
22 Четырехокись азота	N_2O_4	37,3	59,8	79,4	100,3	112,3	121,0	127,0	132,2	158,0	99,0
23 Смесь из 80% HNO_3 98%-ной + 20% N_2O_4	—	58	83	103	124	135	144	155	160	198,0	132,0
24 Вода	H_2O	120,1	152,4	186,5	213,1	234,6	251,1	264,7	270,5	374,15	225,65

1) Substance; 2) chemical formula; 3) pressure in atmospheres; 4) critical parameters; 5) $t_{кр}$, °C; 6) $p_{кр}$, atmospheres; 7) temperature, °C;

8) 100% ethyl alcohol; 9) same, 92%; 10) 100% methyl alcohol; 11) isopropyl alcohol, 100%; 12) aniline; 13) ammonia; 14) kerosene; 15) Tonka-250; 16) hydrazine; 17) asymmetrical dimethylhydrazine; (dimazine); 18) methylhydrazine; 19) liquid oxygen; 20) 100% nitric acid; 21) same, 98%; 22) nitrogen tetroxide; 23) mixture of 80% 98% HNO_3 + 20% N_2O_4 ; 24) water.

SECTION 3. METHODS OF CONVERTING ELEMENTARY WEIGHT COMPOSITIONS OF FUEL COMPONENTS INTO CONVENTIONAL CHEMICAL FORMULAS AND VICE VERSA

In evaluating fuels and making thermodynamic calculations for ZhRD, it is sometimes necessary to convert the elementary weight compositions of the fuel components into conventional chemical formulas and vice versa.

When oxygen-bearing oxidizers are used, the components of a fuel at 100% concentration by weight may, in their general form, have

the following elementary weight compositions.

Fuel: C_g - carbon;*
 H_g - hydrogen;
 O_g - oxygen;
 N_g - nitrogen.

Total 100% or 1 kg

Oxidizer: C_o - carbon;**
 H_o - hydrogen;
 O_o - oxygen;
 N_o - nitrogen.

Total 100% or 1 kg

But the identical compositions of the combustible and oxidizer can be expressed in the form of the following conventional chemical formulas:

a) fuel $C_{c_1} H_{h_1} O_{o_1} N_{n_1}$ and b) oxidizer $C_{c_2} H_{h_2} O_{o_2} N_{n_2}$, where c_1, h_1, o_1, n_1 , and c_2, h_2, o_2, n_2 , are the numbers of atoms of the individual elements in the combustible and oxidizer, respectively.

Similar conventional chemical formulas can be written for a large number of elements forming combustibles and oxidizers, such as $C_{c_2} H_{h_2} O_{o_2} N_{n_2} F_{f_2} Cl_{cl_2}$ for a complex oxidizer.

Conversion of a specified set of weight fractions for the elements of the combustible C_g, H_g, O_g , and N_g and the oxidizer C_o, H_o, O_o, N_o in percent into conventional chemical formulas reduces basically to determining the number of atoms of the individual elements in the fuel components by the following formulas.

Combustible:

$$c_1 = \frac{C_g}{12}; \quad h_1 = \frac{H_g}{1}; \quad o_1 = \frac{O_g}{16}; \quad n_1 = \frac{N_g}{14}. \quad (5.7)$$

Oxidizer:

$$c_2 = \frac{C_o}{12}; \quad h_2 = \frac{H_o}{1}; \quad o_2 = \frac{O_o}{16}; \quad n_2 = \frac{N_o}{14}. \quad (5.8)$$

Conversion of given fuel-component compositions from conventional chemical formulas into the weight fractions of the elements is carried out by the following formulas.

*[r = g = goryucheye = combustible.]
 **[o = o = okislitel' = oxidizer.]

Combustible:

$$\begin{aligned} C_r &= \frac{12c_1}{\mu_r} & H_r &= \frac{h_1}{\mu_r}; \\ O_r &= \frac{16o_1}{\mu_r} & N_r &= \frac{14n_1}{\mu_r} \end{aligned} \quad \text{kg/kg;} \quad (5.9)$$

Oxidizer:

$$\begin{aligned} C_o &= \frac{12c_2}{\mu_o} & H_o &= \frac{h_2}{\mu_o}; \\ O_o &= \frac{16o_2}{\mu_o} & N_o &= \frac{14n_2}{\mu_o} \end{aligned} \quad \text{kg/kg,} \quad (5.10)$$

where $\mu_g = 12c_1 + h_1 + 16o_1 + 14n_1$ is the molecular weight of the combustible;

$\mu_o = 12c_2 + h_2 + 16o_2 + 14n_2$ is the molecular weight of the oxidizer.

If the combustible and oxidizer consist of several different components, the weight fractions of the elements are determined for them by the following formulas.

Combustible:

$$\begin{aligned} C_r &= g_1 C_{r1} + g_2 C_{r2}; & H_r &= g_1 H_{r1} + g_2 H_{r2}; \\ O_r &= g_1 O_{r1} + g_2 O_{r2}; & N_r &= g_1 N_{r1} + g_2 N_{r2}. \end{aligned} \quad (5.11)$$

and

Oxidizer:

$$\begin{aligned} C_o &= g_1 C_{o1} + g_2 C_{o2}; & H_o &= g_1 H_{o1} + g_2 H_{o2}; \\ O_o &= g_1 O_{o1} + g_2 O_{o2}; & N_o &= g_1 N_{o1} + g_2 N_{o2}. \end{aligned} \quad (5.12)$$

and

where g_1 and g_2 are the weight fractions of the combustible mixture in kg/kg, C_{g1} , H_{g1} , and C_{g2} , H_{g2} are the elements of the respective components in the combustible mixture in kg/kg, and C_{o1} , H_{o1} and C_{o2} , H_{o2} are the same for the oxidizer, in kg/kg.

The compositions of the fuel components for specified concentrations in aqueous solution may be expressed by the following conventional chemical formulas:

$$C_r H_{r1} O_{r1} N_{r1} \cdot m_r H_2 O \quad \text{and} \quad C_o H_{o1} O_{o1} N_{o1} \cdot m_o H_2 O; \quad (5.13)$$

and

here, m_g and m_o are the numbers of water molecules per mole of pure fuel and pure oxidizer, respectively, as determined by the formulas:

$$m_r = \frac{\mu_r (100 - \omega_r)}{18 \omega_r} \text{ mole/mole;} \quad m_o = \frac{\mu_o (100 - \omega_o)}{18 \omega_o} \text{ mole/mole,} \quad (5.14)$$

where $\sigma_g\%$ and $\sigma_o\%$ are the concentrations of the combustible and oxidizer, respectively, in aqueous solution.

If $\sigma_g\%$ of combustible and $\sigma_o\%$ of oxidizer are contained in the aqueous solution in question, the weights of the corresponding solutions according to calculation for 1 mole of pure combustible will be:

$$p_r' = p_r + 18m_r = p_r \frac{100}{\sigma_r} \text{ kg}; \quad p_o' = p_o + 18m_o = p_o \frac{100}{\sigma_o} \text{ kg}, \quad (5.15)$$

Example 1. Write the conventional chemical formula for kerosene if the weight fractions of its elements are as follows: $C_g = 86.4\%$ and $H_g = 13.6\%$.

Solution.

1. The numbers of atoms of the individual elements in kerosene of this composition will be

$$c_1 = \frac{C_g}{12} = \frac{86.4}{12} = 7.2 \text{ and } h_1 = \frac{H_g}{1} = 13.6$$

2. Kerosene has the conventional chemical formula $C_{7.2}H_{13.6}$.

Example 2. Determine the elementary weight composition of a combustible consisting of 50% by weight of triethylamine ($C_6H_{15}N$) and 50% by weight of xylidene ($C_8H_{11}N$).

Solution.

1. The molecular weights of the combustible components are:

a) for triethylamine,

$$p_{r_1} = 12c_1 + h_1 + 14n_1 = 12 \cdot 6 + 1 \cdot 15 + 14 \cdot 1 = 101.0;$$

b) for xylidene,

$$p_{r_2} = 12 \cdot 8 + 11 \cdot 1 + 14 \cdot 1 = 121.25.$$

2. The elementary weight fractions of the combustible-mixture components are:

a) for triethylamine,

$$\begin{aligned}
 C_{r_1} &= \frac{12c_1}{\mu_{r_1}} = \frac{12 \cdot 6}{101,2} = 0,7115 \text{ кг} = 71,15\%; \\
 H_{r_1} &= \frac{h_1}{\mu_{r_1}} = \frac{15}{101,2} = 0,1482 \text{ кг} = 14,82\%; \\
 N_{r_1} &= \frac{14n_1}{\mu_{r_1}} = \frac{14 \cdot 1}{101,2} = 0,1403 \text{ кг} = 14,03\%; \\
 &\text{Total 1 kg or 100\%}
 \end{aligned}$$

b) for xylidene,

$$\begin{aligned}
 C_{r_2} &= 12 \frac{c_2}{\mu_{r_2}} = \frac{12 \cdot 8}{121,25} = 0,7939 \text{ кг} = 79,39\%; \\
 H_{r_2} &= \frac{h_2}{\mu_{r_2}} = \frac{11}{121,25} = 0,0907 \text{ кг} = 9,07\%; \\
 N_{r_2} &= 14 \frac{n_2}{\mu_{r_2}} = \frac{14}{121,25} = 0,1154 \text{ кг} = 11,54\%; \\
 &\text{Total 1 kg or 100\%}
 \end{aligned}$$

3. The elementary weight fractions of the combustible mixture are

$$\begin{aligned}
 C_r &= g_1 C_{r_1} + g_2 C_{r_2} = 0,5 \cdot 0,7115 + 0,5 \cdot 0,7939 = 0,7527 \text{ кг}; \\
 H_r &= g_1 H_{r_1} + g_2 H_{r_2} = 0,5 \cdot 0,1482 + 0,5 \cdot 0,0907 = 0,1194 \text{ кг}; \\
 N_r &= g_1 N_{r_1} + g_2 N_{r_2} = 0,5 \cdot 0,1403 + 0,5 \cdot 0,1154 = 0,1279 \text{ кг}. \\
 &\text{Total 1 kg}
 \end{aligned}$$

Example 3. Write the conventional chemical formula for 96% by-weight nitric acid and determine the weight fractions of its elements.

Solution.

1. The water content of the aqueous nitric acid solution is

$$m_0 = r_0 \frac{(100 - c_0)}{18,06} = 63 \frac{(100 - 96)}{18,06} = 0,145 \text{ mole/mole}.$$

2. The conventional chemical formula for this aqueous nitric acid solution takes the form



3. The weight of the aqueous solution, calculated for one mole

of pure nitric acid is

$$H_0 = H_0 \frac{100}{98} = 63 \frac{100}{98} = 69.7 \text{ kg.}$$

4. The elementary weight fractions of the oxidizer-mixture components are

a) nitric acid

$$H_{01} = \frac{1}{63} = 0.016 \text{ kg/kg;}$$

$$N_{01} = \frac{14.1}{63} = 0.762 \text{ kg;}$$

$$O_{01} = \frac{16.3}{63} = 0.222 \text{ kg/kg;}$$

or, taken together,

$$H_{01} + N_{01} + O_{01} = 0.016 + 0.762 + 0.222 = 1 \text{ kg;}$$

b) water

$$H_{02} = \frac{1}{18} = 0.111 \text{ kg/kg and}$$

$$O_{02} = \frac{16.1}{18} = 0.889 \text{ kg/kg;}$$

or, taken together,

$$H_{02} + O_{02} = 0.111 + 0.889 = 1 \text{ kg.}$$

5. The elementary weight fractions of the oxidizer mixture are:

$$H_0 = \xi_1 H_{01} + \xi_2 H_{02} = 0.96 \cdot 0.016 + 0.04 \cdot 0.111 = 0.020 \text{ kg/kg;}$$

$$N_0 = 0.96 \cdot 0.762 = 0.213 \text{ kg/kg;}$$

$$O_0 = 0.96 \cdot 0.222 + 0.04 \cdot 0.889 = 0.762 \text{ kg/kg}$$

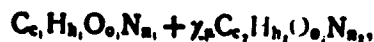
Total 1 kg or 100%

SECTION 4. DETERMINATION OF THEORETICAL AND ACTUAL QUANTITY OF OXIDIZER REQUIRED FOR COMPLETE COMBUSTION OF A UNIT OF COMBUSTIBLE

A fully determinate quantity of oxidizer is theoretically required for complete combustion of a given quantity of combustible.

For example, complete combustion of 1 kg of tractor kerosene theoretically (stoichiometrically) requires 14.8 kg of air, or 7.4 kg of hydrogen peroxide, or 5.4 kg of 98%-by-weight nitric acid, or 3.42 kg of liquid oxygen.

In its general form, therefore, the composition of the fuel for an oxygen oxidizer may be expressed by the following conventional chemical formula:



(5.16)

where χ_{O_2} is the number of moles of oxidizer theoretically required for complete combustion of one mole of combustible, as determined from the equality of the numbers of oxygen atoms before and after complete combustion of the combustible fuel elements (Tables 5.2 and 5.3), i.e.,

$$o_1 + \chi_{\text{O}_2} o_2 = 2(c_1 + \chi_{\text{O}_2} c_2) + 0.5(h_1 + \chi_{\text{O}_2} h_2),$$

from which it follows that

$$\chi_{\text{O}_2} = \frac{2c_1 + 0.5h_1 - o_1}{o_2 - (2c_2 + 0.5h_2)} \quad \text{mole/mole.} \quad (5.17)$$

In this formula, the numerator represents the number of oxygen atoms required for complete combustion of one mole of combustible, while the denominator is the number of oxygen atoms contained in one mole of oxidizer.

Table 5.2

Numbers of Atoms of Individual Elements in Molecule of Combustible, Oxidizer, and Fuel, in General Form

1 Элементы горючего и окислителя	2 В 1 моле горючего	3 В 1 моле окислителя	4 В топливе из расчета на 1 моль горючего
5 Углерод	c_1	$\chi_{\text{O}_2} c_2$	$c_1 + \chi_{\text{O}_2} c_2$
6 Водород	h_1	$\chi_{\text{O}_2} h_2$	$h_1 + \chi_{\text{O}_2} h_2$
7 Кислород	o_1	$\chi_{\text{O}_2} o_2$	$o_1 + \chi_{\text{O}_2} o_2$
8 Азот	n_1	$\chi_{\text{O}_2} n_2$	$n_1 + \chi_{\text{O}_2} n_2$

1) Elements of combustible and oxidizer; 2) in one mole of combustible; 3) in one mole of oxidizer; 4) in fuel, from calculations for one mole of combustible; 5) carbon; 6) hydrogen; 7) oxygen; 8) nitrogen.

Analogous formulas can be written for a fuel consisting of a large number of combustible and oxidizer elements.

The quantity of oxidizer theoretically required for complete combustion of a given unit weight of combustible is frequently referred to as the propellant mixture ratio.

The above formulas enable us to determine the molar stoichio-

metric propellant mixture ratio independently of the combustible and oxidizer concentrations.

For 100%-by-weight concentration of the combustible and oxidizer, the volumetric and gravimetric stoichiometric propellant mixture ratios are determined by the formulas:

$$\chi_s = \frac{O_{s,o}}{O_{s,r}} = \chi_p \frac{r_o}{r_r} = \chi_p \frac{12c_2 + h_2 + 16o_2 + 14n_2}{12c_1 + h_1 + 16o_1 + 14n_1} \text{ kg/kg}; \quad (5.18)$$

$$\chi'_o = \frac{V_{s,o}}{V_{s,r}} = \frac{O_{s,o}/\gamma_o}{O_{s,r}/\gamma_r} = \chi_s \frac{\gamma_r}{\gamma_o} \text{ liters/liter}, \quad (5.19)$$

from which

$$\chi_s = \chi' \frac{\gamma_o}{\gamma_r} \text{ kg/kg}, \quad (5.20)$$

where γ_g and γ_o are the specific gravities of the combustible and oxidizer, respectively, in kg/liter.

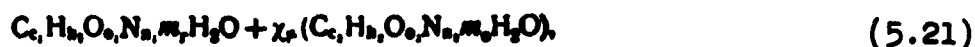
Table 5.3

Number of Oxygen Atoms Required for Combustion of Combustible Fuel Elements and Moles of Combustion Products Obtained with this Number

1 Уравнения сгорания горючих элементов топлива	2 Потребное число атомов кислорода для полного сгорания горючих эле- ментов топлива	3 Получаемое число молей продуктов полного сго- рания 1 моля горючего моля/моль
$C + O_2 = CO_2$ $H_2 + 0,5O_2 = H_2O$ 4 Азот не горит	$2(c_1 + \chi_p c_2)$ $0,5(h_1 + \chi_p h_2)$ 5 Кислорода не требуется	$M_{CO_2} = c_1 + \chi_p c_2$ $M_{H_2O} = 0,5(h_1 + \chi_p h_2)$ $M_{N_2} = n_1 + \chi_p n_2$
6 Всего теоретически тре- буется кислорода и обра- зуется продуктов сгора- ния топлива	$2(c_1 + \chi_p c_2) +$ $+ 0,5(h_1 + \chi_p h_2) =$ $= O_1$	$M_r = M_{CO_2} + M_{H_2O} + M_{N_2} =$ $= c_1 + 0,5 h_1 + n_1 +$ $+ \chi_p (c_2 + 0,5 h_2 + 0,5 n_2)$

1) Combustion equation of combustible fuel elements; 2) number of oxygen atoms required for complete combustion of combustible fuel elements; 3) number of moles of products obtained in complete combustion of one mole of combustible, mole/mole; 4) nitrogen does not burn; 5) oxygen not required; 6) total oxygen theoretically required and total fuel-combustion products formed.

For specified weight concentrations of combustible ($\sigma_g\%$) and oxidizer ($\sigma_o\%$) in aqueous solutions, the fuel composition is given in general form by the following conventional chemical formula:



where m_g and m_o are the numbers of water molecules in one mole of the combustible and oxidizer, respectively, as determined by the formulas given above, in moles/mole.

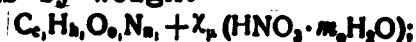
Here, the stoichiometric proportions by weight and volume of the fuel components are determined by the formulas

$$\chi_o = \chi_r \frac{P_o}{P_r} = \chi_r \frac{P_o \frac{100}{P_r} \frac{P_r}{P_o}}{\frac{100}{P_r} \frac{P_r}{P_o}} = \chi_r \frac{P_r}{P_o} \text{ kg/kg} \quad (5.22)$$

$$\chi'_o = \chi_r \frac{P_r}{P_o} \frac{1}{T_o} \text{ liters/liter} \quad (5.23)$$

We may write formulas for determining the coefficients χ_{μ} and χ_o as they apply for specific fuels, for example:

1) for a complex fuel and aqueous nitric acid solution in different concentrations by weight



$$\chi_r = \frac{2c_1 + 0.5b_1 - o_1}{8 - 0.5b_2} \text{ mole/mole};$$

$$\chi_o = \chi_r \frac{63 + 18m_o}{12c_1 + b_1 + 16o_1} \text{ kg/kg};$$

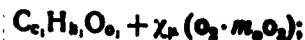
2) for a complex fuel and oxygen,



$$\chi_r = c_1 + 0.25b_1 - 0.5 \cdot o_1 \text{ moles/mole}$$

$$\chi_o = \chi_r \frac{32}{12c_1 + b_1 + 16 \cdot o_1 + 14n_1} \text{ kg/kg}$$

3) for a combustible and a solution of ozone in oxygen,



$$\chi_r = \frac{2c_1 + 0.5b_1 - o_1}{2 + 3m_o} \text{ mole/mole};$$

$$\chi_o = \chi_r \frac{32 + 48m_o}{12c_1 + b_1 + 16 \cdot o_1} \text{ kg/kg};$$

If the fuel is specified in the form of the elementary compositions of the combustible and oxidizer, the stoichiometric mixture ratio by weight will be determined for the fuel by these formulas.

1. For an oxidizer consisting of pure oxygen

$$\chi_o = \frac{8}{3} C_r + 8H_r - O_r \text{ kg/kg}$$

where C_g , H_g , and O_g are the combustible elements in kg/kg.

2. For use of an oxidizer whose composition also includes combustible elements:

$$\chi_o = \frac{\frac{8}{3} C_p + 8H_p - O_p}{O_p - \left(\frac{8}{3} C_p + 8H_p\right)} \text{ kg/kg}$$

Here, in this case, the molar stoichiometric mixture ratio of the fuel will be determined from the formula given earlier:

$$\chi_o = \chi_p \frac{\mu_o}{\mu_p} \text{, i.e., } \chi_p = \chi_o \frac{\mu_p}{\mu_o} \text{ kmole/kmole.}$$

Tables 5.4 - 5.6 list values of the stoichiometric mixture ratios by weight and volume for the most extensively used fuels.

Example 4. Determine χ_μ , χ_o , and χ'_o for a fuel consisting of kerosene of the composition $C_{7.15}H_{13.5}$ and nitric acid of 96% concentration by weight when $\gamma_g = 0.84$ kg/liter, $\gamma_o = 1.5$ kg/liter, and $m_o = 0.184$ kmole/kmole.

Solution.

The mixture ratio for this fuel will be

a)
$$\chi_p = \frac{2c_1 + 0.5h_1 - o_1}{o_2 - 0.5h_2} = \frac{2 \cdot 7.15 + 0.5 \cdot 13.5 - 0}{3 - 0.5 \cdot 1} = 8.16 \text{ kmole/kmole;}$$

b) by weight

$$\chi_o = \chi_p \frac{\mu_o + 18m_o}{12c_1 + h_1 + 16o_1} = 8.16 \frac{63.18 + 0.184}{12 \cdot 7.15 + 13.5} = 5.512 \text{ kg/kg;}$$

c) by volume

$$\chi'_o = \chi_o \frac{\gamma_r}{\gamma_o} = 5.512 \frac{0.84}{1.5} = 3.081 \text{ liter/liter.}$$

Example 5. Determine the theoretical amount of tetranitromethane $C(NO_2)_4$ for complete combustion of one kmole and one kg of kerosene of the following composition: $C_g = 86.4\%$ and $H_g = 13.6\%$.

Solution.

1. The conventional chemical formula of kerosene of this composition takes the form

$$\frac{C_{86.4}}{12} \frac{H_{13.6}}{1} = C_{7.2}H_{12.6}$$

2. The stoichiometric mixture ratio of the fuel will be

a) molar

$$\chi_p = \frac{2.7.2 + 0.5.13.6}{8 - 2.1} = 3.537 \text{ kmole/kmole};$$

b) by weight

$$\chi_o = \chi_p \frac{P_p}{P_r} = 3.537 \frac{196}{100} = 6.933 \text{ kg/kg}.$$

The same results can be obtained by another method.

For this purpose, we compute the elementary composition by weight of tetranitromethane, i.e.,

$$C_o = \frac{12}{196} 100 = 6.12\%; \quad N_o = \frac{4.14}{196} 100 = 20.86\%;$$

$$O_o = \frac{8.16}{196} 100 = 65.39\%.$$

Here, we obtain

$$\chi_o = \frac{\frac{8}{3} C_r + 8H_r - O_r}{O_o - \left(\frac{8}{3} C_o + 8H_o\right)} = \frac{\frac{8}{3} 85.4 + 8.13.6}{65.3 - \frac{8}{3} 6.12} = 6.93 \text{ kg/kg};$$

$$\chi_p = \chi_o \frac{P_r}{P_o} = 6.93 \frac{100}{196} = 3.537 \text{ kmole/kmole}.$$

Example 6. Determine the theoretical consumption of nitric acid at 100 and 90% concentrations by weight for complete combustion of one kmole and one kg of toluene, C_7H_8 .

Solution.

$$1) \quad \chi_p = \frac{2c_1 + 0.5h_1 - o_1}{O_2 - (2c_2 + 0.5h_2)} = \frac{2.7 + 0.5.8}{8 - 0.5.1} = 7.2 \text{ kmole/kmole};$$

$$2) \quad \chi_o = \chi_p \frac{P_p}{P_r} = 7.2 \frac{63}{92} = 4.93 \text{ kg/kg}$$

$$3) \quad \chi_o = \chi_p \frac{P_p \cdot r}{P_r \cdot o} = 7.2 \frac{63 \cdot 100}{92 \cdot 90} = 5.46 \text{ kg/kg}$$

Example 7. Determine the quantity of nitric acid theoretically necessary for combustion of one kg of kerosene if the components have the elementary compositions:

a) kerosene:

$$C_g = 85.6\% = 0.856 \text{ kg}$$

$$H_g = 14.4\% = 0.144 \text{ kg}$$

$$\text{Total } 100\% \text{ or } 1 \text{ kg}$$

b) nitric acid:

$$\begin{aligned}
 H_o &= 1.6 = 0.016 \text{ kg;} \\
 O_o &= 76.2\% = 0.762 \text{ kg} \\
 N_o &= 22.2\% = 0.222 \text{ kg} \\
 \hline
 &\text{Total 100\% or 1 kg}
 \end{aligned}$$

Solution.

$$\lambda_o = \frac{\frac{8}{3} C_r + 8H_r - O_r}{O_o - \left(\frac{8}{3} C_o + 8H_o \right)} = \frac{\frac{8}{3} 85.6 + 8 \cdot 14.4}{76.2 - 8 \cdot 1.6} = 5.4 \text{ kg/kg.}$$

SECTION 5. DETERMINATION OF EXCESS OXIDIZER RATIO FOR FUEL

Calculation and experiment indicate that the highest specific thrusts are developed by an engine in operation on a fuel having a small oxidizer deficiency, since in this case:

- 1) the temperature of the fuel's products of combustion is lowered as a result of dilution by the combustible and, consequently, the heat losses due to dissociation of the gases are reduced;
- 2) the products formed on combustion of the fuel have low molecular weights (gaseous hydrogen and other light gases), and, consequently, higher gas constants;
- 3) conditions for mixing of the fuel components are improved, since the wider the divergence of the fuel-mixture composition from the stoichiometric, the easier will it be to set up agitation and obtain a stoichiometric mixture composition for the component present in deficient quantity. As a result, combustion will be complete and the specific heat yield of the fuel will be higher; in combination with the factors enumerated above, this will raise the specific thrust of the engine.

On the other hand, however, some of the component remains unburned in the combustion products when the combustible is burned with an oxidizer deficiency, and some of the combustible is wasted. In practice, therefore, there must be a reasonable limit to the amount by which the oxidizer proportion in the fuel is reduced below the

stoichiometrically necessary quantity.

The ratio of the quantity of oxidizer actually consumed in burning a unit quantity of combustible is commonly known as the excess oxidizer ratio of the fuel and denoted by the letter α , i.e.,

$$\alpha = \frac{\chi_p}{\chi_o} = \frac{\chi}{\chi_o} = \frac{\chi'}{\chi_o}, \quad (5.24)$$

from which the actual quantity of oxidizer for combustion of a unit of fuel will be

$\chi_{\mu}' = \alpha \chi_{\mu}$ kmole/kmole; $\chi = \alpha \chi_o$ kg/kg and $\chi' = \alpha \chi'$ liters/liter, where χ_{μ}' , χ , and χ' are the actual molar, weight, and volume mixture ratios of the fuel, respectively.

In modern engines, $\alpha \approx 0.70-0.98$.

If the oxidizer contains combustible elements, there will be a considerable difference between the excess oxidizer ratio and the excess oxygen (fluorine, chlorine) ratio.

Table 5.4 lists calculated values of χ and χ' for different α for a fuel consisting of kerosene $C_{7.15}H_{13.5}O_{0.05}$ ($\gamma_g = 0.84$ kg/liter at $20^\circ C$) and aqueous solutions of nitric acid of various concentrations by weight, as computed for standard temperature, taking into account the change in the specific gravity of the nitric acid as a function of its concentration.

Table 5.4

1 Концентрация в %	96	98	100	96	98	100
α	3 χ в кг/кг			4 χ' в л/л		
0.6	2,903	2,953	2,935	1,073	1,043	1,022
0.7	3,577	3,534	3,491	1,300	1,266	1,229
0.8	4,175	4,129	4,083	2,333	2,297	2,248
0.9	4,835	4,780	4,698	2,705	2,643	2,580
1.0	5,512	5,450	5,292	3,081	3,004	2,924

Table 5.5

2 Коэффициент α	3 χ в кг/кг	4 χ' в л/л
0.6	2,054	1,405
0.7	2,307	1,745
0.8	2,798	1,991
0.9	3,083	2,341
1.0	3,424	2,485

1) Concentration in %; 2) coefficient α ; 3) χ in kg/kg; 4) χ' in liters/liter.

Table 5.5 lists calculated values of χ and χ' for a fuel consisting of kerosene $C_{7.15}H_{14.2}$ ($\gamma_g = 0.83$ kg/liter at $20^\circ C$) and liquid oxygen O_2 .

Table 5.6 presents values of χ and χ' for a fuel consisting of aqueous ethyl alcohol solutions of different weight concentrations ($C_2H_5OH \cdot m H_2O$) and liquid oxygen O_2 .

Table 5.6

1	Концентрация C_2H_5OH в %	75	85	95	100	75	85	95	100
2	χ в кг/кг					3	χ' в л/л		
	0,6	0,745	0,892	1,038	1,112	0,558	0,649	0,731	0,768
	0,7	0,950	1,112	1,274	1,355	0,712	0,809	0,797	0,937
	0,8	1,154	1,332	1,509	1,598	0,865	0,969	1,063	1,105
	0,9	1,359	1,552	1,745	1,841	1,019	1,129	1,229	1,273
	1,0	1,564	1,772	1,980	2,085	1,172	1,290	1,395	1,441

1) Concentration of C_2H_5OH , %; 2) χ in kg/kg; 3) χ' in liters/liter.

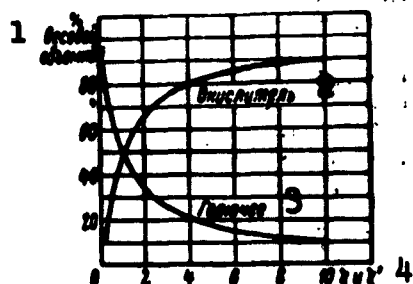


Fig. 5.8. Percentage contents by weight of combustible and oxidizer in fuel as functions of the mixture ratios χ and χ' . 1) % by weight or volume; 2) oxidizer; 3) combustible; 4) χ and χ' .

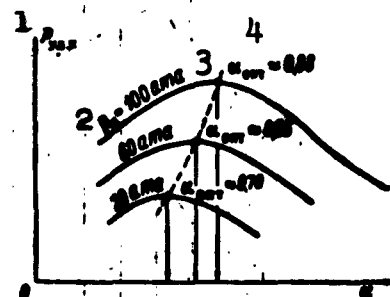


Fig. 5.9. Specific thrust of engine as a function of excess oxidizer ratio in fuel for different combustion-chamber pressures. 1) $P_{ud.k}$; 2) P_k ; 3) atmospheres absolute; 4) α_{opt} .

If we know the proportions of the fuel components by weight or by volume, χ' , the curves of Fig. 5.8 can be used for approximate determination of the combustible and oxidizer contents of the fuel

*[$P_{уд.к} = P_{уд.к} = P_{удел'ное, камерное} = P_{chamber, specific}$; $P_k = P_k = P_{камерное} = P_{chamber}$; $\alpha_{онт} = \alpha_{opt} = \alpha_{оптимальный} = \alpha_{optimum}$.]

in percent by weight or volume.

Less than adequate study has thus far been devoted to the problem of the optimum value α_{opt} for different fuels as a function of combustion-chamber pressure. For a given pressure in the engine's combustion chamber, the optimum value of the excess oxidizer ratio will be that which corresponds to the specific-thrust maximum, and, like the optimum value of this coefficient, the specific thrust depends on the nature of the outflow process of the fuel's combustion products through the nozzle.

As the pressure in the engine's chamber rises, the dissociation of the combustion products is reduced (the combustion process is intensified), so that the value of α increases with respect to the maximum specific thrust (Fig. 5.9).

Calculation indicates that fuels with high combustion temperatures (e.g., kerosene plus liquid oxygen) have specific-thrust maxima in a region of α smaller (Fig. 5.10) than those for fuels with relatively low combustion temperatures (e.g., kerosene plus nitric acid).

For a given pressure in the engine's chamber, the fuel-combustion temperature maximum with respect to α will be closer to unity than the specific-thrust maximum.

Calculations indicate that a 5% change in χ from its optimum value will reduce P_{ud} by 0.5%, while a 2% change in χ will change the temperature of the fuel-combustion products by almost 50°C and the terminal velocity of the missile by approximately 4%.

For approximate determination of the optimum value α_{opt} for a given fuel as a function of engine-chamber pressure, it is necessary to assign certain hypothetical values of α (no fewer than four) and compute the engine's specific thrust for these values, and then construct a diagram of P_{ud} as a function of α .

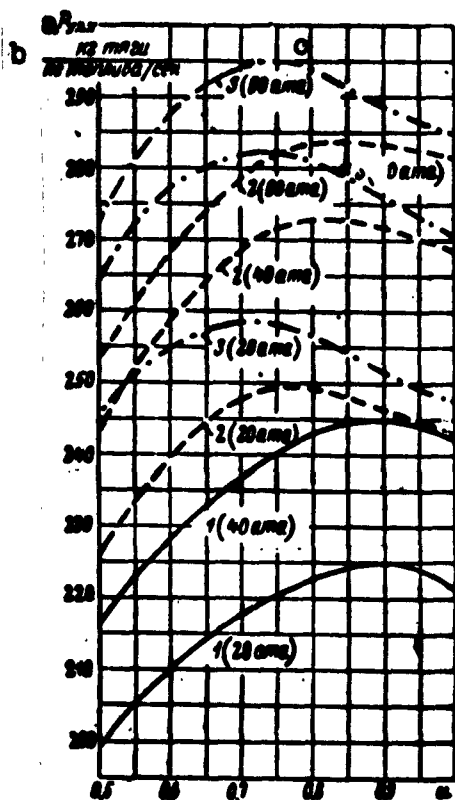


Fig. 5.10. Theoretical specific thrust developed with certain fuels as a function of oxidizer excess ratio with combustion-chamber pressures $p_k = 20, 40,$ and 60 atmospheres absolute. 1) Kerosene + 96% nitric acid; 2) 93.5% ethyl alcohol + liquid oxygen; 3) kerosene + liquid oxygen. a) $P_{ud.t}$; b) kg of thrust/kg of fuel/sec; c) atmospheres absolute.

dizer deficiencies (left branch of curve) or fuel deficiencies (right branch).

This approximation of the two curves is due to reduced dissociation of the fuel-combustion products as the combustion process passes into the region of lower temperatures. The steep descent of the two curves in the region of reduced α (from unity toward zero) is

$$q_{k.n} = q_{k.1} = q_{kamernnyy, ideal'nyy} = q_{chamber, ideal'nyy}$$

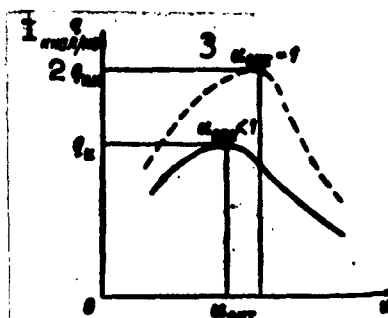


Fig. 5.11. Ideal and actual heat yields of fuel as functions of excess oxidizer ratio. 1) q , kcal/kg; 2) $q_{k.1}$; 3) $q_{k.*}$

Figure 5.11 shows curves of the specific heat yields of a fuel in an ideal engine ($q_{k.1}$) and in a real engine q_k (taking accessory heat losses into account) as functions of the excess oxidizer ratio α of the fuel.

It will be evident from this figure that the curve of q_k has a maximum at $\alpha < 1$, lies below the curve of $q_{k.1}$ and tends to approach closer to it in the low-temperature regions associated with large ox-

accounted for by the steadily increasing oxidizer deficiency and the severely retarded course of the combustion process due to depression of the temperature.

In the region of $\alpha > 1$, these specific heat-yield curves and, consequently, the temperature of the fuel-combustion process as well, drop off more steeply (than in the region of $\alpha < 1$), with the result that the combustion process itself is also inhibited.

As the pressure in the combustion chamber is raised, the specific heat yield q_k increases as a result of the reduced dissociation of the fuel-combustion products.

The elementary composition by weight of one kg of fuel for a given excess oxidizer ratio α is determined by the formulas:

$$\begin{array}{ll} \text{a) Carbon} & \text{c) Oxygen} \\ C_r = \frac{C_r + \alpha L C_o}{1 + \alpha L} \text{ kg/kg;} & O_r = \frac{O_r + \alpha L O_o}{1 + \alpha L} \text{ kg/kg;} \\ \text{b) Hydrogen} & \text{d) Nitrogen} \\ H_r = \frac{H_r + \alpha L H_o}{1 + \alpha L} \text{ kg/kg;} & N_r = \frac{N_r + \alpha L N_o}{1 + \alpha L} \text{ kg/kg;} \end{array} \quad (5.25)$$

Example 8. Determine the elementary composition of a fuel consisting of kerosene ($C_g = 0.86$; $H_g = 0.13$ and $O_g = 0.01$ kg/kg) and nitric acid of 96% concentration by weight ($H_o = 0.020$, $O_o = 0.767$ and $N_o = 0.213$ kg/kg), if the excess oxidizer ratio α of the fuel is 0.8.

Solution.

1. The quantity of nitric acid of the specified concentration by weight required to burn one kg of kerosene is:

a) theoretical

$$L_o = \frac{\frac{8}{3} C_r + 8 H_r - O_r}{O_o - \left(\frac{8}{3} C_o + 8 H_o \right)} = \frac{0.86 + 8 \cdot 0.13 - 0.01}{0.767 - 8 \cdot 0.02} = 5.46 \text{ kg/kg;}$$

b) actual

$$\chi = \alpha L_o = 0.8 \cdot 5.46 = 4.36 \text{ kg/kg.}$$

2. The elementary composition of this fuel will be

$$C_r = \frac{C_r + \gamma C_o}{1 + \gamma} = \frac{0.86}{1 + 4.36} = 0.161 \text{ kg/kg};$$

$$H_r = \frac{O_r + \gamma O_o}{1 + \gamma} = \frac{0.13 + 4.36 \cdot 0.02}{1 + 4.36} = 0.039 \text{ kg/kg};$$

$$O_r = \frac{O_r + \gamma O_o}{1 + \gamma} = \frac{0.01 + 4.36 \cdot 0.767}{1 + 4.36} = 0.626 \text{ kg/kg};$$

$$N_r = \frac{N_r + \gamma N_o}{1 + \gamma} = \frac{4.36 \cdot 0.213}{1 + 4.36} = 0.174 \text{ kg/kg};$$

$$\text{Total} \quad 1.00 \text{ kg}$$

SECTION 6. DETERMINATION OF PROPORTIONS BY WEIGHT AND VOLUME, SPECIFIC GRAVITY, AND SPECIFIC VOLUME OF FUEL

For thermodynamic design of an engine, it is necessary to know the fractions by weight and volume of the combustible and oxidizer and the specific gravity or specific volume of the specified fuel composition.

These characteristics of the fuel may be determined by the formulas:

1) fraction of fuel components by weight:

$$g_r = \frac{r_r}{r_r + \alpha \mu_o} \text{ kg/kg}; \quad g_o = \frac{\alpha \mu_o}{r_r + \alpha \mu_o} \text{ kg/kg}; \quad (5.26)$$

where $\mu_g + \alpha \mu_o$ is the number of kilomoles of fuel calculated for one kmole of combustible, with $g_g + g_o = 1 \text{ kg}$;

2) the specific volumes of the fuel components

$$v_r = g_r / \gamma_r \text{ liters/kg}; \quad v_o = g_o / \gamma_o \text{ liters/kg}, \quad (5.27)$$

where γ_g and γ_o in kg/liter are the specific gravities of the combustible and oxidizer, respectively; these values are taken from the tables and corrected for the specified temperature;

3) the specific volume of the fuel

$$v = v_r + v_o = g_r / \gamma_r + g_o / \gamma_o \text{ kg/liter}; \quad (5.28)$$

4) the specific gravity of the fuel

$$\bar{r}_0 = \frac{1}{\bar{v}_0} = \frac{1}{(g_r/\bar{v}_r) + (g_o/\bar{v}_o)} = \frac{r_r + r_o \bar{v}_r/\bar{v}_o}{(g_r/\bar{v}_r) + (g_o/\bar{v}_o)} \text{ kg/liter}; \quad (5.29)$$

5) the fractions by volume of the fuel [components]:

$$r_r = \frac{v_r}{v_0} = \frac{g_r/\bar{v}_r}{(g_r/\bar{v}_r) + (g_o/\bar{v}_o)} \text{ liters/liter}; \quad r_o = \frac{v_o}{v_0} = \frac{g_o/\bar{v}_o}{(g_r/\bar{v}_r) + (g_o/\bar{v}_o)} \text{ liters/liter}, \quad (5.30)$$

where $r_g + r_o = 1$ liter.

SECTION 7. DETERMINATION OF HEAT VALUE OF FUEL

In ZhRD theory, it is customary to distinguish between complete and incomplete combustion of the fuel.

Complete fuel combustion is a term applied to combustion of fuel during which one of its components (that present in deficient amount with respect to the stoichiometrically required quantity) is completely consumed to form combustion products that are incapable of burning further.

Incomplete fuel combustion is a term applied to combustion during which one of the components (that present in deficient quantity relative to the stoichiometrically required quantity) is consumed partly with formation of complete-combustion products and partly with formation of products that are still capable of burning further under certain conditions.

The quantity of heat evolved in complete combustion of a unit weight or volume of fuel, reduced to standard conditions, is commonly known as the heating value of the fuel.

Since one kilomole, one kg, or one liter is usually taken as the unit quantity of fuel, it is customary to distinguish the molar, unit-weight, and unit-volume heating values of the fuel.

Since the fuel may have the combustible and oxidizer present in stoichiometric and nonstoichiometric effective proportions, it is also necessary to differentiate between the following heating values of a fuel:

1) the stoichiometric (for $\alpha = 1$), which is usually listed in the handbook literature, and the

2) effective (for $\alpha \neq 1$); this is usually determined by calculation in each specific case.

It is also customary to distinguish the following values for a fuel or its components:

1) the gross heat yield — the quantity of heat evolved in combustion of a fuel or fuel-component unit without taking into account the heat lost under standard conditions with the water vapor formed in the fuel-combustion process;

2) the net heat yield — the same, but taking the heat lost with the water vapor into account.

The gross heat yield is not characteristic for purposes of evaluating a fuel or its components, since in practice not all of the heat evolved when the combustion products cool to standard conditions can be used in the engine. For this reason, the value of the fuel's net heat yield is used in the heat calculations for the processes. In the general case, the heat yield of a fuel may be governed by the heat liberated during combustion of the combustible elements of the combustible and oxidizer.

Table 5.7 lists values of the stoichiometric heat yields of certain combustibles.

If the combustible or oxidizer contains water, it will be necessary to expend a certain quantity of heat to evaporate it, and the heat yield of the components must be reduced by this quantity.

The heat yields and enthalpies of petroleum-refinery products are not normally uniform, even for fractions with the same specific gravity. Their values depend on the oilfield and the characteristics of the crude petroleum, as well as on the refining process.

Table 5.7

Heat Yields of Certain Combustibles with Combustion in Oxygen

1 Наименование горючего	2 H_{pr}^v ккал/кмоль	3 H_{pr} ккал/кмоль	4 H_{ug} ккал/кг
5 Водород	62 644	57 785	28 792
6 Углерод	94 051	94 051	7 838
7 Бензол	783 400	751 000	9 809
8 Толуол	933 000	893 000	9 920
9 Скипидар	1 470 000	1 385 000	19 180
10 Этиловый спирт 100%-ный	328 000	296 200	6 440
11 Метиловый спирт 100%-ный	170 900	149 700	4 680
14 Условная формула:			
12 Бензин авиационный грозненский	$C_{7,13}H_{14,5}$		10 500
13 Керосин экспортный	$C_{7,13}H_{14,4}$		10 360
.	$C_{7,13}H_{12,5}O_{0,05}$		10 230
.	$C_{4,23}H_{12,76}O_{0,08}$		10 250

1) Combustible; 2) H_{pr}^v , kcal/kmole; 3) H_{pr} , kcal/kmole; 4) H_{ug} , kcal/kg; 5) hydrogen; 6) carbon; 7) benzene; 8) toluene; 9) turpentine; 10) 100% ethyl alcohol; 11) 100% methyl alcohol; 12) Grozny aviation gasoline; 13) export kerosene; 14) conventional formula.

For this reason, it is frequently necessary to use certain averaged values for the heat yields and enthalpies of petroleum products for practical calculations; these are computed from their elementary compositions and specific gravities.

The net molar stoichiometric heat yield for a temperature of 20°C may be determined by the formulas:

1) combustible:

$$H_{pr} = 94\,051c_1 + 57\,785 \cdot 0.5h_1 - 9718m, \text{ kcal/kmole}; \quad (5.31)$$

2) oxidizer:

$$H_{pr} = 94\,051c_2 + 57\,785 \cdot 0.5h_2 - Q_{p,ox} - 9718m, \text{ kcal/kmole}, \quad (5.32)$$

where 94,051 and 57,785 are the net stoichiometric heat yields of carbon and hydrogen, respectively, for complete combustion in oxygen (see Table 5.7) in kcal/kmole, c_1 , h_1 , and c_2 , h_2 are the number of atoms of carbon and hydrogen, respectively, in one kmole of combustible and oxidizer, $0.5h_1$ and $0.5h_2$ are the numbers of kmoles of water

vapor formed on complete combustion of one kmole of anhydrous combustible and oxidizer, respectively, 9718 is the quantity of heat expended in evaporating one kmole of water at a pressure of one atmosphere and the temperature of the reaction (at one atmosphere, the heat of vaporization of water $r_{isp}^* = 539.4$ kcal/kg), m_g and m_o are the numbers of kilomoles of water in the form of an impurity in one kmole of combustible and oxidizer, respectively, as determined by the formulas given above, and $Q_{\mu obr}^{**}$ is the heat of formation of the oxidizer from the elements H, C, N, and O in kcal/kg; its value may be positive or negative, depending on whether heat is gained or lost in formation of the oxidizer in question.

The heat yield of the oxidizer may be either positive or negative, depending on the quantity of heat liberated in combustion of its combustible elements and the absolute magnitude of its heat of formation. For example, we have the following heat yields for 100% concentration of the oxidizer:

- a) nitric acid HNO_3 with $Q_{\mu obr} = 41,660$ kcal/kmole,
 $H_{\mu O} = 57,785 \cdot 0.5 \cdot 1 - 41,660 = -12,767.5$ kcal/kmole;
- b) hydrogen peroxide H_2O_2 with $Q_{\mu obr} = 44,840$ kcal/kmole,
 $H_{\mu O} = 57,785 \cdot 0.5 \cdot 2 - 44,840 = 12,945$ kcal/kmole.

The heat yield of an oxidizer with a concentration below 100% must be determined with consideration of the heat of solution of water in this component and the heat consumed in evaporating this water. In the majority of cases, the process in which substances dissolve in liquids proceeds exothermically, i.e., with evolution of heat.

The heat of solution of water in a given fuel component can

$$* [r_{\text{resn}} = r_{\text{isp}} = r_{\text{ispareniye}} = r_{\text{evaporation}}.]$$

$$** [Q_{\mu o6p} = Q_{\mu obr} = Q_{\mu obrazovaniye} = Q_{\mu \text{ formation}}.]$$

be determined approximately from the formula

$$Q_{\text{r.pact}} = \frac{Am_0}{a+m_0} \quad (5.33)$$

where m_0 is the number of kilomoles of water per kilomole of the fuel component in question, and A and a are coefficients that are constant for a given substance, e.g., for nitric acid $A = 8974$ and $a = 1.737$.

If the heat $Q_{\mu \text{ rastv}}$ is not separately indicated but is combined with $Q_{\mu \text{ obr}}$, i.e., if for aqueous solutions the quantity $Q_{\mu \text{ obr}}$ is assumed to be larger than it actually is, a special reservation must be made.

The net effective heat yield of a given fuel, calculated for one kmole, one kg, or one liter of combustible, is determined from the formulas:

1) molar

$$H_{\text{pr}} = a(H_{\text{pr}} + \chi_{\text{p}} H_{\text{p.o}}) \text{ kcal/kmole}; ** \quad (5.34)$$

2) unit-weight

$$H_{\text{p}} = \frac{H_{\text{pr}}}{r_{\text{r}} + \sigma_{\text{p}} r_{\text{p.o}}} = \frac{a(H_{\text{pr}} + \chi_{\text{p}} H_{\text{p.o}})}{r_{\text{r}} + aH_{\text{p}} r_{\text{p.o}}} \text{ kcal/kg}; \quad (5.35)$$

3) unit-volume

$$H'_{\text{p}} = \gamma_{\text{p}} H_{\text{p}} \text{ kcal/liter}, \quad (5.36)$$

where γ_{p} is the specific gravity of the fuel in kg/liter.

If we know the net effective unit-weight heat yields of the combustible and oxidizer, the net effective unit-weight heat yield of the fuel may be determined by the formula

$$H_{\text{p}} = \frac{H_{\text{pr}} + \sigma_{\text{p}} H_{\text{p.o}}}{1 + \sigma_{\text{p}}} \text{ kcal/kg}, \quad (5.37)$$

where χ_{p} is the stoichiometric mixture ratio by weight of the fuel.

For an excess oxidizer ratio $\alpha > 1$, the heat yield of the

$$Q_{\text{r.pact}} = Q_{\mu \text{ rastv}} = Q_{\mu \text{ rastovoreniye}} = Q_{\mu \text{ solution}}]$$

**[Subscript $\tau = \text{t} = \text{toplivo} = \text{fuel}$.]

fuel is equal to the chemical energy given by the formulas

$$I_{x,r} = H_{x,r} + \alpha x_r H_{p,0} \text{ kcal/kmole}; \quad (5.38)$$

$$I_{x,r} = \frac{I_{x,r}}{r_r + \alpha x_r p_0} = \frac{H_{x,r} + \alpha x_r H_{p,0}}{r_r + \alpha x_r p_0} \text{ kcal/kg.}^* \quad (5.39)$$

Applying these formulas, we may construct curves of the molecular and unit-weight chemical energies and heat capacities of any specified fuel as functions of the excess oxidizer ratio α (Fig. 5.12).

The net unit-weight stoichiometric heat yield $H_u \approx 1400$ to 2500 kcal/kg for the fuels used in modern engines.

Table 5.8 lists values of the net stoichiometric heat yields of ethyl and methyl alcohols for different concentrations of these alcohols in aqueous solution.

Table 5.8

1 Концентрация %	2 Этиловый спирт (C_2H_5OH)		3 Метиловый спирт (CH_3OH)	
	4 $H_{x,r}$ ккал/кмоль	5 H_u ккал/кг	4 $H_{x,r}$ ккал/кмоль	5 H_u ккал/кг
100	296 200	6440	149 700	4680
95	294 780	6380	148 710	4410
90	293 300	5740	147 680	4180
85	291 850	5880	146 380	3880
80	289 480	5080	145 010	3620
75	287 280	4680	143 440	3360
70	284 650	4330	141 680	3090
65	281 680	3980	139 680	2830
60	278 320	3630	137 200	2570

1) Concentration, %; 2) ethyl alcohol (C_2H_5OH); 3) methyl alcohol (CH_3OH); 4) $H_{x,r}$ g, kcal/kmole; 5) H_u g, kcal/kg.

If liquefied gases, i.e., liquids whose boiling points are lower than the initial reaction temperature conventionally adopted (usually 15-20°C), are used as fuels or oxidizers, it will be necessary in determining the heat yield of the fuel in this case to take into account the heat expended in evaporating this component and heating it to the temperature $t^\circ\text{C}$, using the formula

*[Subscript x.r = kh.t = khimicheskiy, topliva = chemical (energy), fuel.]

$$Q_{\mu \text{ исп} + \text{под}} = \mu_{\text{ком}} [r_{\text{исп}} + c_p (t - t_{\text{кип}})] \text{ kcal/kmole}, * \quad (5.40)$$

where $\mu_{\text{ком}}$ is the molecular weight, $r_{\text{исп}}$ is the latent heat of vaporization in kcal/kg, c_p is the heat capacity in cal/kg $^{\circ}\text{C}$, and $t_{\text{кип}}$ is the boiling point of this component, in $^{\circ}\text{C}$. For example, we have for oxygen $\mu r_{\text{исп}} = 1,630$ kcal/mole, $\mu c_p = 7$ kcal/kmole, and $t_{\text{кип}} = -182.97^{\circ}\text{C}$.

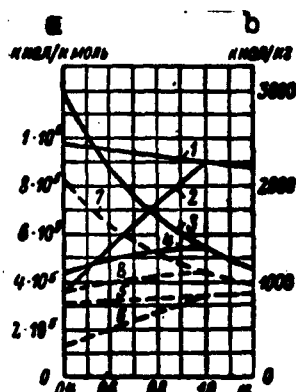


Fig. 5.12. Variation of chemical energy and heat yield of fuel as functions of excess oxidizer ratio. The fuel is kerosene + 95% nitric acid. 1) Molar chemical energy I_{μ} kh.t; 2) molar heat yield $H_{\mu t}$; 3) chemical energy per unit weight, $I_{\text{kh.t}}$; 4) heat yield per unit weight H_u . Fuel: 95% ethyl alcohol + 80% hydrogen peroxide; 5) molar chemical energy I_{μ} kh.t; 6) molar heat yield $H_{\mu t}$; 7) chemical energy per unit weight $I_{\text{kh.t}}$; 8) heat yield per unit weight, H_u ; a) kcal/kmole; b) kcal/kg.

Heats of evaporation of

liquefied oxidizers and the heat required to raise them to normal temperature are as follows [cal/mole]:

Oxidizer:						
O_2	F_2	OF_2	O_2F_2	O_3	FNO_3	NF_3
$Q_{\mu \text{ исп} + \text{под}}$						
3.1	3.0	4.0	5.2	3.6	6.0	4.4

The heat yield is only a static characteristic of a fuel and does not reflect the dynamics of the combustion process in the engine chamber. Under real conditions, two fuels of different types but having almost identical heat yields may develop sharply divergent specific (unit-weight) heat effects. For this reason, heat yield cannot be used as the sole characteristic of fuel quality.

For a given tank capacity of the rocket, it is better to have

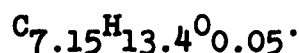
*[Subscripts: исп = испарение = vaporization; под = подогревание = heating, preheating; ком = ком = компонент = component; кип = кип = кипение = boiling.]

a fuel with high specific gravity; for this reason, it is sometimes convenient to refer the heat value of a fuel not to one kilogram but to one liter of fuel. In view of the fact that the weight of the fuel tanks and the engine's fuel-supply system make up a considerable part of the missile's weight, we may take the fuel's unit-volume heating value as a criterion of its calorific value in selecting the fuel components for a rocket engine that we are designing.

Example 9. Determine the net stoichiometric heating value of a fuel ($\alpha = 1$) consisting of kerosene and nitric acid of 98% concentration by weight if $C_g = 85.75\%$, $H_g = 13.50\%$, and $O_g = 0.75\%$; $H_{u g} = 10,230 \text{ kcal/kg}$, $\gamma_g = 0.841 \text{ kg/liter}$, and $\gamma_o (100\%) = 1.520 \text{ kg/liter}$.

Solution.

1. The conventional chemical formula of kerosene of the specified composition takes the form



2. The specific gravity of the specified aqueous solution of nitric acid is

$$\gamma_o = \frac{1}{g_1/\gamma_1 + g_2/\gamma_2} = \frac{1}{0.98/1520 + 0.02/1} = 1.491 \text{ kg/liter.}$$

3. The stoichiometric mixture ratios of the fuel are as follows:

a) molar

$$\lambda_p = \frac{2c_1 + 0.5h_1 - o_1}{o_2 - (2c_2 + 0.5h_2)} = \frac{2 \cdot 7.15 + 0.5 \cdot 13.4 - 0.05}{3 - 0.5 \cdot 1} = 3.4 \text{ kmole/kmole;}$$

b) unit-weight

$$\lambda_o = \lambda_p \frac{P_o}{P_r} = 3.4 \frac{63}{100} = 5.292 \text{ kg/kg.}$$

4. The specific gravity of the fuel is

$$\gamma = \frac{\lambda_r(1 + \lambda_o)}{\lambda_o + \lambda_o \gamma} = \frac{1.520 \cdot 0.841(1 + 5.292)}{1.520 + 5.292 \cdot 0.841} = 1.34 \text{ kg/liter.}$$

5. The quantity of water in one kmole of nitric acid at the specified concentration is

$$m_o = \frac{\mu_o(100 - c_o)}{18.0} = \frac{63(100 - 98)}{18.0} = 0.078 \text{ kmole/kmole.}$$

6. The net molar stoichiometric heat yield of this kerosene with $H_{u g} = 10,230 \text{ kcal/kg}$ (see Table 5.7)

$$H_{\mu g} = \mu_g H_{u g} = 1,023,000 \text{ kcal/kmole.}$$

7. The net molar stoichiometric heat yield of nitric acid of the specified concentration with $Q_{\mu obr} = 41,660 \text{ kcal/kmole}$ and $Q_{\mu rastv} = -325 \text{ kcal/kmole}$ is

$$H_{p.o} = 94.051c_2 + 28.892h_2 - (Q_{p,exp} + Q_{p,perm} + Q_{p,rest+acc}) = \\ = 28.892 \cdot 1 - (41.660 + 325) = -13.093 \text{ kcal/kmole.}$$

8. The net stoichiometric heat yields of the fuel are as follows:

a) molar

$$H_{p.r} = \alpha(H_{p,r} + \chi_p H_{p.o}) - 9718(m_r + \alpha \chi_p m_o) = 1(1,023,000 - 8.4 \cdot 13.093) - \\ - 9718 \cdot 1.84 \cdot 0.078 = 906,653.5 \text{ kcal/kmole;}$$

b) unit-weight

$$H_u = \frac{H_{p.r}}{\mu_r + \alpha \chi_p \mu_o + 18(m_r + m_o)} = \frac{906,653.5}{100 + 8.4 \cdot 63 + 18(0 + 0.078)} = 1437.7 \text{ kcal/kg;}$$

$$H'_u = \gamma_u H_u = 1.34 \cdot 1437.7 = 1928.5 \text{ kcal/liter.}$$

Example 10. Determine the net effective heating value of a fuel consisting of an aqueous solution of ethyl alcohol (concentration 90%) and liquid oxygen if $\gamma_g = 0.818 \text{ kg/liter}$, $\gamma_o = 1.14 \text{ kg/liter}$, $\chi_{\mu} = 2.88 \text{ kmole/kmole}$, and $\alpha = 0.8$.

Solution.

1. The weight fractions of the fuel components are

$$g_r = \frac{\mu_r c_o}{\mu_r c_o + \alpha \chi_{\mu} \mu_o g_r} = \frac{46.100}{46.100 + 0.8 \cdot 2.88 \cdot 32.00} = 0.399 \text{ kg/kg;}$$

$$g_o = \frac{\alpha \chi_{\mu} \mu_o g_r}{\mu_r c_o + \alpha \chi_{\mu} \mu_o g_r} = \frac{0.8 \cdot 2.88 \cdot 32.00}{46.100 + 0.8 \cdot 2.88 \cdot 32.00} = 0.601 \text{ kg/kg.}$$

2. The specific gravity of the fuel is

$$\gamma = \frac{1}{g_r/\gamma_r + g_o/\gamma_o} = \frac{1}{0.399/0.818 + 0.601/1.14} = 0.99 \text{ kg/liter.}$$

3. The number of kilomoles of water in one kilomole of ethyl alcohol of the specified concentration is

$$m_r = \frac{\mu_r(100 - c_r)}{18c_r} = \frac{46(100 - 90)}{18 \cdot 90} = 0.284 \text{ kmole/kmole.}$$

4. The net stoichiometric heat yield of ethyl alcohol at this concentration is

$$H_{p,r} = 296200 - 9718m_r = 296200 - 9718 \cdot 0.284 = 294440 \text{ kcal/kmole.}$$

5. The net effective heat yield of the fuel plus the heat of evaporation of the liquid oxygen plus the heat to raise it to normal temperature equal to $Q_{\mu} \text{ isp} + \text{pod} = 3100 \text{ kcal/kmole}$ will be as follows:

a) molar

$$H_{p,r} = \alpha(H_{p,r} + \gamma_p H_{p,o}) = \alpha(H_{p,r} - \gamma_p Q_{p, \text{evap} + \text{heat}}) = \\ = 0.8(296200 - 2.8 \cdot 3100) = 227370 \text{ kcal/kmole;}$$

b) unit-weight

$$H_u = \frac{H_{p,r}}{\mu_r \frac{100}{c_r} + m_r \frac{100}{c_o}} = \frac{227370}{46 \frac{100}{90} + 0.8 \cdot 2.8832} = 1775 \text{ kcal/kg;}$$

c) unit-volume

$$H'_u = \gamma_u H_u = 0.99 \cdot 1775 = 1755 \text{ kcal/liter.}$$

SECTION 8. DETERMINING ENERGY CONTENT OF FUEL

In computing fuel-combustion processes, it is necessary to know the energy content of one kilomole or one kg of the combustible, the oxidizer, and the fuel (initial substances). By the law of conservation of energy, the energy content of the fuel before combustion is equal to the energy content of the products of complete combustion (gases) from this fuel.

On this basis, the energy-balance equation for one kilomole of combustible with $\alpha = 1$ will be expressed as

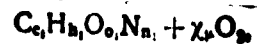
$$I_r + \gamma_p I'_o = I'_{\text{gas}} \text{ kcal/kmole,*} \quad (5.41)$$

from which the energy content of one kilomole of combustible will be

$$I_r = I'_{\text{gas}} - \gamma_p I'_o \text{ kcal/kmole.}$$

*[Subscript gas = gas = gas = gas.]

If oxygen is used as an oxidizer, the composition of the fuel can be expressed in the general case by the formula



and the energy content of the complete-combustion products of this fuel will be

$$I_{rs} = c_1 I_{CO_2} + 0.5 h_1 I_{H_2O} + 0.5 n_1 I_{N_2} + H_{pr} = I_r \text{ kcal/kmole.}$$

From this we obtain a formula for determining the net stoichiometric heating value of one kmole of combustible when oxygen is used as the oxidizer:

$$H_{pr} = I_r - (c_1 I_{CO_2} + 0.5 h_1 I_{H_2O} + 0.5 n_1 I_{N_2}) \text{ kcal/kmole,}$$

where $I_{CO_2}^I$, $I_{H_2O}^I$, and $I_{N_2}^I$ are the energy contents of the carbon dioxide, water vapor, and nitrogen, respectively, in kcal/kmole (taken from the table).

The energy content of one kmole of oxidizer, the composition of which is expressed in the general case by the conventional chemical formula $C_c H_h O_o N_n$, may be determined from the equation

$$I_o = c_2 I_{CO_2} + 0.5 h_2 I_{H_2O} + 0.5 o_2 I_{O_2} + 0.5 n_2 I_{N_2} - Q_{pr} \text{ kcal/kmole.}$$

From this we may also derive a formula for determining the heat of formation of one kmole of oxidizer:

$$Q_{pr} = I_o - (c_2 I_{CO_2} + 0.5 h_2 I_{H_2O} + 0.5 o_2 I_{O_2} + 0.5 n_2 I_{N_2}) \text{ kcal/kmole,}$$

where $I_{CO_2}^I$, $I_{H_2O}^I$, $I_{O_2}^I$, and $I_{N_2}^I$ are the respective energy contents of the carbon, hydrogen, oxygen, and nitrogen in kcal/kmole (taken from the table).

Since there is usually a certain amount of water in some of the fuel components (nitric acid, alcohols, hydrogen peroxide), it is necessary, in computing their energy contents, to take into account the heat liberated when the water dissolves in the fuel component in question (see Table 5.9) by subtracting this amount from the energy content of the component without water. The energy con-

tent of the water is usually taken into account separately.

The water content in the nitric acid depends on its grade and may run as high as 4% by weight.

The energy content of a fuel or oxidizer consisting of several components can be determined by the formula

$$I_{\text{comb}} = \sum g_k I_k + Q_{\text{раств}} \text{ kcal/kg}, \quad (5.42)$$

where g_k is the weight fraction of the k^{th} component in the combustible or oxidizer mixture in kg/kg, I_k is the energy content of the k^{th} component in the combustible or oxidizer mixture in kcal/kg, and $Q_{\text{раств}}$ is the heat of solution of one component in the other in kcal/kg.

For example, the energy content of an aqueous solution of nitric acid is determined by the formula

$$I_{\text{HNO}_3} = g_{\text{HNO}_3} I_{\text{HNO}_3} + g_{\text{H}_2\text{O}} I_{\text{H}_2\text{O}} + g_{\text{H}_2\text{O}} Q_{\text{раств}} \text{ kcal/kg},$$

where g_{HNO_3} and $g_{\text{H}_2\text{O}}$ are the weight fractions of the pure nitric acid and the water in the mixture in kg/kg, I_{HNO_3} and $I_{\text{H}_2\text{O}}$ are the respective energy contents of pure nitric acid and water in kcal/kg, and $Q_{\text{раств}}$ is the heat of solution of water in nitric acid, which is 325 kcal/kg.

Knowing the energy contents of the combustible and oxidizer, we can determine the energy content of the fuel by applying the formulas:

1) molar

$$I' = I'_r + \alpha_{\text{H}_2\text{O}} I'_o \text{ kcal/kmole}; \quad (5.43)$$

2) unit-weight

$$I_1 = \frac{I'_r}{r_r + \alpha_{\text{H}_2\text{O}} r_o + 18(m_r + \alpha_{\text{H}_2\text{O}} m_o)} \text{ kcal/kg} \quad (5.44)$$

or

$$I_1 = \frac{I'_r + \alpha_{\text{H}_2\text{O}} I'_o}{1 + \alpha_{\text{H}_2\text{O}}} \text{ kcal/kg}, \quad (5.45)$$

where I_g and I_o^* are the respective energy contents of one kg of combustible and oxidizer, in kcal/kg.

Table 5.9 lists energy-content values for some of the most widely used fuel components.

If we know the net heating value of one kg of a given fuel component and its elementary weight composition, its energy content can be determined by Formula (5.41).

The energy content of a given substance depends on the system adopted for reckoning its magnitude and on whether the chemical energy is referred to the combustible or oxidizer element or to a substance that forms as a result of chemical reaction.

We encounter various methods for reckoning the energy contents of substances in the literature. In calculations for ZhRD, selection of one or another system for reckoning the energy -content value of a given substance is not of essential importance, since in this case we are interested not in the absolute energy content, but only in its relative change during the process in question. It is only necessary to carry the entire calculation through in the same reckoning system.

We shall henceforth make use of the most common and convenient system of reckoning, which was proposed by A.P. Vanychev.** In this system, the chemical energy (heat of formation) is referred to the substance formed in the chemical reaction. A temperature of 20°C (293.16°K) is taken as the zero reference. Here, all substances possess only chemical energy. Since their physical heat contents are zero, the energy contents of the elements at this temperature are

*[Subscripts: r = g = goryucheye = combustible; o = o = okislitel' = oxidizer.]

**A.P. Vanychev, *Termodinamicheskiy raschet goreniya i istecheniya v oblasti vysokikh temperatur* (Thermodynamic calculation of combustion and discharge in the high-temperature region), Izd. BNT, 1947.

Table 5.9

Energy Contents (total enthalpies) at 20°C for Certain Fuel Components
Used in Foreign Rocket Types

1 Компоненты топлива	2 Формула	3 Энергосодержание ккал/кг.мол. ккал/кг	
6 Горючие			
7 Водород (при -252,8°С)	H ₂	-1 836	-918
8 Керосин состава C ₇ =85,75%, H ₇ =13,5% и O ₇ =0,8%	C _{7.75} H _{12.5} O _{0.05}	-47 000	-470
9 Керосин состава C ₇ =86,76%, H ₇ =12,76% и O ₇ =0,48%	C _{7.26} H _{12.76} O _{0.03}	-43 050	-430,5
10 Этиловый спирт 100%-ный	C ₂ H ₅ OH	-86 486	-1448
11 То же 93,5%-ный	—	—	-1609
12 Метиловый спирт 100%-ный	CH ₃ OH	-57 020	-1778
13 Изопропиловый спирт 100%-ный	C ₃ H ₇ OH	-76 280	-1271
14 Фурфуроловый спирт 100%-ный	C ₄ H ₂ OCH ₂ OH	-63 112	-644
15 Тонка-250 (состоит из 50% ксиандина и 50% триэтилamina)	—	—	-107,7
16 Аммиак	C ₆ H ₇ N	8 450	91
17 Аммиак жидкий (при -33,5°С)	NH ₃	-17 050	-1001,5
18 Гидразин	N ₂ H ₄	12 050	376,5
19 Гидразингидрат	(NH ₂) ₂ ·H ₂ O	-57 950	-1158
20 Диметилгидразин несимметричный (димазин)	C ₂ H ₈ N ₂ (CH ₃) ₂ N ₂	11 125	186
21 Метилгидразин	CH ₃ N ₂	13 445	292
22 Диэтиламин	C ₄ H ₁₁ N	-30 100	-412
23 Метан жидкий (при -164°С)	CH ₄	-17 630	-1102
24 Бензол	C ₆ H ₆	11 700	150
25 Изопропилазидат	C ₃ H ₇ O·NO ₂	-72 828	-476
26 Пентаборан	B ₅ H ₉	7 800	123
27 Окислители			
28 Азотная кислота 100%-ная	HNO ₃	-41 404	-657
29 То же 98%-ная	—	—	-798
30 Четырехокись азота	N ₂ O ₄	-6 740	-73,3
31 Смесь из 80% HNO ₃ 98%-ной + 20% N ₂ O ₄	—	—	-658
32 Тетранитрометан	C(NO ₂) ₄	8 900	45,4
33 Перекись водорода 100%-ная	H ₂ O ₂	-44 500	-1310
34 Кислород жидкий (при -183°С)	O ₂	-3 100	-97
35 Хлорная кислота	HClO ₄	-18 091	-110
36 Озон (при -112°С)	O ₃	+30 200	+829
37 Фтор жидкий (при -188°С)	F ₂	+3 000	+79
38 Монофторид фтора жидкая (при -148°С)	OF ₂	+2 800	+53
39 Трифторид азота жидкий (при -120°С)	NF ₃	-31 900	-449
40 Трифторид хлора	ClF ₃	-32 100	-347
41 Вода (иногда входит в состав компонентов топлива)	H ₂ O	-68 370	-3794
42 Теплота растворения в воде			
43 Азотной кислоты 98%-ной	—	-5 850	-325
44 То же 98%-ной	—	-5 850	-325
45 Этилового спирта	—	-250	-14
46 Перекиси водорода	—	-200	-11

[Key to Table 5.9]

1) Fuel component; 2) formula; 3) energy content; 4) kcal/kmole;
5) kcal/kg; 6) combustibles; 7) hydrogen (at -252.8°C); 8) kerosene
of the composition $C_g = 85.75\%$, $H_g = 13.5\%$, and $O_g = 0.8\%$; 9) kero-
sene of the composition $C_g = 86.76\%$, $H_g = 12.76\%$, and $O_g = 0.48\%$;
10) 100% ethyl alcohol; 11) same, 93.5%; 12) 100% methyl alcohol;
13) 100% isopropyl alcohol; 14) 100% furfuryl alcohol; 15) Tonka-250
(consists of 50% xylidene and 50% triethylamine); 16) aniline;
17) liquid ammonia (at -33.5°C); 18) hydrazine; 19) hydrazine hydrate;
20) unsymmetrical dimethylhydrazine (dimazine); 21) methylhydrazine;
22) diethylamine; 23) liquid methane (at -184°C); 24) benzene; 25)
isopropyl nitrate; 26) pentaborane; 27) oxidizers; 28) 100% nitric
acid; 29) same, 96%; 30) nitrogen tetroxide; 31) mixture of 80% 98%
 $\text{H}_2\text{O}_2 + 20\% \text{N}_2\text{O}_2$; 32) tetranitromethane; 33) hydrogen peroxide, 100%;
34) liquid oxygen (at -183°C); 35) perchloric acid; 36) ozone (at
 -112°C); 37) liquid fluorine (at -188°C); 38) liquid fluorine monoxide
(at -145°C); 39) liquid nitrogen trifluoride (at -129°C); 40) chlorine
trifluoride; 41) water (occurs occasionally in fuel components);
42) heat of solution in water; 43) 96% nitric acid; 44) same, 98%;
45) ethyl alcohol; 46) hydrogen peroxide.

also equal to zero.

The chemical energies of the products formed by combustion of
the fuel in the ZhRD chamber (CO_2 , H_2O , CO , OH , NO , H , O , and N) are
equal respectively to the heats of formation of these substances,
with the chemical energies of the combustion products CO_2 , H_2O , and
 CO negative and those of other gases positive.

The heat of formation of a substance is taken as the actual
heat liberated or absorbed during formation of the substance in ques-
tion from the elements taken in standard states (carbon in the form
of graphite, and oxygen, hydrogen, and nitrogen in the form of the
molecular gases O_2 , H_2 , and N_2).

Heats of formation of combustible and oxidizer elements and
those of the combustion products at 20°C (193.16°K) [sic] are listed
in Table 5.10.

In the reckoning system that we have adopted, the energy con-
tent of a given combustible or oxidizer consists in the general case
of the following components:

TABLE 5.10

Heats of Formation and Dissociation Energies of
Certain Substances at Temperatures of
20°C (293.16°K) and 25°C (298.16°K)

1 Наименование вещества	2 Химическое обозначение вещества	3 Молекулярный или атомный вес	4 Теплота образования ккал/кмоль		5 Энергия диссоциации ккал/кмоль
			293,16° K	298,16° K	
6 Углерод	Графит	12,010	0	0	170 018 (теплота сублимации) 8
9 Водород	H ₂	2,016	0	0	103 242
10 Кислород	O ₂	32,00	0	0	117 946
11 Азот	N ₂	28,16	0	0	225 000
12 Сера	S _{rhomb}	32,00	0	0	—
14 Фтор	F ₂	38,00	0	0	37 000
15 Углекислый газ	CO ₂	44,010	-94 051	-94 052	66 765(CO ₂ =CO+0,5O ₂)
16 Водяной пар	H ₂ O	18,016	-57 785	-57 798	57 102(H ₂ O=H ₂ +0,5O ₂)
17 Окись углерода	CO	28,010	-26 423	-26 426	256 189
18 Сернистый ангидрид	SO ₂	64,07	-70 932	-70 947	67 528(SO ₂ =SO+0,5O ₂)
19 Окись серы	SO	48,035	-2 806	-2 813	118 689
20 Метан	CH ₄	16,042	-17 851	-17 889	392 467
21 Гидроксил	OH	17,008	+8 455	8 456	65 800(H ₂ O=0,5H ₂ +OH)
22 Окись азота	NO	30,008	21 600	21 600	21 481(0,5N ₂ +0,5O ₂ =NO)
23 Атомарные газы:					
24 водород	H	1,008	52 082	52 080	—
25 кислород	O	16,00	59 534	59 542	—
26 азот	N	14,008	112 936	112 944	—
27 углерод	C	12,010	171 312	171 327	—
28 сера	S	32,00	57 441	57 441	—
29 фтор	F	19,00	18 995	19 003	—
30 ацетилен	C ₂ H ₂	26,036	54 197	54 199	388 947
31 этилен	C ₂ H ₄	28,052	12 535	12 496	531 986

1) Substance; 2) chemical formula of substance; 3) molecular or atomic weight; 4) heat of formation, kcal/kmole; 5) dissociation energy, kcal/kmole; 6) carbon; 7) graphite; 8) (heat of sublimation); 9) hydrogen; 10) oxygen; 11) nitrogen; 12) sulfur; 13) S_{rhomb}; 14) fluorine; 15) carbon dioxide; 16) water vapor; 17) carbon monoxide; 18) sulfur dioxide; 19) sulfur monoxide; 20) methane; 21) hydroxyl; 22) nitric oxide; 23) atomic gases; 24) hydrogen; 25) oxygen; 26) nitrogen; 27) carbon; 28) sulfur; 29) fluorine; 30) acetylene; 31) ethylene;

1) the physical heat content, which may be either positive or negative, depending on whether the substance used in the engine is

heated or cooled with respect to the temperature for which its heat of formation has been given;

2) the heat of transition of the substance from one chemically bound state to another, if the heat of formation is referred not to the chemically bound state in which the substance in question is used in the engine (it is necessary to take this heat into account with the proper sign).

The physical heat content is the quantity of heat expended in heating a given unit weight at constant pressure from a selected reference temperature T_0 to the temperature T at which it is used in the engine. This heat is equal to $c_p (T - T_0)$ [kcal/kg], where c_p [kcal/kg, °C] is the mean specific heat capacity of the substance at constant pressure.

The heat of formation is the energy liberated or absorbed in formation of the substance in question from the elements, which are taken in standard states.

Although they are interrelated, the heat of formation and chemical energy are not equal to one another, because a change in the physical heat content invariably occurs in the process of formation of the substance at any temperature other than absolute zero. This is accounted for by the differing heat-capacity values of the substances entering a chemical reaction and the substances produced as a result of this reaction. Only at the absolute zero of temperature does no change in physical heat content take place during a chemical reaction, and here the heat of formation is consequently exactly equal to the chemical energy.

Since the chemical energy of a fuel is determined by the heats of formation of the combustible and oxidizer, the heating value of a fuel will be higher for higher values of the heats of formation of

its components. Since the heats of formation of different substances differ widely and may be either positive or negative, a fuel whose components have positive heats of formation will be superior from this viewpoint.

Example 11. Determine the energy content of water at 20°C.

Solution.

The energy content of liquid water consists of:

a) the heat of formation of water vapor from the elements, which amounts to $Q_{\mu \text{ obr}} = -57,785 \text{ kcal/kmole}$, and

b) the heat of transition of water from the gaseous state into the liquid state at 1 atmosphere absolute and 20°C, which is $Q_{\mu \text{ per}}^* = -106,000 \text{ kcal/kmole}$, i.e.,

$$I_s = Q_{\mu \text{ obr}} + Q_{\mu \text{ per}} = -57,785 + (-106,000) = -163,785 \text{ kcal/kmole}$$

or

$$I_s = \frac{-I_s}{r_s} = \frac{-163,785}{18} = -9,099 \text{ kcal/kg.}^{**}$$

Example 12. Determine the energy content of liquid oxygen at its boiling point (90°K).

Solution.

The energy content of liquid oxygen consists of:

a) the heat withdrawn from oxygen as it cools from 293 to 90°K, which is $Q_{\mu \text{ okhl}}^{***} = c_p (90-293) = 7 (90-293) = -1420 \text{ kcal/kmole}$ and

b) the heat of transition of oxygen from the gaseous to the liquid state, which, at 90°K and atmospheric pressure, is

$$Q_{\mu \text{ per}} = -1680 \text{ kcal/kmole,}$$

$$\text{i.e., } I_{O_2} = Q_{\mu \text{ okhl}} + Q_{\mu \text{ per}} = -1420 - 1680 = -3100 \text{ kcal/kmole}$$

$$* [Q_{\mu \text{ per}} = Q_{\mu \text{ per}} = Q_{\mu \text{ perekhod}} = Q_{\mu \text{ transition}}.]$$

$$** [I_s = I_v = I_{\text{voda}} = I_{\text{water}}.]$$

$$*** [Q_{\mu \text{ okhl}} = Q_{\mu \text{ okhl}} = Q_{\mu \text{ okhlazhdeniya}} = Q_{\mu \text{ cooling}}.]$$

or

$$I_{O_2} = \frac{-I'_{O_2}}{r_{O_2}} = \frac{3160}{32} = -98.9 \text{ kcal/kg.}$$

Example 13. Determine the energy content of 100%-by-weight nitric acid at 20°C.

Solution.

The energy content of nitric acid of 100% concentration by weight at 20°C is equal to the heat of formation in the reckoning system that we have adopted, i.e.,

$$I'_{HNO_3} = Q_{\mu \text{ obr}} = -41,660 \text{ kcal/kmole}$$

or

$$I_{HNO_3} = \frac{-41,660}{88} = -473.4 \text{ kcal/kg.}$$

Example 14. Determine the energy content of 96%-by-weight nitric acid (4% water) at 20°C if the heat of solution of water in it $Q_{\text{rastv}} = -325 \text{ kcal/kg.}$

Solution.

The energy content of nitric acid of the specified weight concentration will be

$$I_{HNO_3} = 0.96 I'_{HNO_3} + 0.04 I'_{H_2O} + 0.04 \cdot Q_{\text{rastv}} = 0.96(-473.4) + 0.04(-3798) + 0.04(-325) = -798 \text{ kcal/kg.}$$

Example 15. Determine the net stoichiometric heating value of a fuel consisting of liquid oxygen O_2 and diethylamine $C_4H_{11}N$, if $C_g = 0.657$; $H_g = 0.152$, and $N_g = 0.191 \text{ kg/kg}$, and $C_t = 0.166$; $H_t = 0.038$, and $N_t = 0.049 \text{ kg/kg}$.

Solution.

1. The quantity of liquid oxygen theoretically required for complete combustion of one kg of diethylamine will be

$$\lambda_o = \frac{8}{3} C_t + 8 H_t = \frac{8}{3} 0.166 + 8 \cdot 0.038 = 2.97 \text{ kg/kg.}$$

2. The energy content of the fuel at 20°C will be determined by the formula

$$I_t = \frac{I_r + \chi_o I_o}{1 + \chi_o} = \frac{-412 + 2,97(-97)}{1 + 2,97} = -176,3 \text{ kcal/kg.}$$

3. The proportions by weight of the combustion products will be

$$\begin{aligned} \varepsilon_{CO_2} &= \frac{11}{3} C_T = \frac{11}{3} 0,166 = 0,608; \\ \varepsilon_{H_2O} &= 9H_T = 9 \cdot 0,038 = 0,343; \quad \varepsilon_{N_2} = 0,049 \text{ kg/kg.} \end{aligned}$$

4. The energy content of the products of complete combustion of the fuel at 20°C is

$$I_{res} = \varepsilon_{CO_2} I_{CO_2} + \varepsilon_{H_2O} I_{H_2O} + \varepsilon_{N_2} I_{N_2} = -2140 \cdot 0,608 + (-3120) 0,343 = -2370 \text{ kcal/kg,}$$

where I_{H_2O} is the energy content of water vapor at 20°C.

5. The net heating value of this fuel will be determined as the difference between the energy contents of the fuel and its combustion products, taken at the specified fuel temperature T_0 , i.e.,

$$H_u = (I_t - I_{gaz}) T_0$$

or

$$H_u = I_{\phi,T} + I_{2,T} - (I_{\phi,res} + I_{2,res}) = (I_{\phi,T} - I_{\phi,res}) + (I_{2,T} - I_{2,res}).^*$$

This formula indicates that the heating value of the fuel is the sum of the differences between the physical and chemical energy contents of the fuel and its combustion products.

Since the heating value of the fuel is usually determined at low temperatures (18-25°C, so that $T_0 \approx 298^\circ K$), the change in the physical and chemical energy contents that takes place under these conditions during combustion of the fuel (its conversion into the products of combustion) is relatively small, and the heating value consists basically of the change in the chemical energies. On this basis, we may assume that

$$H_u \approx I_{2,T} - I_{2,res} = I_t - I_{res} = -176,3 - (-2370) = 2194 \text{ kcal/kg.}$$

Example 16. Determine the energy content of a kerosene if

*[Subscripts: ϕ = f = fizicheskiy = physical; x = kh = khimicheskiy = chemical; τ = t = toplivo = fuel; raz = gaz = gas = gas.]

$C_g = 0.858$, $H_g = 0.135$, and $O_g = 0.007$ kg/kg; $H_{u g} = 10,170$ kcal/kg, the stoichiometric propellant mixture ratio $\chi_o = 3.35$ kg/kg, and $\mu_{ker}^* = 100$.

Solution.

1. The quantity of products of complete combustion of one kg of the kerosene in gaseous oxygen will be

$$G_{CO_2} = \frac{11}{3} C_r = \frac{11}{3} 0.858 = 3.14 \text{ kg/kg};$$

$$G_{H_2O} = 9 \cdot H_r = 9 \cdot 0.135 = 1.21 \text{ kg/kg},$$

or a total of

$$G_r = G_{CO_2} + G_{H_2O} = 3.14 + 1.21 = 4.35 \text{ kg/kg}.$$

2. The energy contents of the complete-combustion products of the kerosene, applying the data of Table 5.10, are:

$$I_{CO_2} = \frac{Q_{r, CO_2}}{\mu_{CO_2}} = \frac{-94051}{44} = -2137.5 \text{ kcal/kg};$$

$$I_{H_2O} = \frac{-57785}{18} = -3210.3 \text{ kcal/kg}.$$

3. The energy content of this kerosene will be determined from the energy balance before and after combustion:

$$I_{ker} + \chi_o I_{O_2} = G_{CO_2} I_{CO_2} + G_{H_2O} I_{H_2O} + H_{u r}$$

i.e.,

$$I_{ker} = G_{CO_2} I_{CO_2} + G_{H_2O} I_{H_2O} + H_{u r} - \chi_o I_{O_2} = -3.14(-2137.5) + 1.21(-3210.3) + 10170 - 0 = -426.2 \text{ kcal/kg}.$$

Example 17. Determine the energy content at 20°C for a fuel consisting of kerosene and nitric acid of 96% concentration by weight if $\chi = 4.2$ kg/kg, $I_{ker} = -426$ kcal/kg, and $I_{HNO_3(96\%)} = 798$ kcal/kg.

Solution.

The energy content of this fuel will be

$$I_r = \frac{I_r + \chi I_o}{1 + \chi} = \frac{-426 + 4.2(-798)}{1 + 4.2} = -724.4 \text{ kcal/kg}.$$

Example 18. Determine the heat content at 2820°K for the pro-

*[Subscript $ker = ker = kerosin = kerosene$.]

ducts of combustion of a fuel of the following composition by volume:

$\text{CO}_2 = 12.1\%$; $\text{CO} = 20.3\%$; $\text{H}_2\text{O} = 41.0\%$; $\text{H}_2 = 10.1\%$; $\text{OH} = 1.8\%$;

$\text{H} = 0.8\%$; $\text{N}_2 = 13.8\%$; and $\text{O}_2 = 0.1\%$.

Solution.

1. According to the tabulated data (Appendix I), the heat content of these components of the fuel's combustion products at 2820°K will be

$$\begin{aligned} I'_{\text{CO}_2}^{2820} &= I'_{\text{CO}_2}^{2980} + \frac{I'_{\text{CO}_2}^{2980} - I'_{\text{CO}_2}^{2820}}{100} 20 - I'_{\text{CO}_2}^{2820} = \\ &= \left[(-60,309 + \frac{-58,81 - (-60,309)}{100} 20 - (-93,990)) \right] 10^3 = \\ &= 33,980 \cdot 10^3 \text{ kcal/kmole}; \\ I'_{\text{CO}}^{2820} &= I'_{\text{CO}}^{2980} + \frac{I'_{\text{CO}}^{2980} - I'_{\text{CO}}^{2820}}{100} 20 - I'_{\text{CO}}^{2820} = \\ &= \left[(-5,803 + \frac{-4,916 - (-5,803)}{100} 20 - (-26,375)) \right] 10^3 = \\ &= 20,749 \cdot 10^3 \text{ kcal/kmole}. \end{aligned}$$

Similarly, $I'_{\text{H}_2\text{O}} = 27.50 \cdot 10^3$ [sic]; $I'_{\text{H}_2} = 19.609 \cdot 10^3$; $I'_{\text{OH}} = 19.854 \cdot 10^3$; $I'_{\text{H}} = 12.519 \cdot 10^3$; $I'_{\text{N}_2} = 10.565 \cdot 10^3$; $I'_{\text{O}_2} = 21.719 \cdot 10^3$ kcal/kmole.

2. The heat content of the combustion products of one mole of combustible at the same temperature is

$$\begin{aligned} I'_x &= \sum r_i I'_i = (0.121 \cdot 33,980 + 0.203 \cdot 20,749 + 0.410 \cdot 27,50 + 0.101 \cdot 19,809 + \\ &+ 0.018 \cdot 19,854 + 0.008 \cdot 12,519 + 0.138 \cdot 20,565 + 0.001 \cdot 21,319) 10^3 = 24,895 \text{ kcal/kmole}. \end{aligned}$$

SECTION 9. SPECIFICATIONS SET FORTH FOR A ZhRD FUEL

Certain properties of the fuel and its components are of decisive importance for the design of the engine, its efficiency in operation, and the range of missiles equipped with this engine.

The following basic specifications are set forth for ZhRD fuels;

1. The highest possible values of the fuel heat yield and the efficiency of the engine operating on this fuel, since this will necessitate smaller specific and per-hour fuel consumption rates and smaller

dimensions and weight for the rocket as a whole. The basic parameter characterizing the quality of a fuel is its heating value. The heating value of the fuel and the efficiency of an engine during operation on this fuel are of critical importance for the discharge rate of the combustion products from the nozzle. It must, however, be remembered that a fuel with a lower heat yield is sometimes preferable to a fuel having a higher heat yield by virtue of its other properties.

2. The highest possible fuel specific gravity, since this enables us to load a greater weight of fuel into tanks of a given capacity and reduce the dimensions and weight of the tanks, the weight of the fuel-supply system, and the aerodynamic drag of the rocket for a given fuel weight; all things equal, this will endow the rocket with a longer flight range. Liquefied fuel components have relatively low specific gravities, and this is their major shortcoming.

The problem of fuel load and its location on the ZhRD-propelled apparatus is of particularly great importance as a result of the very high per-second fuel consumption of the engine.

3. The highest possible specific gas yield of the fuel. All other things equal, the higher the specific volume of the combustion products obtained, the lower will be their reaction temperature and the higher the efficiency.

A gas yield with a high specific volume means a lower specific gravity for these products, which will have higher heat capacities and higher gas constants (all of these parameters are interrelated) and, consequently, signifies that that gas-discharge velocity from the engine's nozzle will be higher, together with the specific thrust, which is proportional to it.

Fuel-combustion products with high specific volumes are

usually obtained using combustibles rich in hydrogen and other light atoms or by the use of hydrocarbon fuels with large combustible excesses, the result of which is formation of a large quantity of gaseous hydrogen that is not bound to oxygen.

This is the fundamental reason why the optimum composition of many bipropellant fuels does not coincide with the stoichiometric composition and usually corresponds to a combustible-rich mixture; the result here is combustion products possessing low molecular weights.

4. The highest possible ratio between the heat capacities of the fuel-combustion products ($k = c_p/c_v$), since an increase in the value of k will, all other conditions the same, result in an increased engine specific thrust.

5. Lowest possible viscosity and surface tension in the fuel components, since this will reduce the energy used in feeding the components into the chamber and improve atomization of the fuel components. The smaller the component surface-tension coefficients, the easier will it be to atomize them. Knowledge of the viscosity coefficient of the fuel components is necessary for hydraulic computation of the engine and its various units.

6. The highest possible heat capacities, thermal conductivities, boiling points, and decomposition points in all fuel components that are intended for use in cooling the engine.

A fuel component must have a thermal stability adequate to prevent boiling at a given pressure, evaporation and chemical decomposition on contact with an engine-chamber liner that has been heated to temperatures of the order of $300-600^{\circ}\text{C}$, and the formation of solid and greasy deposits that interfere with heat transfer from the liner to the fluid. The higher the heat capacity, thermal conductivity, heat

of evaporation, and boiling point of a fuel component, the better will be its performance as a coolant.

7. The possibility of autoignition of the fuel components on mixing in the engine chamber, since it will then be unnecessary to have a fuel-ignition system for starting the engine and the design of the engine-starting system will also be simplified.

8. The shortest possible ignition delay for the components when they are mixed in a wide range of proportions, since in view of the high per-second flow rate of the fuel into the engine's combustion chamber, an ignition delay of only a few fractions of a second may result in a large accumulation of inflammable mixture in the chamber and subsequent explosion, with the attendant damage to the engine.

In order to ensure optimum performance of the fuel in the engine with high efficiency, minimal ignition delay, and the shortest possible residence time of the gases in the combustion chamber, the fuel's flash point must be as low as possible, its ignition range as wide as possible, and its combustion rate as high as possible (all other conditions equal).

9. The highest possible fuel-combustion rate, since this will result in more stable performance on the part of the engine and reduce the residence time of the fuel in question in the combustion chamber, reduce chamber dimensions and weight, and, consequently, all other conditions the same, increase the missile's flight range.

10. The lowest possible fuel-combustion temperature in the engine chamber, coupled with a high specific heat yield; the lower the combustion temperature, the smaller will be the heat loss due to dissociation of the fuel-combustion products and the more favorable will be the conditions under which the combustion chamber and engine

nozzle operate. The fuel combustion temperature should permit arranging a reliable cooling system for the engine.

11. Adequately high physical and chemical stability in the fuel components at operational pressures and temperatures that provide for prolonged storage of these components without deterioration and efficient utilization in the missile engine.

Vaporization of fuel components is particularly undesirable if their vapors present a fire or health hazard.

During prolonged storage, fuel components must not precipitate solid or resinous deposits. To prevent certain fuel components from forming tars, special antioxidants (inhibitors) are added to them.

Storage of liquefied fuel components presents a great problem, since their boiling points are, in the majority of cases, very low (they are highly unstable). It is necessary to bear this circumstance in mind in selecting a fuel for an engine being designed.

12. Lowest possible freezing points in the fuel components (no higher than -40°C) and the highest possible boiling points (no lower than $+50^{\circ}\text{C}$), so that if the temperature should drop slightly during flight, the fuel component will not solidify or become so thick that delivering it to the combustion chamber becomes difficult or altogether impossible, and so that it will not boil if the temperature rises slightly — an important consideration in using the component to cool the engine's combustion chamber and nozzle. This specification does not apply to liquefied and gaseous fuel components.

13. The lowest possible chemical activity (corrosive action) of the fuel components with respect to the materials of the engine, so that the fuel components can be stored in tanks made from non-acid-resistant materials. Nitric acid that is slightly contaminated with water attacks certain metals, undergoing structural changes in

the process that impair its qualities as an oxidizer. Hydrogen peroxide undergoes qualitative changes on contact with metallic surfaces without damaging them. Tanks and plumbing made from special materials are necessary for nitric acid and hydrogen peroxide.

14. Lowest possible hygroscopicity of the fuel components, i.e., they should have the smallest possible tendency to absorb moisture from the atmosphere, which would reduce the concentrations of the components, foul them with crystals on freezing out, and render them aggressive toward many metals.

15. Safety during storage and use, i.e., fuel components should not evaporate violently, explode, or ignite in the presence of atmospheric air.

Vaporization of a fuel in the tank during storage may result in increased pressure and bursting of the tank.

Certain fuel components are unstable (liquid oxygen, liquid ammonia, etc.) and inflammable materials (e.g., hydrogen peroxide, nitromethane, etc.) that are inclined to detonate on contamination, heating, or jarring.

The fire hazard is particularly acute with many oxidizers which form chemical compounds with large numbers of organic substances (e.g., nitric acid and hydrogen peroxide produce autoignition on contact with many organic substances). The majority of combustibles ignite readily on gentle heating in air.

Nitric acid, hydrogen peroxide, aniline and certain other fuel components cause serious burns on contact with the human body. Appropriate precautionary measures are necessary in using such fuel components. The fire hazard involved in handling a combustible is determined by its flash point; the lower this temperature, the greater is the fire hazard that the combustible presents.

16. The fuel components should not be toxic in either the liquid or the gaseous state; this requirement is set forth to avoid poisoning of the attendant personnel. If the appropriate precautionary measures can be taken, however, the toxicity of an efficient fuel component should not represent any obstacle to its use.

17. Abundant supply and low cost of acquiring the fuel components from domestic sources. The fuel components in wide use at the present time, and the oxidizers in particular, cost more than the fuels used in jet and piston engines.

Fuel components may not contain foreign impurities, since these lower the performance and operational dependability of the engine. Solid impurities in fuel components cause wear of jets and pumps, and, according to aviation standards, may not be present in quantities greater than 0.005%.

The above specifications for the fuel determine its technical applications, the specific thrust developed with it, the method used to cool the combustion chamber and nozzle, the fuel-supply system, and the dependability and statistical reliability of engine operation on the fuel in question.

No fuel that fully satisfies all of these specifications enumerated above exists at the present time. For this reason, it is necessary to select combinations that are capable of delivering the best results under specified engine-operation conditions from among the large number of known chemical compounds.

The greatest difficulty is encountered in selecting the oxidizer, since almost all oxidizers are unstable, toxic, and expensive, in addition to presenting an explosion hazard.

The diverse specifications set forth for fuel components have led to a situation at the present time in which only a few of them

are being used in practice. In many cases, it is necessary to dispense with some of the specifications enumerated above in view of other useful properties of a given fuel. For example, it is frequently necessary to overlook toxicity, chemical aggressiveness, and other undesirable properties of fuel components.

SECTION 10. BASIC CHARACTERISTICS OF ZhRD COMBUSTIBLES

In the general case, substances in which the quantities of combustible elements (C, H, Be, Al, etc.) predominate are known as combustibles.

From an engineering viewpoint, any substance characterized by a large evolved heat on combustion of a unit weight or volume, adequate readiness to enter combustion reactions with a given oxidizer, ready availability, and accessibility for large-scale use may be regarded as a combustible.

Existing fuel combustibles are classified as follows in accordance with basic characteristic criteria:

- 1) in accordance with the number of combustible elements — as elementary combustibles, which consist of a single combustible element such as H, Be, B, etc., and complex combustibles, which are formed by various combinations of combustible and noncombustible elements;
- 2) in accordance with physical state at normal temperature — as liquid, gaseous, and solid combustibles;
- 3) in accordance with the number of components making up the combustible — as single-component and multi-component combustibles;
- 4) in accordance with the manner in which the combustible reacts to contact with oxidizers — as nonhypergolic (non-autoreacting) and hypergolic (autoreacting) combustibles;

5) in accordance with the nature of their applications - as basic or working fuel components and auxiliary or starting fuel components, i.e., components used only in starting the engine.

At the present time, complex combustibles are the basic ones in use in ZhRD. The basic complex ZhRD combustibles worthy of the greatest attention include the following:

- 1) hydrocarbon combustibles - kerosene and hydrocarbons similar to it, including benzene, nitrobenzene, and nitrotoluene;
- 2) "oxygenated" hydrocarbon combustibles - the alcohols; these include ethyl, methyl, propyl, and furfuryl alcohols and solutions of them;
- 3) nitrogen-containing hydrocarbon combustibles - the amines: aniline, diethylamine, triethylamine, xylidene, and solutions of them;
- 4) nitrogen-hydrogen combustibles - ammonia and hydrazine and their derivatives (hydrazine hydrate, methylhydrazine, dimethylhydrazine) and
- 5) boron-hydrogen combustibles - pentaborane, diborinamide, etc.

With the exception of ammonia, all of these combustibles are in the liquid state under standard conditions, and this facilitates their use considerably.

Hydrocarbon combustibles. Hydrocarbon combustibles, which are distillation products of petroleum (tractor kerosene, etc.) merit much attention for use as combustibles for ZhRD.

Table 5.11 lists the basic characteristics of hydrocarbon combustibles for combustion in oxygen with $\alpha = 1$.

As a ZhRD combustible, kerosene has important advantages over many other hydrocarbons by virtue of its ready availability and low cost. It possesses a rather high specific gravity, a high flash point,

TABLE 5.11
Heating Value and Energy Content
of Petroleum-Distillation Products at 20°C

1 Наименование угле- водородного горючего	2 Удель- ный вес γ	3 Весовой элемен- тарный состав %		Теплота сгорания при сжигании 6 в кислороде ккал/кг		9
		4 C _r	5 H _r	7 H _u ^v	8 H _u	
10 Бензин авиационный	0,70	84,5	15,5	11370	10580	-536.7
11 То же	0,72	84,8	15,2	11310	10518	-517.4
12 Бензин автомобиль- ный	0,74	85,1	14,9	11249	10472	-500.0
11 То же	0,76	85,4	14,6	11188	10425	-485.2
13 Бензин тракторный (лигроин)	0,78	85,7	14,3	11122	10376	-470.0
11 То же	0,80	86,0	14,0	11055	10328	-457.4
14 Керосин тракторный	0,82	86,3	13,7	10993	10278	-446.6
15 Керосин осветитель- ный	0,84	86,6	13,4	10932	10219	-437.5
16 Газойль	0,86	86,9	13,1	10850	10157	-430.5
.	0,88	87,2	12,8	10779	10106	-424.0

1) Hydrocarbon combustible; 2) specific gravity γ ; 3) elementary composition, % by weight; 4) C_g; 5) H_g; 6) heating value for combustion in oxygen, kcal/kg; 7) H_u^v g; 8) H_u g; 9) energy content I_g, kcal/kg; 10) aviation gasoline; 11) same; 12) automobile gasoline; 13) tractor gasoline (ligroin); 14) tractor kerosene; 15) illuminating kerosene; 16) gas oil.

and a relatively low autoignition temperature — all of which are favorable to its performance in the engine. Nor do shipment and storage of kerosene present any difficulty, and its production has been placed on a firm footing by extensive development of the petroleum-refining industry.

Kerosene can be used as a combustible with all oxidizers based on the oxides of nitrogen. The net stoichiometric heating value of kerosene with nitric acid is $H_u \approx 1450$ kcal/kg.

When kerosene is used as a combustible in a Zhrd, there is a possibility of carbon-deposit formation on the surface of the inner chamber liner, and this will inhibit transfer of heat from the gases to the chamber liner and facilitate cooling of the latter. Carbon-

deposit formation is due to the chemical nature of kerosene and depends on the fuel mixture ratio and the conditions under which it is burned.

In cases where kerosene is used to cool the engine chamber, it is necessary to take into account its tendency to form gums on the cooled surface of the chamber liner at high temperatures; this may interfere to a considerable degree with cooling of the engine. The actual and potential gum contents of kerosene to be used for this purpose must be checked.

In certain cases, it is advisable to use other combustibles for purely operational considerations. Thus, the kerosene fraction boiling between 150 and 280°C during direct distillation of crude petroleum may be used successfully as a ZhRD combustible.

This kerosene has the following basic characteristics:

- 1) elementary composition by weight: $C_g = 86.76\%$, $H_g = 12.76\%$, and $O_g = 0.48\%$;
- 2) net heating value for combustion in oxygen, 10,250 kcal/kg;
- 3) physical properties at 20°C: specific gravity 0.819 kg/liter, viscosity 1.84 cst, heat capacity 0.49 kcal/kg-°C;
- 4) solidification point -60°C, boiling point +150°C, distillation end point (98%) about 280°C;
- 5) heat of formation plus 35 kcal/kmole; heat of evaporation about 79 kcal/kg.

Diesel fuel, which has a minimal delay and a rather low solidification point, should burn somewhat better with oxygen in a ZhRD.

Liquid hydrogen cannot be recommended for use as a ZhRD combustible in view of its extremely low specific gravity and the difficulty of producing, storing, and using it in its liquid state, despite its relatively high heating value.

Oxygenated-hydrocarbon combustibles. Among the oxygen-containing hydrocarbons, an aqueous solution of ethyl alcohol at 75-92% concentration by weight has been most extensively used as a combustible in ZhRD. The ethyl alcohol is diluted with water to lower its combustion temperature and thus render cooling of the engine easier.

Table 5.12 presents the basic characteristics of alcohols and other oxygenated-hydrocarbon combustibles used in ZhRD in one form or another.

A high relative content in fuel mixtures with oxidizers (about 40-50% by volume) is typical for the alcohols. They differ little in specific gravity from the hydrocarbons.

The heating values of the majority of oxygen-containing hydrocarbons are lower than those of the hydrocarbons, due to the high positive values of their heats of formation. However, the use of these expensive combustibles is explained by their low combustion temperatures, which make it possible to design thermally relatively unstressed ZhRD, while the high heat-capacity values allow them to be used successfully for cooling engine chambers; this is also assisted by the high boiling points of the alcohols.

Table 5.13 lists certain characteristics of a fuel consisting of liquid oxygen and aqueous solutions of ethyl alcohol at various concentrations.

Mixtures of other alcohols having the same heating value, combustion temperature, and other characteristics may be used as substitutes for ethyl alcohol; this is of great importance in expanding the operational potential of engines of a given design.

The performance of oxygen-alcohol engines can be forced by converting them to a combustible consisting of alcohol and aviation

TABLE 5.12

Basic Characteristics of Oxygenated-Hydrocarbon Combustibles

1 Горючие 2 Характеристики	3	4	5	6	7	8	9
	Этиловый спирт C_2H_5OH	Метилловый спирт CH_3OH	Изопропиловый спирт C_3H_7OH	Фуриловый спирт $C_4H_3O_2$	Фуриловый спирт $C_4H_3O_2$	Вениловый спирт C_6H_5OH	Фенол C_6H_5O
10 Элементарный состав горючего, %:							
11 углерода	52,2	37,5	59,96	61,3	62,5	66,7	76,6
12 водорода	13,1	12,5	13,42	6,2	4,2	11,1	6,4
13 кислорода	34,7	50,0	26,62	32,5	33,3	22,2	17,0
14 Молекулярный вес	46,07	32,04	60,09	98,10	98,08	72,07	94,1
15 Удельный вес при 20° С кг/л	0,789	0,792	0,781	1,133	1,100	0,754	1,07 (20°)
16 Температура, °С:							
17 плавления	-117,3	-97,9	-88,5	-32	-38,7	-50	-40,8
18 кипения	78,5	64,6	82,26	171,0	161,7	26	180,9
19 Теплота образования, ккал/г-моль	-68,48	-57,82	-76,5	-68,1	—	-46,0	-37,3
20 Удельный вес топлива, кг/л	1,00	0,97	1,01	1,14	1,15	0,99	1,2
21 Низшая теплотворность топлива:							
22 весовая, ккал/кг	2880	1880	2070	2880	—	2280	2180
23 объемная, ккал/л	2910	1790	2080	2340	—	—	2580
24 Газообразование:							
25 л/кг	789	849	789	654	653	728	—
26 л/л	788	841	773	745	789	717	—

*At atmospheric pressure.

1) Combustible; 2) characteristic; 3) ethyl alcohol; 4) methyl alcohol; 5) isopropyl alcohol; 6) furfuryl alcohol; 7) furfural; 8) vinyl [sic] ethyl ether; 9) phenol; 10) elementary composition of combustible, %; 11) carbon; 12) hydrogen; 13) oxygen; 14) molecular weight; 15) specific gravity at 20°C, kg/liter; 16) temperature, °C; 17) melting; 18) boiling; 19) heat of formation, kcal/g-molecule; 20) specific gravity of fuel, kg/liter; 21) net heating value of fuel; 22) unit-weight, kcal/kg; 23) unit-volume, kcal/liter; 24) gas yield; 25) liters/kg; 26) liters/liter.

gasoline (binary combustible mixtures) or mixtures of alcohol, gasoline, and benzene (ternary combustible mixtures), which do not separate into layers at relatively high temperatures. The stratification temperature of the combustible mixture rises when the water content of the alcohols is increased.

Furfuryl alcohol is added to certain combustibles to render

TABLE 5.13

Basic Characteristics of Aqueous Ethyl Alcohol Solutions

Характеристики топлива и его продуктов сгорания при $\alpha=1$	Концентрация спирта в водных растворах, % по весу							
	60	70	75	80	85	90	95	100
3) состав топлива, %:								
4) спирта	44,4	40,7	39,0	37,5	36,1	34,8	33,6	32,4
5) кислорода	55,6	59,3	61,0	62,5	63,9	65,2	66,4	67,6
6) состав топлива, %:								
7) спирта	50,6	47,4	46,0	44,8	43,6	42,6	41,7	40,9
8) кислорода	49,4	52,6	54,0	55,2	56,4	57,4	58,3	59,1
9) коэффициент состава топлива:								
10) по весу	1,251	1,489	1,564	1,609	1,772	1,876	1,981	2,085
11) по объему	0,977	1,111	1,174	1,235	1,292	1,346	1,397	1,443
12) удельный вес, кг/л								
13) спирта	0,789	0,868	0,856	0,844	0,831	0,818	0,804	0,789
14) топлива	1,014	1,011	1,009	1,007	1,006	1,006	1,006	0,998
15) состав продуктов полного сгорания топлива, %:								
CO ₂	59,9	54,4	55,9	57,3	58,6	59,8	60,9	62,0
H ₂ O	49,1	45,6	44,1	42,7	41,4	40,2	39,1	38,0
16) чистая стехиометрическая теплотворность топлива:								
17) весовая, ккал/кг	1590	1709	1770	1820	1869	1909	1959	2010
18) объемная, ккал/л	1590	1720	1780	1840	1899	1959	2009	2060
19) количество при полном сгорании топлива:								
20) л/кг	870	845	834	828	814	805	797	789
21) л/л	882	854	841	829	818	807	797	789

1) Characteristics of fuel and its combustion products at $\alpha = 1$; 2) concentration of alcohol in aqueous solutions, % by weight; 3) composition of fuel by weight, %; 4) alcohol; 5) oxygen; 6) composition of fuel by volume, %; 7) alcohol; 8) oxygen; 9) fuel mixture ratio; 10) by weight; 11) by volume; 12) specific gravity, kg/liter; 13) alcohol; 14) fuel; 15) weight composition of products of complete combustion of fuel, %; 16) net stoichiometric heating value of fuel; 17) unit-weight, kcal/kg; 18) unit-volume, kcal/liter; 19) gas yield from complete combustion of fuel; 20) liter/kg; 21) liters/liter.

them autoigniting on mixing with the oxidizer. It is a colorless aromatic fluid that is slightly soluble in petroleum hydrocarbons and has a flash point of about 91.3°C.

Nitrogen-containing hydrocarbon combustibles. The nitrogen-containing hydrocarbon combustibles include aliphatic and aromatic

TABLE 5.14

Basic Characteristics of Nitrogen-Containing Compounds

1 Горючие	3 Анилин C_6H_7N	4 Диэтиламин $C_4H_{11}N$	5 Триэтиламин $C_6H_{15}N$	6 Ксиландин $C_9H_{11}N$	7 Нитробензол $C_6H_5NO_2$	8 Нитротолуол $C_7H_7NO_2$
2 Характеристика						
9 Вещное содержание элементов горючего, %:						
10 углерода C ,	77,4	65,7	71,2	79,2	58,5	61,3
11 водорода H ,	17,6	15,2	14,9	9,2	4,1	5,1
12 азота N ,	15,0	19,1	13,9	11,6	11,4	10,2
13 кислорода O ,	—	—	—	—	26,0	23,4
14 Молекулярный вес	93,08	73,14	101,07	121,12	123,0	137,1
15 Удельный вес, кг/л	1,022	0,711	0,728	0,977	1,207	1,068
16 Температура, °C:						
17 плавления	-6,2	-38,9	-114,8	-54	5,7	-10,6
18 кипения	184,4	55,9	89,5	210	210,6	222,3
19 Теплота образования, ккал/г-моль	+7,08	30,1	-14,71	-8,42	-3,8	4,0
20 Удельный вес топлива на основе жидкого кислорода, кг/л	1,022	0,99	1,0	1,09	—	—
21 Коэффициент состава топлива:						
22 весовой	2,68	2,95	3,08	2,84	—	—
23 объемный	2,39	1,84	1,97	2,48	—	—
24 Теплотворность топлива:						
25 весовая, ккал/кг	2200	2230	2240	2130	2150	2230
26 объемная, ккал/л	2430	2200	2250	2330	—	—
27 Газообразование:						
28 л/кг	687	775	780	875	—	—
29 л/л	736	787	788	738	—	—

*At atmospheric pressure.

1) Combustible; 2) characteristic; 3) aniline; 4) diethylamine; 5) triethylamine; 6) xylidene; 7) nitrobenzene; 8) nitrotoluene; 9) elementary weight contents of elements in combustible, %; 10) carbon C_g ; 11) hydrogen H_g ; 12) nitrogen N_g ; 13) oxygen O_g ; 14) molecular weight; 15) specific gravity, kg/liter; 16) temperature, °C; 17) melting; 18) boiling; 19) heat of formation, kcal/g-molecule; 20) specific gravity of fuel based on liquid oxygen, kg/liter; 21) fuel mixture ratio; 22) by weight; 23) by volume; 24) heating value of fuel; 25) unit-weight, kcal/kg; 26) unit-volume, kcal/liter; 27) gas yield; 28) liters/kg; 29) liters/liter.

amines. Representatives that have been used as combustibles in ZhRD include aniline, diethylamine, triethylamine, and xylidene. Table 5.14 lists the basic characteristics of certain amines and nitro-compounds.

Aniline and the combustible Tonka-250, which consists of 50% triethylamine and 50% xylidene, have been most extensively used as self-contained combustibles. The rest of the above amines may be used in one quantity or another in the compositions of other combustible mixtures.

Xylidene mixes very poorly with water. Triethylamine mixes well with water and this makes it possible to water the Tonka-250 combustible to a marked degree without precipitating phases.

The basic characteristics of the Tonka-250 combustible are as follows:

- 1) elementary composition by weight: $C_g = 75.252\%$, $H_g = 12.046\%$, and $N_g = 12.702\%$;
- 2) the net heating value for combustion in oxygen is 9095 kcal/kg;
- 3) the solidification point is -50°C and the boiling point is $+85^{\circ}\text{C}$;
- 4) specific gravity 0.845 kg/liter at 20°C , heat capacity 0.55 kcal/kg- $^{\circ}\text{C}$, and kinematic viscosity 1.19 cst (at 20°C);
- 5) the heats of evaporation at temperatures of -60° and $+250^{\circ}\text{C}$ are 80.3 and 59.3 kcal/kg, respectively.

Nitrogen-hydrogen combustibles. Among the nitrogen-hydrogen combustibles (nitrogen hybrids [sic]*), ammonia, hydrazine, and the latter's derivatives (hydrazine hydrate, methylhydrazine, and dimethylhydrazine) merit the greatest attention.

*[The Russian gidridov which appears in the original is probably a typographical error for gidridov, hydrides.]

Ammonia (NH_3) is a colorless gas with a characteristic pungent odor under normal conditions. It is poisonous and irritates the membranes of the eyes and respiratory organs. Concentrations no higher than 0.02 mg per liter of air can be safely tolerated. It can be stored for long periods under pressure in the liquid state. It dissolves well in a large number of organic and inorganic compounds and even in metals.

The basic physicochemical properties of ammonia are as follows:

molecular weight	17.03
melting point, °C	-77.75
boiling point, °C	-33.44
critical temperature, °C	132.4
critical pressure, atmospheres absolute	111.5
specific gravity at -33.44°C, kg/liter	0.68
heat capacity at 20°C, kcal/kg-°C	1.14
thermal conductivity at 20°C, kcal/m-hour-°C	0.42
viscosity at -33.44°C, dyne-sec/cm ²	0.00254
surface tension at 20°C, dynes/cm	66.67
heat of formation at -33.44°C, kcal/kg	-1000.0
heat of evaporation at -33.44°C, kcal/kg	327.65
net heating value, kcal/kg:	
a) for combustion in oxygen	1640
b) for combustion in fluorine	2310

Since ammonia contains only 17.8% by weight of combustible (hydrogen), it is incapable of combustion in air and burns only in oxygen, with a yellow flame; it is autoigniting at 700°C. However, the use of ammonia with oxygen in ZbRD is inconvenient because of its sluggishness in chemical reaction, its low boiling point, and its toxicity, even though it has a low combustion temperature and cooling properties better than those of kerosene (in cases where it is used in cooling the engine chamber).

Hydrazine (N_2H_4) is obtained from ammonia; under standard conditions, it is a colorless, poisonous fluid that fumes in air and absorbs moisture, carbon dioxide, and oxygen from the atmosphere.

It mixes with water, alcohols, ammonia, and other nonpolar liquids.

Hydrazine is unstable; in its anhydrous state, it is liable to catalytic and thermal decomposition into the elements and into a nitrogen-ammonia mixture. It burns with a blue flame in air. Hydrazine is not sensitive to jarring, and its ignition temperature is lower in oxygen than in air and highest of all in nitrogen. It attacks rubber and many other organic materials.

The basic physicochemical properties of hydrazine are as follows:

molecular weight	32.05
melting point, °C	2.0
boiling point, °C	113.5
critical temperature, °C	380
critical pressure, atmospheres absolute	145
specific gravity at 20°C, kg/liter	1.0083
heat capacity at 20°C, kcal/kg-°C	0.735
viscosity at 20°C, dyne-sec/cm ²	0.01038
surface tension at 25°C, dynes/cm	66.67
heat of formation at 25°C, kcal/kg	+374.41
heat of fusion at 2°C, kcal/kg	94.38
heat of evaporation at 113.5°C, kcal/kg	304.52
net heating value, kcal/kg:	
a) for combustion in oxygen	1940
b) for combustion in fluorine	2430

Hydrazine is a most efficient and versatile combustible because it delivers higher P_{ud}^* in combination with almost all oxidizers. To use it, it will be necessary to improve its operational properties and lower the cost of producing it. It would be highly desirable to lower its boiling point by introducing admixtures, e.g., by dissolving water in it or by dissolving it in ammonia, in which it dissolves without limit. The addition of 10% by weight of water to hydrazine lowers its boiling point to -9°C, and 20% of water depresses it almost to -30°C.

Highly promising ZhRD combustibles are methylhydrazine, $(CH_2N_2H_2)$ and unsymmetrical dimethylhydrazine $(CH_3)_2N_2H_2$, which are

$[P_{yn} = P_{ud} = P_{udel'nyy} = P_{specific}]$

derivatives of hydrazine that are liquid under normal conditions. These combustibles have low boiling points, are more stable than hydrazine, and form highly efficient fuels with fluorine monoxide, all of which indicate that they should be thoroughly studied and put to use.

Methylhydrazine is hygroscopic, has a $t_{pl} = -52.4^{\circ}\text{C}$, $t_{kip} = 87^{\circ}\text{C}$ (at 745 mm Hg), $t_{kr} = 257^{\circ}\text{C}$, $p_{kr} = 75$ atmospheres absolute, $\gamma_g = 0.876$ kg/liter, $Q_{obr} = 292$ kcal/kg, $Q_{isp} = 209.78$ kcal/kg, and $Q_{pl} = 54.13$ kcal/kg.*

Unsymmetrical dimethylhydrazine (dimazine) is a colorless, highly hygroscopic fluid with a high mobility under standard conditions and an ammoniacal odor; it is soluble in water, alcohols, hydrocarbons, and amines.

The basic physicochemical properties of dimazine (DMG**) are as follows:

molecular weight	60.08
melting point, $^{\circ}\text{C}$	-58
boiling point, $^{\circ}\text{C}$	63
specific gravity at 20°C , kg/liter	0.795
coefficient of expansion	0.0013
critical temperature, $^{\circ}\text{C}$	249
critical pressure, atmospheres	62
viscosity, centipoises	0.586
flash point (in closed vessel), $^{\circ}\text{C}$	1.1
heat capacity at 20°C , kcal/kg- $^{\circ}\text{C}$	0.653
heat of formation [sic], kcal/kg	184.75
heat of combustion, kcal/kg	7900
heat of evaporation, kcal/kg	40
heat of formation [sic], kcal/kg	134
thermal conductivity at 20°C , kcal/m-hour $^{\circ}\text{C}$	0.18
coefficient of surface tension, kg/m	0.0025
energy content, kcal/kg	218
net thermal conductivity [sic] for combustion in oxygen (at 20°C), kcal/kg	2200

At the present time, dimazine is used as a ZhRD combustible

*[Subscripts: пл = pl = plavleniye = melting; исп = isp = ispareniiye = evaporation.]

**[DMG= DMG = dimetilgidrazin = dimethylhydrazine.]

that is hypergolic when mixed with nitric acid and its derivatives. It can also be used with liquid oxygen; the latter are not auto-igniting when mixed.

Boron-hydrogen combustibles. Elementary boron has a net heating value of about 13,670 kcal/kg and forms a number of compounds (known as boranes) with hydrogen. The best of these are diborane (B_2H_6 , a gas), pentaborane (B_5H_9 , a liquid), decaborane ($B_{10}H_{14}$, a solid), etc.

The net heating value of boron-hydrogen compounds for combustion in oxygen attains 16,300 kcal/kg, while this figure is 10,300 kcal/kg for kerosenes. For this reason, they develop specific thrusts almost 1.6 times greater than those of the kerosenes. Diborane and pentaborane are autoigniting in air. When carbon is added to them, they are stabilized as regards autoignition, but this drops the net heating value to 13,880 kcal/kg. The boron hydrocarbons thus obtained are generally known as alkylboranes or carboranes.

The basic physical properties of the combustibles involved here are as follows:

1) Горючее	2) μ_r	3) γ , г/см ³ при 20°С	4) t_{pl} , °С	5) t_{kip} , °С
6) Керосин	—	0,82	—80	150
7) Диборан (B_2H_6)	27,7	0,42	—165	—92
8) Пентаборан (B_5H_9)	63,2	0,61	—47	60
9) Декаборан ($B_{10}H_{14}$)	122,3	0,97	160	213
10) Карборан	—	0,82	—	200

1) Combustible; 2) μ_g ; 3) γ , g/cm³ at 20°C; 4) t_{pl} , °C; 5) t_{kip} , °C; 6) kerosene; 7) diborane; 8) pentaborane; 9) decaborane; 10) carborane.

These combustibles are many times more expensive than kerosene. In addition, it is extremely difficult to use them for a number of reasons.

Pentaborane,* which is a colorless, toxic, mobile fluid with an unpleasant odor under standard conditions, is of interest as a combustible for ZhRD. Under ordinary conditions, it can be stored for years. It decomposes slowly on heating, for the most part to boron oxide, which is capable of causing corrosion and forming deposits that clog the flow sections of the jets, which makes its utilization very difficult. Pentaborane can be used as an additive to other combustibles, as well as for adjusting the combustion processes of amines and hydrazine derivatives in combination with fluorine monoxide or ammonium-fluoride fuels, which are unstable in ZhRD.

Suspensions of boron in kerosene, which give energy yields only slightly below those of mixtures with pentaborane and are considerably more convenient to work with, must be regarded as the most attractive among the boron-based fuels.

The use of silicon hydrides and trisilicylamine $\text{Si}_3\text{H}_9\text{N}$ (a mobile colorless fluid that is autoigniting in air) is not justified in practice because of the difficulty of producing them.

Analysis of the heat effects obtained with known elementary combustibles and the most efficient oxidizers permits the conclusion that hydrogen, lithium, beryllium, boron, carbon, sodium, aluminum, magnesium, silicon, phosphorous, sulfur, potassium, and calcium have the highest heating values among them. Here, calculations indicate that the most efficient of these elements are hydrogen, lithium, beryllium, and boron, which can be burned in liquid fluorine to increase the flight range of rockets.

The fuels hydrogen fluoride and lithium fluoride develop the highest specific thrusts (about 400 kg of thrust/kg of fuel/sec). Increasing the chamber pressure at the optimum excess oxidizer ratio

*Ekspress-informatsiya AN SSSR, No. 9, ADS-37, 1959.

and redistribution of the gases in the nozzle (the metallic fluorides are in the solid state, while nonmetallic fluorides are gaseous) by the use of these fuels may result in a specific thrust in vacuo of about 450 kg of thrust/kg of fuel/sec, which is obviously the attainable limit for chemical energy sources in oxidation reactions.

Although the use of difficult-to-make and expensive solid combustible elements in ZhRD is technically possible and easiest in the form of suspensions in kerosene, amines, hydrazine, and its derivatives, their practical utilization is in doubt at the present time due to their high viscosity, inadequate stability (they coagulate) and relatively high combustion temperatures, which are an obstacle to operation and cooling of the engine. Due to the high viscosity of the suspensions, the pressure gradient in the jets of the combustion chamber must, all other things equal, be 3 to 6 times higher than for kerosene.

This does not exclude the application of certain metals and nonmetals to activate combustibles or to provide chemical ignition of the sustaining fuel when the engine is started.

SECTION 11. BASIC CHARACTERISTICS OF OXIDIZERS FOR ZhRD COMBUSTIBLES

Substances in which oxidizing elements (O_2 , O_3 , H_2O_2 , etc.) predominate in the weight breakdown are known as oxidizers.

Among all the potential oxidizers, only those that couple adequate efficiency in reaction with combustibles with abundant occurrence and accessibility to use are of technical significance.

The most important oxidizers include the elementary oxidizers — fluorine, oxygen, chlorine — and other complex oxidizers, which are compounds of oxygen, fluorine, chlorine, and nitrogen with one another in different combinations, certain compounds of these elements with combustible elements (carbon, hydrogen, sulfur, etc.), as well

TABLE 5.15

Physicochemical Properties of Certain Oxidizers

1 Наименование окислителя	2 Химичес- кая формула	3 Молеку- лярный вес	4 Удельный вес в жидком состоянии	5 Температура, °C		8 Теплота кал/кмоль		11 Вязкость	
				6 $t_{зам}$	7 $t_{кип}$	9 образо- вания	10 испаре- ния		
17 Азотная кислота 100%-ная	HNO ₃	63,02	1,51(20° C)	-41,60	86,0	-41,40	9,43	0,58 сст (20° C)	12
18 Перекись водорода 100%-ная	H ₂ O ₂	32,02	1,44(20° C)	-1,7	151,4	-45,16	11,67	1,373 с-пуаз (19,6° C)	13
19 Четырехокись азота	N ₂ O ₄	92,02	1,45(20° C)	-11,20	21,15	-6,75	9,11	1,307 сст (18° C)	12
20 Хлорная кислота	HClO ₄	100,46	1,77(20° C)	-112,0	110,0	-18,1	—	—	
21 Тетранитрометан	CN ₄ O ₆	198,04	1,64(20° C)	13,8	126,7	+8,8	+9,2	0,0166 пуаз (18° C)	14
22 Жидкий трифторид азота	NF ₃	71,01	1,55(-129,8° C)	-206,79	-129,06	-31,9	2,77	—	
23 Жидкий нитрат фтора	NO ₂ F	81,01	1,61(-80° C)	-181,0	-80,0	-1,0	4,73	—	
24 Трифторид хлора	ClF ₃	92,46	1,85(12° C)	-76,32	11,75	-32,19	6,58	4,35 с-пуаз (10° C)	13
25 Жидкий кислород	O ₂	32,00	1,14(-183° C)	-218,76	-182,97	-3,10	1,63	0,143 с-пуаз (-170° C)	13
26 Жидкая перекись фтора	O ₂ F ₂	70,00	1,45(-57° C)	-163,5	-57,0	0	4,57	—	
27 Жидкий фторид кисло- рода (окись фтора)	OF ₂	54,0	1,52(-144,3° C)	-223,8	-144,8	2,86	2,65	0,3836 с-пуаз (-145,3° C)	13
28 Жидкий фтор	F ₂	38,00	1,51(-188,4° C)	-219,62	-187,92	0	1,58	0,367 с-пуаз (190° C)	13
29 Жидкий озон	O ₃	48,00	1,35(-112° C)	-192,5	-112,0	30,2	3,5	—	
30 Серная кислота	H ₂ SO ₄	98,00	1,834(18° C)	-10,5	340	193,75 (18° C)	—	20,2 с-пуаз (25° C)	13
31 Вода	H ₂ O	18,00	0,9999(20° C)	0	100	15 539,1 кал/г	539,1 16 кал/г	1 с-пуаз (20,3° C)	13

Note. The solidification and boiling points, as well as the other characteristics of the oxidizers are listed for atmospheric pressure.

1) Oxidizer; 2) chemical formula; 3) molecular weight; 4) specific gravity in liquid state; 5) temperature, °C; 6) $t_{зам}$ *; 7) $t_{кип}$; 8) heat, kcal/kmole; 9) formation; 10) evaporation; 11) viscosity; 12) cst; 13) centipoises; 14) poises; 15) kcal/kmole; 16) cal/g; 17) 100% nitric acid; 18) 100% hydrogen peroxide; 19) nitrogen tetroxide; 20) perchloric acid; 21) tetranitromethane; 22) liquid nitrogen trifluoride; 23) liquid fluorine nitrate; 24) chlorine trifluoride; 25) liquid oxygen; 26) liquid fluorine peroxide; 27) liquid oxygen fluoride (fluorine oxide); 28) liquid fluorine; 29) liquid ozone; 30) sulfuric acid; 31) water.

as solutions of oxidizers in one another.

Presently known oxidizers for ZhRD combustibles may be classified on the basis of the following characteristic criteria.

1. On the basis of their physical state under standard conditions — as liquid, gaseous, and solid oxidizers.

2. On the basis of the oxidant base, as follows:

*[Subscript зам = зам = zamerzaniye = freezing, solidification.]

a) oxygen oxidizers - liquid oxygen, its allotropic modifications, and its compounds with combustible elements;

b) nitrogen oxides and oxidizers containing nitrogen oxides or derived from them;

c) fluorine oxidizers - fluorine and fluorides of oxygen, chlorine, and nitrogen and other fluorine-containing compounds;

d) chlorine oxidizers - chlorine, chlorine oxides, and oxidizers containing chlorine oxides or derived from them.

Solutions of the various oxidizers in one another can be assigned to the various oxidant-base groups listed above in accordance with the oxidizers that are chemically most characteristic.

The presently known most efficient elementary oxidizers can be arranged in the following series in order of diminishing activity in chemical reaction: fluorine, oxygen, chlorine, bromine, and iodine. Only a few oxidizers are currently in use in ZhRD.

Table 5.15 lists the physicochemical characteristics of the most efficient oxidizers, and Table 5.16 the net stoichiometric heating value of toluene with these oxidizers. The heats of evaporation and warming to normal temperature were taken into account in computing the heating values for liquified oxidizers.

Table 5.17 shows the elementary compositions of the oxidizers considered here. It will be seen from this table that nitric acid, hydrogen peroxide, perchloric acid, and tetranitromethane contain combustible elements.

Below we present a brief discussion of the fundamental properties of the oxidizers that are of prime importance in using them.

In its pure form, nitric acid is a colorless, poisonous, hygroscopic liquid that fumes in air and has a highly irritating odor. The use of nitrogen dioxide gives it a yellow to brown coloration.

On coming into contact with the skin, it inflames the tissue and forms yellow spots. If the acid is not washed off immediately and neutralized, lesions will form. When conditions favor it, explosions may occur when it comes into contact with solid combustible materials (dry sawdust, cotton batting in large quantities). It forms snow-white crystals in its solid state.

TABLE 5.16

Efficiency of Basic Oxidizers in Stoichiometric Combustion of Toluene in Them

1 Наименование окислителя	2 Удель- ный вес при 20° C кг/л	3 Низшая стехи- ометрическая теплотворность		5 Удельное газовыделение		8 Газовая постоян- ная кг/м кг °C
		4 ккал/кг		6 л/кг	7 л/л	
9 Азотная кислота	1,34	1400	1970	747	1010	28,3
10 Перекись водорода	1,32	1600	2110	922	1220	31,9
11 Четырехокись азота	1,29	1720	2250	686	800	26,0
12 Хлорная кислота	1,50	1730	2490	640	960	24,2
13 Тетранитрометан	1,47	1700	2510	660	970	25,0
14 Трифторид азота	1,44	1600	2670	499	718	18,9
15 Нитрат фтора	1,33	2050	2730	705	987	26,7
16 Кислород	1,06	2200	2415	650	689	24,6
17 Перекись фтора	1,29	2500	3222	657	847	24,8
18 Окись фтора	1,36	2650	3590	582	791	22,0
19 Фтор	1,30	2600	3700	433	600	16,4
20 Озон	1,25	2730	3530	650	812	24,6

Note. In this table, the oxidizers are arranged in order of increasing unit-weight net stoichiometric heating value of the fuel.

1) Oxidizer; 2) specific gravity at 20°C, kg/liter; 3) net stoichiometric heating value; 4) kcal/kg; 5) specific gas yield; 6) liters/kg; 7) liters/liter; 8) gas constant, kg-m/kg °C; 9) nitric acid; 10) hydrogen peroxide; 11) nitrogen tetroxide; 12) perchloric acid; 13) tetranitromethane; 14) nitrogen trifluoride; 15) fluorine nitrate; 16) oxygen; 17) fluorine peroxide; 18) fluorine oxide; 19) fluorine; 20) ozone.

Hydrogen peroxide is a colorless, poisonous, odorless, low-mobility fluid that appears bluish in thick layers. On coming into contact with the skin, it produces white spots which are accompanied by itching and burning but disappear after a few hours; blisters form after prolonged contact with the skin. Wool, coal, cotton batting, and certain other combustible materials are spontaneously inflammable

TABLE 5.17

Elementary Compositions by Weight of Basic Oxidizers

1 Наименование окислителя	2 Весовое содержание отдельных элементов в окислителе %					
	3 кислорода	4 фтора	5 хлора	6 азота	7 водорода	8 углерода
9 Азотная кислота	76,2	—	—	22,2	1,6	—
10 Перекись водорода	94,0	—	—	—	6,0	—
11 Четырехокись азота	69,6	—	—	30,4	—	—
12 Хлорная кислота	63,7	—	35,3	—	1,0	—
13 Тетранитрометан	55,8	—	—	28,8	—	6,1
14 Трифторид азота	—	80,8	—	18,7	—	—
15 Нитрат фтора	59,2	23,5	—	17,3	—	—
16 Кислород	100	—	—	—	—	—
17 Перекись фтора	45,7	54,3	—	—	—	—
18 Окись фтора	29,6	70,4	—	—	—	—
19 Фтор	—	100	—	—	—	—
20 Озон	100	—	—	—	—	—

1) Oxidizer; 2) contents by weight of individual elements in oxidizer; 3) oxygen; 4) fluorine; 5) chlorine; 6) nitrogen; 7) hydrogen; 8) carbon; 9) nitric acid; 10) hydrogen peroxide; 11) nitrogen tetroxide; 12) perchloric acid; 13) tetranitromethane; 14) nitrogen trifluoride; 15) fluorine nitrate; 16) oxygen; 17) fluorine peroxide; 18) fluorine oxide; 19) fluorine; 20) oxone.

on contact with hydrogen peroxide. It presents an explosion hazard and can be stabilized. It is a colorless crystalline mass in the solid state.

In pure form, nitrogen tetroxide is a colorless, poisonous fluid. This oxidizer is usually yellowish in color, and this coloration intensifies as the temperature rises due to decomposition into nitrogen dioxide. The low boiling point makes it highly volatile, and its vapors asphyxiate. On coming into contact with the skin or combustible materials, it behaves in much the same way as nitric acid; it may autoignite under certain circumstances and presents an explosion hazard. It is a white crystalline mass in the solid state.

In its pure form, perchloric acid is a colorless, hygroscopic, poisonous fluid that fumes in air with corrosive vapor. It forms painful and dangerous lesions on the skin. There is a danger of explosion on contact with combustible materials (coal, paper, wood, etc.); it is stabilized to some extent by addition of about 1 to 2%

of carbon tetrachloride.

In its pure form, tetranitromethane is a colorless and tasteless liquid. It is more highly toxic than any other high-boiling oxidizer, except perhaps for the fluorine-containing oxidizers. It is volatile and causes copious lachrymation. Its vapor is colorless and asphyxiating, possessing the pungent odor of the nitrogen oxides. It irritates the skin on contact with it. Combustibles and solid materials (cloth, wood) do not autoignite on contact with it. It presents an explosion hazard, can be stabilized, and forms white crystals in the solid state.

Nitrogen trifluoride is a liquefied gas. In its gaseous state, it is colorless, highly poisonous, explosive, and stable to heating and various chemical disturbances. It is nearly insoluble in water; it does not react with water under normal conditions. A reaction with water vapor begins only when electrical energy is supplied and then proceeds slowly. It has not been adequately studied up to the present time.

Fluorine nitrate is a liquefied gas. In the gaseous state, it is colorless, poisonous, and has an asphyxiating odor. It decomposes during storage and explodes on contact with certain combustibles (alcohol, ether, etc.). It is soluble in water and decomposes to a minor degree.

Liquid oxygen is a bluish low-boiling liquid (liquefied gas). Gaseous oxygen is colorless, odorless, and tasteless. It can be inhaled for brief periods without danger. Brief contact of liquid oxygen with the human body (fractions of a second) is not dangerous, but freezing occurs on longer contact. Normally, combustible materials do not ignite in oxygen. It presents an explosion hazard and is a white mass in the solid state.

Liquid fluorine is a yellow low-boiling liquid (liquefied gas). It is an extremely [the most] powerful oxidizer, reacting with practically all organic and inorganic substances (with the exception of inert gases) with evolution of heat.

The saturation vapor pressure of fluorine in the boiling-point interval from 53.54-90°K is given by the equation

$$\lg p = 7.08718 - \frac{337.258}{T} - \frac{1.3185 \cdot 10^6}{T^2},$$

where p is the pressure in mm Hg and T is the absolute temperature in degrees.

The critical pressure is 55 atmospheres and the critical temperature is 129°C.

Gaseous fluorine is nearly colorless in a thin layer, but is greenish-yellow in color in thick layers. It is highly poisonous and has a sharp, irritating odor. Brief contact of fluorine vapor with the skin causes inflammation and abscessing. It presents an explosion hazard. It is a white mass in the solid state.

The following fluorine-based oxidizers are possible: liquid fluorine peroxide O_2F_2 , liquid fluorine oxide OF_2 , chlorine trifluoride ClF_3 , bromine pentafluoride BrF_5 , etc. Like fluorine itself, these oxidizers are thermodynamically stable and have indefinite storage lives.

Liquid fluorine peroxide is a low-boiling blood-red liquid (liquefied gas). It has a pale brown color in its gaseous state: at 50°C, it becomes colorless as a result of decomposition into the elements. It forms orange-red crystals in the solid state. It has not been thoroughly studied. It resembles fluorine oxide and fluorine in its behavior.

Liquid fluorine oxide is a yellow low-boiling fluid (liquefied gas). In the gaseous state, it is colorless and has the unpleasant odor of fluorine. It yields little to fluorine as

regards toxicity and aggressiveness toward materials. The efficiencies of fluorine monoxide-based fuels are higher than those of the oxygen fuels but lower than those of the fluorine fuels; however, the production of fluorine monoxide is more complex than that of elementary fluorine.

Brief contact with solid combustible materials does not result in ignition. The explosion hazard is relatively high.

Chlorine trifluoride has a molecular weight of 92.46, a melting point of -76.32°C , a boiling point of $+11.75^{\circ}\text{C}$, a critical temperature of $+153.5^{\circ}\text{C}$, and a specific gravity of 1.885 kg/liter (at 0°C).

Bromine pentafluoride has a molecular weight of 174.92, a melting point of -62.5°C , a boiling point of $+40.3^{\circ}\text{C}$, a critical temperature around 197°C , and its specific gravity is 2.547 kg/liter (at 0°C).

Liquid ozone is a low-boiling, highly poisonous violet fluid (liquefied gas); in the gaseous state it is blue and has a sharp characteristic odor. It is more aggressive toward combustible materials than is fluorine oxide and causes ignition of most liquids (hydrocarbons, alcohols, amines, etc.) and solid combustibles.

It presents a very high explosion hazard, particularly in the gaseous state, and means to stabilize it have not been found. In the solid state it is black with a violet luster.

Consequently, all of these oxidizers are dangerous to operate with for one reason or another, since they are to a greater or lesser extent poisonous and highly inflammable (with the exception of tetranitromethane), while about half of them present explosion hazards.

Liquid oxygen is the safest to work with under operational conditions. All the oxidizers with the exception of fluorine decompose at elevated temperature, and this is their principal shortcoming.

It will be seen from Table 5.15 and the brief characterization of the oxidizers given above that the first five oxidizers are liquids at normal temperature, while the rest are gaseous.

Gaseous oxidizers must be liquefied for operational use. The use of such oxidizers in ZhRD is made difficult by their violent fuming and low temperatures, which cause freezing of engine valves, hardening of rubber gaskets and rubber-and-metal parts, increased danger of cavitation in the pumps, etc.

It will be seen from Table 5.17 that fuels based on oxygen and ozone have the smallest specific gravities (1.07-1.26) while fuels based on tetranitromethane and perchloric acid have the highest gravities (1.48-1.51); here, the specific gravity of the fuels using these oxidizers varies from 1.3 to 1.45.

The low-boiling oxidizers form the lightest fuels and those with the highest heating values, while the high-boiling oxidizers form the heaviest and lowest-yield fuels. However, fluorine, fluorine oxide, and nitrogen trifluoride form heavier fuels than do nitric acid, hydrogen peroxide, and nitrogen tetroxide.

These oxidizers may be arranged in the following series in order of increasing heating value with toluene: nitric acid, hydrogen peroxide, nitrogen tetroxide, perchloric acid, tetranitromethane, nitrogen trifluoride, fluorine nitrate, oxygen, fluorine peroxide, fluorine, and ozone.

The heating value of a fuel based on perchloric acid and tetranitromethane is higher than that of an oxygen-based fuel, but the heating value with nitric acid is smaller than the latter by almost 18% (see Table 5.16). Fuels based on fluorine, fluorine oxide and peroxide, and ozone have considerably higher heating values.

The fuel based on concentrated hydrogen peroxide has the

highest gas yield and the lowest combustion temperature; it is followed by the nitric-acid based fuel (see Table 5.16). Fuels based on perchloric acid, tetranitromethane, and nitrogen tetroxide do not differ essentially as regards their gas yields and combustion temperatures.

The heat yields of the fuels are also practically identical. Fuels based on oxygen, and on ozone in particular, have higher combustion temperatures. Obviously, the rather high efficiencies of these fuels are also to be accounted for by their high combustion temperatures, which are extremely favorable for operation of the engine (for cooling it). This also applies to fluorine and fluorine-containing oxidizers. An advantage of fluorine over oxygen consists in its high activity in reactions and in the volatility of the fluorides, which is coupled with a relatively high heating value.

It is obvious that for a given heating value, the advantage will lie with those oxidizers which, all other things equal, produce fuels with the highest gas yields and the lowest combustion temperatures. Here, however, the other properties of these oxidizers that exert considerable influence on their selection and utilization should not be overlooked.

The content of a given oxidizer in a fuel mixture is usually high, and this creates difficulty in mixing it with the combustible in the ZhRD chamber. In this respect, the low-boiling oxidizers are superior, since they evaporate readily and quickly fill the combustion-chamber space.

The efficiency of oxidizers depends to a considerable degree on the combustible matched to it. For preliminary evaluation of the oxidizer, the combustible, and the fuel as a whole, it is necessary to take into account their specific gravities, the specific thrust,

and the relative fuel load in the missile's tanks.

Calculations indicate that when kerosene is used as the combustible, these oxidizers array themselves in the following series in order of increasing relative efficiency: nitric acid, nitrogen tetroxide, hydrogen peroxide, perchloric acid, tetranitromethane, nitrogen trifluoride, fluorine nitrate, fluorine, ozone, fluorine oxide, and fluorine peroxide. When these oxidizers are used with other combustibles, the efficiency pattern may differ slightly from that for kerosene.

Hydrocarbon fuels based on anhydrous nitric acid and hydrogen peroxide, perchloric acid, nitrogen tetroxide, tetranitromethane, and nitrogen trifluoride deliver virtually identical specific thrusts (with kerosene, about 270-285 kg of thrust/kg of fuel/sec; the difference is less than 6%). Oxygen, fluorine, and fluorine nitrate used with hydrocarbons deliver relatively high and virtually identical specific thrusts (with kerosene, 300-305 kg of thrust/kg of fuel/sec).

Among the oxidizers that are liquid at normal temperatures, nitric acid is of the greatest importance, since it is the most readily available and cheapest product of the chemical industry.

It works satisfactorily in the engines with nitrogen oxides and without them, both with combustibles that are autoigniting on contact and in nonhypergolic mixtures.

The basic shortcomings of nitric acid are as follows:

- 1) the relatively low specific-thrust values;
- 2) its inadequate stability, which makes it difficult to store in hermetically sealed tanks on board the corresponding vehicle at temperatures from 50-60°C;
- 3) its excessively high freezing point (-41.3° for the chemically pure acid and -43 to -45° for 98% technical nitric acid),

which excludes or severely complicates its use at ambient temperatures from -50 to -60°C ;

4) its high aggressiveness toward metals, which necessitates using stainless steels and aluminum alloys with it.

It is advisable to dissolve more efficient high-boiling oxidizers – nitrogen tetroxide and pentoxide and perchloric acid – in nitric acid to improve its quality.

At normal temperature, nitric acid becomes saturated with the tetroxide at 52-54% by weight. The specific-gravity maximum of the solution corresponds to 42% of nitrogen tetroxide in the nitric acid, but this solution has a freezing point of about -20°C and a low boiling point (29°C). When the nitrogen tetroxide content in the solution is reduced, the freezing point is depressed, but the boiling point remains virtually unchanged (Table 5.18).

To produce a solution with a freezing point above -40°C , the nitrogen tetroxide content in the nitric acid should not exceed 35% by weight. Here, the viscosity of the solution at $+20^{\circ}\text{C}$ is 1.6 times that of nitric acid; the corresponding factors for -20°C and -40°C are 4 and 12, respectively.

The use of this solution with kerosene increases P_{ud} by 2.6% and the specific gravity by 3.8%, which corresponds to a 3-5% increase in the fuel's efficiency as compared to nitric acid.

The basic characteristics of an oxidizer composed of 80% HNO_3 (98% concentration) plus 20% N_2O_4 are as follows:

1) physical properties at 20°C : specific gravity 1.600 kg/liter, kinematic viscosity 5.8 cst, heat capacity $0.48 \text{ kcal/kg } ^{\circ}\text{C}$;

2) boiling point $+48.6^{\circ}\text{C}$, freezing point -60°C , decomposition at about 152°C ;

3) heat of evaporation at temperatures from -60°C to $+150^{\circ}\text{C}$,

177.2-152.5 kcal/kg, respectively.

TABLE 5.18

Characteristics of Nitric Acid Solutions of
Nitrogen Tetroxide at Standard Pressure

1 Весовое содержание, %		4 Температура, °C		Удельный вес при 20°C 7 кг/л
2 азотной кислоты	3 диоксида азота	5 замерзания	6 кипения	
0	100	-10,2	22	1,448
30	80	-15	23	1,616
60	40	-21,4	27	1,618
70	30	-58,5	30	1,607
80	18	-73	37	1,580
90	10	-80	50	1,547
100	0	-42	87	1,503

1) Content by weight, %; 2) nitric acid; 3) nitrogen tetroxide;
4) temperature, °C; 5) freezing; 6) boiling; 7) specific gravity
at 20°C, kg/liter.

More efficient fuels are based on nitrogen tetroxide and tetranitromethane. The most important shortcomings of these oxidizers include the low boiling point of nitrogen tetroxide (+22.15°C) and the high solidification temperature of tetranitromethane (+13.8°C). In practice, therefore, they can be used with cooling or heating, respectively, before the missile's tanks are fueled with them, either in the form of solutions in one another or in solution in certain other oxidizers. The use of tetranitromethane in its pure form is also restricted by the explosion hazard which it presents (the detonation-propagation velocity attains 5800 m/sec).

Tetranitromethane may be used as an additive to combustibles with the object of increasing the completeness of combustion and raising the specific gravity, which may result in an increase in the P_{ud} and efficiency of fuels based on liquid oxygen or oxygen compounds. The content of this substance in the combustibles may attain large values and is limited only by the explosiveness of the solution in the working temperature interval (explosive properties are not ob-

served below 5% of tetranitromethane in kerosene and below 60% in benzene and ethyl alcohol).

The basic advantage of hydrogen peroxide is its low combustion temperature, and that of perchloric acid is its high specific gravity and high relative activity in reactions (ignition delay one-tenth that observed with nitric acid). However, concentrated hydrogen peroxide has a high freezing point (-9.4°C at a 90% concentration by weight), while perchloric acid explodes easily at concentrations above 72%.

The injection of nitrogen pentoxide (N_2O_5) into nitric acid in quantities up to 30% depresses its solidification point and raises the specific gravity of the solution; then, however, the boiling point drops considerably. Moreover, a solution of the pentoxide in nitric acid with a 20-30% concentration by weight is not stable enough in prolonged storage if the ambient temperature is above zero.

Solutions of perchloric acid in nitric acid also have increased specific gravities; the activities of these composite oxidizers and the heating values of fuels based on them are also higher, but adequate study has not yet been devoted to these solutions. It is obvious that solutions containing no less than 18% of perchloric acid by weight, which have a crystallization temperature of -40°C at this concentration, may be of practical interest.

The relative accessibility and low cost of liquid oxygen have encouraged its use. In its liquid form, it composes no less than 99% by volume of the total mass. Liquid oxygen does not tolerate mechanical impurities, acetylene, water, oils, etc.: the carbon-dioxide content in one liter of liquid oxygen may not exceed 8 cm^3 .

The most efficient among the oxidizers not containing fluo-

rine is ozone, in its pure form and as an additive to liquid oxygen, but its use in pure form is still made difficult by its instability and the explosion hazard that it presents. It will be evident that adding less than 20% by weight of ozone to liquid oxygen does not give any significant increase in the efficiency of the solution.

The basic advantage of fluorine over oxygen is its high activity in oxidation reactions and the high volatility of the fluorides. However, the aggressiveness of fluorine is still an obstacle to its use as an oxidizer for ZhRD combustibles.

The utilization of fluorine oxide and peroxide, whose boiling points are high and whose specific thrusts exceed those developed by fuels based on liquid oxygen, is of great interest. These oxidizers have almost identical efficiencies for a given combustible. It will be seen that fluorine and oxygen fluorides are the most efficient among the oxidizers under discussion here. Fluorine is more stable than ozone.

The following conclusions may be drawn on the basis of the above exposition.

1. The following oxidizers are best adapted for ZhRD at the present time by virtue of a number of their qualities: nitric acid, liquid oxygen, fluorine oxide, and fluorine.

2. Hydrogen peroxide may be used in the form of a highly concentrated aqueous or nonaqueous solution if it is stabilized, readily available, and inexpensive.

3. Tetranitromethane, which has many good operational properties (high specific gravity, higher-than-average heating value, high boiling point, and negligible aggressiveness toward metals), cannot be used in its pure form because of the great drawback inherent in its high melting point (+13.8°C).

4. The use of anhydrous perchloric acid, which would theoretically deliver somewhat higher P_{ud} than nitric acid, in its pure form is impossible in practice since it decomposes rapidly with formation of lower oxides of chlorine, accumulation of which results in explosion. Moreover, being highly hygroscopic, it absorbs water vigorously and forms the solid monohydrate ($HClO_4 \cdot H_2O$) with a melting point of $+50^\circ C$, which may foul lines, jets, and various other units of the engine.

5. Nitrogen tetroxide may be used as a self-sufficient oxidizer and in nitric-acid solutions.

6. Fluorine peroxide has no important advantage over fluorine monoxide, but this does not exclude its utilization provided that adequate stabilization is ensured.

7. Some oxidizers will be used more frequently in practice as their production is developed and costs are reduced; this applies primarily to perchloric acid and liquid ozone when the problems of stabilizing them are successfully solved.

SECTION 12. BASIC CHARACTERISTICS OF ZhRD FUELS

Each combustible may be matched with an oxidizer which ensures the highest possible efficiency from the fuel that they form.

Calculation and experiment indicate* that combustibles which are highly efficient with one oxidizer are of low efficiency with other oxidizers - e.g., ammonia is inferior to kerosene as regards fuel efficiency when used with oxygen, ozone, or fluorine oxide, but it provides one of the most efficient fuels when used with fluorine. Liquid oxygen is perfectly suitable for combustion of alcohols and their solutions, while liquid oxygen and nitric acid or its solutions

*Express-informatsiya AN SSSR, No. 32, RT-94, 1957.

with nitrogen tetroxide, tetranitromethane, and perchloric acid are useful for kerosenes and other hydrocarbons.

Calculations indicate that the most efficient fuels from the standpoint of flight range are formed by the low-boiling oxidizers and the least efficient fuels by the high-boiling oxidizers.

Fuels consisting of nitric acid and hydrocarbons or amines, liquid oxygen and aqueous solutions of alcohols are being used successfully for ZhRD in a number of countries.

The use of hydrocarbon combustibles other than kerosene that come closer to meeting the specifications set forth is also expedient for ZhRD.

The use of other high-heat-yield combustibles is justified only in cases where it is necessary to obtain a very high specific thrust, limit the missile's fuel load, and secure a high flight altitude or range.

Fluorine oxide with dimethylhydrazine and fluorine with hydrazine are most efficient and promising fuels. When hydrazine and pentaborane become readily accessible, it may be of interest to combine them with nitric acid containing nitrogen oxides as an additive. The most efficient among the possible combinations of the fuel's components is that of hydrazine with fluorine oxide.

The use of fluorine oxide and fluorine results in a considerable increase in flight range over that attainable with an oxygen-kerosene fuel. However, the efficiency advantage of these oxidizers can be achieved only at a high price, since their operational use is not only relatively difficult, but also dangerous as a result of the high aggressiveness and toxicity. Moreover, the use of fluorine oxidizers requires successful solution of an extremely difficult problem — that of cooling the chamber of an engine operating at temperatures

around 4000-4500°K.

The net heating value of these fuels is $H_u \approx 1500$ to 3600 kcal/kg, specific gravity $\gamma_t \approx 1.0$ to 1.5 kg/liter, and the theoretical specific thrust with $p_k/p_v^* = 100$ attains $P_{ud.t} \approx 260$ to 380 kg of thrust/kg of fuel/sec.

Table 5.19 lists approximate theoretical (calculated) values of the combustion temperature $T_{k.t}$ and the specific thrust $P_{ud.t}$ for certain ZhRD fuels having excess oxidizer ratios $\alpha = 0.8$, various values of p_k , and $p_v = 1$ atmosphere absolute, while Table 5.20 shows approximate values of the basic characteristics of a number of fuels with $p_k/p_v = 40/1$ and the optimum α .

If P_{ud} , T_k , and the other characteristics have been determined for specified values of p_k , p_v , and α for a fuel whose oxidizer is nitric acid of a specified concentration by weight in one case and the same nitric acid with nitrogen tetroxide added to it in a quantity $x = 35$ or 40% in another case, the above characteristics for a fuel consisting of the same combustible and an oxidizer in the form of a mixture of nitric acid and nitrogen tetroxide in any other specified quantity may be determined with an accuracy sufficient for practical purposes by the linear interpolation formula

$$N_x = N_0 + \frac{N_{35\%} - N_0}{35\%} \cdot x,$$

where x is the quantity of nitrogen tetroxide added to the nitric acid at the corresponding concentration by weight in percent, N_x is the unknown characteristic of the fuel with the oxidizer in question, and N_0 and $N_{35\%}$ are the same for a fuel whose oxidizer is the nitric acid in question and a mixture of it with $x = 35\%$ by weight of nitrogen tetroxide, respectively.

Linear interpolation may also be employed to determine the
*[Subscripts: $k = k = \text{kamera} = \text{chamber}$; $s = v = \text{vykhod} = \text{exit}$.]

TABLE 5.19

Approximate Calculated Values of Theoretical Combustion Temperature $T_{k.t}$ and Theoretical Specific Thrust $P_{уд.t}$ for Certain Foreign **TRD** Fuels for Different Combustion-Chamber Gas Pressures, an Excess Oxidizer Ratio $\alpha = 0.8$, and a Chamber Nozzle Exit Pressure $p_y = 1$ Atmosphere Absolute

1 Топливо		2 Давление в камере сгорания p_k в атм								
		20	30	40	50	60	70	80	90	100
3	Керосин +HNO ₃ 96%-ная:									
	$T_{к.т}$ $P_{уд.т}$	2910 225	2930 235	2960 242	2960 242	2970 250	2978 254	2985 257	2990 260	2995 262
4	Керосин+HNO ₃ 98%-ная:									
	$T_{к.т}$ $P_{уд.т}$	2965 226	2965 237	3010 244	3025 247	3035 253	3040 256	3050 260	3055 262	3060 264
5	Керосин+80% HNO ₃ 98%-ная и 20% N ₂ O ₄ :									
	$T_{к.т}$ $P_{уд.т}$	3025 228	3055 238	3080 244	3190 250	3100 254	3115 257	3125 260	3130 264	3135 267
6	Керосин+60% HNO ₃ 98%-ная +40% N ₂ O ₄ :									
	$T_{к.т}$ $P_{уд.т}$	3090 230	3120 245	3150 249	3165 255	3180 260	3195 262	3200 265	3210 268	3220 270
7	Топка-250+HNO ₃ 98%-ная:									
	$T_{к.т}$ $P_{уд.т}$	2995 225	3022 236	3045 245	3060 252	3075 256	3083 260	3090 262	3125 264	3160 265
8	Топка-250+80% HNO ₃ 98%-ная и 20% N ₂ O ₄ :									
	$T_{к.т}$ $P_{уд.т}$	3050 205	2983 226	3110 248	3128 253	3145 258	3155 264	3160 265	3166 267	3170 268
9	Топка-250+60% HNO ₃ 98%-ная +40% N ₂ O ₄ :									
	$T_{к.т}$ $P_{уд.т}$	3118 232	3148 243	3175 252	3193 258	3210 262	3222 265	3230 268	3242 272	3250 274
10	Керосин+O ₂ жидкий:									
	$T_{к.т}$ $P_{уд.т}$	3510 256	3560 273	3610 282	3640 288	3655 294	3695 298	3720 302	3742 305	3765 308
11	C ₂ H ₅ OH 93,5%-ный+O ₂ жид- кий:									
	$T_{к.т}$ $P_{уд.т}$	3225 250	3262 265	3300 270	3322 284	3346 284	3358 290	3374 290	3382 293	3395 295
12	Керосин+тетранитрометан 96%-ный:									
	$T_{к.т}$ $P_{уд.т}$	3300 236	3140 250	3380 258	3405 264	3430 268	3445 273	3460 276	3475 278	3490 281
13	Керосин+N ₂ O ₄ 96%-ная:									
	$T_{к.т}$ $P_{уд.т}$	3210 240	3245 250	3280 255	3300 260	3320 265	3335 270	3350 272	3360 276	3370 278

[Key to Table 5.19]

- 1) Fuel; 2) combustion-chamber pressure p_k in atmospheres absolute;
 3) kerosene + 96% HNO_3 ; 4) kerosene + 98% HNO_3 ; 5) kerosene + 80%
 of 98% HNO_3 and 20% N_2O_4 ; 6) kerosene + 60% of 98% HNO_3 and 40% N_2O_4 ;
 7) Tonka-250 + 98% HNO_3 ; 8) Tonka-250 + 80% of 98% HNO_3 and 20% N_2O_4 ;
 9) Tonka-250 + 60% of 98% HNO_3 and 40% N_2O_4 ; 10) kerosene + liquid
 O_2 ; 11) 93.5% $\text{C}_2\text{H}_5\text{OH}$ + liquid O_2 ; 12) kerosene + 96% tetranitro-
 methane; 13) kerosene + 96% N_2O_4 .

$T_{k.t} = T_{k.t} = T_{\text{kamera, teoreticheskij}} = T_{\text{chamber, theoretical}}$;

$P_{\text{уд.т}} = P_{\text{уд.т}} = P_{\text{udel'nyy, teoreticheskij}} = P_{\text{specific, theoretical}}$.

TABLE 5.20

Approximate Theoretical Values of Characteristics of Certain Foreign
 Zhrd Fuels for $p_k = 40$ Atmospheres Absolute and $p_y = 1$ Atmosphere Ab-
 solute and Optimum Excess Oxidizer Ratios α

1 Топливо		4 Характеристики топлива			7 Характеристики продуктов сгорания и равновесного истечения из сопла							15 Удельные площади сопла камеры			
2 горючее	3 окислитель	α	χ кг/кг	I_t ккал/кг	$T_{k.t}$ °K	$\mu_{k.t}$ 9	$T_{v.t}$ °K	$\mu_{v.t}$ 11	k	12 13		$f_{\text{уд.в.т}}$ см ²	$f_{\text{уд.кр.т}}$ см ²		
										$P_{\text{уд.т}}$	β_t				
											14 кгсек/кг				
														16	17
														см ²	см ²
18 Керосин	Азотная кислота 98%-ная	0,9	4,88	-677	3010	25,8	1930	26,7	1,15	245	158	24,5	3,8		
19 То же	60% HNO ₃ 98%-ной + 40% N ₂ O ₄	0,9	4,70	-487	3150	26,0	2110	27,4	1,14	250	161	25,7	3,9		
20 .	Жидкий кислород	0,7	2,36	-198	3610	22,8	2300	21,2	1,15	280	182	28,9	4,4		
21 .	Моноокись фтора	0,7	4,00	-68,5	4530	21,1	2620	22,7	1,20	320	210	29,9	5,0		
22 Тонка-250	Азотная кислота 98%-ная	0,9	4,28	-613	3045	25,6	1960	26,6	1,15	245	160	24,8	3,8		
23 То же	60% HNO ₃ 98%-ной + 40% N ₂ O ₄	0,9	3,90	-426	3175	26,9	2140	27,3	1,14	255	162	26,0	3,9		
24 Этиловый спирт 93,5%-ный	Жидкий кислород	0,9	1,75	-642	3300	24,0	2420	25,7	1,12	270	173	28,7	4,2		
25 Метиловый спирт	То же	0,8	1,12	-952	3110	22,6	1905	23,3	1,16	235	170	25,7	4,1		
26 Изотропный спирт	.	0,8	1,79	-576	3370	23,4	2275	25,0	1,14	275	175	28,0	4,2		
27 Гидразин	.	0,9	1,70	152	3350	19,2	2120	20,3	1,16	298	192	29,5	4,6		
28 .	Жидкий фтор	0,9	2,13	66	4490	19,0	2845	20,7	1,17	345	222	33,5	5,4		
29 .	Трехфтористый азот	0,9	2,65	-224	4105	21,0	2310	22,0	1,21	305	200	28,5	4,8		
30 .	Трифторид хлора	0,9	2,60	-146	3860	22,5	2135	24,0	1,21	285	186	26,0	4,5		
31 Димазин (ДМГ)	Жидкий кислород	0,8	1,70	19	3545	21,4	2465	23,0	1,13	235	188	30,5	4,5		
32 Диэтиламин	Моноокись фтора	0,7	3,49	-73	4410	20,0	2830	22,0	1,17	330	214	32,6	5,2		
33 Аммиак NH ₃	Жидкий фтор	0,9	3,35	-291	4425	19,2	2840	21,0	1,17	340	220	33,4	5,3		
34 60% NH ₃ , 40% N ₂ H ₄	То же	0,8	2,89	-150	4305	18,4	2820	19,7	1,20	342	221	31,6	5,3		

- 1) Fuel; 2) combustibile; 3) oxidizer; 4) characteristics of fuel;
 5) χ , kg/kg; 6) I_t , kcal/kg; 7) characteristics of combustion pro-
 ducts and equilibrium outflow from nozzle; 8) $T_{k.t}$, °K; 9) $\mu_{k.t}$;
 10) $T_{v.t}$, °K; 11) $\mu_{v.t}$; 12) $P_{\text{уд.т}}$; 13) β_t ; 14) kg-sec/kg; 15) specific
 areas of chamber nozzle; 16) $f_{\text{уд.в.т}}$, cm²; 17) $f_{\text{уд.кр.т}}$, cm²; 18) kero-
 [Key Cont'd. next page]

*[Subscripts: уд.в.т = ud.v.t = udel'nyy, vykhod, teoreticheskij =
 specific, exit, theoretical; уд.кр.т = ud.kr.t = udel'nyy, kri-
 ticheskij, teoreticheskij = specific, critical, theoretical.]

[Key to Table 5.20, Cont'd.]

sene and 98% nitric acid; 19) kerosene and 60% of 98% HNO_3 + 40% N_2O_4 ; 20) kerosene and liquid oxygen; 21) kerosene and fluorine monoxide; 22) Tonka-250 and 98% nitric acid; 23) Tonka-250 and 60% of 98% HNO_3 + 40% of N_2O_4 ; 24) 93.5% ethyl alcohol and liquid oxygen; 25) methyl alcohol and liquid oxygen; 26) isotropic* alcohol and liquid oxygen; 27) hydrazine and liquid oxygen; 28) hydrazine and liquid fluorine; 29) hydrazine, nitrogen trifluoride; 30) hydrazine and chlorine trifluoride; 31) dimazine (DMG) and liquid oxygen; 32) diethylamine and fluorine monoxide; 33) ammonia, NH_3 and liquid fluorine; 34) 50% NH_3 + 50% N_2H_4 and liquid fluorine.

characteristics of a fuel whose combustible is ethyl alcohol at various concentrations by weight or a mixture of two different combustibles.

Free radicals (H, N, CH, NH, OH, and others)** may be regarded as promising fuels for ZhRD in the next ten years; these are electrically neutral fragments obtained from ordinary chemical gas molecules as a result of their dissociation at high temperatures.

Free radicals are electrically neutral particles with characteristic unpaired electrons in their outer shells, a result of which is that they possess an exceedingly strong tendency to recombine with liberation of large quantities of energy, basically in the form of heat and partially in the form of light. It is customary to refer to them as metastable substances, i.e., substances that are in a stage of pseudoequilibrium, so that the energy content associated with them considerably exceeds the energy content characteristic for the equilibrium state of the gas molecule in question.

A particularly large quantity of heat may be liberated on recombination of atomic hydrogen (Table 5.21).

*[Translator's note: Russian izotropnyy, isotropic, is presumably an error for izopropilovyy, isopropyl.]

**Ekspress-informatsiya AN SSSR, No. 8, RT-22, 1958.

TABLE 5.21

1 Радикал	Энергия рекомбинации 2 ккал/кг	Эквивалентная скорость истечения 3 м/сек
H	52 300	21 000
CH	10 600	9 300
N	8 200	8 200
NH	5 300	6 600

1) Radical; 2) energy of recombination, kcal/kg; 3) equivalent exhaust velocity, m/sec.

However, the total energies indicated for the radicals in Table 5.21 cannot be realized because of the fact that the recombination reactions (e.g., for atomic hydrogen $H + H \rightleftharpoons H_2$) are actually reversible and can proceed to completion only at very high pressures.

At a pressure of 50 atmospheres in the chamber, only 50% of the hydrogen atoms will recombine as the temperature rises up to nearly 5500°C, but the equilibrium exhaust velocity may be of the order of 15,000 m/sec with a nozzle expansion ratio of 100:1.

It is possible to decompose molecular hydrogen or nitrogen into its atoms in a high-temperature electric field with subsequent freezing to a temperature close to absolute zero (5-30°K) before recombination begins, since monatomic gases can exist for less than a thousandth of a second in the unfrozen state. The free radicals obtained in this way can be stored for as long as several hours. In general, however, development of reliable methods for stabilizing free radicals requires much additional research.

Concentrations of at least 10% are required for practical utilization of free radicals in ZhRD.

The feasibility of producing and storing free radicals on a large scale is still problematical as a result of their extremely high cost and the danger of working with them.

It will probably be impossible to use free radicals as fuels until ways have been found to stabilize them without recourse to the extremely low temperatures and very low pressures at which they can be produced. Another difficulty in the utilization of free radicals in ZhRD consists in selecting materials for the chamber that will be capable of withstanding the infernal temperatures of their recombination.

SECTION 13. METHODS OF IMPROVING THE QUALITY OF ZhRD FUELS

The operational qualities of fuel components can be improved in the following ways:

- 1) lowering the melting points of easily solidified fuel components by adding other substances to them;
- 2) chemical purification to remove undesirable impurities from the fuel;
- 3) stabilizing unstable fuel components to prevent their decomposition or autoignition on contact with atmospheric air;
- 4) activating fuel components by introducing special ignition and combustion catalysts into them;
- 5) "inhibiting" the fuel components with the object of reducing their corrosive aggressiveness toward the metals of the engine;
- 6) introducing suspensions of metals and solutions of high-efficiency additives with the object of raising specific gravity and specific thrust;
- 7) supercooling the fuel components before running them into the fuel tanks, with the object of raising their specific gravities and, consequently, "packing" the fuel components more tightly into the tanks, etc.

The overwhelming majority of autoigniting fuel components are characterized by considerable ignition delays; this applies to both

the oxidizer and the combustible.

Examples of oxidizer activation are:

- 1) nitric-acid solutions of nitrogen tetroxide (up to 30-35% by weight) and nitrogen pentoxide;
- 2) nitric-acid solutions (up to 25%) of perchloric acid (70% concentration by weight);
- 3) solution of up to 4% of ferric chloride (FeCl_3) in nitric acid, so that the melting point of the oxidizer is also depressed (from 42°C [sic] for nitric acid to 50°C [sic] for the resulting oxidizer solution);
- 4) solution of hydrogen fluoride (HF) in the nitric acid to reduce corrosion of the aluminum alloys and stainless steels;
- 5) solution of up to 10-50% of sulfuric acid (H_2SO_4) in nitric acid; this reduces the ignition delay of the combustible and simultaneously reduces the aggressiveness of the oxidizer toward the metals of the engine;
- 6) solution of about 0.5% by weight of potassium permanganate (KMnO_4) in the nitric acid; nitric acid must be thus enriched before it is fed into the combustion chamber, since its activity declines after 2-3 min (for this reason, it is necessary to install a special activator device in the system).

Elements with low heating values such as iron, copper, cadmium, sodium, etc., may also be included among the combustion-process catalysts that are added to fuel components.

The specific gravities of high-boiling and low-boiling oxidizers and combustibles may be raised considerably by cooling to temperatures at which they are still in the liquid state and have acceptable viscosities. In the case of the low-boiling components, it is also possible to achieve a drastic reduction in the loss of expensive

fuel components by evaporation, as well as to improve safety conditions in work with them.

SECTION 14. SELECTION OF FUEL COMPONENTS FOR ENGINE IN DESIGN STAGE

Rational selection of fuel components for a ZhRD that is being designed is an extremely important stage in this design process. As noted earlier, the type of fuel determines the type of engine, its design, economy, and operational reliability. In all cases, the fuel must be selected with an eye to the specific conditions under which the engine will be used.

The following factors must be taken into account at the outset in selecting fuel components for an engine in the planning stage.

Function of the Weapons System

The conditions under which the engine and the rocket operate require that the fuel possess physical and chemical stability (which will permit storage of the fuel components for prolonged periods without special precautionary measures), a high boiling point, and a low solidification temperature. The fuel should not be toxic and should not be aggressive with respect to the materials of the engine. Furthermore, the cost of the fuel should be low.

For antiaircraft missiles, the fuel must first be run into the tanks and stored there for prolonged periods. Such properties as rapid evaporation, corrosive action on the metal of the tanks, tendency to decompose, etc., prevent the utilization of many fuel components for these purposes. The use of liquefied gases as oxidizers in the engines causes freezing of valves and hardening of rubber gasket sleeves and rubber-and-metal parts.

Liquefied oxidizers can be used successfully in the engines of long-range missiles, which are usually launched from rear areas

where there is an opportunity to fill the fuel tanks with rapidly evaporating fuel components before launching.

At the present time, liquid oxygen is used for long-range missiles, chiefly because of its relative availability and low cost.

Oxygen can be produced on the spot by mobile generators, so that it is cheaper than other oxidizers. It can be stored for long periods in thoroughly insulated tanks without creating a danger of autodetonation or boiling out to any significant degree. It is nontoxic and does not autoignite in the presence of organic materials.

However, the low temperature of liquid oxygen imposes certain limitations on the selection of materials for the engine because of cold-shortness phenomena — as is the case with other low-boiling oxidizers (fluorine, fluorine oxides, nitrogen trifluoride, ozone). At the temperature of liquid oxygen, the impact strengths of carbon and medium-alloy steels, magnesium, zinc, and their alloys drop to an intolerably low level.

Practical Possibility of Economical Use of the Fuel in the Engine

At the present time, certain fuels which deliver high heating effects are not used in practice because of the very high temperatures that they develop in the engine's combustion chamber, which make it impossible to cool the engine conveniently and reliably. Kerosene with liquid oxygen and other combinations of combustibles and oxidizers are among the fuels that have not yet come into extensive use for this reason.

Among other things, the use of fluorine oxidizers requires successful solution of the extremely difficult problem of

engine-chamber cooling when the temperature of the products of combustion is of the order of 4000-4500°K.

Fuel-component pairs that meet operational-economy requirements in the engine may, in certain cases, be found unsuitable due to their nonconformity to some other specification set forth for ZhRD fuels.

The thermodynamic characteristics of different fuels must be compared for identical and fully defined combustion conditions in the engine.

Dynamics of the Combustion Process of the Fuel in the Engine

One of the basic parameters characterizing a given pair of fuel components is the engine's operating economy using these components, which is usually characterized by the internal efficiency or specific thrust.

A number of considerations of a practical nature frequently make it necessary to employ not those fuel-component pairs which would be best from a purely thermodynamic standpoint, but only those combinations which are most suitable in practice.

The fuel must make it possible to secure a sufficiently stable combustion process in the chamber, without pressure pulsations in the combustion products, which sometimes set up intolerable vibrations in the engine.

Certain conditions which, as a rule, involve complicating the design of the engine and increasing its weight, particularly in its fuel-supply system, are necessary to ensure sufficiently stable performance of the engine and to prevent sharply expressed pulsation in combustion of the fuel in the chamber. In a number of cases, this circumstance makes it necessary to employ fuel components that ensure

a stable combustion process in the engine when its operation is either throttled or augmented.

Specifications Set Forth for ZhrD Fuel

Fuel components can be selected properly and used efficiently only provided that their characteristic properties and operational and other singularities have been taken into account.

Selection of the oxidizer for the combustible presents the greatest difficulty, since many known oxidizers have low activities in chemical reactions and are unstable, aggressive toward the materials of the engine, poisonous, and expensive.

Highly important factors determining the operational viability of fuel components are their solidification, boiling, and combustion temperatures, heat capacities, thermal conductivities, and specific gravities. Also of great importance is the possibility of using one or both of the fuel components to cool the engine chamber and nozzle.

A fuel that delivers a relatively low specific thrust but possesses a high specific gravity may, in certain cases, be found superior as regards its over-all characteristics (flight effectiveness of the missile) to a fuel that delivers a high specific thrust; having been found optimal for missiles with one tactical mission, it may be completely unsuitable for a missile with a different mission.

In evaluating a missile fuel, therefore, the basic criterion is not exhaust velocity, but primarily the specific gravity or the volume specific thrust, which is the product of the specific thrust by the specific gravity of the fuel.

The specific gravity γ_t of the fuel exerts its primary influence on the weight of the fuel tanks and the dimensions and weight

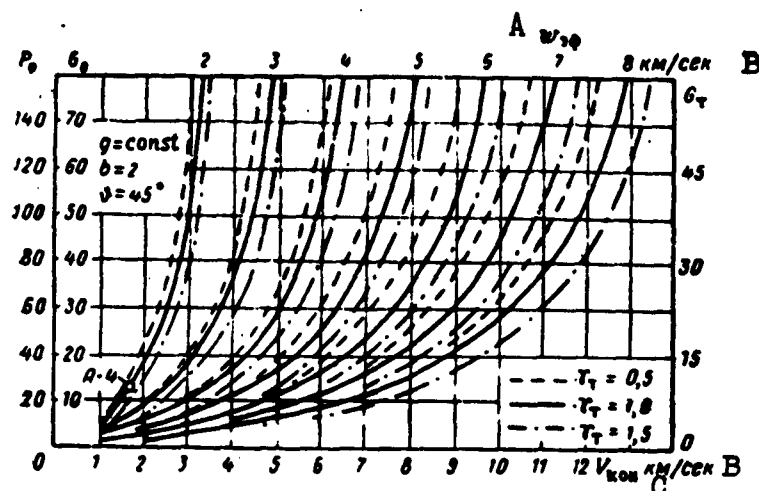


Fig. 5.13. Approximate theoretical values in tons — from specifications of the A-4 missile— of engine thrust P_0 , missile launching weight G_0 , and tank fuel load G_t to obtain the required flight velocity V_{kon} at the end of the powered trajectory with a one-ton payload, a launching angle $\theta = 45^\circ$ with respect to the vertical at a certain altitude, and different fuel specific gravities γ_t and nozzle exhaust velocities w_{ef} . * A) w_{ef} ; B) km/sec; C) V_{kon} .

of the engine's fuel-supply system and, consequently, on the velocity V_{kon} of the missile at the end of its powered trajectory. In each individual case, therefore, we must seek a compromise solution with regard to the exhaust velocity w_{ef} of the gases leaving the chamber nozzle (specific thrust) and the specific gravity γ_t of the fuel; as we know, this interrelationship varies in accordance with the range of V_{kon} under consideration.

For small V_{kon} (~ 1 km/sec), it is better to increase γ_t than w_{ef} . This is what accounts for the preference given to nitric acid as an oxidizer for short-range and antiaircraft missiles. With high V_{kon} (~ 3 km/sec), an increase in the exhaust velocity from 2 to 3 km/sec is many times more effective than a similar increase in

the fuel specific gravity (Fig. 5.13). For this reason, the starting

*[Subscripts: $\tau = t = \text{toplivo} = \text{fuel}$; $\text{kon} = \text{kon} = \text{konechnyy} = \text{end, terminal, final}$; $\text{ef} = \text{effektivnyy} = \text{effective}$.]

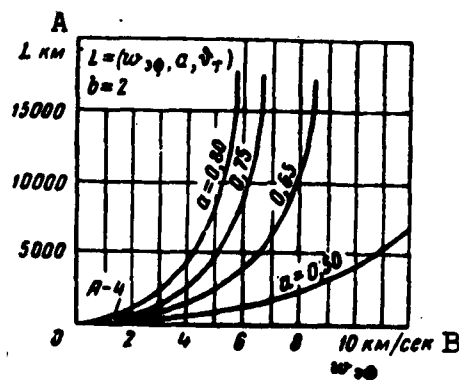


Fig. 5.14. Approximate calculated values (from specifications of A-4 missile) of flight range L for optimum climbing angle (with respect to the vertical) θ_t at the end of the powered trajectory and different values of the relative fuel reserve a in the tanks and the gas-exhaust velocity w_{ef} from the chamber nozzle. A) km; B) km/sec.

figure in the design of high-thrust missiles should be an exhaust velocity higher than 3 km/sec.

Exhaust velocities are still falling far short of the practically possible limit (4.5 km/sec). It is possible at the present time to attain exhaust velocities around 3 km/sec. In the future, the exhaust-velocity range from 3 to 4 km/sec will be of interest from the standpoint of obtaining the necessary V_{kon} ; this will make it possible to design smaller mis-

siles with relatively higher payloads.*

The influence of exhaust velocity and the relative fuel reserve a in the missile's tanks on the range L is shown in Fig. 5.14.

Calculations indicate that as the relative fuel reserve on board the missile is increased, the influence of specific gravity on the range becomes weaker and the influence of the engine's specific thrust becomes more pronounced.

As we know, the use of multi-stage missiles is a more efficient way to increase flight velocity and range than the use of more expensive fuel components in single-stage missiles.

In multi-stage missiles, it is expedient to use a fuel with a high specific gravity in the first stage, even though it may have a smaller specific thrust, and a fuel that possesses a high specific thrust coupled with a relatively low specific weight in the remaining

*Voprosy raketnoy tekhniki (Problems of Rocket Engineering), No. 5, 1959, IL.

stages of this missile, since the specific gravity will now be a secondary factor.

The use of a dense fuel to operate the engine at the beginning of a missile flight makes it possible to minimize the dimensions of the missile. However, practical considerations may sometimes compel us to select a cheap fuel with a low specific gravity for the engine, since the over-all cost of the launching (missile plus fuel) may then be lower, despite the fact that the dimensions and cost of the missile itself will be relatively higher.

The use of expensive fuels that deliver high thrusts for the first stage of a missile may not always be justified: even though in this case the dimensions of the fuel tanks and the weight of the missile may, all other conditions remaining the same, be reduced, the total cost of the launching will be higher as a result of the high fuel cost. The use of such fuels is still efficient for the second and third stages of the missile, where the high cost of the fuel is completely offset by the reduction of the dimensions, weight, and cost of the latter stages of the missile.

When the appropriate precautionary measures are taken, the toxicity of an exotic fuel component may not represent an obstacle to its use. Under operational conditions, the toxic effects of oxidizers and combustibles are manifested primarily when their vapors are inhaled with air, with irritation of the mucous membranes of the respiratory tract as the first symptom. The following concentrations of their toxic vapors in mg/liter of air, which have been adopted in industry as the permissible maxima for prolonged inhalation, may serve as an index to the toxicities of these substances:

fluorine monoxide	0.00001
ozone	0.0001
tetranitromethane	0.005-0.001

fluorine and chlorine	0.001
sulfuric acid	0.002
hydrogen peroxide and nitric acid with nitrogen oxides	0.005
oxygen	700
pentaborane and nitrobenzene	0.00001
nitrotoluene, aniline, and xylidene	0.005
ammonia	0.02
methyl alcohol	0.05
benzene and toluene	0.1
propyl alcohol	0.2
kerosene, gasoline, and turpentine	0.3
ethyl alcohol	1.0

Fluorine monoxide and ozone have the highest toxicities; they are more toxic than phosgene and prussic acid, for which the maximum permissible vapor concentrations in the air are 0.0004 and 0.0003 mg/liter, respectively. The combustibles pentaborane and nitrobenzene are also highly toxic.

Dangerous concentrations of poisonous vapor in the air are developed easily in using low-boiling oxidizers, which possess high volatilities and vapor pressures under standard conditions.

Precautionary measures to be taken in handling the corresponding toxic substances are always spelled out by the special instructions.

SECTION 15. USE OF ATOMIC ENERGY IN ROCKET ENGINES*

The probable specific-thrust limit that can be obtained from ZhRD operating on chemical fuels at the surface is no higher than 400-450 kg-sec/kg with combustion-chamber temperatures about 4000-4500°C. In this case, it will be necessary to use as fuel components expensive and difficult-to-produce combustibles and fluorine oxidizers which are complicated to work with because of their high aggressiveness and toxicity. The use of such exotic fuel components in ZhRD will require successful solution of a number of extremely difficult problems involved in the design of an engine that will operate re-

*Jet Propulsion, Vol. 28, No. 4, 1958; Missiles and Rockets, Vol. 1, No. 1, 1956.

liably. The problem of cooling the engine's combustion chamber and nozzle is particularly complex.

Conversion to nuclear energy sources with the object of increasing the specific thrust of a rocket engine involves even greater difficulties and danger for the servicing personnel. Appropriate warning systems and protective devices must be used if nuclear energy is to be employed with safety. Nevertheless, the use of atomic energy in rocket engines is highly promising.

In this case, it is necessary to deal with enormous quantities of energy coming from sources having very small mass. It may be assumed in approximation that almost $1 \cdot 10^7$ times the amount of energy liberated on combustion of one kg of the chemical fuel having the highest heating value is liberated on fission of the atoms in one kg of uranium-235. When such a highly concentrated energy source is employed in rocket engines, it will be possible in practice to attain exhaust velocities above 10,000 m/sec.

When nuclear energy is used, the reaction thrust may be obtained as a result

1) of direct outflow through the reactor nozzle of a jet of fission products from the atoms of the active material (e.g., uranium-235, plutonium-239, etc.);

2) of outflow of some gaseous mass vehicle (hydrogen, helium, ammonia, etc.) through the reactor nozzle after heating by the thermal energy liberated on fission of atoms of a radioactive material;

3) of outflow of electrically charged particles - the ions of some mass vehicle (cesium, rubium*, etc.) under the influence of an electric field after they have been produced by the use of nuclear energy.

*[Translator's note: presumably an error for rubidium.]

Applications of atomic energy taking the form of direct expulsion of the actual products of fission of the atoms (photons) to produce thrust are not feasible at the present time. If, however, it were possible to achieve practical mastery of this method of using atomic energy, it would be possible to obtain engine specific thrusts almost 1000 times higher than those attainable with ordinary chemical ZhRD, since according to Einstein's law of conservation of equivalence between energy and matter, the maximum exhaust velocity of the atomic fission products has as its possible limit the velocity of light in a vacuum ($3 \cdot 10^8$ m/sec). Such processes are already known — e.g., transformation of an electron and a positron into a photon. In nuclear processes, we observe the disappearance of the electron-positron pair and the appearance of gamma-quanta; however, this phenomenon cannot yet be realized on a large scale for use in engineering. Engines using this type of reaction will probably develop the ultimate specific thrusts. With the nuclear energy used in this way, however, the temperature in the reactor chamber would be phenomenally high, approaching the temperatures attained in explosion of nuclear bombs. For this reason, it is naturally still impossible to produce such an engine in practice.

The atomic rocket engine most easily realized in practice is that type in which the working fluid [mass vehicle] is heated by atomic energy produced in the reactor by fission of molecules of solid uranium or plutonium rods (Fig. 5.15).

In such an engine, a liquid mass vehicle may be pumped from the tanks into the engine's so-called heterogeneous solid-phase reactor, where it is heated, and then flow out into the environment through an expanding nozzle similar to the type used in an ordinary ZhRD operating on chemical fuels. This mass vehicle can also be used

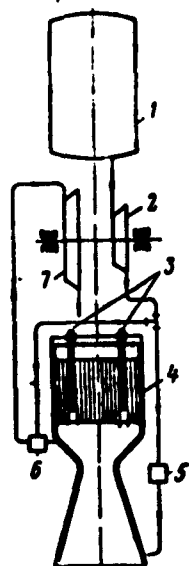


Fig. 5.15. Diagram of atomic reaction-thrust engine with liquid heat carrier. 1) Tank for heat carrier; 2) pump; 3) rods for control of working process in reactor; 4) reactor; 5) device for control of heat carrier supply to reactor; 6) throttling regulator; 7) pump-unit turbine.

prior to pumping into the reactor for purposes of cooling the reactor (chamber) itself and its nozzle. In an atomic rocket engine of this type, the specific thrust is directly proportional to the temperature to which the mass vehicle is heated in the reactor and inversely proportional to the molecular weight of this vehicle. This means that efficient operation of such a thermal atomic engine, i.e., securing the highest possible exhaust velocities (specific thrusts), requires that the molecular weight of the mass vehicle be as low as possible and that it be heated to the highest possible temperature in the reactor.

The temperature to which the working fluid is heated in the reactor and, consequently, its exhaust velocity will depend on how much of the nuclear fuel is used in heating the unit weight of the mass vehicle at a given efficiency (Table 5.22).

The figures in this table indicate that the exhaust velocity of the mass vehicle from the reactor nozzle increases in proportion to the quantity of atomic fuel used in heating a unit of this vehicle to a given temperature.

Since the cost of atomic fuels is high, it would be expedient to produce the highest possible exhaust velocity from the reactor nozzle in the thermal nuclear rocket engine.

However, the mass-vehicle temperature developed in the reactor

TABLE 5.22

Calculated (Theoretical) Nozzle Exhaust Velocities of Gas for Atomic-Engine Reactor as a Function of the Ratio of Atomic Fuel (Plutonium-239) to the Mass of the Working Fluid with the Energy Utilized at 50% Efficiency

Скорость истечения 1 м/сек	Отношение массы атомного горючего к массе рабочего 2 тела
10 000	1
1 000	1/100
100	1/10 000
10	1/1 000 000

1) Exhaust velocity, m/sec; 2) ratio of mass of atomic fuel to mass of working fluid.

presents a practical limiting factor in raising the exhaust velocity. When the working fluid is heated in heterogeneous nuclear reactors, its temperature may not exceed the melting point of the solid radioactive substance used as the source of nuclear energy nor the safely admissible temperature of the reactor's shell.

The upper-limit melting point for uranium is about 1130°C , while the safely permissible temperature for the best materials that can be used at the present time for fabrication of the reactor's inner shell does not exceed $1000\text{--}1100^{\circ}\text{C}$. In practice, however, the maximum permissible temperature for uranium under the operating conditions of a heterogeneous reactor is much lower than the melting point indicated above. Contemporary stationary industrial heterogeneous uranium reactors operate at temperatures of the order of hundreds of degrees Centigrade.

This state of affairs indicates that the efficiency obtained from the uranium nuclear energy used in heterogeneous reactors is very low. If it is assumed that it will be possible in the future to raise the admissible temperature in the heterogeneous reactor to

1500°C, it will probably be possible to produce specific thrusts of the order of 400-700 kg-sec/kg, i.e., thrusts 2 to 3 times that attainable with existing chemical ZhRD.

The only way to produce higher mass-vehicle temperatures in the reactor and, consequently, higher specific thrusts, is to feed the mass vehicle and the atomic fuel into the reactor concurrently, with the latter in a liquid, gaseous, or intermediate state.

Under these conditions, the temperature in the so-called homogeneous liquid-phase, gaseous-phase, or mixed reactor is no longer restricted by the melting point of the solid radioactive substance used in the reactor, in contrast to the solid-phase reactor considered above. The upper limit of this temperature will be delineated only by the higher safety limit of temperature for the materials used in building the engine itself; this limit permits development of specific thrusts of the order of 1500 kg-sec/kg.* For example, the melting points of the carbides of certain metals range around 4000°K.

However, there are important drawbacks inherent even in this method of utilizing nuclear energy: the small quantity of liquid nuclear fuel required as compared with the quantity of mass vehicle, the necessity of conducting the process in the gaseous phase at very high pressures and using for the purpose a reactor of tremendous size so that the reaction will be self-sustaining, the considerable heat losses into the environment, etc.

Since the temperature of the mass vehicle in a heterogeneous atomic-engine reactor is limited in practice, it is necessary to make an expedient selection of the mass vehicle for the engine in order to obtain optimum utilization of the nuclear fuel in the engine

*Jet Propulsion, Vol. 28, No. 4, 1958.

(highest possible cycle efficiency).

It may be assumed that the most effective mass vehicle for a thermal atomic rocket engine will be a substance which:

1) possesses the lowest possible molecular weight and the highest possible specific heat capacity in the gaseous state, since the heat content of the gas at a given temperature will be the higher the higher its heat capacity (it is not necessary for the heat carrier to possess a chemical energy);

2) possesses the highest possible dissociation and ionization [constants] in a given thermal regime, since these properties will contribute to reducing its molecular weight and increasing its heat capacity and, consequently, will result in less heating for a given amount of heat supplied;

3) has a sufficiently high specific gravity and, consequently, a smaller tank capacity for a given heat carrier load;

4) conforms to a number of nuclear characteristics and operational requirements;

5) has a small neutron capture section and, when fast-neutron reactors are used, a small moderating ratio as well.

Molecular hydrogen comes closest to meeting these specifications. A number of its characteristics are not inferior to those of monatomic hydrogen, the more so because the latter is almost useless in view of its great instability.

Atomic rocket engines in which the mass vehicle is heated in the reactor will obviously be much heavier and more massive structures than the ordinary chemical ZhRD, particularly when protective measures are provided in it against gamma rays, neutrons, and alpha particles, as is mandatory for manned missiles. The use of an atomic engine of this type may be found convenient only for the second and

subsequent stages of large missiles to be placed in operation at very high altitudes. Such missiles may be used for a wide variety of purposes.

The development of atomic rocket engines for missiles presents an extremely complex and difficult problem. In designing an engine of this type, it will be necessary to solve extremely complex problems involved in selection of the engine configuration, its mass vehicle, cooling of the reactor, the technique by which the reaction process is controlled, radiation shielding, etc.

Since efficient operation of an atomic engine requires extremely high working-fluid temperatures in the reactor, the utilization of nuclear energy in a thermal rocket engine requires:

1) mastery of new, highly heat-resistant materials for fabrication of the chamber in which the heat carrier is heated and methods of collimating the stream of reacting material with magnetic or electric fields, so that the shell of the engine's chamber (reactor) will be able to withstand the infernal reaction temperatures;

2) mastery of a highly efficient and dependable cooling system for the atomic engines;

3) achievement of very low atomic-fuel consumption rates coupled with very high mass-vehicle flow rates (about 1050 tons of molecular hydrogen are required for one g of uranium-235 with an efficiency of about 60%);

4) design of a reliable system for controlling the reaction process, dependable and lightweight protection for the components of the missile engine and the crew from intense gamma-radiation;

5) attainment of dependable performance in the engine as a whole.

Production of nuclear energy for practical utilization is

possible only provided that a self-developing nuclear-fission chain reaction can be set up; such reactions can be sustained only in a reactor.

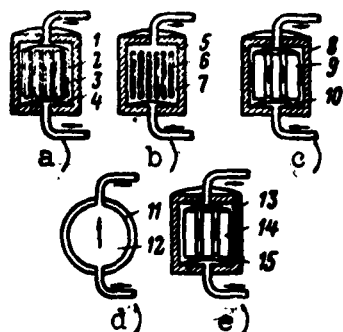


Fig. 5.16. Schematic diagrams of nuclear reactors. a) Heterogeneous reactor: solid fuel and moderator, coolant circulates; 1) reflector; 2) uranium rods in tubes; 3) solid moderator; 4) heat carrier (gas or liquid); b) heterogeneous reactor: solid fuel, moderator circulates and acts simultaneously as heat carrier; 5) reflector; 6) jacketed uranium rods; 7) liquid moderator; c) heterogeneous reactor: solid moderator; liquid nuclear fuel circulates; 8)

reflector; 9) solid moderator; 10) liquid fuel (solution or molten alloy), acting simultaneously as heat source and heat carrier; d) homogeneous reactor: liquid mixture of fuel and moderator circulates; 11) reflector; 12) liquid mixture of uranium and moderator: functioning simultaneously as heat source and heat carrier; e) homogeneous reactor: solid (or liquid) mixture of uranium and moderator; heat carrier circulates; 13) reflector; 14) solid or liquid mixture of uranium and moderator; 15) heat carrier (gas or liquid).

It is customary to classify nuclear reactors into the following types in accordance with the velocities of the neutrons causing the fission:

- 1) reactors operating on slow neutrons (if most of the fission occurs on capture of slow neutrons) and
- 2) reactors operating on fast neutrons (if fission is triggered by fast neutrons).

The minimum neutron velocity attainable as a result of moderation is equal to their velocity of thermal agitation as established at thermal equilibrium with the environment. For this reason, slow-neutron reactors are also known as thermal-neutron reactors.

Uranium-fueled nuclear reactors can be built only for slow neutrons, since it is only in this case that the probability of fission of the isotope uranium-235 is so high that it can predominate over the probabilities of all other processes. As the content of the

uranium-235 isotope in the uranium is raised, it becomes possible to realize reactors of two other types (uranium with its content of the isotope U^{235} elevated over the natural content is known as enriched uranium).

The basic elements of a slow-neutron nuclear reactor are as follows (see Fig. 5.16):

1) the active section (core), i.e., the zone in which the uranium and the neutron moderator are placed; graphite, heavy water (water in which light hydrogen has been replaced by heavy hydrogen) or beryllium oxide, or, in the case of enriched uranium, even water can be used to moderate the neutrons;

2) the reflector, i.e., a device which reflects neutrons projected from the active section; the same materials are used for the reflector as for the moderator;

3) the cooling system, the function of which is to remove the heat liberated in the active section of the reactor; it consists of tubes through which a coolant (heat carrier) is pumped; gases, heavy and ordinary water, or fused metals may be used as coolants;

4) a system for controlling the rate of the nuclear-fission chain reaction, and, consequently, the power setting; this includes sensors that measure the density of the neutron flux in the reactor, regulating rods whose composition includes substances with good neutron-absorbing ability (cadmium, boron), and various electronic and electromechanical devices the function of which is to control absorption by the rods;

5) protective shielding, which protects other parts of the missile engine and the crew from intense radiation.

If the nuclear fuel and moderator represent a homogeneous mixture (e.g., a solution of a uranium salt in water), the reactor

is said to be homogeneous, while if the nuclear fuel is placed in the moderator in the form of individual blocks or rods, the reactor is known as a heterogeneous reactor.

The uranium blocks or rods, which are frequently referred to as fuel elements, are usually arranged in a certain regular order to form a so-called lattice.

In accordance with the type of moderator used, the reactor may be designated as a graphite, heavy-water, or metal-cooled reactor, etc.

The power developed by the reactor depends on the number of uranium nuclei undergoing fission in one second, and this is, in turn, proportional to the number of neutrons in the reactor. In a homogeneous reactor, almost all of the energy liberated on fission of the nuclei is transformed into thermal energy; here, the largest quantity of heat is liberated in the reactor's active section, while this occurs in the uranium rods in the heterogeneous reactor.

Selection of the materials needed for the various elements of the reactor is determined not only by the functions to be performed by each given design element, but also by their nuclear properties, by which we mean their ability to absorb neutrons and become activated (form radioactive isotopes as a result of neutron absorption by stable isotopes). In selecting a material, it is also necessary to take into account the changes that take place in its properties at high temperature and under intensive radioactive bombardment (radiation damage).

As we know, metals tend to lose mechanical strength under irradiation. If the energy transmitted to the metal is larger than the bonding energy of the atoms in its molecules, the atoms may be displaced from their normal positions in the crystal lattice. In com-

plex chemical compounds, there is a possibility of chemical-bond rupture and changes in chemical composition.

A substance with a high slowing-down ability and the smallest possible neutron-capture section should be used for the moderator. The slowing-down ability of a substance is equal to the product of its microscopic neutron-scattering section by a quantity that is proportional to the energy lost in one fission event.

The materials used for reflectors include those used for the moderator and heavy substances that have large scattering sections and small neutron-capture sections.

The protective shield surrounding the reactor has the following functions:

- 1) moderation of fast neutrons that escape the active section through the various slits and gaps in the moderator or reflector;
- 2) absorption of slow neutrons escaping from the outer layer of the reflector;
- 3) attenuation of gamma radiation.

To moderate fast neutrons effectively, the shield must contain elements with high atomic numbers. Neutrons give up their energy as a result of inelastic collisions with the nuclei of these elements. Iron and barium are best suited for these functions. Since the process of inelastic scattering is accompanied by emission of gamma rays, these materials must be concentrated chiefly at the external surface of the protective shield.

High mechanical strength is required of the materials used to make jackets for the uranium blocks, plumbing for the heat carrier, plumbing and containers for liquid nuclear fuels, and the supporting structures. General requirements set forth for the structural materials consist in retention of mechanical strength under irradiation

and at high temperature, corrosion resistance, and low neutron absorption.

In selecting the metal for the uranium-block jackets, an additional specification is high thermal conductivity, which ensures a small temperature gradient between the block and the heat carrier. Here, the use of different metals is not admissible because of the electromotive forces that arise and result in intensified electrochemical erosion.

Stainless steels represent an excellent corrosion-resistant material. They are suitable for fabrication of tubing for liquid-metal heat-exchanger systems and pipelines and containers for reactors operating on aqueous and metallic uranium solutions. The fundamental constituents of stainless steel — iron and the alloying elements — are activated under neutron bombardment and produce long-lived isotopes that emit high-energy gamma rays. It must be remembered that certain components of the system are subject not only to thermal stresses, but also to thermal creep on heating.

The rate of the nuclear reaction increases exponentially with temperature, and if the control system is not sufficiently dependable the process may die out or, on the other hand, turn into a destructive explosion. The engine's cooling system should perform in close coordination with the reaction-temperature control system, since a change in the amount of heat taken from the reactor will influence the reaction rate, and if the rate of heat generation exceeds the rate at which the heat is withdrawn, an explosion may result.

While a cooling-system breakdown in a reaction engine using the chemical energy of the fuel normally results in burnthrough of the chamber without causing any appreciable increase in the temperature of the reaction products in the chamber during the process, a

cooling-system breakdown of an atomic-engine reactor will lead to a temperature rise in the reactor that is accompanied by an explosion. While ordinary ZhRD are potentially dangerous to work with because of a certain probability that they will explode on starting or in operation, the atomic engines, which are distinguished by an even greater concentration of energy per unit volume and complications in controlling the process, which unfolds at relatively high temperatures, present an incomparably greater explosion hazard.

Nuclear reactors presently in operation and those undergoing design have control, monitoring, alarm, and emergency-stop systems which operate in accordance with the intensity of the neutron flux in the reactor. Ionization chambers which sense the intensity of the neutron flux are employed for this purpose. The operating regime of the engine can be controlled by adjusting the inflow of the working substance into the reactor.

It appears that the problem of controlling the operation of the engines by metering will best be solved by feeding the fissionable material into the reactor in much the same way as in the case of the homogeneous reactor. This solution can be sprayed into the reactor chamber around its perimeter in order to produce a concentration at the center of the chamber adequate to sustain the nuclear reaction. As we have already noted, another way to control the reaction is to feed solid rods of a fissionable material into the chamber (reactor) in the same way as electrodes are fed automatically into an electric furnace.

A degree of safety may be ensured in a thermonuclear engine by placing the "fuel" supply outside the reactor, so that it will not be able to participate in the reaction until it is injected into the reactor and heated to a certain temperature. It is then possible

to start the nuclear engine by local excitation of the particles rather than by an atomic explosion.

The primary nuclear fuel is the isotope uranium-235. Although a nuclear-fission chain reaction can be set up under certain conditions in natural uranium, in which the uranium-235 content is only 0.71%, it is helpful in many cases to use uranium with a elevated content of the isotope uranium-235, and, for small reactors, even practically pure uranium-235. Thus, it is necessary to concentrate the uranium-235 (enrichment) for successful development of nuclear power.

The principal sources for extraction of uranium are uranium-rich minerals - uranite (pitchblende) and carnalite (a complex compound of uranium and vanadium). There are also a large number of minerals with low uranium contents. Nor have we excluded the possibility of using plutonium and the man-made isotope uranium U^{233} .

Uranium can be used either in the form of the pure metal or in a solution of metallic uranium in some other low-melting metal, or in a solution of one of its salts in heavy water. If metallic uranium is used as the nuclear fuel, its mechanical strength is of great importance. Metallic-uranium reactors must be designed for a maximum operating temperature of the uranium below 660°C (at temperatures lower than 660°C , uranium exists in the form of the alpha-phase, which has a rhombic crystal lattice with an ultimate strength of about 28 kg/mm^2). At higher temperatures, the uranium becomes softer and loses strength, while at lower temperatures its strength diminishes as a result of radial* damage; under bombardment by neutrons and other fission fragments, the uranium blocks and rods swell

*[Translator's note: radial'nykh, radial is presumably an error for radiatsionnykh, radiation.]

and warp.

When uranium is used in the form of a solution in another low-melting metal, such as bismuth or lead, or in the form of a uranium-salt solution in water, the problem of its mechanical strength is avoided. In the latter case, however, radiation damage to the fuel consists in decomposition of the water into hydrogen and oxygen. If heavy water is used, losses of this product cannot be permitted because of its high cost.

The basic problem in designing an atomic engine for a missile consists in reducing its size and weight to the greatest possible degree. Although the energy-production density in the reactor's active section reaches 10-20 thousand kw/m³, which is approximately 100 times greater than that in ordinary thermal engines, the final unit-volume and unit-weight ratios are nevertheless far from that good for the nuclear installation because of the necessity of having a thick protective shield to counter radiation effects.

The reactor can operate continuously until 0.9 kg of the uranium-235 has undergone fission. We indicated earlier that complete fission of one kg of this uranium liberates about 20 million kilowatt-hours of energy. In consuming one kg of uranium-235, therefore, the reactor can develop about $0.9 \cdot 20 = 18$ million kilowatt-hours of energy and will operate nearly 600 hours in doing so.

Figure 5.17 shows a schematic diagram of an electric-arc-type nuclear rocket engine for a missile. In this engine, the nuclear reactor is the energy source supplying the arc. The result is the creation of the same specific thrust as in a thermonuclear rocket engine with the mass vehicle heated and expanded in the nozzle.

Figure 5.18 shows a schematic diagram of an ion-type rocket engine for a missile.

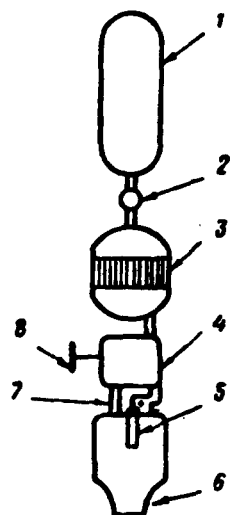


Fig. 5.17. Schematic diagram of electric-arc nuclear rocket engine for missile. 1) Tank for mass vehicle; 2) turbopump set; 3) nuclear reactor; 4) turbogenerator; 5) electric arc; 6) chamber nozzle; 7) mass vehicle; 8) radiator (heat exchange).

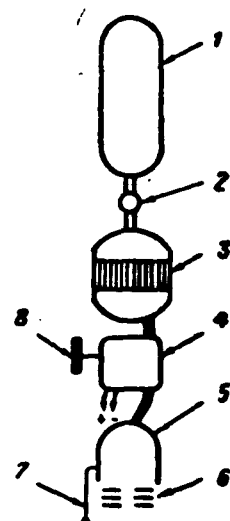


Fig. 5.18. Schematic diagram of ion rocket engine for missile. 1) Tank for mass vehicle; 2) turbopump set; 3) nuclear reactor; 4) turbogenerator; 5) ionization chamber; 6) accelerating grids (or annular accelerating electrodes); 7) electron generator; 8) radiator (heat exchange).

Basically, this engine consists of a nuclear reactor, a system for converting heat into electrical energy, and an ionization chamber with an accelerating electric field.*

The plasma produced in the ionization process, which consists of electrons and positively charged ions, is accelerated to a very high speed by the magnetic field, with the result that the engine creates a reaction-thrust force. To prevent electric charges from clinging to the mass of the missile and exerting a retarding influence on the stream of positively charged ions flowing from the engine, the ions are neutralized by electrons liberated at the cathode of the ionizing unit.

Electric power obtained from galvanic cells or by conversion of solar energy can also be used to ionize the working fluid and

**Ekspress-informatsiya* AN SSSR, No. 45, RT-133, 1958.

accelerate the plasma.

The design of atomic-ionic rocket engines encounters difficulty as a result of the complexity of converting atomic energy into kinetic energy of a working fluid in the form of an ionic plasma.

As with the solar and electric ionic engines mentioned earlier, these engines have an enormous drawback in the fact that if they are to develop large thrusts, it is necessary to expend enormous quantities of electric energy at very high voltages to accelerate the ionized particles of the mass vehicle to the necessary exhaust velocities. Rough calculations indicate that a rated power of 500 Mw per ton of thrust is required to produce exhaust velocities of the order of 100 km/sec for the electrically charged particles of the working fluid leaving the nozzle, i.e., a power station with the same capacity as a normal thermoelectric power station and weighing several thousand tons must be aboard the missile.

It appears that nuclear energy can be used effectively for reactive-propulsion purposes provided that a successful method is found for converting it directly into electrical energy, which would eliminate the necessity of having cumbersome and heavy mechanisms in the power unit. The principles underlying direct utilization [sic] of atomic energy into electrical energy are described in the literature.

An extremely serious problem in the case of the electroatomic rocket engine is removal from the reactor of that fraction of the heat that cannot be converted into electric power because of the imperfect nature of the process.

The principal obstacles to introduction of these engines into aviation and surface transportation are the large dimensions and great weight of the shielding of the engines, the high cost of the nuclear fuel, and the complexity of control.

Chapter VI
CYCLES IN ZhRD CHAMBERS

Qualitative and quantitative data about the mechanism of the cycle in the combustion chamber and nozzle of a ZhRD permit valid selection of optimum parameters and chamber shape and dimensions, and solution of other problems of engine design and construction.

Calculating the kinetics of the phenomena occurring in the combustion chamber and nozzle, together with the thermal and sometimes the gasdynamic calculations, facilitates establishing the picture of temperature, pressure, and velocity distribution in the gas stream in the engine chamber's characteristic sections, and computing the engine's basic parameters (specific thrust, per-second fuel consumption for a given absolute thrust, and others), as well as selecting and computing the systems for fuel atomization, cooling, and propellant feed.

At the present time it is impossible to ascertain the role of the various factors influencing a ZhRD cycle with sufficient accuracy or give them a quantitative evaluation. In calculating the fuel combustion processes in an engine we assume (on the bases of statistical and experimental data which are still extremely limited) the values of certain characteristics of the cycle, such as, for example, the propellants' excess oxidizer coefficient and the physical completeness of combustion, the polytropic exponent for the gases' expansion in the nozzle, etc.

In the present chapter we consider the basic factors affecting the character of the cycles occurring in a ZhRD chamber, set down the method of determining the nature of these processes, and give the approximate limits of their numerical values.

At the same time, we show examples of the numerical calculations for determining temperature and composition of the products of combustion of the fuel in the engine combustion chamber and nozzle outlet section, as well as other thermodynamic parameters. Tables and graphs required for calculating the process of fuel combustion are also given.

SECTION 1. CYCLES OF FUEL PREPARATION AND COMBUSTION IN THE ENGINE CHAMBER

Fuel combustion in the engine chamber is an extremely complicated physical and chemical process, consisting of overlapping cycles of preparation, ignition and combustion of the fuel mixture. The engine characteristics depend on the degree of perfection of these processes.

The cycles for preparing the fuel for combustion include:

- 1) atomization of the propellant components, which are fed to the combustion chamber, into the smallest particles;
- 2) heating and vaporization of these propellant components by means of the heat formed by combustion of the previous portions of the fuel in the chamber, and
- 3) mixing the vapors formed from the fuel components together, chiefly by means of turbulent diffusion.

The completeness of combustion and the stability and reliability of the engine's operation depend on the time and nature of these processes' occurrence, as well as the volume of the combustion chamber occupied by these processes.

The vaporization cycle, whose rate is determined by the parameters of the surrounding medium (temperature and pressure) and the

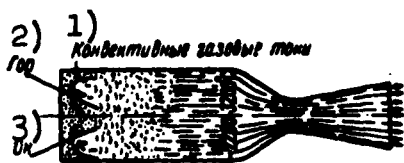


Fig. 6.1. Convective gas flows at head of an engine chamber. 1) Convective gas flows; 2) combustible; 3) oxidizer.

physical and chemical characteristics of the fuel, may be concluded before the time that the drops of fuel arrive in the high-temperature zone. Then combustion will occur in a medium consisting of small amounts of combustible and oxidizer vapors mixed together. If the

drops are not vaporized before the beginning of combustion, a heterogeneous reaction will take place on the surface of the separate liquid particles of the combustible or oxidizer, depending on which of the components vaporizes more easily.

The processes for preheating and vaporizing the propellant components which have arrived in the combustion chamber are accomplished by means of the radiant energy of the seat of combustion, the heat from the heated chamber walls, and convective gas currents flowing back toward the combustion-chamber head as a consequence of some blow-out of the gaseous medium from the head by the streams of injected fuel (Fig. 6.1).

Reverse gas currents always exist in a combustion chamber, especially in the fuel-cone area and between the components' atomization cones, as well as along the walls of the chamber, and play an important part in the fuel-combustion cycle. Their intensity depends on the design of the injectors and the system whereby the latter are arranged in the chamber head. For a given head design, the intensity of the reverse currents may be considered as constant, if unavoidable random fluctuations are ignored.

As the liquid drops of propellant component move in a stream of hot gas, they are preheated and partly vaporized. The speed of this process increases as the temperature difference between the drops and

the products of combustion is increased. Small drops are vaporized more quickly than large ones.

One may assume that in that section of the combustion chamber where about 5-10% of the fuel is vaporized, reverse currents will already have disappeared. Further preheating and vaporization of the drops is provided by the heat produced by combustion occurring simultaneously with vaporization. With vaporization and combustion of about 10-25% of the fuel, the mean velocity of the gas becomes equal to the mean velocity of the fuel drops; in the following sections of the combustion chamber, the gas velocity exceeds the drops'. About 10-15% of the heat liberated by fuel combustion is required for preheating and vaporization of the liquid fuel components.

In existing engines, the propellant component used for cooling the engine chamber receives about 10-25% of the heat required for its heating and vaporization from the surface of the chamber liner; when the pressure in the combustion chamber is 35-40 atm abs, this heat may amount to 50-60%.

The combustion cycles for the fuel mixture include the mutually overlapping processes of kinetic and diffusion fuel combustion, as a result of which a state of chemical and energy equilibrium of the gases obtained by these means, corresponding to their pressure and temperature, is established at the end of the chamber. In accordance with the degree of consumption of the fuel mixture, the temperature in the chamber rises, and attains maximum value toward the end of the combustion chamber. No significant reaction between the oxidizer and the combustible occurs in the liquid phase.

The rate (time) with which the fuel combustion process occurs in the kinetic zone is independent of the hydrodynamic and diffusion factors (stream velocity, dimensions and shape of combustion chamber,

and the design of its head), and is chiefly a function of:

- 1) the properties of the fuel components (their activation energies);
- 2) the temperature and pressure in the combustion chamber;
- 3) the concentration of reagents in the combustion zone.

The rate at which the fuel combustion process takes place in the turbulent-diffusion zone is almost independent of the kinetic factors, if we do not consider the weak dependence of several physical constants on temperature, and is determined primarily by hydrodynamic factors, such as:

- 1) the nature of the gas stream's motion in the combustion chamber (the mixing time of the propellant components depends very little on the stream velocity);
- 2) the distribution of velocities, concentrations of fuel components, and temperatures in this stream;
- 3) the shape and dimensions of the combustion chamber (with a conically converging shape of combustion chamber the turbulence of the gas stream is damped);
- 4) the character of general and local stream turbulence;
- 5) the redistribution of heat inside the stream, especially in the combustion zone, and also between the stream and the external medium (heat transfer caused by the system's being nonadiabatic), and so forth.

The character of the fuel injection into the engine chamber has an important effect on the combustion process.

Depending on the structural shape of the combustion chamber head and the type, number, and arrangement scheme of the fuel injectors, the following things occur in an engine chamber:

- 1) fuel-component injection jets in different directions;

2) a great number of seats of vapor formation and fuel-propellant combustion distributed throughout the volume of the chamber;

3) vortical convective currents of the hot mass toward the head of the combustion chamber, and other phenomena.

The movement of the working fluid in the engine combustion chamber becomes turbulent because of these factors. The effect of all the factors enumerated above leads to the basic mass of the propellant components being vaporized and burning in a short section of the combustion chamber, forming a unique flame front.

Up to the present time, we have not found sufficiently precise methods for determining the propellant-combustion time in the engine chamber.

The means used for developing the combustion cycle depend on the type of propellant components used and the specific situation occurring in the process. In the beginning of the combustion chamber, where, as a consequence of intensive vaporization, the temperature of the mixture is comparatively low, reactions take place slowly. On the other hand, the velocity of the gas stream and intensity of mixing in the beginning of the chamber is considerably less than in the remaining part of the chamber, which is explained by the temperature regime of this section, and also by the fact that part of the fuel in this section is in a liquid state, occupying a much smaller volume of the chamber than vapor. For these reasons, combustion in the beginning of the chamber will be kinetic or compound.

A high temperature, close to the maximum combustion temperature, is found in the remaining part of the chamber, because of which the chemical reactions take place practically instantaneously, and therefore the combustion process has a turbulent-diffusion nature. In a ~~Zhrd~~ molecular diffusion occurs considerably more slowly than turbu-

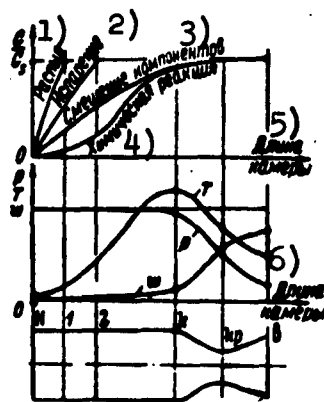


Fig. 6.2. Course of basic cycle stages throughout the length of an engine chamber. 1) Atomization; 2) vaporization; 3) mixing of propellants; 4) chemical reaction; 5) chamber length; 6) chamber length.

lent diffusion, and therefore the speed with which the gases mix, in the final analysis, is determined by the speed of turbulent diffusion.

The heterogeneity of a composition of the gases, on a scale equal to the distance between the injectors, is equalized rather quickly but, in existing engines, inequalities on a scale equal to chamber diameter are hardly equalized even throughout the entire length of the chamber.

Figure 6.2 shows curves which are approximately characteristic of the occurrence of basic cycle stages throughout the length

of the engine combustion chamber and nozzle. On the ordinate of these curves, the quantity G/G_s is the fraction of the fuel, in percentages, whose participation in any process is already concluded. All the basic processes are in operation in section H-1. The atomization process is finished in this section, and the part of the propellant components which have reacted amounts to a very small fraction. In section 2, propellant-component vaporization is almost completed. Here the chemical reaction is still not especially great and the rate of the combustion cycle is limited. High temperatures exist in the last part 2-k of the combustion chamber, and therefore all the fuel which succeeded in mixing is consumed here. The rate of combustion in this section is limited by the mixing of the propellant components. The amount of the mixture which has reacted is increased in the engine nozzle because of the complete combustion of the fuel and recombination of molecules.

Ignoring the partial overlap in the components' mixing and combustion processes, one may conditionally consider that the total time for direct fuel combustion in the engine chamber consists of:

1) the time τ_{fiz}^* required for physical contact between the gaseous combustible and the gaseous oxidizer;

2) the time τ_{khim}^{**} required for the chemical reaction itself (kinetic combustion of the components) to take place, i.e.,

$$\tau_{sg} = \tau_{fiz} + \tau_{khim} \text{ sec.}^{***} \quad (6.1)$$

As pressure in the engine combustion chamber is increased, the fuel-combustion process is intensified, and therefore the time required for fuel combustion is decreased (Figs. 6.3 and 6.4).

Since the rate of the chemical reaction is quite great in the combustion chambers of existing engines, with high temperatures in the developed focus of combustion, and fuel combustion is mainly determined by the speed with which the fuel mixture forms, i.e., τ_{khim} is quite small in comparison to τ_{fiz} , in practice, one may consider that the fuel combustion cycle occurs chiefly in the form of turbulent diffusion, i.e.,

$$\tau_{sg} \approx \tau_{fiz} \approx \tau_{t.d.}^{****} \quad (6.2)$$

The mixing time for the propellant components in the diffusion-combustion zone is little dependent on stream velocity and is determined chiefly by the turbulence, which is a function of the combustion-chamber head's shape and the character of the combustion process itself.

*[$\tau_{физ} = \tau_{fiz} = \tau_{fizicheskiy} = \tau_{physical} \text{ (contact).}$]
 **[$\tau_{хим} = \tau_{khim} = \tau_{khimicheskaya} = \tau_{chemical} \text{ (reaction).}$]
 ***[$\tau_{сг} = \tau_{sg} = \tau_{sgoraniye} = \tau_{combustion.}$]
 ****[$\tau_{т.д} = \tau_{t.d} = \tau_{turbulentnaya.diffuziya} = \tau_{turbulence.diffusion.}$]

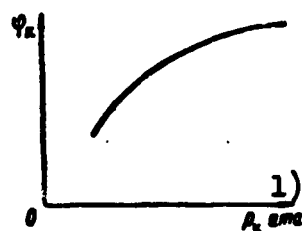


Fig. 6.3. Fuel heat-liberation coefficient as a function of pressure in the combustion chamber. 1) p_k , atm abs.

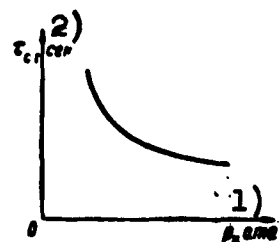


Fig. 6.4. Fuel-combustion time as a function of pressure in the combustion chamber. 1) p_k , atm abs; 2) sec.

Since the complete fuel-combustion cycle in the engine chamber consists of: 1) preparation processes accomplished during time τ_{podg}^* and 2) the processes for turbulent mixture and combustion of the gaseous fuel components during the time τ_{sg} , the total stay time of the working fluid in the engine combustion chamber may be conditionally expressed by the formula

$$\tau_{pr} = \tau_{podg} + \tau_{sg}. \quad (6.3)$$

Stay time varies for different fuels and must be determined by experimental methods. For low-boiling propellant components its value is less than that for high-boiling components. Besides this, the greater the pressure in the combustion chamber, the smaller τ_{pr} , since as p_k is raised the fuel-combustion cycle is intensified.

For a given fuel, τ_{pr} is chiefly a function of the hydrodynamics of the burner cup (injection head) of the engine chamber (the shape of the head, number of injectors, and their type and arrangement in the head, etc.), i.e., it depends on:

- 1) the character of the fuel components' distribution across a cross section of the combustion chamber;
- 2) the components' degree of atomization and the degree to which

*[$\tau_{podg} = \tau_{podg} = \tau_{podgotovka} = \tau_{preparation}$]

they are mixed together, and

3) formation of the reverse convective gas currents mentioned above, which transfer heat from the seat of combustion to the propellant components which have just arrived in the chamber and, thus, heat and vaporize these components.

Fuel stay time in an engine combustion chamber may be determined in accordance with the formula

$$\tau_{np} = \frac{V_k \gamma_k}{G_s} = \frac{V_k p_k}{G_s R_k T_k} \text{ sec.} \quad (6.4)$$

This formula shows that fuel stay time in a combustion chamber at a given per-second flow rate G_s kg/sec depends on the chamber volume V_k , its gas pressure p_k , temperature T_k , and gas constant R_k ; stay time is also a function of combustion chamber shape.

In designing a ZhRD, a rational selection of combustion chamber volume sometimes, actually, amounts to finding a magnitude of τ_{pr} within limits of $\tau_{pr}/\tau_{sg} \approx 2-3$, which is optimum both in regard to physical completeness of fuel combustion and to the engine chamber's specific weight. The shorter τ_{pr} , the smaller the volume, weight, and cost of the engine combustion chamber. Therefore, when designing an engine, one should strive in every possible way to obtain the smallest possible combustion chamber dimensions with the highest operating economy.

The magnitude of τ_{pr} may be decreased without lowering the engine chamber operating economy by means of:

- 1) raising the pressure in the chamber, thus promoting intensification of the fuel combustion cycle;

- 2) improving the quality of propellant-component atomization without significant complication and cost increase in the atomizing unit (using atomization which is fine and even throughout the chamber

section, spray injectors, reverse-flow atomization, etc.);

3) reinforcing gas-stream turbulence by installing cooled turbulence rings in the combustion chamber, etc.

The mechanism of the combustion reaction varies for different fuels in their gaseous phases, but in all cases a fine, uniform mixture of the propellant components is required in order for the combustion process to start.

The speed with which the flame front moves through the chemically reactant mixture is mostly a function of the turbulent mass transfer due to the gas vortices, and only to an insignificant degree is it a function of the true velocity of the flame through the discrete volumes of the mixed gas inside each vortex.

The propagation of the flame front through the unburned gaseous fuel mixture is, probably, partially due to the high rate of diffusion for certain active molecular and atomic groups such as OH, N, H, or CH_2 , which form during the fuel-combustion process. It is probable that these active particles function as carriers of the chain reaction.

Combustion processes for hypergolic fuel components, which ignite when mixed, are considerably different from the combustion processes for nonhypergolic components which are briefly described above. These propellant components, igniting at mutual contact, do not require heat for preliminary preparation for combustion; a relatively smaller τ_{pr} is required for them.

When starting the cycle in an engine combustion chamber, one must always bear in mind that:

1) fuel combustion must always be preceded by fine atomization, preheating, vaporization, and a thorough mixing of the components;

2) mixing the combustible and oxidizer in the liquid form is not

mandatory if their drops are well mixed together before vaporization (in bipropellant emulsion centrifugal-spray injectors);

3) the propellant-component mixing process has a sharply expressed hydrodynamic character and is chiefly determined by the conditions under which turbulent diffusion and heat transfer take place;

4) the speed with which fuel components vaporize is determined by the temperature and pressure in the combustion chamber, size of drops and relative velocity of the fuel components, turbulence in the gas stream, and other factors;

5) in the beginning of the combustion chamber, where the mixture temperature is comparatively low because of intensive component vaporization, fuel reactions take place slowly, and some part of the combustible mixture is formed which, as a consequence, burns almost kinetically, regardless of the hydrodynamic factors;

6) the fields of velocities and concentrations in fuel components across a cross section of the combustion chamber are never completely homogeneous and are basically a function of the atomizing units' design;

7) under practical conditions, the chemical processes rarely reach a state of equilibrium; the level of their completeness is essentially a function of the rate at which the reactions take place, magnitude of thermal effect, rate of heat removal or heat transfer, pressure, temperature, and concentration of reagents;

8) in fuel combustion, the flame front is not a simple surface intersecting the cross section of the combustion chamber, and the speed of its movement through the chemically reacting mixture is basically a function of turbulent mass transfer accomplished by the gas vortices; it is only to an insignificant degree that the flame front moves through discrete volumes of mixed gas within each vortex;

9) the mechanisms of the chemical reactions, in the gaseous state, vary for each specific fuel, especially for hypergolic and nonhypergolic propellant components;

10) the rates with which chemical reactions take place are quite great, and therefore fuel combustion is chiefly determined by the speed with which the combustible mixture (the mixing of the propellant components) is formed;

11) the mixing time for the fuel components in the turbulent-combustion zone depends very little on the velocity of the gas stream and is chiefly determined by the turbulence of the flow, depending on the atomization units of the engine and the character of the combustion itself for the given fuel;

12) when pressure in the chamber is increased, the combustion process is intensified, and therefore combustion time decreases;

13) stay time in the combustion chamber for the given fuel components is determined chiefly by the hydrodynamics of the engine atomizing unit;

14) as the fuel's stay time in the combustion chamber is increased, the fuel is better consumed (the coefficient of completeness of combustion is increased), but the dimensions and specific weight of the chamber are increased.

SECTION 2. HEAT BALANCE FOR AN ENGINE COMBUSTION CHAMBER

Fuel-energy losses in a ~~Zhrd~~ chamber are divided into losses directly in the combustion chamber and in the chamber nozzle.

We will first consider heat losses in the engine combustion chamber.

It is well known that the fuel combustion process in an engine chamber occurs at a very high temperature level and thermal potential.

As a result of this, the molecules of the products of combustion are in a highly excited state and partially dissociate, absorbing heat. Thus, some physical incompleteness of fuel combustion takes place because of the propellant components' imperfect mixing and limited stay time in the combustion chamber. Besides this, the fuel combustion process is accompanied by heat transfer to the surrounding medium and the work of friction between the molecules of the gases and against the surface of the engine chamber liner. The work of this friction is turned into gas heat.

If the combustion-chamber flame tube is cooled by one of the propellant components, the heat $q_{okhl.s}^*$ transferred to this component in the chamber-nozzle coolant passage is brought into the combustion chamber and is an external physical heat increment for the chamber. In medium- and high-thrust engines, this heat usually does not exceed 0.1 to 0.2% of the fuel's lowest operating heating value. Besides this, each kilogram of fuel which arrives in the combustion chamber has some velocity w_t , and, consequently, carries this energy $w_t^2/2g$ with it into the chamber from outside.

However, external energy increments, as the fuel arrives in the engine combustion chamber ($q_{okhl.s}$ and $w_t^2/2g$), like the work of the friction of the gases therein, are relatively small in comparison to the fuel's heating value, and, with sufficient precision for practical purposes, may be ignored in computations, all the more so since their quantitative evaluation at the first stage of designing and planning an engine is impossible.

At the first stage of designing a ZhRD, we most frequently, regardless of method, consider the following fuel energy losses in an en-

$$*[q_{oxl.c} = q_{okhl.s} = q_{okhlazhdeniye.sopla} = q_{cooling.nozzle}]$$

gine combustion chamber (calculating them on the basis of 1 kg), caused by:

- 1) gas dissociation q_{dis}^* in kcal/kg;
- 2) incompleteness q_{nep}^{**} of combustion, in kcal/kg;
- 3) heat transfer q_{okr}^{***} to the surrounding medium, in kcal/kg.

Thus, ZhRD combustion-chamber heat-balance conditions are expressed by the equation

$$H_u = q_k + q_{dis} + q_{nep} + q_{okr} = q_k + q_{pot} \text{ kcal/kg,****} \quad (6.5)$$

where H_u is the fuel's heating capacity in kcal/kg; q_k is the fuel's specific heat liberation in the engine combustion chamber in kcal/kg; and q_{pot} is the heat loss in the combustion chamber, in kcal/kg.

For existing ZhRD, fuel-heat losses in the combustion chamber depend on a great number of factors, and usually vary within the limits of

$q_{dis} \approx 7-14\%$, $q_{nep} \approx 2-5\%$, and $q_{okr} \approx 1\%$ of H_u , which compose the total fuel-heat loss $q_{pot} \approx 10-20\%$ of H_u .

Heat loss q_{dis} may be determined by calculations, but q_{nep} and q_{okr} may be determined only by experiments. In computations, we often neglect the values of q_{okr} and the friction work of the gases because of their negligible amounts.

The processes of complete fuel combustion, recombination of products of dissociation, and gas friction take place within the engine nozzle, and it is here that part of the available heat is converted into the kinetic energy of the gas-stream leaving the nozzle. The remaining part of the available heat remains in the gas

*[$q_{дис} = q_{dis} = q_{dissotsiatsiya} = q_{dissociation}$.]
 **[$q_{неп} = q_{nep} = q_{nepolnota} = q_{incompleteness} \text{ (of combustion)}$.]
 ***[$q_{окр} = q_{okr} = q_{okruzhayushchaya} = q_{surrounding} \text{ (medium)}$.]
 ****[$q_k = q_{chamber}$; $q_{пот} = q_{loss}$.]

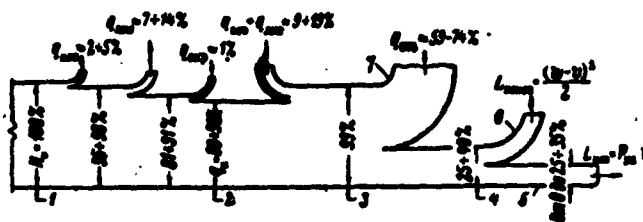


Fig. 6.5. Approximate diagram of the energy balance of the fuel in a ZhRD chamber. 1) Fuel's available heat in the form of effective heating value, $H_u = q_k + q_{nep} + q_{dis} + q_{okr}$; 2) fuel's specific heat liberation in the combustion chamber, $q_k = H_u - (q_{nep} + q_{dis} + q_{okr})$; 3) energy of the gases at the outlet from the nozzle, consisting of thermal and kinetic energy; 4) kinetic energy of the gases at the outlet from the nozzle, $L_{rasp} = w_v^2/2g$; 5) kinetic energy of the gases effectively used for moving the missile, $L_{isp} = p_{ud}v$; 6) kinetic energy of the gases not used by the weapon; 7) thermal energy of the gases at the outlet from the nozzle.

flow and is lost as far as the engine is concerned, which is analogous to the energy loss from the hot exhaust gases in internal-combustion engines (Fig. 6.5).

The combustion-chamber heat balance, which characterizes the result of the fuel-combustion cycle, does not reflect in any obvious form the effect of the dynamic or similar factors which led to this particular result. This statistically balanced equality of heat input and expenditure for the fuel which took part in the engine-chamber cycle, however, has an important significance both for improving the engine and for the technical computation of a newly planned combustion chamber.

In computations for ZhRD chambers, we usually find it more convenient, when considering loss of fuel energy as a consequence of

physical incompleteness of combustion, to use the pressure coefficient $\varphi_{p.k}$ for the gases in the combustion chamber, and to use the velocity coefficient φ_s for the gas outflow from the chamber nozzle when considering fuel energy losses as a consequence of the imperfection of the process for the outflow of products of combustion from the engine chamber nozzle (see Section 3 of this chapter).

SECTION 3. THE FUEL HEAT-LIBERATION COEFFICIENT IN AN ENGINE COMBUSTION CHAMBER

Incomplete liberation of fuel heat occurs in an engine combustion chamber because of physical incompleteness of combustion, dissociation of the products of combustion, and heat transfer to the surrounding medium.

The ratio between the heat liberated by combustion of one kilogram of fuel to the heat available, that is, the calorific value H_u of the fuel, is customarily called the total coefficient of fuel heat-liberation:

$$\varphi_k = \frac{q_k}{H_u} = \frac{I_k}{H_u} = \varphi_{p.k} \varphi_{d.k} \varphi_{st.k} \approx \varphi_{p.k} \varphi_{d.k}^* \quad (6.6)$$

where I_k is the heat content, in kcal/kg, of 1 kg of the fuel's products of combustion, allowing for heat losses as a consequence of incomplete combustion and dissociation (heat losses to the surrounding medium are neglected because of their small amounts); $\varphi_{p.k} = \varphi_k / \varphi_{d.k} = I_k / H_u \varphi_{d.k}$ is the coefficient for physical completeness of fuel combustion (the heat-liberation coefficient for the fuel in accordance with the physical mixing of the components), indicating that part of the heat which is liberated in the engine combustion chamber during

*[$\varphi_{п.к} = \varphi_{p.k} = \varphi_{\text{полнота.камера}} = \varphi_{\text{completeness.chamber}}$;
 $\varphi_{д.к} = \varphi_{d.k} = \varphi_{\text{диссоциации.камера}} = \varphi_{\text{dissociation.chamber}}$;
 $\varphi_{ст.к} = \varphi_{st.k} = \varphi_{\text{стабильности.камера}} = \varphi_{\text{stability.chamber}}$]

fuel combustion, only in the case of heat losses attributable to nonideal mixing and combustion of the fuel components; the quantity $1 - \varphi_{p.k}$ represents that part of the heat, in the form of the chemical energy of the unburned portion of the fuel, which remained in the products of combustion at the end of the combustion chamber; $\varphi_{d.k} = \varphi_k / \varphi_{p.k} = I_k / H_u \varphi_{p.k}$ is the coefficient for completeness of fuel heat liberation in the engine combustion chamber, allowing only for heat losses resulting from dissociation of gases; the quantity $1 - \varphi_{d.k}$ represents that part of the heat, in the form of chemical energy, which remains in the gas dissociation product; $\varphi_{st.k}$ is the stability coefficient for the heat of the products of fuel combustion in the combustion chamber, representing that part of the heat which the products of combustion have in the chamber, allowing only for heat loss to the surrounding medium; and $1 - \varphi_{st.k}$ is the fraction of heat transfer to the surrounding medium.

To determine the heat content of the separate components of the gaseous mixture, one may use the data in the table in Appendix I, subtracting the energy content of the gas at 20°C from the energy content of the gas at a given temperature, i.e. assuming that $I'_i = I'_{ig} - I'_{ig}{}^{20^\circ}$ kcal/kmole.

Consequently, the fuel heat-liberation coefficient φ_k in the combustion chamber represents that part of the heat which is actually liberated during fuel combustion in the chamber, allowing for heat losses caused by dissociation, incomplete combustion, and transfer to the surrounding medium; the quantity $1 - \varphi_k$ represents that part of the heat which is lost in the engine combustion chamber as a result of fuel-heat losses q_{nep} , q_{dis} , and q_{okr} .

In existing engines $\varphi_{p.k} \approx 0.95-0.98$; $\varphi_{d.k} \approx 0.85-0.90$; $\varphi_{st.k} \approx 0.99$, and $\varphi_k \approx 0.70-0.90$.

The coefficient $\varphi_{p.k}$ depends on the type and composition of the fuel, design of the atomizing unit, shape and volume of the combustion chamber, and other factors; it may be determined approximately only by means of experiments, like the coefficient $\varphi_{st.k}$. The coefficient $\varphi_{d.k}$ may be determined analytically with sufficient accuracy.

At the present time experimental data concerning the coefficient $\varphi_{p.k}$ are still extremely limited, which hampers our evaluation of its magnitude when designing engines.

It has been established that as stay time τ_{pr} for the fuel in an engine combustion chamber is increased, the value of $\varphi_{p.k}$, at first, increases sharply, and then, beginning at some magnitude of fuel combustion's dimensionless time ($\tau = \tau_{pr}/\tau_{sg} \approx 2-3$) this increase becomes quite insignificant (Fig. 6.6).

As pressure p_k in the engine combustion chamber is increased, dissociation of the products of fuel combustion decreases, which increases the value of $\varphi_{d.k}$ (Fig. 6.7). Thus the optimum magnitude of the excess oxidizer coefficient α in the fuel is increased, because of which the fuel heat-liberation coefficient φ_k also increases.

Throughout the length of the engine nozzle, the values of φ_p and φ_d^* increase as the consequence of complete fuel combustion and recombination of the molecules of dissociation products, and in a nozzle section, in practice, may attain a value of one. In longer nozzles, the stay time for the products of fuel combustion is increased, as a result of which the processes of complete fuel combustion and recombination of molecules occur more completely.

The phenomena occurring in an engine combustion chamber when $\alpha \neq 1$ and $\varphi_{p.k} < 1$ are very complex and as yet have been little studied. If

*[$\varphi_d = \varphi_{\text{dissociation}}$; $\varphi_n = \varphi_{\text{completeness}}$.]

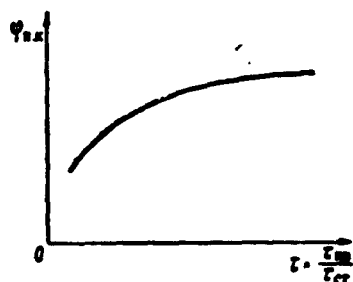


Fig. 6.6. Fuel's completeness of combustion coefficient as a function of dimensionless time.

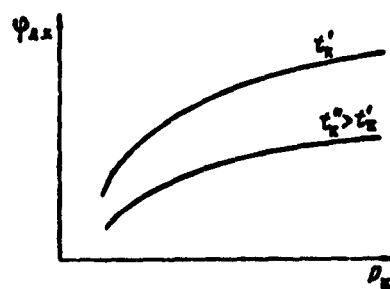


Fig. 6.7. Fuel's heat liberation coefficient, allowing for dissociation, as a function of pressure and temperature in the engine combustion chamber.

there turns out to be more oxidizer in some section of the combustion chamber, and therefore the local value of the excess oxidizer coefficient α_m^* will be greater than the mean value of α for the entire combustion chamber, and the fuel-combustion process in this place will be accomplished more completely.

In the other parts of the combustion chamber, where there is more combustible, i.e., when $\alpha_m < \alpha$, the fuel-combustion process will occur less completely. At a very incomplete atomization and mixing of the fuel components in some parts of the combustion chamber, an almost complete absence of one of the fuel components may occur. The fuel component which is not participating in the combustion process will be heated up, vaporized, and decomposed by means of the heat from the part of the fuel which has burned, increasing the number of products of incomplete combustion.

When such gases leave the nozzle, the unburned part of the combustible close to the boundary of the stream comes into contact with the air of the atmosphere, and continues to burn outside, forming a long tongue of flame. The shock waves, which are observed in the form

$$*[\alpha_m = \alpha_m = \alpha_{\text{mestnoye}} = \alpha_{\text{local}}.]$$

of wide luminescent "packets,"* are another widespread trait of the stream of gases flowing out of an engine nozzle.

SECTION 4. IDEAL, THEORETICAL, AND ACTUAL THERMODYNAMIC TEMPERATURES OF FUEL COMBUSTION

The temperature of the products of fuel combustion in an engine chamber is characteristic of the thermal potential level for these products.

Fuel-combustion product temperature has an important effect on the nature of the engine-chamber cycle, and must be considered in selecting a proper chamber-cooling method. Therefore, the main problem in a ZhRD thermodynamic computation is to determine temperature and composition of the products of fuel combustion in the combustion chamber and nozzle outlet section. These parameters for the fuel combustion cycle are required for planning and designing the engine chamber.

The value of the thermodynamic (static) temperature for the products of combustion of a given fuel in an engine chamber depends on a number of factors, the most important of which are:

- 1) the fuel's specific calorific value, which is characteristic of the chemical composition of its components and their ratio to each other;
- 2) the pressure in the combustion chamber, the value of which is established, when designing an engine, by starting from the economic, operational, and other considerations;
- 3) the heat losses from the fuel to be burned, which depend on the establishment of the engine combustion-chamber cycle and how the cycle proceeds, as well as the chamber design and geometrical parameters, and also other factors.

*["пакеты" = "pakety" = "packets."]

Depending on which fuel heat losses during combustion in a ZhRD chamber are considered, we distinguish between the following thermodynamic temperatures for the products of fuel combustion:

- 1) ideal $t_{k.i}^{\circ}\text{C}^*$ or $T_{k.i}^{\circ}\text{K}$;
- 2) theoretical $t_{k.t}^{**}$ or $T_{k.t}^{\circ}\text{K}$, and
- 3) actual $t_k^{\circ}\text{C}^{***}$ or $T_k^{\circ}\text{K}$.

The ideal temperature of a fuel's combustion is that temperature which the product of complete combustion of this fuel would have at a stoichiometrical component ratio and without any sort of heat losses in the engine combustion chamber. Under this condition, the ideal thermodynamic temperature of the products of fuel combustion is determined from the equation of energy up to and after complete combustion of a given unit of fuel (see Section 5, Chapter VI). For existing ZhRD fuels, $t_{k.i} \approx 3100-4800^{\circ}\text{C}$ or higher.

The ideal combustion temperature is a function of the chemical composition of the fuel only, since only this determines the composition of the products of combustion and the amount of heat which is liberated. The magnitude of this temperature is one of the fuel's characteristics.

At high temperatures, fuel combustion in an engine chamber is, in practice, accompanied not only by an increase in the internal energy of the products of combustion in the form of translational, rotational, and vibrational motion of the molecules and their atomic nuclei, but also by considerable dissociation, accompanied by a great heat loss, and, consequently, by a decrease in the temperature in the engine combustion chamber.

$$*[t_{k.i} = t_{k.i} = t_{\text{kamera.ideal'naya}} = t_{\text{chamber.ideal}}.]$$

$$**[t_{k.t} = t_{k.t} = t_{\text{kamera.teoreticheskaya}} = t_{\text{chamber.theoretical}}.]$$

$$***[t_k = t_{\text{chamber}}.]$$

The theoretical temperature for fuel combustion is that temperature which the products of combustion of a fuel would have at a given pressure in the engine chamber and with only one heat loss, due to gas dissociation. For existing fuels and their combustion conditions in a ZhRD, $t_{k,t} \approx 3000-3800^{\circ}\text{C}$ or higher.

The value of this thermodynamic temperature is always lower than the ideal temperature and depends to a considerable degree on the type and composition of the fuel and its combustion conditions.

Since direct methods do not permit accurate determination of fuel-heat losses due to dissociation of combustion products, one may determine these heat losses analytically, by successive approximation or some other method.

In practice, fuel heat losses also occur in an engine chamber because of physical incompleteness of combustion and transfer to the surrounding medium, which are accompanied by a decrease in the combustion temperature.

The actual temperature is that temperature which the products of combustion for a given fuel actually have in the combustion chamber of a real engine at a given pressure and with heat losses in the form of dissociation, incomplete combustion, and transfer to the surrounding medium. For existing ZhRD and the fuels used in them, $t_k \approx 2800-3300^{\circ}\text{C}$ or higher.

The actual combustion temperature for the new, most thermally efficient chemical fuels is probably 5500°C . In practice, the possibility of using products of combustion with a temperature higher than 4000°C is scarcely probable. The magnitude of this temperature is limited by the heat resistance of the materials used for the engine chamber. The best existing materials can withstand a temperature of the order of $1500-2000^{\circ}\text{C}$ during sustained operation. Magnesium oxide is one of the

strongest materials. The feasible limit for this material, even in short-term engine chamber operation, is a temperature which is not higher than 3000°C . Any engine-chamber liner material will vaporize at a temperature higher than 4100°C .

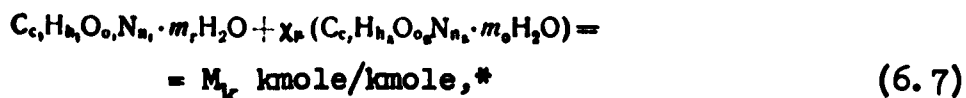
Determining the actual temperature in an engine combustion chamber is extremely complex and cannot be done accurately, since, in practice, it is impossible for us to accurately estimate the effect that a number of factors have on the fuel-combustion cycle.

The temperature level in the engine combustion chamber has an important effect on the fuel combustion process, the degree of gas dissociation, and the engine structure. It is practicable to use propellants with low combustion temperatures and combustion products, and relatively high exhaust velocities, for a ZhRD, since this simplifies engine design.

SECTION 5. DETERMINING THE COMPOSITION AND IDEAL TEMPERATURE FOR PRODUCTS OF FUEL COMBUSTION

If the combustible and oxidizer consist chiefly of carbon, hydrogen, oxygen, and nitrogen, the products of complete combustion for a weight unit of this fuel, when the excess oxidizer coefficient $\alpha = 1$ and there is no dissociation, are CO_2 , H_2O , and N_2 gases.

When water, in the form of an admixture, is present in the combustible and oxidizer, the composition of this fuel may be expressed by the following chemical formula:



where c_1 , h_1 , o_1 , n_1 , and c_2 , h_2 , o_2 , and n_2 are the number of atoms of the different elements in 1 kmole of the combustible and oxidizer, respectively; χ_μ is the molar coefficient of the fuel's composition;
 $*[m_r = m_{\text{combustible}}; m_o = m_{\text{oxidizer}}]$

and m_g and m_o are the number of kilogram molecules of water in 1 kmole of combustible and oxidizer, respectively.

Under this condition, the amount of the products of complete combustion for the fuel mentioned, when $\alpha = 1$, will be:

1) according to computation per kmole

$$M_p = M_{CO_2} + M_{H_2O} + M_{N_2} = \sum M_i \text{ kmole/kmole}, \quad (6.8)$$

where $M_{CO_2} = c_1 + \chi_\mu c_2$ is the number of kmole of carbon dioxide; $M_{H_2O} = 0.5[h_1 + \chi_\mu h_2 + 2(m_g + \chi_\mu m_o)]$ is the number of kmole of water vapor; and $M_{N_2} = 0.5(n_1 + \chi_\mu n_2)$ is the number of kmole of molecular nitrogen;

2) according to computation per kg

$$G_p = G_{CO_2} + G_{H_2O} + G_{N_2} = \sum G_i \text{ kg/kg}, \quad (6.9)$$

where $G_{CO_2} = 11/3(C_g + \chi_o C_o)$ is the amount of carbon dioxide;

$$G_{H_2O} = 9(H_g + \chi_o H_o) \text{ is the amount of water vapor}; \quad (6.10)$$

$$G_{N_2} = N_g + \chi_o N_o \text{ is the amount of molecular nitrogen.}$$

Here C_g , H_g , N_g and C_o , H_o , and N_o are the weight fractions of the elements in 1 kg of combustible and oxidizer, respectively; and χ_o is the stoichiometrical weight coefficient for the fuel composition.

If we know the weight composition C_t , H_t , and N_t^* of the elements in 1 kg of fuel, the weight of the separate components for the products of combustion of this fuel, when $\alpha = 1$, may be determined in accordance with the formulas:

$$g_{CO_2} = (11/3)C_t \text{ kg/kg}, \quad g_{H_2O} = 9H_t \text{ kg/kg}, \quad \text{and} \quad g_{N_2} = N_t \text{ kg/kg}, \quad (6.11)$$

thus

$$g_{CO_2} + g_{H_2O} + g_{N_2} = 1.$$

If $\alpha > 1$ and there is no dissociation, there will also be excess oxygen in the composition of the products of combustion for a given unit of fuel to the amount of:

*[Subscript t = toplivo = fuel.]

$$M_{O_2} = O_2 - \left(\frac{2c_1 + 0.5h_1 - o_1}{\alpha \chi_p} + 2c_2 + 0.5h_2 \right) \text{kmole/kmole}, \quad (6.12)$$

or

$$g_{O_2} = O_2 - \left(\frac{8}{3} C_r + 8H_r \right) \text{kg/kg}, \quad (6.13)$$

where o_1 and o_2 are the numbers of atoms of oxygen in 1 kmole of combustible and oxidizer, respectively; and O_t is the amount of oxygen, by weight, in 1 kg of fuel.

The weight of the products of combustion from 1 kmole of combustible is equal to

$$\begin{aligned} G_{p,r} &= \sum_i M_i = p_r + 18m_r + \chi_p (p_o + 18m_o) = \\ &= p_r + \chi_p p_o + 18(m_r + m_o) \text{kg/kmole}, \end{aligned} \quad (6.14)$$

or

$$G_{p,r} = p_r \frac{100}{\alpha_r} + \chi_p \frac{100}{\alpha_o} \text{kg/kmole}, \quad (6.15)$$

since, as previously stated,

$$p_r + 18m_r = p_r \frac{100}{\alpha_r} \text{ and } p_o + 18m_o = p_o \frac{100}{\alpha_o}.$$

where μ_1 is the molecular weight of the 1-th gas in the mixture.

The following interdependent functions exist between the parameters of each 1-th gas in a mixture of any composition and the parameters of the mixture as a whole:

$$\frac{v_i}{v_n} = \frac{R_i}{R_n} = \frac{\gamma_i}{\gamma_n} = \frac{p_i}{p_n}; \quad (6.16)$$

$$\begin{aligned} v_n &= \sum g_i v_i = \frac{1}{\gamma_n} = \sum \frac{g_i}{\gamma_i} = \frac{1}{\sum g_i \gamma_i} = \frac{1}{\sum r_i \mu_i}; \\ p_n &= \frac{\sum p_i p_i}{p_n} = \sum r_i p_i = \frac{1}{\sum g_i \mu_i} = \frac{848}{R_n} = \frac{\sum p_i M_i}{p_n}; \\ R_n &= \frac{848}{p_n} = \sum g_i R_i = \frac{848}{\sum p_i r_i} = 848 \sum \frac{g_i}{p_i} = \frac{1}{\sum r_i / R_i} = \frac{1}{\sum g_i \mu_i}; \\ g_i &= \frac{G_i}{G_n} = \frac{V_i / v_i}{V_n / v_n} = \frac{V_i}{V_n} \frac{v_n}{v_i} = r_i \frac{v_n}{v_i} = \frac{p_i M_i}{p_n M_n} = \frac{p_i r_i}{\sum p_i r_i}; \\ r_i &= \frac{V_i}{V_n} = \frac{G_i / \gamma_i}{G_n / \gamma_n} = \frac{G_i}{G_n} \frac{\gamma_n}{\gamma_i} = g_i \frac{\gamma_n}{\gamma_i} = \frac{p_i}{p_n} = \frac{M_i}{M_n} = \frac{g_i \mu_i}{\sum g_i \mu_i}; \\ p_i &= p_n \frac{V_i}{V_n} = p_n r_i = p_n \frac{M_i}{M_n} = p_n p_n \frac{g_i}{\mu_i} = p_n \frac{g_i v_i}{v_n} = p_n \frac{g_i R_i}{R_n} = \\ &= p_n \gamma_n \frac{g_i}{\gamma_i}. \end{aligned} \quad (6.17)$$

The subscript "k" in letter symbols shows that the parameters of the gas mixture in the given case refer to the engine combustion chamber.

If we know the composition of the products of complete combustion of 1 kmole or 1 kg of fuel when $\alpha = 1$ and there are no heat losses, we may determine the ideal temperature of these products, using one of the following equations of the balance of energy:

$$I_t = \frac{1}{P_{\text{mix}}} \sum p_i I_i \text{ kcal/kg} \quad (6.18)$$

or

$$H_u = \sum g_i \frac{(\mu c_p)_i}{H_i} \text{ kcal/kg}, \quad (6.19)$$

where I_t is the given fuel's energy content; H_u is the lowest stoichiometric calorific value of this fuel; and I_i is the energy content of the i-th gas in the mixture in kcal/kmole.

The ideal temperature for the products of fuel combustion when $\alpha = 1$ and there are no heat losses would be the temperature value at which the magnitudes for the thermodynamic energy contents I_i or the molecular specific heats $(\mu c_p)_i$ of the different gases in the mixture, taken from the tables, would satisfy the equations of the balance of energy given above.

In practice, fuel-combustion cycles in ZhRD chambers occur when $\alpha < 1$ and at very high temperatures, as a result of which the products of combustion dissociate considerably, with the loss of a significant amount of heat. This heat loss is equivalent to the chemical energy of the products of dissociation which are formed (generally CO, OH, O, H, NO, and N gases) and is usually considered in the thermodynamic calculations for the engine chamber.

In the majority of cases, we perform the thermal computations for a ZhRD for various pressures in the combustion chamber and various ex-

cess oxidizer coefficients in the fuel so that we may select optimum values later on.

SECTION 6. DETERMINING THE ENERGY CONTENT OF PRODUCTS OF FUEL COMBUSTION

The amount of energy contained in a unit of weight of the products of combustion for a given fuel in cycles with constant pressure is called the energy content of the products of fuel combustion.

The energy content I_k of the products of physically complete combustion for a given fuel in an engine combustion chamber, at the corresponding temperature T_k , consists of thermal energy I_{tepl} ,* chemical energy I_{dis} ,* and the kinetic energy I_{kin} * developed by the motion of these products, i.e., $I_k = I_{tepl} + I_{dis} + I_{kin}$.

In present-day ZhRD combustion chambers, gas velocity is negligible, and therefore one may assume $I_{kin} = 0$ and consider that $I_k = I_{tepl} + I_{dis}$.

This sum of energies is sometimes called the enthalpy of the products of fuel combustion.

Due to a high value of T_k , the energy I_{tepl} developed by gas-molecule vibrational motion is a major fraction of the enthalpy, and gas-dissociation energy I_{tepl} is a relatively smaller portion, whose value, for a given fuel, is a function of the pressure p_k in the combustion chamber and the excess oxidizer coefficient α . The higher T_k is at a given p_k , the greater is I_{dis} . As p_k increases, the value of I_{dis} decreases.

To plot the enthalpies for gases formed during fuel combustion,

$$\begin{aligned} &*[I_{тепл} = I_{tepl} = I_{тепловaya} = I_{thermal}; \\ &I_{дис} = I_{dis} = I_{диссоциация} = I_{dissociation}; \\ &I_{кин} = I_{kin} = I_{кинетическая} = I_{kinetic}.] \end{aligned}$$

we use a system in which the enthalpies of gases O_2 , H_2 , N_2 , F_2 , Cl_2 , and C are assumed as equal to zero at a temperature of $20^\circ C$.

The energy contents of gases at a given temperature are given in Appendix I.

We determine the energy content of products of fuel combustion by the following formulas:

1) molar

$$I'_x = \sum M_i I'_i = \frac{M_x}{p_x} \sum p_i I'_i \text{ kcal/kmole}, \quad (6.20)$$

since the number of moles (M_1) of the i-th gas in the mixture $M_1 = (M_k/p_k) p_t$;

2) weight

$$I_x = \frac{I'_x}{p_x + \sigma \gamma_p p_o + 18 (m_r + \sigma \gamma_p m_o)} = \frac{I'_x}{p_x M_x} = \frac{1}{p_x M_x} \sum p_i I'_i \text{ kcal/kg}, \quad (6.21)$$

where p_1 is the partial pressure of the i-th gas in the mixture, in atm abs; I'_1 is the energy content of this gas in the mixture, in kcal/kmole; M_k is the number of kmole of the products of combustion from 1 kmole of combustible; and $p_x = \frac{1}{p_x} \sum p_i p_i$ is the molecular weight of these products.

Computation of the energy content of a fuel and the products of its combustion must be carried out by using this coordinate system.

Example 1. Determine the enthalpy of the products of combustion of kerosene with liquid oxygen when $\alpha = 0.8$; $p_k = 40$ atm, $p_v = 1$ atm, and $T_k = 3600^\circ K$; the composition is as follows: $p_{H_2O} = 12.432$; $p_{H_2} = 2.852$; $p_H = 1.275$; $p_{OH} = 2.632$; $p_{CO} = 12.187$; $p_{CO_2} = 6.513$; $p_{O_2} = 1.324$, and $p_O = 0.785$ atm.

Solution.

1. Molecular weight of the given gas mixture

$$p_k = \frac{1}{p_k} \sum p_i p_i = \frac{1}{40} (18 \cdot 12,432 + 2 \cdot 2,852 + 1 \cdot 1,275 + \\ + 17 \cdot 2,632 + 28 \cdot 12,187 + 44 \cdot 6,513 + 32 \cdot 1,324 + 16 \cdot 0,785) = 23,968.$$

2. Enthalpy of this gas mixture

$$I_k = \frac{1}{p_k p_k} \sum p_i I_i = \frac{1}{23,968 \cdot 40} [12,432 (-20,082,2) + 2,852 \cdot 26,649,6 + \\ + 1,275 \cdot 68,510,0 + 2,632 \cdot 36,913,7 + 12,187 \cdot 1336,4 + \\ + 6,513 (-48,212,2) + 1,324 \cdot 29,287,8 + 0,785 \cdot 75,710,0] = -189,0 \text{ kcal/kg.}$$

SECTION 7. THE ESSENCE OF ZhrD CHAMBER THERMODYNAMIC DESIGN

ZhrD chamber thermodynamic design consists of the determination of the composition, temperature, and other parameters of the products of fuel combustion in the combustion chamber and in the nozzle outlet section, the exhaust velocity, and the specific thrust, from which we compute the basic geometrical dimensions of the combustion chamber and chamber nozzle as well as the volumes of the engine fuel tanks.

Thermodynamic computations for engine-chamber combustion cycles and gas outflows from nozzles are usually based on the following assumptions:

1. Fuel combustion is entirely completed in the combustion chamber and proceeds at a constant pressure, which is valid when $F_k/F_{kr} > 5$.
2. The products of fuel combustion at the end of the combustion chamber are a dissociated gas mixture, in a state of complete chemical and energy equilibrium corresponding to the given pressure in the combustion chamber and the temperature which has been established therein.
3. The excess oxidizer coefficient, which is characteristic for the chemical composition of the products of fuel combustion, is the same across a cross section of the combustion chamber and does not change throughout the length of the nozzle.
4. The kinetic energy of the products of combustion, during their motion in the combustion chamber, is negligible in comparison to the

enthalpy of the gases, and is therefore assumed to be equal to zero.

5. As the products of fuel combustion flow in the chamber nozzle, a complete equilibrium change in the thermodynamic state and composition of the gases takes place in accordance with the change in pressure and temperature.

6. There is no gas friction against the surface of the chamber-nozzle liner and no heat transfer to the liner.

7. The gas stream in the engine chamber nozzle is isentropic, i.e., it occurs at a constant value of entropy; since the reactions of combustion are entirely completed in the combustion chamber, there is no fuel combustion in the surrounding medium or heat transfer from the gas to the surrounding medium.

8. The gas stream in the chamber nozzle is also unidimensional and steady.

The first four conditions mentioned are assumed on the basis of the determination of the temperature and composition of the products of combustion in the engine combustion chamber, and the four latter assumptions describe the schematization for the process of gas outflow from the chamber nozzle.

The basic initial data for thermodynamic design of an engine are usually the following:

- 1) the engine's absolute nominal thrust;
- 2) the engine's designation and operating program;
- 3) the characteristics of the combustible and oxidizer;
- 4) the pressure of the gases in the engine combustion chamber and in the nozzle outlet section.

The parameters and magnitudes which are missing, when designing an engine, are selected in the process of the appropriate computations, starting from the engine operating conditions, and its economic,

structural, and other considerations.

Sometimes the type of fuel is not given; we then select it in accordance with the engine operating conditions and considerations of efficiency, cost, simplicity of engine operation, obtaining the best flight characteristics for the weapon, and so forth.

The correct selection of parameters for designing an engine presents great practical difficulties, since, so far, few experimental data have been accumulated concerning this problem. For some parameters, we may succeed in establishing, with a small error, their limitations of possible change for each specific case by means of computation methods, or we may ascertain the nature of their effect on the basic operating characteristics of the engine, which facilitates computations considerably.

In the majority of cases, an engine thermodynamic computation is performed for several different pressures in the combustion chamber and excess oxidizer coefficients in the fuel. Later on, we use the optimum value of these factors for computing the engine to the second approximation, allowing for the missile's characteristics.

We usually design an engine in accordance with a given operating regime, in the following order.

1. We determine the composition and temperature of the products of fuel combustion in the combustion chamber and in the nozzle outlet section, the exhaust velocity and specific thrust, the gas-pressure impulse in the combustion chamber, and the mean exponent of the adiabatic process of gas outflow from the combustion chamber nozzle (in accordance with the equation associating pressure and the specific volume of gases).

2. We determine the basic geometrical characteristics of the combustion chamber and nozzle (volume, diameter, and length of combustion

chamber, diameter of the critical section [throat] and outlet section, and the length of the nozzle, combustion-chamber shape, and nozzle profile).

3. We perform the computations and construct the curves characterizing the change in gas parameters as a function of pressure in the combustion chamber and excess oxidizer in the fuel.

4. We perform the computations and construct the curves characterizing change in gas parameters throughout the length of the engine chamber nozzle.

Later on, we may compute and construct the curves for the throttle and altitude characteristics of the engine, select and design the fuel-atomizing unit, the cooling system for the combustion chamber and nozzle, and the propellant-feed system, and perform the engine strength computations.

An engine's thermodynamic design may be carried out both by analytic and graphic methods. The graphic method is based on the use of entropy diagrams which were constructed earlier. The analytic method is used in cases when one must design either one or a small number of engines and the graphic method when it is necessary to design a large series of engines using the same fuel.

Although the thermodynamic designing of an engine by the graphic method (by using entropy diagrams) is somewhat faster than the analytic method, constructing the required diagrams (if they are not already available) requires a great expenditure of time.

In designing a ~~ZhRD~~ ZhRD, a number of the problems we have mentioned must be solved as a unit, since only under this condition may we correctly evaluate and select the optimum parameters, perform the required calculations for the engine, and, subsequently, produce the most practicable engine design.

SECTION 8. EQUATIONS OF THE CONSTANTS OF EQUILIBRIUM OF GAS-DISSOCIATION REACTIONS AND EQUATIONS OF MATERIAL BALANCE

O We use the equations of the constants of equilibrium of gas-dissociation reactions and the equations of material balance (the equality between the weights of the separate elements in the fuel and in the fuel's products of combustion) to determine the theoretical temperature and composition of the products of fuel combustion in a combustion chamber or in an engine-nozzle outlet. We will therefore briefly consider these equations.

A fuel, which consists chiefly of carbon C, hydrogen H, oxygen O, and nitrogen N, burns at a high temperature in a ZhRD combustion chamber. The products of fuel combustion thus obtained dissociate considerably and may consist of the following gases: CO_2 , CO, H_2O , H_2 , OH, H, O_2 , O, N_2 , NO, and N. If the fuel contains other elements, the composition of its combustion products will, accordingly, be different.

() The weight content of each of these gases in the mixture is a function of temperature and pressure and may be expressed in the form of partial pressures. To determine n partial pressures of the gases, we must have n equations.

The dependence of the composition of products of fuel combustion on temperature is quite marked, since as temperature increases gas dissociation increases considerably and when it decreases gas dissociation also decreases. Pressure has a smaller effect on the composition of the products of combustion, as an increase in pressure somewhat suppresses gas dissociation and increases the amount of the products of complete combustion.

O At given values of temperature and pressure, a state of chemical equilibrium may be established between the different components of the products of fuel combustion. When temperature or pressure changes,

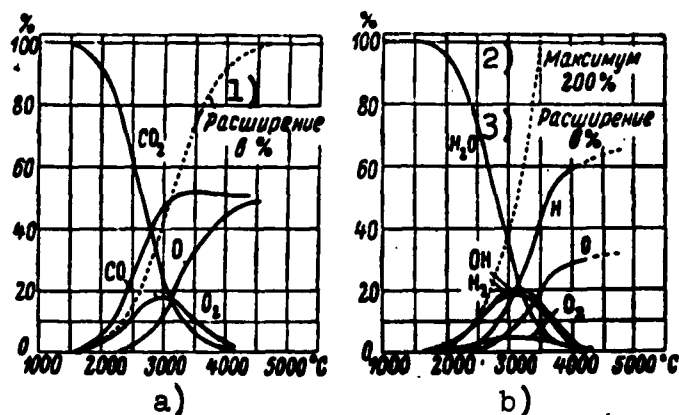


Fig. 6.8. Dissociation of CO_2 and H_2O as temperature rises. 1) Expansion in %; 2) maximum 200%; 3) expansion in %.

this state of equilibrium is disrupted, and the products of combustion, changing their composition, change to a new state of chemical equilibrium. Figure 6.8 shows the computed curves for the change in volume content of the gases in the products of combustion of kerosene ($C_g = 0.87$ and $H_g = 0.13$ kg/kg) with oxygen, when $\alpha = 0.86$ and $p_k = 10$ atm abs, as a function of temperature.

The curves show that if the combustion temperature is lower than 2500°C , one may neglect the dissociation of the molecular gases of oxygen, hydrogen, and nitrogen, as well as NO formation, when performing technical computations. At a temperature lower than 1500°C , dissociation is so insignificant that, in technical computations, a gas whose temperature is below 1500°C may be considered as undissociated.

CO_2 dissociation begins at a temperature of about 1500°C (see Fig. 6.8a), and at about 2000°C almost 10% of the CO_2 has decomposed to CO and O_2 . At 2200°C the decomposition of molecular oxygen into atoms becomes considerable. When temperature is increased further, dissociation increases rapidly. At 2500°C almost half of the original CO_2 is dissociated. At 3000°C the amount of molecular oxygen O_2 attains max-

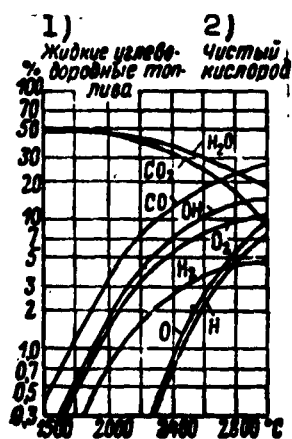


Fig. 6.9. Composition of products of combustion of a hydrocarbon combustible with oxygen at various temperatures. 1) Liquid hydrocarbon fuels; 2) pure oxygen.

imum magnitude, and at even greater temperatures the gas will consist almost entirely of CO and atomic oxygen O.

Because of this molecular decomposition, the products which have been formed expand considerably, i.e., besides expansion as a result of temperature changes, expansion as a consequence of the chemical change of state of the product also occurs.

The corresponding picture of H_2O dissociation (see Fig. 6.8b) is analogous to what we have considered, but is complicated by the earlier appearance of hydroxyl OH and

by molecular hydrogen breaking up into atoms. Here, H_2 and OH appear in almost equal amounts along the entire temperature range.

The curves of these graphs show that atomic products become noticeable even at a temperature of about 2000°C and at 2500°C attain an order of 1%.

Figure 6.9 shows the composition of products of combustion of a liquid hydrocarbon combustible with oxygen. Computations show that for hydrocarbon combustibles, atomic products may be about 20% of the total volume of the products.

The change in chemical composition of the products of fuel combustion as a function of temperature may be characterized by the appropriate equations.

We will consider these equations for a case in which the fuel consists of the elements C, H, O, and N, since this case is most characteristic for the fuels used in ZhRD at the present time.

The general equation of chemical reaction, as a result of which

initial substances A and B change to products C and D, and the reverse, has the form



where a, b, c, and d, are the numbers of molecules of the corresponding substances which participate in the elementary event of the chemical reaction.

At given values of temperature and pressure, the chemical reaction occurs in both directions at a different rate, the magnitude of which is a function of the partial pressures of the reacting gases.

The rate at which the forward chemical reaction (formation of products of fuel combustion) takes place

$$V_1 = K_1 p_A^a p_B^b, \quad (6.23)$$

and the rate for the reverse chemical reaction (the dissociation of combustion products) will be

$$V_2 = K_2 p_C^c p_D^d, \quad (6.24)$$

where K_1 and K_2 are the constants for the rates of the chemical reactions, and p_A , p_B , p_C , and p_D are the partial pressures of the reacting gases.

An equilibrium between the forward and reverse chemical reactions is established upon condition of equality

$$V_1 = V_2 \text{ or } K_1 p_A^a p_B^b = K_2 p_C^c p_D^d. \quad (6.25)$$

The ratio of the constants of the rates at which forward and reverse chemical reactions take place, i.e.,

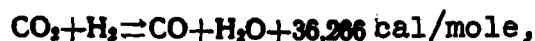
$$\frac{K_1}{K_2} = \frac{p_C^c p_D^d}{p_A^a p_B^b} = K_p, \quad (6.26)$$

is called the constant of the chemical equilibrium, as defined by the partial pressures of the gases.

A change in the chemical composition of the products of fuel combustion mentioned above, representing 11 chemically active gases, may

be characterized as the totality of the equations of reactions of dissociation and constants of equilibrium shown in Table 6.1 (see page 335).

For computing products of fuel combustion, an equation obtained by subtracting Eq. (6-28), contained in this table, from Eq. (6-1) [sic] is convenient, i.e.,



for which the equation of the constant of equilibrium has the form

$$K_{28} = \frac{p_{\text{CO}} p_{\text{H}_2\text{O}}}{p_{\text{CO}_2} p_{\text{H}_2}} = f_{28}(T), \quad (6.34)$$

where T is the absolute temperature, in $^{\circ}\text{K}$, at which an equilibrium of the chemical reaction occurs.

It is easy to see that the value of the square root of p_{O_2} is general for the majority of the constants of equilibrium shown in Table 6.1, namely:

$$\sqrt{p_{\text{O}_2}} = K_{p1} \frac{p_{\text{CO}_2}}{p_{\text{CO}}} = K_{p2} \frac{p_{\text{H}_2\text{O}}}{p_{\text{H}_2}} = K_{p4} \frac{p_{\text{NO}}}{\sqrt{p_{\text{N}_2}}} = \frac{p_{\text{O}}}{\sqrt{K_{p5}}}. \quad (6.35)$$

From this equality it follows that one constant of equilibrium may be replaced by another, for example:

$$K_{p1} = K_{p2} \frac{p_{\text{H}_2\text{O}} p_{\text{CO}}}{p_{\text{H}_2} p_{\text{CO}_2}} = K_{p4} \frac{p_{\text{NO}} p_{\text{CO}}}{p_{\text{CO}_2} \sqrt{p_{\text{N}_2}}} = \frac{p_{\text{O}} p_{\text{CO}}}{p_{\text{CO}_2} \sqrt{K_{p5}}}. \quad (6.36)$$

The values of the corresponding constants K_r^* of chemical equilibrium for the products of fuel combustion depend only on temperature and may be taken from the tables (see Appendices II and III) for computations. When forward reactions are the reactions of dissociation, the values of the constants of equilibrium increase with a rise in temperature.

Analytical determination of the values of K_r as a function of temperature is attended with great difficulties since to do this one must know the change in the system energy as the chemical reaction

$$*[K_p = K_r = K_{\text{равновесие}} = K_{\text{equilibrium}}]$$

TABLE 6.1

Уравнения реакций диссоциации газов с указанием химических энергий в ккал/кмоль 1)	Уравнения констант равновесия реакций диссоциации газов 2)
$\text{CO}_2 \rightleftharpoons \text{CO} + 0.5\text{O}_2 + 1,051$	$K_{p1} = \frac{p_{\text{CO}} p_{\text{O}_2}^{0.5}}{p_{\text{CO}_2}} = f_1(T). \quad (6.27)$
$\text{H}_2\text{O} \rightleftharpoons \text{H}_2 + 0.5\text{O}_2 + 57,785$	$K_{p2} = \frac{p_{\text{H}_2} p_{\text{O}_2}^{0.5}}{p_{\text{H}_2\text{O}}} = f_2(T). \quad (6.28)$
$\text{H}_2\text{O} \rightleftharpoons \text{OH} + 0.5\text{H}_2 + 8,455$	$K_{p3} = \frac{p_{\text{OH}} p_{\text{H}_2}^{0.5}}{p_{\text{H}_2\text{O}}} = f_3(T). \quad (6.29)$
$\text{N}_2 + \text{O}_2 \rightleftharpoons 2\text{NO} + 21,600$	$K_{p4} = \frac{p_{\text{NO}}^2}{p_{\text{N}_2} p_{\text{O}_2}} = f_4(T). \quad (6.30)$
$\text{H}_2 \rightleftharpoons 2\text{H} + 52,082$	$K_{p5} = \frac{p_{\text{H}}^2}{p_{\text{H}_2}} = f_5(T). \quad (6.31)$
$\text{O}_2 \rightleftharpoons 2\text{O} + 80,834$	$K_{p6} = \frac{p_{\text{O}}^2}{p_{\text{O}_2}} = f_6(T). \quad (6.32)$
$\text{N}_2 \rightleftharpoons 2\text{N} + 112,500$	$K_{p7} = \frac{p_{\text{N}}^2}{p_{\text{N}_2}} = f_7(T). \quad (6.33)$

1) Equations of the reactions of gas dissociation, indicating the chemical energies in cal/kmole; 2) equations of constants of equilibrium of reactions of gas dissociation.

takes place, as well as a number of magnitudes which are characteristic of the gas molecules. We may define the values of K_p with greater precision in accordance with the degree to which we study this problem. Therefore, in computations, one should approximate to the later, more precise results.

The equations of material balance equate the amounts of the different elements in the fuel before combustion to their amounts in the products of combustion of this fuel.

If 1 kg of ordinary fuel consists, as a general rule, of the elements C_g , H_g , O_g , N_g , C_o , H_o , O_o , and N_o by weight, the weight fractions of each of these elements may be determined in accordance with

the formulas:

a) carbon

$$C_t = \frac{C_r + \chi C_o}{1 + \chi} \text{ kg/kg};$$

b) hydrogen

$$H_t = \frac{H_r + \chi H_o}{1 + \chi} \text{ kg/kg};$$

c) oxygen

$$O_t = \frac{O_r + \chi O_o}{1 + \chi} \text{ kg/kg};$$

d) nitrogen

$$N_t = \frac{N_r + \chi N_o}{1 + \chi} \text{ kg/kg},$$

where $C_t + H_t + O_t + N_t = 1 \text{ kg}$.

Thus, the equations of material balance for the fuel elements will have the form:

$$C_t = \frac{C_r + \chi C_o}{1 + \chi} = \frac{12}{\sum_i \mu_i p_i} (p_{CO_2} + p_{CO}) \text{ kg/kg}; \quad (6.37)$$

$$H_t = \frac{H_r + \chi H_o}{1 + \chi} = \frac{1}{\sum_i \mu_i p_i} (2p_{H_2O} + 2p_{H_2} + p_{OH} + p_H) \text{ kg/kg}; \quad (6.38)$$

$$O_t = \frac{O_r + \chi O_o}{1 + \chi} = \frac{16}{\sum_i \mu_i p_i} (2p_{CO_2} + p_{CO} + p_{H_2O} + p_{OH} + 2p_{O_2} + p_{O} + p_{NO}) \text{ kg/kg}; \quad (6.39)$$

$$N_t = \frac{N_r + \chi N_o}{1 + \chi} = \frac{14}{\sum_i \mu_i p_i} (2p_{N_2} + p_{NO} + p_N) \text{ kg/kg}. \quad (6.40)$$

To exclude the unknown quantity $\sum_1 \mu_1 p_1$ from these equations, one must divide them term by term by one of these same equations.

If, for example, we divide Equations (6.37), (6.38), and (6.40) by Eq. (6.39) [sic, probably (6.39)], we obtain equations of material balance in the following forms:

$$\frac{C_t}{O_t} = \frac{C_r + \chi C_o}{O_r + \chi O_o} = \frac{12}{16} \frac{p_{CO_2} + p_{CO}}{2p_{CO_2} + p_{CO} + p_{H_2O} + p_{OH} + 2p_{O_2} + p_{O} + p_{NO}}; \quad (6.41)$$

$$\frac{H_t}{O_t} = \frac{H_r + \chi H_o}{O_r + \chi O_o} = \frac{1}{16} \frac{2p_{H_2O} + 2p_{H_2} + p_{OH} + p_H}{2p_{CO_2} + p_{CO} + p_{H_2O} + p_{OH} + 2p_{O_2} + p_{O} + p_{NO}}; \quad (6.42)$$

$$\frac{N_T}{O_T} = \frac{N_T + \gamma N_0}{O_T + \gamma O_0} = \frac{14}{16} \frac{2p_{N_2} + p_{NO} + p_N}{2p_{CO_2} + p_{CO} + p_{H_2O} + p_{OH} + 2p_{O_2} + p_O + p_{NO}} \quad (6.43)$$

If a fuel contains water before combustion, as a general rule the following number of atoms of the different elements are contained in the fuel (by computation per kmole of combustible):

- a) carbon: $c_1 + \alpha \chi_\mu c_2$;
- b) hydrogen: $h_1 + \alpha \chi_\mu h_2 + 2(m_g + \alpha \chi_\mu m_o)$;
- c) oxygen: $o_1 + \alpha \chi_\mu o_2 + m_g + \alpha \chi_\mu m_o$;
- d) nitrogen: $n_1 + \alpha \chi_\mu n_2$,

and equations of material balance may be expressed in the following manner:

$$\frac{C_T}{O_T} = \frac{c_1 + \alpha \chi_\mu c_2}{o_1 + m_r + \alpha \chi_\mu (o_2 + m_o)} = \frac{p_{CO_2} + p_{CO}}{2p_{CO_2} + p_{CO} + p_{H_2O} + p_{OH} + 2p_{O_2} + p_O + p_{NO}}; \quad (6.41')$$

$$\frac{H_T}{O_T} = \frac{h_1 + 2m_r + \alpha \chi_\mu (h_2 + m_o)}{o_1 + m_r + \alpha \chi_\mu (o_2 + m_o)} = \frac{2p_{H_2O} + 2p_{H_2} + p_{OH} + p_H}{2p_{CO_2} + p_{CO} + p_{H_2O} + p_{OH} + 2p_{O_2} + p_O + p_{NO}}; \quad (6.42')$$

$$\frac{N_T}{O_T} = \frac{n_1 + \alpha \chi_\mu n_2}{o_1 + m_r + \alpha \chi_\mu (o_2 + m_o)} = \frac{2p_{N_2} + p_{NO} + p_N}{2p_{CO_2} + p_{CO} + p_{H_2O} + p_{OH} + 2p_{O_2} + p_O + p_{NO}} \quad (6.43')$$

If the fuel does not contain nitrogen, Eqs. (6.30) and (6.33) are not necessary, and Eqs. (6.40) or (6.42) and (6.43) are simplified.

SECTION 9. DETERMINING THE THEORETICAL TEMPERATURE AND COMPOSITION OF PRODUCTS OF FUEL COMBUSTION IN A THIRD COMBUSTION CHAMBER

We determine the theoretical temperature and the composition of fuel combustion products corresponding to it at a given pressure in the combustion chamber in accordance with the following system of equations:

- 1) the equations of constants of equilibrium (6.27)-(6.33);
- 2) the equations of material balance (6.37)-(6.40) or (6.41)-(6.43);

3) the equation of balance of partial pressures for products of fuel combustion (gases);

$$p_z = \sum_i p_i = p_{CO_2} + p_{H_2O} + p_{CO} + p_N + p_{H_2} + p_{O_2} + p_{OH} + p_{NO} + p_H + p_O + p_{H_2O} \quad (6.44)$$

4) the equation of equal enthalpies of a fuel and the products of fuel combustion (equation of conservation of energy):

$$I_1 = I_2 = \frac{1}{\mu_k p_k} \sum_i I_i p_i \text{ kcal/kg}, \quad (6.45)$$

where I_i is the enthalpy of 1 kmole of the i -th gas in the mixture, from the table (see Appendix I); and μ_k is the apparent molecular weight of the products of fuel combustion, determined by using the formula

$$\mu_k = \frac{1}{p_k} \sum_i \mu_i p_i \quad (6.46)$$

here μ_i is the molecular weight of the i -th gas in the mixture.

Computations for determining partial pressures and temperatures of the gases in an engine combustion chamber are most frequently carried out in the following manner.

1. We select three values of assumed gas temperatures (T_{k1} , T_{k2} , and T_{k3}) in the combustion chamber and determine the partial pressures p_i of the different gases in the mixture corresponding to the temperatures by using Eqs. (6.27)-(6.44).

2. We compute the enthalpies (I_{k1} , I_{k2} , and I_{k3}) of the gases in the combustion chamber at these temperatures and at the values of p_i which we have found, by using Eq. (6.45).

3. By means of the three computed points, we construct a curve of I_k as a function of T_k (Fig. 6.10), and by means of it locate the unknown theoretical temperature T_k of the gases in the engine combustion chamber (when fuel burns to a chemical state of equilibrium of the

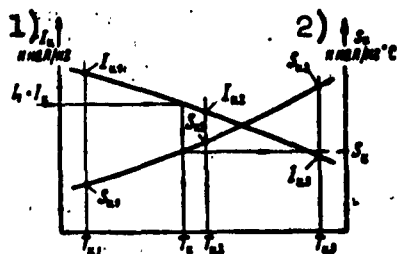


Fig. 6.10. Determining temperature and entropy of the gases in an engine combustion chamber. 1) I_k , kcal/kg; 2) S_k , kcal/kg°C.

composition of the gases, a temperature must be established at which the enthalpy I_k of the gases is equal to the enthalpy I_t of the burning fuel).

4. We determine the theoretical composition of the products of fuel combustion at the temperature T_k found, by means of Eqs. (6.27)-(6.44) or by graphic interpolation of the values of p_1 which were computed earlier at the three selected values of temperature; the latter are used for constructing the corresponding curves of p_1 as a function of T_{k1} , T_{k2} , and T_{k3} , and we may locate the theoretical values of p_1 corresponding to temperature T_k by using these curves.

5. Finally, we determine enthalpies, molecular weights, gas constants, and other theoretical parameters for the products of fuel combustion at this same temperature T_k (Figs. 6.11-6.23).

We may also approximately determine the actual temperature of the gases in the engine combustion chamber by using the curve in Fig. 6.10 if we reduce the calorific values of the combustible and oxidizer, having multiplied them by the coefficient $\varphi_{p,k}$ of physical completeness of fuel combustion, when computing the fuel enthalpy.

The rated values of the theoretical gas temperatures in the combustion chamber are selected by using the computed tables (5.20 and 5.21) or the curves in Figs. 6.11-6.17.

One must bear in mind that gas temperature in a ZhRD combustion chamber is chiefly a function of the type of propellant components, their ratio to each other (the excess oxidizer coefficient), and the pressure in the combustion chamber.

There are several methods for solving the system of equations

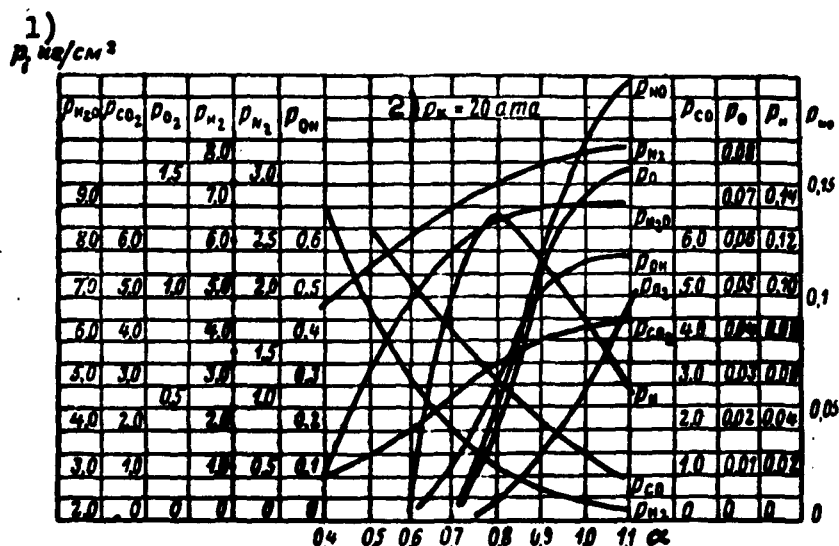


Fig. 6.11. Change in composition for products of combustion of tractor kerosene with nitric acid of 96% concentration as a function of the excess oxidizer coefficient. 1) p_1 , kg/cm²; 2) $p_k = 20$ atm abs.

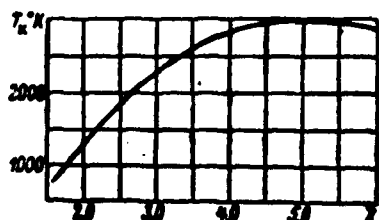


Fig. 6.12. Temperature of products of combustion of kerosene and 96% nitric acid at various values of χ with a p_k of 10-40 atm abs.

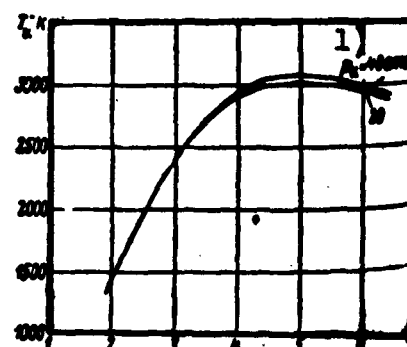


Fig. 6.13. Temperature of products of combustion of kerosene and an oxidizer consisting of 80% HNO_3 of 98% concentration and 20% N_2O_4 at various values of χ and p_k . 1) $p_k = 40$ atm abs.

(6.27)-(6.44) we have given for determining partial pressures of the products of fuel combustion at a selected temperature value and a given pressure in an engine combustion chamber. However, successive approximations are the most convenient method, which, depending on the

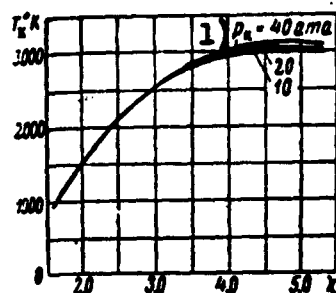


Fig. 6.14. Temperature of product of combustion of kerosene and an oxidizer consisting of 60% HNO_3 of 98% concentration and 40% N_2O_4 at various values of χ and p_k . 1) $p_k = 40$ atm abs.

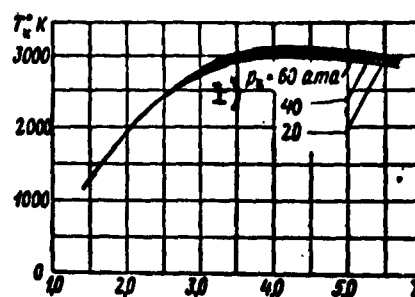


Fig. 6.15. Temperature of products of combustion of Tonka-250 and an oxidizer consisting of 80% HNO_3 of 98% concentration and 20% N_2O_4 at various values of χ and p_k . 1) $p_k = 60$ atm abs.

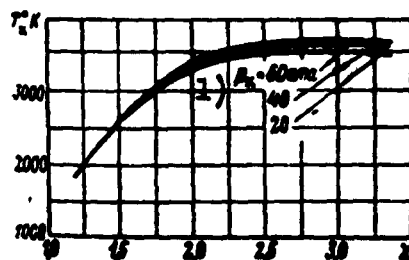


Fig. 6.16. Temperature of products of combustion of kerosene and liquid oxygen at various values of χ and p_k . 1) $p_k = 60$ atm abs.

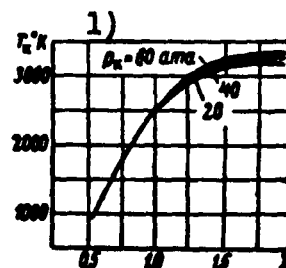


Fig. 6.17. Temperature of products of combustion of 93.5% ethyl alcohol and liquid oxygen at various values of χ and p_k . 1) $p_k = 60$ atm abs.

temperature of the combustion products, may give different results, since the method, giving a convergent sequence of roots in one case, makes a sequence of computations divergent in other cases.

In solving the equations by the method of successive approximations, at first we equate the partial pressures of those gases whose percentage content in the gas mixture, under given fuel combustion

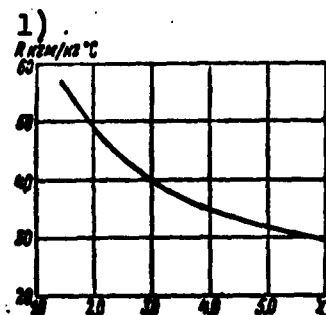


Fig. 6.18. Gas constant of products of combustion of kerosene and nitric acid of 96% weight concentration at various values of χ (for these combustion products, R is practically independent of temperature). 1) R , kg-m/kg°C.

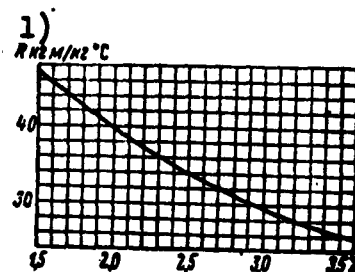


Fig. 6.19. Gas constant for combustion products of kerosene and liquid oxygen at various values of χ (for these combustion products R_k is almost independent of pressure). 1) R , kg-m/kg°C.

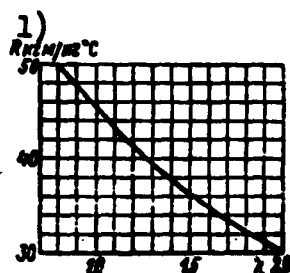


Fig. 6.20. Gas constant for combustion products of ethyl alcohol of 93.5% weight concentration and liquid oxygen at various values of χ . 1) R , kg-m/kg°C.

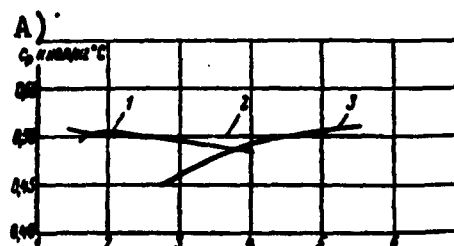


Fig. 6.21. Heat capacity for fuel combustion products at various coefficients of composition: 1) kerosene + 80% HNO_3 of 98% concentration + 20% N_2O_4 ; 2) Tonka-250 + 80% HNO_3 of 98% concentration + 20% N_2O_4 ; 3) kerosene + HNO_3 of 96% weight concentration. A) c_p , kcal/kg°C.

conditions, is assumed to be small, to zero, and compute the partial pressures of the remaining gases. Using the values of p_1 that were found, we determine the partial pressures of those gases whose values at first were assumed as equal to zero; then, using these values of p_1 , we compute the p_1 of the basic gases in the second approximation.

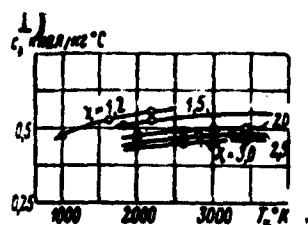


Fig. 6.22. Heat capacity c_p for combustion products of kerosene and liquid oxygen at various values of χ as a function of temperature. 1) c_p , kcal/kg°C.

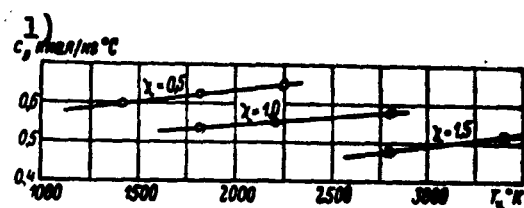


Fig. 6.23. Heat capacity c_p for combustion products of ethyl alcohol of 93.5% weight concentration and liquid oxygen at various values of χ as a function of temperature. 1) c_p , kcal/kg°C.

These operations are repeated until such time as we attain the required exactness in computing p_1 , and by this means we satisfy the condition

$$\sum_1 p_1 = p_k.$$

If the difference in the values of p_1 of the following and previous approximations for a given computation does not exceed about 0.02 atm abs, the computation is completed with that.

The computations' accuracy may be checked by means of:

- a) determining the constants of equilibrium in accordance with the computed p_1 and comparing their values with the initial (table) values;
- b) checking to see if the equations of absolute material balance (6.37)-(6.39) are satisfied by the computed values of p_1 . If these equations are satisfied, there are no errors in the computations which have been carried out.

If the fuel contains nitrogen, we recommend that one reduce the partial pressures of O_2 , NO , N , O , H , and OH gases to zero in the first approximation. Under this condition, five unknown partial pressures of the basic gases remain, altogether, in the system of equations:

$$p_{CO_2}, p_{H_2O}, p_{CO}, p_{N_2}, \text{ and } p_{H_2}.$$

To determine the values of these p_1 , we use Eqs. (6.41)-(6.44). Equation (6.34) serves as a supplementary here.

Solving this system of equations, we determine, in the first approximation, the values of the partial pressures for the basic gases (p_{CO_2} , p_{H_2O} , p_{CO} , p_{N_2} , and p_{H_2}), which we then substitute into Eqs. (6.27)-(6.33), and find pressures p_{O_2} , p_{OH} , p_{NO} , p_H , p_O , and p_N . Later we determine the partial pressures for the basic gases in the second approximation by using Eqs. (6.4)-(6.44).

If the differences between the partial pressures of the first and second approximations turn out to be greater than permitted by the design, we perform the third approximation, and so forth.

To reduce the number of approximations at subsequent, higher selected values of assumed temperature (T_{k2} or T_{k3}) in the combustion chamber, we recommend that after the first approximation one assume the composition of the gases (the values of p_1) that were computed at the previous, lower temperature (T_{k1} or T_{k2}).

This means that, for example, if the values of p_1 were determined at a temperature $T_{k1} = 2800^\circ K$, these values should be assumed for the composition of the gases in the first approximation when computing the partial pressures of the gases at a temperature $T_{k2} = 3000^\circ K$, for example, and p_1 should be determined in the second approximation, then in the third, etc., until the desired exactness in the computation results is obtained.

If a divergent sequence of roots should be observed in the computations, at first one should take the assumed magnitude for the partial pressure of one of the gases (for example, oxygen, p_{O_2}), and then compute the partial pressures of the other gases.

When there is no nitrogen in the fuel, we recommend the following order for solving the system of equations:

1) at temperatures of up to 2300°K, the method which brings results most quickly is that in which we equate the partial pressures p_O , p_H , p_{OH} , p_{CO} , and p_{O_2} to zero, if $\alpha < 1$, or equate p_O , p_H , p_{OH} , p_{CO} , and p_{H_2} to zero if $\alpha > 1$;

2) at temperatures from 2300 to 3000°K, we equate only pressures p_O , p_H , p_{OH} , and p_{O_2} to zero if $\alpha < 1$, or equate p_O , p_H , p_{OH} , and p_{H_2} to zero if $\alpha > 1$;

3) at temperatures above 3000°K, we recommend that pressures p_O , p_H , p_{H_2} , and p_{O_2} be equated to zero, and the remaining four unknown pressures be located from Eqs. (6.41)-(6.44) and the equation obtained by excluding pressures p_{O_2} and p_{H_2} from Eqs. (6.27)-(6.29), i.e.,

$$\frac{K_{p1}K_{p3}}{K_{p2}} = \frac{p_{CO}p_{OH}^2}{p_{CO}p_{H_2}p_O} = K_{eq}. \quad (6.47)$$

Thus, the computations become considerably more complex, since solution of the system of equations leads to an equation of the third degree. In this case, it is more practicable to select one of the partial pressures and solve the system of equations for determining the remaining values of p_i (preferably to assume the value of p_{O_2}). If $\sum p_i < p_k$ is obtained in the first approximation, one should increase p_i of the selected p_i of the second approximation in comparison with p_i of the first approximation, or the reverse, if $\sum p_i > p_k$.

Thus, the system for the first ten or eleven equations for determining p_i may be solved for several selected values of assumed gas temperature in the engine combustion chamber.

To determine the temperature of the gases in the engine combustion chamber, one may also assume only one arbitrary assumed value of T_k and determine the partial pressures of these gases corresponding to this temperature by the method mentioned above, and then compute the enthalpy I_k of the gas mixture according to Formula (6.45).

If the value of I_k that has been found does not agree with the enthalpy I_t of the fuel used, i.e., if $I_k \neq I_t$, one must assume another value of temperature T_k and repeat the computations until such time as the equality $I_k = I_t$ is attained. With a happy choice of temperature T_k , it is enough to perform two or three approximations.

The main difficulty when we perform these computations, as before, is in determining the equilibrium composition for the products of fuel combustion corresponding to the selected temperature in the engine combustion chamber.

In determining partial pressures by means of the system of equations given above, we assume only real and positive roots in our computations. The precision of the computations may be limited to the third or fourth decimal place.

SECTION 10. METHODS FOR SOLVING SYSTEMS OF EQUATIONS FOR DETERMINING THEORETICAL TEMPERATURE AND COMPOSITION OF PRODUCTS OF FUEL COMBUSTION

To simplify computations, the system of equations given above for determining the composition of the products of fuel combustion in an engine combustion chamber by the method of successive approximations may, for practical purposes, be placed in a more convenient form.

If the fuel contains nitrogen, it is practicable to change this system of equations in the following manner.

At first, we express Equations (6.37)-(6.40) in the form of ratios:

$$\frac{C_r}{N_r} = \frac{12}{14} \frac{p_{CO_2} + p_{CO}}{2p_{H_2O} + p_{NO} + p_N} \quad \text{or} \quad \frac{p_{CO_2} + p_{CO}}{2p_{H_2O} + A} = \frac{7}{8} \frac{C_r}{N_r} = Q, \quad (6.48)$$

whence

$$p_{CO_2} + p_{CO} = Q(2p_{H_2O} + A),$$

where $A = p_{NO} + p_N$;

$$\frac{H_r}{N_r} = \frac{1}{14} \frac{2p_{H_2O} + 2p_{H_2} + p_{OH} + p_H}{2p_{H_2O} + p_{NO} + p_N}$$

or

$$\frac{p_{H_2O} + 2p_{H_2} + B}{2p_{N_2} + A} = 14 \frac{H_T}{N_T} = R, \quad (6.49)$$

whence

$$p_{H_2O} + p_{H_2} = \frac{R}{2} (2p_{N_2} + A) - \frac{B}{2}.$$

where $B = p_{OH} + p_H$;

$$\frac{O_T}{C_T} = \frac{16p_{CO_2} + p_{CO} + p_{H_2O} + 2p_{O_2} + p_O + p_{OH} + p_{NO}}{p_{CO_2} + p_{CO}}$$

or

$$\frac{2p_{CO_2} + p_{CO} + p_{H_2O} + L}{p_{CO_2} + p_{CO}} = \frac{3}{4} \frac{O_T}{C_T} = S, \quad (6.50)$$

where

$$L = 2p_{CO_2} + p_O + p_{OH} + p_{NO}.$$

We then give Eq. (6.44) the form

$$p_K = p_{CO_2} + p_{H_2O} + p_{CO} + p_{N_2} + p_{H_2} + E, \quad (6.51)$$

where

$$E = p_{O_2} + p_{OH} + p_{NO} + p_H + p_O + p_N.$$

Having replaced the sums $p_{CO_2} + p_{CO}$ and $p_{H_2O} + p_{H_2}$ in Eq. (6.51) with their expressions taken from Eqs. (6.48) and (6.49), we obtain

$$p_K = Q(2p_{N_2} + A) + \frac{R}{2} (2p_{N_2} + A) - \frac{B}{2} + p_{N_2} + E.$$

whence

$$p_{N_2} = \frac{p_K - E + \frac{B}{2} - A(Q + \frac{R}{2})}{2Q + R + 1}. \quad (6.52)$$

From Eq. (6.22), we find

$$p_{CO} = Q(2p_{N_2} + A) - p_{CO}, \text{ or } p_{CO} = a - p_{CO}, \quad (6.53)$$

where $a = Q(2p_{N_2} + A)$.

Substituting the value of the sum $p_{CO_2} + p_{CO}$ in the numerator and denominator of Eq. (6.50), we obtain

$$\frac{p_{CO_2} + Q(2p_{N_2} + A) + p_{H_2O} + L}{Q(2p_{N_2} + A)} = S,$$

$$p_{H_2O} = Q(2p_{N_2} + A)(S - 1) - L - p_{CO_2} \text{ [sic]}$$

whence $p_{H_2O} = Q(2p_{N_2} + A)(S - 1) - D - p_{CO_2}$ [sic] or

$$p_{H_2O} = b - p_{CO_2}, \quad (6.54)$$

where $b = Q(2p_{N_2} + A)(S - 1) - D$.

From Eq. (6.23), we also find

$$p_{H_2} = \frac{R}{2}(2p_{N_2} + A) - \frac{E}{2} - p_{H_2O}$$

or, considering expression (6.54)

$$\begin{aligned} p_{H_2} &= \frac{R}{2}(2p_{N_2} + A) - \frac{E}{2} - Q(2p_{N_2} + A)(S - 1) + D + p_{CO_2} = \\ &= (2p_{N_2} + A) \left[\frac{R}{2} - Q(S - 1) \right] - \frac{E}{2} + D + p_{CO_2}, \text{ or } p_{H_2} = c - p_{CO_2}, \end{aligned} \quad (6.55)$$

where $c = (2p_{N_2} + A) \left[\frac{R}{2} - Q(S - 1) \right] - \frac{E}{2} + D$.

Since, when determining the composition of the products of fuel combustion in the first approximation, the values of A , B , D , and E are equal to zero, Eqs. (6.53)-(6.55) will have the form

$$\left. \begin{aligned} p_{N_2} &= \frac{p_{N_2}}{2Q + R + 1}; \quad p_{CO} = 2Qp_{N_2} - p_{CO_2}; \\ p_{H_2O} &= 2Qp_{N_2}(S - 1) - p_{CO_2} \text{ and } p_{H_2} = 2p_{N_2} \left[\frac{R}{2} - Q(S - 1) \right] - p_{CO_2}. \end{aligned} \right\} \quad (6.56)$$

These equations, together with Eq. (6.34), are basics for the subsequent solution. The equations of the constant of equilibrium (6.1-6.7) are supplementary; we also give them the form

$$\left. \begin{aligned} p_{O_2} &= \left(K_{p1} \frac{p_{CO_2}}{p_{CO}} \right)^2; \quad p_{OH} = K_{p2} \frac{p_{H_2O}}{\sqrt{p_{H_2}}}; \quad p_{NO} = \sqrt{K_{p4} p_{N_2} p_{O_2}}; \\ p_{H} &= \sqrt{K_{p5} p_{H_2}}; \quad p_{O} = \sqrt{K_{p6} p_{O_2}} \text{ and } p_{N} = \sqrt{K_{p7} p_{N_2}}. \end{aligned} \right\} \quad (6.57)$$

The order for solving the system of equations given here is as follows.

1. We compute coefficients Q , R , and S in accordance with Eqs. (6.48)-(6.50), using the data for the element composition of the fuel.
2. In the first approximation, we assume partial pressures p_{O_2} , p_{OH} , p_{NO} , p_H , p_O , and p_N are equal to zero, as a result of which A , B , D , and E will be equal to zero. Under this assumption, only pressures

p_{CO_2} , p_{H_2O} , p_{CO} , p_{N_2} , and p_{H_2} still remain unknown in the system of equations.

3. Having substituted the expressions for p_{CO} , p_{H_2O} , and p_{H_2} [see Eqs. (6.53)-(6.55)] given above in Eq. (6.34), we obtain

$$K_2 = \frac{p_{CO} p_{H_2O}}{p_{CO_2} p_{H_2}} = \frac{(a - p_{CO})(b - p_{CO})}{p_{CO_2}(c - p_{CO})} \quad (6.58)$$

By solving this quadratic equation, we find the value of p_{CO_2} .

From the two roots for solution of these equations, we choose the one which gives positive values of all remaining partial gas pressures.

Since inaccuracy in determining coefficients a , b , and c strongly hampers further computations, we recommend that the correctness of these computations be checked by the relationship $a + b + c = p_k - p_{N_2}$.

4. In accordance with Eqs. (6.53)-(6.55), we determine the values of p_{CO} , p_{H_2O} , and p_{H_2} , and also check to make sure that no errors have been committed. For this, by means of the value of p_1 which has already been found, we find the value of K_2 , and compare it with the initial data from the table.

5. In accordance with Eqs. (6.57), we compute, in the second approximation, the values of p_1 of these gases that were assumed as equal to zero in the first approximation. Then, by means of the values of p_{O_2} , p_{OH} , p_{NO} , p_H , p_O , and p_N that have been found, we determine the magnitudes of A , B , D , and E .

6. We determine p_{CO_2} , p_{H_2O} , p_{CO} , p_{H_2} , and p_{N_2} in the second approximation, in accordance with Eqs. (6.34) and (6.53)-(6.55).

If the differences between p_1 of the first and second approximations is greater than that permitted in the given design, we perform a third approximation, or following approximations, until we attain the desired accuracy in determining p_1 .

If the fuel does not contain nitrogen, we determine the partial

pressures of the products of combustion at a selected temperature and given pressure in the engine combustion chamber in the following manner.

1. In accordance with the data from existing computations or curves for products of fuel combustion, we select the value of the partial pressure of oxygen for the first approximation ($p_{O_2} = a^2$) and express the partial pressures of the remaining gases as functions of p_{CO_2} and p_{H_2O} in the following manner:

Общий вид исходной системы уравнений 1)	Расчетный вид уравнений, получаемых после соответствующих преобразований исходных уравнений 2)
$K_{p1} = \frac{p_{CO} p_{O_2}^{0.5}}{p_{CO_2}}$	$p_{CO} = K_{p1} \frac{p_{CO_2}}{p_{O_2}^{0.5}} = \frac{K_{p1}}{a} p_{CO_2} = b p_{CO_2}; (1)$ $b = \frac{K_{p1}}{a}$
$K_{p2} = \frac{p_{H_2} p_{O_2}^{0.5}}{p_{H_2O}}$	$p_{H_2} = K_{p2} \frac{p_{H_2O}}{p_{O_2}^{0.5}} = \frac{K_{p2}}{a} p_{H_2O} = c p_{H_2O}; (2)$ $c = \frac{K_{p2}}{a}$
$K_{p3} = \frac{p_{OH} p_{H_2}^{0.5}}{p_{H_2O}}$	$p_{OH} = K_{p3} \frac{p_{H_2O}}{p_{H_2}^{0.5}} = \frac{K_{p3} p_{H_2O}}{\sqrt{c p_{H_2O}}} = d \sqrt{p_{H_2O}};$ $d = \frac{K_{p3}}{\sqrt{c}}; (3)$
$K_{p4} = \frac{p_H^2}{p_{H_2}}$	$p_H = \sqrt{K_{p4} p_{H_2}} =$ $= \sqrt{K_{p4} c p_{H_2O}} = e \sqrt{p_{H_2O}}; (4)$ $e = \sqrt{c K_{p4}}$
$K_{p5} = \frac{p_O^2}{p_{O_2}}$	$p_O = \sqrt{p_{O_2} K_{p5}} = a \sqrt{K_{p5}} = f; (5)$

- 1) General form of initial system of equations;
2) computed form of equations obtained after appropriate transformations in initial equations.

(Continued)

Общий вид исходной системы уравнений	Расчетный вид уравнений, получаемый после соответствующих преобразований исходных уравнений
<p>1)</p> <p>3) Уравнение относительного материального баланса:</p> $\frac{2(p_{H_2O} + p_{H_2}) + p_{OH} + p_H}{p_{CO_2} + p_{CO}} =$ $= 12 \frac{H_T}{C_T} = A$	<p>2)</p> <p>4) После подстановки полученных выше выражений для p_i в исходные уравнения относительного материального баланса и преобразований получим</p> $2(1+e)p_{H_2O} + (d+e)\sqrt{p_{H_2O}} =$ $= A(1+b)p_{CO_2} \quad (6)$ <p>5) где $(1+e)p_{H_2O} = p_{H_2O} + p_{H_2}$; $(d+e)\sqrt{p_{H_2O}} = p_{OH} + p_H$; $(1+b)p_{CO_2} = p_{CO_2} + p_{CO}$</p>
<p>6) Уравнение относительного материального баланса:</p> $\frac{2(p_{CO_2} + p_{CO}) + p_{CO} + p_{H_2O} + p_{OH} + p_{H_2} + p_O}{p_{CO_2} + p_{CO}} =$ $= \frac{3}{4} \frac{O_T}{C_T} = B$	<p>7) Аналогично предыдущему уравнению получим</p> $p_{H_2O} + d\sqrt{p_{H_2O}} + p_{CO_2} + p_{CO} +$ $+ 2p_{CO_2} + p_{CO} = B(1+b)p_{CO_2}$ <p>8) или</p> $p_{H_2O} + d\sqrt{p_{H_2O}} + p_{CO_2} + p_{CO} =$ $= [(B-1)(1+b)-1]p_{CO_2} \quad (7)$ <p>9) где $p_{CO} = (1+b)p_{CO_2} - p_{CO_2}$</p>

1) General form of initial system of equations; 2) computed form of equations obtained after appropriate transformations in initial equations; 3) equation of relative material balance; 4) after substituting the expressions for p_i obtained above in the initial equations of relative material balance and performing the transformations, we obtain; 5) where; 6) equation of relative material balance; 7) analogous to the previous equation, we obtain; 8) or; 9) where.

Note. Equations containing the value of p_1 for gases which contain nitrogen are excluded from the general system of equations, since they are not needed for this computation.

2. Having divided Eqs. (6) by the equation of material balance (7), we obtain

$$\frac{2(1+e)p_{H_2O} + (d+e)\sqrt{p_{H_2O}}}{p_{H_2O} + d\sqrt{p_{H_2O}} + 2p_{CO_2} + p_{CO}} = \frac{A(1+b)}{(B-1)(1+b)-1} = g$$

or

$$h(\sqrt{p_{H_2O}})^2 - n\sqrt{p_{H_2O}} - gm = 0,$$

whence

$$\sqrt{p_{H_2O}} = \frac{n + \sqrt{n^2 + 4hgm}}{2h},$$

where

$$h = 2(1+c) - g; \quad n = d(g-1) - e; \quad m = 2a^2 + f.$$

The quadratic equation obtained has only one positive root, since negative values of p_1 , in actuality, cannot occur.

We determine the values of p_1 for the remaining gases in the mixture by using the appropriate formulas.

For checking the correctness of the values of p_{O_2} which were assumed for the computations, we use the equation $\Sigma p_1 = p_k$. If Σp_1 agrees with the given p_k with sufficient exactness, we conclude the computation with this.

If Σp_1 is greater than the p_k which is permissible in the design, we determine the composition of the products of combustion in the second approximation, and so forth, assuming greater values of $p_{O_2} = a^2$, or if $\Sigma p_1 < p_k$, the reverse.

In selecting a value of p_{O_2} , one may tentatively assume that it is proportional to the value of Σp_1 that has been obtained.

It is convenient to perform computations for determining p_1 in the order shown in Table 6.5.

We determine the composition and temperature of the gases in the nozzle outlet section in an analogous manner. Thus, the only difference is that here, instead of an equality of enthalpies, we try to obtain an equality of entropies in the combustion chamber (S_k) and in the nozzle outlet section (S_v). At comparatively low temperatures for the gases in the nozzle outlet section, the atomic gases will be absent; some partial pressures (for example, p_{OH} , p_{H_2} , p_{O_2} , etc.) will be close to zero.

Beside the methods of successive approximations which we have

laid down for determining compositions of products of combustion for the simplest fuels (consisting of the elements C, H, O, and N) at given values of pressure and temperature, other methods exist which permit computing parameters at high temperatures and small or great amounts of excess oxidizer, at a changing pressure, or changing propellant-component ratio.

In those cases where the propellant includes a large number of elements, the computations become considerably more complex and laborious. However, there are very convenient methods of computation for even these situations. A great series of computations, required, for example, for constructing an I-S diagram, may be performed by means of an electronic computer.

Sample computations for the characteristics of the combustion products of kerosene and nitric acid are shown below.

Example 2. Determine the composition and other parameters for the products of combustion of kerosene ($C_g = 0.865$; $H_g = 0.135$, and $O_g = 0$) and nitric acid of 98% weight concentration when $p_k = 30$ atm abs, $T_k = 2900, 3000$, and $3100^\circ K$, if $C_t = 0.161$; $H_t = 0.040$; $O_t = 0.622$, and $N_t = 0.177$ kg/kg, and $I_t = -677$ kcal/kg.

Solution.

1. We express the given pressure for the gases in the combustion chamber in physical atmospheres:

$$p_k = 30/1.033 = 29 \text{ atm.}$$

2. We compute the constant coefficients, which are functions of the given weight composition of the fuel elements:

$$Q = \frac{7}{6} \frac{C_t}{N_t} = \frac{7}{6} \frac{0.161}{0.177} = 1.06; \quad R = 14 \frac{H_t}{N_t} = 14 \frac{0.04}{0.177} = 3.16$$

and

$$S = \frac{3}{4} \frac{O_t}{C_t} = \frac{3}{4} \frac{0.622}{0.161} = 2.90.$$

First approximation.

3. We determine the partial pressures of the gases in the first approximation:

$$\begin{aligned}p_{N_2} &= \frac{p_k}{2Q + R + 1} = \frac{29}{2 \cdot 1,06 + 3,162 + 1} = 4,62; \\p_{CO} &= 2Qp_{N_2} - p_{CO_2} = 2 \cdot 1,06 \cdot 4,62 - p_{CO_2} = 9,80 - p_{CO_2}; \\p_{H_2O} &= 2Qp_{N_2}(S-1) - p_{CO_2} = 9,80(2,90-1) - p_{CO_2} = 18,60 - p_{CO_2}; \\p_{H_2} &= 2p_{N_2} \left[\frac{R}{2} + Q(S-1) \right] + p_{CO_2} = 2 \cdot 4,62 \left[\frac{3,16}{2} - 1,06(2,90-1) \right] + \\&\quad + p_{CO_2} = p_{CO_2} - 4,07.\end{aligned}$$

Summarizing the coefficients obtained

$$a + b + c = 9,80 + 18,60 - 4,07 = 24,33 \text{ and } p_k - p_{N_2} = 29,00 - 4,62 = 24,38,$$

we are satisfied that they were computed without significant errors.

4. After substituting the expressions for the partial pressures which have been found in Eq. (6.34), we obtain

$$K_{2a} = \frac{p_{CO}p_{H_2O}}{p_{CO_2}p_{H_2}} = \frac{(9,80 - p_{CO_2})(18,60 - p_{CO_2})}{p_{CO_2}(p_{CO_2} - 4,07)}.$$

At the selected value for the presumed temperature of the gases ($3000^\circ K$), we find, in accordance with the table, that $K_{2a} = 7.382$, because of which the last equation for K_{2a} takes the form

$$6,38p_{CO_2}^2 - 1,60p_{CO_2} - 182,3 = 0,$$

whence

$$\begin{aligned}p_{CO_2} &= \frac{1,60 + \sqrt{1,6^2 + 4 \cdot 182,3 \cdot 6,38}}{2 \cdot 6,38} = 5,48; \\p_{CO} &= 9,80 - p_{CO_2} = 9,80 - 5,48 = 4,32; \\p_{H_2O} &= 18,60 - p_{CO_2} = 18,60 - 5,48 = 13,12; \\p_{H_2} &= p_{CO_2} - 4,07 = 5,48 - 4,07 = 1,41.\end{aligned}$$

After checking, we obtain:

a) in accordance with the total pressure in the combustion chamber

$$\sum p_i = 4,62 + 5,48 + 4,32 + 13,12 + 1,41 = 28,95 \text{ atm}; \quad p_k = 29 \text{ atm};$$

b) according to the constant of equilibrium

$$K_{2a} = \frac{p_{CO}p_{H_2O}}{p_{CO_2}p_{H_2}} = \frac{4,32 \cdot 13,12}{5,48 \cdot 1,41} = 7,36 \text{ instead of } 7.382.$$

Second approximation.

5. We determine the partial pressures for the remaining six gases in the second approximation, having taken the constants of equilibrium at temperature 3000°K from the table (see Appendices II and III):

$$K_{p1} = 0,3417; \quad K_{p3} = 0,04841; \quad K_{p4} = 0,01472; \\ K_{p5} = 0,02475; \quad K_{p6} = 0,01441; \quad K_{p7} = 0,1879 \cdot 10^{-4}.$$

Thus, we obtain the following values for the partial pressures of the gases:

$$p_{O_2} = \left(K_{p1} \frac{p_{CO_2}}{p_{CO}} \right)^2 = \left(0,3417 \frac{5,48}{4,32} \right)^2 = 0,188;$$

$$p_{OH} = K_{p3} \frac{p_{H_2O}}{\sqrt{p_{H_2}}} = 0,04841 \frac{13,12}{\sqrt{1,41}} = 0,534;$$

$$p_{NO} = \sqrt{K_{p4} p_{N_2} p_{O_2}} = \sqrt{0,01472 \cdot 4,62 \cdot 0,188} = 0,113;$$

$$p_H = \sqrt{K_{p5} p_{H_2}} = \sqrt{0,02475 \cdot 1,41} = 0,187;$$

$$p_O = \sqrt{K_{p6} p_{O_2}} = \sqrt{0,0144 \cdot 0,188} = 0,052;$$

$$p_N = \sqrt{K_{p7} p_{N_2}} = \sqrt{0,1879 \cdot 10^{-4} \cdot 4,62} = 0,003.$$

6. We determine coefficients A, B, D, E:

$$A = p_{NO} + p_N = 0,113 + 0,003 = 0,116;$$

$$B = p_{OH} + p_H = 0,534 + 0,187 = 0,721;$$

$$D = 2p_{O_2} + p_{OH} + p_{NO} + p_O = 2 \cdot 0,188 + 0,534 + 0,113 + 0,052 = 1,075;$$

$$E = p_{O_2} + p_{OH} + p_{NO} + p_H + p_O + p_N = 0,188 + 0,534 + 0,113 + 0,187 + 0,052 + 0,003 = 1,077.$$

7. We determine the partial pressures for the basic gases in the second approximation:

$$p_{N_2} = \frac{p_N - E + \frac{B}{2} - A \left(Q + \frac{R}{2} \right)}{2Q + R + 1} = \\ = \frac{29 - 1,077 + \frac{0,721}{2} - 0,116 \left(1,06 + \frac{3,16}{2} \right)}{2 \cdot 1,06 + 3,16 + 1} = 4,46;$$

$$p_{CO} = Q(2p_{N_2} + A) - p_{CO_2} = 1,06(2 \cdot 4,46 + 0,116) - p_{CO_2} = 9,58 - p_{CO_2};$$

$$p_{H_2O} = Q(2p_{N_2} + A)(S - 1) - D - p_{CO_2} = 9,58(2,90 - 1) - 1,075 - p_{CO_2} = \\ = 17,12 - p_{CO_2};$$

$$p_{H_2} = (2p_{N_2} + A) \left[\frac{R}{2} - Q(S - 1) \right] - \frac{B}{2} + D + p_{CO_2} = \\ = (2 \cdot 4,46 + 0,116) \left[\frac{3,16}{2} - 1,06(2,90 - 1) \right] - \frac{0,721}{2} + 1,075 + p_{CO_2} = p_{CO_2} - 3,27.$$

Thus, Eq. (6.34) takes the form

$$K_{p2} = \frac{(9,58 - p_{CO_2})(17,12 - p_{CO_2})}{p_{CO_2}(p_{CO_2} - 3,27)} = 7,38$$

or

$$6,38p_{CO_2}^2 + 2,58p_{CO_2} - 164 = 0,$$

whence

$$p_{CO_2} = \frac{-2,58 + \sqrt{2,58^2 + 4 \cdot 164 \cdot 6,38}}{2 \cdot 6,38} = 4,87.$$

From this

$$p_{CO} = 9,58 - 4,87 = 4,71; \quad p_{H_2O} = 17,12 - 4,87 = 12,25;$$

$$p_{H_2} = 4,87 - 3,27 = 1,60.$$

Checking gives the following results:

$$\Sigma p_i = p_{CO} + p_{CO_2} + p_{H_2O} + p_{H_2} + p_{N_2} + E =$$

$$= 4,87 + 4,71 + 12,25 + 1,60 + 4,46 + 1,077 = 28,967 \text{ instead of } p_K = 29 \text{ atm};$$

$$K_{2a} = \frac{4,71 \cdot 12,25}{4,87 \cdot 1,60} = 7,40 \text{ instead of } 7,38.$$

Third approximation.

8. We determine the partial pressures for the six gases, taking the formulas and constants of equilibrium for this from the second approximation:

$$p_{CO_2} = \left(0,3117 \frac{4,87}{4,71}\right)^2 = 0,124; \quad p_{OH} = 0,0484 \frac{12,25}{\sqrt{1,60}} = 0,468;$$

$$p_{NO} = \sqrt{0,0147 \cdot 4,46 \cdot 0,124} = 0,091; \quad p_{H_2} = \sqrt{0,02475 \cdot 1,60} = 0,199;$$

$$p_O = \sqrt{0,0144 \cdot 0,124} = 0,042; \quad p_N = \sqrt{1,88 \cdot 10^{-6} \cdot 4,46} = 0,003.$$

9. We determine the coefficients:

$$A = 0,091 + 0,003 = 0,094; \quad B = 0,468 + 0,199 = 0,667;$$

$$D = 2 \cdot 0,124 + 0,468 + 0,091 + 0,042 = 0,849;$$

$$E = 0,124 + 0,468 + 0,091 + 0,199 + 0,042 + 0,003 = 0,927.$$

10. We determine the partial pressures for the basic gases:

$$p_{N_2} = \frac{29 - 0,927 + 0,333 - 0,094 \cdot 2,64}{6,28} = 4,49;$$

$$p_{CO} = 1,06(2 \cdot 4,49 + 0,094) - p_{CO_2} = 9,64 - p_{CO_2};$$

$$p_{H_2O} = 9,64 \cdot 1,90 - 0,849 - p_{CO_2} = 17,47 - p_{CO_2};$$

$$p_{H_2} = (2 \cdot 4,49 + 0,094)(-0,44) - 0,333 + 0,849 + p_{CO_2} = p_{CO_2} - 3,48.$$

Thus, Eq. (6.34) takes the form

$$7,38 = \frac{(9,64 - p_{CO_2})(17,47 - p_{CO_2})}{p_{CO_2}(p_{CO_2} - 3,48)}$$

or

$$6,38p_{CO_2}^2 + 1,43p_{CO_2} - 168,5 = 0,$$

whence

$$p_{CO_2} = \frac{-1,43 + \sqrt{1,43^2 + 4 \cdot 168,5 \cdot 6,38}}{2 \cdot 6,38} = 5,03;$$

$$p_{CO} = 9,64 - 5,03 = 4,61; \quad p_{H_2O} = 17,47 - 5,03 = 12,44;$$

$$p_H = 5,03 - 3,48 = 1,55.$$

Checking shows:

$$\sum p_i = 4,49 + 5,03 + 4,60 + 12,44 + 1,55 + 0,927 = 29,027 \text{ instead of } p_k = 29 \text{ atm};$$

$$K_{22} = \frac{4,61 \cdot 12,44}{1,55 \cdot 5,03} = 7,39 \text{ instead of } 7,38.$$

Comparing the results of the solution of the second and third approximations (Table 6.2), we see that there is still a considerable difference in the values of p_1 ; it is about 0.2 atm for CO_2 and H_2O . Therefore, we must perform the computations in the fourth approximation.

Fourth approximation.

11. We determine the values of p_1 for the six gases:

$$p_{O_2} = \left(0,3417 \frac{5,03}{4,61}\right)^2 = 0,139; \quad p_{OH} = 0,0484 \frac{12,44}{\sqrt{1,55}} = 0,480;$$

$$p_{NO} = \sqrt{0,0147 \cdot 4,49 \cdot 0,139} = 0,096; \quad p_H = \sqrt{0,02475 \cdot 1,55} = 0,196;$$

$$p_O = \sqrt{0,0144 \cdot 0,139} = 0,045; \quad p_N = \sqrt{1,879 \cdot 10^{-4} \cdot 4,49} = 0,003.$$

12. We determine the coefficients:

$$A = 0,096 + 0,013 = 0,099; \quad B = 0,480 + 0,196 = 0,676;$$

$$D = 2 \cdot 0,139 + 0,480 + 0,096 + 0,045 = 0,899;$$

$$E = 0,139 + 0,480 + 0,096 + 0,196 + 0,045 + 0,003 = 0,959.$$

13. We determine the values of p_1 for the basic gases:

$$p_{N_2} = \frac{29 - 0,959 + 0,338 - 0,099 \cdot 2,64}{6,28} = 4,48;$$

$$p_{CO} = 1,06(2 \cdot 4,49 + 0,099) - p_{CO_2} = 9,60 - p_{CO_2};$$

$$p_{H_2O} = 9,60 \cdot 1,90 - 0,899 - p_{CO_2} = 17,38 - p_{CO_2};$$

$$p_H = (2 \cdot 4,49 - 0,099)(-0,44) - 0,338 + 0,899 + p_{CO_2} = p_{CO_2} - 3,46.$$

Thus, Eq. (6.34) takes the form

$$7,38 = \frac{(9,60 - p_{CO_2})(17,38 - p_{CO_2})}{p_{CO_2}(p_{CO_2} - 3,46)}$$

or

$$6,38p_{CO_2}^2 + 1,46p_{CO_2} - 166,4 = 0.$$

TABLE 6.2

1) № при- ближения	2) Парциальные давления газов p_i в атм										
	N ₂	CO ₂	CO	H ₂ O	H ₂	O ₂	OH	NO	H	O	N
1	4,62	5,48	4,32	13,12	1,41	0	0	0	0	0	0
2	4,46	4,87	4,71	12,25	1,60	0,188	0,534	0,113	0,187	0,052	0,003
3	4,49	5,03	4,61	12,44	1,55	0,124	0,468	0,091	0,199	0,042	0,003
4	4,48	5,00	4,60	12,38	1,54	0,139	0,480	0,096	0,196	0,045	0,003

1) Number of approximation; 2) partial pressures p_i of gases in atm.

whence

$$p_{CO_2} = \frac{-1,46 + \sqrt{1,46^2 + 4 \cdot 166 \cdot 4,6 \cdot 38}}{2 \cdot 6,38} = 5,00;$$

$$p_{CO} = 9,60 - 5,00 = 4,60; \quad p_{H_2O} = 17,38 - 5,00 = 12,38;$$

$$p_{H_2} = 5,00 - 3,46 = 1,54.$$

Checking shows:

$$\sum p_i = 4,48 + 5,00 + 4,60 + 12,38 + 1,54 + 0,96 = 29,07 \text{ instead of } p_k = 29 \text{ atm};$$

$$K_{2a} = \frac{4,60 \cdot 12,938}{5,03 \cdot 1,54} = 7,37 \text{ instead of } 7,38.$$

Comparing the results of the third and fourth approximations (see Table 6.2) shows that the greatest difference in the values of p_i does not exceed 0.06 atm. Further computations are, therefore, impracticable. We assume the composition for the products of combustion obtained in the fourth approximation as final. For further computations, we round off the values of p_i to the second decimal place; thus, we will neglect the partial pressure of atomic nitrogen, since it is very small (altogether 0.003 atm).

14. We construct a curve of the convergence of the partial pressures to a precise value through our approximations; constructing curves of this type is convenient for controlling the course of computations. The curve we have constructed for p_{H_2O} (Fig. 6.24) shows that we could have limited ourselves to three approximations in the



Fig. 6.24. Convergence of values of p_{H_2O} for determining composition of products of fuel combustion by the method of successive approximations. 1) Curve of approximations; 2) precise value of p_{H_2O} ; 3) numbers of approximations; 4) p_{H_2O} , atmospheres.

computations we performed. At higher temperatures, convergence occurs much later, and requires the computation of a large number of approximations or shifting to another, more convenient method of computation.

15. We place the results of the computed values of p_1 in Table 6.3 and make sure there are no errors in the computations, using the equation of material balance for this purpose:

$$C_T = \frac{12}{\sum \nu_i p_i} (p_{CO_2} + p_{CO}) = \frac{12}{716.8} (5.00 + 4.60) = 0.1005$$

instead of 0.161, which was assumed for computation;

$$H_T = \frac{1}{\sum \nu_i p_i} (2p_{H_2O} + 2p_{H_2} + p_{OH} + p_H) = \frac{1}{716.8} (2 \cdot 12.38 + 2 \cdot 1.54 + 0.48 + 0.20) = 0.0338 \text{ instead of } 0.040;$$

$$\begin{aligned} O_T &= \frac{16}{\sum \nu_i p_i} (2p_{CO_2} + p_{CO} + p_{H_2O} + 2p_{O_2} + p_{OH} + p_{NO} + p_O) = \\ &= \frac{16}{716.8} (2 \cdot 5.00 + 4.60 + 12.38 + 2 \cdot 0.14 + 0.48 + 0.10 + 0.06) = \\ &= 0.6215 \text{ instead of } 0.622; \end{aligned}$$

$$N_T = \frac{14}{\sum \nu_i p_i} (2p_{N_2} + p_{NO}) = \frac{14}{716.8} (2 \cdot 4.48 + 0.10) = 0.117,$$

which agrees with the value (0.177) assumed for the computations.

The results of this check show that the composition for the products of fuel combustion determined by means of the values of p_1 is without significant errors.

16. Finally, we determine the other parameters for the products of fuel combustion in the engine chamber at the given pressure $p_k = 30 \text{ atm abs}$ and a temperature of 3000°K , using the data from the appropriate tables for this purpose:

a) enthalpy

$$I_k = \frac{\sum p_i I_i}{\sum \nu_i p_i} = 1000 \frac{-476.1}{716.8} = -665;$$

TABLE 6.3

1)	2)			3)		4)				
Gas	p_i atm	p_i	$p_i p_i$	I_i kcal/mole	$p_i I_i$	S_i kcal/mole	$S_i p_i$	$\lg p_i$	$4.57 p_i \lg p_i$	$S_i p_i - 4.57 p_i \lg p_i$
N ₂	4.48	28	125.5	22.20	99.6	63.77	286.0	0.651	13.3	272.7
CO ₂	5.00	44	220.0	-57.31	-286.5	79.91	399.0	0.698	15.9	383.1
CO	4.60	28	128.5	-4.03	-16.5	65.46	312.0	0.673	14.1	297.9
H ₂ O	12.38	18	123.0	-27.92	-346.0	68.27	845.0	1.093	61.8	783.2
H ₂	1.54	2	3.1	21.24	32.7	48.47	74.5	0.187	1.3	73.2
O ₂	0.14	32	4.5	23.48	3.3	67.98	9.5	-0.854	-0.5	10.0
OH	0.48	17	8.2	31.55	15.2	61.38	29.4	-0.318	-0.7	30.1
NO	0.10	30	3.0	44.36	4.4	68.85	6.9	-1.000	-0.5	7.4
H	0.20	1	0.2	65.53	14.1	38.86	7.8	-0.698	-0.6	8.4
O	0.05	16	0.8	72.69	3.6	50.09	2.5	-0.302	-0.3	2.8
5) $\Sigma \mu_{p_i}$	29.07	-	716.8	-	-476.1	-	-	-	-	1868.8

1) Gas; 2) p_i , atm; 3) I_i , cal/mole; 4) S_i , kcal/kmole-°C; 5) sum.

b) molecular weight

$$\mu_k = \frac{1}{p_k} \sum \mu_i p_i = \frac{716.8}{29.07} = 24.68;$$

c) gas constant

$$R_k = 848/\mu_k = 34.3 \text{ kg-m/kg}^\circ\text{C};$$

d) entropy

$$S_k = \frac{1}{\sum \mu_i p_i} \sum (S_i p_i - 4.57 p_i \lg p_i) \frac{1868.8}{716.8} = 2.605 \text{ kcal/kg}^\circ\text{C}.$$

17. We perform analogous computations for temperatures of 2900 and 3100°K and place the results obtained in Table 6.4.

18. We construct the curves of I_k , S_k , and μ_k as a function of the three values of temperature that we chose (Fig. 6.25) and, when $I_t = -677 \text{ kcal/kg}$, we find the theoretical unknown parameters of the gas in the combustion chamber: $T_k = 2984^\circ\text{K}$, $S_k = 2.597 \text{ kcal/kg}^\circ\text{C}$, $\mu_k = 24.7$, and $R_k = 34.35 \text{ kgm/kg}^\circ\text{C}$.

TABLE 6.4

T_k °K	1) I_k ккал/кг	P_k	2) R_k кг·м/кг·°C	3) S_k ккал/кг·°C
2900	-720	25,12	33,75	2,581
3000	-665	24,68	34,30	2,605
3100	-595	24,03	35,30	2,619

1) I_k , kcal/kg; 2) R_k , kg-m/kg-°C; 3) S_k , kcal/kg-°C.

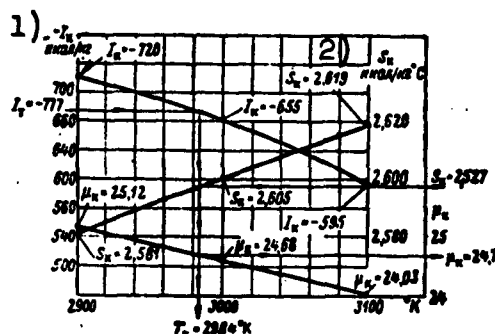


Fig. 6.25. Curves of I_k , S_k , and μ_k as functions of T_k (see Example No. 2). 1) I_k , kcal/kg; 2) S_k , kcal/kg-°C.

With this, computations for the state of the products of fuel combustion in the engine combustion chamber are completed.

Example 3. Determine the temperature and composition for the products of combustion of a fuel consisting of ethyl alcohol of 93.5% weight concentration ($C_2H_6O \cdot 0.178H_2O$) and liquid oxygen (O_2), when $\alpha = 0.82$; $p_k = 35$ atm, and $p_v = 1$ atm.

Solution.

1. We perform the required preliminary computations, select an assumed temperature of 3300°K for the gases in the combustion chamber, and, appropriate for this, assume values of $p_{O_2} = a^2 = 0.95$ and 1.21 atm, and select the numerical values for the constants of equilibrium from the table. Then we compute the values of p_1 for the corresponding

TABLE 6.5

1) № по пор.	$p_{01}=a^2$	0,95	1,21	1,11	1,122
1	a	0,975	1,100	1,054	1,069
2	$p_0=f=a \sqrt{K_{p0}}$	0,296	0,334	0,320	0,322
3	$b=K_{p1}/a$	0,942	0,835	0,871	0,868
4	$1+b$	1,942	1,835	1,871	1,868
5	$A(1+b)$	6,172	5,832	5,946	5,937
6	$(B-1)(1+b)-1$	3,329	3,090	3,170	3,164
7	$g=\frac{A(1+b)}{(B-1)(1+b)-1}$	1,854	1,887	1,876	1,876
8	$c=K_{p2}/a$	0,120	0,106	0,111	0,1106
9	$1+c$	1,120	1,106	1,111	1,1106
10	$2(1+c)$	2,240	2,212	2,222	2,2212
11	$h=2(1+c)-g$	0,386	0,325	0,346	0,3452
12	\sqrt{c}	0,346	0,326	0,332	0,3326
13	$d=K_{p3}/\sqrt{c}$	0,408	0,433	0,425	0,424
14	$d(g-1)$	0,348	0,384	0,372	0,371
15	$e=\sqrt{c}\sqrt{K_{p1}}$	0,126	0,118	0,121	0,121
16	$n=d(g-1)-e$	0,222	0,266	0,251	0,250

1) Number in order.

TABLE 6.5 (continued)

1) № по пор.	$p_{O_2} = a^2$	0,95	1,21	1,11	1,122
17	n^2	0,049	0,071	0,063	0,0625
18	$m = f + 2a^2$	2,196	2,754	2,540	2,562
19	$4hgm$	6,286	6,756	6,594	6,636
20	$\sqrt{n^2 + 4hgm}$	2,517	2,613	2,580	2,588
21	$s = n + \sqrt{n^2 + 4hgm}$	2,739	2,879	2,831	2,838
22	$\sqrt{p_{H_2O}} = s/2k$	3,548	4,429	4,091	4,113
23	p_{H_2O}	12,586	19,612	16,738	16,914
24	$2p_{H_2O}$	25,172	39,224	33,476	33,828
25	$p_{H_2} = c p_{H_2O}$	1,510	2,079	1,858	1,871
26	$2p_{H_2}$	3,020	4,158	3,716	3,742
27	$p_{OH} = d \sqrt{p_{H_2O}}$	1,448	1,918	1,739	1,744
28	$p_H = e \sqrt{p_{H_2O}}$	0,447	0,523	0,495	0,498
29	$t = 2p_{H_2O} + 2p_{H_2} + p_{OH} + p_O$	30,087	45,823	39,426	39,812
30	$p_{CO} = \frac{t}{A(1+\delta)}$	4,875	7,857	6,631	6,706
31	$p_{CO} = b p_{CO_2}$	4,589	6,561	5,776	5,821
32	Σp_i	26,094	40,094	34,667	34,997

1) Number in order.

gases, in the same succession as indicated in Table 6.5.

The data from this table show that when $p_{O_2} = 0.95$ atm, $\Sigma p_1 = 26.694$ atm, and when $p_{O_2} = 1.21$ atm the value of $\Sigma p_1 = 40.094$ atm. This means that a value of p_{O_2} lying somewhere between 0.95 and 1.121 atm is appropriate for the given value of $p_k = 35$ atm.

For further computations, we select an intermediate value of p_{O_2} (see Table 6.5). Then, as the result of additional simple computations, we obtain another composition for the combustion products of the given fuel as follows:

$$\begin{aligned}\Sigma p_i &= p_{CO_2} + p_{CO} + p_{H_2O} + p_{H_2} + p_{OH} + p_{O_2} + p_{H_2} + p_{O_2} = \\ &= 6.707 + 5.821 + 16.916 + 1.871 + 1.744 + 1.121 + 0.498 + 0.322 = 35.000 \text{ atm.}\end{aligned}$$

2. Since the computed value of I_k for these products of fuel combustion at 3300°K as obtained is less than the enthalpy I_t of the given fuel, we perform an analogous computation for another, higher temperature of 3400°K , and find other values of Σp_1 and I_k .

On the basis of the value of I_k that we have found in this manner, we establish the fact that the temperature T_k corresponding to the value of I_t lies within the limits of 3300 - 3400°K .

In this case we use the method of linear interpolation to determine the temperature of the gases. We compute the calculation coefficients M and N required for this, together with the solution of the following two linear equations:

$$M + T_{k1}N = I_{k1} \text{ and } M + T_{k2}N = I_{k2}.$$

Using the interpolation equation $M + T_k N = I_t$, we obtain the unknown temperature of the gases in the engine combustion chamber:

$$T_k = \frac{I_t + M}{N} = 3358^\circ\text{K}.$$

At this temperature, we find, by computations, the following composition for the products of fuel combustion, at which $I_k = I_t$:

$$\sum p_i = p_{CO_2} + p_{CO} + p_{H_2O} + p_{H_2} + p_{OH} + p_{O_2} + p_{H} + p_O = \\ + 6,081 + 16,358 + 2,023 + 1,969 + 1,268 + 0,801 + 0,407 = 35,000 \text{ atm.}$$

This means that the temperature T_k which we have found corresponds to the given value of p_k .

We may then compute the other characteristics for the products of fuel combustion.

An analogous method for determining the composition of products of fuel combustion which do not contain nitrogen is shown in the work of G.B. Sinyarev and M.V. Dobrovol'skiy.*

SECTION 11. DETERMINING THE THEORETICAL TEMPERATURE AND COMPOSITION FOR PRODUCTS OF FUEL COMBUSTION IN AN ENGINE-CHAMBER NOZZLE OUTLET SECTION

In designing ZhRD, we most frequently use a method based on the assumption of complete chemical and energy equilibrium for the composition of the gases throughout the length of the nozzle. However, the required state of equilibrium is somewhat lacking due to the chemical change in the composition of the gases as they flow out of the nozzle, which actually occurs chiefly in the supercritical part of the nozzle, and is usually considered as some decrease in the computed theoretical exhaust velocity or theoretical specific thrust (1-2% when the length of the supercritical part of the nozzle is of the order of 0.1-0.2 m).

To determine the theoretical temperature, and the composition of the products of fuel combustion corresponding to it, in the outlet or in any engine chamber-nozzle cross section at a given pressure p_v by this method, we use the same equations of the constants of equilibrium and equations of material balance as for the combustion chamber (see Chapter VI, Section 10).

*G.B. Sinyarev and M.V. Dobrovol'skiy, Zhidkostnye raketnye dvigateli (Liquid-propellant rocket engines), Oborongiz (State Publishing House of the Defense Industry), 1957.

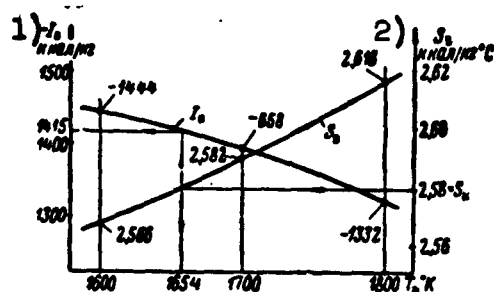


Fig. 6.26. Graphic determination of temperature and enthalpy for products of fuel combustion in an engine nozzle outlet section. 1) I_v , kcal/kg; 2) S_v , kcal/kg-°C.

This system of equations, applicable to the outlet (or any) section of the nozzle, is supplemented by the equation of the isentropic condition for the gas-expansion process:

$$S_k = S_v = \frac{1}{\mu_k p_k} \sum (S_i - R \ln p_i) p_i = \frac{1}{\mu_k p_k} \sum (S_i p_i - 4.57 p_i \lg p_i) \text{ kcal/kg}^\circ\text{C}, \quad (6.59)$$

where S_k and S_v are the absolute entropies for the products of fuel combustion in the combustion chamber and in a nozzle cross section, respectively, in kcal/kg°C; S_1 is the absolute entropy of the i -th gas in the mixture at a temperature T_v and a pressure of 1 atm abs, in kcal/mole°C, selected from Appendix IV; $R = 1.987$ is the universal gas constant for the products of fuel combustion in kcal/mole°C; and p_1 is the partial pressure of the i -th gas in the mixture at the outlet from the engine nozzle, in atm abs.

To determine the composition for the products of fuel combustion in the nozzle outlet section, under conditions of isentropic expansion, we usually assume three values for the presumed temperature T_v of these products, and, as previously (see Chapter VI, Section 10), we determine the partial pressures p_1 corresponding to them. After this, we compute the values for the entropies S_v of the entire gas mixture for each of these temperatures, in accordance with the formula given above. Then we construct a curve showing the value of S_v as a function of the three selected values of temperature T_v (Fig. 6.26).

Since, with isentropic outflow, the entropy S_v of the gas mixture in the nozzle outlet section is equal to its value S_k in the combus-

TABLE 6.6

1)	Продукты сгорания топлива	2) Значение k
3)	Керосин с жидким кислородом	1,12—1,14
4)	Керосин или тонка-250 с азотной кислотой или ее производными	1,16—1,18
5)	Этиловый спирт с жидким кислородом	1,13—1,16
6)	Гидразин с жидким кислородом	1,16—1,19
7)	Гидразин с жидким фтором	1,18—1,20
8)	Гидразин с трифторидом хлора	1,21—1,23
9)	Димазин с жидким кислородом	1,13—1,20
10)	Димазин с моноокисью фтора	1,15—1,17
11)	Аммиак с жидким фтором	1,23—1,27

1) Products of fuel combustion; 2) value of k ;
 3) kerosene and liquid oxygen; 4) kerosene or
 Tonka-250 and nitric acid or its derivatives;
 5) ethyl alcohol and liquid oxygen; 6) hydra-
 zine and liquid oxygen; 7) hydrazine and liq-
 uid fluorine; 8) hydrazine and chlorine tri-
 fluoride; 9) dimazine and liquid oxygen; 10)
 dimazine and fluorine monoxide; 11) ammonia
 and liquid fluorine.

tion chamber, having computed

$$S_z = \frac{1}{p_{u,p_k}} \sum (S_i p_i - 4,57 p_i \lg p_i) \text{ kcal/kg}^\circ\text{C}, \quad (6.60)$$

we may determine the unknown value of T_v from the curve in Fig. 6.26, and then find the corresponding composition of fuel-combustion products, the values of I_v , μ_v , R_v , and γ_v , and other characteristics.

In this case, the task of solving the system of equations for determining the partial pressures of the gases is simplified by the fact that the temperature of the products of combustion in the nozzle outlet section is considerably lower than in the combustion chamber, because of which we may neglect the content of OH, O_2 , O, NO, and N, which is negligible. This assumption does not introduce any significant error into the results of the computations and simplifies them considerably. Computations for determining the value of p_1 may thus be carried out quite rapidly, since the results of the computation are

sufficiently precise in the first approximation.

For approximate selection of the values of assumed temperature for the gases in the nozzle outlet section, we may make use of the well-known formula of adiabatic dependence of gas parameters:

$$T_{\text{b.ox}} = T_{\text{u}} \left(\frac{p_{\text{b}}}{p_{\text{u}}} \right)^{\frac{k-1}{k}}, \quad * \quad (6.61)$$

where k is the isentropic exponent for the gas expansion in the engine-chamber nozzle, whose approximate value may be taken from Table 6.6.

Greater values of the k exponent correspond to higher pressures p_k in the combustion chamber and lower values of the excess oxidation coefficient α in the fuel.

Precise values of k may be taken from the computed tables, depending on the type of fuel and the magnitudes of p_k and α .

The theoretic velocity for the isentropic gas outflow in the engine-chamber nozzle outlet section is determined in accordance with the formula

$$w_{\text{t}} = \sqrt{2g427(I_{\text{u}} - I_{\text{b}})} = 91.53 \sqrt{I_{\text{u}} - I_{\text{b}}} \text{ m/sec.} \quad (6.62)$$

We may assume that the state of the separate gases in the mixture (both in the combustion chamber and in the nozzle) is ideal, i.e., consider that each of them (but not the mixture as a whole) is subject to the equation of state $pv = RT$, where $R(848/\mu)$ is the characteristic gas constant.

The theoretical area of the nozzle outlet section is determined in accordance with the formula

$$F_{\text{t}} = \frac{G_{\text{t}} v_{\text{t}}}{w_{\text{t}}} = \frac{P v_{\text{t}}}{P_{\text{ya}} w_{\text{t}}}, \quad (6.63)$$

where P is the engine thrust, and v_{v} is the specific volume of the products of combustion in this nozzle section.

*[$T_{\text{b.ox}} = T_{\text{v.ozh}} = T_{\text{vykhod.ozhidaemaya}} = T_{\text{outlet.assumed}}$]

To determine the theoretical value of the engine-nozzle throat, as a preliminary, we determine theoretical values of the following gas parameters:

- a) the mean isentropic exhaust exponent

$$k_1 = \lg \frac{p_u/p_n}{v_u/v_n}; \quad (6.64)$$

- b) the pressure in the nozzle throat

$$p_{np} = p_n \left(\frac{2}{k_1 + 1} \right)^{\frac{k_1}{k_1 - 1}}; \quad (6.65)$$

- c) the specific volume in the nozzle throat

$$v_{np} = v_n (p_n/p_{np})^{\frac{1}{k_1}}; \quad (6.66)$$

- d) the velocity in the nozzle throat

$$w_{np} = \sqrt{g k_1 p_{np} v_{np}}. \quad (6.67)$$

Thus, the area of the nozzle throat is determined in accordance with the formula

$$F_{np} = \frac{G v_{np}}{w_{np}}. \quad (6.68)$$

The mean isentropic exhaust exponent, when $R_k = R_v$, is

$$k_2 = \frac{\lg(p_n/p_u)}{\lg(p_n T_u/p_u T_n)}. \quad (6.69)$$

The values of k_1 are somewhat greater than k_2 ; as the excess oxidizer factor in the fuel increases, they decrease; when combustion-chamber pressure is raised, they increase.

The mean exhaust-gas isentropic exponent k_1 may be used in the gasdynamic computation of the engine characteristics, or basic geometrical dimensions, thrust coefficient, specific thrust, specific area for the chamber-nozzle throat and outlet section, etc. The mean exhaust-gas isentropic exponent k_2 may be used for computations connected with determining gas temperatures.

Example 4. Determine the composition and other characteristics

for the products of fuel combustion in an engine-chamber nozzle outlet section according to the data for the previous example if $p_v = 0.9$ atm abs.

Solution.

1. We determine the assumed temperature for the gases in the nozzle outlet section, using for this purpose the value of the isentropic exponent $k = 1.17$ (see Table 5.20):

$$T_{v,ozh} = T_k \left(\frac{p_v}{p_k} \right)^{\frac{k-1}{k}} = 2984 \left(\frac{0.9}{30} \right)^{\frac{1.17-1}{1.17}} = 1670^\circ \text{K}.$$

Proceeding from the value of $T_{v,ozh}$ obtained, for computing the composition of the combustion products, we assume a temperature $T_v = 1600, 1700, \text{ and } 1800^\circ \text{K}.$

2. We express the given gas pressure in the nozzle outlet section in physical atmospheres:

$$p_v = 0.9/1.033 = 0.87 \text{ atm.}$$

3. At first, we perform the computations for a temperature of 1700°K , assuming that partial pressures for the O_2 , OH , NO , H , O , and N gases are equal to zero (because of their small amounts at low temperatures and when $\alpha < 1$).

With this assumption, the products of fuel combustion in the engine-chamber nozzle outlet section will consist of only five basic gases, whose partial pressures, in the first approximation, are equal to:

$$\begin{aligned} p_{N_2} &= \frac{p_v}{2Q + R + 1} = \frac{0.87}{2 \cdot 1.06 + 3.16 + 1} = 0.139; \\ p_{\text{CO}} &= 2Qp_{N_2} - p_{\text{CO}_2} = 2 \cdot 1.06 \cdot 0.139 - p_{\text{CO}_2} = 0.294 - p_{\text{CO}_2}; \\ p_{\text{H}_2\text{O}} &= 2Qp_{N_2}(S-1) - p_{\text{CO}_2} = 0.294(2.90-1) - p_{\text{CO}_2} = 0.554 - p_{\text{CO}_2}; \\ p_{N_2}^* &= 2p_{N_2} \left[\frac{R}{2} - Q(S-1) \right] + p_{\text{CO}_2} = 2 \cdot 0.139 \left[\frac{3.16}{2} - 1.06(2.90-1) \right] + \\ &\quad + p_{\text{CO}_2} = p_{\text{CO}_2} = 0.122. \end{aligned}$$

According to the table, at 1700°K , we find $K_{2a} = 3.56$, and, as a result, we obtain

$$3.56 = \frac{(0.294 - p_{CO_2})(0.554 - p_{CO_2})}{p_{CO_2}(p_{CO_2} - 0.122)}$$

or

$$2.56p_{CO_2}^2 + 0.414p_{CO_2} - 0.164 = 0,$$

whence

$$p_{CO_2} = \frac{-0.144 + \sqrt{0.414^2 + 4 \cdot 2.56 \cdot 0.164}}{2 \cdot 2.56} = 0.184;$$

$$p_{CO} = 0.294 - 0.184 = 0.110; \quad p_{H_2O} = 0.554 - 0.184 = 0.370;$$

A check shows $p_{H_2} = 0.184 - 0.122 = 0.062.$

$$\sum p_i = 0.139 + 0.184 + 0.110 + 0.370 + 0.062 = 0.865 \text{ instead of } 0.87;$$

$$K_{2a} = \frac{0.110 \cdot 0.370}{0.184 \cdot 0.062} = 3.57 \text{ instead of } 3.56.$$

It appears that we have found the composition of the products of fuel combustion in the engine-chamber nozzle outlet section without significant errors.

From Table 6.7 we see, that out of the number of gases whose p_1 we have assumed as being equal to zero, the OH gas has the greatest p_1 ; therefore, we determine its value in the nozzle outlet section:

$$p_{OH} = K_{p3} \frac{p_{H_2O}}{\sqrt{p_{H_2}}} = 0.625 \cdot 10^{-3} \frac{0.370}{\sqrt{0.062}} \approx 0.00001 \text{ atm abs.}$$

The value of the OH gas's p_1 obtained shows that the composition of the products of combustion in the nozzle outlet which we computed in the first approximation was sufficiently precise.

We place the results of the computations in Table 6.7, in which we also place other data.

4. We check the computations, using the equation of material balance for this purpose:

$$C_T = \frac{12}{\sum r_i p_i} (p_{CO_2} + p_{CO}) = \frac{12}{21.74} (0.184 + 0.110) = 0.162 \text{ instead of } 0.161;$$

$$H_T = \frac{1}{\sum r_i p_i} (2p_{H_2O} + 2p_{H_2}) = \frac{1}{21.74} (2 \cdot 0.370 + 2 \cdot 0.062) = 0.039 \text{ instead of } 0.040;$$

$$O_T = \frac{16}{\sum r_i p_i} (2p_{CO_2} + p_{CO} + p_{H_2O}) = \frac{16}{21.74} (2 \cdot 0.184 + 0.110 + 0.370) =$$

TABLE 6.7

1)	2)			3)		4)				
Gas	p_i atm abs	μ_i	$\mu_i p_i$	I_i' kcal/mole	$I_i p_i$	S_i kcal/mole	$S_i p_i$	$\lg p_i$	$4.57 p_i \lg p_i$	$S_i p_i - 4.57 p_i \lg p_i$
N ₂	0,139	28	3,89	10,89	1,52	58,84	8,18	-0,857	-0,55	8,73
CO ₂	0,194	44	8,10	-76,42	-14,02	71,58	13,17	-0,735	-0,62	13,79
CO	0,110	28	3,08	-15,41	-1,70	60,50	6,66	-0,958	-0,49	7,15
H ₂ O	0,370	18	6,65	-43,97	-16,25	61,29	22,68	-0,432	-0,73	23,41
H ₂	0,062	2	0,12	10,27	0,64	43,70	2,71	-0,207	-0,34	3,05
5) Сумма	0,865	—	21,74	—	29,81	—	—	—	—	56,13

1) Gas; 2) p_i , atm abs; 3) I_i' , cal/mole; 4) S_i , cal/mole; 5) sum.

= 0.623 instead of 0.622;

$$N_r = \frac{14}{\sum \mu_i p_i} 2p_{N_2} = \frac{14}{21,74} 2 \cdot 0,139 = 0,179 \text{ instead of } 0,177.$$

This check shows that there were no significant errors in determining p_i .

5. We determine the other theoretical parameters for the products of fuel combustion in the engine-chamber nozzle outlet section:

a) enthalpy

$$I_s = \frac{\sum p_i I_i'}{\sum \mu_i p_i} = \frac{-29,81}{21,74} = -1370 \text{ kcal/kg};$$

b) molecular weight

$$\mu_s = \frac{1}{p_s} \sum \mu_i p_i = \frac{1}{0,865} = 21,74 = 25,12;$$

c) gas constant

$$R_v = 848/\mu_v = 848/25,12 = 33,8 \text{ kg-m/kg}^\circ\text{C};$$

d) entropy

$$S_s = \frac{1}{\sum \mu_i p_i} (S_i p_i - 4,57 p_i \lg p_i) = \frac{56,13}{21,74} = 2,597 \text{ kcal/kg}^\circ\text{C}.$$

TABLE 6.8

T_k °K	1) I_v ккал/кг	2) S_v ккал/кг °C	μ_v	3) R_v кг·м/кг °C
1600	-1440	2,532	25,32	33,5
1700	-1370	2,582	25,12	33,7
1800	-1312	2,640	24,9	34,1

1) I_v , kcal/kg; 2) S_v , kcal/kg°C; 3) R_v , kgm/kg°C.

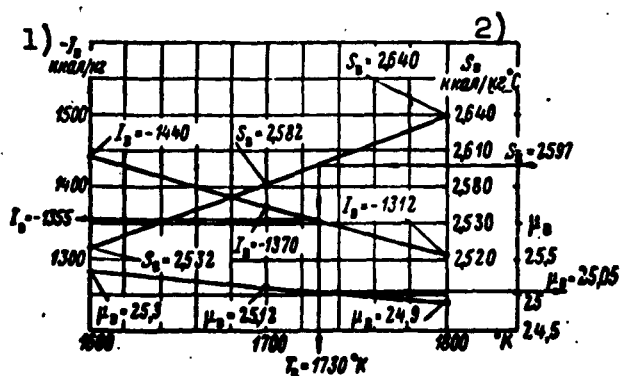


Fig. 6.27. Curves of I_v , S_v , and μ_v as functions of T_k (see Example 4).

1) I_v , kcal/kg; 2) S_v , kcal/kg°C.

6. We perform the computations for gas temperatures 1600 and 1800°K analogously, and place the results obtained in Table 6.8.

7. We construct curves showing I_v , S_v , and μ_v as functions of the selected values of temperature (Fig. 6.27), and by means of this, when $S_k = 2.597$ kcal/kg°C, we find the following theoretical values for the gas parameters in the engine-chamber nozzle outlet section:

$$T_v = 1730^\circ\text{K}, I_v = -1355 \text{ kcal/kg}, \mu_v = 25.05, \\ \text{and } R_v = 33.9 \text{ kg-m/kg}^\circ\text{C}.$$

8. We compute the other theoretical values for the gas in the nozzle outlet section:

a) density

$$\gamma_v = \frac{p_v}{R_v T_v} = \frac{0.9 \cdot 10^4}{33.9 \cdot 1730} = 0.1535 \text{ kg/m}^3;$$

b) exhaust velocity

$$w_e = 91.53 \sqrt{I_k - I_0} = 91.53 \sqrt{-677 - (-1355)} = 2380 \text{ m/sec};$$

c) specific nozzle outlet section

$$f_{y_{1,2}} = \frac{1}{\gamma_0 w_0} = \frac{1}{0.1535 \cdot 2380} = 26.4 \cdot 10^{-4} \text{ m}^2/\text{kg} = 26.4 \text{ cm}^2/\text{kg}.$$

SECTION 12. DETERMINING THE TRUE PARAMETERS AND CHARACTERISTICS OF A ZhRD

In a ZhRD thermodynamic computation, we usually determine the theoretical engine parameters and characteristics upon condition of:

- 1) complete physical combustion of the fuel used in the engine combustion chamber, up to a state of chemical and energy equilibrium for the gases formed;
- 2) chemical and energy equilibrium as the gases flow out from the chamber through the nozzle into the surrounding medium;
- 3) only one additional fuel-energy loss in the combustion chamber, due to gas dissociation, which is considered directly when determining theoretical temperature in the combustion chamber;
- 4) no heat is transferred from these gases to the surrounding medium through the surface of the engine chamber;
- 5) the chemical composition and thermodynamic parameters of the gas stream are the same in any nozzle cross section, from the combustion chamber to the nozzle outlet section;
- 6) the gas stream at the outlet from the nozzle is entirely coaxial;
- 7) fuel-energy loss from the exhaust gases, in accordance with the second law of thermodynamics, is taken into consideration by the engine thermal efficiency (assuming an adiabatic outflow).

Thus, the computed theoretical values of gas temperature in the combustion chamber and in the nozzle outlet section, the exhaust vel-

ocity, and the ~~ZhRD~~ specific thrust are overstated in relationship to their real values, which are obtained during static engine tests.

Under real engine operating conditions, the following things occur:

1) there is some physical incompleteness in fuel combustion because of imperfect mixing of the propellant components and their limited stay time in the combustion chamber, to limit the latter's volume and weight, which leads to a shortage in working gas pressure in the combustion chamber relative to its rated theoretical value;

2) the combustion-chamber thermal resistance to the gas stream, as the chamber heats up when fuel is consumed, also leads to some decrease in the gas-stream pressure throughout the length of the combustion chamber (in existing engine designs, this pressure loss, at the end of the combustion chamber, does not exceed 0.4-1% of the gas pressure at the chamber head);

3) there is some loss in gas energy in the engine nozzle due to incomplete fuel combustion, unequal outflow (insufficient recombination and relaxation of gas molecules), friction of gas molecules against each other and against the nozzle surface, and because of the lines of the gas streams at the nozzle outlet being noncoaxial;

4) there is some heat transfer from the gases to the surrounding medium through the engine-chamber liner surface, whose magnitude is insignificant in existing ~~ZhRD~~ designs (it does not exceed 0.5-1% of the fuel's calorific value) and is therefore frequently neglected in computations.

The level of knowledge which we have attained still does not permit us to compute gas outflow, allowing for all of these complex phenomena, and, consequently, we cannot precisely determine exhaust velocity and the specific thrust proportional to it.

Since the phenomena accompanying the process of transformation of thermal energy into kinetic energy in the nozzle occur chiefly with heat liberation, we may nominally consider that the gas outflow is a polytropic process with a variable exponent throughout the length of the nozzle. Thus, we may characterize the quantitative effect of all factors on the gas expansion cycle in the engine-chamber nozzle by one parameter — the polytropic exponent \underline{n} , whose magnitude varies throughout the nozzle length and may be approximately evaluated on the basis of experimental data. Figure 6.28 shows f_v as a function of \underline{n} for various values of p_v/p_k .

Since, at the present time, it is impossible to compute the quantitative theoretical effects of the factors enumerated above on the operating cycles in the combustion chamber and in the nozzle, we must perform computations for ZhRD being designed in accordance with the theoretical engine parameters and characteristics, employing the appropriate experimental coefficients for this purpose.

In view of the above statement, the dependence of an engine's true specific thrust P_{ud} on the theoretical specific thrust $P_{ud.t}$, which was computed during the thermodynamic design of the engine, is expressed by the equality

$$P_{ya} = \varphi_{ya} P_{ya.t} \quad (6.70)$$

where $\varphi_{ud} = P_{ud}/P_{ud.t} = \varphi_{p_k} \varphi_{f_k} \varphi_s \approx 0.90-0.98$ is the specific thrust correction factor for a real ZhRD chamber, allowing for the loss in specific thrust relative to its theoretical value $P_{ud.t}$ as a consequence of the imperfect cycle in the engine (this coefficient does not allow for a loss in P_{ud} due to nonoptimum gas expansion in the nozzle); $\varphi_{p_k} \approx 0.95-0.99$ is the pressure coefficient for the gases in the combustion chamber, allowing for the decrease in engine-chamber specific thrust relative to its theoretical value due to the shortage

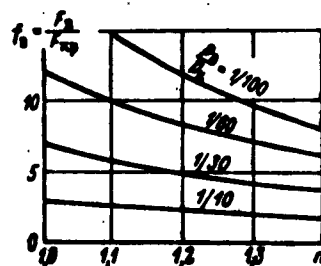


Fig. 6.28. The dimensionless area of an engine nozzle as a function of the pressure difference therein and the polytropic exponent for gas expansion.

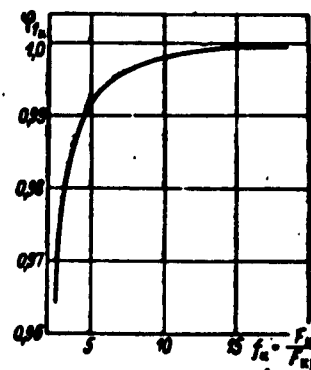


Fig. 6.29. Change in thermal-resistance coefficient φ_{fk} of a combustion chamber as a function of its dimensionless area f_k .

of gas pressure therein due to partial physical incompleteness of fuel combustion; φ_{fk} is the thermal-resistance correction factor for the combustion chamber, i.e., the decrease in engine-chamber specific thrust relative to its theoretical value due to decrease in gas pressure throughout the length of the combustion chamber as a result of the acceleration of the gases as they warm up, which, when $f_k = F_k / F_{kr} \geq 5$, we may assume is equal to one, and when $f_k = 2-4$, is equal to 0.96 to 0.99 (Fig. 6.29); φ_s is the nozzle-efficiency correction factor for the exhaust gases from the chamber nozzle, allowing for the decrease in engine-chamber specific thrust relative to its theoretical value due to gas-energy losses during outflow; its value varies within the limits of $\varphi_s \approx 0.95-0.97$ for conical nozzles, and $\varphi_s \approx 0.98-0.99$ for profiled nozzles.

As an illustration, in Fig. 6.29 we show φ_{fk} as a function of f_k for an engine operating on a propellant mixture of Tonka-250 + 80% HNO_3 of 98% weight concentration, and 20% N_2O_4 , when $p_k = 25-30$ atm abs.

For the gases in the combustion chamber of a bipropellant gas

generator, the pressure coefficient $\varphi_{p_k} \approx 0.85-0.86$, and for the turbine exhaust-pipe nozzle, the nozzle efficiency correction factor $\varphi_s \approx 0.97-0.98$. Thus, the specific thrust correction factor φ_{ud} developed by the exhaust gases of the turbopump unit is approximately equal to 0.82-0.84.

In computations for a ZhRD being designed, the values for the φ_{p_k} and φ_s coefficients are selected on the basis of statistical data, assuming that the structural data for the engine being designed correspond to the structural and operational characteristics for an existing engine, during whose trial the coefficients in which we are interested were obtained.

The pressure coefficient for the gases in a ZhRD combustion chamber is expressed by the formula

$$\varphi_{p_k} = \beta / \beta_t \quad (6.71)$$

where $\beta_t = p_{k.t} F_{kr.t} / G_s$ is the theoretical impulse of the gas pressure in the engine combustion chamber, in kg/(kg/sec), determined from the equation for the theoretical per-second fuel flow rate to an engine combustion chamber:

$$G_{t.r} = \frac{p_{k.t} F_{kr.t}}{\sqrt{R_{k.t} T_{k.t}}} A \text{ kg/sec}, \quad (6.72)$$

i.e.,

$$\beta_t = \frac{\sqrt{R_{k.t} T_{k.t}}}{A} \text{ kg/(kg/sec)}; \quad (6.73)$$

$\beta = p_k F_{kr} / G_s$ is the actual impulse of the gas pressure in the engine combustion chamber, which may be determined for an existing engine from the measured parameters for the cycle during static tests, and for an engine being designed, by selecting a value of the φ_{p_k} coefficient and a computed magnitude of β , i.e., according to the formula

$$*[\beta_t = \beta_t = \beta_{\text{teoreticheskoy}} = \beta_{\text{theoretical}}]$$

$$p_{k.t} = p_{k.t} = p_{\text{kamera.teoreticheskoye}} = p_{\text{chamber.theoretical}};$$

$$F_{kr.t} = F_{kr.t} = F_{\text{kriticheskoye.teoreticheskoye}} = F_{\text{critical.theoretical}}.]$$

$$\beta = \varphi_{p_k} \beta_t \text{ kg/(kg/sec)}. \quad (6.74)$$

For existing fuels and their combustion conditions in a ZhRD, $\beta_t \approx 160\text{-}222 \text{ kg-sec/kg [sic]}$.

In foreign literature, the β_t and β parameters are usually called the theoretical and actual characteristic rates of the fixed fuel-combustion cycle in a ZhRD chamber, respectively, and the parameter $\varphi_{p_k} = \beta/\beta_t$ is the correction factor for conversion of fuel to products of combustion in an engine chamber.

To determine the specific thrust correction factor $\varphi_{ud} = P_{ud}/P_{ud.t}$, we must compute the specific thrust $P_{ud} = P/G_s$ in accordance with the data from the engine's static tests, and then, with the values of gas pressures p_k and p_v measured during these tests, obtain the theoretical specific thrust $P_{ud.t}$ by means of the thermodynamic computations.

All measurements when testing a ZhRD are quite complex, since they are usually performed within a short time and at a great distance (in accordance with safety rules). However, at the present time we can measure the engine's absolute thrust, per-second propellant-component flow rate to the combustion chamber, and the pressure therein with sufficient accuracy for practical purposes. So far, techniques for measuring gas pressure p_v in the nozzle outlet section are poorly developed.

If we do not measure pressure p_v experimentally, it may be computed approximately in accordance with the formula $f_v = F_v/F_{kr}$.

In experimental determination of the φ_{p_k} and φ_s coefficients, it is practicable to perform the theoretical computations for the engine thermal cycle in accordance with the engine's static test data (p_k , G_s , and $\chi = G_{s_o}/G_{s_g}$) because of which the magnitudes of p_k and G_s in the formula

$$\varphi_{p_k} = \frac{\beta}{\beta_r} = \frac{(p_k F_{sp}/G_s)_{acc}}{p_{k,r} F_{sp,r}/G_{s,r}} \quad (6.75)$$

are cancelled out and therefore $\varphi_{p_k} = F_{kr}/F_{kr,t}$.

If, during a ZhrD's static trials, a given operating regime with regard to per-second fuel-flow rate is sustained, so that $G_s = G_{s,t}$, therefore, $\varphi_{p_k} = p_k/p_{k,t}$, and if $p_k = p_{k,t}$, $\varphi_{p_k} = G_{s,t}/G_s$.

Having determined the values of φ_{ud} and φ_{p_k} , and also considering that $\varphi_{f_k} = 1$ for an isobaric combustion chamber, we may compute the nozzle-efficiency correction factor for the gas stream from the engine nozzle, i.e.,

$$\varphi_s = \varphi_{ud}/\varphi_{p_k}. \quad (6.76)$$

Dividing fuel-energy losses into losses in the engine combustion chamber and in the nozzle is convenient because by this means it is easier to ascertain the reasons for a decreased P_{ud} , and plan methods for decreasing energy losses for the fuel used.

We determine engine characteristics in accordance with the experimental coefficients in the following manner:

1. Having assumed the values of the φ_{p_k} and φ_s coefficients, we determine engine specific thrust:

$$P_{ud} = \varphi_{p_k} \varphi_s P_{ud,t} \text{ kg-thrust/(kg-fuel/sec)} \quad (6.77)$$

and per-second fuel-flow rate to the combustion chamber ($p_k = p_{k,t}$):

$$G_s = \frac{P}{P_{sp}} = \frac{G_{s,t}}{\varphi_{p_k} \varphi_s} \text{ kg/sec.} \quad (6.78)$$

2. We determine the area of the nozzle throat under the same conditions ($p_k = p_{k,t}$) in accordance with the equation

$$\frac{p_k F_{sp}}{G_s} = \varphi_{p_k} \frac{p_{k,t} F_{sp,t}}{G_{s,t}} \quad \text{or} \quad \frac{F_{sp}}{G_s} = \varphi_{p_k} \frac{F_{sp,t}}{G_{s,t} \varphi_{p_k}} = \frac{F_{sp,t}}{G_{s,t} \varphi_k},$$

i.e.,

$$F_{sp} = \frac{F_{sp,t}}{\varphi_k} \text{ cm}^2.$$

3. We determine the dimensionless area of the nozzle outlet sec-

tion:

$$f_v = F_v / F_{kr}.$$

4. In accordance with the formulas given above, we compute the coefficients β_t and β .

5. We determine the engine's theoretical thrust coefficient when operating in space:

$$K_{a.r} = \left(\frac{2}{k+1}\right)^{\frac{1}{k-1}} \frac{k}{\sqrt{k^2-1}} \sqrt{1 - \left(\frac{p_a}{p_k}\right)^{\frac{k-1}{k}}} \times$$

$$\times \left[1 + \frac{k-1}{2k} \frac{\frac{p_a^{\frac{k-1}{k}}}{p_k}}{1 - \left(\frac{p_a}{p_k}\right)^{\frac{k-1}{k}}} \right]. \quad (6.79)$$

and then compute the true value for the engine thrust coefficient in accordance with the formula

$$K_p = \varphi_s K_{p.t}.$$

6. We determine the area of the nozzle throat in accordance with the formula for the engine-chamber thrust when operating in the atmosphere:

$$P_a = K_a p_k F_{kp} - F_a p_a = K_a p_k F_{kp} \left(1 - \frac{f_a}{K_a} \frac{p_a}{p_k}\right) = A p_k - B \frac{p_a}{p_k},$$

i.e.,

$$F_{kp} = \frac{P_a}{K_a p_k \left(1 - \frac{f_a}{K_a} \frac{p_a}{p_k}\right)} \text{ cm}^2. \quad (6.80)$$

7. We determine the engine's specific thrust in space and in the atmosphere:

$$P_{ud.p} = P_p / G_s = \beta K_p \text{ kg-thrust / (kg-fuel/sec)} \quad (6.81)$$

and

$$P_{y.a.s} = \frac{P_a}{G_s} = P_{y.a.s} - \frac{F_a p_a}{G_s} = \beta K_a - \frac{F_a p_a}{p_k F_{kp} \beta} = \beta \left(K_a - f_a \frac{p_a}{p_k} \right) =$$

$$= C + D \frac{p_a}{p_k}.$$

The formulas for absolute and specific thrusts given here

$$P_n = Ap_n - B \frac{P_n}{p_n} \text{ and } P_{y,n} = C - D \frac{P_n}{p_n},$$

may be used for computing engine altitude characteristics, assuming A, B, C, and D as constant quantities. By this means, one must assume a number of values for flight altitude and select values of p_n appropriate for them in accordance with the table.

8. We determine the per-second fuel-flow rate to the combustion chamber

$$G_s = \frac{P_n}{P_{y,n}} = \frac{P_n}{P_{y,n}} = \frac{P_n F_{xp}}{\beta} = E p_n \text{ kg/sec.}$$

These formulas may also be used for computing an engine's flow-rate characteristics, assuming E and F_{kr} as constant quantities. Thus, one must assume a number of values of p_k or G_s (from maximum to minimum) and compute G_s or p_k , accordingly.

Because of the difficulties connected with maintaining a constant fuel-flow rate when determining an engine's flow-rate characteristics during its static tests, as a changing magnitude for the flow-rate characteristics we often assume, not the flow-rate, but a magnitude of pressure p_k in the combustion chamber which is proportional to the flow rate.

One must not forget that if there is a considerable decrease in the fuel-flow rate to the engine combustion chamber and nozzle, such a great gas overexpansion may set in that the gas may be detached from the nozzle-liner surface, accompanied by the appearance of a normal gas-compression wave. Thus, the gas velocity at the nozzle outlet will be subsonic and the usual formula for computing the flow-rate characteristics which was derived for a supersonic exhaust, is unsuitable for use.

For approximate computations, we may use the following relationships:

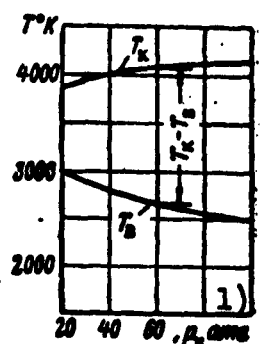


Fig. 6.30. T_k and T_v as functions of the p_k for the fuel-combustion products when $\alpha = 1$ atm abs.
1) p_k , atm abs.

$$G_s = \frac{G_{s,T}}{\gamma_{ya}}; \quad T_k \approx \varphi_{p_k}^2 T_{k,T};$$

$$\varphi_k \approx \varphi_{p_k}^2 \varphi_{k,T}; \quad \gamma_k \approx \frac{\gamma_{k,T}}{\gamma_{p_k}^2} \text{ and } F_s = \frac{F_{s,T}}{\gamma_c}. \quad (6.82)$$

Figures 6.30-6.33 show the effect of gas pressures p_k in the combustion chamber and oxidizer coefficient α on ZIRD parameters.

When p_k is raised, the parameters for the products of combustion of a given fuel and engine-chamber nozzle geometrical dimensions and weight are changed in the following manner:

1) combustion temperature T_k increases only slightly (Fig. 6.30), which is partially explained by some depression in gas dissociation as p_k rises, and, consequently an increase in the fuel heat-liberation coefficient φ_k ;

2) the gas temperature T_v at the outlet from the engine-chamber nozzle decreases (see Fig. 6.30), which is explained by the more considerable decrease in the value of $(p_v/p_k)^{(n-1/n)}$ as p_k rises relative to the change in the ratio T_v/T_k in the formula

$$T_v = T_k \left(\frac{p_v}{p_k} \right)^{\frac{n-1}{n}};$$

3) the value of the β parameter increases very slightly (Fig. 6.31), which is explained by the great decrease in the value of the per-second fuel-flow rate G_s as p_k rises relative to the change in the product of $p_k F_{kr}$ in the formula

$$\beta = p_k F_{kr} / G_s;$$

4) the chamber-nozzle throat is decreased in accordance with the hyperbolic law (see Fig. 6.32), which is chiefly explained by the decrease in per-second fuel-flow rate to the chamber of an engine of

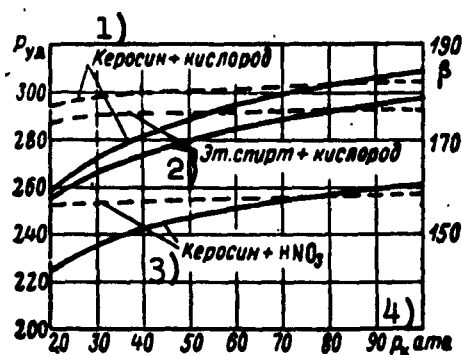


Fig. 6.31. P_{ud} and β as functions of p_k . 1) Kerosene + oxygen; 2) ethyl alcohol + oxygen; 3) kerosene + HNO_3 ; 4) p_k , atm abs.

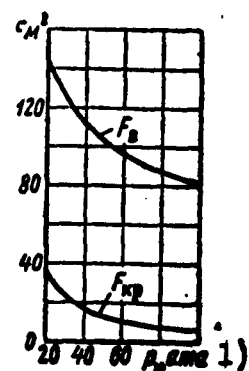


Fig. 6.32. F_{kr} and F_v of a chamber nozzle as functions of p_k when $p_v = 1$ atm abs. 1) p_k , atm abs.

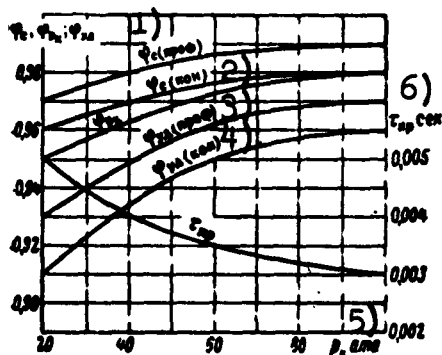


Fig. 6.33. Character of changes in ϕ_p , ϕ_s , ϕ_{ud} , and τ_{pr} as functions of p_k when the cycle is running smoothly, in a chamber with a conical and with a profiled nozzle. 1) ϕ_s (profiled); 2) ϕ_s (conical); 3) ϕ_{ud} (profiled); 4) ϕ_{ud} (conical); 5) p_k , atm abs; 6) τ_{pr} , sec.

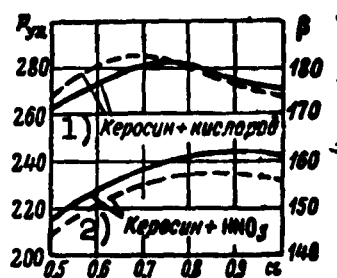


Fig. 6.34. P_{ud} and β as functions of α when $p_v = 1$ atm abs. 1) Kerosene + oxygen; 2) kerosene + HNO_3 .

given thrust as p_k rises;

5) the area of the chamber-nozzle outlet section also decreases (see Fig. 6.32), which is explained by the necessary change in the

ratio F_v/F_{kr} as p_k rises to preserve the given value of the gas pressure p_v at the outlet from the nozzle;

6) the engine-chamber nozzle weight decreases because of the decrease in its dimensions when p_k rises, and as we already know, specific thrust increases;

7) the φ_{p_k} , φ_s , and φ_{ud} coefficients increase and the fuel stay time τ_{pr} in the combustion chamber decreases because of the intensification in the thermal cycle in the engine chamber (Fig. 6.33).

Figure 6.34 shows the change in specific thrust P_{ud} and the β parameter as a function of the excess oxidizer coefficient α for two fuels.

Example 4. Determine the true geometrical nozzle dimensions and specific thrust of an engine with an absolute thrust at ground level of 12,547 kg and operating on kerosene ($C_g = 0.865$ and $H_g = 0.135$) and nitric acid of 98% weight concentration, when $\chi = 4.37$ kg/kg, $\alpha = 0.8$, $p_k = 30$ atm abs, $p_v = 0.9$ atm abs, if $w_{v.t} = 2480$ m/sec, $T_{k.t} = 2970^\circ\text{K}$, $T_{v.t} = 1654^\circ\text{K}$, and $R_{v.t} = 34$ kg-m/kg $^\circ\text{C}$.

Solution.

1. Theoretical parameters for the working fluid and characteristics of the engine:

a) density of the gases at the outlet from the nozzle

$$\gamma_{s.t} = \frac{p_s}{R_{s.t} T_{s.t}} = \frac{0.9 \cdot 10^4}{34 \cdot 1654} = 0.16 \text{ kg/m}^3;$$

b) specific nozzle outlet section

$$f_{yA.s.t} = \frac{1 \text{ m}^2}{\gamma_{s.t} w_{s.t}} = \frac{1}{0.16 \cdot 2480} = 25.2 \cdot 10^{-4} \text{ m}^2/\text{kg} = 25.2 \text{ cm}^2/\text{kg}.$$

2. Actual engine parameters and characteristics:

a) on the basis of the statistical data, we assume $\varphi_{p_k} = 0.96$ and $\varphi_s = 0.98$;

b) specific engine thrust is, therefore,

$$P_{YA} = \eta_{YA} \frac{w_{a,T}}{g} + \eta_{P_k} f_{YA,a,T} (p_a - p_a) = 0,96 \cdot 0,98 \frac{2480}{9,81} + 0,96 \cdot 25,2 (0,9 - 1,0) \approx$$

$$\approx 235,4 \text{ kg-thrust/(kg-fuel/sec)};$$

c) per-second fuel-flow rate

$$G_s = \frac{P}{P_{YA}} = \frac{12547}{235,4} = 53,3 \text{ kg/sec};$$

d) per-second fuel-component flow rate

$$G_{s,r} = \frac{G_s}{1 + \chi} = \frac{53,3}{1 + 4,37} = 9,9 \text{ kg/sec};$$

$$G_{s,o} = \frac{\chi G_s}{1 + \chi} = \frac{4,37 \cdot 53,3}{1 + 4,37} = 43,3 \text{ kg/sec};$$

e) area of the nozzle outlet section

$$F_a = \frac{f_{YA,a,T} G_s}{\eta_c} = \frac{25,2 \cdot 53,3}{0,96} = 1467 \text{ cm}^2;$$

f) mean exponent of isentropic expansion for the gases in the nozzle

$$k = \frac{\lg \frac{p_a}{p_k}}{\lg \frac{p_a T_{a,T}}{p_k T_{k,T}}} = \frac{\lg \frac{0,9}{30}}{\lg \frac{0,9 \cdot 2970}{30 \cdot 1650}} = 1,2;$$

g) critical area of the nozzle when $F_{kr} = 4,96$ (determined from Fig. 3.9 when $p_k/p_v = 33,3$ and $k = 1,2$)

$$F_{up} = \frac{F_a}{f_s} = \frac{1467}{4,96} = 296 \text{ cm}^2.$$

Chapter VII

PLANNING AND DESIGNING ZhRD CHAMBERS

The magnitudes of specific thrust, operational reliability, and cost and specific weight of the engine depend on the structural specifics of the chamber and the processes (cycles) taking place within the chamber.

Calculations of fuel-combustion processes within the chamber, and the discharge of the products of combustion through the nozzle make it possible only to determine specific thrust, the per-second fuel flow rate under given conditions of fuel combustion and given engine thrust, as well as the basic geometric dimensions of the nozzle. However, the structural dimensions of the nozzle and the combustion chamber (including the basic geometric dimensions of the combustion chamber), as well as the most efficient shapes for these are generally determined during the planning, designing, and strength-calculation stages for a chamber.

The basic tasks in planning and designing an engine chamber are the selection and calculation of the operational and structural chamber parameters, as well as design simplicity and low specific weight, operational reliability, and high operational characteristics.

In planning a ZhRD, it is also extremely important to resolve the problem of selecting the ignition system for the nonhypergolic fuel components as the engine is started; in addition, it is also extremely important to resolve the problem of selecting the

materials of which the individual engine parts and elements are to be made, as well as the problems associated with the construction of the engine itself.

The expedient selection of the fuel-ignition system will assure failproof engine starts, and eliminates the possibility of engine breakdown as a result of improper ignition. The expedient selection of materials for engine manufacture, as well as proper construction may result in reliable engine operation at minimum specific weight and cost. In this way the production of the engine is also simplified. The structural adaptation of the ZhRD to the weapon is also a matter of extreme importance.

SECTION 1. ZhRD CHAMBER REQUIREMENTS

A ZhRD chamber, regardless of type and design, must satisfy specific requirements that are based on the conditions under which the chamber is to operate.

The specific features of a ZhRD chamber which distinguish it from other heat-engine combustion chambers are the following:

1) a high rate of combustion-chamber heat liberation (about $0.5 \cdot 10^9 - 5 \cdot 10^9$ kcal/m³ hr), which places great demands on the design of the combustion chamber;

2) high gas pressures and temperatures within the chamber (about 20 to 80 atm abs and 2800-3600°C), which places great demands upon the materials and the cooling system;

3) short time periods for fuel combustion in the chamber (not to exceed 0.005 sec), which calls for extremely good fuel-component vaporization (for the most complete combustion) as the fuel is fed into the combustion chamber;

4) high per-second fuel-component flow rates, which calls

for reliable ignition as the engine is started;

5) pronounced impairment of engine-chamber operating economy and deterioration of cooling conditions, as operating regime falls below the rated regime;

6) rigid limitations in specific weight because of the specifics of ZhRD utilization in conjunction with flying craft, which makes it necessary to use light and high-strength materials (with extremely small strength safety factors) for the manufacture of chambers as well as of other engine elements.

The most important task in planning and designing an engine chamber is to provide for the greatest possible thrust at minimum specific weight and maximum design reliability. In a number of cases, when this is compensated for by corresponding weight reductions, it is fully permissible to reduce specific thrust somewhat. Although such a step would have only an indirect effect and is, at times, associated with considerable engine-design changes, it should, nevertheless, not be ignored.

The design and operational features of a ZhRD are strongly dependent on the type of fuel components used.

In planning an engine chamber it is necessary to provide:

1) for reliable fuel ignition during starting, regardless of atmospheric conditions;

2) for stable fuel combustion (without pressure variations) within the range of established engine-operating regimes;

3) for small fuel-energy losses with combustion in the smallest possible space and a given regime of engine operation;

4) for reliability of cooling (if the engine requires cooling) and for operations within the limits of the established regimes and service lives;

5) for a small fluid-pressure difference across the cooling duct;

6) for chamber-design simplicity, minimum specific weight, minimum cost, etc.

The combustion chambers used in existing engines, designed on the basis of experimental investigations, satisfy, in great measure, the majority of these requirements.

Basically, the perfection of a ZhRD chamber is determined by the magnitude of the specific thrust developed, given a simple, light, and reliable design. The magnitude of the specific thrust of the engine is the most important parameter and the one which determines the range of the weapon for the given degree of design perfection.

The basic factor affecting the magnitude of specific thrust developed by the engine chamber is the quality of the cycle taking place within the chamber. A study of the fuel-combustion processes in ZhRD chambers (for the purpose of their subsequent improvement and perfection) presents an extremely far reaching field for experimental and theoretical investigations.

For improved engine-chamber designs, it is necessary to undertake further investigations of the combustion processes (within the chamber) for given fuels at various component and combustion-pressure relationships as functions of the atomization installation, the spray rates for the fuel components, the configuration of the combustion chamber and the nozzle, as well as of a number of other factors and engine-operating conditions.

SECTION 2. LATERAL AND VOLUMETRIC INTENSITIES OF FLOW RATE AND HEAT LIBERATION IN ENGINE COMBUSTION CHAMBERS

The basic qualitative and quantitative characteristics of combustion-chamber operation in an engine are the following:

1. Coefficient α of excess oxidizer in the fuel, characterizing the maximum temperature level for the combustion-chamber cycle with given conditions of combustion for the given fuel:

$$t_x = \frac{H_{H_2} + \alpha_{H_2} H_{H_2O}}{(1 + \alpha_{H_2}) c_p} ^\circ C,$$

where c_p is the mean heat capacity of the products of fuel combustion, in kcal/kg $^\circ C$.

2. Coefficient φ_k of heat liberation from fuel in combustion chamber, i.e., the number indicating which portion of the heat is liberated in the combustion of the fuel, all secondary heat losses taken into consideration.

3. Coefficient φ_{p_k} of completeness of pressure in combustion chamber, characterizing the degree of physical fuel-combustion completeness.

4. Intensities of flow rate and heat liberation across combustion chamber, i.e., the quantity of fuel or heat directed at one square centimeter or one square meter of maximum combustion-chamber cross section per second or per hour:

$$G_{F_x} = \frac{G_x \cdot 10^3}{F_x} \text{ g/cm}^2 \text{ sec}$$

and

$$Q_{F_x} = \frac{G_x H_{H_2} \varphi_k}{F_x} = G_{F_x} H_{H_2} \varphi_k \text{ kcal/cm}^2 \text{ sec}.$$

5. The flow rate and volumetric rate of heat liberation in the combustion chamber, i.e., the quantity of fuel or heat, respectively, at a unit of combustion-chamber volume per hour or per second:

$$G_{V_x} = \frac{G_x}{V_x} 3600 \text{ kg/m}^3 \text{ hr};$$

$$Q_{V_x} = \frac{G_x H_{H_2} \varphi_k}{V_x} 3600 = G_{V_x} H_{H_2} \varphi_k \text{ kcal/m}^3 \text{ hr}.$$

For a comparative evaluation of the dimensions of engine combustion chambers operating at various gas pressures p_k , the

"reference" values of cross-section and volumetric heat-liberation rates are sometimes used, and these are calculated according to the following formulas:

$$Q_{F_k, \text{пр}} = \frac{Q_{F_k}}{p_k} \text{ kcal/m}^3 \text{ hr abs atm}^* \text{ and } Q_{V_k, \text{пр}} = \frac{Q_{V_k}}{p_k} \text{ kcal/m}^3 \text{ hr abs atm}$$

In contemporary engines (Table 7.1)

$$G_{F_k} \approx 20 + 50 \text{ g/cm}^2 \text{ sec: } Q_{F_k} \approx (0,7 + 5,0) 10^8 \text{ kcal/m}^2 \text{ hr;}$$

$$Q_{V_k} \approx (0,5 + 5,0) 10^8 \text{ kcal/m}^3 \text{ hr and } Q_{V_k, \text{пр}} = \\ = (1,3 + 2,0) 10^8 \text{ kcal/m}^3 \text{ hr abs atm.}$$

TABLE 7.1

Flow-Rate and Volumetric Heat-Liberation Rate Values for Combustion Chambers in Existing Engines

1 Тип двигателя	2 Давление в камере сгорания p_k атм	3 Теплонапряженность камеры сгорания	
		4 поперечная $Q_{F_k} 10^{-8}$ ккал/час м ²	5 объемная $Q_{V_k} 10^{-8}$ ккал/час м ³
6 Керосино-азотнокислотный	20—40	7—15	5—20
7 Спирто-кислородный	15—25	10—17	20—32
8 Керосино-кислородный	25—60	30—50	25—50
9 Прямоточный ВРД дозвуковой	1,3	0,2—0,5	0,3—0,7
10 Турбокомпрессорный ВРД	4,0	0,8—1,2	0,8—1,3

1) Type of engine; 2) pressure p_k in combustion chamber, in abs atm; 3) heat-liberation rate in combustion chamber; 4) cross-section $Q_{F_k} 10^{-8}$, (kcal/hr)/m²; 5) volumetric, $Q_{V_k} 10^{-8}$, (kcal/hr)/m³; 6) kerosene-nitric acid; 7) alcohol-oxygen; 8) kerosene-oxygen; 9) subsonic ramjets; 10) turbojet.

Since the per-second flow rate of fuel to the combustion chamber

$$G_s = \frac{p_k F_{кр}}{\beta} \text{ kg/sec} = \frac{p_k F_{кр}}{\beta} 10^3 \text{ g/sec,}$$

the preceding formula for combustion-chamber unit-weight flow rates

$$* [Q_{F_k, \text{пр}} = Q_{F_k} \text{ пр} = Q_{F_k \text{ камера приведенный}} = Q_{F_k \text{ chamber reference}}.]$$

can be rewritten in the following form:

$$G_{F_k} = \frac{p_k F_{k0}}{\rho F_k} 10^3 \text{ g/cm}^2 \text{ sec},$$

where p_k is the absolute gas pressure in the combustion chamber, in kg/cm^2 .

This formula indicates that the flow rate for a ZhRD combustion chamber (in $\text{g/cm}^2 \text{ sec}$) varies almost in direct proportion with the changes in gas pressure p_k taking place in the combustion chamber, and are numerically almost equal to the pressure value expressed in kg/cm^2 .

Experiments show that with an increase in p_k , the combustion-chamber cycle intensifies, as a result of which the increment of heat into the zone of liquid fuel components increases because of the reverse gas flows. Therefore, without reducing the intensity of the cycles taking place at the front end of the combustion chamber (heating, vaporization of fuel components, and initial mixing), it is possible to deliver a greater quantity of liquid fuel components, i.e., to raise the value of G_{F_k} , to the same chamber cross section F_k per unit of time by raising p_k .

The ratio of ZhRD combustion-chamber flow rate as a ratio to combustion-chamber pressure can approximately be regarded as constant, and the following functions may be used for computational purposes:

a) for nitric-acid engines

$$G_{F_k} \approx (0.8 + 1.0) p_k \text{ g/cm}^2 \text{ sec};$$

b) for oxygen engines

$$G_{F_k} \approx (1.1 + 1.3) p_k \text{ g/cm}^2 \text{ sec};$$

c) for fluorine engines

$$G_{F_k} \approx (0.8 + 0.9) p_k \text{ g/cm}^2 \text{ sec}.$$

In designing a ZhRD, the flow and volumetric heat-liberation rates for the combustion chambers are sometimes used, selecting their values on the basis of available statistics. These resultant cycle characteristics for the combustion chamber in the engine are, doubtlessly, important; however, from the standpoint of setting up a rational cycle and expanding the range of economic regimes for combustion-chamber operations, these characteristics are unusable, since they do not reveal the true picture of the processes taking place in the combustion chamber, nor do they indicate the factors which affect the quality of this cycle when the engine operates at various regimes. These characteristics may serve only as a tentative estimate of the volume required in the combustion-chamber being projected.

Engines with high flow rates and high operating-economy ratings must, clearly, in the case of fuel components exhibit minimum vaporization time, best mixing, and uniform distribution throughout the cross section of the combustion chamber.

A further increase in the flow rate of a ZhRD combustion chamber, evidently, will require:

- 1) a systematic supply of heat to the fuel-component injection zone, in order to accelerate the fuel-component vaporization process;
- 2) intensification of gas-stream turbulence in the combustion chamber through the installation of cooled "turbulizers" or auxiliary spray nozzles, atomizing the fuel into the gas stream;
- 3) the preliminary mixing, in nozzles, of the fuel components into a type of emulsion (using centrifugal emulsion spray nozzles) and other steps.

The concepts mentioned above make it necessary for us to adopt a differentiated approach to the evaluation of combustion-

chamber operations in an engine and particularly to the isolation of those characteristics which could, even if only in approximate terms, reflect the actual qualitative and quantitative cycle diagram in the combustion chamber of a real engine.

Example 1. Determine the volumetric heat-liberation rate in a combustion chamber, without consideration of the physical heat of the fuel being used, if $V_k = 0.383 \text{ m}^3$, $G_s = 127 \text{ kg/sec}$, $H_u = 1568 \text{ kcal/kg}$, and $\phi_k = 0.77$.

Solution.

$$Q_{V_k} = \frac{G_s H_u \phi_k}{V_k} 3600 = \frac{127 \cdot 1568 \cdot 0.77}{0.383} 3600 = 1.43 \cdot 10^8 \frac{\text{kcal/hr}}{\text{m}^3} =$$

$$= 400 \frac{\text{kcal/sec}}{\text{liter}}$$

SECTION 3. DETERMINATION OF COMBUSTION-CHAMBER VOLUME IN ENGINES

In order to burn the fuel to an equilibrium state for the products of combustion, we require appropriate combustion-chamber volume and length in the engine.

The combustion-chamber volume in the engine covers the entire flame tube from the head to the cross section of the converging section of the nozzle (whose area $F = 3F_{kr}$) since, in this portion of the chamber, the most intensive fuel-combustion and complete-combustion processes take place, without any marked reduction in pressure along the length of the chamber.

The following affect the required combustion-chamber volume:

- 1) the type of fuel, its composition, the per-second flow rate, and the atomization system for the fuel-feed system into the chamber;
- 2) the pressure and temperature of the products of fuel combustion;

3) the shape, and length of the combustion chamber, and similar factors.

If the volume of the combustion chamber is less than required, some of the fuel will not be fully consumed and will be carried away by the gases, through the nozzle, into the surrounding medium; if, on the other hand, this volume is excessively large, then the combustion chamber will be too large and heavy, and this will have a negative effect on the flight characteristics of the weapons. In addition, in a combustion chamber that is somewhat too large, there will be significant losses due to friction and heat transfer from the gases to the chamber liner, and in addition, gas-pressure fluctuations are possible, these latter capable of setting up vibrations throughout the entire engine.

Complete fuel combustion and the required combustion-chamber volume, in great measure, depend on the manner in which the fuel mixture is made ready for combustion. The more perfect the atomization of the fuel components and the more uniform the distribution of the fuel components through the cross section of the combustion chamber, the more complete the combustion of the fuel.

In planning a combustion chamber for an engine it is extremely important to select a volume at which it is possible to attain the most complete combustion of the fuel and, consequently, the greatest specific thrust with the lowest specific engine weight.

In view of the fact that the cycles within a combustion chamber of an engine have not been adequately studied, it is, at the present time, impossible to determine the optimum volume and necessary dimensions of the planned combustion chamber with theoretical precision. These parameters must be established in approximate terms only, and here we can make use only of the extremely limited

statistical data.

At the present time, the required volume of an engine combustion chamber can be approximately determined by one of the following methods:

1) according to the reference length of the combustion chamber, i.e., the ratio between combustion-chamber volume V_k and the critical nozzle section F_{kr} ;

$$l_{sp} = \frac{V_k}{F_{kr}},$$

i.e.,

$$V_k = l_{sp} F_{kr} m^3; \quad (7.1)$$

2) according to the stay time τ_{pr} of the fuel in the combustion chamber, i.e.,

$$V_k = G_s \tau_{sp} = G_s \frac{R_s T_s}{P_s} \tau_{sp} = F_{sp} \tau_{sp} \sqrt{g n R_s T_s \left(\frac{2}{n+1} \right)^{\frac{n+1}{n-1}}} m^3; \quad (7.2)$$

3) according to volumetric thrust p_1 (thrust referred to one liter of combustion-chamber volume), i.e.,

$$V_k = P/P_1 \text{ liters}; \quad (7.3)$$

4) according to the heat-liberation rate Q_{v_k} of the combustion chamber, i.e.,

$$V_k = \frac{G_s H_{sp} \tau_{sp}}{Q_{v_k}} 3600 m^3. \quad (7.4)$$

In existing engines, generally $l_{pr} \approx (V_k/F_{kr}) \approx 1.7-4 m$; $\tau_{pr} \approx 0.003-0.005 \text{ sec}$; and $P_1 \approx 70-450 \text{ kg/liter}$.

These parameters do not reflect the effect of combustion-chamber shape on the quantity V_k , although this effect is, in fact, present; neither do we, with these parameters, take into consideration the nature of the cycle within the combustion chamber, and this depends on structural and similar factors. In planning a ZhRD, the values of these parameters must be selected on the basis of statisti-

cal data.

The values of l_{pr} , P_1 , and Q_{V_k} are strongly dependent on the type of fuel and the pressure within the combustion chamber. Therefore, a computation of combustion-chamber volume on the basis of these parameters proves to be extremely inaccurate.

If there are no thoroughly worked out and precise data with respect to these parameters for an engine similar to the one being planned (operating on the same fuel, with the same pressure in the combustion chamber, and exhibiting the same atomization system), then the parameter τ_{pr} , the value of which is a weak function of p_k is the most appropriate for the determination of V_k .

Experiments indicate that with an increase in p_k , the value of τ_{pr} diminishes insignificantly as a result of the increased vaporization rate for the fuel components in view of the heat increment from the backflow of gases to the zone of liquid fuel components (cycle intensification in the combustion chamber). For example, for fuel T-1+80% HNO_3 with 20% N_2O_4 , at $p_k = 20$ abs atm, we may assume $\tau_{pr} \approx 0.0045$ sec, and at $p_k = 60$ abs atm, we may assume $\tau_{pr} \approx 0.003$ sec, which falls within the norms. In alcohol-oxygen engines, τ_{pr} is somewhat smaller than in nitric-acid engines.

A comparison of Eqs. (7.1-7.4) for V_k yields the following expression:

$$V_k = G_s \frac{R_s T_s}{P_k} \tau_{pr} = l_{pr} F_{sp} = \frac{P}{P_s} 10^3 = \frac{G_s H_{sp}}{Q_{V_s}}, \quad (7.5)$$

which indicates that τ_{pr} and l_{pr} , as well as P_1 and Q_{V_k} are, respectively, proportional to one another.

Between the volumetric thrust P_L and the reference length l_{pr} of the combustion chamber, we find the following dependence (at $p_v = p_a$):

$$P_s = \frac{p_k P_{ys}}{I_{sp} \beta}, \quad (7.6)$$

where $\beta = p_k F_{kr} / G_s$, the actual pressure pulse in the combustion chamber of the engine.

Volumetric thrust is a function of the type of fuel used, the design, and the operating regime of the engine.

Figure 7.1 shows volumetric and specific engine thrust as functions of the volume of the combustion chamber. The curves shown in this figure indicate that with an increase in combustion-chamber volume, volumetric thrust diminishes. The optimum volumetric-thrust value is the one which corresponds to the maximum value of P_{ud} .

For an approximate comparison of operational economy in various ZhRD with respect to volumetric thrust (with various p_k values, but identical p_v values) it has been accepted to refer the quantity P_1 to the identical pressure in the combustion chamber (generally to $p_k = 20$ or 30 abs atm) in accordance with the following formula

$$P_{s, \text{прив}}^* = \frac{30}{p_k} P_s \sqrt{\frac{1 - (p_s/30)^{\frac{n-1}{n}}}{1 - (p_s/p_k)^{\frac{n-1}{n}}}}. \quad (7.7)$$

With prechamber atomization of fuel components, the pre-chamber volume is generally 5 to 8% of the combustion-chamber volume.

In view of the inadequate and incomplete experimental materials permitting us to determine optimum volumes for atomization pre-chambers in the combustion-chamber head of the engine, and in view of a lack of reliable data on the applicability of prechamber atomization for the other types of fuel used (with the exception of ethyl alcohol and liquid oxygen — for which this atomization method is

*[Subscript: прив = priv = reference.]

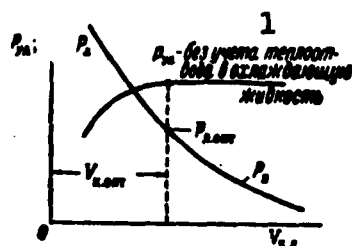


Fig. 7.1. Volumetric and specific engine thrust as functions of combustion-chamber volume. 1) Without consideration of heat transfer to cooling fluid.

presently in use), the selection of the prechamber atomization of fuel components, prechamber volumes, the number of prechambers, and the manner in which they are distributed in the chamber head should be carried out on the basis of existing experimental and statistical data.

In determining the volume of a ZHRD combustion chambers, it is necessary to bear in mind that:

- 1) the optimum volume for a combustion chamber (to provide for complete and stable fuel combustion) is a function of a great many factors whose effect on the volume cannot, for the time being, be taken into consideration in precise terms;
- 2) the volume of the combustion chamber must vary for various types of fuel components, atomization methods, and combustion conditions, since vaporization, activation, and component-combustion rates vary in this case;
- 3) in the case of insufficient combustion-chamber volume, the fuel-combustion process will be incomplete and unstable, and specific thrust will be reduced;
- 4) it is necessary to select the optimum combustion-chamber volume, both in terms of specific thrust, as well as in terms of specific weight;
- 5) the optimum volume of the combustion chamber can be reduced by increasing the gas pressure within the chamber, and through the use of improved atomization devices, and with the installation of special "turbulizers" within the chamber; in addition, there are certain other measures which will serve to speed up the processes of

preparing and burning the fuel;

6) the lower the volume of the combustion chamber, the easier it is to cool the chamber with one of the fuel components, given a small pressure difference across the cooling duct, and the lower the specific weight of the chamber (combustion chambers that are elliptical and spherical in shape have smaller cooled surfaces).

The above-enumerated factors which affect the optimum combustion-chamber volume are contradictory. For example, a combustion chamber that is large in volume and provides for complete fuel combustion cannot, simultaneously, have low specific weight or small pressure losses for the fluid in the cooling duct. Therefore, in determining the required volume of a combustion chamber, it is necessary to adopt a compromise solution which satisfies the majority of the requirements imposed, depending on the designation and operating conditions for the engine.

Example 2. Determine the volume and reference length of an engine-combustion chamber, if the diameter of the cylindrical portion of the chamber is 230 mm, if the length is 320 mm, and if the critical section of the nozzle has a diameter of 92 mm.

1. The area of the critical section of the nozzle is

$$F_{sp} = \frac{\pi d_{sp}^2}{4} = \frac{3.14 \cdot 92^2}{4} = 66.48 \text{ cm}^2.$$

2. The cross sectional area of the converging section of the nozzle, said area used to calculate the volume of the combustion chamber:

$$F = 3F_{sp} = 3 \cdot 66.48 = 199.44 \text{ cm}^2,$$

whence the diameter of this section

$$d = \sqrt{\frac{4F}{\pi}} = \sqrt{\frac{4 \cdot 199.44}{3.14}} = 15.93 \text{ cm} \approx 160 \text{ mm}.$$

3. The length of the converging section of the nozzle, in-

cluded in the volume of the combustion chamber, according to the nozzle drawing is $l_{szh} = 120 \text{ mm.}^*$

4. The volume of the combustion chamber

$$V_k = V_k + V_{cx} = \pi r_{k,k}^2 l_{k,k} + \frac{\pi l_{cx}}{3} (r_{k,k}^2 + r_{k,k} r_{k,k} + r_{k,k}^2) =$$

$$= 3,14 \cdot 1,15^2 \cdot 3,20 + \frac{3,14 \cdot 1,20}{3} (1,15^2 + 1,15 \cdot 1,20 + 1,20^2) = 18,62 \text{ liters.}$$

5. Reference length of combustion chamber

$$l_{sp} = \frac{V_k}{F_{sp}} = \frac{18,62 \cdot 1000}{66,48} = 280 \text{ cm} = 2,8 \text{ m.}$$

SECTION 4. ADVANTAGES AND SHORTCOMINGS OF COMBUSTION CHAMBERS, OF VARIOUS STRUCTURAL SHAPES, AND THEIR HEADS

The design of a ZhRD chamber is based on the over-all assembly and the structural features of the head, the combustion chamber, the nozzle, the cooling duct, the liner thrust frame, etc. A classification of existing combustion chambers for ZhRD is cited in Chapter II.

ZhRD chambers may be constructed with or without a stress-bearing connection between the surfaces of the inner and outer liners.

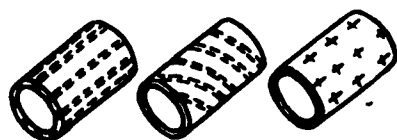


Fig. 7.2. Arrangement of combustion-chamber interliner attachment connections.

To facilitate cooling, the inner liner of the chamber should be made as thin as possible in order to reduce the temperature differences between the gas and liquid surfaces.

However, in this case, because the gas pressure within the combustion chamber exceeds the pressure of the liquid in the cooling duct, it is necessary to fasten this liner to the outer liner of the chamber. In existing ZhRD, the stress-bearing connections between the chamber liners are accomplished by

* $l_{cx} = l_{szh} = l_{suzhayushcheysya} = l_{converging.}$
 ** $[V_u = V_{ts} = V_{tsentr} = V_{center.}]$

means of contact welding or high-temperature "soldering." The contact at the points of welding (soldering) is achieved either through the use of special pads, or by raising sections of the outer liner — the chamber jacket — by means of stamping.

The arrangement of the attachment connections between the chamber liners may run the length of the liner, may be helical, or spot (Fig. 7.2).

In designing ZhRD chambers with connected liners, the selection of the type and arrangement of the stress-bearing elements is of primary importance. The spot connections may be arranged in rectangular or triangular ("chessboard") fashion.

The arrangement of the interliner stress-bearing attachments is based on the load diagrams for the combustion-chamber liners of the engine.

In the case in which the liners are attached to one another, the stress loads are borne by both liners, and therefore the inner liner may be made of much thinner material (lower weight), and this makes the cooling conditions very much easier, and also simplifies the technology required for the manufacture of such chambers. However, given such a liner arrangement, it is difficult, in practice, to provide for high-strength connections between the two liners, and the pressure difference for the cooling fluid in the duct rises substantially when there are spot connections in the form of stamped sections, and this is particularly true in the case of high combustion-chamber pressures.

With liquid being fed (under pressure) into the interjacket chamber space, reaction forces arise at the liner contact points. The stressed state of the inner chamber liner will be determined by the pressure of the liquid in the duct and the magnitudes of these re-

action forces. The latter are, primarily, functions of liquid pressure, as well as of chamber-liner rigidity, the connection arrangement, and the number of connecting elements.

Cylindrical and spherical (or shapes similar to these) combustion chambers are the ones most commonly used. The basic advantage of a cylindrical combustion chamber, relative to combustion chambers of other shapes, is the simplicity of design and manufacture and, consequently, low cost. In addition, this combustion chamber exhibits a smaller diameter.

The basic shortcomings of the cylindrical combustion chamber include the following:

1) given an identical volume, this chamber has great liner surface, thus making the cooling operation complex;

2) all other conditions being equal, this chamber has inferior strength characteristics, thus increasing specific weight and cost;

3) the gas stream in this combustion chamber adheres more closely to the surface of the liner than would be the case in a spherical combustion chamber, and this diminishes turbulence somewhat, causing the laminar gas layer to become thinner at the surface of the liner, and this leads to a reduction in the completeness of fuel combustion and, consequently, to a reduction in specific thrust; moreover, the reduced turbulence serves to increase the transfer of heat from the gases within the liner;

4) lower operational stability because of high-frequency vibrations, limiting flow rate and reducing the range of possible thrust control through variations in fuel flow rate.

Cylindrical combustion chambers are made with demountable or welded heads. These chambers are generally utilized in one-time

or multishot engines of low and medium thrust, where simple and low-cost designs are a primary requirement. In recent times, the combustion chambers that are most frequently used are cylindrical in shape, have a flat head, and single-component centrifugal spray nozzles. As an example of a ZhRD with cylindrical combustion chambers we can cite the German kerosene-nitric-acid engines.

Spherical or the close-to-spherical pearshaped combustion chambers exhibit the following basic advantages relative to combustion chambers of other shapes:

1) for a given volume, they have a smaller liner surface, thus reducing combustion-chamber specific weight, and facilitating cooling of the chamber;

2) for a given pressure within the combustion chamber, these chambers have thinner liners, and this tends to reduce the specific weight of the combustion chamber;

3) the liner of these combustion chambers is more stable against buckling inward under the action of the static pressure of the cooling liquid;

4) the fuel-combustion process within these chambers is more complete as a result of the relatively good turbulization of the gas stream, and this tends to raise specific engine thrust by 2 to 3%;

5) all other conditions being equal, there is, in these chambers, less transfer of heat from the gases to the chamber liner because of the presence, about the surface of the liner, of a thicker laminar layer which reduces heat transfer from the gases to the liner and thus facilitates the cooling of the combustion chamber (comparatively, the gas stream does not press as closely to the surface of the liner).

The basic shortcomings of spherical combustion chambers are the following:

- 1) complexity of design and production technology, which serves to raise cost;
- 2) a comparatively large combustion-chamber diameter, which may require extending the midsection of the missile.

Spherical combustion chambers generally have a welded spherical head. This shape for combustion chambers is used on engines of great thrust, operating for extensive periods of time, when the volume of the combustion chamber is large enough to make prechamber atomization of the components feasible, and also when the gain from weight reduction and improved operational economy (due to shape) exceeds the increased production cost.

As an example of a ZhRD with a spherical combustion chamber we can cite the German A-4 alcohol-oxygen engine.

Combustion chambers that are conical in shape have not come into use because of the great shortcomings that they exhibit and because they demonstrate no advantages whatsoever over other shapes.

Experiments have established that the transition from a spherical or elliptical combustion chamber to a cylindrical combustion-chamber shape has a negative effect on fuel-component mixing and combustion because there is a reduction in the initial "turbulization" of the gas stream in this case and, consequently, the specific thrust of the engine is reduced by 2 to 3%.

Combustion-chamber heads in ZhRD are primarily flat or spherical. Flat chamber heads have various design shapes. Sometimes they are made of three-wall construction with individual planes for the combustible and the oxidizer. The upper plate is generally spherical in shape, whereas the last two plates are flat, and it is in

these plates that the nozzles are mounted. In this case, the fuel component used for the cooling of the chamber enters the lower head cavity formed by the flat plates and passes to the combustion chamber through the spray nozzles. The second fuel component is fed directly into the upper head cavity formed by the spherical upper plate and the flat middle plates, subsequently entering the combustion chamber from this cavity through connector tubes which intersect the flat plates of the head and terminate in spray nozzles. Each of the three plates of the combustion chamber are connected to each other. The upper plate is connected to the middle flat plate by means of variously shaped gusset plates, and for purposes of connecting the flat plates spot-stamped sections or expanded nozzle-frames may be used. Since the number of nozzles is generally high (in the hundreds), the latter method of connecting the liners (plates) is, for all intents and purposes, also quite reliable.

The structural configuration of the head depends primarily on the shape selected for the combustion chamber, on the diameter of the chamber, the type of fuel components used, and also on which of the fuel components is used for the cooling of the chamber. Flat heads are used in chambers of engines developing low or medium thrust. They are most convenient for cylindrical combustion chambers from the standpoint of structural simplicity and convenience of locating jet and centrifugal spray nozzles for the combustible and the oxidizer. Flat heads in combination with a cylindrical combustion chamber provide for good uniformity of velocity field and fuel-component concentration through the cross section of the chamber. The shortcomings of flat heads involve their comparatively limited strength and rigidity in the case of substantial combustion-chamber cross section. Therefore, the heads of large-diameter combustion chambers must

have special stress-bearing elements.

Spherical heads are frequently made with prechambers and are used, primarily, in combustion chambers for alcohol-oxygen engines developing medium and great thrust. This type of head is also suitable from the standpoint of combatting the phenomena associated with lateral sound vibrations characteristic for engines with large-diameter combustion chambers. The advantage of this type of head lies in the fact that it is high in strength and rigidity, and its shortcoming lies in the fact that it is comparatively complex in design.

The installation of prechambers in the head of the combustion chamber facilitates the experimental adjusting of the atomization system, since, in this case, the preliminary adjusting of only a single prechamber is possible, and this is very much simpler and cheaper than attempting to adjust the entire atomization system of the head.

SECTION 5. SELECTION OF SHAPE FOR ZhRD COMBUSTION CHAMBER

The shape of the combustion chamber has a substantial effect on the magnitude of specific thrust as well as on the operating stability of the engine. Therefore, in planning a ZhRD, we must select a shape for the combustion chamber in which we have taken into consideration the general chamber requirements, as well as the advantages and shortcomings of the various shapes of combustion chambers, in addition to the following factors:

- 1) type of fuel components;
- 2) the suggested atomization system for these components;
- 3) the magnitude of absolute thrust and the duration of engine operation;
- 4) the pressure in the combustion chamber;

5) the technology involved in the manufacture of the chamber, etc.

In principle, a combustion chamber in an engine must have a shape which will offer high economy and low specific weight and cost.

During the Second World War, "cold" combustion chambers were made cylindrical in shape to develop low thrust, and had a jet atomization system for the hydrogen peroxide used. If a liquid catalyst is used to decompose the hydrogen peroxide, then a special swirler-mixer is installed inside of the combustion chamber, and in case a solid catalyst is used, the latter "package" is installed directly into the combustion chamber.

It is well known that hypergolic [sic] fuel components begin to react immediately upon mixing, and as a result, the combustion process of these components depends less on temperature, pressure, and combustion-chamber shape, than is the case with hypergolic [sic] fuel components. Therefore, for the first group of fuels it may prove to be more advantageous, from the structural standpoint, to select a simple and inexpensive cylindrical combustion chamber. In addition, for efficient ignition of hypergolic and nonhypergolic fuels, as well as for low-boiling and high-boiling fuel components, various atomization methods may prove to be efficient, and these methods may, in turn, variously influence the selection of optimum combustion-chamber shape in an engine.

The speed of the combustion process for nonhypergolic two-component fuels in the engine chamber, in the region of turbulent diffusion, is basically determined by hydrodynamic factors. In this combustion zone, the properties of the propellant (fuel) and the oxidizer are no longer decisive, nor is the temperature factor significant (if we ignore the weak dependence on the temperature of the

corresponding physical constants). Therefore, it is natural that the shape of the combustion chamber in the engine will have a substantial effect on the fuel-combustion process in the diffusion zone, i.e., on the turbulent intermixing of the components within the chamber, and consequently, on the rate and completeness of combustion.

If absolute thrust and engine operating time are small, preference should be given to a simple design and relatively inexpensive cylindrical combustion chambers with jet or centrifugal atomization of fuel components, since, in this case, the operating economy of the combustion chamber may be of secondary importance. In the opposing case (high absolute thrust and expensive engine operation), the operating economy of the engine assumes great importance, and as a result a more perfect spherical or elliptical shape will be required for the combustion chamber, and the chamber should have prechambers or conventional centrifugal atomization of fuel components; therefore, a slight increase in chamber-design complexity and the resulting increase in cost for the chamber may now become of secondary importance.

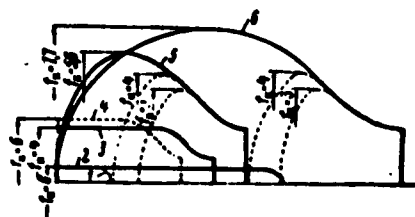


Fig. 7.3. Possible shapes of combustion chambers in ZhRD developing various thrusts.

An increase in the diameter of the combustion chamber as engine thrust increases, or an increase in gas pressure in a combustion chamber developing a given thrust is always associated with an increase in the thickness of the inner chamber liner

and, consequently, with the necessity of reducing the gas temperature in the combustion chamber in order to avoid overheating the combustion liner, and this means that with a drop in P_{ud} and a rise in the

per-second flow rate of the fuel in the engine. This can be explained by the fact that it is more difficult to cool a chamber liner that is thicker because of strength requirements. On the basis of these concepts, we may assume that spherical or elliptical combustion chambers are best suited for such cases, since chambers of such configuration, all other conditions being equal, have an inner liner that is thinner than the inner liner of a combustion chamber that is cylindrical in shape.

Figure 7.3 shows the outlines of several possible combustion-chamber shapes for ZhRD developing various thrusts.

For larger ZhRD (developing thrusts of approximately 50 to 100 tons), evidently, the most suitable chamber profile is profile 5, since the large chamber diameter, for all intents and purposes, eliminates the possibility of using a flat atomization head.

C The effort to preserve a good flow of heat to the head of the combustion chamber, i.e., to maintain a normal flow rate in the head, calls for an increase in the diameter of the combustion chamber, in such an engine, approximately up to 950 mm. As a result, the length of such a chamber will, probably, be approximately 600 to 700 mm. With contemporary mixture formations, such a chamber length may be regarded as excessive; however, it is difficult to reduce the length without impairing the configuration of the converging nozzle section or without reducing the diameter of the chamber.

(For ZhRD of relatively greater thrust and operating on highly efficient fuel components at combustion-chamber pressures of the order of 60 atm abs, the shape of the chamber will be closer to that indicated by profile 6. In this case, because of the large diameter and high pressure, the head of the combustion chamber must be semi-spherical in shape and exhibit a pronounced transition into the com-

bustion chamber which, in turn, must gradually form the nozzle.

In such an engine, the head of the combustion chamber is meant to refer to that portion of the chamber in which the fuel spray nozzles are located. In this case, the diameter of the chamber and the length of the chamber will, as before, be based primarily on the effort to have a head that is not overstressed due to the per-second fuel flow rate. Obviously, the length of the combustion chamber for such an engine will provide the required completeness of fuel combustion.

The ZhRD combustion-chamber profiles examined here may be regarded as typical for engines of various types. In all of these combustion chambers, the diameter is rather large, and therefore the dimensionless areas of these chambers attain values of the order of $f_k = 1.4-7.7$.

Figure 7.3, for combustion-chamber profiles 5 and 6, indicates with dashed lines those profiles which could be used in chambers at $f_k = 3$ and 4. The substantial gain in weight and dimensions for such combustion chambers is obvious. However, the flow rate through the combustion-chamber heads, in this case, increases sharply and exceeds considerably the highest values of G_{F_k} , attained at the present time. The utilization of such high-speed combustion chambers is inexpedient as a result of their limited volume and the difficulty of providing a flow of heat to the head.

In selecting combustion-chamber shapes for a engine in the planning stage, it is important to have the following concepts in mind.

1. The shape of the combustion chamber must provide for small values of optimum volume and specific weight, as well as for high operating economy.

2. The shape of the combustion chamber is significantly affected by the type of fuel used, since this factor is a basic criterion in determining the design of the atomization head of the engine chamber and the nature of the cycle in the latter.

3. The shape of the combustion chamber must, to the extent possible, follow the outline of the flame of fuel burning within it, and here the design of the chamber head must be taken into consideration, as must the atomization method for the components, the type of spray nozzles, the arrangement of the spray nozzles, and other factors.

4. With great thrust and extensive operating time for the engine, a structurally complex and expensive combustion chamber may prove to be economically more suitable than the simple and inexpensive, but less economical, cylindrical chamber.

5. In using elliptical and spherical combustion chambers, we achieve a reduction in liner surface, and the cooling conditions are eased; given this volume, specific weight also is reduced.

6. On the basis of production and design considerations, a combustion chamber of simple geometric shape (cylindrical) is preferred, since with more complex shapes, the design and manufacture of engine-chamber liners involves considerable difficulties; however, the operating efficiency of such a chamber must still be high.

7. Given low thrust and limited operating time for the engine, preference should be given to a structurally simple and relatively inexpensive cylindrical combustion chamber, since, in this case, operating economy may be of secondary importance.

SECTION 6. SELECTION OF RELATIVE AREA IN ENGINE COMBUSTION CHAMBERS

The relative combustion-chamber area $f_k = F_k/F_{kr}$ has a substantial effect on the magnitudes of absolute and specific engine thrust, and, therefore, must, in practice, have rational limits.

In designing a ZhRD the geometric dimensions of the nozzle are frequently determined without taking into consideration the drop in gas pressure across the length of the combustion chamber, which results from the heating of the gases, i.e., given the condition of equality between the gas pressures p_n at the front of the combustion chamber and the pressure p_k at the end of the chamber, which corresponds to $w_k = 0$ and $f_k = ((F_k = \infty)/F_{kr}) = \infty$.

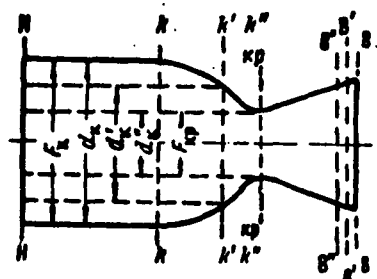


Fig. 7.4. For the selection of the dimensionless area of the combustion chamber (the diameter of the chamber is reduced).

Since a cylindrical combustion chamber for an engine must, in practice, be made with some final f_k , at which $p_k' < p_n$ and $w_k > 0$, the actual thrust for such an engine will be lower than under the condition $p_n = p_k' = p_k$. Therefore, we must set limits for f_k at which it is possible to design an engine

nozzle without taking into consideration the hydrodynamic drop in gas pressure across the length of a cylindrical combustion chamber, i.e., according to data from conventional thermodynamic calculations.

If in the given isobaric combustion chamber for the engine, the diameter d_k is reduced while we have constant values for F_{kr} , the nozzle spray-angle α and the difference between the gas pressure p_n at the front of the combustion chamber and the pressure p_v at the end of the nozzle (Fig. 7.4), then in this case:

1) there is an increase in the pressure difference and the velocity of the gas stream in the combustion chamber and a corresponding reduction in the nozzle; at $f_k = 5$, the loss of gas pressure at the end of the combustion chamber will be negligibly small (about 0.4-0.5%); at $f_k = 4$, about 1%; and at $f_k = 1$, we will obtain

$p_k' \approx 0.455p_n$ (at $f_k = 1$, the chamber is referred to as high-speed or a heat nozzle);

2) there will be a drop in the total gas-pressure difference across the chamber of the engine (p_n/p_v); in order to attain the initial gas pressure p_v at the outlet from the nozzle (with a reduction in p_k) it is necessary to shorten the nozzle correspondingly (see Fig. 7.3);

3) there will be drop in the coefficient φ_k for the fuel heat-liberation rate, as a result of a reduction in the coefficient $\varphi_{p.k}$ for completeness of fuel combustion, due to a lessening in the intensity of the combustion process, a drop in the required stay time τ_{pr}^* , and the influence of other factors on the cycle;

4) there will be an impairment of the conditions under which the nozzles may be positioned on the head of the combustion chamber, as well as a deterioration of fuel-component atomization as a result of a reduction of chamber diameter, which also reduced $\varphi_{p.k}$;

5) there will be a reduction in the exhaust velocity of the gases from the engine nozzle and a proportional drop in specific thrust, since the same gas-pressure difference for a heat nozzle will result in a lower exhaust velocity than would be the case in a purely geometric nozzle;

6) there will be a reduction in absolute engine thrust due to a reduction in the per-second fuel flow rate into the combustion chamber, as a result of a drop in the "flow through" capacity of the critical section of the nozzle, which can be attributed to the increase in the critical specific gas volume at the same time that a pressure drop occurred across the length of the combustion chamber.

Figure 7.5 shows tentative calculation curves for the relation $[\tau_{np}^* = \tau_{pr} = \tau_{prebyvaniye} = \tau_{stay}]$

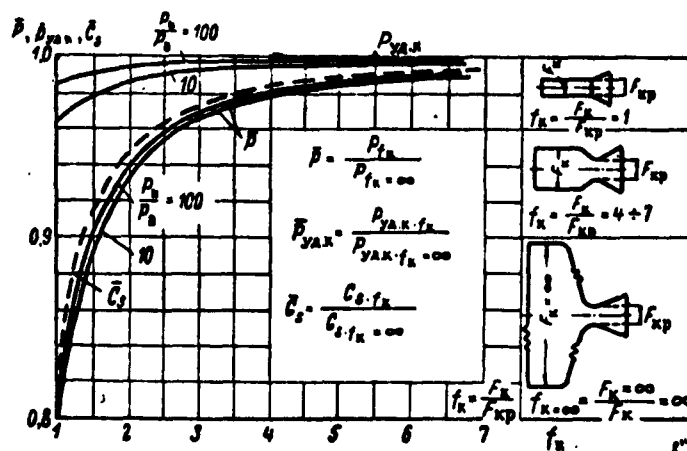


Fig. 7.5. Relative values of the per-second fuel flow rate, absolute thrust, and specific thrust, as functions of the dimensionless area of a combustion chamber in an engine.

tive change in \bar{G}_s , $\bar{P}_{ud.k}$, and \bar{P} as functions of f_k at constant values of f_{kr} , α , p_n/p_v ; $n = 1.2$; $R_k = 30 \text{ kg-m/kg } ^\circ\text{C}$, and $T_k/T_n = 12$. The curves indicate that:

- 1) a high-speed combustion chamber in an engine ($f_k = 1$) relative to an isobaric combustion chamber (with $f_k > 5$) exhibits a series of shortcomings, and therefore the practical utilization of such a chamber is clearly inexpedient;
- 2) with an increase in f_k from 1 to 3, specific and absolute engine thrust increase very markedly, from 3 to 6 the increase is insignificant, and at $f_k > 6$, they remain almost constant;
- 3) at values of $f_k > 3$, the effect of the gasdynamic factors on the processes taking place within the combustion chamber is small, and therefore the design of an engine nozzle must be based on the gas parameters obtained for a combustion chamber in thermodynamic calculations, i.e., at the condition $p_k = p_n$ and $w_k = 0$;
- 4) at values of $f_k < 3$, the above-mentioned assumptions introduce a considerable inaccuracy into the calculations, and this leads to an error in thrust that is greater than 3%. In contemporary en-

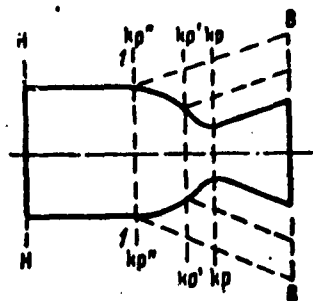


Fig. 7.6. For the selection of the dimensionless area of a combustion chamber (the critical section of the nozzle is increased).

gines, $f_k \approx 4-7.5$ and higher. By increasing the pressure in the combustion chamber, we find that the optimum value of f_k increases. If, however, in the given isobaric combustion chambers of the engine F_{kr} is increased (with F_k , p_n/p_v , and the nozzle flare angle constant [Fig. 7.6]), then:

- 1) specific thrust will be reduced because of the factors cited above;
- 2) there will be an increase in the per-second flow rate of the fuel into the engine chamber, since G_s and p_k are functions of F_{kr} (there will be thrust augmentation in the chamber in terms of the per-second fuel flow rate and thrust); with an increase in f_k , the

TABLE 7.2.

Engine Characteristics for Original and Modified* Versions (through an increase in F_{kr})

1) Вариант двигателя	2) P кг	3) p_k кг/см ²	4) $\frac{P_{ud}}{\text{кг топлива/сек}}$	5) d_k мм	6) d_{kr} мм	7) f_k
8) Первоначальный	1500	41	172	140	57	6.04
9) Форсированный	2000	30	136	140	81	2.98

- 1) Engine version; 2) P , kg; 3) p_k , kg/cm²;
 4) P_{ud} (kg/thrust)/kg fuel/sec; 5) d_k , mm;
 6) d_{kr} , mm; 7) f_k ; 8) original; 9) modified.

flow rate G_s increases more intensively than the specific thrust P_{ud} drop (see Fig. 7.6 and Table 7.2);

- 3) there will be a drop in the specific weight of the chamber (the very lightest is an engine at $f_k = 1$).
 *Literally forced.

The data of this table indicates that with a decrease in f_k from 6 to 3 because of an increase in F_{kr} , the thrust of the chamber increases by 25%. In case of need, the thrust of an existing engine can be increased by raising F_{kr} and G_s . However, it is clearly inefficient to select a value of $f_k < 3$, since, in this case, there would be a substantial drop in engine thrust, i.e., there would be a deterioration of engine-operating economy (see Fig. 7.5).

In planning a ZhRD, we find that for an efficient value of f_k it is necessary to take into consideration the kinetics of the fuel-combustion processes within the chamber, the engine-operating conditions, etc.

The dimensionless area f_k of the combustion chamber is uniquely associated with the flow rate G_{F_k} of the combustion chamber, which is selected at the beginning of the gasdynamic calculation for a ZhRD for purposes of determining w_k , p_k' , and T_k' .

For determination of p_k' and T_k' according to the known p_k and T_k it is necessary to know the state of the gases in the section for which the gasdynamic calculation of the combustion process is being carried out.

Precise experimental data on this point do not exist at the present time, and therefore, for the gasdynamic calculation of an engine it is necessary to select the above-mentioned initial combustion-chamber cross section on the basis of purely theoretical hypotheses and practical considerations. Probably, the truest picture can be gotten in this case if it is assumed that the combustion of the fuel begins in that section of the combustion chamber in which the fuel is vaporized. It should be assumed that the temperature in the zone of this section corresponds to the boiling point for a given partial pressure of the highest-boiling fuel component.

After selection of combustion-chamber shape for the ZhRD has been made, it is necessary to determine the dimensions of the chamber. It is difficult to resolve this problem theoretically, since the chamber dimensions depend on many factors which cannot, at the present time, be calculated quantitatively.

SECTION 7. DETERMINATION OF BASIC GEOMETRIC CHARACTERISTICS OF ENGINE CHAMBER

The basic geometric parameters for a combustion chamber in an engine include:

- 1) diameter of atomization head;
- 2) maximum diameter and length of combustion chamber;
- 3) lateral surface of liner, etc.

To the present time, no rigid rules have yet been set for the determination of the basic combustion-chamber dimensions in an engine. The diameter of the atomization head of the chamber must be adequate to allow the positioning of the fuel spray nozzles. In planning a ZhRD, we must make certain that the diameter of the head for the combustion chamber (of selected shape) can be evaluated approximately on the basis of statistical data.

In designing engines, we may assume the diameter of the atomization head to be:

- 1) for a spherical combustion chamber

$$d_{\text{roz}} \approx d_n^*$$

where d_k is the maximum diameter of the chamber, determined according to the following formula (Fig. 7.7a)

$$d_k = \sqrt[3]{\frac{V_k}{0.5236}} = 1.24 \sqrt[3]{V_k} \text{ m}, \quad (7.8)$$

$$*[d_{\text{роз}} = d_{\text{гол}} = d_{\text{головка}} = d_{\text{head}}.]$$

where V_k is the rated (theoretical) volume for the combustion chamber;

2) for an elliptical combustion chamber (see Fig. 7.7b)

$$d_{\text{roz}} \approx 0,6d_k, \quad (7.9)$$

where d_k is the maximum diameter of the combustion chamber, determined according to the following formula

$$d_k = 1,125 \sqrt{V_k} \text{ cm}$$

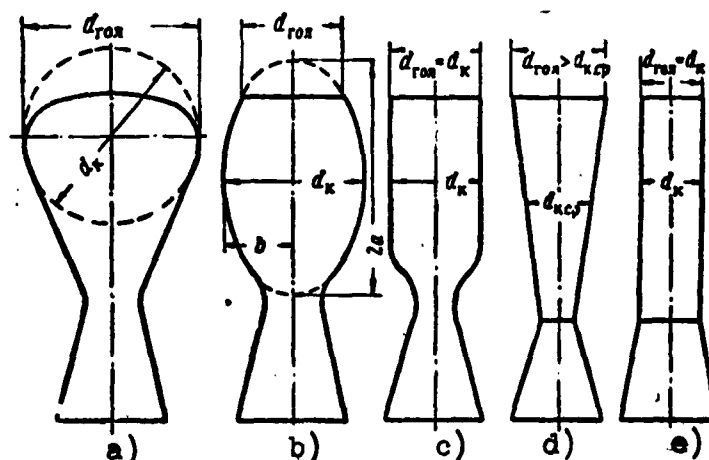


Fig. 7.7. For the determination of the head diameter in combustion chambers of various shapes.

3) for cylindrical and conically converging combustion chambers (see Fig. 7.7c, d, and e)

$$d_{\text{roz}} = d_k, \quad (7.10)$$

where d_k is the diameter of the cylindrical portion of the combustion chamber, determined according to the following formula

$$d_k = \sqrt{\frac{4F_k}{\pi}} = \sqrt{\frac{4G_s}{\pi G_{F_k}}} = \sqrt{\frac{4P}{\pi P_{ud} G_{F_k}}} \text{ cm};$$

here, $F_k = G_s / G_{F_k}$ is the area of the cross section of the combustion chamber, in cm^2 ; G_{F_k} is the area flow rate for the combustion chamber, in $(\text{kg/sec})/\text{cm}^2$; G_s is the rate of fuel flow into the chamber, in kg/sec ; P and P_{ud} are the absolute and specific chamber thrust, in $\text{kg thrust}/(\text{kg fuel/sec})$.

The formula for the determination of d_k of an elliptical combustion chamber is obtained in the following manner.

The volume of an ellipsoid of revolution (spheroid) is expressed by the equation

$$V_{sa} = V_k = \frac{4}{3} \pi abc = \frac{4}{3} \pi ab^2, \quad (7.11)$$

where a is the semimajor axis; b is the semiminor axis of the ellipsoid of revolution, and the axis $c = b$.

On the basis of statistical data, for elliptical combustion chambers it may be assumed that $b = (3/4)a$, i.e.,

$$V_k = \pi \frac{3}{4} a^3,$$

whence

$$a = 0.75 \sqrt[3]{V_k}. \quad (7.12)$$

Then the sought-after formula for the determination of the diameter of the elliptical combustion chamber will take the following form:

$$d_k = 2b = 1.5a = 1.125 \sqrt[3]{V_k}. \quad (7.13)$$

Since the ratio between the combustion-chamber area flow rate and the pressure p_k in the chamber is almost constant, the diameter d_k is inversely proportional to the square root of p_k , i.e., $d_k \approx 1/\sqrt{p_k}$.

The following dependence exists between the diameter of the combustion chamber and the critical nozzle section of contemporary engines:

a) in cylindrical combustion chambers for nitric-acid engines

$$d_k \approx (2.0 + 3.0) d_{np};$$

$$*[\overline{V_{en}} = V_{el} = V_{\text{ellipsoid}} = V_{\text{ellipsoid}}.]$$

b) in spherical combustion chambers for alcohol-oxygen engines

$$d_k \approx (2,3 + 2,5) d_{sp}.$$

The recalculation of the volume of a sphere into the volume of a pearshaped combustion chamber and the determination, approximately, of the length of the chamber can be accomplished in the following manner:

- 1) a circumference of d_k in diameter is drawn to some scale (Fig. 7.8);
- 2) the height $h \approx (0.1-0.2)d_k$ is plotted, to the same scale, on the vertical diameter and a chord — line 2-2, parallel to 1-1 — is drawn, and the diameter d_{gol} of the atomization head of the chamber is plotted on this line.
- 3) this same outline (circumference) is used to determine the height h_1 of the spherical segment intersected by line 2-2;

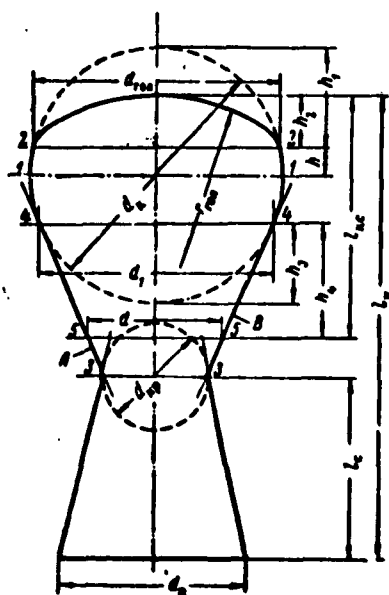


Fig. 7.8. For the determination of the length of a spherical combustion chamber.

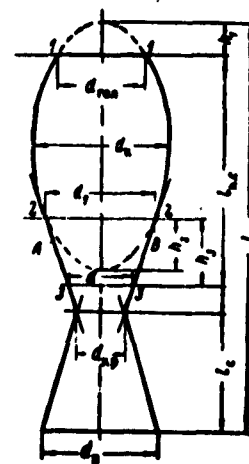


Fig. 7.9. For the determination of the length of an elliptical combustion chamber.

- 4) the height $h_2 \approx 0.1 d_{gol}$ of the tent-shaped combustion

chamber is plotted, to the same scale, up along line 2-2, and the head is drawn with a radius $r = d_k$;

5) the diameter d_{kr} of the critical nozzle section is plotted, to the same scale, on the arbitrary horizontal line 3-3 drawn beneath the circumference, with visual preservation of a certain proportion between the basic geometric chamber dimensions (diameter and length);

6) from the points along 3-3 tangential lines A and B are drawn to the circumference having a diameter of d_k and using the drawing made to the adopted scale, we determine the upper diameter d_1 (along line 4-4) of the truncated cone, and we can also determine the height h_3 of the truncated spherical segment;

7) the diameter of the truncated cone is determined in the same cross section in which the combustion chamber terminates, and determination is also made of the area of this truncated cone ($F = 3F_{kr}$ [line 5-5]);

8) the height of the truncated cone entering the volume of the combustion chamber is calculated:

$$h_4 = \frac{d_1 - d}{2 \operatorname{tg} \frac{\beta}{2}}, *$$

where β is the taper angle for the cone of the converging part of the nozzle;

9) finally, we find the sought length of the combustion chamber:

$$l_{k,c} \approx d_k - (h_1 + h_3) + h_2 + h_4.$$

In this approximate calculation of the length of the combustion chamber, we did not take into consideration the volume of the prechambers in the atomization system adopted for the fuel combustion [tg = tan]

ponents; in precise calculations, this volume must be taken into consideration.

After this calculation, we must undertake the problem of designing the shape of the combustion chamber and nozzle, deviating as necessary from the cited preliminary theoretical diagram for the shape of the engine combustion chamber.

The calculated volume of the ellipsoid of revolution can be distributed into the desired shape of the combustion chamber and the length of the chamber can be determined approximately, in the following manner:

1) the ellipsoid of revolution (Fig. 7.9) is drawn to some scale, using the earlier calculated values of d_k and a (here a is the semimajor axis of the ellipsoid);

2) the diameter d_{gol} of the atomization head of the combustion chamber is plotted, to the same scale, on the drawing of the ellipsoid and the height h_1 of the segment intersected by line 1-1 is determined;

3) determination is made of d_{kr} which, to the same scale, is plotted beneath the drawing of the ellipsoid of revolution, visually preserving a certain proportion between the basic geometric parameters of the chamber;

4) tangential lines A and B are drawn to the ellipsoid of revolution and the height h_2 of the segment cut away from the ellipsoid by line 2-2 is determined from the drawing;

5) similar to the manner in which this was done for the spherical chamber, the diameter of the converging nozzle section is determined for an area of $F = 3F_{kr}$; in addition, the corresponding volumes are determined, as well as the length of the combustion chamber.

The lengths of cylindrical combustion chambers and converging shapes are determined in similar fashion.

The length of the cylindrical portion of the combustion chamber must be such that, for the most part, the fuel-combustion processes can terminate within the chamber.

In combustion chambers of engines developing great thrust, the converging part of the nozzle has substantial dimensions. Therefore, the stay time for the gases in this subcritical nozzle section is high, and this must be taken into consideration in precise calculations of engine-chamber length.

If we know the volume V_k of the combustion chamber, the diameter d_k of the chamber, the diameter d_{kr} of the critical section of the nozzle, and if the profile of the converging part of the chamber (the nozzle) has been constructed, then the length of the cylindrical portion of the combustion chamber may be calculated with sufficient accuracy according to the difference in volumes (see Example 2):

$$V_k = V_k - V_{szh}, \quad (7.14)$$

where V_{szh} is the volume of the converging part of the combustion chamber, determined according to the geometric characteristics (see Section 3, Chapter 7).

It has not yet been established that the length of the cylindrical cross section of the combustion chamber is a function of p_k . However, it may be assumed that with an increase in p_k , the optimum length of this part of the chamber must diminish as a result of the intensification of the processes in the chamber and because of the requirement for an increase in dynamic engine-operation stability.

The length of the cylindrical section of the combustion

chamber in certain contemporary engines ranges from $l_{ts} \approx (1.0-2)d_k$.*

In engines with thrusts in excess of 10 to 15 tons and with increased gas pressure in the combustion chamber, the length of the cylindrical portion of the chamber may be smaller than the chamber diameter.

The structural dimensions of the combustion chamber (regardless of shape) are established in the planning stage and during the strength-calculation process. The theoretical values of the basic geometric combustion-chamber dimensions may be rounded off, since a slight variation has almost no effect on the operating characteristics of the engine.

In selecting the diameter of the cylindrical portion of the engine combustion chamber, it is important to bear in mind that:

1) with an excessively large d_k , it is structurally convenient to position standard-capacity fuel spray nozzles on the chamber head; however, in this case, the contact between the atomized components deteriorates and, therefore, given the theoretical combustion-chamber volume, the completeness of fuel combustion declines;

2) an excessive increase in d_k because of a reduction in l_{ts} may result in the impairment of the processes of heating, vaporization, and combustion for the fuel components;

3) with an excessively small d_k , it is structurally difficult to position standard-capacity fuel spray nozzles on the head. In addition, with little space (pitch) between the nozzles, the supply of heat (for heating and vaporizing the fuel components by a backflow of gases) is impaired, and this reduces the completeness of combustion for the given combustion-chamber volume and may lead to unstable engine operation;

*[$l_u = l_{ts} = l_{tsilindricheskiy} = l_{cylindrical}$.]

4) reducing the required number of standard-capacity spray nozzles to a lesser number, but of greater capacity, is inexpedient, since in this case the dimensions of the atomized fuel-component drops increase, and the completeness of combustion is impaired;

5) an increase in the output of the fuel spray nozzles and an excessive increase in the length of the cylindrical portion of the combustion chamber through a reduction of chamber diameter may result in unstable engine operation (pressure fluctuations within the combustion chamber).

The side liner surfaces of combustion chambers of various geometric shapes are determined by the corresponding formulas cited in mathematics handbooks.

The basic geometric characteristics of an engine-chamber nozzle include:

1) areas and diameters for the critical and outlet sections of the nozzle, which are determined from the data produced in a thermal engine calculation;

2) the length and side surface of the outlet section of the nozzle, which are determined as functions of nozzle profile and dimension, and

3) flare angles of the inlet and outlet sections of the nozzle, whose values are selected from statistical data.

Since the outflow of gases from the engine-chamber nozzle is close to equilibrium and since in this process gasdynamic factors play a major role, ZhRD nozzles may be modeled, i.e., the results obtained in investigations with small-dimension nozzles may be applied to nozzles used in engines developing great thrust.

Example 3. Determine the diameter of the critical and outlet section of the nozzle in an engine chamber, developing a nominal

thrust of $P = 2125$ kg, at $p_k = 22$ abs atm, $p_v = 1$ abs atm, and $n = 1.2$.

Solution.

1. The area of the critical nozzle section is determined from the general thrust formula, i.e.,

$$F_{kp} = \frac{P}{p_k \sqrt{\frac{2n^2}{n-1} \left(\frac{2}{n+1} \right)^{\frac{n+1}{n}} \left[1 - \left(\frac{p_v}{p_k} \right)^{\frac{n-1}{n}} \right]}} =$$

$$= \frac{2125}{22 \sqrt{\frac{2 \cdot 1.2^2}{1.2-1} \left(\frac{2}{1.2+1} \right)^{\frac{1.2+1}{1.2}} \left[1 - \left(\frac{1}{22} \right)^{\frac{1.2-1}{1.2}} \right]}} = 67.8$$

2. The area of the outlet section of the nozzle (see Section 16)

$$F_v = F_{kp} \frac{\left(\frac{2}{n+1} \right)^{\frac{1}{n-1}} \left(\frac{p_k}{p_v} \right)^{\frac{1}{n}}}{\sqrt{\frac{n+1}{n-1} \left[1 - \left(\frac{p_v}{p_k} \right)^{\frac{n-1}{n}} \right]}} =$$

$$= 67.8 \times \frac{\left(\frac{2}{1.2+1} \right)^{\frac{1}{1.2-1}} \left(\frac{22}{1} \right)^{\frac{1}{1.2}}}{\sqrt{\frac{1.2+1}{1.2-1} \left[1 - \left(\frac{1}{22} \right)^{\frac{1.2-1}{1.2}} \right]}} = 263$$

3. The characteristic diameters of the nozzles will be, respectively: $d_{kr} = 9.29$ cm = 92.9 mm, and $d_v = 18.3$ cm = 183 mm.

SECTION 8. SELECTION OF SHAPE AND ANGLE FOR ENGINE-CHAMBER NOZZLE

The shape and flare angles of the nozzle inlet and outlet sections in a ZhRD chamber has a substantial effect on the process of gas expansion and dispersion in the nozzles. Therefore, in chamber designs, the optimum angles must be selected. The better the design, construction, and production of the nozzle, the lower the gas-energy losses in the nozzle and the greater the effective exhaust velocity and specific thrust of the engine.

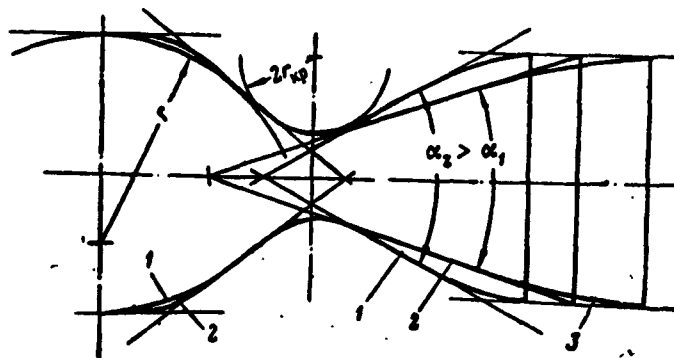


Fig. 7.10. Conical and shaped chamber nozzles. 1) Shaped nozzle with expanded flare angles; 2) conventional conic nozzle; 3) shaped nozzle with a flare angle of a conic nozzle.

Contemporary engines have conic nozzles and nozzles that are shaped along their length (Fig. 7.10).

The nozzles on some existing chambers have an over-all flare angle of 60 to 90° for the inlet section, and an angle of 20 to 40° for the outlet section. Such nozzles are less efficient than nozzles that are shaped along their length.

Nozzles of various shapes and flare angles have not yet been adequately studied for the various operating-regime ranges of existing ZhRD, and this leads to some difficulty in nozzle design.

With the mass production of welded-construction ZhRD chambers, where nozzles blanks are stamped from sheet metal, expenditures on fabricating shaped nozzles will be approximately the same as for a conic nozzle.

In planning nozzles, it is important to make every possible effort to satisfy the following basic requirements as fully as possible:

1) the gas-energy losses in the nozzle should be as small as possible, and their total value is generally taken into consideration

through the magnitude of the coefficient ϕ_s^* for the completeness of exhaust velocity;

2) the surface of the nozzle liner, for the given dimensions of the critical and outlet sections, must be optimum both in terms of efficient nozzle operation as well as in terms of cooling conditions, specific weight, and other indicators;

3) nozzle design and production technology must be kept as simple as possible.

These requirements imposed upon the design of a nozzle are mutually exclusive, since the complete satisfaction of any one of them will result in the impairment of the remaining nozzle properties. Therefore, in designing a nozzle, some compromise solution must be arrived at, this decision to be based on the designation of the engine.

The following gas-energy losses, reducing specific engine thrust, occur in the nozzle of an engine chamber:

1. Losses due to the friction of the gases against the surface of the nozzle liner. These losses are reduced if the inner surface of the nozzle is made smooth and if the outlet section has a large flare angle; the magnitude of these losses, however, cannot be reduced to zero. The greater the nozzle length, the greater the losses due to friction. The magnitude of the energy losses due to friction are taken into consideration through the factor ϕ_{tr}^{**}

The forces of friction in the combustion chamber are negligibly small because of the low gas stream velocities.

2. Losses due to the nonparallelism of the exhaust gases from the nozzle, relative to the nozzle axis. The radial shifting of

*[$\phi_c = \phi_s = \phi_{skorost} = \phi_{velocity}$.]
**[$\phi_{tp} = \phi_{tr} = \phi_{treniye} = \phi_{friction}$.]

the gases in the nozzle cone reduce the momentum of the gases in the axial direction and, consequently, lower the specific thrust of the engine. This loss can be made to vanish if we select a nozzle profile in which the velocities of the gases in the stream at the nozzle outlet are parallel to the axis of the engine. However, nozzles of such a shape are long, and this results in losses due to the friction of the gases against the surface of the liner, and serves to increase the weight and the dimensions of the nozzle (see Fig. 7.9). It is for this reason that it is not advantageous to provide for a completely parallel flow of gases from the nozzle. In practice, the over-all flare angle for a shaped nozzle, at the outlet, is set at from 10 to 16°.

The magnitude of the gas-energy losses resulting from radial gas dispersion within the nozzle (the nonparallelism of the flow at the nozzle outlet) are taken into consideration by the coefficient φ_{ras}^* .

3. Losses resulting from the imperfections in nozzle shape (outlet losses). These losses result from flow discontinuity and compression waves in the supersonic region of the nozzle.

With excessive curvature for the critical section of the nozzle, the peripheral streams may detach from the nozzle surface because of the inertial forces which arise with the transition through the critical section. These discontinuities disrupt the smooth outflow as the speed of sound is exceeded, and lead to the formation of vortices and compression waves. In addition, compression waves may form in the supersonic section of the nozzle at the points at which the nozzle profile is curved excessively. These losses can be diminished if all of the nozzle sections can be given correspond-

*[$\varphi_{\text{pac}} = \varphi_{\text{ras}} = \varphi_{\text{rasseivaniye}} = \varphi_{\text{dispersion}}$.]

ingly smooth outlines.

A series of experiments established that in designing the critical section of the nozzle for a radius equal to the diameter of this section, the outlet losses prove to be insignificant.

The magnitude of losses due to an imperfect nozzle profile are taken into consideration with the coefficient φ_{prof}^* . These losses may also occur with a normal flare angle for the outlet section of the nozzle, if the engine operates with regimes of excessive overexpansion of the gases in the nozzle because of a reduction in the rate of fuel flow into the combustion chamber.

4. Losses resulting from partial nonequilibrium of exhaust gases. These losses are functions of the nature of the products of fuel combustion, their pressure, and the length of the engine nozzle; with a nozzle length of the order of 0.1 meters, these losses do not exceed 1 to 2%. With longer nozzles, these losses, for all intents and purposes, are close to zero, since in this case the stay time for the gases in the nozzle increases and, therefore, the relaxation and recombination processes for the gas molecules in the nozzle are more complete. In calculating the exhaust process, we generally take into consideration the losses resulting from nonequilibrium of the exhaust gases in the nozzle with the mean polytropic exponent.

5. Losses attributable to the transfer of heat from the gases to the surrounding medium. These losses can be reduced if the nozzle exhibits a smaller liner surface, and this can be achieved by increasing the flare angle of the outlet section. The magnitude of the losses to the surrounding medium in a cooled engine are negligibly small (they do not exceed 0.2-0.3%).

(
$$\varphi_{\text{npof}}^* = \varphi_{\text{prof}} = \varphi_{\text{profil}} = \varphi_{\text{profile}}]$$

The above-enumerated gas-energy losses in the chamber nozzle tend to reduce specific engine thrust by 1 to 5% of its theoretical value, calculated for gas outflow from the nozzle without losses.

The basic gas-energy losses in an engine nozzle are taken into consideration with the coefficient of complete exhaust velocity:

$$\varphi_c \approx \varphi_{rp} \varphi_{pac} \varphi_{spc} \varphi_s$$

Engines have $\varphi_s \approx 0.95-0.99$.

The actual gas exhaust velocity from the engine nozzle may be determined according to the following formula:

$$w_{B.T} \approx \varphi_{ys} w_{v.t} \text{ m/sec, *}$$

where $w_{v.t}$ is the velocity of the gas stream in the outlet section of the nozzle, calculated without consideration of radial gas dispersion, according to the conventional formula for isentropic expansion.

The coefficient φ_s for existing ZhRD may be determined experimentally, and for an engine being designed the magnitude of this coefficient should be estimated, in approximate terms, on the basis of statistical data.

The calculation of the gas stream-energy losses due to gas nonparallelism at the nozzle outlet may be taken into consideration, approximately, with the dispersion coefficient φ_{ras} (Table 7.3).

TABLE 7.3.

Values of Coefficient φ_{ras} as Functions of Over-All Flare Angle α_v for Nozzle Outlet

Degrees α_v	0	4	8	12	16	20
φ_{pac}	1,000	0,9997	0,9989	0,9972	0,9951	0,9924
Continuation						
Degrees α_v	24	28	32	36	40	
φ_{pac}	0,9890	0,9851	0,9806	0,9755	0,9698	

$$* [w_{B.T} = w_{v.t}]$$

Here, the mean axial gas-outflow velocity from the nozzle can be expressed by the following formula:

$$w_s = \varphi_{pac} w_s \text{ m/sec,}$$

where $\varphi_{pac} = \frac{1}{2} \left(1 + \cos \frac{\alpha_v}{2} \right)$; here α_v is the over-all flare angle of the outlet section of the nozzle.

Conic nozzles are used in engine chambers developing low and medium thrust, where gas-stream energy losses resulting from radial dispersion may be neglected. The advantage of conic nozzles are their relative simplicity of design and manufacture.

For the conic nozzles in ZhRD chambers being designed, we can presume the following flare angles: a) for the inlet section, $\beta = 60-90^\circ$; b) for the outlet section, $\alpha \approx 25-30^\circ$.

For the radius of profile curvature at the critical nozzle section we may assume

$$r = (0.7 + 1) d_{kr},$$

where d_{kr} is the diameter of the critical section of the nozzle.

With such flare angles, the nozzle has comparatively limited lengths and small weight, and there is no substantial reduction in specific engine thrust relative to the P_{ud} of a perfectly coaxial flow.

Optimum flare angles for the inlet and outlet sections of the nozzle, for a given engine-chamber operating regime, can be established experimentally.

Experiments show that the flare angle and the shape of the inlet section of the nozzle have little effect on the magnitude of specific engine thrust and have practically no effect on the nature of the gas stream in the area beyond the critical section of the nozzle.

The shape of the inlet nozzle section, as well as the angle

of the inlet nozzle section, determine the fields of velocity and pressure in the gas streams for the subcritical section of the nozzle. As a result of the construction of the channel, the gas pressures are greater at the surface of the nozzle than close to the nozzle axis because of centrifugal forces; in the critical section, the opposite is true. The greater the convergence angle for the inlet nozzle section, the greater the gas pressure at the nozzle surface, and the greater the energy losses due to friction. Pronounced changes in the contour of this section of the nozzle may result in the formation of compression waves.

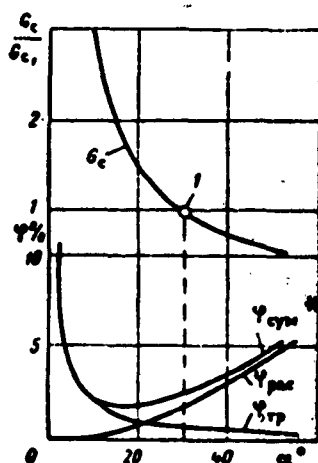


Fig. 7.11. Approximate dependence between weight G_s of conic chamber nozzle developing a given thrust and the magnitude of gas-energy losses within the chamber and the magnitude of the overall flare angle α . 1) Point of initial dependence of nozzle weight G_{s1} of the chamber against which the comparison is being made.

In designing engines, we find it most expedient to prepare the outline of the inlet channel of the nozzle with smooth conjugate curves (with circumferential arcs), which makes it possible to reduce the length of this nozzle section, to simplify the production technology, and to reduce weight. In this case, the radii of the circumferential arcs are selected from the standpoint of the condition for conjugate arcs, so as to impart the smoothest possible outline to the nozzle.

The flare angle for the outlet section of the nozzle, as has already been mentioned above, has a substantial effect on the nature of the cycle within the nozzle

$$*[\varphi_{cym} = \varphi_{sum} = \varphi_{sumarnyy} = \varphi_{total}.]$$

and on the magnitude of specific thrust developed by the engine. In selecting this angle for the engine being designed, it is important to have the following in mind.*

1. The greater the flow angle of the outlet section of the nozzle the shorter and lighter the nozzle, all other conditions being equal, and the smaller the cooling surface, and the smaller the transfer of heat to this surface from the gases (it is easier to cool the nozzle with the given quantity of fluid), and the fluid-pressure losses in the cooling duct will also be smaller, as will the energy losses attributable to the friction of the gases against the nozzle surface. However, in this case, the diameters of the nozzle-outlet section may prove to be excessively large relative to the midsection of the missile, the nonequilibrium conditions for the exhaust gases will be greater, and the gas stream-energy losses will increase substantially as a result of radial dispersion.

2. With an excessively large nozzle flare angle, gas stream-energy losses are possible as a result of the gas stream becoming detached from the nozzle surface, and because of the appearance of vortices, turbulence, and compression waves.

3. As the flare angle is decreased, the nozzle becomes longer, and the outflow of the gases is in a state of greater equilibrium; the energy of the gases is diminished as a result of their radial dispersion at the nozzle outlet. However, in this case, the nozzle-liner surface increases, and this makes cooling more difficult; in addition, gas-energy losses increase due to the friction of the gas against the surface, and moreover, the weight of the nozzle also increases.

The above-enumerated factors which determine the optimum
*D. Satton. Raketnyye Dvigateli. IL, 1950.

values for the flare angle of the diverging part of the nozzle, are mutually contradictory and can, in each specific case, be calculated precisely only through experimentation.

Figure 7.11 shows the change in weight (for a nozzle of a chamber developing a given magnitude of thrust) and gas-energy losses within the nozzle as functions of the flare angle of the diverging part of the nozzle.

The curves on this figure indicate that in terms of gas-energy losses in a conic nozzle, the optimum flare angle must be approximately 20° . However, in order to reduce nozzle weight, the angle may be assumed to be 30° in the design stage. This assumption is valid, since a deterioration in engine efficiency (specific thrust) is permissible by almost as many percentage points as there is for the reduction in engine weight.

The optimum relationship between efficient nozzle operation and nozzle weight depends both on the flare angle and the pressure within the combustion chamber and the outlet section of the nozzle, as well as on the optimum altitude characteristics of the nozzle and the operating time of the engine. This must necessarily be taken into consideration in each specific case in the planning and design of an engine chamber.

The nozzle outlet should not be made to have a sharp edge, since gas overexpansion and increased energy losses because of dispersion may occur as the edge is rounded off.

SECTION 9. GRAPHICAL METHODS TO SHAPE THE NOZZLE OF AN ENGINE CHAMBER

The nozzle of a chamber is usually shaped in engines of medium and great thrust, as well as for engines operating with a high degree of gas expansion, since the utilization of a conic nozzle

C

1



(

(

(

An increase in specific engine thrust of 2 to 3% through the structural parameters of the nozzle alone indicates the feasibility of shaping the nozzles used in ZhRD chambers developing medium and great thrust. The savings in fuel consumption achieved in this case are more than enough to offset the expenditures involved in shaping the nozzle.

There are several different graphical methods of shaping a nozzle for a chamber in an engine. A strict gasdynamic shaping of a nozzle, in which the generatrix of the supersonic portion coincides with the gas stream line is complicated and difficult. Moreover, the length and weight of such a nozzle is comparatively great, and the production techniques are extremely complex. Therefore, for purposes of shaping the nozzle of an engine chamber, it is expedient to use the simplified graphic method.

The initial data for the shaping of the diverging section of a chamber nozzle in an engine are the following:

- 1) the dimensionless nozzle area $f_v = F_v/F_{kr}$;
- 2) the radii r_{kr} of the critical and r_v of the outlet section of the nozzle;
- 3) an angle $\alpha_v/2$ for the nozzle outlet.

Graphically, it is simplest to plot a chamber-nozzle profile along a parabola. In this case, the inlet section of the nozzle, in the area of the critical section, is formed by an arc whose radius is $2r_{kr}$ (Fig. 7.12), and this part of the nozzle is arbitrarily made to meet with the generatrix of the combustion chamber.

The angle $\alpha/2$ ($6-8^\circ$) is selected on the basis of the value of f_v and the tangent AB is drawn to the above-mentioned circumference at this angle. After this, the lengths of the sections AC and AD are determined according to the following formulas:

$$AC = ar_{kp} \text{ and } AD = br_{kp}.$$

For various values of f_v and $\alpha/2$, coefficients a and b have the following values:

f_v	4	6	8
$\alpha/2$	15°	17°	19°
a	5,15	4,82	4,62
b	8,4	9,6	11,2

Then we draw the line DE for the nozzle outlet and line EG which is tangent to the generatrix of the nozzle at the outlet (at angle $\alpha_v/2$), and points E and C are connected with a parabola that is plotted as shown in Fig. 7.12. A table of coordinates is prepared for the working drawing of the nozzle and the nozzle profile is drawn. It is considerably simpler to produce a nozzle of this type since the profile is formed with straight lines and arcs. Figure 7.13 shows the schematic diagram for such a nozzle.

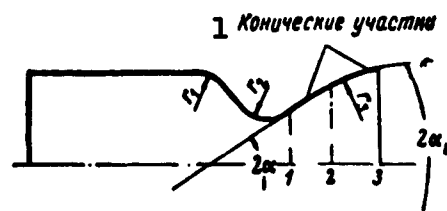


Fig. 7.13. Schematic diagram of nozzle shaped by a simplified graphic method. 1) Conic sections.

The conic section 1-2 of this nozzle is formed by straight lines, and the section 2-3 by a spherical surface of radius r_3 which may terminate in a conic surface.

It should be borne in mind that for engines that develop thrust which can be regulated by controlling the rate of fuel flow into the chamber, a shaped nozzle may prove to be inexpedient. ZhRD combustion chambers and nozzles may be modeled, but in designing new engines this method cannot yet be applied since the development of scientific modeling (similarity) methods for ZhRD are still in the initial stage.

SECTION 10. ENGINE-CHAMBER LINER LOADS

In calculating a ZhRD for strength, the design of the liners

and the chamber head proves to be most difficult and little developed because of the difficulties that arise in calculating the stresses which are present when these elements are in operation at high temperatures and being acted upon by other factors.

In operation, individual engine-chamber elements are subjected to various loads. The inner and outer chamber liners are subjected to particularly diverse load characteristics. These liners are subject to the action:

- 1) of radial and axial hydrostatic-pressure forces;
- 2) of thermal loads, arising as a result of the heating of the inner liner;
- 3) of dynamic and vibration loads occurring during launching, normal operations, and as the engine is stopped;
- 4) of the reaction of the chamber supports which are fastened to the thrust frame of the engine or directly to the weapon.

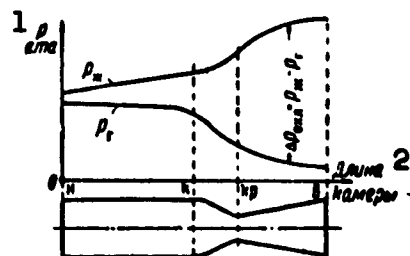


Fig. 7.14. Change in the pressure of the liquid in the cooling duct, along the length of the engine chamber. 1) p , abs atm; 2) length of chamber.

The magnitudes of each of these liner loads for various engine-chamber designs are quite varied, and therefore the strength calculations for combustion-chamber liners and nozzles must be carried out for each specific engine. Since a precise calculation of the loads mentioned in items 2 through 4 is extremely

difficult, the calculations for the liners are generally carried out from the standpoint of general concepts.

Static load on the liner is created by the pressure of the liquid in the cooling duct of the chamber. Under the pressure of this liquid, the outer liner (the jacket) of the chamber is subject to

stretching. In this case, the inner chamber liner is compressed under the action of the pressure difference Δp_{okhl}^* and because of the pressure p_g^{**} in the channel of the chamber (Fig. 7.14).

Since the pressure of the cooling liquid in the duct, moving from the nozzle outlet to the chamber head, diminishes as a result of hydraulic resistance within the duct, and since the gas pressure in the channel of the chamber, to the contrary, drops from the head of the chamber to the nozzle outlet, the maximum fluid-pressure difference for the inner liner appears at the outlet section of the nozzle (in the area at which the fluid enters the cooling duct).

The liner in an uncooled chamber is subjected to radial and axial stretching due to gas pressure; the greatest pressure arises within the combustion chamber, and the least pressure is encountered at the outlet section of the nozzle.

The operating conditions for engine-chamber liners are considerably complicated by the high temperature of the inner liner. Since the strength of the metal depends on temperature, which in the given case diminishes along the length of the liner (from the head to the nozzle outlet), the strength of the inner liner varies throughout the length of the chamber, as well as at various periods of engine operation.

It is possible to calculate, with sufficient accuracy for practical purposes, the stresses arising within individual chamber elements, said stresses arising as a result of static loads. The stresses which arise in the chamber elements as a result of nonuniform heating during operation are not adequately defined.

The inner and outer chamber liners of the engine exhibit

$$^*[\Delta p_{oxl} = \Delta p_{okhl} = \Delta p_{okhlazhdazhdayushchiy} = \Delta p_{cooling}.]$$

$$^{**}[p_r = p_g = p_{gaz} = p_{gas}.]$$

particularly nonuniform heating characteristics, and as a result the inner liner (as the relatively hotter) tends to lengthen, whereas the outer liner which is structurally connected to the inner liner at its ends, hinders this lengthening process. As a result of these phenomena, the inner chamber liner of the engine is subjected to compression, whereas the outer liner is subjected to stretching.

As an example, it should be pointed out that the chamber of the A-4 engine, characteristically 1790 mm long in the cold state, extends up to 5 mm in the axial direction during operation, and up to 4 mm in the radial direction (with respect to the maximum diameter of the combustion chamber).

The nonuniform heating of the thickness of the inner liner leads to the bending of the liner, since as a result of a temperature difference, the hotter liner layers, in their effort to expand, stretch the outer layers, and the latter, resisting this stretching process, compress the inner layers. These temperature stresses attain their maximum values at the gas and liquid surfaces of the liner, whereas they are almost equal to zero in the center of the liner.

If the yield point is exceeded by the temperature stresses arising within the metal of the inner lining as a result of the liner's relative elongation and bending, these stresses may produce plastic deformation within the metal, and this, under certain conditions, will result in premature deformation or even destruction of the liner under the action of other loads.

If there were no temperature stresses within the liner, the permissible stresses resulting only from static load could be greater by a factor of almost two.

Elongation due to temperature and the stresses arising therefrom may also occur in other assembly elements of the engine (TNA, GG) and in the "plumbing," particularly when hot gases are used to

eject the fuel components from the fuel tanks into the combustion chamber.

In order to relieve the chamber liners (made without coordination of the stress-bearing elements) of the temperature loads, arising as a result of nonuniform liner heating and elongation, the outer chamber liner is generally made of shells whose ends are interconnected with some clearance along the axis by means of special compensation rings (similar to an engine of the A-4 type). The installation of temperature compensators on the outer liner is particularly necessary for large-dimension chambers, since the liners of such chambers are subject to considerable temperature elongation.

The compensation rings are affected by the stretching force on the outer chamber liner, said force arising because of the temperature deformations of the inner liner, and because of the pressure of the cooling liquid; the pressure of atmospheric air may be neglected.

However, since the compensators which can, in practice, be made exhibit a certain elasticity if their wall-thickness is substantial and if the diameter of curvature is relatively small, it is generally impossible fully to relieve the chamber liner of the stresses described above.

In view of the above, in the strength calculations for the inner chamber liner of the engine it is necessary to take into consideration the stresses arising within the liner as a result:

- 1) of the difference between the pressure of the cooling liquid across the duct and the gases in the channel of the chamber;
- 2) of the temperature difference through the thickness of the liner;
- 3) of the rigidity of the temperature compensators, resist-

ing the elongation of the inner liner relative to the outer liner, as the former is heated.

These stresses within the liner vary along the chamber length, and as a result it is particularly difficult to take these stresses into account in engine design.

Inner-liner rigidity is extremely important from the standpoint of its reliable operation, since during engine operation the liner is loaded from without by the excess pressure of the cooling liquid. Under the action of the pressure of the cooling liquid and because of the thrust on the nozzle, the inner chamber liner may, at high temperatures, easily become unstable, buckle inward, heat up rapidly, or crumble.

The temperature difference through the thickness is insignificant for the outer chamber liner, and in its strength calculations, therefore, we take into consideration only those stresses arising within it because:

1) of the pressure forces due to the cooling liquid within the duct;

2) of the rigidity of the temperature compensators restricting the elongation of the outer liner, i.e., the temperature elongation of the inner liner which is structurally connected to the outer liner.

The outer chamber liner is regarded as a thin-walled vessel that is subject to internal pressure.

The stresses for the temperature compensators are determined by calculating the bending moments (resulting from the great thickness of their walls, relative to the radius of curvature).

The material of the chamber head is, in practice, also called upon to function at comparatively low temperatures, and as a result

special requirements are imposed.

The head and the chamber liner are to be regarded as a single structure, with a coordinated stress-bearing frame.

When centrifugal spray nozzles are used, the chamber head of the engine is frequently made of two flat plates and one outer spherical plate which form the cavities from which the fuel (combustible) and oxidizer are fed to the spray nozzles.

The structural connection of the flat head plates, in each individual case, may vary. The head in a coordinated stress-bearing frame will, during operation, receive static load in the form of the pressure difference between the mean pressure of the combustible and the oxidizer in the feed cavities and the gas pressure in the combustion chamber.

The head plate that is in contact with the hot gases is strongly heated and linearly elongated. Since the plate is rigidly and structurally connected, by one method or another, to the upper head plate across its entire surface, and connected to the cylinder of the combustion chamber on its periphery, temperature stresses which tend to reduce mechanical properties arise within the material used in the head, and these stresses are in addition to the stresses which may be attributed to static load. It is important for the head of the chamber to be sufficiently rigid and that the required degree of hermetic sealing be maintained at the points at which the spray nozzles have been expanded.

The basic goal in designing a chamber head is the determination of its rigidity for given operating pressures and temperatures. Experiments show that, in practice, the material used in the chamber head is not subject to plastic deformation. In this case, a chamber head may be designed in the usual manner, employing the theory of

elasticity.

In chamber liners with a coordinated stress-bearing frame, the temperature expansions of the inner liner, in both the axial and radial directions, are limited by the fact that it is structurally connected with the outer liner. In this liner design, the distribution pattern for the axial and radial forces is extremely complex and, in practice, the calculation of these forces is extremely difficult.

In addition to high-strength characteristics, chamber elements, as well as the points at which they are connected to one another, must exhibit a certain rigidity because they bear the vibration loads which might arise in an engine, said loads caused by pressure fluctuations in the gases within the combustion chamber, as well as by other factors.

In strength calculations for chambers, gas-pressure fluctuations within the combustion chamber during launching, during operation, and upon stopping the engine, and the thermal and random dynamic loads that have not been taken into consideration to this point must now be accounted for by means of appropriate strength safety factors for the material. If the engine chamber is welded, the thickness of its inner liner must be somewhat greater than rated, in order to make provision for the technically permissible poor weld-seam penetration (up to 25% of liner thickness) and the possible concentration of stresses within the material due to welding.

In planning an engine, frequently the thickness of the inner and outer chamber liners, as well as the chamber head, are assumed; then, during the design stage of the chamber, these are checked for strength. In addition, in order to simplify the equipment needed for the production of the chamber, inner combustion-chamber liners and

nozzles are made in identical thicknesses.

The static internal loads on individual elements of the chamber vary for various operating regimes in the engines, i.e., on launching, during normal operation, and on stopping. The strength-calculation checks for the chamber should be carried out during these most characteristic engine-operating regimes.

As the engine is started, the gas pressure in the combustion chamber is equal to zero, and the pressure of the cooling fluid in the duct attains its highest (complete) value. The inner chamber liner is unheated. At that instant, the chamber liner is loaded to the maximum from without because of the pressure of the fluid. The strength calculations for the liner should be based on the point most heavily loaded (in Section 2, see Fig. 7.12) and in the section with the greatest diameter. In this case, the high-strength properties of the metal used in the liner are taken for normal temperatures. Calculations are carried out for strength and liner stability. The outlet section of the nozzle is the most dangerous with respect to loads. Consequently, this nozzle section must be checked for stability.

During normal engine operation, static fluid load on the liner, from the nozzle outlet to the chamber head, diminishes as a result of the changing gas pressure along the length of the chamber; however, there is, as a result of this, a substantial increase in the liner temperature and, in this connection, liner strength is decreased. In this case, we must take into consideration permissible resistance and the elasticity modulus of the liner material as functions of temperature.

In the calculations, the mechanical properties of the material should be determined at the mean liner temperature, i.e., at

$t_m = \frac{t_{in} + t_{out}}{2}$. The points on the liner for which these calculations

have to be made are the following: the nozzle outlet, the critical section of the nozzle, and the greatest cross section of the combustion chamber. The strength and stability of the liner are also calculated.

As the engine is stopped, the liquid pressure in the cooling duct may be high or low, depending on the setting of the fuel-feed system valves, and the pressure in the combustion chamber drops to atmospheric. The inner chamber liner is heated to a high temperature. This situation could be extremely dangerous for a chamber in which the liquid pressure in the duct does not diminish or drops only slightly, even after a total gas-pressure drop within the chamber. The restarting of the engine is particularly dangerous.

Strength calculations for auxiliary engine elements (tubing, tanks, springs, diaphragms, reduction gears, turbines, pumps, etc.) are carried out according to well-known methods and, as a rule, no serious difficulties are encountered.

SECTION 11. REQUIREMENTS FOR MATERIALS USED IN ENGINE CHAMBERS

The operating conditions for various chamber elements in an engine differ sharply from one another. The outer chamber liner, in practice, functions at low temperatures and therefore no special requirements are imposed on its materials, as is the case with materials used in the chamber head. For the fabrication of these chamber elements, conventional low-carbon steels may be used.

The inner chamber liner functions under extremely difficult conditions and as a result rigid requirements apply to the materials used here.

The material for the inner chamber liner in an engine must exhibit:

1) high heat resistance, since the inner liner operates at high temperatures, despite the steps taken to reduce these;

2) high thermal conductivity and high reflecting power, since this will reduce the temperature of the liner gas surface and increase its strength;

3) easy processing during manufacturing, and if the chamber is of welded design, then with good weldability;

4) high resistance to corrosion with the use of metal-aggressive fuel components, and this is particularly important for multiple-start engines (where the engine is restarted many times);

5) the capacity to resist mechanical and chemical action of the gases flowing past the liner at high speeds;

6) a low coefficient of thermal expansion, which simplifies considerably the design of the outer chamber liner;

7) good resistance to shock, vibration, and thermal loads arising during launching, operation, and the stopping of the engine;

8) the lowest possible specific weight, since the ratio of the ultimate strength σ_b of the material to the specific weight γ_m^* determines the specific strength of the material; the higher σ_b/γ_m , the better the material and the lower the over-all weight of the chamber.

In addition, the material must be inexpensive and readily available.

At the present time, there is no material completely satisfying all of the above-enumerated contradictory requirements. For example, the requirements for high strength and thermal conductivity for the material at substantial temperatures cannot be combined in a single material, since materials exhibiting high strength generally

* $[\gamma_m = \gamma_m = \gamma_{\text{material}} = \gamma_{\text{material}}.]$

have low thermal conductivity, and vice versa.

Materials capable of withstanding substantial stresses at high temperatures (stainless and heat-resistant steels), are best used for the manufacture of liners of limited thickness, in which case satisfactory heat transfer between the gases and the cooling liquid is assured. However, to use these materials for the manufacture of combustion-chamber liners of large dimensions is not always possible, since in this case the heat-transfer conditions require that the thickness of the liner be so small that it would be unsuitable, in terms of stability, even for chambers operating under low loads.

The materials used in ZhRD may have high, medium, and low thermal conductivities.

Materials of high thermal conductivity are copper and aluminum, as well as alloys of these with other materials. These materials, relative to steels, have low permissible stresses, as well as limited resistance to heat. Aluminum alloys lend themselves to processing. Copper exhibits higher thermal conductivity, but just as aluminum, can be used in engine-chamber designs in which the liner is artificially relieved of mechanical loads.

Low-carbon steels exhibiting a coefficient of thermal conductivity of about 40 to 50 kcal/m hr °C are materials of medium thermal conductivity.

These steels lend themselves to stamping and welding. Relative to copper and aluminum alloys, they are more resistant to heat and as a result exhibit a lower thermal conductivity, satisfactory specific strength, are relatively inexpensive, and in adequate supply. These steels are the basic materials used in the fabrication of ZhRD chambers, despite the fact that they have such shortcomings as light oxidizability and little resistance to erosion.

Low-carbon steels are most suitable for the fabrication of multiple-start engine chambers operating on nonaggressive fuel components, and for single-start engines operating on aggressive fuel components. The inner liners of the majority of ZhRD are made of such steels.

Low thermal-conductivity materials include high-alloy and heat-resistant steels. These steels function well at high temperatures and are resistant to erosion. However, as a rule, they do not lend themselves well to stamping and welding. Moreover, they are expensive and in short supply. They are used for engine chambers operating on aggressive fuel components.

In selecting the material for the inner chamber liner it is necessary to bear in mind the requirements for the cooling of the engine, as well as to take into consideration, on the one hand, the changes in specific engine characteristics which occur in a particular engine variant, and, on the other hand, the production and economic considerations.

The operating temperature for the gas surface of liners in contemporary engines generally ranges from 425 to 925°C (with an average of about 650°C). At these temperatures, many of the existing materials exhibit satisfactory strength under normal engine-cooling conditions. However, the necessity of increasing specific engine thrust by using fuels of higher heating value, with high combustion temperatures, makes it necessary to seek out materials for the inner liner of the chamber, which can be heated safely to higher temperatures.

The development of ZhRD required the development of heat-resistant materials: plastics, light alloys of aluminum and titanium, special heat-resistant ferrous- and nickel-based alloys, high-melting

metals (molybdenum, tungsten) with protective coatings, refractory ceramics, and metalloceramic-type compositions (see Section 13, Chapter 9).

At the present time, the problem of seeking out materials for the inner liner of a ZhRD chamber is receiving considerable attention.

The majority of the remaining chamber elements and other engine assemblies can be made of conventional inexpensive and readily available materials. However, they must be selected with an eye to the requirements imposed, and we have reference here to such items as adequate strength at minimum component-part dimensions, low specific weight, limited cost, etc.

The physicomachanical characteristics of the metals and alloys used for the fabrication of engines are cited in the corresponding handbooks.

SECTION 12. DETERMINATION OF OPTIMUM PRESSURE IN ZhRD COMBUSTION CHAMBER

In order to provide the missile with the greatest possible flight range, we can both improve the cycle and the design of the ZhRD, as well as select the optimum engine parameters. One of the

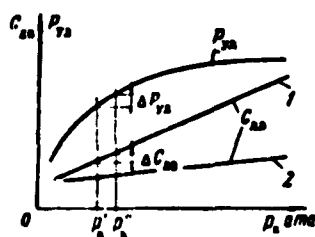


Fig. 7.15. Principal pattern of changes in specific thrust and over-all engine weight as functions of pressure within the combustion chamber. 1) With a pressure-fed fuel-feed system; 2) with a pump-fed fuel-feed system.

basic parameters is the gas pressure p_k in the combustion chamber.

It has already been pointed out above that an increase in gas pressure in the combustion chamber leads, on the one hand, to an increase in specific engine thrust (at first rapidly, and then beginning at 40 to 60 abs atm slowly, and

at about 100 abs atm extremely insignificantly) and, on the other hand, it leads to increased expenditure of energy for the feed, under pressure, of fuel into the combustion chamber, in addition to bringing about an increase in engine weight, particularly of the fuel-feed system as a result of its increased capacity.

For this reason, the velocity at the end of the powered phase and the flight range of the missile will initially increase as p_k is increased, since in this case the increment in specific engine thrust Δp_{ud} is more than enough to offset the energy consumed on carrying a corresponding weight increment ΔG_{dv} for the engine into space, and then after we have attained a certain value of p_k which may be referred to as optimum, the powered-phase velocity and missile-flight range will diminish in view of the fact that the increment Δp_{ud} will no longer be adequate to impart motion to the weight increment (Fig. 7.15).

In designing engines for missiles, the gas pressure in the combustion chamber is frequently taken from statistical data, since there are still too few satisfactory methods for determining its optimum magnitude analytically. Such an approach to the solution of the problem may not always be successful.

In contemporary ZhRD, the gas pressure in the combustion chamber fluctuates over the following ranges:

- a) with a turbopump fuel-feed system, $p_k \approx 15-50$ abs atm, at a feed pressure of $p_p \approx 25-60$ abs atm;
- b) with a pressure-fed fuel-feed system (using VAD or ZhAD) $p_k \approx 25-30$ abs atm and higher at a feed pressure of $p_p \approx 32-40$ abs atm, and with PAD, $p_k \approx 40-50$ abs atm.

Optimum gas pressure in the combustion chamber of the engine depends, basically, on engine thrust, operating time, and the fuel-

feed system and designation of the missile. Approximate calculations indicate that for engines and missiles presently in use, the optimum pressure in the combustion chamber, with respect to flight range, lies within the limits of from 15 to 30 abs atm for pressure-fed fuel-feed systems, and 50 to 70 abs atm for turbopump fuel-feed systems, with gas ejection into the atmosphere behind the turbine.*

The optimum gas pressure in the combustion chamber of an engine being designed must be selected to take into consideration the structural features of the engine, the efficiency and reliability of engine operation, and the factors which affect missile-flight range, i.e., proceeding from the condition of obtaining the best flight characteristics for a missile of variable weight.

In first approximation, this condition is met by the transformation of the formula after K.E. Tsiolkovskiy for the determination of missile-flight velocity at the end of the powered phase:

$$V_{\text{кон}} = gP_{\text{га}} \left(\ln \frac{1}{1-a} - \frac{a}{b} \right) \text{ m/sec, **} \quad (7.15)$$

where $a = G_t/G_0$ is the fuel-weight ratio for the missile; $b = P/G_0$ is the thrust-weight ratio for the missile; G_0 is the starting weight of the missile, consisting of the structural weight of the missile, payload weight, and the weight of the engine with the fuel and the working fluids of the fuel-feed system (compressed gas, exhaust gas, etc.).

In this case, the conditional weight of the engine is expressed by the following formula:

$$G_{\text{дв}} = \gamma_{\text{дв}} P + G_{\text{с}} + G_{\text{раб.тел}} + G_{\text{г}}$$

*Dzh. Khemfris [G. Humphreys]. Raketnyye dvigateli i upravlyayemye snaryady. IL [Rocket Engines and Guided Missiles], 1958.

**[$V_{\text{кон}} = V_{\text{кон}} = V_{\text{конets}} = V_{\text{end}}$.]

***[$G_{\text{раб.тел}} = G_{\text{раб.тел}} = G_{\text{рабочее тело}} = G_{\text{working fluid}}$.]

or

$$G_{AB} = \gamma_{AB} P + (\gamma_B + q + 1) G_t, \quad (7.16)$$

where γ_{dv} is the specific weight of the engine without fuel tanks (chambers, turbopump assembly with gas generator or pressure accumulator [gas-pressure generator] etc.); $\gamma_B = G_B/G_t$ is the specific weight of the fuel tanks, primarily a function of thrust and engine-operating time; $q = G_{rab.tel}/G_t$ is the specific weight of the auxiliary working fluids in the fuel-feed system (compressed gas, exhaust gas, etc.).

If we refer the conditional weight of the engine to the starting weight G_0 of the missile, we obtain the following expression for the relative weight of the engine:

$$\frac{G_{AB}}{G_0} = \frac{\gamma_{AB} P}{G_0} + (\gamma_B + q + 1) \frac{G_t}{G_0} \text{ or } \bar{G}_{AB} = b\gamma_{AB} + (\gamma_B + q + 1)a,$$

whence

$$a = \frac{\bar{G}_{AB} - b\gamma_{AB}}{\gamma_B + q + 1}. \quad (7.17)$$

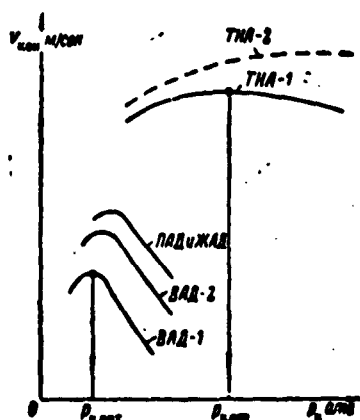


Fig. 7.16. For the determination of optimum gas pressure in the combustion chamber of an engine.

The term in parentheses in Formula (7.15) for V_{kon} was introduced for purposes of accounting for the effect of missile weight on velocity as the missile climbs. The effect of air drag on the magnitude of V_{kon} in the flight of a missile is not taken into consideration with this formula, since this formula, in great measure, depends on the engine-operating regime, the flight trajectory, and the aerodynamic characteristics of the missile; therefore, in this case, this effect cannot be expressed analytically. For pur-

*[$\gamma_B = \gamma_B = \gamma_{Bak} = \gamma_{Tank}$.]

poses of a comparative evaluation of various fuel-feed systems, no serious errors are introduced into the calculations as a result.

Having selected a quantity \underline{b} for this type of missile, and having assigned a series of values for p_k (for example, 20, 30, 40, 50, 60 atm abs, etc.), and calculating the corresponding values of P_{ud} and \bar{G}_{dv} for the given thrust and engine-operating time, we can find the maximum velocity $V_{kon\ max}$, which will correspond to the optimum value of pressure $p_{k.opt}$ (Fig. 7.16).

The practical solution of this problem is fraught with great difficulties, since a correct preliminary evaluation of a series of quantities is required when these values are selected as initial calculation data. In this case, it is particularly difficult to determine, in advance, the dry weight of the engine being planned.

Calculations indicate that when pressurized fuel-feed systems are used, the terminal flight velocity V_{kon} changes significantly with respect to the pressure p_k within the combustion chamber of the engine, and has a pronounced maximum in the region of $p_k \approx 15-30$ atm abs; whereas for a turbopump fuel-feed system, there is a relatively weak dependence and an almost horizontal maximum in the region of pressures exceeding $p_k = 70$ atm abs.

The pronounced dependence between V_{kon} and p_k in the pressurized fuel-feed system can be explained by the fact that the weight of this system (the fuel tanks and the pressure accumulator - gas-pressure-generator) is directly proportionate to the pressure within the combustion chamber. As a result, in the region of high pressures, despite a certain increase in specific thrust, the relative weight of the fuel-feed system increases so markedly, that V_{kon} is reduced.

The turbopump fuel-feed system raises the relative weight as p_k is increased because of the increase in the weight of the pump unit

and the engine chamber. However, since this increase is comparatively small, the region of the greatest values of V_{kon} shifts toward the higher values of p_k and can be presented in a relatively flat curve.

With an increase in p_k , the weight of the combustion chamber diminishes, whereas the weight of the diverging section of the nozzle increases as a result of the necessary elongation of the nozzle which is needed to generate a high pressure difference for the gases; however, in this case, the over-all weight of the engine chamber increases insignificantly.

Since with an increase in p_k gas temperature readings within the combustion chamber rise as does the quantity of heat transferred to the chamber liner, which limits the liner's strength, makes cooling more difficult, and is associated with structural and technological difficulties, the design of the chamber for the engine being planned is best carried out with a p_k that is somewhat below the optimum value. This remark is particularly to the point in the case in which a turbo-pump fuel-feed system is used, when the curve representing V_{kon} as a function of p_k is almost completely horizontal.

Using the values of V_{kon} (or flight range L) for the missile at $p_{k.opt}$, we can construct curves for V_{kon} and L in working at optimum regimes for various ZhRD designs, and these are functions of the values of P , \bar{G}_{dv} , and \underline{b} .

Approximate calculations indicate that in the case of pressurized fuel-feed systems, an increase in the thrust-weight ratio \underline{b} for the missile, at a given value for the relative weight \bar{G}_{dv} of the engine, increases the optimum pressure $p_{k.opt}$ in the combustion chamber, and with a given value for \underline{b} and an increase in \bar{G}_{dv} the pressure $p_{k.opt}$ diminishes (Fig. 7.17). Also, for a turbopump fuel-feed system, with an increase in engine thrust P for a given value of \underline{b} the pressure

$p_{k.opt}$ increases, and here the greater the increase, the lower \bar{U}_{dv} (Fig. 7.18). However, for the given values of P and \bar{U}_{dv} , the increase in b reduces $p_{k.opt}$, and in this case the greater the increase, the lower thrust P ; the greater P , the higher $p_{k.opt}$.

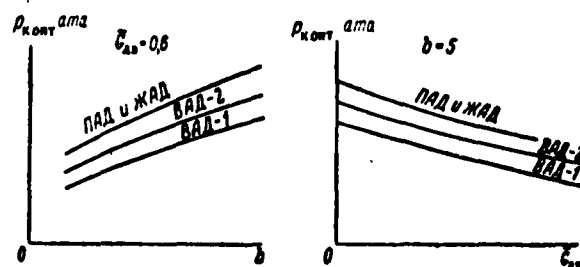


Fig. 7.17. Optimum combustion-chamber pressure as a function of the thrust-weight ratio for the missile (left-hand curves) and of the relative engine weight (right-hand curves) for the pressurized fuel-feed systems.

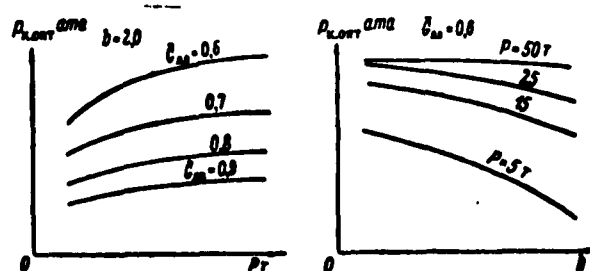


Fig. 7.18. Optimum combustion-chamber pressure in the engine as a function of thrust (left-hand curves) and of the thrust-weight ratio for the missile (right-hand curves) for a turbopump fuel-feed system.

Through the use of an engine chamber and fuel-feed system with improved weight and economic characteristics, optimum pressure in the combustion chamber may be increased up to 80-100 atm abs, which increases the specific thrust of the engine by 8-15% relative to the specific thrust developed at $p_k = 30$ atm abs, i.e., yields as much of

a gain as would be possible through the use of more efficient fuels.

SECTION 13. DETERMINATION OF ENGINE WEIGHT

The weight of a ZhRD depends on its type and design, the pressure within the combustion chamber and the outlet section of the nozzle, the magnitude of absolute thrust, the selected fuel-feed system, and many other factors.

With an increase in pressure p_k in the combustion chamber, the weight of an engine of given nominal thrust increases. This increase in G_{dv} is high with a pressurized fuel-feed system and small in the case of a turbopump fuel-feed system; in this case the weight G_k of the chamber diminishes, whereas the weight $G_{s.p}$ of the fuel-feed system* increases (Fig. 7.19), since the latter must be made stronger in view of the movement of the fuel components to the points at which they are used, and this under great pressure.

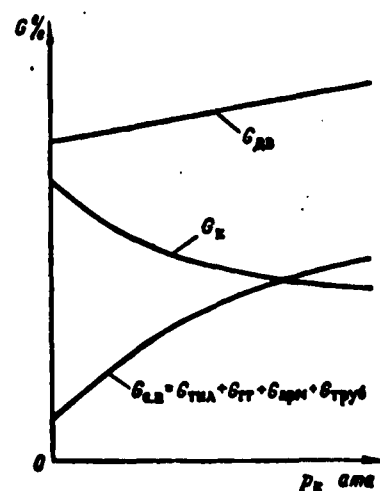


Fig. 7.19. Chamber weight G_k , fuel-feed-system weight $G_{s.p}$, and the weight G_{dv} of the entire engine as approximate functions of the pressure p_k in the combustion chamber.

A drop in G_k with an increase in p_k can be explained by the reduction of optimum volume and, consequently, of the dimensions because of the per-second rate of fuel flow into the chamber developing a given thrust and specific volume for the products of combustion. The per-second rate of fuel flow into the combustion chamber developing the given thrust diminishes as a result of the increase in operating efficiency due to the diminished dissociation of the products of combustion, the raising of their temperature,

*[$G_{c.n} = G_{s.p} = G_{\text{системы топливopодachi}} = G_{\text{fuel-feed system}}$]

and the increased efficiency of the engine.

Calculations show that as p_k is increased, for example, by a factor of two, the cross-sectional area of the combustion chamber also diminishes by a factor of two, and its diameter becomes equal to about 70% of its initial value, if, in this case, the gas flow rate within the chamber remains constant.

With an increase in p_k , the thickness of the chamber liners increases in almost direct proportion and, therefore, the weight of the liners increases per unit area. However, a reduction in combustion-chamber weight as a result of reduced dimensions is more significant and, therefore, the over-all weight of the combustion chamber diminishes as p_k is increased.

An increase in engine thrust for a given p_k is accompanied by increased combustion-chamber and nozzle dimensions and weight (Fig. 7.20), and this can be explained by a corresponding increase in the per-second rate of fuel flow into the chamber and, consequently, by an increase in the dimensions and thickness of the walls. Calculations show that an increase in G_k takes place somewhat more slowly than the increase in thrust.

It should be borne in mind that not all of the units within the chamber and the fuel-feed system of an engine permit proportional variations in dimensions with a change in p_k or thrust. In particular, for a combustion chamber, this is associated with a required time period to achieve the cycle within the chamber, certain mechanical limitations, and the conditions of engine operation.

With an increase in p_k , the weight G_g of the chamber nozzle also diminishes (Fig. 7.21), since, in this case, there is a significant reduction in the areas of the critical and outlet nozzle sections. The insignificant simultaneous increase in liner length and thickness

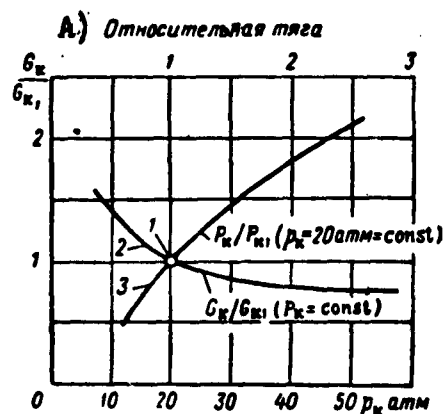


Fig. 7.20. Chamber weight G_k as approximate function of its absolute thrust P_k and combustion-chamber pressure p_k . 1) Point of initial values for thrust P_{k1} and of chamber weight G_{k1} at $p_k = 20$ atm, relative to which the comparison is being made; 2) curve of relative change in G_k as function of p_k ; 3) curve of relative change in G_k as function of P_k , with a given $p_k = 20$ atm. A) Relative thrust.

(weight per unit area) has little effect on the quantity G_s . However, at low engine thrust, this theoretical gain in nozzle weight, is, for all intents and purposes, insignificant.

Given increased altitude characteristics for the nozzle, the dimensions and weight of the nozzle increase, as do the gas-energy losses within the nozzle, this due to the friction of the gases against the walls. A reduction in the weight and length of a high-altitude nozzle is possible by increasing the flare angle of its outlet section; however, this will result in increased gas-energy losses due to the dispersion of the gas stream at the outlet, and the detaching of the gas stream from the walls. Therefore, in selecting the flare angle for the outlet section of the chamber nozzle, in this case, it is necessary

to 4; σ_b is the ultimate strength of the liner material at ambient temperature.

With normal engine operations, the outer chamber liner is subject to a liquid pressure p_{zh} , and the inner liner is subject to the action of the pressure difference between the cooling liquid in the duct and the gases within the chamber, i.e.,

$$\Delta p_{oxa} = p_{\kappa} - p_r \quad (7.20)$$

In this case, the thickness of the inner flame tube of the engine chamber (or a section of it) can be determined according to the following formula:

$$\delta = \frac{d \Delta p_{oxa} R}{\sigma_{bt}} \text{ mm}, \quad (7.21)$$

where σ_{bt} is the ultimate strength for the material used in this liner, at average heating temperature.

The head of the engine chamber developing low and medium thrusts is frequently made of two flat steel plates, each approximately 2.5 to 3 mm thick, on which are mounted the spray nozzles and one steel spherical plate with a radius $r_{sf} \approx 0.7 d_k$ [sic],* where d_k is the diameter of the combustion chamber. The flat plates of the head are fastened to the spherical plate by means of gusset plates (fins). The strength safety factor for the head is $n_{gol} \approx 1.5$. The thickness of the chamber-head plates may be assumed to remain constant with a change in combustion-chamber pressure.

The thickness of the flame tube of the chamber may be taken to be identical along its length, but not less than 1-1.5 mm with a coordinated stress-bearing liner system, and approximately 2-3 mm in the case of a noncoordinated stress-bearing system.

If the liners are connected to one another by means of special

*[$r_{c\phi} = r_{sf} = r_{sfericheskiy} = r_{spherical}$.]

stress-bearing elements, the weight of this element can be taken into consideration by a certain fictitious increase in the thickness of the flame tube.

This thickness for the inner chamber liner may be calculated according to the following formula:

$$\delta_{\text{фикт}} = \delta + k\delta_{\text{св}} \quad (7.22)$$

where δ and $\delta_{\text{св}}$ represent the thickness of the inner liner and the linking element for the two liners, respectively; $k = 2$ is the fictitious increase in thickness for the liner, for purposes of calculating the weight of the connecting element.

The weight of the engine chamber can, approximately, be determined according to the following formula:

$$G_{\text{к}} = G_{\text{об}}(1 + \beta_{\text{ст}}) \quad (7.23)$$

where $\beta_{\text{ст}}$ is the coefficient which takes into consideration the weight of the atomization head, the structural elements of the combustion chamber and nozzle, as well as the tubing and fittings which come into play here, said data not taken into consideration in conventional strength calculations.

The coefficient $\beta_{\text{ст}}$ is determined on the basis of statistical data (according to the data for that existing type of engine which serves as a model for the new engine being planned); for engines developing low or medium thrust, this coefficient may amount to approximately 75% of the total weight of the two chamber liners.

The method cited here for the determination of $G_{\text{об}}$ refers to the noncoordinated liner system for an engine chamber. The weight of the liners in a coordinated system can, approximately, be evaluated on the basis of statistical data.

$$*[\delta_{\text{фикт}} = \delta_{\text{фikt}} = \delta_{\text{фиктивны}} = \delta_{\text{fictitious}}]$$

The weight of the remaining engine elements can be determined, approximately, on the basis of the following formulas:

$$\left. \begin{aligned} G_k &= \gamma_k P; & G_{TNA} &= \gamma_{TNA} N_t; \\ G_{gr} &= \gamma_{gr} P; & G_{ch} &= \gamma_{ch} P, \end{aligned} \right\} \quad (7.24)$$

where P is the nominal thrust of the engine, in kg; N_t is the power of the turbine in the pump unit, in hp; $\gamma_{TNA} = G_{TNA}/N_t$ is the conditional TNA specific weight; $\gamma_{gg} = G_{gg}/P$ is the conditional specific weight of the gas generator; γ_k is the specific weight of the chamber, in kg/kg of thrust; γ_{dv} is the specific weight of the engine, in kg/kg of thrust.

For design of the planned engine, the values of γ_{TNA} , γ_{gg} , γ_k , and γ_{dv} are taken on the basis of statistical data.

The specific weights are, on the whole, extremely important characteristics of chambers and engines. With an increase in absolute thrust, with a drop in combustion-chamber pressure, and with improved design, the specific weight of the engine is diminished. The lower the specific weight of the chamber and the engine on the whole, the more perfect the engine from the standpoint of design. With identical specific weights, the better engine is the one, all other conditions being equal, whose specific fuel consumption is the lowest.

When the specific weight is not the sole determining factor, structurally simpler and less expensive engine elements, even if these are less efficient, should be selected. Such a solution to the problem can be justified on the basis of the fact that 1 kg of engine is almost 100 times as expensive as 1 kg of consumed fuel.

In order to calculate the weight of an engine chamber, it is generally divided into the following elements (sections): the head, the cylindrical portion of the combustion chamber, the converging portion of the combustion chamber (nozzle) and the diverging nozzle section.

There are indications in foreign literature that with a given pressure in the combustion chamber, the weight of the chamber nozzle changes in proportion to the change in thrust, whereas the weight of the combustion chamber changes in proportion to the square root of the thrust (Fig. 7.22). With an increase in thrust up to 25 to 30 tons, the specific weight of the engine chamber diminishes, and then increases, primarily, as a result of an increase in the weight of the chamber head.

Figure 7.23, citing the same sources, shows an approximate change in the weight characteristics of a single-chamber engine with a turbopump unit and a gas generator as a function of thrust.

The weight of the turbopump fuel-feed system (pumps, turbine, gas generator, tubing) increases almost proportionately with the increase in the pressure required to feed the fuel components into the combustion chamber. Therefore, in order to reduce the weight of this fuel-feed system, the pressure difference between the fuel components in the spray nozzles and the cooling liquid in the interliner chamber space is expediently reduced to its minimum values.

The dry weight of a single-chamber A-4 engine (without fuel tanks), developing a thrust of about 25 tons on the ground, at $p_k = 15.0$ atm abs, is 920 kg, and the weight of the engine chamber is 446 kg.

For purposes of coarse calculations, the weight of the individual ZhRD elements as found in the A-4 can be estimated in percent of the total weight G_{dv} of the engine (without taking the fuel tanks into consideration):

- 1) of the chamber

$$G_c \approx (0,45 + 0,50) G_{dv};$$

- 2) of the turbopump unit

$$G_{THA} \approx (0,15 + 0,17) G_{dv};$$



Fig. 7.22. Change in specific engine-chamber as function of magnitude of thrust. 1) Chamber head; 2) chamber nozzle; 3) γ_k , kg/kg of thrust; 4) combustion chamber; 5) engine chamber; 6) chamber head; 7) chamber nozzle; 8) combustion chamber.

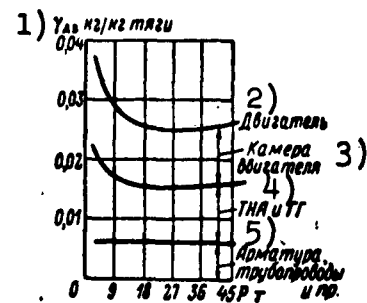


Fig. 7.23. Change in specific engine weight as function of magnitude of thrust. 1) γ_{dv} , kg/kg of thrust; 2) engine; 3) engine chamber; 4) TNA and QG ; 5) fittings, tubing, etc.

3) vapor-gas generator

$$G_{пгг} \approx (0,10 + 0,15) G_{ab}; *$$

4) auxiliary devices (other elements)

$$G_{s,y} \approx (0,20 + 0,21) G_{ab}. **$$

Consequently, using these data and the relative coefficients taken from the statistics available from contemporary ZhRD, we can, in approximate terms, estimate the weight of the engine being planned, as well as that of its individual elements.

The methods used to the present time for the preliminary determination of the weight, the dimensions, and the structural parameters of the engine being planned, and this applies equally to the individual elements of the engine, are still, in a number of instances, not optimum and require continuous refinement and improvement because of a shortage in statistical data, and this applies equally to the methods

$$*[G_{пгг} = G_{пгг} = G_{парогазогенератор} = G_{vapor-gas generator}.]$$

$$**[G_{s,y} = G_{v,u} = G_{вспомогател'ные устройства} = G_{auxiliary device}.]$$

employed in design.

A reduction in weight for a planned engine developing a given thrust is, for all intents and purposes, possible through improved designs for its individual elements, the use of materials with high specific strength, and the selection of the minimum permissible strength safety factors; in addition, other methods have to be carried out and these are spelled out in the corresponding sections of the present work.

The weight of the pump-fed fuel-feed system can be reduced by using fuel tanks of lightened design with increased pressure (within the tanks) to provide for stability and by taking steps to reduce the weight of the fuel-component residues within the tanks and in the engine "plumbing" at the end of the powered phase of the flight.

A significant reduction in weight for the planned engine can be achieved by selecting an optimum thrust-weight ratio for the missile. At the present time, there is a tendency to reduce the thrust-weight ratio for a missile. Vertical take-off missiles (long-range) frequently have an initial acceleration of less than 1.5 g; however, under certain conditions this acceleration can be approximately 1.2 g.* The optimum acceleration for small antiaircraft missiles generally ranges between 3 and 8 g.

In planning long-range missiles, we may regard a thrust-weight ratio $b \approx 1.5$ as acceptable for the first stage, and 1.3 for the later stages.

In the process of improving the ZhRD, particular attention has also been devoted to reducing cost and, primarily, to raising the quality, reliability, and control precision for the operations of the individual units.

*Voprosy raketnoy tekhniki, Issue 4, IL, 1958.

SECTION 14. DETERMINATION OF ENGINE DIMENSIONS

The dimensions of a ZhRD are characterized by its great diameter and length. The preliminary determination of the dimensions for a planned engine are possible only in approximate terms. The greatest diameter of an engine is a function of the tactical designation and the initial weight G_0 of the missile.

To determine the diameter of the engine, we may make use of the following formulas:

- 1) for lateral missile load

$$c = G_0 / F_{sn} \text{ kg-m}^2; * \quad (7.25)$$

- 2) for relative engine thrust

$$b = P_0 / G_0 \text{ kg/kg.} \quad (7.26)$$

If we replace the value of G_0 in (7.25) with the value taken from (7.26) we obtain, for the midsection of the missile,

$$F_{cn} = \frac{P_0}{bc} = \frac{\pi D_{cn}^2}{4}, \quad (7.27)$$

whence the maximum missile diameter will be

$$D_{cn} = \sqrt{\frac{4P_0}{\pi bc}} = 1,127 \sqrt{\frac{P_0}{bc}}. \quad (7.28)$$

In this case, the maximum engine diameter for the given missile can be expressed by the following formula:

$$D_{an} = k D_{cn}, \quad (7.29)$$

where $k \approx 0.86$ is the coefficient by which we take into consideration the dimensions of the bulkheads and the production clearances for the "tail" liner of the missile.

Substituting the value of D_{sn} from (7.28) into (7.29), we will finally obtain

$$D_{an} \approx 0,972 \sqrt{\frac{P_0}{bc}}. \quad (7.30)$$

*[$F_{ch} = F_{sn} = F_{snaryad} = F_{missile}$.]

Consequently, assuming values for b and c, on the basis of statistical data, for a corresponding type of missile and its tactical designation, the last formula may be used to determine approximately the maximum diameter of the engine being planned for this missile.

The length of the engine, without fuel tanks, is generally a function of its type and designation, magnitude of thrust, and other factors; therefore, the preliminary estimates for the engine are extremely difficult. In missile planning, the preliminary length of the engine can be determined, approximately, through the use of statistical data.

SECTION 15. METHODS OF IGNITING FUEL ON ENGINE START

At the instant of engine start, nonhypergolic fuel components require powerful outside energy sources for the initial ignition and continuation of the combustion until the starting regime is attained. Then, as the combustion of the starting fuel flow has been established, the need for the ignition source is eliminated and the engine can be transferred from the starting regime to the nominal regime. The installation which is used for fuel ignition in ZhRD starts is referred to as the engine-ignition system.

The ignition system for single-shot ZhRD is intended to function only during the starting period, and afterwards it is automatically shut off or jettisoned, since the continued combustion of the fuel entering the combustion chamber is accomplished by the heat of the preceding burning fuel injections. The thermal energy needed for this is approximately 10% of the potential heat of the fuel being ignited.

ZhRD ignition systems are called upon to provide the following:

- 1) the ignition must be strong and reliable enough at ambient temperatures of -50°C , since the initial vaporization, mixing, and ig-

dition of the fuel components in a cold combustion chamber are considerably inferior to the case in which the engine is operating normally;

2) the ignition must be achieved prior to the inflow of the basic fuel components to the combustion chamber, and in this case the time difference between the influx of the oxidizer and the combustible must be small enough in order to eliminate the possibility of weakening the ignition focus through cooling (flooding) by one or the other of the fuel components;

3) the fuel ignition must take place close to the combustion-chamber head so that the starting fuel mixture will be employed for the ignition operation; moreover, the ignition should not impair or interfere with the steady-state fuel-combustion process;

4) the ignition system must be simple and inexpensive from the structural standpoint;

5) the ignition system for a multiple-start engine must permit repeated starts.

Certain additional requirements may be placed upon individual ignition systems.

The igniters presently in use on ZhRD cannot simultaneously satisfy the requirements for multiple starts, limited delay in igniting fuel components, and engine starts at great altitudes.

In the case of low power or "nonnormal" ignition-system operation, a great quantity of the chemically unreacted fuel mixture may accumulate in the combustion chamber of the engine. The danger of the explosion of the fuel mixture that is associated with this is extremely great. Therefore, the engine must have a system of control which would make it possible to restrict the accumulation of fuel within the combustion chamber, in the event that the starting ignition operation

does not function properly.

Various ignition systems may be used, depending on the type of fuel components used, the type of engine, and the conditions under which it is operated.

Ignition systems in contemporary engines can be divided according to a series of basic indicators, such as:

1) according to the designation of the system: a) single-start operations, used in single-start engines (missiles, torpedoes, etc.); b) multiple-start operations, used in engines for multiple starts (aircraft, test stand);

2) according to the point at which the ignition installation is mounted on the engine: a) with the mounting of the ignition installation on the head of the combustion chamber; b) with the introduction of the ignition installation within the combustion chamber from the side of the nozzle (similar to the A-4 engine);

3) according to the method used to ignite the starting or operating fuel components: a) electrical ignition, i.e., with the use of electrical devices - electric spark plugs, voltaic arcs; b) "pyrotechnical" ignition, i.e., through the use of one or more "pyrocartridges" and c) chemical ignition, i.e., through the use of hypergolic fuel components - starting or basic.

Ignition by means of electric spark plugs is structurally simple and if properly carried out can provide for an unlimited number of engine starts. The electric spark plug is generally mounted in the head of the combustion chamber.

Ignition by means of conventional electric spark plugs exhibits the following shortcomings:

a) comparatively low heat power on the part of the electric spark plug and, consequently, inadequate reliability for fuel combustion at

low ambient temperatures;

b) the need for a source of electric energy, which cannot always easily be situated in the weapon;

c) limited operational capacity in the acid-hydrocarbon media, in view of the bridging of the spark gap by the electrically conductive acid.

Conventional electric spark-plug ignition is used in engines developing low thrust or in small experimental chambers which are used for test-stand purposes.

In order to ignite the fuel on starting the engine, a spark-ignition system of high power, using semiconductors, may be employed. In this case, the spark plug consists of two concentrically situated electrodes, insulated from one another, and whose ends are situated in one plane with the insulator, the surface of the latter covered with a semiconductor layer near the electrodes. As the electrodes receive voltage, a current flows through the semiconductor; since the semiconductor is nonuniform, a more powerful current passes through the point at which the conductor resistance is lowered. This section of the conductor heats up. At the same time, the current increases and leads to a continued increase in conductor temperature. An accumulation of current of this sort sets up an electric-circuit section within the semiconductor, and the temperature here is adequate to bring about the ionization of the fuel mixture in the vicinity of the electrodes, and as a result a powerful spark discharge between the electrodes takes place.

Depending on the magnitude of the voltage, this phenomena may be repeated with a period of the order of $1 \mu\text{sec}$. If the voltage in the system is 2 kv, then relative to a conventional high-voltage ignition system, corona and surface-discharge losses are reduced.

The "pyrotechnical" ignition system, depending on the design and dimensions of the engine chamber, is installed in the head of the combustion chamber (similar to the electric spark plugs) or within the combustion chamber, from the side of the nozzle, on a special holder. In the latter case, after the ignition of the working fuel components, the ignition installation is ejected from the chamber to the outside by means of the gas stream.

In the A-4 engine, the ignition of the fuel during launching was carried out through the introduction, into the combustion chamber through the nozzle, of a special turntable on which the pyrocartridges were situated tangentially about the circumference. With the ignition of the pyrocartridges, the turntable started rotating, and the entire chamber was filled with a powerful burning flame and gases of high temperature; then, a small amount of fuel entered the combustion chamber, and this fuel was ignited, and subsequently the fuel feed increased.

The pyrocartridges are generally ignited by means of an electric filament, and operate reliably at ambient temperatures of $\pm 60^{\circ}\text{C}$, burn rather uniformly for a number of seconds and yield a combustion flame with a temperature of from $2000\text{--}2500^{\circ}\text{C}$. Therefore, "pyrotechnical" ignition is sufficiently reliable both on the ground and at any altitude.

At the present time, pyrotechnical ignition is used in engines of various thrusts, with single- or multiple-start operation, and a single launch stage.

Chemical ignition systems, in a number of cases, may successfully compete with the structurally simple and operationally adequately reliable system of pyrotechnical ignition because of their great power and operational duration. This ignition method may be used in engines developing various thrusts, for single- and multiple-start operations.

For the chemical ignition of nonhypergolic fuel components in the fuel-feed system of the engine, a special starting system is installed, and on launch this system is used to supply the hypergolic fuel components to the combustion chamber initially, and then, after the formation of a powerful burning flame within the combustion chamber, the basic components are fed to the chamber. Such a launch sequence is structurally simple and makes it possible to transfer smoothly and reliably from the starting fuel components to the basic components.

Single-start chemical ignition is possible also at the chamber-nozzle end; however, in this case, the ignition installation is structurally more complex than in the case of ignition from the combustion-chamber head end, i.e., through the operating spray nozzles. In this case, the ignition flame is directed toward the working fuel components and ignition is kept reliable without additional starter devices within the engine.

For the chemical ignition of nonhypergolic fuel components it is sometimes expedient to select a special starter combustible which is hypergolic with the basic fuel oxidizer for the engine. The selection of such a combustible presents no particular difficulties in practice. This combustible must ignite spontaneously with a delay of no more than 0.03 seconds, it must be high in heating value, nontoxic, and inexpensive. The liquid Tonka-250 and other liquids may be used as the ignition combustible.

There are a great many hypergolic fuels of various composition. They are used in ZhRD as starter and basic fuels. The fundamental shortcomings of these fuels are their low heating value, high cost, and short supply.

In order to obtain uniform ignition of the working mixture without shocks, the chemical ignition system for the engine must satisfy

the following additional requirements as the working mixture enters the combustion chamber.

1. The ignition installation must produce an intensive flame that fills the entire volume of the combustion chamber into which the working components of the fuel enter, and there can be no "dark" zones, at least in that section of the chamber into which the working components are sprayed.

The ignition system cannot be considered independently of the mixture-formation system, since high-quality mixture formation may significantly ease the requirements imposed on the ignition system for the engine. The permissible ignition lag for the starter fuel components is closely associated with the quality of atomization; the greater the ignition lag, the more perfect mixture formation has to be.

2. The starter combustible (fuel) mixture must have optimum composition not in terms of specific thrust but in terms of low ignition lag, requiring a small quantity of heat from the ignition source in order to attain the temperature at which intensive combustion can begin. The fuel-mixture compositions that are close to the stoichiometric generally exhibit high heating value and, consequently, provide for the more rapid establishment of thermal equilibrium for the chamber walls and gases than is the case with mixtures of other compositions.

We must select the starter fuel components from the standpoint that the starting regime for the engine has a significant effect on the ignition lag for the starter components and on the nature of the rise in pressure within the combustion chamber. The lower the ignition lag and the smoother the increase in pressure, the safer the start and the transition to the operating regime, and accordingly we can set a higher value for the ratio of fuel consumption in the operating regime

and the start regime. Low-quality starter hypergolic fuel components, as a rule, result in the explosion of the engine, either during starting, or in the transition regime.

In the operating regime, the quality of the starter components has less effect on the operation of the engine. The nature of the pressure increase in the combustion chamber, in the case of starter combustible (fuel) mixtures, is equally as important as the ignition lag. A slow increase in pressure makes the starting of the engine safer and makes it possible to use starter components with a greater ignition lag. The selection of an ignition method depends on a variety of considerations, particularly on whether or not the ignition will involve a single start or multiple starts.

Of the ignition systems presently in use, the greatest guarantee of failproof ignition is offered by the chemical "charge" ignition system for a one-shot engine (see Section 3, Chapter XII). Explosions and engine breakdown in case of ignition failure, in this case, are prevented by a reliable "autoblocking" system which prevents the combustible (fuel) mixture from entering the combustion chamber in such cases.

With the "charge" starting system for the engine, explosions may be quite accidental and are caused, primarily, by unsatisfactory quality of starter fuel components. The use of this system for starts is generally accompanied by a pronounced increase in gas pressure within the combustion chamber of the engine.

In engines operating on hypergolic fuel components, chemical ignition during starting is accomplished by mechanical means. In this case, it becomes unnecessary to build in any sort of ignition system. However, the use of hypergolic fuel components has serious limitations.

For the reliable starting of an engine, the ignition lag for the

hypergolic fuel components must not exceed 0.01 to 0.03 sec. In order to ascertain such ignition lags for the hypergolic fuels, sufficiently active hypergolic combustibles (fuels) are selected, and oxidizer activation is employed. For example, the addition of nitrogen tetroxide (N_2O_4) to the nitric acid reduces the freezing point of the oxidizer to a certain limit, raises the activity of the oxidizer, increases the heating value of the fuel, and eases the starting conditions for the engine. The addition of concentrated sulfuric acid (H_2SO_4) reduces the aggressive properties of the nitric acid with respect to the structural materials used in the engine, and improves the starting conditions, particularly in the case of hypergolic combustibles (fuels); however, in this case, there is a slight drop in the heating value of the fuel. The addition of ferric chloride (Fe_2Cl_3) also reduces the freezing point of nitric acid and increases its activity, in conjunction with a limited reduction in the heating value of the fuel.

With engine starts at great altitudes, where the pressure and the temperature of the surrounding medium are relatively lower, this ignition lag may be even greater. The combustible (fuel) mixture accumulating within the combustion chamber because of the ignition lag may suddenly ignite and burn up, thus raising the pressure excessively, resulting in the explosion of the engine.

SECTION 16. GENERAL PROBLEMS IN PLANNING AND DESIGNING ZORD CHAMBERS

Preliminary calculations for individual engine-chamber elements, for purposes of establishing their strength dimensions, in the majority of cases are impossible or practically unsatisfactory, since it is not possible to plan designs and dimensions in advance. Therefore, in planning an engine chamber it becomes necessary, first of all, to select the structural configuration of the chamber (following general

considerations), the material of which the chamber is to be made, and tentatively to set structural and strength dimensions for the individual elements; subsequently, the over-all assembly of these elements is carried out, and the strength calculations are then checked.

In order to undertake the over-all assembly of the engine chamber it is necessary to select an expedient shape for the chamber, as well as for the chamber head, and in addition expedient types of fuel-spray nozzles must be chosen, as must the location pattern of these nozzles on the chamber head; in addition, the chamber-cooling method, the shape, and the proposed geometric dimensions for the cooling duct must also be chosen. Simultaneously, a number of other problems must be resolved. In particular, in planning the chamber head, we must clarify which additional devices (with the exception of the spray nozzles) must be positioned on the head, in view of the necessity for providing fuel ignition for one-shot or multiple-start engines, providing for a supply of fuel components to the combustion chamber, etc.

After these problems have been resolved, we can start on the calculations to determine the reliability of chamber cooling and carry out the strength calculations for the remaining chamber elements. This stage of the operation terminates with the final geometric assembly of the chamber and the necessary repeat calculations. In this case, it is generally necessary to select the most suitable methods of supplying the fuel components to the chamber and to drain the liquid from the cooling duct; in addition, we must select the methods by which we interlink the individual chamber elements and fasten the chamber either to the thrust frame or directly to the weapon.

Welding or jointing may be used to attach the head to the combustion chamber (depending on the designation of the engine and the selected atomization method for the fuel components). Welding is always

expedient to interlink the remaining engine elements, since this method is the simplest and least expensive, and the entire chamber construction becomes comparatively lighter. Jointed construction may prove to be preferable only for certain multiple-start engine component parts.

In engines developing low thrust, the fuel components are generally fed to the chamber through separate tubes. In contemporary engines, elastic tubing is used. At high per-second fuel flow rates to the chamber, each of the components can be carried through several tubes in order to provide for a more uniform feed to the spray nozzles. The fuel components used for chamber cooling are frequently delivered to the chamber-nozzle manifold through three or more tubes in order to provide uniform initial liquid flow within the cooling duct.

The fuel manifold to the coolant passage (cooling duct) of the chamber serves as the joint for the nozzle. The manifold supply tubes must be as simple in configuration as possible. The liners of a welded chamber must be joined to the head as simply and as inexpensively as possible, without using special machined rings.

The removal of the fuel (liquid) from the passage (duct) to the chamber head may be direct (similar to the A-4 engine) or through the use of several supply tubes (in the case of a demountable chamber head).

In the space in front of the spray nozzles situated in the head of the engine chamber it is sometimes expedient to set up a fuel distributor in order to avoid nonuniform liquid pressure in front of the spray nozzles, which can be attributed to the velocity head at the outlet from the supply tube.

In building a ZhrD chamber, we should take into consideration the requirements imposed, the difficult operating conditions for individual elements, and also the necessity of precision fabrication. The expan-

sion of individual chamber parts due to temperature should be taken into consideration in order to avoid reducing the strength safety factors for the metal because of the appearance of temperature stresses during engine operation.

In designing a ZhRD chamber, regardless of shape, it is extremely important to provide for high strength and to prevent the burning out of the chamber during operation. The strength of the chamber and the stability of shape are generally provided by selecting the required liner thickness and using various types of fastening elements. As the latter, we can use either longitudinal fins on the liner, or fins which are made in the form of multiple-start square threads with small pitch; these fins also facilitate the cooling of the engine chamber. It may sometimes turn out that such fastening is inadequate. In this case, "band"-type binding may be used as the fastening element.

Since the engine is a component part of the weapon, it must have an efficiently designed system by which it is adapted to the weapon. The joints for fastening the chamber to the thrust frame or the weapon are generally placed close to the chamber head where the strength of the metal is not weakened as much due to heating. These joints must withstand reliably the thrust, inertial, and vibration loads which arise during flight. The fastening of the chamber to the thrust frame must permit the free thermal expansion of the heated engine parts as well as the turning of the engine relative to its centering axis aboard the missile.

The engines used on weapons designed for rapid changes in flight direction and subject, as a result, to great lateral acceleration (antiaircraft missiles, aircraft), should be fastened close to their center of gravity if only possible, thereby reducing the magnitudes of the bending moments within the fastening supports.

The fastening of the engine to the weapon depends on the design, engine dimensions, and magnitude of thrust, as well as on the type of weapon and similar factors; therefore there is a variety of structural designs. In a number of existing weapons, this fastening is accomplished by means of special frame beams or gusset plates.

The problems associated with the planning and designing of an engine chamber are generally resolved in the following sequence:

- 1) the volume of the combustion chamber is determined;
- 2) the shape of the combustion chamber is selected as is the shape of the combustion-chamber heads, and selection is made of the type of fuel spray nozzles and the location pattern for these on the chamber head;
- 3) the method of fastening the head to the combustion chamber is chosen;
- 4) the over-all geometric assembly of the engine chamber is carried out;
- 5) the cooling system for the chamber is selected, as are the shape and dimensions of the coolant passage; a check calculation is carried out to determine cooling reliability;
- 6) the chamber-liner construction is selected, as are the structural materials for the liners, for the chamber head, and for other chamber elements;
- 7) selection is made of the methods to compensate the linear elongation of chamber elements due to temperature and decisions are taken as to their structural realization;
- 8) selection is made of the methods to supply the coolant to the chamber nozzle and to remove the coolant from the coolant passage to the head;
- 9) hydraulic calculations for the coolant passage of the chamber

are carried out;

10) the starting method for the engine is selected and the structural elements which, in this connection, must be situated on the chamber head are refined;

11) selection is made of the method and the points at which the chamber is fastened to the thrust frame or directly to the weapon;

12) selection is made of the production process involved in the fabrication of the chamber, and the production adaptability of the design is determined;

13) final engine chamber assembly is carried out and calculations to check strength and operating stability are performed.

This list does not exhaust all of the problems which are resolved in planning and designing an engine chamber.

Chapter VIII

THEORY AND DESIGN OF ATOMIZING DEVICES FOR ZhRD

Atomization of the fuel components exerts great influence on the performance of ZhRD, since the volume of the combustion chamber, its specific weight, economy, ruggedness, and operational dependability depend on the quality of the atomization function. Little study has as yet been devoted to fuel-atomization processes in these engines, due to their extreme complexity.

Theoretical investigations of the mechanism by which fuel components are atomized in the working engine with simultaneous heating, vaporization, intermixing, and partial diffusive-turbulent combustion are extremely difficult. For this reason, research and development work on new designs and executions for the atomizing heads of chambers is carried out by experiment with operational engines in each specific case.

The planning and calculations for chamber atomizing heads represent an extremely important stage in the creation of an effective engine design.

The present chapter is devoted to consideration of existing methods for atomizing fuel components in ZhRD, gives an account of specifications set forth for atomizing devices, and analyzes the factors that influence the quality of the atomizing function. This includes a brief list of prerequisites for design of atomizing en-

gine-chamber heads and information pertaining to the selection of the optimum design parameters.

SECTION 1. SPECIFICATIONS SET FORTH FOR ATOMIZING DEVICE OF ZhRD

For effective combustion of a liquid fuel, provision must be made for its complete vaporization within a specified time interval and in the proper position in the engine's combustion chamber. For this purpose, the entire mass of fuel fed into the combustion chamber must have the highest possible surface area at the correct instant of time. A considerable increase in the surface area of a component can be obtained by atomizing it into extremely fine particles. For this reason, the atomizing device of a ZhRD must ensure that liquid fuel components fed into the combustion chamber at a definite pressure and in the appropriate quantities will be broken up into extremely fine droplets and that they will mix with one another rapidly and thoroughly. The proficiency with which these processes are realized determines to a significant degree the rate and completeness of combustion of the fuel mixture formed, the volume required for the combustion chamber, its dimensions, specific weight, operational stability, and other characteristics. The more perfect the mixture formation, the more economical, stable, and dependable will be the performance of the engine.

The atomization process for liquid fuel components depends on their physical properties, the type and design of the spray nozzles, their operating regimes, and other factors.

The engine's spray nozzles break up the fuel component into billions of drops having a [total] surface area reckoned in tens of square meters.

If, for example, one liter of liquid has a diameter of about 0.124 m and an area of about 0.0483 m² before delivery into the com-

bustion chamber, its total surface area will be increased by a factor of nearly 1240 on atomization into droplets 100μ (10^{-4} m) in diameter and will come to about 60 m^2 .

The present state of mixture theory and the theory of fuel combustion in ZhRD does not yet enable us to carry out exact calculations for these processes. For this reason, it is necessary in designing engine-chamber heads to proceed from the necessity of satisfying certain basic mixture-formation specifications, making use of the results of research and operational experience.

The atomizing device (chamber head) of a ZhRD must meet the following specifications.

1. The fuel components must be broken up into sufficiently fine and uniform droplets, since the quality of the mixing function and the uniformity and rate of fuel combustion depend on the fineness of the atomizing function.

In normal ZhRD designs, the fineness to which the fuel components are atomized depends on the type, design, and throughput capacity of the spray nozzles, their geometrical characteristics, the pressure gradient in the spray nozzles, and other factors.

The fineness to which the fuel components are atomized is a qualitative criterion of mixture formation and is characterized by the weight-averaged diameter of the droplets formed. The smaller the average droplet diameter, the better is the atomization and the more complete will be combustion of the fuel.

The uniformity of atomization is characterized by the variation in the droplet diameters in the spray of atomized fuel component. The narrower the range over which the diameters of the atomized fuel-component droplets are scattered, the greater is the atomization uniformity.

The so-called median droplet diameter d_m ,* i.e., the figure corresponding to the diameter of half the total mass of all the droplets, is frequently introduced as a characteristic of the fineness to which fuel components are atomized.

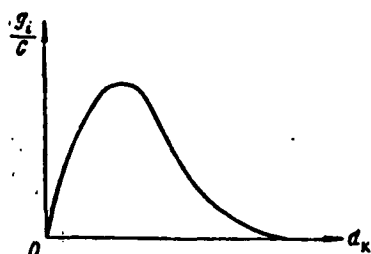


Fig. 8.1. Weight-distribution curve of droplets in atomized fluid, plotted against their diameters (the area under the curve corresponds to 100%).

This means that in the entire mass of droplets, half the weight will have diameters greater than d_m , while half will have diameters smaller than d_m , so that $G_{d_m} = 0.5$.

Sometimes the fineness of atomization of the fuel components is characterized by the so-called average droplet diameter, which implies the diameter that the drops would have if they were all of the same size, i.e., if their total surface area and total volume were the same as in a spray consisting of droplets of different sizes.

For a given fuel-nozzle design, the droplet diameter depends on the nozzle diameter, the injection rate of the liquid, its viscosity, density, and surface tension, and the density of the gaseous medium into which it is injected.

Figure 8.1 shows a diameter distribution curve for these droplets, with the droplet diameter d_k ** plotted against the axis of abscissas and the relative weight fraction of drops of diameter g_1/G [%], where G is the total weight of all the droplets and g_1 is the weight of droplets of a specified diameter, plotted against the axis of ordinates.

In contemporary ZhRD, the atomized fuel-component droplets

*[$d_m = d_m = d_{\text{medianny}} = d_{\text{median}}$.]

**[$d_k = d_k = d_{\text{kapelya}} = d_{\text{droplet}}$.]

have diameters of about 25-250 μ . This means that 1 cm^3 of the fluid to be atomized is broken up into approximately $6 \cdot 10^6$ droplets. In nitric-acid engines, the weight-averaged droplet diameters of kerosene occur in the range from 120 to 150 μ .

A fuel consisting of extremely large drops will be late in completing mixture formation and, consequently, in completing the process of diffusive-turbulent combustion. When the spray is too coarse, as may happen as a result of improper execution of the atomizing device or when the engine thrust is regulated by varying the pressure gradient for the fuel components, the result may be a sharp drop in the efficiency of the combustion process and unstable operation.

As will be shown below, however, breaking the fuel components up into a fine spray is not in itself the only way to improve the quality of the cycle in the engine's combustion chamber. The mixing system must ensure not only fine atomization and thorough mixing of the fuel components, but also an "organized" supply of heat for preheating, vaporizing, and igniting them.

2. The concentration of the atomized fuel components must be uniform over the cross section of the combustion chamber, since otherwise their combustion will not go to completion.

A coarsely mixed fuel mixture is usually produced at the head of the combustion chamber, and this undergoes further mixing as it moves down the chamber and becomes more uniform. Preheating and evaporation of the atomized components and combustion of the resulting fuel mixture take place concurrently with this process.

The completion time of the fuel-combustion process is determined chiefly by the speed at which the fuel components are mixed. All other conditions the same, mixing will take place more rapidly

with finer gaseous fuel-component sprays and high relative rates of movement of these components. In the last analysis, the completeness of combustion of the fuel will be determined by the ratio of the residence time of the working fluid in the combustion chamber to the time required to complete the fuel-combustion process.

Local deviations of the fuel-mixture ratio in the combustion chamber from the theoretical value always results in incomplete combustion, and, consequently, in a drop in the engine's specific thrust.

It has been shown that initial nonuniformity of the fuel-component composition in the regions of the spaces between the spray nozzles is quickly equalized without any noticeable loss of specific engine thrust, while fuel-composition nonuniformities on a scale larger than the spray-nozzle interval usually do not have time to equalize and lower the P_{ud} significantly.

To protect the engine's chamber liner from overheating, the combustible mixture is sometimes intentionally enriched near the liner surface by a special feed system which injects about 2-4% of the total combustion-chamber consumption of combustible through peripheral nozzles. Here, the engine head ensures constancy of the excess oxidizer ratio α_{ya}^* in the middle of the combustion chamber and a lower value α_p^{**} at the surface of the chamber liner.

In a number of nitric-acid engines that were actually built, α_p averages $0.6 \cdot \alpha_{ya}$.

3. The flow intensity of the fuel must be uniform over the cross section of the combustion chamber, since the combustion process will be incomplete where the fuel flow is greater than the calculated value and the combustion-chamber volume will not be utilized

*[$\alpha_{\pi} = \alpha_{ya} = \alpha_{yadro} = \alpha_{core}$.]

**[$\alpha_{\pi} = \alpha_p = \alpha_{poverkhnost} = \alpha_{surface}$.]

fully where this flow rate is lower than that specified.

The uniformity of fuel-flow rate over the cross section of the combustion chamber is a quantitative criterion of fuel-component atomization. This criterion influences the selection of the shape of the engine's chamber.

4. The zone of fuel-mixture formation should extend down the shortest possible length of the combustion chamber, since otherwise a relatively large combustion-chamber volume would be required, and this might increase its dimensions and specific weight.

The component-atomization zone is located near the chamber head, determined by the type and design of the spray nozzles, and characterized by the distance from the chamber head to the point at which droplets of the weight-averaged diameter enter the gaseous medium. This zone is longer with ordinary spray nozzles than for centrifugal nozzles.

The shape of the spray is governed basically by the design of the chamber's atomizing head and by the range of the atomized-fuel jet.

5. The final atomizing spray of the fuel components must be symmetrical with respect to the combustion-chamber axis, since if the spray of burning fuel strikes the surface of the chamber liner and burns there, it may overheat and burn it. The jet of oxidizer must not strike the surface of the chamber liner, since this will cause rapid burnthrough as a result of oxidation of the metal. The spray nozzles must be arranged in the head in such a way that the resultant fuel-stream direction will be parallel to the chamber axis after all of the jets have met. This requirement applies particularly to spray nozzles having intersecting jets.

The problem of the designer is to distribute the nozzles on

the chamber head in such a way that no great amount of oxidizer will strike the walls and the fuel components will be distributed uniformly over the combustion-chamber cross section.

The amounts of the fuel components striking the chamber-liner surface on atomization by the nozzles can be reduced by appropriate aiming of the nozzles, using nozzles with angled faces,* etc.

6. The pressure gradients of the fuel components in the spray nozzles must be optimum both from the standpoint of physical completeness of the fuel's combustion and from the viewpoint of the specific weight of the engine's fuel-supply system. When the pressure gradient of the liquid being atomized in the spray nozzles is lowered, the feed pressure of the fuel into the combustion chamber and, consequently, the capacity and weight of the fuel-supply system are also reduced; then, however, the mixture-formation and fuel-combustion processes deteriorate. The opposite is the case when the pressure gradient in the spray nozzles is raised.

Meeting this specification often involves great difficulty in practice, and for this reason the fuel-component nozzle pressure gradient is usually specified on the basis of statistical data for designing ZhRD.

7. The engine's atomizing system must be simple in design and cheap to manufacture and must not be sensitive to changes in the engine's operating regime or to the vibrations that may arise. Additional requirements are set forth for atomizing devices to be used in engines with controllable thrust.

Experiments have shown that nozzle pressure gradients smaller than 2 kg/cm^2 , such as prevail with small numbers of nozzles, result in unsatisfactory atomization of the fuel components and, consequently, in unstable performance from the engine.

*[Translator's note: literally, "with cutoff at angle."]

If the pressure gradient of the fuel components in the nozzles is assumed equal to $2-3 \text{ kg/cm}^2$ for operation of the engine at minimum power, the spray-nozzle pressure gradient in the maximum-thrust regime will be found to be much higher (perhaps 5-10 times that for the minimum-thrust regime), and this is highly unfavorable because of the relatively great weight of the fuel-supply system. For this reason, regulation of engine thrust by varying the fuel-component nozzle pressure gradients can be justified only in a narrow range.

All of the specifications enumerated above for ZhRD atomizing devices can be met by proper planning and design of the engine chamber head, i.e., by appropriate selection of its shape, the type of nozzles, their parameters and number, their arrangement in the head, etc.

In practical solution of this problem, the designer must be thoroughly familiar with the mixture-formation and combustion processes of various fuels in the chamber and make correct allowances for various factors influencing the course of these processes. Only if this is done will it be possible to design a highly efficient atomizing device for the engine.

A proper fuel-component atomizing setup in the ZhRD makes it possible to reduce combustion-chamber displacement, dimensions, and specific weight and to increase the dependability, safety margin, economy, and stability of the engine's performance. A high-quality mixture-forming function also ameliorates the conditions under which the fuel is ignited when the engine is started and reduces the number of malfunctions.

SECTION 2. METHODS OF ATOMIZING FUEL COMPONENTS IN ZhRD

The atomizing technique depends on the design of the atomiz-

ing device (chamber head). The following basic fuel-component atomizing methods are used in contemporary ZhRD.

1. Jet atomization, i.e., atomization through small holes 1-2.5 mm in diameter that are drilled either directly in the engine chamber head in such a way that the jets of combustible and oxidizer collide and break up into fine droplets, or in special spray nozzles installed in the chamber head.

This atomization method is used in low- and medium-thrust engines because it is simple, mixes satisfactorily, and distributes the fuel components uniformly over the cross section of the combustion chamber. It can be used for atomization of various types of fuels.

2. Centrifugal atomization, i.e., atomization by centrifugal spray nozzles (Fig. 8.2).

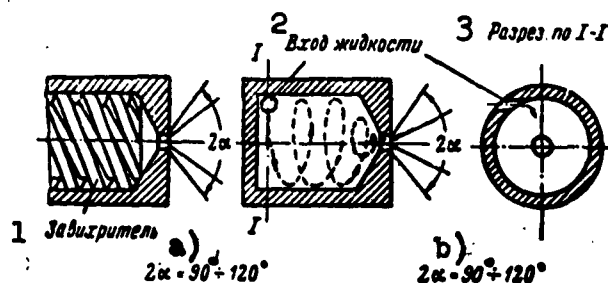


Fig. 8.2. Schematic diagrams of centrifugal nozzle with vanes (left) and tangential nozzle (right). 1) Swirler; 2) liquid input; 3) section through I-I.

This method of atomization is obviously the best, and for this reason it is given preference in nitric-acid and other types of engines. The nozzles are set in the chamber head in such a way as to ensure the best possible mixing of the combustible and oxidizer; the number of spray nozzles is increased for the same purpose.

3. Prechamber atomization, i.e., fuel-component atomization partly through the usual holes in the prechamber walls of the engine chamber and partly through special spray and centrifugal nozzles

screwed into the walls of these same prechambers (in the same way as in the A-4 engine). The combustible and oxidizer are mixed by diffusion and turbulence before entering the combustion chamber. This atomization method is quite effective, but it is a relatively complex matter to set it up.

4. Combinations of centrifugal and jet atomization.

None of the presently existent atomizing methods applied to fuel components in ZhRD can be regarded as perfect and successfully applicable in all cases. The atomizing method must be selected in each specific case with consideration of a number of specific conditions.

The following factors may influence the selection of one or another atomization method and engine-chamber atomizing-head design:

- 1) the properties of the fuel components;
- 2) the absolute thrust, burning time, and operating program of the engine;
- 3) the combustion-chamber gas pressure;
- 4) the production process used to make the atomizing head of the chamber, etc.

The atomizing device strongly influences intensification of the fuel-combustion process, operational stability and efficiency, and the dimensions and specific weight of the engine's combustion chamber.

An efficiently worked-out design for a chamber atomizing head is characterized by the following criteria during operation of the engine:

- 1) the absence of "banding" or localized combustion of the fuel;
- 2) smooth starting and stable combustion of the fuel over a

wide range of combustion-chamber pressure (per-second fuel flow rate) variation;

3) a small pressure gradient for injection of the fuel components into the combustion chamber and atomization quality independent of this factor;

4) low specific heat fluxes from the gases to the engine's combustion-chamber liner;

5) a high degree of completeness of fuel combustion.

In practice, these indicators can be achieved only provided that the rigorous specifications set forth for the engine's atomizing device are met.

SECTION 3. TYPES OF FUEL SPRAY NOZZLES

The ZhRD's fuel-spray nozzles are extremely important units for mixing the combustible and oxidizer fed into the combustion chamber. The quality of the mixing function depends to a major degree on the type and design of these nozzles.

In the majority of cases, the spray nozzles used in the engines have no special device for regulating the fineness of the spray, and some of them possess generally low qualitative characteristics.

ZhRD fuel-spray nozzles can be classified on the basis of the following characteristic criteria.

1. By the number of fuel components atomized by a single spray nozzle:

a) single-component nozzles, which are designed to atomize a single fuel component, and

b) two-component nozzles, which are designed to atomize two fuel components simultaneously.

2. On the basis of the nozzle's operating principle:

a) jet nozzles, which supply liquid into the combustion chamber in the form of streams directed along their axes;

b) centrifugal nozzles, in which a fluid moving under a pressure head is "swirled" and flows into the combustion chamber in the form of a thin and easily shattered conical film as a result of the centrifugal effect thus achieved;

c) centrifugal-jet nozzles (mixed type). Two-component jet nozzles and all types of centrifugal and centrifugal-jet nozzles are executed physically in the form of individual units that can be installed in holes in the engine's chamber head.

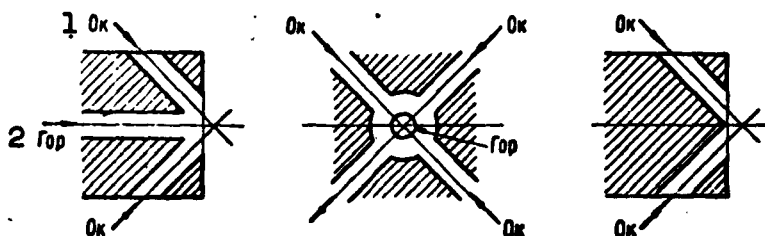


Fig. 8.3. Schematic diagrams of elements in jet atomization of fuel components. 1) Oxidizer; 2) combustible.

Injector designs are classified as follows:

1) single-jet types, which are calibrated holes in the chamber head with diameters from 0.8 to 2.5 mm where the fluid enters the combustion chamber;

2) double-jet types, which are designed to atomize a single given fuel component into two impinging jets (Fig. 8.3);

3) three-jet types, which are designed to atomize two fuel components in a single central jet of combustible and two lateral jets of oxidizer, all situated in the same plane and intersecting at one point (see Fig. 8.3);

4) four- and five-jet types, which are designed respectively to atomize two fuel components into a single central jet of combus-

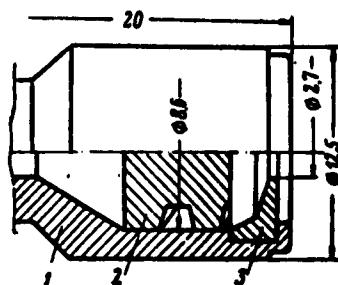


Fig. 8.4. Single-component centrifugal worm injector.
1) Body; 2) vane (swirler);
3) injector nozzle.

tible or four jets of oxidizer located in the same plane and intersecting at a single point (see Fig. 8.3);

5) slot-type injectors, which are designed for simultaneous atomization of two components and structurally take the form of concentric slots in the engine's chamber head.

Centrifugal nozzles are classified as follows on the basis of the method used to swirl fluid in them:

a) tangential types, in which the liquid enters the cavity of the injector through a hole whose axis is perpendicular to the axis of the nozzle but does not intersect with it, so that the liquid being atomized is swirled around the nozzle axis and is easier to break up into droplets (see Fig. 8.2);

b) worm-type nozzles, in which the liquid is swirled by a special swirler (worm insert) which has spiral channels cut into its outer surface (Fig. 8.4).

Figure 8.5 shows prechamber alcohol injection nozzles of the A-4 engine's combustion chamber.

In two-component centrifugal nozzles, the combustible and oxidizer are mixed at the nozzle orifice or in a special mixing chamber and arrive in the combustion chamber in the form of an emulsion. There are various designs for nozzles of this type, but their operating principle remains the same.

Jet nozzles are characterized by design simplicity and relatively low manufacturing cost coupled with inferior fineness of atomization. The length of the atomization zone is also greater for

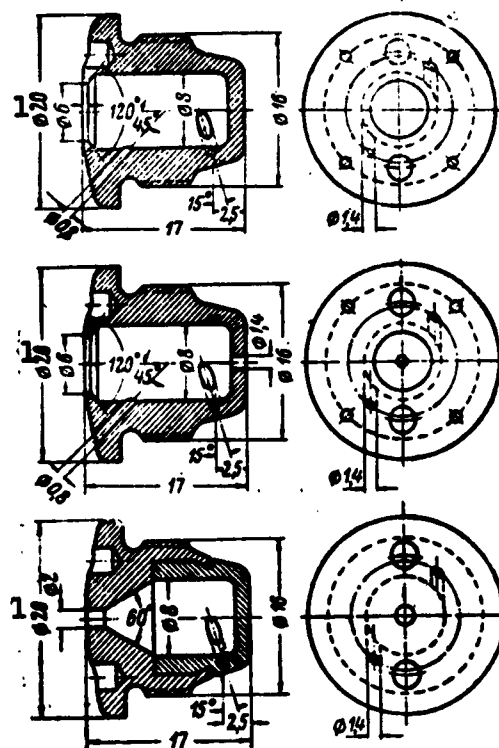


Fig. 8.5. Prechamber alcohol injector nozzles of A-4 engine. 1) ϕ - diameter.

these nozzles, and this increases the volume and specific weight required for the combustion chamber.

The spray angle of the jet-type nozzle is extremely small ($5-10^\circ$; see Fig. 8.6), and the zone in which the decay of the jet into drops terminates is at a great distance from the chamber head. This angle is measured from the face of the injector's nozzle plate and characterizes the shape of the atomized-liquid spray. The size of this angle depends basically on the ratio of the orifice length to its diameter, the amount of turbulence set up in the expanding

spray, and the combustion-chamber pressure.

In order to shorten the atomization zone and obtain finer atomization and uniform distribution of the fuel components over the cross section of the combustion chamber, jet nozzles are usually located in such a way that the jets of atomized liquids will impinge. Moving the points of impingement of the jets closer to the head makes it possible to utilize the combustion-chamber volume most fully and set up more stable combustion for the fuel mixture formed as a result of the minimized nonreacting gaseous dead zones near the chamber head and the superior mixture formation obtained when this is done.

The angles that determine the direction of the fuel-component spray injection from single-jet nozzles must be selected in such a way that the resultant momentum vector after impingement of the jets

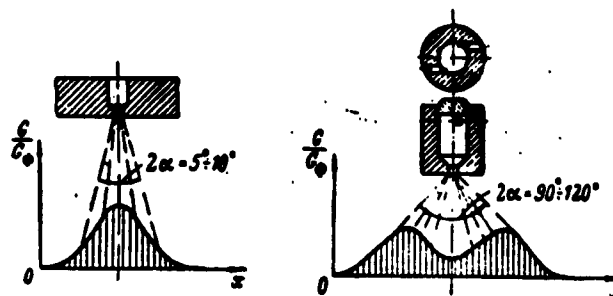


Fig. 8.6. Schematic plots of flow rates versus cross section of atomization sprays from jet centrifugal injector nozzles.*

will have an axial direction, i.e., will run parallel to the engine-chamber axis.

If the impingement angle of the jets is increased, the average drop diameter diminishes as a result of the increased relative velocities of the jets at the point of impingement. This contributes to more uniform distribution of the fuel over the spray cross section. The uniformity of the mixed liquids is improved simultaneously.

Angles of 80 to 100° should be regarded as optimal for the impingement of jets created by jet nozzles, since with larger angles much of the atomized liquid is thrown off toward the sides of the head, so that mixing deteriorates, while smaller jet-impingement angles (60° and less) give rise to distinct flow-rate nonuniformity in the core of the spray and elongate the combustion chamber because of the enlarged component-mixing zone.

Centrifugal nozzles have relatively large liquid-spray angles (about 70-120°) with short spray lengths, and give finer atomization than jet nozzles; however, they are more difficult to manufacture. Basically, the shape of the spray produced by these nozzles depends on the amount of swirl imparted to the atomized liquid in them.

*[Subscript ϕ = f = forsunka = nozzle, injector.]

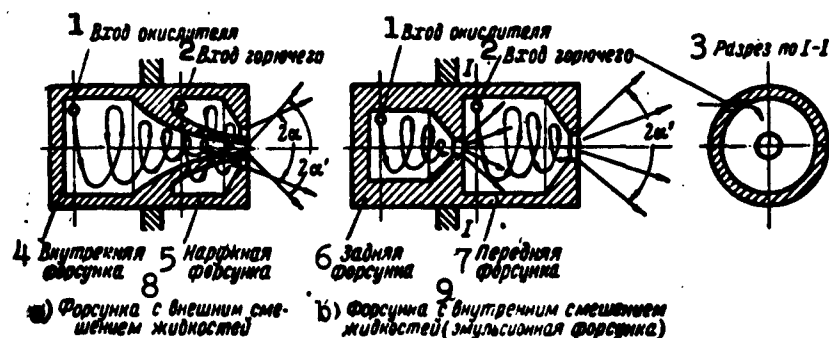


Fig. 8.7. Schematic diagrams of two-component centrifugal nozzles. 1) Oxidizer input; 2) combustible input; 3) section through I-I; 4) inner nozzle; 5) outer nozzle; 6) rear nozzle; 7) front nozzle; 8) nozzle with external mixing of liquids; 9) nozzle with internal mixing of liquids (emulsion nozzle).

In a centrifugal nozzle, the liquid arrives in the swirl chamber through tangential channels the axes of which are offset with respect to the orifice axis (see Fig. 8.2). The liquid is set in rapid rotary motion in the swirl chamber and proceeds thence into the nozzle orifice.

On emerging from the injector orifice, the thin film of liquid, which is no longer being acted upon by centripetal forces, is broken up into drops that disperse along rectilinear trajectories to form the spray cone. The spray angle and flow rate of a centrifugal nozzle are determined by the law of conservation of the momentum of the liquid particles about the nozzle axis. These parameters can be manipulated by appropriate selection of the relationships between the dimensions of the nozzle plate, the swirl chamber, and the entry channels.

At the present time, single-component centrifugal nozzles are used most extensively in engines because of their dependable performance and adequate atomizing effectiveness. In addition, the atomization angle can be varied over a wide range in these nozzles to achieve the most uniform possible distribution of fuel components over the

cross section of the combustion chamber.

Two-component centrifugal nozzles are classified into two types in accordance with the fuel-component mixing method used:

- 1) those with the fuel components mixed outside the nozzle (Fig. 8.7a);

- 2) those with the fuel components mixed inside the nozzle in a special mixing chamber (emulsion nozzles) (Fig. 8.7b).

There are also two-component nozzle designs in which the fuel components are mixed in the orifice of the nozzle.

Nozzles of the former type are made coaxial, with one inside the other. The mouthpiece of the inner nozzle is inscribed, with clearance, into the swirl chamber of the outer nozzle. To ensure good mixing of the fuel components, the spray angle of the inner nozzle (2α) must be larger than the spray angle of the outside nozzle ($2\alpha'$).

Nozzles of the second type consist of two nozzles arranged in tandem. The rear nozzle is used for the oxidizer and is designed in the usual manner.

The dimensions of the atomizing part of the two-component injector must be matched in such a way as to ensure safety in firing it even when one of the fuel components enters the swirl chamber before the other.

It is necessary to exclude the possibility of penetration of one of the fuel components into the other's chamber in order to avoid bursting a two-component injector; for this purpose,

- 1) the spray angle of the rear nozzle must be selected in such a way that the inlet holes of the front injector are outside the impact cavity of the spray cone on the wall of the rear [sic] injector;

2) the diameter of the front-nozzle gas swirl must be greater than the diameter of the rear-injector orifice.

The moment of momentum in the front nozzle propagates through the entire mass of mixed and atomized liquid.

Use of two-component emulsion-type centrifugal nozzles considerably improves mixture formation and compresses the atomization zone, since they ensure mixing of the fuel components in the specified weight proportions before they are fed into the combustion chamber. Moreover, a fuel emulsion possesses lower viscosity and surface tension and can therefore be shattered easily to extremely fine droplets.

The use of emulsion atomization of fuel components in ZhRD confers the following advantages:

a) the combustion-chamber length is reduced as a result of the shorter atomization zone;

b) nearly complete combustion of the fuel is achieved with relatively small combustion-chamber volumes, and, consequently, with small chamber specific weights;

c) a smaller number of injector nozzles is required;

d) it is no longer necessary to have a large fuel-component pressure gradient in the nozzles, a fact of essential importance for high-thrust single-shot engines, where the problems of simplicity and low-cost design are of decisive importance.

When nozzles of this type are used, it is somewhat more difficult to use the combustible to protect the chamber liner from overheating by the burning gases. In this case, the liner must be protected by setting peripheral single-component jet-type or centrifugal nozzles into the chamber head.

In all types of nozzles, the surfaces that come into contact

with the moving liquid must be smoothly machined. Jet nozzles must have precision-cut angles to direct the axis of the nozzle relative to the engine-chamber axis. Inferior nozzle quality has a particularly strong detrimental effect on the quality of the atomizing function when the engine's operating regime drops below the nominal level.

All types of fuel injectors are characterized by the following hydraulic parameters:

- 1) per-second flow rate;
- 2) the fluid pressure gradient in the nozzles;
- 3) the spray angle of the atomized fluid, which is measured at the tip of the nozzle (root angle of the spray);
- 4) the fineness of the spray and the uniformity with which the fluid is distributed about its axis and across its radius;
- 5) the flow-rate factor, which appears in the flow-rate equation.

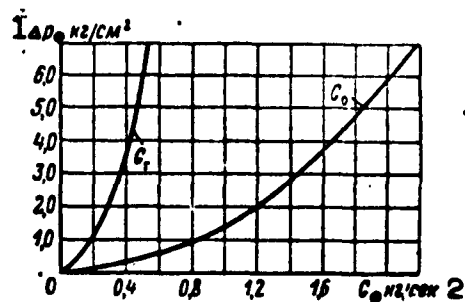


Fig. 8.8. Calibrating curves of engine-chamber head with 85 single-component centrifugal nozzles (31 for kerosene and 54 for nitric acid). 1) Δp_f , kg/cm²; 2) G_f , kg/sec.

The output through individual single-component centrifugal ZhRD nozzles in cylindrical combustion chambers with flat heads is about 20-80 g/sec of combustible and 50-200 g/sec of oxidizer, and the nozzle pressure gradient is of the order of 3.5-12 kg/cm².

The hydraulic parameters of nozzles and chamber atomizing heads are determined by testing them cold by pouring water through them. The performance of the engine chamber is evaluated on an operating engine.

The quantities determined in water testing of the nozzles

are their throughputs as a function of the pressure gradient of the atomizing fluid inside them, the atomization spectrum, the fineness and angle of the spray, and the flow rate over the cross section of the spray cone.

The variation of nozzle throughput as a function of the pressure gradient of the fluid to be atomized inside them is expressed by a parabolic curve (Fig. 8.8).

The spray fineness achieved with a given component can be determined with sufficient accuracy by photography, which is an applicable method both for the use of a single nozzle and with simultaneous operation of two or more nozzles.

The engine chamber heads are subjected to hydraulic testing to study the relationship between the nozzle spray cone and the uniformity of distribution of the component proportions and their flow rates over the cross section of the chamber.

The larger the number of nozzles set into the engine chamber head, the better will be the fuel-component atomization that they provide. For this reason, there may be as many as several hundred nozzles in medium- and high-thrust engines.

In practice, the number of engine spray nozzles is limited by design and other considerations, including the necessity of having a sufficiently large flow section for each nozzle. With small flow sections, the nozzles are easily fouled by any mechanical impurities that may accidentally have gotten into the fluid to be atomized or formed in it as a result of its physical and chemical instabilities.

Various types of materials, ranging from low- and high-alloy steels to bronze and brass, are used to make fuel nozzles in the form of individual units.

The selection of a material for the nozzles is governed by

the type and state of the fuel components to be atomized, the duration and conditions of the engine's operation, the number of times it is started, strength specifications, and other factors.

In the event that chemically active fuel components (e.g., nitric acid, liquid fluorine, etc.) are used, the inside surface of the nozzles must possess high resistance to oxidation and corrosion. If considerable turbulence is induced in the hot gases in the engine chamber head, resulting in heating of the nozzles to 1300-1400°C at various points, the material of these nozzles must also possess high strength. Melting of the nozzle tips and impaired nozzle performance, with the possible consequence of malfunctioning of the engine, are possible at high temperatures.

During operation of the engine, the nozzles are cooled by the stream of liquid flowing through them for atomization. The temperature of this liquid before it enters the nozzles may be either negative (in cases where liquefied fuel components are used), or positive, and, in cases where the liquid has first been used to cool the engine chamber, even close to the boiling point for the working pressure in question.

SECTION 4. FACTORS EXERTING QUALITATIVE INFLUENCE ON ATOMIZATION OF FUEL COMPONENTS

The following factors influence the quality of fuel-component atomization in ZhRD:

- 1) the shape of the combustion-chamber head;
- 2) the type, design, number, and throughput of the fuel spray nozzles;
- 3) the layout of the spray nozzles in the chamber head;
- 4) the pressure gradient of the fuel components to be atomized down the nozzles;

5) the properties and state of the fuel components (viscosity, surface tension, vapor pressure, temperature, heat of evaporation, heat capacity, etc.);

6) the pressure, temperature, and other physical properties of the gaseous medium in the combustion chamber and the nature of its motion;

7) the shape of the combustion chamber and its geometrical parameters;

8) the stability of fuel-feed-system performance;

9) the engine's operating regime, etc.

The shape of the engine head exerts a strong influence on the quality of fuel-component atomization, since the freedom for placing the spray nozzles depends on it to a major degree.

Basically, the engine chamber head determines the distribution of each of the fuel components across the chamber section, the fineness with which they are atomized and the intimacy with which they are mixed with one another; it also determines the intensity of the gas combustion currents that transfer heat from the spray cone to preheat and evaporate the combustible mixture. A flat head with evenly distributed nozzles usually ensures uniform initial distribution of the fuel components over the chamber cross section.

Nonuniform distribution of the fuel components over the combustion-chamber section and concentration of these components in isolated zones usually results in combustion proceeding nonuniformly throughout the available volume, and basically at points where the fuel mixture is concentrated, i.e., only part of the combustion-chamber capacity is used for combustion. A similar phenomenon may arise in cases in which a small number of nozzles is arrayed across a flat chamber head.

As a result, the rates of evaporation, mixing, and combustion of the fuel components in the combustion-chamber volume are nonuniform. As a result, the flame front observed in the ZhRD combustion chamber is not solid and steady, but intermittent, lashing about in its volume; for this reason, the most intensive fuel burning takes place locally, at isolated foci in which the composition of the combustible mixture is close to stoichiometric and ready to burn at the instant in question.

Incidentally, this is what explains the continuous pulsations that can be observed spectroscopically in a ZhRD flame and determined from pressure readings taken from the combustion chamber, even during nonsteady operation of the engine.

Consequently, the uniform distribution of the combustible mixture over the combustion-chamber section that is obtained when a large number of nozzles are evenly distributed across a flat chamber head results in better utilization of combustion-chamber volume and, consequently, more complete combustion. Almost complete conversion of the fuel's chemical energy into heat energy takes place in a relatively small part of the chamber volume in engines in actual operation when satisfactory mixing is ensured. Beyond a certain point, increasing the combustion-chamber volume does not appreciably improve the completeness of fuel combustion or the engine's specific thrust.

Increasing the number of nozzles to a certain limit at the expense of reducing their throughput capacity results in finer atomization and more uniform distribution of the fuel components over the combustion-chamber cross section and, consequently, more rapid evaporation and mixing of the fuel components and more rapid combustion of the fuel mixture. Here, P_{ud} first rises sharply and then

shows no further increase after a certain limit to the number of nozzles has been reached (Fig. 8.9).

0.

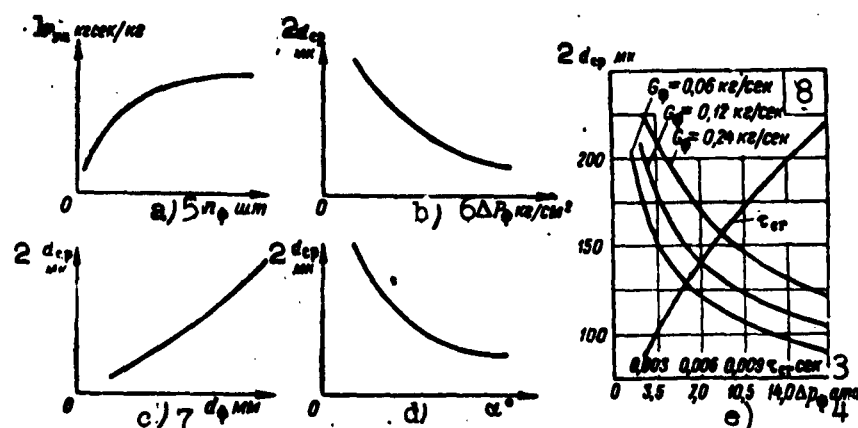


Fig. 8.9. Influence of certain factors on quality of nozzle performance in atomizing fuel components. Typical change in average diameter d_{sr}^* of kerosene droplets on atomization by centrifugal worm-type spray nozzle as a function of nozzle pressure gradient; combustion time τ_{sg}^{**} of fuel mixture as a function of the diameter d_{sr}^{sg} . 1) P_{ud} , kg-sec/kg; 2) d_{sr} , μ ; 3) τ_{sg} , sec; 4) ΔP_f , atmospheres absolute; 5) number of nozzles; 6) ΔP_f , kg/cm²; 7) d_f , mm; 8) $G_f = 0.06$ kg/sec, etc.***

Perfect initial mixing and virtually complete combustion of the fuel components can be achieved, just as in the case of centrifugal nozzles, by selecting a group of jet nozzles with sufficiently small jet diameters that ensure good mixing of the components. When the fuel is fed through single-component centrifugal nozzles, the components are mixed to some extent in the gaseous phase.

It is advantageous to begin mixing the fuel components even before they have left the liquid phase, since a considerably greater volume is required to mix gases than liquids. For this purpose, it is preferable to use two-component emulsion nozzles, which ensure almost perfect initial mixing of the fuel components before they enter

*[Subscript: cp = sr = srednyy = average.]
 **[Subscript: cr = sg = sgoraniye = combustion.]
 ***[Subscript: ϕ = f = forsunka = nozzle, injector.]

the combustion chamber. Here, excellent atomization is achieved with a small number of nozzles and does not require intensive mixing of the atomized components in the combustion chamber. During operation of the engine, the nozzles feed combustible and oxidizer into the medium composed of combustion products and unburned gases that is found near the engine chamber head. The fuel-component droplets formed in this process entrain the adjacent layers of gases, giving rise to convective currents of the gases between the nozzles, inside the spray cones issuing from them, and at the chamber walls; these currents are the basic sources of the heat necessary to evaporate and ignite the combustible mixture.

On the other hand, however, these convective currents disturb the gaseous combustible film on the walls of chambers having the usual configurations. In addition, bands may form at the chamber heads of such engines at the points at which the spray cones from the fuel-component nozzles impinge; these bands may result in detonation under certain conditions.

Above a certain number of smaller-capacity nozzles, the concentration of liquid phase at the chamber head increases and the intensity of the convective gas currents arising in the combustion-chamber head drops off. The amount of heat transferred by these currents from the focus of combustion to the atomized fuel components diminishes. As a result, it becomes more difficult to develop combustion because the time required for the fuel-priming processes has increased. In addition, placement of a large number of nozzles in the chamber head entails a great deal of technological complication, since it is very difficult in practice to drill spray-nozzle holes smaller than 0.8 mm in diameter (in the case of jet nozzles) or to arrange centrifugal and multiple-jet nozzles on the head with

less than 10-11 mm between them.

With a smaller number of high-throughput nozzles, the fuel components are atomized coarsely and distributed nonuniformly over the cross section of the combustion chamber. The result is that the fuel does not burn completely, chamber capacity is poorly utilized, and the engine may even operate in a pulsating regime.

The proficiency of the mixing function depends not only on the parameters and design characteristics of the nozzles and their number, but also on the layout of the nozzles in the head. The proportion by weight of oxidizer to combustible and the manner in which this proportion is distributed over the combustion-chamber cross section strongly influence selection of the nozzle-layout pattern. In the event that excessive heat currents arise in the chamber, its head must also ensure constancy of the excess oxidizer ratio in the center of the combustible mixture and lower values of this ratio at the surface of the combustion-chamber liner. The arrangement of the nozzles in the chamber head also depends on which fuel component is used to cool the engine's combustion chamber and nozzle.

As the fuel-component pressure gradient in the nozzles is raised, mixture formation improves because they are broken up into finer droplets (see Fig. 8.9). This also improves the stability of the engine's performance. The rate at which the fuel components are sprayed into the engine chamber depends on the pressure gradient in the nozzles. The higher the speed at which the fuel components are injected into the gaseous medium and the higher the density and viscosity of this medium, the more finely and uniformly will they be atomized. But the component feed pressure and the capacity and weight of the fuel-feed system also increase when the nozzle pressure gradient is raised. Under certain conditions, this may result in zero gain

from increasing the injection speed.

Moreover, experiments have shown that when the pressure gradient in the nozzles is raised, the droplet size of the atomized fuel components first increases rapidly, then more slowly, and then practically not at all in the region of high gradients (6 kg/cm^2 and higher). For this reason, there exists a nozzle pressure gradient beyond which it is pointless to increase the gradient further. This explains the efforts on the part of ZhRD designers to achieve high-quality fuel-component atomization at minimal nozzle pressure gradients by efficient design of the nozzles and the engine's entire atomizing system. Mixture formation deteriorates considerably and the operation of the engine becomes more unstable with small nozzle pressure gradients (smaller than 2 to 3 kg/cm^2).

The lower the viscosity and surface tension and the lower the density of the fuel components to be atomized, the finer will be the atomization and the more perfect the mixing function. The lower the boiling points of the fuel components, the smaller their heat capacities and the higher their heat yields, the easier will it be to vaporize, mix, and burn them and the shorter will be the time of residence in the combustion chamber; this will make it possible to use smaller chamber volumes.

The density of the gaseous medium strongly influences the quality of fuel-component atomization. Higher chamber pressures contribute to finer atomization of the fuel components (extremely fine droplets), and this improves mixing, accelerates preheating, vaporization, and combustion of these components. As a result, fuel combustion is more complete and the fuel residence time in the combustion chamber is shorter.

When the density of the gaseous medium in the combustion

chamber drops, as may occur when the engine's operating regime changes and when small pressure gradients prevail in the nozzles (gradients of the order of 2-3 atmospheres), the component droplets become larger and the processes of preheating, vaporizing, and burning them deteriorate.

The jets of combustible and oxidizer issuing from the nozzles usually impinge with one another in the engine's combustion chamber, are retarded by the gaseous medium, and subjected to a number of other disturbances, with the result that they are shattered into droplets, with the droplets finer for higher viscosities, densities, and turbulences in this medium.

Basically, the decay of the jets issuing from the nozzles is governed by the drag of the medium into which the liquid is sprayed, together with initial small disturbances on the surface of the jet, which are propagated along it in the form of waves. When centrifugal nozzles are used, these disturbances are compounded by the centrifugal forces which appear as a result of the rotary motion of the liquid particles about the axis of the jet.

The higher the pressure and viscosity of the gases in the combustion chamber, the more finely will the fuel components be atomized, the better will they be mixed, preheated, vaporized, and burned, and, consequently, the higher will be the physical completeness of the fuel combustion.

The resistance to the movement of the liquid droplets in the gaseous medium will be higher the greater the ratio of the droplet's volume to its weight. For this reason, acceleration and deceleration of the droplets in the gaseous medium will occur at higher rates as the droplets become smaller. The larger droplets "forge ahead" to greater distances from the nozzle. The fuel charge carried by the

larger droplets is delayed in completing its mixture-formation and combustion process.

If the nozzle atomizes the fuel in the direction of the gas stream, as is the case in the majority of existing engines, the liquid droplets are decelerated (or accelerated) in the direction of the stream's flow in accordance with the magnitude and direction of their relative velocity in the stream. Here, the finest droplets of liquid are decelerated almost instantaneously and are carried along with the stream.

If, however, atomization takes place in the upstream direction, the fluid droplets, which possess a certain volume-to-weight ratio, enter the stream, are first decelerated by this stream, and then move in the reverse direction with the stream of gas. The path length of the droplets in upstream atomization is approximately 30-35% shorter than the path length in downstream atomization.

The inherently nonuniform atomization of the fuel components by the nozzles sets up an uneven, vibrating ignition and combustion front in the combustion chamber, and this gives the impression of a stable spatial distribution of successive zones in the seat of combustion.

The turbulence set up in the gas flow in the combustion chamber by the design of the engine chamber's atomizing head also influences the quality of the initial and subsequent mixing of the fuel components. As a result of this turbulence, the processes of vaporization and mixing of the fuel components proceed with high intensity in the initial zone near the combustion chamber [sic], in both the liquid and gaseous phases. This is also assisted by the convective gas currents carrying heat into this region from the focus of combustion. Further mixing of the fuel components takes

place in the gaseous phase.

In the event of unstable operation of the engine's fuel-feed system, the pressure gradient of the fuel components in the nozzles varies and, consequently, so does the quality of the atomizing function.

A change in the engine's regime of operation involves a change in the fuel flow rate through the combustion chamber. Here, the conditions under which the fuel spray nozzles are operating may deviate from the optimum, and the nozzles may not ensure satisfactory atomization of the fuel components.

In cases where engine thrust is regulated by varying the fuel flow in the chamber, it is necessary to specify the pressure gradient in the nozzles for operation of the chamber in its minimal regime. The nozzle pressure gradient may rise to an extremely high value (by a factor of 5 to 10) when the engine is switched to operation in the nominal- or maximum-thrust regime. This indicates that this method of engine-thrust regulation is not advisable when wide thrust ranges are involved.

SECTION 5. DESIGN OF JET-TYPE ATOMIZING SYSTEM

The following are initial data for the design of a jet-type atomizing system for an engine:

- 1) the types of combustible and oxidizer, their specific gravities, and their per-second flow rates in the combustion chamber;
- 2) the design configuration and diameter of the chamber head;
- 3) the gas pressure in the combustion chamber.

The per-second flow rates of the combustible and oxidizer in the chamber are determined in making the thermodynamic calculations for the engines. The specific gravities of the fuel components are computed for the temperature at which they enter the combustion cham-

ber. The shape of the chamber head and its dimensions are selected as functions of the engine's thrust, the parameters of the combustion chamber, the method selected to atomize the fuel, the type of spray injector used, and other considerations.

The atomizing device is designed taking into account specifications set forth for the atomization function and statistical and experimental data, and consists in the following.

1) The fuel-component nozzle pressure gradients are specified, remembering that their values in existing engines frequently vary over the range

$$\Delta p_f = 3 \text{ to } 8 \text{ kg/cm}^2 = (3 \text{ to } 8) 10^4 \text{ kg/m}^2.$$

The speeds at which the component in question is injected into the combustion chamber are determined for the selected nozzle pressure gradients, using the following formula, which will be remembered from the course in hydraulics:

$$w_{np} = \varphi \sqrt{2g \frac{\Delta p_f}{\gamma}} \text{ m/sec.}^* \quad (8.1)$$

Frequently, $w_{vpr} \approx 15 \text{ to } 40 \text{ m/sec}$ in existing engines. For a given Δp_f , this velocity is a function of the diameter, length, and shape of the entry and outlet parts of the nozzle orifice and the finish to which its surface is machined.

2. The combined areas necessary for the combustible and oxidizer nozzle orifices are determined, applying another familiar formula for the flow rate of a fluid:

$$\begin{aligned} \text{i.e.,} \quad Q &= F \varphi \sqrt{2g \Delta p_f \gamma}, \\ F &= \frac{Q}{\varphi \sqrt{2g \Delta p_f \gamma}} \text{ m}^2. \end{aligned} \quad (8.2)$$

3. The diameters of the combustible and oxidizer nozzle open-
*[Subscript: np = vpr = vprisk = injection.]

ings (d_g and d_o) are selected and the number of nozzles n determined by the formula

$$n = \frac{F}{\frac{\pi d_\phi^2}{4}} = \frac{4F}{\pi d_\phi^2} \quad (8.3)$$

The diameters of the outlet holes of the spray injectors are selected in accordance with the over-all dimensions of the engine chamber and the type of nozzle selected, and lie somewhere between 0.8 and 2.5 mm. It is not recommended that the injectors be made with diameters less than 0.8 mm, since they would be easily clogged and are difficult to manufacture. To facilitate drilling holes with such small diameters, most of the material's thickness is drilled out to a larger diameter, leaving only a small thickness in the specified diameter. With injectors larger than 2.5 mm in diameter, atomization of the fuel component being fed deteriorates considerably because the jet is excessively thick and shatters poorly.

The flow-rate factor μ of the jet-type nozzle depends on the following factors:

- 1) the way in which the exit edge of the hole is machined (sharp or well-rounded) and the surface finish of the holes;
- 2) the ratio of the length l_f of the nozzle orifice to its exit diameter d_f ;
- 3) the properties of the liquid being atomized and its parameters (viscosity, pressure, velocity, etc.).

The value of μ must be taken on the basis of statistical data in the calculations.

The shape of the injector orifice must be selected in such a way that the flow-rate factor will be maximal and vary only slightly upon significant variation of the per-second fuel flow rate in the

combustion chamber. This condition is particularly important in cases in which the engine must operate in low-thrust regimes.

Experiments have shown that the most suitable among the great number of different nozzle-orifice shapes is the cylindrical orifice with a smoothly rounded exit edge (see Fig. 8.6). With the exit edge shaped in this way, the liquid holds to the surface of the bore during outflow and the flow-rate factor has a higher value than with any other shape. For this shape of the injector orifice, we have $\mu \approx 0.7$ to 0.75 for $l_f/d_f = 0.8$ to 2 , and $\mu \approx 0.75$ to 0.85 for $l_f/d_f = 2$ to 3 .

Since the per-second flow of oxidizer into the engine chamber is usually greater than that for the combustible, the diameters of the oxidizer injector orifices are made larger than those for the combustible. For a given spray-nozzle diameter, the number of nozzles for the oxidizer is greater than that for the combustible.

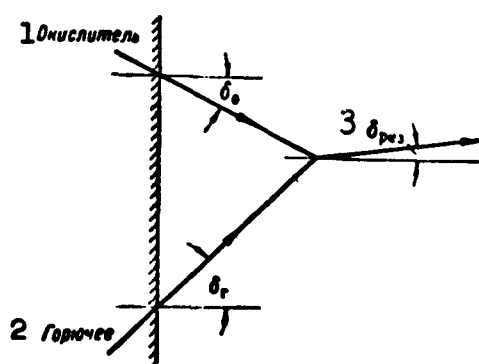


Fig. 8.10. Illustrating determination of resultant momentum in jet atomization of fuel components. 1) Oxidizer; 2) combustible; 3) δ_{rez} .*

In single-jet atomization of the fuel components, the injector orifices are placed in the chamber head in such a way that the jets of combustible and oxidizer will impinge at certain angles and create a combustible mixture that is uniform over the cross section of the combustion chamber and well-primed for combustion.

Since the weight of oxidizer in the fuel mixture is almost 2-5 times the weight of combustible (depending on the type of fuel), and its specific weight is also

*[Subscript: $pez = rez = rezul'tiruyushchiy = resultant$.]

greater, the nozzle pressure gradient for the combustible should be made larger than that for the oxidizer so that the resultant momentum vector of the impinging jets produced by the single-jet nozzles will have an approximately axial direction. With the same objective, the combustible and oxidizer injectors are arranged at different angles relative to the combustion-chamber axis.

The resultant magnitude of the momentum vector after impingement of the combustible and oxidizer jets is determined from relationships based on the law of conservation of momentum.

If the total momentum of the two jets does not change upon impingement, the angle between the chamber axis and the resultant jet will be given by the formula (Fig. 8.10):

$$\operatorname{tg} \delta_{\text{res}} = \frac{G_o w_o \sin \delta_o - G_r w_r \sin \delta_r}{G_o w_o \cos \delta_o - G_r w_r \cos \delta_r}. \quad (8.4)$$

If the resultant momentum vector of the impinging jets has an approximately axial direction, i.e., for $\delta_{\text{rez}} = 0$ and $\tan \delta_{\text{rez}} = 0$, the angular relationship reduces to the equality

$$G_o w_o \sin \delta_o = G_r w_r \sin \delta_r. \quad (8.5)$$

The relationships between the angles δ_g , δ_o , and δ_{rez} may be obtained from these expressions.

The resultant impingement vector of the combustible and oxidizer jets can be directed axially with a small inclination of the combustible injector to the chamber axis, if the pressure gradient in it is made larger than that in the oxidizer injector.

Atomization using multiple-jet injectors gives rather good results and does not involve design complications.

Jets of the same fuel component impinge in a two-jet nozzle, while in the three- and four-jet nozzles a single jet of combustible collides with two or (respectively) with four or five jets of oxidizer.

The three-jet injector delivers extremely poor mixing of the fuel components in the liquid phase if the velocities of all three jets are approximately equal. In this case, we observe a considerable excess of oxidizer in the core of the spray, while its periphery contains a large excess of combustible; this is accounted for by shattering of the central combustible jet when it is struck by the lateral oxidizer jets. This remark also applies to the four-jet injector nozzle.

To achieve uniform distribution of the fuel components in the spray produced by these nozzles, it is necessary to increase the velocity of the central combustible jet by approximately 50-60% over the velocity of the lateral oxidizer jets.

The advantage of the three- and four-jet injectors consists in the fact that no liquid is thrown back toward the engine-chamber head when they are used for the atomizing function, even with large impingement angles between the jets. The fuel-component atomization quality is almost the same for these two types of nozzles.

It must be assumed that the three-jet nozzles will be most efficient with oxidizer-to-combustible weight ratios equal to 2-3, while the four-jet nozzles will be preferable with fuel-component ratios around 3-5.

In selecting the type of nozzles and the optimum parameters for the design, as well as the arrangement of the nozzles in the chamber head, it is necessary to take into account factors which influence the quality of fuel-component atomization in ZhRD and the specifications for the atomizing function. It is also necessary to consider the results of detailed analysis of the atomizing devices used in existing engines.

The above scheme for designing a jet-atomization system can

also be used for [concentric]-slot atomization, using other values for the flow-rate factors of the nozzles.

Example 1. 0.590 kg/sec of aniline at 15°C ($\gamma_g = 970 \text{ kg/m}^3$) and 1630 kg/sec of nitric acid at 132°C ($\gamma_o = 1500 \text{ kg/m}^3$) are being fed into a combustion chamber, each through eight nozzles. The nozzle pressure gradient is 5.6 kg/cm^2 and the flow rate factor $\mu = 0.75$.

Determine the total flow sections for the combustible and oxidizer in the chamber head, the corresponding injector diameters, the exit velocity of the liquids from them, and the inclination of the impinging jets to give an axial resultant vector.

Solution.

1. Flow-section areas of combustible and oxidizer injector orifices:

$$F_r = \frac{G_r}{\mu_r \sqrt{2g\Delta p_r \gamma_r}} = \frac{0.590 \cdot 10^4}{0.75 \sqrt{2 \cdot 9.81 \cdot 5.6 \cdot 10^4 \cdot 970}} = 0.240 \text{ cm}^2;$$

$$F_o = \frac{G_o}{\mu_o \sqrt{2g\Delta p_o \gamma_o}} = \frac{1.630 \cdot 10^4}{0.75 \sqrt{2 \cdot 9.81 \cdot 5.6 \cdot 10^4 \cdot 1500}} = 537 \text{ cm}^2.$$

2. The diameters of the combustible and oxidizer spray nozzles:

$$d_r = \sqrt{\frac{4F_r}{\pi n_r}} = \sqrt{\frac{4 \cdot 0.240}{3.14 \cdot 8}} = 0.195 \text{ cm} = 1.95 \text{ mm};$$

$$d_o = \sqrt{\frac{4F_o}{\pi n_o}} = \sqrt{\frac{4 \cdot 0.537}{3.14 \cdot 8}} = 0.294 \text{ cm} = 2.94 \text{ mm}.$$

3. The fuel-component velocities at exit from the spray nozzles into the combustion chamber:

$$w_r = \mu_r \sqrt{\frac{2g\Delta p_r}{\gamma_r}} = 0.75 \sqrt{\frac{2 \cdot 9.81 \cdot 5.6 \cdot 10^4}{970}} = 20.3 \text{ m/sec};$$

$$w_o = \mu_o \sqrt{\frac{2g\Delta p_o}{\gamma_o}} = 0.75 \sqrt{\frac{2 \cdot 9.81 \cdot 5.6 \cdot 10^4}{1500}} = 25.2 \text{ m/sec}.$$

4. We set the inclination of the oxidizer jet to the chamber axis arbitrarily equal to 20° and determine the corresponding inclination of the combustible jet to obtain an axial resultant vector:

$$\sin \delta_r = \frac{G_o w_o}{G_r w_r} \sin \delta_o = \frac{1,630 \cdot 20,8}{0,590 \cdot 25,2} \sin 20^\circ = 0,75,$$

from which $\delta_g = 48.5^\circ$.

SECTION 6. DESIGN OF SINGLE-COMPONENT CENTRIFUGAL SPRAY NOZZLES

The basic difference between centrifugal and jet-type spray nozzles consists in the fact that the fluid flowing through a centrifugal nozzle possesses a moment of momentum about the nozzle axis. This causes the formation of a whirlpool running down the nozzle axis and results in a low flow-rate factor and a large atomization-spray angle.

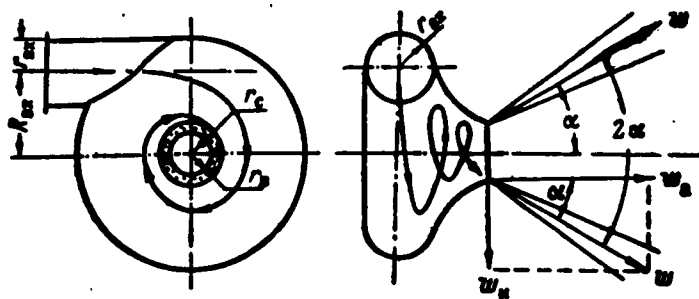


Fig. 8.11. Illustrating design of single-component centrifugal nozzle.*

In a tangential centrifugal nozzle, the fluid to be atomized enters at a velocity w_{vkh} into the nozzle cavity through an entry hole having a radius r_{vkh} (Fig. 8.11). This hole is so located that its axis is tangential to a circle of radius R_{vkh} with its center on the nozzle-nipple axis. As a result of its injection in this manner, the liquid swirls inside the inner cavity of the nozzle. Here, centrifugal forces arise in the liquid and compress it to the inside surface of the nozzle, forming a thin ring-shaped film where it exits through the nipple. A gas whirlpool in which the pressure is equal to that of the environment, i.e., to the combustion-chamber gas pressure, forms inside this liquid film. On leaving through the nozzle opening,

*[Subscripts: $bx = vkh = vkhodnoy = \text{entry}$; $c = s = \text{soplo} = \text{nipple}$; $b = v = vikhr' = \text{whirlpool}$; $a = \text{axial}$; $u = u = \text{tangential}$.]

the liquid particles, which are no longer acted upon by the centripetal forces governed by the reaction of the nozzle walls, fly out along rectilinear trajectories to form a spray cone.

The "live" [effective] cross section of the annular liquid film flowing through the nipple is determined by the nipple radius r_s and the radius r_v of the gas whirlpool (see Fig. 8.11), i.e.,

$$f_{\pi} = \varphi \pi r_c^2 = \pi (r_c^2 - r_v^2), \quad (8.6)$$

where $\varphi = 1 - (r_v^2/r_s^2)$ is the factor to which the nipple cross section is filled with liquid.

The thickness of the liquid film at exit from the nipple is

$$\delta = \frac{1}{2} (d_c - d_v),$$

where d_s and d_v are the diameters of the nipple and the gas whirlpool, respectively.

The diameter of the gas whirlpool at exit from the nipple is

$$d_v = d_c \sqrt{1 - \varphi}.$$

The relative thickness of the film in the exit section of the nipple is

$$\frac{\delta}{d_c} = \frac{1}{2} (1 - \sqrt{1 - \varphi}).$$

The liquid pressure in the nozzle declines and reaches the gas-whirlpool pressure at exit from the nipple.

The full pressure gradient Δp_f of the liquid in the nozzle is expended in setting up the velocity w_{vkh} in the entry hole and the axial component w_a of the velocity in the nipple.

The higher the entry velocity w_{vkh} of the liquid into the nozzle as compared to the axial velocity w_a , the higher will be the tangential velocity w_u of the fluid at exit from the nipple and the

*[Subscript: π = zh = zhidkost' = liquid.]

greater will be the part of the gradient Δp_f expended in creating the entry velocity. The higher the intensity with which the liquid is swirled in the nozzle (the greater the ratio of tangential to axial velocity) the smaller will be the cross-sectional area f_{zh} of the liquid film in the nipple; r_v increases as the swirling intensity rises.

According to Equation (8.2), the flow rate of the liquid through the nozzles is

$$G_\phi = f_\phi \mu \sqrt{2g\Delta p_\phi} \text{ kg/sec},$$

where μ is the flow-rate factor, the value of which depends on the intensity with which the liquid is swirled in the nozzle.

The value of μ will be smaller for higher swirling rates, since this reduces the area of the annular section of the fluid jet in the nipple and the pressure gradient in the nozzle.

It has been demonstrated theoretically* that the following relationships obtain between the geometrical characteristic A of the nozzle, the factor ϕ to which the cross section of the exit orifice is filled with fluid, the flow-rate factor μ , and the atomization semiangle α for an ideal liquid (disregarding friction):

$$A = \frac{(1-\phi)\sqrt{2}}{\sqrt{\phi^3}} = \frac{R_{ex}r_c}{lr_{ex}^3} = \frac{R_{ex}r_c}{lr_{ex}^3} = \frac{R_{ex}r_c}{lf_l} = \frac{D_{ex}r_c}{lr_{ex}^3}; \quad (8.7)$$

$$\mu = \sqrt{\frac{\phi^3}{2-\phi}} = \frac{1}{\sqrt{\frac{A^2}{1-\phi} + \frac{1}{\phi^3}}}; \quad (8.8)$$

$$\operatorname{tg} \frac{\alpha}{2} = \frac{(1-\phi)\sqrt{8}}{(1+\sqrt{1-\phi})\sqrt{\phi}}. \quad (8.9)$$

*G.N. Abramovich. Teoriya tsentrobezhnoy forsunki (Theory of the centrifugal nozzle). Promyshlennaya aerodinamika (Industrial aerodynamics), TsAGI (Central Aerohydrodynamics Institute), 1944.

**[Subscript: z_{akp} = z_{akr} = $z_{akrutka}$ = swirl.]

where R_{vkh} is the swirl radius of the fluid in the nozzle, in mm; i is the number of tangential entry holes in the nozzle; f_1 is the cross-sectional area of the nozzle entry hole, and d_{vkh} and D_{zakr} are the respective diameters of the nozzle entry hole and the swirl diameter of the liquid jet, which is equal to twice the distance from the nozzle axis to the exit of the nozzle's tangential entry hole.

As the geometrical characteristic varies from $A = 0$ to $A = \infty$, the flow-rate factor μ diminishes from unity to zero. The coefficient μ and the angle α are governed by the law of conservation of the moment of momentum of the liquid particles relative to the exit-hole axis. These parameters may be manipulated by appropriate selection of the ratios between the dimensions of the nipple, the nozzle's swirl chamber, and the entry canals.

In nozzles with worm-type swirl members, R_{vkh} should be understood as the distance from the center of gravity of the liquid cross section in one channel of the worm to the nozzle axis, while r_{vkh} should be understood as the radius of a circle having an area equal to that of the cross section of one channel of the worm.

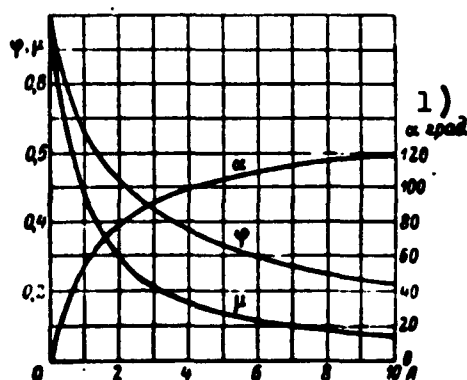


Fig. 8.12. Filling factor ϕ of nipple, flow-rate factor μ , and total atomization angle α of single-component centrifugal nozzle as functions of its geometrical characteristic. 1) Degrees.

Figure 8.12 shows curves of ϕ , μ , and α as functions of A , as computed from the formulas given above (without taking the hydraulic resistance of the liquid in the nozzle into account).

For an ideal liquid, the external moment of force acting on the liquid in the swirl chamber is zero, and the flow is subject to the law of conservation of moment of momentum.

In a real liquid, frictional forces opposing the flow arise at the liquid-wall interface as a result of viscosity. This frictional moment reduces the moment of momentum of the fluid leaving the nipple below the moment that it possesses at entry into the swirl chamber. Here, the radius of the gas whirlpool and the spray-cone angle are found to be smaller than in the case of the ideal liquid, while the flow-rate factor increases (the thickness of the annular liquid film in the exit nipple increases).

Thus, fluid friction on the swirl-chamber wall of the centrifugal nozzle causes an increase in the flow rate of the fluid as compared with the ideal case.

In addition to reducing the moment of momentum, friction of the liquid against the walls of the nozzle swirl chamber also gives rise to energy losses which, however, are relatively small and can be disregarded in practical calculations.

Applying the principle of maximum flow rate for a viscous fluid, we obtain an expression for the geometrical characteristic of the real nozzle, i.e., for the equivalent characteristic*:

$$A_{\text{ex}} = \frac{(1-\varphi) \sqrt{2}}{\sqrt{\varphi}} = \frac{R_{\text{ex}} r_c}{lr_{\text{ex}}^2 + \frac{f}{2} R_{\text{ex}} (R_{\text{ex}} - r_c)} \quad ** \quad (8.10)$$

Thus, the expressions establishing the relationships prevailing in the real nozzle differ from those presented above for the ideal nozzle only in the fact that it is necessary to replace A by the value of A_{ek} , which is related to A by the formula (denoting $R_{\text{vkh}}/r_{\text{vkh}}$ by B):

$$A_{\text{ex}} = \frac{A}{1 + \frac{f}{2} \left(\frac{B^2}{l} - A \right)} = \frac{R_{\text{ex}} r_c}{lr_{\text{ex}}^2 + \frac{f}{2} R_{\text{ex}} (R_{\text{ex}} - r_c)} \quad (8.11)$$

*I.V. Astakhov. Vliyaniye vyazkosti topliv i drugikh faktorov na melkost' raspylivaniya (Influence of fuel viscosity and other factors on fineness of atomization), "Dizelestroyeniye" (Diesel engineering), 1937, No. 2.

**[Subscript: эк = ek = ekvivalentnyy = equivalent.]

where f is the coefficient of friction of the liquid flowing through the nozzle and may be determined from the empirical formula

$$\lg f = \frac{25.8}{(\lg Re)^{2.58}} - 2. \quad (8.12)$$

Here, Re is the Reynolds number at entry of the fluid into the swirl chamber, as computed by the formula

$$Re = \frac{w_{vkh} d_{ex}}{\nu}. \quad (8.13)$$

Since $w_{vkh} = G_f / F_{vkh}$ is the entry velocity of the liquid, $F_{vkh} = \pi d^2 / 4$ is the area of the entry channels, and $\nu = \eta / \rho = \eta g / \gamma$ is the coefficient of kinematic viscosity of the liquid, the above formula for the Reynolds number can be rewritten in the following form:

$$Re = \frac{w_{vkh} d_{ex}}{\nu} = \frac{4G_f}{\eta g d_{ex}} = \frac{4G_f}{\eta g d_{ex}}.$$

where η is the liquid's dynamic viscosity coefficient, g is the acceleration of gravity, and γ is the specific gravity of the liquid being atomized.

A curve showing f as a function of Re is shown in Fig. 8.13.

Taking fluid friction in the nozzle into consideration increases the flow-rate factor μ and makes it a function of the liquid pressure gradient in the nozzle; however, this does not introduce any essential change into the spray-angle determination because the interrelationships between the gaseous medium in the combustion chamber and the spray cone are not being taken into account in this case.

The diagram of Fig. 8.12 may be used to determine the flow-rate factor of a real centrifugal nozzle if the values of A_{ek} are plotted against the axis of abscissas instead of A .

The value of A_{ek} is always smaller than A . The curve of μ as

* $\lg = \log$.

a function of A (or of A_{ek}) indicates that the flow-rate factor μ increases with diminishing A .

Thus, the flow-rate factor of the centrifugal nozzle increases in accordance with the increase in the coefficient of friction f and the number $(B^2 - 1) - A$ on transition from the ideal to a viscous liquid.

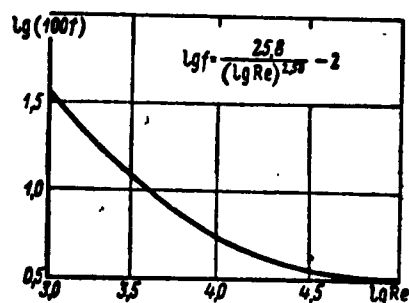


Fig. 8.13. Coefficient of friction of fluid in centrifugal nozzle as a function of Reynolds number.

Disregarding the negligible energy losses, we obtain an expression of the form (8.9) for determining the atomization spray angle for outflow of a viscous liquid; this expression is different only in the fact that the geometrical characteristic of the nozzle has been replaced in it by the equivalent character-

istic, i.e.,

$$\operatorname{tg} \frac{\alpha}{2} = \frac{2\mu A_{ek}}{\sqrt{\left(1 - \frac{r_v}{r_e}\right)^2 - 4\mu^2 A_{ek}^2}}, \quad (8.14)$$

where $r_v/r_e = s$ is the dimensionless radius of the whirlpool at the exit face of the nipple.

Thus, the angle of the atomization spray for a viscous liquid is also determined by the curve of Fig. 8.12, with the quantity A_{ek} laid off on the axis of abscissas instead of A . Since $A_{ek} < A$, the spray angle for a viscous fluid is smaller than that for the ideal fluid. Consequently, the hydraulic parameters of the centrifugal nozzle are determined by the equivalent characteristic for atomization.

The geometrical dimensions of the nozzle have the following effects on its hydraulic characteristics [see Eq. (8.11)]:

1) as R_{vkh} increases and the other parameters remain unchanged, A_{ek} and α first increase and then decrease; μ varies in the

opposite sense;

2) as r_s increases with the other parameters remaining the same, A_{ek} and α increase, while μ diminishes;

3) as r_{vkh} increases with the other parameters held constant, A_{ek} and α diminish, while μ increases;

4) as the velocity increases, Re , A_{ek} , and α diminish, and the coefficients f and μ increase;

5) as r_s is reduced and R_{vkh} is increased, the thickness of the liquid film at the exit from the nipple diminishes, with the result that the droplet diameter and the evaporation time are reduced and the atomization cone contracts.

The contraction of the liquid stream in the nipple can be taken into account by using the equivalent effective nozzle characteristic.

In the case of the ideal liquid, the expression for the effective characteristic is the same as that for the geometrical characteristic, with replacement of the area of the inlet canals by the stream cross section in these canals, i.e.,

$$A_s \frac{A}{s} = \frac{R_{s\sqrt{f}}}{\sqrt{f}} = \frac{R_{s\sqrt{f}}}{\sqrt{f}} \quad * \quad (8.15)$$

The flow-rate factor and the cone angle depend on A_d in the same way as on A .

The equivalent effective nozzle characteristic for a real liquid is given by the formula

$$A_{s,d} = \frac{A_s}{1 + \frac{f}{2} \left(\frac{B^2}{s^2} - A_s \right)} \quad ** \quad (8.16)$$

Here, the value of the contraction factor of the jet may be set equal to $\epsilon \approx 0.85-0.90$ for abrupt entry of the liquid into the

*[Subscript: $d = d = \text{deystvuyushchiy} = \text{effective}$].

**[Subscript: $s.d = e.d = \text{ekvivalentnyy, deystvuyushchiy} = \text{equivalent, effective}$].

tangential canal. When the liquid flows smoothly in the entry canals, $\epsilon = 1$.

As we see, the liquid pressure and the parameters of the main stream do not influence the flow-rate factor and the atomization-cone angle of the nozzle.

The manner in which the liquid flows in a centrifugal nozzle having a worm-type swirl insert differs in no respect from the way in which it moves in a tangential-entry nozzle. Thus, all of the conclusions presented above are equally applicable for these two types of nozzles.

The geometrical dimensions of nozzles in the design stage are usually established on the basis of the above theoretical premises, and on the basis of design considerations. A nozzle designed in this way is corrected on the basis of experimental data after fabrication.

It is sufficient to have 2-4 entry canals (1 is frequently made equal to 2) to ensure uniform distribution of the fluid in the nozzle swirl chamber.

The nozzle swirler is usually made long enough so that the liquid will complete from 1/4 to 1/3 revolution, since a fluid-pressure loss is suffered without any compensating gain in atomization quality when longer swirlers are used.

The ratio of the swirl radius R_{vkh} for the fluid in the nozzle to the radius of the nipple orifice r_s can be set equal to $C = R_{vkh}/r_s = 2.5$. The value of R_{vkh} is usually selected to conform to the over-all dimensions of the nozzle.

As C is reduced, the radial velocity of the liquid rises, its axial velocity diminishes accordingly, and, consequently, the flow-rate factor μ drops off and the spray angle increases.

The radius of the entry hole for the fluid may be determined

from the formula

$$r_{sz} = \frac{R_{sz}}{B}. \quad (8.17)$$

The quantity B is computed using the formula for the geometrical characteristic A of the nozzle, after substitution of $r_s = R_{vkh}/C$ in it, i.e.,

$$A = \frac{R_{sz} r_c}{r_{sz}^2} = \frac{R_{sz} R_{sz}}{1 C r_{sz}^2} = \frac{B^2}{1 C},$$

from which

$$B = \sqrt{A 1 C}. \quad (8.18)$$

In designing and computing nozzles, an effort is usually made to have $(B^2/1) \cdot A$ equal to or less than 5 to 10. The fluid-friction losses in the nozzles increase with excessively high values of this parameter, while excessively low values give smaller absolute dimensions for the atomizer and, consequently, complicate manufacture and lower the precision to which the nozzles can be made.

The diameter of the nozzle's swirl chamber may be set equal to

$$D_s = 2(R_{sz} + r_{sz}) \text{ mm.}^* \quad (8.19)$$

The outside diameter of nonadjustible nozzles is selected on the basis of design considerations:

$$D_\phi = D_s + 3 \text{ mm.}$$

The cylindrical part of the outlet nipple of the nozzle should be as short as possible. Normally, the ratio l_s/d_s is set equal to or less than 1, since the atomization spray angle becomes smaller when the nipple length l_s is too great.

For $A_{ek} \leq 4-5$, we may set $l_s/d_s = 0.5-1$, while the corresponding figure for $A_{ek} \geq 4-5$ is 0.25-0.5.

The angle of the swirl-chamber cone of the nozzle where it

*[Subscript: $\kappa = k = \text{kamera} = \text{chamber}$].

enters the nipple is placed between 60 and 120° .

The nozzles of a given set must have the same flow characteristics. With this object in mind, nozzles are manufactured to the second and third precision classes. Here, the tolerance for passage of a given liquid through the nozzle must not amount to more than 3-5%.

If it is necessary to control the engine's thrust by varying the flow rate of the fuel into the combustion chamber, it is possible to use two-stage centrifugal nozzles. In this nozzle design, the liquid is supplied to the first and second stages from two cavities, either of which may be cut in or out of operation without any significant disturbance to atomization quality.

The initial data for design of a centrifugal nozzle are the following:

- 1) the angle α of the atomization cone;
- 2) the nozzle throughput G_f ;
- 3) the pressure gradient Δp_f in the nozzle;
- 4) the physical constants of the liquid being atomized (specific gravity, viscosity).

The design of centrifugal nozzles (tangential types and those with swirl inserts) follows the following procedure.

1. Knowing the approximate dimensions of existing nozzles, we determine the number of nozzles n that can be located in the engine-chamber head in question. In existing nitric-acid engines, about 20-30 nozzles are required for one ton of thrust.*

With the object of securing good atomization of the fuel components, an effort is usually made to place as many nozzles as possible in the chamber head, although a limitation is placed on this by

*Ekspress-informatsiya AN SSSR, No. 6, RT-16, 1957.

design and production considerations.

At the present time, single-component centrifugal nozzles are arranged on larger chamber heads at intervals $t = 15-20$ mm with a ratio $D_f/t \leq 0.75$, where D_f is the outside diameter of the nozzle. Nozzles with very low throughput are not used because of technological difficulties.

2. Knowing the number of nozzles and the per-second flow rates of the combustible and oxidizer into the combustion chamber (G , kg/sec), we determine the flow rates of these components through a single nozzle:

$$G_f = \frac{G}{n} \text{ g/sec.} \quad (8.20)$$

3. We select the liquid-atomization angle α desired for the nozzle and use the diagram of Fig. 8.12 to determine the geometrical characteristic A of the nozzle, with subsequent determination of the flow-rate factor μ from the same figure as a function of this characteristic.

It is desirable to make the atomization angle as large as possible. It must be remembered, however, that as the atomization angle is increased, the nozzle dimensions also increase, so that it may become difficult to locate the selected number of nozzles on the head.

If, however, it is found that the desired number of nozzles cannot be fitted into the head for the range of fuel-component atomization angles of interest to us, we may specify a slight increase in the head diameter or the nozzle pressure gradients of the components or the number of inlet channels into the nozzles. It is not recommended that recourse be taken to using a larger number of nozzles with lower throughputs, since in this case the dimensions of the nozzles increase more rapidly than the size of the interval between

them (it would be even more difficult to locate the smaller number of nozzles on the head).

4. The diameters of the oxidizer and combustible nipples are determined from the equation for the flow rate of the liquid through a single nozzle:

$$d_c = \sqrt{\frac{4G_\phi}{\pi \sqrt{2g\Delta p_\phi}}}. \quad (8.21)$$

In contemporary engines, $\Delta p_f = 2.5-7.5 \text{ kg/cm}^2 = (2.5 \text{ to } 7.5) \cdot 10^4 \text{ kg/m}^2$.

5. Proceeding from design considerations, we select the number of entry canals \underline{i} and the radius R_{vkh} of the corresponding nozzle by the formula $R_{vkh} = Cr_s$ [mm].

6. We determine the radius of the inlet canals of the nozzles:

$$r_{sz} = \frac{R_{sz}}{B} = \frac{R_{sz}}{\sqrt{A/C}} = \sqrt{\frac{R_{sz}r_c}{iA}}. \quad (8.22)$$

If necessary, we determine the actual nozzle characteristic by the formula

$$A_s = \frac{A}{\epsilon} = \frac{R_{sz}r_c}{\epsilon r_{sz}^2}. \quad (8.23)$$

7. When \underline{i} and R_{vkh} have been selected, we determine the diameter of the input canals:

$$d_{sz} = 2 \sqrt{\frac{R_{sz}r_c}{\epsilon i A_s}}. \quad (8.24)$$

This completes the elementary calculation of the nozzle for an ideal fluid. It is followed by evaluation of the influence of friction and various design factors on the hydraulic parameters of the nozzle and correction for the ideal fluid as a first approximation.

8. We determine the Reynolds number at entry into the swirl chamber:

$$Re = \frac{4G_\phi}{\gamma v d_{sz}}. \quad (8.25)$$

9. We find the coefficient of fluid friction in the nozzle:

$$\lg f = \frac{25.8}{(\lg Re)^{2.85}} - 2. \quad (8.26)$$

To avoid repeating these tedious calculations in each specific case, it is advisable to construct a graph of $f = \varphi(Re)$ from this formula, as shown in Fig. 8.13.

10. We compute the value of the equivalent effective nozzle characteristic:

$$A_{e,d} = \frac{R_{ex} f_c}{u r_{ex}^2 + \frac{f}{2} R_{ex} (R_{ex} - r_c)}. \quad (8.27)$$

Obviously, the calculated value of $A_{e,d}$ will be smaller than A_d . If the difference between $A_{e,d}$ and A_d is small, i.e., if the values of the flow-rate factor and the spray angle corresponding to $A_{e,d}$ and A_d differ by no more than a few percent and can be satisfied, we should rest content with the results of the first-approximation calculations. This will be the case when fluid friction does not exert a strong influence on the hydraulic parameters of the nozzle [with small values of f and the parameter $(B^2/i) - A$].

11. If, however, the difference between $A_{e,d}$ and A_d is large, it is necessary to carry the calculation through the next approximation. Assuming that the coefficient of friction is equal to the calculated value f , and solving the equation of $A_{e,d}$ for r_{vkh} , we find a new value for the diameter of the entry holes:

$$d_{ex} = 2 \sqrt{\frac{R_{ex} f_c}{u A_{e,d}} - \frac{f}{2u} R_{ex} (R_{ex} - r_c)}. \quad (8.28)$$

Then we determine the number Re' and the value of the coefficient of friction f' , from which we then compute the value of the equivalent characteristic $A'_{e,d}$ corresponding to entry channels with the diameter d'_{vkh} :

$$A'_{e,k} = \frac{R_{ex} r_c}{d r_{ex}'^2 + \frac{f'}{2} R_{ex} (R_{ex} - r_c)} \quad (8.29)$$

We again compare $A'_{e,d}$ and $A_{e,k}$ and, if the difference is greater than the allowable difference, carry the calculation to the next approximation. Normally, two or three approximations are sufficient.

12. Having found the diameter of the entry canals, we determine the remaining parameters of the nozzle:

a) the diameter of the swirl chamber

$$D_s = 2(R_{ex} + r_{ex});$$

b) the height of the cylindrical part of the swirl chamber

$$z \approx d_{ex};$$

c) the nipple length

$$l_c = (0.25 - 1.0) d_c;$$

d) the inlet-canal length

$$l_{ex} = (1.5 - 3.0) d_{ex}.$$

Finally, we draw the nozzles and refine their geometrical dimensions in such a way as to obtain nozzles with the specified parameters. If, however, it is impossible in designing the nozzle to hold to the dimensions adopted for it, the calculations must be repeated using other initial data.

The parameters required in nozzles of existing designs for atomization of selected fuel components are selected on the basis of calibration for water.

Example 1. Determine the geometrical dimensions of a nozzle for an oxidizer consisting of 60% of 98% HNO_3 and 40% N_2O_4 ($\gamma_o = 1627.3 \text{ kg/m}^3$) and a kerosene combustible nozzle ($\gamma_g = 830 \text{ kg/m}^3$), if the throughput of these nozzles with $\Delta p_f = 4 \text{ atm}$ must be

$$G_o = 63.3 \text{ g/sec and } G_g = 25.7 \text{ g/sec.}$$

Solution.

Computation of oxidizer nozzle:

1. We specify the atomization-cone angle at $2\alpha = 90^\circ$ and determine $A_o = 2.65$ and $\mu_o = 0.24$ from the diagram of Fig. 8.12.

2. The diameter of the nozzle nipple will be

$$d_{\phi o} = \sqrt{\frac{4G_{\phi o}}{\mu_o \pi \sqrt{2g\Delta p_{\phi o}} \gamma_o}} = \sqrt{\frac{4 \cdot 0.0633}{0.24 \cdot 3.14 \sqrt{2 \cdot 9.81 \cdot 4 \cdot 1627.3}}} = 0.00306 \text{ m} = 3.06 \text{ mm.}$$

3. We assign the characteristic $C = R_{vkh}/r_s = 2.5$ and determine the swirl radius of the fluid in the nozzle:

$$R_{sx} = Cr_c = 2.5 \cdot 1.53 = 3.82 \text{ mm.}$$

4. We assume three inlet openings in the nozzle and compute the quantity

$$B = \sqrt{A/C} = \sqrt{2.65 \cdot 3.25} = 4.46.$$

5. We compute the radius of the nozzle entry hole

$$r_{sx} = \frac{R_{sx}}{B} = \frac{3.82}{4.46} = 0.855 \text{ mm.}$$

6. We determine the diameter of the nozzle swirl chamber:

$$D_x = 2(R_{sx} + r_{sx}) = 2(3.82 + 0.855) = 9.35 \text{ mm.}$$

7. The outside diameter of the nozzle will be

$$D_\phi = D_x + 3 = 9.35 + 3 = 12.35 \text{ mm.}$$

At this point, we have completed the calculation of the nozzle for an ideal liquid. The next step is to convert the geometrical dimensions of the nozzle to take into account the coefficient of fluid friction f .

8. On computing the Reynolds number, we obtain $Re \approx 16,700$.

9. We use the diagram of Fig. 8.13 to determine the coefficient of friction in the nozzle in accordance with the value of Re ,

obtaining as a result

$$\lg Re = 4.223; \lg(100 f) = 0.615 \text{ and } f = 0.0412.$$

10. We compute the equivalent geometrical characteristic of the nozzle:

$$A_{ex} = \frac{R_{ex} r_c}{r_{ex}^2 + \frac{f}{2} R_{ex} (R_{ex} - r_c)} = \frac{3.82 \cdot 1.53}{3 \cdot 0.855^2 + \frac{0.0412}{2} (3.85 - 1.53)} = 2.47.$$

11. From the value of A_{ek} on the diagram of Fig. 8.12, we find new values for the flow-rate factor $\mu'_0 = 0.28$ and the spray angle $2\alpha'_0 = 88^\circ$ and compare them with the initial values μ_0 and $2\alpha_0$:

$$\frac{\mu'_0}{\mu_0} = \frac{0.28}{0.24} = 1.082 \text{ and } \frac{\alpha'_0}{\alpha_0} = \frac{90}{88} = 0.968.$$

Since only small discrepancies have been obtained between the original and subsequent values of the flow-rate factor and spray angle, we shall not recompute the geometrical dimensions of the nozzle.

Calculation for combustible nozzle:

1. We set the values of $2\alpha_g$, μ_g , and A_g equal to those for the oxidizer and obtain $d_g = 0.00229 \text{ m} = 2.29 \text{ mm}$.
2. Setting $C = 2.5$, we find $R_{vkh} = 2.86 \text{ mm}$.
3. Assigning $i = 3$ and computing B , we obtain $r_{vkh} = 0.641 \text{ mm}$.
4. After further similar calculations, we obtain:

$$D_x = 7.002 \text{ mm}; D_\phi = 10.002 \text{ mm}; f = 0.0588; A_{ex} = 2.32; \mu'_r = 0.265;$$

$$\frac{\mu'_r}{\mu_r} = 1.103; 2\alpha'_r = 87^\circ \text{ and } \frac{\alpha'_r}{\alpha_r} = 0.964.$$

In view of the considerable discrepancies between the original values of μ_g and α_g and the results just obtained, we recompute the geometrical parameters of the nozzle, taking into account the coefficient of fluid friction in it, i.e.,

$$d_{ex} = 2 \sqrt{\frac{R_{ex} r_c}{i A_{ex}} - \frac{f}{2} R_{ex} (R_{ex} - r_c)} = 1.203 \text{ mm}.$$

Here, we obtain $f = 0.0575$; $A_{ek} = 2.66$; $r_{vkh} = 0.71$ mm;
 $D_k = 8.928$ mm and $D_f = 11.928$ mm.

Finally, we set the spray angle equal to 90° , for which
 $\mu_g = 0.24$ and $d_s = 2.29$ mm.

SECTION 7. DESIGN OF TWO-COMPONENT CENTRIFUGAL EMULSION-TYPE NOZZLES

Calculations for two-component centrifugal emulsion-type nozzles are based on the theory of single-component centrifugal nozzles and reduce basically to determination of the nipple diameter, the swirl radius of the fluid, and diameters of the oxidizer and combustible entry holes that will ensure the specified proportions between them, as well as the required injector throughput and angle of spray,

In the emulsion-type nozzle, the oxidizer enters the swirl chamber through tangential openings arranged on the surface of the swirl radius R_{vkh} (Fig. 8.14), while the combustible enters through holes arranged around the same surface and inclined at an angle δ to the plane perpendicular to the axis of the injector nipple.

Since the entry canals for the two fuel components emerge into a common swirl chamber in the nozzle, we assume the same pressure gradient $\Delta p_f = p_p - p_k$ for them and apply the Bernoulli equations

$$p_s = p_k + \frac{\gamma_r w_r^2}{2g} = p_o + \frac{\gamma_o w_o^2}{2g}$$

for the flow of the liquids in the entry canals; this gives

$$\frac{w_o}{w_r} = \sqrt{\frac{\gamma_r}{\gamma_o}}$$

or

$$w_r = w_o \sqrt{\frac{\gamma_o}{\gamma_r}}, \quad (8.30)$$

where γ_o and γ_g are the specific weights of the oxidizer and combus-

tible, respectively, and w_o and w_g are the entry velocities of these fuel components.

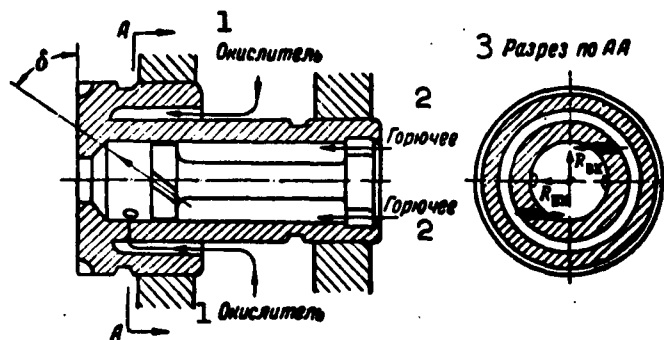


Fig. 8.14. Schematic diagram of emulsion-type centrifugal nozzle. 1) Oxidizer; 2) combustible; 3) section through AA.

Here, the mixture ratio of the fuel mixture in the swirl chamber of the nozzle will be

$$\chi = \frac{G_{f.o}}{G_{f.r}} = \frac{F_{f.o} w_o \gamma_o}{F_{f.r} w_r \gamma_r} = \frac{\frac{\pi d_o^2}{4} w_o \gamma_o}{\frac{\pi d_r^2}{4} w_r \gamma_r} = \frac{d_o^2 \gamma_o w_o}{d_r^2 \gamma_r w_r}$$

or, applying Eq. (8.30) for the velocity relationship w_o/w_g

$$\chi = \frac{d_o^2 \gamma_o}{d_r^2 \gamma_r} \sqrt{\frac{\gamma_r}{\gamma_o}} = \frac{d_o^2 \gamma_o}{d_r^2 \gamma_r} \sqrt{\frac{\gamma_o}{\gamma_r}}, \quad (8.31)$$

where $G_{f.o}$ and $G_{f.g}$ are the per-second flow rates of the oxidizer and combustible, respectively, through the nozzle, i_o and i_g are the numbers of entry canals in the injector for these components, d_o and d_g are the diameters of the fuel-component inlet canals, and $F_{f.o}$ and $F_{f.g}$ are the total areas of these canals.

Knowing χ and having selected i_o and i_g previously, we may determine the ratio d_o/d_g from Formula (8.31).

The per-second flow of fuel through the nozzle will be (remembering that $G_{f.g} = G_{f.o}/\chi$)

$$G_\phi = G_{\phi.o} + G_{\phi.r} = G_{\phi.o} + \frac{G_{\phi.o}}{\chi} = \frac{1+\chi}{\chi} G_{\phi.o} = \frac{1+\chi}{\chi} \pi r_o^2 i_o w_o \gamma_o. \quad (8.32)$$

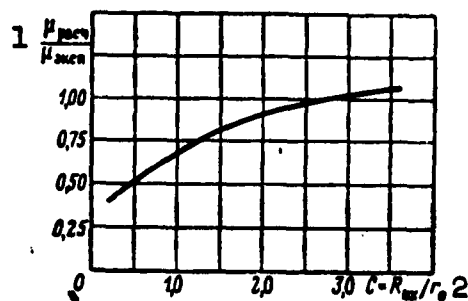


Fig. 8.15. Ratio $\mu_{\text{rasch}}/\mu_{\text{eksp}}^*$ as a function of R_{vkh}/r_s .
1) $\mu_{\text{rasch}}/\mu_{\text{eksp}}$; 2) $C = R_{\text{vkh}}/r_s$.

On the basis of the theory of the single-component centrifugal nozzle, we may arrive at the conclusion that the flow-rate factor μ , the atomization-cone angle α , and the nozzle fill factor ϕ of the two-component emulsion-type centrifugal nozzle are determined by a geometrical characteristic of the form

$$A_{e.m} = \frac{\chi \left(\chi + \sqrt{\frac{\gamma_o}{\gamma_r} \cos \delta} \right)}{(1 + \chi) \left(\chi + \frac{\gamma_o}{\gamma_r} \right)} \times \frac{R_{\text{vkh}} r_c}{l_o^3} \quad (8.33)$$

where r_o is the radius of the entry canals for the oxidizer.

The dependences of μ , ϕ , and α on $A_{e.m}$ remain the same as for the single-component centrifugal nozzle and, consequently, can be determined from the diagrams presented above (see Fig. 8.12).

The flow rate of fuel mixture through the two-component emulsion-type nozzle is determined from the familiar formula for outflow of a liquid through a nozzle:

$$G_\phi = f_\phi \sqrt{2g \Delta p_\phi \gamma_r} \quad (8.34)$$

where $f_\phi = \pi d_s^2/4 = \pi r_s^2$ is the area of the exit section of the injector nipple and γ_t is the specific weight of the fuel mixture computed by the formula

$$\gamma_r = \frac{\gamma_o \gamma_r (1 + \chi)}{\gamma_o + \chi \gamma_r}.$$

Knowing G_f , Δp_f , α , χ , γ_o , and γ_g , we may use Formulas (8.33)

*[Subscripts: pacu = rasch = raschetnyy = calculated;
эксп = eksp = eksperimental'nyy = experimental.]
**[Subscript: э.м = e.m = emul'sionnyy = emulsion-type.]
***[Subscripts: ф = f = forsunka = nozzle; c = s = soplo = nipple]
т = t = toplivo = fuel.]

and (8.34) for $A_{e.m}$ and G_f to determine the diameter d_s of the injector nipple, the swirl radius, and the diameter d_o of the entry canals for the oxidizer, and then determine the diameter d_g of the combustible entry holes from Formula (8.31) for χ .

The calculation presented above for the ideal centrifugal emulsion-type nozzle gives satisfactory results for ratios $R_{vkh}/r_s = C > 3$. If, however, the nozzle must have a large flare angle at the nipple ($C < 3$), it is necessary to correct the calculation using the curves of Fig. 8.15.

SECTION 8. PLACEMENT OF FUEL NOZZLES AND OTHER DEVICES ON ENGINE-CHAMBER HEAD

The nozzles are laid out on the chamber head after selection of the head's design, the most efficient type of fuel nozzles and the number of nozzles, and determination of their geometrical imensions.

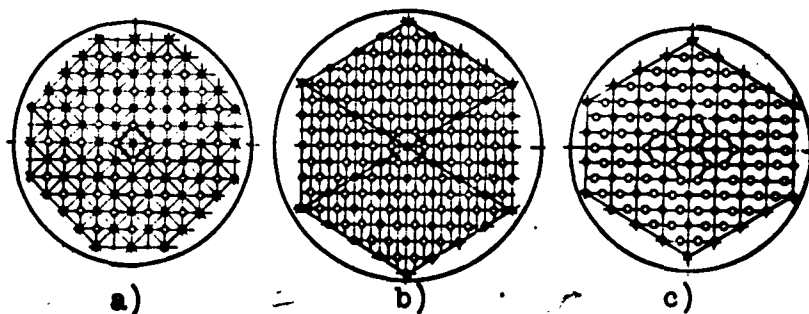


Fig. 8.16. Schematic diagrams of fuel-nozzle arrangements on engine-chamber head.

In selecting an arrangement of the nozzles on the chamber head of a ZhRD in the design stage, it is necessary to take into account the specifications set forth for atomization of the fuel components and atomization data from existing engines.

At the present time, the combustible and oxidizer nozzles are arranged on the ZhRD's chamber head in chessboard, honeycomb, and

annular arrangements.

In the chessboard arrangement, the combustible and oxidizer nozzles alternate (see Fig. 8.16a). Here, each combustible nozzle is surrounded by four oxidizer nozzles.

A deficiency of this nozzle placement consists in the fact that the number of combustible nozzles is approximately equal to the number of higher-throughput oxidizer nozzles, since there is almost two to five times as much oxidizer in the fuel as there is combustible. As a result, the thick oxidizer jet mixes poorly with the thin combustible jet, deflecting it to one side, with the resulting detrimental effects on mixture-formation performance.

The honeycomb injector arrangement is the most highly perfected.

In the honeycomb arrangement, the number of oxidizer nozzles is larger than the number of combustible nozzles (see Fig. 8.16b). Here, each combustible nozzle is surrounded by six oxidizer nozzles, with the result that mixture formation improves over that obtained with the chessboard arrangement. In this case, the number of individual droplet bundles formed is the same as the number of individual nozzle groups laid out on the chamber head.

Two variants of the honeycomb arrangement of injectors on a flat chamber head are possible:

- 1) symmetrical honeycomb arrangement of the nozzles with respect to two axes (see Fig. 8.16b);
- 2) symmetrical honeycomb arrangement of the nozzles with respect to one axis (see Fig. 8.14c [sic]).

The honeycomb arrangement permits only a fully determined number of combustible and oxidizer nozzles.

The chessboard and honeycomb nozzle arrangements can be set

up by using a flat head with two cavities situated one above the other. Such a head ensures approximately identical pressure gradients in the nozzles for the two fuel components.

For design reasons, the fuel component used to cool the engine chamber is usually fed into the lower cavity of the head.

In the concentric nozzle arrangement, i.e., when the nozzles are arranged in belts around the chamber head, combustible and oxidizer nozzles alternate. The advantage of this method consists in the fact that its use simplifies supplying the fuel components to the nozzles. However, this method is not often used. The chessboard and honeycomb nozzle arrangements are the basic ones used for flathead engine chambers.

It is characteristic for all engines with ordinary flat heads and centrifugal nozzles that much of the working mixture (up to 30% of the total flow) strikes the surface of the combustion-chamber liner as the mixture ratio is lowered. The presence of heat exchange between the gases and the liner and the increased flow rate near the wall as compared with the core of the stream tend to draw out development of the working process at the wall, causing it to lag behind the stream core.

Striking the wall of the combustion chamber, a certain amount of the fuel components ricochets off it and flows along it in the form of a liquid shroud, with part of it forming a thick layer of clustered droplets; they are heated and evaporated as a result of heat exchange with the combustion products in the core.

As the pressure in the combustion chamber rises, evaporation of the fuel-component droplets is accelerated, both in the stream core and in the layer at the wall. This phenomenon cuts short the flow of the liquid shroud down the liner surface and contributes to

transfer of heat from the stream core to the liner.

Reacting with one another and with the combustion products in the stream core, the vaporized fuel components form a layer of combustion products at the wall as they burn out. The fuel-component ratio in the wall layer at the end of the working process is determined to a major degree by the initial proportions of the components striking the wall.

As the gases move through the wall layer, the component proportions in them may vary as a result of mixing with the stream core.

The chamber liner can be protected from excessive heating and burning by arranging the combustible and oxidizer nozzles on the head in a way that promotes creation of a combustible excess around the liner surface. In this case, it is necessary to depart slightly from the alternation principle adopted for the nozzles and to place an excessive number of combustible nozzles around the periphery of the head, so that it will be possible to create a combustible curtain around the liner surface.

To reduce the amount of combustible expended in forming the protective curtain, these peripheral injectors are sometimes made with fuel flow rates lower than those of the main injectors.

It is simpler to protect the liner from overheating when the honeycomb arrangement is used. With the chessboard nozzle arrangement, it is necessary to install nozzles with reduced combustible flow rates around the periphery of the head; if the distance from the peripheral nozzles to the chamber liner is great, powerful convective gas currents form near the liner surface and will wash away the layer of combustible at the wall, which is serving to protect the liner from overheating.

In calculations, it may be assumed in first approximation

that the interval t between the centrifugal nozzles is proportional to the square root of the diameter d_{gol}^* of the flat chamber head, i.e.,

$$t \approx \sqrt{d_{\text{roz}}}.$$

In the case of a cylindrical combustion chamber, d_{gol} is equal to the combustion-chamber diameter d_k .

In modern engines, the average interval between centrifugal nozzles on a flat engine-chamber head varies from $t = 12$ to 20 mm.**

It follows from the expression of the form

$$V_k = \frac{G_k R_k T_k}{p_k} = \frac{n G_{\phi} R_k T_k}{p_k} = \frac{\pi d_k^2}{4} l_{k.c}$$

for the volume of a cylindrical chamber head that the number of nozzles n , of the selected throughput G_{ϕ} and step t between them is almost inversely proportional to p_k for given values of d_k and $l_{k.s}$ or, with the values of p_k and $l_{k.s}$ remaining unchanged, directly proportional to d_k^2 , while G_{ϕ} is inversely proportional to p_k when the other parameters of this formula remain unchanged.

If the interval between nozzles is not changed when the engine thrust is increased, the length of the fuel-component mixing paths will also remain almost constant. In this case, purely technical difficulties may arise on transition to very high thrusts in connection with the necessity of making a chamber head with several thousand nozzles.

Since the flow rate in the chamber increases accordingly when the combustion-chamber pressure is raised, the throughput of each nozzle should increase if the interval between the nozzles remains constant. The result is that the engine requires a great combustion-chamber length if the working process is to be completed in it. However,

*[Subscript: roz = gol = golovka = head.]

**Ekspress-informatsiya AN SSSR, No. 36, RT-108, 1957.

relatively long combustion chambers are not feasible because of the possibility that longitudinal acoustic vibrations may arise in them. Consequently, two-component emulsion-type nozzles are recommended with the object of reducing combustion-chamber length, since their use reduces the length of the fuel-component mixing zone required.

The physical design of the system supplying fuel components to the nozzles depends to a major degree on the type of nozzles and the chamber-head shape selected for the engine.

For example, a high-throughput jet-type nozzle with a large number of holes for oxidizer feed is installed in the center of each prechamber or head of a ZhRD with a prechamber head (such as the A-4 engine), with jet-type and centrifugal-jet combustible nozzles around it.

In nitric-acid engines, the chamber head may consist of three plates, of which the two flat ones form a lower cavity for supplying the nozzles with the fuel component used to cool the chamber, while the third — a spherical plate — forms the second head cavity with the central head plate of this engine; the second fuel component is fed into this cavity from the tank for distribution among the nozzles.

In chamber heads with concentric nozzle arrangement, the fuel components are fed into corresponding manifolds which connect the individual belts of nozzles. This ensures approximately uniform pressure gradients for the component in the nozzles of a given concentric belt.

If it is necessary to install a firing device, devices for chamber blowout, etc., in the chamber head, it is necessary to minimize the area occupied by these devices, since they preempt useful nozzle-placement area, upset the equilibrium fuel-component distribution over the chamber cross section, and interfere with utilization

tion of its volume. In addition, the fuel components emerging from the spray nozzles form a "cold" zone in front of the head which protects it from the high thermal fluxes. When the head surface includes large areas that are not protected by the components from the effects of high temperatures, the head may easily burn through at those points where the above devices are located, since external cooling of the head is ineffective because of the low rate at which the liquid moves in it. For this reason, it is necessary to avoid if at all possible installation of any devices other than the nozzles in the chamber head.

When the method for arranging the nozzles on the chamber head has been selected, the general geometrical configuration of the chamber head is worked out and the necessary check calculations are made.

After design and execution, the chamber head must ensure the calculated fuel composition even when the total flow rate of the fuel components through the nozzles varies slightly, i.e., the chamber head must meet the condition

$$\chi_{\text{fuel}} = \frac{G_{s.o}}{G_{s.r}} = \frac{\mu_o F_{\phi.o} \sqrt{2g \Delta p_o \gamma_o}}{\mu_r F_{\phi.r} \sqrt{2g \Delta p_r \gamma_r}} = \frac{\mu_o F_{\phi.o} \sqrt{\Delta p_o \gamma_o}}{\mu_r F_{\phi.r} \sqrt{\Delta p_r \gamma_r}} = \text{const.} \quad (8.35)$$

In hydraulic (water) testing of the chamber head to determine its hydraulic resistance and ascertain the manner in which the jets impinge, the sizes of the droplets formed, the mixture composition, and other atomization characteristics, $\gamma_g = \gamma_o$ and $\Delta p_g = \Delta p_o$, so that Eq. (8.35) for the weight composition of the mixture assumes the form

$$\chi = \frac{\mu_o F_{\phi.o}}{\mu_r F_{\phi.r}}. \quad (8.36)$$

The quantity χ , which is measured during hydraulic testing of the head with water, is converted for the working fuel components by

multiplying it by the expression $\sqrt{\Delta p_o \gamma_o / \Delta p_g \gamma_g}$.

After arriving at the design layout of the engine, the shape of the chamber and its head, the number of nozzles, and their arrangement, it is necessary to carry out check calculations for the combustion chamber to determine the fuel mixture ratio over its cross section and the average engine specific thrust.

This brief survey has not exhausted the subject of the design features of the atomizing devices used in contemporary engines.

It is necessary to rely on statistical data in planning and designing ZhRD atomizing devices. The design features of the atomizing devices of certain contemporary engines are illuminated in brief in the papers by G.V. Sinyarev and M.V. Dobrovol'skiy, D. Satton, V.I. Feyodos'yev and G.V. Sinyarev.*

It is necessary to design and configure engine-chamber atomizing devices with consideration of the recommendations set forth above, following approximately the following procedure:

- 1) select the chamber-head shape and make a preliminary sketch of its physical configuration;
- 2) ascertain which devices must be installed in the chamber head in addition to the nozzles, so that installation space can be provided for them;
- 3) select the type of centrifugal fuel nozzles, the interval between them, and their arrangement on the chamber head;
- 4) make scale drawings of the nozzle arrangement on a chamber head of the diameter in question and determine the number of combustible and oxidizer nozzles; here, the chamber-head diameter may be slightly increased or decreased;
- 5) determine the nozzle throughput from their number and the

*See list of references at end of book.

per-second flows of combustible and oxidizer into the engine's combustion chamber;

6) calculate the geometrical and over-all dimensions of the nozzles and ascertain the practical possibility of placing them on the head;

7) if necessary, introduce the required corrections into the calculations and configuration of the nozzles and make the final drawing of the engine chamber head; if necessary, change the throughput and number of nozzles for the fuel components;

8) select the expedient variants for the nozzle mounting in the chamber head and refine the physical configuration.

The problems of mating the head to the combustion chamber are solved during the process of designing and configuring the entire engine chamber, and the necessary corrections are introduced into these designs to take other factors into account (methods of supplying fuel components to the chamber head, igniting the fuel when the engine is started, etc.).

Like the joints between their various parts, the joints between the head and the combustion chamber may be either welded or separable. Preference should always be given to welded constructions, and the inclusion of elements requiring machining in them should be avoided, since welded designs are always lighter and cheaper to manufacture. Only in multistart engines and engines with relatively large working margins is it necessary to use certain separable joints for convenience in inspecting their components and elements after a certain operating time interval and replacement of damaged parts with new ones before the engine is restarted.

Chapter IX

PLANNING AND DESIGNING ZhRD COOLING SYSTEMS

Reliable chamber cooling is the most important problem in developing sustained-operation engines, and the most difficult problem to solve. This is explained by the fact that a huge amount of fuel usually burns in a ZhRD combustion chamber within a very short time, at high pressures (about 15-60 absolute atmospheres) and temperatures (approximately 3000-4450°K), and with great gas-stream velocities (from 40-300 meters per second in the combustion chamber and up to 2000-3000 meters per second in the nozzle outlet) as well. The heat formed per unit of combustion-chamber volume by this means attains enormous magnitudes (up to 10^6 - 10^9 kcal/m³ hr).

The enormous heat flows from the gas to the chamber liner, sometimes attaining magnitudes of $28 \cdot 10^6$ kcal/m² hr in the nozzle throat, which correspond to these engine operating conditions, cause the chamber to heat up rapidly and lose its required strength even if it is made of the most heat-resistant materials.

In practice, removing so many powerful specific heat flows from the chamber liner presents enormous difficulties. In the future, these difficulties will increase as the consequence of the continuous aspirations of ZhRD designers to raise specific engine thrust by increasing gas pressure in the combustion chamber, using fuels of high calorific value, and carrying out a number of other measures.

As we design and perfect a ZhRD, the complexity of solving the cooling problem is aggravated still more by the fact that heat-

transfer processes in the chamber depend on a great number of factors, and the quantitative evaluation of these heat-transfer factors is still extremely difficult. Heat transfer in liquid-propellant rocket engines, as yet, has been investigated very little.

Since, at the present time, it is impossible to theoretically completely establish the physical properties of the gases throughout the length of the engine combustion chamber and nozzle, taking into account the work of friction and other phenomena therein, it is also impossible to design an engine-chamber cooling system with accuracy. For the same reason, there is still no established methodology for designing ZhRD-chamber cooling systems.

Existing methods of designing ZhRD cooling systems, based on hydrodynamic and gasdynamic theories, still do not give satisfactory results, and therefore are of little use in practical design work. Moreover, designing cooling systems in accordance with these methods is cumbersome and laborious. The greatest difficulties lie in determining the specific convective and radiation heat flows from the gas to the engine-chamber liner.

It is for these reasons that we now design chamber-cooling systems in approximation for ZhRD being planned, chiefly by using experimental formulas of the theory of heat transfer, developed in conformity with the operating conditions of industrial heat-power plants.

The greatest difficulties encountered when designing ZhRD-chamber cooling systems lie in determining the coefficient of heat transfer from the gas to the chamber liner; at the present time, we have still not found a fully valid method for computing this factor.

The demand for increased operating economy (specific thrust), which is evident in ZhRD development trends, intensifies the need for a precise method of designing cooling systems for engine combustion chambers and

nozzles. This extremely urgent problem may be solved only as the result of further thorough theoretical and experimental investigations of the processes of heat transfer in engine chambers, considering the particulars of the combustion of various fuels therein under different conditions, the design particulars of combustion chambers and nozzles, and the nature of the gas currents therein.

The cooling system for an engine-chamber inner liner must provide for removing heat, thus preventing the liner from heating up to a temperature at which the strength properties of the material are considerably reduced.

The reliability and operating time of an engine depend upon the degree of success with which the problem of cooling the combustion chamber and nozzle has been solved.

SECTION 1. METHODS OF PROTECTING ZhRD CHAMBERS AGAINST OVERHEATING; THEIR ADVANTAGES AND SHORTCOMINGS

One of the basic problems of rocket engineering is the development of ZhRD with a high specific thrust and a long service life.

According to data from the foreign literature, specific thrust amounts to 215-240 kg of thrust/ (kg of fuel/second) in contemporary ZhRD, while the power potential of existing and prospective fuels would permit obtaining a P_{ud} of the order of 280-340 kg of thrust/ (kg of fuel/second).

The reason for such a great gap between the attained and potential values of P_{ud} lies in the exceptional complexity of developing a method of protecting the engine-chamber inner liner against the effects of high-temperature products of combustion.

The basic complexity of this problem lies in the fact that the heat flow from the hot gases to the chamber liner is proportional to the difference in temperatures between the gas and the liner surface, and therefore any rise in gas temperature causes an increase in heat flows,

and, consequently, a rise in the chamber-liner gas-side surface temperature.

The methods of protecting the chamber liner against overheating and burnout used at the present time are, in a number of cases, of little use, or, if of satisfactory efficiency, cause the operating cycle in the chamber to become impaired, and, consequently, reduce P_{ud} .

The principal (and most economical) method of protecting the engine-chamber liner against overheating from the hot gas is by external cooling, using one or both propellants for this purpose.

This method of cooling an engine is called regenerative, since, in this case, the heat transferred from the chamber liner to the coolant is almost entirely returned to the combustion chamber. Usually, we use the propellant component which has minor corrosive properties and the highest heat capacity, thermal conductivity, and boiling point as an engine-chamber coolant. We find the most effective cooling agent is frequently the oxidizer, since its per-second flow rate in the engine is as much as twice to four times the size of the combustible flow rate.

If one component is inadequate for purely regenerative engine-chamber cooling, we may use both propellant components (assuming that the second component is suitable for use as a coolant). Since we cannot mix them outside the combustion chamber, one of the propellant components may be used for cooling the nozzle and the other for cooling the combustion chamber. However, using both propellant components for cooling the engine is, in practice, difficult from the design viewpoint.

It is not desirable to use liquified propellant components for cooling the chamber. At the pressures and temperatures which occur in an engine-chamber coolant passage, hydrazine and nitromethane may decompose and explode.

Water has good cooling properties because of its high values of heat capacity, thermal conductivity and thermal diffusivity, as well as its low viscosity, but it is not practicable to use it for missile ZhRD, since a great supply of water is required in the missile for cooling the engine chambers, and this makes the missile too heavy. Water is often used as a coolant for combustion chambers on experimental test stands.

Regenerative cooling of ZhRD chambers may be intensified, within certain limits, by increasing the velocity of the liquid in the coolant passage by means of decreasing the flow area of the latter. As velocity increases the laminar layer of liquid at the liner surface becomes thinner, and as a result of this the thermal resistance between the liner and the coolant is reduced. However, if it is necessary to remove great amounts of heat from the liner, such intensification of regenerative cooling may be, in practice, disadvantageous, since, if the velocity of the liquid is increased considerably, the hydraulic resistance in the passage is unavoidably increased; to prevent this resistance, we require a considerable increase in coolant-feed pressure and, consequently, an increase in the weight and capacity of the engine fuel-feed system. Besides, the manufacture of a coolant passage with an extremely small flow section is very difficult to accomplish, owing to production problems.

In practice, it is possible to decrease heat transfer from the gases to the chamber liner by an artificial increase in the thermal resistance of the gas-side surface of the liner — by introducing a relatively cold body (of liquid or gas) into the boundary layer of gases.

If the gas pressure in the combustion chamber is increased or propellants of high calorific value are used to increase specific thrust, the cycle in the engine is intensified, as a result of which the heat

flows from the gases to the inner chamber liner increase and may attain such great magnitudes that it becomes disadvantageous or impossible to remove the required amount of heat from the liner by purely regenerative cooling. Moreover, many propellant components, because of their physical and chemical properties, are of little use for regenerative engine cooling (liquid oxygen is an example).

In these cases, as well as when it is necessary to relieve the conditions of regenerative engine cooling, in addition to the latter we often protect the chamber liner against overheating by means of:

- 1) developing a vapor-gas or liquid curtain (film) around the flame-tube surface by constantly feeding combustible, in small amounts, to the chamber wall-side gas layer either through injectors installed along the periphery of the chamber head or through special slots or orifices arranged in belts around the chamber liner (Fig. 9.1);
- 2) insulating the inner surface of the chamber liner from the hot gases by a special coating (of ceramic, graphite, tungsten carbide, silicon, or metallic oxides);
- 3) deliberately impairing the cycle in the combustion chamber (when operating on a given fuel) by excessive increase in the excess coefficient of one of the propellant components or by adding water to a component to decrease the combustion temperature.

Protecting the chamber liner against overheating by means of a film of combustible is quite effective. The efficiency of this method depends on the type of liquid used, the amount of liquid used to form the film, and the method and place of film formation.

For example, in an engine with a ground-level thrust of 10 tons, operating with a value of $p_k = 25$ atm abs and using a combustible of Tonka-250 and an oxidizer consisting of 80% of HNO_3 + 20% of N_2O_4 , a curtain of combustible on the chamber-head side provides a decrease in

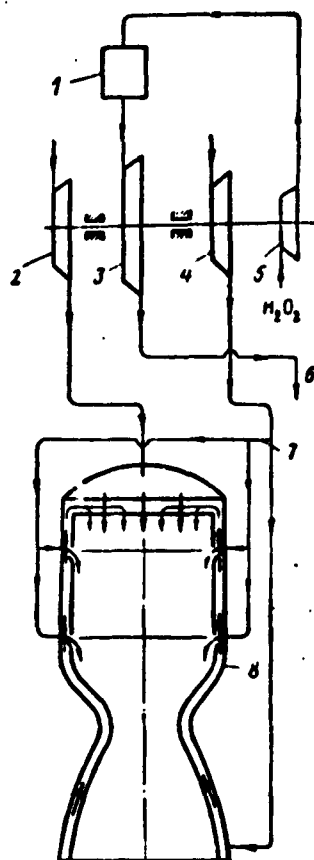


Fig. 9.1. Simplified diagram of an engine with belt method of protecting the chamber liner against overheating:
 1) Hydrogen-peroxide vapor-gas generator; 2) oxidizer pump; 3) vapor-gas turbine; 4) combustibile pump; 5) hydrogen-peroxide pump; 6) turbine-exhaust vapor gas; 7) feeding of combustibile to form protective curtains; 8) engine chamber with two belts of slots for internal protection of the liner against overheating by means of a film of combustibile.

Reverse gas currents always occur close to the head, and these also

$$* [X_{ct} - X_{st} - X_{stenka} - X_{wall}.]$$

$$** [X_R - X_{ya} - X_{yadro} - X_{core}.]$$

gas temperature in the wall-side layer of the combustion chamber of up to 1300-1400°K, when the value of the fuel-composition coefficient $X_{st}^* = 1.3-1.5$ whereas, in the core of the stream, the gas has a temperature of about 2600-3000°K, when $X_{ya}^{**} = 3.8-4.4$.

The development of a continuous thin protective layer on the entire surface of the combustion-chamber and nozzle liners presents the greatest difficulties in developing the curtains. It is obvious that the closer to each other the belts for feeding the liquid to the curtain are located, the easier it is to develop a continuous thin film curtain with a small amount of liquid.

A curtain developed by injecting a small amount of combustibile through the chamber-head injector is of little use, since it is blown away by the turbulent stream of the gas core.

tend to wash the protective curtain away. Besides, a small amount of the atomized basic fuel components (combustible and oxidizer) fall on the chamber walls, and the curtain mixes with these and is partially consumed, as a consequence of which its operating efficiency is decreased still further. However, this method of developing a protective curtain is extremely simple from the structural point of view and is therefore recommended for use in engines which have flat combustion-chamber heads.

When protective curtains are used, the engine operating economy is somewhat decreased, since the combustible expended in forming the curtains usually does not burn and, in general, is a fuel-energy loss for the engine.

A film curtain developed by means of special belts in the chamber liner is more economical, but, structurally, relatively complex. Water or gas also may be used for formation of the curtains. By internal protection, the chamber liner is, at the same time, preserved from the corrosive and erosive effects of gases.

The use of a solid coating to insulate the internal liner surface from gas heat is accompanied with great difficulties of a technological and operational nature, since it is difficult to preserve the strength of such a coating. As a rule, the use of refractory materials (ceramics and the like) for this purpose is limited by their sensitivity to the chemical reaction of the products of fuel combustion and to a heat "shock." Unavoidable changes in the temperature of the insulating material may lead to liner cracking or chipping, which cause local chamber-liner burnouts.

The efficiency of this method of protecting the chamber liner against overheating depends on the physical properties of the insulating materials (thermal expansion, thermal conductivity, temperature

diffusivity, mechanical strength, etc.).

The use of chamber-liner gas-side surface coatings that are resistant to high temperatures will not be further considered, since we lack sufficient data concerning the structural, technological, and operational properties of such coatings.

At high temperatures, the most stable materials are the oxides of magnesium (melting point 2800°C), thorium (2800°C), and hafnium (2812°C).

The materials with the highest melting points are the carbides of zirconium (3550°C), niobium (3500°C), tantalum (3900°C), and hafnium (4160°C); the nitrides and borides of hafnium have melting points of 2307 - 3062°C .

Graphite is exceptionally stable at high temperatures (up to 3800°C), but, unlike the other materials mentioned above, it has a high thermal-conductivity coefficient and cannot be used as an insulator.

Deliberate combustion-cycle impairment was used in the early stages of ZhRD development, when the cooling problem appeared insurmountable, but is now justified only in exceptional cases.

At the contemporary stage of ZhRD development, we must seek more radical means of protecting the liner from overheating.

Obviously, the sweat method of cooling an engine chamber may be quite effective. In this method, the inner liner of the chamber or nozzle is made of a porous material.* The coolant penetrates into the chamber through the pores in this liner, thereby cooling the liner and forming a vapor curtain around the surface of the flame tube.

* Ekspress-informatsiya, AN USSR, No. 2, RT-58, 1957.

which decreases the heat transfer from the gases. Although this method of cooling has passed preliminary tests, so far it has not been perfected.

The prospects of using porous materials for inner chamber liners depend on their properties and on the technology of their manufacture. The great shortcoming of porous materials lies in the fact that as the engine operates their pores rapidly become dirty and clogged, so that the liner may burn through in this place.

The efficiency of sweat cooling depends on the nature of the porous liner material and the physical properties of the coolant. The greater the density of the coolant, the lower the temperature of the surface of the porous flame tube will be. At a given density of liquid, cooling efficiency is a function of the temperature and velocity of the gases inside the engine chamber.

The consumption of liquid for cooling a porous engine nozzle amounted to about 2% of the flow rate, by weight, of the combustible to the combustion chamber in one of the experiments.*

In practice, the efficiency of the film and the sweat methods of cooling may become perfected to such a degree that extremely high temperatures will be safe for the inner liner.

Under the same conditions, film cooling and sweat cooling can provide about the same decrease in heat transfer from the gases to the liner. However, they are uneconomical and therefore may be recommended only in case of extreme necessity, when one cannot manage with purely

* Ekspress-informatsiya, AN USSR, No. 2, RT-58, 1957

regenerative cooling or it is expedient to relieve the operating conditions of the engine-chamber inner liner.

By knowing how to use all methods of protecting the chamber liner against overheating, one may plan and develop an engine which is reliable and economical in operation, with a small specific weight for the fuel-feed system and a small expenditure of energy in servicing it.

It is possible to cool the zone of the nozzle throat in the presence of great local heat flows ($q_{\max} > 14 \cdot 10^4$ kcal/m² hr) even without protective curtains of combustible, using, in this case, a special thin-walled engine-chamber construction, or making the inner liner of copper (for alcohol-oxygen engines), but in the majority of cases a copper chamber liner is very complex from the technological point of view and does not give any noticeable gain in comparison to a steel-chamber liner.

With a connected system of steel chamber liners, the thickness of the inner liner for an engine of any thrust can be 1 mm, although for great thrusts it is advisable to make the liner thicker than 1 mm.*

As we develop a ZhRD cooling system, decisions made regarding type of cooling system and coolant, additional cooling by film-cooling methods, etc., depend on general engine plan, thrust magnitude, type of propellant, combustion-chamber pressure, and engine designation, as well as combustion-chamber pressure, and engine designation, as well as combustion-chamber and nozzle design.

Each engine-cooling problem must be individually solved in each separate case, as we have not yet found an efficient method for solving them in totality.

* G. B. Sinyarev and M. V. Dobrovol'skiy. Zhidkostnye raketnye dvigateli [Liquid-propellant rocket engines], Oborongiz [State Publishing House of the Defense Industry], 1957.

If the engine operating time is not long (up to 5-15 seconds) or if the thermal regime is insignificant, one can get along without cooling the chamber, using a material with either a small or a large thermal-conductivity coefficient for the chamber liner. With a small thermal-conductivity coefficient, the liner material, of some thickness, will gradually warm up, melt, and be blown away by the gas stream; this is accepted, if the liner thickness does not decrease below a safe minimum, nor the liner overheat, losing its strength. The geometrical dimensions and parameters of the engine chamber are changed at the same time. A chamber liner of considerable thickness, made of heat-conducting material, is capable of heating up and accumulating heat in itself for some time without increasing the gas-side surface temperature above a permissible limit.

One can greatly increase engine operating time by using refractory materials with a comparatively small thermal conductivity. Many materials are known to have very high melting points, but this is not the only criterion for selecting a construction material.

Graphite gives relatively good results, especially when it has a sheathing to absorb mechanical stresses. Nozzles made of the carbides of tungsten and silicon operate satisfactorily up to temperatures somewhat lower than their melting points. Judging by melting temperatures, some refractory carbides and nitrides could resist the highest temperatures developed in ordinary ZhRD. One may considerably increase the operating time for uncooled ZhRD by the use of refractory materials. Thus, for some fuels, engine operating time may be increased to 60 sec.

Uncooled ZhRD chambers differ from cooled chambers in their structural simplicity and cheapness. The inner surface of uncooled combustion chambers is usually protected from the hot gas blasts by

appropriate materials, for the purpose of increasing engine operating time.

SECTION 2. HEAT-TRANSFER PROCESSES IN A ZhRD CHAMBER.

Heat transfer, in a liquid-propellant rocket engine, is a complex physical process, consisting of;

- 1) the processes of heat transfer by heat conduction, convection, and radiation from the hot moving gas to the inner chamber liner;
- 2) the process of heat transfer by heat conduction through the chamber liner;
- 3) the process of convective heat transfer from the liner to the liquid moving in the chamber coolant passage.

In an engine, these processes occur simultaneously under conditions of the work of friction; continuous feeding, heating, and vaporization of fuel; and chemical, thermal, and geometrical reactions on the parameters of the gas stream, with a turbulent motion of the gases in the chamber and of the liquid in the coolant passage.

We ordinarily refer to heat transfer from the gases to the chamber liner by means of conduction (thermal conductivity) and convection as convective heat transfer or contact heat transfer.

Heat is transferred by conduction of the heat across the boundary dividing the gas (or liquid) from the liner.

With a turbulent stream, convection is accomplished by means of random motion of the particles of gas or of liquid, which carry heat. A thin laminar layer of gas, where heat is transferred by means of molecular conduction of heat and turbulent mixing of the gas particles, is located only in close proximity to the surface of the liner. Gas particles, as they approach the chamber wall, transfer their

physical heat and kinetic energy and the heat liberated by their recombination to this layer of gas.

One may assume that the processes of dissociation and recombination of the gases occur very rapidly in the boundary layer, as the gases are mixed, heated, and cooled; therefore the composition of the gas may be considered as being in a state of equilibrium.

Since the gases have a low thermal conductivity and mix poorly, a considerable temperature difference occurs in the laminar layer of gas at great heat flows.

In contemporary engines, the fraction of convective heat transfer from the gas to the chamber liner amounts to 60-80%; the remaining part of the heat is transferred from the gas by radiation.

Thermal radiation is the process of transferring heat from one body to another by means of electromagnetic waves.

The greatest specific radiation heat flow occurs in a combustion chamber with the greatest gas temperature, and in some engines amounts to $(1.2-2)10^6$ kcal/m² hr.

As the gas temperature decreases along the length of the chamber, the relative fraction of radiation heat flow also decreases, and in the converging part of the nozzle its magnitude is insignificant.

The role of convection and radiation in an engine heat-transfer process depends on the type of fuel and its mixture ratio, the method of atomization, the nature of fuel combustion, and a number of other factors.

Thus, for example, a noncarbon-bearing fuel (hydrogen with oxygen or hydrogen peroxide) usually yields weakly luminous flame, which contains chiefly diathermic gases. Only the water vapor yields a noticeable radiation. In this case, convective heat transfer con-

siderably exceeds radiation heat transfer even in the combustion chamber.

A carbon-bearing fuel (for example, alcohol with oxygen and, chiefly, hydrocarbons with nitric acid) gives a strongly luminous flame, which contains, to some amount, hot particles of carbon which did not burn. Naturally, in this case, heat transfer by radiation may be of great significance in the combustion chamber; radiation from a luminous flame is considerably more complex than gas radiation.

Short-wave chemiluminescent radiation (excited as the direct result of propellant chemical reaction) is a function only of the thermal effect of the reaction; its intensity increases directly with density. If we consider partial fuel combustion in the engine nozzle, which leads to the appearance of a luminous flame, radiation also may be of considerable importance in the divergent part of the nozzle.

We call the process of transferring heat from the gases to the coolant through the engines-chamber liner the process of heat transfer.

In contemporary ZhrD, about 5-10% of the gas heat is transferred to the coolant.

The intensity of the process of heat transfer in an engine is given by the magnitude of specific heat flow q , by which is meant the amount of heat which is transferred during an hour or a second from the burning gas to one square meter of the liner surface, or from the latter to the coolant (q kcal/m² hr or q kcal/m² sec).

The establishment of the cycle in a combustion chamber has a very strong effect on heat transfer therein. The cycle is unequal throughout the length of the combustion chamber.

The total specific heat flow throughout the length of the engine combustion chamber and nozzle has a variable magnitude, and usually

attains its greatest value just before the critical section of the nozzle, as a result of which the liner in this section has a very high temperature.

In contemporary engines, the convective specific heat flow attains a value of $1 \cdot 10^6 - 28 \cdot 10^6$ kcal/m² hr in the nozzle throat.*

Since the heat-release rate of the chamber liner varies throughout its length, when designing ZhRD cooling systems we differentiate:

- 1) local (actual) specific heat flows, corresponding to fixed places (points) of the chamber liner, and
- 2) mean specific heat flows, which refer to a chamber liner of given length.

Determining local specific heat flows from the gas to the engine-chamber liner is attended with very great difficulties, which is explained by the complexity of the processes which occur in the gas boundary layer. Gas temperature, pressure, and velocity are continuously changing in this layer because of fuel combustion and consumption, heat transfer to the liner, recombination of gas-dissociation products, friction, and other phenomena. In practice, we find that complete quantitative evaluation of these phenomena is impossible.

For this reason, when designing an engine cooling system, we must use empirical formulas and experimental data which are still not sufficiently validated.

Since it is impossible to determine accurately the composition and parameters of the gas throughout the length of the combustion chamber, when designing ZhRD cooling systems, we must consider the specific heat flow from the gas to the liner as constant through-

* Jet Propulsion, v. 28, No. 1, 1958

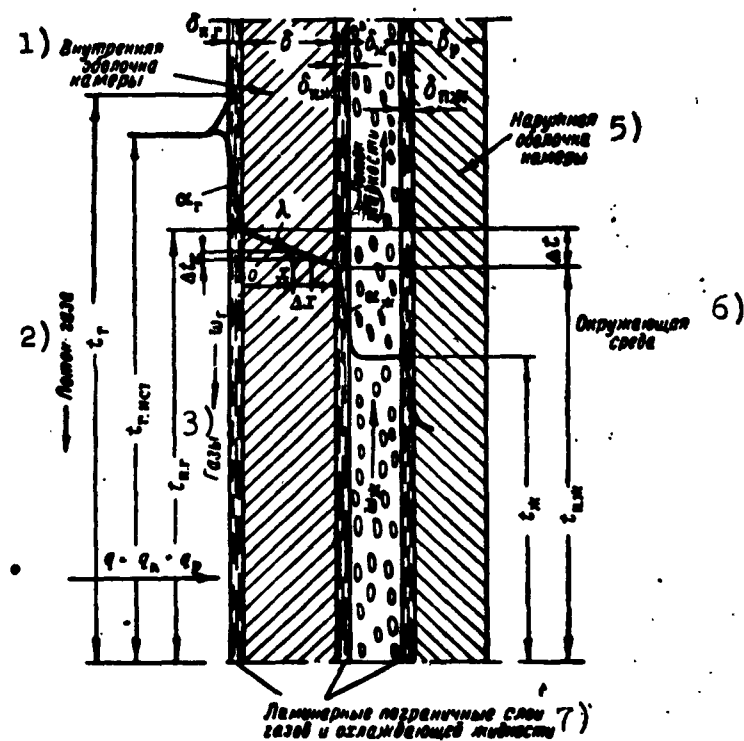


Fig. 9.2. Scheme of temperature distribution in the heat-transfer system of a ZhRD chamber with a solid inner liner.

- 1) Inner chamber liner; 2) gas stream;
- 3) gases; 4) liquid stream; 5) outer chamber case; 6) surrounding medium;
- 7) laminar boundary layers of the gases and the coolant.

out the length of the combustion chamber, and equal to the heat-flow value which was computed in accordance with the parameters of the gas at the end of a cylindrical combustion chamber, or across the largest cross section of a spherical or elliptical combustion chamber.

One may determine the parameters of the gas throughout the length of the nozzle, in approximation, by using the formulas given in Section 6, Chapter 3.

Methods for determining specific heat flows throughout the length of an engine-chamber nozzle are given below.

Since, as we mentioned above, the thickness of combustion-chamber and nozzle liners of contemporary engines is very small in comparison to liner diameter, in computing heat transfer in an engine we neglect

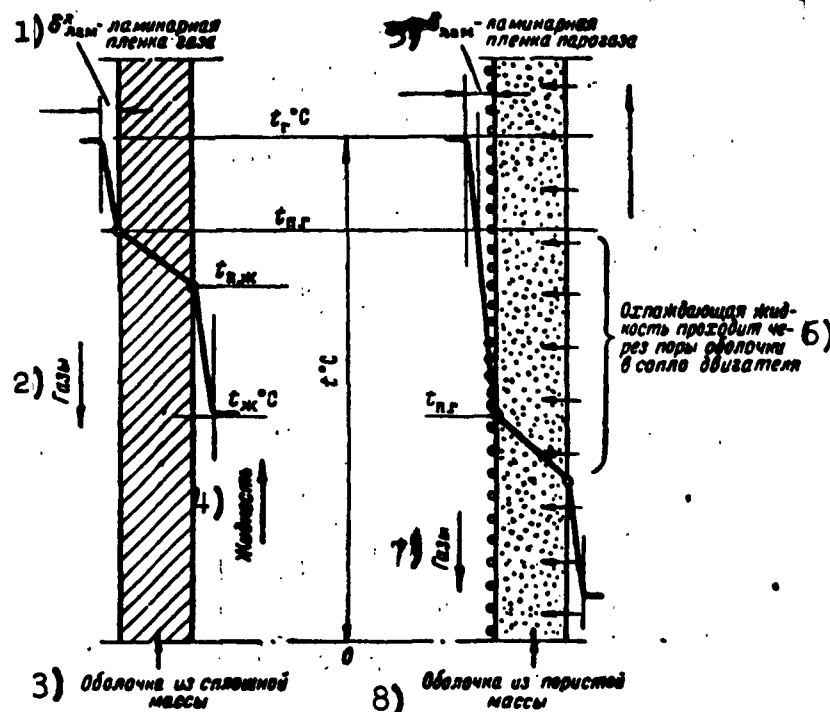


Fig. 9.3. Scheme of temperature distribution in the heat-transfer system of a ZhRD chamber with a porous inner liner.

1) δ_{lam} - laminar gas film *; 2) gases; 3) solid liner; 4) liquid; 5) δ_{lam} - laminar vapor-gas film; 6) coolant passes through liner pores into engine nozzle; 7) gases; 8) porous liner.

the effect of liner curvature on the process of heat transfer, and consider the liner as being flat.

The temperature in the separate parts of the system (according to the thickness of the heat layer) is also included among the number of the basic characteristics of heat transfer in ZhRD.

Figures 9.2 and 9.3 show the change in temperature in the heat-transfer system of a ZhRD, assuming flat solid and porous chamber liners.

The following designations are used in these figures:

t_g^{**} - temperature of the gas, determined by the appropriate computation;

* δ_{lam} - δ_{lam} - $\delta_{laminarnyy}$ - $\delta_{laminar}$
 ** $t_r - t_g - t_{gaz} - t_{gas}$

t'_g - actual temperature of the moving gas;
 $t_{p.g}^*$ - temperature of the gas-side surface of the chamber liner;
 $t_{p.zh}^{**}$ - coolant-side (liquid side) temperature of the surface of the chamber liner.

t_{zh}^{***} - coolant temperature (mean temperature throughout a section of the flow in a given portion of the liner length);

w_{zh} - velocity of coolant flow in m/sec (the mean velocity across a section of the coolant flow and in a given section of the liner length);

w_g - gas velocity in the engine combustion chamber or in the nozzle;

δ - thickness of the combustion-chamber or nozzle liner, in meters [sic];

δ_r^{****} - thickness of the outer case (jacket);

δ_{zh} - inter-jacket clearance for coolant flow;

$\delta_{p.g}$ - thickness of laminar gas film;

$\delta_{p.zh}$ - thickness of liquid film;

α_g - coefficient of heat transfer from the gas to the liner, numerically equal to q when $t_g - t_{p.g} = 1^\circ\text{C}$, and characterizing the intensity of heat transfer between the gas and the liner surrounding it (the amount of heat which is transferred from the gas to one square

* $t_{n.r} - t_{p.g} - t_{\text{poverkhnost' gazovaya}} - t_{\text{surface gas-side}}$

** $t_{n.x} - t_{p.zh} - t_{\text{poverkhnost' zhidkostnaya}} - t_{\text{surface coolant-side}}$

*** $t_x - t_{zh} - t_{\text{zhidkost'}}$ - t_{coolant}

**** $\delta_p - \delta_r - \delta_{\text{rubashka}} - \delta_{\text{jacket}}$

meter of the liner surface during an hour at a temperature difference between the gas and the liner surface of 1°C), in $\text{kcal}/\text{m}^2 \text{ hr}^{\circ}\text{C}$;

α_{zh} - coefficient of heat transfer from the liner surface to the coolant;

γ - liner thermal-conductivity coefficient (the amount of heat transferred within one hour across a liner area of 1 m^2 , with a liner thickness of 1 m [sic] and a temperature difference between the liner surfaces of 1°C) in $\text{kcal}/\text{m hr}^{\circ}\text{C}$; and

q - specific heat flow from the gas to the liner and from the liner to the coolant in a direction perpendicular to the surface, in $\text{kcal}/\text{m}^2 \text{ hr}$.

The curves in figures 9.2 and 9.3 show that resistance to the heat flow in the engine is the sum of the resistances of the layer of hot gas, the liner material, and the layer of coolant.

The change in temperature across the thickness of a flat liner. is characterized by some curve, slightly convex or concave, depending upon whether the liner-metal thermal-conductivity coefficient increases or decreases with a change in temperature.

For simplicity in computations, we assume that a change in temperature throughout the length of the flat engine-chamber liner occurs in accordance with the linear law.

At great heat flows, the temperature difference between the gas-side and the liquid-side surfaces of the chamber liner may become substantial, commensurable with the temperature difference in the boundary layers.

Some common temperature is established on the surfaces where the two adjacent layers (liner surface - gas or liquid) are in contact. A sharp decrease in temperature occurs in the laminar layers of gas and

liquid, close to the liner surface.

The basic temperature difference is found at the boundary layer of gas at the surface of the liner. The gas moves turbulently along the liner surface, shifting closer to it, to a laminar motion. If there were no heat transfer from the gas to the liner, the gas temperature around the liner surface would be raised almost to the deceleration temperature appropriate for a case when there was no heat transfer (to the value of the thermodynamic temperature in the combustion chamber obtained during the thermodynamic computations for the engine). In a real engine chamber, heat is transferred from the gas to the liner, because of which the thermodynamic gas temperature close to the liner does not rise to the value of the temperature of an adiabatically decelerated gas, but, passing some maximum value, is sharply decreased by several hundred degrees in the thin laminar gas layer, corresponding to its proximity to the surface, and adhering to the ordinary temperature profile, as described earlier, at the surface of the liner itself (See Fig. 9.2).

Because a simultaneous quantitative evaluation of the effect of various factors on heat transfer in a ZhRD chamber is not possible, in the design of a chamber-liner cooling system, we generally proceed from the hypothesis that convective and radiative specific heat flows are independent of each other, that the averaged temperature remains constant throughout the entire volume of the moving stream; moreover, we do not take into consideration the features of heat transfer associated with the hydrodynamics of the stream, which in fact plays an important role in the formation of the temperature field.

A temperature field in a heat-transfer system may be a function of

one, two, or three coordinates, and therefore is called a one-dimensional, two-dimensional or three-dimensional temperature field, respectively.

The equation of a one-dimensional temperature field has the simplest form:

$$t = f(x). \quad (9.1)$$

In general, temperature is a function of spatial coordinates x , y , z and of time τ , i.e.,

$$t = f(x, y, z, \tau). \quad (9.2)$$

In ZhRD designing, we must deal with a one-dimensional temperature field.

If the temperature in each point of the system does not change with regard to time, the temperature field, and the heat-transfer process corresponding thereto, is called steady-state or stationary, or in the opposite case, unsteady-state or nonstationary.

In cooled engines, operating in fixed regimes, the heat-transfer system has steady-state temperature fields, and in uncooled engines, unsteady-state temperature fields.

The geometrical locations of the points of a system having the same temperature form isothermal surfaces. A change in temperature, in a heat-transfer system, occurs only in directions intersecting isothermal surfaces (in direction x , Fig. 9.2).

The limit of the ratio of temperature change Δt to the distance Δx between isotherms along the normal is called the temperature gradient.

The temperature difference between isothermal surfaces in a system being studied is called the temperature difference and is designated as Δt (see Figures 9.2 and 9.3).

The rate at which temperature levels off in a uniformly heated body is characterized as the coefficient of thermal diffusivity:

$$a = \frac{\lambda}{C\gamma} \text{ m}^2/\text{hr},$$

where C is the mean heat capacity of the body at a constant pressure, in kcal/kg°C; and γ is the specific weight of this body in kg/m³.

The higher the thermal-diffusivity coefficient is for a given body (gas, liquid, or metal), the greater the rate of temperature distribution therein.

Assuming a steady-state heat-transfer process in a ZhRD, the specific heat flow from the gases to the chamber liner is equal to the specific heat flow across the liner to the coolant.

Because of this fact, specific heat flows in a ZhRD may be expressed by formulas.

1. From the gases to the chamber liner:

a) convective

$$q_k = \alpha_k (t_r - t_{n,r}) \text{ kcal/m}^2 \text{ hr}, \quad (9.3)$$

b) radiation

$$q_p = \alpha_p (t_r - t_{n,r}) \text{ kcal/m}^2 \text{ hr}; \quad (9.4)$$

c) total

$$\begin{aligned} q &= q_k + q_p = \alpha_k (t_r - t_{n,r}) + \alpha_p (t_r - t_{n,r}) = \\ &= (\alpha_k + \alpha_p) (t_r - t_{n,r}) = \alpha_r (t_r - t_{n,r}) \text{ kcal/m}^2 \text{ hr}. \end{aligned} \quad (9.5)$$

2. Across the chamber liner:

$$q = \frac{\lambda}{\delta} (t_{n,r} - t_{n,x}) \text{ kcal/m}^2 \text{ hr}. \quad (9.6)$$

3. From the chamber liner to the coolant:

$$q = \alpha_n (t_{n,x} - t_n) \text{ kcal/m}^2 \text{ hr}, \quad (9.7)$$

where α_r^* is the coefficient of radiation heat transfer from the gases to the chamber liner, in kcal/m² hr°C.

* $\alpha_p = \alpha_r = \alpha_{\text{radiatsionnyy}} = \alpha_{\text{radiation}}$

From these equations of specific heat flows, we obtain the following temperature differences in an engine heat-transfer system:

$$t_r - t_{n,r} = q \frac{1}{a_r}; \quad t_{n,r} - t_{n,x} = q \frac{\delta}{\lambda} \text{ and } t_{n,x} - t_x = q \frac{1}{a_x}.$$

Adding this system of equations, we obtain formulas for determining, in a ZhRD heat-transfer system:

1) Total temperature difference

$$t_r - t_x = q \left(\frac{1}{a_r} + \frac{\delta}{\lambda} + \frac{1}{a_x} \right) = \frac{q}{k}; \quad (9.8)$$

2) Heat flow from the gases across the liner to the coolant

$$q = \frac{1}{\frac{1}{a_r} + \frac{\delta}{\lambda} + \frac{1}{a_x}} = k(t_r - t_x) \text{ kcal/m}^2 \text{ hr} \quad (9.9)$$

where $k = \frac{1}{\frac{1}{a_r} + \frac{\delta}{\lambda} + \frac{1}{a_x}}$, which is the coefficient of heat-transfer from the gas through the chamber to the coolant, in kcal/m² hr°C.

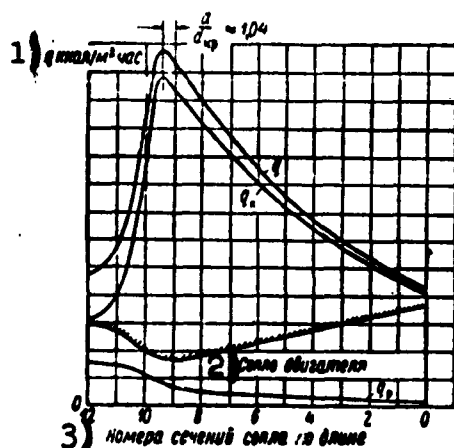


Fig. 9.4. Approximate distribution of specific heat flows throughout the length of an engine nozzle.

- 1) q , kcal/m² hr
- 2) engine nozzle
- 3) number of nozzle sections in accordance with length

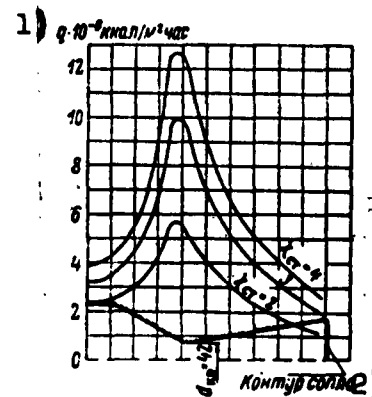


Fig. 9.5 Approximate distribution of specific heat flows throughout the length of a chamber nozzle for a nitric-acid engine, at $p_k = 40$ atmospheres absolute and various fuel-mixture ratios, that is, χ_{st} , at the chamber-liner wall.

- 1) $q \cdot 10^{-6}$ kcal/m² hr
- 2) nozzle contour

The quantity that is the reciprocal of the coefficient of heat transfer k , i.e.,

$$\frac{1}{k} = \frac{\delta_1}{\alpha_1} + \frac{\delta}{\lambda} + \frac{1}{\alpha_2}, \quad (9.10)$$

is called the thermal resistance of heat transfer.

Figure 9.4 shows the distribution pattern of specific heat flows throughout the length of an engine-chamber nozzle at a given fuel-mixture ratio χ , and Figure 9.5 shows the same for different values of χ .

SECTION 3. REQUIREMENTS IMPOSED ON A ZhRD REGENERATIVE COOLING SYSTEM.

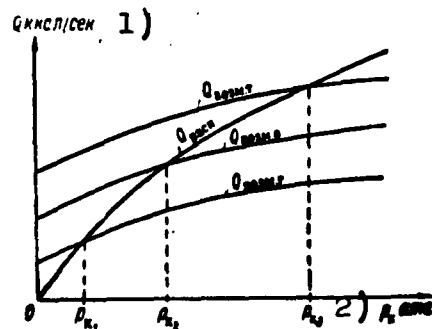


Fig. 9.6. Change in total available heat flow ($Q_{\text{расп}}$ kcal/sec) to be removed from a liner and total maximum possible heat removal by means of given quantity of the combustible ($Q_{\text{возм.г}}$ kcal/sec), the oxidizer ($Q_{\text{возм.о}}$ kcal/sec), or the propellant ($Q_{\text{возм.т}}$ kcal/sec), as a function of p_k : 1) Q , kcal/sec; 2) p_k , atm abs.

The stability and reliability required for prolonged operation of ZhRD may be provided only by reliable cooling for the engine-chamber inner liner.

An engine-cooling system may be reliable only if it is made with due regard to the following imposed requirements:

1. the temperature of the gas-side surface of the combustion-chamber and nozzle liners must not exceed a safe permissible limit, which is selected by assuming the required strength, and by making due allowance for possible erosion by the gas stream. Otherwise, the chamber-liner material will, on the burner side,

become softened and blown away by the gas stream, which may result in wrecking the engine.

Consequently, in designing a ZhRD, we must know the temperatures at which the various structural elements of the engine, all of which are subjected to erosion by the hot gases, begin to melt, become plastically deformed, and are strongly eroded. The values of these parameters, as well as the erosional activity, are functions of the physical properties of the metal, the gas velocity and composition, and of other factors.

In practice, a safe permissible temperature for the engine-chamber liner surface must not exceed:

- a) 550-560°C for carbon steels;
- b) 700-900°C for special heat-resistant alloy steels;
- c) 350-450°C for copper;
- d) 350-400°C for aluminum alloys of the AL4 type.

The working temperature of the gas-side liner surface, in contemporary engines, is usually within the limits of 400 to 900°C (on the average, about 650°). At these temperatures, many materials have a satisfactory strength. However, the requirement for increasing specific engine thrust by raising gas pressure in the combustion chamber and using fuels of increased heat capacity, which have high combustion temperatures, obliges us to search for inner chamber-liner materials that permit liners to be safely heated to higher temperatures.

2. In the usual plans for regenerative engine-cooling systems, it is necessary for the coolant to remove as much heat from the chamber liner as was transferred from the hot gases to the liner, and that the temperature of the coolant in the passage does not exceed its boiling point at the given pressure. Otherwise, a vapor film may form on

the liquid-side liner surface, which sharply decreases heat removal from the liner and leads to the latter being overheated and burned out.

This requirement is filled when the available heat flow (Fig. 9.6) from the gases to the chamber liner

$$Q_{\text{расп}} = \sum q_i S_i \text{ kcal/sec}^*$$

is less than the total maximum possible removal of heat by the given amount of coolant

$$Q_{\text{возм}} = G_{\text{ожл}} C (t_{\text{кип}} - t_{\text{вх}}) \text{ kcal/sec}^{**}$$

i. e.,

$$Q_{\text{расп}} < Q_{\text{возм}}$$

when q_i is the specific heat flow in the i -th section of the liner, whose surface is equal to $S_i \text{ m}^2$, in kcal/m² per second; C is the mean heat capacity of the coolant in the passage, in kcal/kg°C; $G_{\text{ожл}}$ is the coolant flow rate, to the engine-chamber passage, in kg/sec; $t_{\text{вх}}$ is coolant temperature at the inlet to the coolant passage; and $t_{\text{кип}}$ is the boiling temperature of this liquid at the pressure in the passage.

$$*[Q_{\text{расп}} = Q_{\text{расп}} = Q_{\text{располagayemyy}} = Q_{\text{available}}]$$

$$**[Q_{\text{возм}} = Q_{\text{возм}} = Q_{\text{возможnyy}} = Q_{\text{possible}};$$

$$G_{\text{ожл}} = G_{\text{ожл}} = G_{\text{okhlazhdayushchaya}} = G_{\text{coolant}};$$

$$t_{\text{кип}} = t_{\text{кип}} = t_{\text{kipeniye}} = t_{\text{boiling}};$$

$$t_{\text{вх}} = t_{\text{вх}} = t_{\text{vhkod}} = t_{\text{inlet}}.]$$

The maximum possible specific heat removal for any propellant component is a function of the boiling point and heat capacity of the component at a given local pressure in the coolant passage of a chamber of reactor.

Figure 9.6 shows that an engine may be cooled by means of combustible alone if combustion-chamber pressure does not exceed p_{k1} ; by means of oxidizer alone if p_k does not exceed p_{k2} ; or by means of both components (for example, kerosene and nitric acid) if p_k does not exceed p_{k3} . However, if combustion-chamber pressure is higher than p_{k3} , one must use some special method of protecting the chamber against overheating, in addition to regenerative cooling.

3. The temperature of the liquid-side chamber-liner surface, in the ordinary slotted coolant-passage design, must not exceed the coolant boiling point, to avoid forming local vapor locks, which are capable of causing the liner to overheat and burn out. However, if the coolant flows through a sufficiently narrow insulated channel and the engine service life is short, in some cases the liquid-side liner-surface temperature may exceed the coolant boiling point, at any given coolant pressure in the passage, by approximately 30-50°C.

One must bear in mind that increasing coolant velocity in the passage is accompanied by an increase in hydraulic resistance.

4. The engine-cooling system must not only be reliable, but also economical, as well as easily accomplished from the viewpoints of production and operation.

In planning and designing engine-chamber cooling systems, one must strive for the following:

1) developing reliable inner-liner cooling throughout the entire length of the combustion chamber and nozzle;

2) using low-alloy or even relatively cheap carbon steels for this liner;

3) establishing minimum inner chamber-liner thickness in accordance with the conditions required for reliable cooling and strength;

4) simplifying the technology of chamber manufacture.

The requirements for ZhRD cooling systems which have been enumerated must be borne in mind when determining specific heat flows from the gases to the chamber liner and from the latter to the coolant. If the computed parameters do not satisfy the requirements set down, we must use other methods to attain the required results when we design an engine-cooling system.

Our attempts to reduce engine dimensions may well result in further increase in combustion-chamber pressure, even in spite of the complexities involved in constructing and operating plumbing that works at high pressures.

If high pressure (for example, above 40 absolute atmospheres) is used in a combustion chamber, it may be advisable to use two- or three-stage engine-chamber regenerative cooling systems - low-, medium-, and high-pressure cooling stages (using two- or three-stage centrifugal fuel pumps).

The selection of such an engine-cooling system may be conditional upon a high liner heat-release rate in the nozzle-throat section, aside from high gas pressure in the combustion chamber and nozzle. Although this cooling method makes the system for feeding the coolant more complex, since high gas pressures (of the order of 40 absolute atmospheres or above) in the combustion chamber require the use of two- or three-stage centrifugal fuel pumps, the system of regenerative cooling, in general, does not become significantly more complex, and, under certain conditions, may be entirely advantageous.

A low-pressure cooling stage may be used for the divergent part of the engine nozzle. When $p_k = 40$ absolute atmospheres, gas pressure in this nozzle section may change within the limits of approximately 10 - 0.75 absolute atmospheres, and gas temperature, 2500-2000°C. With such gas parameters in the nozzle channel, it may be reliably cooled at a coolant pressure, in the nozzle passage, of about 15 absolute atmospheres. The relatively small pressure of the liquid in the coolant passage facilitates using thin-walled (of the order of 1.5-2 mm) inner and outer chamber liners, which, with a great nozzle length, considerably decreases engine-chamber weight.

If a one-stage cooling system were used, coolant pressure in the passage would be of the order of 45 atmospheres absolute, and the thickness of an inner nozzle liner, unconnected with a stress-bearing system, about twelve mm. This, of course, would lead to a considerable increase in nozzle weight.

A medium-pressure cooling stage may be used for the subcritical part of the nozzle. This nozzle section, when $p_k = 40$ absolute atmospheres, would be characterized by a great linear gas-pressure change (of the order of 36-10 absolute atmospheres) and by a large inner nozzle-liner heat-release rate. To decrease this heat-release rate, it is advisable to make the liner as thin as possible, as well as to relieve it from external static load as far as possible. Besides this, for better heat removal from the liner to the coolant it is necessary that liquid pressure throughout passage length be changed in accordance with gas-pressure change in the chamber channel.

Evidently, regenerative cooling is inadequate at high gas pressures. It may, therefore, be necessary to use some special method of protecting the liner against overheating in conjunction with regenerative cooling.

It is advisable to use a high-pressure cooling stage for the combustion chamber. In this area of the engine chamber, the gases have the greatest pressure; for an example under consideration, $p_k = 40$ atm abs and $t_k = 3000-3500^\circ\text{C}$.

A coolant flows from a high-pressure passage to a chamber head and then through the injectors to the combustion chamber. Thus, liquid pressure in the passage will be of the order of 45-50 absolute atmospheres.

The designing of each engine-cooling stage should be performed separately, since initial data, cooling conditions, and requirements for each of the stages are different. In this case, designing a cooling system consists chiefly of determining the level of coolant heating in the passage for each stage, and the minimum inner-liner thickness throughout the length of the engine chamber.

SECTION 4. FACTORS AFFECTING HEAT TRANSFER IN A ZHRD CHAMBER

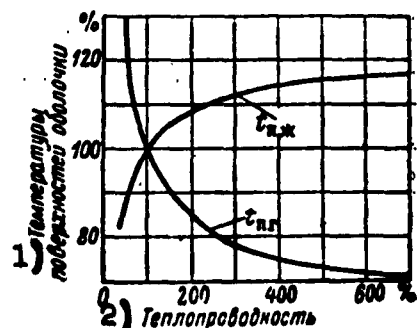


Fig. 9.7. Change in temperatures of liquid-side and gas-side liner surfaces as a function of thermal conductivity (computed data).

- 1) liner-surface temperatures
- 2) thermal conductivity

crease and the temperature of the gas-side liner surface rises.

For example, a pressure rise in a combustion chamber, other things

The magnitude of total specific heat flow from the gas to the chamber liner, and of gas-side liner-surface temperature, is most significantly affected by the following factors:

1. Gas pressure, temperature, and velocity throughout chamber length. As these parameters are increased, the fuel-combustion cycle intensifies considerably, as a result of which local specific heat flows from the gas to the liner in-

being equal, increases gas density and mass velocity, with some rise in temperature, and, consequently, raises total specific heat flow from the gas to the liner, as well as gas-side and liquid-side liner-surface temperatures.

Experiments show that specific heat flow from the gases to the chamber liner changes in accordance with the linear law, almost proportional to $p_k^{0.8}$. A rise in gas temperature in a combustion chamber by means of using a more efficient type of fuel leads to the same results as raising p_k .

The fact that $t_{p.g}$ is a function of engine operating conditions shows that the use of higher values of p_k and high-efficiency fuels is attended by the necessity of extremely intensive engine-chamber cooling.

As gas velocity in the chamber increases, the thickness and, consequently, the heat resistance, of the laminar gas layer at the liner surface decreases, which intensifies convection heat transfer from the gases to the chamber liner and leads to an increase in the values of q , $t_{p.g}$, and $t_{p.zh}$.

Convective heat transfer is also affected by the physical properties of the gases, combustion-chamber and nozzle dimensions and shape, and many other factors.

2. Chamber-liner material thickness and thermal conductivity.

At a given specific heat flow, the feasibility of local chamber-liner cooling is also determined by liner thickness and the material thermal conductivity, coolant physical properties, and permissible hydraulic loss in the coolant passage.

The thinner the liner and the greater the thermal conductivity of the liner material, the less the temperature difference across the

liner thickness and the greater the heat transferred from the liner, per unit time, to the coolant. Thus, $t_{p.zh}$ is somewhat increased and $t_{p.g}$, somewhat decreased (Fig. 9.7). This means that if the gas-side liner-surface temperature, at any place, exceeds a maximum permissible value, this boundary for reliable engine operation may be raised by using liner material with a higher coefficient of thermal conductivity.

Consequently, it is advisable to make the inner chamber liner as thin as possible, from a material with the greatest possible thermal-conductivity coefficient. However, one must bear in mind that metals having a large thermal-conductivity coefficient, as a rule, have limited strength. In practice, one may develop an engine chamber with a relatively thin liner by making the liner structurally interconnected with a stress-bearing system, or by making the liner of rectangular nickel (or even copper) tubing. After having bonded such shaped tubing together along its length, one may develop the required chamber contour with a smooth burner-liner surface.

The coolant flows inside these tubes.

In order to increase tubing rigidity and resistance to the pressure of the coolant inside, we cover the tubing segments with special jacketing rings made of welded steel or of plastic reinforced with fiber-glass.*

According to data from the foreign press**, when this tubing has a wall thickness of 0.75 - 1.25 mm, one may safely develop gas temperatures of up to 3400-4000°C in such a combustion chamber, with a con-

* Problems of Rocket Engineering, No. 6, IL, 1956

** loc. cit.

siderable increase in pressure and a relatively small specific weight. Another advantage for tube construction of the coolant passage and inner chamber liner lies in the fact that it may be used in engines of great thrust without a significant change in tube dimensions and thickness.

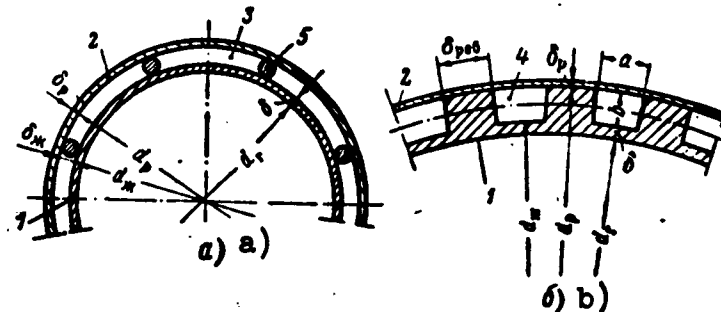


Fig. 9.8. ZhRD-chamber coolant passage shapes.

- 1) inner chamber liner; 2) outer chamber liner
- 3) clearance for coolant; 4) coolant channel
- 5) adjusting rod.

3. Structural shape and degree of finishing of engine-chamber and nozzle coolant-passage surface. These factors have a significant influence on the nature of the coolant movement in the passage and the magnitude of heat transfer from the chamber liner. For example, a spiral chamber-coolant passage has a greater heat-transfer surface from the liner to the coolant than a slotted passage (Fig. 9.8) which leads to some increase in q and $t_{p.zh}$, as well as a decrease in $t_{p.g}$.

With a smoother chamber-liner surface, a thinner liquid laminar layer is attained, which facilitates convective heat transfer between the liner and the liquid and leads to the same results as using a spiral passage for cooling the liner.

Thus, with a spiral passage and a smooth liquid-side liner sur-

() face, we can somewhat relieve engine-chamber cooling-system conditions. However, we must remember that using a special passage almost always entails an increased complexity in engine-chamber structure, as well as higher cost.

4. Coolant physical properties and velocity in the coolant passage. The physical properties of a coolant (thermal conductivity, heat capacity, specific weight, thermal diffusivity, and viscosity) have a considerable influence on heat transfer in a ZhRD chamber.

If a liquid has higher thermal conductivity, heat capacity, specific weight, and boiling point at a given pressure in the chamber coolant passage, and has a lower viscosity than other liquids, it will have better cooling properties than these other liquids.

As we have already mentioned above, water has the best cooling properties, and after it, in descending order, methyl alcohol, nitric acid, ethyl alcohol, and kerosene.

By raising coolant temperature, we decrease the viscosity and increase the quantity of heat transferred by conduction and convection from the liner, as a result of which $t_{p.g}$ is somewhat decreased. This indicates that a hotter liquid has better cooling properties.

As we increase coolant velocity in the passage, we decrease the thickness of the laminar liquid layer around the liner, and, as a result of this, heat removal increases and $t_{p.g}$ decreases, with some increase in the value of q .

(Thus, by decreasing the flow-through section of the coolant passage, and, by this means, increasing velocity, we may maintain a given value of $t_{p.g}$. However, one must bear in mind that, in practice, it is possible to increase w_{zh} only by increasing liquid pressure difference across the coolant passage, and, consequently, by in-

creasing the fuel-feed system weight and cost.

The higher the coolant pressure in the passage, the higher its boiling point, and the greater the maximum possible specific heat removal (maximum possible removal of heat per kilogram of liquid).

5. Engine-chamber liquid-side liner-surface temperature.

In the process of heat transfer from the chamber liner to the coolant, at a given coolant pressure in the passage, instances are possible when $t_{p.zh}$ is not greater than t_{kip} or $t_{p.zh}$ is greater than t_{kip} .

In the first case, ($t_{p.zh}$ is not greater than t_{kip}) it is impossible for the liquid in the passage to begin to boil. In the second case, ($t_{p.zh}$ is greater than t_{kip}) the coolant can begin to boil on the liner surface. If, in this case, the coolant temperature, in the basic core, is lower than the boiling point, the friable bubbles of vapor which have been formed on the liner surface will be washed away by a denser and hotter turbulent liquid flow and condensed therein.

Because of this nucleate boiling of the liquid on the liner surface, the heat-transfer coefficient α_{zh} increases considerably if the value of the coolant velocity in the passage remains unchanged (Fig. 9.9). Thus, $t_{p.g}$ will decrease slightly and q will increase considerably. However, after heating has reached a certain temperature limit, intensive liquid boiling on the liner surface may lead to a violent formation of a vapor film that will not be washed away by the liquid flow, and the film, due to poor thermal conductivity, causes heat removal from the liner to deteriorate considerably, which, as a result, may cause the liner to overheat and burn out.

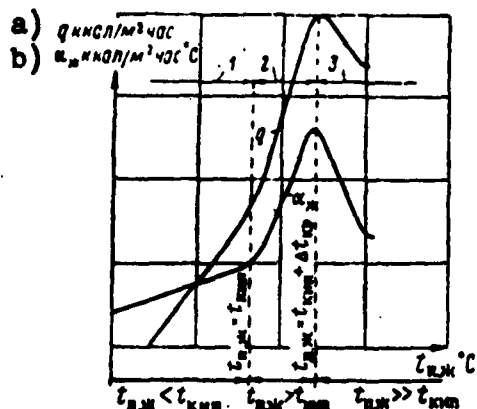


Fig. 9.9. Nature of change in specific heat flow and heat-transfer coefficient from liner to coolant as a function of difference in temperature between liner and coolant. 1) zone where liquid heats up to boiling point; 2) coolant nucleate-boiling zone; 3) coolant film-boiling zone a) q , kcal/m² hr; b) α_{zh} , kcal/m² hr⁰C.

it may well be feasible to use a nucleate-boiling ZhRD cooling regime under which heat removal from the liner is increased several times in comparison with a heat-transfer regime to the liquid when the latter is not boiling. By knowing how to use the phenomenon of nucleate coolant boiling, one may considerably decrease the capacity and weight of the engine fuel-feed system.

6. Engine-chamber injection-head design. The engine-chamber head design and the type and number of fuel injectors and their distribution system in the head control the quality of fuel-mixture formation and fuel-combustion cycle, the nature of the gas-flow movement in the chamber, and also the distribution of temperatures and velocities therein, which, to a considerable degree, affect heat transfer

The probability of vapor-film formation is also a function of the coolant velocity and the degree of chamber-liner surface finishing, as a rough surface makes the flow turbulent. At present it is impossible to ascertain accurately the conditions under which a vapor film occurs on the liner surface, since this effect on ZhRD operating conditions has been studied very little, when using different coolants. For this reason, at the present time, cooling engines by means of producing a nucleate boiling of the liquid in the passage is practically never used. In general,

between the gas and chamber liner and, consequently, affect t_{p.g.}

The chamber head chiefly determines the distribution for each propellant component across a combustion-chamber section, the degree of fineness to which components break down and mix, and also the possibility of developing convection backflows of gas, which transfer heat from the hot spray for heating and vaporizing the fuel mixture.

Uniform propellant-component distribution across a combustion-chamber cross section, with uniform distribution of a large number of fuel injectors on a flat head, leads to a better use of combustion-chamber volume and to increased completeness of fuel combustion.

An unfortunate chamber injection-head design may cause propellant components to burn on the liner surface and overheat it. A small number of injectors in the head, as well as nonuniform injector distribution in the head, causes a nonuniform propellant-component distribution across a combustion-chamber cross section, and, because of this, a poor use of chamber volume. This leads to incomplete fuel combustion and, in some cases, to an oscillating engine-operation regime, at which increased heat transfer between the gas and chamber liner is possible, and, as a rule, the liner will burn out.

Burnouts in various engine combustion-chamber and nozzle locations are almost always associated with the injector distribution system in the chamber head. Burnouts in the nozzle are usually formed in places lying opposite to places where the oxidizer injectors in the head lie closest to the wall. The results of special experiments also testify to the great influence that chamber-head design has on heat transfer in ZhRD. Comparison of the available data concerning the effect that the combustion-chamber cycle has on heat transfer allows us to con-

clude that the basic cause of burnout in an engine nozzle is the inconstancy in propellant-component ratios across a chamber section; gas of variable composition and different temperature flows along various generatrices of nozzles.

A fortunate chamber injector-head design facilitates not only increasing the completeness of fuel combustion and thus increasing engine specific thrust, but also decreasing heat transfer from the gases to the liner, in spite of the relative increase in the temperature of products of combustion.

To decrease oxidizer flow rate at engine-chamber walls, we may use:

- 1) injectors with a displaced nozzle axis (twisted in relationship to the chamber axis); a change in eccentricity permits changing distribution of liquid flow rate within rather wide limits;

- 2) injectors of the ordinary type with a one-sided face toward the nozzle outlet section, and also with a single-entry worm;

- 3) injectors with a nozzle cross section canted toward the axis; this method also allows us to have wide limits for regulating flow-rate distribution for the atomized liquid.

We may use bipropellant injectors for a peripheral row with a tentative distribution of oxidizer, which may be attained by one of the methods indicated above. The advantage of this lies in the fact that they may be arranged independently of the rule for injector distribution in the chamber head, and easily permit a shift from one scale to another.

By the way, one should mention that a shift to high-thrust engines operating on the same fuel need not be accompanied by a proportional increase in number of injectors.

Besides this, an increase in engine thrust by increasing combustion-chamber and head diameter need not cause a change in distance between injectors or a shift to larger injectors.

7. Engine thrust magnitude and operating regime. A change in per-second fuel-flow rate to the combustion chamber for regulating engine thrust has a marked effect on the characteristics of the cycle in the chamber, and on heat-transfer conditions between the gas and the liner.

Experiments and computations show that it is more difficult to cool an engine in a minimum thrust regime than in regimes of nominal and maximum thrust. This is explained by the fact that when fuel-flow rate to the combustion chamber is decreased in order to reduce engine thrust, coolant-flow rate is decreased and, consequently, coolant velocity in a passage of given flow section and coolant heat removal from the liner, since the flow of heat from the gas to the liner is, by this means, decreased to a considerably smaller value, which, at some limit, may lead to the engine-chamber liner overheating and burning out.

As engine thrust is increased, heat removal by the liquid from a unit of liner surface is increased. This indicates that it is easier to cool an engine chamber of great thrust than an engine of small thrust (Fig. 9.10). In particular, it is entirely impossible to cool an engine with a thrust of 50-100 kg with propellant components. An engine of such small thrust may be cooled only by water. This is explained by the fact that raising engine thrust P only by means of increasing the per-second fuel-flow rate G_g leads to an increase in chamber volume V directly proportional to G_g , i.e.,

$$\frac{V_{g,s}}{V_{g,n}} = \frac{G_{g,s}}{G_{g,n}}, \quad (9.11)$$

and, in this case, the combustion-chamber liner surface increases relatively slowly.

Consequently, a relatively greater amount of coolant arrives for every square meter of liner surface for a large combustion chamber than for a small chamber, because of which it is easier to cool.

Other things being equal, the heating surface of a spherical combustion chamber is smaller than that for a cylindrical one, and, therefore, is easier to cool with propellant components.

The brief survey we have given does not exhaust the analysis of the factors affecting ZhRD heat transfer. The basic factors we have studied indicate the extreme complexity of this process and the impossibility of analyzing these factors accurately when we are designing an engine-chamber cooling system.

On the basis of the facts given above, one may conclude that the basic means for achieving a high gas temperature t_k in a combustion chamber without increasing gas-side liner-surface temperature $t_{p.g}$ above a safely permissible limit, or for decreasing temperature $t_{p.g}$ at a given value of t_k , and thus relieving the chamber-cooling system, are as follows.

1. Decreasing flame-tube thickness δ to the minimum, commensurable

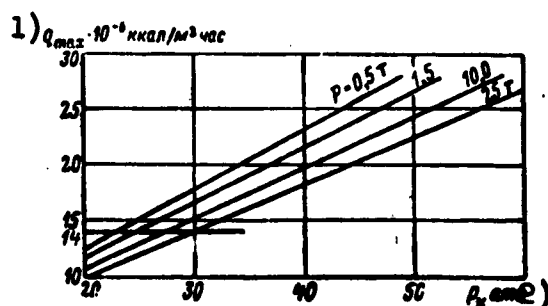


Fig. 9.10. Examples of maximum specific heat flow in a nozzle as a function of combustion-chamber pressure for kerosene-nitric-acid engines of different thrusts. 1) q_{max} , 10^{-6} kcal/m² hr; 2) p_k , absolute atmospheres.

with ultimate strength, by fabricating the liner in the form of an interconnected system of separate rectangular tubing.

By a fortunate design solution to this problem, one may also considerably decrease engine-chamber weight.

From the viewpoint of the necessary strength, it is feasible to make the chamber flame tube in the form of separate liners of various thickness.

2. Using material with a large thermal-conductivity coefficient λ for the flame tube, which, allowing for the factors mentioned in the previous point, will decrease thermal resistance $R_{ob} = \delta/\gamma^*$ and liner thermal conductivity H according to the following ratio:

$$\frac{H_1}{H_2} = \frac{\delta_2}{\delta_1} \frac{\lambda_1}{\lambda_2} \quad (9.12)$$

Here, subscripts 1 and 2 refer to the two different thicknesses for the liner, which is manufactured from materials of different thermal conductivity.

3. Decreasing wall-side laminar liquid layer thermal resistance $R_{zh} = 1/\alpha_{zh}$ by increasing the velocity w_{zh} in the passage, for which we decrease the equivalent diameter d_{ek}^{**} for the chamber passage (flow-through section area).

However, in practice, this measure is limited by the magnitude of liquid hydraulic-pressure loss in the passage, and thus is attended by an increase in the capacity and weight for the engine fuel-feed system.

4. Selecting a coolant with the best physical properties for this purpose, such as density ρ , viscosity η , heat capacity c and thermal-

* $R_{os} = R_{ob} + R_{obshchiy} + R_{total}$

** $d_{3K} = d_{ek} = d_{ekivalentnyy} = d_{equivalent}$

conductivity coefficient λ , which increases coolant thermal conductivity H_{zh} in accordance with the following ratio (for two different liquids):

$$\frac{H_{x1}}{H_{x2}} = \left(\frac{\lambda_1}{\lambda_2}\right)^{0.645} \left(\frac{d_{x1}}{d_{x2}}\right)^{0.2} \left(\frac{\gamma_2}{\gamma_1}\right)^{0.445} \left(\frac{c_1}{c_2}\right)^{0.335} \left(\frac{\rho_1 w_{x1}}{\rho_2 w_{x2}}\right)^{0.8}$$

This ratio may be changed within wide limits for various liquids.

However, the possibility of selecting the most efficient liquid for engine-chamber cooling may, in practice, often be limited, if one of the propellant components is of little use for cooling.

5. Decreasing the engine-chamber heating surface by means of using a spherical combustion chamber and a greater nozzle outlet-section divergent angle, as well as increasing chamber cooling surface by means of using a coolant passage of spiral shape in the places where the chamber has the highest heat release rate.

These measures are attended by well-known design complications and increased cost for the hardware.

6. Decelerating heat flow from the gases to the chamber liner by means of using protective gas or liquid curtains of combustible, by which we also increase the wall-side laminar gas layer thermal resistance $R_g = 1/\alpha_g$ and decrease layer thermal conductivity.

This measure is limited by the magnitude of engine specific thrust loss because of combustible expenditure in forming the protective curtain for the chamber liner.

For contemporary heat-resistant steels, which are used to manufacture a chamber flame tube with a purely regenerative cooling system, the permissible temperature $t_{p.g}$ (of the order of 900°C for alloy steels) is conditional upon a gas temperature in the combustion chamber of not higher than 3000°C .

Approximate computations show that for maintaining a constant value of $t_{p.g} = 900^\circ\text{C}$, at an increase in the value of t_k , the value

of R_{zh} is decreased to half of the initial value, corresponding to $t_k = 2500^\circ\text{C}$, which permits an increase in heat transfer from the liner to the liquid of almost 30%, and when R_{ob} is decreased by a factor of 2, heat transfer increases by 55%.

At such a great heat-transfer rate, the liquid may begin to boil in the chamber passage, which lowers, within wide limits, the practical use of such augmented heat transfer.

The quantitative values of heat-transfer parameters given here are approximate, since, in estimation of these parameters, we considered neither combustion-chamber pressure nor specific thrust, nor a number of other factors.

Because the analytical method has limited possibilities in computation, heat-transfer processes are usually studied experimentally. The scientific basis for these experiments, in studying heat transfer in an engine, is the theory of similarity of physical phenomena, showing proper methods for statement and generalization of the results in the form of criteria of similarity, i.e., dimensionless groups composed of quantities characterizing a physical phenomenon.

The law governing heat similarity determines the conditions under which geometrically and mechanically similar systems are also similar with regard to heat; by this, we mean that temperature fields and heat flows are similar.

The basic criteria for the theory of similarity of physical phenomena, during heat transfer in an engine, are the Reynolds number Re , Peclet number Pe , Prandtl number Pr , and Nusselt number Nu , whose physical essence is as follows.

1. A purely convective flow (which is the product $G = w\gamma$ kg/sec of the amount of gas or liquid passing, per unit time, across a unit

of area for a channel cross section, multiplied by heat capacity C_p kcal/kg°C and change in temperature Δt in this case):

$$q'_k = w\gamma C_p \Delta t \text{ kcal/m}^2 \text{ hr} \quad (9.13)$$

2. A conductive flow (by means of heat conduction, since a heat-conduction flow occurs only in the boundary layer of gas or liquid moving along the liner, in a direction normal to the surface): surface:)

$$q_r = -\lambda \frac{\partial t}{\partial x} = \lambda \frac{\Delta t}{d} \text{ kcal/m}^2 \text{ hour} \quad (9.14)$$

where w is the mean velocity in meters per second; γ is the specific weight in kg/m³; λ is the thermal conductivity of the gas or liquid in kcal/m hr°C; and d is the mean diameter of the section of the chamber liner or nozzle liner being studied, in m.

The ratio of q'_k to q_t is designated as the Peclet number, i.e.

$$Pe = \frac{q'_k}{q_r} = \frac{w\gamma C_p \Delta t}{\lambda \frac{\Delta t}{d}} = \frac{dw\gamma C_p}{\lambda} = \frac{wd}{a} = \text{idem}, \quad (9.15)$$

where $a = \lambda/C_p\gamma$ is the coefficient of thermal diffusivity, in m²/hr.

The Peclet number Pe is the measure of convective heat transfer; it characterizes the ratio of convective and conductive heat flows at a convective heat transfer.

The Reynolds number Re is the criterion of dynamic similarity of phenomena, since it characterizes the ratio of velocity and forces of viscosity for the gas or liquid:

$$Re = \frac{wd}{\nu} = \frac{wd}{\eta/\rho} = \text{idem}, \quad (9.16)$$

where η is the coefficient of dynamic viscosity in kg per second/m²;
 $\nu = \eta g / \gamma = \eta / \rho$ is the coefficient of kinematic viscosity for the gas or liquid, in m²/sec.; $g = \gamma / \rho$ is the acceleration of gravity in m/sec²;
 here ρ is the density of the gas or liquid in kg sec²/m⁴.

The ratio of Pe to Re is called the Prandtl number, i.e.,

$$Pr = \frac{Pe}{Re} = \frac{\frac{wd}{\rho}}{\frac{wd}{\rho}} = \frac{\nu}{\alpha} = \frac{\eta g C_p}{\lambda} = \frac{\eta C_p}{\lambda} = \text{idem.} \quad (9.17)$$

Thus, the Peclet number may be expressed by the formula

$$Pe = Re Pr.$$

The Prandtl number Pr is a characteristic of the physical properties for the gas or liquid. For gases of identical atomicity, this number is a constant magnitude, independent of pressure and temperature. For monatomic gases $Pr = 0.67$, for biatomic gases $Pr = 0.7$, for triatomic gases $Pr = 0.8$, and for tetratomic gases or greater $Pr = 1$.

The convective specific heat flow is generally expressed by the formula

$$q_k = q'_k + q_r = \alpha \Delta t \text{ kcal/m}^2 \text{ hour} \quad (9.18)$$

The relationship of q_k to q_t is called the Nusselt number, i.e.,

$$Nu = \frac{q_k}{q_r} = \frac{\alpha \Delta t}{\frac{\lambda}{d} \Delta t} = \frac{\alpha d}{\lambda} = \text{idem.} \quad (9.19)$$

whence the coefficient for convective heat transfer from the gas to the liner or from the liner to the coolant will be

$$\alpha = \frac{Nu \lambda}{d} \text{ kcal/m}^2 \text{ hour}^\circ\text{C} \quad (9.20)$$

The Nusselt number Nu is a measure of heat transfer, in that it characterizes the intensity of heat transfer on the border between the gas or liquid and a solid surface.

With thermal similarities between two or several systems, for any similar point, the curves of Pe and Nu criteria of similarity have the same value. In experimental studies of heat transfer, the unknown magnitude is usually the heat-transfer coefficient α . For a steady-state, forced turbulent motion of a gas or a liquid, the criterion equation assumes the form

$$Nu = f(Re, Pe) \text{ or } \frac{\alpha d}{\lambda} = f\left(\frac{wd}{\nu}, \frac{\nu}{\alpha}\right), \quad (9.21)$$

The form of this function is determined experimentally; complete study of the problem is facilitated by the fact that it is necessary to seek only the dependence of Nu on the two changing magnitudes of Re and Pe , as Nu is not a function of all the separate quantities included in the detailed expression of the latter equation.

SECTION 6. DETERMINING SPECIFIC CONVECTIVE HEAT FLOWS FROM THE GAS TO THE ENGINE-CHAMBER LINER

So far, a completely valid method for accurately determining specific convective heat flows from gases to Zhrd-chamber liners does not exist. This is explained by the complexity of the cycle which occurs in the combustion chamber and nozzle, and, because of this, the extraordinary difficulty of experimental heat-transfer studies under engine operating conditions.

Specific convective heat flows from the gases to the liner for a given section of engine-chamber length, or in separate engine-chamber sections, may be determined in accordance with the formula

$$q_c = \alpha_c (t_c - t_{\text{lin}}) \text{ kcal/m}^2 \text{ hr}^\circ\text{C}, \quad (9.22)$$

where t_g is the temperature of the adiabatically decelerated gas stream, in $^{\circ}\text{C}$; $t_{p.g}$ is the gas-side chamber-liner surface temperature, whose value, in computations, is assumed as a function of the strength properties for this liner material; α_k is the convective coefficient of heat transfer from the gases to the liner, which most authorities, in the existing literature, recommend be determined in accordance with the following formula, which is derived on the basis of experimental data processed in criteria of similarity:

$$\alpha_k \approx 74,3 C_{p_{n.r.}} (G \eta_{n.r.})^{0.18} \frac{Q^{0.82}}{d_r^{1.82}} \left(\frac{T_r}{T_{n.r.}} \right)^{0.38} \text{ kcal/m}^2 \text{ hr } ^{\circ}\text{C}, \quad (9.23)$$

where G is the gas-flow rate in the engine, equal to the fuel-flow rate to the combustion chamber, in kg/sec; d_g is the mean liner diameter along the gas-side surface of the given chamber-length section, in m; $T = 273 + t_g$ is the absolute temperature of the adiabatically decelerated gas stream; this temperature value is usually assumed as being the same for the entire length of the engine chamber, and as being equal to the thermodynamic temperature ($T_k^{\circ}\text{K}$ or $t_k^{\circ}\text{C}$) of the gases in the combustion chamber, since gas velocity is very small, in close proximity to the solid wall (in the boundary layer), and the gas-stream deceleration temperature at the liner surface almost coincides with the thermodynamic temperature*; $T_{p.g} = 273 + t_{p.g}$ is the mean absolute liner-surface temperature for a given chamber-length section, in $^{\circ}\text{C}$,

* Actually, the laminar boundary layer of a rapidly moving gas stream is not completely retarded and, therefore, has a temperature $T'_g >$

$> T_g$, which, for an insulated system, may be expressed by the formula

$$T'_g = T_{\text{термод}} + r \frac{A w_c^2}{2g C_p} \quad ** \quad (9.24)$$

where r is the recovery factor, whose value is less than unity.

** $T_{\text{термод}} = T_{\text{термод}} = T_{\text{термодинамическая}} = T_{\text{thermodynamic}}$

whose value, in first-approximation computation, is assumed as not exceeding the safely permissible limit for the assumed liner material, considering this temperature as constant throughout the length of a cylindrical combustion chamber; $C_{p.p.g}$ is the mean gas heat capacity, in kcal/kg °C, computed at the gas-side liner-surface temperature by means of the formula

$$C_{p.p.g} = \sum g_i C_{p,i.p.g} \quad (9.25)$$

$g = 9.81 \text{ m/sec}^2$ is the acceleration of gravity; $\eta_{p.g}$ is the mean dynamic viscosity coefficient of the gases, in kg-sec/m², computed in accordance with the formulas

$$\frac{1}{\eta_{p.g}} = \sum \frac{g_i}{\eta_{i.p.g}} \text{ and } \frac{1}{g \eta_{p.g}} = \sum \frac{g_i}{g \eta_{i.p.g}}; \quad (9.26)$$

$C_{p,i.p.g}$ and $\eta_{i.p.g}$ are the mean values for the heat capacity and dynamic viscosity, respectively, of the i-th gas in the mixture, taken from Tables 9.1 and 9.2 as functions of the gas-side chamber-liner surface temperature; g_i is the weight fraction of the i-th component in the gas mixture, computed in accordance with the formula

$$g_i = \frac{\mu_i p_i}{\sum \mu_i p_i}; \quad (9.27)$$

p_i is the partial pressure of the i-th gas in the mixture, in atm abs; and μ_i is the molecular weight of the i-th gas.

Here, gas heat capacity and viscosity are referred to gas-side liner-surface temperature, since this temperature is usually given, while it is not always possible to determine accurately gas temperatures in given sections of the chamber.

In computing $C_{p,i.p.g}$ and $\eta_{i.p.g}$, we neglect the heat capacity and viscosity of those gases which are present in small amounts in the mixture. These components are usually O, OH, H, NO, and N. When we compute

TABLE 9.1

Mean Heat Capacity C_{p_g} for Gases at a Constant Pressure, inkcal/kg $^{\circ}$ C, as a Function of Temperature

1) Наименование газа	2) Хими- ческая формула	3) Температура газа в °C												
		0	100	200	300	400	500	600	700	800	900	1000	1100	1200
4) Кислород	O ₂	0,218	0,223	0,230	0,2376	0,2445	0,2504	0,2553	0,2593	0,2627	0,2656	0,2682	0,2703	0,2723
5) Азот	N ₂	0,248	0,2489	0,2512	0,2554	0,2607	0,2664	0,2721	0,2774	0,2822	0,2864	0,2902	0,2935	0,2964
6) Водород	H ₂	3,390	3,4509	3,4643	3,4712	3,4826	3,5020	3,5298	3,5660	3,6101	3,6572	3,7063	3,7584	3,8095
7) Окись углерода	CO	0,248	0,2495	0,2528	0,2580	0,2641	0,2704	0,2763	0,2816	0,2863	0,2904	0,2939	0,2970	0,2996
8) Окись азота	NO	0,238	0,2381	0,2414	0,2472	0,2534	0,2594	0,2648	0,2695	0,2736	0,2770	0,2799	0,2824	0,2845
9) Двуокись углерода	CO ₂	0,194	0,2182	0,2371	0,2524	0,2652	0,2758	0,2847	0,2921	0,2984	0,3037	0,3081	0,3119	0,3152
10) Водяной пар	H ₂ O	0,444	0,4515	0,4635	0,4778	0,4931	0,5092	0,5258	0,5429	0,5601	0,5769	0,5929	0,6080	0,6220

1) Name of gas; 2) chemical formula 3) gas temperature, in $^{\circ}$ C; 4) oxygen; 5) nitrogen; 6) hydrogen; 7) carbon dioxide; 8) nitric oxide; 9) carbon monoxide; 10) water vapor.

g_1 , the values of p_1 are assumed in accordance with the data from the thermodynamic computation of the engine.

All quantities included in Eq. (9.23) must be expressed in the same measurement-unit system.

This equation shows that convective heat transfer between a gas and a chamber liner is affected by per-second gas-flow rate, physical heat-transfer parameters, geometrical gas-passage dimensions and other factors.

In the subcritical part of the nozzle, mass transfer of gases increases considerably and the wall-side laminar gas layer becomes thinner,

TABLE 9.2

Dynamic Viscosity $g \cdot 10^5$ kg/m sec of Gases as a Function of Temperature

1) Наименование газа	2) Химиче- ская формула	3) Температура газа в °C												
		0	100	200	300	400	500	600	700	800	900	1000	1100	1200
4) Кислород	O ₂	1,943	2,460	2,910	3,312	3,677	4,014	4,327	4,622	4,900	5,164	5,416	5,657	5,889
5) Азот	N ₂	1,667	2,101	2,478	2,815	3,121	3,402	3,664	3,911	4,143	4,364	4,575	4,777	4,970
6) Водород	H ₂	0,850	1,062	1,226	1,381	1,521	1,651	1,771	1,884	1,991	2,093	2,190	2,283	2,373
7) Окись углерода	CO	1,656	2,087	2,462	2,797	3,100	3,380	3,640	3,885	4,116	4,336	4,545	4,746	4,939
8) Окись азота	NO	1,352	1,825	2,257	2,653	3,020	3,362	3,683	3,986	4,272	4,546	4,807	5,057	5,298
9) Двуокись углерода	CO ₂	1,384	1,816	2,262	2,642	2,991	3,316	3,620	3,906	4,177	4,435	4,681	4,917	5,143
10) Водяной пар	H ₂ O	0,818	1,208	1,605	2,000	2,390	2,772	3,145	3,510	3,864	4,210	4,447	4,674	4,894

1) Name of gas; 2) chemical formula; 3) gas temperature, in °C;
4) oxygen; 5) nitrogen; 6) hydrogen; 7) carbon monoxide; 8) nitric oxide; 9) carbon dioxide; 10) water vapor.

as a result of which convective heat transfer from the gas to the liner is increased here.

As engine-chamber dimensions are increased, without a change in gas parameters, the coefficient α_k decreases, since its magnitude is a function of the diameter d_g of the gas channel (see formula 9.23). This circumstance indicates that an engine of large thrust (large dimensions) is easier to cool than an engine of small thrust (small dimensions).

The equation given for determining the value of α_k experimentally has been verified for subsonic velocity in a gas stream in a cylindrical tube.* However, for rocket engines, we must consider other factors.

* A. A. Gukhman and N. V. Il'yukhin. Osnovy ucheniya o teploobmene pri techenii gaza s bol'shoy skorost'yu [The Bases for Studying Heat Transfer in High-Speed Gas Streams], Mashgiz [State Scientific and Technical Publishing House of Literature on Machinery], 1951.

Actually, chamber nozzles have conical (or nearly conical) shapes, because of which a supersonic gas-exhaust velocity is obtained. Besides, this equation does not consider effects on heat transfer due to the features of the cycle in the combustion chamber (design of the head, type and number of injectors, injector-distribution system on the head, etc.) or to phenomena occurring in the wall-side gas layer. Close to the chamber liner (in the wall-side layer), gas temperature rises due to gas deceleration; gas molecules recombine intensively and transform chemical energy into heat, partially transferring heat to the liner; and gases diffuse from the zone of higher temperature to the zone of lower temperature. All these factors strongly affect heat transfer in a ZhRD.

Because of the facts given above, the formula (9.23) mentioned above is suitable only for extremely approximate determination of the value of α_k , upon condition that the nozzle, throughout its length, is divided into a number of sections, the diameters of which are equal to the mean diameter for the conical part of the section.

In this case, it is convenient to perform the computations in the following order:

1. We select safely permissible values of temperature $t_{p.g}$ in the characteristic engine-chamber sections. In contemporary engines, the gas-side surface temperature for a steel liner, in the majority of cases, has the following values:

- a) at the outlet from the combustion chamber to the nozzle - about 450-600°C;
- b) in the nozzle throat - about 700-850°C;
- c) at the outlet from the nozzle, about 350-500°C.

For a copper liner, temperature values are 300-350, 450-550, and 150-200°C, respectively.

Gas-side surface temperature for the cylindrical part of a com-

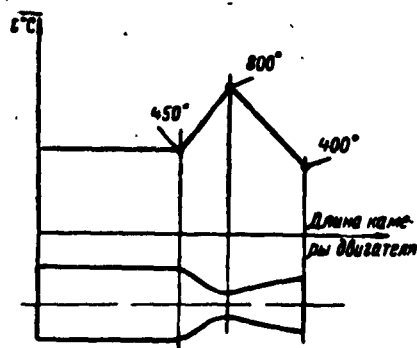


Fig. 9.11. Approximate gas-side surface-temperature distribution for a steel liner throughout the chamber length, for designing a cooling system.
1) Engine-chamber length.

bustion chamber is considered as constant, and as equal to the temperature at the entrance to the convergent part of the nozzle. Temperature distribution ($t_{p.g.}$) between characteristic sections may be assumed as linear (Fig. 9.11), in the first approximation, throughout the length of the chamber.

2. We compute heat capacity and viscosity for the products of fuel combustion at the gas-side liner-surface temperature at the inlet to the nozzle section, considering heat capacity and viscosity as constant throughout the entire length of the engine chamber.

The values of $C_{p.p.g.}$ and $\eta_{p.g.}$ are functions of combustion-product temperature for the gas-side liner surface, but, since the computation is approximate, we may assume that their values are constant throughout the length of the chamber.

When using tabular materials, we must pay attention to the dimensionality of the quantities, and, if necessary, translate them into the dimensions which were assumed for using the particular formula.

3. We divide the length of the engine-chamber nozzle into about 10-15 sections (depending on the desired accuracy of computation) and, for each of these sections, we compute the value of α_k , as if for an equivalent tube, assuming tube diameter and the given temperature as the mean for each chamber section.

4. Knowing the value of α_k , we determine the value of q_k for each nozzle section. In accordance with the results of the computations, we construct a curve of the change in q_k throughout the length of the

engine chamber (see Fig. 9.4).

Since an engine head usually develops a nonuniform fuel-component distribution throughout a combustion-chamber cross section, specific heat flows in a ZhRD may be determined more accurately by taking into consideration the presence of a layer of gases, enriched by combustible, at the chamber-liner surface, and the fact that the gas-layer temperature is lower than that of the stream core.

In such computations, it is recommended that one determine specific heat flows for various engine-nozzle generatrices, in conformity with these formulas, as though the fuel-mixture ratio χ were constant throughout the section; in this case, the magnitude of the fuel-mixture ratio is assumed as being equal to χ_{st} . In this case, we assume the composition of the wall-side layer developed by the chamber head is preserved to a considerable degree throughout the entire extent of the chamber, up to the outlet from the nozzle.

Specific convective heat flows from the gases to the liner, allowing for the presence of a gas layer, enriched by combustible, at the chamber wall, may be determined in accordance with a special method.

In approximation, one may consider that, in the cylindrical part of the combustion chamber, the value of q_k is constant, and equal to its value at the entrance to the convergent part of the nozzle.

The gas parameters in the stream core are determined in conformance with the fuel-mixture ratios in the stream core (χ_{ya}) and in the wall-side layer (χ_{st}).

The fuel-mixture ratios in the wall-side layer are determined by the fuel-injector distribution scheme in the head, which varies for different chamber shapes.

A decrease in the magnitude of χ at the chamber wall leads to a decrease in heat flows, and alleviates engine-cooling conditions. How-

ever, such a decrease in the value of χ , as already mentioned above, decreases specific thrust. In solving the problem of establishing ZhRD cooling, it is important to know the connection between a decrease in heat flows and the corresponding decrease in specific thrust.

SECTION 7. DETERMINING SPECIFIC RADIATION HEAT FLOWS FROM A GAS TO AN ENGINE-CHAMBER LINER

A transfer of thermal energy from one body to another by means of radiation is accomplished in the form of electromagnetic waves with a length of 0.8 to 40 μ .

Solid bodies radiate and absorb radiant energy of all wavelengths, but gases do so only within fixed intervals of wavelengths, which vary for different gases. Such radiation and absorption by gases is called selective.

Biatomic gases have very low radiation and absorption capacities and are therefore almost transparent for thermal radiation. These gases have very narrow spectral bands for radiation and absorption. Most of the radiation of products of combustion in a ZhRD is radiation associated with vibratory and rotational motion of gas molecules.

The greatest selectivities in radiation and absorption are those exhibited by H_2O , CO_2 , SO_2 , CO , and OH gases (these gases are enumerated in descending order for their degree of radiation intensity).

The natural radiation of a body, added to the radiation reflected to the body from other bodies, is called the effective radiation of the body.

Contemporary ZhRD operate on hydrocarbon combustibles and on oxidizers containing oxygen as a basic element.

In these engines, radiation consists of three types:

- 1) radiation from high-temperature gases;
- 2) radiation from solid atomized particles of carbon, which are in suspension in the gases;

TABLE 9.3

1) Форма камеры и ее размеры	2) Значение l м
3) Шарообразная с диаметром d	0,60d
4) Цилиндрическая с диаметром d и длиной $l_x = d$	0,75d
5) $l_x = 1,5d$	0,85d
6) $l_x = (2+3)d$	0,90d
7) Эллиптическая с небольшим диаметром и длиной $l_x = (3+4)d$	0,70d

1) Chamber shape and dimensions; 2) value of l , m; 3) spherical, with a diameter d ; 4) cylindrical, with a diameter d and length $l_x = d$; 5) $l_x = 1.5d$; 6) $l_x = (2-3) d$; 7) elliptical, with a small diameter and a length $l_x = (3-4) d$.

3) radiation from the thermal effect of the chemical reaction of fuel combustion (chemiluminescent radiation).

In a typical ZhRD, radiant heat transfer is caused primarily by radiation from water vapor, and, partially, from carbon dioxide. SO_2 gas is often entirely lacking in the products of fuel combustion, or, sometimes, is a very small percentage of the entire amount of the gases. The remaining gases included in the composition of the products of combustion are assumed to be transparent to radiation. Radiation from particles of soot and chemiluminescence has an extremely weak effect on radiant heat transfer in a ZhRD and, therefore, is usually not considered in computations. The majority of solid bodies and liquids are not transparent to thermal radiation. Radiation and absorption, in solid opaque bodies, occur only in the surface layer, but in gases they occur throughout the entire volume. Throughout the length of a ZhRD combustion chamber, radiant heat flows increase, but throughout the length of the nozzle, they decrease.

Radiant heat transfer, in any section of a ZhRD chamber, is essentially a function of:

1) composition, temperature, and pressure of the gases, which determine thermal-radiation efficiency;

(2) geometrical shape and dimensions for the given section of the engine chamber, which determine selection of the characteristic dimension for computing radiation and absorption capacities of the gas for the volume under consideration;

3) propellant-component ratio across an engine combustion-chamber cross section, which determines the nature of the chamber cycle, and fields of temperature and velocity of the gases;

4) position of the engine-chamber section under consideration, since factors affecting radiant heat transfer change throughout the chamber length.

Initial data for determining specific radiant heat flows in an engine chamber are:

1) the combustion-chamber and nozzle shape and dimension;

2) the pressure, the temperature, and the partial pressures for the gases in the combustion chamber;

3) the type of chamber-liner material and the effective degree of gas-side liner-surface blackness;

4) the supplementary curves for several rated parameters.

Since, in gases of different volumetric shape, the length of rays varies according to direction, when we wish to determine the specific radiant heat flow, we must replace the given volumetric shape for the radiating gases with a hemispherical shape of equivalent volume, in which the length of the rays to the center of a flat base will be the same in all directions. The radius of such a gas hemisphere will also be a certain mean effective ray length l, which is characteristic of the radiation and absorption capacities of the gases for the given volumetric shape.

TABLE 9.4

Degree of Chamber-Liner Gas-Side Surface Blackness, With Liner in Oxidized State, Within Temperature Limits of 200-600°C

1) Материал оболочки камеры	$\epsilon_{ст}$
2) Сталь	0,75-0,85
3) Медь	0,57-0,87
4) Латунь	0,59-0,61
5) Алюминиевый сплав	0,11-0,19
6) Керамика огнеупорная	0,80-0,90

1) chamber-liner material; 2) steel; 3) copper; 4) brass; 5) aluminum alloy; 6) refractory ceramics.

For approximate determination of the effective ray length for gases of different volumetric shape, M. A. Mikheyev* recommends the formula

$$l = 3,6 \frac{V}{S} \text{ м}, \quad (9.28)$$

where V is the volume of the gases for the given shape, in m^3 ; and S is the liner surface for this volume of gases, in m^2 .

Table 9.3 shows the values of \underline{l} for gases in channels of different shapes (with radiation to the lateral face).

The radiating power of a corresponding gas is a function of the temperature and the effective thickness of the gas layer (the optical density) is, in effect, the product $p_1 \underline{l}$ atm abs \cdot m or $\rho_1 \underline{l}$, where p_1 is the partial pressure of the i -th gas in the mixture, $\rho_1 = \gamma_1/g$ is the density of the gas in $\text{kg-sec}^2/\text{m}^4$, and \underline{l} is the effective ray length in m, determined by the shape and the dimensions for the gas volume under consideration.

* A. M. Mikheyev [sic; probably M. A. Mikheyev]. Osnovy teploperadachi [The Bases of Heat Transfer], Gosenergoizdat [State Power Engineering Publishing House], 1956.

The total radiation for the gas mixture is not equal to the sum of the radiations of its separate components taken separately. Thus, the degree of blackness for a mixture of carbon dioxide and water vapor is less than the sum of the individual degrees of blackness for the gases. This phenomenon is due to the partial mutual absorption of radiation by both gases in the wave-length region in which their spectral lines overlap each other.

Experimental determination of radiant heat flows in ZhRD chambers is extremely difficult due to the complexity of the cycle in the combustion chamber and nozzle.

To determine the radiation from water vapor and carbon dioxide under ZhRD operating conditions, at the present time we use extrapolation data for the greater temperatures and pressures obtained in standard industrial furnaces at a pressure of 1 atm abs and at temperatures of up to 2000°C.* Thus, we usually consider that the fraction of specific radiant heat flow from the gases to a ZhRD-chamber liner is not large (especially in the chamber nozzle), and, therefore, in practice, such an extrapolation has sufficient accuracy, although, in fact, cases are possible when this type of heat transfer may play an important part in the total heat transfer in an engine chamber.

Because of the fact that gas-side surface temperature for a steel or copper liner, in contemporary ZhRD chambers, is usually not high, we may neglect radiation from the liner to the layer of gases. On this basis, the total specific radiant heat flow from the gases to the combustion chamber liner, when there is no protective curtain, may be

* A. M. Mikheyev [sic], op. cit.

computed, in approximation, according to the formula*

$$q_{p.r} = \epsilon_{st.ef} C_0 \left(\frac{T_k}{100} \right)^4 \text{ kcal/m}^2 \text{ hr}, \quad (9.29)$$

where $\epsilon_{st.ef} = (1 + \epsilon_{st})/2$ is the effective degree of blackness for the gas-side surface of the combustion-chamber liner (with radiating gases) and there is an inequality $1 > \epsilon_{st.ef} > \epsilon_{st}$; here $\epsilon_{st} \approx 0.75-0.85$ is the degree of blackness for the gas-side surface of a steel chamber liner, depending on the condition of this surface, i.e., the degree to which the surface is oxidized (see Table 9.4); and $\epsilon_g = \epsilon_{H_2O} + \epsilon_{CO_2} - \epsilon_{H_2O} \epsilon_{CO_2}$ is the degree of blackness for the triatomic gases, depending on the parameters of these gases and on the effective ray length \underline{l} ; $C_0 = 4.96$ is the radiation coefficient for a conditionally ideal black body, in $\text{kcal/m}^2 \text{ hr}^\circ\text{K}$; and T_k is the thermodynamic temperature for the gases in the engine combustion chamber, in $^\circ\text{K}$.

A. M. Gurvich**** recommends that the total radiation capability of H_2O and CO_2 be determined by an exponential function of the following form

$$\epsilon_g = 1 - e^{-k_r p l}, \quad (9.30)$$

* N. V. Inozemtsev and V. K. Koshkin. Protsessy sgoraniya v dvigatelyakh [Combustion Cycles in Engines], Mashgiz [State Scientific and Technical Publishing House of Literature on Machinery], 1949.

** $\epsilon_{st.ef} = \epsilon_{st.ef} = \epsilon_{stepen' \text{ effektivnaya}} = \epsilon_{\text{effective degree}}$

*** $\epsilon_{st} = \text{degree}$

**** A. M. Gurvich. Teploobmen v topkakh parovykh kotlov [Heat Transfer in Steam-Boiler Furnaces], Gosenergoizdat [State Power Engineering Publishing House], 1950.

where $p_g = p_{H_2O} + p_{CO_2}$ is the sum of partial pressures for water vapor and carbon-dioxide gas in the combustion chamber, in atm abs; k_g is the effective coefficient of weakening of the rays of these gases as a consequence of the fact that the wavelengths for their radiation spectra somewhat overlap each other, which is determined in accordance with the formula

$$k_g = \frac{0.8 + 1.6p_{H_2O}}{\sqrt{p_g}} (1 - 0.00038T_g); \quad (9.31)$$

and l is the effective ray length, in m.

In ZhRD chambers which operate at high gas temperatures or on fuels of high calorific value, as well as those chambers which have a heat-resistant liner (for example, if the liner is coated with ceramics), the gas-side liner-surface temperature may be high, and, therefore, the specific radiant heat flow from the gases, in this case, may play an important part in the total heat transfer of the engine.

Specific radiant heat flow from the gases to the chamber liner, when the liner is radiating and there is no protective curtain, may be determined, in approximation, in accordance with the formula

$$q_{p,g} = \epsilon_{cr} \epsilon_g C_0 \left(\frac{T_g}{100} \right)^4 - \epsilon_{cr} C_0 \left(\frac{T_{p,g}}{100} \right)^4 [1 - \epsilon_{cr}(1 - \epsilon_g)] \text{ kcal/m}^2 \text{ hr}, \quad (9.32)$$

where $\epsilon'_g \approx 0.7-0.8$ is the coefficient characterizing gas absorption of that part of the radiant energy, which is reflected from the combustion-chamber liner (the magnitude of this coefficient is greater than ϵ_g); and $T_{p,g}$ is the absolute combustion-chamber gas-side liner-surface temperature, in $^{\circ}\text{K}$.

The degree of blackness of CO_2 and H_2O decreases as temperature increases. Therefore, the radiation of these gases does not increase in accordance with the Fourth Power Law, but somewhat more slowly.

Experiments show that radiation and absorption for water vapor is

proportional to T_g^3 , and for carbon dioxide it is proportional to $T_g^{3.5}$.

However, for convenience, in determining radiation from H_2O and CO_2 we frequently use the Fourth Power Law for the absolute temperature, i.e., the Stefan-Boltzmann law.

To determine specific radiant heat flows from H_2O and CO_2 to the engine combustion-chamber liner, the following formulas are recommended in existing literature*:

a) for water vapor

$$q_{H_2O} = 35 p_{H_2O}^{0.8} \left[\left(\frac{T_g}{100} \right)^4 - \left(\frac{T_{gr}}{100} \right)^4 \right] \text{kcal/m}^2 \text{ hr}; \quad (9.33)$$

b) for carbon-dioxide gas

$$q_{CO_2} = 3.5 \sqrt{p_{CO_2}} \left[\left(\frac{T_g}{100} \right)^{3.5} - \left(\frac{T_{gr}}{100} \right)^{3.5} \right] \text{kcal/m}^2 \text{ hr}. \quad (9.34)$$

Thus, the total specific radiant heat flow is equal to

$$q_{p.k} = q_{H_2O} + q_{CO_2} \text{ kcal/m}^2 \text{ hr}. \quad (9.35)$$

In determining the value of q_r in the characteristic chamber section, it is necessary to consider not only the change in gas-stream geometrical dimensions but also the changes in temperature, pressure and composition for the gases throughout the length of the chamber, which, in practice, is accompanied by cumbersome computations and does not give satisfactory accuracy.

Therefore, for the entire combustion chamber length of existing ZhrD, with the exception of the initial section, about 50-100 mm in length, it is more practicable to assume the specific radiant heat flow as being constant, and equal to the value of $q_{r.k}$, which is computed in accordance with the gas parameters at the end of the combustion chamber, and to consider that $q_r \approx 0.25 q_{r.k}$ at the chamber head.

* A. V. Bolgarskiy and V. K. Shchukin. *Rabochiye Protsessy v zhidkostno-raketnykh dvigatelyakh* [Cycles in Liquid-Propellant Rocket Engines], Oborongiz [State Publishing House of the Defense Industry], 1953. G. B. Sinyarev and M. V. Dobrovol'skiy. *Zhidkostnyye raketnyye dvigateli* [Liquid-Propellant Rocket Engines], Oborongiz, 1957.

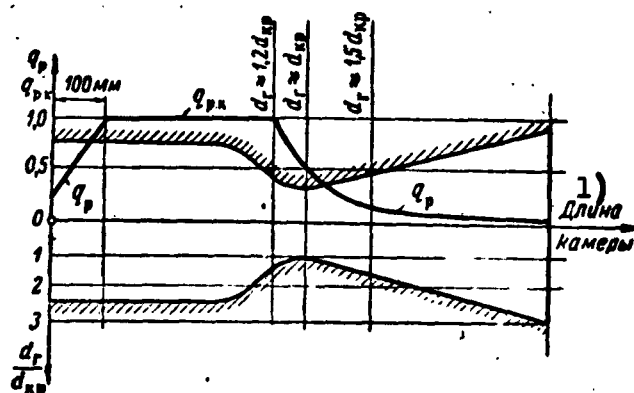


Fig. 9.12. Distribution of specific radiant heat flow throughout engine-chamber length. 1) chamber length.

In determining specific radiant heat flows from the gases to the chamber-nozzle liner, we also may consider that:

- 1) in the subcritical part of the nozzle, up to a section with a diameter $d_g \approx 1.2 d_{kr}$, the specific radiant heat flow is constant, and equal to $q_{r.k}$ at the end of the combustion chamber;
- 2) in the nozzle throat $q_r \approx 0.5 q_{r.k}$, and
- 3) in the supercritical part of the nozzle in a section where $d_g \approx 1.5 d_{kr}$, $q_r \approx 0.15 q_{r.k}$, and in a section where $d_g = 2.5 d_{kr}$, q_r is about $0.04 q_{r.k}$.

Radiation from the gases located in the combustion chamber, in practice, entirely fails to reach the liner of the supercritical nozzle section.

Thus, it is simple to compute and to construct a curve for rapid determination of the value of q_r throughout the entire length of the chamber, upon condition that the propellant components are uniformly distributed across a chamber cross-section (Fig. 9.12).

Radiant heat transfer in a ZhRD also is essentially a function of the parameters of the wall-side gas layer, which is formed from the combustible or from a relatively cold gas fed from the head or through

special belts of slots for protecting the liner against overheating by the hot gases. In this case, the gas stream in the chamber is divided into two layers, each of which is distinctive in gas properties and gas parameters; these two layers are the flow core and the wall-side layer. If film cooling, as described above, is used in an engine, part of the energy radiated by the stream core is absorbed by the relatively cold wall-side layer of gases, especially if those gases whose radiation composes the basic part of gas radiation in the core are maintained in considerable amounts in the wall-side layer (Fig. 9.13). To determine specific radiation heat flow in this case, it is necessary to consider the absorption of the energy emitted from the core by the intermediate and wall-side layers, the internal radiation of the intermediate layer and its absorption by the wall-side layer and, finally, the radiation from the latter.

If the area flow rate throughout the chamber-head field has an even distribution, the initial thickness of the wall-side gas layer, as combustible is fed through the injectors, is approximately proportional to the distance between the injectors, and at a given distance the thickness of the layer somewhat depends on the engine scale.

If the distance between the injectors is 11-20 mm, the initial thickness of the wall-side layer for nitric-acid engines of a 2-5 ton-thrust with centrifugal injectors of the same flow rate, is equal to approximately 15-30 mm. At such an initial thickness for the wall-side layer, the strength of gas-core radiation is already considerably reduced in the intermediate and in the wall-side gas layers, and the intensity of the radiant flux incident on the chamber walls is reduced by approximately 20-70% (as a function of the fuel-mixture ratio χ_{st} in the wall-side layer). Thus, for engines of various thrusts and combustion-chamber pressures, it is possible, in approximation, to

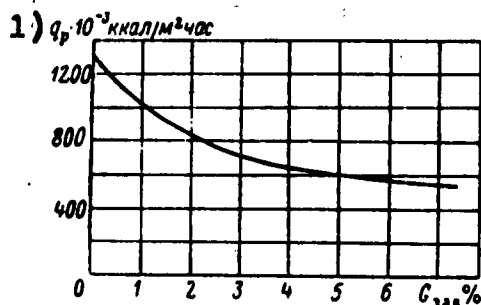


Fig. 9.13. Computed value of q_r as a function of kerosene flow rate G_{zav} in forming protective curtains, when $p_k = 20$ atm abs, and $\chi_{gol} = 4.4$.
1) $q_r \cdot 10^{-3} \text{ kcal/m}^2 \text{ hr}$.

assume the same decrease in radiation intensity as that which would be produced by a protective curtain of medium capacity at the liner surface (when $\chi_{st}/\chi_{ya} = 0.3-0.6$).

On this basis, specific radiant heat flow from the gases to the combustion-chamber liner, when there is a protective curtain of combustible at the liner, may be determined, in approximation, in accordance with the formula

$$q_{r,ms} = q_{r,k} \cdot \epsilon_{st,es} \cdot \varphi_1 \cdot \varphi_2 \text{ kcal/m}^2 \text{ hr}, \quad (9.36)$$

where $q_{r,k}$ is the specific radiant heat flow in the combustion chamber when there is no protective curtain, computed by the method given above; $\epsilon_{st,es} \approx 0.8$ is the effective degree of blackness for a steel combustion-chamber liner; $\varphi_1 \approx 0.60-0.70$ is the coefficient by which we consider the decrease in gas-core radiation intensity due to the presence of the curtain; φ_2 is the coefficient by which we consider the decrease in specific radiant heat flow due to reduced hot radiant gas-core surface (because of the cold wall-side curtain layer) relative to combustion chamber surface; this coefficient may be determined, in approximation, in accordance with the formula

$$\varphi_2 = \frac{(d_k - 2t)(l_{k,s} - 2t)}{d_k l_{k,s}}, \quad (9.37)$$

where d_k and $l_{k,s}^*$ are the diameter and length of a cylindrical combustion chamber, respectively; and t is the distance between the centrifugal injectors.

* $l_{k,c} = l_{k,s} = l_{\text{kamera sgoraniya}} = l_{\text{combustion chamber}}$

The distribution of specific radiant heat flows throughout the entire length of an engine combustion chamber, when a gas curtain is present, may be determined, with sufficient accuracy for practical purposes, in accordance with the method given above, having first computed the values of $q_{r.k}$ when there is no protective curtain of combustible in the chamber.

In the given case, there is no point in introducing any changes, associated with the presence of an intermediate and a wall-side gas layer along the chamber, into this method for determining the distribution of the values of q_r , since determining gas composition and gas parameters, which are required for computing the values of q_r for a gas stream with gas parameters that change across a section, is, at the present time, possible only in extreme approximation.

SECTION 8. SELECTING SHAPES AND DIMENSIONS FOR AN ENGINE-CHAMBER COOLANT PASSAGE

In designing a regenerative engine-cooling system, we must select an appropriate shape for the coolant passage and establish coolant-passage dimensions throughout the chamber length.

An engine-chamber coolant passage should be made so that:

- 1) the passage is structurally simple and efficient;
- 2) the coolant, at a given per-second flow rate, removes a specific quantity of heat from the liner;
- 3) the pressure difference for the liquid in the coolant passage is at a minimum, for the purpose of decreasing hydraulic resistance in the passage, and, consequently, decreasing the capacity and weight of the engine fuel-feed system.

At the present time, ZhRD coolant passages are made in slotted, spiral, and spiral-slotted shapes (see Fig. 9.8), depending on the coolant and the required structural strength of the chamber, and bearing

in mind the considerations given earlier. A chamber coolant passage may also be made in the form of longitudinal rectangular channels, formed by the helices (ribs) of the chamber flame tube, or by tubes which are shaped and bonded together directly forming a "tubular" engine-chamber liner.

A smooth slotted (annular) passage is the simplest to manufacture. The shortcomings of a slotted engine-chamber coolant passage are:

- 1) poor chamber rigidity, which makes it necessary to reinforce the inner liner by fastening it to the outer liner (outer case), or, sometimes, using thin longitudinal reinforcing ribs, about 1 mm in thickness and several mm apart, on the outer surface of the liner;

- 2) the necessity of using a very small annular-slot clearance at a small per-second coolant-flow rate, in order to develop the required coolant velocity in the passage for the purpose of reliable heat withdrawal from the liner, which increases the pressure difference across the passage, the weight of the fuel-feed system and the expenditure of energy in servicing the fuel-feed system; besides this, there are production difficulties in making a uniform slot clearance with a height of 0.8 mm, if the chamber is machined, or a height of less than 1.5 mm if the chamber is of welded construction.

We must bear these remarks in mind when selecting coolant-passage shapes and designing engine-chamber cooling systems.

Structural coordination between chamber liners may be of many different forms. It is very difficult to make a strong connection between the inner and outer chamber liners, as is required at great pressures in the combustion chamber (up to 40-60 atm abs) and in the coolant passage (up to 60-80 atm abs).

In a slotted-passage structure, the inner and outer chamber liners of an uncoordinated stress-bearing system are usually fixed

together by longitudinal metal rods (or bands), arranged at a certain distance from one another (resembling the A-4 alcohol-oxygen engine).

Spiral and spiral-annular passages are used when it is necessary to increase the heat removal from the liner to the liquid by increasing the cooling surface of the liner. This type of passage is a series of square-thread channels, cut spirally into the outer surface of the chamber flame tube. Such a passage shape is often used only in the throat section of the nozzle, which has a greater magnitude of thermal stress, while, in the remaining parts of the combustion chamber, it is more practicable to use the relatively simple slotted passage.

The flow-through section that we select for the spiral channel depends on the coolant velocity; the usual channel height is 2-3 mm, with a helix thickness of about 1 mm.

All-welded chambers made of sheet metal, even if well fitted (by mandrels, templates, etc.), may have deviations in the measurement of the inter-jacket clearance of the order of plus or minus 0.4 mm, commensurable with the rated clearance. Insignificant deviations from the rated clearance will give either a sharp local increase in the coolant velocity, which leads to the liner burning through, or an impermissibly high passage resistance, and, if the walls close, the liner will burn out. We often observe all these defects at a time when the engine is nearly completed, or even while observing static engine tests. For these reasons, a slot clearance of not less than 1.5 mm between engine-chamber liners is advisable.

In some cases, it is expedient to use a spiral passage for the coolant flow, at the same time allowing a clearance between the liners of 1.5-2.0 mm or more. A spiral coolant passage is more advantageous than a slotted passage for engines with a thrust of about 0.5-1.5 tons.

The intensification of regenerative cooling must be accompanied by the general increase in manufacturing precision of the coolant passage, especially in the nozzle-throat area.

The essential difficulty associated with regenerative cooling when using a slotted passage lies in achieving and maintaining the required coolant velocity with reasonable accuracy.

A spiral engine-chamber coolant passage has the following inherent shortcomings:

1) the complexity of cutting the spiral threads on the liner, especially on the conical section of the nozzle, which increases the cost of the chamber in relationship to a chamber with a slotted passage;

2) the relatively great coolant hydraulic losses in the passage at a quite insignificant decrease in inner-liner temperature, due to the use of helices, which makes it necessary to raise coolant pressure at the entrance to the passage, as well as feed pressure.

After selecting coolant-passage shapes, it is necessary to establish passage dimensions which will provide reliable and economical engine cooling. Thus, the necessary preliminary condition is to provide the required liquid velocity in the nozzle-throat section.

If an excessively great coolant velocity in the passage is required for reliable regenerative engine cooling, which would be accompanied by a considerable loss in coolant pressure, the need for a heavier and more powerful fuel-feed system, we must use one of the well-known special methods of protecting the liner against overheating.

In existing engines, coolant pressure difference across the passage usually amounts to 5-20 kg/cm^2 or more, and coolant velocity is*:

*Ekspress-Informatsiya, AN USSR, No. 23, RT-68, 1958. A. V. Satton [sic, possibly G. P. Sutton]. Raketnyye dvigateli [Rocket Engines], IL, 1950.

- a) in combustion chambers - about 2-6 m/sec;
- b) in a nozzle throat - about 6-15 m/sec, or higher.

In particular, the following coolant velocities exist in the coolant passage for the A-4 alcohol-oxygen engine.

- a) in the maximum-diameter region of the combustion chamber - about 3 m/sec;
- b) in the nozzle-throat section - about 12 m/sec;
- c) in the nozzle-outlet section - about 4 m/sec.

If absolutely necessary, coolant velocity in a chamber nozzle-throat passage may be raised to 25-30 m/sec.

Coolant velocity in an engine-chamber coolant passage must not be greater than that required by the conditions for removing specific heat flows from the liner, since, otherwise, coolant pressure difference across the passage would be needlessly increased. For this purpose, the clearance of the annular slots in an engine coolant passage is made smaller in those places where the specific heat flows from the gas to the liner are greater.

Coolant pressure difference across an engine-chamber coolant passage usually amounts to 1/3 of the pressure p_k in the combustion chamber, i.e.,

$$\Delta p_{охл} \approx \frac{p_k}{3}^*$$

When designing ZhRD-chamber cooling systems, we may assume that $\Delta p_{охл} \leq 0.3p_k$ when cooling is accomplished by the combustible and $\Delta p_{охл} \leq 0.2p_k$ when cooling is accomplished by the oxidizer.

The assumption of these values of $\Delta p_{охл}$ does not require introducing any complexities of principle into the chamber design.

* $\Delta p_{охл} = \Delta p_{охл} = \Delta p_{охл\text{azhdayayushchaya}} = \Delta p_{coolant}$.

An analysis of Formula (9.57), used to determine the value of the heat-transfer coefficient α_{zh} , shows that increasing the value of Δp_{okhl} by 30-40% would lead to an increase in the value of the heat-transfer coefficient α_{zh} by only 10-14%, since this coefficient changes in proportion to coolant velocity to the power of 0.8 ($w^{0.8}$), while the change in the value of Δp_{okhl} is proportional to the square of w ; under this condition, there is no essential change in the results of the computation. Therefore, we usually assume that the maximum coolant velocity in the chamber-nozzle throat section is not higher than 20-25 m/sec.

The required preliminary condition, when we design an engine chamber, is to provide for a certain coolant velocity in the nozzle-throat section.

In contemporary engines, the clearance (height) of the annular coolant-passage slot ranges from 1 to 5 mm.

When designing a ZhRD-cooling system, we often assume the magnitude of the inter-jacket clearance on the basis of statistical data, and thus determine coolant velocity within the passage; we judge the reliability of engine cooling by the magnitude of coolant velocity.

An insignificant deviation from normal clearance magnitude gives either a sharp (local) increase in coolant velocity within the passage, which leads to the chamber liner burning through, or an impermissibly high passage resistance, and if the liners close together, the engine chamber may burn out.

As we consider the conditions for reliable cooling for engines with a thrust of 1 to 10 tons, we must acknowledge that an inter-jacket clearance of 1.5 or even 1 mm. is advisable. Practice shows that, in a welded construction with a diameter of more than 150 mm, this clearance is maintained with a precision of ± 0.3 mm. However, to avoid an accidental change in the magnitude of the slot clearance,

which might disrupt normal liner-cooling conditions, an inter-jacket clearance of about 1.5-2 mm, or, in some cases, even greater, should be selected.

An inter-jacket clearance may also be determined by computation, having assumed, tentatively, the magnitude of and the nature of the change in coolant velocity throughout the length of the passage, beginning with due consideration of the quantity of heat to be removed from the liner and the permissible coolant-pressure difference across the passage in this particular case.

The area of the coolant-passage cross section (channel) may be determined in accordance with the following formulas (see Fig. 9.8):

a) slotted

$$F_{\Sigma} = \frac{Q_{\text{out}}}{w_1} = \pi (d_{\Sigma} + \delta_{\Sigma}) \delta_{\Sigma}; \quad (9.38)$$

b) spiral and rectangular

$$F_{\Sigma} = \frac{Q_{\text{out}}}{w_1} = abl. \quad (9.39)$$

If $a = b$, which often is the case, $F_{\Sigma} = b^2 l$.

We may determine coolant velocity in the passage by using these formulas.

The equivalent (hydraulic) diameter of the coolant passage, which is required for determining the coefficient of convective heat transfer from the liner to the coolant, is determined in accordance with the following formulas:

a) for a smooth slotted passage

$$d_{\Sigma} = \frac{4F_{\Sigma}}{\pi} = \frac{4\pi d_{\Sigma} \delta_{\Sigma}}{\pi d_{\Sigma}} = 4\delta_{\Sigma}; \quad * \quad (9.40)$$

* $d_{\Sigma} = d_{\text{ek}} = d_{\text{ekvivalentnyy}} = d_{\text{equivalent}}$

b) for a spiral or slotted passage with longitudinal ribs

$$d_{ex} = \frac{4F_{ex}}{\pi} = \frac{4ab l}{(a+2b)l} = \frac{4ab}{a+2b} \quad (9.41)$$

If $a = b$, $d_{ek} = 4/3(b)$, where a is the width of the channel between two ribs (helices), b is the height of the rib, l is the number of channels (entries), and p is the perimeter of heat transfer from the liner to the coolant.

Thus, for a spiral passage

$$b = \sqrt{\frac{G_{ox}}{w\gamma l}} \text{ and } d_{ex} = \frac{3}{4} \sqrt{\frac{G_{ox}}{w\gamma l}},$$

where w is the mean coolant velocity in the passage, in m/sec; and γ is the specific weight of this liquid, at the corresponding temperature in the passage, in kg/m³.

SECTION 9. DETERMINING DEGREE OF COOLANT PREHEATING THROUGHOUT ENGINE-CHAMBER COOLANT-PASSAGE LENGTH.

With a steady-state heat-transfer process in a Zhrd, and negligible heat transfer to the surrounding medium, all heat transferred by the gas to the chamber liner must enter into preheating of the coolant.

Coolant preheating across a given section of the chamber passage may be determined from the equation of heat balance

$$S_1 q_1 = G_{okhl} C_1 \Delta t_1,$$

i.e.,

$$\Delta t_1 = \frac{S_1 q_1}{G_{okhl} C_1}, \quad (9.42)$$

where S_1 is the surface of the 1-th section of the liner, in m²; q_1 is the mean specific heat flow across this section, in kcal/m² hr; G_{okhl} is the coolant-flow rate, in kg/hr; and C_1 is the mean coolant heat capacity across the 1-th section of the liner, in kcal/kg °C;

since liquid preheating across the section is not great, one may use the value of C_1 at the temperature $t_{1_vkh}^*$ of the liquid at inlet to the passage.

By means of this equation, we may compute:

1) coolant temperature at the outlet from the passage of the 1-th section

$$t_{1_out} = t_{1_in} + \Delta t_1, ^\circ C; ** \quad (9.43)$$

2) mean coolant temperature in the passage of this section

$$t_x = \frac{t_{1_in} + t_{1_out}}{2}, ^\circ C; \quad (9.44)$$

3) total liquid preheating in the chamber passage

$$\Delta t_x = \sum \Delta t_i = t_{out} - t_{in}; \quad (9.45)$$

4) coolant temperature at the outlet from the chamber passage

$$t_{out} = t_{in} + \Delta t_x, ^\circ C, \quad (9.46)$$

where t_{vkh} is coolant temperature at the inlet to the chamber coolant passage.

For the cylindrical section of a combustion chamber, the previous formula for computing coolant preheating in the passage takes the form

$$\Delta t_x = t_{out} - t_{in} = \frac{\pi d_k l_{k.ts}}{G_{out} C_{cp}} ^\circ C, \quad (9.47)$$

where d_k and $l_{k.ts}^{***}$ are the diameter and length of the cylindrical

$$* t_{1_in} = t_{1_vkh} = t_{1_vkhod} = t_{1_inlet}$$

$$** t_{1_out} = t_{1_outlet}$$

$$*** l_{k.ts} = l_{k.ts} = l_{kamera, tsilindricheskaya} = l_{cylindrical\ chamber}$$

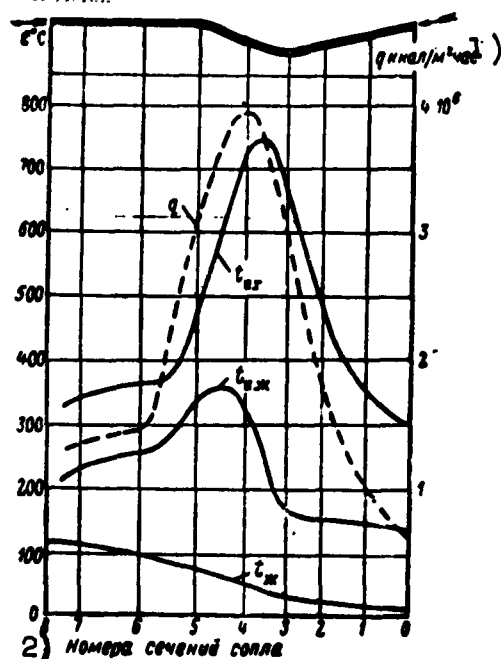


Fig. 9.14. Approximate pattern of change in temperature for gas-side and liquid-side liner surfaces and of coolant, in the passage, throughout chamber length. 1) $q, \text{kcal/m}^2 \text{ hr}$; 2) numbers of nozzle sections.

part of the combustion chamber, respectively, in m; and C_{sr} is the mean coolant heat capacity, at a given temperature interval, in the combustion-chamber coolant passage, in $\text{kcal/kg } ^\circ\text{C}$.

We then construct the curve of the change in the value of t_{zh} throughout the engine-chamber length in accordance with the computed data (Fig. 9.14).

The specific heat capacity of certain liquids, as a function of temperature, is given in Section 2, Chapter V.

For reliable regenerative engine cooling, it is necessary for

the coolant to remove as much heat from the chamber liner as was transferred to the liner from the hot gases, and that the temperature of this coolant does not exceed its boiling point, at the given pressure, at the outlet from the passage. If this requirement is not satisfied, in order to remove the available quantity of heat from the liner

$$Q_{\text{рас}} = \sum S q_i \text{ kcal/hr} \quad (9.48)$$

one must either use both propellant components (if the second component is suitable for this purpose), or protect the liner against overheating by injecting combustible from the chamber-head side, or through special belts, if more convenient methods do not exist. As engine thrust increases and pressure across the combustion chamber decreases, the value of $Q_{\text{рас}}$

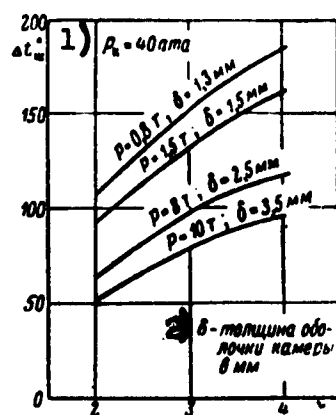


Fig. 9.15. Approximate pattern of change in degree of pre-heating for nitric acid in an engine coolant passage, when $p_k = 40$ atm abs, as a function of thrust and fuel-mixture ratio X_{st} for liner walls of different thickness.

- 1) $p_k = 40$ atm abs;
- 2) δ = thickness of chamber liner, in mm.

efficiency of the combustible-film method of protecting the inner chamber liner against overheating also depends on heat of combustible vaporization; the higher the value of this heat of vaporization, the more efficient the liner protection.

To determine the possibility of regenerative engine cooling by means of one or both propellant components, it is necessary to determine the maximum permissible specific heat Q_{ud} (referred to 1 kg of coolant) and the total possible per-second propellant-component heat Q_{vozm}^* to be removed, by using the following formulas:

- 1) if cooling is accomplished by means of the combustible

$$Q_{y.z.r} = C_r(t_{доп} - t_{ст}) \text{ kcal/kg}^{**} \quad (9.49)$$

* $Q_{возм} = Q_{vozm} = Q_{vozmozhnny} = Q_{possible}$

** $t_{доп} = t_{dop} = t_{dopustimaya} = t_{permissible}$

decreases.

Coolant preheating temperature in the passage may be somewhat decreased by using, instead of a cylindrical shape, a spherical combustion chamber, which, other things being equal, has a relatively smaller heating surface.

The greatest quantity of heat that a given quantity of coolant can remove from a chamber liner is determined by the coolant heating up, at the given pressure, to boiling point $t_{kip}^{\circ}\text{C}$. The higher coolant boiling point and heat capacity are, the more heat may be transferred from the chamber liner to the liquid, and the more efficient the cooling system. The effi-

$$Q_{\text{BOHM},T} = G_s Q_{yA,T} \text{ kcal/sec;} \quad (9.50)$$

2) if cooling is accomplished by the oxidizer

$$Q_{yA,O} = C_o (t_{\text{don}} - t_{\text{ox}}) \text{ kcal/kg;} \quad (9.51)$$

$$Q_{\text{BOHM},O} = G_o Q_{yA,O} \text{ kcal/sec;} \quad (9.52)$$

3) if cooling is accomplished by means of both propellant components

$$Q_{yA,T} = \frac{Q_{yA,T} + Q_{yA,O}}{1 + \chi} \text{ kcal/kg;} \quad (9.53)$$

$$Q_{\text{BOHM},T} = G_s Q_{yA,T} \text{ kcal/sec;} \quad (9.54)$$

where C_g and C_o are the mean heat capacities of the combustile and oxidizer, respectively, in kcal/kg °C; t_{dop} is the permissibly safe coolant preheating temperature in the passage, at the given pressure in °C; and $\chi = G_{s\ o}/G_{s\ g}$ is the actual fuel-mixture ratio, by weight.

Preheating for the liquid in an engine-chamber coolant passage is usually permissible up to the quantity

$$\Delta t_{\text{pre}} = t_{\text{pre}} - (20 + t_{\text{ox}}).$$

At a pressure of 20-60 atm abs, kerosene may be preheated to 250-300°C; therefore, the permissible specific heat removal, when $t_{\text{vkh}} = 0^\circ\text{C}$, may, accordingly, amount to 150-185 kcal/kg.

The heat capacity of nitric acid is less than the heat capacity of kerosene; therefore the maximum specific heat removal of nitric acid is less. However, if we consider the fact that the per-second nitric-acid flow rate in the engine is greater than the kerosene flow rate by almost a factor of 4, we see that the total maximum heat removal for nitric acid is considerably greater than the total heat removal of kerosene.

Figure 9.15 shows curves for an example of a change in degree of

nitric-acid preheating in a combustion-chamber coolant passage, when $p_k = 40$ atm abs, as a function of thrust and the fuel-mixture ratio χ_{st} at the wall of the chamber liner.

SECTION 10. DETERMINING LIQUID-SIDE AND GAS-SIDE ENGINE-CHAMBER LINER TEMPERATURES

The liquid-side chamber-liner surface temperature is chiefly a function of the thermal conductivity λ and thickness δ of the chamber-liner material, as well as of the conditions under which this surface is flushed by the coolant.

The more intensively the coolant flushes the liner surface, the better the coolant will remove heat, and the lower the temperature $t_{p.zh}$ °C of the liquid-side liner surface will be.

A decrease in the value of $t_{p.zh}$, in turn, entails a decrease in the value of $t_{p.g}$, and the latter leads to a change in the entire heat flow from the gases to the liner. Thus, there is a definite interdependence between chamber-liner surface temperatures and heat flows.

The liquid-side engine-chamber liner-surface temperature in given sections may be determined from the equation of specific heat flow through the liner:

$$q = \frac{\lambda}{\delta} (t_{n,r} - t_{n,x}) \text{ kcal/m}^2 \text{ hr},$$

i.e.,

$$t_{n,x} = t_{n,r} - \frac{\delta}{\lambda} q \text{ } ^\circ\text{C}, \quad (9.55)$$

where $t_{p.g}$ is the gas-side liner-surface temperature, the value of which, when computing specific heat flows from the gas to the liner, in the first approximation, must be assumed in accordance with the considerations of engine heat resistance, strength, and service life; δ is the chamber-liner thickness in the given section, in m [sic]; the magnitude of δ , in the first approximation, may be assumed on the

basis of statistical data; and λ is the mean thermal-conductivity coefficient for the liner metal, in kcal/m hr $^{\circ}\text{C}$, determined in accordance with the curves (Figs. 9.16 and 9.17) or from the appropriate formula.

As we determine the value of $t_{p.zh}$, in accordance with Formula (9.55), we must aim for the corresponding change in the magnitudes of $t_{p.g}$ and λ for the material, so that the liner will be of high strength and stability, and the value of $t_{p.zh}$, when using the ordinary slotted passage, does not exceed coolant boiling point, to avoid local vapor locks (if the coolant flows through a sufficiently narrow, insulated channel and if engine service life is short, the value of $t_{p.zh}$ may exceed coolant boiling point, in the corresponding section, by approximately 50°C).

When the value of $t_{p.g}$ changes in comparison to its value that was assumed when computing specific convective heat flow q , it is necessary to bear in mind that a change of temperature by 100°C causes the value of q to change by 5-10%.

Computation of the value of $t_{p.zh}$ is performed in the following order:

- 1) we determine the value of λ , in the first approximation, at a temperature $t_{sr} = (t_{p.g} + t_{p.zh})/2$, having assumed the anticipated temperature $t_{p.zh}$ in advance;
- 2) we compute the value of $t_{p.zh}$, in the first approximation in accordance with Formula (9.55);
- 3) we refine the magnitude of $t_{p.zh}$ in accordance with the computed values and the appropriate curves showing the thermal-conductivity coefficient of the metal as a function of temperature;
- 4) we refine the value of $t_{p.zh}$ in accordance with the refined value of λ .

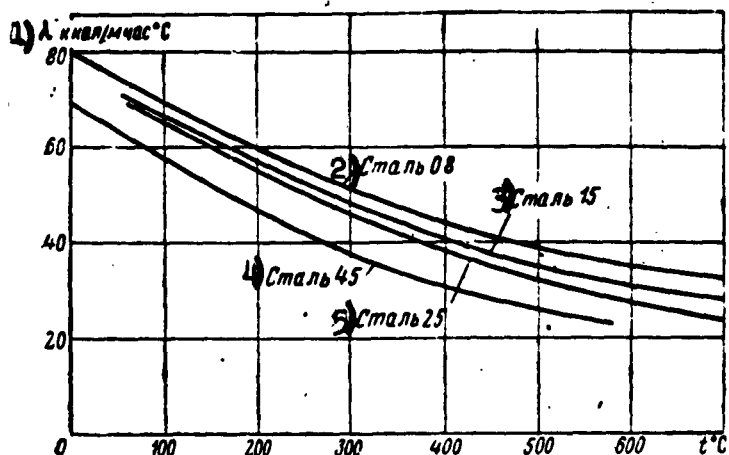


Fig. 9.16. Thermal-conductivity coefficients for carbon steels, as a function of temperature. 1) λ , kcal/m hr $^{\circ}\text{C}$; 2) steel 08; 3) steel 15; 4) steel 45; 5) steel 25.

In accordance with the results of the computations, we can construct a curve of the change in the value of $t_{p.zh}$ throughout the engine-chamber length (see Fig. 9.14).

The liquid-side engine-chamber liner-surface temperature, in the given section of the chamber, also may be determined in accordance with the formula

$$t_{l.x} = t_{\infty} + \frac{q}{k_{2x}} \text{ } ^{\circ}\text{C}, \quad (9.56)$$

where t_{zh} is the mean coolant temperature in the passage of the chamber section being studied;

$$k = 1 + \frac{2\delta}{d_g}$$

is the coefficient by which we consider the increase in efficiency for the surface of heat transfer from the liner to the coolant, relative to the inner gas-side liner surface, to which the magnitude of specific heat flow pertains; here d_g and δ are the inner diameter along the gas-side surface, and the thickness of the chamber liner, for the section being studied, respectively; α_{zh} is the coefficient of heat transfer from the liner to the coolant, as the coolant moves turbulently and is heated, which is computed in accordance with the

empirical formula*:

$$\alpha_x \approx 75,6B \frac{1}{d_{ek}^{0,2}} \left(\frac{G_{okhl}}{F_x} \right)^{0,8} \beta \text{ kcal/m}^2 \text{ hr}^\circ\text{C}; \quad (9.57)$$

where d_{ek} is the equivalent coolant-passage diameter, in m; G_{okhl} is the coolant-flow rate, in kg/sec; F_{zh} is the coolant-passage flow area, in m^2 ;

$$B = \lambda_x^{0,57} \frac{C_x^{0,48}}{(g\eta_x)^{0,4}}$$

is a coefficient which is a function of the type of coolant and mean coolant temperature (Fig. 9.18); and

$$\beta = \left(\frac{Pr_x}{Pr_{n,x}} \right)^{0,25} = \left(\frac{g\eta_x C_x / \lambda_x}{g\eta_{n,x} C_{n,x} / \lambda_{n,x}} \right)^{0,25}$$

is a coefficient by means of which we consider the direction of the heat flow and temperature head, which is the ratio of the Prandtl numbers, respectively, of coolant temperature in the passage (numerator) and of mean liquid-side liner-surface temperature of this passage (denominator), where η_{zh} kgsec/m², C_{zh} kcal/kg^oC, and λ_{zh} kcal/msec ^oC are, respectively, coolant viscosity, heat capacity, and thermal conductivity at mean coolant temperature in the passage of the section being studied; and $\eta_{p,zh}$, $C_{p,zh}$, and $\lambda_{p,zh}$ are coolant viscosity, heat capacity, and thermal conductivity, respectively, at the liquid-side chamber-liner surface temperature.

The coefficient α_{zh} , to a considerable degree, is a function of coolant properties, which, at present, have still been very little studied for certain combustibles and oxidizers.

The physical constants of certain liquids used in ZhRD are given in Section 2, Chapter V.

The curves in Fig. 9.21 [sic, probably Fig. 9.18] show that:

*A. M. Mikhaylov [sic]. Osnovy teplooperadachi [The Bases of Heat Transfer], Gosenergoizdat [State Power Engineering Publishing House], 1956.

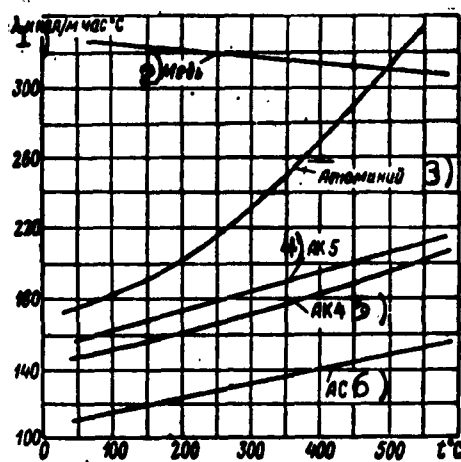


Fig. 9.17. Thermal-conductivity coefficients for copper, aluminum, and aluminum alloys, as a function of temperature. 1) kcal/m hr °C; 2) copper; 3) aluminum; 4) AK 5; 5) AK 4; 6) AS 1.

1) a hot liquid, other conditions being equal, cools a liner better than one which is less heated; this fact is explained by the change in the physical constants of the liquid at a change in temperature;

2) water is the most efficient coolant, better than kerosene, approximately by a factor of 5-6, and better than nitric acid by almost a factor of 1.5, and nitric acid is better than kerosene by a factor of almost 1.5-2.

For different liquids the thermal-conductivity coefficient $\lambda \approx 0.08-0.60$ in kcal/m hr °C. For the majority of liquids (except water and glycerine), the value of λ increases as temperature rises.

At great specific heat flows, the formula given above for determining the value of α gives understated computation results. In existing engines, the value of $\alpha_{zh} \approx 10^4-10^6$ kcal/m² hr °C.

If the temperature $t_{p.zh}$ has been determined in accordance with Formula (9.55), the coefficient of heat transfer from the liner to the coolant may be determined in accordance with the formula

$$\alpha_x = \frac{q}{t_{n,x} - t_x} \text{ kcal/m}^2 \text{ hr}^\circ\text{C}$$

By using this formula, together with the Nusselt formula, for determining α_{zh} , we may obtain an expression for determining the required area of the engine-chamber coolant-passage flow section:

$$F_x = G_{ox} \left[\frac{75.6B (t_{n,x} - t_x)^{1.25}}{\alpha_{zh}^{0.75}} \right]^{1.25} \quad (9.58)$$

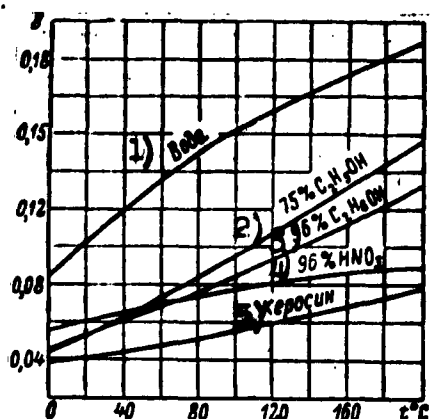


Fig. 9.18. The B complex, as a function of temperature, for different liquids (C_{zh} kcal/kg $^{\circ}\text{C}$, λ kcal/m sec $^{\circ}\text{C}$, and η kg sec/m²).
 1) water; 2) 75% $\text{C}_2\text{H}_5\text{OH}$;
 3) 96% $\text{C}_2\text{H}_5\text{OH}$; 4) 96% HNO_3 ;
 5) kerosene.

For determining the value of F_{zh} in accordance with this formula, we must tentatively assume the anticipated approximate value of coolant-passage equivalent diameter d_{ek} , and then check to see if the computed value of d_{ek} does not vary too greatly from this value. If this divergence is considerable, we must repeat the determination of F_{zh} , having assumed, at the same time, a new computed value of d_{ek} .

We usually determine the value of F_{zh} for the most characteristic

sections of the chamber nozzle, thus simplifying coolant-passage shape for design and manufacturing considerations. Thus, we determine coolant velocity in the passage in accordance with the already well-known formula:

$$w = \frac{Q_{rzh}}{F_{zh}} \text{ m/sec.}$$

As a result of the computations, it may appear that the dimensions of the interjacket space are too small and too difficult to accomplish, from a production standpoint, within the limits of the required tolerances. Then we must either use a spiral coolant passage or use special methods to decrease specific heat flows q . If the coolant velocity in the passage is too great, from the viewpoint of hydraulic losses, we must either increase temperature $t_{p.zh}$ to permissible limits, or decrease the value of q , by taking appropriate measures.

In chamber coolant passages made in the form of spiral or longitudinal channels, heat is transferred to the coolant both from the

cylindrical parts of the flow-channel liner surfaces and from the side surfaces of these channel-helices. Since the efficiency of heat transfer from the helices is less than the efficiency of heat transfer from the cylindrical surface of the liner, in order to determine the value of α_{zh} , we must somewhat decrease the cooled perimeter of the helices.

The temperature of the gas-side engine-chamber liner surface, within selected sections, may be determined in accordance with Formula (9.55)

$$t_{n,r} = t_{n,x} + q \frac{\delta}{\lambda} = t_x - q \frac{1}{\alpha_r} = \frac{t_x}{1 + \delta \alpha_r / \lambda} + \frac{t_{n,x}}{1 + \delta \alpha_r / \lambda} \text{ } ^\circ\text{C.}$$

If the temperature $t_{p,g}$ obtained by this means differs by more than 5% from the temperature value that was ~~assumed~~ earlier, when determining specific heat flows, it is necessary to find the values of the specific heat flows at this temperature and repeat all the computations from the beginning.

In the second approximation, we usually do not recalculate specific radiant heat flows from the gases to the chamber liner, since a small change in the value of $t_{p,g}$ has a quite insignificant effect on the magnitudes of specific radiant heat flows; therefore, for further computations, we assume that $q_{r2} = q_{r1}$.

The computed values of t_{zh} , $t_{p,zh}$, and $t_{p,g}$ must satisfy the requirements set forth.

If the value of $t_{p,g}$ obtained exceeds the permissible limits for the given chamber-liner metal, then, to decrease $t_{p,g}$ to a possibly safe limit, one must decrease the value of F_{zh} , or, if possible, decrease chamber-liner thickness. If these measures are inadequate or impracticable, we must use a special method of protecting the liner against overheating by the hot gases.

The result of the computations for changes in magnitudes of q_k , q_r , q , t_{zh} , $t_{p,zh}$ and $t_{p,g}$, throughout the length of the combustion

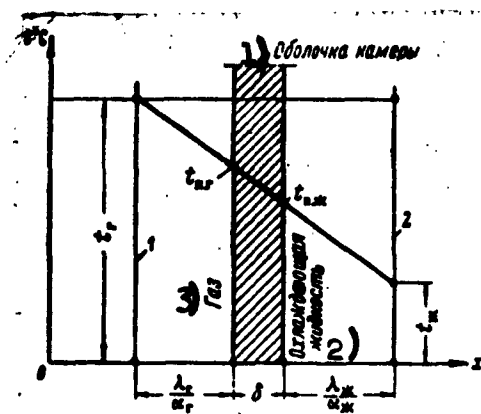


Fig. 9.19. For determining liquid-side and gas-side chamber-liner surface temperatures by the graphic method. 1) chamber liner; 2) coolant; 3) gas.

chamber and nozzle are usually placed in tables and presented in the form of the corresponding curves.

Since, according to Equation (9.8), the total temperature head in a ZhRD heat-transfer system is expressed by the equation

$$t_r - t_x = q \left(\frac{1}{\alpha_r} + \frac{\delta}{\lambda} + \frac{1}{\alpha_{\text{ж}}} \right),$$

after multiplying and dividing the right-hand part of this equation by the liner-material thermal-conductivity coefficient λ , we obtain

$$t_r - t_x = \frac{q}{\lambda} \left(\frac{\lambda}{\alpha_r} + \delta + \frac{\lambda}{\alpha_{\text{ж}}} \right) ^\circ\text{C},$$

where λ/α_g is the effective (overall) thermal resistance for heat transfer from the gases to the chamber liner, in m [sic]; $\lambda/\alpha_{\text{zh}}$ is the same for heat-transfer processes from the chamber liner to the coolant; and

$$\frac{\lambda}{\alpha_r} + \delta + \frac{\lambda}{\alpha_{\text{ж}}}$$

is the same for the total thermal-resistance thickness.

The equation which we have stated shows that the temperature, across the entire thickness of an engine heat-transfer system heat layer, changes according to the linear law. This permits determining gas-side and liquid-side chamber-liner surface temperatures by the graphic method.

The graphic method of determining the values of $t_{p.g}$ and $t_{p.zh}$ is based on the idea of replacing the layer of gas and coolant by an equivalent solid chamber liner with a thermal-conductivity coefficient equal to the value of λ for the metal of a real liner, and consists of the following steps (Fig. 9.19):

- 1) we draw chamber-liner thickness δ , in m [sic], in an arbitrary

scale, and from there along the x-axis, in the same scale, we plot to the left, the value of λ/α_g , in m [sic], and the value of λ/α_{zh} , in m [sic], and then drop the boundary perpendiculars 1 and 2 to the x-axis;

2) we plot the appropriate values of gas temperature t_g °C and coolant temperature t_{zh} °C on the perpendiculars mentioned, also to an arbitrary scale;

3) we connect the points t_g and t_{zh} obtained on the perpendiculars by a straight line, which intersects the gas-side and liquid-side liner surfaces, and in the adopted scale, yields the unknown values of temperatures $t_{g.p}$ [sic, probably $t_{p.g}$] and $t_{p.zh}$.

Then, if necessary, we recompute the heat flows as indicated above.

The change in the temperature of the thermal field of the heat-transfer system in an engine also may be presented graphically as a function of the thermal resistances of the system: $1/\alpha_g$, δ/λ , and $1/\alpha_{zh}$.

SECTION 11. PROTECTIVE CURTAINS FOR AN ENGINE-CHAMBER INNER LINER

Films of combustible are used to protect an engine-chamber liner against overheating when:

- 1) the influx of heat from the gases to the liner is so great that it cannot be removed by one or both propellant components;
- 2) the magnitudes of the specific heat flows in separate sections of the chamber liner (especially in the nozzle throat) are so great that they also cannot be removed by a purely regenerative method, given moderate coolant velocities;
- 3) it is advisable to reduce heat flows from the gases to the liner and thus ease the conditions of regenerative cooling, or to reduce hydraulic losses in the engine coolant passage with a small

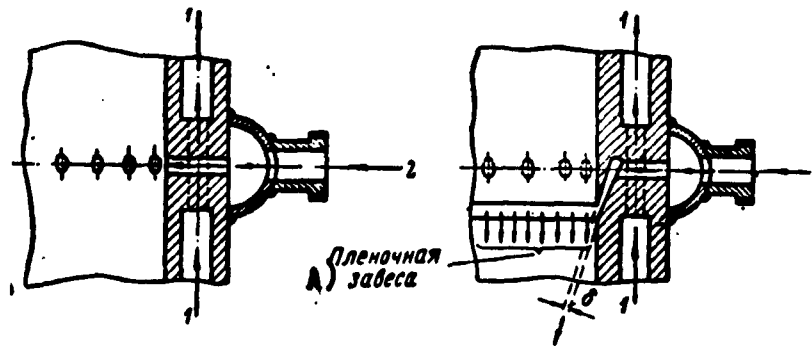


Fig. 9.20. Design of belt for protecting engine-chamber liner against excessive heating by hot gases. 1) Coolant flow in inter-jacket space; 2) feeding of combustible to form protective curtain; δ , thickness of film curtain; A) film curtain.

decrease in specific thrust;

4) it is necessary to increase the engine service life considerably, if more economical methods of protecting the chamber liner from the hot gases do not exist;

5) it is advisable to use inexpensive and light materials such as, for example, carbon steels or aluminum, in fabricating the chamber liner;

6) we must protect the chamber liner against the corrosive action of products of fuel combustion.

Protective curtains for the engine-chamber liner may be created by feeding a certain quantity of combustible along the inner-liner surface by means of:

1) peripheral injectors in the combustion-chamber head or by an annular slot between the combustion-chamber head and the liner;*

2) a special belt (or several belts) which are located directly in the chamber liner, in the form of an annular row of orifices or an annular slot (Fig. 9.20).

Liner protection with combustible by means of peripheral head injectors is called a gas curtain, and cooling by means of special

*Problems of Rocket Engineering, No. 1, 1958, IL.

chamber-liner belts is called a film curtain (or curtains).

With sufficient protective-curtain intensity, reliable ~~ZhRD~~ chamber cooling with propellant components is always possible. However, the use of protective curtains decreases specific engine thrust.

The following requirements (from the viewpoint of economy and reliability of operation) are imposed on chamber-liner protective curtains:

- 1) the curtain must fit the inner surface of the chamber liner tightly and uniformly;
- 2) losses in specific engine thrust, which are caused by the use of protective curtains, must be kept at a minimum;
- 3) the curtain must satisfy engine-operating conditions, i.e., it must be stable and must not be sensitive to flight loads (including lateral loads) or to gas-stream perturbations;
- 4) the curtain must be created by devices that are sufficiently simple from the design viewpoint.

A gas curtain created by peripheral chamber-head injectors satisfies the requirements for stability and nonsensitivity to flight loads if the injectors used for this purpose are not excessively small or inclined to clog. Also, this method is extremely simple from the design viewpoint. Therefore, with a short combustion-chamber, in engines developing low or medium thrust it is practicable to set up a gas curtain from the flat head through peripheral combustible injectors. At an engine thrust of 1-2 tons, the combustible used in forming the gas curtain, by means of peripheral injectors, usually does not exceed 1% of the flow rate to the combustion chamber.

In engines developing great thrust, or if a small amount of combustible is used to form the curtain, the latter is efficient at the head and up to a certain distance from the head; here the gas-

core temperature is relatively low; however, the curtain is of little use in the nozzle-throat section, which is farthest from the head and exhibits the greatest heat-liberation rate. Such a curtain is flushed away by the turbulent gas-core stream while en route from the head to the nozzle throat, and is consumed to a considerable degree.

In order to ensure the least effect of the gas curtain on the magnitude of specific engine thrust, it is necessary to feed combustible for forming the curtain in such a way as to ensure that, after combustible vaporization, the wall-side gas layer thus formed has minimum thickness, is pressed against the liner surface, and is flushed as little as possible by the turbulent gas-core of the stream.

Combustible feed for the curtain by means of head injectors, evidently, does not satisfy this requirement.

The process of forming a wall-side gas curtain in this case, and the mixing of the curtain with the turbulent gas-stream core, is schematically presented in the following form.

Some of the basic combustible and oxidizer impinges on the combustion-chamber surface in a liquid state, or enters a zone close to the liner. These components, including the additional combustible which was fed to the chamber for forming the curtain, are partially mixed when they meet at the liner surface and as they move along the liner surface in the form of a liquid film. Vaporization and combustion of this mixture is completed at some distance from the head, and a wall-side gas layer is formed from the mixture. In approximation, one may consider the composition of this layer initially constant along the normal to the liner and the composition is determined by the mixture ratio of the fuel reaching the liner or a zone close to the liner. As it moves along, this layer mixes with the gases in the

stream core, as a result of which an intermediate layer with a variable composition across its thickness forms between the core and the wall-side layer.

This concept is schematic, but apparently correctly reflects the real processes and is convenient for computations. In the literature it is indicated that as the products of combustion move along the chamber and the nozzle, they mix relatively slowly in the radial directions across the chamber section.*

The layer that adjoins the liner and is constant in composition across its thickness is denoted as the wall-side layer, and if, as the result of mixing, its composition is changed in comparison to the initial composition, or if the layer has a variable composition, we call it the intermediate layer, even if it extends to the liner itself.

Thus, in the general case, the stream core is separated from the liner by an intermediate layer with variable parameters and by a wall-side layer with parameters that are constant across its thickness.

For engines developing great thrust, the belt method of film cooling for the chamber liner is more economical, but from the design viewpoint, relatively complex; this system is made in the form of one or several special belts of slots for the tangential feeding of the combustible into the combustion chamber. The use of such film curtains is especially advisable for engines with prechamber propellant-component atomization (for chambers with a spherical head).

Computations show that the belt method of protecting the chamber liner against overheating is quite efficient and relatively economical up to very high pressures in the engine combustion chamber (up to

*Problems of Rocket Engineering, No. 4, 1956, IL.

$p_k = 100 \text{ atm abs}$).

It is advisable to use the combustible for the purpose of forming the film curtain at the end of the combustion chamber (at the beginning of the converging section of the nozzle) to protect the liner in the nozzle-throat section.

If it is necessary to reduce the heat flows from the gases to the liner both in the nozzle and in the combustion chamber, in this case the first belt for the film curtain should be in approximately the same combustion-chamber section where propellant-component vaporization is completed. If chamber design permits, it is better to feed the combustible for the film curtain into several separate belts. The range of effective operation for each curtain is established by appropriate computations. The intervals between the belts for different curtains may be increased by making each curtain thicker.

In designing and adjusting the systems of protective curtains, we must strive to attain a uniform combustible feed around the entire circumference of the combustion chamber and nozzle, as well as to meet the requirements imposed on the curtain.

Belt curtains in the form of small orifices in the liner are of little use because of the difficulty of feeding combustible for forming the curtain, without the combustible jet gushing into the gas-stream core; the orifices may also clog with scale and sediments, especially in nitric-acid engines.

As yet, the formation of curtains with belts of porous material has been little studied, and is probably efficient only for engines developing great thrust.

In existing engines, the expenditure of combustible for the formation of protective curtains amounts to 1-20% of the basic flow

rate to the combustion chamber. We may assume that in a number of existing ZhRD the consumption of liquid for inner-liner protection is unjustifiably great because of the inefficient method by which the liquid is fed to the inner-liner surface and is several times the amount of the consumption of liquid that was calculated on the basis of the power potentials of the liquid in this case.

If correctly established, protective curtains may be sufficiently economical and capable of reducing specific heat flows from the gases to the chamber liner (up to 70%), but for all that, they do not remove the requirement for external regenerative engine cooling. By means of efficient regenerative cooling and internal protective combustible curtains, one may increase P_{ud} when using steel chamber liners, and increase the liner service life sharply.

Protective-curtain design is usually reduced to the determination of the liquid-flow rate required for protecting the given chamber-liner section and the additional combustible-flow rate required for forming the protective curtains.

A precise method of computing the quantity of liquid required for forming the protective curtains is, as yet, lacking in the literature. This is explained by the fact that when a curtain is present, it is still impossible to determine accurately the available specific heat flows q_1 from the gases to the liner, as well as the temperature of the wall-side gas-layer.

One may determine G'_{zav} by approximate computations in accordance with the parameters computed in the absence of a protective curtain.

One may consider, in approximate terms, that if a protective curtain is formed, the excess heat flow from the gases to the chamber liner, which the coolant cannot remove by purely regenerative cooling,

is equal to

$$Q_{\text{изб}} = \sum S_i q_{i, \text{пачн}} - \sum S_i q_{i, \text{ночн}} \text{ kcal/hr}^*$$

or

$$Q_{\text{изб}} = Q_{\text{пачн}} - Q_{\text{ночн}} \text{ kcal/hr};$$

this excess heat flow is used to heat and vaporize the curtain, and also to superheat the vapor formed here, to the local temperature of the products of fuel combustion.

Under this condition, the quantity of liquid required for forming the curtain is determined from the equation of heat balance:

$$Q_{\text{изб}} \approx G_{\text{изб}} [C(t_{\text{кип}} + t_{\text{ночн}}) + r_{\text{исп}} + C_p(t_g - t_{\text{кип}})] \text{ kcal/sec}^{**}$$

i.e.,

$$G_{\text{изб}} = \frac{Q_{\text{изб}}}{C(t_{\text{кип}} - t_{\text{ночн}}) + r_{\text{исп}} + C_p(t_g - t_{\text{кип}})} \text{ kg/sec} \quad (9.59)$$

where C and C_p are the mean heat capacities of the liquid and of the gas formed from the liquid, respectively, in kcal/kg °C; $t_{\text{под}}$ and $t_{\text{кип}}$ are the temperature of the liquid as it is fed for the purpose of forming the curtain, and its boiling point at the local pressure in the chamber, respectively, in °C; t_g is the local gas temperature in the chamber, at the point where the curtain is formed; and $r_{\text{исп}}$ is the heat of liquid vaporization, at the local gas pressure in the chamber, in kcal/kg.

We must bear in mind that even if coolant feed for film-curtain formation is uniform and the chamber-liner flame tube has a uniform degree of finish, the length of the liquid film along the liner generatrix is not uniform or constant, and this is explained by the non-

$$*[Q_{\text{изб}} = Q_{\text{изб}} = Q_{\text{избыток}} = Q_{\text{excess}}.]$$

$$**[t_{\text{под}} = t_{\text{под}} = t_{\text{подача}} = t_{\text{feed}}; r_{\text{исп}} = r_{\text{исп}} = r_{\text{испарение}} = r_{\text{vaporization}}.]$$

uniformity of the cycle in the combustion-chamber volume and the unavoidable nonuniformity of local film heating resulting from the nature of chamber-head operation. Therefore, when protecting an engine-chamber liner by liquid films alone (without using regenerative cooling), the distance between the slots in the chamber flame tube must be less than the distance at which the liquid film is entirely vaporized.

Besides this, there is no proportional interdependence between mean film length \underline{l}_{pl}^* and the liquid-flow rate G'_{zav} needed for forming the film (for a given increase in \underline{l}_{pl} , a more than proportional increase of G'_{zav} is required), because the liquid is partially carried away into the flow of products of fuel combustion in view of the turbulence of these products, the presence of intensive oscillating waves on the surface of the film, and the difference in velocities between the liquid film and the products of fuel combustion.

These factors lead not only to partial detachment of the liquid film from the chamber-liner surface, but also cause intensive film vaporization.

In this connection, the actual flow rate G_{zav} of liquid for the formation of the chamber-liner film curtain must be greater than the theoretical flow rate G'_{zav} that was computed in accordance with Formula (9.59), i.e.,

$$G_{zav} = \frac{G'_{zav}}{\epsilon_{zav}} \text{ kg/sec,} \quad (9.60)$$

where ϵ_{zav} is the coefficient by means of which we consider the efficiency of the liquid film; it is determined experimentally and is a function of curtain-ring design (the nature of the method used

$$*\underline{l}_{пл} = \underline{l}_{pl} = \underline{l}_{plenka} = \underline{l}_{film}.$$

to supply liquid for forming the film), the initial layer thickness, the properties of the liquid, the design of the injector head and the nature of its operation, the combustion-chamber shape, the degree of finish of the liner flame tube, and of other factors. The value of ϵ_{zav} may vary within wide limits (from 0.80 to 0.95).

For a fine and reliable film curtain, the liquid must be fed through the slots, and at a definite velocity; otherwise, the curtain will be of little use since it will be flushed away by the gas stream, detached from the liner surface, and intensively vaporized.

If a liquid velocity w_{pl} for forming a film curtain through a slot has been selected, the required slot clearance δ_{shch}^* is determined from the equation of mass balance

$$G_{gas} = \pi d_g \delta_m w_{gas} \gamma_g$$

i.e.,

$$\delta_m = \frac{G_{gas}}{\pi d_g w_{gas} \gamma_g} \quad (9.61)$$

where d_g is the chamber-liner diameter along the slot generatrix; and γ_g is the specific weight of the combustible at the temperature at which it is fed into the chamber.

When film curtains are used to protect the liner, specific chamber thrust and thrust losses in this case are determined in accordance with the following formulas:

$$P_{ya, gas} = \frac{P}{G_g + G_{gas}} \quad (9.62)$$

$$\Delta P_{ya} = 100 \frac{P_{ya} - P_{ya, gas}}{P_{ya}} \quad (9.63)$$

and where P is the absolute engine-chamber thrust; G_g is the per-second propellant-flow rate to the engine chamber; P_{ud} is the effective

$$*[\delta_m = \delta_{shch} = \delta_{shchel} = \delta_{slot}]$$

specific engine-chamber thrust at zero combustible-flow rate for forming a curtain; and $P_{ud\ zav}$ is effective specific engine-chamber thrust when there is a combustible-flow rate for the purpose of forming a curtain.

The approximate method given above for designing an engine-chamber regenerative cooling system, with liquid curtains, is performed in the following sequence:

- 1) we compute the available specific heat flows $q_{1\ rasp}$ throughout the engine chamber, when there is no protective curtain;

- 2) we determine the excess heat flow Q_{1zb} which cannot be removed from the entire liner, or from separate parts of the liner where there is a greater heat-release rate, by purely regenerative cooling; we then compute the quantity G_{zav} of liquid required for forming the curtain, for efficient operation in the selected section;

- 3) we refine the design of the regenerative cooling system for the engine combustion chamber and nozzle, making allowance for the curtains.

SECTION 12. THE SEQUENCE OF DESIGNING A ZhrD-CHAMBER COOLING SYSTEM

The designing of ZhrD-chamber cooling systems consists basically of determining the nozzle and combustion-chamber inner-liner surface temperatures, the coolant temperature, the geometrical dimensions of the coolant passage, and the hydraulic losses in the passage.

Draft and control methods for designing engine-chamber cooling systems exist.

In the draft design, we determine feasible structural shape and optimum dimensions for the coolant passage throughout the length of the chamber, which will provide for reliable chamber cooling.

The control calculations give relatively less accurate results,

but they are not as laborious as the draft method.

In the control calculations, we tentatively select the design and dimensions for the flow section of the coolant passage through the chamber, on the basis of which we determine coolant velocity in the passage and the other characteristics, which permit us to evaluate the reliability and operating economy of the chamber under given operating conditions.

The initial data required for designing a ZhRD-chamber cooling system usually consists of:

- 1) combustion-chamber and nozzle configuration and the dimensions required (the chamber drawing);

- 2) inner-liner thickness throughout the chamber, and liner material, with the required physical characteristics (thermal-conductivity coefficient, ultimate strength, temperature-expansion coefficient, etc.);

- 3) per-second gas-flow rate in the engine and gas parameters throughout chamber (pressure, temperature, specific weight, velocity, etc.). Chamber coolant-passage flow section and coolant velocity therein may be tentatively assumed or determined from computations;

- 4) per-second propellant-component flow rate and propellant physical properties (heat capacity, thermal conductivity, viscosity coefficient, corrosiveness in relationship to the structural materials, etc.);

- 5) chamber injector-head design (head drawing), with injector characteristics (type, capacity, arrangement on the head, etc.).

The designing of a ZhRD-chamber cooling system is usually performed in approximately the following sequence.

1. Proceeding from the considerations of engine strength and the established service life, we tentatively assume the desired tem-

perature distribution for the gas-side liner surface throughout the length of the chamber. In the following computations, this temperature distribution is refined.

2. We divide the engine-chamber nozzle longitudinally into several (10-15) sections in each of which the specific heat flow may be assumed as constant and equal to the mean value of the specific heat flows at the boundaries of the chamber section under consideration. Close to the nozzle throat, where specific heat flow changes most rapidly, the sections must be of relatively shorter length; one of the chamber sections must pass through the nozzle throat.

3. We assume a number of values for the proposed gas-pressure distribution throughout the chamber and determine the other basic parameters (temperature, specific weight, and velocity), which correspond to these values of gas pressure, in accordance with the formulas in Section 6, Chapter III. In accordance with these parameters, we simultaneously compute the corresponding chamber gas-channel cross-section areas. The parameters and areas that are found are then presented in the form of curves, as functions of chamber length.

4. We determine convection, radiation, and total specific heat flows from the gases to the liner, in the selected chamber sections, in accordance with the corresponding formulas.

In accordance with the results of these computations, we derive the curves for the changes in q_k , q_r , and \underline{q} throughout the engine chamber.

We may assume that \underline{q} is constant throughout the combustion chamber and equal to the value of \underline{q} at the beginning of the convergent part of the nozzle. If appropriate experimental data are available, the values of \underline{q} may be accepted as variable throughout chamber length.

In practice, we sometimes use the method of recalculating specific heat flows, which were found by experimental methods in an existing engine chamber, for the engine chamber that is being designed. For such a recalculation, it is desirable to use experimental data for a chamber which operates on the same fuel as the chamber that is being designed, and has gas parameters in the combustion chamber that are close to the parameters for the chamber that is being designed.

This recalculation may be sufficiently rigorous only for the the chamber nozzle, where convection heat transfer between the gases and the engine-chamber liner plays an important part.

5. We determine, in succession, the areas S_1 of the gas-side liner surfaces for each selected chamber section, and multiplying them by the appropriate mean values of specific heat flows Q_1 (which were computed earlier) we find the quantity of heat which must be taken up by the coolant in each separate chamber section, i.e., we compute $\Delta Q_1 = S_1 q_1$. After this, we determine coolant preheating Δt_1 in the passage for each section and coolant preheating Δt_{zh} for the entire chamber.

Coolant temperature at the outlet from the chamber passage must not exceed the coolant boiling point or coolant decomposition (coking) temperature at the local pressure in the passage.

This condition must be observed particularly when the chamber is operating in a minimum regime, when coolant preheating is greater than in other, higher operating regimes.

If, from the condition for total coolant preheating, regenerative engine-chamber cooling appeared adequate, the following stage of design is the determination of liquid-side liner-surface temperature throughout the nozzle and combustion chamber.

6. We tentatively assume the interliner clearance along chamber

length, and compute clearance area and coolant velocity within the clearance (passage) for several (5-6) of the most characteristic passage sections.

It is desirable to make the interliner clearance uniform throughout the entire length of the chamber; however, if necessary, it may be variable in separate chamber sections, or throughout its entire length.

7. We determine liquid-side liner-surface temperature in the selected characteristic chamber sections. This temperature must be greater than coolant temperature throughout the entire length of the chamber. It is desirable that the value of $t_{p.zh}$ around the nozzle throat be close to coolant boiling point or decomposition temperature at the given pressure in the passage, or even somewhat higher than this limit (by 20-50°C), so that the heat-transfer coefficient α_{zh} may be increased and, by this means, the required coolant velocity in the passage be reduced, and consequently pressure losses in the passage may be reduced.

Repeated computations are usually required in order to obtain the desired value of this temperature throughout chamber length. Here, we change slightly the values of temperature $t_{p.g}$ that were assumed for computation. If the computed temperature $t_{p.g}$ differs from the value that was assumed earlier for computation by more than 5%, we must repeat the computations, having assumed a new intermediate value for this temperature (between the initially selected value and the value obtained as the result of the computations).

After this, it is necessary to provide the most feasible change in the interliner clearance, throughout the length of the chamber, from the viewpoint of structural and production considerations. Then, we may again determine the coolant velocity in the passage, the heat-

transfer coefficient α_{zh} , and finally, we find the values of $t_{p.zh}$ and $t_{p.g}$.

8. Finally, we determine coolant-pressure losses in the separate sections of the passage and throughout the entire chamber length, which are required for designing the engine fuel-feed system, using the corresponding formulas (see Section 13, Chapter X) for this purpose;

$$\Delta p_i = \xi \frac{l_i}{d_{ex i}} \frac{\gamma_i w_i^2}{2g} \text{ and } \Delta p_{\text{tot}} = \sum \Delta p_i,$$

where ξ is the loss coefficient, computed in accordance with formulas

$$\xi = \frac{0.3164}{\sqrt[4]{Re}} \text{ at } Re = 3 \cdot 10^3 + 10^5;$$

$$\xi = 0.0032 + \frac{0.221}{Re^{0.337}} \text{ at } Re = 10^5 + 10^6.$$

If ZhRD thrust is regulated, we must design the chamber-cooling system for two operating regimes — maximum and minimum. In a maximum engine-operating regime, heat-flows from the gases to the chamber liner are greater, as a result of which gas-side liner-surface temperature may exceed its permissible limits. When the engine shifts into a minimum operating regime, coolant-flow rate (propellant-flow rate to the combustion chamber) is reduced almost proportionally to gas pressure in the combustion chamber, and heat flows decrease approximately proportionally to a power of 0.8 in relationship to gas pressure. Higher coolant preheating is obtained when the engine operates in a minimum regime than when it operates in a maximum regime, which also may cause excessive inner chamber-liner heating.

If, through computations, we establish the fact that gas-side liner-surface temperature, coolant heating in the passage, or liquid-side chamber-liner surface temperature is higher than the safely

permissible limit, we may, in addition to regenerative cooling, protect the inner chamber liner against overheating by means of one or several curtains of combustible. This is usually associated with some change in engine-chamber design in relationship to the initially selected version.

An example of the designing of a ZhRD-chamber regenerative cooling system, performed in approximation, is shown in the work of G. D. Sinyarev and M.V. Dobrovol'skiy.*

SECTION 13. DETERMINING TEMPERATURE STRESSES IN A ZhRD-CHAMBER LINER

Temperature stresses in an engine-chamber flame tube are, to a considerable degree, a function of liner design and of the thermal conductivity of the material.

Thermal conductivity is one of the most important characteristics of the thermal properties of a metal; the other important thermal properties are strength and rigidity at high temperatures. Therefore, when selecting a material for the inner chamber liner, and designing the chamber-cooling system, we must pay special attention to the thermal-conductivity coefficient for this material, as well as to this coefficient as a function of temperature.

For industrial metals at ordinary temperatures, $\lambda \approx 10$ to 340 kcal/m hr $^{\circ}\text{C}$. The most efficient heat-conducting metal is red copper ($\lambda = 300-340$), and then, in descending order: aluminum (180-200), brass (80-100), carbon steels (40-80), bronze (30-40), and alloy steels (10-20).

As the carbon content in steel is increased, λ is reduced. Additions to steel, for the purpose of increasing its resistance to heat and its capability to maintain its strength at high tempera-

*G.B. Sinyarev and M.V. Dobrovol'skiy. Zhidkostnyye Raketnyye Dvigateli [Liquid-propellant Rocket Engines], Oborongiz [State Publishing House for Defense Industry], 1957.

tures, decreases λ .

The thermal-conductivity coefficient is, essentially, a function of metal composition and temperature. As temperature increases, the value of λ , for carbon steels and copper, is reduced, and for alloy steels, aluminum, and aluminum alloys, λ is increased (see Figs. 9.16 and 9.17).

The value of λ as a function of temperature is determined experimentally for different metals. If accurate experimental data are lacking, the thermal-conductivity coefficient for tempered carbon steels within temperature limits of 0 to 500°C, may be determined, in approximation, in accordance with the following empirical formula*

$$\lambda = a + b \Sigma + c \Sigma^2 \text{ kcal/M m}^\circ\text{C} \quad (9.64)$$

where $a = 66 - 5.74 \cdot 10^{-2}t$; $b = 29.4 - 8.5 \cdot 10^{-2}t + 0.7 \cdot 10^{-4}t^2$; $c = 8.0 - 3.4 \cdot 10^{-2}t + 0.36 \cdot 10^{-4}t^2$; t is the temperature at which the thermal-conductivity coefficient is determined; and $\Sigma = \text{Si} + \text{Mn} + \text{P} + \text{S}$ is the total quantity of admixtures, of corresponding elements, to the iron, in weight percentages.

This formula is suitable for determining the value of λ for steels containing admixtures to the amount of $\Sigma = 0.1 - 2.0\%$ (Table 9.5); the formula is accurate to $\pm 4\%$.

The thermal-conductivity coefficient for chrome-nickel austenitic steels, within temperature limits of 100 to 900°C, may be determined, in approximation, in accordance with the formula**

$$\lambda = 13.3 - a + (1.1 + b) 10^{-2} \text{ kcal/M m}^\circ\text{C} \quad (9.65)$$

where $a = 10(\sigma - 0.5)$; $b = 1.15(\sigma - 0.5)$; t is the temperature at which the thermal-conductivity coefficient is determined;

*"Теплоэнергетика" [Heat and Power Engineering], VTI [All-Union Heat Engineering Institute of the] USSR, 1955, No. 9.

**op cit.

$$\sigma = \frac{C}{12} + \frac{Si}{28} + \frac{Mn}{55} + \frac{Cr}{52} + \frac{Ni}{59} + \frac{W}{184} + \frac{Nb}{93} + \frac{Mo}{96} + \text{etc.}$$

is the characteristics of the steel composition, representing the total amount of grams of the elements, with the exception of iron, contained in 100 g of steel.

TABLE 9.5

Values of λ for Carbon Steels when $\Sigma = 0.1-2.0\%$ for Temperature Intervals of 0-500°C

$\Sigma\%$	0,1	0,2	0,4	0,6	0,8	1,0	1,2	1,4	1,6	1,8	2,0
$t^\circ\text{C}$											

1) Коэффициент теплопроводности λ в ккал/м час °C

0	63,1	60,4	55,5	51,2	47,6	44,6	42,2	40,5	39,5	39,1	39,2
50	60,6	58,3	54,0	50,3	47,0	44,3	42,1	40,3	39,0	38,4	38,1
100	58,1	56,1	52,3	49,0	46,1	43,6	41,5	39,8	38,4	37,6	37,0
200	52,9	51,5	48,7	46,2	43,9	41,8	39,9	38,2	36,8	35,4	34,4
300	47,8	46,8	44,9	43,1	41,2	39,6	38,0	36,5	35,3	33,7	32,4
400	42,3	41,7	40,4	39,1	37,8	36,6	35,4	34,2	32,9	31,8	30,6
500	36,9	36,4	35,5	34,7	33,8	32,9	32,0	31,1	30,2	29,5	28,7

1) Thermal-conductivity coefficient λ , in kcal/m hr °C.

Here C, Si, Mn, etc., are the elements in the steel (in percentages by weight); the denominators in the formula are the atomic weights of these elements.

This formula is acceptable for determining the λ of steels containing $\sigma = 0.5-0.8$.

Low-alloy steels have a $\sigma = 0.048-0.99$; in stainless chrome steels, $\sigma = 0.273-0.63$; and in chrome-nickel austenitic steels, $\sigma = 0.5-0.9$.

Table 9.6 shows the values of λ for chrome-nickel steels, computed in accordance with Formula (9.65) (for these steels, the accuracy of the formula is $\pm 4\%$); for chrome-manganese austenitic steels, the value of λ is approximately 10% lower than the tabular data.

Table 9.7 shows the approximate values of thermal conductivity λ ,

heat capacity C , and thermal-diffusivity coefficient a (cm^2/sec) for several heat-resistant materials, and Figs. 9.21 and 9.22 give ultimate strength σ_b and linear-expansion coefficients α , respectively, as functions of temperature.

TABLE 9.6

Values of λ for Chrome-Nickel Steels for a Temperature Interval of 100-900°C.

$t, ^\circ\text{C}$	100	200	300	400	500	600	700	800	900
$\sigma\%$									
1) Коэффициент теплопроводности λ в $\text{ккал/м час } ^\circ\text{C}$									
0,5	14,3	15,4	16,5	17,7	18,8	19,9	21,0	22,1	23,2
0,55	14,0	15,1	16,3	17,4	18,6	19,7	20,9	22,1	23,2
0,60	13,5	14,7	16,0	17,2	18,4	19,6	20,8	22,0	23,2
0,65	13,0	14,2	15,6	16,8	18,2	19,4	20,7	21,9	23,2
0,70	12,6	14,0	15,3	16,6	18,0	19,3	20,6	21,9	23,2
0,75	12,2	13,6	15,0	16,4	17,7	19,1	20,5	21,9	23,2
0,80	11,8	13,2	14,6	16,1	17,5	19,0	20,4	21,9	23,2

1) Thermal-conductivity coefficient λ , in $\text{kcal/m hr } ^\circ\text{C}$.

The greater the value of λ , the less the temperature difference in the chamber liner, which is expressed by the formula

$$\Delta t = t_{n,r} - t_{n,m} = \frac{q\delta}{\lambda},$$

and the more favorable liner operating conditions will be from the viewpoint of liner temperature stresses.

From the equation given above we obtain the ratio

$$\frac{q}{\lambda} = \frac{\Delta t}{\delta} \text{ degrees/mm} \quad (9.66)$$

which is called the liner temperature gradient.

Here, λ represents the mean temperature-conductivity coefficient for the metal, determined at the mean temperature

$$t_{cp} = \frac{t_{n,r} + t_{n,m}}{2} \text{ } ^\circ\text{C}.$$

The enormous heat-flows originating in the liner lead to great temperature gradients across liner thickness, which, for a steel liner,

amount to several hundred degrees (Fig. 9.23).

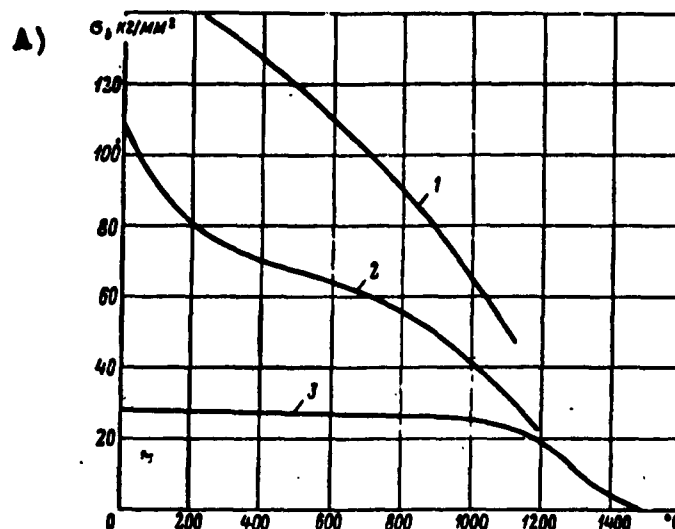


Fig. 9.21. Ultimate strength σ_b as a function of temperature. 1) Tungsten; 2) molybdenum; 3) aluminous [sic] oxide; A) σ_b kg/mm².

In steel chambers for contemporary engines, $q/\lambda \approx 100-300^\circ/\text{mm}$. These figures show that as an engine operates, extremely large thermal stresses originate in the chamber liner, and this reduces liner strength. The hotter liner layers, attempting to expand, stretch the outer liner layers, and the latter, resisting the stretching, compress the inner liner layers (the hotter liner layers are compressed and the cooler liner layers are stretched). For this reason, temperature stresses have maximum values at the gas-side and liquid-side liner surfaces, and in the center of the liner they are close to zero. Since the gas-side surface temperature is higher than the liquid-side surface temperature, the greatest temperature stresses occur at the gas-side surface.

If temperature stresses exceed the yield point for the liner material, they may cause marked plastic deformation of the metal, which, under certain conditions will lead to permature liner destruction under the action of static load.

The greater the liner-material thermal-conductivity coefficient, the smaller the temperature stresses, other things being equal [see Formula (9.66)]. Therefore, it is advisable to select the material with the highest possible thermal-conductivity coefficient for the chamber liner. The greater the value of λ , the more favorable the liner operating conditions (other things being equal). This also explains the fact that, in some cases, ZhRD designers try to make the inner chamber liner of copper.

TABLE 9.7

Approximate Values of Thermal-Conductivity Coefficient λ , Heat Capacity C and Thermal-Diffusivity Coefficient a as Functions of Temperature

t, °C	1) Вольфрам спеченный (пористый)			2) Молибден спеченный			3) Окись алюминия (пористая)			4) Карбид кремния (пористый)		
	λ	C	a	λ	C	a	λ	C	a	λ	C	a
20	0,38	0,026	0,76	0,33	0,060	0,53	—	—	—	—	0,14	—
100	—	—	—	0,32	0,065	0,50	0,033	0,20	0,047	0,0595	0,233	0,079
200	0,35	0,026	0,69	0,30	0,063	0,46	0,025	0,20	0,0357	—	—	—
300	—	—	—	0,29	0,0645	0,43	0,021	0,23	0,026	0,0500	0,277	0,0564
400	0,31	0,027	0,59	0,28	0,066	0,41	0,019	0,23	0,0236	0,046	0,282	0,050
500	—	—	—	0,27	0,0675	0,38	0,016	0,247	0,0185	0,0425	0,275	0,0480
600	0,28	0,027	0,53	0,26	0,069	0,36	0,015	0,247	0,0174	—	—	—
700	—	—	—	0,255	0,070	0,35	0,0143	0,256	0,016	—	—	—
800	0,26	0,028	0,49	0,248	0,0715	0,33	0,014	0,256	0,0155	0,0365	0,225	0,050
900	—	—	—	0,240	0,073	0,32	0,013	0,263	0,014	—	0,129	—
1000	0,25	0,028	0,47	0,235	0,075	0,30	0,0128	0,263	0,0138	—	—	—
1100	—	—	—	0,23	0,077	0,29	0,0123	0,269	0,013	—	—	—
1200	0,24	0,029	0,43	0,225	0,078	0,28	0,012	0,269	0,0127	—	—	—
1300	—	—	—	0,22	0,080	0,26	0,012	0,275	0,0125	—	—	—

1) Sintered tungsten (porous); 2) sintered molybdenum; 3) aluminum oxide (porous); 4) silicon carbide (porous).

Among copper alloys for engine-chamber liners, the special bronzes (cadmium and chromium), which exhibit high strength and electrical conductivity, deserve attention: their thermal-conductivity coefficients have, as yet, been little studied.

Temperature stresses in a cylindrical liner, which do not exceed the limit of proportionality for the material, may be determined in accordance with the formula for the theory of elasticity:

$$Z_{oces} = \frac{E\alpha}{2(1-\mu)} \Delta t = \frac{E\alpha q b}{2(1-\mu)\lambda} \text{ kg/mm}^2 \quad (9.67)$$

where Z_{osev}^* represents the temperature stresses in the liner, in the axial direction (it is assumed that the chamber-liner section under

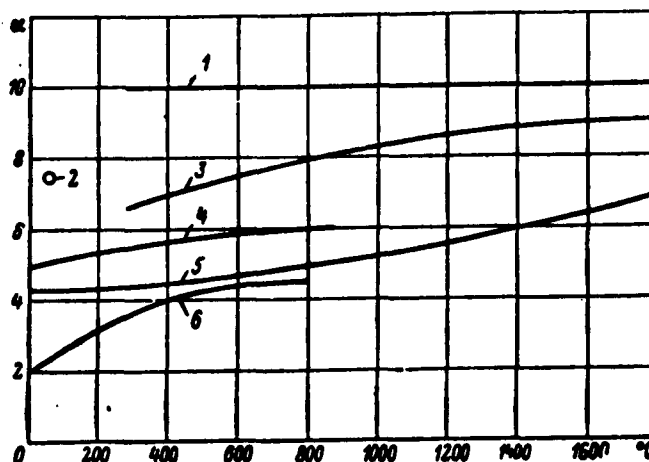


Fig. 9.22. Linear-expansion coefficient α as a function of temperature. 1) α -graphite; 2) graphite; 3) aluminum oxide; 4) molybdenum; 5) tungsten; 6) silicon carbide.

investigation is a tube of sufficient length to permit us to neglect the effect of the free ends); E is the modulus of elasticity for the liner material, in kg/mm^2 , taken from the table; α is the linear-expansion coefficient for this material; μ is the Poisson coefficient; and Δt is the temperature difference across the liner thickness.

This formula may be used only in those cases in which the condition $Z_{osev} \leq \sigma_s$ is not violated (where σ_s is the yield point for the liner material, also a function of temperature). When $Z_{osev} > \sigma_s$, the formula mentioned above is not suitable for computing temperature stresses in a chamber liner.

$$*[Z_{oces} = Z_{osev} = Z_{osevoye} = Z_{axial}.]$$

The change in the yield point for the material of the liner section being studied, as a function of temperature, may, with sufficient accuracy for practical purposes, be considered as linear, i.e.,

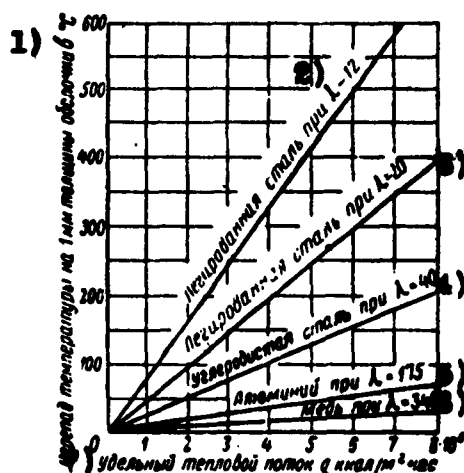


Fig. 9.23. Approximate temperature difference across 1 mm of chamber-liner thickness (liners made of different materials) as a function of specific heat flow. 1) Temperature difference across 1 mm of liner thickness, in °C; 2) alloy steels, when $\lambda = 12$; 3) alloy steels, when $\lambda = 20$; 4) carbon steel, when $\lambda = 40$; 5) aluminum, when $\lambda = 175$; 6) copper, when $\lambda = 340$; 7) specific heat flow q , kcal/m² hr.

$$\sigma_s = \sigma'_s - k_s \Delta t = \sigma'_s - k_s \frac{q^0}{\lambda} \text{ kg/mm}^2, \quad (9.68)$$

where σ'_s is the extrapolated yield point for the liner material at liquid-side surface temperature; and k_s is the coefficient of proportionality for this material.

Since the yield point σ_s is lower at the gas-side liner surface than at the liquid-side liner surface, the first plastic deformation may originate at the gas-side surface.

The magnitude of the heat flow, at which plastic deformation appears in the chamber liner, is determined from the equation

$$z_s = Z_{\text{огн}} = \frac{F q^0}{2(1-\mu)\lambda}.$$

i.e.,

$$q = \frac{\sigma_s 2\lambda(1-\mu)}{E z_s} \text{ kcal/m}^2 \text{ hr.} \quad (9.69)$$

If the quantity q is greater than that computed in accordance with this formula, a plastic compression zone is formed in the liner, on the gas-side surface. As the value of q increases still further, a plastic deformation zone is also formed at the liquid-side liner surface, which will be a zone of elongation. Only a narrow strip in the central part of the liner thickness will remain elastic.

SECTION 14. SELECTING MATERIAL FOR ENGINE-CHAMBER INNER LINER AND DETERMINING LINER THICKNESS

If the thickness for the inner engine combustion-chamber and the nozzle liner is not given, it may be determined by computation. In the liner, under the action of the pressure difference Δp between the coolant in the jacket and the gas inside the conditional cylindrical combustion-chamber or nozzle section under investigation, the following stress arises:

$$\sigma = \frac{\Delta p r}{\delta} \text{ kg/mm}^2 \quad (9.70)$$

where δ is the liner thickness for the section being studied, in mm; and r is the mean diameter (radius) of this liner, in mm.

The force operating on 1 mm of liner-surface for the section being studied, according to the previous equation, may be expressed by the formula

$$P = \sigma \delta = \Delta p r \text{ kg/mm}$$

If we denote liner thickness by dx , we obtain

$$P = \int \sigma dx.$$

The ultimate strength σ_b , in kg/mm^2 , can also serve as a liner-material characteristic.

Since the strength of the material is not constant across liner thickness because of temperature stresses, calculations of liner strength must be performed, not in accordance with permissible stresses, but in accordance with permissible loads.

The maximum permissible load on a liner, per mm of length, may be expressed by the formula

$$P_{\text{max}} = \int \sigma_b dx \text{ kg/mm}$$

where σ_b is the ultimate strength for the given liner material, in kg/mm^2 under standard conditions; it is taken from the table or from

the curve that shows the ultimate strength as a function of temperature.

Since the liner temperature varies across liner thickness, the value of σ_b must be determined by taking temperature change into consideration.

One may assume, with sufficient accuracy for all practical purposes, that the ultimate strength of the liner metal changes as a function of temperature, in accordance with the linear law;

$$\sigma_b = \sigma'_b - k_b \Delta t \text{ kg/mm}^2 \quad (9.71)$$

where σ'_b is the extrapolated ultimate strength of the liner metal, at the liquid-side liner-surface temperature; k_b is a coefficient of proportionality for the liner material; $\Delta t = qx/\lambda$ is the temperature difference across the liner; and λ is the thermal-conductivity coefficient for the liner material.

Substituting the expression for Δt into the last formula, we finally obtain

$$\sigma_b = \sigma'_b - k_b \frac{qx}{\lambda} \text{ kg/mm}^2 \quad (9.72)$$

In this case, the formula for the value of p_{dop} takes the form

$$P_{don} = \int_0^{\delta} \sigma_b dx = \int_0^{\delta} \left(\sigma'_b - k_b \frac{qx}{\lambda} \right) dx$$

or

$$P_{don} = \sigma'_b \delta - \frac{k_b q \delta^2}{2 \lambda} \text{ kg/mm} \quad (9.73)$$

Assuming various values of q and λ for the liner, we may construct a curve showing p_{dop} as a function of δ (Fig. 9.24).

By determining the values of q and P_{dop} for each liner section by computations, using this curve, one may determine liner thickness δ for the selected material, taking into account the temperature stresses caused by the temperature difference across liner thickness.

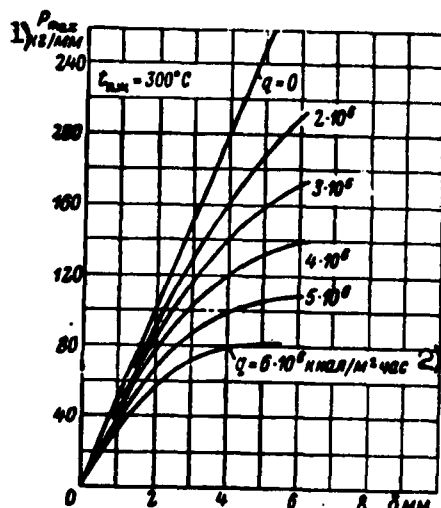


Fig. 9.24. Maximum permissible tensile stress for a steel liner at various thicknesses and specific heat flows when $t_{p.zh} = 300^\circ\text{C}$. 1) p_{max} , kg/mm; 2) $q = 6 \cdot 10^6$ kcal/m² hr.

When the value of q is increased, the optimum thickness for a steel liner must be reduced, and when $q \approx 10^7$ kcal/m² hr, liner thickness is 1 mm.

The liner carrying capacity for an unreinforced design, under existing ghRD operating conditions, is extremely small, and is clearly inadequate for reliable chamber operation. The use of reinforced liners makes it possible to design an efficient engine chamber with a steel inner liner of quite small thickness (of the order of 1 mm) and by this means, to provide for a high value of $t_{p.zh}$ at considerable heat flows. Because of this, external chamber cooling, with a reinforced liner design, makes it possible to develop engines with a higher P_{ud} than is possible with unreinforced designs.

If we also consider the longitudinal temperature stresses for the inner chamber liner, the required liner thickness will be somewhat greater.

Formula (9.73) shows that as heat flow increases, the maximum permissible load capacity of the inner chamber liner (the liner carrying capacity) is reduced sharply, since to maintain a high temperature $t_{p.zh}$ (when $\delta = \text{const}$) we require an increase in $t_{p.g}$, which causes a marked deterioration in the liner-metal mechanical properties. Therefore, if

At relatively higher heat flows, a further increase in the value of $t_{p.g}$ and a reduction of inner chamber-liner thickness are required in order to make the external cooling system more efficient. However, at the present time, the potentials for raising $t_{p.zh}$ by means of increasing $t_{p.g}$ and reducing liner thickness are, in practice, quite small, since in contemporary chambers, δ is already 1 mm, and the value of $t_{p.g}$ is 1000°C .

Computations show that purely regenerative cooling for a steel engine-chamber inner liner can, in practice, be feasible for heat flows of not more than $10^7 \text{ kcal/m}^2 \text{ hr}$. At higher heat flows, chamber cooling is possible only upon condition that one uses an inner liner made of a material that conducts heat better than steel, by means of which we attain a small difference in temperatures ($t_{p.g} - t_{p.zh}$) and consequently, a lesser reduction in the liner strength properties due to the temperature difference across liner thickness.

Since the thermal conductivity of copper and copper alloys is several times greater than that of any brand of steel, the carrying capacity of a copper chamber liner, as heat flows increase, is reduced less than that of a steel liner. For just this reason, a copper chamber liner, other things being equal, may be made with a relatively greater thickness, and, consequently, with a greater carrying capacity, even at heat flows above $3 \cdot 10^7 \text{ kcal/m}^2 \text{ hr}$.

The use of steel for fabrication of inner chamber liners makes it possible to develop ZhRD that are relatively cheap and simple to produce and operate.

Many brands of steel are corrosion-resistant to oxidizers based on nitric acid. In this respect, steel chambers satisfy the requirements set forth for mass-produced ZhRD missiles. At the same time, however, external cooling does not provide for an increase in specific

chamber thrust when a steel chamber is used.

The use of internal liner protection by means of combustible made it possible to develop steel-liner chambers with a greater P_{ud} than is possible with external cooling alone.

One may draw the following conclusions on the basis of the material given above:

1. The basic criteria for evaluating the mechanical properties of a material for an inner combustion-chamber or nozzle liner are the ultimate strength and the thermal conductivity of the material, at liner operating temperature.

2. Liner strength increases up to a certain thickness, above which temperature stresses due to the great temperature difference across liner thickness bring the safety factor evolved by the additional liner thickness to naught.

3. The lower the thermal conductivity of the material at a given heat flow, the more rapidly the ultimate strength of the material is reduced by a rise in temperature (the lower the heat resistance of the material), the lower the liner-thickness limit (according to item 2).

4. If the magnitude of specific heat flow is less than $5 \cdot 10^6$ kcal/m² hr, copper is more suitable for the liner than other materials; copper yields to steel in strength, specific weight, and resistance to corrosion.

5. For heat flows of the order of 10^7 kcal/m² hr or above, copper and its alloys (brass and bronze) are the most suitable materials for a liner, since other materials are not capable of conducting such quantities of heat with a liner thickness of more than 1 mm (a thinner liner is difficult to manufacture).

6. The suitability of a material for an engine combustion-chamber

or nozzle inner liner and the required liner thickness may be determined by deriving curves in coordinates of liner strength and liner thickness for different materials at various liquid-side wall temperatures and heat flows.

7. When selecting a material for a liner, it is also necessary to consider liner-material plasticity, weight, heat resistance, manufacturing properties, cost, etc.

8. As an engine operates, the inner liner is subjected to considerable thermal and static loads; therefore, it is necessary to select a liner material that has high stability. The liner-material stability is a function of thermal conductivity and heat resistance. The greater the thermal conductivity of the material, the more favorable liner operating conditions will be.

An increase in liner-material heat resistance permits reducing liner thickness and relieving liner operating conditions.

Chapter X

PLANNING AND DESIGN OF ZhRD FUEL-FEED SYSTEMS

The next stage in developing the engine is design and planning of the system to feed fuel into the combustion chamber.

Delivery of the theoretically required per-second fuel-component flow rates from the tanks into the ZhRD combustion chamber under the specified constant pressure is an extremely important and complex problem in the design of the engine.

At the present time, there are several different types and configurations of ZhRD fuel-feed systems; these possess various advantages and disadvantages, by virtue of which one or another of these feed systems may prove most suitable under fully defined utilization conditions.

The fuel-feed system is of very great importance for normal and economical operation of the ZhRD. However, little study has as yet been devoted to the operation of the various fuel-feed systems. Most neglected of all are the processes that involve the working gas in pressure-fed fuel-feed systems, with consideration of the heat exchange between this gas and the pipeline and tank walls, and with the liquid - with its surface variable during flight of the missile, the variable nature of the washing of this liquid by the gas, partial evaporation and mixing of the vapors formed with the gas, condensation of the latter's vapors in the tank, etc.

The ZhRD's fuel-feed system should be not only simple in design,

compact, and efficient in operation, but should also have a small specific weight, i.e., weight per 1 kg of fuel used.

The weight characteristic of each fuel-feed system is a function of many different factors, such as: feed pressure, thrust and operating time of the engine, its function, etc.

For rational selection of a fuel-supply system, it is necessary to give a comparative evaluation with existing systems for the specified physical operating conditions of the engine being designed. Here, the most difficult matter is to establish the weight of the proposed system, which does not yet exist. Theoretical solution of this problem is not always possible, while the existing statistical data on which the determination might be based to some extent are still inadequate. At the present time, only approximate solution of this problem is possible.

The present chapter presents a brief discussion of existing ZhRD fuel-feed systems and their advantages and disadvantages, and sets forth the fundamentals of their design, as well as illuminating other problems, so that the total content may be of assistance in designing an efficient fuel-feed system.

SECTION 1. BASIC TYPES OF ZhRD FUEL-FEED SYSTEMS, THEIR ADVANTAGES, DISADVANTAGES, AND RANGES OF APPLICATION

The combustible and oxidizer are usually delivered from the tanks into the ZhRD's combustion chamber either by a gas under pressure or by means of pumps.

The aggregate of engine components that ensure delivery of the fuel components from the tanks into the combustion chamber is normally known as the fuel-feed system.

The ZhRD's fuel-supply system must make provision for fueling the engine, storage of the fuel in its tanked state, starting the engine,

and subsequent delivery of the fuel components from the tanks into the combustion chamber in the specified weight proportions and quantities during operation, as well as necessary drainage of the liquids from the system.

In the general case, the engine's fuel-supply system consists of the following elements:

- 1) tanks for the combustible, oxidizer, and auxiliary substances;
- 2) a unit to set up feed pressure behind the working substances to deliver them to their point of application;
- 3) pipelines and fittings (inside-tank fuel intake units, filler and drain plugs, cutoff and nonreturn valves, etc., gate valves, pressure relays, pressure reducer, burst diaphragms, throttling disks, and other elements).

Physically, the elements of the ZhRD fuel-feed system may take a wide variety of forms and may be combined in different ways; for this reason, there is, at the present time, a large number of fuel-supply-system combinations.

The main element in the engine's fuel-supply system, and that which determines all of its other elements, is the unit that sets up the necessary pressure to feed the working components to their places of utilization.

In accordance with the type of unit used here, there are now two basic and most characteristic ZhRD fuel-feed systems: the pressure-fed and fuel-fed types.

The pressure-fed ZhRD fuel-feed system may incorporate one of the following units:

- a) a gas pressure accumulator (GAP)*, which is a tank containing

* [ГАП = GAP = газовый аккумулятор давления = (compressed gas pressure accumulator.)]

a reserve of the compressed gas (air, nitrogen, helium) necessary to force the combustible and oxidizer from the tanks into the engine combustion chamber (see Fig. 10.1);

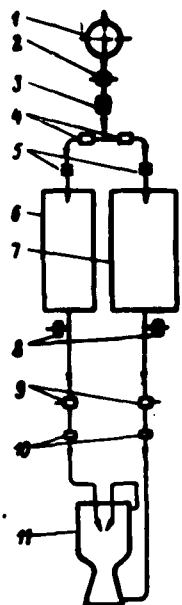


Fig. 10.1. Schematic diagram of pressure-fed ZhRD system with GAD.
1) Compressed air tank; 2) release valve with power cartridges; 3) compressed-air pressure reducer; 4) nonreturn valves; 5) free-burst diaphragms; 6) combustible tank; 7) oxidizer tank; 8) pressure relay; 9) cutoff valves with powder cartridges; 10) regulating disks; 11) engine chamber.

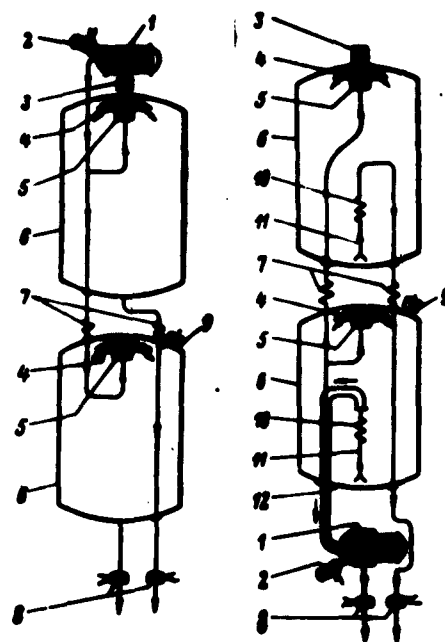


Fig. 10.2. Schematic diagram of pressure-fed ZhRD fuel-feed system with PAD.
1) Solid-propellant pressure accumulator (PAD); 2) starting powder chamber with electric ignition; 3) constant-pressure valve; 4) gas reflector; 5) nonreturn valve; 6) propellant tanks; 7) compensators in propellant pipelines; 8) forced-burst diaphragms; 9) pressure relays; 10) bellows of rotary-type intake; 11) rotary intake; 12) gas tubing.

b) a solid-propellant pressure accumulator (PAD), which is a unit capable of producing hot gas at a definite pressure in the form of the products of slow combustion of a powder charge, as required to pressurize the combustible and oxidizer from the tanks into the engine's combustion chamber (Fig. 10.2);

c) a liquid-propellant pressure accumulator (ZhAD)*, which is a

* [ПАД = PAD = porokhovoy akkumulyator davleniya = powder (solid-propellant) pressure accumulator (gas generator).]

unit that generates a hot gas at a definite pressure in the form of the combustion products of the fuel components, as necessary to displace the combustible and oxidizer from the tanks into the engine combustion chamber (Fig. 10.3).

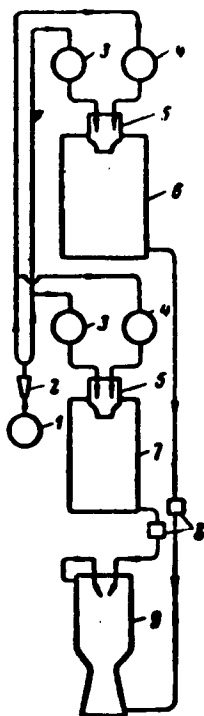


Fig. 10.3. Schematic diagram of pressure-fed ZhRD fuel-feed system with ZhAD.
1) Compressed-air bottle;
2) air-pressure reducer;
3) and 4) tanks for auxiliary fuel components;
5) gas generator; 6) tank for main oxidizer; 7) tank for main combustible;
8) cutoff (control) valves or burst diaphragms; 9) engine chamber.

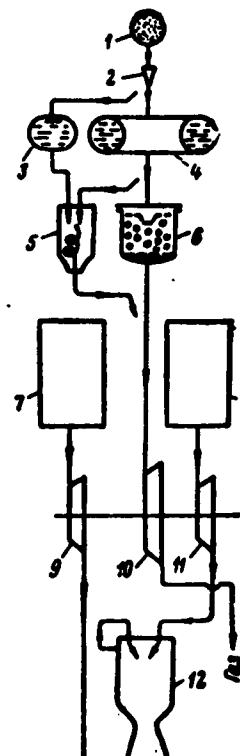


Fig. 10.4. Schematic diagram of turbopump assembly of ZhRD fuel-feed system with hydrogen-peroxide vapor-gas generator (with solid and liquid catalysts for the hydrogen peroxide).
1) Compressed-air bottle;
2) pressure reducer; 3) tank for aqueous solution of sodium permanganate; 4) tank for aqueous solution of hydrogen peroxide; 5) reactor for hydrogen peroxide and liquid catalyst; 6) reactor for hydrogen peroxide and solid catalyst; 7) combustible tank; 8) oxidizer tank; 9) combustible centrifugal pump; 10) vapor-gas turbine; 11) oxidizer centrifugal pump; 12) engine chamber. A) Gas.

Pressure-fed fuel-feed systems with the above three types of pressure accumulators are sometimes known respectively as the gas-bottle, gas-powder, and gas-generator fuel-feed systems.

A pump-fed ZhRD fuel-feed system may have:

1) mechanical pump drive off the main engine of the missile (in much the same way as in certain aircraft ZhRD - the superperformance rockets),

2) independent pump drive in the form of a vapor-gas turbine or other type of engine.

The systems of fuel feed by turbine-driven centrifugal or screw pumps are generally known as turbopump fuel-feed systems.

In principle, the following may be used as working gases to feed the turbine of a TNA;

1) a vapor gas obtained by decomposition of 80-82 percent hydrogen peroxide in a "cold-type" vapor-gas generator (Fig. 10.4);

2) the gas obtained as a result of combustion of the basic or auxiliary fuel components in a "hot-type" vapor-gas generator (Fig. 10.5);

3) gas scavenged from the engine combustion chamber (Fig. 10.6);

4) powder gas obtained by slow combustion of a powder charge in a special chamber;

5) compressed gas loaded onto the missile in a special bottle.

The fuel tanks in any pressure-fed ZhRD fuel-feed system are pressurized to a level slightly higher than the combustion-chamber pressure. In the turbopump system, on the other hand, the fuel tanks are virtually free of gas pressure (the gas pressure in the tanks generally does not exceed $2-3.5 \text{ kg/cm}^2$), with the result that their weight is relatively low.

Before entry into the turbine, the products of fuel combustion

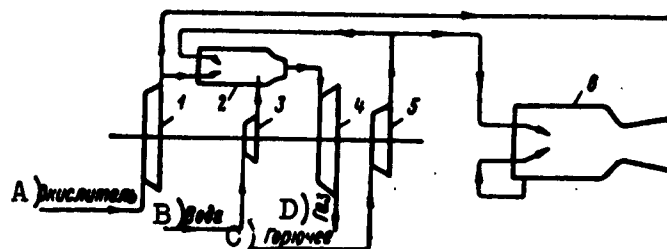


Fig. 10.5. Schematic diagram of turbopump-type fuel-feed system with "hot" gas generator.

- 1) Oxidizer-feed pump; 2) gas generator;
3) pump feeding water into reactor; 4) vapor-gas turbine; 5) combustible-feed pump;
6) engine chamber. A) Oxidizer; B) water;
C) combustible; D) gas.

in a vapor-gas generator or combustion products withdrawn directly from the combustion chamber must be cooled to a temperature (500-850°C) that can be safely tolerated by the turbine blades.

One of the most important problems with which it is necessary to deal in using turbopump feed systems is cavitation in the centrifugal pumps. To ensure cavitation-free operation of the pumps with a sufficiently high number of rpm, it is necessary to provide a head in front of them; the greater this head, the higher the speed of the pumps that can be used and the smaller will be the weight and dimensions of the TNA.

In accordance with their operating principles, contemporary ZhRD fuel-feed systems are classified as single-shot systems that frequently do not provide for regulation of fuel-flow (thrust) and are used in missile and aerial-torpedo engines and multiple-use systems, which provide regulation of fuel flow in the majority of cases and are usually used in aviation sustainer engines.

The most important characteristic of any ZhRD fuel-feed system is its specific weight, which is defined as the ratio of the total system weight $G_{s.p}$ to the fuel-tank volume V_B^* , i.e.,

* [Subscript B = B = Bak = tank.]

$$\gamma_{\text{tot}} = \frac{G_{\text{tot}}}{V_{\text{tot}}} \text{ kg/liter.} \quad (10.1)$$

The total weight of the fuel-feed system can also be referred to the weight of the fuel margin in the tanks:

$$G_t \approx \gamma_t V_t \text{ kg,} \quad (10.2)$$

where γ_t is the specific weight of the fuel in the tanks in kg/liter.

The following basic specifications are laid down for any type of fuel-feed system:

- 1) simplicity, compactness, and low design weight;
- 2) uniformity in the feed of the working components to their point of application and ease of controlling the engine;
- 3) high economy and operational dependability;
- 4) low manufacturing cost and convenience in operation.

Fig. 10.6. Schematic diagram of turbopump ZhRD fuel-feed system with withdrawal of gas from combustion chamber of engine and cooling of gas to specified temperature by addition of a certain quantity of combustible.

1) Combustible tank; 2) oxidizer tank; 3) combustible pump; 4) gas turbine; 5) oxidizer pump; 6) gas starter of turbine; 7) mixture chamber (hot gas with supplementary combustible); 8) engine chamber.

Since the engine must sometimes vary its developed thrust stepwise and cut in and out of operation periodically, it is further required in this case that the fuel-feed system ensure a strictly determined thrust-variation pattern and dependable starting and stopping of the engine when operating conditions require it.

The weight and economy characteristics of the different types of fuel-feed systems vary differently with variation of the engine's combustion-chamber pressure and thrust (per-second fuel component flow rates) and its elapsed operating time (propellant reserve in tanks)

and accordingly have different optimum values for the parameters and different ranges of most effective application in accordance with the mission of the device.

The ranges and limits of expedient application of one or another ZhRD fuel-supply system and its individual units have not yet been precisely established.

The prime factor in determining selection of the type of fuel-feed system and the individual elements in it is specific weight, while the comparative design complexity, cost, and economy of operation follow in importance.

In the design of an engine, the appropriate type of fuel-feed system and the design features of its individual elements are usually governed by the mission, thrust, operating time, and operating regime of the engine, as well as weight, production, economy, operational, and other considerations. In this connection, it will be advisable to devote brief attention to the basic advantages and disadvantages of existing ZhRD fuel-supply systems.

The advantages of the pressure-fed fuel-feed systems with GAD, ZhAD, and PAD are as follows:

- 1) simplicity and low cost of construction;
- 2) small dimensions and specific weight, if the engine is a low-thrust engine with a short operating time;
- 3) stability in the feed of the fuel components into the combustion chamber, if the gas accumulator is equipped with a pressure reducer or the powder-type accumulator is equipped with a high-sensitivity release valve for the excess powder-gas pressure, etc.

The basic deficiencies of these fuel-feed systems are:

- 1) the high specific weight of the fuel tanks, which results from the necessity of making them stronger for operation under the

rather high gas pressure, particularly in cases where hot gases are used (when PAD or ZhAD are used in the system);

2) high specific weight of the pressure accumulator with the compressed gas in it (in cases where GAD are used);

3) large heat losses from the hot gases into the surrounding medium (in cases where PAD or ZhAD are used); this increases the specific weight of the powder charge or fuel required to generate the gas;

4) the rate of powder combustion depends on the temperature of the environment, with the result that its combustion surface must be determined proceeding from the rate of combustion for the lowest possible ambient temperature - which necessitates installing a pressure-release valve in the accumulator and losing part of the energy of the powder;

5) when the operating time of the engine is lengthened, the weight of these fuel-feed systems rises sharply, which makes them unsuitable for engines with high thrusts and long operating times.

If the compressed gas is preheated before entry into the fuel tanks, the weight of gas stored in the system's bottle can be reduced by a factor equal to that by which the temperature is raised.

Due to the special properties noted above, the pressure-fed fuel-feed system is useful only for low- and medium-thrust engines with short operating times. This system is also used with GAD in stationary experimental units and in starting and sustainer aircraft engines. However, the positive features inherent in this system may, in some cases, make its use expedient even for relatively high-thrust and long-burning engines.

The advantages of the turbopump fuel-feed system include:

1) lighter-weight fuel-tank design, since the tanks operate at low gas pressure;

2) the weight of the TNA does not depend on the operating time of the engine;

3) fully satisfactory constancy in the feed of the fuel components into the engine's combustion chamber;

4) the possibility of utilizing the spent turbine gases for flight-control and stabilization of the missile;

5) high engine specific thrust, since the optimum gas pressure in the combustion chamber of an engine using this system is usually found to be higher than in pressure-fed fuel-feed systems.

The deficiencies of the turbopump fuel-feed system include complexity of design, which lowers dependability and raises the cost of the engine, as well as the torque developed by the turbopump assembly, which is transmitted to the apparatus and may require special compensation.

The turbopump fuel-feed system has been used in engines for long-range missiles with thrusts above 18-25 tons and operating times longer than 60 sec. With lightweight and economic design of the TNA, this fuel-feed system may be found expedient for lower-thrust engines with shorter operating times.

It must be remembered that the creation of a fuel-feed turbopump system is an extremely complex and difficult problem, particularly in those cases where it is necessary to deal with highly aggressive fuel components. The problems of making metering and regulating devices for this system are also complex and have not yet been adequately studied.

The time for the TNA to come up to the rated regime may run to 2 sec with the total time for the engine to come up to regime no greater than 2.3 sec.

After selection of efficient types and designs for the individual elements of the fuel-feed system, the ignition, control, and self-

blocking systems are selected for the ZhRD. Successful solution of these problems guarantees dependable starting, operation, and stopping of the engine.

SECTION 2. FUNDAMENTALS OF PLANNING AND DESIGN OF ZhRD FUEL TANKS

The fuel tanks of the ZhRD are the reservoirs which hold its combustible and oxidizer. The following problems must be resolved in their design:

1. Selection of the tank type in accordance with technical specifications.
2. Selection of the arrangement of the tanks on the missile.
3. Selection of the fuel-baffling devices for the interior of the tanks.
4. Determination of the required fuel-tank volumes.
5. Strength calculations for the tanks and their individual elements.
6. Determination of fuel-tank weight.
7. Selection of the structural materials for the tanks, etc.

1. Fuel-tank types and specifications set forth for them. In accordance with the method used to feed the fuel components into the engine's combustion chamber, fuel tanks are classed into two basic groups:

Stressed tanks, i.e., tanks that are under high pressure during operation of the ZhRD and usually form a component part of a pressure-fed fuel-feed system.

Unstressed tanks, i.e., tanks that are under only moderate pressure ($2-3.5 \text{ kg/cm}^2$ and up) during operation of the ZhRD and usually form a component part of the missile.

Since the dimensions of the fuel tanks usually make up most of the

length of the missile, they are frequently used as the thrust framework to absorb the forces acting on the missile. Such tanks are known as bearing tanks. Tanks of this type are extremely sensitive to external pressures, since the ratio of their wall thickness to their diameter is very small (about 1 to 500).

The specifications set forth for the materials and design of the fuel tanks depend on the type of pressure accumulator used in the feed system and the physicochemical properties of the fuel components used in the ZhRD.

If fuel components with low boiling points (liquid oxygen, etc.) are used for the engine, the tanks must have special heat insulation. Tanks for corrosive fuel components must be made from special corrosion-resistant materials.

If a hot-tank pressure accumulator is used in the system, it is necessary to take into account the thermal stresses that arise in the material of the tanks as a result of their becoming heated by the hot gas, as well as the changes in the strength properties of the material that take place when this happens.

The following basic specifications are set forth for the design of fuel tanks of any type or construction.

The tanks must have the smallest possible specific weight, since the flight characteristics of the missile improve as their weight is reduced. It is particularly important to bear this requirement in mind in designing ZhRD with stressed tanks, since their weight always makes up the major part of the design weight of the entire missile.

Minimum tank design weight can be achieved by using materials with high mechanical properties and low specific gravities in their manufacture.

In the case of the pump-fed fuel-feed system, the tanks make up

only a small percentage of the total weight of the missile and are frequently relatively simple from a design standpoint. In the case of the pressure-fed system, the tank weight may compose approximately 20-30 percent of the total dry weight of the missile.

The tanks must be highly corrosion-resistant. This specification assumes particular importance when the ZhRD operates on corrosive fuel components, particularly when it is necessary to store them in the engine's tanks for long periods.

The tanks must be simple to manufacture and convenient to work with. For the most part, fuel tanks are fabricated by welding. High strength, plasticity, tightness, and corrosion-resistance properties are required in the weld seams of the tanks.

Welding must be carried out in such a way that the deformation undergone by the metal will be minimal.

Bearing tanks must have smooth outlines that conform to the outlines of the missile. The tanks must be located on a single axis with the missile (when the tandem placement system is used). The fuel-tank design must also satisfy a number of operational specifications: the possibility of rapid evacuation in emergency situations, measurement of the liquid level in the tank, and rapid blowoff of pressure. In certain cases, it is necessary to provide windows for hydrostatic testing, cleaning, and inspection of the interiors of the tanks.

2. Geometrical shapes and relative placement of tanks on missile.

The fuel tanks of a ZhRD are normally made cylindrical in shape and arranged separately (one after the other) or concentrically (one inside the other) on board the missile.

The generally accepted model for placement in a reaction-thrust missile is tandem location of cylindrical fuel tanks forward of the engine chamber.

In selecting one or another fuel-tank shape and the scheme for locating them on the missile, it is necessary to take into account the weight characteristics of the tanks, their positions, and the technological, economy, and other factors involved here.

If it is possible to use long tanks, it is advisable to select the simpler tandem arrangement, while when the missile has a relatively large diameter, preference may sometimes be given to concentric-system tanks (Fig. 10.7c). The concentric fuel-tank arrangement can be justified only by the necessity of ensuring the specified weight and flight characteristics for the missile, since it is a relatively complex arrangement to execute.

Bearing fuel tanks are frequently of the "combined" configuration (see Fig. 10.7b). As with the concentric tank arrangement, the basic deficiency of this design consists in the danger of explosion of hypergolic fuel components in the event that the hermetic partition between the two tanks is broken.

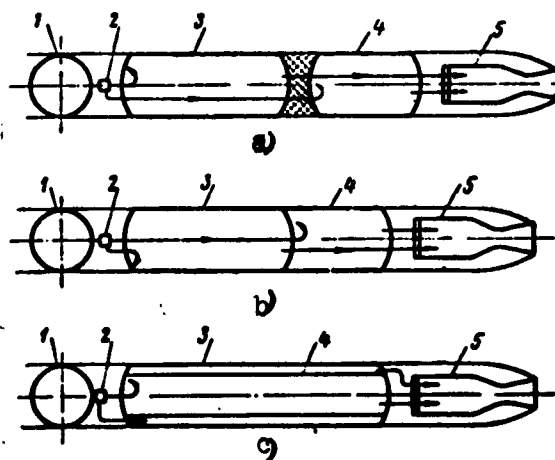


Fig. 10.7. Schematic diagram showing arrangement of engine fuel tanks on board missile.

a) Separate (tandem) tank arrangement;
 b) combined tank construction with tandem arrangement; c) concentric tank arrangement: 1) Pressure accumulator; 2) pressure reducer; 3) and 4) fuel tanks; 5) engine chamber.

For engines with turbopump fuel-feed systems, it is sometimes advisable from the viewpoint of pump operation to place the oxidizer tank forward. In general, however, the tank arrangement may be varied; the tanks are located in such a way that the missile will be stable. In resolving the question of tank placement aboard the missile, it is necessary to give preference to the variant with which the center of gravity of the tanks will shift least with respect to its initial position as the fuel is burned out. With this object in mind, the fuel tanks are usually located as close as possible to the missile's center of gravity.

The diameters of the fuel tanks are determined by the design and mission of the missile, and their length by the fuel reserve required to operate the engine. The ratio of tank length to diameter is frequently 2-5, and has even reached 8-12 in certain designs of recent years ("Aerobee" and "Corporal" rockets, etc.).

The fuel-tank bases are frequently made spheroidal in shape. Sometimes, however, it may prove expedient to use a funnel-shaped taper. This base shape on the liquid-takeoff end guarantees a higher fluid-flow rate in front of the turbine drive, as well as eliminating the necessity of using intake devices inside the tanks.

Placement of one tank partly inside the other makes it possible to reduce the excess pressure on the tapered base and the fuel-intake line of one of the tanks and make them thinner and lighter in weight.

3. Inside-tank intake devices. It is necessary that the design of each tank incorporate certain devices that are important for its operation: devices for fueling, drain and safety valves, etc. A pressure-relief valve is sometimes installed in reusable stressed tanks. Large-volume tanks frequently have windows for inspection of their internal parts and for repair.

When the missile maneuvers, liquid fuel components in the tanks may be sloshed away from the intake tube as a result of the centrifugal forces, particularly when the tanks contain only small quantities of liquid. This may result in stalling of the engine and even explosion. in cases when hypergolic fuel components are being used.

Furthermore, the liquid in the tanks may foam under the impingement of the gas jet from the pressure accumulator, and the gas may mix violently with the liquid and form bubbles in it, to the considerable detriment of normal engine performance.

Under certain conditions, the liquid issuing from the tank may swirl and form a whirlpool, so that the working gas may be sucked out of the tank into the offtake pipeline until the liquid is completely exhausted, so that the engine stalls.

Baffles, diaphragms, and special funnel quenchers are installed to protect the liquid in the tanks from the jet of gases at entry, suppress sloshing and foaming as the missile maneuvers or comes under overload, and as a countermeasure against formation of whirlpools at the entry into the intake device.

Special inside-tank intake devices are employed to prevent starvation of the side intake tube during maneuvers by the missile.

The following basic designs are known for inside-tank fuel-intake devices (Fig. 10.8):

- 1) flexible hose-type intakes;
- 2) rotary trunk-type intakes;
- 3) sliding tank pistons;
- 4) flexible pressurizing bags.

In the case of pressure-fed fuel-feed systems with PAD or ZhAD, it is necessary to limit the temperature of the gases fed into the fuel tanks to a certain range (normally no higher than 800-900°C) in

order to avoid excessive heating of the tank walls and lowering of their strength.

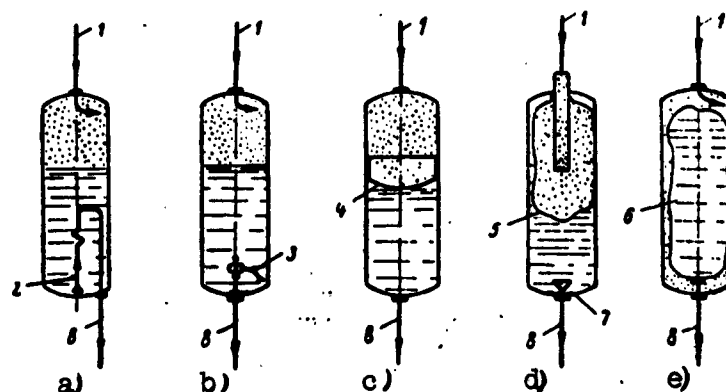


Fig. 10.8. Schematic diagrams of fuel-intake devices in fuel tanks.

a) Tank with hose intake; b) tank with trunk intake; c) tank with piston impeller; d) and e) tanks with pressurizing bags. 1) Gas supply; 2) hose trunk; 3) swivel trunk; 4) piston; 5) and 6) pressurizing bags; 7) quencher; 8) propellant outlet.

The hot gases may be cooled by spraying a certain amount of water into them or by cooling the gas pipeline with one of the fuel components. When ZhAD are used, the temperature of the combustion products may also be reduced by varying the fuel mixture ratio.

4. Determining required fuel-tank volume. The required tank volume for a given fuel component is determined by the formula

$$V_B = V_{\text{pac}} + V_{\text{rap}} + V_{\text{pod}} \text{ m}^3, *$$

where $V_{\text{rasch}} = G\tau_{\text{dv}}/\gamma^{**}$ is the calculated volume of the propellant in question (G is the per-second flow in kg, γ is the specific gravity of this propellant, and τ_{dv} is the engine's operating time in sec), $V_{\text{gar}} \approx (0.02 \text{ to } 0.05) V_{\text{rasch}}$ is the guaranteed fuel-component reserve needed to start the engine and ensure dependable operation during the

* [Subscripts: pac = rasch = raschetnyy = calculated; rap = gar = garantiynyy = guaranteed; pod = pod = podushka = cushion.]

** [Subscript дв = dv = dvigatel' = engine.]

established operating time, since in practice a certain noncorrespondence between the actual and calculated per-second fuel flow rates is possible, and, moreover, not every inside-tank device can guarantee complete scavenging of the component from the tank; $V_{pod} \approx (0.03 \text{ to } 0.06)V_{rasch}$ is the gas-cushion volume required in the tank to prevent an excess pressure rise in it as a result of volume expansion of the fuel component when the temperature rises after fueling and the evolution of gas that takes place as a result of the chemical reactions that unfold in it, as well as to soften the sharp impact of the incoming gas on the surface of the liquid on starting when pressure-fed fuel-feed systems are used.

The value of V_{gar} will be higher for superior inside-tank mechanisms and longer missile-launching and climbing times. The time of the ZhRD's operation on the starting device is basically determined by the engine's starting system. With pyrotechnic ignition this time comes to about 0.2 sec; with stepped ignition of the engine, it attains 2-3 sec.

The volume of the gas cushion in a given tank must be determined with consideration of possible pressure elevation in the tank as a result of increases in the fuel-component temperature under the engine's operating conditions. The value of this pressure is governed by the design of the fuel tanks and the special characteristics of the engine's fuel-feed hydraulic system; in pressure-fed systems, it must not exceed the bursting pressure of the sealing diaphragms (5-8 atm abs), since the engine might otherwise start by itself.

The temperature of the atmospheric air may vary from -40 to $+50^{\circ}\text{C}$, depending on the conditions under which the ZhRD-equipped missile operates. When this temperature changes, the temperature and volumes of the fuel components and air cushions in the tanks usually change too.

The required tank volume for a given fuel component may be determined as follows, with consideration of air-cushion volume.

If the fuel component is run into the tank at a temperature of -40°C , its volume will be

$$V_{\text{ком}}(-40^{\circ}) = \frac{G_{\text{ком}}}{\gamma(-40^{\circ})}, \quad *$$

and the free volume in the tank (air cushion) will be expressed by the formula

$$V_{\text{с}}(-40^{\circ}) = V_{\text{Б}} - V_{\text{ком}}(-40^{\circ}) = V_{\text{Б}} - \frac{G_{\text{ком}}}{\gamma(-40^{\circ})},$$

where $G_{\text{ком}}$ is the weight of the fuel component in question for operation of the engine for a specified interval of time, $V_{\text{Б}}$ is the required tank volume for this fuel component, taking into account the air-cushion volume, and $\gamma(-40^{\circ})$ is the specific gravity of this component at -40°C .

On heating of the fuel component, the free volume in the tank (air cushion) becomes smaller and will be

$$V_{\text{с}}(+50^{\circ}) = V_{\text{Б}} - \frac{G_{\text{ком}}}{\gamma(+50^{\circ})},$$

at a temperature of $+50^{\circ}\text{C}$; here $\gamma(+50^{\circ})$ is the specific gravity of the component at a temperature of $+50^{\circ}\text{C}$.

Since the tank is airtight, the same quantity of air remains in it at $+50^{\circ}\text{C}$ as was there at -40°C , while its pressure has risen to some value $p_{\text{под}}$ that is safely admissible for the tank, i.e.,

$$G_{\text{воз}} = G_{\text{воз}}(-40^{\circ}) = G_{\text{воз}}(+50^{\circ}).$$

The weight of the air cushion at temperatures of -40 and $+50^{\circ}\text{C}$ may be expressed by the following equations of state:

* [Subscript ком = komp = komponent = component .]

$$G_{\text{нол}}(-40^{\circ}) = \frac{p_a V_a(-40^{\circ})}{R_a T_a(-40^{\circ})} = \frac{p_a \left[V_B - \frac{G_{\text{комн}}}{\gamma(-40^{\circ})} \right]}{R_a T_a(-40^{\circ})};$$

$$G_{\text{нол}}(+50^{\circ}) = \frac{p_{\text{нол}} V_{\text{нол}}(+50^{\circ})}{R_{\text{нол}} T_{\text{нол}}(+50^{\circ})} = \frac{p_{\text{нол}} \left[V_B - \frac{G_{\text{комн}}}{\gamma(+50^{\circ})} \right]}{R_{\text{нол}} T_{\text{нол}}(+50^{\circ})},$$

where p_a , T_a and R_a are the pressure, temperature, and gas constant of atmospheric air at -40°C , and $p_{\text{нол}}$, $T_{\text{нол}}$ and $R_{\text{нол}}$ are the same quantities for the air cushion in the tank at a temperature of $+50^{\circ}\text{C}$.

On comparing the right members of these equations and making the appropriate conversions for $R_a = R_{\text{нол}}$, we obtain a formula for determining the tank volume required for the fuel component in question:

$$V_B = \frac{\frac{p_{\text{нол}}}{\gamma(+50^{\circ})} T_a(-40^{\circ}) - \frac{p_a}{\gamma(-40^{\circ})} T_{\text{нол}}(+50^{\circ})}{p_{\text{нол}} T_a(-40^{\circ}) - p_a T_{\text{нол}}(+50^{\circ})} G_{\text{комн}}$$

or

$$V_B = \frac{233 \frac{p_{\text{нол}}}{\gamma(+50^{\circ})} - 323 \frac{1}{\gamma(-40^{\circ})}}{233 p_{\text{нол}} - 323} G_{\text{комн}}$$

This formula does not take into account the partial vapor pressures of the fuel component and the pressure that may be generated in the tank as a result of decomposition of the component during storage.

The design may call for running the components into the tanks either from the top or from the bottom (depending on the type of missile, the conditions under which it starts, etc.). It is advisable to fill a tank with liquid oxygen from the bottom in order to avoid the violent evaporation of the substance. The gas cushions communicate with the atmosphere through bleeders when the tanks are filled with propellant.

In computing tank volumes, it is also necessary to take into account the volume occupied by tubing, intake devices, etc.

In cases where the engine stops as a result of exhaustion of the propellant supply in the tanks, it is advisable to use propellant tanks

of volumes such that the oxidizer will be exhausted first and the engine will stop with some combustible left. When this is done, the guarantee component margin is found to be smaller, while the conditions under which the engine stops are more favorable.

5. Strength calculations for tanks. Strength calculations for the tanks are based on the formulas of the theory of thin-walled vessels.

With the turbopump fuel-feed system, the calculated fuel-tank pressure may, in first approximation, be assumed equal to 2-3.5 kg/cm².

With the pressure-fed fuel-feed system, the theoretical tank pressure is made 15-25 percent higher than the necessary feed pressure, which is "refined" after final elaboration of the engine's entire hydraulic system.

In the case of the pressure-fed system, the pressure necessary to feed a given fuel component into the engine's combustion chamber is given by the formula

$$p_s = p_k + \Delta p_{s.p} \text{ kg/cm}^2, * \quad (10.3)$$

where p_B is the propellant pressure in the tank, p_k is the gas pressure in the engine's combustion chamber, and $\Delta p_{s.p}$ is the total pressure gradient in the propellant in the engine's fuel-feed system (Δp_f in the nozzles, Δp_{okhl} in the cooling system, Δp_{tr} in the pipelines, Δp_{kl} at the valves, throttling disks, etc.).

All of these fluid-pressure losses between the tank and the combustion chamber are determined together by the usual hydraulic formulas.

In designing the hydraulic system of the engine, it is necessary that the tank pressures of the two fuel components be the same, since this simplifies the design of the fuel-feed system. Unequal hydraulic

* [Subscripts $n = p = \text{podacha} = \text{feed}$; $B = B = \text{Bak} = \text{Tank}$; $k = k = \text{kamera} = \text{chamber}$; $c.n = s.p = \text{summaryy perepad} = \text{total gradient}$.]

resistances in the combustible and oxidizer systems are usually eliminated by inserting throttling disks into the lines. These disks are also used to ensure the necessary flow rate of the fuel components into the combustion chamber in the specified weight proportions.

The thickness of the fuel-tank walls is determined by the pressure exerted on the fuel components in them, as well as by the mechanical properties of the material from which these tanks were made.

Knowing the theoretical tank pressure p_B , we can determine the necessary tank-wall thickness δ_B . For example, we have for a cylindrical tank

$$\delta_B = \frac{p_B d_B n_B}{2\sigma_{bB}}, \quad (10.4)$$

where d_B is the inside diameter of the tank, σ_{bB} is the ultimate strength of the material selected for the tank, in kg/cm^2 , and n_B is the strength safety margin of the tank material.

The thickness of the bases of cylindrical tanks depends on their shape. The wall thickness of a spherical tank base is determined by the formula

$$\delta_{dn} = \frac{p_B d_B n_B}{4\sigma_{bB}}. \quad (10.5)$$

The most common tank-base shape is elliptical or near-elliptical, described by a radius $r_{dn} > d_B/2$.

The thickness of the tank-base wall can be determined in this case by the formula

$$\delta_{dn} = \frac{p_B r_{dn} n_B}{2\sigma_{bB}}, \quad (10.5a)$$

where r_{dn} is the radius of the base sphere.

When the tanks are designed, it is necessary to make allowances for the loss in strength that takes place on heating.

* [Subscript dn = dn = $dnishche$ = base.]

The most severe conditions for the tank metal arise during fuel feed by hot gases (from PAD or ZhAD). In this case, the metal must be sufficiently strong for feed pressures of the order of 35-60 atm abs and temperatures around 400-800°C.

If the fuel tanks bear stresses, it is necessary, in addition to the stresses that arise in the metal due to the pressure of cold or hot gases inside them, to take into account the external loads experienced by the tanks during launching and flight of the missile (weight of the liquid column in the tank, acceleration effect, etc.).

In modern fuel-tank designs, which are executed in steel and stressed by the pressure of a cold gas, the strength margin $n_B \approx 1.5$ to 2.0. If the fuel tanks operate under the pressure of hot gases or are used as load-bearing structural members of the missile, the strength safety margin of the tank material must be raised to $n_B \approx 2.5$ and higher. The strength margin of the tank material also takes into account the increase in the pressure in the tanks due to the liquid column and the inertial forces that arise in it during the flight of the missile.

Cylindrical fuel tanks and the gas accumulators are sometimes wire-wound to permit making them lighter. The weight of a cylindrical tank wound with steel wire is almost equal to the weight of a spherical tank of the same capacity (such as the gas bottles of the German V-1 missile).

Unpressurized fuel tanks used in engines with pump-fed fuel systems are usually made thin-walled (shell thicknesses up to 2 mm) from magnesium-aluminum alloy with a short-time breaking strength $\sigma_{bB} < 20 \text{ kg/mm}^2$ and a specific weight of 2700 kg/m^3 . The strength safety margin of tanks made from this material may be set at $n_B = 1.8$ to 2.

6. Determining fuel-tank weight. The dry weight of a cylindrical

tank for a given component may be expressed by the following formula, without consideration of the effects of the liquid column in it and acceleration forces:

$$G_B = \epsilon_B \pi d_B l_B \delta_B \gamma_{m.B} \text{ kg, *} \quad (10.6)$$

where $\epsilon_B \approx 1.2$ to 1.4 is an encumbrance factor which takes into account the weight of the bases, flanges, mountings, and fittings of the tank (fueling valve, scavenging devices, etc.), $l_B = 4V_B/\pi d_B^2$ is the length of the cylindrical tank, and $\gamma_{m.B}$ is the specific gravity of the material from which the tank is made.

Substituting values of δ_B from (10.5) and l_B in (10.6), we obtain finally

$$G_B = 2\epsilon_B \frac{p_B V_B n_B}{\sigma_{b.B} \gamma_{m.B}}. \quad (10.7)$$

The specific weight of the fuel tanks will be

$$\gamma_B = \frac{G_B}{V_B} = \frac{2\epsilon_B p_B n_B}{\sigma_{b.B} \gamma_{m.B}}. \quad (10.8)$$

Thus, the fuel-tank specific weight is proportional to the pressure p_B and depends on shape, design, and the strength properties of the tank materials, with γ_B diminishing as the material's strength factor $\sigma_{b.B}/\gamma_{m.B}$ increases.

For rough calculations, use may be made of data on existing tanks of similar types made from the same material, taking into account the values of the pressure p_B and the volume V_B .

Assuming that the strength and design characteristics of the tanks being compared are identical, we obtain

$$G'_B = G_B \frac{V'_B p'_B}{V_B p_B}. \quad (10.9)$$

In computing the weight of an unpressurized high-capacity tank, it is necessary to take into account the weight of the transverse

* [Subscript m = material = material.]

framing (bulkheads) necessary to give the tank rigidity and the weight of the fittings, baffles, and insulation.

The tank fill factor depends on the mission of the missile and may vary in practice from 0.6 to 0.8. This means that the fuel reserve in the tanks amounts to about 60-80 percent of the missile's weight at launching, and, consequently, that the fuel tanks are normally relatively large in dimensions and rather heavy.

With pump-fed fuel systems, the tanks represent a small percentage of the total weight of the missile and are frequently relatively simple from a design standpoint. In the case of the pressure-fed fuel system, the tank weight may represent about 20-30 percent of the missile's total weight without fuel and approximately 70 percent of the engine dry weight. For this reason, fuel-tank design is frequently subordinated to the general planning conception of the missile.

7. Materials for the tanks. In selecting a material for the tanks, we usually proceed from the specifications set forth for it, taking into consideration

- 1) the nature of the fuel components (their corrosive action);
- 2) the method of feeding the propellants into the engine's combustion chamber (pumps, cold gases, hot gases);
- 3) the positioning of the tanks in the missile (load-bearing or nonbearing tanks);
- 4) the period for which the fuel component will be stored in the tank, etc.

Practical experience has established the most suitable materials for a number of specific cases; usually, these are various types of steel and aluminum alloys. Given the appropriate welding technique and heat-treatment, tanks may be made from carbon steels and magnesium for certain fuel components. However, the use of these materials for

tanks to hold a number of oxidizers is possible only provided that they are given special protection from surface corrosion. Oxidizer tanks are frequently made from stainless steels.

Many special steels possess high mechanical properties: with appropriate heat treatment, these steels can withstand stresses up to 120 kg/mm^2 . However, the difficulty of employing such steels consists in the fact that it is difficult to produce weld seams with strengths equal to that of the basic material. Furthermore, the tanks require heat treatment after welding, and this involves considerable difficulty with large tank sizes. Finally, such steels are expensive.

It is necessary to use readily available materials in the design of single-shot ZhRD so as to lower the cost of the entire design.

Since the majority of combustibles do not require tanks with high corrosion resistance, high-strength steels are normally used in their manufacture. In selecting gaskets and other accessories for these tanks, it should be remembered that the majority of combustibles in use at the present time possess active solvent properties. For this reason, plastics are often used as the materials for the gaskets.

By their nature, all oxidizers are more or less aggressive substances with respect to many structural materials. For this reason, tanks for aggressive oxidizers must possess high corrosion resistance. Moreover, the material of a hydrogen-peroxide tank may not contain elements that catalyze its decomposition (especially copper). In cases where liquid oxygen, etc., are used, the tank material must retain the necessary strength at low temperatures.

Metallic and nonmetallic materials that have adequate resistance to oxidizers and can be used for ZhRD tanks are known at the present

time.

Engines operating on fuels in which the oxidizer is nitric acid or one of its derivatives have recently come into widespread practical use in various defense and aviation fields. In this connection, the problem of materials for the manufacture of ZhRD tanks has become an acute one.

Alloy steel may be used for tanks to hold nitric acid and its derivatives, nitrogen tetroxide, hydrogen peroxide, and tetranitromethane.

Carbon steels can also be used for hydrogen peroxide, provided that a coating of some sort is used with them (paint, wax, or oxide film).

Stainless steels and aluminum alloys are useful for liquid-oxygen and ozone tanks. As with other low-boiling liquids, the low temperature of liquid oxygen imposes certain limitations on the selection of materials for the tanks as a result of the cold-shortness phenomenon.

Nickel, copper, aluminum, and their alloys, and alloy steels can be used for tanks to hold liquid fluorine and fluorine oxides and nitrate.*

Chromium steels and aluminum and its alloys are applicable for perchloric-acid tanks.

SECTION 3. DESIGN OF GAS PRESSURE ACCUMULATOR FOR ENGINE FUEL-FEED SYSTEM

The gas pressure accumulator (GAD) is a bottle with the appropriate fittings used to concentrate a supply of compressed air or some other gas as necessary to pressurize the fuel components from the tanks into the engine's combustion chamber.

*Missiles and Rockets, September 1957.

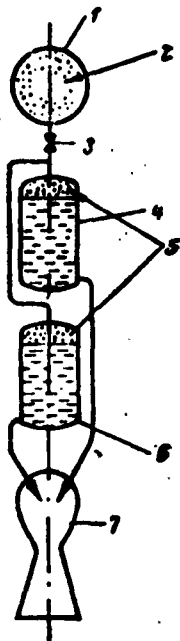


Fig. 10.9. Illustrating the design of gas pressure accumulator of pressure-fed ZhRD fuel-feed system.

1) GAD; 2) gas; 3) pressure reducer; 4) combustile tank; 5) gas; 6) oxidizer tank; 7) engine combustion chamber.

The following problems must be solved in planning and designing GAD for fuel-supply systems:

1) selection of the accumulator-bottle shape and the working gas for the system;

2) selection of the initial gas pressure in the bottle;

3) determination of the gas temperature in the bottle and in the fuel tanks when the system's operation terminates;

4) determination of the volume of the bottle and the gas reserve required;

5) strength calculations for the gas accumulator and determination of its weight.

1. Selecting shape of accumulator bottle and working gas for the system. The gas bottle of the pressure accumulator is usually made spherical in shape, since its weight will then be smaller than a cylindrical bottle under the same conditions. Cylindrical bottles with spherical bases are used only in cases in which the diameter of a spherical bottle would exceed the computed midsection of the missile.

Compressed-gas bottles are made from high-strength, high-weldability steels.

Figure 10.9 shows a schematic representation of a fuel-feed system with GAD. The following symbols have been adopted for the

parameters of the gas:

V_{1a} , G_{1a} , p_{1a} , and T_{1a} - the initial parameters for the gas in the pressure accumulator;

$V_{2a}=V_{1a}$, G_{2a} , p_{2a} , and T_{2a} - the final parameters for the gas in the pressure accumulator;

V_{1B} , G_{1B} , p_{1B} , and T_{1B} - the initial parameters in the fuel tanks;

V_{2B} , G_{2B} , p_{2B} , and T_{2B} - the final parameters for the gas in the fuel tanks;

here, V is the volume of the gas, G is its weight, p is its pressure, and T is the temperature of the gas.

The initial gas pressure in the pressure accumulator is generally specified for the design of the system on the basis of the following considerations:

- 1) an increase in the initial pressure p_{1a} of a given volume of gas in the bottle exerts virtually no influence on the weight of the bottle and reduces its volume and dimensions (see Fig. 10.9);
- 2) the higher p_{1a} , the smaller will be the amount of unused passive gas in the system at the end of the engine's operation;
- 3) the higher p_{1a} , the more expensive will it be to produce 1 kg of compressed gas;
- 4) the p_{1a} of the gas is limited by the head developed by the fueling facilities.

The maximum pressure is set equal to 250-330 atmospheres when the bottle is charged with gas using a compressor, since raising the pressure above these values complicates the design of the compressor. This consideration is eliminated when the bottle is filled by evaporation of a liquefied gas, and the initial pressure of the gas in the bottle may be made higher than when a compressor is used for the charging operation; it is now limited by the feasibility of fabricating thin-walled bottles and fittings for very high pressures.

Thus, the initial gas pressure in the bottle of the feed-system accumulator is determined by the conditions under which the bottle is charged and normally varies between 150 and 350 kg/cm², i.e., exceeds the feed pressure p_B by a factor of nearly 4-8.

Normally, the gas bottle is charged with compressed gas before starting through a charging stopcock the design of which makes it possible to release pressure manually if the necessity arises. The pressure is monitored from a gauge. A safety valve which releases the air into the atmosphere is usually installed in the main line to protect the tubing from elevated pressures.

The gas is almost invariably throttled down through a pressure reducer to the feed pressure p_B on its way from the bottle into the fuel tank. A relatively cheap throttling disk may also be used for this purpose, but it will not guarantee constancy of the feed pressure (Fig. 10.10).

The gas-pressure regulator holds the feed of the fuel components from the tanks into the combustion chamber at a constant level and, consequently, also holds the engine's operating regime constant.

In the calculations, the gas pressure in the bottle at the end of the system's operation is assumed equal to*

$$p_{2n} = p_1 + \Delta p_{\text{red}}, \quad ** \quad (10.10)$$

where $\Delta p_{\text{red}} \approx 5$ to 10 kg/cm² is the minimum required gas pressure gradient in the pressure reducer that guarantees normal operation of the latter during the last few seconds of the engine's operation.

2. Selection of initial gas pressure in bottle. Air, nitrogen, helium, or carbon dioxide may be used as the working compressed gas in the system. Selection of the type of gas for a gas-bottle fuel-

*G.B. Sinyarev and M.V. Dobrovol'skiy. Zhidkostnyye raketnyye dvigateli (Liquid-fuel rocket engines), Oborongiz, 1950.

**[Subscript: p_{red} = red = reduktor = reducer.]

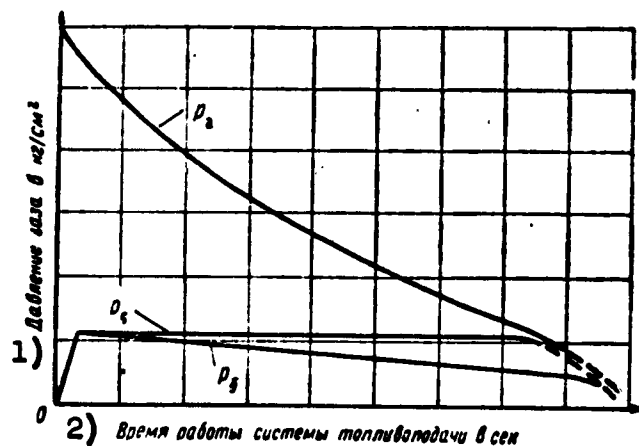


Fig. 10.10. Gas pressure p_a in pressure accumulator, pressure p_B after reducer, and pressure p_b after throttling disk as functions of operating time of fuel-feed system.* 1) Gas pressure in kg/cm^2 ; 2) operating time of fuel-feed system, in sec.

feed system depends on the nature of the fuel components, temperature, the solubility of the gas in them, and other factors.

As a relatively cheap material that is always available in sufficient quantity, compressed air is frequently used in contemporary systems. Nitrogen is employed in cases in which the fuel components may enter chemical reactions with air and disrupt normal fuel feed.

Helium may be used when it is necessary to pressure-feed liquefied fuel components at such low temperatures that air or nitrogen would be capable of condensing and dissolving in the cold liquid on contact with it. A further advantage of helium over other gases consists in the fact that it has smaller molecular and specific weights. As a result, the weight of helium necessary to displace 1 m^3 of liquid will, all other conditions equal, be little more than $1/7$

*[Subscripts: a = a = akkumulyator = accumulator; B = B = Bak = Tank; b = b (unidentified in text - Trans.).]

of the corresponding weight of nitrogen. Moreover, when helium is throttled through the reducer, its temperature rises (in contrast to the situation with air and nitrogen), reducing the necessary weight of pressurizing gas still further.

More compressed gas is required to displace cold liquefied fuel components than for displacement of the same quantity of nonliquefied liquid component at normal temperature; this is accounted for by cooling of the gas in the tanks. For example, approximately 2.5 times the amount of nitrogen is required to feed liquid oxygen than to feed the same quantity of nitric acid or kerosene.

3. Determination of gas temperature in bottle and in fuel tanks at end of system's operation. As the gas flows from the bottle into the fuel tanks, the gas remaining in the bottle expands with a decline in temperature and an influx of heat from the warmer walls of the bottle. Since this influx of heat is insignificant, however, the gas temperature in the bottle shows a net decline, i.e., the gas in the bottle undergoes polytropic expansion with an exponent n smaller than that for adiabatic expansion of the gas ($1 < n < k$).

Since it is impossible to estimate the value of n exactly, it is customary to make the calculations for a system with a gas pressure accumulator on the basis of the ratio of specific heats k . Consequently, the gas temperature in the bottle at the end of the system's operation will be determined from the adiabatic-expansion equation for the gas in the system:

$$T_2 = T_1 (p_2/p_1)^{\frac{k-1}{k}} = T_1 x^{\frac{k-1}{k}} = T_1 C_1 \text{ } ^\circ\text{K.} \quad (10.11)$$

The temperature of nitrogen declines somewhat on throttling, while that of helium rises slightly. The throttled gas is heated slightly in the fuel tanks as a result of the higher temperature of the tank walls and the liquid fuel component in it.

It is difficult to make a theoretical allowance for the variation of the gas temperature in the fuel tanks because of the inadequate study that has been devoted to the heat-exchange process in the system. The temperature of the gas in the bottle and in the fuel tanks at the end of the system's operation is determined from the equation of conservation of the energy of the gas in the system, with the condition that it expands adiabatically (see Fig. 10.9):

$$U_1 = U_2 + AL \quad (10.12)$$

or

$$G_{1a}C_{v1a}T_{1a} + G_{1B}C_{v1B}T_{1B} = G_{2a}C_{v2a}T_{2a} + G_{2B}C_{v2B}T_{2B} + AL, \quad (10.13)$$

where $U_1 = G_{1a}C_{v1a}T_{1a} + G_{1B}C_{v1B}T_{1B}$ is the internal energy of the gas in the bottle and in the fuel tanks before the system goes into operation; $U_2 = G_{2a}C_{v2a}T_{2a} + G_{2B}C_{v2B}T_{2B}$ is the same at the end of the system's operation; $A = 1/427$ is the heat equivalent of the mechanical work in kcal/kg-m;

$$L = \int_{V_{1B}}^{V_{2B}} p_B dV_B = p_{1B}(V_{2B} - V_{1B}) = p_{1B}V_{2B} - p_{1B}V_{1B} = G_{2B}R_{2B}T_{2B} - G_{1B}R_{1B}T_{1B}$$

is the mechanical work expended in displacing the fuel components from the tanks to the engine's chamber

with $p_{1B} = p_{2B} = p_B = \text{const}$; $G_{2B} = G_{1a} + G_{1B} + G_{2a}$ is the weight of the gas in the fuel tanks at the end of the system's operation; it is obtained from the equation of the weight balance of the gas in the system, $G_{1a} + G_{1B} + G_{2a}$;

$$G_{2a} = \frac{p_{2a}V_{2a}}{R_{2a}T_{2a}} = \frac{p_{2a}V_{1a}}{R_{2a}T_{1a}x^{\frac{k-1}{k}}} = \frac{p_{2a}}{x^{\frac{k-1}{k}}} = \frac{V_{1a}}{R_{1a}T_{1a}} = \frac{p_{1a}}{x^{\frac{k-1}{k}}} \frac{G_{1a}}{p_{1a}} = \frac{p_{1a}}{p_{1a}} \frac{G_{1a}}{x^{\frac{k-1}{k}}} = x \frac{G_{1a}}{x^{\frac{k-1}{k}}} = G_{1a}x^{1/k},$$

since $V_{2a} = V_{1a} = V_a$ and it follows from the equation of state of the gas in the bottle before the system goes into operation that $p_{1a}V_{1a} = G_{1a}R_{1a}T_{1a}$ so that $V_{1a}/R_{1a}T_{1a} = G_{1a}/p_{1a}$.

Substituting the resulting expression for G_{1a} , T_{2a} , G_{2B} , and L in Equation (10.13), assuming (without incurring a large error) in the calculations that the respective heat capacities C_v and constants R of the gas are equal during the system's operation and that $p_{1B} = p_{2B} = \text{const}$ (gas-pressure reducer installed in the system, see Fig. 10.10), and remembering the familiar expression $AR/C_v = k-1$, we obtain the final equation for determination of the gas temperature in the fuel tanks at the end of the system's operation:

$$T_{2B} = \frac{G_{1a}T_{1a}(1-x) + kG_{1B}T_{1B}}{k[G_{1a}(1-x^{1/k}) + G_{1B}]} \text{ } ^\circ\text{K.} \quad (10.14)$$

Disregarding (again, without incurring any significant error in the calculations) the insignificantly small quantity G_{1B} in this equation, we obtain

$$T_{2B} \approx T_{1a} \frac{1-x}{k(1-x^{1/k})} = T_{1a} C_2 \text{ } ^\circ\text{K.} \quad (10.15)$$

where C_2 is a coefficient taken from Table 10.1.

If special provision is made for preheating the gas in the system,

$$T_{2B} \approx T_{1a} \frac{1-x}{k(1-x^{1/k})} + \frac{q_{ya}}{C_p}. \quad (10.16)$$

where q_{ud} is the unit heat supply to the gas in kcal/kg and C_p is the heat capacity of the gas at constant pressure in kcal/kg $^\circ\text{C}$.

TABLE 10.1.

Values of Coefficients C_1 and C_2 as Functions of p_{1a}/p_{2a} for $k = 1.33$.

$x = p_{1a}/p_{2a}$	10	8.5	7	5.5	4	3	2
C_1	0.56	0.60	0.61	0.65	0.70	0.76	0.84
C_2	0.75	0.77	0.80	0.83	0.87	0.88	0.90

If we take into account the change in the temperature of the air

during the throttling process, C_2 will be slightly smaller than the tabulated values, or, in the case of helium, slightly larger. For purposes of calculation, the value of C_2 must be increased by 10% over the tabulated values.

4. Determination of full capacity and required gas reserve. In designing a gas-bottle fuel-feed system, it is necessary to determine the capacity of the bottle and the load of compressed gas required to displace the fuel components from the tanks into the engine's combustion chamber under a pressure p_B .

The initial data used here are:

- 1) the total capacities of the combustible and oxidizer tanks;
- 2) the feed pressure of the components, i.e., the pressure in the fuel tanks;
- 3) the nature of the working gas and its initial parameters — pressure and temperature.

The capacity required in the pressure-accumulator gas bottle may be determined using Equation (10.13) if we make the substitution $GT = pv/R$. With this condition, the above energy equation takes the form

$$V_{1a}(p_{1a} - p_{2a}) = p_{2a}V_{2a} - p_{1a}V_{1a} + \frac{AR}{C_v} \int_{V_{1a}}^{V_{2a}} p_B dV_B. \quad (10.17)$$

For constant feed pressure (with $p_{1B} = p_{2B} = \text{const}$), this equation is reduced to the form

$$V_{1a}(p_{1a} - p_{2a}) = p_{2a}(V_{2a} - V_{1a}) \left(1 - \frac{AR}{C_v}\right), \quad (10.18)$$

from which, applying the expressions $AR/C_v = k-1$ and $p_{2a} = p_{1a}x$, we obtain

$$V_{1a} = \frac{k p_{2a} (V_{2a} - V_{1a})}{p_{1a} - p_{2a}} = \frac{k p_{2a} (V_{2a} - V_{1a})}{p_{1a} (1 - x)}. \quad (10.19)$$

Disregarding the insignificant quantity V_{1B} in this equation

with the object of simplifying the calculations and introducing the symbols $V_{1a} = V_a$, $p_{1a} = p_a$, $p_{2B} = p_B$, and $V_{2B} = V_B$, we finally obtain an expression for determining the capacity of the pressure-accumulator gas bottle:

$$V_a = \frac{kp_B V_B}{p_a(1-x)} \quad (10.20)$$

This expression is also suitable for determining V_a for variable fuel-tank pressures if we make the substitution

$$p_B = \frac{p_{1B} + p_{2B}}{2}.$$

G.B. Sinyarev and M.V. Dobrovolskiy give another expression for determination of V_a , which they derive as follows.

The weight of gas in the bottle at the end of the system's operation is determined from the equation of the weight balance of the gas before and after operation of the system:

$$\begin{aligned} G_{1a} + G_{1B} &= G_{2a} + G_{2B}, \\ \text{i.e., } G_{2a} &= G_{1a} + G_{1B} - G_{2B}, \end{aligned}$$

where $G_{1a} = p_{1a} V_{1a} / R_{1a} T_{1a}$ is the weight of the gas in the bottle at the beginning of the system's operation; $G_{1B} = p_{1B} V_{1B} / R_{1B} T_{1B}$ is the same for the fuel tanks, and $G_{2B} = p_{2B} V_{2B} / R_{2B} T_{2B} = p_{2B} V_{2B} / R_{2B} T_{1a} C_2$ is the weight of the gas in the fuel tanks at the end of the system's operation.

On substitution of the expressions for G_{1a} , G_{1B} , and G_{2B} in the original equation of the weight balance, we obtain

$$G_{2a} = \frac{p_{1a} V_{1a}}{R_{1a} T_{1a}} + \frac{p_{1B} V_{1B}}{R_{1B} T_{1B}} - \frac{p_{2B} V_{2B}}{R_{2B} T_{1a} C_2}.$$

Substituting the value of G_{2a} from the earlier expression for it in the equation of state of the gas in the bottle for the end of the system's operation

$$p_{2a} V_{2a} = p_{2a} V_{1a} = G_{2a} R_{2a} T_{2a} = G_{2a} R_{2a} T_{1a} C_1$$

we find

$$P_{2a} V_{1a} = \left(\frac{P_{1a} V_{1a}}{R_{1a} T_{1a}} + \frac{P_{1B} V_{1B}}{R_{1B} T_{1B}} - \frac{P_{2B} V_{2B}}{R_{2B} T_{2B}} \right) R_{2a} T_{2a} C_1;$$

from which, after cancelling the R (assuming that the gas constant of the gas in the system does not vary) and other manipulations, we obtain

$$V_{1a} = \frac{\left(\frac{P_{2B} V_{2B}}{C_2} - P_{1B} V_{1B} \frac{T_{1a}}{T_{1B}} \right) C_1}{P_{1a} C_1 - P_{2a}}.$$

Assuming, as above, that $V_{1a} = V_a$, $P_{1a} = P_a$, $P_{2B} = P_B$, and $V_{2B} = V_B$, we finally obtain the desired form of the equation for determining the capacity of the gas bottle:

$$V_a = \frac{\left(\frac{P_B V_B}{C_2} - P_{1B} V_{1B} \frac{T_{1a}}{T_{1B}} \right) C_1}{P_a C_1 - P_{2a}} \quad (10.21)$$

The above equations indicate that the capacity of the pressure-accumulator gas bottle is directly proportional to the feed pressure and the fuel-tank capacity.

Knowing the capacity of the gas bottle and the initial pressure in it, we may determine the amount of gas necessary for the system's operation by applying the equation of state, i.e.,

$$G_{1a} = \frac{P_{1a} V_{1a}}{R_{1a} T_{1a}}.$$

Substituting $C_{1a} = G_a$, $R_{1a} = R_a$, $T_{1a} = T_a$, and $V_{1a} = V_a$ in this equation, we finally obtain [applying

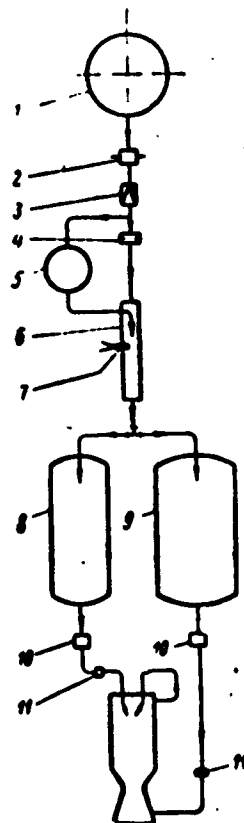


Fig. 10.11. Schematic diagram of pressure-fed fuel-feed system with preheating of compressed air. 1) Compressed-air bottle; 2) starter valve with outer cartridge; 3) pressure reducer; 4) throttling disk; 5) small combustile tank; 6) preheating chamber; 7) firing plug; 8) combustile tank; 9) oxidizer tank; 10) cutoff valves; 11) throttling disks.

Equation (10.20)]

$$G_a = \frac{k p_2 V_2}{R_2 T_2 (1-x)} \quad (10.22)$$

Since theoretical evaluation of the heat exchange that takes place in the fuel-feed system is extremely difficult and can be done only approximately, it is recommended that the theoretically required weight G_g of gas be increased by 5% to allow for errors in the calculations and ensure normal delivery of fuel components into the chamber.

If a special provision is made in the system to preheat the gas (Fig. 10.11), the required quantity of gas will be determined as follows.

If we disregard the small quantity G_{1B} (to simplify the derivation), the equation of the weight balance for the gas in the system takes the form

$$G_{1a} = G_{2a} + G_{2B}$$

Substituting the expressions for $G_{2a} = G_{1a} x^{1/k}$ and $G_{2B} = \frac{p_{2B} V_{2B}}{R_{2B} T_{2B}}$ in this equation, with the subsequent substitution

$$T_{2B} = \frac{T_{1a}}{k} \frac{1-x}{1-x^{1/k}} + \frac{q_{ya}}{C_p},$$

we obtain finally

$$G_{1a} = \frac{k p_{2B} V_{2B}}{R_{1a} T_{1a} (1-x) + (k-1) (1-x^{1/k}) \frac{q_{ya}}{C_p}}$$

or, using our adopted symbols

$$G_a = \frac{k p_2 V_2}{R_2 T_2 (1-x) + (k-1) (1-x^{1/k}) \frac{q_{ya}}{C_p}} \quad (10.23)$$

where q_{ud} is the specific amount of heat supplied to the gas in kcal/kg.

This equation indicates that special preheating of the gas in the fuel-feed system reduces the quantity of this gas that must be

stored and, consequently, the weight of the bottle to hold it. For $q_{ud} = 0$, as may be assumed in approximation for a VAD* with preheating of the air, this equation becomes identical to Equation (10.22).

In practice, the air may be preheated in a special heat exchanger, making use of the heat of products of combustion taken from the engine chamber; however, preheating in this manner is rendered inefficient by the considerable weight and design complexity of the heat exchanger. When the air is preheated in a special preheater by using the heat of a small quantity of ignited combustible in the air stream, the preheater becomes simple in design and lightweight, permitting use of a simple system to control the temperature of the gas.

If the gas temperature in the fuel tanks is maintained constant by some device ($T_{1B} = T_{2B} = T_B = \text{const}$), we obtain the following values:

- 1) required gas charge in accumulator:

$$G_s = \frac{p_s V_s}{R_s T_s (1 - x^{1/k})}; \quad (10.24)$$

- 2) the amount of heat that must be supplied to a unit weight of the gas:

$$q_{ys} = C_p T_s - \frac{C_p T_s}{k} \frac{1-x}{1-x^{1/k}} + q_{\text{pot}} \text{ kcal/kg}, \quad (10.25)$$

where q_{pot} ** is the specific loss of heat in the system.

Knowing the heating value H_{ug} of the combustible, we can determine its specific flow (for 1 kg of gas):

$$C_{ys} = \frac{q_{ys}}{\varphi_p H_{us}} = \frac{1}{\varphi_p H_{us}} \left(C_p T_s + q_{\text{pot}} - \frac{C_p T_s}{k} \frac{1-x}{1-x^{1/k}} \right) \text{ kg/kg}, \quad (10.26)$$

where $\varphi_p \approx 0.90$ to 0.95 is the theoretical-to-ideal correction factor

*[BAD = VAD = Vozdushnyy Akkumulyator Davleniya = (Compressed-) Air Pressure Accumulator.]

**[$q_{\text{pot}} = q_{\text{pot}} = q_{\text{poterya}} = q_{\text{loss}}$.]

***[Subscripts: $y_d = ud = udel'nyy$ = specific; $r = g = goryucheye$ = combustible; $n = p = polnota$ = completeness.]

for burning of the combustible in the air of the preheater.

In the fuel-feed system, the hot gases lose part of their heat by heating the metal walls of the system and the liquid in the tanks. If powder-generated gases are used, some of them burn to completion with evolution of heat (the gases H_2 and CO are oxidized), the combustion being supported by the oxygen in the fuel-tank air cushion and the oxygen in the fuel component.

The nature of these processes is influenced by:

- 1) the chemical and physical properties of the hot gas;
- 2) the design of the fuel-feed system;
- 3) the volume of the air cushions in the tanks;
- 4) the physicochemical properties and the temperature of the fuel components displaced from the tanks into the engine chamber;
- 5) the feed pressure and feed time of the fuel components.

It is impossible in practice to take these processes into account quantitatively. For this reason, the design of a pressure-fed feed system using hot gases usually takes the effect of the above processes into account by using an over-all heat-utilization factor η_{tepl}^* for the hot gas, the value of which may be established by experiment.

In the calculations, the thermal efficiency of a preheated-gas system may be set equal to

$$\eta_{tma} = \frac{q_{ya} - q_{not}}{q_{ya}} \approx 0.3 - 0.4.$$

Since $q_{ud} = \varphi_p H_{ug} C_{ud.g}$, Expression (10.26) for $C_{ud.g}$ may be given the form

$$C_{ya.r} = \frac{C_p}{\eta_{tepl}} \left(T_s - T_s \frac{1-x}{k(1-x^{1/k})} \right) \text{ kg.} \quad (10.27)$$

The necessary pressure-accumulator gas-bottle capacity may,
*[Subscript: репл = tepl = teplota = heat.]

provided that the gas constant R in the preheater does not vary, be determined by the formula

$$V_a = \frac{G_a R T_a}{p_a} = \frac{p_B T_a}{p_a T_B} \frac{V_B}{1-x^{1/k}} \quad (10.28)$$

5. Strength calculation for gas pressure accumulator and determination of its weight. The strength and weight characteristics of a spherical gas pressure accumulator are determined by the formulas:

1) wall thickness of bottle:

$$\delta_a = \frac{p_a d_a n_a}{4 \sigma_{\delta a} \gamma_{M.a}} \quad (10.29)$$

2) dry weight of accumulator

$$G_{ak} = \epsilon_a \pi d_a^2 \delta_a \gamma_{M.a} = \frac{3}{2} \frac{\epsilon_a n_a p_a V_a}{\sigma_{\delta a} \gamma_{M.a}}$$

or, after substitution of V_a by the expression used previously,

$$G_{ak} = \frac{3}{2} \frac{k \epsilon_a p_B V_B n_a}{(1-x) \sigma_{\delta a} \gamma_{M.a}} \quad (10.30)$$

where $n_a \approx 1.5$ to 2.5 is the strength safety margin of the material of the gas bottle, which depends on the properties of the material and the way in which it is used, and $\epsilon_a \approx 1.2$ to 1.5 is the encumbrance factor of the gas bottle, which takes into account the weight of its fittings, attachments, etc; in the case of a cylindrical bottle, ϵ_a also includes consideration of the bottle's bases and may be as large as 1.5 - 2.5 .

The wall thickness of a cylindrical gas bottle and the dry weight of the pressure accumulator are then determined by the same formulas as used for cylindrical fuel tanks.

Since the accumulator bottle must withstand high gas pressures, it must be manufactured to a high degree of perfection.

The total weight of the pressure accumulator consists of the weight G_a of the compressed gas and the weight G_{ak}^* of the bottle for
*[Subscript: ak = ak = akkumulyator = accumulator.]

this gas, i.e.,

$$G_{\underline{\underline{GAD}}} = G_a + G_{ak}.$$

The specific weight of a spherical pressure accumulator, i.e., the weight per one liter capacity of the tanks for the basic fuel components, is determined by the formulas:

1) without preheating of the gas in the system (e.g., in the case of a VAD-1)

$$\begin{aligned} \gamma_{\text{ГAA}} &= \frac{G_{\text{ГAA}}}{V_B} = \frac{k p_B}{R_s T_s (1-x^{1/k})} + \frac{3}{2} \frac{\epsilon_a p_B n_a}{(1-x) \sigma_{\theta a} / \gamma_{\text{н.а}}} = \\ &= \frac{k p_B}{1-x} \left(\frac{1}{R_s T_s} + \frac{3}{2} \frac{\epsilon_a n_a}{\sigma_{\theta a} / \gamma_{\text{н.а}}} \right) \text{ kg/liter}; \end{aligned} \quad (10.31)$$

2) with a special gas preheater present in the system (e.g., in the base of the VAD-2)

$$\gamma_{\text{ГAA}} = \frac{p_B}{1-x^{1/k}} \frac{T_s}{T_B} \left[\frac{3}{2} \frac{\epsilon_a n_a}{\sigma_{\theta a} / \gamma_{\text{н.а}}} + \frac{1-C_{\text{ГAA}}}{R_s T_s} \right] \text{ kg/liter}. \quad (10.32)$$

In the case of a special gas preheater in the system, the weight of the fuel with its "canister" and the weight of the preheater can be taken into account by increasing the encumbrance factor ϵ_a of the pressure accumulator.

The weight of the fuel-feed system is composed of the weight $G_{\underline{\underline{GAD}}}$ of the gas pressure accumulator and the weight of the cylindrical main fuel tanks, i.e.,

$$G_{\text{c.н}} = G_{\text{ГAA}} + G_B. \quad (10.33)$$

The specific weight of a pressure-fed fuel-feed system with a gas pressure accumulator is:

1) without special preheating of the gas in the system

$$\gamma_{\text{c.н}} = \frac{G_{\text{c.н}}}{V_B} = p_B \left[\frac{k}{1-x} \left(\frac{1}{R_s T_s} + \frac{3}{2} \frac{\epsilon_a n_a}{\sigma_{\theta a} / \gamma_{\text{н.а}}} \right) + \frac{2 \epsilon_B n_B}{\sigma_{\theta B} / \gamma_{\text{н.Б}}} \right] \text{ kg/liter}; \quad (10.34)$$

2) with special preheating of the gas in the system,

$$\gamma_{\text{c.н}} = p_B \left[\frac{T_s}{T_B (1-x^{1/k})} \left(\frac{1-C_{\text{ГAA}}}{R_s T_s} + \frac{3}{2} \frac{\epsilon_a n_a}{\sigma_{\theta a} / \gamma_{\text{н.а}}} \right) + \frac{2 \epsilon_B n_B}{\sigma_{\theta B} / \gamma_{\text{н.Б}}} \right] \text{ kg/liter}. \quad (10.35)$$

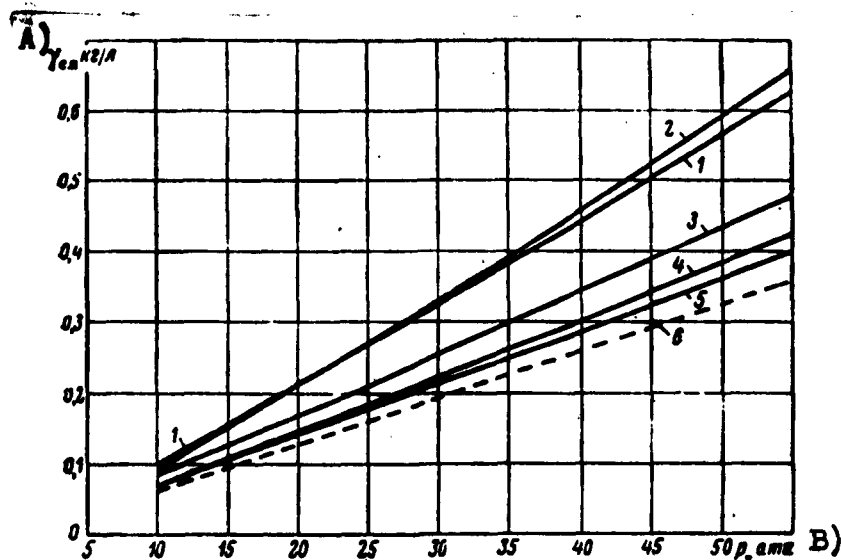


Fig. 10.12. Specific weight of pressure-fed fuel-feed system using different energy sources as a function of the strength properties of the tanks, feed pressure, and other factors. 1) VAD-1;

2) ZhAD with $R_k T_k = 10,000$ kg-m/kg; 3) ZhAD with $R_k T_k = 25,000$ kg-m/kg and VAD-2 with air pre-heated to 325°C ; 4) ZhAD with $R_k T_k = 50,000$ kg-m/kg; 5) PAD with $R_k T_k = 75,000$ kg-m/kg; 6) fuel tanks taken alone. A) $\gamma_{s.p}$, kg/liter; B) p_B , atm abs.

Figure 10.12 shows the specific-weight curve of a feed system with a VAD-1 as a function of the pressure in the fuel tanks, as computed by Formula (10.34) for $p_a = 325$ atmospheres, $T_a = 293^\circ\text{K}$, $R_a = 29.27$ kg-m/kg $^\circ\text{C}$; $k = 1.4$; $\epsilon_a = 1.7$; $\epsilon_B = 1.4$; $\sigma_{ba} = \sigma_{bB} = 110$ kg/mm²; $n_a = 1.7$; $n_B = 2.5$; $\gamma_{m.a} = \gamma_{m.B} = 7900$ kg/m³. The same figure shows the curve of $\gamma_{s.p}$ as a function of p_B in a feed system with a VAD-2 for a fuel-tank air temperature $T_a = 600^\circ\text{K}$ and $H_{ug} = 10,250$ kcal/kg; $\varphi_p = 0.94$; $\eta_{tepl} = 0.4$; $n_B = 3$ (the fuel-tank strength is lowered as a result of heating, and this is taken into account by raising the strength margin from 2.5 to 3) and other data.

The pressure-fed fuel-feed system using a VAD is simple and dependable in operation, and has therefore been used both in ZhRD and in experimental test-stand installations.

A major deficiency of the VAD-equipped pressure-fed fuel-feed system consists in the heavy fuel tanks and gas bottle. Thus, for example, about 50 kg of compressed air at 300 atm abs is required to feed 1 m³ of fuel from the tanks to the engine chamber with a tank pressure of 35-45 kg/cm². A bottle with a capacity of 150 liters is required to hold this air on board the missile. A steel spherical bottle of this type weighs about 150 kg and has a diameter of 680 mm.

This makes perfectly natural the tendency of designers to use solid or liquid substances with relatively low specific weights and high combustion-product temperatures as the working bodies in pressure accumulators. One of the systems for producing a high-temperature gas from a condensed solid substance is the use of a powder [solid-propellant] pressure accumulator for the fuel-feed system.

SECTION 4. DESIGN OF POWDER PRESSURE ACCUMULATOR FOR ENGINE FUEL-FEED SYSTEM

The powder pressure accumulator (PAD) is an apparatus which generates a hot gas in the form of the products of combustion of a powder in a special chamber as necessary to displace the fuel components from the tanks to the engine's combustion chamber.

PAD are classified on the basis of the powder-gas pressure in the chamber as subcritical types without and hypercritical types with a nozzle to reduce the gas pressure to the feed pressure in the tanks. The pressure in a hypercritical PAD reaches 200-250 atm abs.

ZhRD normally employ subcritical PAD, since they have superior weight characteristics and generate a gas with a lower temperature. The gas pressure in the chamber of this PAD is almost equal to the feed pressure in the tanks and is held constant in the system by a

pressure-relief valve.

Normally, PAD employ smokeless powder in armored caps having a constant combustion area and burning from one or both ends. The powder used in the PAD should burn steadily at low temperatures and moderate pressures. The caps are installed in a thick-walled chamber from which the powder gases escape through a nozzle into the fuel tanks. A special ignition charge of fine type DRP smokeless powder ignited electrically is generally used to fire the main powder charge in starting the engine.

The end combustion surface of the main powder charge may be specially channeled or fluted to reduce the weight of the starting powder charge. This enlarges the combustion surface of the basic powder charge while the engine is coming up to thrust and, consequently, also increases the amount of powder gas formed per unit time. The result is that the starting powder charge can be reduced by 40-60% and the weight of the canister for it by 15-30%. Here, the length of the basic powder charge increases only insignificantly, without affecting the dimensions of the basic PAD chamber.

A special reflector (screen) is installed in each fuel tank at the powder-gas inlet, so that the jet of hot gas will not strike the surface of the liquid in the tank and roil it during the early phase of the system's operation, or undergo significant cooling. In the absence of such a screen, the volume of the hot gas entering the tank will be considerably smaller, with the result that a large quantity of it will be required to pressurize the specified quantities of fuel components from the tanks into the combustion chamber. When the hot-gas input unit is unsuccessfully designed, the time required for the engine to come up to thrust may increase and the weight of the working body generating the gas will be relatively high.

The principal advantages of the PAD over the VAD consist in the compactness of its design and the lower specific weight resulting from the relatively small volume of the quantity of powder required.

The PAD has a shortcoming in the fact that the majority of powders burn steadily only at rather high chamber pressures (over 40-50 atm abs), while the combustion rate and hence the rate of gas evolution depend heavily on the temperature at which combustion begins, i.e., on the external atmospheric conditions. Moreover, the heat losses of the powder gases in the fuel tanks and, consequently, the temperature of the gases vary over time and are functions of the fluctuations of the component surface area during the missile's flight.

The powder gases in the system cool from 2300-3300 to 700-900°C as a result of dissipation of heat into the surrounding medium through the walls of the combustion chamber, pipelines, and fuel tanks, as well as to the liquid fuel components. With the objective of reducing heat losses into the surrounding medium, engine designers usually make an effort to shorten the powder-gas lines.

To protect fuel-tank upper bulkheads from the action of the high-temperature powder gases, they may be fitted with screening in the form of a thin-walled metal tube, as in the case of the combustion-chamber screen of the English launching booster "Super Sprite." The most severe thermal stresses arise at the tops of the tanks, at the end into which the hot gases are fed. The temperature in the oxidizer tank is usually higher than in the fuel tank as a result of completion of powder-gas combustion within them (H, CO, etc.).

As a result of the impossibility of making an exact allowance for the heat losses from the gas into the environment, the design of a PAD-equipped fuel-feed system can be only approximate in practice.

It is sometimes convenient to equip each of a group of tandem fuel tanks with an individual powder pressure accumulator.

The use of inside-tank pressure accumulators is the result of efforts to reduce their weight and the heat losses from the powder gases into the environment, as well as to solve the problem of cooling the accumulator in cases in which the engine operates for a long period. However, in cases where corrosive fuel components are used, an inside-tank solid-propellant pressure accumulator must be made from acid-resistant and, consequently, more expensive steels. Furthermore, installation of the accumulator inside the tank is a relatively complex job.

If the engine burns longer than 30-40 sec, the PAD combustion chamber must be cooled by one of the fuel components that is not used to cool the engine chamber. The slight drop that occurs in the pressure of the components in the accumulator's cooling system is of no essential importance, since it is frequently necessary to reduce this pressure to conform to the pressure of the component with which the engine chamber is cooled by installing a throttling disk in its main pipeline. The heat taken from the solid-propellant combustion chamber of the accumulator by the coolant fuel component (heating of the latter) must be taken into account in the thermodynamic calculations for the engine and in the design of the combustion-chamber atomizing head.

The following special requirements are set forth for any form of the PAD-equipped feed system:

- 1) simplicity of design and low specific weight;
- 2) convenience in cooling the PAD chamber with one of the fuel components;
- 3) simple and dependable actuation of the PAD;

4) the shortest possible gas-line length;

5) coincidence (or minor noncoincidence) of the feed-system center of gravity with the pressure center of the missile during flight;

6) uniform displacement of the fuel components from the tanks, even through the vibrations and overloads that are possible in flight and through fluctuations in the ambient temperature.

In the general case, the PAD-equipped fuel-feed system may consist of the following principal elements (see Fig. 10.2):

1) the main PAD chamber, in which the main powder charge is stored and burned;

2) an actuating chamber equipped with a nozzle; this holds the actuating powder charge for combustion when the engine is started (its function is to ignite the main powder charge and fill the free volumes of the tanks and pipelines with powder gases quickly);

3) a constant-pressure powder-gas valve in the feed system; this functions to release excess quantities of the powder gas formed into the surrounding medium;

4) nonreturn valves, which function to prevent one of the fuel components from getting into the other's tank through the main PAD chamber;

5) the pipelines along which the powder gas is fed into the fuel tanks;

6) burst diaphragms and other small elements.

Some of the PAD elements listed above may be lacking (e.g., the additional powder chamber for the initiating powder, the nonreturn valves, the device for forced bursting of the diaphragms, etc.), depending on the type of the fuel components used, the layout of the feed system, and other factors. In the absence of the additional

chamber, its functions are performed by an actuating charge placed directly in the main chamber of the PAD.

Various schemes are possible for the adaptation of the gas-powder fuel-feed system in accordance with the weight and operational characteristics of the engine and the design features of the missile as a whole.

For feed systems designed for prolonged operation, it is advisable to place the gas tubes inside the fuel tanks and cool them with the fuel components. Gas tubes situated outside the tanks for cooling by the combustible or the oxidizer are complex to manufacture and use and have relatively high weights per unit length.

The following problems are solved in designing and making the calculations for a PAD:

- 1) selection of the accumulator's design layout and the type of powder to be used in it;
- 2) calculation of the necessary weight, maximum surface, and length of the powder caps;
- 3) determination of the geometrical dimensions and weight of the accumulator design;
- 4) selection and design of the fittings and connecting and other elements of the pressure accumulator.

For normal operations of a fuel-feed system with a PAD, it is necessary that

- 1) the per-second volume flow rate $V_{sg} = G_{sp}/\gamma_{g.B}$ of the powder gases formed in the combustion chamber of the PAD and entering the fuel tanks under a pressure p_B be equal to the per-second volume flow rate of the fuel in the engine's combustion chamber, $V_{st} = G_{st}/\gamma_t$;

- 2) the combustion time τ_{sg} of the powder charge be equal to the

engine's operating time τ_{dv} .

Here, $\gamma_{gB} = p_B / R_B T_B$ is the specific gravity of the powder gases in the fuel tanks.

To obtain the necessary weight of powder gases at the specified pressure, the powder charge must have a certain definite combustion surface, and the powder-cap lengths must correspond to the specified operating time of the engine.

Since the specific weight of the powder is a constant quantity ($\gamma_p = 1.4$ to 1.7 g/cm^3), the quantity of gas formed will depend on the velocity and combustion area of the powder.

For uniform combustion of the powder charge over the specified surface area, and to obtain a powder-gas volume that is constant over time in the process, the powder charge (caps) are armored; the powder caps are wound with asbestos sheet about 3-4 mm thick on all sides except for the one or two ends that are intended for combustion, and then inserted into a thin-walled steel shell or wound over the asbestos sheet with fine steel wire and placed inside the cylindrical combustion chamber of the PAD. This is not the only method of armoring PAD powder caps.

The combustion rate of the powder depends on its composition and structure and the initial temperature and pressure of combustion. The burn rate of the powder charge depends only to a very minor degree on the initial temperature, and this has a strong influence on the weight of powder gas formed in the temperature range $\pm 50^\circ\text{C}$, which is characteristic for various times of year and different climatic conditions. An increase in pressure facilitates supplying heat to the powder charge and accelerates the reactions taking place on its surface.

When the powder charge is burned at the ends, the gas output of

the PAD is more or less constant over time. Powder charges that burn along an internal canal generally show a gradual increase in combustion surface and, consequently, an increase in the PAD's gas output; charges that burn along the outside cylindrical surface, on the other hand, give a gradually decreasing gas output, which is extremely undesirable.

The weight of the powder charge and the dimensions of the powder caps necessary for normal feed of the theoretical quantity of fuel components from the tanks into the engine chamber are determined by the formulas:

- 1) weight of powder charge

$$G_n = \frac{p_B V_B}{R_B T_B} = \frac{p_B V_B}{R_a T_a \gamma_{renn}} = \frac{p_B V_B}{f_a \gamma_{renn}}; \quad (10.36)$$

- 2) the per-second flow rate of the powder gases into the fuel tanks

$$G_{s,r} = G_{s,n} = F_n u_{ps} \tau_n = \frac{V_{s,r}}{\tau_B} = \frac{V_{s,r} p_B}{R_B T_B} = \frac{G_n \tau p_B}{\tau R_a T_a \gamma_{renn}} \text{ kg/sec} \quad (10.37)$$

- 3) the burn surface of the powder

$$F_n = \frac{G_n \tau p_B}{\tau R_a T_a \gamma_{renn} u_{ps} \tau_n} = \frac{G_n \tau p_B}{\tau f_a \gamma_{renn} u_{ps} \tau_n} \text{ m}^2; * \quad (10.38)$$

- 4) length of powder cap

$$l_n = u_{ps} \tau_n \text{ cm, **} \quad (10.39)$$

where V_B is the volume of the tanks for the basic fuel components; p_B , T_B , γ_B , and R_B are the pressure, temperature, specific gravity, and gas constant, respectively, of the powder gas in the fuel tanks, T_a and R_a are the temperature and gas constant, respectively, of the powder gases in the PAD chamber, $f_a = R_a T_a$ is the reduced power of the selected type of powder which is taken from tables for the

*[Subscript: π = p = porokh = powder.]

**[Subscript: π = sh = shashka = cap.]

majority of existing smokeless powders ($f_a = 80,000$ to $100,000$ kg-m/kg), i is the number of burn faces of the powder cap, τ_{dv} is the operating time of the engine, $\eta_{tepl} \approx 0.3$ to 0.4 is a coefficient taking into account the heat losses of the powder gases in the fuel-feed system, u_{tp_a} is the linear burn rate of the smokeless powder, which depends on its composition and the initial temperature of combustion t_{nach}^* in $^{\circ}\text{C}$, and on the combustion pressure p_a , which is given approximately by the formula

$$u_{tp_a} = u_{15^{\circ}} p_a^v [1 + 0.0028(t_{nach}^* - 15^{\circ})] \text{ cm/sec}; \quad (10.40)$$

here, $u_{15^{\circ}}$ is the linear burn rate of the given type of powder at a pressure of 1 atm abs and a temperature of 15°C , as taken from the table; v is an experimental coefficient that characterizes the composition of the powder and is also taken from the table (for existing smokeless powders, we have $v = 1.45$ to 1.75).

Jacketed charges of type NM are sometimes used for PAD. The efficiency of this powder with $\eta_{tepl} = 3.5$ attains

about 28,500 kg-m/kg at 25 atm abs;

about 31,100 kg-m/kg at 40 atm abs.

In determining the required burn surface of the powder charge, the value of u_{tp_a} is taken for the lowest possible initial combustion temperature of the powder with the objective of guaranteeing the specified powder-gas pressure in the fuel tanks even in the event that the initial temperature of the powder's combustion is, in accordance with atmospheric conditions, the lowest of the possible temperatures for operation of the engine, i.e., when the linear burn rate of the powder and the rate of generation of the powder gases are at their minima. In practice, operation of the engine will inevitably occur also at higher ambient temperatures (with the temperature $t_{nach} = t_{nach} = t_{nachal'nyy} = \text{initial.}$)

ture of powder initiation higher than the theoretical level). As a result, the burn rate and the quantity of gases formed will be larger than the theoretical values. For this reason, a valve that releases excessive quantities of gas into the atmosphere is usually installed in the PAD system to prevent elevation of the gas pressure in the fuel tanks above the calculated value, thereby maintaining the pressure in the PAD combustion chamber at a constant level. One of the basic specifications in designing gas-line valves for PAD-equipped fuel-feed systems is protection of their resilient elements (springs) from attack by the hot gases.

In determining the length of the powder caps, the value of u_{tp_a} is chosen for the highest possible powder-combustion initiation temperature under operating conditions in order to ensure normal operation of the feed system for the specified length of time, even in cases where the temperature of powder-combustion initiation and, consequently, the burn rate of the powder are at their highest values in accordance with atmospheric conditions. Naturally, the charge will not be able to burn until the system has ceased to operate if the initial temperature of powder combustion is lower than the calculated value. This means that the weight of the PAD powder charge will have a guarantee margin when the length of the powder caps is determined in this way.

It must be remembered that when the powder burns in a chamber with a nozzle, as is sometimes the case in a PAD, data for the burn rates of unarmored powder caps cannot be used because it has been established that their burn rates depend heavily on scavenging of the surface by the powder gases, which does not occur when powder burns in a PAD.

Combustion of the majority of smokeless powders proceeds normally

only at rather high combustion-chamber pressures (above 40-50 atm abs). At lower pressures, the powder burns slowly with incomplete decomposition (the heat of decomposition is now entirely liberated).

Entering the oxidizer tank and mixing there with oxidizer vapors, the powder gases may complete combustion (since the excess oxidizer ratio α in the powders is normally less than 1), with a slight increase in the temperature of the powder gases over their temperature in the combustible tank, where such combustion cannot take place. For this reason, the value of η_{tepl} for the oxidizer tank will be smaller than for the combustible tank. In such cases, we may set

$$\eta_{tepl.o} \approx (0.8 \text{ to } 0.9) \eta_{tepl.g}.$$

In designing the PAD, it is necessary to provide measures to prevent entry of unburned solid powder particles into the propellant tanks, where they may become centers of ignition and result in detonation or, at the very best, foul the propellant nozzles of the combustion chamber, to the considerable detriment of the effectiveness with which the propellants are atomized.

The weight of the initiating powder charge influences the nature of the process at the start of powder combustion. When there is an insufficient quantity of this powder, the pressure in the PAD combustion chamber rises slowly, and when a large quantity is present, the pressure rises at once to a value exceeding the normal combustion-chamber pressure and then drops off. Experiments have shown that the basic powder charge also contributes to the formation of a peak in this pressure.

The weight of the PAD powder charge is determined by the formula

$$G_{\text{пуск}} = \frac{p_E V_{\text{своб}}}{R_0 T_{\text{своб}}}, \quad (10.41)$$

*[Subscript: $\text{пуск} = \text{pusk} = \text{puskovoy} = \text{initiating}$; $\text{своб} = \text{svob} = \text{svobodnyy} = \text{free}$.]

where V_{svob} is the "free" volume of the fuel-feed system and $\eta_{tepl} \approx 0.15$ to 0.2 is a coefficient taken into account for the heat losses of the powder gases in the system at the engine's minimal operating temperature.

It is necessary to compute the length of the powder cap by the formula

$$L_m \approx u_{tp_a} \tau_{pusk} \quad (10.42)$$

where u_{tp_a} is the linear burn rate of the powder type in question at a chamber pressure p_a , and τ_{pusk} is the starting-conditions time of the engine.

The amount of the initiating powder charge must be such that the "free" volume of the engine will be filled with powder gases at the feed pressure p_B from the fuel tanks at the beginning of the work done by the basic powder charge.

A quick-burning powder is used as the initiating charge of the PAD to bring the engine up to its operating regime quickly.

The chamber of the initiating PAD is usually left uncooled (in view of its short operating time) and with a hypercritical nozzle. The critical-section area of the nozzle is determined here by the formula

$$F_{n.kp} = \frac{G_{s,uzen}}{\gamma_c a p_a}, \quad * \quad (10.43)$$

where φ_s is the flow-rate factor of the nozzle and a is a coefficient which depends on the properties of the powder gases and their pressure drop in the nozzle.

The combustion chambers of the main and initiating PAD are usually made cylindrical with spherical bases. Their geometrical dimensions are determined by the calculated dimensions of the powder charges.

*[Subscript: n.kp = p.kr = ploshchad', kriticheskaya = critical area.]

The wall thickness of a cylindrical accumulator combustion chamber is expressed by the formula

$$\delta_a = \frac{p_a d_a n_a}{2 \sigma_{ba} / \gamma_{m.a}}, \quad (10.44)$$

where $n_a \approx 2.5$ to 3.0 is the strength margin of the combustion-chamber material, which depends on the operating time of the pressure accumulator (on the degree to which it becomes heated).

The weight of a PAD with a cylindrical combustion chamber may be expressed by the formula

$$G_{ak} = \epsilon_a \pi d_a l_a \delta_a \gamma_{m.a} b_a, \quad (10.45)$$

where $\epsilon_a \approx 2$ to 2.5 is an encumbrance factor taking into account the weight of the bases, fittings, connecting parts, and other small components of the accumulator, d_a and l_a are the diameter and length, respectively, of the cylindrical powder-combustion chamber, $\gamma_{m.a}$ is the specific gravity of the chamber material, b_a is the fill factor of the combustion-chamber volume with the powder charge (this takes into account the free volume of the chamber and the volume occupied by the armored powder caps), which, for purposes of calculation, may be set equal to

$b_a \approx 1.05$ to 1.5 for burning of the powder from one end and

$b_a \approx 1.5$ to 2.5 is the same for combustion from two ends.

Since the volume of the cylindrical powder-combustion chamber may be expressed approximately by the formula $V_a = (\pi d_a^2 / 4) l_a$, from which $\pi d_a^2 l_a = 4V_a$, and the fluctuation of the gas pressure in the powder-combustion chamber as a result of nonuniform gas evolution may be taken into account by a coefficient C_a , Equation (10.45) may be rewritten as

$$G_{ak} = 2 \epsilon_a V_a \frac{p_a n_a b_a C_a}{\sigma_{ba} / \gamma_{m.a}}, \quad (10.46)$$

where $C_a \approx 1.2$ to 1.4 in the absence of a pressure-relief valve and

$C_a \approx 1.02$ to 1.05 in the presence of a pressure-relief valve.

The weight of the components connecting the accumulator to the fuel tank depends on the type of tank, its position, output, and other factors, and is normally evaluated on the basis of design considerations and statistical data.

The approximate weight of the PAD with its powder charge is

$$G_{\text{ПДЛ}} = G_a + G_{\text{ш}} = \frac{p_B V_B}{f_a \gamma_{\text{гснл}}} + \frac{2z_a p_a V_a n_a b_a C_a}{\sigma_{ba} / \gamma_{\text{м.а}}} = \frac{p_B V_B}{f_a \gamma_{\text{гснл}}} \left(1 + \frac{2z_a p_a n_a b_a C_a}{\gamma_{\text{гснл}} \sigma_{ba} / \gamma_{\text{м.а}}} \right), \quad (10.47)$$

where $V_a = G_p / \gamma_p = p_B V_B / \gamma_p f_a \eta_{\text{тепл}}$ is the powder-charge volume.

It is necessary to burn about 12-15 kg of powder to pressurize one cubic meter of fuel from the tanks to the engine chamber (taking into account cooling of the gas in the system). Since the powder has a high specific gravity in its solid state, the volume of the powder chamber to hold the quantity of powder indicated will be approximately 12-15 liters, and its weight without the powder charge will come to about 25 kg (the weight of the chamber also depends on the powder-gas pressure).

The specific gravity of the PAD, including the powder charge, is

$$\gamma_{\text{ПДЛ}} = \frac{G_{\text{ПДЛ}}}{V_B} = \frac{p_B}{f_a \gamma_{\text{гснл}}} \left(1 + \frac{2z_a p_a n_a b_a C_a}{\gamma_{\text{гснл}} \sigma_{ba} / \gamma_{\text{м.а}}} \right) \text{ kg/liter}. \quad (10.48)$$

The specific gravity of the PAD-equipped fuel-feed system is

$$\gamma_{\text{с.а}} = \frac{G_B + G_{\text{ПДЛ}}}{V_B} = p_B \left[\frac{2z_B n_B}{\sigma_{bB} / \gamma_{\text{м.В}}} + \frac{1}{f_a \gamma_{\text{гснл}}} \left(\frac{2z_a p_a n_a b_a C_a}{\gamma_{\text{гснл}} \sigma_{ba} / \gamma_{\text{м.а}}} \right) \right] \text{ kg/liter}; \quad (10.49)$$

Figure 10.12 shows curves of the specific weight of a PAD-equipped fuel-feed system as a function of the pressure p_B in the fuel tanks for $\epsilon_B = 1.4$, $\epsilon_a = 2.5$, $n_B = 3$, $n_a = 2.5$, $b_a = 1.2$, $C_a = 1$, $\sigma_{bB} = \sigma_{ba} = 110 \text{ kg/mm}^2$, $\gamma_{\text{м.В}} = \gamma_{\text{м.а}} = 7900 \text{ kg/m}^3$, $f_a = 75,000 \text{ kg-m/kg}$, $\eta_{\text{тепл}} = 0.33$, $p_a = 100 \text{ atm abs}$, and $\gamma_p = 1600 \text{ kg/m}^3$.

SECTION 5. CALCULATIONS FOR LIQUID-PROPELLANT PRESSURE ACCUMULATOR FOR FUEL-FEED SYSTEM

The liquid-propellant pressure accumulator (ZhAD) is a unit which generates a hot gas from two hypergolic fuel components for displacement of the main fuel components from the tanks into the engine's combustion chamber. The fuel components are fed into the ZhAD from special storage tanks by compressed air supplied from the pneumatic unit of the system.

The basic deficiency of ZhAD-equipped fuel-feed systems is their higher design complexity as compared with VAD or PAD-equipped feed systems.

A ZhRD fuel-feed system pressure fed by a ZhAD may consist of the following four basic units (see Fig. 10.3):

- 1) the oxidizer-feed unit;
- 2) the combustible-feed unit;
- 3) the system's pneumatic unit;
- 4) tanks for the basic propellants.

The basic elements of the feed units for the respective fuel components are:

- a) the reactor, which is usually installed in the appropriate tank for the basic fuel component;
- b) small tanks for the combustible and oxidizer (the auxiliary fuel components);
- c) fittings and tubing.

The system's pneumatic block is shared by the two feed units for the fuel components. The basic element in each feed block is the reactor (the auxiliary-propellant combustion chamber). The reactors for the two main-propellant tanks are physically almost identical.

Each reactor may consist of the following units:

- a) a chassis, which is the basic element of the gas generator and the one on which all the other elements are mounted;
- b) nozzles for atomization of the propellants as they are fed into the reactor;
- c) a diaphragm unit, the function of which is to block communication between the reactor cavity and the tanks while the latter are being filled with the propellants and during storage of the engine (the unit consists of a body, a filter, a diaphragm, a disk, and a pressure screw);
- d) a cutoff valve;
- e) a diaphragm-equipped reactor cap, which, together with the body, forms a chamber for mixing and combustion of the fuel components;
- f) a number of other small elements.

The top of the reactor housing serves as a head for placement of the fuel nozzles.

A detailed description of the design features of the ZhAD, its starting process, and its operating principle is outside the scope of the present discussion.

In principle, any combination of combustible and oxidizer can be used to operate a ZhAD. However, efforts to ensure simple and dependable starting of the accumulator, stable operation, and convenient maintenance have reduced the number of fuels that can be used expediently for ZhAD. Hypergolic fuel components are most suitable. In cases where nonhypergolic fuel components are used for this purpose, it is advisable to use a spark-fired powder cartridge to ignite them when the engine is started. The range from 800 to 900°C may be regarded as the operationally most suitable combustion

temperature of the propellants in the ZhAD reactor.

To obtain a vapor gas at the above temperature, the fuel-mixture ratio $X_{B.g}$ for the ZhAD's combustible tank must be made lower and that for the oxidizer ($X_{B.o}$) considerably higher than the stoichiometric value in order to avoid combustion of the gases in the tanks. The combustible-tank reactor normally operates at an excess oxidizer ratio $\alpha_{B.g} \approx 0.3$ to 0.4 , while that of the oxidizer tanks works at $\alpha_{B.o} \approx 3$ to 6 .

Limits are usually imposed on the mixture ratios of the propellants fed into the ZhAD reactor to prevent exceeding the adopted temperature value, e.g., 900°C .

As we know, the temperatures of the base t_{dn} and shell t_{obech}^* of the tank at the reactor end and the specific flow rate of the fuel into the reactor will depend on the fuel mixture ratios. When the fuel composition changes toward the stoichiometric value, the temperature of the main-propellant tanks will rise and the specific flow rate of the fuel will decline, and vice versa. The optimum mixture ratios for the ZhAD will be those values at which the wall temperature of the main-propellant tanks does not exceed the safely admissible limit ($480-500^{\circ}\text{C}$) at the end of the engine's operation.

During the engine's operation, the shell and bottom of the combustible tank are heated to a temperature $80-100^{\circ}$ higher than the corresponding parts of the oxidizer tank. The tank bases are heated by almost the same number of degrees above the temperatures of their shells. The degree to which the bases and shells of the engine fuel tanks are heated depends on the material of which they are made, the gas temperature and the heating period, the physical properties of the components to be pressurized, and a number of other factors.

*[Subscript: o6ey = obech = obechayka = shell.]

Since analytical determination of the temperature to which the tank walls are heated involves great difficulty and is not always possible with the accuracy required for practical purposes, the values of t_{dn} and t_{obech} must be assigned for the calculations on the basis of statistical and experimental data.

The feed pressure p_B of the main fuel components is composed of the engine's combustion-chamber pressure plus the pressure lost in the form of hydraulic resistance in the pipelines on the way from the tank to the engine's injectors. To insure stable feed of the propellants into the combustion chamber and reduce the fluctuations in engine thrust, a definite tolerance for the value of p_B must be established by the technical specifications for the design of the system.

The following basic data are necessary for calculation of a ZhAD for an engine fuel-feed system:

- 1) the type and per-second flow rates of the basic propellants for operation of the engine chamber;
- 2) the capacities of the tanks for these propellants, with an indication as to the volumes of the "guarantee" propellant margins and air cushions in the tanks after fueling;
- 3) the pressure p_B feeding the main propellants into the engine's combustion chamber (the pressure in the fuel tanks);
- 4) the temperature to which the fuel-tank walls may safely be heated during the time in which the system is operating;
- 5) the type of the hypergolic fuel components used to operate the ZhAD;
- 6) the engine's operating program.

Basically, the design of the ZhAD reduces to determination of:

- 1) the necessary fuel mixture ratio χ required to operate the ZhAD at a selected gas temperature in the reactors — which is done

by thermodynamic calculation of the compositions of the combustion products of the fuel in question for a series of selected values of χ with subsequent construction of curves of T_k and $R_k T_k$ as functions of χ or by the use of existing diagrams;

2) the necessary per-second flow rates of the fuel components in the combustible tank and the oxidizer tank for operation of the ZhAD;

3) the volumes of the tanks for these fuel components;

4) the number and dimensions of the nozzles for atomization of the fuel components as they are fed into the reactor;

5) the required reserve of air in the bottle of the system's pneumatic unit for the initial pressure selected for it and the dimensions of this bottle.

When the calculations have been completed, the necessary fittings are selected for the feed units of the ZhAD and laid out for it, and the necessary strength calculations are made for the system. The most difficult part is thermodynamic calculation of the composition of the products of fuel combustion in the reactors for different χ .

It has been established that the products of combustion of a fuel composed of Tonka-250 + 80% HNO_3 and 20% N_2O_4 consist of the gases CO_2 , CO , H_2 , H_2O , N_2 , C_2H_6 , CH_4 , C_2H_4 , and C_2H_2 and C in the solid phase for small χ . The composition of these combustion products is determined by solution of a system of equations consisting of

a) the mass-balance equations in ratio form:

$$\frac{C_r + \chi C_o - n_c}{O_r + \chi O_o} = \frac{12}{16} \frac{p_{\text{CO}_2} + p_{\text{CO}} + p_{\text{CH}_4} + 2p_{\text{C}_2\text{H}_6} + 2p_{\text{C}_2\text{H}_4} + 2p_{\text{C}_2\text{H}_2}}{2p_{\text{CO}_2} + p_{\text{H}_2\text{O}} + p_{\text{CO}}}$$

$$\frac{H_r + \chi H_o}{O_r + \chi O_o} = \frac{1}{16} \frac{2p_{\text{H}_2\text{O}} + 2p_{\text{H}_2} + 4p_{\text{CH}_4} + 2p_{\text{C}_2\text{H}_6} + 2p_{\text{C}_2\text{H}_4} + 6p_{\text{C}_2\text{H}_2}}{2p_{\text{CO}_2} + p_{\text{H}_2\text{O}} + p_{\text{CO}}}$$

$$\frac{N_r + \chi N_o}{O_r + \chi O_o} = \frac{14}{16} \frac{2p_{\text{N}_2}}{p_{\text{CO}_2} + p_{\text{H}_2\text{O}} + p_{\text{CO}}}$$

where η_C is the weight fraction of carbon in the solid phase;

b) the equation of the sum of the gas partial pressures in the mixture,

$$p_r = \sum p_i = p_{CO_2} + p_{CO} + p_{H_2O} + p_{H_2} + p_{CH_4} + p_{C_2H_2} + p_{C_2H_4} + p_{C_2H_6};$$

c) the equation of the chemical-equilibrium constants (see Appendix V).

In solving the above system of equations by the method of successive approximations, the partial pressures of the gases C_2H_2 , C_2H_4 , and C_2H_6 may be set equal to zero in the first approximation because of their smallness.

If nitrogen is present in the fuel in question, the weight fraction of the solid-phase carbon may also be determined from the following balance equation:

$$\frac{g_C - \eta_C}{g_N} = \frac{12}{14} \frac{p_{CO_2} + p_{CO}}{2p_{N_2} + p_{NO} + p_N},$$

where g_C and g_N [kg/kg] are the respective weight fractions of carbon and nitrogen in one kilogram of fuel.

In this case, the energy content of 1 kg of fuel-combustion products is determined by the formula

$$I_r = \frac{1 - \eta_C}{\mu_r} \sum p_i I_i + \frac{\eta_C}{\mu_C} I_C,$$

where I_i and I_C are the respective energy contents of the i^{th} gas and the solid carbon (condensed phase) in the mixture, referred to 1 kmole and μ_C is the molecular weight of the carbon in the solid phase.

The entropy of 1 kg of combustion products is computed by the formula

$$S_r = \frac{1}{\mu_r p_r} \sum (S_i - R \ln p_i) p_i + \frac{\eta_C}{\mu_C} S_C,$$

where S_i and S_C are the standard entropies of the i^{th} gas and the

solid carbon, referred to 1 kmole.

Calculations indicate that there is about 4-5% of carbon in the solid phase in 1 kg of combustion products from the above fuel with $\chi = 1.8$ and a temperature of 900°C .

As the fuel-mixture ratio χ is increased above the stoichiometric value, the combustion temperature of the fuel begins to drop off. This is accompanied by a corresponding decline of the content of the dissociation products O, H, and OH in the combustion products and a sharp decline in the H_2 and CO contents of the gas mixture.

It has been established that for large values of χ , the combustion products of the fuel under consideration consist of the products of complete combustion CO_2 and H_2O , free oxygen O_2 , and nitrogen N_2 .

Much time is required to determine the composition and temperature of the combustion products of a fuel heavily ballasted with combustible. For this reason, design of the combustion chamber for fuels with very low excess oxidizer ratios ($\alpha = 0.15$ to 0.4) may be based on the value of $R_k T_k$ (see page 766).

The usual system of equations is employed to determine the composition of these products at the selected temperature in the reactor; its solution is highly simplified by the small number of gases.

In this case, the mass-balance equations take the form

$$\begin{aligned} 1) \quad & \frac{C_r + \chi C_o}{O_r + \chi O_o} = \frac{12}{16} \frac{p_{\text{CO}_2}}{2p_{\text{CO}_2} + p_{\text{H}_2\text{O}} + 2p_{\text{O}_2}}; \\ 2) \quad & \frac{H_r + \chi H_o}{O_r + \chi O_o} = \frac{1}{16} \frac{2p_{\text{H}_2\text{O}}}{2p_{\text{CO}_2} + p_{\text{H}_2\text{O}} + 2p_{\text{O}_2}}; \\ 3) \quad & \frac{N_r + \chi N_o}{O_r + \chi O_o} = \frac{14}{16} \frac{2p_{\text{N}_2}}{2p_{\text{CO}_2} + p_{\text{H}_2\text{O}} + 2p_{\text{O}_2}}. \end{aligned}$$

The calculations also make use of the equality between the energy contents of the fuel and the products of its combustion, taking into account the loss due to the incompleteness of combustion and dissipation of heat from the reactor into the surrounding medium

(the energy losses are determined experimentally).

The composition of the combustion products of a fuel ballasted with oxidizer in the necessary quantity for operation of the ZhAD (up to the temperature of the combustion products $T_k = 1100$ to 1200°K) may also be determined by the formulas

$$g_{\text{CO}_2} = \frac{11}{3} C, \text{ kg/kg } g_{\text{H}_2\text{O}} = 9H, \text{ kg/kg};$$

$$g_{\text{O}_2} = O - \left(\frac{8}{3} C + 8H\right) \text{ kg/kg}; g_{\text{N}_2} = N, \text{ kg/kg};$$

where

$$g_{\text{CO}_2} + g_{\text{H}_2\text{O}} + g_{\text{O}_2} + g_{\text{N}_2} = 1.$$

The fuel mixture ratio χ which guarantees the necessary temperature T_k of the evolved gas is determined as follows.

We assign three proposed values to the oxidizer-to-combustible weight ratio χ (e.g., $\chi = 10, 15$, and 20 kg/kg) and compute the following values corresponding to them:

1) the elementary weight composition of the fuel (C_t, H_t, O_t , and N_t in kg/kg) and its energy content I_t in kcal/kg ;

2) the weight compositions of the combustion products of the fuel in question in the form of the partial pressures p_i or weight fractions g_i and the energy content I_k of these products at the selected temperature T_k [$^\circ\text{K}$] by the formula

$$I_k = \frac{1}{\sum g_i} \sum g_i I_i \text{ kcal/kg}$$

or

$$I_k = \sum g_i I_i \text{ kcal/kg}.$$

Then we construct combined diagrams of $I_t = f(\chi)$ and $I_k = f(\chi)$ and, since $I_t = I_k$ according to the first law of thermodynamics, the point of intersection of the curves of I_t and I_k will correspond to the unknown theoretical value χ_{rasch} that corresponds to the selected working temperature T_k [$^\circ\text{K}$].

Similarly, χ is determined for the fuel ballasted with combus-

tible; in this case, it is necessary first to assign $\chi = 0.5, 1.0,$ and 1.5 .

The required auxiliary-fuel flow rate for operation of each ZhAD of the system is determined by the formula

$$G_s = \frac{p_B (V_B + V_{kl})}{R_k T_k \eta_{\text{tepl}}} \text{ kg,} \quad (10.50)$$

where V_{kl} is the volume of gas lost through the constant-pressure valve, which is determined by experiment in each specific case, $R_k T_k$ is the reduced power of the gas, which is determined in the thermodynamic calculations for the reactor in kg-m/kg, and $\eta_{\text{tepl}} \approx 0.2$ to 0.3 is a coefficient taking into account the heat losses from the gas in the fuel-feed system; this is also determined experimentally.

The above formula indicates that the required auxiliary-fuel flow rate into the ZhAD reactor is inversely proportional to the gas temperature in the engine tank. The necessary reserves of fuel components should be determined for the feed units of the ZhAD with consideration of the probable departures from tolerance in the feed pressure p_B , tank volume, the quantity $R_k T_k$, and the coefficient χ .

The fuel-flow rate into the ZhAD of a fuel-feed system is approximately 1.5-2% of the fuel flow rate into the engine combustion chamber.

The general specifications apply for atomization of the fuel components at delivery into the reactors. The reactor injectors are designed in the usual manner.

In certain cases, it is highly important to reduce the time taken for the fuel-tank pressure to come up to the operating values when the engine is started (when air cushions are present in the tanks). Powder caps that burn during the first seconds after the "fire" signal may be used for this purpose. The weight and burn area

of these caps are computed on the basis of the condition that the free volume of the tanks must be filled to the feed pressure by the powder gases. Burning of the caps must be completed before the ZhAD reactor goes into operation.

The weight of the ZhAD consists of the fuel weight G_t , the weight G_{bach}^* of the small tanks for the fuel, the weight G_{bal}^{**} of the compressed-gas bottles, and the weight G_g^{***} of the compressed gas, i.e.,

$$G_{ЖАД} = G_t + G_{bach} + G_{bal} + G_g. \quad (10.51)$$

Since there are not at the present time any exact data concerning the weights of ZhAD combustion chambers, its weight must be taken into account in approximate calculations by a slight increase in the coefficient ϵ_a (in figuring the weights G_{bach} and G_{bal}).

Assuming that the small fuel tanks and gas bottles of the ZhAD are made spherical and of the same material and have identical volumes, i.e.,

$$V_{bach} = V_{bal} = \frac{G_t}{\gamma_t} = \frac{p_B V_B}{R_g T_g \gamma_{t,trans}},$$

the specific weight of the ZhAD may be expressed as follows by analogy to the VAD-equipped pressurized fuel-feed system:

$$\begin{aligned} \gamma_{ЖАД} &= \frac{G_{ЖАД}}{V_B} = \frac{G_t + G_{bach} + G_{bal} + G_g}{V_B} = \frac{p_B}{R_g T_g \gamma_{t,trans}} \left[\gamma_t + \frac{3}{2} \frac{\epsilon_a n_a (p_B + \Delta p_B)}{\epsilon_B s / \gamma_{m,a}} + \right. \\ &\quad \left. + \frac{3}{2} \frac{k s_a n_a (p_B + \Delta p_B)}{(1-x) \epsilon_B s / \gamma_{m,a}} + \frac{k (p_B + \Delta p_B)}{R_g T_g (1-x)} \right] = \\ &= \frac{p_B}{R_g T_g \gamma_{t,trans}} \left[\gamma_t + \frac{3}{2} \frac{\epsilon_a n_a (p_B + \Delta p_B)}{\epsilon_B s / \gamma_{m,a}} \left(1 + \frac{k}{1-x} \right) + \frac{k (p_B + \Delta p_B)}{R_g T_g (1-x)} \right] \text{ kg/liter,} \end{aligned} \quad (10.52)$$

where k is the polytropic exponent of gas expansion in the system, γ_t is the specific gravity of the fuel in the ZhAD, Δp_B is the pres-

- * [Subscript: $\sigma_{ach} = bach = bachok = (\text{small}) \text{ tank.}$]
 ** [Subscript: $\sigma_{al} = bal = ballon = \text{bottle.}$]
 *** [Subscript: $r = g = gaz = \text{gas.}$]

sure drop between the ZhAD bottles and the tanks holding the basic fuel components, and R_a and T_a are the gas constant and temperature of the gas in the ZhAD tanks when the system goes into operation.

The specific weight of a ZhAD-equipped pressure-fed fuel-feed system (pressure accumulator and cylindrical tanks for basic fuel) is

$$\gamma_{c.s} = p_B \left\{ \frac{1}{R_a T_a \gamma_{m.a}} \left[1 + \frac{3}{2} \frac{\epsilon_a n_a (p_B + \Delta p_B)}{\gamma_{m.a} / \gamma_{m.B}} \left(1 + \frac{k}{1-x} \right) + \frac{k (p_B + \Delta p_B)}{\gamma_{m.a} (1-x)} \right] + \frac{2 \epsilon_B n_B}{\epsilon_B / \gamma_{m.B}} \right\} \text{ kg/liter.} \quad (10.53)$$

Figure 10.12 presents curves showing the specific weight of the ZhAD-equipped fuel-feed system as computed by Eq. (10.53) for $R_k T_k = 10,000 \text{ kg-m/kg}$ and $R_k T_k = 50,000 \text{ kg-m/kg}$, $\eta_{tepl} = 0.28$, $\gamma_t = 1300 \text{ kg/m}^3$, $\epsilon_a = \epsilon_B = 1.4$, $n_a = 1.7$, $n_B = 3$, $\Delta p_B = 0.2 p_B$, $k = 1.4$, $x = 0.2$, $\sigma_{ba} = \sigma_{bB} = 110 \text{ kg/mm}^2$, $\gamma_{m.a} = \gamma_{m.b} = 7900 \text{ kg/m}^3$, $R_a = 29.27$ and $T_a = 293^\circ \text{K}$.

Calculations indicate that the γ_{sp} of a ZhAD-equipped pressure-fed fuel-feed system is close to the specific weight of a PAD-equipped fuel-feed system with adequately high gas temperatures.

The basic deficiency of the ZhAD-equipped fuel-feed system is its complexity of design as compared with systems equipped with VAD and PAD.

SECTION 6. METHODS OF POWERING TNA TURBINES AND THEIR ADVANTAGES AND DISADVANTAGES

During recent years, according to the foreign literature, a general tendency toward increasing the economy of high-thrust ZhRD's by increasing the combustion-chamber pressure has been noted. The turbopump fuel-feed system is usually used in such engines.

Various methods may be used to obtain the working fluid to power the pump-set turbine. The following types of gas generators

(GG*) may be used for this purpose:

- 1) one-shot solid-fuel gas generators, which are distinguished by relative design simplicity and ease of starting;
- 2) single-component gas generators, which work on single-component liquid fuels and can be restarted;
- 3) two-component gas generators, which operate on the basic fuel components and can be restarted.

The appropriate slow-burning powders may be used as the solid gas-generator fuel, while hydrogen peroxide (H_2O_2), isopropyl nitrate ($C_3H_7ONO_2$), ethylene oxide (CH_4O), ammonia (NH_3), hydrazine (N_2H_4), etc., may be used as single-component fuels. Some of the single-component fuels require use of appropriate catalysts to accelerate their decomposition.

In cases where hydrogen peroxide is used to generate the gas, the generator is frequently referred to as a hydrogen-peroxide vapor-gas generator (PGG**).

A number of existing turbopump-fed ZhRD use single-component vapor-gas generators operating on hydrogen peroxide of 80-90% concentration by weight, with expulsion of the spent vapor gas into the atmosphere (see Fig. 10.4).

A vapor gas at a temperature of about 380-480°C is formed on decomposition of 80% hydrogen peroxide. The discharge velocity of this vapor gas from the nozzle attains $c_1 = 950$ to 1100 m/sec at a pressure of 25-30 atm abs in front of the nozzle.

In practice, the turbine blades make it possible to use a vapor gas at a relatively high temperature and, consequently, with a high discharge velocity of this gas from the turbine nozzle. The turbine's

economy of operation, i.e., the specific vapor-gas consumption, which

*[$\Pi T = \underline{GG}$ = gazogenerator = gas generator.]

**[$\Pi T = \underline{PGG}$ = parogazogenerator = vapor-gas generator.]

is the ratio of the per-second flow of vapor gas into the turbine to its net power, depends on the velocity c_1 . The method of powering the turbine has been well-mastered in practice, as compared to other methods, and is simple from a design standpoint. A drawback to it is the low operating economy of the turbine.

In the case of the TNA, the temperature of the vapor gas obtained at a given pressure in the PGG is determined by the hydrogen-peroxide concentration. As a result, it is no longer necessary to have a temperature regulator for the vapor gas or to ignite the components in the vapor-gas generator on starting, and this simplifies the generator's design and insures dependable operation.

The hydrogen-peroxide vapor-gas generator starts automatically and does not require special initiating devices; it is capable of operating dependably on a very small amount of hydrogen peroxide. If, however, the thrust of the engine must be controllable, the generator must have provision for varying the output in order to reduce the number of TNA rpm's.

As one of the engine's vital units, the turbopump set is subject to dependability and economy requirements. Increasing the efficiency of the turbines for low- and medium-thrust ZhrD has no significant effect, since the fuel consumed to drive the TNA in these cases composes an insignificant fraction of the total fuel consumed in the engine's combustion chamber. For this reason, even a very large increase in turbine efficiency has here only a very slight effect on over-all engine economy. However, the prospective development of the ZhrD promises to create high-thrust engines with enormous fuel-flow rates in the chambers. In these cases, the problem of TNA operating economy acquires considerably greater importance.

The use of a vapor gas at higher temperatures (of the order of

700-800°C) should be noted as one of the possible methods of increasing the turbine efficiency.

It is possible to obtain a vapor gas at such temperatures working with hydrogen peroxide by increasing the latter's concentration to 90%. However, the use of H_2O_2 of such high concentration raises the cost of the vapor gas considerably due to the relatively high cost of the peroxide and involves certain difficulties with its application as a result of the higher freezing point. For example, 80% H_2O_2 has a freezing point of $-27.7^{\circ}C$, while 90% peroxide freezes at $-11^{\circ}C$.

The temperature of the vapor gas may also be increased by adding to hydrogen peroxide of lower concentration certain organic additives (methanol, phenol, glycerine, etc.) that are capable of burning in it to liberate a considerable additional quantity of heat due to the gaseous oxygen formed from the peroxide on its decomposition. In this case, a vapor gas at a pressure of 25-30 atm abs and a temperature of $1000^{\circ}C$ may have a discharge velocity of about $c_1 \approx 1300-1400$ m/sec. This way of producing the vapor gas for the turbine is more convenient in practice because, with proper selection of the additives to the peroxide, it is possible simultaneously to obtain a vapor gas at higher temperature and depress the freezing point of the initial hydrogen peroxide solution. Moreover, the cost of this vapor gas will be reduced as a result of the use of additives that are cheaper than the H_2O_2 .

However, this advantage is retained only provided that the turbine-powering system remains simple in design and dependable in operation. The explosion hazard presented by such mixtures must be investigated with particular care.

Naturally, hydrogen-peroxide catalysts used to produce a high-

temperature vapor gas must be thermally stable within the indicated temperature range (they must retain their activity and mechanical cohesion under these conditions) and be capable of promoting the reaction at the necessary rate. The catalysts presently known for decomposition of hydrogen peroxide have been developed for application with low vapor-gas temperatures. The necessity of producing vapor gas at relatively high pressure and temperature naturally requires catalysts of higher thermal stability and mechanical cohesiveness for decomposition of hydrogen peroxide with the organic additives.

It is possible to power the turbine with gas taken directly from the combustion chamber at the point where the basic stage of the fuel-combustion process culminates (e.g., at the end of the combustion chamber in front of the nozzle). However, this method of powering the turbine involves considerable difficulty in practice, since the materials of which the turbine components are made cannot withstand the high temperature of the scavenged gas (of the order of $2600-3100^{\circ}\text{C}$). For this reason, this gas must be cooled to $650-850^{\circ}\text{C}$ before it is fed into the turbine, using a special cooling chamber with water sprayed into it; this water must be taken on board the missile. Moreover, it is very difficult in practice to regulate the temperature of the vapor-gas mixture in front of the turbine and to obtain a sufficient quantity of fully reacted gas from the combustion chamber. Apparently, this method of powering TNA turbines has not been used because of these difficulties.

It is also possible to reduce the temperature of the gas withdrawn from the engine's combustion chamber to the safely admissible limit for the turbine blades by subsequent pumping of a certain quantity of combustible into it (from the engine tank), but this measure entails additional consumption of the component and also re-

quires precise metering of it (see Fig. 10.6).

It is also possible to power the turbine with gas obtained by burning a combustible of the type used to power the engine in a special gas generator. This method of powering the turbine differs from the preceding only in that the process of producing the hot gas is isolated from the engine's combustion chamber and is therefore more easily controlled. However, the gas that forms in cases where a fuel of stoichiometric composition is burned has a high temperature, and water injection is necessary to reduce this to the admissible limit. Calculations and experiment have shown that a change of a few percent in the rate at which water is fed into the gas changes the vapor-gas temperature by an inadmissible margin.

This circumstance makes it difficult to control the gas generator together with the engine and require a special complex automatic-control system to ensure stability in the parameters of the vapor gas produced.

It is expedient to power the turbine with gas formed in a gas generator from the same fuel components used to operate the engine, but this must be done with a very small excess oxidizer ratio (of the order of $\alpha = 0.2$ to 0.3).

In this case, the weight of the TNA turns out to be of the same order as that of systems with expulsion of the spent gas into the atmosphere behind the turbine; however, the weight of the PGG may be estimated from the weight of the ZhRD chamber for the appropriate flow rates and pressures.

The gas obtained in this case has a temperature (about 700-900°C) that can be withstood safely by the turbine blades. After being used in the turbine, this gas can either be expelled directly into the environment or burned to the optimum component proportions

in the same chamber or in a special chamber, participating in the generation of engine thrust or, finally, used to protect the chamber liner from overheating (Fig. 10.13).

Expulsion of this generator gas into the atmosphere behind the turbine naturally involves an unproductive expenditure of heat in servicing the feed system, i.e., a loss in the effective thrust of the $ZhRD$, since the latter is defined as the ratio of engine thrust to the over-all consumption of fuel in it.

One of the possible ways to improve the characteristics of the $ZhRD$ is to raise p_k , which results in an increase in P_{ud} . As P_{ud} increases, however, there is a proportional increase in the specific flow rate of the mass vehicle to drive the TNA turbine (the specific flow rate is proportional to the pressure at which the fuel components are fed into the combustion chamber of the engine).

A closed system may be used to cool the engine chamber and power the turbine (Fig. 10.14) for high-thrust (over 100-120 tons) $ZhRD$ that have rather long operating times. However, it will evidently be difficult to set up such a system for high-thrust engines with high combustion-chamber pressures, particularly in cases in which dependable cooling of the chamber requires a fuel-component ratio χ_{st}^* at the wall that is considerably lower than the average, χ_{sr} .

From a thermodynamic standpoint, the best working fluid for this system is water, since it possesses much better cooling properties than the fuel components. The basic drawback to the use of water is its high freezing point, which makes it necessary to heat it with special units in winter. It is also possible to use water-alcohol mixtures with lower freezing points as the mass vehicle in the closed circuit of this system. In this system, the mass vehicle is heated

*[Subscript: $cr = st = stanka = wall$.]

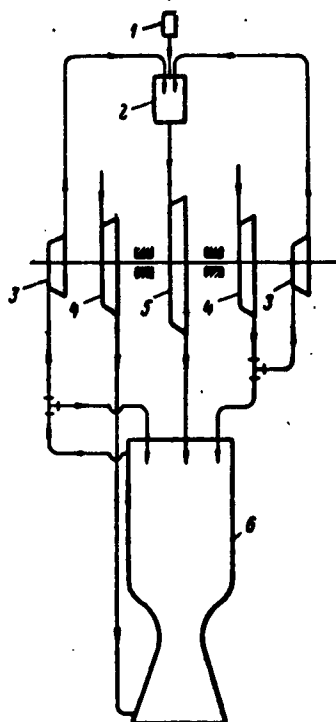


Fig. 10.13. Schematic diagram of turbopump-fed fuel-feed system with two-component PGG and further combustion of the vapor gas after the turbine in the engine combustion chamber. 1) Chamber with powder charge for starting twist of turbine by powder gases; 2) two-component vapor-gas generator; 3) pressurizing pumps; 4) pumps for main fuel components; 5) vapor-gas turbine; 6) engine chamber.

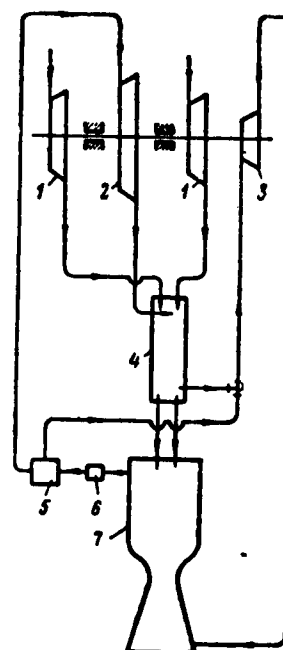


Fig. 10.14. Schematic diagram of closed system for cooling and supplying turbine with vapor gas with water-throttling device and separation of the vapor before the turbine. 1) Fuel-component pumps; 2) vapor turbine; 3) circulation pump; 4) water-vapor condenser; 5) moistened-vapor separator; 6) hot-water pressure regulator; 7) engine chamber.

and vaporized in passage through the engine's coolant passages and then enters the vapor turbine, from which it proceeds to a refrigerating unit where it is condensed and redirected into the engine chamber's coolant passages. If there is insufficient heat to evaporate the liquid taken from the chamber liner, it can be vaporized in a special vaporizer installed for this purpose in the engine's combustion chamber. The water vapor that has been used in the turbine passes through surface-type condensers and is cooled by the fuel com-

ponents entering the engine combustion chamber.

However, when this system is used to cool the engine chamber and power the turbine, we encounter the problem of ensuring stable operation of the vaporizer system, since it is known from operating practice with direct-flow steam boilers that such systems require special measures to ensure stable operation (sliding disks, etc.).

Powering the turbines with powder gases or compressed air is of no practical interest because of the essential shortcomings that are inherent in it; however, these products may be used for giving the turbine its initial twist or powering it with energy from another source.

SECTION 7. DESIGN OF HYDROGEN-PEROXIDE VAPOR-GAS GENERATORS FOR ZhRD

At the present time, there exist single-component hydrogen-peroxide vapor-gas generators (PGG) with liquid and solid catalysts that accelerate decomposition of the peroxide.

Below we present thermochemical calculations for these vapor-gas generators.

Calculations for Hydrogen-Peroxide Vapor-Gas Generator with Liquid Catalyst

This type of vapor-gas generator was used in the engine of the A-4 long-range missile. Eighty-percent hydrogen peroxide was used in it as the working gas-generating substance, and an aqueous solution of sodium permanganate (NaMnO_4) was used as the liquid catalyst.

Potassium permanganate KMnO_4 , calcium permanganate $\text{Ca}(\text{MnO}_4)_2$, barium $\text{Ba}(\text{MnO}_4)_2$ and other substances may also be used as liquid catalysts for hydrogen peroxide.

An aqueous solution of sodium permanganate at 28-32% concentration by weight gives the most active response with hydrogen peroxide (in the sense of the latter's decomposition). For economical utiliza-

tion of this catalyst, the weight proportions of the aqueous hydrogen-peroxide and sodium-permanganate solutions must lie in the range from 12 to 26. In existing PGG, the amount of liquid catalyst consumed runs to about 7-8% of the amount of 80% hydrogen peroxide.

The corrosive action exerted on the aluminum elements of the engine turbine by the sodium hydroxide formed in the chemical reaction of the hydrogen peroxide with sodium permanganate is insignificant. Calcium and barium hydroxides are less aggressive toward the metals, as will be seen from comparison of the solubilities of these substances. On the other hand, however, their low solubility represents a disadvantage, since the engine turbine becomes fouled with the products MnO_2 , Ba(OH)_2 , and Ca(OH)_2 .

This circumstance is one of the factors that have compelled engine designers to abandon the use of liquid catalysts for hydrogen peroxide in ZhRD fuel-feed systems and to develop PGG with solid catalysts.

The liquid-catalyzed hydrogen-peroxide vapor-gas generator is a system (see Fig. 10.4) consisting of a reactor (mixing chamber), a hydrogen-peroxide tank, a tank for the sodium permanganate, a compressed-nitrogen bottle to pressurize the components from the tanks into the reactor, a pressure reducer, metering safety valves, pipelines, and other small elements.

The aqueous solutions of hydrogen peroxide and sodium permanganate are sprayed, under the pressure of the gas in their tanks, through special jet nozzles into the PGG reactor, where they are mixed together and react chemically, with the result that a vapor gas of the specified parameters is formed.

Basically, the design of a hydrogen-peroxide vapor-gas generator for a liquid catalyst reduces to the determination of

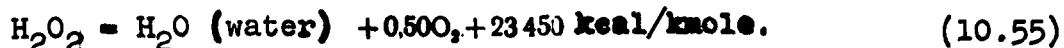
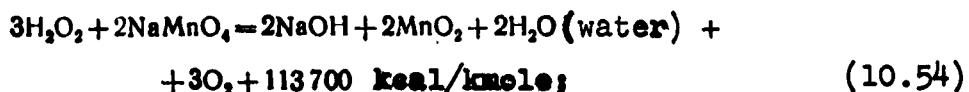
1) the composition and parameters of the vapor gas obtained with the specified reactor pressure and the velocity selected for the working components;

2) the basic geometrical dimensions of the chamber of the vapor-gas generator (reactor) and the automatic-control devices, including plumbing.

The design and capacity of the reactor must provide for sufficient mixing of the components and the most rapid possible reaction between them, while the automatic system controlling the vapor-gas generator must ensure stability of the specified operating regimes. The ratio of the length of the cylindrical reactor to its diameter does not exceed 2 in existing PGG designs.

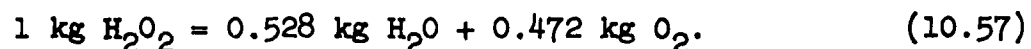
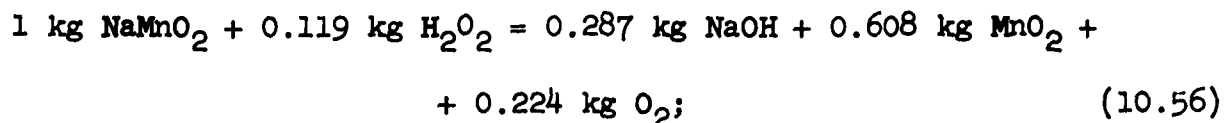
Since dissociation of the peroxide-decomposition products does not occur at the temperatures prevailing in the reactor, the vapor gas consists of water vapor and gaseous oxygen (if we disregard the relatively small content of the solid products formed).

Decomposition of hydrogen peroxide on mixing with sodium permanganate proceeds in accordance with the following equations when both are present in 100% concentrations by weight:



On reaction of the hydrogen peroxide with sodium permanganate, the chemical reaction first proceeds in accordance with the first equation to form manganese dioxide MnO_2 , which then acts as a catalyst on the hydrogen peroxide and decomposes it in accordance with the second equation. Here, the quantity of manganese dioxide formed during the first reaction is so large that it is adequate for subsequent decomposition of a large amount of hydrogen peroxide.

Consequently, the function of the first of these reactions consists in formation and activation of the catalyst MnO_2 , while that of the second reaction is to evolve the heat necessary to evaporate the water and heat the forming vapor gas to a specified temperature. On conversion from kilomoles to one kilogram of the reacting components, Eqs. (10.54) and (10.55) assume the form:



These equations may be used as a basis for the appropriate calculations to obtain the following formulas for determination of the per-second quantities of vapor-gas products formed:

$$G_{\text{H}_2\text{O}} = a_{\text{nep}}(1 - 0.471\sigma_{\text{nep}}) + b_{\text{kat}}(1 - 0.937\sigma_{\text{kat}}) \text{ kg/sec};^*$$

gaseous oxygen

$$G_{\text{O}_2} = 0.471a_{\text{nep}}\sigma_{\text{nep}} + 0.168b_{\text{kat}}\sigma_{\text{kat}} \text{ kg/sec};$$

manganese dioxide

$$G_{\text{MnO}_2} = 0.608b_{\text{kat}}\sigma_{\text{kat}} \text{ kg/sec};$$

sodium hydroxide

$$G_{\text{NaOH}} = 0.287b_{\text{kat}}\sigma_{\text{kat}} \text{ kg/sec},$$

which gives a total of

$$G_{\text{nr}} = G_{\text{H}_2\text{O}} + G_{\text{O}_2} + G_{\text{MnO}_2} + G_{\text{NaOH}} \text{ kg/sec}^{**}$$

where a_{per} and b_{kat} are the per-second flow rates of the hydrogen peroxide and sodium permanganate, respectively, into the vapor-gas generator, and σ_{per} and σ_{kat} are the weight concentrations of the hydrogen peroxide and sodium permanganate in the aqueous solutions.

Figure 10.15 presents the results of thermochemical calcula-

*[Subscripts: nep = per = perekis' = peroxide; kat = kat = katalizator = catalyst.]

**[Subscript: nr = pg = parogas = vapor gas.]

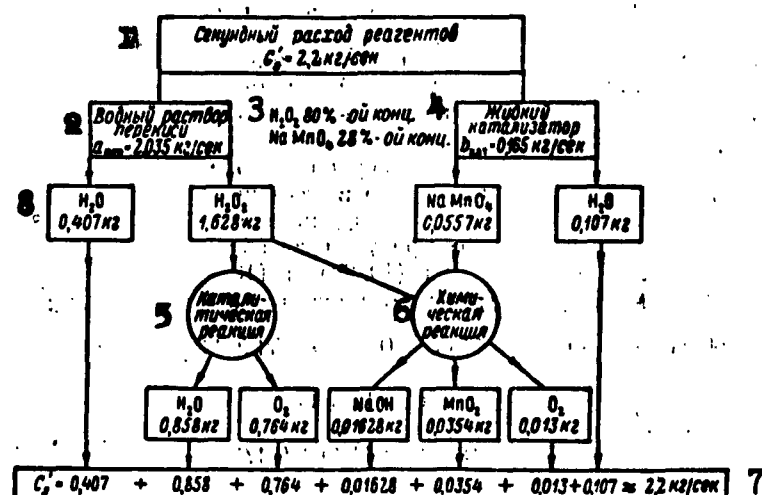


Fig. 10.15. Results of calculation for decomposition products of hydrogen peroxide (80% concentration by weight) with 28% sodium permanganate. 1) Per-second consumption of reagents, $G'_s = 2.2 \text{ kg/sec}$; 2) aqueous peroxide solution, $a_{\text{per}} = 2.035 \text{ kg/sec}$; 3) 80% $\text{H}_2\text{O}_2 + 28\% \text{ NaMnO}_4$; 4) liquid catalyst, $b_{\text{kat}} = 0.165 \text{ kg/sec}$; 5) catalytic reaction; 6) chemical reaction; 7) 2.2 kg/sec; 8) H_2O , 0.407 kg.

tions for the vapor-gas composition with the per-second flow rates $a_{\text{per}} = 2.035 \text{ kg/sec}$ for 80%-by-weight hydrogen peroxide and $b_{\text{kat}} = 0.165 \text{ kg/sec}$ for 28%-by-weight sodium permanganate.

The calculations indicate that different sodium permanganate concentrations and different weight proportions of the permanganate to the hydrogen peroxide have little effect on the composition of the vapor gas obtained; this is accounted for by the low specific weight of the reaction (10.54) in the process in which the vapor gas is formed. The composition of the vapor gas is determined basically by the specified hydrogen peroxide concentration.

In engineering calculations, the manganese dioxide and sodium hydroxide contents in the vapor gas are usually disregarded because of the small quantities involved.

Table 10.2 presents average values of the weight and volume

TABLE 10.2

1 Состав паровая %	2 σ_{per} %				
	70	75	80	85	90
$\varepsilon_{\text{H}_2\text{O}}$	68,2	65,9	63,6	61,4	59,1
ε_{O_2}	31,8	34,1	36,4	38,6	40,9
$r_{\text{H}_2\text{O}}$	79,0	77,3	75,6	73,7	71,8
r_{O_2}	21,0	22,7	24,5	26,3	28,2

1) Composition of vapor gas, %; 2) σ_{per} , %.

composition of the vapor gas for various concentrations by weight of the hydrogen peroxide and sodium permanganate in the aqueous solutions.

The vapor gas produced in the PGG is characterized by its pressure, temperature, and heat content.

In the calculations, the pressure in the vapor-gas generator's reactor is usually assigned and the temperature and heat content of the vapor gas determined on the basis of the heat-balance equation for decomposition of hydrogen peroxide with the specified liquid catalyst. The temperature of the resulting vapor gas depends on

- 1) the pressure in the vapor-gas generator's reactor;
- 2) the physicochemical properties of the working components (reagents);
- 3) the concentration factors of these components in the aqueous solution;
- 4) the weight proportions of the working components.

If we disregard the small quantity of heat expended in heating the solid products NaOH and MnO_2 , the theoretical temperature of the vapor gas (assuming a complete decomposition reaction for the hydrogen peroxide and the absence of heat losses into the surrounding medium) may be determined from the following heat-balance equation:

i.e.,

$$[M_{H_2O}(\mu C_p)_{H_2O} + M_{O_2}(\mu C_p)_{O_2}] t_{nr, \tau} = Q_{BMA}^*$$

$$t_{nr, \tau} = \frac{Q_{BMA}}{M_{H_2O}(\mu C_p)_{H_2O} + M_{O_2}(\mu C_p)_{O_2}} \text{ } ^\circ\text{C}, \quad (10.58)$$

where $M_{H_2O} = G_{H_2O}/18$ and $M_{O_2} = G_{O_2}/32$ are the number of kmoles of water vapor and gaseous oxygen, respectively, $(\mu C_p)_{H_2O}$ and $(\mu C_p)_{O_2}$ are the molar heat capacities at constant pressure, in kcal/kmole $^\circ\text{C}$ for the water vapor and gaseous oxygen, respectively; these are taken from tables in accordance with the proposed vapor-gas temperature, and

$$Q_{BMA} = 10750 \left(4.025 - 18.20 \chi_{\text{per}} \frac{\sigma_{\text{nep}}}{\sigma_{\text{kat}}} - M_{H_2O} \right) \text{ kcal/kmole}.$$

Here, χ_{per} is the weight ratio between the aqueous hydrogen peroxide and sodium permanganate solutions, and σ_{per} and σ_{kat} are the weight concentrations of these components.

The actual temperature of the vapor gas obtained will be

$$t_{nr} = \varphi_k t_{nr, \tau} \text{ } ^\circ\text{C}, \quad (10.59)$$

where $\varphi_k \approx 0.92$ to 0.95 is a coefficient taking into account the actual heat evolved in the vapor-gas generator reactor and the dissipation of heat into the environment.

The heat content of the vapor gas is determined by the usual formula:

$$I_{nr} = g_{H_2O} I_{H_2O} + g_{O_2} C_{pO_2} t_{nr} \text{ or } I_{nr} = \frac{Q_{BMA}}{18M_{H_2O} + 32M_{O_2}} \text{ kcal/kg}, \quad (10.60)$$

where I_{H_2O} is the heat content of the water vapor in kcal/kg, as determined from the I-S diagram as a function of its pressure and temperature, and C_{pO_2} is the heat capacity of gaseous oxygen at constant temperature in kcal/kg $^\circ\text{C}$; this is taken from a table as a function of the vapor-gas temperature t_{pg} $^\circ\text{C}$.

The quantity of vapor gas formed in one second depends on the
*[Subscripts: nr, \tau = pg, t = parogaz, teoreticheskiy = vapor gas, theoretical; BMA = vyd = vydelenny = evolved.]

flow rate of the liquid components during a similar period of time in the vapor-gas generator reactor. Here, since the per-second flows of components into the reactor are determined for practical purposes by the pressure of the gas fed from the accumulator into the hydrogen-peroxide and permanganate tanks through the pressure reducer, the pressure and flow rate of the vapor gas from the reactor to the TNA turbine are regulated by the pressure reducer.

The A-4 engine's liquid-catalyst hydrogen-peroxide vapor-gas generator has the following specifications:

- 1) working components: 80%~~by-weight~~ H_2O_2 and 28%~~by-weight~~ $NaMnO_4$
- 2) component flow rate: 2.035 kg/sec for the hydrogen peroxide and 0.165 kg/sec for the sodium permanganate
- 3) parameters of vapor gas produced: pressure, 28 atm abs; temperature, $380 \pm 40^\circ C$
- 4) output of vapor gas generator, 2.2 kg/sec
- 5) operating period, 60 sec
- 6) total weight of components in tanks of installation: 169 kg of hydrogen peroxide and 14 kg of sodium permanganate
- 7) geometrical dimensions of reactor: volume, 2.3 liters; diameter, 115 mm; length, 200 mm
- 8) dry weight of entire PGG unit 72 kg

Calculations for Solid-Catalyst Hydrogen-Peroxide Vapor-Gas Generator

Vapor-gas generators in which hydrogen peroxide is decomposed by a separate catalyst are simple in design and economical and dependable in operation.

Since the solid catalyst is placed directly in the reactor in this PGG, it is no longer necessary to use a series of automatic-

control valves and other elements that are present in the liquid-catalyst PGG.

Hydrogen peroxide at an 80-82% concentration by weight is also used in this case to produce vapor gas.

Solid catalysts are characterized by their

1) activity (vigor of reaction), i.e., by the quantity of hydrogen peroxide that can be decomposed by one kilogram of catalyst in one second;

2) total yield (total operating margin), i.e., the quantity of hydrogen peroxide that can be decomposed by one kilogram of catalyst before the latter's catalytic properties are fully exhausted;

3) mechanical cohesiveness under operating conditions.

It is an extremely difficult problem to prepare a solid catalyst for hydrogen peroxide; it must decompose hydrogen peroxide rapidly, retain its activity for a long period, and not crumble. This last property is extremely important, since the vapor gas flowing out of the reactor at high velocity may quickly break the catalyst down into small particles that accelerate wear of the turbine when they get into it.

Some of the best solid catalysts used by the Germans for ZhRD during the Second World War were made of porous porcelain that had been impregnated with solutions of calcium permanganate or potassium chromate.

A catalyst consisting of nickel chloride NiCl_2 , cobalt chloride CoCl_2 , barium permanganate $\text{Ba}(\text{MnO}_4)_2$, and barium bichromate BaCr_2O_7 has also been used.

With a pressure of 25 atm abs in the vapor-gas generator reactor, 1 kg of this catalyst can decompose about 0.15-0.2 kg of 80%-by-weight hydrogen peroxide in one second and has a total yield as high

as 1800-2000 kg.*

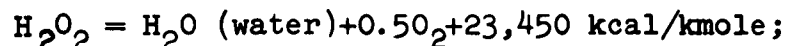
Other substances (aqueous solutions of the permanganate KMnO_4 , soda) can also be used as catalysts for hydrogen peroxide.

Solid catalysts for hydrogen peroxide may take the form of ceramic cubes or plates impregnated with the appropriate catalytic substances, or special briquettes produced by pressforming and subsequent sintering of the appropriate substances (following powder-metallurgical practice).

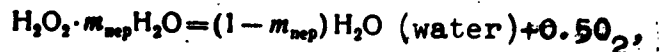
Metallic lead or iron, aluminum, copper and other metals in powdered form may be used as binding agents for the briquettes (catalyst vehicles). Potassium nitrate KNO_3 , boric acid H_3BO_3 , cobalt oxide Co_2O_3 , and nickel oxide Ni_3O_3 , which are simultaneously hydrogen-peroxide catalysts, are added to the mixture to raise the porosity of the briquettes.

In the presence of a solid catalyst, the hydrogen peroxide decomposes, evolving heat in accordance with the equations:

a) in the case of 100% concentration by weight,



b) in the case of a $\sigma_{\text{per}}\%$ concentration by weight,



where m_{per} is the number of kmoles of water in 1 kmole of hydrogen peroxide, as determined by the formula

$$m_{\text{per}} = \frac{\mu_{\text{H}_2\text{O}}(100 - c_{\text{per}})}{18c_{\text{per}}} = 1.89 \frac{100 - c_{\text{per}}}{c_{\text{per}}} \text{ kmole/kmole}.$$

*Voprosy raketnoy tekhniki, No. 3, 1958, IL.

The weight of the decomposition products of 1 kmole of hydrogen peroxide at $\sigma_{\text{per}}\%$ concentration is

$$\mu'_{\text{nep}} = \mu_{\text{H}_2\text{O}_2} + 18m_{\text{nep}} = 34 + 18 \cdot 1,89 \frac{100 - \sigma_{\text{nep}}}{\sigma_{\text{nep}}} = \frac{3400}{\sigma_{\text{nep}}} \text{ kmole/kmole}$$

Anhydrous 100% hydrogen peroxide consists of 5.9% hydrogen and 94.1% oxygen by weight. Almost half of this oxygen remains bound to the hydrogen in the form of water.

The quantity of heat evolved on decomposition of 1 kg of hydrogen peroxide is, according to the equation of the reaction,

$$Q_{\text{sum}} = \frac{23450}{\mu_{\text{nep}}} = \frac{23450}{3400} \sigma_{\text{nep}} = 6,9 \sigma_{\text{nep}} \text{ kcal/kg} \quad (10.61)$$

where $\sigma_{\text{per}}\%$ is the concentration of the hydrogen peroxide by weight.

This heat is expended on heating and vaporizing the water of the components and in heating the vapor gas that is formed. As the hydrogen peroxide concentration declines, the temperature of the resulting vapor gas also diminishes, since this increases the amount of heat spent in evaporating the water.

Consequently, the following are formed on decomposition of 1 kg of 100%-by-weight hydrogen peroxide:

1) Water vapor

$$g_{\text{H}_2\text{O}(100\%)} = 0,528 \text{ kg} = 52,8\%;$$

2) Gaseous oxygen

$$g_{\text{O}_2(100\%)} = 0,472 \text{ kg} = 47,2\%$$

and the amount of heat evolved

$$Q_{\text{sum}(100\%)} = 690 \text{ kcal/kg}$$

while decomposition of 1 kg of hydrogen peroxide of $\sigma_{\text{per}}\%$ concentration by weight gives correspondingly

$$g_{\text{H}_2\text{O}} = g_{\text{H}_2\text{O}(100\%)} + g_{\text{O}_2(100\%)}; (1 - \sigma_{\text{rep}}) = 1 - 0,00472\sigma_{\text{rep}} \text{ kg.}$$

$$g_{\text{O}_2} = g_{\text{O}_2(100\%)} \sigma_{\text{rep}} = 0,472\sigma_{\text{rep}} \text{ kg.}$$

$$Q_{\text{BMA}} = Q_{\text{BMA}(100\%)} \sigma_{\text{rep}} \text{ kcal/kg}$$

where σ_{per} is the peroxide concentration expressed in weight units.

The quantity of heat $Q_{\text{vyd}}(100\%)$ is adequate to vaporize the water of the components at a pressure of 1 atm abs and raise the temperature of the resulting vapor gas nearly to 960°C (Fig. 10.16). The heat of decomposition of hydrogen peroxide increases linearly from zero (pure water) to 690 kcal/kg (100% H_2O_2).

At first, this heat is expended on heating the liquid, but then, beginning at a concentration of 13.5% H_2O_2 , it goes to vaporize the water. At a peroxide concentration of 64.5%, the quantity of heat evolved is adequate to vaporize the liquid completely, i.e., to form a dry saturated vapor. From this point on, the heat of decomposition of the peroxide is further expended in heating the vapor gas. When 80% H_2O_2 is used, the temperature of the vapor gas at a pressure of 1 atm abs is about 460°C .

When a solid catalyst is used, a vapor gas at a rigidly determined temperature may be obtained simply by varying the hydrogen peroxide concentration; this is one of the merits of this catalyst.

Figure 10.17 shows a diagram of the temperature and heat content of the vapor gas as functions of the hydrogen peroxide concentration

and the pressure in the reactor.

This diagram can be used in designing hydrogen-peroxide vapor-gas generators.

Figure 10.18 shows the thermodynamic decomposition characteristics of hydrogen peroxide H_2O_2 for various concentrations and solid and liquid catalysts.* The liquid catalyst referred to here is sodium permanganate $NaMnO_4$ at a concentration $\sigma_{kat} \approx 0.35$.

The curves of this figure indicate that a hydrogen peroxide concentration $\sigma_{per} = 0.7$ to 1.0 ensures a vapor-gas temperature range all the way up to the maximum permissible at the present time for gas turbines. Use of the solid catalyst is preferable.

Figure 10.19 shows the results of calculation for the decomposition of ethylene oxide C_2H_4O at various pressures in the reactor chamber.* The curves of this figure show that the temperature of the gaseous mixture can be tolerated by contemporary turbines, while the parameter $R_k T_k$, which characterizes the work capacity of 1 kg of gas, is quite large. This is also characteristic for other liquid single-component fuels: hydrazine N_2H_4 , isopropyl nitrate $C_3H_7ONO_2$, and others.

If the vapor-formation process in the reactor is to proceed normally, it is necessary to have the appropriate reactor volume, the optimum value for which can be determined only by experiment. It has been established that 1 liter of reactor volume can decompose about 1 kg of 80% hydrogen peroxide per second with excellent completion. Approximately 65-75% of this volume is filled by the solid catalyst.

The design and layout of the nozzles for injection of the hydrogen peroxide, the placement of the catalyst with respect to the nozzles,

*Izvestiya vysshikh uchebnykh zavedeniy MVO SSSR (Bull. Higher Educ. Inst. Ministry of Higher Education USSR), Aviatsionnaya tekhnika (Aviation Engineering), No. 1, Kazan', 1958.

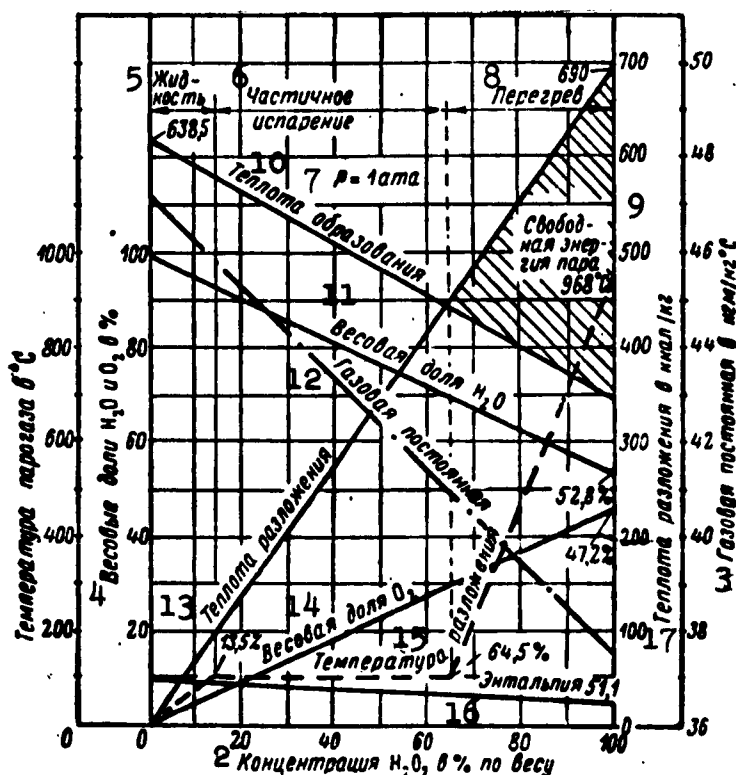


Fig. 10.16. Physicochemical characteristics of hydrogen peroxide at a pressure of 1 atm abs and different concentrations by weight. 1) temperature of vapor gas in $^{\circ}C$; 2) concentration of H_2O_2 in % by weight; 3) gas constant in $kg\cdot m/kg\cdot^{\circ}C$; 4) weight fraction of H_2O and O_2 in %; 5) liquid; 6) partial evaporation; 7) $p = 1$ atm abs; 8) superheating; 9) free energy of vapor, 968 $^{\circ}C$; 10) heat of formation; 11) weight fraction of H_2O ; 12) gas constant; 13) heat of decomposition; 14) weight fraction of O_2 ; 15) decomposition temperature; 16) enthalpy 51.1; 17) heat of decomposition in $kcal/kg$.

and other factors influence the reactor volume.

The design of the reactor and the placement of the catalyst package may strongly influence both the hydrogen peroxide decomposition process and the total yield from the catalyst.

The catalyst's working life may be increased by appropriate placement of steel screens in the reactor to protect the catalyst from erosion by hydrogen peroxide when the latter is injected into the reactor and prevent grains from being entrained by the stream of vapor gas. Moreover, the screens present an additional catalyzation surface.

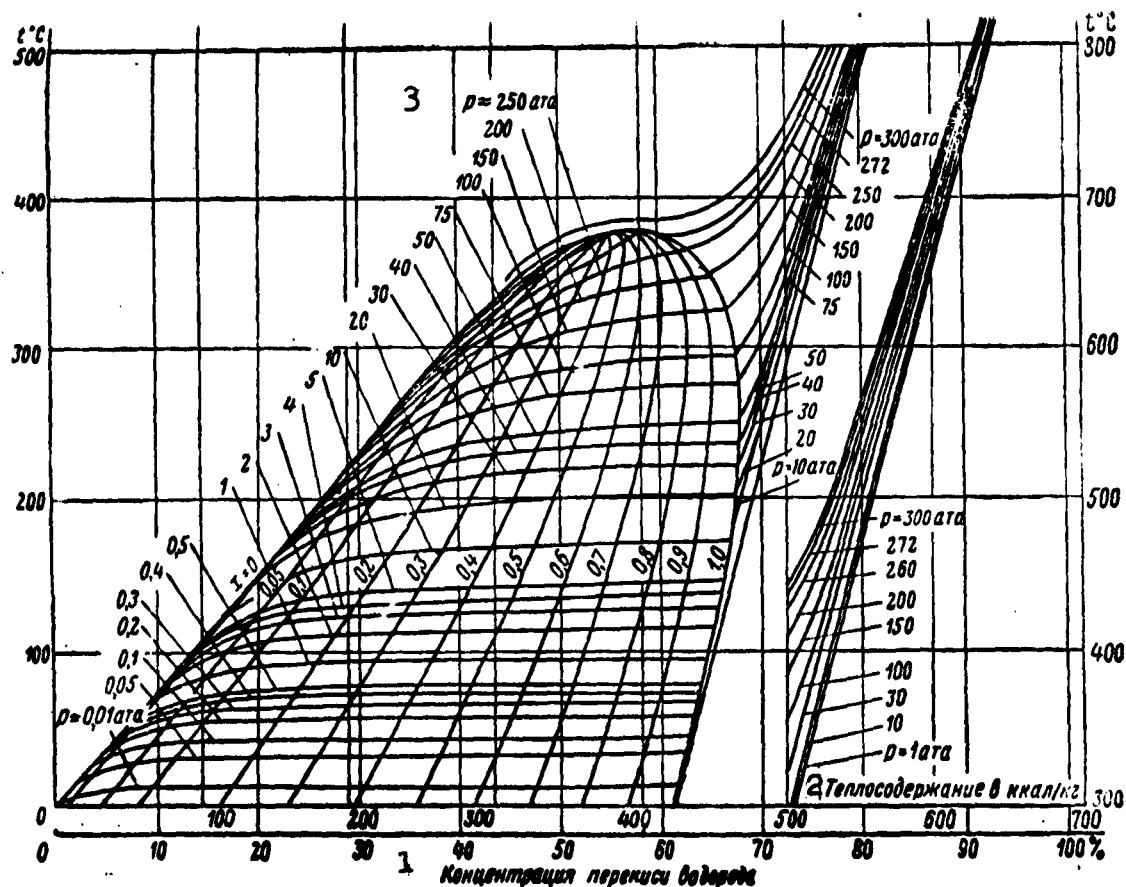


Fig. 10.17. Temperature and heat content of vapor gas as function of hydrogen peroxide concentration and pressure in reactor. 1) hydrogen peroxide concentration; 2) heat content in kcal/kg; 3) $p \approx 250$ atm abs.

The weight of the required solid-catalyst package for a given PGG yield may be determined by the formula.

$$G_{\text{kat}} = G_{\text{pg}}/S_1 \text{ kg}, \quad (10.62)$$

where G_{pg} is the quantity of vapor gas formed in kg/sec and S_1 is the permissible per-second hydrogen peroxide load for 1 kg of solid catalyst in kg/sec/kg (when hydrogen peroxide of 80% concentration by weight is used, certain contemporary catalysts tolerate $S_1 \approx 2.5$ to 2.8 kg/sec/kg; their S_2 for full stable-performance margins at the 480°C temperature of the vapor gas formed is about 600 to 700 kg/sec/kg).

To ensure normal operation of the PGG during the specified period of time τ_{dv} , it is necessary to observe the condition

$$G_{\text{pg}} \tau_{\text{dv}} \leq S_1 G_{\text{kat}} \quad (10.63)$$

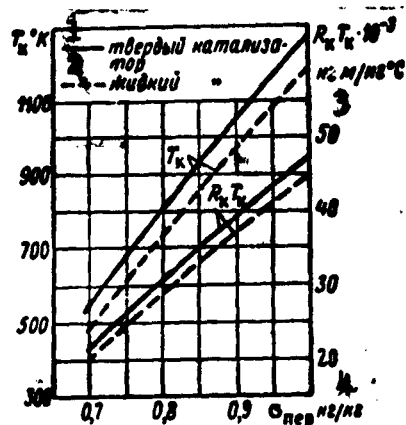


Fig. 10.18. Thermodynamic characteristics of decomposition products of H_2O_2 for different concentrations by weight and with solid and liquid catalysts. 1) solid catalyst; 2) liquid catalyst; 3) $kg\text{-}m/kg\text{ }C$; 4) $\sigma_{per}, kg/kg$.

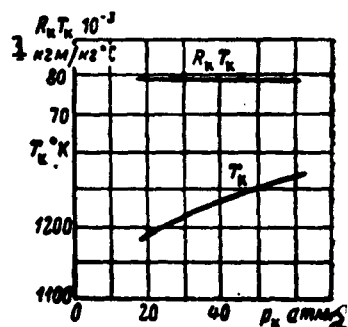


Fig. 10.19. Thermodynamic characteristics of decomposition products of C_2H_4O for different chamber pressures. 1) $kg\text{-}m/kg\text{ }C$; 2) atmospheres.

The volume of the catalyst package is determined by the formula

$$V_{kat} = \frac{G_{per}}{\gamma_{kat}}, \quad (10.64)$$

where γ_{kat} is the loose-bulk weight of the solid catalyst in $kg/liter$; for certain existing catalysts,

$$\gamma_{kat} \approx 1.3 \text{ to } 1.4 \text{ kg/liter.}$$

The geometrical dimensions of the catalyst package are determined from the condition that the ratio of its length l_{kat} to its diameter d_{kat} must be equal to 0.7 - 1. The thickness of the solid-catalyst layer in the PGG must not be smaller than 70 mm. The remaining dimensions of the reactor are determined on the basis of design considerations.

The volume of the total hydrogen-peroxide reserve is determined by the formula

$$V_{per} = \frac{G_{per}}{\gamma_{per}}, \quad (10.65)$$

where γ_{per} is the specific gravity of the hydrogen peroxide and depends on temperature; it may be taken from the diagram or table for purposes of calculation.

The values for the quantities of components to be used in the PGG may be used as a basis for computing the tank volumes required for them.

Knowing the vapor-gas pressure at entry into the turbine, we may determine the pressure necessary to feed the working components into the PGG reactor and make the calculations for its units (the gas bottle and pressure reducer in the case of gas-bottle feed of the hydrogen peroxide or the pump in the case of pump feed).

SECTION 8. TWO-COMPONENT ZhRD GAS GENERATORS

The first highly original and dependable two-component gas generator was designed and built in the USSR in 1937. This gas generator produced a gas at a pressure of 20 - 25 atm abs as a result of combustion of kerosene with nitric acid and water injection into the products with the object of lowering their temperature to 450 - 550°C (see Fig. 10.5).

The basic drawback to a GG of this type is the high temperature of the vapor gas formed on combustion of a fuel of stoichiometric composition. The greatest difficulty encountered in practice is in controlling the temperature of the gas by injection of water into it.

It may be most convenient to feed the TNA turbine with hot gases obtained in a two-component gas generator from the basic fuel components with a lower excess oxidizer ratio (with the object of producing a gas at a temperature admissible for the turbine lathes).

After operating the turbine, a gas produced in this manner can either be exhausted directly into the environment or burned to the optimum fuel-component proportions in the engine chamber.

In this case the TNA turbine can be given its initial twist when the engine is to be started at the expense of the energy of gases from a combustible powder charge or that of compressed air. For this purpose, the reserve of powder charge must be selected in such a way that the inflow of vapor gas from the GG will attain its calculated value at the instant at which the work of the powder chamber has been completed.

The merits of the ZhRD equipped with a two-component GG consists

in the facts that

1) there are no auxiliary fuel components for production of the gas, so that we may dispense with tanks to hold them and their feed and control systems; this simplifies the design of the engine and lowers its cost;

2) it is possible to produce a vapor gas at a temperature that can be safely tolerated by the working turbine blades (in the range from 650 to 900°C);

3) the gas can be burned efficiently in the combustion chamber after passage through the TNA turbine, thus raising the engine's operating economy and, consequently, all other things equal, increasing the range of the missile.

These advantages are also inherent to ZhRD with GG operating on one of the fuel components.

The following specifications are set forth for two-component gas generators in ZhRD fuel-feed systems:

1) the highest possible specific work capacity, which is characterized by the parameter $R_k T_k$ of the gas produced:

2) uniformity of the temperature field across the chamber cross section;

3) minimum amounts of solid phase (soot and coke) in the gas produced;

4) simplicity of design and the shortest possible gas-generator chamber length.

A distinctive feature of the two-component GG is the fact that it operates at very small excess oxidizer ratios in the fuel with the object of producing a gas at a temperature that can be safely tolerated by the turbine blades.

For alloy-steel turbine blades, a temperature of about 800°C can be regarded as a safe working level. Approximate calculations indicate that this gas temperature can be obtained in practice with fuel mixture ratios of the order of $\chi \approx 0.7$ to 1.0. Under these conditions, the gas is a mixture of fuel-combustion products and excess-combustible decomposition products.

The kinetics of the process taking place in two-component GG has been illuminated only to a very slight extent in the literature. The process of gas generation in a two-component gas generator can be broken down roughly into two basic processes that unfold simultaneously and therefore somehow influence one another: the process of fuel combustion and the cracking process of the hydrocarbons.

In setting up the working process in this GG, it is necessary to try to make the chemical reaction in the chamber sufficiently long for evaporation of the fuel components and their decomposition into lighter hydrocarbons, without liberation of large quantities of soot and coke in the gas. The completeness of the combustible's reaction with the oxidizer depends basically on the temperature and time involved in the chemical reaction. For this reason, the problem of the time taken by the working process in the gas generator is of central importance.

The production in the GG of a gas of the specified or selected temperature and the highest possible gas constant (specific work capacity $R_k T_k$) is highly important. Naturally, the gas constant R_k of the gas formed will have its maximum only at a fully determined stay time of the fuel in the gas-generator chamber. If the fuel droplet has a short stay time in the chamber, it will not be able to vaporize completely, and if this time is excessively long, soot, heavy gums, and coke will form from the combustible vapors, and this will lower the gas constant of the gas produced. Moreover, the gas may contain a

significant quantity of hydrocarbons that are liquid under standard conditions, while no hydrocarbons other than methane are observed in the gas according to the normal thermodynamic calculation.

This indicates that there is not sufficient time for establishment of chemical equilibrium in the combustion products in a two-component gas generator. The gas temperature is also nonuniform over the gas-generator chamber cross section.

In working out a GG design, it is necessary to attempt to create the most uniform possible temperature field over the cross section of the chamber, particularly in zones with large combustible excesses, since local high-temperature foci in these zones will contribute to more rapid precipitation of soot. Formation of heavy gums and coke is possible when the temperature field is smoothed out.

The following basic problems must be resolved in designing a two-component gas generator and making the calculations for it:

- 1) selection of an expedient design layout for the gas generator;
- 2) selection of the working pressure in the gas-generator chamber and the necessary fuel-component proportions;
- 3) thermodynamic calculation of the gas-generator chamber;
- 4) design for mixture formation in the chamber;
- 5) determination of the basic geometrical dimensions of the chamber;
- 6) design of the fuel injectors;
- 7) determination of the vaporization time and trajectories of the droplets in the chamber.

The physical design of two-component GG depends on the schematic diagram adopted for the working process in the gas-generator chamber and is similar in many respects to that of the combustion chamber of an ordinary ZhRD.

The gas pressure in the gas-generator chamber is determined with

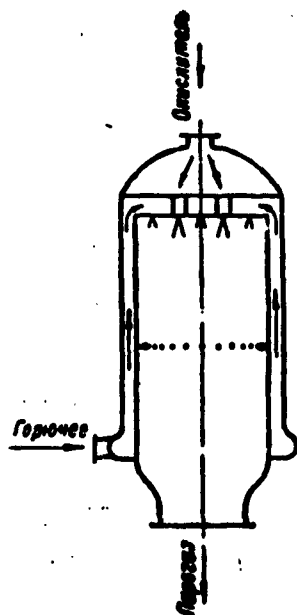


Fig. 10.20. Schematic diagram of chamber of two-component vapor-gas generator. 1) oxidizer; 2) combustible; 3) vapor gas.

consideration of the TNA turbine's operating economy, the weight of the design, the stability of combustion in the chamber, and the dynamic stability of the operating regime for the engine as a whole. The gas pressure in the combustion chambers of existing two-component ZhRD gas generators attains $30 - 50 \text{ kg/cm}^2$.

Two practically possible and fundamentally different systems are known at the present time for setting up the working process in a two-

component gas generator; these also differ in physical design.

The combustion of fuel in a two-component gas generator may take place in one stage or in two stages - in the zones of primary and secondary mixing of the components.*

In this connection, we may draw a distinction between the following basic design layouts of the two-component gas generator:

1) the GG-A, the design of which is analogous to that of an ordinary ZhRD, in which the fuel components are fed into the chamber only at the head end (Fig. 10.20);

2) The GG-B, which is characterized by the fact that the combustible is fed into the chamber partly through the head with an excess oxidizer ratio $\alpha_{\text{gol}} \approx 0.4$ to 0.6 and partly through a peripheral belt located approximately halfway down the chamber length, with a view to making the over-all excess oxidizer ratio $\alpha_{\text{obshch}} = 0.07$ to 0.18 at

* D. Satton. *Raketnyye dvigateli* (Rocket engines), IL, 1950.

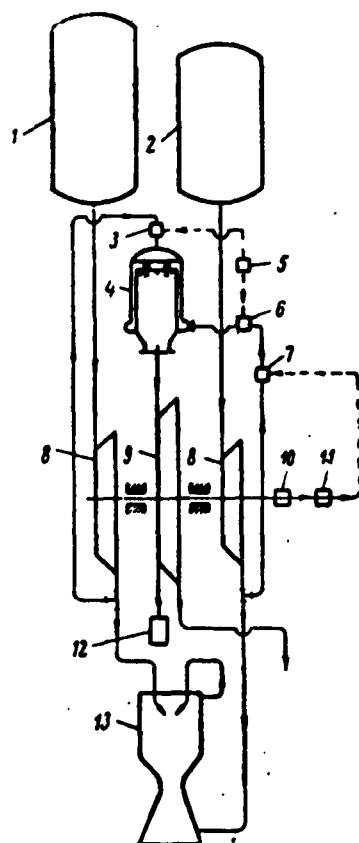


Fig. 10.21. Schematic diagram of turbopump fuel-feed system with two-component vapor-gas generator. 1) oxidizer tank; 2) combustible tank; 3) flow-control valve; 4) gas-generator chamber; 5) follow-up mechanism of PGG's fuel-mixture-ratio controller; 6) flow-speed measuring unit; 7) control valve; 8) pumps for basic fuel components; 9) vapor-gas turbine; 10) rpm sensor; 11) follow-up mechanism of rpm controller; 12) powder chamber with electric initiator for twisting turbine when engine is fired; 13) engine chamber.

the exit of the gas from the chamber (Fig. 10.21).

Since combustion of the fuel at a small excess oxidizer ratio is characteristic for two-component GG, the use of the GG-A is advisable only for easily vaporized and easily inflammable fuel components, ignition and combustion of which does not require a large quantity of heat or a high temperature. These fuels include Tonka-250+80% of 98% HNO_3 and 20% N_2O_4 as well as ethyl alcohol+liquid oxygen.

The GG-A can operate dependably with $\alpha = 0.10$ to 0.25 . This gas generator is not suitable for fuel components of the type kerosene+nitric acid or its derivatives.

The basic drawback to such a gas generator is the relatively low temperature throughout the chamber volume, a consequence of which is that the working gas-generation process

proceeds relatively slowly, and a large chamber volume is required to produce the gas at the specified temperature. For this reason, more favorable conditions for the polymerization and condensation processes of the hydrocarbons are created in this generator than prevail in the GG-B, which is a highly important consideration.

The most suitable design layout for fuels of the type kerosene+ nitric acid or its derivatives is the GG-B gas generator. In the first zone of this generator's chamber, the fuel burns at a temperature at which chemical equilibrium is established in the fuel-combustion products (of the order of $1900-2200^{\circ}\text{C}$). As a result, the fuel-combustion process proceeds relatively rapidly, without liberation of soot and coke.

As these combustion products approach entry into the second zone of the chamber, a certain additional quantity of water or combustible is fed into them with the result that a gas of the required temperature is formed; this is then fed into the engine's fuel-feed turbine. It may be stated as a simplified presentation that as the additional combustible vaporizes and decomposes and the gas proceeding from the head cools, the chemical reaction between this gas and the evaporation and decomposition products of the combustible proceeds so rapidly that there is time for establishment of equilibrium under the conditions in the chamber. However, this continues until the gas temperature has decreased to a value at which the rate of the above chemical reactions is so slow that they cannot reach equilibrium under the operating conditions of the gas-generator chamber. The chambers of both types of gas generator are usually cooled by one of the fuel components.

At the present time, exact thermodynamic calculations for the working process in the chamber of a two-component gas generator, i.e., exact determination of the temperature and gas constant of the gas formed at the end of the chamber, is impossible because of the complexity and our inadequate knowledge of the combustion kinetics of fuels at low excess oxidizer ratios.

The usual method of thermodynamic calculation for a ZhRD are not applicable for the two-component gas generator because chemical

equilibrium is not established in the combustion products of a fuel with a very small excess oxidizer ratio (at temperatures below 1300 - 1400°K).

The theoretical specific work capacities of certain liquid fuels for $\alpha = 0.15$ and $p_k = 40$ atm abs are characterized by the following values:

$$R_k T_k$$

- 1) Kerosene+98% nitric acid ($T_k = 1155^\circ\text{K}$)..... $63.75 \cdot 10^3$
- 2) Same+80% 98% HNO_3 and 20% N_2O_4 ($T_k = 1165^\circ\text{K}$)..... $65.20 \cdot 10^3$
- 3) Kerosene+60% of 98% HNO_3 and 40% of N_2O_4 ($T_k = 1180^\circ\text{K}$)... $66.65 \cdot 10^3$
- 4) Tonka-250+98% nitric acid ($T_k = 1205^\circ\text{K}$)..... $67.35 \cdot 10^3$
- 5) Tonka-250+80% 98% nitric acid and 20% N_2O_4 $68.90 \cdot 10^3$
($T_k = 1220^\circ\text{K}$)
- 6) Tonka-250+60% 98% HNO_3 and 40% N_2O_4 ($T_k = 1235^\circ\text{K}$)..... $70.45 \cdot 10^3$
- 7) Kerosene+liquid oxygen ($T_k = 1250^\circ\text{K}$) $80.30 \cdot 10^3$
- 8) 93.5% ethyl alcohol+liquid oxygen ($T_k = 1080^\circ\text{K}$)..... $59.50 \cdot 10^3$

Here, $T_k [^\circ\text{K}]$ is the calculated theoretical temperature of the combustion products of the fuel in question.

Figure 10.22 shows values of the theoretical combustion temperature $T_k [^\circ\text{K}]$ and the parameter $R_k T_k$ of the combustion products of kerosene and nitric acid at a chamber pressure $p_k = 40$ atm and different values of the excess oxidizer ratio.

The curves of this diagram indicate that the gas temperature in the gas-generator chamber may be reduced by an excess of combustible ($\alpha < 1$) and an oxidizer excess ($\alpha > 1$). For small α , the specific work capacity $R_k T_k$ of the gas is considerably larger. The gaseous mixture obtained at small α is a reducing medium that is safe for the materials of the engine, while the combustion products obtained with large α contain much free oxidizer that is active with respect to the materials. Finally, in the excess-combustible zone ($\alpha < 0.3$), the temperature of the combustion products varies less intensively with

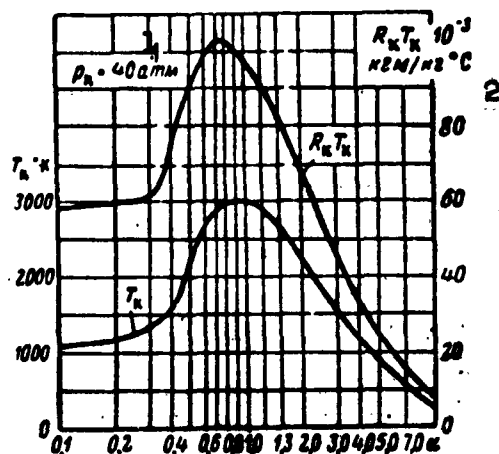


Fig. 10.22. Thermodynamic characteristics of combustion products of kerosene with nitric acid for different excess oxidizer ratios α . 1) $p_k = 40$ atm; 2) $\text{kg-m/kg}^\circ\text{C}$.

respect to α than in the excess-oxidizer zone. This ensures greater safety for the turbine blades during operation.

The picture remains fundamentally the same for other combustion-chamber pressures because of the total absence of thermal dissociation of the gases at high α and its low rate in the zone of small α .

A general deficiency of the method of gas generation with large excesses of one of the fuel components is incomplete utilization of the fuel's chemical energy, and this is reflected in the engine's economy. For this reason, it has been suggested that a system be used in which the working fluid is burned further after utilization in the engine's auxiliary system. Burnout may be accomplished under conditions that do not limit the combustion temperature.*

Figure 10.23 shows curves of $R_k T_k$ as a function of α when water is used to lower the temperature of the fuel-combustion products whose characteristics are shown in Fig. 10.22 to 1100°C .

In this figure, the upper curve indicates the quantity of water required when it is fed into the gas-generator chamber through nozzles installed in the chamber head, while the lower curve indicates the same figure when the water is fed into the fuel-combustion products as they leave the chamber on their way to the point of application. These curves indicate that for a given temperature depression in the fuel-combustion

* Izvestiya vysshikh uchebnykh zavedeniy MVO SSSR, Aviatsionnaya tekhnika, No. 1, Kazan', 1958.

products (in this case, to 1100°C), the required water flow rate is smaller when it is fed directly into the combustion products. The specific work capacities $R_k T_k$ of the vapor gases formed in these two water-injection methods are practically the same and increase slightly when a fuel with a small excess oxidizer ratio α is employed; this is accounted for by the formation of gases with low molecular weights.

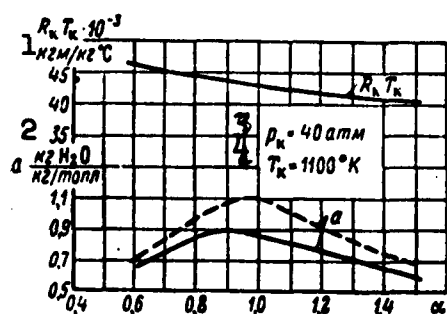


Fig. 10.23. Thermodynamic characteristics of vapor gas formed in combustion of basic fuel with various excess oxidizer ratios and injection of water to lower the temperature. 1) $\text{kg-m/kg}^{\circ}\text{C}$; 2) $\text{kg of H}_2\text{O/kg of fuel}$; 3) $p_k = 40 \text{ atm}$; 4) $T_k = 1100^{\circ}\text{K}$.

In spite of the difficulty encountered here in producing a uniform and stable temperature field in the vapor gas produced and the complexity of the system controlling the output of the turbine being fed, there exist examples of practical application of three-component gas generators.

Operational experience with ZhRD gas generators has shown that centrifugal nozzles are advisable for atomization of the fuel components, since they give a finer and more uniform spray. The finer and more uniform the fuel-component spray, the shorter will be the time required for vaporization of the droplets. For a given temperature in the GG chamber, this time must not exceed the time required for formation of soot and coke from the decomposition products of the vaporized combustible.

The basic geometrical dimensions of a two-component gas generator are the diameter and length of the chamber. The diameter of the cylindrical chamber of a gas generator may be determined approximately from the over-all weight-flow rate of the fuel, setting its value

$$G_{F_k} \approx (1.0 \text{ to } 1.1) p_k \text{ g/cm}^2\text{-sec}, \quad (10.66)$$

where p_k is the absolute pressure in the gas-generator chamber in kg/cm^2 .

Having selected a value for the weight-flow rate for the cylindrical GG chamber, we may determine the diameter of this chamber by using the equation

$$d_k = \sqrt{\frac{4G'_s}{\pi G_{F_k}}} \text{ or } d_k = \sqrt{\frac{4G'_s}{\pi p_k}} \left(\text{at } \frac{G_{F_s}}{p_k} = 1 \right), \quad (10.67)$$

where G'_s is the fuel flow rate in the gas-generator chamber in g/sec.

The length of the GG chamber must be such that the processes of evaporation and decomposition of fuel components will have time to go to completion in it, and that the gas constant of the gas obtained at the temperature selected for it will be maximal (the maximum of R_k will probably occur at the end of complete evaporation of the fuel-component droplets).

In designing the engine, the length of the GG chamber may be determined by the appropriate approximate calculation or from experimental data. A stay time of the fuel in the chamber in the range from 0.003 - 0.004 sec may be used for this purpose.

It may be assumed that the length of the gas-generator chamber should not exceed 250 - 350 mm (in cases where the fuel is fed in from the head end) for fuels based on nitric acid or its derivatives when the chamber pressure is about 30 - 50 atm abs. Calculations indicate that about 0.3 - 0.5 kg of fuel can be burned with adequate completeness in 1 liter of the chamber volume of a two-component gas generator.

The centrifugal nozzles for the GG are designed on the basis of the usual theory, which was discussed earlier.

The strength calculations for the gas generator are also carried out on the basis of the familiar theory.

The fuel components may be fed into either the gas generator of a turbopump set or into the pressurizing reactors of the fuel tanks through nonreturn valves which, in addition to performing their direct functions, also serve as regulators for the fuel mixture ratio in the combustible and oxidizer pipelines. In addition to this, the nonreturn valves prevent entry of gas into the pipelines when the engine is being started and stopped.

When a two-component gas generator is used, the ZhRD's fuel-feed system may consist of TNA with an exhaust tube terminating in a nozzle, the gas generator, a nonreturn-valve unit with throttling disks, a constant-pressure valve, pipelines with burst membranes at their joints (in some cases), plugs and mounting components.

A special flow-and pressure-regulating system of the same type as is used in the engine's program mechanism (thrust regulator) can be employed to guarantee constancy in the operation of the gas generator. With this mechanism, pressurization of the fuel tanks does not depend on the engine's operating regime, since now the delivery of the fuel components into the tank reactors will be determined by the pressure set up in the tank.

It should be noted in conclusion that the most desirable gas-generation system for the apparatus will be the one that couples performance of its functions with simpler design, lowest possible weight, and higher thermodynamic efficiency - the latter characterized by the parameter $R_k T_k$ of the gas - as well as being simpler and more dependable to operate with, etc. The higher the value of $R_k T_k$, the smaller will be the reserve of auxiliary fuel required to generate the gas and the smaller will be the tank volume required for the fuel and the weight of the entire system.

Comparison of the various gas-generation systems as regards their

parameters $R_k T_k$ for the same working pressures and temperatures of the gas formed indicates that the method of gas generation with high excess oxidizer ratios has the lowest thermodynamic efficiency. The efficiency with which the powder gases are produced is almost equivalent to that of forming a vapor gas from 80 - 90%-by-weight hydrogen peroxide. The method in which the gas is produced by burning the basic fuel components at high temperature, with subsequent depression of this temperature to the required limit by injecting a second quantity of water into the gas is also efficient. However, as was noted above, this method has not been mastered adequately in practice from the design and operations standpoints. Production of gas from the basic fuel components with small excess oxidizer ratios or from a single-component liquid fuel of the ethylene-oxide type represents the most efficient method. In practice, these two gas-generation methods do not encounter fundamental design or operational difficulties.

Since the operating margin of a ZhRD turbine is not large, the use of a gas at elevated temperature may be justified in a number of cases. A higher-temperature gas can be produced conveniently from the basic fuel components with a low excess oxidizer ratio or from an auxiliary single-component liquid fuel having good operational and economy characteristics.

SECTION 9. DETERMINING POWER OF TNA TURBINE AND PER-SECOND FLOW OF GAS REQUIRED TO FEED IT

In a number of contemporary ZhRD, the fuel is fed into the engine chamber and sometimes even into the gas generator of the fuel-feed system by means of centrifugal pumps driven directly from the gas turbine and differing considerably from stationary pumps as regards design, quality of the materials from which they are manufactured, and precision and care in manufacture. The turbine is usually installed

between the main centrifugal pumps and on a common shaft with them.

Depending on the schematic diagram adopted for the ZhRD, the fuel pumps may either service only the engine chamber, in which case the fuel-feed system's gas generator has its own feed system (as in the A-4 engine) or service the engine chamber and the fuel-feed system's gas generator simultaneously. The turbopump set and gas generator can also service several ZhRD chambers simultaneously.

The power of the turbines to drive the fuel pumps of the engine's fuel-feed system is determined by the total output required from the pumps, i.e.,

$$N_T \approx N_{n.r} + N_{n.o} \quad (10.68)$$

where $N_{n.g}$ and $N_{n.o}$ are the required powers for the combustible and oxidizer pumps, respectively.

The powers required for the fuel pumps are determined by the following formulas:

1) in the case of fuel feed only into the engine chamber and exhaust of the turbine gases into the atmosphere,

$$N_{n.r} = \frac{G_{t.r} \Delta p_{n.r}}{\gamma_{t.r}} \text{ kgm/sec} \quad (10.69)$$

$$N_{n.o} = \frac{G_{t.o} \Delta p_{n.o}}{\gamma_{t.o}} \text{ kgm/sec} \quad (10.70)$$

2) in the case of fuel feed simultaneously into the chamber and a two-component gas generator and exhaust of the turbine gases into the atmosphere,

*[Subscripts: $r = t$ = turbina = turbine; $n.r.$ = n.g. = nasos goryuchego = combustible pump; $n.o$ = n.o = nasos okislitelya = oxidizer pump.]

$$N_{n.r} = \frac{G_{s.r} + G'_{s.r}}{\gamma_r \eta_{n.r}} \Delta p_{n.r} = \left(\frac{G_s}{1 + \gamma_k} + \frac{G'_s}{1 + \gamma_{kr}} \right) \frac{\Delta p_{n.r}}{\gamma_r \eta_{n.r}} \text{ kg-m/sec;} \quad (10.71)$$

$$N_{n.o} = \frac{G_{s.o} + G'_{s.o}}{\gamma_o \eta_{n.o}} \Delta p_{n.o} = \left(\frac{\gamma_k G_s}{1 + \gamma_k} + \frac{\gamma_{kr} G'_s}{1 + \gamma_{kr}} \right) \frac{\Delta p_{n.o}}{\gamma_o \eta_{n.o}} \text{ kg-m/sec;} \quad (10.72)$$

where G_{sg} and G_{so} are the flow rates of the combustible and oxidizer into the engine chamber in kg/sec, G'_{sg} and G'_{so} are the corresponding rates into the gas generator of the engine's fuel-feed system, γ_g and γ_o are the specific gravities of the combustible and oxidizer, $\eta_{n.g}$ and $\eta_{n.o}$ are the efficiencies of the pumps feeding the combustible and oxidizer, and $\Delta p_{n.g}$ and $\Delta p_{n.o}$ are the heads developed by these pumps, which are computed, respectively, as

$$\Delta p_{n.r} = p_k + \Delta p_{c.n.r} - p_{sc.r} \text{ and } \Delta p_{n.o} = p_k + \Delta p_{c.n.o} - p_{sc.o};$$

here, p_k is the gas pressure in the engine's combustion chamber, $\Delta p_{s.p.g}$ and $\Delta p_{s.p.o}$ are overall pressure gradients for the combustible and oxidizer in the engine's feed system (Δp_f in the injectors, Δp_{okhl} in the cooling passages, Δp_{tr} in the pipelines, Δp_{kl} in the valves and throttling disks, etc.), and $p_{vs.g}$ and $p_{vs.o}$ are the combustible and oxidizer intake pressures at the pumps (the heads in the tanks holding the fuel components).

Single-stage centrifugal fuel pumps used in existing ZhRD have $\eta_{n.g} \approx 0.45$ to 0.70 and $\eta_{n.o} \approx 0.56$ to 0.75 . For low-thrust aviation engines, $\eta_n = 0.3$ to 0.4 .

The pump efficiencies must be specified on the basis of statistical

*[Subscripts: c.n.r = s.p.g = summarnyy perepad, goryucheye = total gradient, combustible; sc.r = vs.g = vsasivaniye, goryucheye = intake, combustible; c.n.o = s.p.o = summarnyy perepad, okislitel' = total gradient, oxidizer; sc.o = vs.o = vsasivaniye, okislitel' = intake, oxidizer.]

data in the design of engine TNA.

The feed pressure necessary to force a given fuel component into the engine combustion chamber is expressed by the following formula in the case of a pump-fed system:

$$p_n = p_s + \Delta p_n + p_{sc}. \quad (10.73)$$

The fuel flow rate into the TNA turbine of the engine's fuel-feed system may be determined from the turbine power equation

$$N_t = \Delta I_t \eta_t G_t \text{ kg/sec}$$

i.e.,

$$G_t = \frac{N_t}{\Delta I_t \eta_t} \text{ kg/sec} \quad (10.74)$$

where η_t is the relative net efficiency of the turbine, which is determined by thermodynamic calculation; usually, $\eta_t \approx 0.35$ to 0.50 . ΔI_t is the energy-content drop in 1 kg of gas in the turbine, in kcal/kg, as determined by the formulas

$$\begin{aligned} \Delta I_t = I_1 - I_2 &= \frac{k}{k-1} AR_1 T_1 \left[1 - \left(\frac{p_2}{p_1} \right)^{\frac{k-1}{k}} \right] - \\ &= c_p T_1 \left[1 - \left(\frac{p_2}{p_1} \right)^{\frac{k-1}{k}} \right] \text{ kcal/kg;} \end{aligned}$$

here, I_1 and I_2 are the energy contents of the gas at entry into the turbine and at exit from it, respectively; these values may be taken from the tabulated calculations for combustion and equilibrium of flow of the products of combustion under the conditions specified for the fuel in question; R_1 and T_1 are the gas constant and absolute temperature of the gas at the entry into the turbine, p_1 and p_2 are the pressures of the gas at entry into the turbine and exit from it, in atmospheres absolute, and c_p is the average heat capacity of the gas at constant pressure, in kcal/kg°C.

The quantity of hydrogen peroxide of the specified weight concentration required to operate the fuel-feed system depends basically on the pressure in the engine's combustion chamber and the specific gravity of the fuel to be fed.

Figure 10.24 shows curves for approximate evaluation of the amount of 80% hydrogen peroxide consumed per kilogram of basic fuel in the engine as a function of combustion-chamber pressures and the specific gravity of the fuel.

If there is a constant-pressure valve for the gas in the fuel-feed system, the consumption of fuel in the gas generator is determined by the formula

$$G'_s = G_{\text{typ6}} + G_{\text{ka}} = \frac{G_{\text{typ6}}}{1-\delta} \text{ kg/sec} * \quad (10.75)$$

where $\delta = G_{\text{kl}}/G'_s \approx 0.1$ is the fraction of the gas deflected by the valve into the exhaust pipe of the turbine and G_{kl} is the quantity of gas deflected through the constant-pressure valve in kg/sec.

The gas spent in the turbine enters the nozzle of the exhaust pipe at a pressure that sets up critical conditions for its outflow in the nozzle throat. As a result, the turbine operates at constant gas pressure at its intake and outlet and, consequently, at a constant power that does not depend on flight altitude.

The type of fuel pumps and their operating modes are selected for a ZhRD in the design stage on the basis of analysis of rpm factor and weight and cavitation characteristics, taking into account the specifications set forth for the pumps (high efficiency, low weight and small dimensions, operational reliability, etc.).

Proper selection of the fuel-pump type and its characteristics will ensure normal operation of the TNA and the engine as a whole.

*[Subscript typ6 = turb = turbina = turbine.]

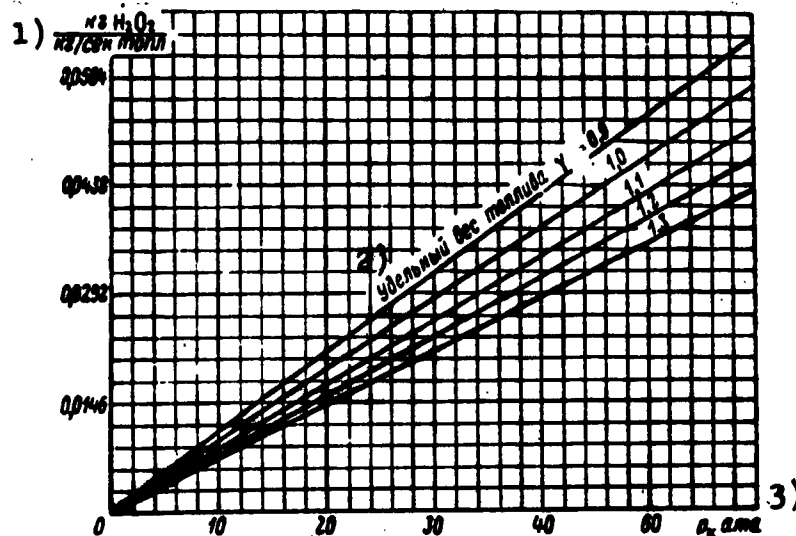


Fig. 10.24. Required consumption of 80%-by-weight hydrogen peroxide to feed 1 kg of fuel into engine combustion chamber, as a function of combustion-chamber pressure and specific gravity of fuel delivered. 1) kg of H_2O_2 per kg/sec of fuel; 2) specific gravity of fuel $\gamma_t = 0.9$; 3) p_k , atm abs.

SECTION 10. CHARACTERISTICS OF ZhRD FUEL-FEED SYSTEM TURBINES AND SPECIAL POINTS FOR THEIR DESIGN

The following basic specifications are set forth for the turbo-pump set of a ZhRD fuel-feed system:

- 1) good pickup on starting (ability to come up to the operating regime rapidly and smoothly);
- 2) stability in feeding the fuel components into the combustion chamber at the specified composition;
- 3) high efficiency and operational dependability;
- 4) simplicity of design;
- 5) minimal weight and dimensions.

The efficiency of the turbine depends basically on its power, the available vapor-gas heat difference, number of rpm's and other factors.

Since the efficiency of the turbine is almost directly proportional to its number of rpm's, it is advisable to design the pump for the highest possible speed (up to 40,000 rpm). However, with the object of achieving design simplicity and reducing weight, the turbine is

frequently mounted on the same shaft with the centrifugal pumps. This makes it necessary to reduce the turbine's rpm from the value optimal from the viewpoint of its efficiency to the relatively low optimum pump speed corresponding to cavitation-free operation of the latter. The turbine then operates uneconomically with a sharply depressed efficiency, with the result that almost one-and-one-half times as much working fluid is required to operate it.

High turbine efficiency can be achieved by appropriate selection of its operating and design parameters and careful finishing of the nozzle and working blades, as well as by appropriate selection of its basic dimensions, clearances in the working parts, etc.

Dependable turbine operation is insured primarily by the use of materials that resist high temperature and creep for the nozzle blades and for the working blades in particular.

The disks of the bladed wheel and the casing of a TNA turbine are sometimes made from aluminum alloy for low working-gas temperatures. In this case, only the intake pipe, the shaft, and a certain number of minor parts are made of steel. Cast iron and carbon steels can be used for the nozzles of turbines for one-time use.

Since the basic turbopump-fed ZhRD used in long-range missiles actually operate only for short times, the economy of TNA-turbine operation is not of essential importance. In this case, the prime factors are simplicity of design, low specific weight and operational dependability.

Naturally, the gas-generator unit of the ZhRD's feed system must then be simple in design, compact, and lightweight.

While the weight of a pressure-fed fuel-feed system depends basically on the reserve of fuel components carried in the tanks (on the operating time and thrust of the engine), the weight of a turbopump-

fed fuel system is basically determined by engine thrust and the feed pressure displacing the fuel components into the engine's combustion chamber. The weight of the TNA also depends on the number of turbine rpm's, the properties of the fuel components, the material of which the components of the turbopump set are made, and the mission of the vehicle.

The weight of a ZhRD turbopump set for one-time operation can be determined approximately from the formula

$$G_{TNA} = (a + bp_k) G_s, \quad (10.76)$$

where p_k is the combustion-chamber pressure, G_s is the flow rate of the fuel into the chamber, and a, b , and v are statistical coefficients for which values of $a \approx 4$ to 5 , $b \approx 0.065$ and $v \approx 0.5$ may be assumed for orientational calculations.

The parameters of the turbine depend on its power, the parameters of the working fluid, the method by which it is produced, and the manner in which it is used in the engine.

The working principle and design of turbines to be used to drive fuel pumps in ZhRD are almost the same as those of ordinary steam and gas turbines, detailed information concerning which can be found in the general handbooks for gas and steam turbines.

The turbine is designed for a definite set of theoretical operating conditions. The highest operating economy of the turbine corresponds to this regime.

The initial data for design of the turbine are the following:

- 1) the turbine's power in the theoretical regime and its number of rpm's;
- 2) the per-second flow of the vapor gas into the turbine, and its initial and final parameters (pressure, temperature).

The design of the turbine reduces to determination of its flow sections, the dimensions of the nozzle blades and main wheel, its overall dimensions, etc. These dimensions are usually fixed in such a way as to ensure the specified turbine power with a minimal vapor-gas consumption and small over-all turbine dimensions.

The theoretical operating regime of the turbine characterizes its most favorable working cycle. On changes in the flow rate of the vapor gas into the turbine or in its initial parameters (pressure, temperature), the turbine's economy of operation will deteriorate, since it will not be operating under the calculated conditions.

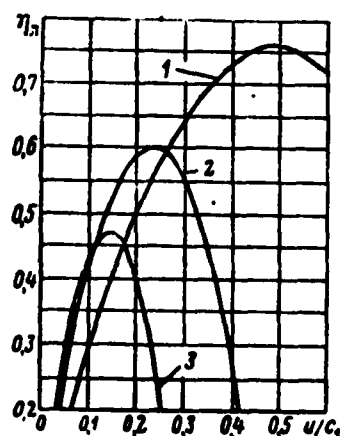


Fig. 10.25. Variation of blade efficiency of single-ring (curve 1), two-ring (curve 2), and three-ring (curve 3) velocity turbines as a function of vapor-gas velocity with discharge at 17° angle from nozzle onto turbine blades. 1) η_1 .*

ZhRD normally use single- or two-stage turbines with one pressure stage and two velocity stages. This turbine is simple in design and has a low specific weight (per horsepower), as compared with other turbine types. Two-ring turbines frequently have about ten-fifteen per cent reaction for more uniform loading of the working blades on the two rings of the wheel.

The slant angles of the turbine nozzles are usually selected in such a way as to deliver optimum turbine efficiency.

The height of the working blades on the wheels of modern turbines $h_1 = 15$ to 28 mm, while the ratio of height to average wheel diameter, $h_1/D_{sr} = 0.05$ to 0.12 , i.e., the blades are short and therefore do not require special shaping over their length. The step between the blades is 6 to 10 mm at the average wheel diameter (for rotors with a blade assembly). The ratio

of the blade step to blade width $t_{sr}/b_1 \approx 0.6$ to 0.85. In operational turbines, the blades are secured to the wheel disc by T-shaped mounts.

The gaps between the injector apparatus and the wheel blades are about 1.2-1.5 mm. The gap between the blade faces and the turbine housing (for unshrouded blading) is 0.15-0.4 mm.

The use of working blades that are unit-cast with the rotor or welded to it may considerably simplify the process of manufacturing the turbines.

It is desirable to design the turbine for the highest possible efficiency in order to reduce the specific consumption of vapor gas in the turbine, and consequently lower its specific weight.

As we know from the theory of turbines, the efficiency of a velocity turbine attains its maximum value at a fully defined ratio u/c_1 of the circumferential velocity of the turbine blades at the average wheel diameter to the velocity of the vapor gas at entry onto the working buckets of the turbine (Fig. 10.25). However, it is impossible to use this most favorable velocity ratio in practice because

- 1) of the deterioration of fuel-pump operation at high rpm's (it is convenient to mount the turbine and centrifugal pumps on a common shaft, without using reducing gearing);

- 2) of the limited ultimate strength of the materials of the moving turbine parts when they operate at high temperatures;

- 3) of the necessity of reducing the dimensions and weight of the turbine.

For these reasons, the fuel-system turbines of modern ZhRD are usually made to have efficiencies $\eta_t \approx 0.30$ to 0.50 at a velocity ratio $u/c_1 \approx 0.10$ to 0.15. As an example, the turbine of the A-4 engine has

$u/c_1 = 0.1$. The circumferential speed u of a TNA turbine may reach 150-250 m/sec.

The use of three gas-velocity stages in the turbine enables us to raise its efficiency slightly over that of the two-ring type and reduce the specific consumption of gas in it. However, this is accompanied by an increase in weight and design cost of the turbine, and this is not always expedient because of the short period of time during which the ZhRD fuel-feed system operates.

The velocity at which the gas is discharged from the turbine's nozzle apparatus is increased by increasing the heat difference of the gas in the turbine by raising the pressure or temperature at entry or using a fuel with a high heat yield for the gas generator, but the power gained when this is done is insignificant because the efficiency of the turbine must be lowered to maintain the adopted ratio u/c_1 and the design is usually complicated.

Consequently, no significant gain is achieved by raising the gas temperature at entry into the turbine, while the low temperature of the gases (380-500°C) permits extensive use of aluminum in manufacturing the turbine and thereby saves a significant amount of weight and reduces the chances of failure and warping of the components.

No warmup period is permitted for ZhRD turbines. When the full flow rate of hot gas suddenly bursts into the turbine, severe thermal shock and temperature strains may arise in its components, and this raises the probability of detrimental friction of the moving parts of the turbine.

The time taken by the TNA unit and the 2-component gas generator to come up to the operating regime (attain the specified TNA shaft rpm's) may amount to 2 sec.

The advantages connected with higher turbine efficiency and, consequently, with lower gas consumption in it, can be realized only provided that the design of the turbopump set admits of high circumferential velocities of the turbine blades, e. g., on introduction of a cooled reducing gear between the turbine and the pumps or with the use of pumps having high shaft rpm's. However, this measure complicates the design of the turbopump set, lowers its operational reliability, and raises its weight and cost, in addition to involving an additional loss in driving it.

Having selected the turbine type for the pump drive and established the optimum velocity ratio $u/c_1=a$ for it on consideration of the appropriate factors, we may determine the wheel-blade circumferential velocity of the turbine being designed, i. e., $u=ac_1$ m/sec.

Knowing the circumferential velocity of the turbine blades and having determined its number of rpm n , we can determine the average wheel diameter for the turbine by the familiar formula

$$D_{cp} = \frac{60u}{\pi n}. \quad (10.77)$$

Certain aluminum-alloy turbines used in modern ZhRD have circumferential blade velocities (at the average wheel diameter) of about 150 m/sec with vapor-gas temperatures in the range from 400-450°C.

In the single-shaft TNA system, the optimum turbine rpm's must be selected with consideration of the cavitation characteristics of the combustible and oxidizer pumps; the determining factor is the oxidizer pump.

The turbines of contemporary ZhRD have $n \approx 3000$ to 10,000 rpm and higher. The number of TNA turbine rpm's is established on the basis of determination of the maximum rpm's of the pump that is most dan-

gerous from the viewpoint of cavitation.

Since the total time during which the turbopump set of a fuel-feed system operates in military systems is relatively short, the influence of creep and fatigue in the structural materials can, in many cases, be disregarded in the design work and the gas temperature at entry into the turbine and the circumferential blade velocity increased over the values adopted for ordinary turbines designed for prolonged operation.

Installation of the turbine between the fuel pumps on a common shaft with them encounters various design and operational difficulties in certain cases. For example, one of the pumps in engines of the A-4 long-range missile supplies low-temperature (-183°C) liquid oxygen.

In this case, it is necessary to provide not only heat insulation between the heated turbine and the liquid oxygen, but also dependable sealing, in order to prevent penetration of the basic fuel components of the engine into the turbine housing.

The vibration problems encountered with ZhRD turbines are more complex than in the case of ordinary stationary turbines as a result of their proximity to the exceptionally powerful vibration source represented by the ZhRD proper. As a result, it is necessary that the TNA's critical rpm figure not only differ from its working speed, but also correspond to the lower segment of the engine's amplitude-frequency vibration spectrum.

For high-thrust ZhRD and engines operating at high combustion-chamber pressures, it will probably be expedient to use TNA of the reducing-gear type (Fig. 10.26), since it is beneficial to raise the number of turbine rpm's at optimum centrifugal-pump rpm's in the case of high-powered ZhRD.

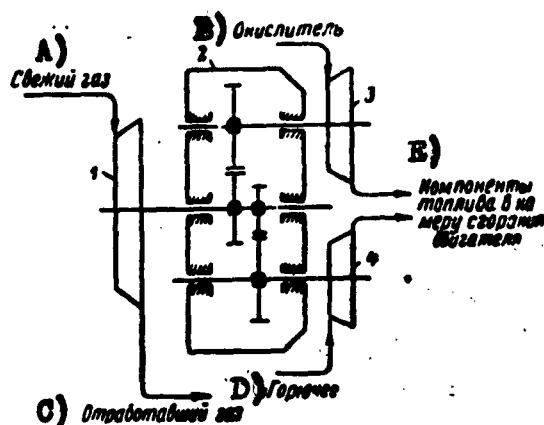


Fig. 10.26. Diagram of TNA with reducing-gear transmission to pumps. 1) gas turbine; 2) reducing gear; 3) oxidizer pump; 4) combustibile pump. A) fresh gas; B) oxidizer; C) spent gas; D) combustibile; E) fuel components to engine combustion chamber.

Velocity regulators (see Fig. 10.21, item 11) are normally employed to control the number of TNA rpm's. The rotary speed of the TNA shaft may be held constant; for this purpose, the regulator's control signal should be made proportional to shaft speed or varied in such a way that the feed pressure of the fuel components into the engine chamber will remain constant. In the latter case, the control signal should be proportional

to feed pressure.

Table 10.3 shows the basic specifications of the TNA used in the A-4 engine, which developed a thrust of 25 tons at the surface (Fig. 10.27), while Table 10.4 lists the materials used to fabricate the same turbopump.

TABLE 10.3
Basic Specifications of TNA of A-4 Engine

1) Характеристики и расчетные данные элементов ТНА	2) Размерность	3) Данные
5) Тип турбины	4) Парогазовая турбина	6) Однодисковая двухвечная активная с парциальным подводом пара (типа Кертинс)
7) Мощность	8) л. с.	465
9) Число оборотов	10) об/мин	3800
11) Рабочий газ	—	12) Продукты разложения 80%-ной H_2O_2

TABLE 10.3 (continued)

13) Расход парагаза	14) кг/сек	2,2
15) Давление парагаза на входе в турбину	16) кг/см ²	28
17) То же на выходе из турбины	.	1,5
18) Температура парагаза на входе в турбину	°C	385
19) Коэффициент полезного действия	—	0,32
20) Средний диаметр колеса	21) мм	447
22) Количество сопловых сегментов	23) шт.	4
24) . сопел в сегменте	.	4
25) Степень парциальности	—	0,884
26) Высота сопла	21) мм	11,5
27) Ширина сопла	.	38
28) Количество рабочих лопаток в одном венце	23) шт.	177
29) Размеры рабочих лопаток: ширина	21) мм	11,5
30) высота $A_{1\text{вх}} = A_{2\text{вх}}$.	16,5
30a) $A_{\text{н. вх}}$.	17
30b) $A_{\text{н. вых}}$.	23
30c) $A_{2\text{вх}}$.	25
30d) $A_{2\text{вых}}$.	30
31) Шаг между рабочими лопатками	.	8,4
32) Торцевой зазор между рабочими лопатками	.	2
33) Диаметр вала турбины у диска	.	38
34) Наружный диаметр корпуса турбины	.	575
35) Наружная ширина корпуса	.	125
36) Коэффициент заполнения турбины металлом при удельном весе 2700 кг/м ³	—	0,72
37) сс турбины	38) кг	60

39) Насос для горючего

40) Горючее	—	75% этилового спирта
41) удельный вес горючего при температуре 15°C	43) кг/м ³	41) +25% H ₂ O 864
44) Производительность	45) кг/сек	5
46) Давление подачи	47) кг/см ²	21,7
48) Давление на всасывании	.	1,08
49) Мощность	7) л. с.	270
50) Число оборотов	51) об/мин	3800
52) Коэффициент полезного действия	—	0,66
53) Диаметр крыльчатки	21) мм	320
54) Количество лопастей крыльчатки	23) шт.	7

TABLE 10.3 (continued)

55) Насос для окислителя

56) Окислитель	—	57) Жидкий кислород
58) Удельный вес горючего при -183°C	43) кг/м^3	1140
44) Производительность	45) кг/сек	69,3
46) Давление подачи	47) кг/см^2	17,5
48) Давление на всасывании	—	2,1
49) Мощность	7) л. с.	190
50) Число оборотов	51) об/мин	3900
52) Коэффициент полезного действия	—	0,86
53) Диаметр крыльчатки	21) мм	282
54) Количество лопастей крыльчатки	23) шт.	7
59) Общий вес ТНА	38) кг	180

1) Characteristics and theoretical data of TNA elements; 2) dimensions; 3) specifications; 4) vapor-gas turbine; 5) type of turbine; 6) single-disk two-row velocity turbine with partial vapor-gas supply (Curtis type); 7) power; 8) horsepower; 9) rotary speed; 10) rpm; 11) working gas; 12) decomposition products of 80% H_2O_2 ; 13) vapor-gas consumption; 14) kg/sec ; 15) vapor-gas pressure at entrance into turbine; 16) kg/cm^2 ; 17) same, at exit from turbine; 18) vapor-gas temperature at entrance into turbine; 19) efficiency; 20) average wheel diameter; 21) mm; 22) number of nozzle segments; 23) units; 24) number of nozzles in segment; 25) degree of partiality*; 26) nozzle height; 27) nozzle width; 28) number of working buckets in one row; 29) dimensions of working buckets: width; 30) height $h_{1vkh} = h_{2vykh}$; 30a) $h_{n.vkh}$; 30b) $h_{n.vykh}$; 30c) h_{2vkh} ; 30d) h_{2vykh} [Subscripts: $n = n = \text{nasos} = \text{pump}$; $vx = vkh = \text{vykhod} = \text{entrance}$; $vyx = vykh = \text{vykhod} = \text{exit}$.]; 31) step between working buckets (blades); 32) end gap between working blades; 33) diameter of turbine shaft at disk; 34) outside diameter of turbine casing; 35) outside width of casing; 36) fill factor of turbine with metal at specific gravity of 2700 kg/m^3 ; 37) turbine weight; 38) kg; 39) pump for combustible; 40) combustible; 41) 75% ethyl alcohol + 25% H_2O ; 42) specific gravity of combustible at 15°C ; 43) kg/m^3 ; 44) output; 45) kg/sec ; 46) feed pressure; 47) kg/cm^2 ; 48) intake pressure; 49) power; 50) rotary speed; 51) rpm; 52) efficiency; 53) impeller diameter; 54) number of impeller blades; 55) pump for oxidizer; 56) oxidizer; 57) liquid oxygen; 58) specific gravity of combustible at -183°C ; 59) total weight of TNA.

*[Literal rendition.]

TABLE 10.4.

Materials of A-4 Engine TNA

1) Детали ТНА	Прочность на разрыв 2) кг/см ²	3) Химическая характеристика материала
4) Литые корпуса турбины, насосов и их крыльчаток	2000	5) Алюминиевый сплав: 10-13% Si 0,2-0,5% Mg 0,3-0,7% Mn
6) Поковка диска турбины	1790	5) Алюминиевый сплав: 2,0-2,5% Mg 1,0-2,0% Mn 0,0-0,2% Sb
7) Рабочие лопатки турбины	2490	5) Алюминиевый сплав: 0,5-1,5% Mg 0,5-1,5% Si 0,3-1,3% Mn
8) Вали, болты	6300	9) Сталь: 0,45% C 10) менее 0,1% P и S
11) Сопловой аппарат турбины	2190	12) Серый чугун
13) Подшипники кислородного насоса	-	14) Свинцовистая бронза: 18-26% Pb 0,3% Sb 0,3% Sn 15) Остальное Cu

1) TNA part; 2) tensile strength, kg/cm²; 3) chemical characterization of material; 4) cast casing of turbine, pumps, and their impellers; 5) aluminum alloy; 6) turbine-disk forging; 7) working turbine buckets; 8) shafts and bolts; 9) steel; 10) less than 0.1% P and S; 11) turbine nozzle unit; 12) gray iron; 13) bearings of oxygen pump; 14) leaded bronze; 15) remainder Cu.

SECTION 11. CHARACTERISTICS OF PUMPS FOR ZhRD FUEL-FEED SYSTEM AND SPECIAL POINTS IN THEIR DESIGN

The design of pumps that are simple in design, small in size, and reliable in operation to feed combustible and oxidizer into a ZhRD chamber is one of the basic problems encountered in planning, building, and refining these engines. Up to now, the literature has cast very little light on the problems of designing pumps for ZhRD.

Missile ZhRD normally employ single-stage centrifugal pumps because of their small dimensions, light weight, and satisfactory operation at high rpm's on the same shaft with the turbine; high pressures

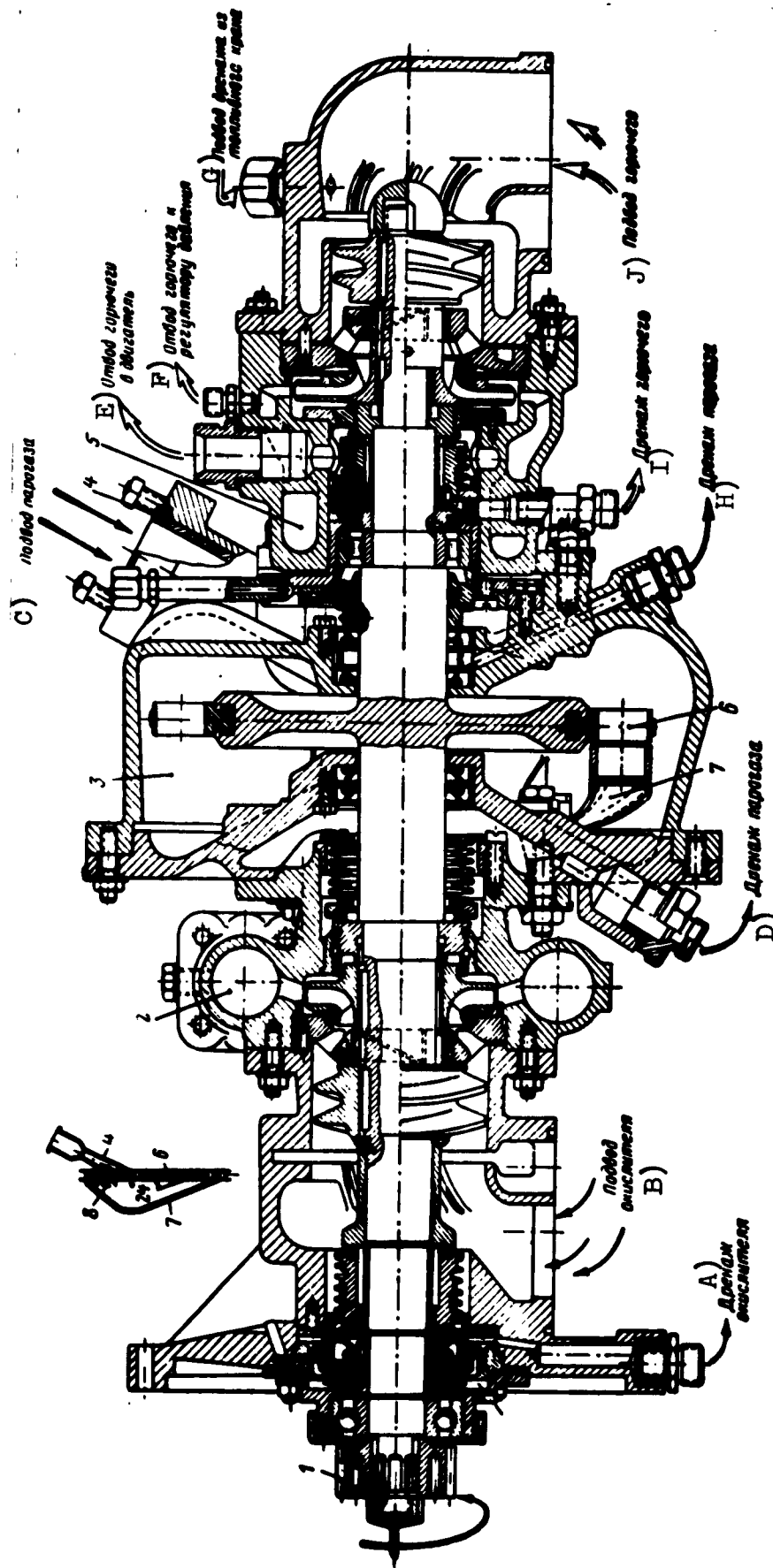


Fig. 10.27. Section through TNA of "Walter" ZhrD. 1) Gear; 2) oxidizer pump; 3) turbine; 4) nozzle; 5) combustible pump; 6) turbine wheel with blades; 7) rotary chamber; 8) entrance buckets. A) Oxidizer drainage; B) oxidizer supply; C) vapor-gas supply; D) vapor-gas drainage; E) combustible takeoff to engine; F) combustible takeoff to pressure regulator; G) drainage supply from fuel cock; H) vapor-gas drainage; I) combustible drainage; J) combustible supply.

can be generated and large quantities of liquid fed in for prolonged periods.

During operation of the TNA, an axial force directed toward the entry of the liquid into the pump arises in each of its centrifugal pump units, since the fluid pressure is not the same on the front and rear surfaces of the working wheel of each pump. To reduce the axial forces, it is necessary to place the pumps of a single-shaft TNA on the shaft in such a way that their entry ducts will be directed counter to one another (toward the turbine, as in the A-4 engine, or away from it, as with the "Walter" engine). This also takes into consideration a slight possible axial force in the gas turbine. If the axial forces of the TNA are not completely offset, it is necessary to compensate them by installing a thrust bearing.

The general techniques of planning and designing ordinary-type centrifugal pumps are also applicable to ZhRD pumps. The basic problem in developing centrifugal pumps for engine fuel-feed systems is that of creating high-output, lightweight, and miniature designs.

Simplicity of design in a turbopump set makes it possible to minimize the likelihood of failure in operation and simplify work with it, while small dimensions make it easier to adapt the unit to the engine, since the spaces reserved for its installation aboard the missile are usually quite small.

The turbopump set must possess excellent pickup properties and not require a long warmup period; it must come up to the design number of rpm's (30-40 thousand) in one second or an even shorter interval of time.

Normally, ZhRD pumps do not require special starting devices; in starting, the fuel components can be moved to the pumps by gravity feed alone or under the static pressure head in the tanks.

The necessary feed pressure for the corresponding pump is determined from the gas pressure in the combustion chamber and the hydraulic losses in the pipelines from the pump to the combustion chamber, i.e.,

$$p_s = p_k + p_{\text{pot}} \text{ kg/cm}^2 \quad (10.78)$$

The following basic parameters of the pump are used in making calculations for it and evaluating its quality:

- 1) total output

$$Q = \frac{G}{\gamma} \text{ m}^3/\text{sec}; \quad (10.79)$$

- 2) the head developed by the pump,

$$H = \frac{10 \Delta p_n}{\gamma} \text{ m} \quad (10.80)$$

- 3) the pump rotary speed n in rpm,

where G is the weight output of the pump in kg/sec, γ is the specific gravity of the fluid in kg/m³, $\Delta p_n = p_p - p_{vkh} = p_k + p_{\text{pot}} - p_{vkh}$ is the fluid pressure set up by the pump in kg/cm²; here, $p_{vkh} = p_B - p_{st}^{**}$ is the fluid pressure at entrance into the pump and p_{st} is the pressure of the column of fluid in the tank.

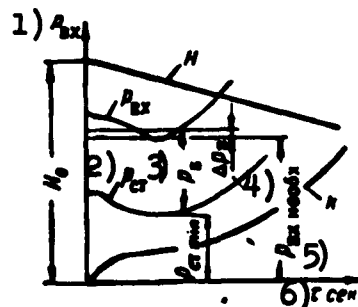


Fig. 10.28. Typical variation of H , p_{vkh} , p_{st} , p_B and k during flight of missile.

- 1) p_{vkh} ; 2) p_{st} ; 3) p_B ;
- 4) Δp_p ; 5) p_{vkh} , necessary;
- 6) τ , seconds.

*[Subscripts: $\pi = p = \text{podacha} = \text{feed}$; $\kappa = k = \text{kamera} = \text{chamber}$;

$\text{not} = \text{pot} = \text{poteri} = \text{losses}.$]

**[Subscript: $st = st = \text{stolb} = \text{column}.$]

In missile ZhRD, the fuel tanks are normally located above the engine, so that p_{st} is positive. In aircraft ZhRD, the fuel tanks may be installed below the engine, so that p_{st} may be negative. During the missile's flight, p_{st} varies as a result of the decrease in the liquid column in the tank as the fuel is

consumed and as a result of longi-

tudinal acceleration of the missile.

As a result, the pressure p_{st} of the fuel component in question in front of the pump will consist of the static pressure of the liquid column and the inertial force of the same column, i.e.,

$$\begin{aligned} p_{st} &= H\gamma \sin \theta + H\rho j = H\rho(j + g \sin \theta) = \\ &= H\gamma(k + \sin \theta), \end{aligned} \quad (10.81)$$

where θ is the inclination of the missile to the horizon during flight and $k = j/g$ is the axial overload on the missile.

Figure 10.28 shows a typical variation of the pressure p_{st} over the operating time of the engine as a function of the liquid column in the tank and the flight acceleration of the missile. It will be seen from this figure that the minimum liquid pressure $p_{st.min}$ in front of the pump will occur after the engine is started; it will be slightly smaller than the pressure $p_{st.zap} = H_0\gamma$ that obtains when the engine is started.*

Consequently, it is necessary to know the missile's flight trajectory and acceleration in order to determine $p_{st.min}$. The cavitation calculations for the pump must be made for this pressure.

If $p_{vkh.neobkh}^{**}$ has been determined in the cavitation calculations for the pump, the required tank pressure p_B must be such that the required pressure p_{vkh} will be ensured at minimum liquid-column pressure, i.e.,

$$p_B = p_{st.neobkh} - p_{st.min} + p_{atm} \quad (10.82)$$

In missiles that are subject to large accelerations, such as antiaircraft missiles, or in rocket-powered interceptor aircraft, special measures should be taken to maintain the minimum required liquid head for the pump intake (e.g., installation of ejectors to

*[Subscript: zap = zapusk = starting, firing.]

**[Subscript: neobkh = neobkhodimyy = necessary.]

evacuate steam and air bubbles from the intake line of the pump).

The above pump parameters Q , H , and n , taken in a definite combination, give a similarity criterion for the pump, i.e., a quantity that determines its basic properties irrespective of the absolute geometrical parameters, the head, and the number of rpm's.

The pump's rpm factor

$$n_s = 3.65 \frac{n \sqrt{Q}}{H^{0.75}}. \quad (10.83)$$

is such a similarity criterion for a centrifugal pump.

A special property of ZhRD centrifugal pumps is their very small rpm factor, $n_s \approx 15$ to 90. Specifically, the rpm factor of the alcohol centrifugal pumps of the A-4 engine is $n_s = 55$, and that of the oxygen pump is $n_s = 82.7$.

The low values of n_s are responsible for the very low efficiency of the pump, because of the large frictional losses that take place in them and leakage of the liquid through the gaps between the impeller and casing of the pump. The size of the gap in the labyrinth packing of the nitric-acid pump is usually 0.2 to 0.25 mm. To some extent, the hydraulic losses depend on the case with which the surfaces of the pump wheel are machined.

The design output Q of the pump for a given head H is usually fine-adjusted by introducing the appropriate resistance in the form of a throttling disk, etc., into the pump circuit. It is necessary to regulate the head and output of the pump in this way because of the tolerances admitted for the hydraulic parameters and characteristics of the pumps, valves, injectors, etc.

The characteristics of the pump for various rpm's may be determined from their known values for some single rpm figure, proceeding from the following relationships: liquid flow rate $Q = f(n)$, head

$H = f(n^2)$, and power $N_n = f(n^3)$, where f is a function dependent upon the design of the pump.

The head, liquid flow rate, and efficiency of the pump also depend on the design of the impeller, the shape of its buckets, and the geometry of the pump casing.

The head developed by a centrifugal pump is approximately proportional to the square of the circumferential velocity u_2 at the outer diameter D_2 of the pump wheel:

$$\Delta p_n = \gamma H = f(u_2^2) = \left(\frac{\pi D_2 n}{60} \right)^2, \quad (10.84)$$

where n is the pump shaft rpm's.

The circumferential velocity of the centrifugal-pump wheel is limited by strength considerations and usually does not exceed $u_2 = 100$ to 200 m/sec. If it is necessary to produce large heads, a switch is made to multiple-stage centrifugal pumps.

Selection of the rpm figure for a centrifugal pump is a rather complex matter. As we know, raising the number of rpm's of a pump of this type has a favorable influence on the design of the entire turbopump set, since it results in a decrease in its dimensions and weight and in an improvement of the turbine's operating conditions (increases its efficiency). However, raising the number of pump rpm's above a definite limit is restricted in practice by the phenomenon of cavitation under a given set of pump-operation conditions, i.e., by vapor formation in the fluid at entry into the pump, since the liquid pressure is lowest at this point and may even be lower than the saturation vapor pressure at the liquid temperature in question.

Cavitation causes fluctuations in pump output and makes the engine's operation unstable and unsafe, since it may result in severe vibrations and even explosion in the engine. For this reason, it is not permissible to operate ZhRD pumps in their cavitation regime.

The maximum admissible cavitation-free number of rpm's for a centrifugal pump is determined by the formula

$$n_{\max} = \frac{c_{kp}}{\sqrt{Q}} \left(\frac{H_{\text{ex}} - H_s}{10} \right)^{0.75} = \frac{c_{kp}}{\sqrt{Q}} \left(\frac{p_{\text{ex}} - p_s}{\gamma} \right)^{0.75} \quad (10.85)$$

where c_{kr}^* is the pump's experimental critical cavitation coefficient, which depends on the hydraulic characteristics and design of the entrance part of the pump; in the design work, it may be evaluated approximately on the basis of the pump's rpm factor n_s :

for $n_s = 50-70$	$c_{kp} \approx 600-750$;
70-80	750-800
80-150	800-1000
150-300	1000-1200;

$H_{vkh} = p_{vkh}/\gamma$ is the liquid head at entry into the pump, in meters, $H_s = p_s/\gamma$ is the head at which vapor begins to form in the liquid, and p_s is the saturated vapor pressure at the liquid temperature in question.

This formula can also be used to determine the head necessary in the fuel tank to ensure cavitation-free pump operation at the specified number of rpm's n , i.e.,

$$H_{\text{ex.needed}} = H_s + 10 \left(\frac{n \sqrt{Q}}{c_{kp}} \right)^{0.75} m, \quad (10.86)$$

or

$$p_{\text{ex.needed}} = \gamma H_{\text{ex.needed}} = p_s + \gamma \left(\frac{n \sqrt{Q}}{c_{kp}} \right)^{0.75} \text{ atm-abs},$$

where γ is the specific gravity of the fluid.

In making the cavitation calculations, therefore, it is necessary to know the saturation vapor pressure p_s of the liquid being pumped, since the lower this pressure, the easier will it be for cavitation to arise.

The pressure p_s depends on the nature of the liquid and its temperature. [Subscript: $kp = kr = \text{kriticheskiy} = \text{critical}$.]

perature. As the temperature increases, p_g rises sharply, and this must be taken into account in making the cavitation calculations for the pump. In the calculations, p_g , γ , and Q must be taken for a temperature of $+50^\circ\text{C}$, which corresponds to the worst possible operating conditions of the pump. Data concerning p_g as a function of temperature are normally presented in courses on ZhRD fuels and in certain physics and chemistry handbooks.

It follows from Expression (10.85) that the maximum admissible number of pump rpm's will be smaller for the oxidizer pump than for the combustible pump, since the oxidizer's volume flow rate will always be higher than that of the combustible. For this reason, the number of TNA rpm's in single-shaft turbopump sets is determined by the value of n_{\max} for the oxidizer pump.

A liquid head at entrance into the pump is usually created artificially in the tanks of pump-fed ZhRD in order to raise the maximum admissible number of pump rpm's. In practice, the liquid head at entry into the pump may be set up by any of the following methods:

- 1) excess pressure in the tanks due to the velocity head of the atmospheric air;
- 2) by pressurizing the tank with compressed gas from special bottles or with gas produced at a definite pressure in a special gas generator;
- 3) by injection apparatus;
- 4) by pumps.

Figure 10.29 presents schematic diagrams of ZhRD with different methods of feeding the pump-set turbine and pressurizing the fuel tanks.

It is inefficient to pressurize the fuel tanks by means of the velocity head. In practice, the head is most simply set up by com-

pressed-air pressurization, although this increases the weight of the system.

If special gas generators are used to pressurize the fuel tanks, the tanks must be pressurized with compressed air before these generators go into operation. As the tank pressurizing pressure rises above the established value, the excess of air or gas must be released into the atmosphere through a safety valve.

It may be found efficient to pressurize the tanks by the use of injector apparatus and screw pumps. However, use of these pumps is possible only provided that their designs ensure cavitation-free operation at high rpm's of the main pumps. For this purpose the auxiliary pump must have either a special design (e.g., worm-type) or a lower number of rpm's, i.e., must be driven off the turbine via a reducing gear.

Figure 10.30 shows curves of the maximum pump rpm as a function of its output and pressure head, as computed by Formula (10.85) for $c_{kr} = 560$ and a liquid with a specific gravity $\gamma = 1000 \text{ kg/m}^3$.

The curves of this figure indicate that the creation of high-speed, high-output pumps requires large liquid heads at entrance into the pump (about 5 to 10 atmospheres). In case the component flow rates are moderate (below 40-50 kg/sec), however, it is obvious that high-speed pumps ($n \approx 10,000$ to 18,000 rpm) may be used with relatively small heads (about 1 to 3 atmospheres).

The amount of pressurization tolerated is determined by the strength of the lightweight tank, the weight of the gas used for pressurization, and the weight of the system feeding this gas. Since an increase in the fuel-tank pressurization pressure results in an increase in the weight of the pressurization system with the gas, and also makes it necessary to build stronger and relatively heavy fuel

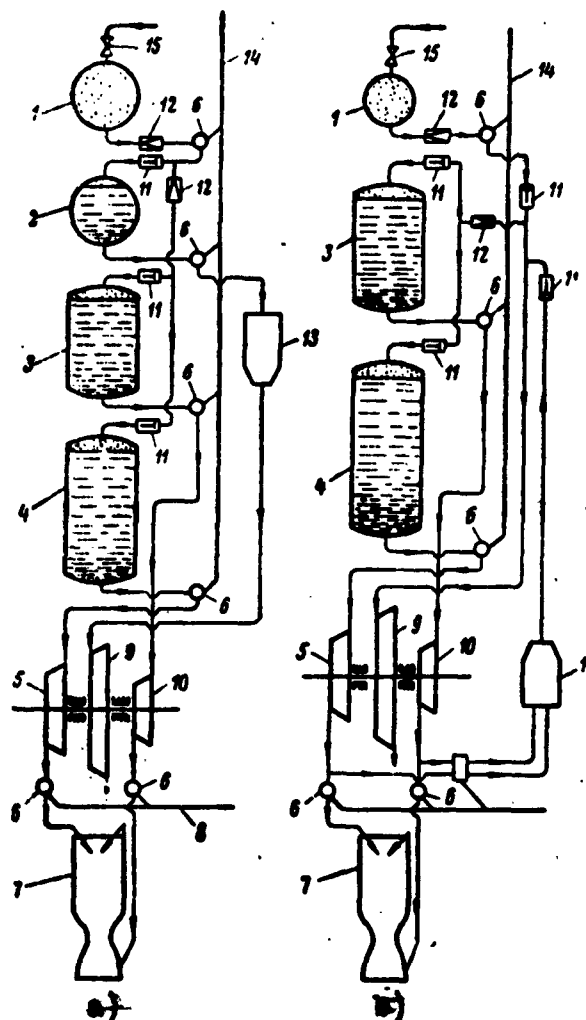


Fig. 10.29. Schematic diagrams of ZhRD with independent (a) and dependent (b) pump-set turbine feed and fuel-tank pressurization. 1) Compressed-air bottle; 2) tank for single-component fuel to feed gas generator; 3) main combustible tank; 4) oxidizer tank; 5) oxidizer pump; 6) controllable valve; 7) engine chamber; 8) engine thrust control; 9) gas turbine; 10) combustible pump; 11) nonreturn valve; 12) pressure reducer; 13) single-component gas generator; 14) control main for starting engine; 15) gate valve; 16) two-component gas generator.

tanks, the practice of raising the gas-pressurization pressure over the tanks must not be abused in establishing the maximum permissible pump speed for a ZhRD because it may result in a general increase in the engine's weight.

Since the oxidizer pump is more liable to cavitation than the combustible pump, the oxidizer-tank pressurization pressure must be

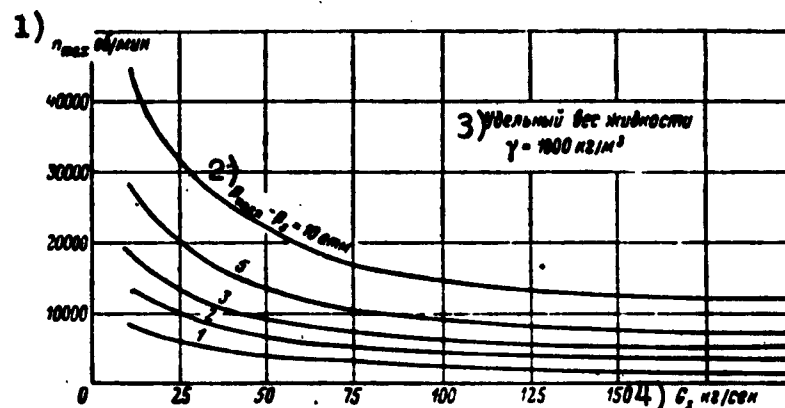


Fig. 10.30. Maximum pump speed as a function of pressure head and liquid flow rate through pump. 1) n_{max} , rpm; 2) $p_{podp} - p_s = 10$ atmospheres; 3) specific gravity of liquid $\gamma = 1000 \text{ kg/m}^3$; 4) G_s , kg/sec.*

larger than that for the combustible tank. If the oxidizer tank is located in the nose section of the missile, the pressurization pressure must, accordingly, be made smaller than when the tank is located near the engine chamber, because part of the pressure at entry into the pump can be obtained from the pressure of the liquid column in front of the pump.

Various measures, such as swirling the liquid stream at entry into the pump impeller by installing fixed directing blades, installing an auxiliary screw or vane-wheel booster pump in front of the main centrifugal pump, etc., are usually taken to improve pump performance and raise its speed without incurring an excessive increase in the tank pressurization pressure.

The use of a screw pump to pressurize the fluid in front of the usual centrifugal pump is of considerable interest (stable operation of this pump begins only at 9000-10,000 rpm; below these speeds, the pump operates unevenly, with pulsations).

Tests of a screw pump showed that the head developed by it is

*[Subscript: подп = podp = podpora = boost.]

extremely large and composes approximately 30% of the total head developed by this group. Installation of a screw pump makes it possible to reduce the weight and size of the entire unit by a considerable margin. Moreover, it becomes possible to achieve a considerable increase in the diameter of the intake pipelines and thereby reduce the losses in them to a minimum. This, in turn, enables us to minimize the heads in the fuel tanks. The velocity of the fluid at entry into the pump impeller is usually adjusted between 3 and 6 m/sec, and the velocity at the output from the impeller is 3-15 m/sec.

Since the use of certain liquid fuel components involves a danger of explosion when they come into contact with one another, special measures must be taken to eliminate leakage of fluid through the shaft packings or stuffing boxes of the pump. In cases where hypergolic fuel components are used, leakage may result in fire and explosion of the engine and the entire missile. If fuel components with high corrosive properties are employed, extremely rigid specifications are imposed on the material and design of the pump packings.

The design measures taken against liquid seepage in the pump may be different in different existing TNA designs.

Bellows-type packings are recommended for the pumps. To lighten the load on the packing units, the fluid intake into the pumps should be made at the drive end.

In designing turbines for the engines, it is necessary to devote attention to the critical number of rpm's, the axial and radial loads on the bearings, and the stresses that arise in the rotating parts. Since the engine pumps are not usually rigidly mounted to a heavy foundation, but have resilient suspensions and are located near the powerful vibration source represented by the ZhrD, these vibrations may seriously affect pump performance (e.g., cause shaft

breakage or local friction between the rotating and stationary parts).

In cases where the pressure in the engine's combustion chamber is high (above 40 atm abs), the liquid head set up by a single-stage pump may be found inadequate or off-optimum. For this reason, two- and three-stage centrifugal pumps are required to set up high fuel-component pressure heads.

In planning and designing fuel pumps for ZhRD, every effort must be made to raise their over-all efficiencies. The following may be listed as basic methods of raising the efficiencies of TNA centrifugal pumps:

- 1) raising the pump speed by dividing each pump into two stages:
 - a) a preliminary stage operating at a low speed selected on the basis of cavitation conditions and a low head selected on the basis of the operating conditions of the main stage and b) a stage operating at higher rpm's, a setup which corresponds to the use of a reducing-gear TNA design;

- 2) increasing the number of pump stages with the rpm's held constant;

- 3) increasing the liquid head at entry into the pump;

- 4) improving the anti-cavitation properties of the pump (installation of preliminary screw pump in front of main pump, utilization of energy of pumped fluid for ejection, oversized entrance to wheel, etc.).

The rpm factor of the pump and, consequently, its over-all efficiency may be increased by application of one of these measures or a combination of them.

SECTION 12. FITTINGS, PIPELINES, AND OTHER ELEMENTS OF ZhRD FUEL-FEED SYSTEM

In developing a ZhRD design, a highly important step is the selec-

tion of the necessary fittings, instruments, and other elements for the fuel-feed system in such a way as to provide for starting, normal operation, and stopping of the engine.

For a one-shot ZhRD, these elements of the fuel-feed system include:

- 1) automatically operated cutoff valves;
- 2) burst membranes of the spontaneous-burst or forced-burst (powder-cartridge) types;
- 3) constant-pressure relays;
- 4) nonreturn valves;
- 5) compressed-gas pressure reducers;
- 6) throttling disks;
- 7) drainage valves;
- 8) fueling and drain plugs or the appropriate shutoff-valve substitutes;
- 9) inside-tank fuel-intake devices;
- 10) safety valves;
- 11) pipelines, bellows, etc.

Selection of the elements for the fuel-feed system, their number, and their design depend to a major degree on the mission and thrust of the engine and other factors. In all cases, it is necessary to try to minimize the number of mechanical devices such as valves, relays, and pipelines in the fuel-feed system in order to improve the safety and dependability of its operation.

Cutoff valves (OK*) function to regulate the flow of the fuel components into the combustion chamber, are usually automatically operated, and work in the same way as stop valves. The feed of the fuel components and the gas can be controlled by opening and closing

*[OK = OK = Otsechnyy Klapa = Cutoff Valve.]

these valves (starting and stopping the engine).

Since large quantities of liquid flow under high pressures through the cutoff valves, considerable effort is required to operate them. The force necessary to close and open ZhRL cutoff valves is usually developed by an electromagnet or servo-piston (pneumatic or hydraulic) loaded with the control pressure. Due to their high consumption of electricity, electromagnetically operated cutoff valves are used only for small-diameter pipelines. Servo-piston valves are most convenient for large-diameter pipelines. Here the engine may develop its top thrust about 1.5 seconds and stop (zero thrust) approximately 0.5 second after application of the appropriate pulse to the valve.

The basic elements of any cutoff-valve design are its seat, the actual valve covering the pipeline, and the drive to this valve.

In the design of a cutoff valve, special attention must be devoted to its trouble-free operation. This is achieved through the use of various valve designs that guarantee tight leakage-free seating and by the use of stainless steels for the seat inserts, the bodies of the valves, the springs, and the other parts in order to prevent failure in operation of the valve because of corrosion.

Cutoff-valve designs are classified into the following types in accordance with the position of the valve [poppet] relative to the seat before and during engine operation:

- 1) normally closed valves, i.e., valves that are closed when no current is flowing in the circuit and open when current is fed;
- 2) normally closed valves with drainage, i.e., with a hole that bleeds pressure from the line behind the valve when the current stops flowing;
- 3) normally opened valves, i.e., valves that are open in the

absence of current in the circuit and closed when the current is thrown into it;

4) normally closed follow-up valves with hydraulic or pneumatic servo-pistons, i.e., valves that are closed in the absence of pressure on the servo-piston and open when pressure is applied;

5) normally closed [sic] follow-up valves with servo-pistons.

The physical designs and operating principles of existing cutoff valves and those of other elements of ZhRD fuel-feed systems are described in detail in the available literature.*

In designing a ZhRD's fuel-feed system, it must be borne in mind that although cutoff valves are simple in design, great difficulties are sometimes encountered in working out certain of their components, in selecting the materials for the valve seat and determining the gaps, and with sticking in the open position.

Cutoff valves must operate dependably, since any damage to the valve may put the entire engine out of commission. Leakage in a fuel valve and sticking in the open or closed position may result in malfunction of the engine and the weapon system as a whole.

Duplex or triplex valves, in which a single servo-piston opens two or three valves in the lines of different components or in parallel lines of the same component, are also encountered in modern ZhRD systems. In this case, the movement is transmitted from the servo-piston to the valves through rocker arms.

Before installation in the engine, cutoff valves must pass hydraulic tests for leakage through the seat or guides and for operating precision.

In selecting the size of a cutoff valve, we proceed from the assumption that its diameter should be equal to the open diameter of

*G.E. Sinyarev and M.V. Dobrovol'skiy. Zhidkostnyye raketnyye dvigateli (Liquid-Fuel Rocket Engines), Oborongiz, 1957.

the corresponding pipeline. Here, the valve lift should be no greater than $1/4$ of its diameter.

The force necessary for dependable closing of the valve is determined from airtightness calculations for it.

Plastics and light metals may be used for the packing inserts of the valve (in accordance with the type and function of the valve). Ground-to-seat valves are sometimes used for particularly aggressive liquids.

Diaphragms of the spontaneous- and forced-burst types (MR*), [the latter] opened by an electrically ignited powder charge, represent extremely simple and relatively lightweight stop-flow units that are frequently used as substitutes for cutoff valves in single-shot fuel-feed systems. They ensure dependable sealing. When the specified pressure is attained, the diaphragm bursts and gives the fuel component access to the place at which it will be used. Here, interchangeable throttling disks are used to regulate the flow rates of the components.

Once started, an engine equipped with stop-flow membranes cannot be stopped until one or both of the fuel components has been completely exhausted.

The diaphragm designs have either ring-shaped or cross tear patterns. It is along these patterns that the diaphragm bursts when the specified pressure is reached in the system, since the strength of the diaphragm is lowest along these lines. After a membrane of the first type has burst along the tear pattern, its "petal" bends back and opens the way to the liquid or gas. In membranes of the second type, bursting also takes place along the marks, and a number of petals bend back.

*[MP = MR = Membrana Razryva = Burst Diaphragm.]

The diaphragm is usually hand-picked for the required burst pressure, since the force required to tear the thin material of the membrane depends to a major degree on the tolerances for the thickness at the burst lines.

The function of the constant-pressure relay (RPD*) is to switch electric circuits when a definite pressure has been reached in the pipeline or tank being serviced and to reverse-switch the circuit when the pressure has dropped below the specified limit. Pressure relays may be of the normally open or normally closed type.

Nonreturn valves (OK**) function to prevent motion of the liquid or gas in the backward direction along the pipeline. In the idle state, the head of this valve is compressed to its seat by spring tension. On entering the connecting piece containing the valves, the component opens it by pressure on the head and passes into the outlet section. The reverse motion of the liquid or gas is impossible, since it always results in closing of the valve. The motion of the valve head is limited by a stop shoulder.

The pressure reducer (RD***) functions to lower the pressure of the gas moving from the pressure accumulator into the tanks to displace the fuel components from them into the engine's combustion chamber to a specified limit, and is one of the basic elements of pressure-fed fuel-feed systems.

Gas-pressure reducers are also frequently used in feed systems supplying automatic control elements with gas at a required pressure for feeding components into the vapor-gas generator, and for other purposes.

The amount by which the gas pressure is reduced during throttling

*[РПД = RPD = Rele Postoyanstva Davleniya = Constant-Pressure Relay.]

**[OK = OK = Obratnyy Klapen = Nonreturn Valve.]

***[РД = RD = Reduktor Davleniya = Pressure Reducer.]

in the reducer is governed by the size of the opening between the valve and the seat.

The reducer design is determined to a major degree by the direction in which its valve opens. Pressure reducers are classified into direct-action and reverse-action types on the basis of this criterion. In a direct-action pressure reducer, the valve opens in the direction of the force developed by a high-pressure gas (in the direction of gas flow). In the reverse-action reducer, the valve opens against the force developed by the high-pressure gas (against the gas flow).

Reverse-action pressure reducers are normally used in ZhRD.

The pressure reducer not only lowers the gas pressure to the level required to displace the components from the tanks, but also simultaneously acts as a regulator to hold the fuel-tank pressure almost constant even though the gas pressure at entry into the reducer is constantly diminishing as a result of the loss of gas from the pressure accumulator.

Like most other types of reducers, the reverse-action pressure reducer operates with a certain nonuniformity, i.e., when the gas pressure at the inlet into the reducer changes, the gas pressure at its output also changes slightly. The dependence of the output gas pressure on the gas pressure at the inlet into the reducer is known as the reducer's characteristic. We distinguish between two types of reducer characteristics. The gas pressure at the reducer output as a function of the inlet pressure in the absence of gas flow is known as the static characteristic. The same relationship for gas flowing through the reducer is known as the dynamic characteristic.

The gas pressure at the outlet from the reducer must be constant and independent of the pressure at the reducer inlet (the bottle pressure). When the component feed into the combustion chamber ceases, the

reducer must automatically block access of the gas to the working fluids.

The throttling disks (DSh*) function to regulate the flow rates of the components in the system's pipelines. The resistance of the system can be reduced or increased by a considerable margin by plugging a throttling disk with a larger or smaller flow section in it, and this results in a corresponding change in the component flow rate. Installation of such throttling disks in the component-feed lines is inevitably necessary in calibrating a ZhRD feed system, since it is only through the use of these chokes that both the absolute flow rates of the combustible and oxidizer and their proper weight proportions can be maintained.

Drainage valves (DK**) serve to permit drainage of the various systems when the fuel components are taken aboard and to bleed excess pressure from the fuel tanks when the system is stored in fueled condition.

In designing the engine, it is necessary to strive to minimize its specific gravity. The smaller the flow sections of the pipelines, cocks, etc., the lighter will they be. As the flow sections of the pipelines are reduced, however, the pressure losses in the fuel components increase and to ensure the necessary per-second flow it becomes necessary to raise the flow pressure, and this results in an excessive increase in the weight of the fuel-feed system. The engine designer's problem consists in finding the optimum flow sections for the pipelines and starting-control apparatus.

For aggressive fuel components, it is necessary to use pipelines made from stainless steel or aluminum, depending on the pressure

*[DSh = DSh = Drossel'naya Shayba = Throttling Disk.]

**[DK = DK = Drenazhnyy Klapan = Drainage Valve.]

applied to the component.

The designer must devote particular attention to fabrication of the valves and other monitoring and control components for high working-fluid flow rates; this applies particularly to ZhRD where extremely slight working-fluid seepage may result in malfunction of the engine and the system as a whole. This is accounted for by the fact that various substances ranging from nontoxic gases such as nitrogen or air to boiling corrosive fluids such as liquid oxygen or liquid fluorine, ammonia, etc. are usually employed in ZhRD. The working temperatures of these fluids also vary over wide ranges: from -183°C for liquid oxygen to plus several hundred degrees for the gases used in the pump-set turbine.

Stop, throttling, nonreturn, and reducing valves are the types most frequently used in ZhRD; burst diaphragms are relatively infrequent. The conditions under which these units operate may be extremely severe: the transition from the completely closed state to the completely opened state must be effected in a very short time (no longer than 10-20 msec). Initiation, ignition, and cutoff of high fuel-component flow rates also represent very complex operations. In designing the engine, therefore, it is necessary to make provision for its dependable and on-design operation in the specified regimes and to avoid rupture of the pipelines, the chamber, and the engine as a whole when the above operations are being performed.

An effort must be made to reduce the cost of the individual elements of the engine in the design stage. The valves that regulate feed of the basic fuel components normally have large flow-section areas because of the high flow rates involved and therefore require rather large working loads. To produce these loads, for example, when solenoid valves are used, it is necessary to beef up the valves and

increase their consumption of electricity. Since there is usually a high-pressure gas source in the ZhRD, pneumatically operated valves may also be used. Only the valves feeding the working gas must be of small dimensions; they may be of the piston or aneroid type.

When the ZhRD is fired, the fuel components must enter the engine's combustion chamber either together or in a definite sequence. Duplex valves, which consist of two valves and are opened by a third air-operated valve working through a cross shaft that is set up to open one valve earlier than the other.

In controllable-thrust ZhRD, it is also necessary to have special monitoring valves to throttle the fuel-component flows. Such valves may turn out to be extremely complex in design, as in the case of the rotating slide valve with balancing system (German Walter engine).

The number of different types of valves and other control units usually increases in cases where engine thrust and fuel-mixture ratio are automatically controlled.

The diameters of the pipelines for the ZhRD's fuel-feed system are selected on the basis of the permissible flow velocity of the components in them. The fluid-flow velocity in the engine's pipelines is normally set at 6-10 m/sec. It is not advisable to raise the velocity above 10 m/sec because the hydraulic resistance in the pipelines, which is proportional to the square of velocity, will be very high, i.e., will cause large hydraulic losses. It is also undesirable to lower the velocity below 6 m/sec, since the result is larger pipeline diameters.

The pipeline elements of the engine are usually connected with nipples or flanges (in accordance with the diameter of the pipeline and the pressure in it). For small diameters (less than 25 mm), the nipple-type pipeline joint is most commonly used.

For large pipeline sections (pipe diameters of the order of 100 mm), the tubing elements are connected by means of bellows. Connections of this type make it easy to compensate for manufacturing imprecision, as well as for temperature elongations of the pipes and machine components. Flanges are used to connect two sections of pipe with the throttling disk or diaphragm inserted between them.

When hypergolic fuel components are used, the combustible and oxidizer lines should be passed through different ducts of the missile to avoid fire. For the same reasons, the fueling and drainage accesses to the component tanks should be separated by a great distance.

The electrical equipment of the system may consist of power sources (batteries), the appliances (the electric heaters for the initiating fuel components, etc.), communication apparatus, and a cable network.

Fuel-feed and control-system designs for ZhRD having different missions are discussed and their operation described in detail in the book by G.B. Sinyarev and M.V. Dobrovol'skiy, "Zhidkostnyye raketnyye dvigateli" (Liquid-Fuel Rocket Engines), Oborongiz, 1957.

SECTION 13. HYDRAULIC CALCULATIONS FOR ZhRD FUEL-FEED SYSTEM

By hydraulic calculation of a ZhRD fuel-feed system we mean determination of the pressure drop in the moving fluid (fuel components, gas, etc.) in the engine's plumbing as a result of fluid viscosity, friction, and local drag.

Exact determination of the hydraulic losses becomes possible only after the sketch design of the ZhRD has been completed, at which point the method to be used in cooling the chamber and the fuel-feed system have been selected and the dimensions and shape of the pipelines are known, as well as the type and number of valves and other elements in the fuel-feed and engine-control system.

The fluid-pressure drop in the engine's main pipelines depends on the nature of its motion. The motion of a fluid in a given section of pipeline may be either laminar or turbulent.

The nature of fluid motion in the channel is determined from the familiar formula for the Reynolds number:

$$Re = \frac{w d_{ek}}{\nu} = \frac{w \gamma d_{ek}}{\eta g} = \frac{G}{F} \frac{d_{ek}}{\eta g} = \frac{4G}{\Pi \eta g}, *$$

where d_{ek} is the equivalent (hydraulic) diameter of the channel, as determined by the formula

$$d_{ek} = \frac{4F}{\Pi} \text{ m};$$

F is the cross-sectional area of this channel in m^2 , G is the flow rate of the coolant through the same channel in kg/sec , w [m/sec], η [kg-sec/m^2], ν [m^2/sec], and γ [kg/m^3] are the average values of the corresponding velocity of motion, coefficients of dynamic and kinematic viscosity, and the specific gravity of the liquid, g is the acceleration of gravity in m/sec^2 , and Π is the perimeter of the channel at which the fluid friction occurs, in meters.

For $Re_{kr} < 2300$ (for smooth channels), the motion of the fluid is laminar, but it is turbulent for $Re_{kr} > 2300$. Re is smaller for rough-walled channels than for smooth channels.

The total pressure drop in a given fuel component in the engine's fuel-feed system is expressed by the formula

$$\Delta p = \sum \Delta p_{tp} + \sum \Delta p_{u.c} + \sum \Delta p_{ck} ** \quad (10.87)$$

where $\Delta p_{tp} = \xi_{tr} \frac{l}{d_{ek}} \frac{w^2}{2g}$ [kg/m^2] is the fluid-pressure loss in the channel on the straight segment in question; here, l is the length of this channel in meters and ξ_{tr} is the coefficient of fluid friction on the

*[Subscript: $ek = ek = \text{ekivalentnyy} = \text{equivalent}$; $\Pi = P = \text{Perimeter}$.]
 **[Subscripts: $tp = tr = \text{treniye} = \text{friction}$; $u.c = m.s = \text{mestnoye soprotivleniye} = \text{local resistance}$; $ck = sk = \text{skorost' = velocity}$.]

wall of the channel for a fluid moving with a velocity of w m/sec, which is determined as a function of the nature of fluid flow using the familiar formulas of the hydraulics curriculum, $\Delta p_{\text{tr}} = \xi_{\text{tr}} \frac{\rho w^2}{2g}$ is the fluid-pressure loss resulting from local resistances in the engine's main pipelines (abrupt expansion and constriction of the channels, elbows, branch points, valves, throttling disks, etc.); here, ξ_{tr} is the local-resistance coefficient, which is determined by the appropriate formulas or taken from the tables usually included in hydraulics textbooks and in the special handbooks, and $\Delta p_{\text{ex}} = \frac{\rho w_2^2 - \rho w_1^2}{2g}$ is the drop in fluid pressure in the channel as a result of the increase in its velocity.

In exact calculations, it is also necessary to take into account the buoyant force that arises in the fluid when it is heated.

Fluid-pressure drops may occur in the ZhRD on the segments

- 1) of the engine-chamber cooling passage;
- 2) of the fuel injectors;
- 3) of the pipelines with their fittings.

The fluid-pressure loss in the engine's coolant passages is usually determined as the sum of the resistances of the individual segments into which the chamber was subdivided in determining the specific heat flows. The theoretical parameters for each of these segments are assumed equal to those for the middle of the segment and constant over its entire length.

The formulas for determining Re and d_{ek} may be reduced to the following forms (see Fig. 9.8) for different cooling-passage shapes of the engine chamber:

- 1) in the case of a smooth-walled annular passage (assuming $d_{sr} = d_{zh}$ by virtue of the small gap δ_{zh}):

$$Re = \frac{4G}{\pi \eta g} = \frac{4G}{2\pi \eta g} \quad \text{and} \quad d_{ek} = \frac{4F}{\pi} = \frac{4\pi d_{zh}^2}{2\pi d_{zh}} = 2d_{zh};$$

2) in the cases of the annular passage with longitudinal ribs and the spiral passage

$$Re = \frac{4G_1}{\pi_1 \eta_g} = \frac{4G_1}{2(a+b)\eta_g} \text{ and } d_{\text{eq}} = \frac{4F_1}{\pi_1} = \frac{4ab}{2(a+b)} = \frac{2ab}{a+b},$$

where $G_1 = G/i$ is the coolant flow rate through the i^{th} channel, $F_1 = ab$ is the cross-sectional area of the i^{th} channel, and $P = 2(a+b)$ is the perimeter of this channel.

The hydraulic resistance of the entire cooling passage of chambers with spiral and longitudinal ribs is equal to the hydraulic resistance of some single i^{th} channel.

The coefficient of fluid friction in a spiral channel of the chamber's cooling jacket is determined by the formula*

$$\xi_{\text{sp},s} = \xi_{\text{sp}}, \quad **$$

where β is a correction factor computed from the formula

$$\beta = 1 + 3,5 \frac{d_{\text{sp}}}{d_s};$$

here, d_v is the average diameter of the spiral line of the i^{th} channel.

The length of the cooling-passage spiral channel in a given segment of the chamber is determined by the formula

$$l_s = \frac{l}{\sin \varphi_{\text{sp}}},$$

where l is the length of the passage segment in question and φ_{sp} is the average inclination of the helical line on this segment of the chamber.

The fluid-pressure loss in the chamber's cooling passage is composed basically of the frictional loss $\Delta p_{\text{tr.okhl}}$ and the losses

*G.B. Sinyarev and M.V. Dobrovolskiy. Zhidkostnyye raketnyye divigateli (Liquid-Fuel Rocket Engines), Oborongiz, 1957.

**[Subscript: s = v = vintovaya liniya = spiral line.]

$\Delta p_{m.s.okhl}$ resulting from local resistances, i.e.,*

$$\Delta p_{oxl} = \Delta p_{tp.oxl} + \Delta p_{m.c.oxl}. \quad (10.88)$$

Normally, $\Delta p_{m.s.okhl}$ is much smaller than $\Delta p_{tr.okhl}$, but the first of these losses may attain a considerable magnitude in certain chamber-cooling passage designs and even exceed the value of the latter.

The total fluid-pressure drop in the cooling passage of a ZhRD chamber may reach $\Delta p_{okhl} \approx 5$ to 20 kg/cm^2 .

The fluid-pressure drop in the engine's injectors is determined from the familiar formula

$$\Delta p_{\phi} = \frac{1}{2g} \left(\frac{G_{\phi}}{F_{\phi}} \right)^2 \text{ kg/m}^2.$$

The fluid (gas)-pressure drop in the engine's plumbing is composed of losses due to fluid friction at the walls and local losses and, as already noted, is determined from the formula and data of the hydraulics handbooks. Here, the local-resistance coefficients are determined as functions of the nature of the barriers on the path of the fluid (gas).

The fluid-pressure loss in the various valve designs is determined by pouring water through the valves.

In contemporary ZhRD, the over-all pressure differences in the individual fuel components in the engine's feed system attain $\Delta p_{s.p} \approx 8$ to 25 kg/cm^2 .

Knowing the value of $\Delta p_{s.p}$, we can establish the feed pressure forcing the fuel components into the engine's combustion chamber and make the strength calculations for the fuel-feed and automatic-control systems of the engine.

*[Subscripts: $tp.oxl = tr.okhl = \text{treniye, okhlazhdayushchiy trakt} =$ = friction, cooling passage; $m.c.oxl = m.s.okhl = \text{mestnoye soprotivleniye, okhlazhdayushchiy trakt} =$ local resistance, cooling passage.]

SECTION 14. TUNING OF ZhRD TO OPERATE AT DESIGN PARAMETERS

A ZhRD is usually adjusted to the specified thrust and optimum fuel mixture ratio in accordance with the system and layout adopted for the fuel feed.

In certain existing engines, the necessary thrust value is established as follows:*

for fuel feed by GAD - by adjusting the spring in the pressure reducer feeding the fuel components from the tanks to the combustion chamber of the engine (this reducer is installed at the compressed-gas bottle of this system); the engine is started by opening a stop valve in front of the reducer and programmed opening of the valves to pass the fuel components into the combustion chamber;

for fuel feed by ZhAD - by adjusting the spring in the pressure reducer feeding the auxiliary fuel components (this reducer is installed at the compressed-gas bottle of the same system); the engine is started by opening a stop valve in front of the reducer and programmed opening of the fuel valves to let the auxiliary fuel components into the gas generator;

for fuel feed by PAD - by adjusting the spring of the excess-pressure release valve in the chamber of the solid-propellant accumulator feeding hot powder gases into the fuel tanks; the engine is set in operation by sparking the PAD powder charge;

for fuel feed by TNA fed by a gas from a monoreactant hydrogen-peroxide gas generator with a liquid catalyst - by adjusting the spring of the pressure reducer feeding the hydrogen peroxide and liquid catalyst from the tanks into a reactor (mixing chamber) mounted at the compressed-gas bottle of the same system; the engine is started by opening a stop valve in front of the reducer and programmed opening

*Jet Propulsion, Vol. 27, No. 6, 1957.

of the gas-generator valves and the valves for the basic fuel components to admit them to the combustion chamber;

for fuel feed by TNA fed by a gas from a monoreactant hydrogen peroxide gas generator with a solid catalyst and pump feed of the peroxide into the reactor — by setting the regulator's turbopump set to the rotary speed that meters the required flow of vapor gas into the pump-set turbine; the engine is started by spinning the turbopump set with powder gases or compressed air from a bottle carried aboard the missile or mounted on the launching pad;

for fuel feed by TNA fed by gas from a bireactant gas generator operating on the basic fuel components — by setting the regulator's turbopump set to a number of rpm's that meters the necessary flow of gases into the pump-set turbine and by calibrating the units of the gas generator's feed system with the object of establishing the necessary fuel-mixture ratio; the engine is started by spinning the turbopump set by the pressure of hot gases from a solid-propellant gas generator or with compressed air from a bottle mounted on board the missile or on the launching pad.

Contemporary ZhRD are usually started by means of a programming mechanism which provides for stopping the countdown and, among other things, automatic stopping of the engine if a malfunction in some individual unit of the system is detected as it is being started.

It is preferable to mount the launching-regime control units for guided missiles on the launching towers, etc., with the object of reducing the weight of the engine.

The ZhRD is tuned for operation at the design fuel-mixture ratio by calibrating the units of the engine's hydraulic systems and by experimental adjustment of the system resistances to compensate for production tolerances.

The magnitudes of the necessary corrections are usually determined from the data obtained in hydraulic testing of the engine with water, with subsequent conversion of the results of these tests to the equivalent differences for the fuel components.

These operations are commonly known as tuning the engine to optimum operating parameters (technical adjustment of the engine).

The magnitudes of the hydraulic resistances in the combustible and oxidizer main pipelines can be varied by varying the flow sections of the throttling disks to obtain the required pressures, per-second flow rates, and proportions between the fuel components entering the engine chamber as they apply to the fuel-feed system, etc.

The tuning equation is written to apply to the specific engine design. The corrections to be applied to the initial pressure-loss values for the flow disks are usually determined from special diagrams which give the corrections as functions of the corresponding parameters. The diameters of the flow disks are also determined from special diagrams as functions of the pressure gradient required. The numerical values of the coefficients appearing in the tuning equation are computed on the basis of the calculations used to determine the influence of the corresponding units of the engine on thrust and fuel-mixture ratio.

The principle of tuning a TNA-fed engine consists in compensating any deviations of the hydraulic parameters characterizing the operation of the turbopump set and the constant-pressure valve from the rated values by varying the flow-disk resistances in the main pipelines of the fuel system. Specifically, by varying the dimensions of the flow disks in the fuel-pump lines, we may vary the feed pressure, output, and required power, and thereby attain steady operation of the TNA for the specified adjustment of the constant-pressure

valve passing the excess of vapor gas around the turbine into the exhaust pipe of the gas generator.

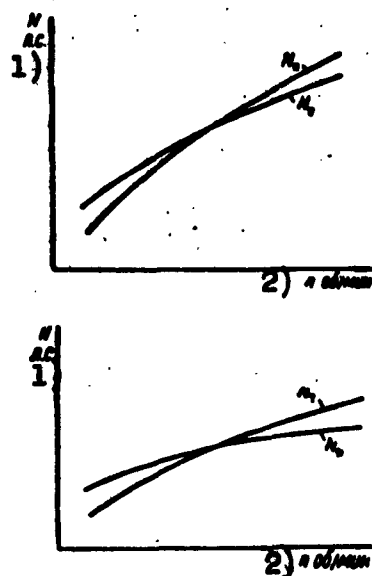


Fig. 10.31. Diagrams of functions $N_n = f(n)$ and $N_t = f(n)$ corresponding to stable and unstable operation of ZhRD turbopump installation.
1) N , horsepower; 2) n , rpm.

Diagrams showing pump power as a function of the diameters d_1 and d_2 of the throttling disks, i.e., $N_n = f(d_1, d_2)$ are usually constructed for this purpose.

For specified pump outputs and feed pressures, the number of TNA rpm's is usually selected on the basis of the intersect of the curves showing the powers as functions of the number of rpm's n of the pumps and turbine, i.e., $N = f(n)$.

The operation of the TNA may be either stable or unstable in accordance with the form of these characteristics (Fig. 10.31).

If stable TNA operation is achieved with the required pump output, i.e., $N_n = N_t$, an accidental increase in the TNA speed over the specified value will result in the pump power N_n becoming larger than the turbine power N_t , and acceleration of the TNA will be impossible. When n accidentally drops below the specified value, the pump power N_n will be found smaller than the turbine power and it will be impossible to stop the TNA.

If, however, the operation of the TNA is unstable, i.e., $N_n \neq N_t$, an accidental increase in the rotary speed n over the specified value will result in N_t becoming larger than N_n and the TNA will run wild, while an accidental decrease in n results in the value

of N_n becoming larger than N_t , and the TNA will stop.

Consequently, tuning of a TNA-fed engine is carried out on the basis of the torques — the active moment of the turbine and the hydraulic resistance of the fuel pumps. Here, the necessary calculations are simplified, the data for a two-component engine design are replaced by single-component data, the fluids and gases are regarded as ideal, and the design of the engine as absolutely rigid.

All working equations are normally retained as they apply to the design operating regime of the engine. In cases where there is a constant-pressure regulator in the fuel-feed system, the calculations are made after the Bernoulli equation for nonsteady flow and the mass-balance and moment-of-momentum equations.

Here, the instability of the engine's operation that results from combustion of the fuel in the combustion chamber (dynamic operating instability of the engine) is not usually considered, since full analysis of this phenomenon encounters great difficulty.

An engine that has been tuned to an optimum stable operating regime by the use of throttling disks or other elements in the fuel-feed system will operate in this regime only provided that the per-second flow rates of the fuel components into the engine chamber and their parameters (pressure, temperature, mixture ratio, etc.) are constant.

Under flight conditions, the characteristics of an engine tuned in static tests will differ from the design values due to a number of factors that influence the engine's working parameters (feed pressure and per-second flow rates of fuel components into chamber, etc.) in one way or another (see Section 11 of Chapter IV).

Under flight conditions, these deviations of the engine's basic characteristics from the nominal values may significantly influence

the flight characteristics of the system (velocity at the end of the powered segment, flight range, etc.).

A precise and complex automatic control system is required for the engine to ensure small spreads in the basic characteristics of the engine during flight (to maintain the necessary operating regime or vary it in a defined manner) and improve the flight characteristics of the missile. For example, the influence of the difference between the inertial pressures of the fuel components on the mixture ratio during flight may be reduced by installing a special automatic choke valve in the main oxidizer line; if the system is TNA-fed, it may be found expedient to use a bypass valve instead of the choke.

SECTION 15. COMPARISON OF DIFFERENT ZhRD FUEL-FEED-SYSTEM LAYOUTS

One of the most complex problems in designing a ZhRD for a specified mission is proper selection of the fuel-feed system layout.

In the majority of cases, the heaviest part of the engine is its fuel-feed system, which, together with its automatic controls, governs the starting and stopping conditions for the engine. All other things equal, the lower the weight of the engine's fuel-feed system, the greater will be the flight range of a missile equipped with this engine.

The fuel-feed system of a ZhRD is normally selected after comparison of various systems as they influence the missile's characteristics, and primarily with respect to weight and operating economy, with secondary emphasis on design complexity and cost.

Figure 10.12 presents comparative curves showing the specific weights of various pressure-fed fuel systems, from which the advantages of systems with PAD and ZhAD hot-gas accumulators, which have specific weights 20-30% lower than systems with ordinary VAD-1 (without preheating of the air before delivery into the fuel tanks)

will be evident. The VAD-2-fitted pressure-fed system (with pre-heated air) occupies an intermediate position between the two hot-gas fuel-feed systems.

The different turbopump-fed fuel-feed systems differ from one another basically in economy, which depends on the thermodynamic parameters of the vapor gas used in the turbine, and in slight differences in design complexity and cost. Comparison will show the distinct advantage of high-temperature vapor gas, particularly when it is burned further behind the turbine.

The various fuel-feed-system layouts can also be compared as regards the ratio of the fuel-feed system's weight $G_{s.p}$ to the absolute engine thrust P , i.e., as regards the so-called specific weight of the feed system with respect to engine thrust:

$$\gamma_{c.s} = \frac{G_{c.s}}{P} \text{ kg/kg}, \quad (10.89)$$

Here, the weight of the turbopump-fed fuel-feed system can be determined approximately by the formula

$$G_{c.s} = G_{TNA} + G_{GG} + G_B, \quad (10.90)$$

where G_{TNA} is the weight of the turbopump set, $G_{GG} \approx 12\%$ of G_{TNA} is the weight of the gas generator, and $G_B \approx 7\%$ of G_t is the weight of the fuel tanks (G_t is the weight of the fuel in the tanks).

The weight of a pressure-fed fuel-feed system with the appropriate pressure accumulator can be computed by the formula

$$G_{c.s} = \gamma_{c.s} V_B \approx \gamma_{c.s} \frac{G_t}{\gamma_t} \text{ kg}, * \quad (10.91)$$

where $\gamma_{s.p}$ is the specific weight of the fuel-feed system in kg/liter, V_B is the fuel-tank capacity of this system in liters, and G_t and γ_t are the weight of the fuel in the tanks and its specific gravity,

*[Subscripts: c.n = s.p = sistema podachi = feed system; B = B = Bak = Tank; t = t = toplivo = fuel; pod = pod = podushka = cushion.]

respectively, and ξ_{pod} is a coefficient taking into account the volume of the air cushion in the tanks.

The above formulas indicate that the specific weight of the fuel system depends basically on the thrust and operating time of the engine. When the engine's operating time is lengthened, the specific weight of all fuel-feed systems increases almost linearly, with the most rapid increase in $\gamma_{s.p}$ shown by the VAD-1-equipped system and the slowest by the TNA-equipped system. When the engine thrust increases, the specific weight $\gamma_{s.p}$ of pressure-fed systems increases slightly, while that of the turbopump-fed system drops by a considerable margin.

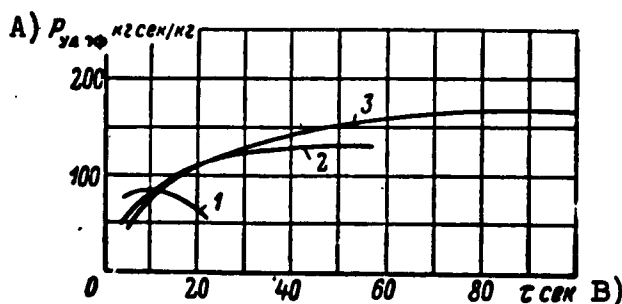


Fig. 10.32. Effective specific thrust of engine as function of operating time. 1) Solid-propellant engine; 2) ZhRD with gas-bottle fuel-feed system; 3) ZhRD with turbopump-fed fuel system.

A) $P_{ud.ef}$, kg-sec/kg; B) τ , sec.

Comparison of the curves of Fig. 10.12 [sic] shows that the best weight characteristics for engines with short flight times (less than 10 sec) are conferred by pressure-fed systems with hot-gas pressure accumulators. For medium-thrust engines with rather long operating times, the weight advantage clearly lies with the turbopump system.

However, purely relative comparison of fuel-feed systems as regards their weight characteristics alone is inadequate, since it does not take into account the differing operating economies of these

systems. Moreover, the weight and economy indices of the fuel-feed system influence the characteristics of missiles with different thrusts and missions in different ways. For this reason, the formula for determining the flight velocity V_{kon} (or the range L corresponding to it) at the end of its powered path may be used as the basic parameter for comparison of different ZhRD fuel-feed systems.

J. Humphries* recommends comparison of the different ZhRD fuel-feed systems on the basis of the so-called "effective specific thrust," which is defined by the formula

$$P_{y\lambda\phi} = \frac{P_{\tau_{dv}}}{G_t + G_{dv}} \text{ kg of thrust / sec, **}$$

where P is the average thrust of the engine during an operating period τ_{dv} , in sec, G_t is the weight of fuel in the tanks, and G_{dv} is the dry weight of the engine, including the tanks and the working fluids (fuel, gases, etc.).

The curves in Fig. 10.32 give a general idea as to which fuel-feed system will be most conveniently used to produce the maximum effective specific engine thrust.

These curves have reference to an engine with a surface thrust of 2270 kg, but they may be useful for preliminary analysis of fuel-feed systems. The curve for a solid-propellant engine is presented for comparison.

It will be seen from Fig. 10.32 that a given engine operating on liquid fuel possesses superior performance from the standpoint of effective specific thrust when compared to a solid-propellant engine with operating times of the order of 10 sec and higher. Moreover, ZhRD with gas-bottle fuel-feed systems have better $P_{ud.ef}$ char-

*J. Humphries. *Raketnyye dvigateli i upravlyayemye snaryady* (Rocket engines and guided missiles), IL, 1958.

**[Subscripts: $y\lambda\phi$ = $ud.ef$ = $udel'nyy$, $effektivnyy$ = specific effective; dv = $dvigatel'$ = engine.]

acteristics than ZhRD with turbopump systems for operating times of 10-20 sec; for longer engine operating times, it is more expedient to use the turbopump-fed fuel system.

In solving this problem, however, it should not be forgotten that TNA-equipped ZhRD are complex in design, so that this feed system is more expensive than the pressure-fed system; moreover, a working fluid is required to drive the turbine, and to obtain this fluid it is usually necessary to have a gas-generator apparatus or some other facility. For this reason, the possibility of using the pressure-fed fuel system is not excluded, in spite of the fact that in this case the turbopump feed system may endow the engine with a relatively higher effective specific thrust.

Taking the above exposition into account, we may draw the following conclusions:

- 1) the use of the turbopump fuel-feed system is most attractive for ZhRD with total impulses above 250-270 thousand kg-sec;
- 2) for long-range missiles (SDD*), the turbopump fuel-feed system is most efficient;
- 3) for missiles with low thrusts but large payloads (for ZURS†*), the best results are given by PAD- and ZhAD-equipped pressure-fed fuel-feed systems;
- 4) in aircraft ZhRD, pump feed of the propellants is more attractive, since it results in a lower total engine weight than gas-bottle feed. If the ZhRD is being designed as an aircraft super-performance unit, the pumps may be driven through a gearbox off a main aircraft engine of another type.

In working out the layout for the engine's fuel-feed system and

*СДМ = SDD = Snaryad Dal'nego Deystviya = Long-Range Missile.]

**ЗУРС = ZURS = Zenitnyy Upravlyayemyy Raketnyy Snaryad = Guided Antiaircraft Rocket Missile.]

its control, it is necessary to select:

- 1) the elements of the fuel-feed system and their adaptation to the engine being designed;
- 2) the locations of the fuel-tank and gas-bottle connections for loading the system with fuel components and other working fluids, as well as the stop-flow, safety, and other units for the fueling lines;
- 3) the points of connection of the lines for air bleeding and the stop-flow and other units in the drainage mains;
- 4) devices to prevent admission of fuel components from the tanks into the combustion chamber before the engine is fired;
- 5) units to ensure dependable firing, normal operation, and stopping of the engine (also including the fuel-ignition system) and their placement;
- 6) the method and sequence (program) of operation for the units of the engine's starting and stopping system, as well as the energy source to operate them;
- 7) elements to be used in tuning the engine to the specified operating regime, and their operating principles;
- 8) automatic-control units of the fuel-feed system for metering delivery of the working fluid (fuel components, gas) in starting, for normal operation of the engine, and for control of its operating regime in accordance with a specified program;
- 9) the automatic-blocking system for the engine's fuel feed, its elements, and the location and method of its installation.

The number of elements in the system being designed must be as small as possible in order to improve its operating dependability and lower the cost of the engine.

Chapter XI

STABLE AND UNSTABLE ZhRD REGIMES AND AUTOMATIC OPERATING CONTROL

One of the most important problems arising in the planning of a ZhRD, regardless of type and designation, is the matter of providing for operating stability in given regimes, and the dissemination of the conditions under which the engine can work with dynamic stability, even with the action of unavoidable perturbations and variable control-system commands.

The planning of a stably functioning ZhRD calls for the design of an engine in which the fluctuations in gas pressure in the combustion chamber, the per-second fuel-component flow rates to the chamber, and the thrust, caused by the perturbations, will not exceed the permissible limits.

The mechanism to which unstable ZhRD operation may be attributed is extremely complex and therefore, as yet, little studied.

In order to increase the dynamic stability of the ZhRD, various structural and similar measures are employed, and one of these is automatic control.

The development of a control system for the ZhRD can only succeed if the factors responsible for nonstable engine operations and the theoretical bases of control are fully known.

The present chapter cites the basic factors responsible for nonstable ZhRD operations, and there is an examination of the measures

for controlling these factors, and these measures may prove to be of practical interest in the design of stably functioning systems; in addition, there is an examination of the methods involved in experimental investigation of stability, said methods useful in the development and adjustment of new engines and their individual assembly. Moreover, the basic principles of automatic control of liquid-rocket engines are discussed.

SECTION 1. STABLE AND NONSTABLE ZhRD OPERATING REGIMES

The records of gas pressures within the combustion chamber and in the fuel components in front of the spray nozzles, in the case of the steady-state functioning of the ZhRD, indicate that there are always gas-pressure oscillations occurring within the combustion chamber, said oscillations having various frequencies and amplitudes which change with a change in the operating regime of the engine. This circumstance indicates that the operating regime of a ZhRD, regardless of type and design, is not at all stable and periodically varies with respect to time as a result of a series of perturbation factors inherent in the engine cycle.

A detailed analysis of the cycles within contemporary engines makes it possible to draw the conclusion that the basic factor responsible for ZhRD operating-regime fluctuations is the delay in converting the liquid fuel components into gaseous products, and this [delay] is of the order of the fuel-component stay time within the combustion chamber, since it is precisely during this period that the fuel is consumed.

Should excess gas pressure develop in the combustion chamber, for any reason whatsoever, at the instant τ , the per-second rate G_s of fuel flow through the spray nozzles (Fig. 11.1) will diminish correspondingly, and the gas-flow rate from the combustion chamber

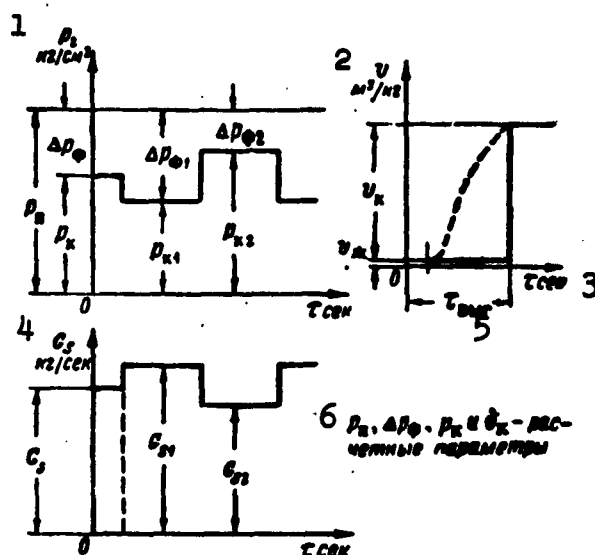


Fig. 11.1. Oscillations in pressure p_k in the combustion chamber and in the per-second fuel flow rate G_s (the feed pressure p_p is assumed to be constant).
 1) p_2 , kg/cm²; 2) v , m³/kg; 3) τ_{sec} ;
 4) G_s , kg/sec; 5) τ_{useful} ; 6) p_p , Δp_f , p_k and v_k are design parameters.

through the nozzle will increase. Since the actual volume of the liquid components is negligibly small relative to the actual volume of the gases, this change in fuel-flow rate leads to a drop in the inflow of gases only at the instant of time $\tau + \tau_{\text{zap}}^*$, where τ_{zap}^* is the delay time. At this instant, the pressure within the combustion chamber may drop, and this will also lead to a pressure rise at $\tau + 2\tau_{\text{zap}}$.

Consequently, a change in pressure p_k leads to a change in the flow rate G_s which, in turn, has an effect on the magnitude of p_k . As a result, this interrelationship leads to fluctuations in these two parameters. If the fluctuations in these parameters tend to damp out, the engine operation will be stable, whereas if they increase with respect to time the operation of the engine will be unstable.
 * [$\tau_{\text{zap}} = \tau_{\text{zap}} = \tau_{\text{zapazdyvaniye}} = \tau_{\text{delay}}$.]

The further the cycle takes place from the boundary (threshold) of instability, the more rapidly will these fluctuations be damped. The instability boundary for engine operation is characterized by a rapid increase in oscillation amplitude, frequently accompanied by pronounced changes in frequency.

In fact, the processes taking place within the combustion chamber of a ZhRD are substantially more complex than in the primitive diagram presented here. Unstable engine operation is possible even in the case of an ideal fuel-feed system which does not react at all to a change in gas pressure within the combustion chamber.

We are dealing here with the fact that the time during which the fuel-component drops are converted into the products of combustion depends on the pressure within the combustion chamber, the temperature of the gases within which these drops move, as well as a series of similar factors, such as:

- 1) the presence of foci of vapor formation and fuel-component combustion (random and sudden flashes of combustion caused by the basic atomization head of the engine chamber) distributed throughout the volume of the combustion chamber, and as a result there are deviations from the mean in the gas pressure within the chamber;

- 2) an increase or decrease in the flow rate of the fuel components to the chamber and their ignition lag as a result of the gas-pressure fluctuations within the combustion chamber as well as the resulting regular increased and decreased fuel-component pressure differences across the spray nozzles and, consequently, impairment of the atomization quality for the fuel components;

- 3) the unavoidable changes in the fuel-composition factor resulting in a temperature change for the combustion-chamber cross section, and the resulting change in the ignition-lag time period;

4) the hydraulic fluctuations within the fuel-feed system, caused by the following: the changing fuel-component pressure difference across the nozzles, pump pulsations, nonrigid elements in the system, pulses, gas bubbles, friction in the elements of the automatic-control system, and other factors.

Instability, in some measure, may appear in engines operating on any practically conceivable fuel components. The use of certain fuels is still so limited that it is not possible, in practice, to design a stable engine to operate on these fuels (for example, kerosene and liquid oxygen).

With an unstable operating regime, there is a pronounced impairment of the engine characteristics, and the elements of the engine are subject to dangerous static and thermal loads. In the case of unstable fuel combustion, the gas pressure within the combustion chamber, at individual instants of time, may exceed the rated value by a factor of 2 to 3, as a result of which there is the possibility of the explosion of the engine chamber.

In the case of gas-pressure fluctuations in the chamber, the transfer of heat from the gases to the chamber liners may be greater by a factor of 1.5 to 2.5 than would be the case with stable engine operation, and in this connection the overheating and burning out of the chamber liner becomes possible and, consequently, engine breakdown. In addition, the gas-pressure fluctuation in the combustion chamber leads to pulsations in exhaust velocity, i.e., engine thrust, and this leads to engine vibrations which can break the fastening devices by which the engine is connected to the missile, and it can also lead to the disruption of the tubing, etc.

A fluctuation in engine thrust may lead to missile vibrations, including the tanks containing the working components and the supply

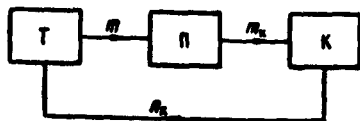


Fig. 11.2. The simplest structural diagram of a ZhRD with a single-loop closed circuit. $n_k = (p_k - p_{kl})/p_k$ is the pressure fluctuation within the combustion chamber (the output coordinate of the link K); $m = (G_s - G_{sl})/G_s$ is the fluctuation in the fuel-flow rate as a result of the pressure fluctuations within the combustion chamber (acts on link P); $m_k = (G_k - G_{kl})/G_k$ is the fluctuation in the gas-formation rate in the combustion chamber because of the changes in the fuel-flow rate (this is the input coordinate of the closure link K).

tubing, and this will have an effect on the process of fuel combustion within the chamber and on the functioning of the missile-flight-control instruments. Consequently, the mounting of an unstable engine on the flying craft cannot be permitted.

The capacity of a ZhRD to self-excitation of vibrations can, primarily, be attributed to the sensitivity of the fuel-feed system to pressure changes in the combustion chamber, resulting from a time shift between the inflow of the liquid fuel components to the chamber and the

process of converting the fuel components to gaseous products of combustion (the rate of fuel flow through the spray nozzles is a function of the gas-pressure pulsations within the combustion chamber). Consequently, a ZhRD (with respect to design and principle of operation) is a self-oscillation system with a delay link (closed loops exist between the combustion chamber and the fuel-feed system).

The structural diagram of the ZhRD takes the form, in the simplest case, of a single-loop closed circuit consisting of three links (Fig. 11.2).

The links, denoted by \underline{T} , \underline{P} , and \underline{K} , respectively, represent the fuel-feed system, the process of converting the fuel into the products of combustion, and the combustion chamber as the gas volume.

The rate of fuel feed to the combustion chamber, the rate of gas formation, and the pressure in the combustion chamber are taken

as the input and output variable links. Feedback reflects the action of pressure within the chamber on the feed rate for the liquid fuel components.

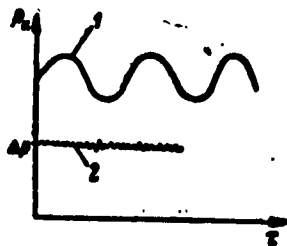


Fig. 11.3. Low-frequency (1) and high-frequency (2) gas-pressure oscillations within the combustion chamber of the engine.

Investigations have shown that during the operation of a ZhRD, gas-pressure fluctuations within the combustion chamber may be of the following types (Fig. 11.3):

low-frequency (from 30 to 50 up to 180 to 220 cps), resulting from the delay between the processes of

fuel-component inflow to the combustion chamber and the instants of their combustion (pressure oscillations with the natural frequency of the fuel-combustion process);

high-frequency (from 600 to 1200 cps and higher) representing resonance (acoustic) oscillations down the combustion chamber in the gas with which the chamber is filled;

detonation (unstable), arising the instant the engine is started; this type of fluctuation has not yet been thoroughly studied.

Not a single unstable ZhRD type exists in its pure form. Generally, during engine operation there are gas-pressure fluctuations of various types.

All types of oscillation frequencies and amplitudes depend, to some degree, on:

1) the design and parameters of engine head and chamber, combustion-chamber shape, and the relationships between their geometric dimensions;

2) the design and parameters of the fuel-feed system and the auxiliary engine elements;

- 3) precision of engine fabrication and interaction of all engine elements;
- 4) chemical and physical properties of fuel components;
- 5) design and parameters of weapon, as well as its flight conditions;
- 6) engine-operating regime and other factors.

The system consisting of the gases within the combustion chamber, and the fuel within the feed system, as well as the mechanical parts of the entire engine, tend to unstable operation even when the fuel-combustion process is completely stable. Such processes as gas fluctuations within the combustion chamber and liquid fluctuations within the fuel-feed system or the vibrations of the mechanical parts of the engine may occur even in the presence of extremely small perturbations.

Experiments indicate that pressure and fuel-component rate oscillations in the supply tubes of the engine exhibit this same frequency as the pressure oscillations in the combustion chamber, but the amplitude is smaller. The laws governing the conversion of the fuel into gaseous products of combustion, both with respect to time and, in space, with respect to the volume of the combustion chamber, play an important role in the mechanism of unstable ZhRD operation.

Low-frequency instability predominates in those cases in which the ZhRD functions with small pressure differences for the fuel-component spray and with low pressures within the combustion chamber. At relatively high gas pressures within the combustion chamber, high-frequency forms of acoustic oscillations (which in certain cases may be dominant) can develop simultaneously with the low-frequency oscillations.

The high-frequency stability of the ZhRD is characterized by the

presence of gas compression waves that move periodically along the combustion chamber, from the head to the nozzle, and back.

The physicochemical processes occurring within the combustion chamber during the delay time develop at rates which are affected by the pressure and temperature of the gases and liquids, their relative flow rates through the length of the chamber, etc.

With changes in the above-mentioned factors, there are also changes in these rates, and at the same time, there are changes in the delay time; high rates lead to short delay time.

The fluctuation of the above-mentioned factors about their mean values produce fluctuations in the delay time of the corresponding volumes (particles) of fuel. If, for example, the delay time increases at a particular point in the chamber, this will extend the process with respect to time and space, i.e., lead to the reduction of the fuel-combustion rate. On the other hand, the fuel-combustion rate increases if the delay time is shortened. Consequently, changes in the factors affecting the rate at which the physicochemical processes occur within the combustion chamber produce a change in the fuel-combustion rate or fluctuations in the power of the hot-gas source, even with a constant rate of fuel-component spray into the combustion chamber.

As a result, periodic longitudinal pressure pulses (compression waves) may arise within the combustion chamber, from the head to the nozzle, and back. If these pulses attain high values, self-intensification self-oscillation conditions are established, longitudinal shock waves of relatively greater amplitude appear, and here the operation of the engine chamber becomes unstable.

The cycle period for these fluctuations is approximately equal to the conversion delay time, the time required for the distribution

of temperatures from the front of the flame, and the pressure-pulse propagation time from the head to the nozzle and back.

Acoustic gas-pressure oscillations within the combustion chamber of the engine are capable of establishing lateral acoustic velocities for the atomized fuel-component particles and thus to affect their intermixing; the jets of fuel vapors undergo sinusoidal deformation. Given sufficiently great deformation of these jets, the concentration of heat or mass within them is changed, and this leads to marked periodic variations in the local coefficients of excess oxidizer throughout the entire mixing zone, with all of the consequences that follow from this.

Longitudinal self-oscillation in the combustion chamber of the engine, under certain conditions, may result in local overheating and burning out of the chamber flame tube.

Instability of engine operations may be the result of such processes as the propagation of eddies in space at certain frequencies, fluctuations in liquid flows through the spray nozzles and in the atomization of two impinging jets, combustion phenomena within the eddies, fluctuations resulting from chemical kinetics, the conversion of the gas stream within the converging part of the nozzle, etc.

All of these processes may be characterized by time constants that are different from relaxation or the period of natural oscillations, and the processes can lead to unstable regimes at frequencies differing from the frequencies characteristic of low-frequency and high-frequency instability.

The problem of ZhRD instability can be reduced to the problem of designing an engine in which, during operation, there are no deviations from the rated values (in excess of the permissible magnitudes) in combustion-chamber pressure, specific flows of heat from

the gases to the chamber liner, and in thrust.

It is only possible to design an engine that functions in a stable manner within the required range of regimes by undertaking a thorough study of the mechanisms involved in the development of unstable pressure fluctuations within the combustion chamber and within the fuel-feed system, and this can, at the present time, be achieved basically through experimentation.

Experiments indicate that an increase in the ignition lag τ_{zad}^* for the fuel components diminishes the oscillation frequency for the gas pressure within the combustion chamber and increases the amplitude of the oscillations (Fig. 11.4). With a rise in combustion-chamber pressure, there is a drop in the conversion delay time for the liquid fuel components to gaseous products, and in this connection the oscillation frequency increases, whereas the amplitude diminishes (Fig. 11.5). The physical processes within the combustion chamber of the engine, during the delay period, are extremely complex and, as of the moment, inadequately studied. The frequency of pressure oscillations also increases with a drop in the reference length of the engine combustion chamber ($l_{\text{pr}} = V_k / F_{\text{kr}}$).

It has been established that spherical and elliptical combustion-chamber shapes are more stable with respect to high frequency oscillations than is the case with cylindrical chambers. An increase in the combustion-chamber fuel-flow rate and a drop in engine thrust by reducing the fuel-flow rate brings the operation of the engine to the boundary of instability. A decrease in the liquid-pressure difference across the spray nozzles also leads to unstable engine operation, this caused by a change in the spray regime and a deterioration of atomization quality.

* $[\tau_{\text{zad}} = \tau_{\text{zad}} = \tau_{\text{zaderzhka}} = \tau_{\text{lag}}]$.

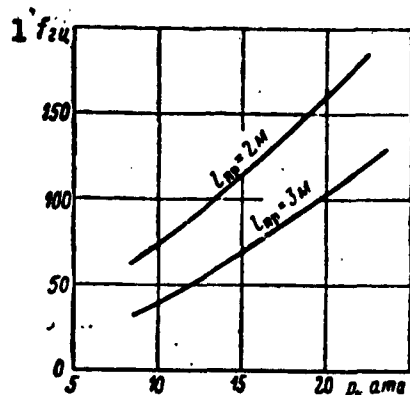


Fig. 11.4. Oscillation frequency as function of combustion-chamber pressure, at $l_{pr} = 2$ and 3 m. 1) f_{cps} .

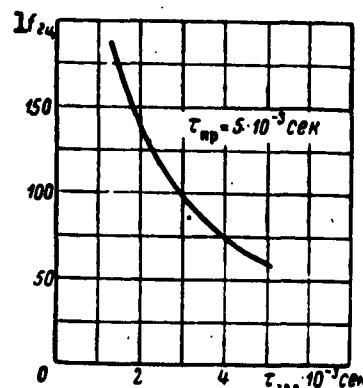


Fig. 11.5. Oscillation frequency as function of fuel-combustion delay time. 1) f_{cps} .

Pressure fluctuations in the combustion chamber may arise from a variety of random factors (effect of design and aerodynamic forces of the missile, etc.).

In the case of improper engine design, the engine having been made without the specific features of the fuel components that are used in the engine having been taken into consideration, fluctuations can attain a destructive force and can even be accompanied by detonation phenomena. Generally, within a wide spectrum of frequencies two to three, and sometimes even four basic frequency oscillations stand out, and these are measured in tens, hundreds, and thousands of cycles per second.

As a missile accelerates in flight, inertial forces act on the feed pressure and may lead to operational engine instability. Missile vibrations may be caused by aerodynamic forces, which, in turn, has a substantial effect on the stability of engine operation. A change in the temperature of the surrounding medium from -50 to $+70^\circ\text{C}$ may affect not only the chemical and physical properties of the fuel, but the operation of certain engine elements as well.

Experiments indicate that in a short combustion chamber the

intensity of longitudinal compression (shock) waves is lower than would be the case in a long chamber. The frequency of these oscillations changes in inverse proportion to the length of the combustion chamber.

The length and the shape of the converging portion of the nozzle also affects the longitudinal stability of engine-chamber operation. A chamber with a long (relative to the combustion chamber) subsonic nozzle portion is more stable than one that is relatively shorter.

The stabilizing effect of the diffuser section of the nozzle depends on the manner in which the waves are reflected from the nozzle to the chamber head. The reflection of the waves at each point is determined by the corresponding velocity gradient. The greater the gradient and frequency, the more dispersed the reflection pattern, and the smaller the probability of resonance and the appearance of instability.

The supersonic outlet section of the nozzle has no arbitrary effect on the processes taking place within the combustion chamber, if that section of the nozzle does not violate the operating conditions within the critical section of the nozzle.

Finally, it should be pointed out that the gas-pressure fluctuations within the combustion chamber variously affect the combustible and oxidizer flow rates within the chamber. This leads to a change in the weight relationships between the components and, consequently, to a change in the delay time (combustion rate), specific rate of heat liberation, as well as gas temperature and pressure, which have a substantial effect on engine operating stability.

In order to eliminate this perturbation factor from engine operation and to reduce its effect, the fuel-feed system can be made with

an automatic fuel-component regulator, in the form of a servomechanism with feedback. Such feed control can be accomplished with one or more feedback loops, although theoretically it would be enough to regulate only the feed of the oxidizer or the combustible. If a fuel-feed system for the engine is selected with only one feedback loop, this should be connected to the oxidizer manifold, since this manifold is more sensitive to the pressure fluctuations within the combustion chamber.

With servo control, the ZhRD can be stable in operation in the low-frequency region, for all values of the delay time. However, it should be borne in mind that this control method for the engine imposes a serious practical problem with reference not only to the mathematical design of the feedback loop but with reference to the regulator circuit which, in the final analysis, converts the amplified electrical signal into mechanical oscillations of sufficient amplitude in the frequency interval being examined.

For stable engine operation it is necessary to implement a series of measures which are frequently associated with a deterioration of other engine characteristics.

It is possible to raise ZhRD operating stability substantially by:

- 1) the use of an expedient design for the atomization head of the engine chamber;
- 2) an increase in the pressure difference across the spray nozzles and an increase in the number of spray nozzles by reducing their capacity, since in this case the sensitivity of the fuel-system to pressure changes within the combustion chamber diminishes;
- 3) increasing the pressure in the combustion chamber, since in this case the vaporization and fuel-combustion processes become more

intense, the delay time in the conversion of the liquid fuel components into the gaseous products of combustion is reduced, and the phase shift between the inflow of the fuel components to the chamber and their combustion narrows, and this results in a greater gas-pressure oscillation frequency in the combustion chamber, and also leads to a reduction in amplitude;

4) a well organized cycle within the combustion chamber through special structural measures (the use of devices augmenting the back-flow of hot gases in the area of the atomization head of the chamber, which reduces the delay time; various types of spray nozzles in a single atomization head, which increases the nonheterogeneity of the delay time for various sizes of fuel-component drops and improves engine operating stability, etc.);

5) a change in combustion-chamber volume by increasing chamber diameter, since a greater chamber volume serves to damp the gas-pressure pulsations during engine operation;

6) an increase in the dimensionless area of the combustion chamber, since, in this case, the area flow rate of the chamber drops, and the preparation processes and conditions for stable fuel combustion improve up to a certain point; in certain contemporary engines, the dimensionless area of the chamber attains $f_k = F_k / F_{kr} = 7.8$, and the reference length l_{pr} of the combustion chamber is 4 meters;

7) the utilization of certain types of combustibles (fuels) [Tonka-250, etc.), which exhibit a small ignition lag and provide for a stable combustion process in the engine with selected oxidizers, whether in the case of throttling, or with augmented engine operation;

8) a decrease in the ignition lag period for the fuel components

by heating them, and using special catalysts;

9) the proper selection of fuel-feed system manifold length and flowthrough sections and the most advantageous installation of this system on the engine;

10) the selection of the type and designs for valves and other elements in the fuel-feed and control system;

11) automatic control of the fuel-mixture ratio as a function of changes in gas pressure in the combustion chamber.

By varying the design of the elements in the fuel-feed system as well as the parameters of these elements (the length and diameter of the tubing, the hydraulic resistance of the units, etc.), it is possible partially to stabilize engine operation and, in case of need, to expand the range over which engine thrust may be varied.

Engine operating stability can also be improved by increasing the speed at which the fuel components are fed to the combustion chamber, and this can be accomplished by reducing the diameters of the tubing.

Not only is the operating characteristic of the regulation element (cock, valve, etc.) important, but its dimensions as well. The valve must be designed so that it is half open during normal engine operations, since an excessively small valve will always be open, whereas an extremely large valve will, for the most part, be closed. Under these conditions, the valves may cause instability in engine operation.

For purposes of controlling the pressure in the combustion chamber or in order to control the fuel-flow rate, it is expedient to use valves with exponential characteristics, since they operate less as functions of the operating conditions (static fluid pressure, flowthrough sections, and lengths of tubing), than do valves with

linear characteristics.

Any measure which leads to the more rapid conversion of the fuel into the products of combustion (reducing the area flow rate, improving atomization conditions for the fuel components, improving the transfer of heat to the atomized drops of these components, using chemically more active components, heating them, and other measures) will serve to stabilize engine operation.

However, it should be borne in mind, that localization or partial reduction of anomalous, at times destructive gas-pressure pulsation forces within the combustion chamber, and detonation phenomena which arise on starting the engine or within large-dimension combustion chambers, by employing structural measures is usually accompanied by increasing the complexity of engine design. An increase in the fuel-component pressure difference across the "plumbing" of the engine, including the spray nozzles, leads to an increase in the capacity and weight of the fuel-feed system.

The development of design methods for ZhRD, these providing for stable operating systems, is an extremely important task, since experimental adjustment of engines is extremely time- and labor-consuming, and requires, in addition, tremendous expenditures.

Of greatest importance is the possibility of carrying out analytical computations for the stability of low-frequency pressure oscillations in the combustion chamber, since these oscillations occur most frequently in the design of new types of engines, and great difficulties are encountered in attempting to control these. The mechanism whereby high-frequency oscillations and shock oscillations arise has, apparently, much in common with the mechanism by which low-frequency oscillations are excited.

SECTION 2. AUTOMATIC REGULATION OF ZhRD OPERATING REGIME

In order to attain certain values of the dependent variable parameters during engine operation under flight conditions (per-second flow rates for combustible and oxidizer, their relationship, pressure in combustion chamber, engine thrust, or change in these according to preset program) and to improve the flight characteristics of the weapon, a complex automatic regulation system is necessary, as are mechanical, hydraulic, and electrical systems, or combinations of these.

In contemporary ZhRD, wide use is made of devices for the automatic regulation of engine thrust, the relationship between fuel components, and extensive use is also made of devices for start preparation, start, engine shutoff, operating safety, etc. Automatic regulation has a stabilizing effect on engine operation.

The most important problem in ZhRD regulation is to provide for timely fuel ignition on starting the engine, and maintaining the combustion of the fuel during the transition regimes from start to rated engine operating regime. Operational reliability during starting for certain ZhRD is still low and does not exceed 80%, whereas their reliability in the operating regime attains 95 to 100%.

Fuel-ignition reliability as the engine is started is achieved most simply by increasing the number of ignition sources, i.e., through the use of a number of grain (powder) igniters, a separate and corresponding supply of hypergolic fuel components or a powerful electric-spark generator. However, in order to prevent a dangerous accumulation of unconsumed fuel within the combustion chamber of the engine, we require the physical and functional consolidation of the system used to spray the fuel components into the combustion chamber with the system used to control the feed of fuel from the devices

which are set to react should the engine fail to function properly. A high reaction rate and the reproducibility of the regulation system action is of great importance.

In the transitional starting regimes it is possible to regulate a ZhRD as a function of time, TNA rpm, or the fuel-component pressure at the pump outlets. The use of the last two parameters is most logical, since this makes it possible directly to act against certain maladjustments in engine operation. Action against such maladjustments as fuel-combustion instability or the breaking off of the flame must be taken independently.

In contemporary ZhRD, the systems used to regulate combustion are based on the use of hydromechanical feedback, reacting to the magnitude of pressure*. Disruption of the combustion process instantly acts on the fuel-feed regulator. Thus, continuous action can be maintained both for the initial ignition process as well as for the subsequent transitional combustion processes.

The next most important problem is the matter of regulating ZhRD thrust. Unlike the system used to regulate the processes of ignition and fuel combustion for which we require reaction to high-frequency oscillations, the thrust-regulation system must be limited to a frequency of 10 cps or less. The purpose of such regulation is the prevention of substantial pressure fluctuations within the combustion chamber of the engine.

The precision with which thrust is regulated depends on the type and designation of the engine. For example, for starter engines and aviation vernier engines which develop fixed thrust there is a permissible range of $\pm 5\%$ for the limit values of fluctuations in regulated thrust. For guided missiles, in some cases, a more precise

*Ekspress-informatsiya AN SSSR, Issues 4 and 7, RT, 1958.

regulation of thrust magnitude and engine shutoff is required.

Thrust, combustion-chamber pressure, feed pressure from one or both fuel components, and the rpm of the turbopump unit serve as feedback for the regulation of ZhRD operation.

For direct measurements of thrust, a complex design for engine suspension and special pickups are needed; all of this equipment is generally too heavy. The selection of the pressure in the combustion chamber for purposes of feedback requires a connection to the hot-gas source in the combustion chamber and does not provide for the direct regulation of the starting transitional regimes. The combustible- or oxidizer-feed pressure provides the required, although indirect, change in pressure within the combustion chamber and can generally be used for purposes of regulation in starter regimes. The TNA rpm is best used as feedback only to balance the capacities of several TNA in a multichamber engine.

At the present time, the complex automatic regulation of the engine operating regime may be justified only for ballistic guided missiles. For missiles of limited range, where design simplicity and low cost are basic requirements, such regulation of ZhRD operation is inefficient.

Automatic regulation of ZhRD operating regime in flight makes it possible:

- 1) to improve the engine characteristics during flight by keeping the regulated parameters constant during operation;
- 2) to raise the economy of engine operation through the use of an optimum fuel-mixture ratio and to increase, as a result of this, the engine operating time through the more complete utilization of the fuel reserves aboard the missile;
- 3) to compensate for lack of fabrication precision in the fuel-

feed system elements and in the adjustment of the engine to the operating regime under static conditions;

4) to raise dynamic stability and engine service life by maintaining normal operating processes in the fuel-feed system and in the combustion chamber throughout the entire time of operation, at all load variations and for all perturbations acting on the missile during flight (acceleration, interruption of smooth functioning of individual units, etc.);

5) to compensate for the scattering of the fuel-feed system characteristics (pumps, pressure reducers, etc.);

6) to simplify operation and increase operational reliability for the engine;

7) to expand the range of stable engine operation with thrust regulation by varying the rate at which the fuel flows into the chamber.

The ZhRD regulation system is similar to other regulation systems in that it represents a definitively combined group of links, and if any link is improperly designed (calculated), the entire system will prove to be ineffective.

Each element within the system must be selected and designed not only from the standpoint of its adaptability for its assigned function, but also from the standpoint of its joint functioning with elastic elements.

Specific physical limitations are imposed on the elements which satisfy the required characteristics. Some links of the system are relatively constant (for example, the fuel manifolds, the combustion chamber, the turbine, the pumps); the parameters for these links are determined by the requirements for a steady-state regime and the conditions of static stability. However, frequently certain param-

eters, even of relatively constant elements, may undergo change within narrow limits. The final determination (fixing) of these parameters must be based on an evaluation of their influence on the characteristics of the entire system. The variable elements of the regulation system must be designed so as to satisfy the transitional characteristics and provide for dynamic stability in the engine.

The object whose operation must be completely or partially regulated automatically is referred to as the regulated object, whereas the individual quantities subject to regulation are referred to as regulated quantities.

The main element in a regulated ZhRD are the following: the combustion chamber, the fuel pumps, the fuel manifold, the turbine, the fuel-flow regulation valves, and the thrust regulator.

The characteristics of the turbine, the pumps, the manifold, and the combustion chamber are, for the most part, given, since their parameters are set by engine thrust, the type of fuel, and materials used.

The basic elements of the regulation system are the regulators. The signal that is sent as a result of a change in a regulated quantity acts on a regulator, and the latter, in turn, acts to change the regulated quantity by means of a regulation element. The link which closes the followup circuit at any point is referred to as main or basic feedback.

Depending on the requirements imposed on the engine cycle, the regulator must maintain the value of the regulated quantity constantly and at a specific preset level or change it, again in accordance with a specific preset program. In the latter case, we have the so-called program regulation.

The object and the regulator form a closed system of automatic

regulation. One or several quantities (parameters) can be controlled (regulated) on the given object.

Automatic regulation systems involving several regulated quantities can be divided into noncoordinated and coordinated regulation systems. Noncoordinated regulation systems are those in which the regulators which serve to regulate various quantities are not inter-coordinated and can interact only through the object common to them. The coordinated regulation systems are those in which the regulators of the various regulated quantities are mutually coordinated, interacting outside of the object being controlled.

The regulation (control) process can be continuous or periodic. The principal technical solution is generally presented in the form of a feedback control system.

In planning, the following basic requirements are imposed on a ZhRD regulation system.

1. A high degree of control with the minimum number of system elements and the minimum expenditure of energy on servicing these elements.
2. High operational reliability for the system as the engine is started, in transitional regimes, and in the rated regime.
3. The devices performing analogous functions, such as the turbopump units, the fuel-component-feed control valves, etc., must have direct mechanical linkage.
4. Since the required power for servicing the control system of a ZhRD may be considerable in view of the presence of large fuel-throttling valves operating at high pressures and great velocities, it is desirable to use the simplest hydromechanical systems for control purposes; the utilization of electric power should be reduced to the minimum, and the use of air as an energy source should

also be restricted in order to eliminate the need or in order to reduce the requirement for high pressure within the flask.

5. In order to reduce the weight of the ZhRD and to simplify its design, auxiliary power systems (pneumatic, electrical, and hydraulic) should be, to the extent possible, excluded from the control system; it is necessary, to the greatest extent possible, to utilize the potentials to be gained through the installation of engine-starting regime regulation units directly on the missile launch pad.

The selection of the ZhRD operating control method depends on the requirements imposed on the engine; for example, constancy of fuel-mixture ratio as the fuel components are fed to the engine chamber, constancy of pressure in the combustion chamber, or change in pressure according to a given program, etc.

The fuel-mixture ratio is generally controlled by calibrating the hydraulic systems of the engine and through experimental adjustment of the system resistances to compensate for production allowances.

In starter and auxiliary-aircraft ZhRD, fuel is generally fed from the main aircraft system. In these cases, the duration of engine operation and magnitude of thrust are not the main factors for the aircraft characteristics. Therefore, for such engines, no special regulation is required for fuel-mixture composition through the metering out of the fuel components.

The fuel-mixture ratio is generally regulated when it is important for the missile to attain its maximum possible velocity at the instant that the entire supply of fuel in the tanks is exhausted, or when the maintenance of the given fuel-mixture ratio during engine operation guarantees the most complete utilization of fuel energy

with the greatest dynamic operating stability.

A number of factors affect the deviation of the fuel composition from the rated optimum values, i.e.,

a) change in component density due to change in component temperature during flight as a result of the effects of atmospheric conditions on the components;

b) the effect of missile acceleration during flight on the engine fuel-feed system (Figs. 11.6 and 11.7);

c) pressure fluctuation in the fuel-component feed due to scattered pump characteristics and fabrication allowances for parts within the fuel-feed system, etc.

If a constant rated fuel-mixture ratio is not maintained during engine operation, the conditions for and completeness of combustion are violated and the gas-exhaust velocity from the engine nozzle diminishes, thus leading to a drop in P_{ud} , and at the instant that the engine stops working a certain amount of one of these components remains in the tanks. This will lead to an increase in the final weight of the missile and thus impair mass transfer. Simultaneously, the operating time for the engine will decline, and this will lead to a drop in total momentum.

In order to maintain a constant fuel-mixture ratio, while at the same time moving the fuel out of the tanks, we have the following three ZhRD operating control methods.

1. An element to sense gas pressure in the combustion chamber of the engine is connected, by means of a transducer and an amplifier, to a servo-valve installed in the combustible (fuel) and oxidizer manifolds. In the case of a change in the gas pressure in the combustion chamber due to disruption of the established per-second fuel-component flow rates and their weight relationships the servo-valves

vary the fuel-component flow rates so that the rated pressure at an optimum fuel-mixture ratio will be established within the combustion chamber (according to the method of hydraulic analogy).

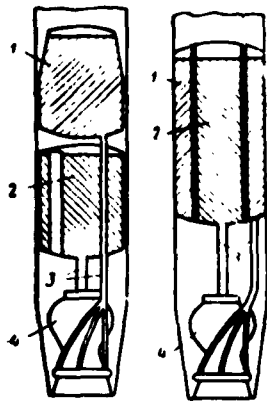


Fig. 11.6. In-line and concentric positioning of fuel tanks aboard the missile. 1) Ethyl-alcohol tank; 2) liquid-oxygen tank; 3) tubing; 4) engine chamber.

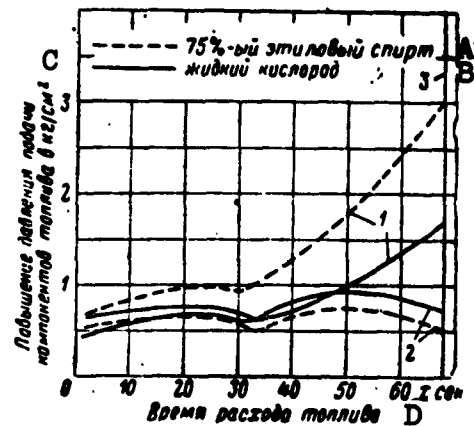


Fig. 11.7. Increase in pressure for spraying fuel components into combustion chamber because of acceleration during flight of missile. 1) With in-line positioning of fuel tanks; 2) with concentric positioning of fuel tanks; 3) termination of burning of fuel reserve in tanks; A) 75% ethyl alcohol; B) liquid oxygen; C) increase in feed pressure for fuel components, in kg/cm^2 ; D) fuel-consumption time.

2. Volumetric flowmeters and controlled servo-valves are installed in the combustible and oxidizer supply tubes. Through the use of special computers, the fuel-mixture ratio is determined, and if this ratio deviates from the given values, this device transmits a signal, through an amplifier, to the servo-valve which varies the component flow rates.

3. The fuel-component level in the tanks is kept constant by differential pressure-sensing elements, and if there is a change in the flow rate or if the weight relationship is disrupted, a special electric circuit controls the servo-valves installed in the combustible and oxidizer supply tubes, varying the per-second flow rates.

Figure 11.8 shows the approximate effect of deviation in the

fuel-mixture ratio from the rated value, at maximum velocity V_{kon} and total flight altitude H_p^* for the missile**.

We can see from this curve that the shortage of oxidizer in the fuel has a predominantly greater effect on reducing the above-mentioned missile characteristics, than does a shortage in the combustible. Simple calculations will demonstrate that in the case of in-line positioning of the fuel tanks aboard the missile, the fuel-mixture ratio increases after starting, and then diminishes; at the end of the engine operation, the value of the fuel-mixture ratio drops below its starting value; this may yield a deviation of up to 10% from the rated ratio in the region of a lean fuel mixture, and in the case of a rich mixture, the deviation may be as high as 6%. Such a change in the fuel-mixture ratio relative to the rated value is particularly intolerable for missiles developing great thrust.

Calculations indicate that a 5% variation in the fuel-mixture ratio relative to its optimum value reduces specific engine thrust by a factor of almost 0.5%. With a 2% deviation in χ from the rated value during the flight of the missile, there will be a corresponding failure to burn up completely one of the fuel components and as a result we will have a drop of almost 4% in the final velocity of the missile.

Figure 11.9 shows the principal diagram for a system of automatic control of the fuel-mixture ratio which changes because of acceleration during the flight of the missile.

With this circuit, the combustible and oxidizer flow rates per given unit time and their ratio are measured and compared with the rated values. A deviation in the ratio from the rated values causes

*[$H_n = H_p = H_{polnaya} = H_{total}$.]

**Zeitschrift, VDI, Bd. 99 [Journal, Association of German Engineers] No. 2, 1957.

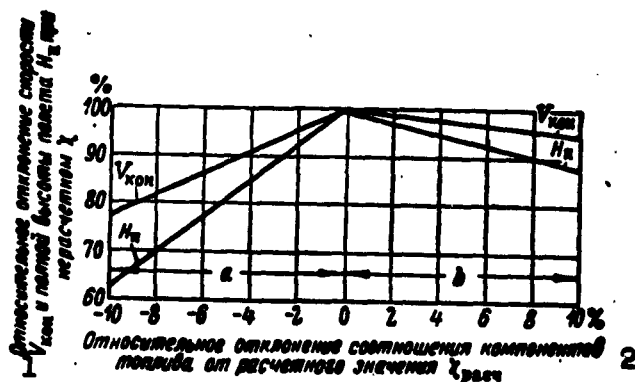


Fig. 11.8. Effect of deviation in fuel-mixture ratio from rated value of X_{rasch} on velocity V_{kon} at end of powered phase and on total flight altitude H_p for missile (fuel, ethyl alcohol + liquid oxygen). a) Region of excess combustible; b) region of excess oxidizer; 1) relative deviation in velocity V_{kon} and in total flight altitude H_p with nonrated X ; 2) relative deviation in fuel-mixture ratio from rated value of X_{rasch} .

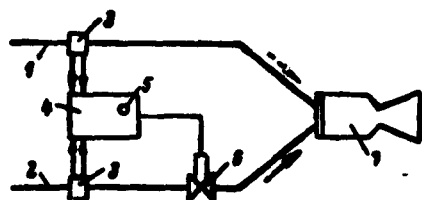


Fig. 11.9. Diagram of engine with automatic fuel-mixture ratio control. 1) Oxidizer tubing; 2) combustible tubing; 3) sensing element; 4) regulator; 5) nominal sensing element; 6) hydraulic throttle; 7) engine chamber.

a control signal to be sent, and in this way the combustible feed (or oxidizer feed) is increased or reduced by means of the control link to the point at which the deviation attains tolerable magnitudes. With such circuits, we can use devices that are kept under stepped or continuous control.

Figure 11.10 shows a convenient circuit for an automatic fuel-mixture-ratio control system which employs the method of measuring the hydrostatic-pressure differences for the components in the tanks.

Given a pressure difference, this control circuit employs mercury differential manometers housed in the oxidizer and combustible tanks, and the manometer surface is used to short the loops of wire-

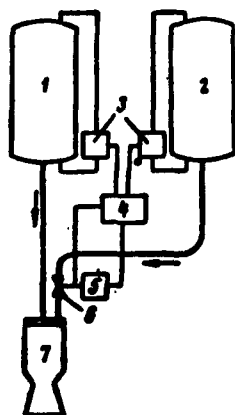


Fig. 11.10. Fuel-mixture-ratio control circuit employing method of measuring pressure differences across engine fuel tanks of high-altitude missile. 1) Oxidizer tank; 2) combustible tank; 3) differential manometer; 4) fuel-mixture ratio regulator; 5) actuator throttle drive; 6) hydraulic throttle; 7) engine chamber.

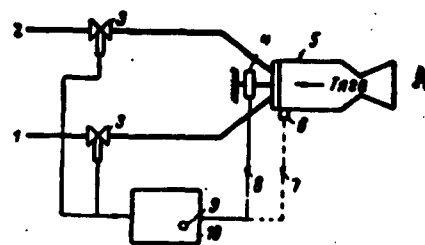


Fig. 11.11. Automatic engine-thrust control circuit employing the method of comparing thrust magnitude or combustion-chamber pressure against given values. 1) Combustible supply tube; 2) oxidizer supply tube; 3) control valves; 4) instrument measuring thrust; 5) engine chamber; 6) sensing element for gas pressure in combustion chamber; 7) signal of pressure in combustion chamber; 8) signal of thrust magnitude; 9) given value for engine thrust (pressure); 10) thrust regulator; A) thrust.

wound resistors situated in the manometer bands, and this affects the measuring mechanism of the regulator.

Constancy of engine thrust can be controlled by changing the rate of fuel flow into the combustion chamber or by varying the gas pressure in the chamber. In the simplest case, the spray pressure for the fuel components and, consequently, the fuel feed can be varied mechanically through the use of a throttling device (Fig. 11.11). The pressure in the combustion chamber is generally the parameter to be regulated. When it becomes necessary to maintain constant engine thrust with respect to flight altitude, the ambient pressure must serve as an additional parameter. The effect of a change in thrust will be taken into consideration when engine thrust serves as a control parameter. In special cases, total missile acceleration may be employed for purposes of regulation.

At the present time, engines using turbopump units attain the

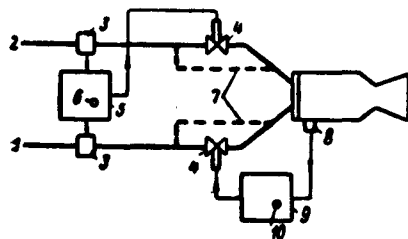


Fig. 11.12. Automatic thrust and fuel-mixture-ratio control circuit. 1; 2) The same as in Fig. 11.11; 3) flowmeter; 4) control valves; 5) fuel-mixture-ratio regulator; 6) given value of fuel-mixture ratio; 7) bypass device; 8) sensing element for gas pressure in combustion chamber; 9) gas-pressure regulator in combustion chamber; 10) given value of pressure in combustion chamber.

required changes in fuel feed by reducing the rpm of the TNA. In this case, the pressure in the combustion chamber is received and compared with the feed pressure proportional to the magnitude of required thrust. The pressure difference is transmitted to the corresponding regulator situated at the inlet to the gas generator in order to provide coordination between actual thrust and the thrust for the given feed. This TNA control method has a serious shortcoming, i.e., substantial system inertia.

An automatic control system must prevent changes in the given turbine rpm of more than 5% and the system must also stabilize engine operation for a given thrust.

If several variable engine parameters have to be controlled simultaneously (for example, thrust, fuel-mixture ratio), then multiple control is employed (Fig. 11.12). The principle behind this control method also involves the regulator comparison of the given value of the parameter against its measured value and action on the positions of the fuel throttle valves or TNA rpm. It is most effective to control the TNA rpm, since in this case the pumps change rpm by an equal amount, and this prevents substantial deviations in the quantity χ .

The corresponding block diagram for multiple control (Fig. 11.13) indicates that there are side links which can subsequently affect

engine operating stability. In this case, the thrust-control parameter p_k is determined not only by the control sector 4 but through the side link 6 as well, i.e., by the parameter controlling the fuel-mixture ratio. The perturbation factor (for example z_1) acts not only on p_k , but also acts on the magnitude of the fuel-mixture ratio χ through side link 7.

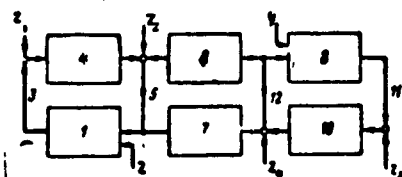


Fig. 11.13. Block diagram for simultaneous fuel-mixture-ratio and thrust control. 1) Thrust regulator; 2) input of nominal value of pressure p_k in combustion chamber; 3) output value of thrust-control parameter; 4) pressure-control sector; 5) input of true value of pressure in combustion chamber; 6) side link between 4 and 8; 7) side link between 1 and 10; 8) fuel-mixture-ratio regulator; 9) input of nominal value for fuel-mixture ratio; 10) fuel-mixture-ratio control sector; z_1-z_4) perturbation factors; 11) output of fuel-mixture-ratio control parameter; 12) input of true value of fuel-mixture ratio.

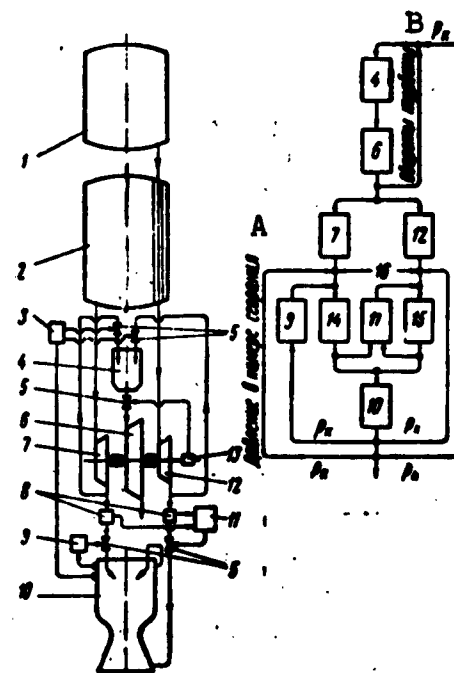


Fig. 11.14. Principal diagram of ZhRD with TNA, employing automatic thrust and fuel-mixture-ratio control (at left) and the block diagram of the automatic control system (at right). 1) Combustible tank; 2) oxidizer tank; 3) gas-generator fuel-flow rate regulator; 4) two-component gas generator; 5) control cock; 6) gas turbine; 7) oxidizer pump; 8) fuel flowmeter; 9) thrust regulator; 10) combustion chamber; 11) fuel-mixture-ratio regulator; 12) combustible pump; 13) turbine rpm regulator; 14) oxidizer supply tube; 15) combustible supply tube; 16) transmission of perturbation due to missile acceleration; A) combustion chamber; B) turbine rpm.

Figure 11.14 shows the principal diagrams for ZhRD with a turbopump fuel-feed system, automatically regulated for thrust and fuel-mixture ratio (at left) and the right-hand side of the figure shows a block diagram of the automatic control system. The circuit incorporates several feedbacks which make up a complex system of dynamic interaction between various units. Thrust is controlled by changing pressure in the combustion chamber, and the fuel-mixture ratio is controlled by changing the combustible flow rate; the operation of the gas generator is regulated by varying the TNA rpm. All in all, there are six closed control loops with their corresponding side links in the system. The various pressure regulators used in the system form auxiliary parallel control circuits which, in the case of unstable engine operation, act on the basic control circuits as perturbation factors.

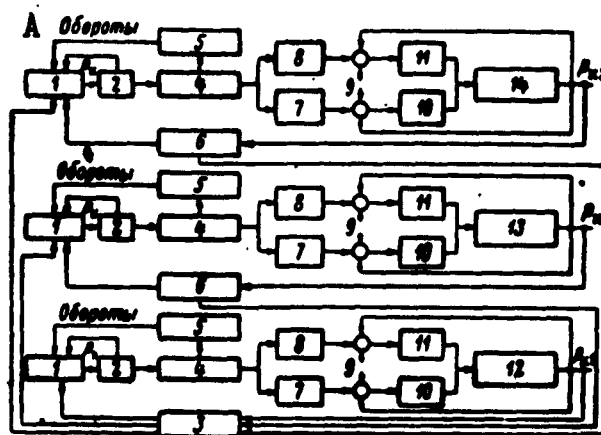


Fig. 11.15. Block diagram of automatic control system for multichamber ZhRD (with the exception of fuel-mixture-ratio control). 1) GG [gas generator] valve; 2) gas generator; 3) main regulator; 4) gas turbine; 5) turbine rpm regulator; 6) thrust regulator; 7) oxidizer pump; 8) combustible pump; 9) action of flight-acceleration factor; 10) oxidizer supply tube; 11) combustible supply tube; 12, 13, and 14) first, second, and third combustion chambers, respectively; A) rpm.

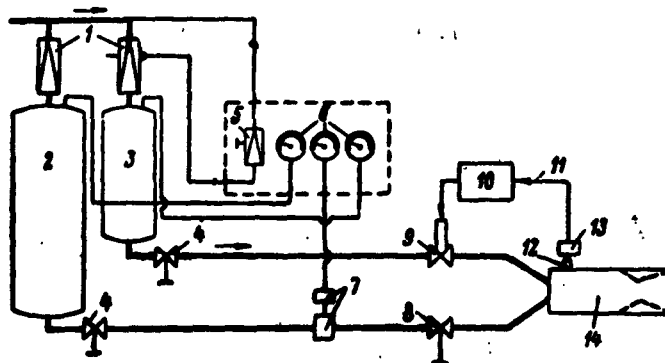


Fig. 11.16. Diagram of test stand for engine employing regulation of pressure constancy in combustion chamber. 1) Pressure reducers; 2) oxidizer tank; 3) combustible tank; 4) shut-off valves; 5) pressure-reducer control; 6) manometers; 7) receiver and transmitter elements; 8) manual control valve; 9) automatic control valve; 10) pressure regulator; 11) input of gas pressure to combustion chamber; 12) point at which pressure is checked; 13) pressure sensing element; 14) engine chamber.

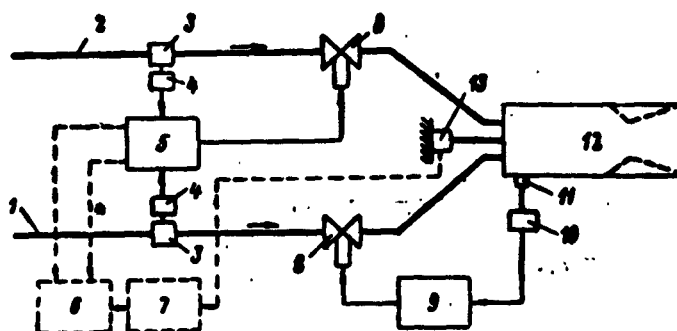


Fig. 11.17. Diagram of test stand for engine employing regulation of fuel-mixture ratio and pressure in combustion chamber. 1) Combustible tubing; 2) oxidizer tubing; 3) flowmeters; 4) flow-rate sensing elements; 5) fuel-mixture-ratio regulator; 6) computer for determination of flow rate; 7) computer for determination of gas exhaust velocity $w_v = P/G_s$ from engine-chamber nozzle; 8) control valve; 9) regulator of gas pressure in combustion chamber; 10) pressure-sensing element; 11) point at which pressure-sensing element is installed; 12) engine chamber; 13) thrust meter.

In the example cited here, we were dealing with the problem of the automatic control of only a single engine chamber. In practice,

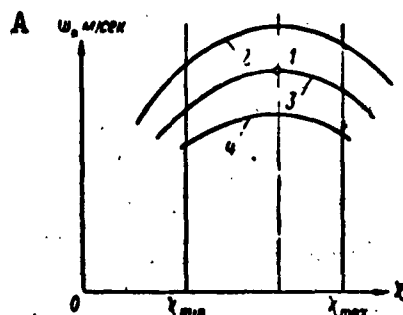


Fig. 11.18. Change in gas exhaust velocity from engine-chamber nozzle as function of changes in fuel-composition factor and gas pressure in combustion chamber. 1) Nominal value of p_k and w_v ; 2, 3, and 4) curves of three various values of $p_1 = \text{const}$; χ_{\min} and χ_{\max}) boundaries of stable engine operation; A) w_v , m/sec;

it is possible to combine several engine chambers into a single overall control circuit. In multichamber ZhRD, in order to avoid nonsymmetry in the thrust being controlled, it is necessary to maintain strict conformity between the thrusts of the individual chambers (engines). The block diagram for a multichamber engine without a fuel-mixture-ratio control system is shown in Fig. 11.15.

The methods examined above are useful only for the control of thrusts within narrow limits, within

which the stability of the combustion process is not substantially disturbed as a result of the indirect changes in fuel-component pressure differences across the spray nozzles.

In determining ZhRD characteristics on a test stand, it is expedient to make extensive use of automatic control and auxiliary computers which make it possible to eliminate possible errors which arise in "manual" control; in addition, the computers make it possible to obtain all of the necessary engine characteristics without any additional calculations. Automatic control in experimental investigations of an engine also yield fuel economy, as well as more complete and more precise determination of the necessary characteristics, while, at the same time, reducing the amount of labor required. As an example, below are presented diagrams of equipment in which the gas pressure in the combustion chamber, the fuel-composition factor, etc., are used as control parameters.

The device shown in Fig. 11.16 makes it possible to obtain exhaust velocity as a function of the fuel-mixture ratio.

Figure 11.17 shows a diagram of a test stand, employing regulation of the fuel-mixture ratio and the pressure in the combustion chamber. This device makes it possible to determine P_{md} as a function of X for variable values of p_k and P_{ud} as a function of p_k at various values of X , as well as to carry out control engine tests with constant values for p_k and X (Fig. 11.18).

A test stand with a device for the automatic control, in addition to the pressure in the tanks, of thrust, fuel-flow rate, pressure in the combustion chamber, the latter all measured directly, makes it possible to bring out a series of other factors which can be calculated by means of the computers shown in Fig. 11.17 by the dashed lines (devices 6 and 7).

Chapter XII

CERTAIN PROBLEMS ENCOUNTERED IN ZhRD OPERATION

The concluding stage in the development of a ZhRD is the starting system, operational control, and the stopping of the engine. This stage of the planning is closely associated with the development of the fuel-feed system for the combustion chamber of the engine.

With improper functioning of the ignition and starter systems, both engine breakdown and the destruction of the entire flying craft are possible. Therefore, in planning a ZhRD particular attention must be devoted to the problems of reliable starts, engine operation, and engine shut-off.

The starting and stopping system for the engine primarily depends on the tactical designation of the engine and the magnitude of the thrust developed. For single- and multi-shot engines, structurally different systems may be employed; for example, the requirement for repeated engine starts imposes additional conditions on the functioning of the fuel-ignition system and the automation equipment.

For smooth and rapid engine start, the ignition-control system must be accurate and precise, and the servicing personnel must be completely familiar with the corresponding technical data (instructions).

This chapter presents short reviews of the basic fuel-ignition methods employed, as well as the rules governing the starting and

the stopping of a ZhRD; in addition, certain other problems encountered in the operation of engines are also discussed.

SECTION 1. ENGINE OPERATING RELIABILITY

ZhRD engine operation during its guaranteed service life is one of its basic characteristics. This factor must, of necessity, be taken into consideration in designing a new type of rocket engine.

Engine failure occurs primarily during starting, and as a result:

- 1) of the nonreliability of the ignition unit in the automatic starter equipment;
- 2) of the low quality of the starter or working fuel components, as a result of which they initially do not burn satisfactorily;
- 3) of improper exploitation of the material portion of the engine (deviations from given regimes of starting and stopping, failure to carry out starting instructions, etc.);
- 4) of operating-regime instability, caused by unsatisfactory functioning of thrust-control units; because of these units, the engine may not develop total thrust, and this, during starting, may lead to the explosion of the engine.

The explosion of the engine is extremely dangerous, since it sometimes leads to considerable destruction, particularly if the explosion is transmitted to the fuel components in the tanks.

Explosions and breakdowns, occurring at times in engines operating in normal regimes (or as the engine is stopped), may be attributed to the same factors as engine failure during starting, as well as to the unsatisfactory functioning of the cooling system, improper operation, inadequate structural strength of the individual engine elements, an unsatisfactory fuel-feed system, a non-normal combustion

process, etc.*

The explosion of the engine during starting can be avoided by imposing more rigid requirements on the ignition system, reducing the fuel-flow rate to the chamber during starting, etc. Starting reliability for the engine, in great measure, depends on the starting system.

The danger of explosions in ZhRD follows directly from the operating conditions for these engines. The greatest danger of engine explosion exists during starting. Non-normalcy in the functioning of the starting and ignition system, leading to an ignition lag for the fuel components being sprayed into the combustion chamber, unavoidably leads to explosion. When this ignition lag is insignificant, the explosion can be of smaller or greater force. Given a significant ignition lag for the mixture, or in the case of a large start fuel consumption, or with an unreliable ignition system in the engine, explosions are possible in the mixture and these can destroy the engine as well as the weapon. Ignition lag may be caused as a result of the fact that the initial vaporization and mixing of the combustible (fuel) mixture in the cold combustion chamber of the engine is substantially less thorough than is the case for a normal heat regime in the chamber, and at a number of points in the chamber, a large number of excessively lean or rich fuel mixture zones are formed.

On starting the ZhRD using high-boiling fuel components, the formation of an explosive fuel mixture is most likely with the least possible ignition lag. In the case of low-boiling oxidizers, especially in the case of liquefied gases, there is less possibility of explosion, since the first batches of such an oxidizer vaporize

*Jet propulsion, Vol. 6, No. 6, 1957.

easily.

For satisfactory ignition of the fuel components, with permissible ignition lag, it is necessary to have high-quality mixture formation for the component batches fed to the combustion chamber.

The type of fuel and its capacity to ignite play significant roles. The easier a fuel ignites, the lower its ignition point, and the "softer" the start of the engine. Therefore, the addition of several substances to the oxidizer and combustible activate the ignition of the fuel.

An explosive combustible-oxidizer mixture (one inclined to detonation), accumulating within the combustion chamber during the ignition lag, is capable of producing tremendous destruction on ignition. It is precisely for this reason that the overwhelming majority of engine explosions occur during engine start. However, on stopping the engine, we find that destructive explosions sometimes also take place as a result of imperfections in engine design; for example, in the mixture-formation system, in the automation system, or because of similar factors.

Engine start, in great measure, depends on the fuel-component-feed pressure, the hydraulic shock in the atmospheric-pressure system, and on similar factors. The greater engine thrust, the more difficult the conditions for safe start and reliable operation; however, here we are dealing with great fuel-flow rates, and high temperatures and pressures in a system of large stressed volumes. Therefore, in ZhRD developing great thrust the role of automation in the control of all starting, operational control, and engine-shut-off processes must be increased. Highly developed automation must provide for reliable double blocking where this is called for, and control all of the elements involved in the starting process with minute precision.

There are particularly serious difficulties encountered in the development of engines to function on a monopropellant fuel containing both the oxidizer and the combustible; in addition, there are difficulties in the development of engines employing separate supply systems for the combustible and oxidizer when these fuel components explode on contact. In this case, an explosion in the combustion chamber may lead to the explosion of the fuel in the tanks or in the feed system.

Fuel components that explode can be permitted only if a special, particularly powerful, exciter (not encountered in the process of using these components) is required in order to initiate explosion in these components. As a rule, unstable monopropellant components must not be used, since even a well designed engine cannot eliminate the possibility of nonuniform shocks and explosions with the use of such fuels, particularly if the engine is started improperly.

In such cases, the fuel tanks and the engine must be situated in the immediate vicinity of one another for structural reasons, and this makes it necessary to impose particularly rigid requirements on the fuel components in terms of their stability. It is precisely these considerations of chemical stability that make it necessary to store the fuel components in separate tanks.

At the present time, the control process for fuel combustion in the engine has already been mastered, so that the case of an explosion in a perfected design is extremely rare after the engine has started functioning and entered its normal regime. In a steady-state operating regime, the engine may explode as a result of a break in the hermetic sealing of the assemblies and "plumbing," or as a result of breaks due to poor fabrication or installation quality, or because of other factors (vibrations, inadequate strength of individual

elements).

The engine must be made so as to prevent any hydraulic shocks or pulsations within the feed system at the instant that the engine is started.

Increased ZhRD operating reliability is possible through the method of duplication, which involves the design of several auxiliary assemblies and systems which can replace the basic assemblies, and automation systems for the engine, should the basic assemblies fail to operate. This is expedient only when the increased weight of the engine resulting from duplication can be compensated by substantially improved operating reliability.

SECTION 2. START AND STOPPING THE ZhRD

The starting and stopping of engines rank among the more complex stages of engine operation. Therefore, in planning ZhRD, we should devote particular attention to problems of reliable engine starts and stops. The engine is generally started from a panel, if the entire weapon is ready for flight.

The basic requirement for starting and stopping an engine can be summed up in the need to provide for the reliable and smooth transfer of the engine to the basic operating regime and to shut the engine off on command. In addition, the starting process should not overload the chamber and should require a minimal expenditure of time.

At the present time, there are hypergolic fuels which provide high efficiency (specific thrust); however, starting engines with these fuels (employing the "charge" method) results in extreme combustion-chamber overloads (see Fig. 11.1). The duration of the starting process depends, primarily, on the time needed to actuate the automation system and the rapidity at which the required fuel-component feed pressure can be built up. The time from the instant at

which the liquid leaves the spray nozzle to the time at which total pressure in the combustion chamber is attained is 0.05 to 0.1 sec., and this makes up only part of the total time (1-2 sec) generally allotted to starting.

For the reliable starting of a ZhRD it is necessary to meet the following conditions.

1. As the engine is started, it should not be permitted that a large amount of one or both of the fuel components accumulate in the combustion chamber. It is particularly dangerous for both components to accumulate in the combustion chamber, since the combustible and oxidizer mixtures used in ZhRD are explosive. If at the start of ignition, a large amount of the fuel (combustible) mixture accumulates in the combustion chamber, the gas pressure will suddenly increase to extremely high magnitudes as the engine is started, i.e., a shock of excessive strength will take place, and this shock may lead to the destruction of the engine.

In order to prevent this, the starting system of the engine must provide for fuel-component ignition in no more than 0.03 seconds after the fuel components enter the combustion chamber.

In order to reduce the accumulation of the combustible mixture in the combustion chamber at the instant of starting, in engines developing great thrust the starting flow rate of the fuel components should be set considerably below that of the basic flow rate, i.e., a step-by-step fuel-component feed to the combustion chamber should be introduced, with the subsequent stage (step) attained after the engine enters its first operating stage in normal fashion. In the A-4 engine, the preliminary stressed stage develops 8 tons.

Step-by-step engine starting refers to the preliminary ignition of a small quantity of fuel, with subsequent transition to total flow

rate.

The magnitude of the starting fuel flow rate, in each specific case, is determined by the period of ignition lag for the fuel components and the nature of the increase in gas pressure in the combustion chamber. A sufficiently stable engine operation (without substantial vibrations and shocks) is possible, in practice, if the initial flow rate for the combustible (fuel) mixture makes up no less than 20 to 30% of the total combustible flow rate to the combustion chamber. In certain cases, this flow rate can be less than indicated, and this is determined by the type of starting system employed.

A smooth increase in combustion-chamber pressure during engine start can also be achieved by gradually changing the fuel composition, as is the case with the "charge" starting method.

2. In engine starts, the sequence in which the fuel components enter the combustion chamber must be strictly observed. It is desirable that the fuel components enter the combustion chamber simultaneously, but since this is, in practice, almost impossible to achieve because of the imperfect synchronization of the automatic starter equipment of the engine, it is generally permitted that one of the fuel components enter the combustion chamber ahead of the other by a fraction of a second.

The sequence in which the fuel components enter the combustion chamber may vary for various engines and depends on the ignition system employed during starting, the method of mixture formation, and the type of fuel components used.

The sequence (in which the fuel components enter the combustion chamber) required for normal engine start may be achieved through the use of burst diaphragms which are sometimes installed in the tubing joints, separating the feed unit from the chamber, or through the

appropriate regulation of cut-off valves which can be used instead of the burst diaphragms.

3. The starter fuel components must be replaced by working fuel components in the case of a high thermal potential in the combustion chamber, and at a specific gas pressure and temperature within the chamber, i.e., if there is, in the combustion chamber, a powerful burning starter flame adequate to ignite the increasing flow of the combustible mixture. This thermal potential for the combustion chamber is determined by the flow rate for the starter and working fuel components and their preparation for combustion.

In addition, the replacement of the starter fuel components with the basic components must be continuous and smooth, since even a slight discontinuity in the feed (with a great ignition lag) can lead to the disruption of the combustion process and the subsequent explosion of the accumulated combustible mixture.

In nitric-acid ZhRD, the ignition of the basic fuel components during starting is possible through the use of only a single combustible which is hypergolic together with the oxidizer (a mixture of triethylamine and xylidine, Tonka-250, etc.).* This starter combustible is generally placed in the main combustible-supply tube, in a separate tank (in the form of tubing) of relatively large diameter*. The input and output channels to this tank are closed by burst diaphragms in order to avoid having the starter combustible pour through the supply tube.

Subsequently, when the shut-off valve is opened to permit the compressed air to flow out of the flask, through the reducer, into the tanks containing the combustible and the oxidizer, the latter, under pressure in the supply tubes, burst the diaphragms and enter

*Voprosy raketnoy tekhniki, Issue 1, IL, 1957.

the combustion chamber. In this case, the starter combustible enters the combustion chamber of the engine first, under the pressure of the basic combustible, i.e., kerosene. As a result, there is an almost instantaneous ignition, in the chamber, of the combustible and the oxidizer, and subsequently the basic combustible is ignited as it enters the combustion chamber after the starter combustible.

The engine starting system, on the whole, (the ignition system and the fuel-feed system) must operate without fail; however, in case of engine failure provision must be made for an automatic control and blocking system which prevents the restarting of the engine until the defect causing the failure has been eliminated.

It is necessary that the fuel residues be removed from the combustion chamber before each start and prior to the subsequent start or attempt to start. Even in the case of a vertical combustion chamber, the inner cavities of the chamber must be flushed.

In the case of engines that are used repeatedly, the service life of their starting and control systems must be raised to correspond to the required service life of the engines.

By starting ZhRD developing great thrust only on the ground, we can simplify the design of the engine and reduce its weight, since the ignition units and the machinery required to set the turbine into motion for purposes of starting the engine (starters) can structurally be separated from the engine and be included in the complex of the ground equipment of the starting platform.

Starters are necessary when turbines are fed by pumps that have to be driven by the turbine itself. In this case, the starting procedure and the control system are considerably more complex. However, an independent compressed-air starting and control system for an engine cannot be used for powerful engines that expend tremendous

quantities of fuel, in view of the problems of weight and size. Therefore, for engines developing thrust in excess of 50 tons, evidently, a more perfect self-servicing turbine must be adopted, a turbine which does not require any air.

Since the given thrust for a ZhRD may change in stages, a specific requirement imposed on the engine-control system in this case involves the fact that it must provide for a definite procedure for change in thrust and engine shut-off, when this is called for in accordance with the conditions of the missile flight.

4. Starting and stopping processes in the engine must be completely automated, and only highly skilled personnel may be employed for this purpose.

Depending on the operating conditions and the design of the ZhRD, the engine is stopped either after the opening of the fuel-component-feed cut-off valves, or after the complete exhaustion of the fuel supply in the tanks. In certain cases, the engine is stopped in stages, i.e., the engine is first reduced to lower thrust and only afterwards completely shut off.

As the engine is stopped, just as in the case of starting the engine, an accumulation of fuel components within the combustion chamber is intolerable. An accumulation of fuel components in the combustion chamber, after the stopping of the engine, is possible as a result of the gradual draining of the fuel components (in the form of residue) from the various supply-tube cavities and cut-off valves, as well as because of imperfect closing of the latter. The fuel that accumulates in the hot combustion chamber can suddenly ignite and produce a strong shock, frequently resulting in the explosion of the engine. In order to diminish the accumulation of fuel components, it is necessary to set the cut-off valves as close as possible to the

spray nozzles. In addition, the design of these valves must guarantee complete component-feed cut-off.

For reliable stopping of the engine, i.e., in order to avoid the accumulation of fuel components in the hot combustion chamber and in order to prevent the explosion of the fuel components after the stopping of the engine, the chamber is flushed with air or nitrogen.

On test stands, after the chamber is shut down, the air from the auxiliary supply tubes available at the stand is generally used for flushing purposes. The engine can also be flushed by one of the fuel components or, in the case of a pressure-fed fuel-feed system, by the gas used to force the fuel components from the tanks to the combustion chamber.

The air pressure for flushing must exceed the working pressure of the fuel components in the "plumbing" by 0.5 to 1.0 atmospheres.

A high-quality combustible (fuel) mixture, improved engine design, and technically accurate engine operation eliminates the possibility of explosions in ZhRD and makes it possible to use these engines with a high degree of reliability.

Instances of engine explosion because of inadequate engine strength or unsatisfactory cooling are a generally infrequent occurrence and can be explained either by poor weld seams between the combustion-chamber liners and the nozzle, or because of deviations from the technical conditions called for in their fabrication.

A drainage facility must be provided for in the tubing, both in order to remove the fuel components, as well as to eliminate air bubbles (plugs). The tubing must be strong and elastic, and there may be no sections in which a sharp change in the direction of liquid motion is called for, since such a change can lead to hydraulic shocks and the bursting of the tubing system.

SECTION 3. "CHARGE" ZhRD STARTING, WITH HYPERGOLIC FUEL COMPONENTS*

In order to carry nitric-acid ZhRD antiaircraft missiles into their operating regime, a so-called "charge" engine start method is sometimes employed (similar to the German missile "Taifun").

With such a method of starting the engine, pressure is initially generated in the fuel tanks, said pressure equal or close to the working feed pressure. Subsequently, the diaphragms or cut-off valves which block the entry of the fuel components into the combustion chamber prior to engine start are burst or open quickly, respectively.

Under pressure, the fuel components move from the tanks to the empty tubing sections and into the cavities of the engine-chamber head. One of the components also passes through the coolant passage of the chamber. In this case, the liquid moves through the "plumbing" of the system at fluctuating velocities, because of local resistances and collisions, along the way, with the air and gas formed during the combustion of the "pyrocartridges," used to burst the diaphragms. The mean flow rates for the liquid vary with respect to time as a function of the "plumbing" design in the engine and the points at which local resistance arises within the "plumbing." The greatest hydraulic resistance is generated by the combustion-chamber spray nozzles.

The fuel components do not enter the combustion chamber from all of the spray nozzles simultaneously; one of the components generally is first to enter the head. In this case, the fuel-composition factor changes as a function of the lead of oxidizer or combustible feed, and the factor varies from infinity to the given value.

The lack of excess pressure within the combustion chamber at
*Voprosy raketnoy tekhniki, 1957, No. 1, IL: Ekspress-informatsiya, AN SSSR, Issue 18 RT-53, 1957.

the time the engine is started and the resulting substantial hydraulic shock in front of the spray nozzles leads to the entry of an excessively large quantity of fuel, through the spray nozzles into the combustion chamber, at the beginning of the starting process. During the ignition lag (of the components in the combustion chamber) a large quantity of combustible (fuel) mixture is accumulated (at $p_k = 30$ atm abs; the rate of fuel flow into the engine chamber may reach approximately 250% of the nominal value, in which case the pressure difference across the spray nozzles is equal to ~ 7 atm abs).

The interaction between two hypergolic fuel components can, during the period of engine start, conditionally be divided into three stages.

The first stage takes place in the liquid phase and, primarily, at the separation boundary between the liquids (the contact surface), as a result of which intermediate products are liberated in the form of an opaque cloud containing both vapor-like, liquid-drop, and solid materials, i.e., "vapor gas." The second stage of the process takes place within the vapor gas, and terminates with the appearance of one or several ignition foci.

The third stage of the process is characterized by the propagation of the flame throughout the entire vapor gas, with the formation of the final products of reaction. It is in this stage that there is a sharp rise in pressure within the combustion chamber, and the rate of gas flow through the chamber nozzle increases; the rate of fuel flow through the spray nozzles diminishes.

Under certain conditions, the starting pressure of the forming gases within the combustion chamber can exceed the nominal pressure by a factor of more than 2, corresponding to a steady-state nominal operating regime for the engine. After a short time, the pressure in

in the combustion chamber should drop, and then there is a new increase in the rate of flow through the spray nozzles, etc.

If the operation of the engine is stable, one to four periods of pronounced fluctuations (which then are rapidly attenuated) appear after the first "peak" of pressure in the combustion chamber.

The processes encountered in "charge" engine starts are extremely complex and therefore cannot yet be calculated.

Extremely important in the start of ZhRD is the rapidity with which the vapor-gas and droplet mixture burns up after the expiration of the ignition lag. It may be assumed that not all of the vapor-gas participates in this combustion, that the liquid particles (droplets) have not yet been heated, and that they vaporize slowly. In the middle of the process, combustion proceeds most intensively, since it involves the vaporization of the basic mass of the gas and droplets. Finally, the concluding stage of the ignition must be characterized by comparatively weak final (complete) combustion.

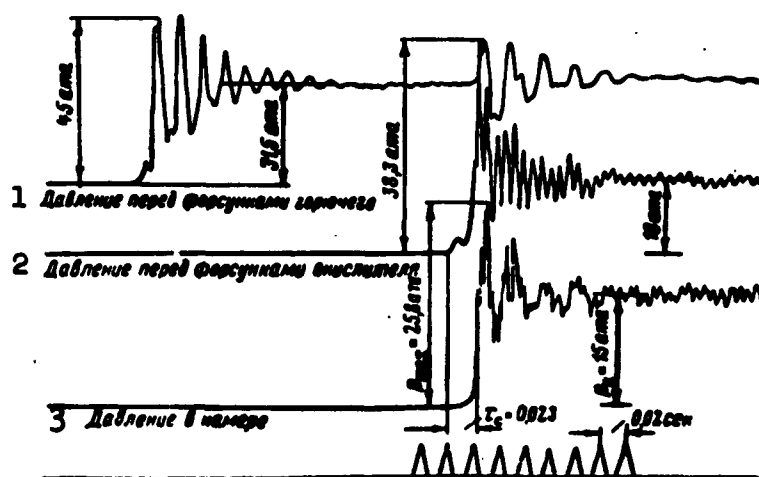


Fig. 12.1. Change in pressure on starting ZhRD.
 1) Pressure in front of combustible spray nozzles;
 2) pressure in front of oxidizer spray nozzles;
 3) pressure in chamber.

Consequently, the "charge" starting of a ZhRD operating on hyper-

golic fuel components is generally accompanied (Fig. 12.1) by:

1) considerable hydraulic shocks in front of the spray nozzles, with damped pressure fluctuations, as a result of which excessively large quantities of fuel enter the combustion chamber (at this instant, the pressure in the combustion chamber does not exceed 1 atm abs);

2) a sharp rise in pressure in the combustion chamber, due to sudden ignition and combustion of hypergolic combustible (fuel) mixture accumulated within the chamber during the ignition lag, as a result of which there is a temporary delay in the normal entry of a new supply of fuel to the combustion chamber, and sometimes the engine may be destroyed.

The main task in planning a fuel-feed system for a ZhRD is the effort to:

1) reduce the duration of engine start to its minimum;

2) avoid excessive starting overload of combustion chamber due to the pressure of the gases forming within the chamber at the instant of engine start.

The duration of the start depends primarily on the time required to actuate the automatic equipment and the rapidity with which the necessary pressure for the feed of the components to the combustion chamber can be generated. The time from the instant at which the components leave the spray nozzles to the time at which total pressure in the combustion chamber of the engine is attained is, for all intents and purposes, equal to 0.05 to 0.1 seconds, and this makes up only part of the total time (1-2 sec), generally set aside for the starting of the engine, in the case of the "charge" method.

Starting combustion-chamber overload is the ratio of maximum

pressure p_{push}^* in the combustion chamber at the instant of engine start to the pressure p_k in the combustion chamber during normal engine operation, i.e.,

$$n_{\text{exp}} = \frac{p_{\text{push}}}{p_k} \quad (12.1)$$

In the case of "charge" engine start, it is possible to avoid substantial combustion-chamber overload only with certain starter fuels. The most useful fuel for this purpose is xylidine or the combustible Tonka-250 and a melange (a mixture of nitric and sulfuric acids) as the oxidizer (this oxidizer is a 40 or 50-% solution of fuming sulfuric acid, H_2SO_4 , in nitric acid). These fuels are not very efficient for the basic operating regime of the engine because of their low heating value.

At the present time, there are other hypergolic fuel components which provide for relatively high specific thrusts; however, using these fuels to start engines, with the "charge" system, yields high combustion-chamber overload.

Basically, the following factors affect the starting ZhRD combustion-chamber overloads.

1. Ignition lag τ_{zad}^{**} for the fuel mixture, and this lag represents an interval of time from the instant at which the combustible comes into contact with the oxidizer in the combustion chamber to the instant at which excess pressure appears within the chamber.

The magnitude of this lag determines the possibility of and technical conditions for starting ZhRD with the given fuel, and also to a considerable degree, it prescribes the continued combustion process for the fuel mixture in the combustion chamber. The lower τ_s for the fuel components, the less fuel will accumulate in the

$$^* [p_{\text{push}} = p_{\text{push}} = p_{\text{pushovaya}} = p_{\text{start}}.]$$

$$^{**} [\tau_{\text{zad}} = \tau_{\text{zad}} = \tau_{\text{zaderzhka}} = \tau_{\text{lag}}.]$$

combustion chamber at the instant of start, and the lower the chamber overload.

2. The weight accumulation of fuel in the combustion chamber during the start of the engine

$$G_{\text{факт}} = G_{\text{норм}} \psi \text{ kg/sec,}$$

where $G_{\text{факт}}$ is the actual quantity of fuel delivered to the combustion chamber at the instant of start, in kg; $G_{\text{норм}}^*$ is the quantity of fuel which would normally be fed to the combustion chamber in the absence of hydraulic shocks in front of the spray nozzle;

$\psi \approx G_{\text{факт}}/G_{\text{норм}}$ is the coefficient characterizing the hydraulic shock in the cavity in front of the spray nozzles, as well as the character of the opening of the cut-off valves or diaphragms, given the condition that the combustible and the oxidizer enter the combustion chamber simultaneously, in which case the magnitude of the flow rate of these two components would be determined by the feed pressure in the fuel tanks.

The magnitude of the first liquid-pressure maximum in front of the spray nozzles, as a result of the hydraulic shock, has a substantial effect on the coefficient ψ . The softening of the hydraulic shock, by any method whatsoever, can reduce the combustion-chamber overload at the start. The conversion of a substantial quantity of liquid, on its way from the tanks to the spray nozzles, on coming into contact with the air and gas of the burning pyrocartridges used for the burst diaphragms, serves somewhat to reduce the hydraulic shock at the chamber head.

3. Quality of fuel-component atomization, since vigorous mixing increases the combustion time τ_{sg} for the combustible mixture formed at the start, thus reducing the overload on the combustion chamber

$$* [G_{\text{норм}} = G_{\text{норм}} = G_{\text{норм, no}} = G_{\text{норм}}.]$$

of the engine.

However, this method of reducing n_{per} is, in practice, unusable since mixture formation in ZHRD is, first of all, based on the principle of attaining high economy and operating stability for the engine, for which purpose good fuel atomization and component mixing is necessary. Therefore, there is little likelihood that any recommendations to reduce n_{per} by impairing the process of mixture formation can be applied in practice if they contradict the requirements of economy and stability for the operating processes taking place within the combustion chamber of the engine.

4. The heating value of the fuel, characterized by the properties of its components, and the composition factor χ .

It is well known that the heat balance has a substantial effect on the rate at which the combustible (fuel) mixture burns in the combustion chamber at the instant that the engine is started. The heat balance of the fuel mixture is, to a great extent, determined by the heating value of the fuel, the concentration of the products of reaction, and the heat losses within the combustion chamber at the instant that the engine is started. The lower the heating value of the starter fuel mixture, the lower the pressure in the combustion chamber at the instant of start.

5. External engine-operating conditions, i.e., the pressure and temperature of the surrounding medium, since it is on these that the ignition lag for the fuel mixture depends in part on starting, and consequently, it is also on these that the starting combustion-chamber overload depends. A reduction in the temperature of the atmospheric air reduces the chemical activity of the fuel mixture and increases the delay lag. A reduction in atmospheric pressure intensifies the hydraulic shock in front of the spray nozzles as a result of the drop

in the counterpressure to the liquid flow, moving from the tanks to the combustion chamber. This will lead to an increase in ψ_{uzk} and n_{per} . The total effect of a drop in atmospheric pressure and temperature (altitude conditions) impair the starting conditions for a ZhRD.

6. The pressure p_B required to feed the fuel components into the combustion chamber, the magnitude of the free space in front of the combustion-chamber head, its reference length l_{pr} and similar factors.

An investigation into the factors effecting the nature of the pressure increase within the combustion chamber is of great practical significance.

The law governing the burning up of the combustible mixture on engine start can, theoretically, be taken as close to sinusoidal, in which case the combustion ceases (is equal to zero), at the instant the combustion lag is completed, and is equal to unity at the end of the reaction process.

The feasibility of purely structural measures designed to reduce ψ and, consequently, n_{per} , are now fully apparent. For example, a reduction in the coefficient ψ can be achieved through the simple structural division of the engine-chamber head into several sections, arranging the design so that these sections would begin to function in stages. Other methods may be used to delay the liquid for a short time (for the period required for engine start). For example, in one of the nitric-acid engines used in antiaircraft missiles* the fuel-component feed to the combustion chamber at the instant of engine start is controlled by special hydromechanical starter valves. In each of these valves, the shift of a small piston is calculated to open, within one second, a flowthrough section for the fuel com-

*Ekspress-informatsiya, AN SSSR, Issue 44 RT-132, 1957.

ponent being fed into the combustion chamber, to permit a flow ranging from zero to total consumption.

Given such a system of gradual fuel-component feed into the combustion chamber, the engine easily and quickly enters its regime, and maximum thrust is developed within 0.6 seconds after the engine has been started.

Thus, the starting reliability of a ZhRD is determined by the systems. The reliability of operating and starting a ZhRD is determined by a series of other factors. The reliability of stopping the engine on the test stand can be thoroughly checked only if the same method of engine shut-off is used as would be the case with a real missile engine.

The basic factors affecting the stability of the steady-state process in the ZhRD are the process of converting the fuel into gaseous products and the characteristics of the hydraulic system in the engine and the combustion chamber.

SECTION 4. ENGINE SERVICE LIFE

ZhRD service life is meant to refer to the period of reliable engine operation in the nominal regime, as guaranteed by the plant-supplier.

The service life of the engine is affected by a series of various factors, of which the most important are the following:

1. The type of fuel used; the physicochemical properties of the fuel and the high combustion temperature, more or less, tend to corrode the structural materials used in the engine, thus determining the service life of the materials in question (in conjunction with the other factors). Such oxidizers as nitric acid, fluorine, and its derivatives, are particularly aggressive for the majority of structural materials. Fluorine and its derivatives, in

addition, burn at comparatively high temperatures.

2. The atomization method for the fuel components; the quality of the mixture formation in the combustion chamber affects the nature of heat transfer, the thermal and vibrational loads on the engine, and consequently, the service life of the engine.

3. Pressure in the combustion chamber; with an increase in pressure, the temperature of the products of combustion for the given fuel increases, and this promotes the chemical and mechanical tendency of these products to corrode the structural materials used in the engine (the flushing of the material in the inner chamber liner, by means of the gas stream, is accelerated).

4. Engine operating regime; with a drop in the rate of fuel flow to the combustion chamber in order to control thrust, there is an impairment in the conditions under which the combustion chamber and nozzle are cooled, and this, under certain conditions, may result in pulsations in fuel combustion, overheating, and the burning out of the flame tube. Therefore, in practice the changing of the operating regime for the engine should be carried out within strictly defined limits, established by the plant-supplier.

5. Engine-chamber design; in good designs, static, thermal, and vibrational loads can be reduced to the minimum, and this would increase the service life of the engine.

6. Quality of engine fabrication; in the case of production defects (low-quality fabrication or installation of individual engine elements), excessive overheating of the inner chamber liner is possible, as is the operational failure of the automatic systems, and in addition there may be other consequences which can reduce the established service life of the engine, and even result in the explosion of the engine.

The practicality of producing an engine with increased specific thrust and a substantial service life depends, in great measure, on how efficient a chamber-cooling system can be employed.

The service life of cooled ZhRD is not great and is generally measured in terms of minutes, tens of minutes, and, at the very most, in hours.

Under the conditions prevailing with one-shot missiles, the service-life requirements for the engine are extremely limited. In this case, the service life of the engine must be equal to the operating time required for the engine during the powered phase of the missile flight. Although this greatly eases attaining the required service life, it should not be forgotten that the heat capacity of the hot sections of the engine and the intensity of the heat flows within the engine are such that the thermal regime is established within the engine within about 10 to 15 seconds after start, and in engines with a thin chamber liner, even more rapidly. Therefore, an engine with inadequate cooling intensity will burn out after 15 to 20 seconds after start, i.e., ahead of its shortest service life.

The service-life requirements for ZhRD mounted on aircraft (winged missiles) and intended for repeated starts are increasing greatly. The service life of such engines must be measured in terms of hours.

The service life of uncooled engines, in great measure, depends on the fuel used and the conditions under which the fuel is burned; the service life may reach 10 to 15 seconds, at combustion-chamber temperatures of approximately 3000°K.

Chapter XIII

STAGES IN THE PLANNING AND FINAL TESTS OF ZhRD

Planning and design is an extremely important stage in the development of new ZhRD. The basic problems which must be resolved in this case are the overcoming of the physical obstacles which retard the development of ZhRD (the operation of the engine at high temperatures, control of engine-operating instability, protection of the chamber flame tube against overheating, and the utilization of new fuels and atomic energy).

This chapter presents brief descriptions of the stages involved in the planning of a ZhRD in its entirety, and the basic types of tests to which the engine is subjected on a test stand; in addition, there are sections on the testing centers and the instruments and measuring equipment used during the tests.

SECTION 1. STAGES IN THE PLANNING OF A ZhRD

The planning and design of a ZhRD is generally based on specific technical conditions (TU*), which determine the designation and program of engine operation, its nominal, maximum, and minimum thrust, the type of fuel to be used, economy requirements, specific weight, ability to withstand extended storage, etc.

The selection of the fuel components, basic operating parameters, the type and basic engine diagram, the structural materials, *TU = TU = Tekhnicheskiye Usloviya = Technical Conditions.]

and the assembly of the engine elements are extremely important in planning a ZhRD.

The type and design of the engine, its characteristics, and the type of fuel used in the engine are, basically, determined by the design, dimensions, weight, and flight characteristics of the flying craft. It is therefore extremely important to plan an engine for the craft (of given designation), which will be reliable, economical, and, all other conditions being equal, provide the best characteristics for the craft.

To plan an engine of a given designation means:

- 1) to make advantageous selection for purposes of developing and laying the groundwork for the construction diagrams of the engine, as well as to make expedient selection of the structural materials required for the engine;

- 2) to set the optimum operating and structural parameters for the future engine;

- 3) to carry out properly the required calculations of the geometric and operational characteristics;

- 4) to make the structural diagrams for individual engine elements, to carry out the strength calculations for these elements, to handle the necessary assembly, and to resolve a series of other problems, associated with engine design.

There is no uniform method of selecting the type of engine. In each individual case, this or that factor may prove to be the most important, determining the advantages of a given engine version. It is the task of the designer to make proper evaluations of all these factors, to analyze the effect of these factors on a given engine version, and to select, on the basis of this analysis, that diagram which would offer the greatest advantages with respect to

the basic data, over the other versions.

The rational selection of a design for the engine and its automatic equipment must be based on existing theoretical and experimental materials and statistical data, in which are taken into consideration the engine-design diagrams and elements, and with which operational parameters great specific thrust, operational reliability, and the best weight and flight characteristics for the craft can be achieved. In each specific case, for flying craft of various designations, it is necessary to use well defined and the most rational engine design and engine-instrument types, since with a change in the designation of the craft, the requirements imposed on the engine also undergo change.

In selection of engine design, the adaptability of the design to production must serve as one of the basic criteria, since the best design would be the one which can be mass produced, with the lowest production costs.

The design of the engine must provide for the smallest possible number of component parts. Where this is possible, use should be made of component parts that have been completely adjusted and checked in operation.

The duplication of systems and component parts in order to increase engine-operating reliability must be done with an eye to the shortcomings which this [duplication] introduces (for example, increased weight and dimensions).

The choice of materials depends on the requirements imposed on the materials, on the type of engine design, the designation of the individual assemblies, the component parts included in these assemblies, and the operating conditions. The cataloguing of materials should, desirably, be reduced to the minimum, especially insofar as

this pertains to the component parts fabricated of raw materials that are in short supply. We must make every effort to use the least expensive materials which are readily available and make it possible to employ the least expensive mass-production methods.

The weight and strength of the design elements are closely associated with one another and, therefore, in a comparison of material characteristics, both of these factors have to be taken into consideration at the same time. In order to facilitate this comparison, we have introduced the concept of the coefficient of specific material strength, by which we mean the ratio between the strength characteristic of the material and the specific weight of the material. This coefficient varies as a function of the nature of component-part load and deformation.

In the production of ZhRD, alloy and carbon steels, as well as light-weight alloys are used.

The use of inappropriate materials, incomplete utilization of the strength properties of the material, and inexpedient designs for individual engine elements, might lead to excessive weight for the engine.

Substantial improvements in ZhRD cannot be achieved through the introduction of various production measures alone, unless the design of the entire engine is reworked. By reworking of engine design we mean the designing of an engine which provides for the performance of all assigned functions within the established service life, and still exhibits minimum dimensions, engine weight, and material expenditures.

The design of an engine and its adaptability to production must be confirmed through a detailed economic analysis of the technical and economic indicators (output, cost, utilization of capital, and

other factors).

Since materials, equipment, personnel, and time are necessary for the mass production of engines, in the planning of a new engine the designer must always take into consideration, in addition to the TU, the requirements of production and economics.

The basic economic and production requirements imposed on the engine being designed, are the following:

- 1) utilization of domestic raw materials;
- 2) adequacy of supply and cost of materials used;
- 3) simplicity of design and production adaptability for component parts;
- 4) standardization of design elements (component parts, units);
- 5) cost (inexpensiveness) of production, on the whole.

The cost of the finished product is generally determined by taking into consideration such costs as materials, labor, equipment, overhead, and other expenses associated with the given item being produced. Pricing and expenditure norms for all categories are established in accordance with the corresponding departmental standards.

We can recommend the following approximate sequence for planning and developing an engine.

1. Sketch of engine:

- a) selection of simplest version of principal diagram and basic working and design parameters for the engine;
- b) establishment, to the extent possible, of the production base required for the engine being planned;
- c) standardization of units and basic component parts contained within the product being planned, and of the products already in production;
- d) laying out the product into independent assembly units;

- e) providing for production adaptability in key component parts;
- f) selection of rational (efficient) blanks for key component parts.

The sketch of the ZhRD is the first stage in the job of designing an engine, and it is the stage in which the principal layout, and the basic operating and design parameters appear. This stage is concluded with the preparation of calculation curves, and the drawings of the over-all view of the engine, in several projections, and in assembled form.

It is in this stage of the planning that the coordination of all design elements is carried out. If the engine is to be used to control the flight of the missile by turning the chamber relative to its axis in order to change the thrust vector, provision has to be made for appropriate units and mechanisms, and all of the factors determining the operation of the engine under the given conditions have to be taken into consideration.

2. The technical stage of planning an engine involves the determination of the designs for the products and units used in the engine, as well as the determination of the structural shape of all engine elements.

It is at this stage of the operation that the basic technological problems are resolved, i.e., blanks, machining, welding, assembly:

- a) selection of simplest design for units and component parts;
- b) selection of assembly bases for products;
- c) calculation of the most important dimensioning circuits;
- d) meeting the requirements for assembly equipment;
- e) meeting the basic production requirements from the standpoint of processing and the standpoint of basic blank dimensions.

3. The working stage of engine design is the process in which

the problems of production adaptability for the design of each component part and the entire product as a whole are worked out. In this case, particular attention is devoted to:

- a) the selection of the production bases for the component parts, in accordance with the design and assembly bases;
- b) the establishment of dimensions and designation of optimum tolerances and limits of mechanical characteristics for the metals;
- c) the selection of the most inexpensive and most readily available materials, as well as the preparation of a catalogue listing of same;
- d) the adherence to the requirements imposed on the elements of the structural blanks;
- e) the adherence to all requirements imposed on the production of the design elements;
- f) the maximum standardization of design elements.

The drawings made in the drafting of a ZhRD can generally be divided into the following two groups:

design drawings, for over-all views of the engine and its basic elements; these drawings give a general presentation of the installation, the operating principles, and the dimensions of the product being planned, and contain the initial data required for the working drawings;

working drawings containing all development data for the production processes of fabrication and product control.

The finishing precision required for parts is shown in the drawings in accordance with GOST 2789-51. Tolerances are indicated with all working drawing dimensions (diametrical, linear, and angular, as well as with the distances between axes or between axes and planes) in accordance with GOST 3457-46.

The designer is not merely responsible for high operational characteristics for the future engine, but also for the development of a design that will permit the use of the most economical production processes.

ZhRD design can be improved on the basis of data gained from experience in rocket-engine operation, production, and from the results of special tests.

When we design ZhRD, we must consider the unequal temperature expansion in separate parts of the engine during operation; this is necessary to avoid reducing the strength safety factor of the metal because of the appearance of excessive thermal stresses.

The operating conditions for the separate units of an engine do not always make it possible for us to design an engine that will entirely satisfy all the requirements imposed. We therefore must often accept compromises in the process of designing an engine.

In the process of planning and designing an engine, it is necessary to check the geometric shapes and dimensions of the separate elements and units for strength by using "preliminary" strength calculations based on the theory of the usual patterns of resistance for materials and machine parts.

Contemporary one-shot and multi-shot ZhRD consist of a great many parts including complex and expensive units and assemblies. These parts, units, and assemblies pass through many tests and control operations (external inspection, measurements, etc.). First of all, the purpose of the control operation is to check conformity of dimensions obtained, and tests are conducted to check the hermetic sealing of units, "plumbing," chamber elements, and fuel tanks.

The assembled engine and its fuel-feed system undergo pneumatic and hydraulic tests and are subjected to functional tests as a unit;

in these tests we check the separate units for correct operation and test automation devices, valves, propellant-component feed system, etc., to ensure that they operate without fail.

After a complete and thorough check, we commence the static firing tests of the engine and check the most important engine parameters against the theoretical data. We adjust the engine to a reliable operating condition in accordance with these tests.

When we design and produce an engine we must pay particular attention to the following basic requirements:

1. The surfaces of the inner engine-chamber liner must be smooth, without projections or depressions in joints or machined sections, etc., in order to avoid hydraulic losses inside the chamber or in the coolant passage, as well as to avoid possible local liner overheating, excessive thermal stresses, and warping.

2. The weld seams of the chamber liner must be hermetically sealed and sufficiently strong.

3. The nozzle throat and the injector orifices must have smooth surfaces and strictly defined dimensions, since an insignificant change in these dimensions causes a marked change in engine operating characteristics.

4. The coolant-passage slot must be uniform throughout its circumference, since an insignificant change in its dimensions can lead to the disruption of normal engine-chamber cooling conditions and to overheating and burning out of the inner chamber liner.

5. The axes of the chamber nozzle and of the injector orifices must be made with rigid tolerances in order to avoid noncoaxial thrust direction and unsatisfactory propellant-component atomization.

6. The automation and control devices for engine operation must have rigid and precise tolerances, since any inaccuracy in the fabri-

cation of these devices can lead to a considerable disruption in the operating regime of the engine and sometimes even to breakdown.

The precision of engine fabrication should be established by starting from strictly valid technical requirements, since a shift to a higher class of precision increases the time and the cost of processing to a marked degree. However, an increase in fabrication precision for blanks is advantageous in some cases, since this permits savings in subsequent production operations.

The requirements for the design and production of a ZhRD and its separate automation devices are quite different in each separate case and are usually dictated by special conditions.

The basic requirements imposed on the assembly of the elements for a ZhRD of any designation or design are compactness, convenience in adapting the engine to the weapon, insignificant effect on weight and flight characteristics of the weapon, and simplicity and cheapness of installation techniques.

The assembly of the separate subassemblies for an engine being planned depends on:

- 1) the designation of the weapon;
- 2) the magnitude of engine thrust and the engine operating time;
- 3) the type of propellant components and the system for feeding the components to the combustion chamber;
- 4) considerations of design, operation, and economy.

These factors determine the design features of the engine, the operating regime, the operating conditions, and, consequently, the number of subassemblies required for the engine, as well as their design and assembly.

It is impossible to give general recommendations with respect to the assembly of the separate units of the engine, even in a weapon

of the same designation, since this problem can be solved expediently only upon condition of the simultaneous assembly of the given weapon, which is characterized by a variety of design in almost every separate case. To solve this problem, we must try to design a weapon that is simple, inexpensive, and reliable in operation and has minimum weight and good flight characteristics.

It is well known that ZhRD development is moving toward an increase in absolute thrust, in operating time, and in specific thrust by means of the improvement of operating cycles, the use of new high-efficiency chemical fuels, and so forth.

Because ZhRD development is associated with the development of new types of weapons, in most cases accurate data concerning the newest types of engines for long-range and super-long-range missiles are lacking at the present time. The literature reports that the USAF is working on the development of a single-chamber ZhRD with a thrust of 450 tons and on a multi-chamber ZhRD with a thrust of 700 tons;* ammonia-fluorine, hydrazine-fluorine, hydrogen-fluorine, hydrogen-ozone, and others are under study by the USAF as possible engine fuels;** the USAF has developed stands for testing engines with thrusts of up to 1,000 tons*** and with combustion-chamber diameters of up to 3.5 m; in addition, they are developing plans of missiles with engines developing extremely great thrusts. In particular, the design for the three-stage missile "Meteor Junior"****, intended for a flight to the moon, includes a first stage with a block-type engine of 17 chambers, each with a thrust of 59.2 tons; a second stage with an engine of 6 chambers, each with a thrust of 20 tons; and a third stage with an engine of four chambers, each with

*Ekspress-informatsiya, AN USSR, No. 20, ADS-78, 1958.

**Ekspress-informatsiya, AN USSR, No. 11, ADS-42, 1958.

***Ekspress-informatsiya, AN USSR, No. 7, RT-13, 1958.

****Ekspress-informatsiya, AN USSR, No. 8, RT-23, 1958.

a thrust of 2.25 tons. Five engines are mounted on "propeller" shafts with hydraulic drive for controlling the flight of each missile stage. Liquid fluorine is the oxidizer proposed for the engine of this missile.

When selecting the type and plan for an engine, we must first of all bear in mind that the production of a single-chamber engine with great thrust is extraordinarily difficult, requires much time, and is accompanied by enormous expenditures of funds. It is economically more advantageous to use a block-type engine in the form of a cluster of chambers made in accordance with earlier designs for single-chamber engines of smaller thrusts.

However, a single-chamber engine of the same thrust is simpler from the design viewpoint and has a smaller external diameter. Nevertheless, because the reliability of single-chamber ZhRD is still not high, and for the purpose of weight reduction for the design, these engines are designed and fabricated with minimum strength safety factors; even an insignificant disruption in starting conditions or a small irregularity in operation can cause an explosion and missile breakdown. Besides the destruction of parts, an explosion can disrupt the sequence of certain operations, especially the ignition of the fuel at engine start. The difficulties of fuel ignition at engine start increase in the later stages of the multi-stage missile because of the low pressures and temperatures at high altitudes, in comparison to the temperatures and pressures at ground level when the first-stage engine is started.

From this viewpoint, a multi-chamber (block-type) engine is more reliable, since a breakdown in one of its chambers need not cause the breakdown of the entire engine.

The basic difficulties in throttle control for engines of great

thrusts are caused by the disruption of the normal fuel-combustion cycle, the cooling conditions, and the stabilization of engine operation. At a partial load, a multi-chamber engine with thrust regulated by means of a variation in fuel-flow rate apparently has a greater specific thrust than a single-chamber engine of the same thrust, since the range of load variation for each small chamber of a block-type engine is narrower and losses in specific thrust caused by regulation of fuel-flow rate are relatively smaller.

Included in the shortcomings of a multi-chamber engine are the necessity of maintaining strict mutual conformity of thrust for the separate chambers in order to avoid asymmetry in the resultant engine thrust, and also the presence of a branched "plumbing" system and a relatively complex regulation system to provide for the given operating characteristics, as well as to suppress possible vibrations and self-oscillations. We must also bear in mind that multi-stage missiles are considerably less reliable than single-stage missiles.

When we develop ZhRD of great thrust, we must pay particular attention to the solution of such problems as an increase in the operational reliability of the separate chambers, a method of starting these chambers in space, a considerable convergence of scatter limits of the basic characteristics for the separate engine chambers, the development of reliable engines developing great thrust without an excessive increase in the number of chambers, the introduction of high-efficiency fuels, etc.

SECTION 2. STATIC TESTS OF ZhRD

Newly built engines are subjected to cold-calibration and hot-firing tests on stands, in accordance with special programs.*

*D. Satton [sic, possibly G.P. Sutton], Raketnyye dvigateli [Rocket Engines], IL, 1952.

The cold-calibration tests of a ZhRD involve hydraulic and pneumatic engine tests for the purpose of checking the strength of the separate elements and the hermetic sealing of the weld seams, "plumbing" connections, etc.

During static hot-firing tests of a ZhRD, we adjust the engine to the given parameters in regard to thrust, economy, and reliability of operation; we also establish the permissible ranges of operation in various regimes, determine operating time, and check on the safety of starting and stopping the engine.

The adjustment of an engine is always attended by enormous difficulties. In practice, the adjustment of a ZhRD is frequently accompanied by new maladjustments, after the engine has been subjected to tens of firing starts in order to check the absence of shocks and the reliability of starts.

Hot-firing tests of ZhRD are very dangerous for servicing personnel because of possible explosions and fires. A reliable personnel shelter is required and the engine undergoing tests must be kept at a distance from the personnel, with strict observation of safety precautions; also, preliminary studies and model tests of the separate units and assemblies on special benches are mandatory.

Thus, for example, it is better to test the turbine separately with water vapor or compressed gas before the final test of the turbopump assembly; the pumps can be adjusted for the given operating regime by the use of less dangerous liquids than liquid oxygen, nitric acid, or the like (such as water, for example).

We can determine the characteristics of the chamber head by hydraulic tests with water and then by hot-firing tests of the engine chamber. Testing the chamber head with water permits us to ascertain the nature of the injector-jet interaction, and of the atomiza-

tion, mixing, and distribution of the liquid throughout a cross section of the engine combustion chamber. Although such tests are carried out under conditions very different from the real engine operating conditions, they can be useful for improving the operation of the engine-chamber head.

We can also use water to check the engine propellant-component flow rate, which depends on the operational nature of the various assemblies, elements, and units of the fuel-feed system. Since this type of testing is very important, a special laboratory is sometimes equipped for this purpose. To test fuel-feed systems for explosive components, we sometimes require installations as complex as those used for testing entire ZhRD.

We can also study the problem of cooling an engine chamber (especially when using new propellant components) to a considerable degree by the use of models, which can be made more simply and more rapidly.

Hot-firing tests of the entire engine are usually preceded by tests of the separate assemblies under more difficult operating conditions than the normal operating regime in the engine (such as, for example, with regard to load, operating time, etc.). In these tests, we must be particularly careful not to destroy the assemblies, since they are always designed and manufactured to operate with a small strength safety factor for the purpose of reducing weight. At first, an engine chamber can be tested with water cooling and then with cooling by means of the propellant component selected for this purpose.

The first test-firings of an engine are of short duration (several seconds) and are followed by careful inspection of all the elements and assemblies, either partially or entirely dismantled. The specific

programs for these tests depend on the features and the designation of the ZhRD. We usually introduce many changes based on the results of the previous tests during the final tests of the assembled engine.

An engine that has been brought to the given operating parameters by the designer is presented to the departmental commission for hot-firing tests. The basic purpose of these tests is to check the conformity of the actual engine operating parameters with the technical aspects of its construction. In these tests particular attention is devoted to the operational features of the engine.

If the results of these tests are favorable, the engine is presented to a special commission for static firing and flight tests. During these tests we check the basic and operational characteristics of the engine and make recommendations concerning the feasibility of placing the engine in series production in accordance with the results of the tests.

Proving-ground flight tests of an engine installed in a corresponding weapon are performed under conditions that are quite different from those of static tests. Here the engine begins to operate for the first time under the effect of gravity, which can disrupt propellant-component feeding to the combustion chamber and the operation of the valves in the fuel-feed and control systems.

We perform flight tests both for the purpose of the determination of engine characteristics under operating conditions and for the evaluation of the vibrational effect of engine operation on the instruments and on the entire structure of the weapon.

It is very difficult to obtain data concerning missiles in flight; we usually use a system of telemetric control for this purpose. In missile tests we should try to ensure that we obtain all the required data from each missile launching, since a missile is a

one-shot object. Data concerning the operation of an aircraft engine in flight can be recorded by conventional automatic recording devices.

In most cases, ZhRD are used in large and expensive rockets for which special flight tests to check reliability are often barred because of the enormous cost. For this reason, in most cases the designer has no opportunity to obtain information on the way various elements of the engine operate under various real flight conditions. We can evaluate the surrounding medium in which a ZhRD and its elements must operate only approximately before the flight tests. Also, the corresponding telemetric information concerning engine operation during a flight test cannot always be obtained. Besides this, in each new case of the use of an engine in rockets, the ambient flight conditions usually vary.

Sometimes we can resolve this difficulty by the use of a ZhRD in an aircraft, for flight tests of an engine in an aircraft are not so limited with respect to cost; a piloted aircraft is an economical flying laboratory, in which the separate units and assemblies can be studied for the purpose of improving them under real operating conditions.

It is feasible to use sleds for natural flight tests of engines for objects operating at supersonic flight speeds (Fig. 13.1).^{*} This method of testing engines and missiles is gaining ever increasing importance, since at the present time natural tests of objects in wind tunnels at supersonic speeds is practicable only for small objects. When computing flight trajectories, especially for long-range ballistic missiles, we must have all aerodynamic characteristics that can be obtained by sled tests.

As we can see, the development of each engine assembly as a ^{*}Jet Propulsion, 1956, No. 2.

whole from the prototype to the series model is a long and a very difficult process. This is particularly true of the engine chamber because of the necessity of burning great per-second flow rates of fuel efficiently within a small volume. Consequently, we are not always successful in designing and fabricating any engine assembly (the chamber, the turbine, or even the simplest valve) in such a way that it satisfies the requirements imposed, without experimental improvements.



Fig. 13.1. Sled for natural tests of ZhRD.

The task of the design and the perfection of a ZhRD with a thrust of several hundred tons is particularly difficult. At the contemporary level of development in reaction engineering, we conceive of such an engine as being multi-chambered.* It could be a "cluster" of a certain number of larger or smaller chambers with independent fuel-feed systems, or one or several "clusters" of multi-chamber engines with a common feed system for several chambers, i.e., with a common TNA and a common gas generator.

Because the development of a ZhRD is usually associated with the development of new forms of armament, there are no accurate data con-
*Aviation Daily, Vol. 114, No. 35, 1958.

cerning the newest types of engines for long-range and super-long-range missiles. However, reports published in the foreign press concerning, for example, the construction of test stations for ZhRD permit us to assume that engines with a thrust of 200 tons and more have already been developed. We can also assume that a further increase in ZhRD thrust will be attained by means of the use of "clusters" of engines operating in unison. Therefore, we could develop engines with a thrust of several hundred tons in a single unit, on the basis of existing chambers with thrusts of 20-100 tons. According to data from the American press,* the USAF has ordered a ZhRD with a thrust of 450 tons from the firm "North American" and has been conducting studies on the construction of a multi-chamber engine with a thrust of 700 tons since 1954.

In industrial series production, every engine undergoes brief hydraulic, pneumatic, and production hot-firing tests on a stand, in accordance with special programs. The final tests are performed for the determination and the refinement of the basic rating-plate data for the engine.

If the fabrication of the engine chambers is of good quality, about 5-10% of the fabricated batch must pass through production test-firings. If the production of engines is properly organized, this form of chamber tests should be entirely unnecessary. Besides, the testing of chambers of great thrusts is quite expensive.

Therefore, it is advisable to limit static tests for engines with particularly simple designs and short one-shot service life to the checking of the operation of the electrical and the pneumatic systems.

Aircraft ZhRD undergo about the same tests as conventional turbo-
*Interavia, No. 4038, 1958.

jet engines. We test each assembly for its entire thrust range and check the fuel ignition and combustion and the operating characteristics in order to ensure that they satisfy the technical conditions. We also perform tests under special conditions, such as, for example, testing the ignition system under high-altitude flight conditions. In tests of the Me-163, the Germans filled the fuel tanks with water and supplied the turbopump assembly with steam from an external generator. By this means it was possible to check the operation of the valves without using expensive fuel.

We can also carry out static hot-firing tests of an engine in accordance with a tremendous variety of programs entirely for the purpose of research (to study fuel-combustion cycles, to determine the value of P_{ud} as a function of α , or to study economy of operation in corresponding regimes to check the efficiency of methods for the atomization of propellant components, etc.).

Special experimental installations for experimental checks of theoretical computations of the specific thrust developed by an engine, operating on various fuels, are often set up.

Considering the difficulties encountered in preparing the fuels under investigation in large enough quantities and in order to reduce the expenditures for the experiments to the minimum, we have these installations made to develop low thrust (of the order of 100-250 kg). In order to use the results of the experiments for an objective evaluation of the efficiency of the different fuels under investigation, the chambers of experimental installations are made for high pressures (within the limits of 20-60 atm abs), since the completeness of fuel combustion increases in direct proportion to the pressure in the combustion chamber. The use of high pressures for fuel combustion gives rise to extremely rigid requirements for the

chamber-cooling system. Water, which has good cooling properties, often serves as a cooling agent in these cases.

Hot-firing tests of engines require special experimental stands and accurate measuring equipment.

The structure, equipment, and methodology for these stands and the duration of the tests depend on the type of engine and the designation of the hot-firing tests in each specific case. Since engines developing great thrusts have enormous per-second propellant-component flow rates, stands and measuring equipment for these engines are designed and constructed in such a way as to provide for completion of tests and measurements within the shortest possible time.

Either open or closed stands are built for hot-firing tests of engines developing comparatively small thrusts; sometimes the fuel tanks in these stands are partitioned from the test cell or, for the purpose of safety, the tanks may be separated from the cell by a wall reinforced with brick or concrete. In these stands, we can control and observe engine tests from small observation ports (usually made of plexiglas); from "pyroscopes" or a system of mirrors; from an adjacent compartment separated from the test cell by an armored wall; or from a concrete bunker located at some distance from the stand. A pit filled with water for dilution of propellant components can be dug below the stand.

We can build special open or closed test stands for tests of medium-thrust engines. In the first case, the stand is usually dug in the earth and surrounded by an earth revetment. A light shed is often built to protect the stand and the measuring equipment above the stand. In the second case, each firing pit (cell) of the stand is surrounded by concrete walls on three sides and covered by a roof. The cell has two compartments: one for installation of all the control and guidance devices and the other for the propellant-component tanks.

We often use a pressurized fuel-feed system for simplicity and

ease in control of experiments. A compressed gas (air or nitrogen) under a pressure of about 250-300 kg/cm² is fed through a system of "plumbing" from flasks located in a different compartment through reduction valves into the control room and then through other valves into the fuel tanks. A sprinkler system is installed in case of engine explosion or a fire in the test cell; when the sprinkler system is turned on, water immediately floods the entire apron and then drains into a sump.

The instrument panel is usually very simple and is installed in such a way as to make it convenient for the operator to control the instruments. Here, one of the main precautionary measures is to prevent valves and other electrically controlled equipment from being switched on accidentally. For this purpose, electric power is fed to the control panel through a fuse box equipped with a demountable "safety link" that has male plugs at each end. These plugs are inserted into rosettes that are so arranged that the instrument panel is switched on only at a certain (correct) position of a switch controlled by the person responsible for conducting the engine test.

The arrangement of the equipment in these stands depends on the type of test, but the engine is always mounted at the open end of the cell in order to prevent great destruction in case of an explosion. If a measurement of engine thrust is not required during the test, the stand can be of simple rigid construction; otherwise, a stand permitting some displacement of the engine is required.

In these cases, the test stand is usually designed as a movable parallelogram (Fig. 13.2). A fixed parallelogram is more complex, but has the advantage that engine thrust can be measured at any position of the movable [sic] parallelogram unlike a movable [sic] parallelogram, in which any displacement in the line of thrust transmission makes a

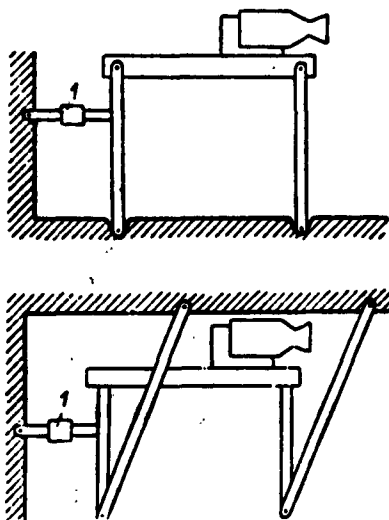


Fig. 13.2. Movable parallel-ogram for hot-firing tests of ZhRD.

new thrust calibration necessary.

A contemporary station for tests of ZhRD developing great thrusts may include:

1. A test cell (or sometimes several cells), occupying a special building and consisting of a special bench for installation and testing of an engine, and of instruments and equipment for measurement of thrust, per-second propellant-component flow rates, pressures, temperatures, etc.
- The fuel tanks and certain instruments and equipment are often installed in a special compartment of the test cell.
2. The control room for engine tests, which is often a separate building reinforced with concrete or brick and contains the instruments and control devices; a system for communications between the operator and the servicing personnel who work in the test cell during installation, checking, and preparation of the engine for tests and during dismounting of the engine after tests.
3. The auxiliary building of the station, in which the engine is prepared for tests (the technical condition of the engine, the documentation, etc. are checked).
4. The machine shop, which contains equipment for servicing and repairing the test station and the engine itself.
5. Warehouses for storage of propellant components and other liquids used in engine tests (these warehouses are located at some distance from the test cell).
6. The personnel building of the station for engineering, technical

and servicing personnel.

Other variations and construction plans for test stations are also possible.

As a rule, test stations for ZhRD developing great thrusts are located at a great distance from densely populated areas. Local relief is often used for convenience in the location of a test station.

A test stand of special construction is required for tests of engines intended for small guided missiles, in which the chamber and the fuel tanks are one unit (Fig. 13.3). In this case, a possible explosion during engine tests would be more powerful because of the great amount of fuel in the chamber.

We must pay particular attention to the safety of the servicing personnel when designing a station for testing ZhRD. Care in the handling of propellant components is most important, since many of them are toxic and noxious to the human organism. This is especially true of nitric acid and hydrogen peroxide. The danger involved in handling liquid oxygen is also well known.

Servicing personnel must be in bunkers separated from the test cell during engine tests. A test station is always supplied with reliable firefighting equipment.

As we have already mentioned above, the test-cell compartment has concrete or reinforced-brick walls on all sides except the side from which we observe the engine tests and from the open side provided for escape of exhaust gases; the cells are built in this way so that safety precautions will not interfere with the experiment being carried out. The control room for engine tests is located close to the test cell (often on the left side of the cell). The control room has several inspection holes in the test-cell side for visual observation of the testing process. The panes of these sight holes are made of rather

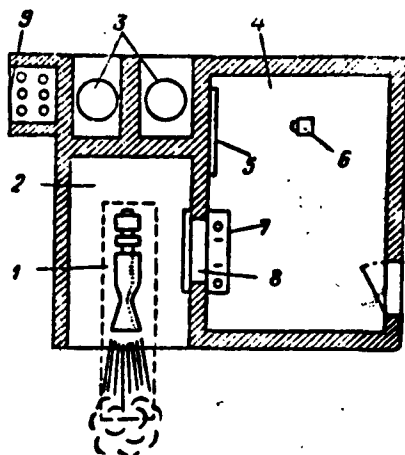


Fig. 13.3. Schematic plan of a station for firing tests of small engines. 1) drainage sump; 2) test cell; 3) fuel tanks; 4) control room; 5) instrument panel; 6) camera for photographing instrument readings during engine tests; 7) control panel; 8) device for indirect observation of engine behavior during tests or armored window (with a thick pane made of plexiglas) for visual observation; 9) flasks of compressed gas.

thick plexiglas.

The engine is started by remote control.

The organization of static tests provides for strict observation of safety precautions. The servicing personnel are instructed in detail concerning the rules of procedure and the sequence of operations is regulated. The operator gives a signal (usually a siren) before the engine is started to warn all hands that hot-firing engine tests are beginning.

The following engine parameters are usually measured in hot-firing

static engine tests:

- 1) the absolute engine thrust;
- 2) the per-second flow rates of combustible, oxidizer, and auxiliary working fluids to the combustion chamber;
- 3) the pressure of the combustible and the oxidizer to the injectors in the pressurized and pump-fed "plumbing";
- 4) the pressure in the combustion chamber;
- 5) the temperature of the propellant components at the inlet to the engine and the temperature of the cooling agent at the inlet to and the outlet from the chamber;
- 6) the temperature of the gas in the combustion chamber and of the walls of the inner combustion-chamber and nozzle liners;
- 7) the pressure and the velocity of the gases at the outlet from

the nozzle;

8) the chemical composition of the products of fuel combustion.

We measure the parameters enumerated above as the engine is started and stopped as well as during the steady-state engine operating regime.

At the present time we can measure thrust and flow rate and pressure of liquid and gases with a sufficient degree of accuracy.

Spring dynamometers, hydraulic or pneumatic dynamometers, or pickups of the tensometer type can be used as instruments for the measurement of thrust. We often use a dynamometer installation for the measurement of thrust; this consists of a hinged parallelogram from which thrust force is transmitted to a pendulum dynamometer.

As we have already mentioned above, the conventional design of a bench for the installation of an engine and the measurement of its thrust is a movable or a fixed parallelogram, or a cradle suspended on elastic steel bands. In these test-stand installations thrust force is transmitted directly to a thrust transmitter — a dynamometer (Fig. 13.4) or an instrument of some other type. The pressure in the dynamometer is measured by a first precision class manometer. The accuracy of thrust measurement by means of the elastic elements and the diaphragm of the flow dynamometer usually does not exceed 0.5% at an error in the manometer (that measures the pressure in the dynamometer) of no more than 0.35%. The calibration of a dynamometer is usually performed with the aid of standard loads and an articulated lever.

Test stands are so equipped as to permit the installation and the testing of an engine within the shortest time. Sometimes it becomes necessary to measure the lateral components of thrust or even the torque developed by the gas rudders of an engine chamber. This requires

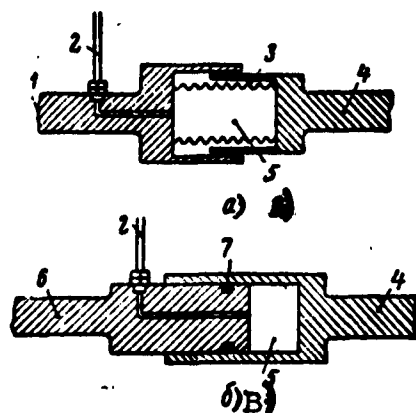


Fig. 13.4. The dynamometer — a thrust transmitter for a test stand. 1) fixed element; 2) lead to manometer; 3) diaphragm; 4) movable element; 5) dynamometer chamber; 6) fixed element; 7) packing.

a very complex measurement installation resembling the aerodynamic balances.

The measurement of working-fluid flow rates during engine tests is a rather complex task. Propellant-component flow rates are often determined by means of throttle plates.

In this case we ordinarily use differential mercury manometers,

which are the most accurate and re-

liable among instruments of this type. The throttle plates are designed so that the height of the mercury in the differential manometer is about 600-1200 mm; this permits making readings with an accuracy of 0.2-0.3%.

We can successfully use a rotary flow meter (Fig. 13.5) for the measurement of the flow rate of liquids, including those that cause corrosion, at various temperatures (from the temperature of liquid oxygen up to several hundred degrees) and at various pressures. A flow meter consists of three basic parts:

1) the flow meter pickup, installed in the "plumbing"; electric pulses are generated in the pickup with a frequency proportional to the flow rate of the liquid in the "plumbing";

2) an electronic relay that converts the electrical pulses into direct current proportional to the frequency;

3) an indicator of standard type representing a one-milliampere milliammeter, selected in accordance with the characteristics needed; the scale can be graduated in any sort of units.

A flow-meter receiver is a tube inside of which a four-vaned screw

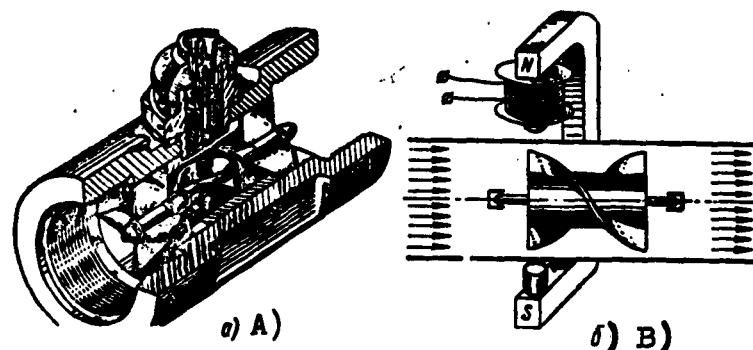


Fig. 13.5. Basic diagram of a rotation flow meter A) overall view; B) turbine.

rotor is located. One of the vanes of this rotor has a magnetic insert; the opposite vane is counterbalanced in the corresponding way.

A flow-meter inductor is a coil with an iron core located in a casing that is screwed into the receiver tube in such a way that the coil lies within the field of the rotor magnet.

A signal pulse is induced within the coil at every revolution of the rotor; the frequency of pulses is proportional to the flow rate of the liquid. The pulse is amplified and fed into the pulse-counter circuit.

The flow rate is measured in units of volume or, if the specific weight of the liquid remains constant, in units of weight. If the indicator of the flow meter is calibrated in weight units, variations in the specific weight of the liquid will cause an error in the flow-rate readings. In such cases we can use different methods of calibration.

The determination of per-second propellant-component flow rate by the method of reading the level in the test-stand tanks before and after the engine is started is seldom used, since the readings given by this method during the period of nonsteady engine operation are distorted.

In hot-firing tests of ZhRD, the mean square accuracy in the measurement of thrust and of the per-second flow rates of the combustible and the oxidizer must not exceed 1% of the measured magnitude.

Pressures are the most important working parameters of the engine. We often measure pressure with first precision class manometers. Any system of measurement readings based on mechanical motion has one very serious shortcoming: unsatisfactory frequency characteristics. For example, a Bourdon diaphragm gauge indicates only the mean pressure at oscillations with a frequency above 1-2 cps. We measure small excess pressures or a vacuum (in the nozzle outlet section) with a mercury vacuum manometer. Pickups are also used to measure pressures (Fig. 13.6)*. They operate on the principle of the conversion of the work performed by pressure of the liquid or the gas into an electrical signal which, in turn, is transformed, amplified, and recorded. The most common of these is the carbon pickup, whose sensing element is composed of special carbon discs that change their electrical conductivity as a function of the load developed by a diaphragm.

Pickups operating on the principle of a variation in capacitance are also used. In these, the pressure on a diaphragm changes the volume between the diaphragm and an immovably fixed plate. This change in capacity varies the strength of the signal which is transmitted to an instrument with fixed frequency modulation. If the pickup must operate in high-temperature gases, it is cooled by water. The pickup must be strong and capable of withstanding the high shock loads obtained during the starting of an engine; it must operate reliably without errors; it must not be sensitive to temperature variations and must provide for a linear interdependence between the pressure and the thrust of the engine.

Since an engine is usually designed and constructed to operate with a minimum strength safety factor for its separate parts, the temperatures of the working fluids are very important for an engine.

We can measure the temperatures of the propellant components and

* Ekspress-Informatsiya, AN USSR, No. 17, ADS-67, 1958.

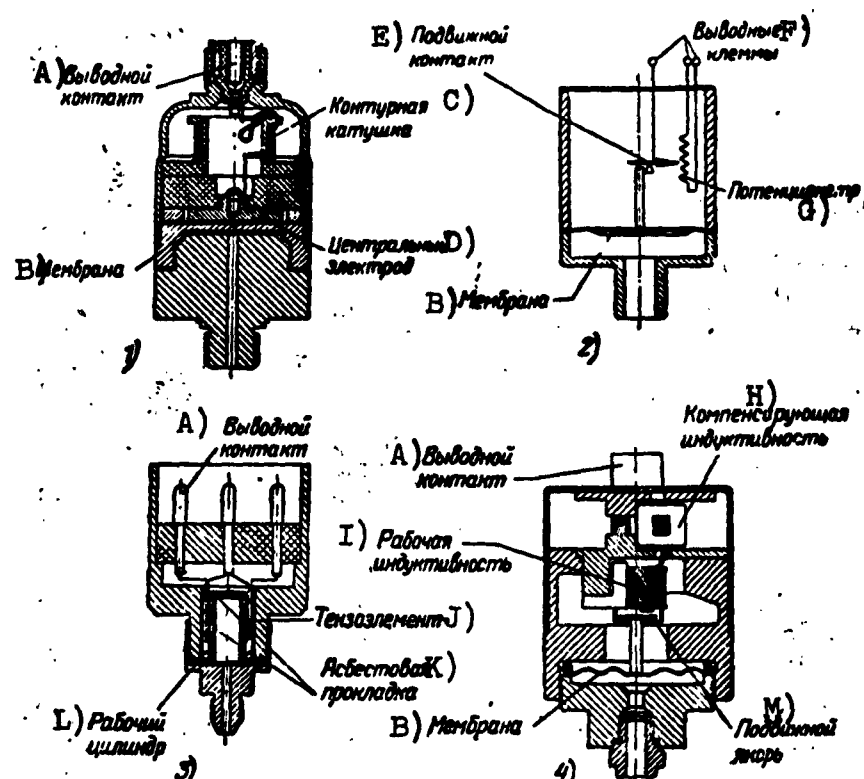


Fig. 13.6. Schematic cross section of pressure pickups. 1) capacity pickup; 2) potentiometer pickup; 3) tension pickup; 4) induction pickup. A) lead contact; B) diaphragm; C) circuit coil; D) central electrode; E) slide contact; F) lead terminals; G) potentiometer; H) compensating inductance; I) working inductance; J) tension element; K) asbestos packing; L) working cylinder; M) movable armature.

the temperatures of the inner-liner walls throughout the chamber by the use of thermocouples. We place these thermocouples in the liner in advance in order to measure inner chamber-liner temperatures. However, these measurements are not very accurate, since a considerable temperature difference occurs across the liner and the thermocouple has dimensions commensurate with the thickness of the liner.

We often assume that the temperature of the propellant components at the engine is equal to the temperature of the liquid in the tank, since the temperature in the "plumbing" before the engine is started differs very little from the temperature of the compartment in which the tanks are located. We measure the temperature of the coolant at the outlet from the cooling jacket of the chamber by means of thermocouples.

The measurement of the gas temperature at the outlet from the

engine-chamber nozzle is a complex problem. The high temperature and the great velocity of the gas in this section of the nozzle make these measurements inaccurate and difficult to obtain. We use optical pyrometers for this purpose. We can use the spectroscopic method, based on the Doppler effect, to determine the temperatures and exhaust velocities of the gases.

The velocity of the gas stream in the outlet section of the engine-chamber nozzle is a variable across a cross section of the nozzle. Therefore, it is easy to determine the mean effective velocity for the exhaust gases of a given ZhRD nozzle in accordance with the measured thrust and the per-second fuel-flow rate to the combustion chamber.

All measuring instruments are usually calibrated just before and immediately after the engine is started in order to eliminate any deviation from the readings of the control instrument.

At the station, we customarily use highly sensitive electronic equipment with automatic registration of instrument readings (by photography, recording, etc.) with a simultaneous notation of time for the purpose of studying the nature of the rapid cycles occurring in an engine during starting, operation, and stopping.

The instruments are usually grouped on one panel and the readings are photographed at fixed intervals of time. With such a method of recording the readings, we can use instruments of the ordinary type and read directly from a photographic film without deciphering. Some time is required to develop the film, to plot the results of the experiment on a diagram and to analyze the results; this is a real shortcoming when the results of the analysis are urgently needed to correct the conditions for the next experiment.

For the most important measurements, we often use devices operating in parallel with direct recording of the readings that can be processed

and studied after the engine test. At the present time industry is producing electronic recording devices that permit us to record the readings of as many as 50 information channels simultaneously.

For some time past we have been working towards the introduction of computers into test-stand measurement systems that would permit us to obtain processed data immediately during engine tests.

Finally, we should mention that an experienced test engineer can judge engine operation, fuel-mixture ratio, fuel-flow rate, injector-head operation, stability or instability of engine operation in this or that regime, etc., by the nature of the flame and the noise of the engine as it operates.

If the head operates well and the chamber volume is appropriate, fuel combustion is almost entirely completed in the chamber and the flames at the outlet from the nozzle are short. Otherwise, fuel combustion can continue even behind the chamber nozzle. Different maladjustments in head operation can be detected from the nature of the flame behind the nozzle. For example, light or dark streaks appear in the flame, depending on the regime and the operating conditions of the engine, when the chamber-head injectors are partially clogged.

Photographs of the flame behind the engine-chamber nozzle permit us to control the instrument readings during the engine test. Therefore, we usually photograph the flames behind the chamber nozzle during a test and subsequently we use these photographs as auxiliary material to evaluate the quality of engine operation.

We sometimes analyze gases taken from the rear of a chamber nozzle for a detailed study of the operating characteristics of an engine-chamber head. However, it is very difficult to take samples of gases because of their high temperatures and velocities. In order to obtain a complete picture of the composition of products of fuel combustion in

an engine-chamber nozzle, we must take a number of samples at different places across and along the nozzle. Probes cooled with water can be used to take samples.

SECTION 3. PROCESSING DATA FROM HOT-FIRING STATIC TESTS OF AN ENGINE

We process and analyze the data from static test firings of a ZhRD and measure the basic dimensions of the chamber after tests in the appropriate manner.

We construct the throttle characteristics of the engine in accordance with the values of P , G_s , and p_k that were measured in the experiments. We usually draw a curve showing P , G_s , and P_{ud} as functions of p_k ; since the basic parameter characterizing the engine operating regime is the gas pressure in the combustion chamber, it is convenient both for computing the characteristics and for controlling engine operation during tests on the stand and in flight. These curves permit us to compare the results of the separate startings of the engine; if we obtain noncorresponding data, these curves make it possible for us to ascertain which of the parameters was improperly measured during the experiments.

We usually test one-regime engines at constant values of p_k and χ .

To avoid accidental errors at multiregime static test-firings of an engine, which are possible when the engine is stopped and again started, it is feasible to take the characteristics of the engine during continuous operation. In this case, the value of p_k can be varied in accordance with a fixed program, such as, for example, at first it is increased by stages and then decreased in the same sequence; a coincidence of measurement results from the appropriate instrument readings at a uniform value of p_k permits us to judge the quality of engine operation.

As we plot the experimental points of P_{ud} on a curve, we must not

forget the possibility of considerable deviation in specific thrust at starting in cases of variable values of α , since P_{ud} , as a function of α , is a maximum curve. To avoid additional scattering of the points because of the affect of α on the magnitude of P_{ud} , we must limit the magnitudes of P_{ud} to fixed limits of α ; for example, at a given $\alpha = 0.75$ we must limit the values of $\alpha = 0.70-0.80$.

We usually analyze the degree of perfection of engine combustion-chamber and nozzle operation by a comparison of the actual values of P_{ud} , β , K_p , etc., with the theoretical values of $P_{ud.t}$, β_t , $K_{p.t}$, etc.

The theoretical characteristics of the fuel used in the engine and of the combustion process under appropriate conditions can be taken from the tables or the curves or computed in accordance with the thermodynamic computations for the engine chamber, assuming that there are no additional losses of energy in the burning fuel, except those due to gas dissociation.

To evaluate the completeness of fuel combustion in the combustion chamber of the engine being tested, we can use the parameter

$$\beta = \frac{P_{ex} F_{ex}}{G_s}, \quad (13.1)$$

which consists of the quantities measured during the engine tests.

If the measured value of G_s is equal to the theoretical per-second fuel-flow rate G_{st} to the combustion chamber, we can express the physical completeness of fuel combustion in the engine in the form of the ratio of actual β and theoretical β_t impulses of the gas pressure in the combustion chamber, i.e.,

$$\frac{\beta}{\beta_t} = \frac{P_{ex}}{P_{ex.t}} = \eta_{P_{ex}}, \quad (13.2)$$

where p_k and $p_{k.t}$ are the measured and theoretical values of the gas pressure in the combustion chamber; and p_k is the pressure coefficient

for the gases in this combustion chamber.

Since, from the expression of the gas-pressure impulse $\beta = p_k F_{kr} / G_s$ in the combustion chamber we have $G_s = p_k F_{kr} \beta$, and from the equation for the thrust coefficient $K_p = P / p_k F_{kr}$ we find $P = K_p p_k F_{kr}$, we can express the actual specific thrust of the engine undergoing test by the formula

$$P_{ya} = \frac{P}{G_s} = \frac{K_p p_k F_{kr}}{p_k F_{kr} \beta} = \beta K_p. \quad (13.3)$$

On this basis, we can compare the quality of operation for different injector heads in the same chamber at the same pressure by means of

$$\frac{P_{ya1}}{P_{ya2}} = \frac{\beta_1}{\beta_2}, \quad (13.4)$$

where subscripts 1 and 2 refer to the first and the second engine-chamber heads tested.

This equation also permits us to control the accuracy of the measurement of thrust or gas pressure in the combustion chamber during an experiment by a comparison of the measured magnitudes with the data from other engine starts.

Energy losses in the gases in the engine-chamber nozzle as a consequence of an imperfect exhaust cycle (some nonuniformity in the cycle in the subcritical part of the nozzle, friction, noncoaxial velocities in the outlet section and compression waves) can be determined by a comparison of K_p and $K_{p.t}$, i.e.,

$$\frac{K_p}{K_{p.t}} = \eta_c, \quad (13.5)$$

here

$$K_p = \frac{P}{p_k F_{kp}} = \frac{P - F_g p_k}{p_k F_{kp}},$$

where φ_g is the nozzle-efficiency coefficient; and P is the measured thrust of the engine.

The value of K_p is a function of the geometric dimensions of the chamber and of the polytropic exponent \underline{n} for the expansion of the gases in the nozzle; the value of K_p is computed in accordance with the test data for the engine. The averaged value of \underline{n} can be determined from the curve in Fig. 3.9 as a function of the relative area $f_v = F_v/F_{kr}$ of the outlet section of the chamber nozzle and the values of p_k and p_v that were measured during the test (Fig. 13.7). At the present time this is the only method for the determination of \underline{n} and is entirely reliable.

We can determine the losses in specific thrust relative to the theoretical value of $P_{ud.t}$ on the basis of processed data from static hot-firing tests of an isobaric engine chamber by the use of the formula

$$\Delta\varphi_{ya} = 1 - \varphi_{ya} = 1 - \frac{P_{ya}}{P_{ya,t}}. \quad (13.6)$$

This loss in specific engine thrust at optimum chamber-nozzle operation (at $P_v = P_a$) [sic] depends on the energy losses in the burning fuel as a consequence of:

- 1) physical incompleteness of combustion

$$\Delta\varphi_{pe} = 1 - \varphi_{pe} = 1 - \frac{\beta}{\beta_r};$$

- 2) imperfect chamber-nozzle operation

$$\Delta\varphi_c = 1 - \varphi_c = 1 - \frac{K_p}{K_{p,t}};$$

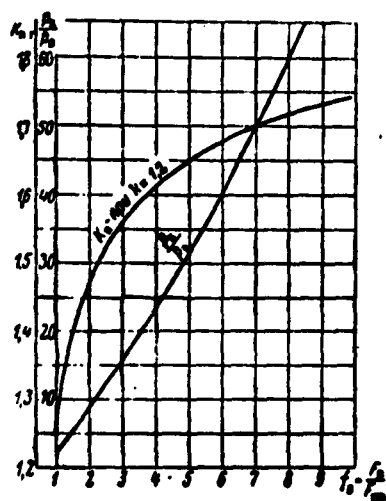


Fig. 13.7. K_p as a function of f_v at $k = 1.2$. 1) K_p at $k = 1.2$.

If $p_v \neq p_a$, a loss of energy in the burning fuel occurs as a consequence of the nonoptimum conditions of gas expansion in the chamber nozzle:

$$\Delta \varphi_a = 1 - \varphi_a = 1 - \frac{P_{ya}}{P_{ya, \text{opt}}},$$

where $P_{ud, \text{opt}}$ is the specific thrust of the engine chamber at optimum conditions of nozzle operation (at $p_v = p_a$), computed in accordance with the formula

$$P_{ya, \text{opt}} = \beta \varphi_c K_{n, T, \text{opt}} - f_{n, \text{opt}} \frac{F_{np} p_a}{G_s} = \beta \frac{K_n}{K_{n, T}} K_{n, T, \text{opt}} - f_{n, \text{opt}} \frac{F_{np} p_a}{G_s};$$

here $K_{p, t, \text{opt}}$ and f_v are the theoretical coefficient of thrust and the relative area of the nozzle outlet section, respectively (at $p_v = p_a$ the value of this quantity is taken from the curves in Figs. 3.9, 4.10, and 4.11).

We can also determine the value of p_v at known values of p_k , f_v , and k or n from the curve in Fig. 4.10.

A number of examples showing the processing of results from hot-firing tests of ZhRD are shown below.

3) transfer of heat from the chamber flame tube to the cooling water

$$\Delta \varphi_s = \Delta \varphi_{ya} - (\Delta \varphi_{p_k} + \Delta \varphi_c).$$

In some cases losses $\Delta \varphi_{p_k}$ and $\Delta \varphi_{p_s}$ are so small that it is difficult to determine them at the accuracy of the experiments.

Example 1. Determine the losses in specific thrust relative to $K_{p.t}$ for an engine chamber having a $d_{kr} = 222.7$ mm and a $d_v = 559$ mm, if the measured values of $P = 10,850$ kg, $G_s = 44.6$ kg/sec, $p_k = 20.5$ atm abs and $p_a = 1$ atm abs were obtained during static test-firings on a propellant of kerosene and liquid oxygen at $\alpha = 0.7$.

Solution.

1. In accordance with the data obtained during the chamber tests, we obtain;

a) specific chamber thrust;

$$P_{ya} = \frac{P}{G_s} = \frac{10850}{44.6} = 243 \text{ kg sec/kg};$$

b) specific pressure impulse

$$\beta = \frac{p_k F_{kp}}{G_s} = \frac{20.6 \cdot 389.21}{44.6} = 180.5 \text{ kg sec/kg};$$

c) thrust in space

$$P_s = P + F_a p_a = 10850 + 2440 \cdot 1 = 13290 \text{ kg};$$

d) thrust coefficient in space

$$K_s = \frac{P_s}{p_k F_{kp}} = \frac{13290}{20.6 \cdot 389.21} = 1.65;$$

e) specific thrust in space

$$P_{yLs} = \frac{P_s}{G_s} = \frac{13290}{44.6} = 298 \text{ kg sec/kg}.$$

2. From the curve

$$f_0 = f\left(\frac{p_s}{p_a}, k\right) \text{ at } f_0 = \frac{F_s}{F_{kp}} = \frac{d_v^2}{d_{kr}^2} = \frac{559^2}{222.7^2} = 6.3 \text{ and } k = 1.18$$

we find that $p_k/p_v = 41$, and then $p_v = (p_k/41) = (20.5/41) = 0.5$ atm abs (the value of $k = 1.18$ is taken from the table of data for the thermodynamic computation for the chamber at $p_v = 1$ atm abs).

3. In accordance with the table or the thermodynamic computation

for the chamber at the measured operating parameters (p_k and G_s) and $p_v = 0.5$ atm abs as computed earlier, we find that $P_{ud} = 257$ kg sec/kg, $\beta_t = 181$ kg sec/kg, and $K_{p.t} = 1.685$.

4. From the curve mentioned earlier, $f_v = (p_k/p_v, k)$ at optimum chamber-nozzle operation $p_k/p_v = 20.5$ and $k = 1.18$, we find that $f_{v.opt} = 3.8$ and $K_{p.t.opt} = 1.60$.

5. The specific thrust at an optimum chamber-nozzle operating regime (at $p_v = p_a$)

$$P_{ya.opt} = \beta \eta_c K_{n.t.opt} - \frac{F_{xp} p_a}{G_s} f_{n.opt} = \beta \frac{K_n}{K_{n.t}} K_{n.t.opt} - \frac{F_{xp} p_a}{G_s} f_{n.opt} = 180.5 \frac{1.65}{1.685} 1.60 - \frac{389.21 \cdot 1}{44.6} 3.8 = 251.4 \text{ kg sec/kg.}$$

6. The loss in specific engine-chamber thrust relative to the theoretical value of specific engine-chamber thrust

$$\eta_{ya} = 1 - \eta_{ya.t} = 1 - \frac{P_{ya}}{P_{ya.t}} = 1 - \frac{243}{257} = 1 - 0.945 = 0.055 = 5.45\%.$$

This loss in specific chamber thrust depends on:

a) physical incompleteness of fuel combustion

$$\Delta \eta_{p_x} = 1 - \eta_{p_x} = 1 - \frac{180.5}{181} = 1 - 0.997 = 0.003 = 0.3\%;$$

b) imperfect nozzle operation

$$\Delta \eta_c = 1 - \eta_c = 1 - \frac{K_n}{K_{n.t}} = 1 - \frac{1.65}{1.685} = 1 - 0.979 = 0.02 = 2\%;$$

c) nonoptimum nozzle operation

$$\Delta \eta_n = 1 - \eta_n = 1 - \frac{P_{ya}}{P_{ya.opt}} = 1 - \frac{243}{251.4} = 1 - 0.966 = 0.033 = 3.3\%.$$

which, in totality, comprises

$$\Delta \eta_{ya} = \Delta \eta_{p_x} + \Delta \eta_c + \Delta \eta_n = 0.3 + 2 + 3.3 = 5.6\%$$

(earlier $\Delta \eta_{ud} = 5.4\%$).

If part of the heat of the gases is transferred through the liner

to the flowing water used as a coolant during the chamber tests, in this case there is an additional loss in specific thrust that can be approximately determined in accordance with the formula

$$\Delta \varphi_{\text{oxl}} = \Delta \varphi_{\text{ya}} - (\Delta \varphi_{\text{p}_k} + \Delta \varphi_{\text{r}} + \Delta \varphi_{\text{a}}).$$

We can compute $\Delta \varphi_{\text{okhl}}$ more accurately with respect to the quantity of heat carried off by the flowing water used as a coolant during a fixed period of time as the engine is being tested in a given operating regime. For this purpose, it is necessary to measure the flow rate of the cooling water during the test and the water temperature at the inlet to and the outlet from the chamber coolant passage.

Example 2. Determine the polytropic exponent \underline{n} for the gas expansion in an engine chamber nozzle if the measured values of $p_k = 22$ atm abs and $p_v = 1$ atm abs were obtained during static hot-firing tests; the relative outlet area of the nozzle $f_v = 3.88$.

Solution.

1. We assume values of $\underline{n} = 1.1, 1.2, \text{ and } 1.3$ and compute the corresponding values of f_v in accordance with the formula

$$f_v = \frac{F_s}{F_{\text{np}}} = \frac{\left(\frac{2}{n+1}\right)^{\frac{1}{n-1}} \cdot \sqrt{\frac{n-1}{n+1}}}{\sqrt{\left(\frac{p_k}{p_v}\right)^{\frac{2}{n}} - \left(\frac{p_v}{p_k}\right)^{\frac{n+1}{n}}}}.$$

2. We construct a curve $f_v = f(n)$ in accordance with the result of the computations and in accordance with this curve, at $f_v = 3.88$, we find the sought value of $\underline{n} = 1.21$.

Example 3. Determine the loss in engine-chamber thrust relative to the rated value as well as the loss in rated theoretical thrust as a consequence of an angle $\alpha_v = 16^\circ$ for nozzle taper at the outlet section if the measured chamber thrust is ($P = 10$ tons) and the rated theoretical thrust is $P_t = 10.8$ tons at the corresponding measured operating parameters (p_k, p_v, α, G_s).

Solution.

1. Thrust loss in the experimental chamber relative to the rated theoretical value

$$\Delta P_{\text{th}} = 1 - \frac{P}{P_r} = 1 - \frac{10}{10,8} = 1 - 0,926 = 0,074 = 7,4\%.$$

2. Rated theoretical chamber thrust with allowance for loss in energy of gases as a consequence of angle of nozzle taper.

$$P_{r,\text{nos}} = P_{r,\text{pac}} = P_r \frac{1}{2} \left(1 - \cos \frac{\alpha_2}{2} \right) = 10,8 \frac{1}{2} \left(1 - \cos \frac{16^\circ}{2} \right) = 10,8 \cdot 0,995 = 10,746.$$

3. Loss in rated theoretical chamber thrust as a consequence of angle of nozzle taper at outlet section.

$$\Delta P_r = 1 - \eta_{\text{pac}} = 1 - \frac{P_{r,\text{nos}}}{P_r} = 1 - \frac{10,747}{10,8} = 1 - 0,995 = 0,005 = 0,5\%, \text{ i.e., } 0,054 \text{ tons.}$$

Example 4. Determine the velocity of gases flowing out of an engine-chamber nozzle if measured values of $P = 50$ tons, $p_v = 1,2$ atm abs, $p_a = 1$ atm abs, and $G_g = 218$ kg sec/kg were obtained during static test-firings; $F_v = 3200$ cm².

Solution.

1. Effective exhaust velocity

$$w_{\text{ef}} = \frac{P}{G_g} g = \frac{50000}{218} 9,81 = 2250 \text{ m/sec.}$$

2. Increase in velocity of gases flowing out of the chamber nozzle because of the static thrust number

$$\Delta w = \frac{F_v (p_v - p_a)}{G_g} g = \frac{3200 (1,2 - 1)}{218} 9,81 = 28,8 \text{ m/sec.}$$

3. Exhaust velocity of the gases in the outlet section of the chamber nozzle.

$$w_e = w_{\text{ef}} - \Delta w = 2250 - 28,8 = 2221,2 \text{ m/sec.}$$

We can also determine this velocity in accordance with the thrust formula in its general form, i.e.,

$$w_s = \frac{P - F_s(p_s - p_s)}{G_s} g = \frac{50000 - 3200(1.2 - 1)}{218} 9.81 = 2250 \text{ m/sec.}$$

Example 5. In approximation, determine the actual combustion temperature T_k of liquid ammonia and liquid fluorine at $p_k = 100$ atm abs and $\alpha = 1$ if $T_{k.t} = 4600^\circ \text{ K}$.

Solution.

1. We assume that $\varphi_{p_k} = 0.98$.
2. We determine the gas-temperature coefficient φ_T in the engine combustion chamber in accordance with the expression

$$\varphi_{p_k} = \frac{\beta}{\beta_T},$$

where

$$\beta = \frac{R_k T_k}{A_k} \text{ and } \beta_T = \frac{\sqrt{R_{k.t} T_{k.t}}}{A_{k.t}}.$$

Assuming (with a small error) that $R_k \approx R_{k.t}$ and $A_k = A_{k.t}$ we obtain

$$\varphi_{p_k} \approx \sqrt{\frac{T_k}{T_{k.t}}} = \sqrt{\varphi_T},$$

whence the gas-temperature coefficient will be

$$\varphi_T = \frac{T_k}{T_{k.t}} = \varphi_{p_k}^2 = 0.98^2 = 0.9604.$$

3. The actual temperature of the products of combustion for the given fuel is equal to

$$T_k \approx \varphi_T T_{k.t} = 0.9604 \cdot 4600 \approx 4418^\circ \text{ K}.$$

APPENDICES

APPENDIX I

ENERGY CONTENT OF PRODUCTS OF FUEL COMBUSTION I' kcal/kmole*

T°K	CO ₂	H ₂ O	CO	OH	NO	H ₂
300	-93990,0	-57731,4	-26375,1	10107,9	21645,2	46,9
400	-93049,8	-56919,4	-25676,8	10815,0	22359,2	741,4
500	-92021,8	-56087,9	-24970,6	11520,4	23082,3	1439,9
600	-90922,2	-55231,2	-24251,1	12226,2	23819,6	2139,0
700	-89763,3	-54341,9	-23514,8	12932,3	24575,0	2841,9
800	-88555,2	-53423,8	-22760,8	13643,8	25348,0	3547,8
900	-87304,7	-52478,7	-21990,0	14362,8	26138,9	4258,4
1000	-86022,6	-51505,4	-21204,1	15091,4	26944,4	4976,2
1100	-84709,6	-50505,1	-20404,6	15830,0	27762,9	5702,7
1200	-83371,8	-49477,2	-19593,3	16579,6	28592,1	6438,5
1300	-82013,4	-48423,2	-18771,7	17340,3	29430,5	7184,3
1400	-80637,2	-47344,3	-17941,0	18112,0	30276,7	7940,5
1500	-79245,6	-46242,2	-17102,6	18894,4	31129,6	8707,3
1600	-77840,4	-45118,3	-16257,6	19686,8	31988,3	9484,4
1700	-76423,0	-43974,5	-15406,8	20488,7	32852,0	10271,7
1800	-74995,0	-42812,4	-14550,7	21299,6	33720,1	11068,8
1900	-73557,4	-41633,7	-13690,1	22118,9	34592,1	11875,2
2000	-72111,2	-40440,1	-12825,5	22945,9	35467,6	12690,4
2100	-70657,4	-39232,8	-11967,3	23780,2	36346,2	13514,0
2200	-69196,4	-38013,1	-11085,9	24621,3	37227,6	14345,5
2300	-67729,0	-36782,1	-10211,5	25468,6	38111,6	15184,5
2400	-66255,6	-35540,7	-9334,4	26321,9	38997,9	16030,8
2500	-64776,6	-34289,9	-8454,9	27180,6	39886,4	16883,9
2600	-63292,4	-33030,3	-7573,2	28044,5	40776,8	17743,5
2700	-61803,2	-31762,6	-6689,5	28913,1	41669,1	18609,5
2800	-60309,3	-30487,6	-5803,9	29786,4	42563,2	19481,3
2900	-58811,1	-29205,7	-4916,6	30664,0	43458,9	20358,9
3000	-57308,8	-27917,4	-4027,6	31545,8	44356,3	21242,1

* G. B. Sinyarev and M. V. Dobrovol'skiy. Zhidkostnyye raketnyye dvigateli [Liquid-propellant Rocket Engines], Oborongiz [State Publishing House of the Defense Industry], 1957.

APPENDIX I (CONTINUED)

O ₂	N ₂	H	O	N	T° K
47,9	47,6	52115,6	59183,1	85591,6	300
758,0	744,9	52612,4	59701,0	86068,4	400
1489,1	1447,5	53109,2	60211,5	86585,2	500
2244,4	2160,5	53606,0	60717,8	87082,0	600
3022,3	2887,8	54102,8	61221,6	87578,8	700
3819,9	3631,1	54599,6	61723,7	88075,6	800
4634,0	4390,5	55096,4	62224,8	88572,4	900
5461,5	5165,0	55593,2	62724,9	89069,2	1000
6300,3	5953,2	56090,0	63224,5	89566,0	1100
7148,6	6753,7	56586,8	63723,7	90062,8	1200
8005,1	7565,1	57083,6	64222,5	90559,6	1300
8869,0	8386,0	57580,4	64721,0	91056,4	1400
9739,6	9215,1	58077,2	65219,3	91553,2	1500
10616,5	10051,6	58574,0	65717,4	92050,0	1600
11499,4	10894,5	59070,8	66215,4	92546,8	1700
12388,1	11743,0	59567,6	66713,2	93043,6	1800
13282,6	12596,6	60064,4	67211,1	93540,5	1900
14182,7	13454,7	60561,2	67708,8	94037,4	2000
15088,3	14316,8	61058,0	68206,6	94534,3	2100
15999,5	15182,5	61554,8	68704,4	95031,3	2200
16916,1	16051,5	62051,6	69202,3	95528,5	2300
17838,2	16923,4	62548,4	69700,4	96025,8	2400
18765,7	17798,0	63045,2	70198,6	96523,4	2500
19698,4	18675,1	63542,0	70697,1	97021,4	2600
20636,4	19554,5	64038,3	71195,9	97519,8	2700
21579,4	20436,0	64535,6	71695,0	98018,9	2800
22527,3	21319,5	65032,4	72194,6	98518,6	2900
23480,0	22204,7	65529,2	72694,8	99019,2	3000

APPENDIX I (CONTINUED)

T° K	CO ₂	H ₂ O	CO	OH	NO	H ₂
3100	-55802,6	-26623,4	-3136,0	32431,6	45255,1	22130,6
3200	-54292,7	-25324,1	-2244,0	33321,1	46155,4	23024,4
3300	-52779,2	-24020,0	-1350,7	34214,2	47057,1	23923,3
3400	-51262,4	-22711,4	-456,2	35110,7	47960,2	24827,2
3500	-49742,4	-21398,7	+439,6	36010,6	48864,5	25736,0
3600	-48219,2	-20082,2	1336,4	36913,7	49770,0	26649,6
3700	-46693,2	-18762,1	2234,4	37819,9	50676,7	27568,0
3800	-45164,4	-17438,7	3133,4	38729,1	51584,6	28491,0
3900	-43632,8	-16112,2	4033,4	39641,2	52493,6	29418,5
4000	-42098,6	-14782,8	4934,4	40556,0	53403,8	30350,5
4100	-40561,8	-13450,7	5836,3	41473,6	54315,0	31286,9
4200	-39022,6	-12116,1	6739,2	42393,8	55227,3	32227,6
4300	-37480,9	-10779,1	7643,0	43316,6	56140,6	33172,5
4400	-35936,8	-9439,9	8547,7	44241,9	57054,9	34121,7
4500	-34390,5	-8098,6	9453,2	45169,7	57970,2	35074,9
4600	-32841,8	-6755,2	10359,5	46099,9	58886,5	36032,1
4700	-31291,0	-5409,8	11266,5	47032,5	59803,8	36993,4
4800	-29737,8	-4062,4	12174,3	47967,5	60722,1	37958,6
4900	-28182,6	-2713,2	13082,9	48904,8	61641,4	38927,7
5000	-26625,0	-1362,0	13992,1	49844,3	62561,7	39900,5
5100	-25065,4	-9,0	14902,1	50786,0	63483,0	40877,2
5200	-23503,4	+1346,0	15812,7	51729,7	64405,3	41857,6
5300	-21939,4	2702,8	16724,1	52675,6	65328,5	42841,6
5400	-20373,0	4061,4	17636,1	53623,5	66252,6	43829,3
5500	-18804,6	5422,0	18548,7	54573,4	67177,7	44820,5
5600	-17233,8	6784,3	19462,1	55525,3	68103,8	45815,1
5700	-15661,0	8148,5	20376,1	56479,1	69030,9	46813,5
5800	-14085,8	9514,5	21290,7	57434,9	69958,9	47815,1
5900	-12508,6	10882,3	22206,0	58392,5	70887,8	48820,1
6000	-10929,0	12261,9	23121,9	59361,9	71817,7	49828,5

APPENDIX I (CONTINUED)

O ₂	N ₂	H	O	N	T° K
24437,8	23091,6	66026,0	73195,5	99520,9	3100
25399,1	23980,2	66522,8	73696,8	100023,3	3200
26365,2	24870,2	67019,6	74198,9	100528,0	3300
27335,5	25761,6	67516,4	74701,8	101033,9	3400
28309,7	26654,3	68013,2	75205,4	101541,6	3500
29287,8	27548,3	68510,0	75710,0	102051,4	3600
30269,5	28443,5	69006,8	76215,5	102563,3	3700
31254,7	29339,3	69503,6	76722,0	103077,7	3800
32243,2	30237,2	70000,4	77229,5	103594,8	3900
33234,8	31135,6	70497,2	77738,1	104114,7	4000
34229,4	32035,0	70994,0	78247,8	104637,7	4100
35226,8	32935,4	71490,8	78758,6	105164,0	4200
36226,8	33836,6	71987,6	79270,6	105693,8	4300
37229,3	34738,8	72484,4	79783,8	106227,3	4400
38234,1	35641,9	72981,2	80298,1	106764,6	4500
39241,2	36545,8	73478,0	80813,7	107305,9	4600
40250,4	37450,6	73974,8	81330,5	107851,4	4700
41261,6	38356,2	74471,6	81848,5	108401,1	4800
42274,6	39262,6	74968,4	82367,7	108955,4	4900
43289,3	40169,8	75465,2	82888,1	109514,1	5000
44306,7	41077,8	75962,0	83409,7	110077,6	5100
45323,7	41986,5	76458,8	83932,5	110645,8	5200
46343,1	42896,1	76955,6	84456,6	111218,9	5300
47363,9	43806,3	77452,4	84981,8	111796,9	5400
48386,0	44717,4	77949,2	85508,2	112380,0	5500
49409,9	45629,1	78446,0	86035,8	112968,1	5600
50433,8	46541,6	78942,8	86564,6	113561,4	5700
51459,4	47454,9	79439,6	87094,5	114159,9	5800
52485,9	48368,8	79936,4	87625,5	114763,7	5900
53513,4	49283,5	80433,2	88157,7	115372,8	6000

APPENDIX II

CONSTANTS OF CHEMICAL EQUILIBRIUM FOR PRODUCTS OF FUEL COMBUSTION*

$T^{\circ} K$	$K_{p1} = \frac{P_{CO} P_{O_2}^{1/2}}{P_{CO_2}}$	$K_{p2} = \frac{P_{H_2} P_{O_2}^{1/2}}{P_{H_2O}}$	$K_{p3} = \frac{P_{CO} P_{H_2O}}{P_{CO_2} P_{H_2}}$	$K_{p4} = \frac{P_{OH} P_{H_2}^{1/2}}{P_{H_2O}}$
300	$0,1825 \cdot 10^{-44}$	$0,1637 \cdot 10^{-39}$	$0,1115 \cdot 10^{-4}$	$0,5140 \cdot 10^{-46}$
400	$0,3895 \cdot 10^{-32}$	$0,5759 \cdot 10^{-29}$	$0,6764 \cdot 10^{-3}$	$0,1237 \cdot 10^{-33}$
500	$0,9886 \cdot 10^{-25}$	$0,1302 \cdot 10^{-22}$	$0,7593 \cdot 10^{-2}$	$0,3518 \cdot 10^{-26}$
600	$0,8624 \cdot 10^{-20}$	$0,2333 \cdot 10^{-18}$	$0,3696 \cdot 10^{-1}$	$0,3400 \cdot 10^{-21}$
700	$0,2900 \cdot 10^{-16}$	$0,2614 \cdot 10^{-15}$	$0,1109$	$0,1265 \cdot 10^{-17}$
800	$0,1277 \cdot 10^{-13}$	$0,5156 \cdot 10^{-13}$	$0,2475$	$0,6119 \cdot 10^{-15}$
900	$0,1445 \cdot 10^{-11}$	$0,3185 \cdot 10^{-11}$	$0,4537$	$0,7568 \cdot 10^{-13}$
1000	$0,6331 \cdot 10^{-10}$	$0,8728 \cdot 10^{-10}$	$0,7254$	$0,3604 \cdot 10^{-11}$
1100	$0,1389 \cdot 10^{-8}$	$0,1314 \cdot 10^{-8}$	$1,0560$	$0,8519 \cdot 10^{-10}$
1200	$0,1814 \cdot 10^{-7}$	$0,1267 \cdot 10^{-7}$	$1,4320$	$0,1193 \cdot 10^{-8}$
1300	$0,1591 \cdot 10^{-6}$	$0,8648 \cdot 10^{-7}$	$1,8400$	$0,1116 \cdot 10^{-7}$
1400	$0,1020 \cdot 10^{-5}$	$0,4501 \cdot 10^{-6}$	$2,2600$	$0,7603 \cdot 10^{-7}$
1500	$0,5087 \cdot 10^{-5}$	$0,1885 \cdot 10^{-5}$	$2,6990$	$0,4016 \cdot 10^{-6}$
1600	$0,2074 \cdot 10^{-4}$	$0,6615 \cdot 10^{-5}$	$3,1350$	$0,1726 \cdot 10^{-5}$
1700	$0,7131 \cdot 10^{-4}$	$0,2005 \cdot 10^{-4}$	$3,5550$	$0,6250 \cdot 10^{-5}$
1800	$0,2135 \cdot 10^{-3}$	$0,5383 \cdot 10^{-4}$	$3,9670$	$0,1964 \cdot 10^{-4}$
1900	$0,5687 \cdot 10^{-3}$	$0,1303 \cdot 10^{-3}$	$4,3630$	$0,5475 \cdot 10^{-4}$
2000	$0,1371 \cdot 10^{-2}$	$0,2892 \cdot 10^{-3}$	$4,7410$	$0,1378 \cdot 10^{-3}$
2100	$0,3035 \cdot 10^{-2}$	$0,5954 \cdot 10^{-3}$	$5,0970$	$0,3178 \cdot 10^{-3}$
2200	$0,6240 \cdot 10^{-2}$	$0,1149 \cdot 10^{-2}$	$5,4300$	$0,6797 \cdot 10^{-3}$
2300	$0,1203 \cdot 10^{-1}$	$0,2094 \cdot 10^{-2}$	$5,7460$	$0,1361 \cdot 10^{-2}$
2400	$0,2195 \cdot 10^{-1}$	$0,3634 \cdot 10^{-2}$	$6,0390$	$0,2573 \cdot 10^{-2}$
2500	$0,3810 \cdot 10^{-1}$	$0,6037 \cdot 10^{-2}$	$6,3110$	$0,4625 \cdot 10^{-2}$
2600	$0,6333 \cdot 10^{-1}$	$0,9649 \cdot 10^{-2}$	$6,5630$	$0,7947 \cdot 10^{-2}$
2700	$0,1013$	$0,1490 \cdot 10^{-1}$	$6,7940$	$0,1312 \cdot 10^{-1}$
2800	$0,1565$	$0,2233 \cdot 10^{-1}$	$7,0080$	$0,2091 \cdot 10^{-1}$
2900	$0,2345$	$0,3256 \cdot 10^{-1}$	$7,2020$	$0,3228 \cdot 10^{-1}$
3000	$0,3417$	$0,4628 \cdot 10^{-1}$	$7,3820$	$0,4841 \cdot 10^{-1}$

* G. B. Sinyarev and M. V. Dobrovol'skiy. Zhidkostnyye raketnyye dvigateli [Liquid-propellant Rocket Engines], Oborongiz [State Publishing House of the Defense Industry], 1957.

APPENDIX II (CONTINUED)

$K_{p4} = \frac{p_{NO}^2}{p_{N_2} p_{O_2}}$	$K_{p5} = \frac{p_{H_2}^2}{p_{H_2O}}$	$K_{p6} = \frac{p_{O}^2}{p_{O_2}}$	$K_{p7} = \frac{p_{N}^2}{p_{N_2}}$	$T^\circ K$
0,6653 · 10 ⁻³⁰	0,1813 · 10 ⁻⁷⁰	0,8191 · 10 ⁻⁸⁰	0,216 · 10 ⁻¹¹⁸	300
0,4898 · 10 ⁻²³	0,1811 · 10 ⁻⁵¹	0,3084 · 10 ⁻⁶⁸	0,3359 · 10 ⁻⁸⁷	400
0,2587 · 10 ⁻¹⁷	0,4899 · 10 ⁻⁴⁰	0,2944 · 10 ⁻⁴⁵	0,1879 · 10 ⁻⁶⁸	500
0,3648 · 10 ⁻¹⁴	0,2153 · 10 ⁻³²	0,1387 · 10 ⁻³⁶	0,6218 · 10 ⁻⁶⁴	600
0,6489 · 10 ⁻¹²	0,6425 · 10 ⁻²⁷	0,2240 · 10 ⁻³⁰	0,5633 · 10 ⁻⁴⁷	700
0,3163 · 10 ⁻¹⁰	0,8426 · 10 ⁻²⁸	0,1034 · 10 ⁻²⁵	0,3010 · 10 ⁻⁴⁰	800
0,6495 · 10 ⁻⁹	0,1369 · 10 ⁻¹⁹	0,4450 · 10 ⁻²²	0,5230 · 10 ⁻³⁵	900
0,7302 · 10 ⁻⁸	0,5148 · 10 ⁻¹⁷	0,3631 · 10 ⁻¹⁹	0,8239 · 10 ⁻³¹	1000
0,5277 · 10 ⁻⁷	0,6676 · 10 ⁻¹⁵	0,8820 · 10 ⁻¹⁷	0,2262 · 10 ⁻²⁷	1100
0,2752 · 10 ⁻⁶	0,3886 · 10 ⁻¹³	0,8630 · 10 ⁻¹⁵	0,1673 · 10 ⁻²⁴	1200
0,1112 · 10 ⁻⁵	0,1220 · 10 ⁻¹¹	0,4191 · 10 ⁻¹³	0,4503 · 10 ⁻²²	1300
0,3680 · 10 ⁻⁵	0,2356 · 10 ⁻¹⁰	0,1173 · 10 ⁻¹¹	0,5478 · 10 ⁻²⁰	1400
0,1039 · 10 ⁻⁴	0,3087 · 10 ⁻⁹	0,2113 · 10 ⁻¹⁰	0,3527 · 10 ⁻¹⁸	1500
0,2575 · 10 ⁻⁴	0,2944 · 10 ⁻⁸	0,2657 · 10 ⁻⁹	0,1354 · 10 ⁻¹⁶	1600
0,5738 · 10 ⁻⁴	0,2162 · 10 ⁻⁷	0,2486 · 10 ⁻⁸	0,3393 · 10 ⁻¹⁵	1700
0,1170 · 10 ⁻³	0,1277 · 10 ⁻⁶	0,1819 · 10 ⁻⁷	0,5961 · 10 ⁻¹⁴	1800
0,2213 · 10 ⁻³	0,6267 · 10 ⁻⁶	0,1080 · 10 ⁻⁶	0,7761 · 10 ⁻¹³	1900
0,3926 · 10 ⁻³	0,2631 · 10 ⁻⁵	0,5376 · 10 ⁻⁶	0,7829 · 10 ⁻¹²	2000
0,6595 · 10 ⁻³	0,9658 · 10 ⁻⁵	0,2299 · 10 ⁻⁵	0,6349 · 10 ⁻¹¹	2100
0,1057 · 10 ⁻²	0,3155 · 10 ⁻⁴	0,8624 · 10 ⁻⁵	0,4263 · 10 ⁻¹⁰	2200
0,1625 · 10 ⁻²	0,9313 · 10 ⁻⁴	0,2885 · 10 ⁻⁴	0,2429 · 10 ⁻⁹	2300
0,2410 · 10 ⁻²	0,2516 · 10 ⁻³	0,8738 · 10 ⁻⁴	0,1198 · 10 ⁻⁸	2400
0,3391 · 10 ⁻²	0,6284 · 10 ⁻³	0,2423 · 10 ⁻³	0,5206 · 10 ⁻⁸	2500
0,4840 · 10 ⁻²	0,1464 · 10 ⁻²	0,6215 · 10 ⁻³	0,2023 · 10 ⁻⁷	2600
0,6592 · 10 ⁻²	0,3207 · 10 ⁻²	0,1487 · 10 ⁻²	0,7114 · 10 ⁻⁷	2700
0,8786 · 10 ⁻²	0,6649 · 10 ⁻²	0,3345 · 10 ⁻²	0,2289 · 10 ⁻⁶	2800
0,1148 · 10 ⁻¹	0,1312 · 10 ⁻¹	0,7117 · 10 ⁻²	0,6797 · 10 ⁻⁶	2900
0,1472 · 10 ⁻¹	0,2475 · 10 ⁻¹	0,1441 · 10 ⁻¹	0,1879 · 10 ⁻⁵	3000

APPENDIX II (CONTINUED)

$T^{\circ}K$	$K_{p1} = \frac{P_{CO}P_{O_2}^{1/2}}{P_{CO_2}}$	$K_{p2} = \frac{P_{H_2}P_{O_2}^{1/2}}{P_{H_2O}}$	$K_{p3} = \frac{P_{CO}P_{H_2O}}{P_{CO_2}P_{H_2}}$	$K_{p4} = \frac{P_{OH}P_{H_2}^{1/2}}{P_{H_2O}}$
3100	0,4854	$0,6436 \cdot 10^{-1}$	7,5430	$0,7074 \cdot 10^{-1}$
3200	0,6744	$0,8770 \cdot 10^{-1}$	7,6900	0,1009
3300	0,9179	0,1173	7,8210	0,1410
3400	1,2280	0,1544	7,9410	0,1933
3500	1,6100	0,2000	8,0480	0,2601
3600	2,0810	0,2556	8,1430	0,3444
3700	2,6520	0,3222	8,2280	0,4492
3800	3,3340	0,4017	8,2990	0,5780
3900	4,1410	0,4951	8,3640	0,7343
4000	5,0870	0,6042	8,4180	0,9217
4100	6,1810	0,7303	8,4650	1,1450
4200	7,4420	0,8750	8,5060	1,4070
4300	8,8740	1,0400	8,5310	1,7130
4400	10,5000	1,2280	8,5570	2,0670
4500	12,5300	1,4370	8,5760	2,4750
4600	14,3600	1,6730	8,5880	2,9400
4700	16,6200	1,9340	8,5920	3,4680
4800	19,1100	2,2240	8,5920	4,0610
4900	21,8400	2,5430	8,5880	4,7290
5000	24,8300	2,8940	8,5780	5,4730
5100	28,0600	3,2780	8,5670	6,2980
5200	31,5800	3,6940	8,5490	7,2090
5300	35,3700	4,1480	8,5310	8,2130
5400	39,4100	4,6340	8,5040	9,3110
5500	43,7500	5,1600	8,4780	10,5100
5600	48,3700	5,7270	8,4450	11,8100
5700	53,2700	6,3330	8,4120	13,2300
5800	58,4800	6,9810	8,3770	14,7600
5900	63,9800	7,6700	8,3390	16,4000
6000	69,7400	8,4050	8,2980	18,1800

APPENDIX II (CONTINUED)

$K_{p4} = \frac{P_{NO}^2}{P_{N_2} P_{O_2}}$	$K_{p5} = \frac{P_{H_2}^2}{P_{H_2O}}$	$K_{p6} = \frac{P_{O_2}^2}{P_{O_3}}$	$K_{p7} = \frac{P_{H_2}^2}{P_{H_2O}}$	T° K.
0,1858 · 10 ⁻¹	0,4485 · 10 ⁻¹	0,2786 · 10 ⁻¹	0,4866 · 10 ⁻⁵	3100
0,2310 · 10 ⁻¹	0,7836 · 10 ⁻¹	0,5174 · 10 ⁻¹	0,1189 · 10 ⁻⁴	3200
0,2833 · 10 ⁻¹	0,1324	0,9253 · 10 ⁻¹	0,2751 · 10 ⁻⁴	3300
0,3431 · 10 ⁻¹	0,2170	0,1600	0,6064 · 10 ⁻⁴	3400
0,4115 · 10 ⁻¹	0,3459	0,2680	0,1278 · 10 ⁻³	3500
0,4882 · 10 ⁻¹	0,5374	0,4364	0,2587 · 10 ⁻³	3600
0,5736 · 10 ⁻¹	0,8186	0,6928	0,5042 · 10 ⁻³	3700
0,6677 · 10 ⁻¹	1,2120	1,0730	0,9491 · 10 ⁻³	3800
0,7720 · 10 ⁻¹	1,7630	1,6240	0,1731 · 10 ⁻²	3900
0,8851 · 10 ⁻¹	2,5190	2,4080	0,3063 · 10 ⁻²	4000
0,1008	3,5380	3,5050	0,5276 · 10 ⁻²	4100
0,1141	4,8890	5,0100	0,8857 · 10 ⁻²	4200
0,1283	6,6580	7,0480	0,1452 · 10 ⁻¹	4300
0,1436	8,9390	9,7540	0,2330 · 10 ⁻¹	4400
0,1598	11,8500	13,3100	0,3680 · 10 ⁻¹	4500
0,1770	15,5200	17,9800	0,5641 · 10 ⁻¹	4600
0,1952	20,0800	23,8300	0,8541 · 10 ⁻¹	4700
0,2143	25,7200	31,3200	0,1272	4800
0,2343	32,6200	40,7000	0,1863	4900
0,2553	40,9800	52,3400	0,2699	5000
0,2771	51,0100	66,6500	0,3828	5100
0,2997	62,9800	84,1000	0,5379	5200
0,3234	77,1400	105,2000	0,7484	5300
0,3478	93,7800	130,5000	1,0330	5400
0,3731	113,2000	160,6000	1,3890	5500
0,3988	135,7000	196,3000	1,8640	5600
0,4258	161,7000	238,1000	2,4750	5700
0,4533	191,5000	287,0000	3,2610	5800
0,4812	225,5000	343,8000	4,2560	5900
0,5100	264,0000	409,4000	5,5080	6000

APPENDIX III

COMMON LOGARITHMS FOR CONSTANTS OF CHEMICAL EQUILIBRIUM FOR PRODUCTS OF FUEL COMBUSTION*

T° K	$\lg K_{p1} = \lg \frac{P_{CO_2}^{1/2}}{P_{CO}}$	$\Delta \lg K_{p1}$	$\lg K_{p2} = \lg \frac{P_{H_2O}^{1/2}}{P_{H_2}}$	$\Delta \lg K_{p2}$	$\lg K_{p3} = \lg \frac{P_{CO} P_{H_2O}}{P_{CO_2} P_{H_2}}$	$\Delta \lg K_{p3}$	$\lg K_{p4} = \lg \frac{P_{CO} P_{H_2O}^{1/2}}{P_{H_2O}}$	$\Delta \lg K_{p4}$
300	-44.7389	12.3295	-39.7860	10.5464	-4.9529	1.7831	-46.2890	12.3814
400	-32.4094	7.4044	-29.2396	6.3542	-3.1698	1.0502	-33.9076	7.4539
500	-25.0050	4.9407	-22.8854	4.2534	-2.1196	0.6873	-26.4537	4.9852
600	-20.0643	3.5268	-18.6320	3.0494	-1.4323	0.4774	-21.4685	3.5706
700	-16.5375	2.6434	-15.5826	2.2949	-0.9549	0.3485	-17.8979	2.6846
800	-13.8941	2.0541	-13.2877	1.7909	-0.6064	0.2632	-15.2133	2.0923
900	-11.8400	1.6415	-11.4968	1.4377	-0.3432	0.2038	-13.1210	1.6779
1000	-10.1985	1.3412	-10.0591	1.1779	-0.1394	0.1633	-11.4431	1.3735
1100	-8.8573	1.1160	-8.8812	0.9838	0.0239	0.1322	-10.0696	1.1463
1200	-7.7413	0.9428	-7.8974	0.8343	0.1561	0.1085	-8.9233	0.9710
1300	-6.7985	0.8069	-7.0631	0.7164	0.2846	0.0905	-7.9823	0.8333
1400	-5.9916	0.6980	-6.3467	0.6220	0.3551	0.0760	-7.1190	0.7228
1500	-5.2936	0.6194	-5.7247	0.5452	0.4311	0.0652	-6.3962	0.6331
1600	-4.6832	0.5563	-5.1795	0.4817	0.4963	0.0546	-5.7631	0.5590
1700	-4.1469	0.4763	-4.6978	0.4288	0.5509	0.0475	-5.2041	0.4973
1800	-3.6706	0.4255	-4.2690	0.3841	0.5984	0.0414	-4.7068	0.4452
1900	-3.2451	0.3821	-3.8549	0.3461	0.6398	0.0360	-4.2616	0.4009
2000	-2.8630	0.3451	-3.5388	0.3136	0.6758	0.0315	-3.8607	0.3629
2100	-2.5179	0.3131	-3.2252	0.2856	0.7073	0.0275	-3.4978	0.3301
2200	-2.2048	0.2852	-2.9396	0.2606	0.7348	0.0246	-3.1677	0.3016
2300	-1.9198	0.2610	-2.6790	0.2394	0.7594	0.0216	-2.8661	0.2766
2400	-1.6586	0.2396	-2.4396	0.2204	0.7810	0.0191	-2.5895	0.2546
2500	-1.4191	0.2207	-2.2192	0.2037	0.8001	0.0170	-2.3349	0.2351
2600	-1.1984	0.2039	-2.0155	0.1889	0.8171	0.0150	-2.0998	0.2178
2700	-0.9945	0.1890	-1.8266	0.1755	0.8321	0.0135	-1.8820	0.2024
2800	-0.8065	0.1756	-1.6511	0.1637	0.8456	0.0119	-1.6796	0.1885
2900	-0.6299	0.1635	-1.4874	0.1528	0.8575	0.0107	-1.4911	0.1760
3000	-0.4684	0.1525	-1.3346	0.1432	0.8682	0.0093	-1.3151	0.1648

* G. B. Sinyarev and M. V. Dobrovolskiy. Zhidkostnyye raketnyye dvigateli [Liquid-propellant Rocket Engines], Oborongiz [State Publishing House of the Defense Industry], 1957.

APPENDIX III (CONTINUED)

$\lg K_M = \frac{P_{NO}^2}{P_N P_{O_2}}$	$\Delta \lg K_M$	$\lg K_{ps} = \lg \frac{P_H^2}{P_{H_2}}$	$\Delta \lg K_{ps}$	$\lg K_{ps} = \lg \frac{P_O^2}{P_{O_2}}$	$\Delta \lg K_{ps}$	$\lg K_{p'} = \lg \frac{P_H^2}{P_N}$	$\Delta \lg K_{p'}$	T° K
-30,1770 -22,3100 -17,5872	7,8670 4,7228 3,1492	-70,7414 -51,7421 -40,3099	18,9993 11,4322 7,6430	-80,0867 -58,5109 -45,5311	21,5758 12,9798 8,6731	-118,6656 -87,4738 -68,7259	31,1918 17,7479 12,5196	300 400 500
-14,4380 -12,1878 -10,4998 -9,1874 -8,1366	2,2502 2,6880 1,3124 1,0508 0,8590	-32,6669 -27,1921 -23,0744 -19,8636 -17,2883	5,4748 4,1177 3,2108 2,5753 2,1128	-36,8580 -30,6499 -25,9854 -22,3515 -19,4400	6,2081 4,6645 3,6339 2,9115 2,3855	-56,2064 -47,2492 -40,5214 -35,2815 -31,0841	8,9572 6,7278 5,2399 4,1974 3,4386	600 700 800 900 1000
-7,2776 -6,5604 -5,9540 -5,4342 -4,9836	0,7172 0,6064 0,5198 0,4506 0,3944	-15,1755 -13,4105 -11,9185 -10,6275 -9,5105	1,7650 1,4970 1,2860 1,1170 0,9794	-17,0545 -15,0640 -13,8777 -11,9307 -10,6752	1,9905 1,6863 1,4470 1,2555 1,0996	-27,6455 -24,7766 -22,3466 -20,2614 -18,4526	2,8689 2,4301 2,0851 1,8088 1,5842	1100 1200 1300 1400 1500
-4,5892 -4,2412 -3,9318 -3,6550 -3,4060	0,3480 0,3094 0,2708 0,2400 0,2252	-8,5311 -7,6652 -6,8941 -6,2029 -5,5798	0,8659 0,7711 0,6912 0,6231 0,5647	-9,5756 -8,6044 -7,7403 -6,9665 -6,2695	0,9712 0,8641 0,7738 0,6970 0,6311	-16,8684 -15,4694 -14,2247 -13,1101 -12,1063	1,3990 1,2447 1,1146 1,0088 0,9090	1600 1700 1800 1900 2000
-3,1808 -2,9760 -2,7892 -2,6180 -2,4606	0,2048 0,1868 0,1712 0,1574 0,1454	-5,0151 -4,5010 -4,0309 -3,5994 -3,2018	0,5141 0,4701 0,4315 0,3976 0,3674	-5,6384 -5,0643 -5,5398 -4,0586 -3,6157	0,5741 0,5245 0,4812 0,4429 0,4091	-11,1973 -10,3703 -9,6147 -8,9218 -8,2835	0,8270 0,7556 0,6829 0,6383 0,5995	2100 2200 2300 2400 2500
-2,3152 -2,1810 -2,0620 -1,9404 -1,8322	0,1342 0,1248 0,1158 0,1082 0,1012	-2,8344 -2,4938 -2,1772 -1,8821 -1,6064	0,3406 0,3166 0,2951 0,2757 0,2582	-3,2066 -2,8277 -2,4756 -2,1477 -1,8415	0,3789 0,3521 0,3279 0,3062 0,2866	-7,6940 -7,1479 -6,6404 -6,1677 -5,7261	0,5461 0,5075 0,4727 0,4416 0,4133	2600 2700 2800 2900 3000

APPENDIX III (CONTINUED)

$\lg K_{PI} = \frac{P_{PI}^2}{P_N P_{O_2}}$	$\Delta \lg K_{PI}$	$\lg K_{PS} = \lg \frac{P_{PI}^2}{P_{H_2}}$	$\Delta \lg K_{PS}$	$\lg K_{PM} = \lg \frac{P_{PI}^2}{P_{O_2}}$	$\Delta \lg K_{PM}$	$\lg K_{PT} = \lg \frac{P_{PI}^2}{P_{N_2}}$	$\Delta \lg K_{PT}$	$T^\circ K$
-1,7310	0,0946	-1,3482	0,2423	-1,5550	0,2688	-5,3128	0,3878	3100
-1,6364	0,0888	-1,1059	2,2278	-1,2862	0,2525	-4,9250	0,3645	3200
-1,5476	0,0830	-0,8781	0,2146	-1,0337	0,2377	-4,5605	0,3433	3300
-1,4646	0,0790	-0,6635	0,2025	-0,7960	0,2242	-4,2172	0,3239	3400
-1,3856	0,0742	-0,4610	0,1913	-0,5718	0,2118	-3,8933	0,3061	3500
-1,3114	0,0700	-0,2697	0,1812	-0,3600	0,2005	-3,5872	0,2898	3600
-1,2414	0,0660	-0,0885	0,1717	-0,1595	0,1899	-3,2974	0,2747	3700
-1,1754	0,0630	0,0832	0,1630	0,0304	0,1802	-3,0227	0,2609	3800
-1,1124	0,0594	0,2462	0,1550	0,2106	0,1712	-2,7618	0,2480	3900
-1,0530	0,0564	0,4012	0,1475	0,3818	0,1629	-2,5138	0,2361	4000
-0,9666	0,0538	0,5487	0,1405	0,5447	0,1552	-2,2777	0,2250	4100
-0,9428	0,0512	0,6892	0,1341	0,6999	0,1480	-2,0527	0,2148	4200
-0,8916	0,0488	0,8233	0,1280	0,8479	0,1413	-1,8379	0,2052	4300
-0,8428	0,0464	0,9513	0,1223	0,9892	0,1351	-1,6327	0,1962	4400
-0,7964	0,0444	1,0736	0,1171	1,1243	0,1292	-1,4365	0,1879	4500
-0,7520	0,0424	1,1907	0,1122	1,2535	0,1237	-1,2486	0,1801	4600
-0,7096	0,0406	1,3029	0,1075	1,3772	0,1186	-1,0685	0,1728	4700
-0,6690	0,0388	1,4104	0,1031	1,4658	0,1138	-0,8957	0,1659	4800
-0,6302	0,0372	1,5135	0,0991	1,6096	0,1092	-0,7298	0,1595	4900
-0,5930	0,0356	1,6126	0,0951	1,7188	0,1050	-0,5703	0,1533	5000
-0,5574	0,0342	1,7077	0,0915	1,8238	0,1010	-0,4170	0,1477	5100
-0,5232	0,0330	1,7992	0,0881	1,9248	0,0972	-0,2698	0,1423	5200
-0,4902	0,0316	1,8873	0,0848	2,0220	0,0935	-0,1270	0,1372	5300
-0,4586	0,0304	1,9721	0,0818	2,1156	0,0902	0,0102	0,1324	5400
-0,4282	0,0290	2,0539	0,0788	2,2058	0,0870	0,1426	0,1278	5500
-0,3992	0,0284	2,1327	0,0760	2,2928	0,0840	0,2704	0,1235	5600
-0,3708	0,0272	2,2087	0,0735	2,3768	0,0811	0,3939	0,1195	5700
-0,3436	0,0260	2,2822	0,0709	2,4579	0,0784	0,5134	0,1156	5800
-0,3176	0,0252	2,3531	0,0685	2,5363	0,0758	0,6290	0,1120	5900
-0,2924		2,4216		2,6121		0,7410		6000

APPENDIX III (CONTINUED)

T, K	$\lg K_{p1} = \lg \frac{p_{CO} p_{O_2}^{1/2}}{p_{CO_2}}$	$\Delta \lg K_{p1}$	$\lg K_{p2} = \lg \frac{p_{H_2} p_{O_2}^{1/2}}{p_{H_2O}}$	$\Delta \lg K_{p2}$	$\lg K_{p3} = \lg \frac{p_{CO} p_{H_2O}}{p_{CO_2} p_{H_2}}$	$\Delta \lg K_{p3}$	$\lg K_{p4} = \lg \frac{p_{O_2} p_{H_2O}}{p_{H_2O}}$	$\Delta \lg K_{p4}$
3100	-0,3139	0,1428	-1,1914	0,1344	0,8775	0,0084	-1,1503	0,1545
3200	-0,1711	0,1339	-1,0570	0,1265	0,8859	0,0074	-0,9958	0,1452
3300	-0,0372	0,1257	-0,9305	0,1191	0,8933	0,0069	-0,8506	0,1363
3400	0,0885	0,1183	-0,8114	0,1125	0,8999	0,0058	-0,7138	0,1290
3500	0,2068	0,1115	-0,6989	0,1064	0,9057	0,0051	-0,5848	0,1219
3600	0,3153	0,1052	-0,5925	0,1007	0,9108	0,0045	-0,4629	0,1154
3700	0,4235	0,0994	-0,4918	0,0957	0,9153	0,0037	-0,3475	0,1094
3800	0,5229	0,0942	-0,3961	0,0908	0,9190	0,0034	-0,2381	0,1040
3900	0,6171	0,0893	-0,3053	0,0865	0,9224	0,0028	-0,1341	0,0987
4000	0,7064	0,0847	-0,2188	0,0823	0,9252	0,0024	-0,0354	0,0940
4100	0,7911	0,0806	-0,1365	0,0785	0,9276	0,0021	0,0686	0,0896
4200	0,8717	0,0764	-0,0580	0,0751	0,9297	0,0013	0,1482	0,0855
4300	0,9481	0,0731	0,0171	0,0718	0,9310	0,0013	0,2337	0,0817
4400	1,0212	0,0696	0,0889	0,0686	0,9323	0,0010	0,3154	0,0781
4500	1,0908	0,0664	0,1575	0,0659	0,9333	0,0005	0,3935	0,0748
4600	1,1572	0,0634	0,2234	0,0631	0,9338	0,0003	0,4683	0,0716
4700	1,2206	0,0607	0,2865	0,0607	0,9341	0,0000	0,5399	0,0688
4800	1,2813	0,0580	0,3472	0,0582	0,9341	-0,0002	0,6087	0,0660
4900	1,3393	0,0556	0,4054	0,0561	0,9339	-0,0005	0,6747	0,0635
5000	1,3949	0,0533	0,4615	0,0539	0,9334	-0,0007	0,7382	0,0610
5100	1,4482	0,0512	0,5155	0,0521	0,9327	-0,0008	0,7992	0,0587
5200	1,4994	0,0492	0,5675	0,0501	0,9319	-0,0010	0,8579	0,0566
5300	1,5485	0,0470	0,6176	0,0484	0,9309	-0,0013	0,9145	0,0545
5400	1,5956	0,0454	0,6660	0,0467	0,9296	-0,0014	0,9690	0,0526
5500	1,6409	0,0435	0,7127	0,0452	0,9282	-0,0015	0,0216	0,0508
5600	1,6846	0,0420	0,7579	0,0437	0,9267	-0,0017	1,0724	0,0492
5700	1,7265	0,0405	0,8016	0,0423	0,9249	-0,0018	1,1216	0,0474
5800	1,7670	0,0389	0,8439	0,0409	0,9231	-0,0020	1,1690	0,0459
5900	1,8059	0,0376	0,8848	0,0397	0,9211	-0,0021	1,2149	0,0445
6000	1,8435		0,9245		0,9190		1,2594	

In the columns for the differences in the common logarithms of the equilibrium constants ($\Delta \log K_{p1}$, $\Delta \log K_{p3}$, etc.) is presented the difference in the values of the common logarithms of the equilibrium constants for the subsequent and current temperatures. For example, in the line $T = 3400^\circ K$ we are given the difference in the value of $\log K_p$ at 3500 and 3400°K.

Using the difference tables, we can determine the values of the equilibrium constants (by linear interpolation of the logarithms of the equilibrium constants) regardless of the intermediate temperature.

APPENDIX IV

ENTROPY S_1 OF PRODUCTS OF FUEL COMBUSTION IN kcal/kmole $^{\circ}$ C*

T° K	CO ₂	H ₂ O	CO	OH	NO	H ₂
298,16	51,061	45,106	47,301	43,888	50,339	31,211
300	51,116	45,154	47,342	43,934	50,384	31,253
400	53,815	47,490	49,352	45,978	52,436	33,250
500	56,113	49,314	50,927	47,553	54,048	34,809
600	58,109	50,903	52,238	48,840	55,392	36,084
700	59,895	52,269	53,373	49,927	56,556	37,167
800	61,507	53,490	54,379	50,877	57,589	38,108
900	62,980	54,599	55,287	51,723	58,520	38,946
1000	64,3310	55,6180	56,1160	52,4910	59,3700	39,7040
1100	65,5822	56,5712	56,8779	53,1949	60,1500	40,3963
1200	66,7461	57,4654	57,5837	53,8470	60,8715	41,0365
1300	67,8334	58,3090	58,2413	54,4559	61,5425	41,6334
1400	68,8532	59,1084	58,8569	55,0278	62,1696	42,1938
1500	69,8132	59,8687	59,4353	55,5675	62,7580	42,7227
1600	70,7200	60,5939	59,9806	56,0788	63,3122	43,2248
1700	71,5792	61,2873	60,4964	56,5650	63,8358	43,7016
1800	72,3955	61,9515	60,9857	57,0285	64,3319	44,1571
1900	73,1727	62,5887	61,4510	57,4714	64,8034	44,5931
2000	73,9145	63,2010	61,8945	57,8956	65,2524	45,0112
2100	74,6238	63,7900	62,3181	58,3027	65,6811	45,4130
2200	75,3034	64,3574	62,7234	58,6939	66,0912	45,7998
2300	75,9557	64,9045	63,1121	59,0705	66,4841	46,1728
2400	76,5828	65,4328	63,4854	59,4337	66,8613	46,5329
2500	77,1865	65,9434	63,8444	59,7842	67,2240	46,8812
2600	77,7687	66,4374	64,1902	60,1230	67,5732	47,2183
2700	78,3307	66,9159	64,5238	60,4508	67,9100	47,5451
2800	78,8740	67,3796	64,8458	60,7684	68,2351	47,8622
2900	79,3997	67,8294	65,1572	61,0764	68,5494	48,1702
3000	79,9090	68,2661	65,4586	61,3753	68,8537	48,4696

* G. B. Sinyarev and M. V. Dobrovolskiy. Zhidkostnyye raketnyye dvigateli [Liquid-propellant Rocket Engines], Oborongiz [State Publishing House of the Defense Industry], 1957.

APPENDIX IV (CONTINUED)

O ₂	N ₂	H	O	N	T° K
49,011	45,767	27,3927	38,4689	36,6145	298,16
49,056	45,809	27,4232	38,5010	36,6450	300
51,098	47,818	28,8524	39,9915	38,0742	400
52,728	49,385	29,9610	41,1308	39,1828	500
54,105	50,685	30,8667	42,0540	40,0885	600
55,303	51,805	31,6326	42,8307	40,8544	700
56,368	52,797	32,2959	43,5011	41,5177	800
57,327	53,692	32,8811	44,0914	42,1029	900
58,1990	54,5090	33,4045	44,6183	42,6263	1000
58,9983	55,2601	33,8780	45,0945	43,0998	1100
59,7364	55,9565	34,3103	45,5288	43,5321	1200
60,4220	56,6060	34,7079	45,9281	43,9297	1300
61,0622	57,2143	35,0761	46,2975	44,2979	1400
61,6628	57,7863	35,4188	46,6413	44,6406	1500
62,2287	58,3261	35,7395	46,9628	44,9613	1600
62,7640	58,8371	36,0407	47,2646	45,2625	1700
63,2719	59,3221	36,3246	47,5492	45,5464	1800
63,7585	59,7836	36,5932	47,8184	45,8151	1900
64,2172	60,2237	36,8480	48,0737	46,0699	2000
64,6590	60,6443	37,0904	48,3166	46,3124	2100
65,0829	61,0471	37,3215	48,5481	46,5436	2200
65,4904	61,4333	37,5424	48,7695	46,7646	2300
65,8828	61,8044	37,7538	48,9814	46,9763	2400
66,2614	62,1614	37,9566	49,1848	47,1794	2500
66,6272	62,5054	38,1515	49,3803	47,3747	2600
66,9812	62,8373	38,3390	49,5686	47,5628	2700
67,3241	63,1579	38,5196	49,7501	47,7443	2800
67,6568	63,4679	38,6940	49,9254	47,9197	2900
67,9797	63,7680	38,8624	50,0950	48,0894	3000

APPENDIX IV (CONTINUED)

T° K	CO ₂	H ₂ O	CO	OH	NO	H ₂
3100	80,4079	68,6904	65,7506	61,6658	69,1484	48,7609
3200	80,8822	69,1029	66,0338	61,9482	69,4342	49,0447
3300	81,3180	69,5042	66,3087	62,2230	69,7117	49,3213
3400	81,8008	69,8949	66,5757	62,4906	69,9813	49,5911
3500	82,2414	70,2754	66,8354	62,7515	70,2434	49,8545
3600	82,6705	70,6463	67,0880	63,0059	70,4985	50,1119
3700	83,0886	71,0080	67,3340	63,2542	70,7469	50,3635
3800	83,4963	71,3609	67,5738	63,4966	70,9891	50,6097
3900	83,8941	71,7054	67,8076	63,7336	71,2252	50,8506
4000	84,2826	72,0420	68,0357	63,9652	71,4556	51,0866
4100	84,6620	72,3710	68,2584	64,1917	71,6806	51,3178
4200	85,0329	72,6926	68,4760	64,4135	71,9005	51,5445
4300	85,3957	73,0071	68,6887	64,6306	72,1154	51,7668
4400	85,7507	73,3150	68,8966	64,8434	72,3256	51,9850
4500	86,0982	73,6164	69,1001	65,0518	72,5312	52,1992
4600	86,4386	73,9117	69,2993	65,2563	72,7326	52,4096
4700	86,7721	74,2011	69,4944	65,4569	72,9299	52,6164
4800	87,0991	74,4847	69,6855	65,6537	73,1232	52,8196
4900	87,4198	74,7629	69,8728	65,8470	73,3128	53,0194
5000	87,7344	75,0359	70,0565	66,0368	73,4987	53,2159
5100	88,0433	75,3038	70,2367	66,2233	73,6812	53,4093
5200	88,3466	75,5669	70,4136	66,4065	73,8602	53,5997
5300	88,6445	75,8254	70,5872	66,5867	74,0361	53,7871
5400	88,9373	76,0794	70,7576	66,7639	74,2088	53,9717
5500	89,2251	76,3290	70,9251	66,9382	74,3786	54,1536
5600	89,5081	76,5745	71,0897	67,1097	74,5454	54,3328
5700	89,7865	76,8159	71,2514	67,2785	74,7095	54,5095
5800	90,0601	77,0535	71,4105	67,4447	74,8709	54,6837
5900	90,3301	77,2873	71,5670	67,6084	75,0297	54,8555
6000	90,5955	77,5175	71,7209	67,7697	75,1860	55,0250

APPENDIX IV (CONTINUED)

O ₂	N ₂	H	O	N	T° K
68,2936	64,0588	39,0253	50,2592	48,2539	3100
68,5990	64,3409	39,1830	50,4183	48,4135	3200
68,8963	64,6148	39,3359	50,5728	48,5687	3300
69,1859	64,8809	39,4842	50,7229	48,7197	3400
69,4683	65,1397	39,6282	50,8689	48,8669	3500
69,7439	65,3915	39,7681	51,0111	49,0105	3600
70,0128	65,6368	39,9043	51,1496	49,1508	3700
70,2756	65,8758	40,0368	51,2846	49,2880	3800
70,5323	66,1089	40,1658	51,4165	49,4223	3900
70,7834	66,3364	40,2916	51,5452	49,5539	4000
71,0290	66,5585	40,4142	51,6711	49,6830	4100
71,2693	66,7754	40,5340	51,7942	49,8099	4200
71,5046	66,9875	40,6509	51,9147	49,9345	4300
71,7351	67,1949	40,7651	52,0326	50,0572	4400
71,9609	67,3979	40,8767	52,1482	50,1779	4500
72,1822	67,5965	40,9859	52,2615	50,2969	4600
72,3993	67,7911	41,0928	52,3727	50,4142	4700
72,6122	67,9818	41,1973	52,4817	50,5299	4800
72,8210	68,1687	41,2998	52,5888	50,6442	4900
73,0261	68,3520	41,4002	52,6939	50,7571	5000
73,2273	68,5318	41,4985	52,7972	50,8687	5100
73,4250	68,7082	41,5950	52,8988	50,9790	5200
73,6192	68,8815	41,6896	52,9986	51,0882	5300
73,8100	69,0516	41,7825	53,0968	51,1962	5400
73,9975	69,2188	41,8736	53,1933	51,3032	5500
74,1819	69,3831	41,9632	53,2884	51,4092	5600
74,3632	69,5446	42,0511	53,3820	51,5142	5700
74,5416	69,7034	42,1375	53,4742	51,6183	5800
74,7171	69,8596	42,2224	53,5649	51,7215	5900
74,8898	70,0134	42,3059	53,6544	51,8238	6000

APPENDIX V

COMMON LOGARITHMS FOR CONSTANTS OF CHEMICAL EQUILIBRIUM FOR PRODUCTS OF INCOMPLETE FUEL COMBUSTION

T °K	1 Метан CH ₄		2 Ацетилен C ₂ H ₂		3 Этилен C ₂ H ₄		4 Этан C ₂ H ₆		5 Бензол C ₆ H ₆		T °K
	$\lg K_p = \lg \frac{P_{H_2}}{P_{CH_4}}$	$\lg K_p = \lg \frac{P_{CO}^2 P_{H_2}}{P_{CO_2} P_{CH_4}}$	$\lg K_p = \lg \frac{P_{H_2}}{P_{C_2H_2}}$	$\lg K_p = \lg \frac{P_{CO}^2 P_{H_2}}{P_{CO_2} P_{C_2H_2}}$	$\lg K_p = \lg \frac{P_{H_2}}{P_{C_2H_4}}$	$\lg K_p = \lg \frac{P_{CO}^2 P_{H_2}}{P_{CO_2} P_{C_2H_4}}$	$\lg K_p = \lg \frac{P_{H_2}}{P_{C_2H_6}}$	$\lg K_p = \lg \frac{P_{CO}^2 P_{H_2}}{P_{CO_2} P_{C_2H_6}}$	$\lg K_p = \lg \frac{P_{H_2}}{P_{C_6H_6}}$	$\lg K_p = \lg \frac{P_{CO}^2 P_{H_2}}{P_{CO_2} P_{C_6H_6}}$	
300	—	-29,6859	—	-5,2588	—	-29,8082	—	-47,3837	—	-102,3830	300
400	-5,5377	-18,8198	+26,5150	-0,0589	+9,6074	-16,9616	-1,9506	-28,5194	+19,0158	-60,6907	400
500	-3,4585	-12,2102	20,6101	+3,1040	8,3639	-9,1422	+0,4580	-17,0481	17,0437	-35,4746	500
600	-2,0339	-7,7620	16,6801	5,2221	7,5818	-3,8762	2,1233	-9,3346	15,8154	-18,5586	600
700	-0,9808	-4,5551	13,8806	6,7312	7,0454	-0,1040	3,3704	-3,7790	14,9836	-6,4646	700
800	-0,1738	-2,1367	11,7856	7,8596	6,6629	+2,7369	3,3123	+0,3863	14,3670	+2,5891	800
900	+0,4671	-0,2494	10,1646	8,7319	6,3788	4,9462	5,0680	3,6352	13,9098	9,6117	900
1000	0,9901	+1,2705	8,8642	9,4218	6,1513	6,7089	5,6843	6,2418	13,5264	15,1984	1000
1100	1,4320	2,5176	7,8107	9,9833	5,9712	8,1438	6,2003	8,3729	13,2512	19,7688	1100
1200	1,7992	3,5546	6,9277	10,4402	5,8254	9,3378	6,6191	10,1316	13,0109	23,5183	1200
1300	2,1058	4,4248	6,1905	10,8333	5,6990	10,3388	6,9855	11,6253	12,8000	26,7191	1300
1400	2,3616	5,1602	5,5523	11,1515	5,5969	11,1961	7,2862	12,8855	12,6334	29,4311	1400
1500	2,5713	5,7828	5,0114	11,4364	5,5028	11,9274	7,5409	13,9659	12,4628	31,7379	1500

1) Methane CH₄; 2) acetylene C₂H₂; 3) ethylene C₂H₄; 4) ethane C₂H₆; 5) benzene C₆H₆.

APPENDIX VI

THERMODYNAMIC CHARACTERISTICS OF CERTAIN GASES

$T^{\circ}K$ \ 1Gas	CH_4	C_2H_2	C_2H_4	C_2H_6	C_6H_6
A 1. Энергосодержание (полная энтальпия) I_1 ккал/кмоль					
300	-17871	+54212	+12519	-20210	+19870
400	-16945	55346	13690	-18795	22200
500	-15919	56592	15075	-17062	25170
600	-14743	57931	16705	-15104	28710
700	-13419	59330	18483	-12816	32710
800	-11978	60804	20439	-10339	37040
900	-10409	62378	22529	-7686	41680
1000	-8709	63886	24729	-4816	46570
1100	-6939	65497	27039	-1796	51680
1200	-5049	67139	29429	+1314	56990
1300	-3119	68861	31889	4614	62480
1400	-1169	70561	34469	7964	68030
1500	+801	72361	37049	11384	73640
B 2. Энтропия S_1 ккал/кмоль $^{\circ}C$					
300	44,56	48,07	52,52	54,94	64,607
400	47,18	51,30	55,92	58,99	71,267
500	49,47	54,07	59,00	62,83	77,927
600	51,65	56,51	61,95	66,43	84,327
700	53,69	58,67	64,70	69,91	90,447
800	55,61	60,633	67,29	73,25	96,227
900	57,46	62,402	69,74	76,38	101,707
1000	59,22	64,076	72,06	79,38	106,927
1100	60,86	65,603	74,27	82,22	111,747
1200	62,47	67,060	76,34	84,95	116,357
1300	64,01	68,404	78,32	87,56	120,767
1400	65,49	69,682	80,22	90,08	124,847
1500	66,94	70,890	82,02	92,50	128,807
C 3. Молярные теплоемкости μC_{p1} ккал/кмоль $^{\circ}C$					
300	8,543	10,500	10,44	12,66	19,68
400	9,743	11,978	12,91	15,69	26,71
500	11,130	12,947	15,15	18,66	32,80
600	12,537	13,709	17,11	21,32	37,74
700	13,875	14,352	18,74	23,69	41,71
800	15,091	14,925	20,185	25,807	45,06
900	16,210	15,441	21,454	27,686	47,77
1000	17,196	15,909	22,556	29,279	50,14
1100	18,063	16,343	23,516	30,632	52,11
1200	18,877	16,734	24,364	31,840	53,81
1300	19,576	17,088	25,123	32,956	55,27
1400	20,179	17,406	25,763	33,968	56,54
1500	20,700	17,692	26,338	34,883	57,69

1) Gas; A) 1. Energy content (total enthalpy) I_1 , kcal/kmole; B) 2. Entropy S_1 , kcal/kmole $^{\circ}C$; C) 3. Molar heat capacities μC_{p1} , kcal/kmole $^{\circ}C$.

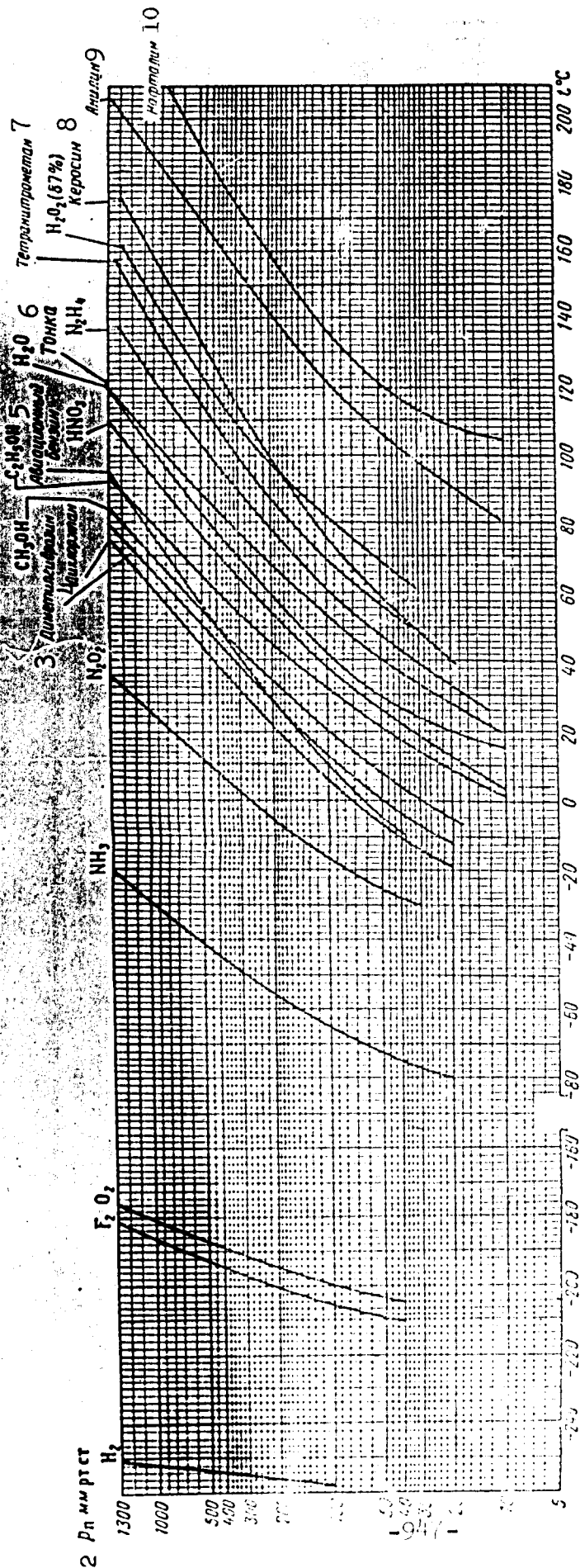
APPENDIX VII

AUXILIARY THERMODYNAMIC-FUNCTION DATA AT DIFFERENT EXPONENTS FOR ISENTROPY OR POLYTROPY EQUATIONS

k	$\frac{1}{k-1}$	$\frac{k}{k-1}$	$\frac{k+1}{k-1}$	$\frac{2}{k+1}$	$\frac{2}{k-1}$	$\frac{k+1}{k-1}$	$\frac{1}{k-1}$	$\sqrt{\frac{k+1}{k-1}}$	$\frac{1}{\left(\frac{k+1}{2}\right)^{\frac{k-1}{2}}}$
1.10	10,000	11,000	1,050	0,952	20,000	21,000	0,0476	4,582	1,628
1.11	9,090	10,090	1,055	0,948	18,182	19,182	0,0526	4,380	1,626
1.12	8,333	9,333	1,060	0,943	16,666	17,666	0,0566	4,103	1,625
1.13	7,692	8,692	1,065	0,939	15,384	16,384	0,0611	4,046	1,623
1.14	7,143	8,143	1,070	0,934	14,286	15,286	0,0654	3,890	1,621
1.15	6,666	7,666	1,075	0,930	13,333	14,333	0,0697	3,786	1,615
1.16	6,250	7,250	1,080	0,926	12,500	13,500	0,0741	3,674	1,618
1.17	5,882	6,882	1,085	0,921	11,765	12,765	0,0778	3,573	1,616
1.18	5,555	6,555	1,090	0,917	11,111	12,111	0,0826	3,479	1,615
1.19	5,263	6,263	1,095	0,913	10,526	11,526	0,0867	3,395	1,612
1.20	5,000	6,000	1,100	0,909	10,000	10,000	0,0909	3,316	1,610
1.21	4,762	5,762	1,105	0,904	9,524	10,524	0,0950	3,244	1,609
1.22	4,545	5,545	1,110	0,901	9,091	10,091	0,0991	3,178	1,607
1.23	4,348	5,348	1,115	0,896	8,696	9,696	0,1031	3,113	1,605
1.24	4,166	5,166	1,120	0,893	8,333	9,333	0,1071	3,055	1,603
1.25	4,000	5,000	1,125	0,888	8,000	9,000	0,1111	3,000	1,602
1.26	3,846	4,846	1,130	0,885	7,692	8,692	0,1150	2,949	1,600
1.27	3,704	4,704	1,135	0,881	7,408	8,408	0,1193	2,900	1,599
1.28	3,572	4,572	1,140	0,877	7,143	8,143	0,1252	2,854	1,597
1.29	3,448	4,448	1,145	0,873	6,896	7,896	0,1266	2,653	1,596
1.30	3,333	4,333	1,150	0,869	6,666	7,666	0,1317	2,768	1,593
1.32	3,125	4,125	1,160	0,862	5,250	7,250	0,1379	2,692	1,590
1.34	2,941	3,941	1,170	0,856	5,882	6,882	0,1453	2,623	1,587
1.36	2,777	3,777	1,180	0,847	5,554	6,555	0,1525	2,560	1,584
1.38	2,692	3,692	1,190	0,840	5,263	6,263	0,1596	2,502	1,581
1.40	2,500	3,500	1,200	0,833	5,000	6,000	0,1666	2,449	1,575
1.50	2,000	3,000	1,250	0,800	4,000	5,000	0,2000	2,236	1,563

APPENDIX VII (CONTINUED)

$\frac{1}{2} \left(\frac{k-1}{k+1} \right)$	$\frac{k}{k+1}$	$\frac{k}{2} \left(\frac{k-1}{k+1} \right)$	$\frac{2}{k+1}$	$\frac{k+1}{2} \left(\frac{k-1}{k+1} \right)$	$\sqrt{\frac{2g}{k-1}}$	$\sqrt{\frac{k+1}{gk} \left(\frac{2}{k+1} \right)}$	$\sqrt{\frac{k+1}{2k^2} \left(\frac{2}{k+1} \right)}$
0,6139	1,712	0,5841	0,3767	0,3588	14,6801	1,978	0,6590
0,6146	1,718	0,5821	0,3775	0,3579	14,0680	1,984	0,6640
0,6153	1,724	0,5804	0,3784	0,3571	13,3381	1,988	0,6690
0,6160	1,730	0,5784	0,3792	0,3562	13,0591	1,993	0,6440
0,6168	1,736	0,5762	0,3800	0,3553	12,6125	1,998	0,6790
0,6175	1,744	0,5744	0,3809	0,3545	12,2637	2,000	0,6848
0,6182	1,749	0,5723	0,3818	0,3536	11,9261	2,009	0,6898
0,6188	1,754	0,5705	0,3826	0,3527	11,6190	2,014	0,6946
0,6195	1,761	0,5685	0,3835	0,3519	11,1175	2,018	0,6997
0,6202	1,767	0,5665	0,3844	0,3510	11,0851	2,024	0,7052
0,6209	1,771	0,5645	0,3852	0,3501	10,8570	2,030	0,7104
0,6216	1,779	0,5621	0,3860	0,3493	10,6323	2,034	0,7153
0,6223	1,785	0,5603	0,3869	0,3485	10,4302	2,040	0,7204
0,6230	1,790	0,5588	0,3878	0,3477	10,2435	2,045	0,7251
0,6237	1,796	0,5569	0,3886	0,3469	10,0672	2,050	0,7302
0,6243	1,801	0,5549	0,3894	0,3462	9,9044	2,055	0,7356
0,6250	1,818	0,5532	0,3903	0,3454	9,7484	2,061	0,7404
0,6257	1,813	0,5513	0,3911	0,3446	9,6067	2,066	0,7453
0,6264	1,820	0,5494	0,3919	0,3437	9,4740	2,072	0,7500
0,6271	1,825	0,5475	0,3927	0,3430	9,3418	2,078	0,7552
0,6276	1,832	0,5457	0,3936	0,3423	9,2495	2,083	0,7598
0,6289	1,838	0,5421	0,3953	0,3407	8,9961	2,094	0,7695
0,6302	1,856	0,5386	0,3968	0,3392	8,7931	2,105	0,7792
0,6314	1,868	0,5352	0,3985	0,3377	8,6280	2,111	0,7906
0,6327	1,880	0,5317	0,4001	0,3362	8,4403	2,129	0,7992
0,6339	1,893	0,5283	0,4018	0,3348	8,2867	2,140	0,8102
0,6401	1,953	0,5120	0,4096	0,3277	7,6720	2,210	0,8586



- 1) Appendix VIII; 2) p_p , mm Hg; 3) dimethyl hydrazine; 4) dichloroethane;
5) aviation gasoline; 6) Tonka; 7) tetranitromethane; 8) kerosene; 9)
aniline; 10) naphthalene.

BIBLIOGRAPHY

- Abramovich, G. N. Teoriya tsentrobezhnoy forsunki [The Theory of the Centrifugal Injector], Promyshlennaya aerodinamika [Industrial Aerodynamics], TsAGI [Central Aero-Hydrodynamical Institute (im. N. Ye. Zhukovskiy)], 1944.
- Astakhov, I. V. Vliyaniye vyazkosti topliv i drugikh faktorov na melkost' raspylivaniya [The Effect of Fuel Viscosities and Other Factors on the Fineness of Atomization], "Dizelestroeniye" [Diesel-Engine Building], 1937, No. 2.
- Bogomolov, L. P. Forsunki nizkogo davleniya dlya zhidkogo topliva [Low-Pressure Injectors for Liquid Fuel]. Byuro Tekhproma VOMT [Technical and Industrial Bureau, All-Union Heavy Machinery Association], Moscow, 1933.
- Bolgarskiy, A. V., and Shchukin, V. K. Rabochiye protsessy v zhidkostno-raketnykh dvigatelyakh [Cycles in Liquid-Propellant Rocket Engines], Oborongiz [State Publishing House of the Defense Industry], 1953.
- Vanichev, A. P. Termodinamicheskiy raschet goreniya i istecheniya v oblasti vysokikh temperatur [The Thermodynamic Calculation of Combustion and Exhaust in a High-Temperature Zone], Izd. BNT [BNT Press], 1947.
- Vanichev, A. P., and Knorre, G. F. Obobshchennyye raschetnyye formuly gazovogo analiza [Generalized Calculation Formulas for Gas Analysis], Izd. BNT, 1946.
- Gukhman, A. A., and Il'yukhin, N. V. Osnovy ucheniya o teploobmene pri techenii gaza s bol'shoy skorost'yu [The Bases for Studying Heat Transfer in High-Speed Gas Streams], Mashgiz [State Scientific and Technical Publishing House of Literature on Machinery], 1951.

- Zel'dovich, Ya. B., and Polyarnyy, A. I. Raschety teplovykh protsessov pri vysokoy temperature [Calculations of Heat Processes at High Temperatures], Izd. BNT, 1947.
- Kalikhman, L. Ye. Gazodinamicheskaya teoriya teploobmena [The Gasdynamic Theory of Heat Transfer], Prikladnaya matematika i mekhanika [Applied Mathematics and Mechanics], 1946, Vol. X, No. 4.
- Key, D., and Lebi, T. [sic]. Spravochnik fizika-eksperimentatora [A Handbook for the Experimental Physicist], IL, 1949.
- Knorre, G. F. Topochnye protsessy [Furnace Cycles], Gosenergoizdat [State Power Engineering Publishing House], 1951.
- Kooy, I., and Yutenbogart, I. Dinamika raket [The Dynamics of Rockets], Oborongiz, 1950.
- Mikheyev, M. A. Osnovy teploperedachi [The Bases of Heat Transfer], Gosenergoizdat, 1956.
- Novikov, I. I. Drobleniye zhidkostey v tsentrobezhnykh forsunkakh [Liquid Drop-Formation in Centrifugal Injectors], ZhTF [Journal of Technical Physics], Vol. XVIII, 1948.
- Rogozin, N. A. Spravochnik po aviatsionnym i avtomobil'nyim toplivam [Handbook of Aviation and Automobile Fuels], Gostoptekhizdat [State Scientific and Technical Publishing House of the Petroleum and Mineral-Fuel Industry], 1947.
- Satton, D. [sic]. Raketnyye dvigateli [Rocket Engines], IL, 1950.
- Sinyarev, G. B., and Dobrovol'skiy, M. V. Zhidkostnyye raketnyye dvigateli [Liquid-Propellant Rocket Engines], Oborongiz, 1957.
- Fedos'yev, V. I., and Sinyarev, G. B. Vvedeniye v raketnyuyu takhniku [Introduction to Rocket Technology], Oborongiz, 1956.*

* An English edition of this book, translated from the Russian by S. N. Samburoff, was published by the Academic Press, New York and London, in 1959.

Khemfris, D. [sic]. Raketnyye dvigateli i upravlayemye snaryady
[Rocket Engines and Guided Missiles], IL, 1958.

Tsander, F. A. Problemy poleta pri pomoshchi reaktivnykh apparatov
[Flight Problems of Reaction Aircraft], Oborongiz, 1947.

Tsiolkovskiy, K. E. Trudy po raketnoy tekhnike [Works on Rocket
Engineering], Oborongiz, 1947.

Izvestiya vysshikh uchebnykh zavedeniy MVO SSSR [Reports of Higher
Educational Institutions, Ministry of Higher Education of the
USSR] Aviatsionnaya tekhnika [Aviation Engineering], No. 1,
Kazan', 1958.

Voprosy goreniya [Problems of Combustion]. Sbornik statey [Collec-
tion of Articles], parts 1 and 2, Translations, IL, 1953.

Journal "Reaktivnaya tekhnika" [Reaction Engineering], No. 2-6,
1937.

Journal "Voprosy raketnoy tekhniki" [Problems of Rocket Engineering].
1956, No. 1, 3, and 4; 1957, No. 1, 3, 5, and 6, IL.

Spravochnik khimika [A Handbook for the Chemist], Vol. 1 and 2,
Gostekhzdat [State Publishing House of Theoretical and Tech-
nical Literature], 1951.

"Teploenergetika" [Heat and Power Engineering], VTI SSSR [All-Union
Heat Engineering Institute (im. F. Dzerzhinskiy) of the USSR]
1955, No. 9.

Fizika i khimiya reaktivnogo topliva [Physics and Chemistry of
Reaction Fuel], Collections No. 1 and 2, IL, 1948.

Ekspress-informatsiya, AN USSR, No. 2, RT-58, 1957.

Ekspress-informatsiya, AN USSR, No. 4, RT-32, 1957.

Ekspress-informatsiya, AN USSR, No. 6, RT-16, 1957.

Ekspress-informatsiya, AN USSR, No. 18, RT-53, 1957.

Ekspress-informatsiya, AN USSR, No. 32, RT-94, 1957.

Ekspress-informatsiya, AN USSR, No. 8, RT-22, 1958.

Ekspress-informatsiya, AN USSR, No. 8, RT-23, 1958.

Ekspress-informatsiya, AN USSR, No. 7, RT-20, 1958.

Ekspress-informatsiya, AN USSR, No. 23, RT-68, 1958.

Ekspress-informatsiya, AN USSR, No. 20, ADS-78, 1958.

Anson, D. Vliyaniye kachestva raspylivaniya na ustoychivoye gorenije zhidkikh toplivnykh struy [The Effect of the Nature of Atomization on Steady Combustion of Liquid-Fuel Sprays], Fuel, Vol. 32, No. 1, 1953.

Kelle, G. K opredeleniyu optimal'nogo davleniya v kamere sgoraniya raketnogo dvigatelya [A Method for Determining the Optimum Pressure for the Combustion Chamber of a Rocket Engine], Welt-raumfahrt, 1953, No. 1.

Krokko, L. [sic]. Voprosy ustoychivosti sgoraniya v zhidkostnykh raketnykh dvigatelyakh [Problems of Stability of Combustion in Liquid-Propellant Rocket Engines], Journal of the Am. Rock. Soc., 1952, No. 22.

Otbor v ZhRD moshchnosti dlya privoda vspomogatel'nykh agregatov [Tapping Power Sources to Drive Auxiliary Units in Liquid-Propellant Rocket Engines], Aviation Age, Vol, 25, No. 4, 1956.

Khurden, D. [sic]. Konstruirovaniye raketnykh dvigateley [The Designing of Rocket Engines], J. Brit. Interpl. Soc., Vol. II, No. 3, 1952.

Shteling, K. [sic]. Forsunochnyy vprysk i gidravlicheskiye faktory v analize raketnogo dvigatelya [Spray Injection and Hydraulic Factors in the Analysis of a Rocket Engine], Journ. of Am. Rock. Soc., Vol. 22, No. 3, 1952.

Aeroplane, 7, Vol. 91, Nos. 2349 and 2347, 1956.

Aviation Daily, Vol. 114, No. 35, 1958.

Interavia, No. 4038, 1958.

Jet Propulsion, Vol. 27, No. 6, 1957.

Jet Propulsion, Vol. 6 [sic]. No. 6, 1957.

Jet Propulsion, Vol. 28, No. 4, 1958.

New Scientist, Vol. 3, No. 66, 1958.

Missiles and Rockets, Vol. 1, No. 1, 1956.

DISTRIBUTION LIST

DEPARTMENT OF DEFENSE	Nr. Copies	MAJOR AIR COMMANDS	Nr. Copies
		AFSC	
		SCFTR	1
		ARO	1
HEADQUARTERS USAF		ASTIA	10
		TD-Bla	3
AFCIN-3D2	1	BSD (BSF)	1
		AFPTC (PTY)	1
		ASD (DCF)	1
OTHER AGENCIES			
CIA	1		
NSA	2		
AID	2		
OTS	2		
AEC	2		
PWS	1		
POB	1		
RAND	1		
SPECTRUM	1		